QC
851
.G73
v.10

Air Ministry
Meteorological Research Committee
MRP 952-1001 (non-inclusive)

MRP No.	Title	Author
952 AD 117799	Convection From a Small, Continuous Source of Heat in a Calm, Neutral Atmosphere (With an Appendix on the Bent-over Plume).	P.J. Meade
953 AD 133971	The Success Achieved in Forecasting Upper Winds by Orthodox and Statistical Techniques.	D.H. Johnson
955 AD 133330	Comments on Statistical and Orthodox Forecasting.	C.S. Durst
956	The Use of a Stream Function in the Sawyer-Bushby Two-Parameter Model of the Atmosphere.	F.H. Bushby V.M. Huckle
960 AD 223098	Development of Thermometers for High-speed Aircraft.	D.D. Clark
961 AD 223097	A Technique for Studying the Local Atmospheric Diffusion of Airborne Material (Porton Technical Paper No. 527).	J.S. Hay F. Pasquill
965 AD 223096	Objective Analysis.	D.H. Johnson
970 AD 223095	The Harmonic Representation of the Annual Temperature Variation in Different Parts of the British Isles.	J.M. Craddock
971 AD 139534	Variation of Visibility in Fog at Exeter Airport, and the Time of Fog Dispersal.	W.E. Saunders
972 AD 223109	Water Loss From Various Cropped Surfaces.	N.E. Rider
973 AD 223108	Evaporation From a Saturated Rough Surface into a Turbulent Air Stream (Porton Technical Paper No. 533).	J.S. Hay
974 AD 223107	A Vertical Gustiness Recorder for Use With a Captive Balloon (Porton Technical Paper No. 536).	J.I.P. Jones
976	Further Observations of Humidity up to 50,000 Feet Made From Aircraft of the Meteorological Research Flight in 1955.	N.C. Helliwell J.K. Mackenzie M.J. Kerley
977 AD 223105	An Electrical Dewpoint Hygrometer Suitable for Routine Meteorological Use.	J. MacDowall

MRP No.	Title	Author
978 AD 223126	Long-period Averages for the Upper Air.	J.K. Bannon
979 AD 131894	Further Observation of Condensation Trails.	N.C. Helliwell J.K. Mackenzie
980	Further Observations of Large Cumuliform Clouds by the Meteorological Research Flight.	G.J. Day
981 AD 208840	Average Height of the Standard Isobaric Surfaces Over the Area From the North pole to 55 degrees N. in July.	H. Heastie
983 AD 223123	The Measurement of Humidity at Britannia Soe 1952-53.	R.A. Hamilton
984 AD 223124	Variation With Height of Rainfall Below the Melting Level.	W.G. Harper
985 AD 139535	A Preliminary Study of Atmospheric Waves Using Radiosonde Data.	G.A. Corby
986 AD 147514	The Objective Analysis of Some 500 mb. Charts.	F.H. Bushby
987 AD 139536	Equivalent Head-wind Statistics for Variable Tracks.	P. Graystone
988 AD 147513	On the Development of an Improved Daylight Illumination Recorder.	M.J. Blackwell D.B.B. Powell
989 AD 223125	The Measurement of Surface Wind.	R. Frith
990 AD 131893	The Exhaust Trail From Jet Engines.	R.F. Jones
991 AD 147512	Droplet Sampling in Cumulus Clouds. A Note on M.R.P. 991.	W.G. Durbin B.C.V. Oddie
994 AD 147511	A Synoptic Study of Anomalies of Surface Air Temperature Over the Atlantic Half of the Northern Hemisphere.	J.M. Craddock C.A.S. Lowndes
995 AD 147510	Meteorological Research in Aircraft.	R.J. Murgatroyd
996	Condensation Trails Formed by Jet Aircraft.	J. Briggs
997 AD 223117	A Simple Method for Measuring Atmospheric Attenuation of Light ("Meteorological Optical Range" or Visibility) at Night.	K.H. Stewart

MRP No.	Author	Title
998 AD 223119	The Measurements of Natural Freezing Nuclei Made by the Meteorological Research Flight During January, 1956.	R.J. Murgatroyd M.P. Garrod
1001 AD 223118	Index of M.R.P.'s Approved for General Distribution.	

M.R.P. 952
S.C. III/196
28th November, 1955

AD 117799

Convection from a small, continuous source of heat in a calm, neutral atmosphere (with an appendix on the bent-over plume)

by

P. J. Meade
(Meteorological Office)

AIR MINISTRY
METEOROLOGICAL RESEARCH COMMITTEE

At the time of issue this report has not been published. Any author desiring to quote this paper should refer to it as "A paper of the Meteorological Research Committee (London), M.R.P. No. 952 by Mr. P.J. Meade. A copy is available in the Library of the Meteorological Office."

M.R.P. 952
S.C.III/196
28th November, 1955

AIR MINISTRY
METEOROLOGICAL RESEARCH COMMITTEE

Convection from a small, continuous source of heat in a calm, neutral atmosphere (with an appendix on the bent-over plume)

by

P. J. Meade (Meteorological Office)

Summary

The problem of the free convection jet from a continuous source of heat in a neutral atmosphere at rest is discussed and formulae are derived which give the variation of the vertical velocity, w, the potential temperature excess, θ', and the radius of the jet with height, z. It is believed that the formulae may have a useful application in such problems as the rising plume of heated gas emitted from factory chimneys.

The solutions to the basic equations incorporate the usual power law features but one set, in particular, contains an exponential term which leads ultimately to a fairly rapid decay of vertical velocity with height. This should provide a more realistic picture in application to practical problems than the much slower rate of decay indicated by the simple power laws generally used.

Comparison of the theory with data from laboratory experiments suggests that, for small scale phenomena, the effects of vertical shearing stress may be neglected. The solutions, thus modified, give results in close agreement with laboratory data and include, as special cases, a number of formulae derived by dimensional and other arguments.

1. General discussion

We consider the velocity and temperature fields and also the vertical variation of radius in the ascending plume or jet of air which results when heat is supplied continuously from a point or a small circular source. In its most general terms the problem is intractable and can only be discussed in a descriptive manner. The difficulty consists largely of accounting for both thermal and dynamic instability, their causes and effects, in a rising air column which is surrounded by an atmosphere in motion and possessing its own thermal characteristics.

It is in consequence necessary to impose some limitations on the type of problem to be studied and, following the normal practice, we postulate that the atmosphere is at rest, except near the boundary of the rising air where turbulent mixing occurs, and in neutral equilibrium. The heated air may then be considered to rise vertically and to be symmetrical about a vertical axis in regard to lateral extent, velocity and temperature excess. At any level above the source, the upward velocity and the temperature excess have their maximum values on the axis of the jet and become smaller and smaller as the horizontal distance from the axis increases.

It is further assumed that while the temperature differences between the jet and the surrounding air are sufficient to produce vertical motion, the associated differences in density are small enough, in comparison with the density itself, to be ignored. Observational evidence supports this assumption since it is well known that a density variation of a few per cent may produce important vertical currents while the inertia of the fluid remains practically unaffected.

The problem is thus formulated as one of free convection and we apply the theories developed in fluid dynamics in relation to boundary layers, jets and wakes (see, for example, Goldstein: Modern Developments in Fluid Dynamics). This approach has also been used by Rouse, Yih and Humphreys (1952) and by Priestley and Ball (1955). These papers contain a discussion of the basic differential equations in their meteorological context.

The following notation is used:-

z = vertical distance above source
r = horizontal distance from z-axis
R = lateral extent of jet = $R(z)$
w = vertical velocity along z-axis = $w(z)$
θ_e = environment potential temperature (assumed constant)
θ = potential temperature
θ' = excess potential temperature along z-axis, $(\theta - \theta_e) = \theta'(z)$
τ = vertical shearing stress

At points removed from the z-axis the velocity and temperature excess are given by:-

$$w(z,\ r) = w(z)\ f(r/R)$$

$$\theta'(z,\ r) = \theta'(z)\ h(r/R)$$

These expressions are justified by considerations of dynamical similarity which suggest that the lateral variation of w has the same form at all heights and similarly for the lateral variation of θ'.

It is further assumed that the vertical shearing stress τ is proportional to the square of the velocity, thus

$$\tau = \tfrac{1}{2}\ \rho\ w^2\ j(r/R)$$

The functions f, h and j of (r/R) are unknown but for most of what follows it is sufficient that their integrals, separately or in combination or in powers, should be finite.

As Rouse et al (1952) and Priestley and Ball (1955) have shown, the equations for momentum and of energy integrated over a horizontal plane from $r = 0$ to $r = \infty$, give the following differential equations governing R, the radius of the jet, and w and θ', the axial values of the vertical velocity and the temperature excess:-

$$\frac{d}{dz}\,(R^2w^2) = a\,R^2\,\frac{\theta'}{\theta_e}\,g \qquad (1)$$

$$\frac{d}{dz}\,(R^2w^3) = b\,R^2w\,\frac{\theta'}{\theta_e}\,g - c\,Rw^3 \qquad (2)$$

In these equations a, b and c are numbers which could be derived directly if the functions f, h and j were known.

Another equation follows from our assumption that the atmosphere has constant potential temperatures. If the heat output Q (calories per second) at the source is constant, then the flow of heat across any horizontal cross-section must also be a constant. We may therefore write

$$R^2w\,\theta' = \text{constant, } A \qquad (3)$$

Priestley and Ball (1955) have shown that equation (3) holds only if the atmosphere is in neutral equilibrium. Using this equation, we may write equations (1) and (2) as follows:-

$$w \frac{d}{dz} (R^2 w^2) = a \frac{Ag}{\theta_e} \qquad (4)$$

$$\frac{d}{dz} (R^2 w^3) = b \frac{Ag}{\theta_e} - c R w^3 \qquad (5)$$

From these two equations $\frac{Ag}{\theta_e}$ can be eliminated and a single differential equation is obtained:-

$$(3a - 2b) \frac{1}{w} \frac{dw}{dz} + 2(a - b) \frac{1}{R} \frac{dR}{dz} = - \frac{ac}{R} \qquad (6)$$

The solution of equation (6) and its significance will depend largely on the relative values of a and b. A fairly wide range of possibilities may be considered but in what follows attention is mainly confined to those considered likely to have an application to practical problems. Equation (6) could have been derived directly from equations (1) and (2) without the aid of equation (3), and in the following two sections equation (3) is not invoked although it does hold for some of the examples discussed.

2. Radius of the jet increasing linearly with height

In several papers on the free convection jet, linear spreading has been deduced at an early stage in the development or assumed. This law for the variation of R can be conveniently discussed as follows:-

(i) $3a - 2b = 0$

If $3a = 2b$, equation (6) reduces simply to

$$R = cz + \text{constant} \qquad (7)$$

This is the solution found by Priestley and Ball (1955) for a neutral atmosphere and their solutions for w and θ' then follow from equations (3) and either (4) or (5).

The condition that $3a - 2b = 0$ requires that the functions $f(r/R)$ and $h(r/R)$ should be the same, that is, both w and θ' should have identical laws of lateral decay. It appears unlikely that this condition would hold in practice and, in the absence of experimental support for it, a certain degree of scepticism can hardly be avoided. For example, if this condition were to be fulfilled, the value of w for large values of z would be virtually proportional to $z^{-\frac{1}{3}}$ yielding velocities far larger than experience would lead us to expect.

(ii) $3a - 2b \neq 0$; $R \propto z$

Let $R = \varepsilon z$

where ε is a constant. Substitution in equation (6) and integration lead to the result

$$w = w_o \left(\frac{z}{z_o}\right)^{-\frac{2(a - b) + \frac{ac}{\varepsilon}}{3a - 2b}} \qquad (8)$$

In the special case of c and ε being equal, as in the solution examined in (i) above, the expression for w would reduce to

$$w = w_o \left(\frac{z}{z_o}\right)^{-1} \qquad (9)$$

and we should also have

$$\theta' = 0 \qquad (10)$$

/On

On practical grounds the simultaneous solutions for w and θ' given by equations (9) and (10) are considered improbable.

Excluding the case when c and ε are equal, there remains the possibility of a variety of solutions depending on the ratio c/ε as well as on the ratio a/b. Because of the assumption of linear spreading of the jet, all these solutions for w, and hence θ', are power law solutions.

If a = b, the expressions for w and θ'

are

$$w = w_o \left(\frac{z}{z_o}\right)^{-c/\varepsilon}$$

$$\theta' \propto z^{-(2 - c/\varepsilon)}$$

One would then expect to find c less than ε because $c > \varepsilon$ would indicate that w decreased more quickly and θ' more slowly than could reasonably be expected. Thus if, as we have assumed from the outset, a and b maintain their values at all heights reached by the jet, experimental data, not necessarily very refined, can assist in the rejection of a number of theoretically possible solutions. However, the likelihood that the ratio a/b may vary from one level to another should not be excluded since a complete solution of the rising jet problem must take account of acceleration from rest in addition to what is normally the sole consideration - the deceleration from the maximum velocity attained.

Before leaving equation (8) it may be remarked that if the following condition were satisfied

$$\frac{a}{b} = \frac{4}{3(1 + c/\varepsilon)},$$

then the set of solutions would be

$$\left.\begin{array}{l} w \propto z^{-\frac{1}{3}} \\ R \propto z \\ \theta' \propto z^{-5/3} \end{array}\right\} \quad (11)$$

This set of solutions is in agreement with the results derived by Schmidt (1941), using a mixing length hypothesis, and by Rouse et al in the paper already referred to. The latters' experimental observations made in a closed room and using a gas burner as a source of heat, give the following approximate values of a and b.

$$a = 2.7; \quad b = 3.5$$

$$\text{i.e. } 3a - 2b > 0$$

With the radius of the jet increasing linearly with height, equation (8) should describe the velocity distribution. Using the value found for a and b, this requires

$$\frac{c}{\varepsilon} = \frac{7}{9}$$

Batchelor (1954) applied dimensional analysis to the problem of a continuous point source and, for turbulent flow, also obtained the set of solutions given in equations (11). His results for laminar flow are referred to in section 4.

3. Non-linear spreading of the jet

The object now is to investigate the solutions to equation (6) which arise when the radius of the jet increases with height but not in accordance with a linear law. Suppose the origin of z is taken at a point where $R = R_0$ and $w = w_0$. This point $z = 0$ need not and normally would not coincide with the point source of heat. The law of variation of R with height may be written

$$R = R_0 \left(\frac{z + z_0}{z_0}\right)^p \qquad (p \neq 1)$$

and equation (6) becomes

$$\frac{1}{w}\frac{dw}{dz} + \frac{2(a-b)}{(3a-2b)}\frac{p}{(z+z_0)} = -\frac{ac}{(3a-2b)}\frac{z_0^p}{R_0}(z+z_0)^{-p} \qquad (12)$$

Here we have divided through by (3a-2b) which cannot equal zero in this context since we are considering only values of p not equal to unity (see section 2(i)).

Equation (12) can be integrated and the set of solutions is given by

$$w = w_0\left(\frac{z+z_0}{z_0}\right)^{-\frac{2(a-b)}{(3a-2b)}p} \exp\left[-\frac{ac\,z_0^p}{(3a-2b)(1-p)R_0}\left\{(z+z_0)^{1-p} - z_0^{1-p}\right\}\right]$$

$$R = R_0\left(\frac{z+z_0}{z_0}\right)^p \qquad (13)$$

$$\theta' \propto \left(\frac{p}{z+z_0} - \frac{c}{R}\right)w^2$$

Here once more there is the possibility of a wide variety of solutions, depending on the values of c and p and on the ratio a/b. However, given suitable values of a, b and c and if $0 < p < 1$, the expression for the vertical velocity contained in equations (13) offers prospects of obtaining a realistic picture of velocity decay, approximating to the usual power law in the lower levels but with a more rapid rate of decay at greater heights as the exponential factor increases in importance.

Simple power law expressions for velocity decay indicate, as does the formula in (13), that the rate of ascent of the heated air approaches zero asymptotically. This is, of course, to be expected following the assumption of a neutral atmosphere but it appears that the ultimate rate of decay of the upward velocity predicted by a simple power law is too slow. Existing theories of the free convection jet may thus give disappointing results when applied, for instance, to the question of the height attained by the heated smoke plume discharged from a factory chimney. In conditions of light wind and of very small or zero gradient of potential temperature, the plume can be seen to become almost horizontal at a height substantially lower than power law theories would predict.

In the preceding section reference was made to papers in which the radius of the convection jet increases linearly with height. By contrast, Sutton (1950) drew a close analogy between the spread of a stream of hot gas and the diffusion of a cloud of cold smoke in the atmosphere and assumed that the radius of the jet, in a neutral atmosphere, would be proportioned to $z^{7/8}$, i.e. non-linear spreading. The following set of solutions was then obtained

$$w \propto z^{-7/24}$$
$$R \propto z^{7/8}$$
$$\theta' \propto z^{-35/24}$$

These solutions for w and R are contained in equations (13), except for the exponential term, provided that

$$p = \frac{7}{8}\ ; \quad \frac{a}{b} = \frac{4}{3},$$

but the solution for θ' reduces to $\theta' \propto z^{-35/24}(Kz^{-1/8} - 1)$ where K is constant.

In the same paper, Sutton took account of the slow rate of velocity decay given by the power law. He considered the ascent of the heated gas to take place in a horizontal wind, thus relaxing the condition of an atmosphere at rest, and assumed that the decay law operated along the trajectory instead of along the vertical. A limit was set to the height attained by the plume by means of the assumption that the ascent came to an end when the trajectory was inclined at an angle of 10° to the horizontal. Even with these modifications of the power law hypothesis, the predicted rise of the plume, as has been shown by Best (1954), may greatly exceed the height observed.

The interpretation of equations (13) and their application calls for a fairly comprehensive series of observations of smoke plumes in the atmosphere in order to permit the determination of a/b, c and p for general use and of z_o, w_o, Θ_o' and R_o for individual cases. The writer is not aware that any programme of observations of the kind required has ever been carried out. However, the velocity formula of equations (13) can be tested in a very approximate manner by making use of some measurements of the height attained by a smoke plume at various distances downwind from the chimney stack in a steady wind of 10 feet per second. The observations were made by Bosanquet, Carey and Halton (1950) and have been used by Best (1954) in a comparison of various formulae for the assessment of ground level concentrations from a heated source.

By converting the distances downwind into times elapsed, a graph of elevation against time can be plotted and the upward velocities at various heights estimated. For application of the formula the values of p and a/b were taken as 7/8 and 4/3 respectively and, by trial, values of z_o, R_o and c were obtained so as to give reasonable agreement with the two lowest velocities, i.e. at 0 and 10 feet above the stack. The velocities for the remaining heights were then calculated. Table I provides a comparison between the vertical velocities (1) estimated from the observations, (2) calculated by means of equations (13), and (3) calculated from the power law, i.e. with the exponential term excluded but using a separate value for z_o in order to ensure agreement with the estimated velocities at 0 and 10 feet.

TABLE I

Comparison of vertical velocities estimated and calculated

Velocity (feet per second)

Height (ft.)	Estimated from Observations	Calculated from:	
		Equations (13)	Power Law
0	28	28	28
10	14	13	14
20	8	8.4	11.6
30	5	6.3	10.3
40	3	4.8	9.5
50	1.7	3.9	8.9
60	1	3.3	8.5

It is not, of course, claimed that Table I represents an entirely valid comparison between different formulae. In the first place the atmosphere was not at rest and, in addition, it is not known whether or not the atmosphere was neutral at the time at which the observations were made. Nevertheless the comparison in Table I is encouraging and suggests that the formulae given in equations (13) may have a useful application to practical problems.

4. Approximate formulae for small scale convection jets

The results derived in the preceding section and given in equations (13) incorporate an exponential factor which becomes more and more important as the vertical distance from the heat source increases. At points along the z-axis near to the source the value of

$$(z+z_0)^{1-p} - z_0^{1-p}$$

is small and especially so the smaller the value of the positive quantity (1-p).

It may seem reasonable to suppose, therefore, that for small scale experiments such as those carried out in a laboratory, the exponential factor in equations (13) will approximate to unity and may be omitted. It is to be noted that the quantity c, which expresses the effects of vertical shearing stress, appears only in the exponential part of the solutions at equations (13) and so, in practice, neglect of the exponentials, in the case of fairly narrow jets studied over a limited range of heights, is equivalent to an assumption that the effects of vertical shearing stress are small. In other words equations (13) with the exponential factors omitted are solutions of equations (3), (4) and (5) with c put equal to zero in equation (5). It is convenient to write the solutions of the basic equations, thus modified, in the following form:-

$$\left.\begin{aligned} w &= w_0\left(\frac{z+z_0}{z_0}\right)^{-\beta} \\ R &= R_0\left(\frac{z+z_0}{z_0}\right)^{\frac{1+3\beta}{2}} \\ \theta' &= \theta'_0\left(\frac{z+z_0}{z_0}\right)^{-(1+2\beta)} \end{aligned}\right\} \qquad (14)$$

In these equations $\beta = \frac{a-b}{b}$ and exact equivalence with equations (13) (excluding the exponential factors) is obtained by putting $p = \frac{3a-2b}{2b}$, a limitation on the value of p which results from neglecting the term containing c in equation (5).

Although this approximate treatment has been approached by means of the results of the preceding section with its assumption of non-linear spreading of the jet, it is possible now to relax this condition and regard equations (14) simply as solutions of the differential equation (6) with c = 0. It can then be seen that if $\beta = \frac{1}{3}$ is substituted in equations (14), the results given in equation (11) are reproduced, i.e. the laws of variation for w, R and θ' found by Schmidt, Rouse et al and by Batchelor.

Again if $\beta = 0$, i.e. a = b, a possibility already discussed in section 2(ii), equations (14) reduce to the form

$$\begin{aligned} &w = \text{constant} \\ &R \propto z^{\frac{1}{2}} \\ &\theta' \propto z^{-\frac{1}{2}} \end{aligned}$$

These are the solutions found by Batchelor for the case of laminar flow from a continuous point source of heat.

The application of the solutions given in equations (14) depends on the determination of a number of constants such as β and z_0, the distance from the origin of the theoretical point source. Since the values of a and b are not known from the outset, the solutions cannot be expressed in closed form and recourse must therefore be had to experimental data. Provided these are available, a portion of the data may be used for the determination of the necessary constants and the remainder may be used to check the accuracy of the solutions. Laboratory experiments under neutral conditions have been carried out by Railston (1954) and by Schmidt (1941), both of whom used small jets and whose results refer to a range of height of less than one metre. Since equations (14) were derived for small jets, the results of Railston and of Schmidt are particularly relevant and these have been used in the following sections for a quantitative test of the theory.

5. Comparison with Railston's experimental results

Railston used three different heat outputs - 4.87, 9.92 and 20.37 watts - and measured the temperature excess along the central axis of the rising plume at 5 cm. intervals up to a distance of 70 cm. from the source which was a square-shaped piece of fine mesh wire gauze of side 3.5 cm. In addition, for the strongest heat output, he measured the excess temperature at a number of points from the axis of the jet at the levels 20, 40 and 60 cm. above the source. This enabled graphs to be drawn showing the form of lateral temperature decay across the jet.

A point of great interest that emerged from Railston's work was that with these small jets of naturally convected air, large disturbances appeared at irregular intervals even though the jets were carefully screened and the heat supply was maintained at a constant rate. Schlieren methods were therefore used to render the air stream visible so as to ensure that measurements were made in conditions of steady flow. Railston also took steps to eliminate the effects of conduction and radiation and thus, as far as practicable, the observations referred to convection alone.

Railston made an empirical analysis of his measurements of axial excess temperature and arrived at the following relation:-

$$\theta' = h\, Q^{0.675} (z + 10.2)^{-1.52}$$

where Q is the heat output and h a constant. The theoretical point source from which the airstream originated was thus found to be at a position 10.2 cm. below the heated gauze.

Comparing the theoretical results derived above with Railston's empirical formula it will be seen that the power to which $(z + 10.2)$ is raised, -1.52, corresponds with a value of β equal to .26. This value was verified and, using the observations for $z = 20$ cm., the appropriate form of equations (14) for θ', the temperature excess, was worked out for each heat output. The resulting formulae and a comparison with Railston's observations are set out in the following Tables I, II and III.

TABLE I

Heat output 20.37 watts

z (cm.)	5.0	10.0	15.0	20.0	25.0	30.0	35.0	40.0	45.0	50.0	55.0	60.0	65.0	70.0
θ' (Observed)°C	20.5	12.2	9.2	7.2	5.4	4.3	3.8	3.1	2.6	2.1	2.0	1.7	1.4	1.2
θ' (Calculated)°C	20.5	13.3	9.7	7.2	5.7	4.6	3.9	3.3	2.8	2.6	2.3	2.0	1.8	1.7

TABLE II

Heat output 9.92 watts

z (cm.)	5.0	10.0	15.0	20.0	25.0	30.0	35.0	40.0	45.0	50.0	55.0	60.0	65.0	70.0
θ' (Observed)°C	12.9	7.7	5.8	4.7	3.4	2.8	2.3	2.1	1.7	1.4	1.3	1.1	1.0	0.9
θ' (Calculated)°C	13.4	8.7	6.3	4.7	3.7	3.0	2.5	2.2	1.8	1.7	1.5	1.3	1.2	1.1

/TABLE III

TABLE III

Heat output 4.87 watts

z (cm.)	5.0	10.0	15.0	20.0	25.0	30.0	35.0	40.0	45.0	50.0	55.0	60.0	65.0	70.0
θ' (Observed)°C	7.8	5.2	3.4	2.7	2.1	1.6	1.4	1.3	1.1	0.9	0.8	0.8	0.7	0.6
θ' (Calculated)°C	7.7	5.0	3.6	2.7	2.1	1.7	1.5	1.2	1.1	1.0	1.0	0.9	0.7	0.6

Railston's empirical formula shows θ' proportional to $Q^{0.675}$ or $Q^{2/3}$ approximately, a law predicted by Priestley and Ball as well as other writers. From the results in the above tables it can also be confirmed that the calculated θ' is roughly proportional to $Q^{2/3}$.

6. Comparison with Schmidt's experimental results

Schmidt used one heat output, the value of which was not given in his paper, and used a spiral coil as the source. He reported the same difficulties as Railston in obtaining a steady jet in spite of the precautions taken to exclude draughts from the laboratory.

Schmidt used a hot-wire anemometer and a small thermocouple to measure the wind and temperature in the jet and took readings at 40, 50, 60, 70 and 80 cm. above the finite source of heat. Since this was not a true point source, he used the observations to calculate from his theoretical analysis that the equivalent imaginary point source was 11.1 cm. below the actual heat source.

Schmidt's values of wind speed and temperature excess along the axis of the jet were applied to the formulae of equations (12). The value of β was found to be 0.29 and of z_0 10.2 cm. The velocity and temperature excess along the axis were then calculated from the formulae. The results together with Schmidt's observations are shown in the following Table IV.

TABLE IV

	w		θ'	
z cm.	Observed	Calculated	Observed	Calculated
40	64	64	13.95	13.95
50	61	61	10.5	10.4
60	58	58	8.2	8.2
70	56	56	6.5	6.6
80	53	54	5.49	5.51

In this application to Schmidt's results, the value obtained for β (0.29) gives a velocity decay law in agreement with that of Sutton's theory, but the index for temperature decay ($-$ 1.58) differs from Sutton's ($-$ 1.46).

7. Conclusion

The approximate solutions given in equations (14) for small jets over a limited range of height have given satisfactory agreement when applied to the experimental data presented by Railston and by Schmidt. The agreement is significantly better than that obtained by Priestley and Ball in testing their solution (section 2(i)) against Railston's results.

The data of Railston and Schmidt, combined with the theory, indicate that the values of a and b, which depend upon the lateral decay functions f(r/R) and h(r/R) are related as follows:-

(Railston) $a = 1.26\ b$
(Schmidt) $a = 1.29\ b$

/Additional

Additional laboratory data would be valuable in order both to test the formulae and to gain further insight into the magnitudes of a and b. It is considered that experiments of the type carried out by Railston but extended to the measurement of velocity as well as of temperature excess would be well worth while.

With regard to the more general formulae, equations (13), these could be tested quantitatively if comprehensive observations were made, in the appropriate atmospheric conditions, of the ascent of heated gas discharged from a chimney. The initial conditions - temperature excess at the orifice, discharge velocity, etc. - would need to be accurately measured.

References:-

Schmidt	1941	Z. agnew Math. Mech. 21, 351-363.
Sutton	1950	J. of Met., Vol 7, No.5, 307-312.
Rouse, Yih, Humphreys	1952	Tellus, 4, p.201.
Railston	1954	Proc. Phys. Soc., B, 67, p.42.
Batchelor	1954	Q.J.R. Met. Soc., 80, p.339.
Best	1954	Meteorological Research Papers, Air Ministry, London, No.878.
Priestley and Ball	1955	Q.J.R. Met. Soc., 81, p.144.
-	1953	A Meteorological Survey of the Oak Ridge Area (1948-52). U.S. Atomic Energy Commission, Weather Bureau, Oak Ridge, Tenn. Report ORO-99.
Bosanquet, Carey and Halton	1950	Proc. Inst. Mech. Engrs., 1950, 162, 355.

APPENDIX

Application to ascent of plume when atmosphere is in horizontal motion

The theoretical discussion has been concerned with ascent in a neutral atmosphere at rest, but since the ultimate objective is to obtain formulae that would be useful in the practical problems associated with chimney stacks, it is desirable to investigate the possible application of the results to a plume ascending through an environment in horizontal motion. Anything in the nature of a thorough test is at present out of the question because observations in the necessary detail are not available. However, a Report entitled "A Meteorological Survey of the Oak Ridge Area" (1953) describes photographic measurements of the height at which the plumes from different chimney stacks became horizontal. The observations were made in atmospheric conditions of small or zero temperature gradient and in various wind velocities. The Report gives a reasonable number of observations relating to two of the stacks and the data have been used to test whether the velocity formula of equations (13) could be satisfactorily applied.

The following are the design details of the two chimneys:-

	Watts Bar Steam Plant	X-10 Steam Plant
Stack Height	160 ft.	180 ft.
Orifice Diameter	14 ft.	9 ft.
Exit Velocity	34 m.p.h.	5 m.p.h.
Exit Temperature	350°F	400°F
Volume Emission Rate	300,000 cu.ft./min.	27,200 cu.ft./min.
Heat Emission Rate	6.6×10^6 cal./sec.	7.1×10^5 cal./sec.

Since the observational data on the plumes consisted solely of the height at which they became horizontal, it was necessary to consider carefully the values to be given to the undetermined quantities in the velocity formula.

For the spreading index, p, it seemed best to use the value 0.875 found by Sutton from numerous observations of the diffusion of smoke clouds. The quantities a and b are important only in their ratio to each other and $\frac{a}{b} = \frac{4}{3}$ was chosen following the discussion in sections 3 and 4 where it is implied that this value is appropriate to fully turbulent motion.

The Oak Ridge data gave little definite indication of the values of the constants z_0 and R_0. The radii of the chimneys are given in the Report but it cannot be assumed that these are the appropriate values to use for R_0. The experimental results of Railston and of Schmidt were confined to a small range of height but appear to offer the only guidance available and suggest that the value of z_0/R_0 is about 4. For jets on a larger scale the ratio may be greater but probably by not more than a factor of 2.

The quantity c expresses the effects of vertical shearing stress and appears only in the exponential part of the velocity formula. In sections 5 and 6 it was shown that satisfactory comparisons with experimental data could be obtained for laboratory experiments in which the range of height is necessarily small and in which reasonable precautions may be taken to ensure that the ambient air is still. It appeared, therefore, that the value of c might be related to the horizontal velocity of the environment and the test of the velocity formula was carried out on the assumption that c would increase as the external wind speed increased. Reference to the formula shows that the effect of increasing c is to increase the rate of velocity decay and this assumption is therefore supported by experience since it is well known that chimney smoke rises higher in a light wind than in a strong wind.

Another question was to decide the criterion for the termination of ascent. The formula for velocity indicates that the rate of ascent approaches zero asymptotically but in practice one is clearly justified in assessing a limit beyond which the residual velocity of ascent may be ignored. It was therefore decided to assume that ascent comes to an end when the upward velocity of the jet has fallen to a value equal to 10 per cent of the horizontal velocity of the environment. This condition is an exacting one and may be considered to lean to the safe side.

The attached figures showing observed plume heights plotted against wind speed are copied from the Oak Ridge Report except that the curve shown by a broken line in each graph is the result of applying the velocity formula of equations (13) adapted in the manner suggested in the preceding paragraphs. Curves in black show tests made at Oak Ridge of other theoretical formulae. Curves (1), (2) and (3) are derived from the work of Bosanquet, Carey and Halton (1950); curves (4) and (5) are based on formulae deduced from wind tunnel experiments.

The figures show that the velocity formula is capable of predicting fairly successfully the heights attained by the plumes from two very different chimneys in conditions of small temperature gradient and in a horizontal wind. However, comparisons with data from other chimneys and, when possible, with comprehensive data (observed velocity decay, increase of radius, etc.) from at least one chimney are required before the formula could be applied generally. Comparisons on these lines will be undertaken as soon as data become available.

M.R.P.952

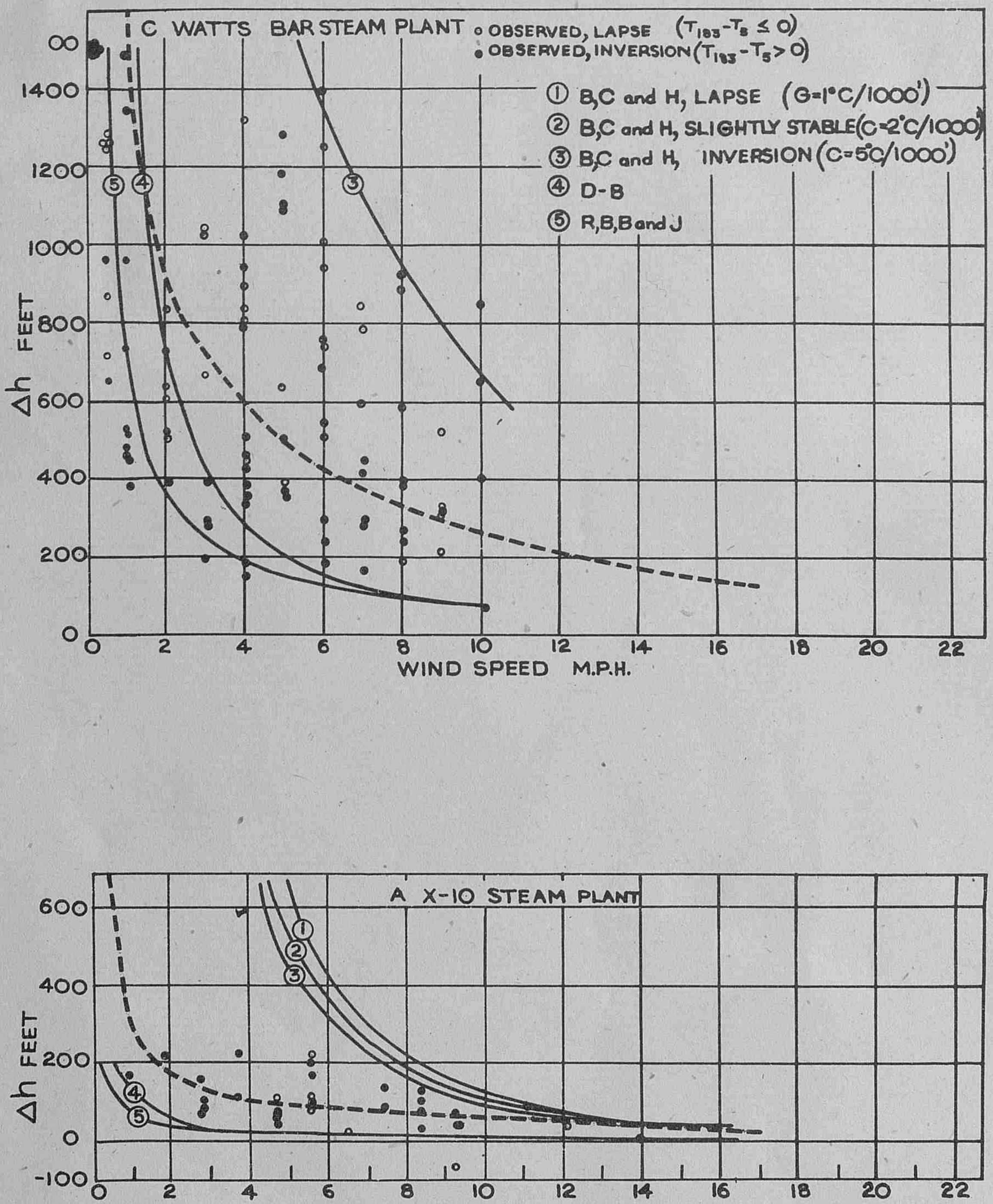

OBSERVED AND CALCULATED PLUME HEIGHTS

M.R.P. 953
S.C. 11/202
31st December, 1955

AD133971

The success achieved in forecasting upper winds by orthodox and statistical techniques

by

D.H. Johnson

(Meteorological Office)

AWSSS
ROUTING SLIP

FILE	INFO	ACTION				
	2,1		DIRECTOR			
			DEP. DIRECTOR			
	2		[illegible] DIRECTOR			
	3		CONSULTANTS			Wg Jth
	4		TRSD		CHF	RLH
				✓	TSS	L.A.C. [illegible]
				✓	RRB	
					EDB	
					SEC	
	1		EDD		CHF	CAS
				✓	HLFB	
					STB	
					SPFB	
					CU	
					SEC	
	5		TIPD		CHF	
				✓	PUE	
					TECH INFO	
					SEC	

AIR MINISTRY
METEOROLOGICAL RESEARCH COMMITTEE

At the time of issue this report has not been published. Any author desiring to quote this paper should refer to it as "A paper of the Meteorological Research Committee (London).
M.R.P. No. 953 by Mr. D.H. Johnson.
A copy is available in the Library of the Meteorological Office."

M.R.P. 953
S.C.II/202
31st December, 1955

AIR MINISTRY
METEOROLOGICAL RESEARCH COMMITTEE

The success achieved in forecasting upper winds by orthodox and statistical techniques

by
D.H. Johnson (Meteorological Office)

1. Introduction

C. S. Durst has explored the possibility of forecasting upper winds by linear regression equations, which exploit judiciously the temporal serial correlation of the wind (1). Forecasting trials were held, during the first four months of 1955, to provide data for a strict comparison between the success of the statistical method and the successes of the techniques currently in use at the Central Forecasting Office and at London Airport. The results of the trials are analysed in this paper.

2. Techniques

Five types of forecast were made: London Airport (L.A.P.), Central Forecasting Office (C.F.O.), Prontour, Statistical and Persistence. The techniques by which these forecasts were made are explained below. Winds forecast were:

(i) point winds at Liverpool and O.W.S. Station 'J' for the 700, 500, 300, 200 and 100 mb. levels (London Airport made no forecasts for 100 mb.);

(ii) mean tailwind components (as distinct from equivalent tailwinds) over approximately great circle routes from Shannon to Gander at 500 mb., and from O.W.S. Station 'A' to London at 200 mb.

C.F.O. and L.A.P. forecasts were made before 0300 G.M.T. on each day, all forecasts being valid for the following 1500 G.M.T.

(a) Orthodox techniques

At C.F.O. and London Airport established practice in forecasting upper winds rests largely on the use of prontours (forecast contour charts), but there are differences between the techniques in use at the two stations, which it is useful to bear in mind when assessing the results of the trial. Up to 200 mb., the C.F.O. contour charts are built up from the 1000 mb. charts by the successive graphical addition of the isopleths of thickness of the layers, 1000-700 mb., 700-500 mb., 500-300 mb. and 300-200 mb. London Airport follows a similar procedure for charts up to 300 mb., but the L.A.P. 200 mb. charts are drawn directly from the 200 mb. observations without reference to the 300-200 mb. thickness pattern. London Airport makes some use of reports from civil aircraft operating at levels up to 500 mb. These reports are not studied as a routine at C.F.O.

C.F.O. prontours are produced by graphical addition of forecast thickness patterns, up to 200 mb. L.A.P. prontours are based upon forecast thickness patterns up to 500 mb.: above that level the technique largely consists of direct extrapolation of contour patterns.

Routine prontours prepared at London Airport for operational purposes are composite charts, that is, the time of validity of the prontour varies from east to west across the chart. The trial route forecasts were of the instantaneous mean winds over the routes. Consequently, the L.A.P. forecasters elected on most occasions, to construct special fixed-time prontours for the purposes of the trial.

Prontours are constructed to meet a schedule which allows a certain balance to be attained between accuracy and speed of production. At C.F.O. uniform attention is given to all parts of the area to which the prontours relate. In framing a specific forecast, the C.F.O. forecaster may have been led to amend the geostrophic value which the prontours imply for one of the following reasons:

(i) to allow for the 3-hr. difference between the time of validity of the routine prontour (1200 G.M.T.) and the time of reference of the trial forecasts (1500 G.M.T.);

(ii) to allow for ageostrophic effects;

(iii) as a result of more detailed consideration of conditions near to the reference point of the forecast;

(iv) in order to reduce the risk of making very large errors by avoiding the prediction of large changes or unusual values.

The value written down by the practising forecaster has been taken as the "C.F.O." forecast. A geostrophic wind measured from a C.F.O. prontour has been termed a "prontour" forecast. Prontour forecasts were obtained after the event, in the Forecasting Research Division.

(b) Statistical forecasts

The statistical forecasts were prepared in the Forecasting Research Division. They were based upon the latest available wind observation, i.e., upon the 2100 G.M.T. observation, or in the absence of a 2100 G.M.T. observation, upon a 1500 G.M.T. wind or a geostrophic estimate of the 1500 G.M.T. wind. So that no use should be made of observations which were not available to the orthodox forecaster, a log was kept of the times of receipt, in the forecast room at C.F.O., of relevant observations: those received later than 0300 G.M.T. were discarded.

The basic principles of the statistical method are discussed in Geophysical Memoir No. 93. Details of how the statistical forecasts were made are given in Appendix I to this report. Values of the regression co-efficient etc., were provided by C. S. Durst.

(c) Persistence forecasts

The forecasting success of a current wind observation provides a useful standard against which to judge the value of more subtle techniques. For both route and point winds estimates of wind at 1500 G.M.T. or 1500 G.M.T. wind observations have been used as forecasts valid for the following 1500 G.M.T. These are referred to as persistence forecasts.

3. Winds over the routes

(a) Estimated "actuals"

Estimates of the mean wind over the route, the "actuals", against which the route forecasts were verified, were made by three methods:

(i) London Airport used a template to obtain from their working charts the average geostrophic wind over a band, approximately 300 miles wide, centred on the route;

/(ii)

(ii) the F.R. Division averaged spot winds, estimated at a series of points equally spaced along the route. Both geostrophic and observed winds were taken into account;

(iii) statistical estimates were made using equation (B) of Appendix I. Means and standard deviations for each type of estimate are given in Table 1.

Table 2 contains details of comparisons between the estimates. The agreement between the C.F.O. and L.A.P. estimates was evidently close: the mean differences were negligible, the correlation co-efficients were high, and the mean square differences between the estimates were small in comparison with the variances of the estimates themselves. The C.F.O. and L.A.P. estimates were averaged to give a further value, which has been termed the "best" estimate. This latter value was the one used in verifying the forecasts. The statistical estimates agree well with the other three, although they contain a systematic error of about 2 kt. for the route Shannon-Gander.

(b) Properties of the statistical forecasts

In assessing the value of the statistical forecasts, and in discussing their behaviour, it is necessary to refer to a number of formulae, most of which are not quoted in published work. These are listed below. The derivation of one of the relationships is given: the remainder are readily derived by similar algebra.

The basic prediction equation is of the form

$$F_t - U = P(V_o - U) \qquad \ldots (1)$$

where V_o = wind observed at time t = o, F_t = wind forecast for time t, and U and P are constants. Durst (1) shows that for such a prediction equation the forecast errors will be a minimum if U is identified with $\bar{V}$, the mean wind for the period over which forecasts are made, and P is identified with R_t, the correlation between observations made t hours apart. Equation (1) and the following relations apply both to route wind forecasts, which are scalar quantities, and to the vector point winds. For vector winds the correlation co-efficients refer to stretch vector correlations. Values for U and P have to be chosen before the event and so they will not generally be identical with $\bar{V}$ and R_t.

From equation (1), taking mean values over n occasions,

$$\bar{F}_t = U + P(\bar{V} - U) \qquad \ldots (2)$$

and

$$\bar{F}_t - \bar{V} = (U - \bar{V})(1 - P) \qquad \ldots (3)$$

The variance of n statistical forecasts may be written as $\frac{1}{n}\sum(F_t - \bar{F}_t)^2$, which on substitution for F_t and $\bar{F}_t$ from (1) and (2) becomes, $\frac{1}{n}P^2\sum(V_o - \bar{V})^2$. Thus, if σ_F is the standard deviation of the statistical forecasts, and σ is the standard deviation of winds observed during the period of the trial, we have,

$$\sigma_F = P\sigma \qquad \ldots (4)$$

P is less than one, so the standard deviation of the statistical forecasts should be appreciably less than that of the observed winds.

The following relationships may be similarly obtained.

Root-mean-square error of statistical forecasts =

$$\left\{\sigma^2\left(1-2PR_t+P^2\right)+\left(U-\bar{V}\right)^2(1-P)^2\right\}^{\frac{1}{2}} \qquad \ldots (5)$$

Standard deviation of statistical forecast errors =

$$\sigma\left(1-2PR_t+P^2\right)^{\frac{1}{2}} \qquad \ldots (6)$$

Root-mean-square error of persistence forecasts =

$$\left\{2\sigma^2\left(1-R_t\right)\right\}^{\frac{1}{2}} \qquad \ldots (7)$$

Co-efficient of correlation between a t-hr. statistical forecast and the wind at time t =

$$\frac{1}{n}\sum\left(F_t-\bar{F}_t\right)\left(V_t-\bar{V}_t\right)\Big/P\sigma^2 = R_t \qquad \ldots (8)$$

Serial correlation in statistical forecast errors =

$$\frac{\sigma^2\left(P^2R_t-P+R_t-PR_{2t}\right)+\left(U-\bar{V}\right)^2(1-P)^2}{\sigma^2\left(1+P^2-2PR_t\right)+\left(U-\bar{V}\right)^2(1-P)^2} \qquad \ldots (9)$$

Serial correlation in persistence forecast errors =

$$\left(2R_t-R_{2t}-1\right)\Big/2\left(1-R_t\right) \qquad \ldots (10)$$

(c) Route forecasts

In forecasting winds over the routes, both C.F.O. and L.A.P. used templates to obtain from the prontours a mean geostrophic wind. The "prontour" forecasts were the average of spot geostrophic measurements made at points along the route. The F.R. Division's estimates of mean winds over the routes were used as persistence forecasts.

Table 3 gives the mean values and standard deviations of the five types of forecast, together with statistics relating to the forecast errors. An important statistic for assessing the success of wind forecasts is the root-mean-square error. Values of the r.m.s. error are set out in Table 3, but for this analysis it was convenient to break the r.m.s. error down into its component parts, (i) bias and (ii) standard deviation.

(i) Bias. The term bias has been used to denote the systematic error (i.e., the difference between the mean forecast value and the mean actual). Over the route Shannon-Gander the bias in the orthodox forecasts was negligible, but in the statistical forecasts there was a bias of nearly 6 kt. Equation (3) shows that the bias, $(\bar{F}_t - \bar{V})$, in the statistical forecasts is proportional to the difference $U-\bar{V}$. Table 4 contains, for comparison, values of U and $\bar{V}$: $U-\bar{V}$ averaged 17 kt. during the four months of the trial. For the route O.W.S. 'A' - London the statistical forecast bias of 2 kt. can be explained similarly. The 2 kt. biases in the orthodox forecasts of wind over the 200 mb. route were tested for statistical significance.* It was found that the C.F.O. bias was significant at the 3% level and the L.A.P. bias was significant at the 6% level, which suggests that there is a real tendency for the orthodox forecasters slightly to under-estimate the 200 mb. tailwinds.

It is clear from Table 3 that in every case except that of the 500 mb. statistical forecasts, the bias made a negligible contribution to the r.m.s. error.

(ii) Standard deviations of the forecast errors. The following comparisons can be drawn between the standard deviations of forecast errors given in Table 3.

(i) The difference between the L.A.P. and C.F.O. values for 500 mb. was negligible but at 200 mb. the L.A.P. value exceeded the C.F.O. value by 1.3 kt. The 200 mb. difference was found to be significant at the 7% level.

(ii) The C.F.O. and statistical values differed by 1.4 kt. at 500 mb. (11% significance level), and by 1.9 kt. at 200 mb. (2% significance level), the C.F.O. value being the smaller in each case.

(iii) Correlation co-efficients. The last column of Table 3 gives the correlations of the forecasts with the actuals. The orthodox forecasts obtained higher correlation co-efficients than did persistence or statistical forecasts.

(iv) Frequency distributions of error. Figure 1 contains histograms which give the frequency of occurrence of errors of given magnitudes. The histograms show clearly the effects of bias. Table 5 shows the frequencies of occurrence of errors greater than specific magnitudes. The figures given in the last two columns of Table 5 indicate that there was little to choose between the orthodox and statistical techniques as far as the avoidance of extreme errors was concerned, although conclusions drawn from the last two columns alone could not be regarded as having a sound statistical basis. In the remainder of the table, frequencies for statistical forecasts exceed those for the orthodox forecasts.

(v) Individual errors. The graphs in Figures 2 and 3 give daily values of C.F.O., L.A.P., and statistical forecasts for comparison with the estimated actuals.

The L.A.P. and C.F.O. graphs suggest that, while there was a high correlation between the two forecasts, the forecast errors were not correlated to the same degree. On calculation, the co-efficient of correlation between the C.F.O. and L.A.P. errors was found to be .61 for the 500 mb. route and .58 for the 200 mb. route. It is thus possible to reduce the standard deviation of the forecast errors by combining the two forecasts, the theoretical reduction amounting to about 10 per cent.†

The statistical forecast graph shows the systematic errors to which the regression equation gave rise over short periods. See, for example, values for the first half of January at 500 mb. Table 6 gives details of occasions when errors greater than 27 kt. were made by one or more of the forecasts. On nine of the fifteen occasions when persistence gave a large error, either C.F.O. or L.A.P. committed an error greater than 20 kt.

/4.

* The tests of significance, which were complicated by serial correlations in the forecast errors, are discussed in detail in Appendix II.

† It is also theoretically possible to improve the statistical forecasts by basing the regression equation on the orthodox forecasts, instead of on the latest actuals.

4. Winds at a point

Point forecasts were normally verified against wind observations. In the absence of a wind observation an estimate was made from the appropriate C.F.O. working chart. At 500 mb., one wind was estimated for Liverpool and eleven for O.W.S.'J'. At 100 mb. 14 winds were estimated for Liverpool and 77 for O.W.S.'J'.

Mean values of the south and west wind components for each type of forecast, corresponding standard vector deviations and statistics relating to the forecast errors are listed in Table 7.

The C.F.O. forecast winds tended to have smaller standard vector deviations than did the observed winds, especially at 300 mb. This did not apply to C.F.O. route forecasts.

(a) Bias. For reasons similar to those discussed under section 3(c) for route forecasts, the statistical point forecasts contained a small bias. The bias in the orthodox forecasts was negligible and for all types of forecast the contribution of the bias to the r.m.s. vector error was small.

(b) Standard vector deviation of errors. The following features emerge from a comparison of the standard deviations of forecasts errors, given in Table 7.

(i) There was little to choose between C.F.O. and London Airport at 700 mb. and 300 mb. At 500 mb., the L.A.P. values for both stations were about a knot lower than those obtained by C.F.O. At 200 mb. C.F.O. bettered the L.A.P. values by about a knot at Liverpool and four knots at the ship.

(ii) C.F.O. achieved smaller standard deviations of error than the statistical method for all levels up to 200 mb. At 100 mb., there was nothing to choose between C.F.O. and statistical values for Liverpool, but C.F.O. had an advantage of one knot at O.W.S.'J'.

(iii) C.F.O. failed to improve upon their prontours up to 300 mb., although at 200 mb. and at 100 mb. (Liverpool) the prontours were bettered. Persistence plays a very large part in the orthodox technique of forecasting at 100 mb. and the gain over the prontours at Liverpool was due partly to the weight being given to the wind observations rather than to measured geostrophic winds.

(iv) In assessing the improvement upon persistence, it must be borne in mind that the values given in Table 7 refer to 24-hr. persistence forecasts. The forecaster could make use of 2100 G.M.T. observations from Liverpool on 118 out of 120 occasions at 200 mb., and 110 of these observations were available at 100 mb. (Corresponding figures for the ship are: 200 mb., 59 occasions; 100 mb., 25 occasions). Making use of equation 8, which shows that the serial correlation in the statistical forecasts should be identical with the serial correlation in the observations on which they are based, it is possible to estimate that if 2100 G.M.T. observations had been used for the persistence forecasts whenever they were available, the persistence errors would have been reduced by about ten per cent. At 100 mb., persistence would have attained approximately the same success as the orthodox and statistical methods, although at all other levels the forecasters would still have shown substantial gains.

Table 8 gives levels of statistical significance of the differences between pairs of the standard deviations of error.

(v) Frequency distributions of the errors. Figure 4 contains histograms showing frequencies of vector errors in 10 kt. ranges for each forecasting technique. In Table 9 are tabulated the frequencies of occurrence of errors greater than 50 kt. and 70 kt. respectively. Neglecting persistence, it does not appear that any one method was less liable to give large errors than the others.

(vi) Individual large errors. In Table 10 the outstanding errors are catalogued. It is remarkable that only one of the cases listed in Table 10 is also quoted in the corresponding table for the routes (Table 6).

5. General assessment

In drawing conclusions it is necessary to assess how far the results of the trials are likely to be of general validity. The statistical significance tests were made with this end in view, but we must also consider whether the conditions obtaining during the trial were such as to affect the representativeness of the samples of forecast errors. In Table 4 the mean winds, the standard vector deviations and serial correlations for the period of the trial are compared with longer period values and with the corresponding statistical prediction parameters. The column headed "Frequency of 1955 departure" gives the percentage of years when a departure of the mean wind from normal, equal to or greater than the departure which was observed in 1955, can be expected to occur. For reasons given at the end of Appendix II, these percentage frequencies must not be taken too literally, but they do give grounds for the belief that while the mean winds over the British Isles, during the period of the trial, were not particularly abnormal, the flow over parts of the Atlantic was far from normal. For O.W.S. 'J', then, and for the 500 mb. route, the biases in the statistical forecasts must be abnormally large. For the point winds, the effect of this was practically negligible in comparison with the non-systematic forecast errors, but for the 500 mb. route, the bias in the statistical forecast was relatively so large as to cancel out the expected gain over persistence. In view of the abnormality of the trial period, the poor success of the statistical forecasts for the 500 mb. route must be considered to be unrepresentative. While the value of U, used for the statistical forecasts, cannot be expected to agree precisely with long period means, it is considered unlikely that, if statistical forecasts were made over a long period, there would be a sufficient difference between U and $\overline{V}$ to give rise to appreciable bias. (Nevertheless, if the use of the statistical method in making special forecasts over a very limited period were contemplated, then the probable bias might require assessment). For the above reasons it is considered that a comparison of the standard deviations of the forecast errors gives a better guide to the relative success of the different techniques than a comparison of the r.m.s. errors, for the 500 mb. route.

Comparison of values given in the last two columns of Table 4 shows that whilst, for the point forecasts, P_{24} was taken as .55 at all levels, the observed serial correlations increased with height. It is considered that the trial period was not abnormal in this respect and that above 300 mb., P_{24} could, with advantage, be increased. Long period values of the serial correlations are not known, but even if P had been given values equal to the serial correlations actually observed, the statistical forecast errors would not have been reduced by more than half per cent at 300 mb. and five per cent at 100 mb.

At O.W.S.'J' the 1955 standard deviations are somewhat less than the normals given by Geophysical Memoir No. 85. Results given for the ship are less accurate than those obtained for Liverpool, partly because the ship observations themselves were sometimes of dubious accuracy and partly because, at the higher levels, a large percentage of the "observed" winds were, in fact, estimates made from the working charts. It is known that both orthodox and statistical forecasts achieve slightly smaller successes relative to persistence during periods when the standard deviation of the observed winds is below normal, but there is no reason to suppose that either technique gains in relation to the other.

It can be concluded, then, that a comparison of the standard deviations of the forecast errors for the trial period is likely to give a fair indication of the relative success, over longer periods, of the different techniques. The results given in Table 8 regarding the comparison between the standard deviations can therefore be summed up in the following terms.

(i) the C.F.O. errors were smaller than the statistical forecast errors over the route and at Liverpool for levels up to 200 mb., the significance levels of the differences varying from 2% to 11%. Taken together these results provide sound evidence that the orthodox method of forecasting as applied in everyday practice is capable of giving significantly smaller forecasting errors than the statistical method for levels up to 200 mb. At 100 mb. there is nothing to choose between the two techniques.

(ii) there is no significant difference between accuracies attained at London Airport and C.F.O. for levels up to 300 mb. At 200 mb., where C.F.O. and L.A.P. techniques differ, there is a reasonably strong suggestion that the C.F.O. technique is superior to that employed by London Airport.

6. Monthly values

Monthly values of the statistics relating to the forecast errors have not been discussed in this paper, but they are held for reference in M.O.21. For the routes, data relating to the success of the forecasts when compared with the individual C.F.O. and L.A.P. estimates of the actuals, are also available in M.O.21.

7. Summary of conclusions

(1) Orthodox techniques of forecasting are capable of giving, under operational conditions, smaller forecasting errors than the statistical technique proposed by C. S. Durst at levels up to 200 mb. There is no evidence that one technique is superior to the other in avoiding extreme errors.

(2) Orthodox and statistical techniques both give appreciably smaller errors than a persistence forecast at levels up to 200 mb. At 100 mb. neither technique improves significantly upon a persistence forecast over the British Isles, but both techniques effect some improvement at Ocean Weather Ship Station 'J'.

(3) C.F.O. and London Airport attain similar degrees of success in forecasting winds up to 300 mb. There is some suggestion that the (modified) thickness technique employed by C.F.O. at 200 mb. is superior to the technique of direct extrapolation practised by London Airport at that level.

(4) The C.F.O. forecasters do not better geostrophic measurements made from their prontours, except for forecasts of wind at a point at 200 mb. and 100 mb.

8. Acknowledgements

The statistics given in Tables 1, 2, 3, 7 and 8 and in Appendix III were obtained by electronic computation on Messrs. Elliot Bros'. 401 machine, at the Rothamsted Experimental Station, Harpenden. Thanks are due to Dr. F. Yates, Head of the Department of Statistics at Rothamsted, for permission to use the facilities of his department, and to his staff, for their valuable assistance. We are particularly grateful to Mr. M. J. R. Healy, of Rothamsted, who designed the programmes and supervised operations.

/References

References

1.	Durst, C.S.	1954	Geophysical Memoir No. 93
2.	Lewis, R.P.W. and McIntosh, D.H.	1952	Met. Mag., Vol. 81, p.242
3.	-do-	1953	Ibid, Vol. 52, p. 239
4.	Brooks, C.E.P. and Carruthers, N.	1953	Handbook of Statistics in Meteorology, p. 323
5.	-do-		Ibid, p. 194
6.	-do-		Ibid, p. 233
7.	Johnson, D. H.	1955	Quart J.R. Met.Soc., Vol. 81, p.1
8.	Brooks, C.E.P. and Carruthers, N.	1953	Handbook of Statistics in Meteorology, p. 200
9.	Yule, G.U. and Kendall, M.G.	1937	Introduction to the Theory of Statistics, p. 403
10.	Jenkinson, A.F.	1955	Met. Mag., Vol. 84, p. 140

Tables 1 and 2

Comparison between estimates of winds over the routes for the four-month period January to April, 1955

Table 1

Route	Estimate	Mean (kt.)	Standard deviation (kt.)
Shannon -Gander 500 mb.	L.A.P.	-13.2	18.7
	C.F.O.	-13.5	19.2
	"Best"	-13.4	18.9
	Statistical	-15.1	17.5
O.W.S. 'A' -London 200 mb.	L.A.P.	20.3	20.4
	C.F.O.	19.9	20.9
	"Best"	20.1	20.5
	Statistical	19.7	20.1

Table 2

Route	Estimates compared	Mean difference (kt.)	Standard deviation of difference (kt.)	r.m.s. difference (kt.)	Correlation co-efficient
Shannon -Gander 500 mb.	C.F.O. - L.A.P.	0.3	5.9	5.9	.95
	C.F.O.-Statistical	1.6	7.6	7.7	.92
	L.A.P.-Statistical	1.9	7.4	7.6	.92
	"Best"-Statistical	1.7	6.9	7.1	.93
O.W.S.'A'. -London 200 mb.	C.F.O. - L.A.P.	0.4	6.1	6.1	.96
	C.F.O.-Statistical	0.2	4.0	4.0	.98
	L.A.P.-Statistical	0.6	6.6	6.6	.95
	"Best"-Statistical	0.4	4.6	4.6	.97

Table 3 Verification of forecasts of wind over the routes. January to April, 1955.

Route	Statistic	Mean (kt.)	Standard deviation (kt.)	Bias (kt.)	Standard deviation of forecast errors (kt.)	r.m.s. error (kt.)	Correlation co-efficient
Shannon -Gander 500 mb.	Actual	-13.4	18.9				
	L.A.P. f/c	-13.4	18.0	0.0	11.1	11.0	0.82
	C.F.O. f/c	-13.7	19.5	0.3	10.9	10.9	0.84
	Prontour f/c	-13.1	19.1	-0.3	11.4	11.4	0.82
	Statistical f/c	-19.2	12.3	5.8	12.3	13.6	0.77
	Persistence f/c	-13.5	19.2	0.1	13.4	13.4	0.75
O.W.S. 'A' -London 200 mb.	Actual	20.1	20.5				
	L.A.P. f/c	18.2	19.9	1.9	12.2	12.3	0.82
	C.F.O. f/c	18.1	19.9	2.0	10.9	11.1	0.85
	Prontour f/c	17.7	18.9	2.4	10.6	10.8	0.86
	Statistical f/c	22.3	16.1	-2.2	12.8	12.9	0.78
	Persistence f/c	19.9	20.9	0.2	14.7	14.7	0.75

Table 4. Comparison between winds observed January - April, 1955 and normal values for January - April

Location	Mean observed wind, $\overline{V}$		Statistical forecast parameter, U	Frequency of 1955 departure	s.v.d. of observed winds (kt.)		Serial correlations	
	1955 (kt.)	1948-55 (kt.)			1955	G.M. 85*	Observed 1955	Statistical value, P
Route Shannon							(24-hr.)	(18-hr.)
- Gander 500 mb.	-13	-	-30	-	18.9	-	.75	.75
Route O.W.S. 'A'							(24-hr.)	(18-hr.)
- London 200 mb.	20	-	29	-	20.5	-	.75	.80
Liverpool							(24-hr.)	(24-hr.)
700 mb.	300°8	280°14	270°13	16%	27.0	29.0	.59	.55
500 mb.	295°16	287°20	280°26	42%	39.9	37.5	.61	.55
300 mb.	295°25	294°27	285°37	> 75%	56.1	53.0	.63	.55
200 mb.	295°24	296°26	285°34	> 75%	39.1	41.0	.70	.55
100 mb.	300°20	295°19	275°25	> 75%	23.5	23.0	.79	.55
O.W.S. 'J'							(24-hr.)	(24-hr.)
700 mb.	235°9	254°21	250°18	< 1%	27.7	30.7	.58	.55
500 mb.	245°13	258°29	270°30	< 1%	35.5	39.1	.57	.55
300 mb.	255°23	263°38	270°40	7%	49.2	54.5	.56	.55
200 mb.	250°23	266°34	260°41	9%	39.9	44.0	.63	.55
100 mb.	255°17	269°23	270°27	15%	22.2	26.0	.69	.55

* Averages for the six months December - May, derived from Geophysical Memoir No. 85, as amended by M.O.9

G. 37808/PC/12/55/50

Table 5. Frequencies of occurrence of errors greater than specified magnitudes

Route	Type of forecast	Error size (kt.)							
		2½	7½	12½	17½	22½	27½	32½	37½
Shannon -Gander 500 mb.	L.A.P.	93	62	32	13	6	1	0	0
	C.F.O.	98	56	33	13	6	1	0	0
	Prontour	94	64	36	17	4	1	0	0
	Statistical	102	68	47	26	12	4	1	1
	Persistence	103	72	40	21	12	3	2	1
O.W.S. 'A' -London 200 mb.	L.A.P.	101	63	37	20	6	3	3	0
	C.F.O.	98	59	32	14	4	2	1	1
	Prontour	94	52	25	13	6	2	2	1
	Statistical	103	66	43	21	8	4	1	0
	Persistence	110	77	44	30	17	8	3	0

Table 6. Occasions when large errors were made

Route	Date	Estimated actual	Forecast wind (kt.)					Forecast errors (kt.)				
			L.A.P.	C.F.O.	Prontour	Statistical	Persistence	L.A.P.	C.F.O.	Prontour	Statistical	Persistence
Shannon	Jan. 27	-5	-36	-30	-33	-43	-40	31	25	28	38	35
- Gander	Mar. 26	3	-13	-10	-12	-27	-29	16	13	15	30	32
500 mb.	Mar. 29	-6	5	22	19	- 4	- 5	-11	-28	-25	- 2	- 1
	Apr. 3	-2	-25	- 8	- 5	-33	-29	23	6	3	31	27
	Apr. 13	2	-14	-21	-21	-24	-36	18	23	23	26	38
	Apr. 18	18	2	15	20	-10	- 9	16	3	- 2	28	27
O.W.S.'A'	Jan. 11	74	38	50	60	44	44	36	24	14	30	30
-London	Jan. 22	53	38	45	45	31	25	15	8	8	22	28
200 mb.	Feb. 16	49	34	36	31	23	14	15	13	18	26	35
	Feb. 27	33	-4	-5	-5	15	8	37	38	38	18	25
	Mar. 3	46	19	25	23	18	18	27	21	23	28	28
	Mar. 6	-19	-9	-10	-13	17	15	-10	-9	-6	-36	-34
	Mar. 8	15	-18	0	-3	-1	-16	33	15	18	16	31
	Apr. 8	3	3	0	2	25	35	0	3	1	-22	-32
	Apr. 9	38	33	30	28	9	4	5	8	10	29	34
	Apr. 10	60	40	30	26	56	40	20	30	34	4	20

errors occur
10% of time
at 200mb

G. 37808/PC/12/55/50

Table 7. Verification of forecasts of wind at a point. January - April, 1955

(a) Liverpool

Level (mb.)	Statistic	Mean component (kt.)		Standard vector deviation (kt.)	Bias in component (kt.)		Standard vector deviation of errors (kt.)	r.m.s. error (kt.)	Correlation co-efficient
		S.	W.		S.	W.			
700	Actual	-3.8	7.0	27.0					
	L.A.P.	-3.1	8.2	28.2	-0.7	-1.2	19.0	18.9	0.77
	C.F.O.	-2.9	8.3	26.5	-0.9	-1.3	18.5	18.5	0.76
	Prontour	-2.1	7.3	26.9	-1.7	-0.3	18.8	18.8	0.76
	Statistical	-2.6	8.7	17.2	-1.2	-1.7	20.1	20.1	0.67
	Persistence	-3.8	6.8	27.0	0	0.2	24.5	24.4	0.59
500	Actual	-7.4	15.3	39.9					
	L.A.P.	-6.7	15.2	39.3	-0.7	0.1	25.5	25.4	0.79
	C.F.O.	-6.3	14.3	35.7	-1.1	1.0	26.6	26.5	0.76
	Prontour	-6.4	12.3	35.7	-1.0	3.0	24.8	24.9	0.79
	Statistical	-7.4	16.7	25.7	0	-1.4	28.9	28.8	0.69
	Persistence	-7.5	15.0	39.9	0.1	0.3	35.2	35.1	0.61
300	Actual	-9.9	22.6	56.1					
	L.A.P.	-9.0	25.1	51.1	-0.9	-2.5	35.3	35.2	0.79
	C.F.O.	-9.9	22.0	47.9	0	0.6	36.6	36.5	0.76
	Prontour	-9.4	19.7	47.3	-0.5	2.9	36.5	36.5	0.76
	Statistical	-11.2	26.8	36.5	1.3	-4.2	40.3	40.3	0.70
	Persistence	-10.0	22.3	56.0	0.1	0.3	48.3	48.1	0.63
200	Actual	-11.2	21.5	39.1					
	L.A.P.	-11.8	23.7	42.1	0.6	-2.2	25.4	25.4	0.81
	C.F.O.	-10.1	21.8	37.7	-1.1	-0.3	24.1	24.1	0.80
	Prontour	-10.0	19.4	38.2	-1.2	2.1	25.7	25.7	0.78
	Statistical	-11.0	26.1	23.5	-0.2	-4.6	26.2	26.5	0.76
	Persistence	-11.4	21.3	39.0	0.2	0.2	30.1	30.0	0.70
100	Actual	-10.4	17.5	23.5					
	L.A.P.	-	-	-	-	-	-	-	-
	C.F.O.	-10.0	18.4	22.0	-0.4	-0.9	13.8	13.7	0.82
	Prontour	-10.9	19.9	25.1	0.5	-2.4	15.2	15.3	0.81
	Statistical	- 8.9	19.9	15.1	-1.5	-2.4	13.6	13.9	0.84
	Persistence	-10.5	17.4	23.5	0.1	0.1	15.1	15.0	0.79

G. 37808/PC/12/55/50

Table 7. Verification of forecasts of wind at a point. January - April, 1955

(b) O.W.S. Station 'J'

Level (mb.)	Statistic	Mean component (kt.)		Standard vector deviation (kt.)	Bias in component (kt.)		Standard vector deviation of errors (kt.)	r.m.s. error (kt.)	Correlation co-efficient
		S.	W.		S.	W.			
700	Actual	5.3	7.2	27.7					
	L.A.P.	8.5	7.4	29.3	-3.2	-0.1	21.0	21.1	0.73
	C.F.O.	6.5	8.7	27.4	-1.2	-1.5	19.9	19.9	0.74
	Prontour	6.4	7.9	27.9	-1.1	-0.6	20.0	19.9	0.74
	Statistical	5.9	11.1	18.5	-0.6	-3.9	22.2	22.4	0.60
	Persistence	5.5	7.2	27.9	-0.2	0.1	25.4	25.3	0.58
500	Actual	5.5	12.3	35.5					
	L.A.P.	9.4	13.3	38.5	-3.9	-1.1	27.1	27.3	0.73
	C.F.O.	7.2	15.1	35.5	-1.7	-2.8	28.3	28.4	0.68
	Prontour	7.1	14.1	34.9	-1.6	-1.8	27.4	27.4	0.70
	Statistical	3.8	19.3	21.8	1.7	-7.0	29.3	30.0	0.57
	Persistence	5.9	12.3	35.7	-0.4	0	32.9	32.8	0.57
300	Actual	6.0	21.6	49.2					
	L.A.P.	10.3	24.0	49.9	-4.4	-2.3	37.9	38.1	0.71
	C.F.O.	8.0	21.6	46.6	-2.1	0	37.3	37.1	0.70
	Prontour	8.0	21.3	44.9	-2.1	0.3	37.4	37.3	0.69
	Statistical	3.9	26.5	30.0	2.0	-4.9	39.4	39.6	0.60
	Persistence	6.2	21.4	49.2	-0.2	0.2	46.2	46.0	0.56
200	Actual	6.7	21.4	39.9					
	L.A.P.	9.1	24.0	42.1	-2.4	-2.6	33.4	33.4	0.67
	C.F.O.	7.0	21.8	36.9	-0.2	-0.4	29.5	29.4	0.71
	Prontour	7.2	22.5	37.1	-0.5	-1.1	30.2	30.1	0.69
	Statistical	6.3	27.1	24.4	0.5	-5.7	31.3	31.7	0.62
	Persistence	7.0	21.3	40.0	-0.3	0	34.4	34.2	0.63
100	Actual	3.6	16.9	22.2					
	L.A.P.	-	-	-	-	-	-	-	-
	C.F.O.	3.8	16.9	20.9	-0.2	-0.0	14.8	14.7	0.77
	Prontour	4.5	17.9	20.6	-0.9	-0.9	14.7	14.7	0.77
	Statistical	1.9	21.1	12.9	1.7	-4.2	16.1	16.6	0.70
	Persistence	3.8	16.8	22.3	-0.2	0.2	17.6	17.5	0.69

G.37808/PC/12/55/50

Table 8. Levels of significance of difference between standard deviations of the forecast errors

Location	C.F.O. - Statistical		C.F.O. - L.A.P.	
	Difference (kt.)	Significance level	Difference (kt.)	Significance level
Route Shannon - Gander 500 mb.	-1.43	11%	negligible	-
Route O.W.S. 'A' - London 200 mb.	-1.85	2%	-1.24	7%
Liverpool 700 mb.	-1.58	5%	negligible	-
" 500 mb.	-2.34	4%	1.08	27%
" 300 mb.	-3.64	4%	1.36	35%
" 200 mb.	-2.07	7%	-1.27	13%
" 100 mb.	negligible	-	-	-

Table 9. Frequencies of errors greater than 50 kt., and greater than 70 kt. in point forecasts

Number of cases. Divide by 2,4 to get %

Forecast	700 mb.		500 mb.		300 mb.		200 mb.	
	>50 kt.	>70 kt.	>50 kt.	>70 kt.	>50 kt.	>70 kt.	>50 kt.	>70 kt.
L.A.P.	2	1	12	2	35	9	16	4
C.F.O.	2	1	14	0	31	13	12	3
Prontour	2	1	10	0	35	11	12	5
Statistical	1	0	14	0	47	12	17	4
Persistence	7	0	38	6	62	33	25	7

Table 10. Large errors in point forecasts

(a) Winds forecast and observed

Date	Level (mb.)	Station	Wind observed (kt.)	Winds forecast (kt.)				
				L.A.P.	C.F.O.	Prontour	Statistical	Persistence
Jan. 15	300	Liverpool	250° 141	275° 85	300° 70	280° 72	298° 112	290° 96
" 28	200	J	190° 30*	240° 90	250° 90	255° 115	240° 51	240° 48
" 30	300	Liverpool	260° 53	170° 95	210° 45	205° 43	220° 69	200° 83
Feb. 6	300	Liverpool	320° 148	315° 50	300° 70	295° 57	290° 38	260° 18
" 7	300	J	230° 150*	245° 105	250° 75	240° 81	245° 61	235° 78*
" 14	200	J	070° 91	040° 30	010° 20	010° 16	315° 7	060° 30
" 26	500	J	310° 114	280° 60	220° 30	240° 26	280° 27	340° 39
" 26	300	J	310° 142	280° 85	220° 30	220° 43	290° 46	330° 79
" 27	300	J	250° 60	250° 130	240° 80	240° 80	285° 80	310° 142
" 27	300	Liverpool	350° 120	360° 15	300° 20	320° 23	315° 19	010° 14
March 1	300	J	310° 50	225° 80	270° 80	260° 78	220° 73	220° 114
" 2	300	J	230° 39	240° 85	220° 130	225° 108	275° 41	220° 33
" 31	200	J	250° 84	Calm	160° 35	150° 28	270° 15	260° 9

* Winds estimated

Table 10. Large errors in point forecasts

(b) Forecast errors

Date	Level (mb.)	Station	Magnitude of vector forecast error (kt.)					Comments
			L.A.P.	C.F.O.	Prontour	Statistical	Persistence	
Jan. 15	300	Liverpool	73	109	86	107	90	Position of wind maximum in a complex westerly jet stream and the location and amplitude of a short wave in the southern half of the jet, were critical for forecasting Liverpool winds.
" 28	200	J	74	80	106	39	37	C.F.O. forecast the westward extension of a zonal jet, but in the event a major trough developed in the jet at about 27°W.
" 30	300	Liverpool	108	42	45	44	72	Forecasters underestimated the speed of translation of a short wave in the upper westerlies.
Feb. 6	300	Liverpool	96	86	99	116	139	Forecasters erred in timing the passage of a northwesterly jet on the forward side of a developing upper ridge.
" 7	300	J	55	82	71	91	72	Statistical regression towards the normal changed the wind in the wrong sense.
" 14	200	J	66	83	84	94	61	C.F.O. underestimated the development of a trough in northerly upper current. Statistical method gave a change in the wrong sense.
" 26	500	J	68	117	106	91	82	The development and subsequent eastward translation over the eastern Atlantic of a major upper ridge was not forecast by C.F.O. The prontour error for 26th at 300 mb. was the highest of the trial.
" 26	300	J	79	144	148	99	72	
" 27	300	J	70	23	23	46	124	
" 27	300	Liverpool	106	108	100	106	106	
Mar. 1	300	J	90	52	60	88	124	Eastward translation of southwesterly jet gave large persistence error.
" 2	300	J	47	91	69	31	9	Orthodox forecasters brought the main upper westerlies too far south over the Atlantic.
" 31	200	J	84	90	93	71	74	Decline of a blocking anticyclone and the development of a fresh upper ridge over the eastern Atlantic was not forecast.

The success achieved in forecasting upper winds by orthodox and statistical techniques

Appendix I: Statistical forecasts

The equation used in making the statistical forecasts was,

$$F_t - U = P(V_o - U) \qquad \text{... (A)}$$

where F_t was the wind forecast for time t, V_o was the wind observed at time t = 0 and P and U were pre-determined constants.

Winds over the route

A statistical estimate, E, of the actual mean tailwind component over the route was obtained using the formula,

$$E - U = \sum_i a_i (v_i - u_i) \qquad \text{... (B)}$$

where the V_i were winds observed at chosen stations along the route, the a_i were regression co-efficients and U and the u_i were constants. It can be shown that to minimise the forecast errors, U is best chosen to be the normal tailwind component along the route and the u_i are best chosen to be normal tailwind components of wind at the selected stations.

Substituting E for V_o in equation (A), the prediction equation is obtained in the form used in practice,

$$F_t = U + P \sum_i a_i (v_i - u_i) \qquad \text{... (C)}$$

Values of U and u_i are given in Table A. Table B gives the bearings of the routes at selected stations. Regression co-efficients: a_i for the estimated actuals; Pa_i for the forecasts; are contained in Table C.

To obtain E for 1500 G.M.T. in the absence of a 1500 G.M.T. observation, a geostrophic estimate, made from the 1500 G.M.T. chart, was used in equation B.

For the forecasts, the winds u_i were normally 2100 G.M.T. observations. In the absence of a 2100 G.M.T. observation the previous 1500 G.M.T. observation was used. If neither a 2100 G.M.T. nor a 1500 G.M.T. observation was available then a geostrophic estimate was made from the 1500 G.M.T. contour chart. For the Irish and Canadian stations (route Shannon - Gander) the rules were:

(i) if Valentia is not available at 2100 G.M.T.: use the Aldergrove wind; but if neither is available at 2100 G.M.T.: use the mean of the two 1500 G.M.T. winds;

(ii) for Newfoundland, either Argentia or Stephenville can be used, but if both are received for the same hour, the mean of the two is taken.

Winds at a point

The point forecasts were made using equation (A). Forecasts were normally based on the 2100 G.M.T. observed wind, when P was taken to be 0.65. If a 2100 G.M.T. observation was missing, the previous 1500 G.M.T. observation was used, when P was taken as 0.55. In the absence of both observations a geostrophic estimate was made from the 1500 G.M.T. chart. Table D contains values of U.

Table A

Normal tailwind components along track

(a) Route O.W.S. 'A' - London 200 mb.

Month	u_i in kt.					U in kt.
	O.W.S. 'A'	O.W.S. 'I'	Aldergrove	Liverpool	Crawley	
January	32	32	33	33	33	33
February	29	30	30	29	28	30
March	26	29	27	25	23	27
April	23	28	24	21	18	24

(b) Route Shannon - Gander 500 mb.

Month	u_i in kt.				U in kt.
	Valentia/Aldergrove	O.W.S. 'J'	O.W.S. 'C'	Stephenville/Argentia	
January	-30	-31	-37	-41	-35
February	-27	-28	-33	-39	-32
March	-24	-25	-29	-36	-28
April	-21	-22	-25	-34	-25

Table B

Bearings of the routes at selection stations

	O.W.S. 'A'	O.W.S. 'I'	Aldergrove	Liverpool	Crawley
O.W.S. 'A' - London	110°	120°	130°	135°	135°
Shannon-Gander	Gander 240°	O.W.S. 'C' 260°	O.W.S. 'J' 270°	Shannon 285°	

Table C

(a) Regression co-efficients for route Ship 'A' - London 200 mb.

	O.W.S. 'A'	O.W.S. 'I'	Aldergrove	Liverpool	Crawley
Actual (all observations 1500Z)	0.15	0.39	0.22	0.16	0.05
Forecast (all observations 2100Z)	0.12	0.32	0.17	0.13	0.04
F/c (O.W.S. 'A' 1500Z, others 2100Z)	0.10	0.34	0.18	0.13	0.04
F/c (O.W.S. 'I' 1500Z, others 2100Z)	0.18	0.23	0.23	0.13	0.03
F/c (Aldergrove 1500Z, others 2100Z)	0.12	0.34	0.08	0.24	0.03
F/c (Liverpool 1500Z, others 2100Z)	0.12	0.32	0.23	0.04	0.09
F/c (Crawley 1500Z, others 2100Z)	0.12	0.32	0.17	0.15	0.03
F/c (O.W.S. 'A' and 'I' 1500Z, others 2100Z)	0.09	0.30	0.24	0.13	0.03

Table C

(b) Regression co-efficients for route Shannon - Gander 500 mb.

	Valentia/ Aldergrove	O.W.S. 'J'	O.W.S. 'C'	Stephenville/ Argentia
Actual (all observations 1500Z)	0.12	0.22	0.39	0.20
F/c (all observations 2100Z)	0.09	0.17	0.29	0.15
F/c (Val./Ald. 1500Z, others 2100Z)	0.07	0.18	0.28	0.15
F/c (O.W.S. 'J' 1500Z, others 2100Z)	0.11	0.13	0.30	0.15
F/c (O.W.S. 'C' 1500Z, others 2100Z)	0.07	0.19	0.25	0.15
F/c (Ste./Arg. 1500Z, others 2100Z)	0.09	0.16	0.29	0.13
F/c (Val./Ald. O.W.S. 'J' 1500Z, others 2100Z)	0.08	0.14	0.30	0.15
F/c (Val./Ald. O.W.S. 'C' 1500Z, others 2100Z)	0.06	0.20	0.23	0.15
F/c (Val./Ald. Ste./Arg. 1500Z, others 2100Z)	0.07	0.18	0.28	0.13
F/c (O.W.S. 'J', O.W.S. 'C' 1500Z, others 2100Z)	0.10	0.14	0.25	0.15
F/c (O.W.S. 'J', Ste./Arg. 1500Z, others 2100Z)	0.11	0.13	0.30	0.13
F/c (O.W.S. 'C', Ste./Arg. 1500Z, others 2100Z)	0.08	0.19	0.25	0.13
F/c (Val./Ald. 'J', 'C' 1500Z, others 2100Z)	0.08	0.14	0.25	0.15
F/c (Val./Ald. 'J', Ste./Arg. 1500Z, others 2100Z)	0.08	0.14	0.30	0.13
F/c (Val./Ald. 'C', Ste./Arg. 1500Z, others 2100Z)	0.06	0.20	0.24	0.13
F/c ('J', 'C', Ste./Arg. 1500Z, others 2100Z)	0.10	0.14	0.25	0.13

Table D

Normal values*, U, of wind at O.W.S. 'J' and Liverpool

Height (mb.)	O.W.S. 'J'								Liverpool							
	Jan.		Feb.		Mar.		Apr.		Jan.		Feb.		Mar.		Apr.	
	deg.	kt.	deg.	kt.	deg.	kt.	deg.	kt.	deg.	kt.	deg.	kt.	deg.	kt.	deg.	kt.
100	265	35	270	30	270	25	275	20	280	30	280	27	275	23	275	20
200	260	48	260	43	265	38	265	32	295	40	290	37	285	33	270	30
300	260	48	270	43	270	38	280	32	290	41	285	38	285	34	280	31
500	270	37	270	33	270	28	270	23	280	30	280	27	285	24	285	21
700	250	22	250	19	250	16	250	13	270	15	270	14	270	12	170	11

---

* These values were obtained from Reference 10

Success achieved in forecasting upper winds by orthodox and statistical techniques

Appendix II: Significance tests

The series of forecast errors discussed in this paper contain small but significant serial correlations, and furthermore the errors of one forecasting technique are correlated with the errors of each of the other forecasting techniques. The usual criteria of statistical significance, which depend upon assumptions of independence of the samples, do not therefore apply.

A device commonly adopted in dealing with a serially correlated set of observations is to estimate the number of independent observations to which they are equivalent. Lewis and McIntosh (2) compare the standard error of the mean of n independent observations, namely $\sigma/\sqrt{n}$, where σ is the population standard deviation, with the standard error of the mean of n serially correlated observations which is,

$$\sigma\left[1+\frac{2}{n}\left\{(n-1)p_1+(n-2)p_2+\cdots+p_{n-1}\right\}\right]^{\frac{1}{2}}\Big/\sqrt{n} \quad \ldots \text{(i)}$$

where p_1 is the correlation between consecutive terms, p_2 is the correlation between alternate terms, p_3 is the correlation between every third term, and so on. They suggest that the number, n', of effectively independent terms be reckoned for statistical purposes as $n\Big/\left[1+\frac{2}{n}\left\{(n-1)p_1+(n-2)p_2+\cdots+p_{n-1}\right\}\right]$. The standard error of the persistent series can then be written as $\sigma/\sqrt{n'}$. Strictly, the use of an n' so obtained, in computing standard errors, is only justified rigorously when mean values are to be dealt with, but it also provides a working basis for assessing the significance of other statistical parameters such as the standard deviation.

By analogy with the conception of an "equivalent number of independent observations" there can be defined "an equivalent number of independent comparisons" for use when two series which are correlated with each other have to be compared. Lewis and McIntosh (3) give $\left[2\sigma^2(1-r)/n\right]^{1/2}$ as the standard error of the difference between the means of two series, of n terms, which are related to each other with co-efficient of correlation r, but which individually have no serial correlation. The two series are assumed to have a common standard deviation σ. In this case an equivalent number of independent comparisons, n'', can be defined equal to $n/(1-r)$. The standard error of the difference between the means is then $(2\sigma^2/n'')^{1/2}$. If series to be dealt with contain serial correlations, then as a first step the equivalent number of independent observations can be obtained for each one; but difficulties then arise in obtaining n'' if n' is not the same for each series. It is therefore necessary to derive an expression for the standard error of the difference between the means ab initio.

Given two series, $x_1 \ldots\ldots\ldots\ldots x_n$ and $y_1 \ldots\ldots\ldots\ldots y_n$ with correlation r between x and y, and serial correlations p_1, p_2 etc. in the x and q_1, q_2 etc. in the y. Let $\bar{x}$, $\bar{y}$ be the sample means and X, Y be population means for x and y. Let $t_{i,j}$ be the correlation between x_i and y_j.

Define

$$P = \frac{1}{n}\left\{(n-1)p_1+(n-2)p_2+\cdots+p_{n-1}\right\};$$

$$Q = \frac{1}{n}\left\{(n-1)q_1+(n-2)q_2+\cdots+q_{n-1}\right\};$$

$$T = \frac{1}{n}\left\{(n-1)t_{1,2}+(n-2)t_{1,3}+\cdots+t_{1,n}\right\}.$$

Then, $\left[\text{standard error of } (\bar{x}-\bar{y})\right]^2 = \frac{1}{m}\sum\left[(\bar{x}-\bar{y})-(X-Y)\right]^2$,

the sum being taken over m samples,

$$= \frac{1}{m}\sum_m(\bar{x}-X)^2 + \frac{1}{m}\sum_m(\bar{y}-Y)^2 - \frac{2}{m}\sum_m(\bar{x}-X)(\bar{y}-Y) \quad \dots \text{(ii)}$$

The first two terms of (ii) are the squares of the standard errors of the sample means and by (i) are equal to $\sigma_x^2(1+2P)/n$ and $\sigma_y^2(1+2Q)/n$ respectively. The third term of (ii) may be expanded as,

$$-\frac{2}{mn^2}\sum_m\left[(x_1-X)+(x_2-X)+\dots+(x_n-X)\right]\left[(y_1-Y)+\dots+(y_n-Y)\right],$$

which when m is large, reduces to,

$$-\frac{2}{n^2}\left[nr\sigma_x\sigma_y + 2(n-1)\sigma_x\sigma_y t_{1,2} + 2(n-2)\sigma_x\sigma_y t_{1,3} + \dots + 2t_{1,n}\right]$$

(assuming that $t_{i,j} = t_{j,i}$), which expression may be written as

$$-\frac{2\sigma_x\sigma_y}{n}(r+2T).$$

Equation (ii) may then be written,

$$\left[s.e.(\bar{x}-\bar{y})\right]^2 = \frac{\sigma_x^2}{n}\left[1+2P\right] + \frac{\sigma_y^2}{n}\left[1+2Q\right] - \frac{2\sigma_x\sigma_y}{n}(r+2T)$$

$$= \frac{\sigma_x^2+\sigma_y^2}{n}\left[1+\frac{2\{P\sigma_x^2+Q\sigma_y^2-\sigma_x\sigma_y(r+2T)\}}{\sigma_x^2+\sigma_y^2}\right]$$

$$= (\sigma_x^2+\sigma_y^2)/n''$$

where $$n'' = n\Big/\left[1+\frac{2\{P\sigma_x^2+Q\sigma_y^2-\sigma_x\sigma_y(r+2T)\}}{\sigma_x^2+\sigma_y^2}\right] \quad \dots \text{(iii)}$$

In the case where there are no serial correlations and r = 0

$$\left[s.e.(\bar{x}-\bar{y})\right]^2 = (\sigma_x^2+\sigma_y^2)/n$$

and so n'' can be defined as the equivalent number of independent comparisons. Table (i) gives values of serial correlations and correlations between the variates, for forecast errors of wind over the routes and of wind at the points. For the points the correlations are stretch vector correlations. A serial correlation greater than .18 is inconsistent at the 5% level with an assumption that the forecast errors are uncorrelated. The serial correlations quoted are the correlations between consecutive terms (i.e., p_1 or q_1):

in the work which follows it has been assumed that $p_2 = p_1^2$, $p_3 = p_1^3$ etc.

There are theoretical grounds for making this assumption (see for example Brooks and Carruthers (4)), and some practical justification for expecting the assumption to be valid for wind statistics may be found in a study of the temporal correlations given by Durst (1). In this work, the p_1's were usually so small that it was not necessary to take into account correlations of a higher order than p_2.

Values of $t_{i,j}$ were not computed from the variates themselves: they were derived from the known correlations p, q, r. $t_{1,2}$ was obtained as follows. With the usual notation for partial correlations,

$$r_{x_1y_2\cdot x_2y_1} = \frac{\left(r_{x_1y_2\cdot y_1} - r_{x_1x_2\cdot y_1}\, r_{y_2x_2\cdot y_1}\right)}{\sqrt{\left(1 - r^2_{x_1x_2\cdot y_1}\right)\left(1 - r^2_{y_2x_2\cdot y_1}\right)}}$$

since x_1 and y_2 are related only through x_2 and y_1, $r_{x_1y_2\cdot x_2y_1}$ can be taken to be zero and so,

$$r_{x_1y_2\cdot y_1} = r_{x_1x_2\cdot y_1}\, r_{y_2x_2\cdot y_1}$$

Expanding the last relation in terms of the total correlations

$$(t_{1,2} - rq)(1 - t_{1,2}^2) = (p - r\,t_{1,2})(r - q\,t_{1,2})$$

when $t_{1,2}$ is taken equal to $t_{2,1}$.

The required $t_{1,2}$ is a root of the cubic

$$t_{1,2}^3 - (pq + r^2 + 1)\,t_{1,2} + r(p + q) = 0\ .$$

In the present work, the values of p, q and r were such that all the roots of this cubic were real, but two of the roots were numerically greater than one, leaving only one physically meaningful solution. $t_{1,3}$ can be obtained as a root of the cubic

$$t_{1,3}^3 - (p^2q^2 + r^2 + 1)\,t_{1,3} + r(p^2 + q^2) = 0,$$ and so on.

In assessing the significance of the correlations it is helpful to consider how they can arise in the case of statistical and persistence forecasts.

Equation (9), Section 3 of the main paper gives the formula for the serial correlation in the statistical forecast errors. If it is assumed that there is no bias in the forecasts ($U = \overline{V}$) and that P has been chosen approximately equal to the serial correlation, R_t, then the expression (9) reduces to $R_t(R_t^2 - R_{2t})/(1 - R_t^3)$ which vanishes when $R_t^2 = R_{2t}$. ($P_2 = P_1^2$ in the notation of the previous paragraph). It follows that there will be little or no serial correlation in the statistical forecast errors unless they contain a bias: this explains why the statistical forecast error correlation given in Table (i) is appreciable for the 500 mb. route but is negligible for the 200 mb. route. Equation (10) is the expression for the persistence forecast errors. Substituting values of R_{24} and R_{48} quoted by Durst (1) for Larkhill in expression (10), values for the serial correlation in persistence forecasts of -.21 and -.20 are obtained for winds at 200 mb. and 100 mb. respectively. These are comparable with correlations of -.16 and -.21 given for Liverpool in Table (i).

Route winds

Significance levels of the bias in the C.F.O. and L.A.P. 200 mb. forecasts, given in Section 4 of the main paper, were assessed using expression (i) of this appendix.

The standard error of the difference between the standard deviations of two normally distributed variates is $[(\sigma_1^2/n_1 + \sigma_2^2/n_2)/2]^{1/2}$. To obtain the levels of significance given in Table 8 for the routes, n_1 and n_2 were taken equal to the appropriate n'', which was itself calculated from equation (iii) above.

Point winds

For the points, the forecast errors are vector errors. Brooks and Carruthers (5) state that the observed winds conform to a normal circular distribution, and it can be expected that the forecasts, both statistical and orthodox, will also conform to this distribution: but it does not follow that the forecast errors should. It can be shown that the standard deviation S_x of the x components of the persistence forecast errors is given by $S_x^2 = 2\sigma_x^2(1-R_x)$ where R_x is the serial correlation in the x components of the observed winds. So $S_W \neq S_S$, the subscripts referring to west and south components, unless $R_W = R_S$ and $\sigma_W = \sigma_S$. Calculations were made of R_W and R_S for the Liverpool winds at 500 mb. and 200 mb. At 500 mb. R_W was .67 and R_S was .55, the difference between the two being not significant. At 200 mb. R_W was .85 (lower 5% confidence limit 0.77), and R_S was .54 (upper 5% confidence limit .68): here the difference was clearly significant.

In view of the considerations of the previous paragraph, tests were made for circularity in the distributions of each type of forecast error at 500 mb. and 200 mb. The test used was that developed by Mauchly and quoted in Brooks and Carruthers (6). The values of the ellipticity statistic which were obtained were not significant at the 5% level for statistical, persistence and orthodox forecasts at 500 mb., but values obtained for the 200 mb. forecasts were all significant at the 5% level.

The elliptic nature of the distribution of 200 mb. errors is evidently due largely to an interesting property of the wind flow at high levels, namely that the west component of the wind varies more slowly with time than does the south component. This feature has been noticed previously in connexion with 100 mb. wind statistics, e.g. in calculating the standard errors of 6-hr. variations of west and south components of 100 mb. wind, it was found that the variance of the west component variations was smaller than the variance of the south component variations (7). For present purposes it has been assumed that the non-circularity occurs only in the lower-stratospheric regime, and that the tropospheric forecast errors conform to a normal circular distribution.

For a normal circular distribution of vectors it is convenient to sum the departures from the vector mean over all directions to obtain a scalar variate V. The equation to the frequency curve of V is, $f(V) = \frac{2N}{\sigma^2} V e^{-V^2/\sigma^2}$ (Brooks and Carruthers (8)).

The second moment, μ_2, or variance of this distribution is given by $\int_0^\infty \frac{2}{\sigma^2} V^3 e^{-V^2/\sigma^2}$ and the fourth moment, μ_4, is $\int_0^\infty \frac{2}{\sigma^2} V^5 e^{-V^2/\sigma^2}$.

Integration yields $\mu_2 = \sigma^2$ and $\mu_4 = 2\sigma^4$. This distribution is obviously not normal. The standard error of the difference between the standard deviations of two such distributions may be obtained using the formula,

$$\left[\text{s.e. of } (\sigma_1 - \sigma_2)\right]^2 = \frac{\mu_4 - \mu_2^2}{4\mu_2 n_1} + \frac{\nu_4 - \nu_2^2}{4\nu_2 n_2} \quad \text{.... (Yule and Kendall (9))}$$

$$= \frac{1}{4}\left\{\frac{\sigma_1^2}{n_1} + \frac{\sigma_2^2}{n_2}\right\} \quad \text{... (iv)}$$

The significance levels quoted in Table 8 for Liverpool forecasts at 700 mb., 500 mb. and 300 mb. have been calculated using equation (iv), where $n_1 = n_2 = n''$, obtained from equation (iii).

For Liverpool 200 mb. errors, the south and west components were treated as two separate normal distributions. The correlations between south and west component errors were: .09 for persistence, .12 for C.F.O., and .16 for statistical forecasts (5% significance level was .22). The probabilities, p_i and q_i, of occurrence of the observed differences between relevant pairs of standard deviations of forecast errors, were computed for each component. The values given in Table 8 for 200 mb. are the probabilities, $p_i q_i$, of simultaneous occurrence of the observed differences of standard deviation in the two components together, the two component distributions being treated as mutually independent.

Tests for the representativeness of the 1955 data

The percentage frequency with which deviations from the normal of sample mean winds, equal to or greater than the deviation which occurred for the trial period, can be expected to occur, are given in Table 4 of the paper, in the column headed "Frequency of 1955 departure". To obtain these values, (a) the 1948-55 means for January to April were taken as the normals, and (b) the standard error of the 1955 mean was calculated using a form of equation (i) derived by Brooks, viz.,

$$\left[\text{s.e. mean}\right]^2 = \frac{\sigma^2}{n}\left\{1 + \frac{2R_t}{1-R_t}\left(1 - \frac{1}{n}\cdot\frac{1-R_t^n}{1-R_t}\right)\right\}$$

This expression is derived assuming that $R_{nt} = R_t^n$. As previously mentioned, this assumption is probably reasonable in the case of wind data where t = 24 hr. for small n, i.e., n = 2 or 3, but in the absence of practical confirmation, it becomes increasingly dubious as n increases. Steps (a) and (b) are both by no means satisfactory, but are made in the absence of further data. Consequently, as mentioned in Section 5 of the paper, the percentage frequencies given in Table 4 must be treated with some reserve, but they do give a guide to the normality of the trial period.

/Table (i)

Table (i). Correlations in forecast errors

(a) Serial correlations in forecast errors

Forecast error	Routes		Liverpool *	
	500 mb.	200 mb.	500 mb.	200 mb.
L.A.P.	.16	-.01	-.08	.11
C.F.O.	.22	.08	-.00	.15
Statistical	.23	.04	-.05	.22
Persistence	.03	-.13	-.21	-.16

(b) Correlations between forecast errors

Forecast errors	Routes		Liverpool *	
	500 mb.	200 mb.	500 mb.	200 mb.
C.F.O. v. Statistical	.47	.44	.58	.54
C.F.O. v. L.A.P.	.61	.58	.66	.53

* Liverpool correlations are stretch vector correlation co-efficients

Fig. 1

Frequencies of forecast errors — route forecasts

January - April 1955

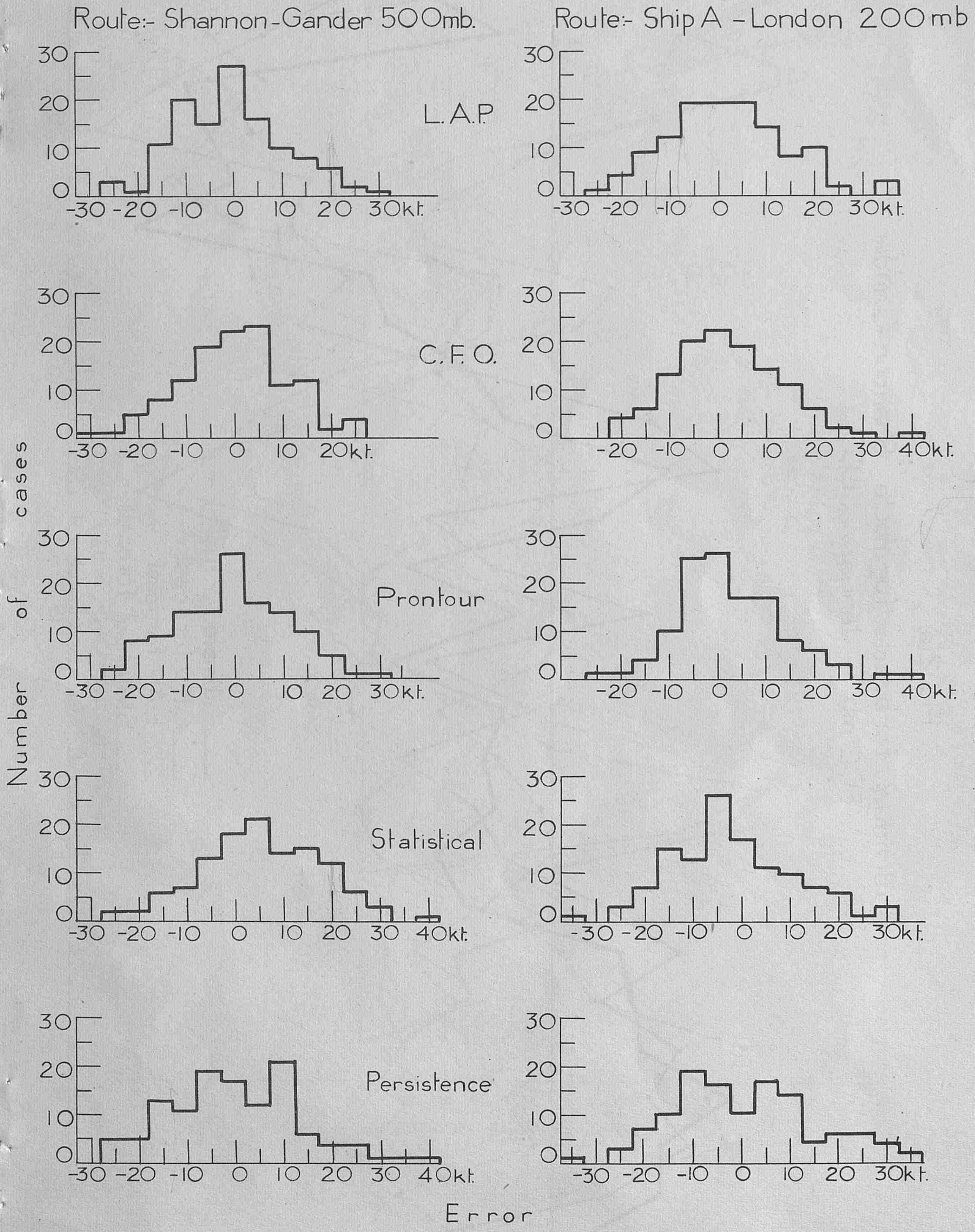

Fig. 2(a)

Individual forecasts for route Shannon-Gander
500 mb. — January, 1955

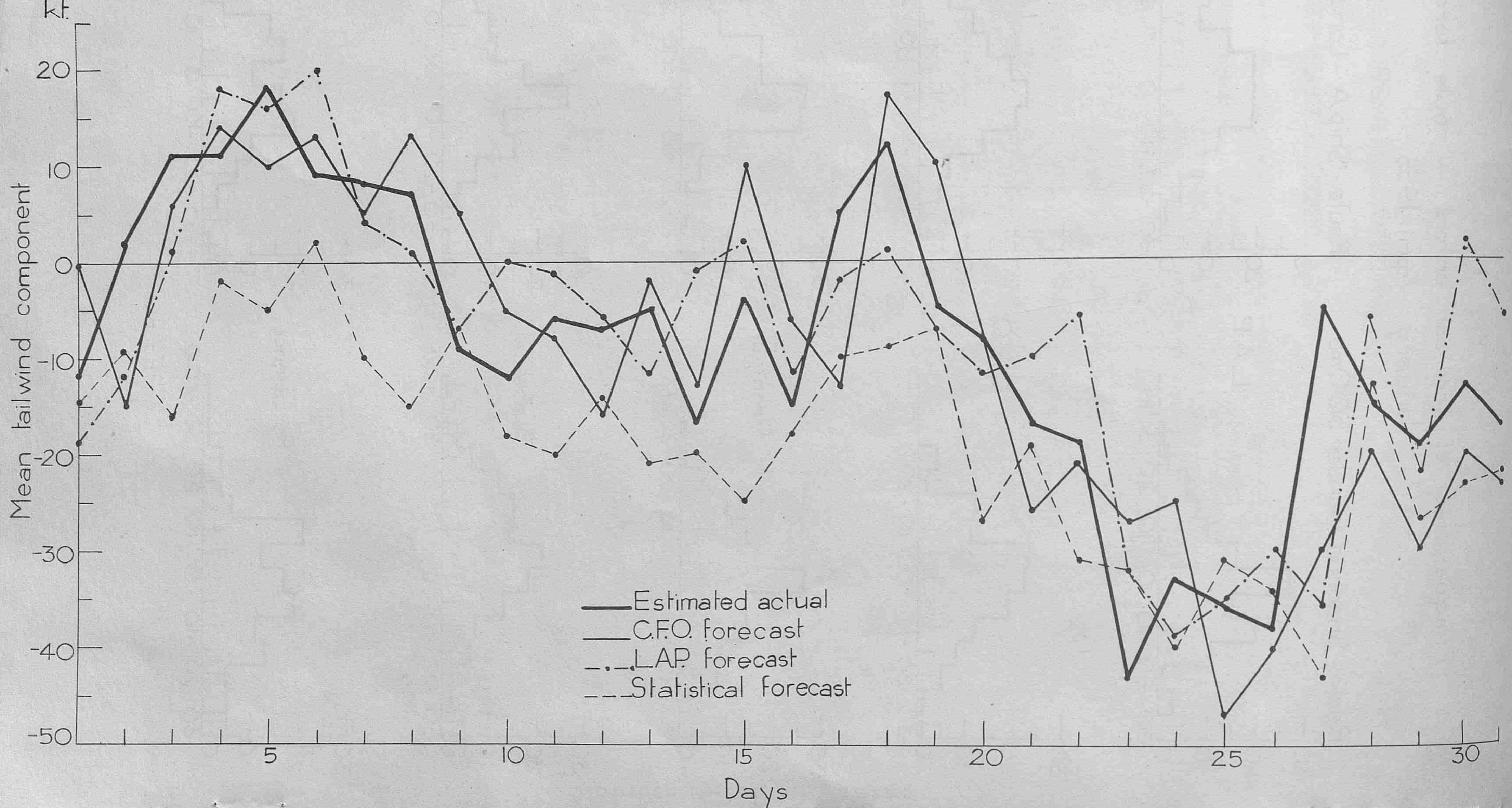

Fig. 2 (b)

Individual forecasts for route Shannon-Gander
500 mb. — February 1955

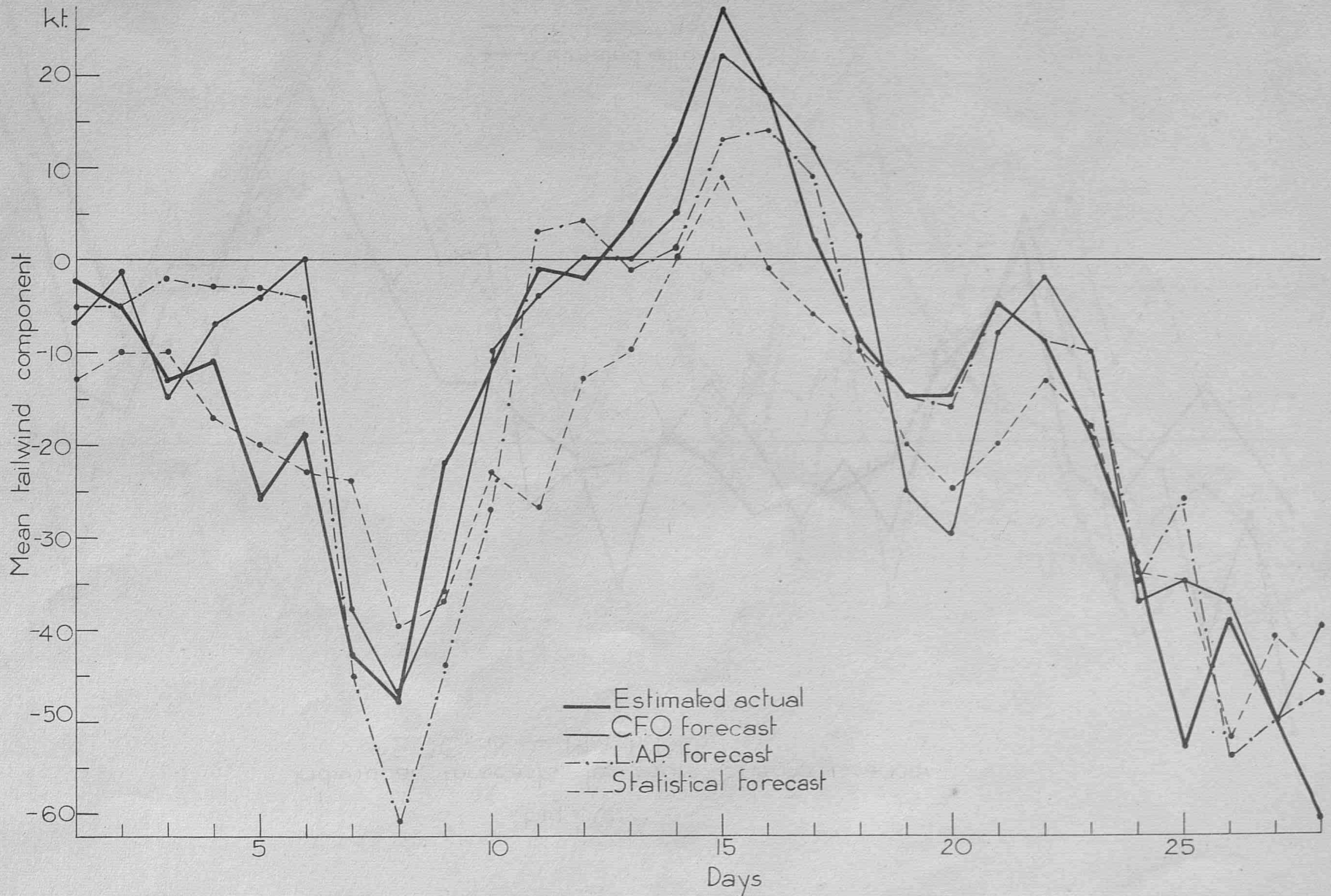

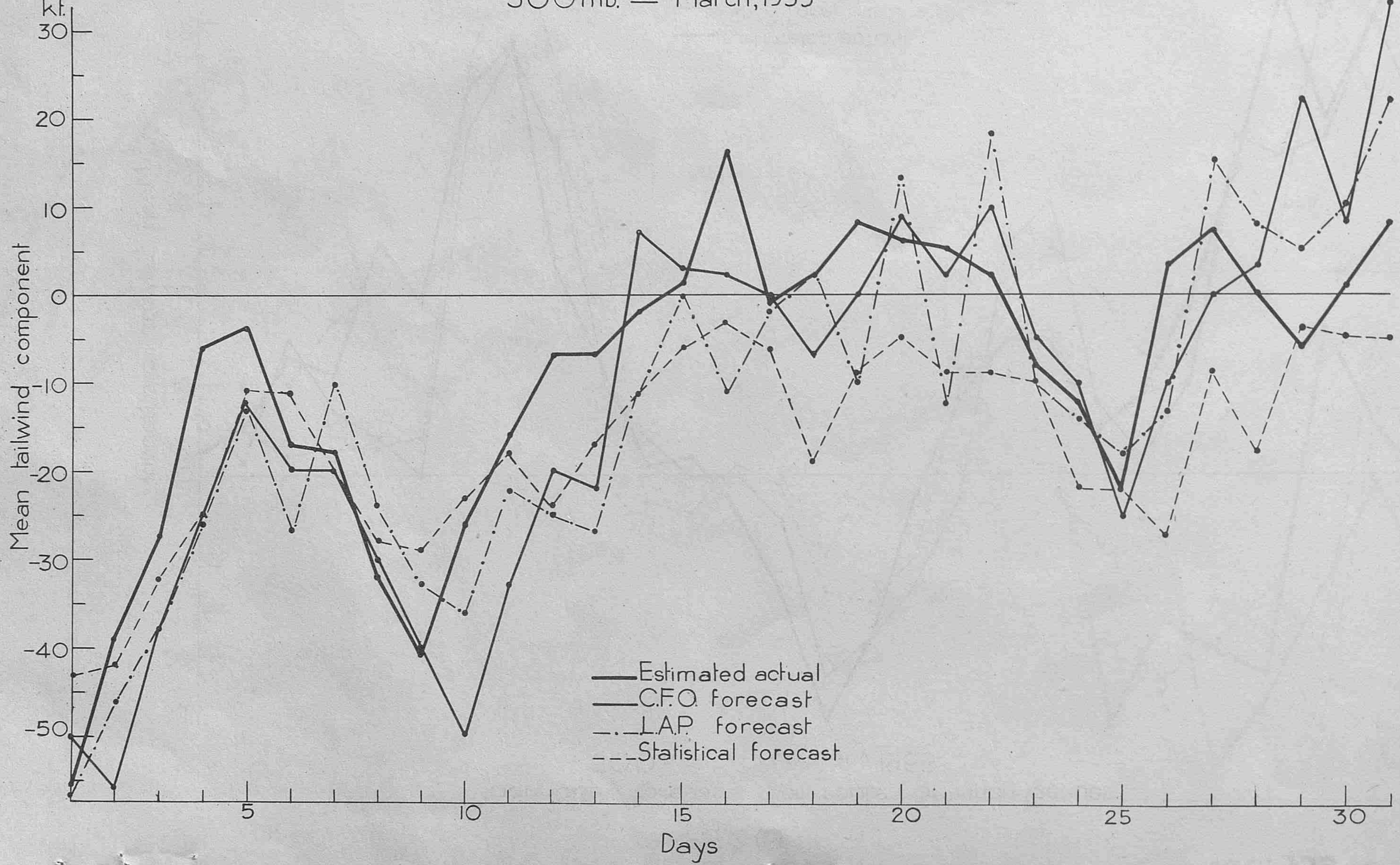

Fig. 2 (c)

Individual forecasts for route Shannon-Gander
500 mb. — March, 1955

Fig. 2(d)

Individual forecasts for route Shannon-Gander
500mb. — April, 1955

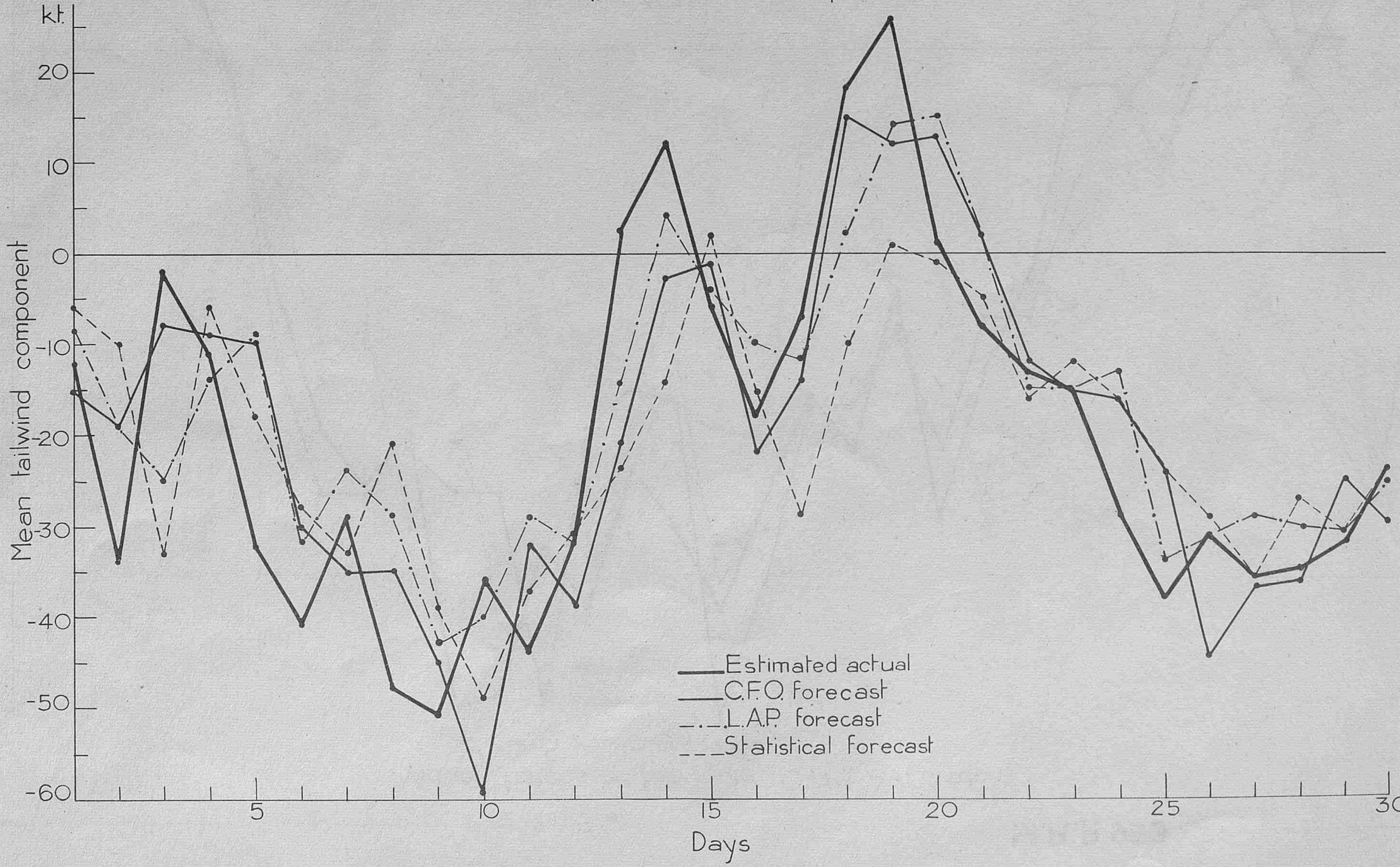

Fig. 3(a)

Individual forecasts for route O.W.S. "A"-London
200mb. —January, 1955

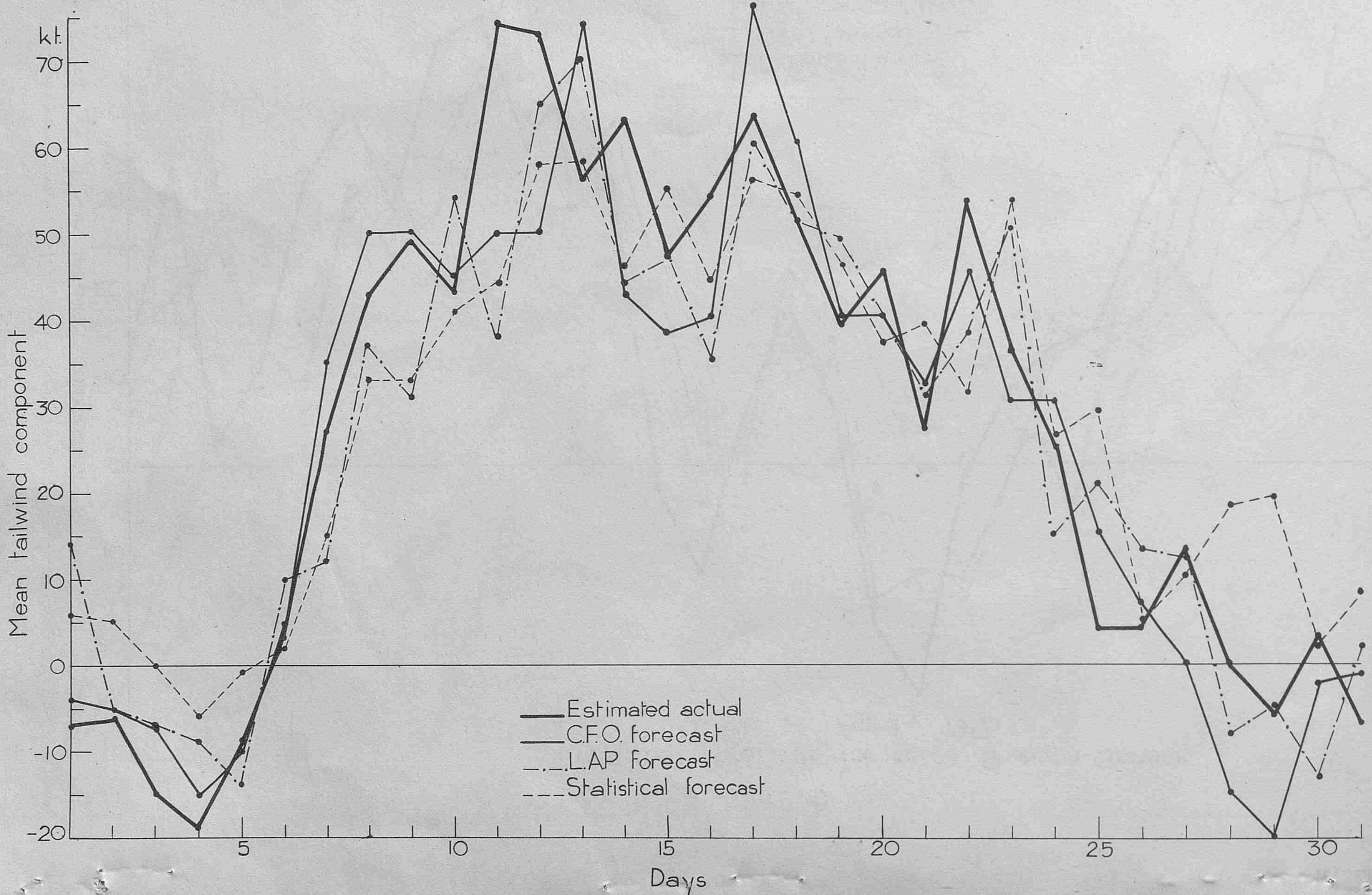

Fig. 3(b)

Individual forecasts for route O.W.S. "A" - London
200 mb. — February 1955

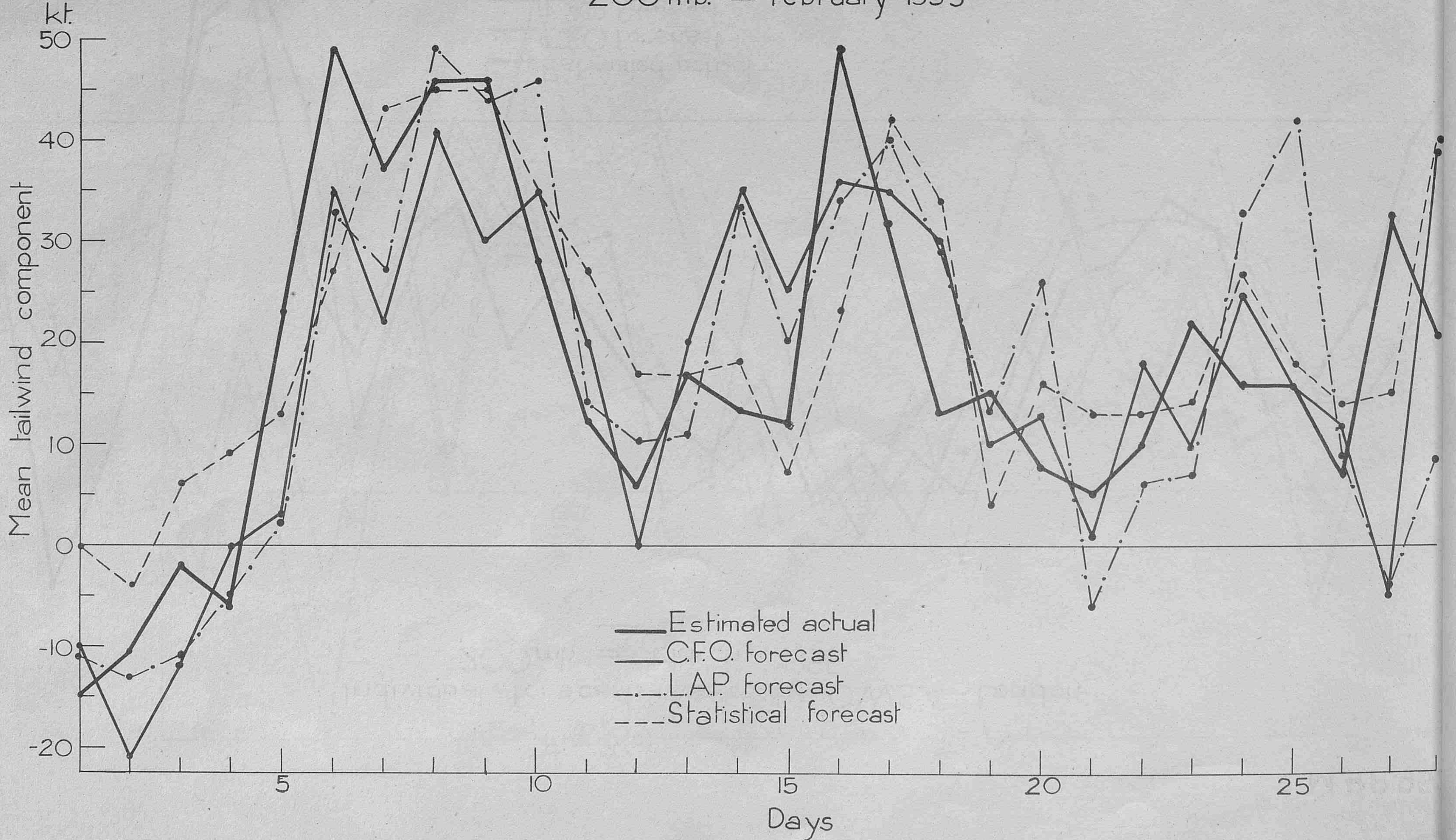

Fig. 3(c)

Individual forecasts for route O.W.S."A" - London
200mb. — March, 1955

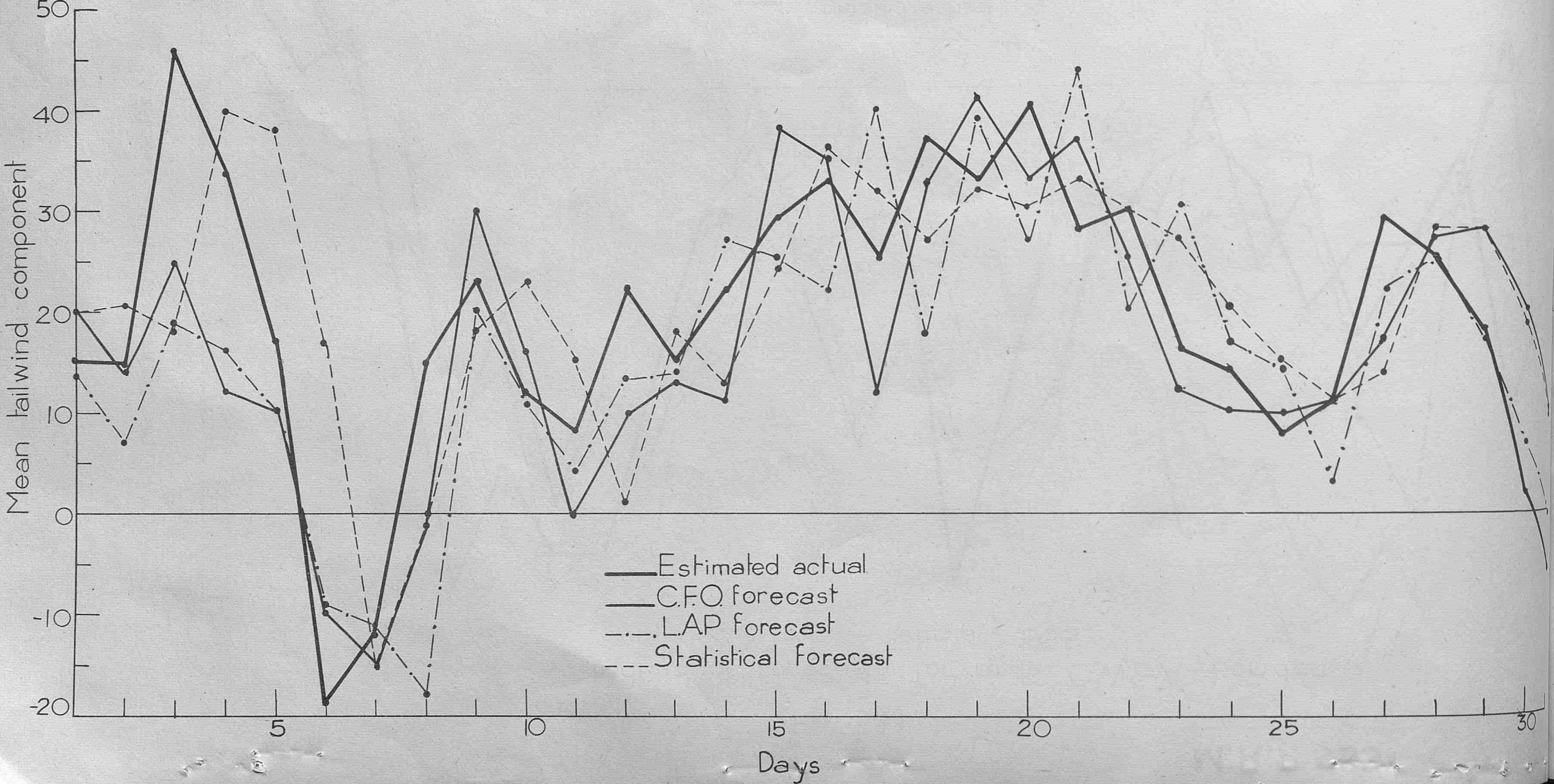

Fig. 3(d)

Individual forecasts for route O.W.S."A"-London
200 mb. - April, 1955

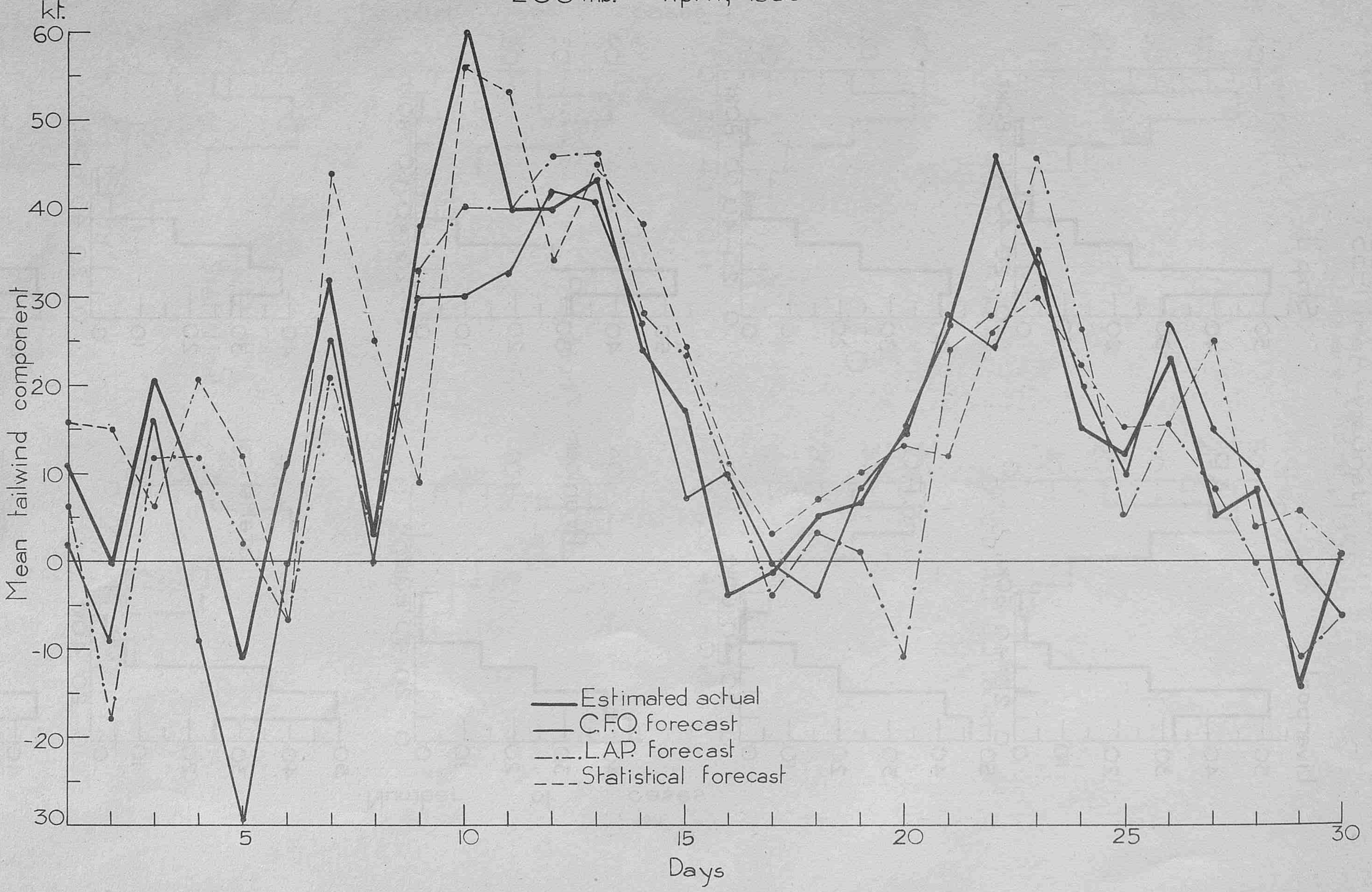

Fig. 4(a)

Frequencies of forecast errors – point forecasts, 700 mb.

January-April 1955

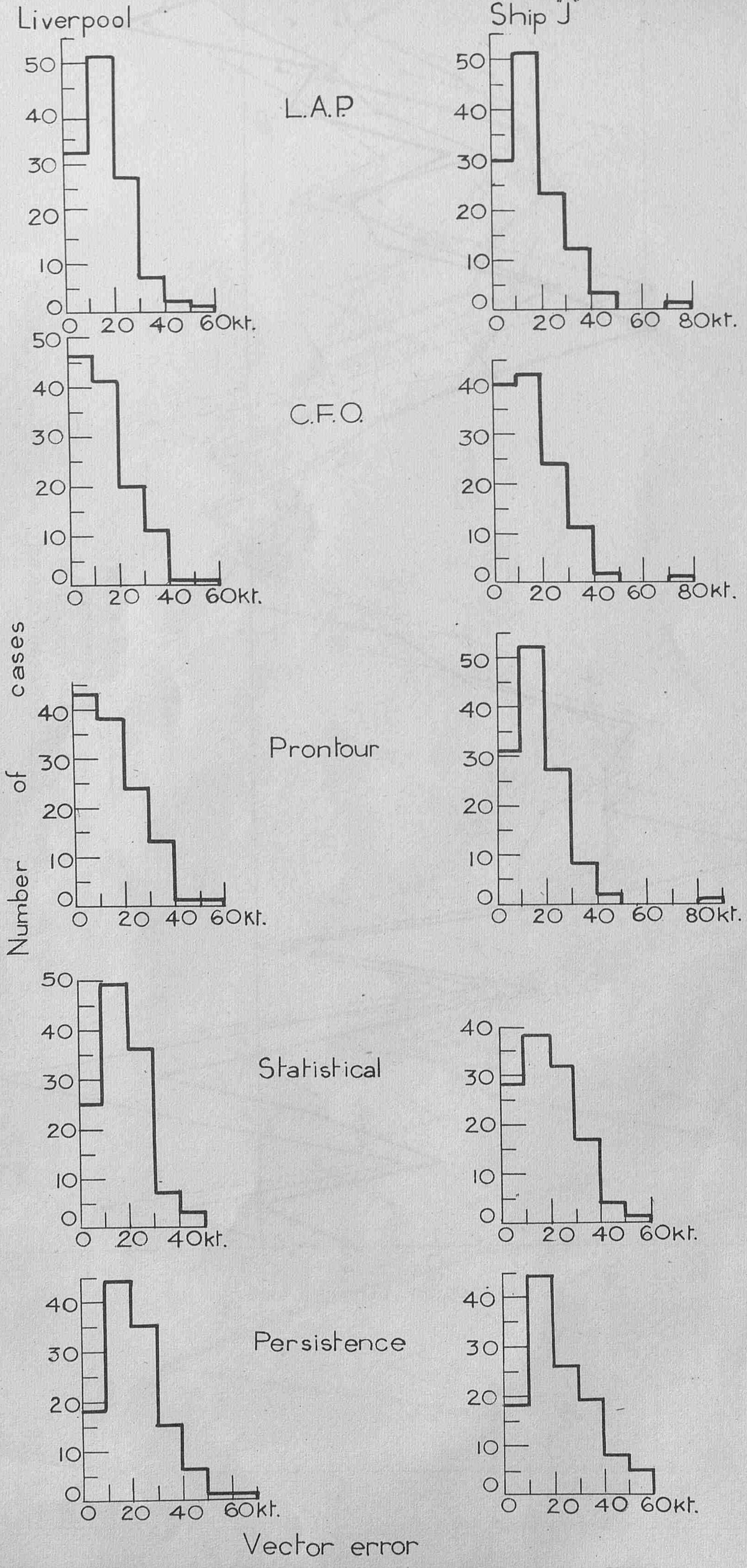

Fig. 4 (b)

Frequencies of forecast errors – point forecasts, 500 mb.
January – April, 1955

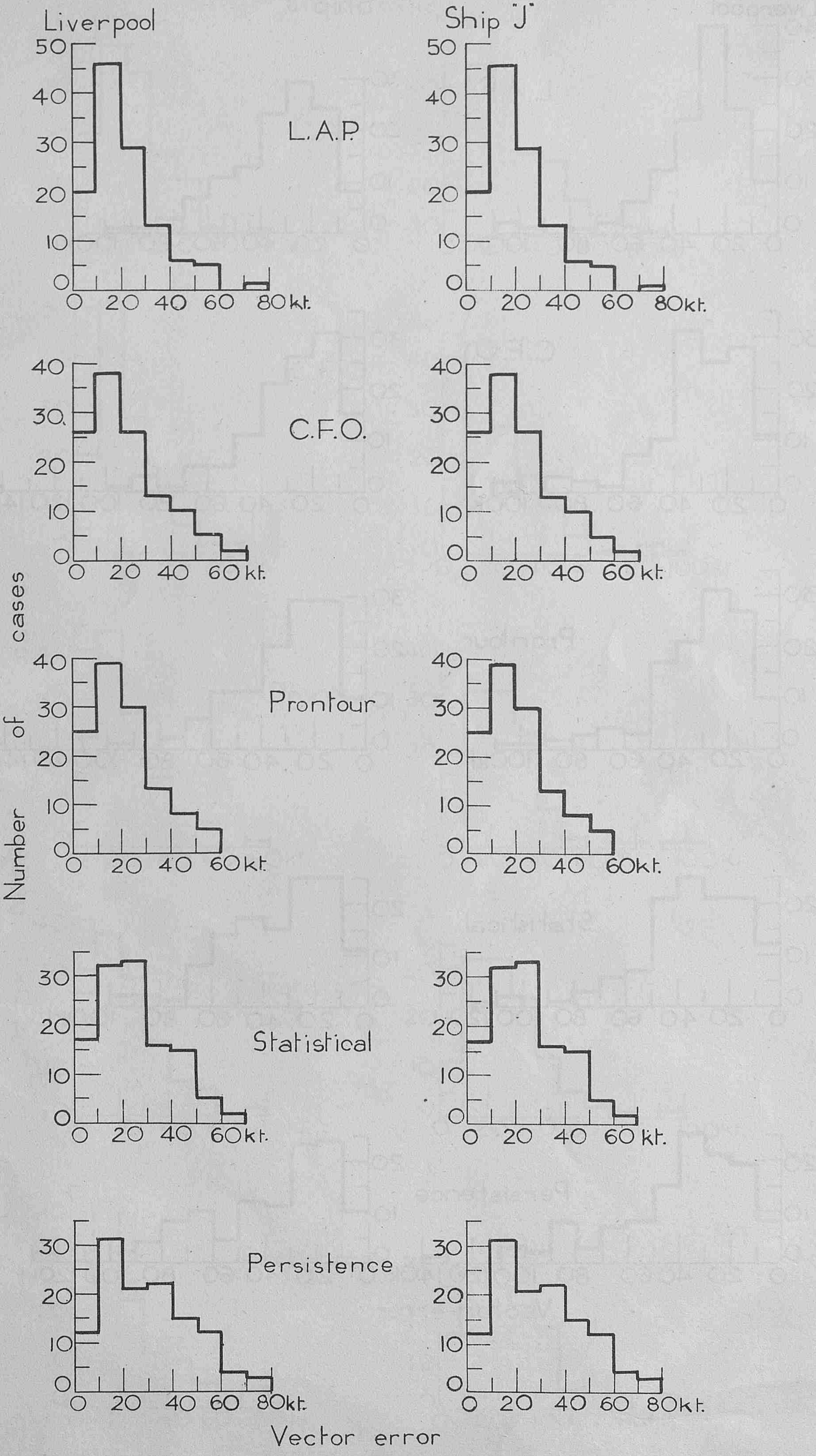

Fig. 4 (c)

Frequencies of forecast errors – point forecasts, 300 mb.
January – April, 1955

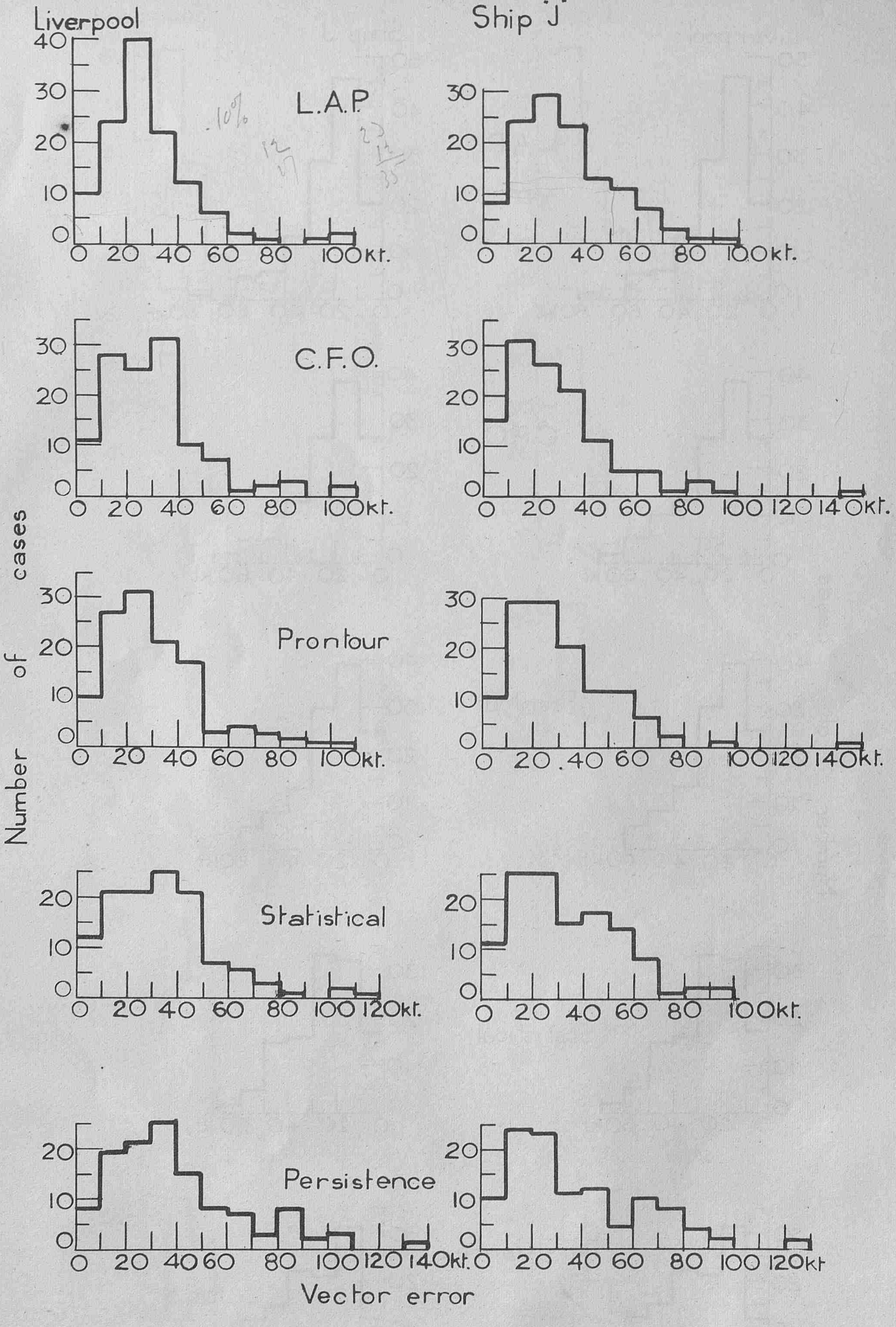

Fig. 4 (d)

Frequencies of forecast errors – point forecasts, 200mb.
January – April, 1955

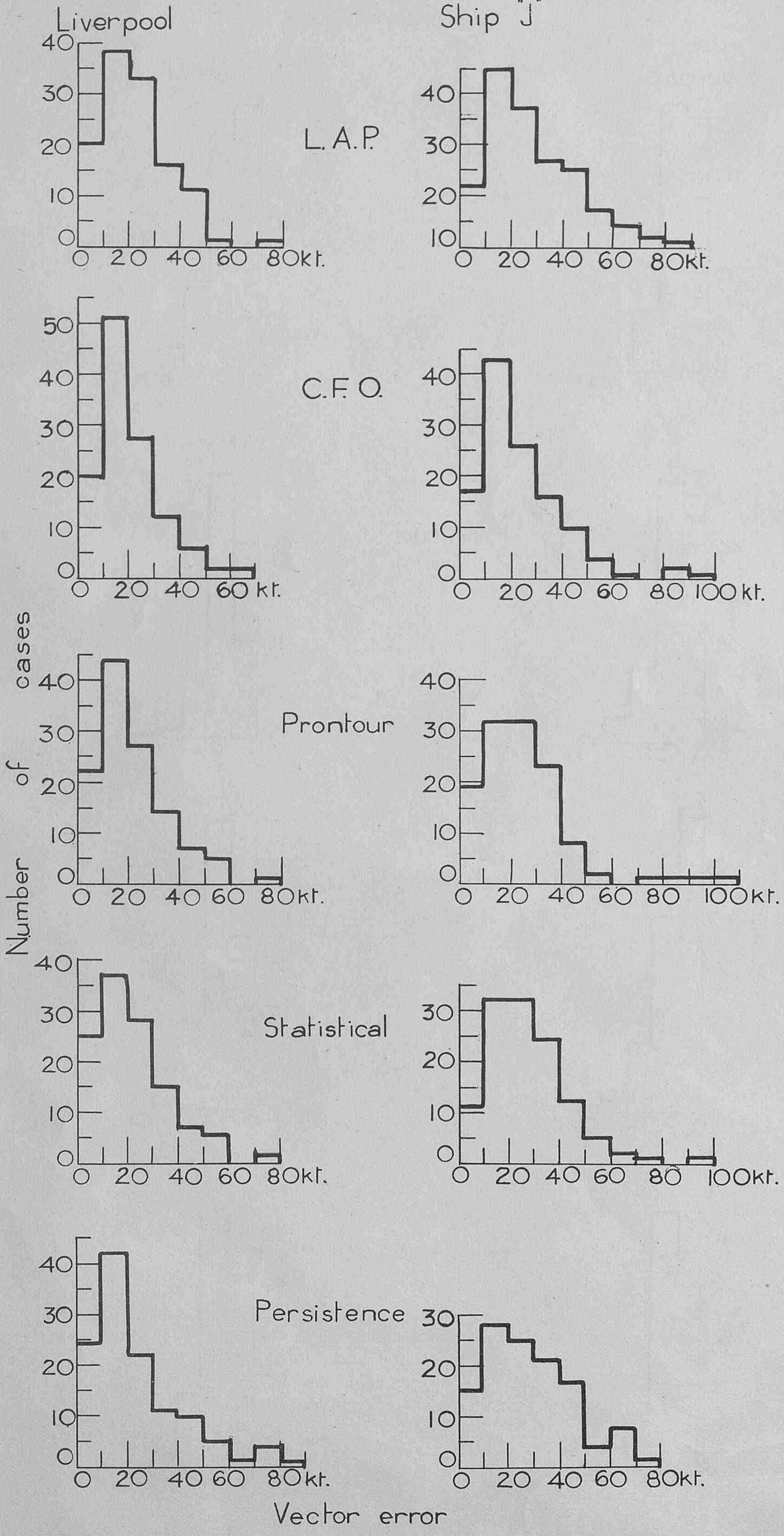

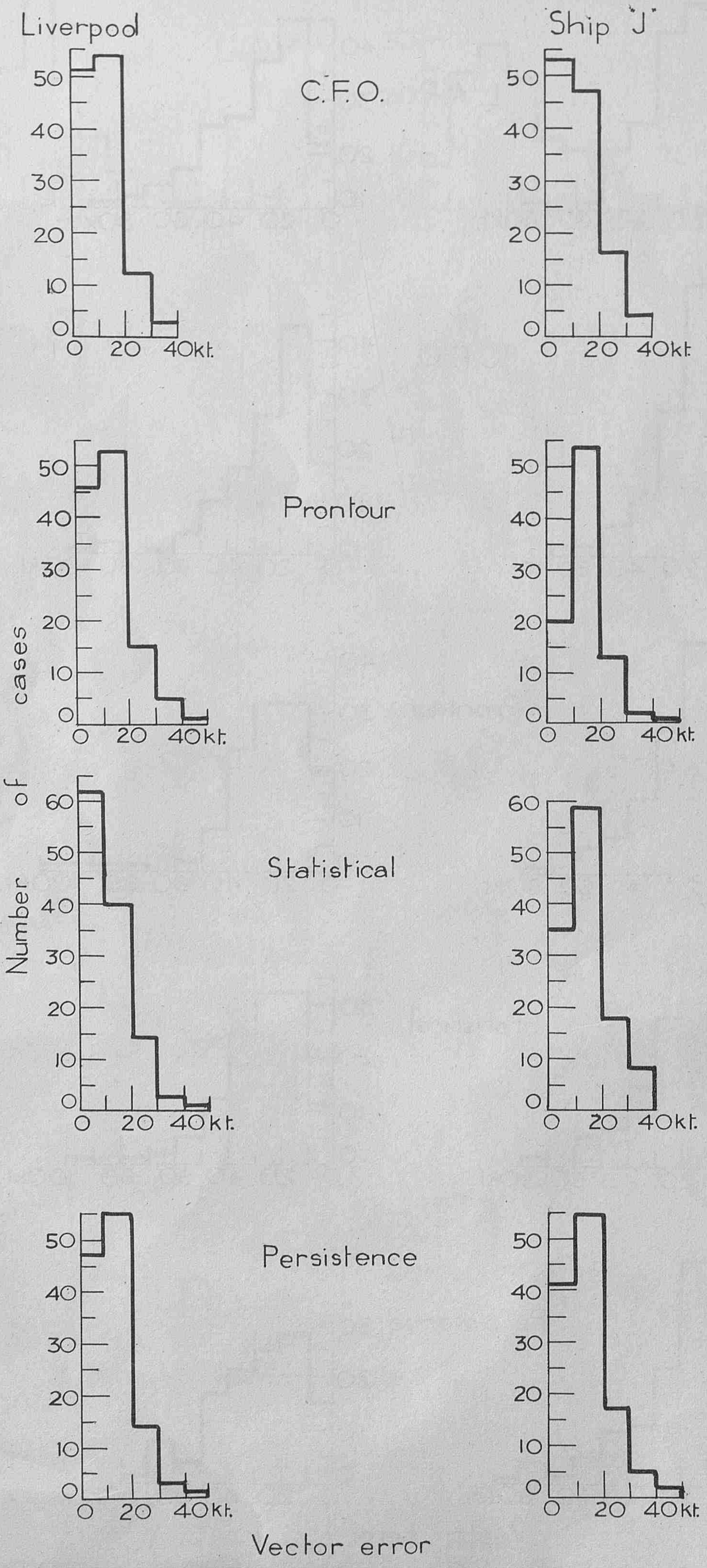

Fig. 4 (e)
Frequencies of forecast errors – point forecasts, 100mb.
January – April, 1955

M.R.P. 955

S.C. II/203

9th January, 1956

AD133330

Comments on statistical and orthodox forecasting

by

C. S. Durst

(Meteorological Office)

AWSSS
ROUTING SLIP

FILE	INFO	ACTION				
	2.1		DIRECTOR			
			DEP DIRECTOR			
	2		[illegible] DIRECTOR			
	3		[illegible]			
	4		TRSD		CHF	
				✓	TSS	
				✓	RRB	
					EDB	
					SEC	
	1		EDD		CHF	
					HLFB	
					STB	
					SPFB	
					CU	
					SEC	
	5		TIFD		CHF	
				✓	PUE	
					TECH INFO	
					SEC	

AIR MINISTRY

METEOROLOGICAL RESEARCH COMMITTEE

At the time of issue this report has not been published. Any author desiring to quote this paper should refer to it as "A paper of the Meteorological Research Committee (London).
M.R.P. No. 955 by Mr. C.S. Durst.
A copy is available in the Library of the Meteorological Office."

M.R.P. 955
S.C.II/203
9th January, 1956

AIR MINISTRY
METEOROLOGICAL RESEARCH COMMITTEE

Comments on statistical and orthodox forecasting
by
C.S. Durst (Meteorological Office)

1. About eighteen months ago I wrote a somewhat lengthy paper on the possibilities of statistical forecasting which led, early in 1955, to the experiment described by Mr. Johnson (1955). The results of that experiment seem to be very much what I had anticipated. For instance the standard errors expected on statistical grounds from 24-hour statistical forecasts on London-Gander route with three intermediate observations are set out below:-

Table I Expected R.M.S. errors of statistical forecasts

	Winter	Spring	Summer	Autumn
500 mb.	13 kt.	12 kt.	9½ kt.	11½ kt.
700 mb.	9 kt.	8½ kt.	6½ kt.	8½ kt.

In my original paper I computed some comparisons. For these I got from London Airport their forecasts of equivalent headwinds for the Shannon-Gander route at 500 mb. and their actuals as estimated from their contour charts for 22nd December, 1952 to 4th April, 1953. I made statistical forecasts also for the same occasions. The result was as follows:-

Table II Root mean square differences between actuals at 500 mb. measured off contour charts and forecasts prepared in various ways for routes across the Atlantic

	R.M.S. difference	R.M.S. difference after correction for contour errors
Orthodox forecasts (24 hours)	9.9 kt.	8.2 kt.
Statistical forecast (0 hours)	7.7 kt.	5.4 kt.
" " (12 hours)	9.0 kt.	7.1 kt.
" " (24 hours)	10.6 kt.	9.0 kt.

The last column probably gives the true errors, as I found by comparison of London Airport's and Prestwick's contour measurements that the root mean square error of measurements of wind over such a route at 500 mb. was about 5½ kt. (Johnson in Table 2 found the R.M.S. difference between L.A.P. and C.F.O. measurements to be 5.9 which gives a R.M.S. error of one set of measurements to be 4.2 kt.)

In Johnson's Table 3 the R.M.S. errors of his trials are given as follows for 500 mb. for Shannon-Gander route, January to April, 1955.

/Table III

Table III — Johnson's figures for forecast errors

	Standard deviation of forecast errors	R.M.S. error
L.A.P. forecast	11.1 kt.	11.0 kt.
C.F.O. forecast	10.9 kt.	10.9 kt.
Statistical forecast (24 hours)	12.3 kt.	13.6 kt.

It may be noted that, since the actuals were the mean of C.F.O. and L.A.P., the R.M.S. error of the actuals used as yard stick was about 3 kt. and provided there is no correlation between the C.F.O. and L.A.P. errors this would make very little difference to the R.M.S. errors of the forecasts. From these tables one can deduce that the season January to April, 1955 was somewhat more difficult for forecasters than December to April, 1953, (probably because the variability of winds was greater). As Mr. Johnson points out, the effect of bias prejudiced the statistical forecast in 1955 but nevertheless the proportionality of the statistical and orthodox forecasts is broadly the same in the two periods, and so the conclusions I reached in my original paper are not disproved.

2. In the planning of the 1955 experiments I wished to have had forecasts made of equivalent head winds rather than of fixed time route winds, for then by comparison with aircraft observation we could have gained knowledge of whether the contour charts drawn at C.F.O. and L.A.P. were both in error in the same sense. However, the estimation of the equivalent head winds presented such difficulties that that scheme was deemed impossible.

However, I obtained from Prestwick the logs of a considerable number of aircraft flying from Gander to Prestwick together with estimates of the actual winds which would have been expected from the contours allowing for the differences in time. The aircraft observations were selected so that two or more were crossing at the same time. Thus (after a statistical correction for small differences in time and position) there were comparisons available (a) between winds found by two aircraft and (b) between winds found from contours and by aircraft. Two periods were examined in this way; in one there were 64 pairs of aircraft, in the other 72 pairs. If we assume that the errors in the aircraft measurements are uncorrelated with each other and also with the contour measurements we can obtain estimates of the probable errors in the aircraft observations and in the geostrophic winds. Further, on 34 occasions I got two estimates made of the geostrophic winds off independent maps by independent estimators. The result was as follows:-

Table IV — R.M.S. of vector errors of winds over a route across the Atlantic at 500 mb. determined in various ways

	Period 1	Period 2	Total
R.M.S. error in aircraft winds	4.8 kt.	8.8 kt.	7.2 kt.
R.M.S. error in geostrophic winds	6.4 kt.	8.8 kt.	7.9 kt.
Apparent R.M.S. error in geostrophic wind derived by comparison of two independent estimates	-	-	7.0 kt.
Number of aircraft pairs	64	72	136

The conclusion which can be drawn from this table is that the winds measured by aircraft over such a route have about the same error as that made by the meteorologist in estimating from his charts and secondly by the comparison of 7.9 kt. and 7.0 kt., that about four fifths of the meteorologist's error is due to incorrect drawing of the contour lines and inaccurate measurements but that one fifth (in this case equivalent to a R.M.S. error of 3½ kt.) is due to consistent errors in drawing, i.e. to faulty pressure readings or to lack of observations or other such biases which lead to the meteorologist's maps being incorrect, however skilfully drawn.

It is of interest that such consistent errors do exist but in the present experiment one can easily see that they do not materially modify the result.

3. British European Airways Corporation requested in 1951 that 33-hourly forecasts of route winds should be given for a number of routes over the Continent. These forecasts were made by orthodox methods and by the use of a regression equation, the latter being done by an assistant without recourse to a highly trained scientist.

Initially a trial was made and showed that the forecasts from the regression equation were less in error than those by orthodox methods and the regression equation was adopted as a routine. Later, however, after more effort had been put into the preparation of the orthodox forecasts a further comparison was made with the following result. Mean route-winds?

Table V Comparison of forecasts for 33 hours ahead made by orthodox and statistical methods

WHAT HEIGHT?

Route	Root mean square errors	
	Orthodox forecasts	Statistical forecasts
London to Bordeaux	13.1 kt.	15.7 kt.
London to Nice	12.5 kt.	12.8 kt.
London to Copenhagen	17.1 kt.	18.7 kt.

The experiment was abandoned because B.E.A.C. operators ran into difficulties, not because the forecasts were found to be of no value.

4. From these examples it is clear that the improvement of orthodox forecasts over statistical is not very great. From Table II and other examples quoted in my original paper it seems that the statistical forecasts could improve on the accuracy of the orthodox forecast if the data on which it were based were 12 hours later than those of the orthodox forecast, and would be but little worse than the orthodox forecast if the data were 6 hours earlier. The time taken to produce a statistical forecast is of the order of 10 minutes after the last observation has been received; the time taken to produce an orthodox forecast is much greater. The orthodox forecasts in this trial were completed before 0300 G.M.T. and referred to an epoch 12 hours later; the statistical forecasts were based on 2100 G.M.T. (or 1500 G.M.T.) observations and an allowance of 6 hours was given for transmissions. It should further be noticed that the orthodox forecasts issued between 0300 G.M.T. and 0900 G.M.T. would be based in the main on the same information as that issued at 0300 G.M.T. whereas the statistical forecast could be brought up to date as each fresh piece of information was received. An improvement of the speed of transmission of data from selected points on the routes (e.g. from weather ships for the Atlantic route) would improve the statistical more than the orthodox forecasts.

5. Apart from the greater speed of the preparation of the statistical forecasts, the advantage of the method is likely to be found (a) in forecasting winds at high levels where the orthodox prontours become increasingly inaccurate and take longer to prepare, (b) in forecasting winds for assessing pay loads; these forecasts (b) are required 24 to 36 hours ahead, they are not operational, and could be made as a routine by assistants, thus saving highly paid staff such as had to be used in the B.E.A. experiment to compete with the accuracy of the forecast by regression equations.

Reference

Johnson, D.H. 1955 Meteorological Research Papers, Air Ministry, London, No. 953.

M.R.P. 956

S.C. 11/204

23rd January, 1956

The use of a stream function in the Sawyer - Bushby two parameter model of the atmosphere

by

F. H. Bushby and Vera M. Huckle

(Meteorological Office)

AWSSS
ROUTING SLIP

FILE	INFO	ACTION		
			DIRECTOR	
			DEP DIRECTOR	
			[illegible] DIRECTOR	
	1		CONSULTANTS	
	2		TRSD	CHF
				TSS
				RRB
				EDB
				SEC
	3		EDD	CHF
				HLFB
				STB
				SPFB
				CU
				SEC
	4		TIPD	CHF
				PUE
				TECH INFO
				SEC

AIR MINISTRY

METEOROLOGICAL RESEARCH COMMITTEE

send to AWS/CL

At the time of issue this report has not been published. Any author desiring to quote this paper should refer to it as "A paper of the Meteorological Research Committee (London).
M.R.P. No. 956 by Mr. F. H. Bushby
and Mrs. V. M. Huckle
A copy is available in the Library of the Meteorological Office."

M.R.P. 956
S.C.II/204
23rd January, 1956

AIR MINISTRY

METEOROLOGICAL RESEARCH COMMITTEE

The use of a stream function in the Sawyer - Bushby two parameter model of the atmosphere

by

F. H. Bushby and Vera M. Huckle (Meteorological Office)

1. Introduction

Most of the recent work on numerical weather prediction has been characterized by the use of the geostrophic approximation to the wind field. An examination of about twenty computed forecasts based on the Sawyer-Bushby (1) two parameter model of the atmosphere suggested that in one or two situations the use of the geostrophic approximation was possibly responsible for a large part of the difference between computed and actual charts.

This paper describes an attempt to improve upon the geostrophic approximation by representing the wind field in an isobaric surface by a stream function which differs from the geopotential. The stream function is derived from an equation similar to the balance equation derived by Charney (2) which relates the horizontal velocity field at a given pressure level with the contours of the same isobaric surface. Three 24-hr. forecasts have been computed applying this technique to the two parameter model and the results compared with previous computations in which no attempt had been made to improve upon the geostrophic approximation.

2. The derivation of the stream function

Since the significant motions of the free atmosphere are characterized by small horizontal divergences we can adequately express the velocity components u and v in terms of a stream function ϕ by

$$u = -\frac{g}{l}\frac{\partial\phi}{\partial s}, \qquad v = \frac{g}{l}\frac{\partial\phi}{\partial r} \qquad \text{---- (1)}$$

where r and s are orthogonal curvilinear distance co-ordinates on the sphere. If the rather slow variation of the Coriolis parameter l with latitude is ignored, this velocity field is non-divergent.

Ignoring the vertical motion terms and the variations of l, substituting from Eq. (1) and taking the horizontal divergence of the equations of motion, we obtain (when pressure is used as the vertical co-ordinate),

$$\frac{2g}{l^2}\left\{\left(\frac{\partial^2\phi}{\partial r\,\partial s}\right)^2 - \frac{\partial^2\phi}{\partial r^2}\frac{\partial^2\phi}{\partial s^2}\right\} - \nabla_e^2\phi = -\nabla_e^2 h \qquad \text{---- (2)}$$

where h is the height of the contour surface and ∇_e^2 is the two-dimensional Laplacian operator on the sphere. This equation is of the Monge-Ampère type and can be solved for ϕ as a boundary value problem provided that

$$g\,\frac{\nabla^2 h}{l} + \frac{l}{2} > 0 .$$

In the analysis given by Charney (2) he does not need to ignore the variation of the Coriolis parameter with latitude as he uses a stream function such that

$$u = -\frac{\partial\phi}{\partial s} \qquad v = \frac{\partial\phi}{\partial r} \qquad \text{---- (3)}$$

Charney then derives an equation similar to Eq. (2) but including a term grad ϕ grad l. Although Charney's equation can be derived with one less approximation than Eq. (2), it is more difficult to obtain suitable boundary values for ϕ when Eq. (3) is used to define the stream function than if Eq. (1) is used for that purpose.

Representing the earth's surface by a stereographic projection of the northern hemisphere on to a plane perpendicular to the earth's axis passing through the north pole, Eq. (2) becomes approximately

$$2\frac{\beta^2 g}{l^2}\left\{\left(\frac{\partial^2\phi}{\partial x\partial y}\right)^2 - \frac{\partial^2\phi}{\partial x^2}\cdot\frac{\partial^2\phi}{\partial y^2}\right\} - \nabla^2\phi = -\nabla^2 h \qquad \text{---- (4)}$$

where β is the magnification factor $\sec^2(\pi/4 - \theta/2)$ and x and y are the rectangular Cartesian co-ordinates on the plane. The ratio of the small terms neglected in deriving Eq. (4) from Eq. (2) to the smallest terms which appear in Eq. (4) is of the same order as the ratio of the wavelength of the characteristic patterns of the stream function to the circumference of the earth.

Eq. (4) can be written as the following finite difference approximation:-

$$\sum_1^4\phi_i - 4\phi_0 + 4h_0 - \sum_1^4 h_i - \frac{2\beta_0^2 g}{a^2 l_0^2}\left\{\frac{1}{16}(\phi_A+\phi_C-\phi_B-\phi_D)^2 - (\phi_1+\phi_3-2\phi_0)(\phi_2+\phi_4-2\phi_0)\right\} = 0 \qquad \text{--- (5)}$$

where a = grid length and the suffixes refer to points relative to the origin O as shown in Fig. 4. Eq. (5) is a quadratic equation in ϕ_0 and can be re-written as

$$\phi_0 = \frac{4K + 2\sum\phi_i \pm \sqrt{16K^2 + 4(\sum\phi_i)^2 - 16Ka^2\nabla^2 h + (\phi_A+\phi_C-\phi_B-\phi_D)^2 - 16(\phi_1+\phi_3)(\phi_2+\phi_4}}{8} \qquad \text{---- (6)}$$

where $K = \dfrac{a^2 l_0^2}{2\beta_0^2 g}$.

It is clear that the solution we require is the one with the negative sign outside the square root; e.g., consider the case of parallel equidistant straight contour lines.

Given ϕ on the boundary we can obtain a solution to Eq. (5) by making an initial guess at the answer (say $\phi = h$) and then using Eq. (6) in a systematic point to point manner over the grid, continuing the process until there is no longer any significant change in ϕ. Since the stream function is defined by Eq. (1) it is possible to use $\phi = h$ on the boundary as the boundary condition. The iterative process is slowly convergent. 15 to 20 iterations were usually needed to obtain the necessary accuracy in the answer when an 18 x 14 grid was used.

The above procedure is not possible if the quantity under the radical (say A) in Eq. (6) is negative. In practice this difficulty was overcome by replacing a negative A by zero. If we consider a stream function ϕ consisting of a series of concentric circles then A not negative implies $\frac{g}{l}\nabla^2 h + \frac{l}{2} \geq 0$, the condition necessary for Eq. (2) to be solved as a boundary value problem. With circular isobars this is equivalent to the condition that the actual absolute vorticity must not be negative.

3. Application of the stream function to the two parameter model

We can represent the horizontal velocity by a stream function only if the flow is approximately non-divergent, and therefore it would appear difficult to make use of a stream function in any model other than the simple barotropic one.

However the two parameters h_m, h' of the Sawyer-Bushby model refer to the height of the mean level of the layer considered and the thickness of the layer. h_m is used solely to represent the flow at the mean level (which even in the two parameter model is thought to be approximately non-divergent, consistent with the assumption of a parabolic vertical motion profile) and we therefore decided to replace h_m by ϕ_m in the prognostic equations. h' however, besides representing the wind shear, does in fact represent the mean temperature of the layer, and it was therefore decided to leave the parameter h' unaltered.

Three time integrations were performed in which ϕ_m was first computed from the initial h_m, ϕ_m was subsequently used instead of h_m during the time integration, and finally h_m at time t = 24 was computed from ϕ_m at that time by solving Eq. (5) as a Poisson equation for h_m given ϕ_m and boundary values for h_m. The boundary values of h_m were taken as $h_m = \phi_m$.

The particular form of the Sawyer-Bushby model used for this experiment was the one which took 600 mb. as the mean level of the layer, included the effect of sea surface heating and used the actual changes that occurred on the boundary as boundary conditions. The results have been compared with time integrations not using the stream function but otherwise using the same version of the two parameter model.

4. The results of the time integration

(a) 1500 GMT 27 January, 1952.

The computation for this situation without use of the stream function has been discussed by Bushby and Hinds (3). Figs. 1a - 1d show the actual charts at the beginning and end of the period. The computed charts not using and using the stream function are also shown in Figs. 1e - 1h.

The introduction of the stream function has made little difference to the forecast charts. At the 500 mb. level a closed circulation has been introduced over Scandinavia, but the position and central values are not very accurate. Over most of the area the introduction of the stream function has led to a reduction in the height of the 500 mb. level by something of the order of 100 - 200 ft. This is not an improvement on the earlier computation and may have been brought about by a reduction in the total anticyclonic vorticity in the forecast area as a result of replacing a negative A by zero.

It is evident by comparing charts 1f and 1h that the use of the stream function has only had a slight effect on the thickness. Thus the difference between the two computed 1000 mb. charts is almost the same as the difference between the computed 500 mb. charts.

(b) 1500 GMT 30 January, 1952.

Although previous computations had been made for this situation they had been made with other variations of the Sawyer-Bushby model than that used here. (Bushby and Hinds (3) and (4)). Thus it is important to note that when this variation is used (without stream function) there are certain differences from the previous numerical forecasts. The trough from south of Iceland to the Faroes now turns down over the eastern North Sea (Fig. 2e) rather than continuing eastwards over Norway and Sweden and there is now no cut-off 500 mb. depression in the vicinity of the Faroes. The axis of the jet is now west-east over the British Isles. The thickness and 1000 mb. patterns (Fig. 2f) are also slightly different from those produced in previous numerical forecasts.

The results of the calculations using the stream function technique are given in Figs. 2g and 2h. The 500 mb. trough is now forecast to be over the western North Sea which is better than the forecast without the stream function. Also, the axis of the jet stream is further south although still not far enough and is orientated west north west - east south east. Fig. 2e shows pronounced ridging over the southwestern seaboard of Europe whereas this is minimised to a large extent in Fig. 2g.

Again there is only very little difference between the computed thickness charts shown in Figs. 2f and 2h, and the improvement in the 1000 mb. pattern in Fig. 2h compared with the 1000 mb. chart shown in Fig. 2f is similar to that already described relative to the 500 mb. pattern.

(c) 1500 GMT 30 January, 1953.

The synoptic situation in the vicinity of the British Isles at this time (Figs. 3a and 3b) is of particular interest because within 24 hours large areas of east and southeast England and the Low Countries were being affected by a severe gale and coastal flooding was the worst for many years.

Numerical integrations previously performed on this data (Bushby and Hinds (3, 4)) had used 500 mb. as the level representing the mean tropospheric flow and had used no change on the boundary as the boundary condition. In these earlier computations the main features producing the gale had been indicated quite well, but an anticyclone west of Ireland had been grossly exaggerated, leading to too strong wind gradients over the British Isles.

Figs. 3e and 3f show the result of a time integration which used the 600 mb. level to represent the mean flow and which used the actual changes round the boundary as the boundary condition. These charts show a marked improvement west of Ireland where the intensity of the surface anticyclone is much more realistic and almost correct, but an upper closed anticyclonic circulation is still wrongly forecast (although it is much weaker than in the previous computations) southwest of Ireland. The trough over the North Sea is still broadly correct at 500 mb., although the main trough line is now too far west and in this respect the previous computations were better, both at the 500 mb. level and at the surface where the strong northerly winds are computed too far west over the British Isles. However, the position and intensity of the depression between Scotland and Norway (Fig. 3d) is almost exactly forecast.

The result of using the stream function technique in this particular situation is shown in Figs. 3g and 3f. The upper anticyclonic circulation has now almost completely disappeared, and the region west of Ireland is now correctly dealt with apart from the fact that the contour heights along the axis of the ridge are about 200 ft. too low. This again is probably due to the fact that a negative A is replaced by zero, thus giving less anticyclonic geostrophic vorticity in the forecast area than there should be. The fact that this is not replaced at the end of the computation when the h_m field is computed from the ϕ_m field does imply that the mean value of h_m inside the forecast area is less than it should be. This again probably accounts for the depression east of Scotland being a little too deep in Fig. 3h.

In this particular situation a somewhat better answer (apart from the position of the 500 mb. trough line near the British Isles) has been obtained by using 600 mb. rather than 500 mb. as the operative level and by using the actual changes along the boundary rather than assuming no change along the boundary. The introduction of the stream function technique has made a further slight improvement in the forecast in the anticyclonic region west of Ireland.

5. Conclusions

This experiment has shown that it is quite practicable to carry out the solution of the Monge-Ampère equation on an electronic computing machine by using the iterative procedure described in Section 2. The use of the stream function technique extends the length of the computation from about 3½ hours to 4 hours on the Manchester University electronic computer.

Apart from a systematic tendency to produce lower forecast values than actually occurred due to an initial reduction of the total anticyclonic geostrophic vorticity in the forecast area, there was no indication in any of the three situations examined that the use of the stream function made the computed forecast worse. In the first situation there was little difference in the forecasts with and without the stream function. On the other two occasions the computed forecasts using the stream function were better than the corresponding forecasts without the stream function.

It is impossible to decide on the basis of the three situations so far examined whether or not it would be desirable to extend the length of the computation by 10% in order to make use of the stream function in the two parameter model in the crude manner described in this paper. Nevertheless the authors believe that in cases of strong winds the technique described in this paper would often make a significant improvement in the forecast, whereas in other cases it would make little difference.

6. References

1. Sawyer, J.S. and Bushby, F.H. 1953 J. Met., 10, p. 54.

2. Charney, J. 1955 Tellus, 7, No. 1.

3. Bushby, F.H. and Hinds, M.K. 1955 Quart. J. R. Met. Soc., 81, No. 349.

4. Bushby, F.H. and Hinds, M.K. 1954 Meteorological Research Papers, Air Ministry, London, No. 863.

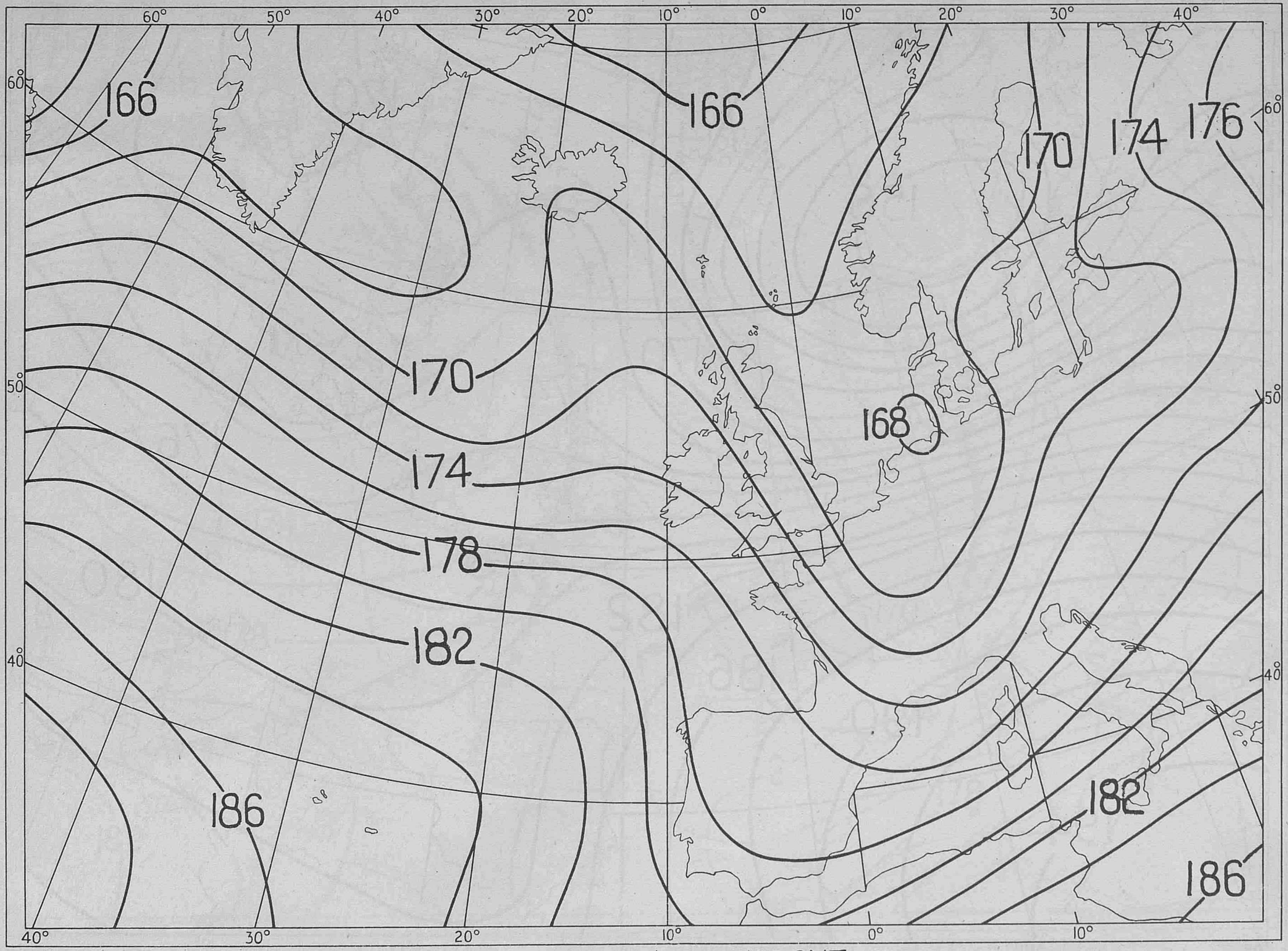
166
166
170
174
176
168
170
174
178
182
186
182
186
60°
50°
40°
30°
20°
10°
0°
10°
20°
30°
40°
60°
50°
40°
40°
30°
20°
10°
0°
10°
60°
50°
40°

Fig 1(a) Actual 500mb. contour chart for 1500 G.M.T. 27:1:52

M.R.P. 956

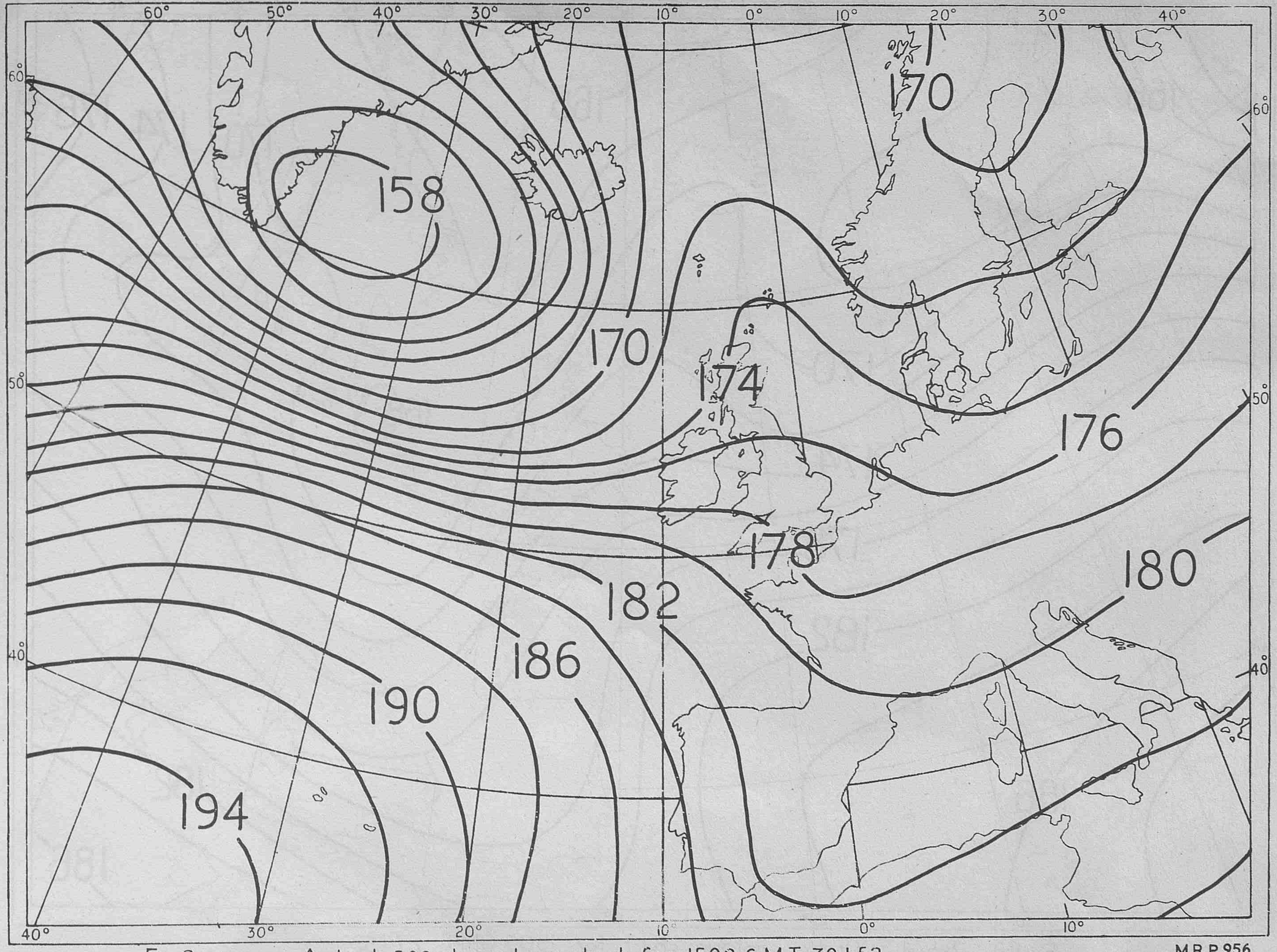
60°
50°
40°
30°
20°
10°
0°
10°
20°
30°
40°
60°
50°
40°
158
170
170
174
176
178
180
182
186
190
194
40°
30°
20°
10°
0°
10°

Fig.2(a) Actual 500mb. contour chart for 1500 G.M.T. 30.1.52

M.R.P. 956

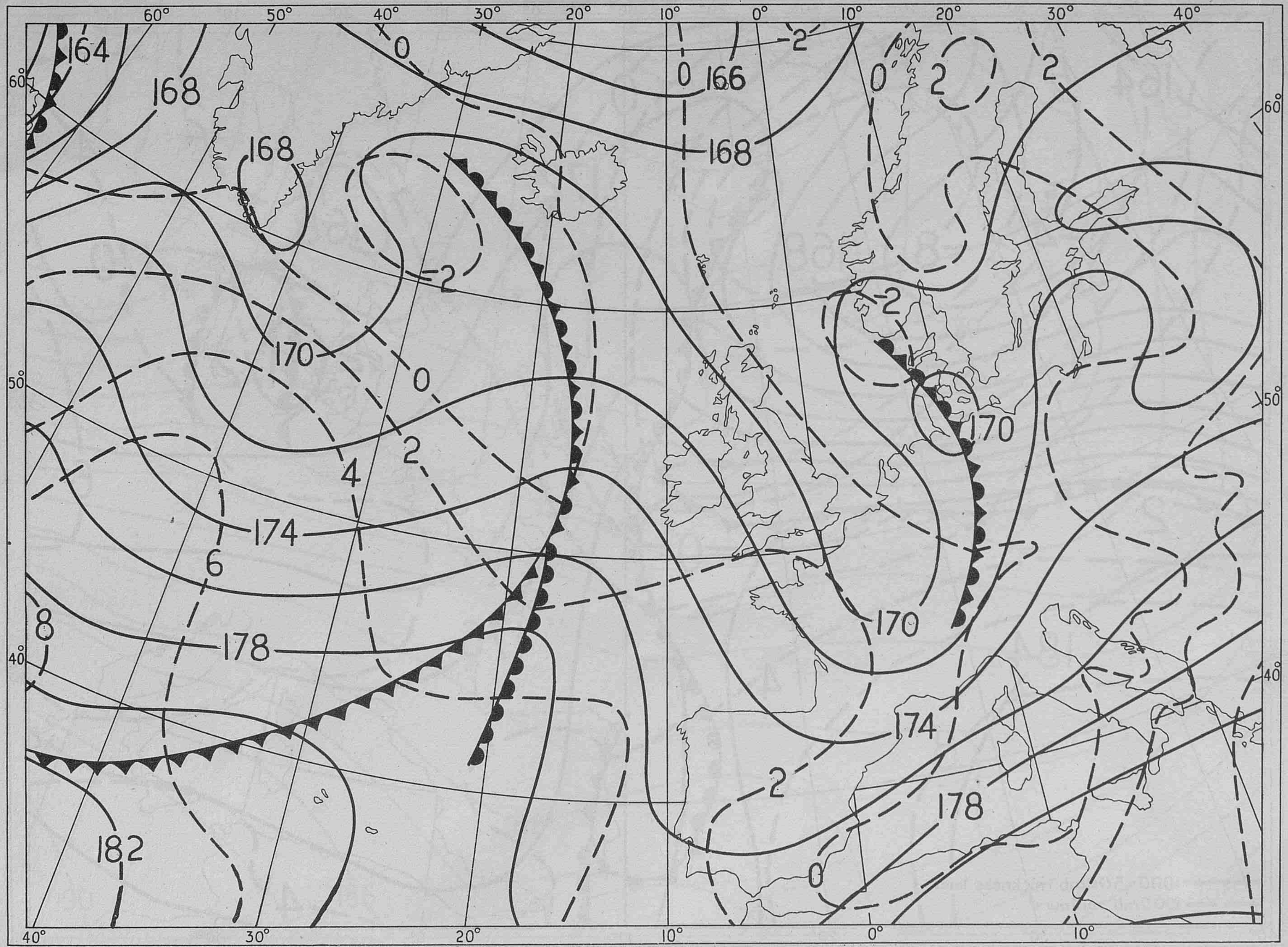
164
168
168
170
174
178
182
166
168
170
170
174
178
0
2
4
6
8
60°
50°
40°
30°
20°
10°
0°

Fig. 1(b) Actual 1000-500mb. thickness and 1000mb. contour charts for 1500 G.M.T. 27:1:52

M.R.P. 956

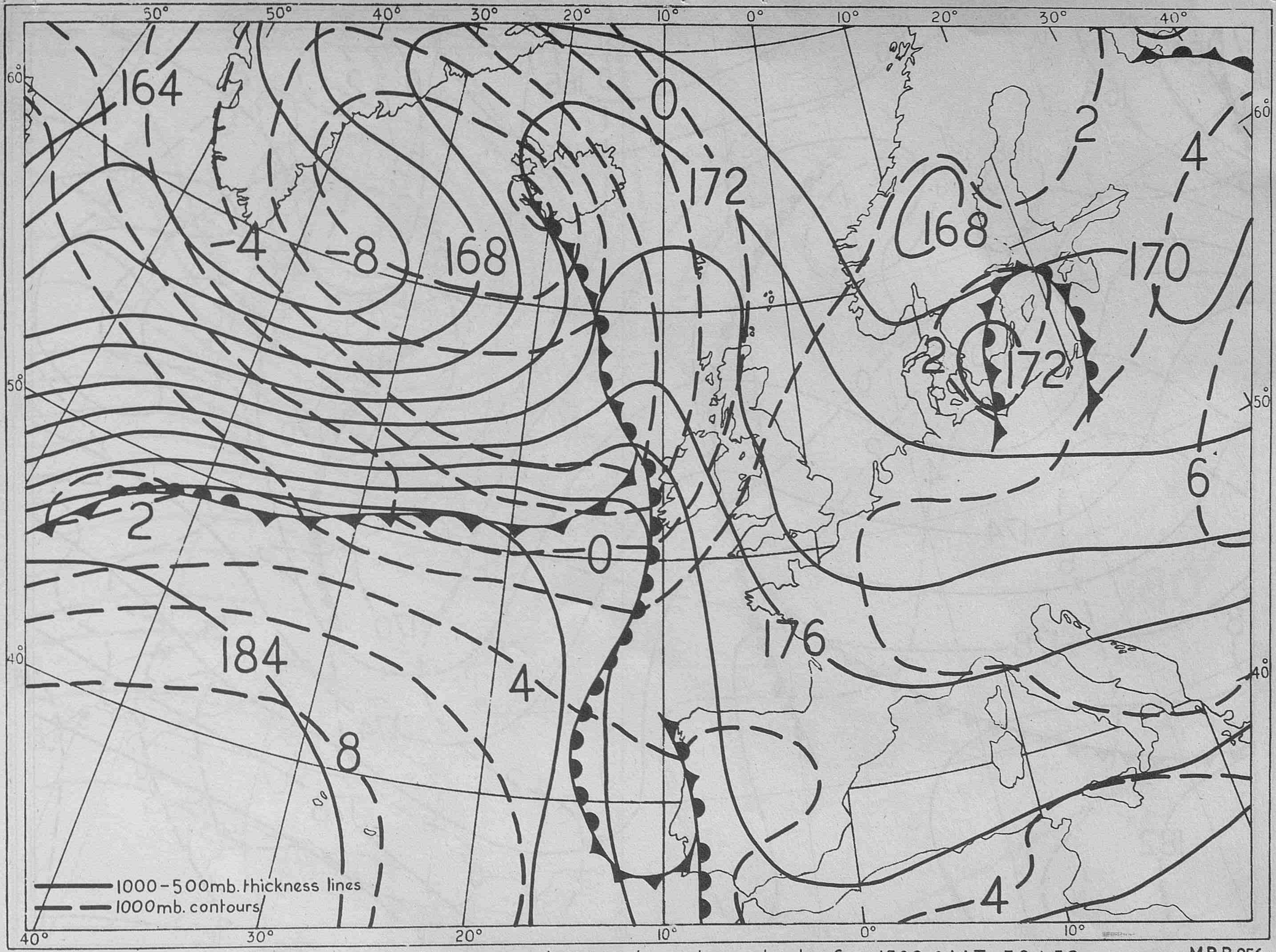
164
-4
-8
168
0
172
168
2
4
170
2
172
6
2
0
176
184
4
8
4
1000-500mb. thickness lines
1000mb. contours
60°
50°
40°
30°
20°
10°
0°

Fig.2(b) Actual 1000-500mb. thickness and 1000mb. contour charts for 1500 G.M.T. 30.1.52

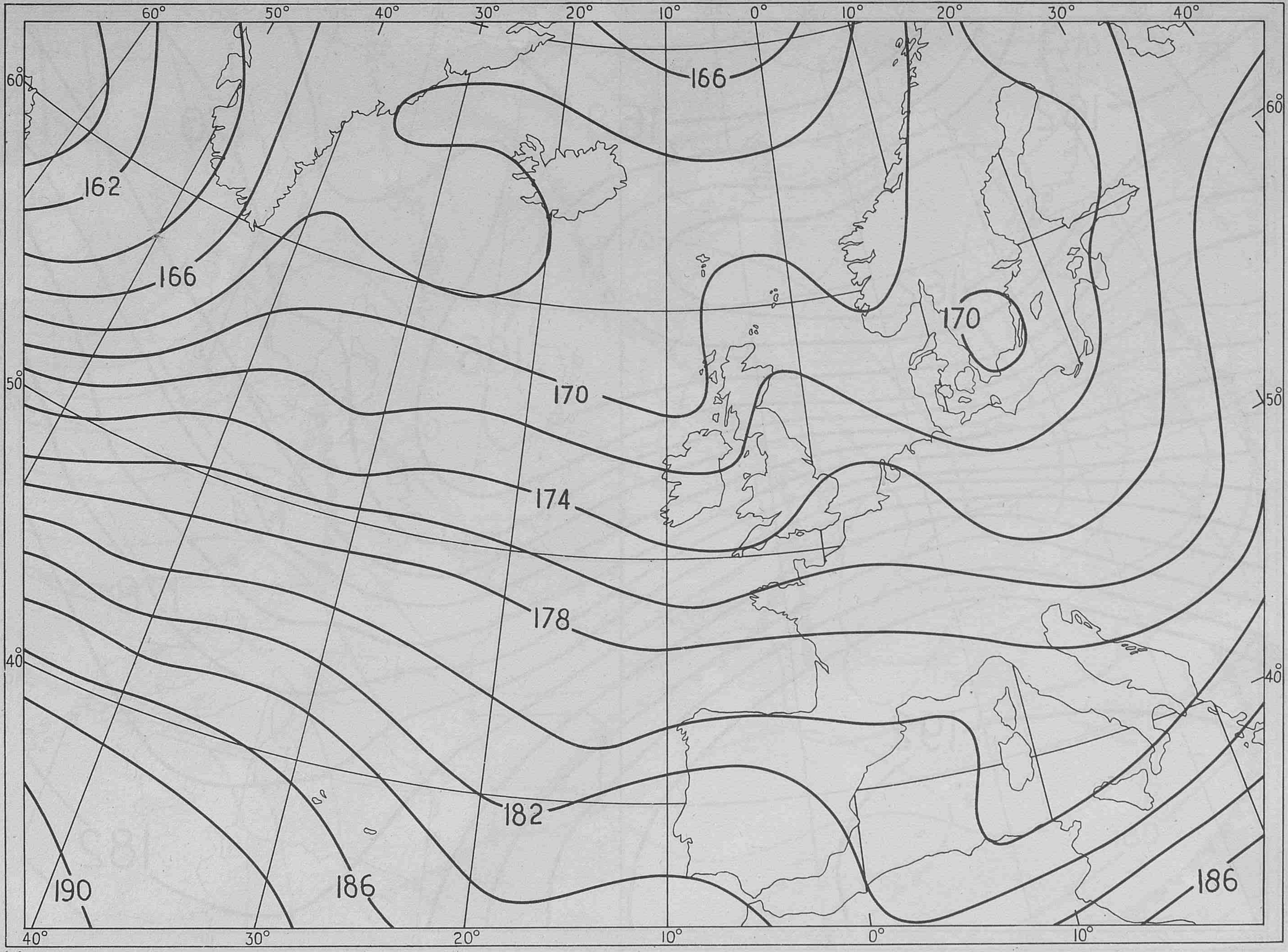
60°
50°
40°
30°
20°
10°
0°
10°
20°
30°
40°
60°
50°
40°
162
166
166
170
170
174
178
182
186
186
190
40°
30°
20°
10°
0°
10°

Fig 1(c) Actual 500 mb contour charts for 1500 G.M.T. 28:1:52

M.R.P. 956

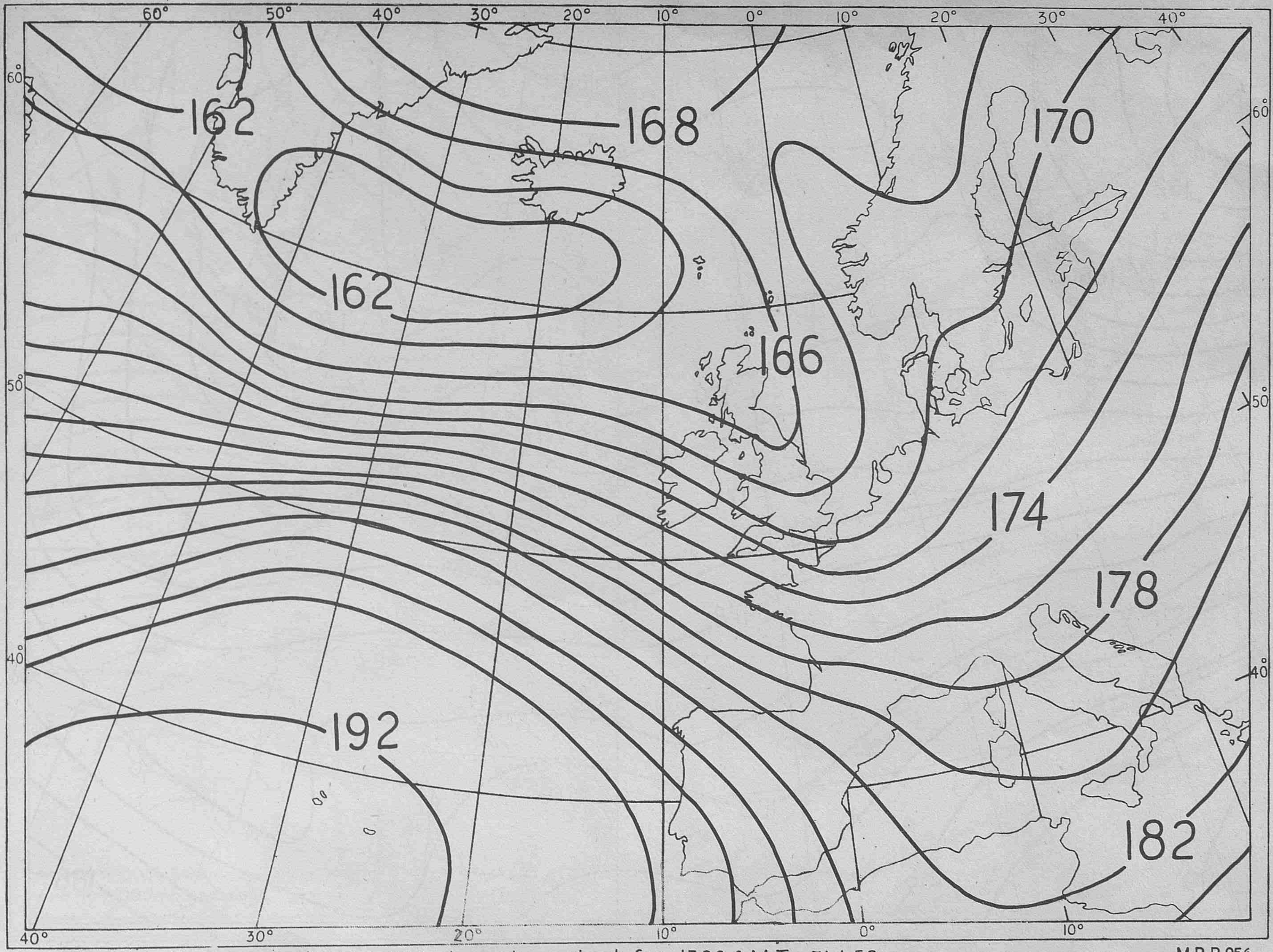
162
162
168
166
170
174
178
182
192
60°
50°
40°
30°
20°
10°
0°
10°
20°
30°
40°
60°
50°
40°
60°
50°
40°
40°
30°
20°
10°
0°
10°

Fig.2(c) Actual 500mb. contour chart for 1500 G.M.T. 31.1.52

M.R.P. 956

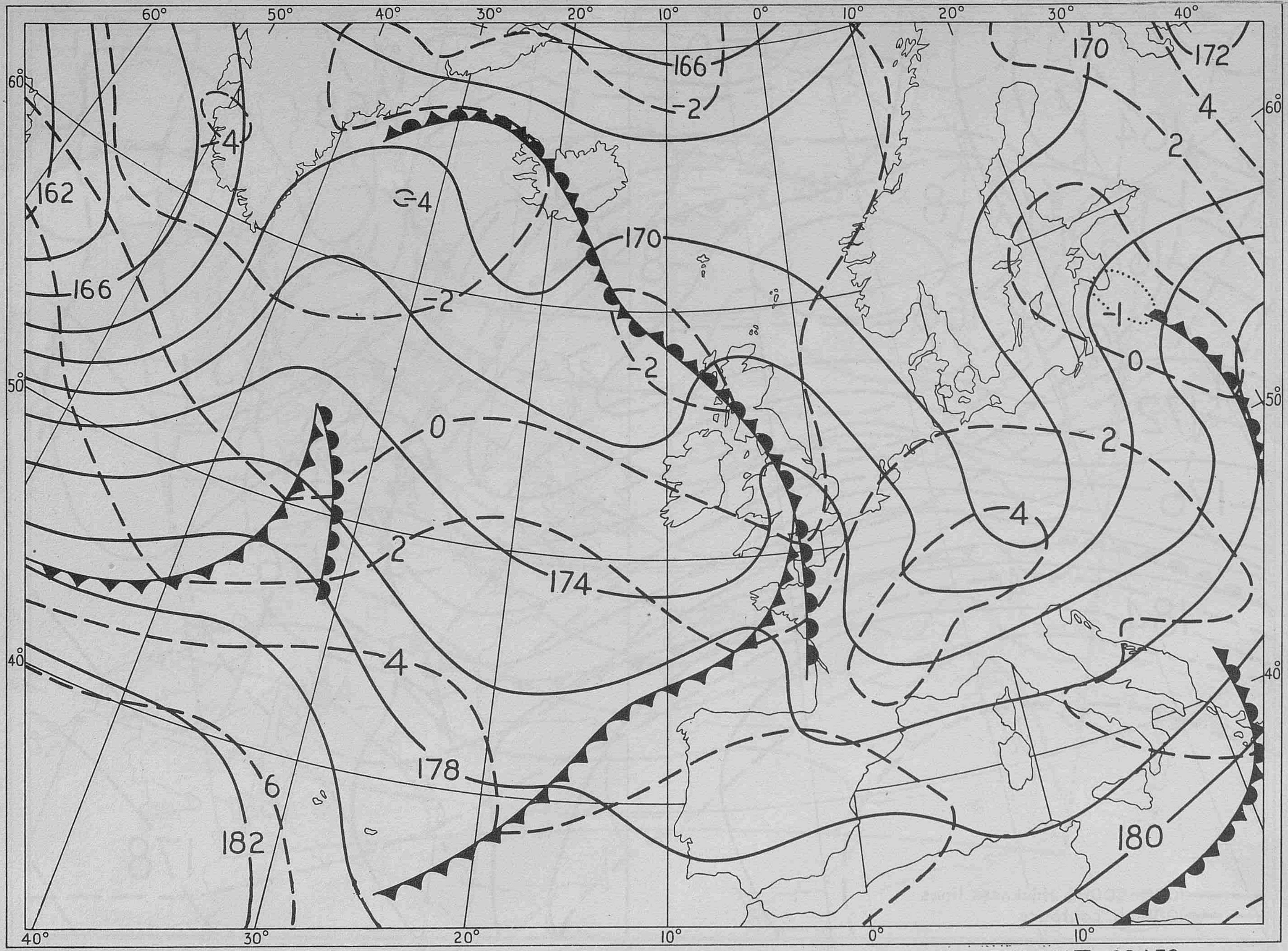
60°
50°
40°
30°
20°
10°
0°
10°
20°
30°
40°
60°
50°
40°
60°
50°
40°
40°
30°
20°
10°
0°
10°
162
166
-4
4
-2
170
166
-2
-2
0
2
174
-4
178
4
6
182
170
172
4
2
-1
0
2
-4
180

Fig 1 (d) Actual 1000-500 mb. thickness and 1000 mb. contour charts for 1500 G.M.T 28:1:52

M.R.P. 956

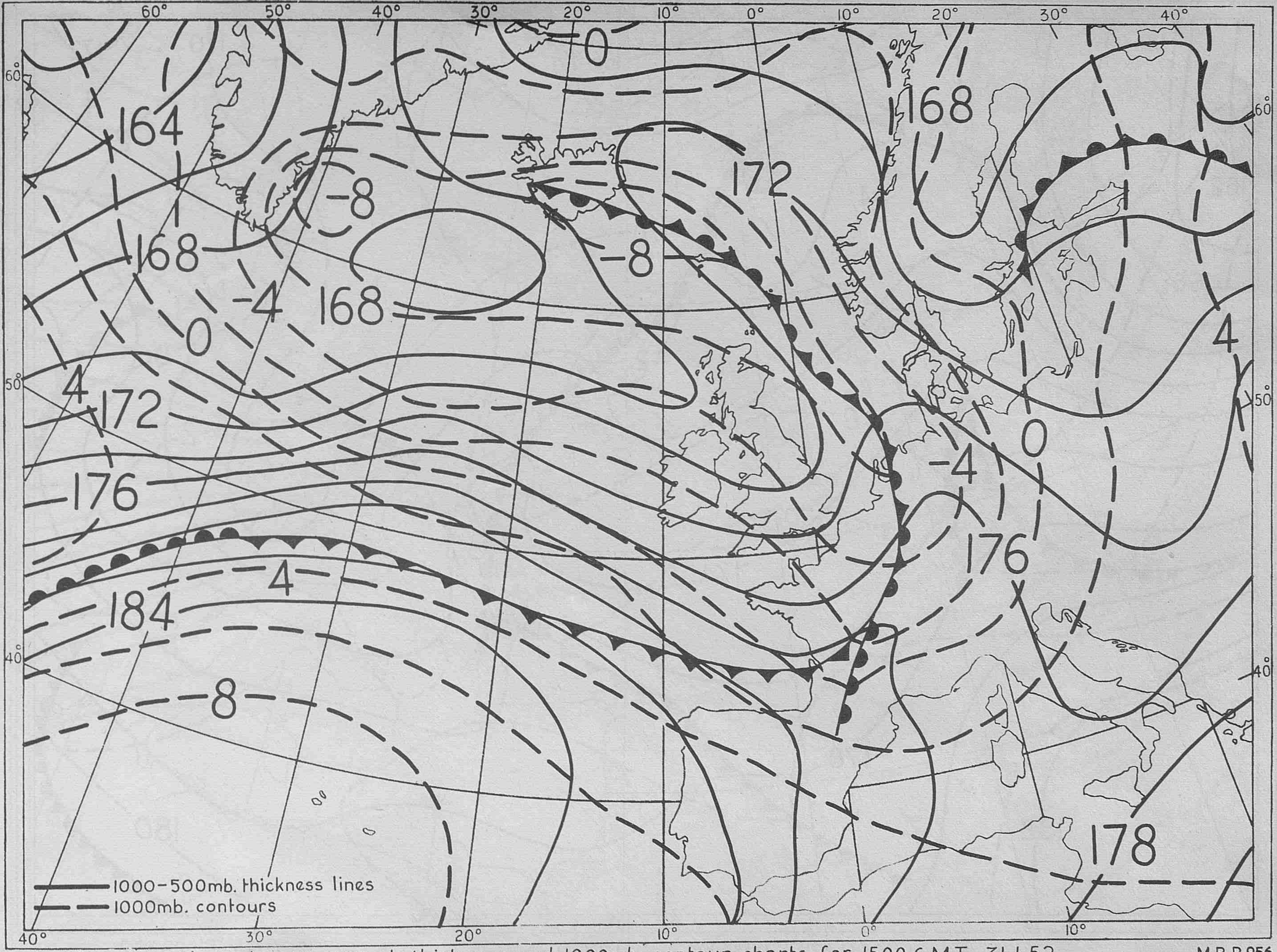
60°
50°
40°
30°
20°
10°
0°
10°
20°
30°
40°
164
168
168
172
172
176
176
184
178
-8
-8
-4
-4
0
0
4
4
4
8
1000-500mb. thickness lines
1000mb. contours

Fig. 2(d) Actual 1000-500mb. thickness and 1000mb. contour charts for 1500 G.M.T. 31.1.52

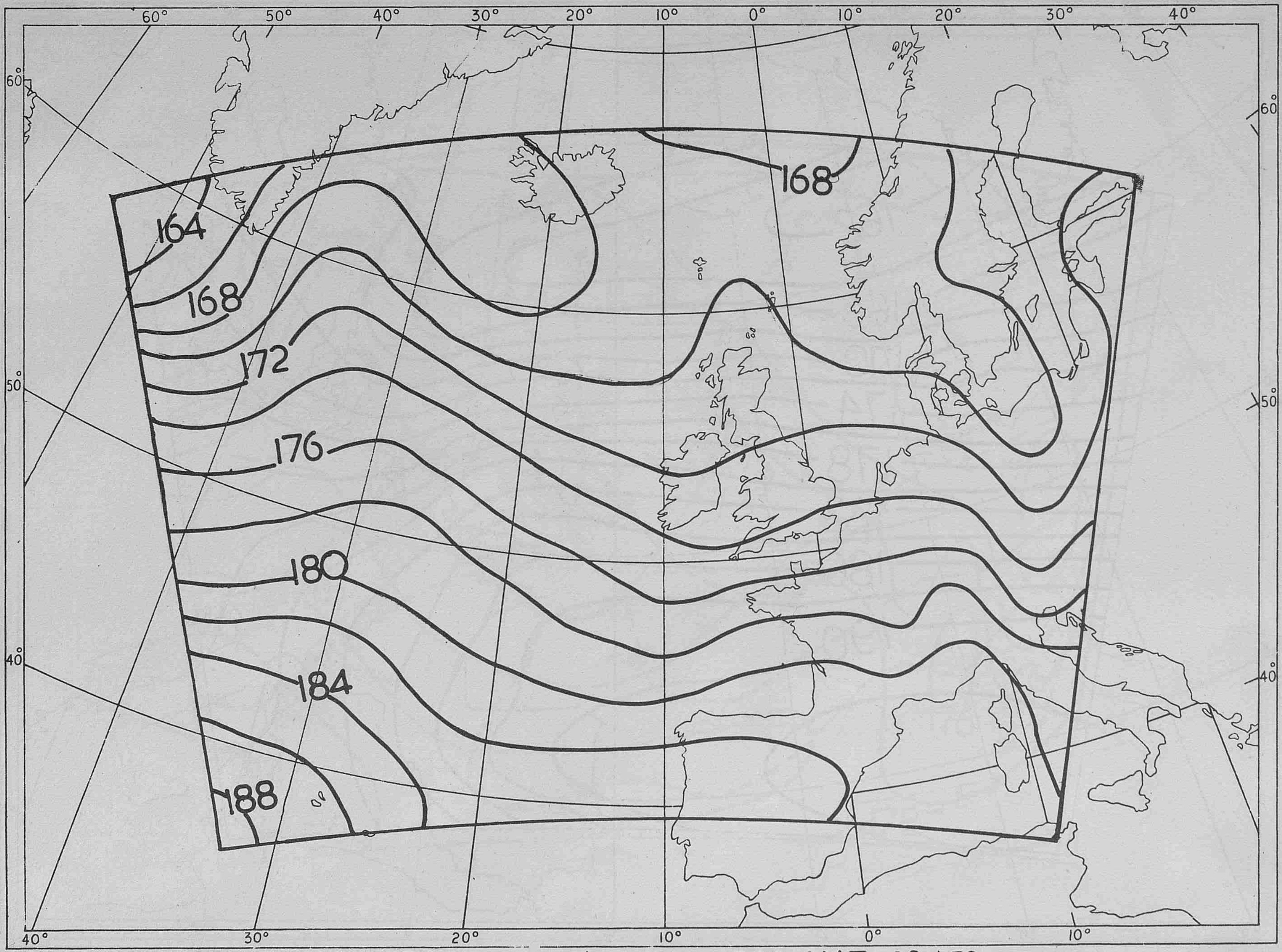
60°
50°
40°
30°
20°
10°
0°
10°
20°
30°
40°
60°
50°
40°
164
168
172
176
180
184
188
168
40°
30°
20°
10°
0°
10°

Fig. 1(e) Computed 500 mb. contour chart for 1500 G.M.T. 28:1:52

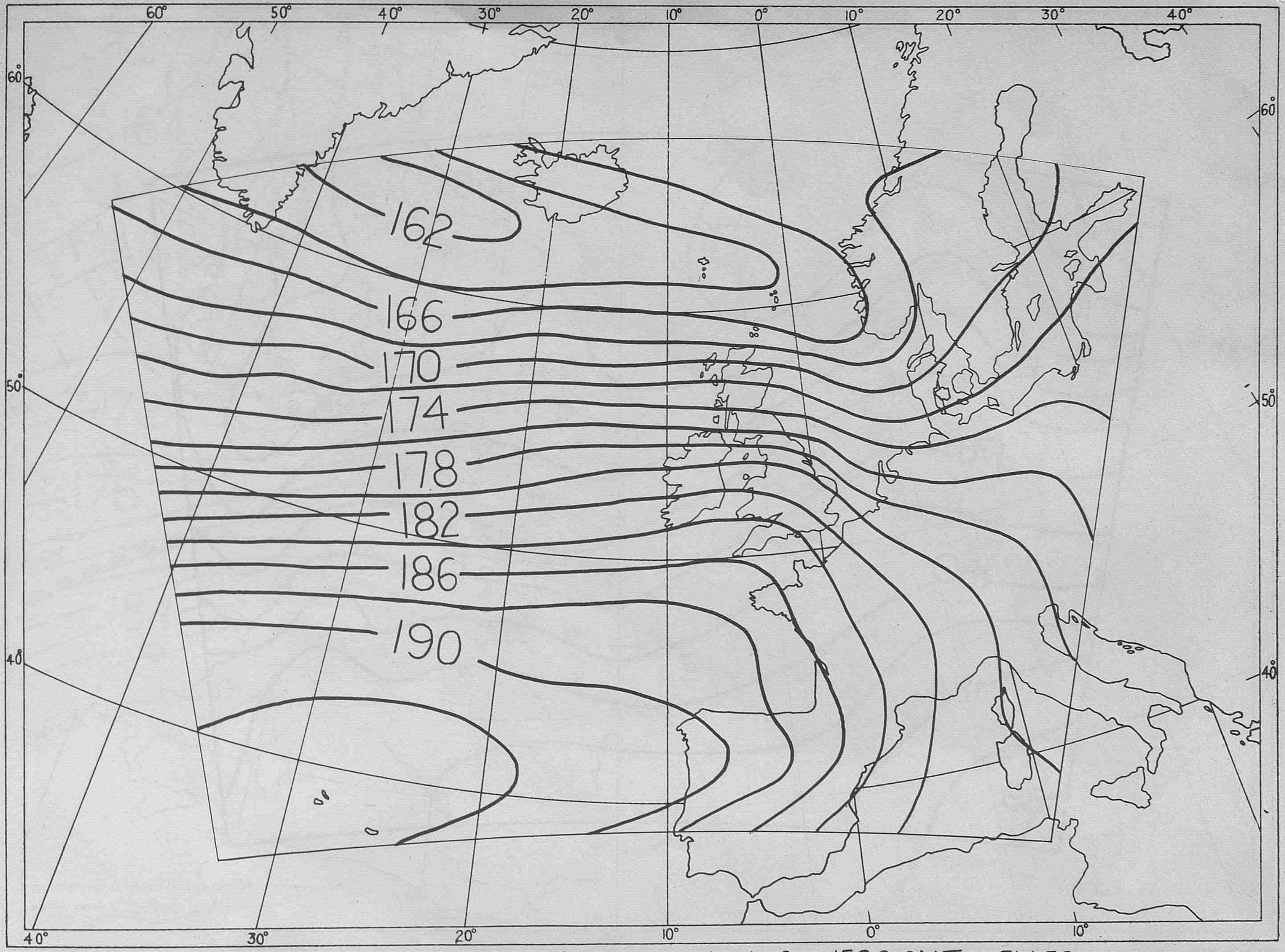
162
166
170
174
178
182
186
190
60°
50°
40°
30°
20°
10°
0°
10°
20°
30°
40°
60°
50°
40°
60°
50°
40°
40°
30°
20°
10°
0°
10°

Fig 2(e) Computed 500mb. contour chart for 1500 G.M.T. 31:1:52

M.R.P. 956

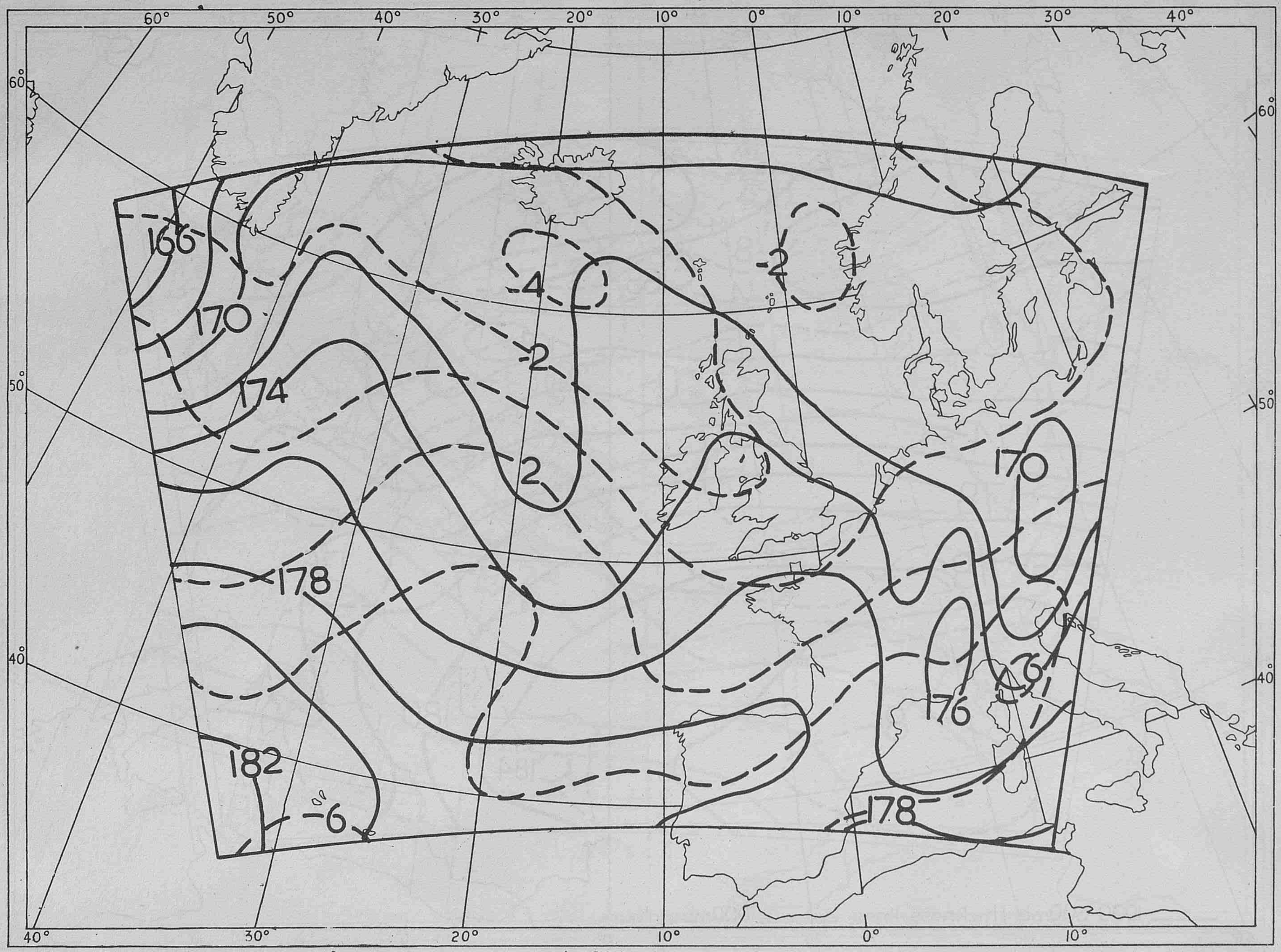
60°
50°
40°
30°
20°
10°
0°
10°
20°
30°
40°
60°
50°
40°
166
170
174
178
182
-6
-4
-2
-2
2
170
176
6
178
40°
30°
20°
10°
0°
10°

Fig.1(f) Computed 1000-500mb. thickness and 1000mb. contour charts for 1500 G.M.T. 28:1:52

M.R.P. 956

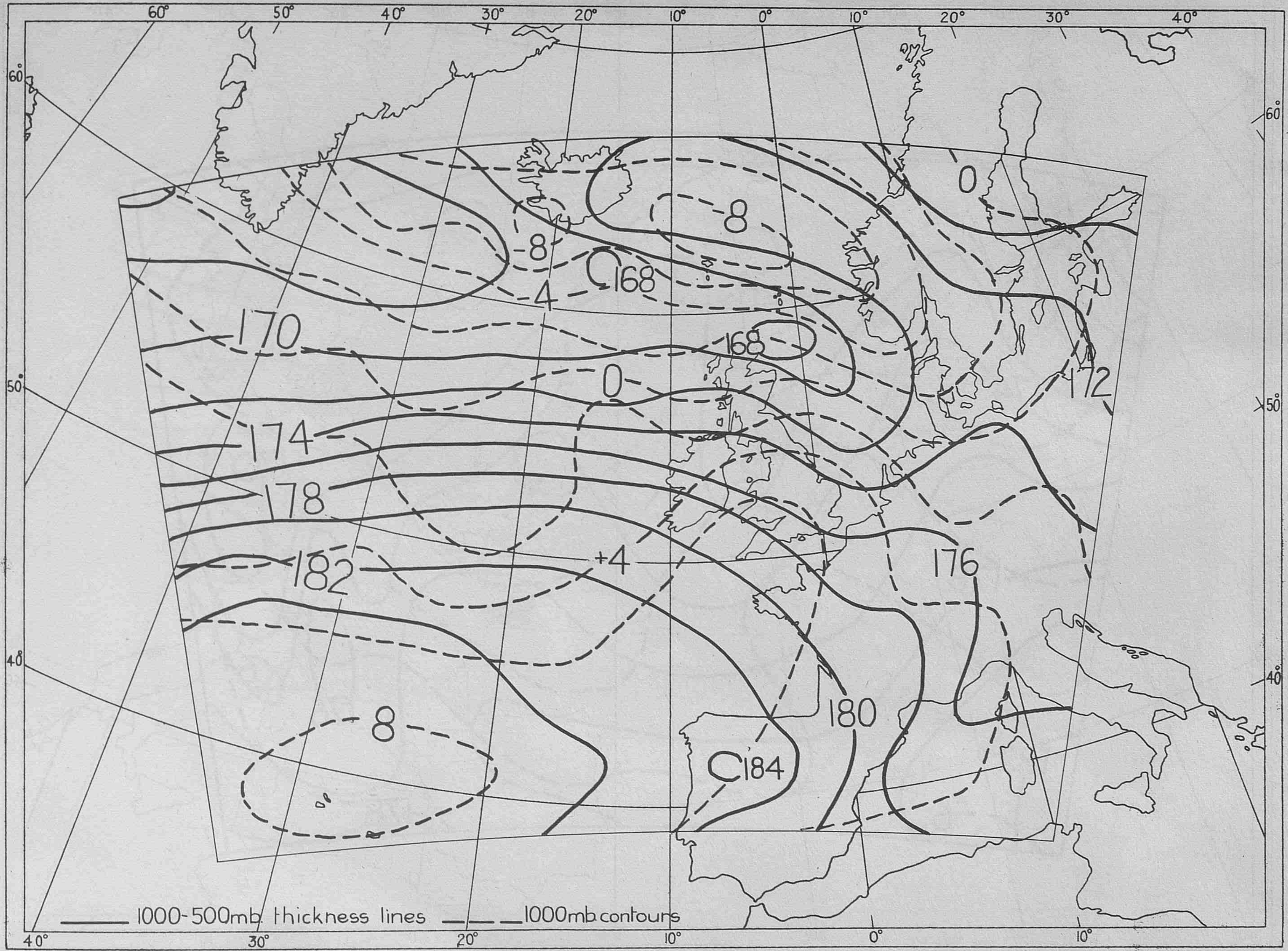

60°
50°
40°
30°
20°
10°
0°
10°
20°
30°
40°
-8
-8
C168
-4
0
170
168
174
178
182
+4
0
172
176
180
C184
8
1000-500mb thickness lines
1000mb contours

Fig 2(f) Computed 1000-500mb. thickness and 1000mb. contour charts for 1500 G.M.T. 31:1:52

M.R.P. 956

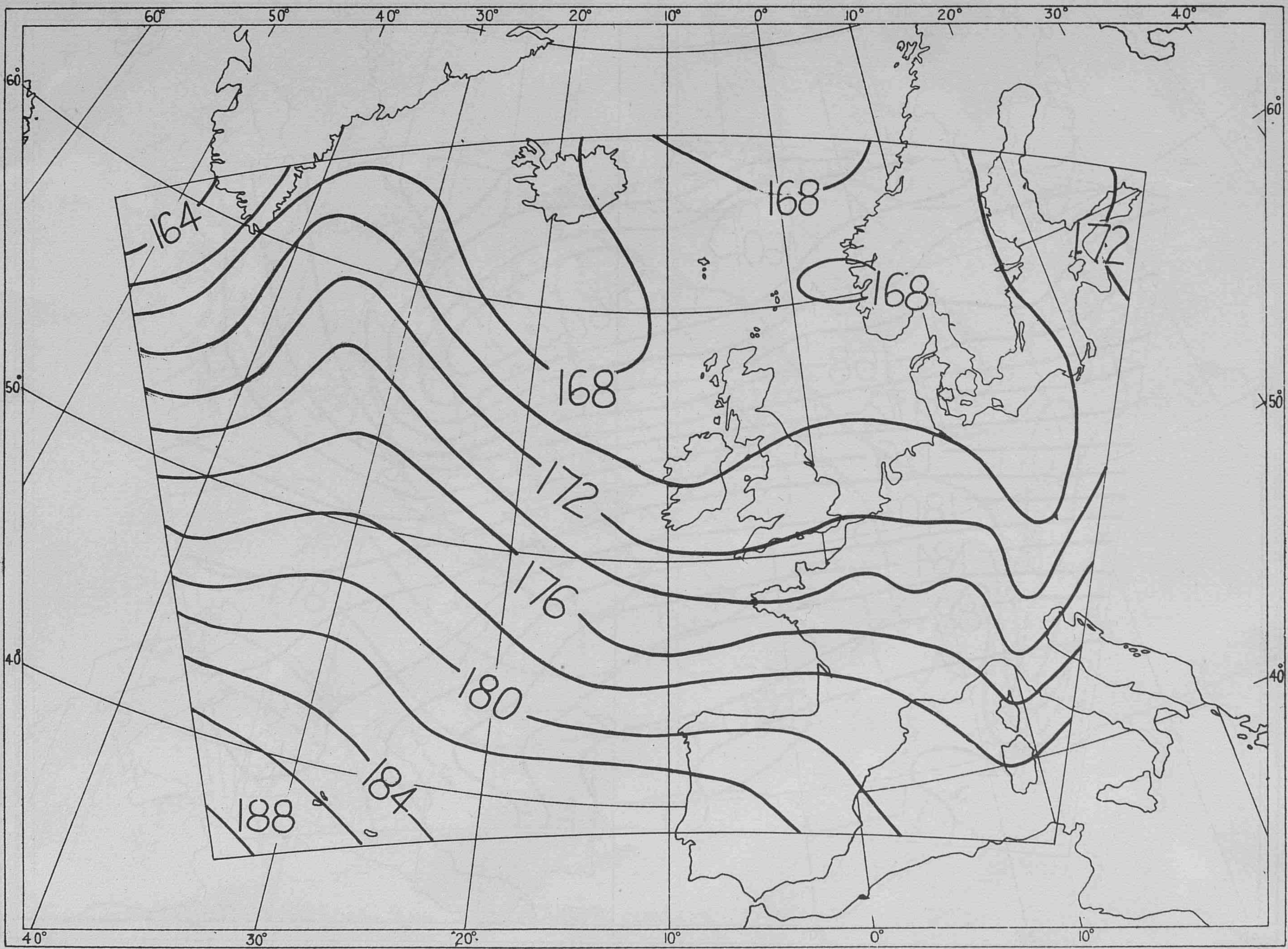
164
168
168
168
168
172
172
176
180
184
188
60°
50°
40°
30°
20°
10°
0°
10°
20°
30°
40°
60°
50°
40°
60°
50°
40°
40°
30°
20°
10°
0°
10°

Fig 1(g) Computed 500mb. contour chart (using stream function) for 1500 G.M.T. 28: 1: 52

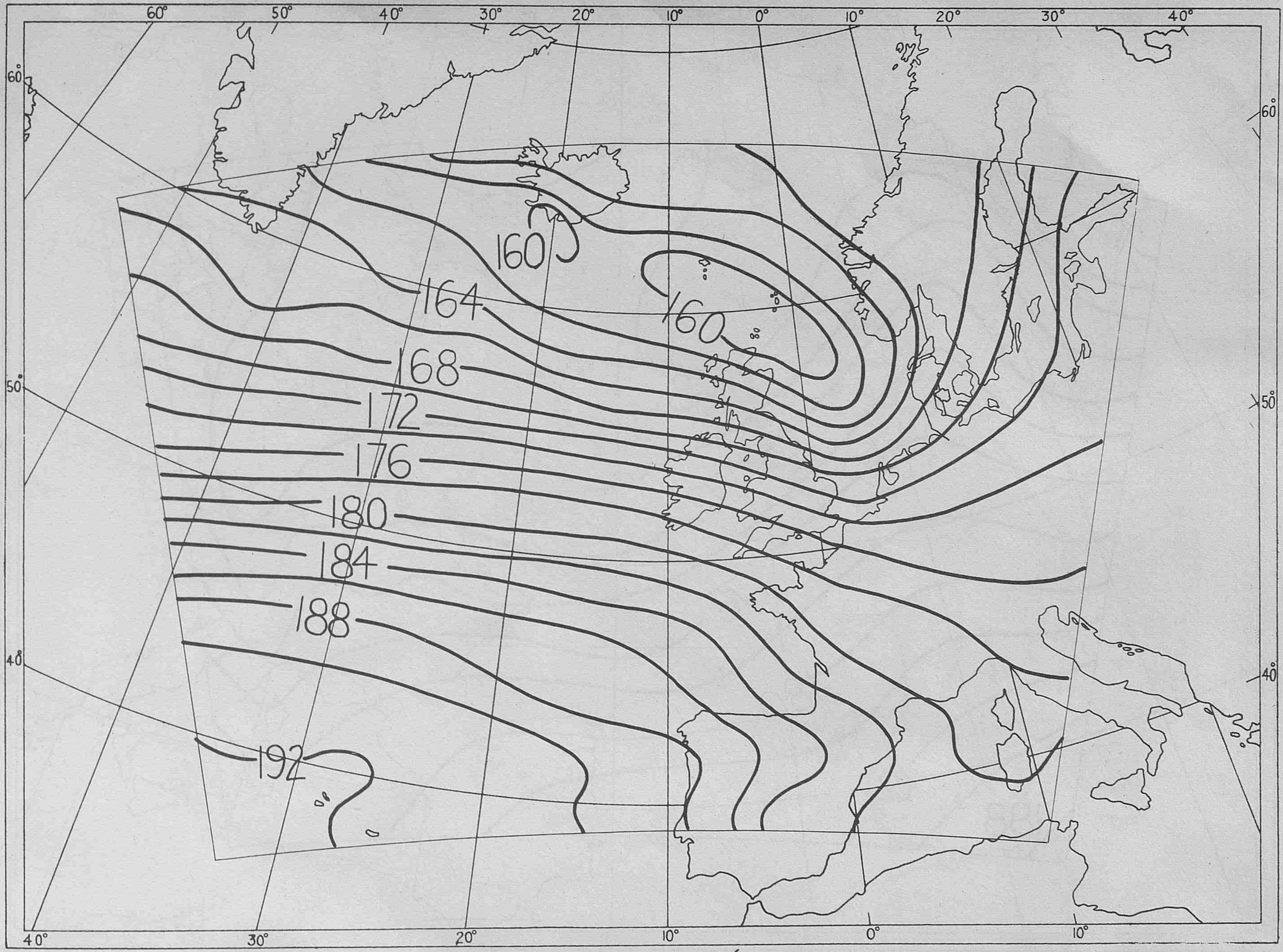
60°
50°
40°
30°
20°
10°
0°
10°
20°
30°
40°
160
160
164
168
172
176
180
184
188
192

Fig 2(g) Computed 500mb. contour chart (using stream function) for 1500GMT. 31:1:52

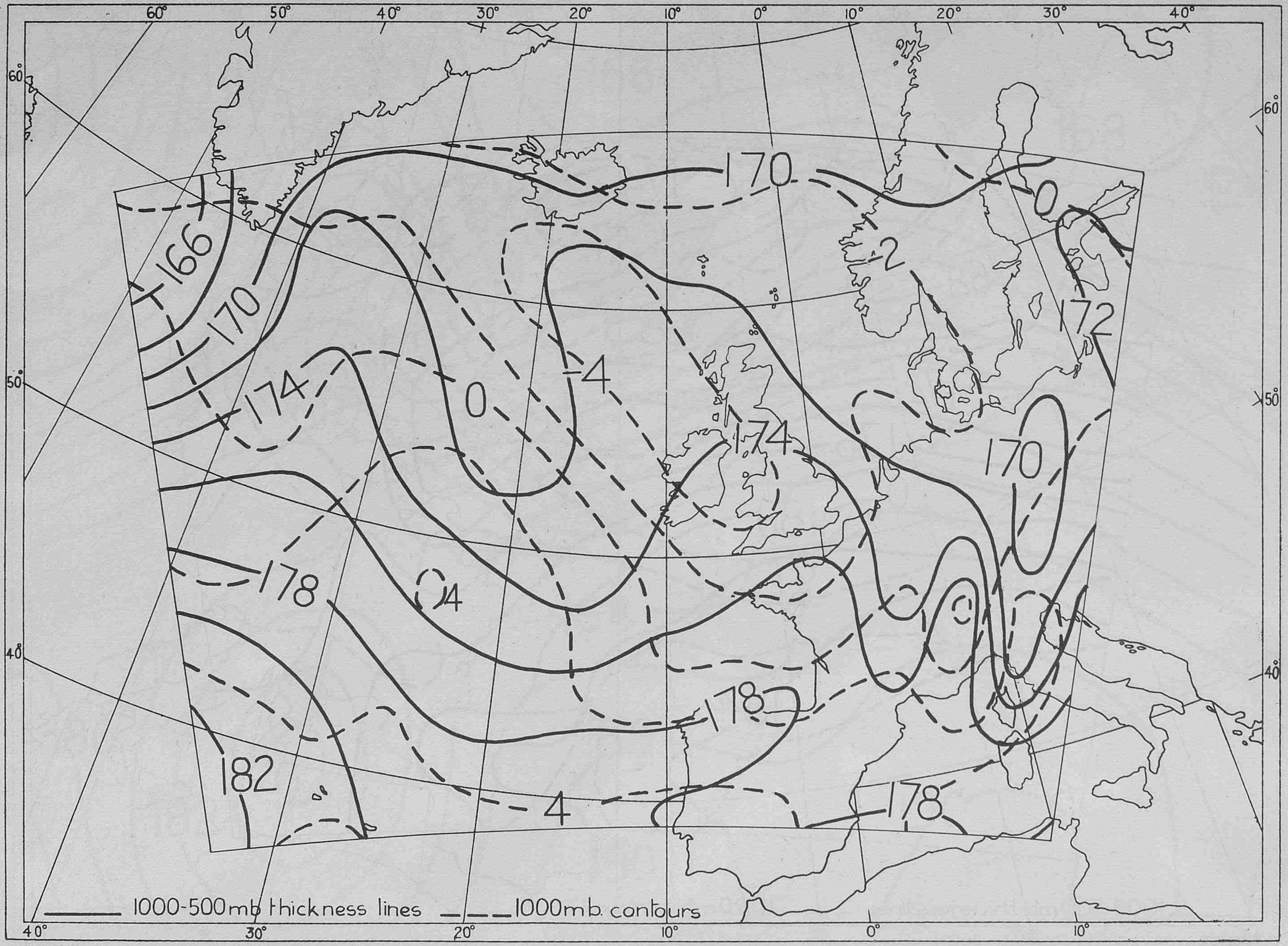
60°
50°
40°
30°
20°
10°
0°
10°
20°
30°
40°
60°
50°
40°
166
170
174
178
182
0
-4
4
2
0
172
170
174
178
178
4
1000-500mb thickness lines
1000mb. contours

Fig 1(h). Computed 1000-500mb. thickness and 1000mb contour charts (using stream function) for 1500 G.M.T. 28:1:52.

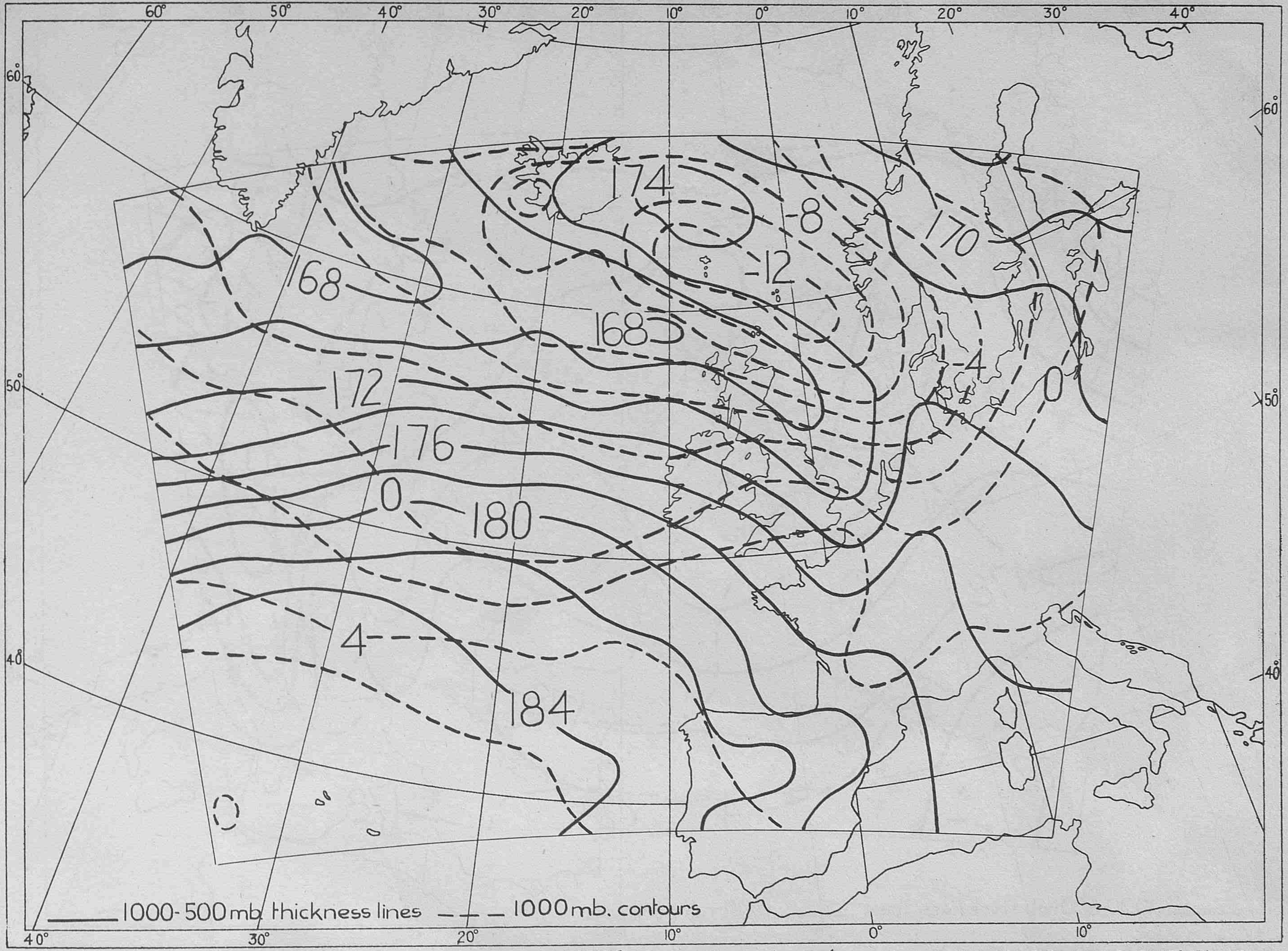
60°
50°
40°
30°
20°
10°
0°
10°
20°
30°
40°
168
174
-8
-12
170
168
172
176
0
180
4
184
-4
0
1000-500 mb thickness lines
1000 mb. contours

Fig 2(h) Computed 1000-500mb. thickness and 1000mb. contour charts (using stream function) for 1500 G.M.T. 31:1:52

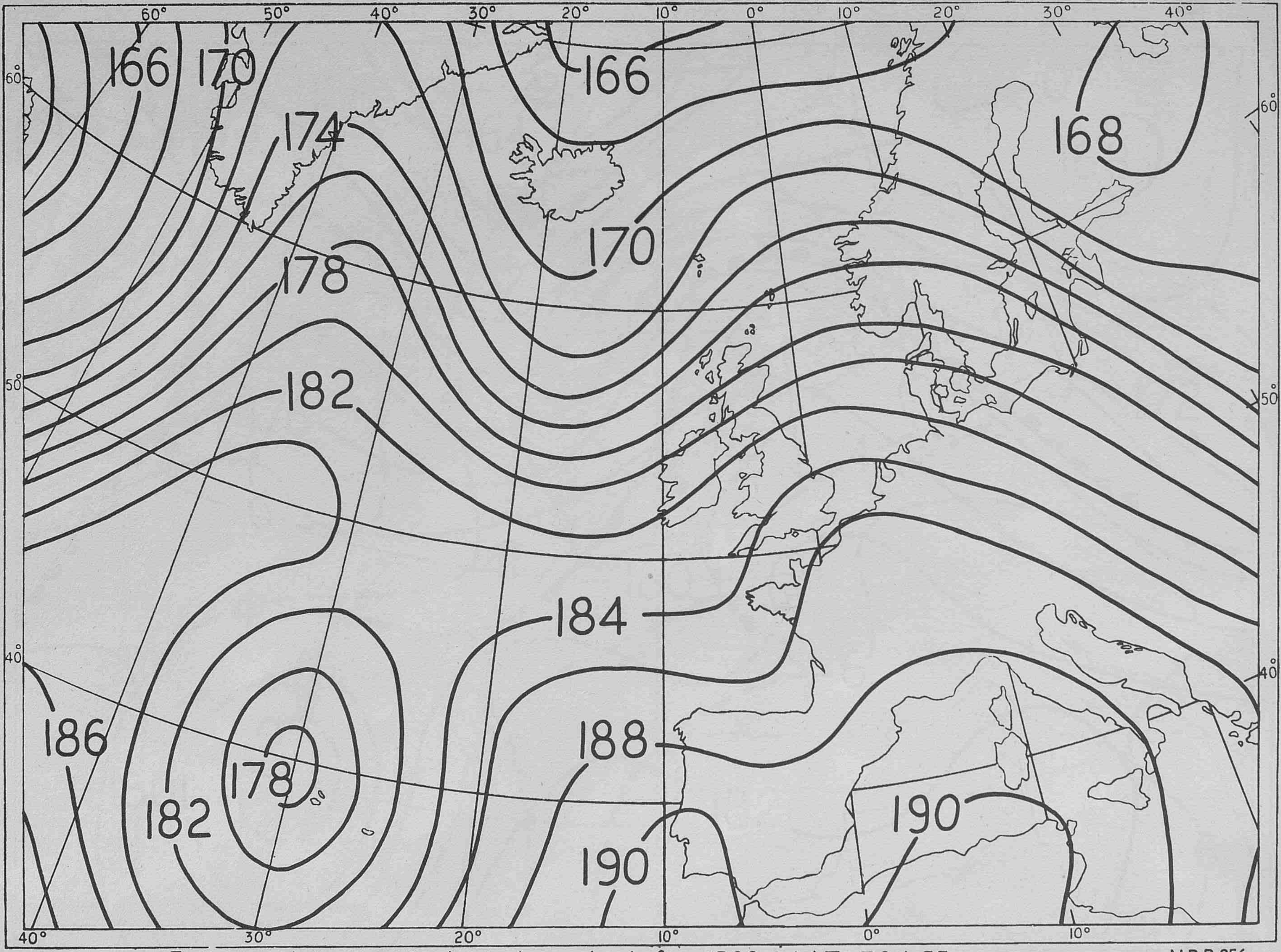
166
170
174
178
182
186
178
182
166
170
184
188
190
190
168
60°
50°
40°
30°
20°
10°
0°
10°
20°
30°
40°
60°
50°
40°
40°
30°
20°
10°
0°
10°

Fig.3(a) Actual 500mb. contour chart for 1500 G.M.T. 30.1.53

M.R.P. 956

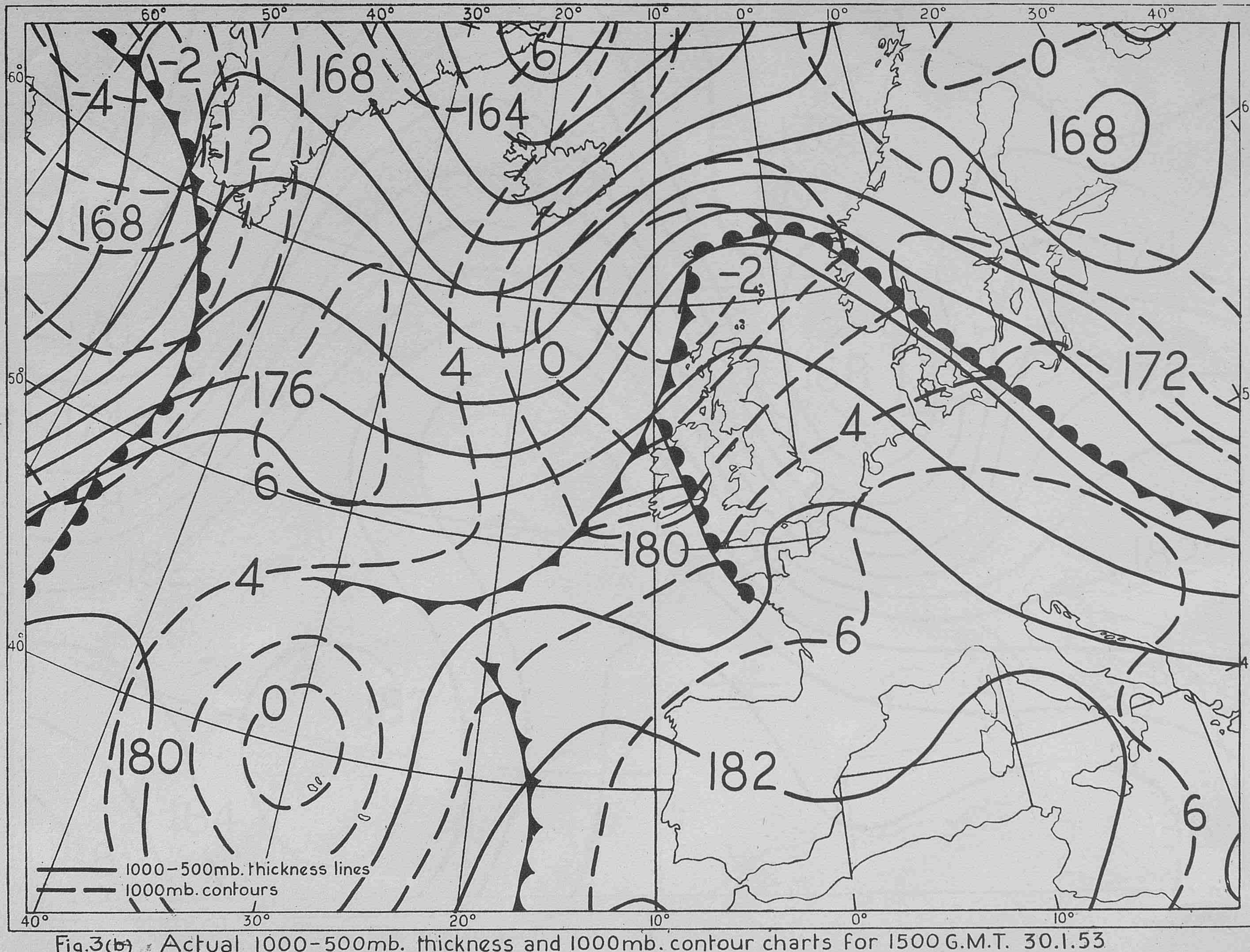
60°
50°
40°
30°
20°
10°
0°
10°
20°
30°
40°
60°
50°
40°
-2
-4
2
168
168
164
6
0
168
0
-2
172
176
4
0
4
6
180
4
6
0
1801
182
6
1000-500mb. thickness lines
1000mb. contours
40°
30°
20°
10°
0°
10°

Fig.3(b) Actual 1000-500mb. thickness and 1000mb. contour charts for 1500 G.M.T. 30.1.53

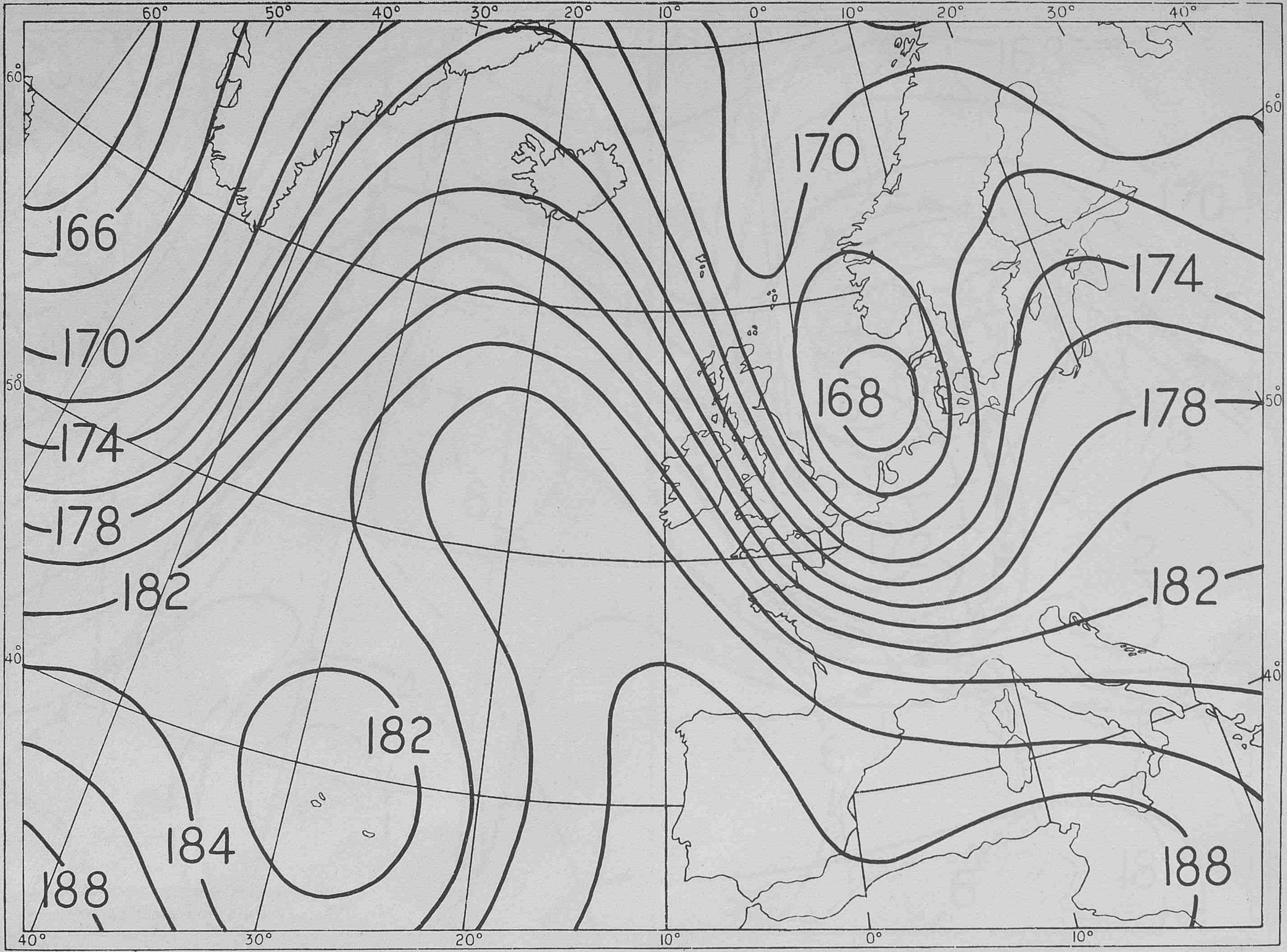
60°
50°
40°
30°
20°
10°
0°
10°
20°
30°
40°
60°
50°
40°
60°
50°
40°
166
170
174
178
182
170
168
174
178
182
182
184
188
188
40°
30°
20°
10°
0°
10°

Fig. 3(c) Actual 500mb. contour chart for 1500 G.M.T. 31.1.53

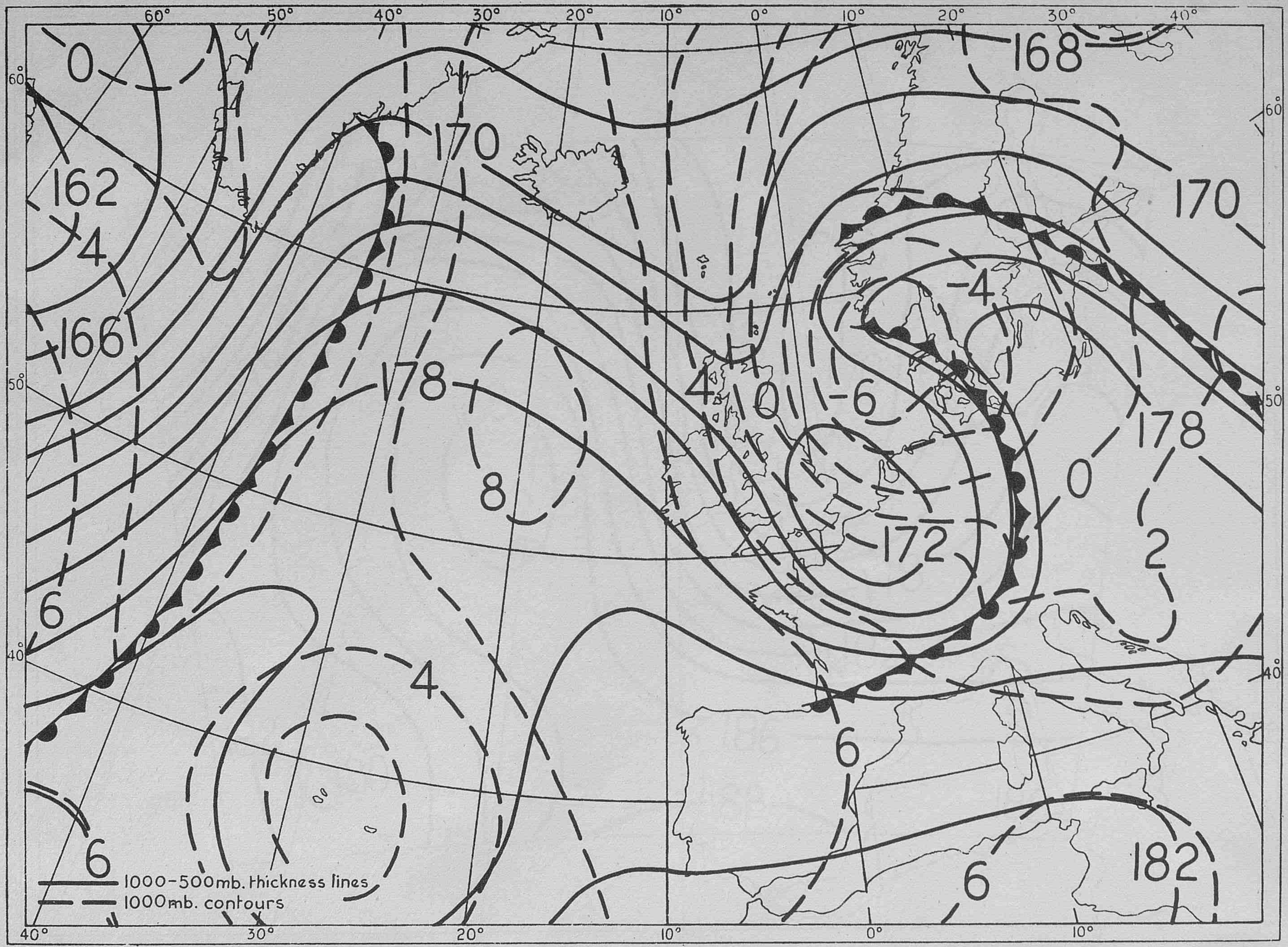
60°
50°
40°
30°
20°
10°
0°
10°
20°
30°
40°
60°
50°
40°
30°
20°
10°
0°
10°
0
162
4
166
6
6
170
178
8
4
4
0
-6
-4
-172
168
170
178
0
2
6
6
182
1000-500mb. thickness lines
1000mb. contours

Fig. 3(d) Actual 1000-500mb. thickness and 1000mb. contour charts for 1500 G.M.T. 31.1.53

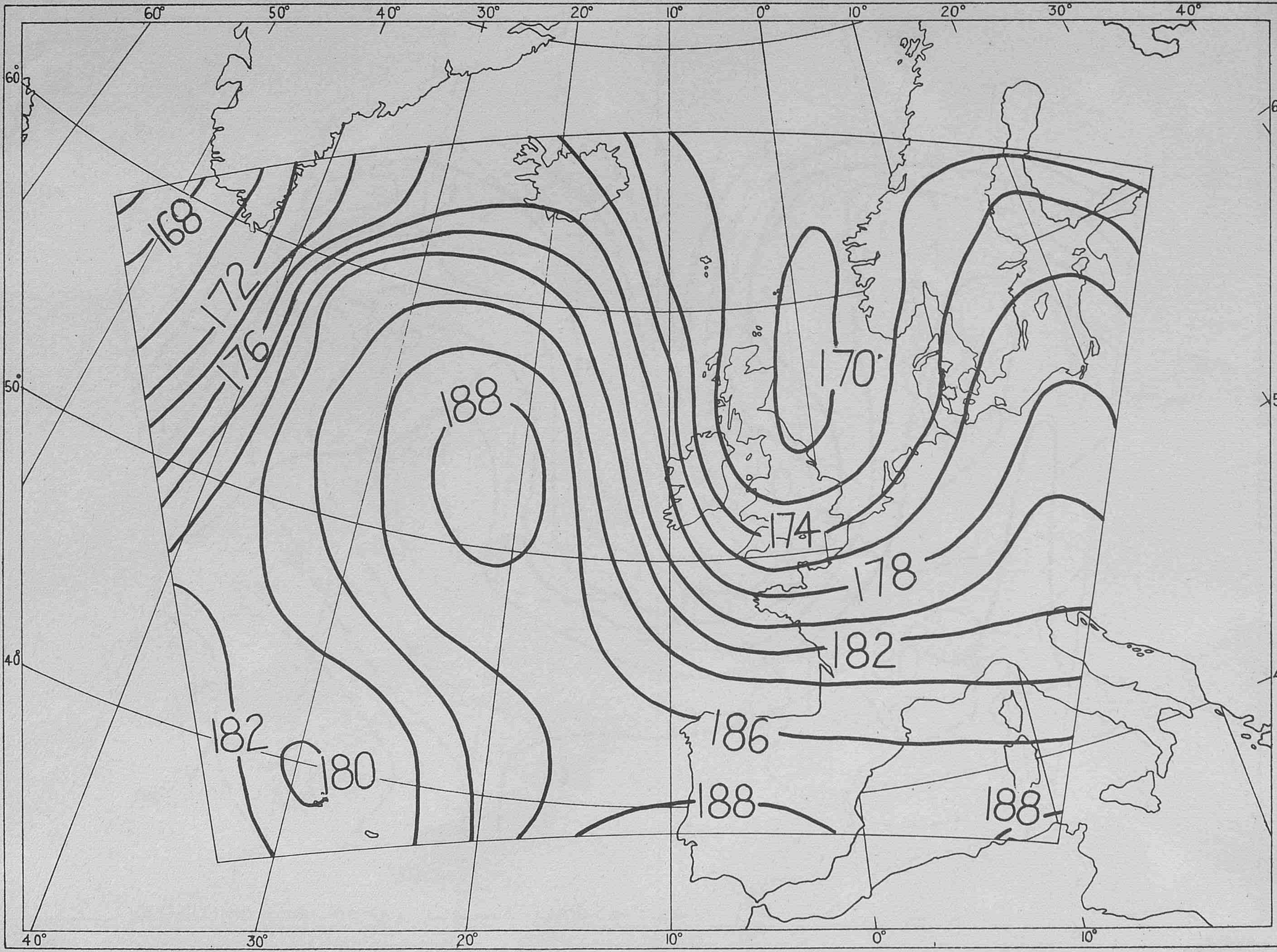
60°
50°
40°
30°
20°
10°
0°
10°
20°
30°
40°
60°
50°
40°
60°
50°
40°
40°
30°
20°
10°
0°
10°
168
172
176
188
170
174
178
182
186
188
182
180
188

Fig. 3(e) Computed 500mb. contour chart for 1500 G.M.T. 31:1:53

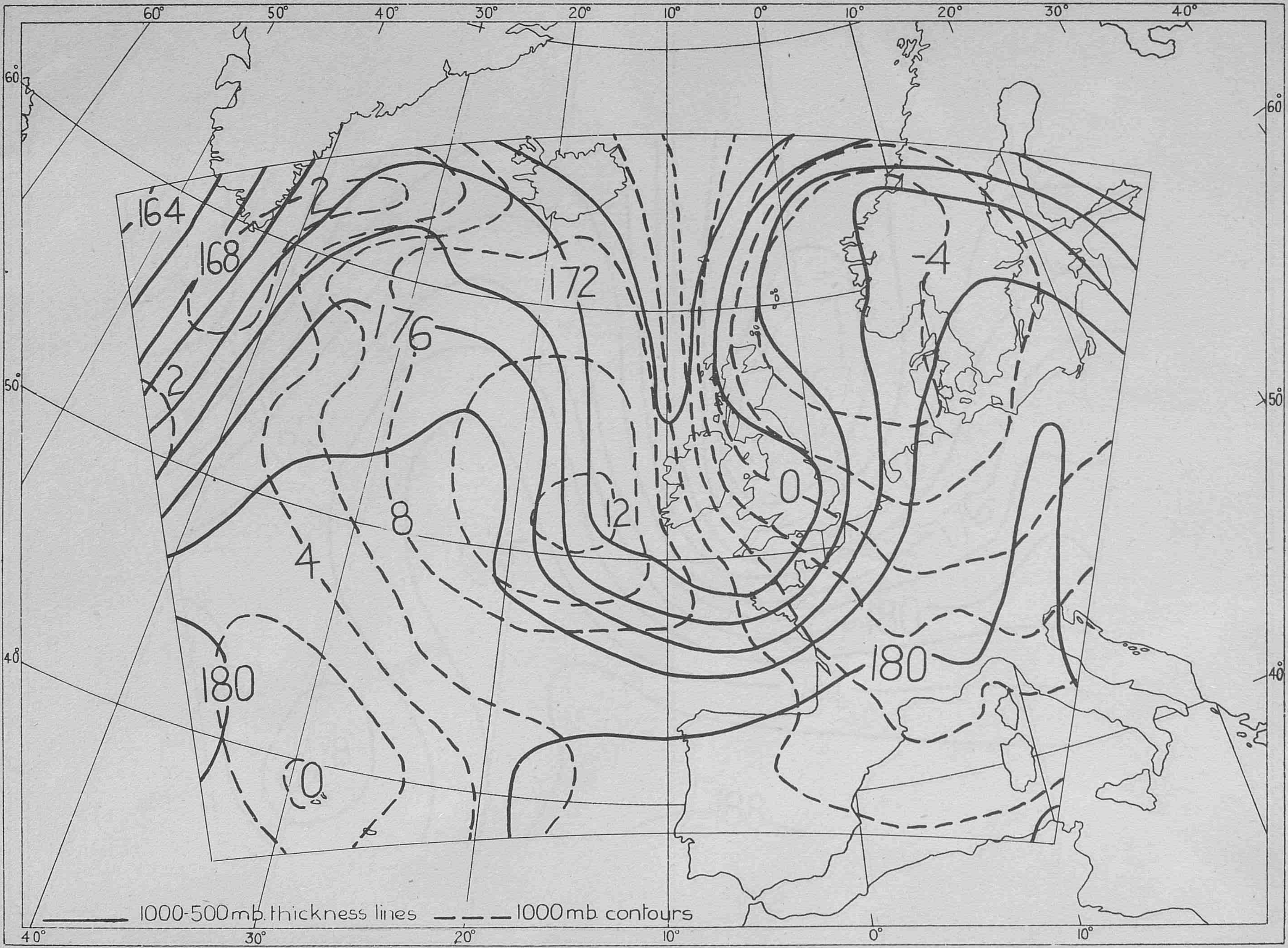
60°
50°
40°
30°
20°
10°
0°
10°
20°
30°
40°
60°
50°
40°
164
168
2
2
172
176
-4
0
8
12
4
180
180
0
40°
30°
20°
10°
0°
10°
1000-500 mb. thickness lines
1000 mb. contours

Fig. 3(f) Computed 1000-500 mb. thickness and 1000 mb. contour charts for 1500 G.M.T. 31:1:53

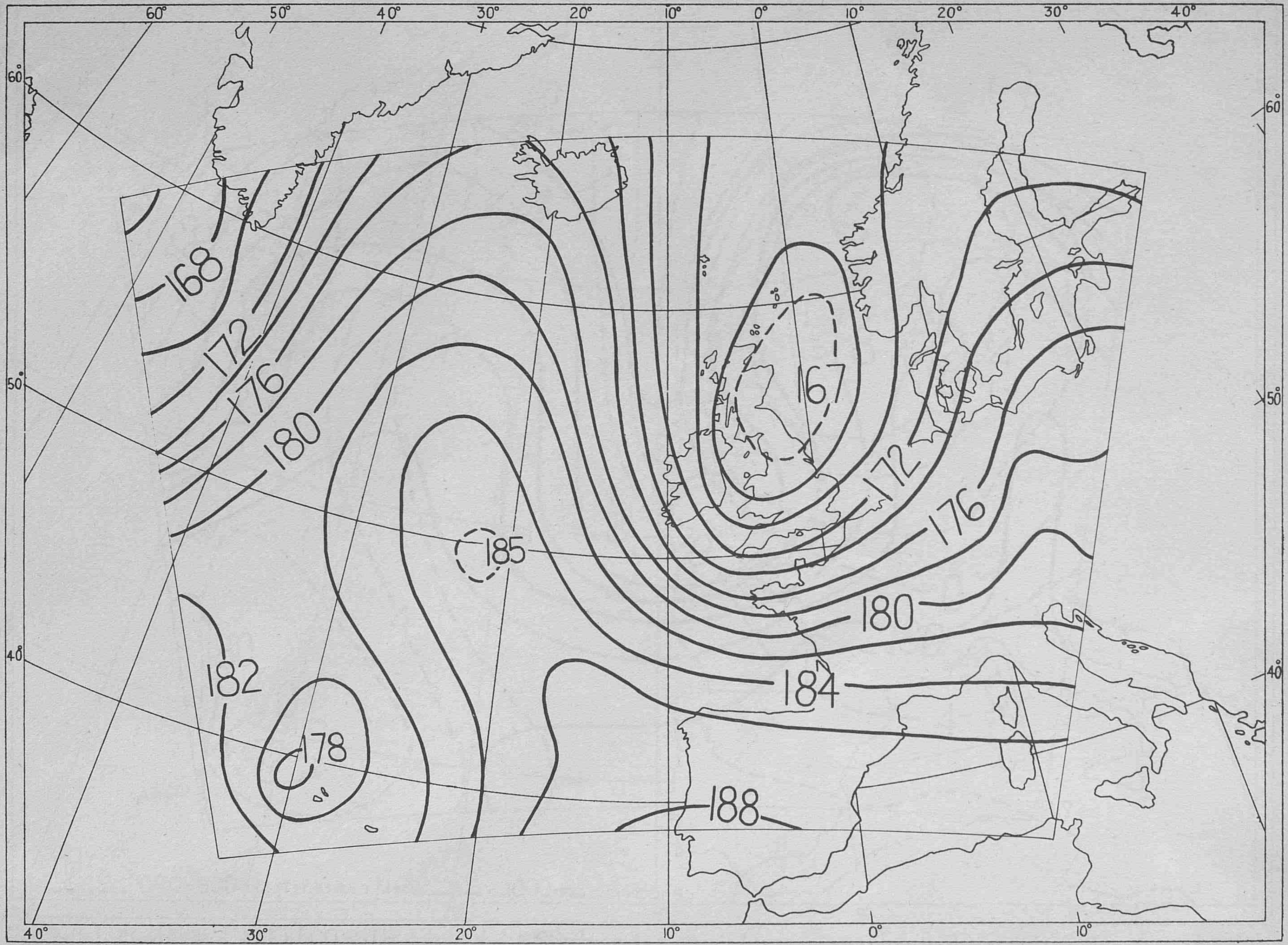
60°
50°
40°
30°
20°
10°
0°
10°
20°
30°
40°
60°
50°
40°
60°
50°
40°
40°
30°
20°
10°
0°
10°
168
172
176
180
185
182
178
167
172
176
180
184
188

Fig. 3(g) Computed 500 mb. contour chart (using stream function) for 1500 G.M.T. 31:1:53

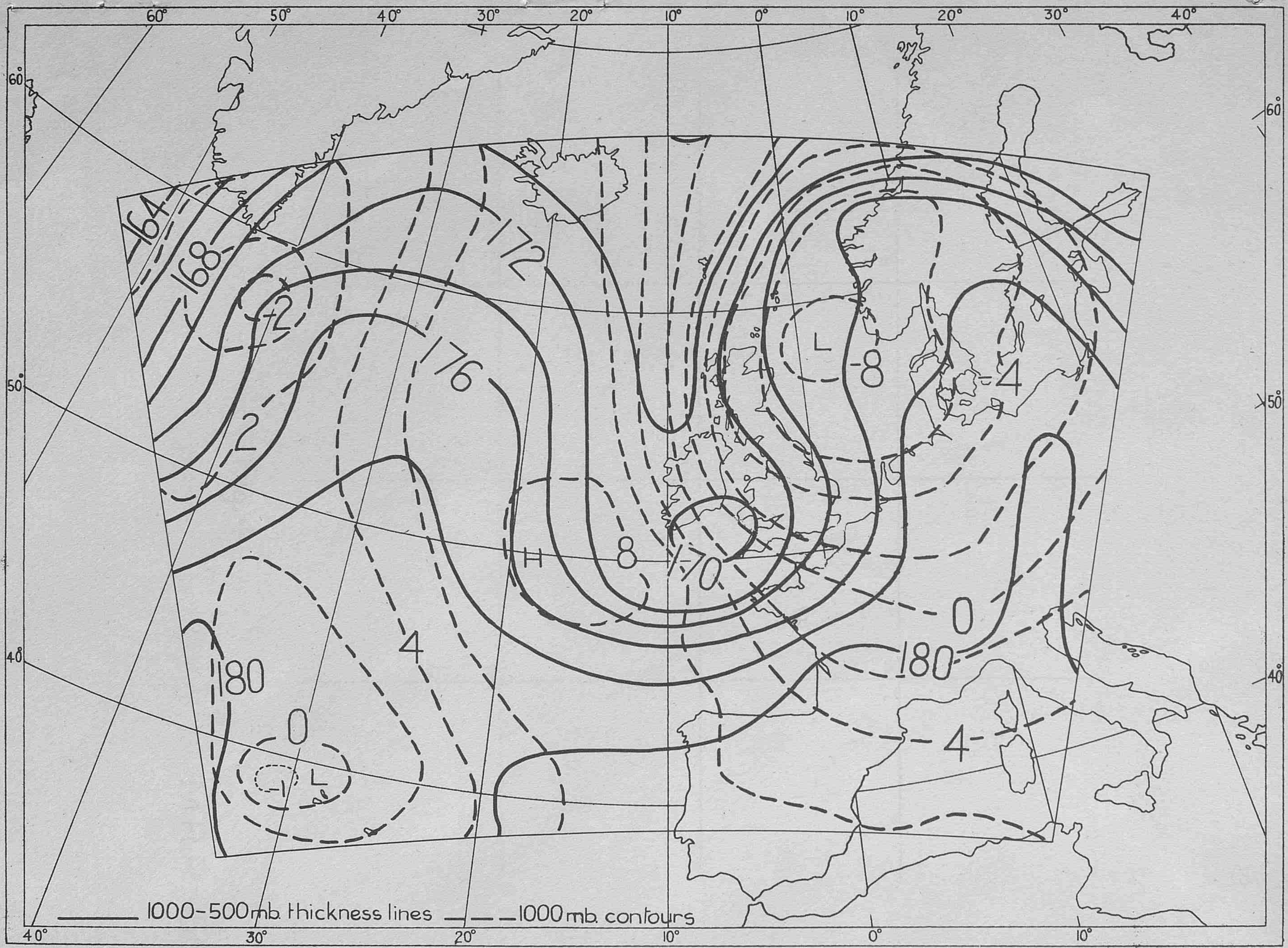
60°
50°
40°
30°
20°
10°
0°
10°
20°
30°
40°
60°
50°
40°
164
168
-12
172
2
176
-8
L
-4
8
H
-170
0
180
4
180
0
L
-4
4
1000-500mb. thickness lines
1000 mb. contours
40°
30°
20°
10°
0°
10°

Fig. 3(h) Computed 1000-500mb. thickness and 1000mb. contour charts (using stream function) for 1500 GMT. 31:1:53

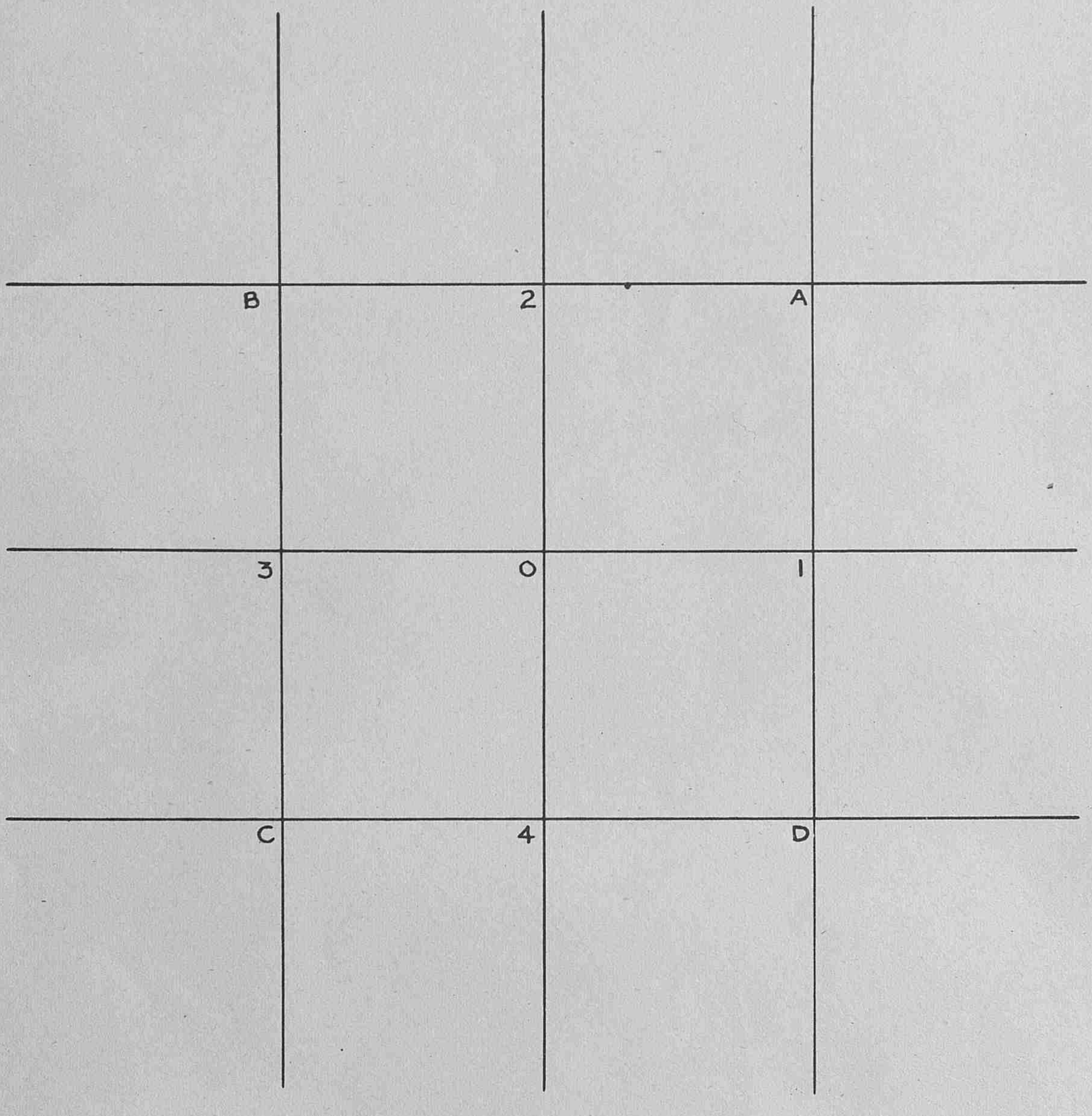

Fig. 4

M.R.P. 960
S.C. 1/110
26th January, 1956

AD 223098

Development of thermometers for high-speed aircraft

by

D. D. Clark
(Meteorological Office)

AIR MINISTRY
METEOROLOGICAL RESEARCH COMMITTEE

At the time of issue this report has not been published. Any author desiring to quote this paper should refer to it as "A paper of the Meteorological Research Committee (London), M.R.P. No. 960 by Mr. D. D. Clark. A copy is available in the Library of the Meteorological Office."

M.R.P.960
S.C.I/110
26th January, 1956

AIR MINISTRY

METEOROLOGICAL RESEARCH COMMITTEE

Development of thermometers for high-speed aircraft

by

D. D. Clark (Meteorological Office)

Summary. The principles of thermometer design are reviewed. Three models were made and tested in a wind tunnel; the results are given in tables and graphs. The model having the best performance (a conical type) was developed further into a production prototype. The lag and radiation errors are calculated and the extension of the use of the thermometer to supersonic flight is discussed.

General principles. A thermometer mounted on an aircraft to measure air temperature does not indicate true air temperature but a temperature higher than true air temperature by an amount which in the ideal case depends only on the square of the air speed. This relationship can be expressed as

$$T_1 - T_o = \frac{\lambda}{2C_p} U^2$$

where T_o is the true air temperature, T_1 the thermometer temperature, U the air speed in cm.sec.$^{-1}$ and C_p the specific heat of air at constant pressure. λ is referred to by most authors as the 'recovery factor' since it can be expressed as the proportion of temperature rise to total temperature rise of completely arrested air, i.e.,

$$\lambda = \frac{T_1 - T_o}{T_2 - T_o}$$

where T_2 is the temperature of air arrested adiabatically. The 'recovery factor' should not be confused with the 'speed-correction coefficient' which is usually expressed in the form

$$T_1 - T_o = \alpha\left(\frac{V}{100}\right)^2$$

where α is the speed-correction coefficient and V is the air speed in knots. Whereas λ depends solely on the characteristics of the thermometer, α depends also on C_p. Since C_p does not vary much, very nearly $\lambda = \frac{3}{4}\alpha$.

It is assumed that λ remains constant; then for air speeds up to about 200 m.p.h. the errors which would arise from small variations in λ are not important. However at high speeds, say 500 m.p.h., an error of 0.1 in λ would give rise to an error in temperature of about 3 degrees Celsius. The effects of variations in λ can be mitigated to some extent by calibrating the thermometer for different heights and Mach numbers; nevertheless it is much better to try to eliminate the variations in λ.

The causes of variations in λ have been dealt with by the present writer (Clark, 1951). An attempt will now be made to describe the development

/work

G.45201/JEK/1/56/50.

work arising out of these two reports to produce a thermometer with a constant recovery factor.

Choice of design. There are in effect two possible forms that the thermometer can take. Either it can arrest the air completely, causing an adiabatic temperature rise corresponding to the resulting compressional heating, or else it can interfere with the air stream as little as possible so that the air speed past the thermometer is unchanged and the temperature rise depends on the thermal dissipative and conductive processes taking place within the boundary layer on the surface.

The first variety has been studied very thoroughly by several authors, of whom it is sufficient to mention E. Brun and Max Plan (1949) and L. Malmquist (1948). Although the total-head thermometer, as this type is sometimes called, has generally been favoured for laboratory and wind-tunnel work, nevertheless for meteorological purposes it has certain disadvantages.

In construction the total-head thermometer consists of a hollow chamber open at the forward end and with leak vents at the rear to maintain a slight air movement inside. The temperature of the arrested air is measured by a rapid response element such as a bare resistance wire or thermocouple junction. It is difficult to make a design of this nature robust without sacrificing speed of response and it is essential that response be rapid owing to the low ventilation rate within the chamber. As has been shown also by Malmquist (1948) the recovery factor of these thermometers suffers significant changes with Mach numbers attributed to the nature of the flow inside the chamber. The recovery factor, which is always slightly less than it would be if the air were completely arrested, is dependent on the rate of ventilation which bears a non-linear relationship to the free air speed. This thermometer is also vulnerable to ice formation and once iced up takes some time to clear unless heaters are fitted for de-icing. Although the total-head thermometer appears at first sight to have the advantage of representing a fundamental approach to the problem of temperature measurement in a moving air stream, in as far as it is dependent only on the total energy of the air and not on local stream velocity, nevertheless the constructional compromises required in the engineering of this thermometer make it inferior to a well designed thermometer of the second type, usually referred to as the flat-plate thermometer.

One advantage possessed by the flat-plate thermometer is the high rate of heat exchange existing at the surface when following temperature change which enables a more robust construction to be employed.

For these reasons it was decided to develop the flat-plate type of thermometer for use at high speeds.

Characteristics of flat-plates. A flat-plate thermometer, designed originally by Brewer (1947), has been in regular use aboard meteorological reconnaissance and research aircraft for many years and gives reliable readings to the nearest half degree Celsius at air speeds up to about 300 m.p.h. It consists essentially of a $\frac{1}{2}$ in. metal tube flattened to $\frac{1}{8}$ in. thick and containing a platinum resistance wire element insulated by mica strips. At the sides and underneath there is a radiation shield made of thin metal sheet, all of which offers small resistance to forward motion. Shellard (1949) however has shown that the speed-correction coefficient of this thermometer is less when measured at high altitudes than at low altitudes. The present author (1951) put forward a theory to explain this variation of speed-correction coefficient based on the well-substantiated phenomenon of separation of the boundary layer at the line of adverse pressure gradient behind the leading edge on narrow section aerofoil shapes, which, it was suggested, took place at the high Reynolds numbers associated with low level flying, but not at the lower Reynolds numbers of high level flight. This theory seemed reasonable as the observed variation in speed-correction coefficient agreed with that to be expected, assuming turbulent or laminar boundary layer flow, and, in confirmation, photographs were obtained of separation of the boundary layer taking place on the flat-plate thermometer during wind-tunnel tests carried out at the National Physical Laboratory.

As a further test an experimental flate-plate thermometer was made up with suction slots cut into the surface behind and parallel with the leading edge to keep the boundary layer on the surface and prevent separation. Suction was provided by connecting the duct from the slots to a Venturi tube. This thermometer was flown on one of the Meteorological Research Flight's aircraft; the speed-correction coefficients for the Fahrenheit scale, measured at two altitudes, are given in Table 1. For comparison the speed-correction coefficients for a standard flat-plate thermometer are given as well.

Table 1. Speed-correction coefficient of flat-plate with suction slots

	Height ft.	S.C.C.	Standard deviation	No. of runs
Flat-plate with suction slots	5,500 21,000	1.59 1.60	.10 .03	14 15
Standard flat-plate (for comparison)	5,500 21,000	1.66 1.62	.07 .06	14 15

The variation of S.C.C. is small in the case of the slotted flat-plate compared with the standard flat-plate over the same height range.

In view of the strong evidence that boundary layer changes can cause variations in S.C.C. in flat-plate thermometers, care must be taken in the development of this type of thermometer to maintain constancy in the boundary layer state through careful attention to aerodynamic design.

Temperature gradients. When a thermometer is in thermal equilibrium with the air stream the condition that there be no heat exchange taking place between the air and the thermometer surface (neglecting small losses) is that there be no temperature gradients anywhere on the thermometer surface, because if temperature gradients are present then heat will be conducted from the warmer parts to the cooler parts of the thermometer, requiring heat to be taken up from the air at the warmer parts to compensate this loss and to be given out to the air at the cooler parts warmed by conduction. Since the rate of heat exchange, which is proportional to $k/\nu^{\frac{1}{2}}$, where k is the thermal conductivity and ν the kinematic viscosity of the air, is less at high altitudes than it is at low altitudes, the temperature gradients will also change with altitude becoming less pronounced the higher up we go. Since mean temperature depends on the surface distribution of temperature it also must follow variations in surface temperature gradients. The result therefore of the presence of temperature gradients on the thermometer is an apparent variation in speed-correction coefficient with altitude which, however, only becomes noticeable when these gradients are well-marked. Care must therefore be taken to avoid designs which give rise to pronounced temperature gradients and to reduce the effects of such temperature gradients as exist to a minimum.

Speed of response. Because the lag coefficient of a thermometer is inversely proportional to the square root of the air speed, in order to maintain the same degree of accuracy in reading at high speeds as at low speeds, the thermometer for use at high speeds must be faster in response than that for low speeds in the ratio of the square roots of the air speeds.

In the atmosphere there can exist temperature changes in the horizontal of about 2°C every 5 miles or so and occasionally extreme variations of 4°C can occur in only one mile. If a thermometer is being designed to read to within $\frac{1}{2}$°C of true indicated temperature in an atmosphere having a variation of as much as 4°C in one mile then, at 200 m.p.h., the lag coefficient would have to be less than 2.25 sec. and, at 500 m.p.h., less than 1 sec. The thermometer with a lag coefficient of 2.25 sec. at 200 m.p.h., however, would have it reduced to 1.4 sec. at 500 m.p.h. and would therefore be too sluggish at that

/speed.

speed. The lag coefficient of 1 sec. at 500 m.p.h. on the other hand becomes 1.58 sec. at 200 m.p.h. and that thermometer would be acceptable.

Besides the variation with air speed the lag coefficient varies approximately inversely with the square root of the air density, therefore the lag coefficient of 1 sec. at 500 m.p.h. at low altitudes becomes 2.75 sec. at 500 m.p.h. at 100 mb.

In the design which was finally adopted a compromise between robustness and speed of response gave a lag coefficient of about 2 sec. at low levels at 200 m.p.h. or 1.3 sec. at 500 m.p.h. which becomes 5.5 sec. at 100 mb. at 200 m.p.h. and 3.5 sec. at 100 mb. at 500 m.p.h. These lag coefficients correspond to the temperature errors, given in Table 2, calculated for temperature gradients in the line of flight of 4°C in one mile and also of 0.4°C in one mile at pressure levels of 900 mb. and 100 mb. and for air speeds of 200 and 500 m.p.h., using the formula from the Meteorological Air Observers Handbook (1945), Appendix 3, namely

$$\Delta T = U g L$$

where ΔT is the lag error, U is the air speed, g the temperature gradient and L the lag coefficient.

Table 2. Temperature errors depending on thermometer lag for lag coefficient of 2 sec. at 900 mb. at 200 m.p.h. calculated for temperature gradients in line of flight of 4°C per mi. and 0.4°C per mi.

Speed m.p.h.	Pressure level mb. 900		100	
	Temperature gradient 4°C/mi.	0.4°C/mi.	Temperature gradient 4°C/mi.	0.4°C/mi.
200	.44	.04	1.22	.12
500	.69	.07	1.93	.19

Experimental models. Summarizing all these points the problem was to design a flat-plate thermometer with the following characteristics:-

(a) The boundary layer of the air flow over the thermometer must be discouraged from separating from the surface and must be encouraged to stay laminar, i.e., there must not be a negative pressure gradient but preferably there should be a slight positive pressure gradient.

(b) There should be no temperature gradients or, if that is impossible because of (a), their effects should be kept to a minimum.

(c) The speed of response to temperature changes must be rapid.

(d) It must be robust and simple in construction.

Starting from the flat-plate there were two lines of development: one was to concentrate on making the flat-plate as thin and small as possible, the other was to incline the working faces to the air stream to provide the necessary positive pressure gradient. Both these lines were followed up but only the second was continued to completion.

A very slender and miniaturized flat-plate was made, .038 in. thick, $\frac{1}{4}$ in. across and $1\frac{3}{8}$ in. long containing a platinum wire wound on mica but insulated from the outside case by anodized aluminium strips. The series of tests on this thermometer was not completed as the radiation shield collapsed during a run at M = 0.6. Since the miniature flat-plate design presented no advantage over the conical design no further work was done on it.

The other line of development, requiring an inclined working face, meant either a wedge shape or a cone. As a cone is easier to make it was decided to develop a conical shaped thermometer. A cone of 20° angle was chosen as providing a convenient size and the velocity component on the surface was calculated and plotted to provide an indication of the temperature gradient. See Fig. 7 and Laitone (1947). Details of these calculations are not given here but it suffices to say that the temperature gradient on the surface was found to be least about one third the length of the cone from the tip. To reduce the effects of the gradient, therefore, the temperature sensitive part of the surface had to occupy as small an area as possible in this region. Two conical models were made; one had the temperature sensitive part of the surface restricted to a band of $\frac{1}{4}$ in. depth situated one third the cone's length from the tip, the other had an all metal nose extending up to one third the length of the cone from the tip, the temperature element being inside the metal nose. Photographs of these two models are shown in Fig. 1.

Wind-tunnel tests. All three models were tested in the 8 x 18 in. wind tunnel of the Aerodynamics Division of the National Physical Laboratory.

The recovery factor λ is defined in the equation

$$T_1 - T_o = \lambda \frac{U_o^2}{2C_p} \qquad \text{\_\_\_\_\_\_}(1)$$

$$= \frac{\gamma-1}{2} \lambda T_o M^2$$

where $0 < \lambda < 1$, T_1 is the thermometer temperature, T_o is the air temperature, U_o the air speed in cm./sec., C_p the specific heat of air at constant pressure, $\gamma = C_p/C_v = 1.4$ and M is Mach number, also $T_2 - T_o = \frac{\gamma-1}{2} T_o M^2$ where T_2 is the total temperature corresponding to the temperature of completely arrested air assuming adiabatic compression.

Hence $$T_2 - T_1 = (1-\lambda) \frac{\gamma-1}{2} M^2 T_o$$

$$= \frac{(1-\lambda) \frac{\gamma-1}{2} M^2 T_2}{1 + \frac{\gamma-1}{2} M^2}$$

Therefore $$1-\lambda = \frac{T_2 - T_1}{T_2} \; \frac{\left(1 + \frac{\gamma-1}{2} M^2\right)}{\frac{\gamma-1}{2} M^2} \qquad \text{\_\_\_\_\_\_}(2)$$

Equation 2 expresses λ in terms that can be measured in the wind tunnel. T_2 is the temperature in the intake chamber which was measured by a bare-wire thermometer, T_1 is the temperature, measured by the thermometer model, in the working section and M is the Mach number measured on the tunnel Mach number gauge and corrected for tunnel interference effects.

During each run the total-head temperature drift was never more than about one degree Celsius and the air in the intake chamber was sufficiently near stagnation for no correction to T_2 for air movement to be necessary even at the highest Mach numbers.

The values of λ for each Mach number for the two conical-head thermometer models calculated using formula 2 are given in Table 3 and are shown plotted in Figs. 3 and 4. The corresponding Reynolds numbers are also given in Table 3 and the variation with Reynolds number is illustrated in Figs. 5 and 6.

The total calibration and reading error in T_1 was found to lie within $\pm.043°C$ and that of T_2 within $\pm.015°C$, whence values of the standard deviation of λ were calculated by the method used earlier by the author. These are given in Table 3, column 11, and apply to both models. From Table 3 it is seen that the values of λ for each Mach number show a slight variation. The importance of this variation has been assessed by calculating the errors in true air temperature which would arise if a constant value were assumed for λ throughout. For this calculation the constant value of λ chosen was the mean λ for M = .4 to M = .9, namely .881 for Model I and .877 for Model II and the true air temperature was assumed to be 281°A. The formula for the temperature error is

$$\delta T_o = \delta\lambda . T_o \frac{(\gamma-1)}{2} M^2$$

The results are given in columns 6 and 10 of Table 3.

Table 3. Wind tunnel results. Values of recovery factor

1	2	3	4	5	6	7	8	9	10	11
		Model I				Model II				I and II
Mach No.	Re.10^{-5}	λ	No. of readings	$\sigma_1(\lambda)$	δT	λ	No. of readings	$\sigma_1(\lambda)$	δT	$\sigma_2(\lambda)$
					°C					
.2	.46	.844	18	.012	.08	.717	22	.035	.37	.016
.3	.67	.866	15	.004	.08	-	-	-	-	.007
.4	.87	.875	16	.002	.05	.859	13	.005	.16	.004
.5	1.05	.880	14	.000	.01	.873	13	.002	.06	.003
.6	1.20	.882	11	.001	.02	.877	14	.001	0	.002
.7	1.32	.882	13	.000	.03	.873	14	.001	.11	.001
.8	1.43	.880	18	.001	.04	.876	9	.000	.04	.001
.9	1.50	.886	15	.002	.23	.884	10	.001	.32	.001

$\sigma_1(\lambda)$= standard deviation of λ

$\sigma_2(\lambda)$= standard deviation calculated from limits of accuracy of T_1 and T_2

Re = Reynolds number

δT = error in true air temperature which would arise from taking λ = .881 for Model I and λ = .877 for Model II.

The error for Model I is negligible for M = .2 to .8 and is still small at M = .9. There is justification therefore in assigning a constant recovery factor of .881 to the Model I thermometer.

Production prototype. Of the two thermometers, Model I has the better performance and therefore was chosen for development as a prototype. In its final form this thermometer has been reduced to four separate parts shown in Fig. 2.

The body of the thermometer consisting of part of the conical surface and a parallel-walled section with a turned down length for mounting is made of a synthetic resin bonded paper (Tufnol). The sensitive element is made up of a platinum resistance wire of 50 SWG wound on to a thin-walled former made of super-pure aluminium base alloy anodized for electrical insulation, on which had been cut a thread of 200 threads per inch. The problem of providing leads and anchoring points for the platinum wire without adding appreciably to the thermal capacity of the element was solved by clamping copper foil strips to the inside of the former by turning down the ends of the foil into end recesses on the face of the former. These copper foil strips then provided anchoring points for both platinum wire and leads.

The thermometer head when assembled is held in a brass adapter piece which enables it to be mounted in a steel tube sting of 1 in. outside diameter, 17 gauge (see Fig. 2). On a later model the tip, which in Figs. 1 and 2 is shown in synthetic bonded paper, was made in one piece with the threaded rod of K-Monel D and was insulated from the temperature element by a Tufnol collar cemented to the tip with Araldite.

Radiation protection. It is normal practice to protect a thermometer from radiation by surrounding it with a radiation shield. The presence of a shield round a flat-plate thermometer, however, gives rise to an increment in air speed over the thermometer. In incompressible flow this increment is a constant proportion of the free air speed and therefore is of no importance in as far as variations in speed-correction coefficient are concerned, but at high Mach numbers this is no longer so as the interference effects are no longer linear with respect to air speed. At high Mach numbers also there is the additional disadvantage of interference from shock waves formed on the shield. Outrigging such as a shield is, besides, always unpopular with aircraft designers because of the drag it represents and the turbulence it introduces into the airstream ahead of the supporting aerofoil. Flat-plate thermometers, therefore, apart from special types such as the sonic-suction thermometer, due to Dunning (1947), must rely on other means of protection from radiation. Protection for the conical head thermometer was therefore provided by making the outer cover of the temperature element as highly reflecting as possible.

The outer cover made of a super-pure aluminium base alloy was anodized to give electrical insulation on the inside. The outside was polished mechanically and anodized and polished electrolytically to give a hard reflecting surface. Good results were obtained with BA SP 16 - WP aluminium alloy which contains small percentages of magnesium and silicon for hardness and ease of machining. When electrolytically polished, the absorptivity for visual wave lengths, according to the manufacturers, is in the region of .15. It is not known yet how long the good reflecting properties of the surface will survive exposure in flight and if it is found that reflectivity decreases considerably during use it may be necessary to renew the outer cover from time to time to maintain a good reflecting surface.

The thermometer will be exposed to solar radiation both direct and reflected and also to long-wave radiation from below; it will also lose heat by radiation from itself. The error in temperature from these effects will depend on the rate of heat exchange per degree of temperature difference between the thermometer and the air stream. Some calculations for various pressure heights and at two different air speeds have been made and are given in Table 5. The intensity of solar radiation at the top of the atmosphere was taken as .032 cal. cm.$^{-2}$sec.$^{-1}$ and allowance for diminution due to passage through the atmosphere has been made by use of a diagram provided by Väisälä (1948). In calculating the effect of the reflected solar radiation the albedo of the earth's surface has been taken as .35 following Scrase (1953), and two solar altitudes have been considered, namely 60 and 30 degrees. The emissivity of the earth's surface for long-wave radiation has been taken as .95 after Houghton and Brewer (1955). Absorptivity of the reflecting outer cover of the thermometer for visual radiation was taken as .15 but, for comparison, calculations have also been made for an absorptivity of .33 which might represent the state of the reflecting surface after some time in use. The emissivity for long-wave radiation (10μ)

was also taken from Scrase (1953) as .03, as no figures were available from the manufacturers.

The following formulae and assumptions were used:-

(i) Direct solar radiation

$$Q_1 = \varepsilon_1 \; I_p \, S_1$$

(ii) Reflected solar radiation

$$Q_2 = K \varepsilon_1 \, R \, I_s \sin h. \; S_1$$

Allowance was made for loss in reflected radiation by re-transmission from ground level to the thermometer.

(iii) Long-wave radiation exchange with earth

$$Q_3 = B \varepsilon_2 \, (\varepsilon_3 T_3^4 - T_1^4) \frac{S_2}{2}$$

(iv) Long-wave radiation upwards: (downwards radiation from above assumed negligible)

$$Q_4 = B \varepsilon_2 \, (- T_1^4) \frac{S_2}{2}$$

(v) Rate of heat exchange with air stream: (considering the thermometer as a flat-plate, see Goldstein (1943))

$$Q_5 = \frac{.686 \sigma^{\frac{1}{3}} k \, S_2}{l} \left(\frac{U_1 \, l \rho}{\mu} \right)^{\frac{1}{2}} . \Delta T$$

Meaning of symbols used:-

ε_1 : emissivity of thermometer surface considered as grey body.

ε_2: ditto for long-wave radiation (10μ), assumed to be .03 after Scrase (1953).

ε_3: emissivity of earth's surface for long-wave radiation, assumed .95 after Houghton and Brewer (1955).

I_p: intensity of solar radiation at pressure level p in atmosphere.

I_o: ditto at top of atmosphere (.032 cal./cm.^{2}).

I_s: ditto at ground level.

S_1: projected area of temperature sensitive surface of thermometer (.45 cm.^{2}).

S_2: total exposed area of temperature sensitive area of thermometer (.46 cm.^{2}).

σ : Prandtl number (values taken from Clark, 1951).

/B:

B: Stefan-Boltzmann coefficient, 1.37×10^{-12} cal. cm.$^{-2}$ sec.$^{-1}$ deg. C.$^{-4}$.

T_1: Temperature in degrees absolute of thermometer surface.

T_3: ditto of earth's surface.

k: coefficient of thermal conductivity, after Taylor and Johnston (1946).

U_1: air speed in cm. sec.$^{-1}$ at the surface of the thermometer deduced from Fig.7 as .95 of free stream air speed.

l: length of exposed surface of temperature sensitive surface of thermometer in direction of air stream, 0.7 cm.

μ: coefficient of viscosity of air at thermometer surface, after Johnston and McCloskey (1940).

ρ: density of air at thermometer surface.

K: shape and orientation factor of thermometer. For horizontal surface $K = 1$, for sphere $K = 2$; as a compromise K was taken as 1.5.

R: albedo of the earth's surface, .35.

h: solar altitude.

/Table 5.

Table 5. Heat economy and radiation errors of a conical-head thermometer

Rate of heat exchange	Solar altitude	PRESSURE LEVEL (mb.)															
		100				300				500				900			
		U (m.p.h.)				U (m.p.h.)				U (m.p.h.)				U (m.p.h.)			
		200		500		200		500		200		500		200		500	
		ε_1		ε_1		ε_1		ε_1		ε_1		ε_1		ε_1		ε_1	
(cal. x 10^{-3})	h	.15	.33	.15	.33	.15	.33	.15	.33	.15	.33	.15	.33	.15	.33	.15	.33
Q_1	60	2.14	4.70	2.14	4.70	2.07	4.56	2.07	4.56	1.96	4.32	1.96	4.32	1.75	3.85	1.75	3.85
	30	2.10	4.61	2.10	4.61	2.01	4.42	2.01	4.42	1.86	4.08	1.86	4.08	1.62	3.57	1.62	3.57
Q_2	60	2.02	4.45	2.02	4.45	2.07	4.56	2.07	4.56	2.17	4.78	2.17	4.78	2.44	5.37	2.44	5.37
	30	1.02	2.25	1.02	2.25	1.05	2.30	1.05	2.30	1.10	2.41	1.10	2.41	1.23	2.71	1.23	2.71
Q_3		.13		.10		.11		.07		.07		.02		-.06		0	
Q_4		-.07		-.10		-.09		-.13		-.13		-.18		-.20		-.25	
$Q_5/\Delta T$		5.17		8.18		8.95		14.15		11.46		18.12		15.22		24.07	
$Q_1+Q_2+Q_3+Q_4$	60	4.22	9.21	4.16	9.15	4.16	9.14	4.08	9.06	4.07	9.04	3.97	8.94	4.05	8.96	3.94	8.97
	30	3.18	6.92	3.12	6.86	3.08	6.74	3.00	6.66	2.90	6.43	2.80	6.33	2.71	6.02	2.60	6.03
ΔT °C	60	.82	1.78	.51	1.12	.46	1.02	.29	.64	.36	.79	.22	.49	.27	.59	.16	.37
	30	.62	1.34	.38	.84	.34	.75	.21	.47	.25	.56	.15	.35	.18	.40	.11	.25

Pressure levels of 100, 300, 500 and 900 mb. and air speeds of 200 and 500 m.p.h. have been considered.

The following values of air temperature were chosen corresponding to the different pressure levels:-

Pressure level (mb.)	100	300	500	900
Air temperature (°A)	216	229	252	281

For speeds of 500 m.p.h., 24 degrees were added to give the surface temperature of the thermometer, and at 200 m.p.h., 4 degrees were added.

From Table 5 it is seen that the greatest errors occur at high altitudes where the rate of heat exchange with the air stream is least. To ensure that errors are kept to ½ degree or less a good reflecting surface must be maintained and the fastest speeds used.

Mounting for thermometer. Whereas a total-head thermometer may be mounted on any forward facing site clear of engine exhaust or induced turbulence, a flat-plate thermometer must be mounted in an air stream undisturbed by the aerodynamics of the aeroplane. To obtain absolute independence of aerodynamic influence would require an elaborate platform not justified for routine measurement work. The conical-head thermometer therefore has been mounted on a sting which will carry it some 2 ft. in front of the point of fixture to the aircraft. It is intended where permissible to mount the thermometer and sting protruding from the leading edge of a narrow section aerofoil such as a wing or tail. The shortness of the sting makes it inadvisable to place it on the forward end of a large shape such as the fuselage.

Supersonic speeds. Although the conical-head thermometer was designed with subsonic speeds in mind, the conical shape is suitable for use in supersonic flow. Taylor and Maccoll (1933) showed that for a 20° angle cone in axial supersonic flow, for Mach numbers greater than 1.035, the shock wave is attached at the nose of the cone and the pressure field is uniform over the surface of the cone. It follows of course that the velocity field is also uniform over the conical surface. Now the relationship which exists in subsonic flow between the temperature rise on a flat-plate and the square of the local surface air speed has been shown by Eber (1952) to hold also in supersonic flow up to Mach number 5 at least.

This means that the formula for the recovery factor in laminar flow namely

$$\lambda = 1 - \left(\frac{U_1}{U_0}\right)^2 (1 - \sigma^{1/2}) \quad \text{(see Clark, 1951)}$$

holds at least up to M 5.

Tables for the flow speed along conical surfaces at supersonic speeds have been published by Kopal (1947) of the Massachusetts Institute of Technology. Using the values of U_1 obtained from these tables for a 20° angle cone and using the value for $\sigma^{1/2}$ from Clark (1951) for 500 mb., namely .846, λ has been calculated for various Mach numbers: the results are given in Table 4.

Table 4. Recovery factor at supersonic speeds for a 20° angle conical thermometer in axial flow

U_1/U_c	.4	.45	.50	.55	.60	.65	.70	.75	.80	.85	.90
M	1.0902	1.2330	1.4028	1.5957	1.8165	2.0750	2.3869	2.7794	3.3041	4.0748	5.4223
λ	.8730	.8675	.8649	.8631	.8616	.8604	.8591	.8580	.8569	.8556	.8543

U_c is the velocity of the air if allowed to expand into a vacuum.

$U_c = U_o^2 \cdot \left\{ 1 + \frac{2}{\gamma - 1} \frac{1}{M^2} \right\}$, subscript $_o$ indicates free stream values.

Acknowledgements. In this work I gratefully acknowledge the help given by the staff of the Aerodynamics Division of the N.P.L. during the wind tunnel tests. I also have pleasure in acknowledging the skill of Mr. A. L. Alexander who made the experimental models and the first prototype and who overcame many difficulties in construction. In particular, the idea of using copper foil strip clamped on the former for anchoring leads and wire was due to him.

REFERENCES

Brewer, A.W. 1947 'Distant reading electrical air temperature thermometer for use on aircraft'. J. Sci. Inst., Vol. 24, pp. 47-50.

Brun, E. and Plan, Max 1949 'La mesure de la temperature d'arrêt dans les courants gazeux rapides'. J. Rech. Cent. Nat. Rech. Sci., Paris, No. 8, pp. 231-237.

Clark, D.D. 1951 'An assessment of the probable causes of the variation of the speed-correction coefficient of aircraft thermometers'. Meteorological Research Papers, Air Ministry, London, No. 677.

Dunning, J.E.P. 1947 'A suggested method of measuring high temperatures in high velocity gas streams at low pressure conditions'. R.A.E. Tech. Note, Aero. 1872, S.D.54.

Eber, G.R. 1952 'Recent investigations of temperature recovery and heat transmission on cones and cylinders in axial flow in the N.O.L. aeroballistics wind tunnel'. J. Aeron. Sci., Vol. 19, p. 1.

Goldstein, S. (Ed.) 1943 'Modern developments in fluid dynamics'. Clarendon Press, Oxford.

Houghton, J.T. and Brewer, A.W. 1955 'Measurements of the flux of long-wave radiation in the upper air 1953-54'. Meteorological Research Papers, Air Ministry, London, No. 914.

Johnston, H.L. and McCloskey, K.E. 1940 J. Phys. Chem., Vol. 44, pp. 1038-1057.

Kopal, Z. 1947 'Supersonic flow of air around cones'. Massachusetts Institute of Technology, T. Rep., No. 1.

Laitone, E.V. 1947 'The subsonic flow about a body of revolution'. Quart.Appl. Maths., Vol. 5, p. 227.

Malmquist, L. 1948 'Temperature measurements in high velocity gas streams'. Trans. Roy. Inst. Tech., Stockholm, No. 15.

Scrase, F.J. 1953 'Radiation and lag errors of the Meteorological Office radiosonde and the diurnal variation of upper-air temperature'. Meteorological Research Papers, Air Ministry, London, No. 836.

Shellard, H.C. 1949 'Variation with altitude of the speed-correction coefficients of aircraft thermometers'. Meteorological Research Papers, Air Ministry, London, No. 527.

Taylor, G.I. and Maccoll, J.W. 1933 'The air pressure on a cone moving at high speeds'. Proc. R. Soc.,A, Vol. 139, p. 278.

Taylor, W.J. and Johnston, H.L. 1946 J. Chem. Phys., Vol. 14, pp. 219-233.

Väisälä, V. 1948 'Solar radiation intensity at the ascending radiosonde'. Geophysica, Helsinki, Vol. 3, p. 49.

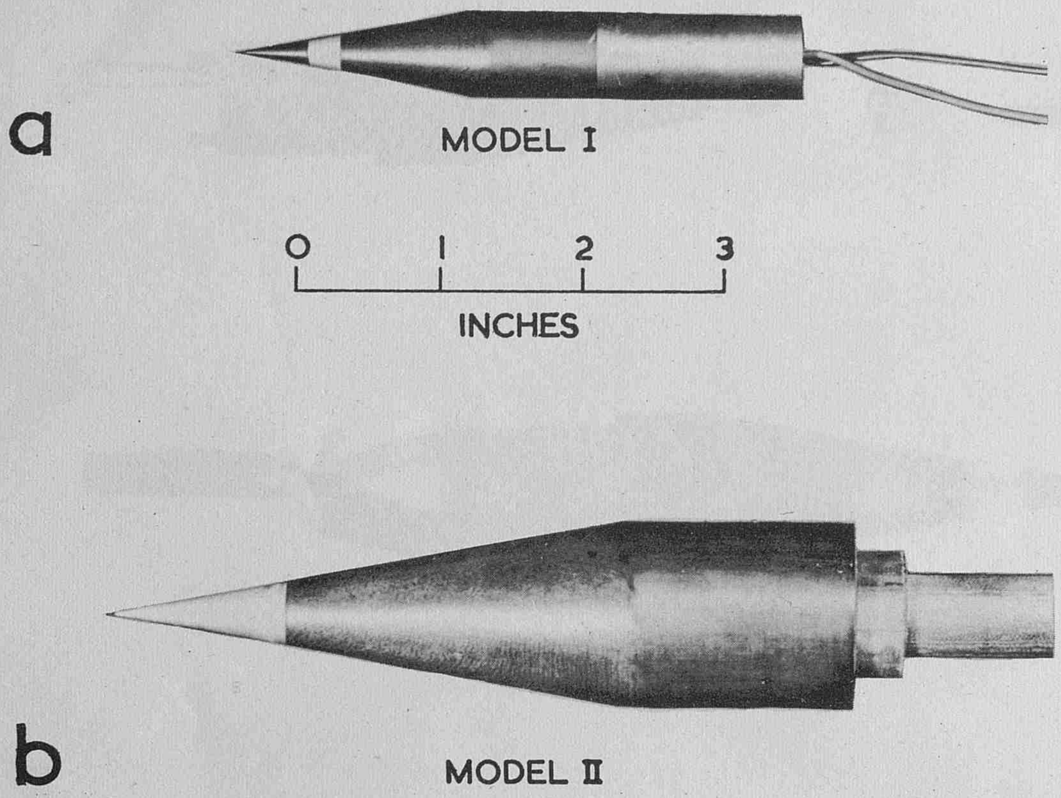
a
MODEL I
0
1
2
3
INCHES
b
MODEL II

Fig.1. Wind tunnel models

(a) Conical thermometer Model I

(b) Conical thermometer Model II

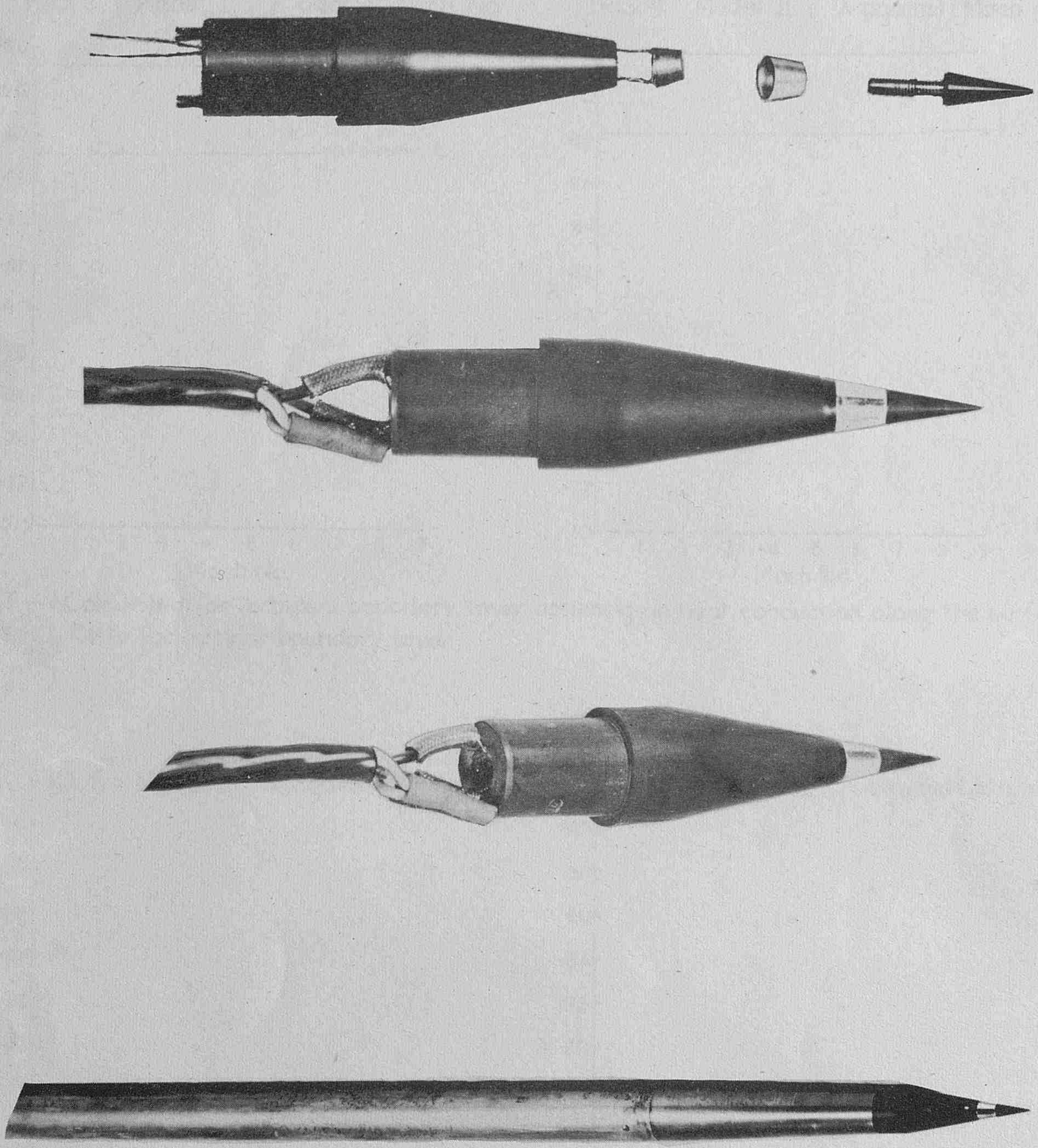

Fig.2. Conical head thermometer - prototype

(a) Exploded view showing parts before assembly

(b) and (c) Assembled thermometer. The two free leads shown are compensating leads

(d) Thermometer mounted on a sting

FIG. 3 Model I : λ against Mach No.

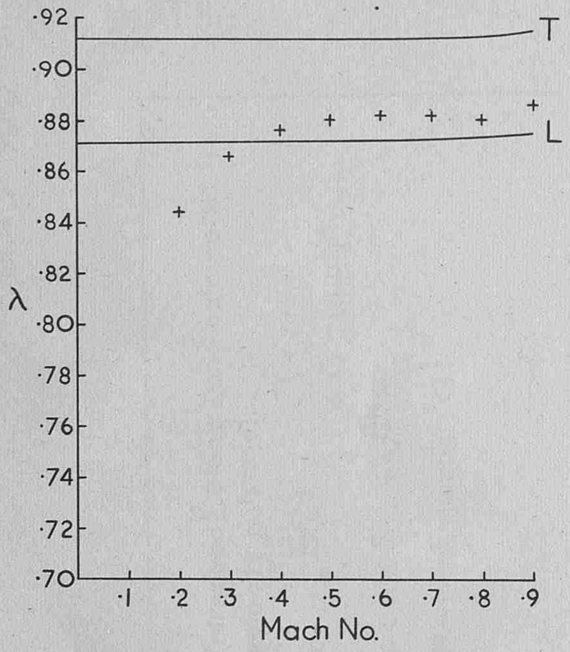

FIG. 4 Model II : λ against Mach No.

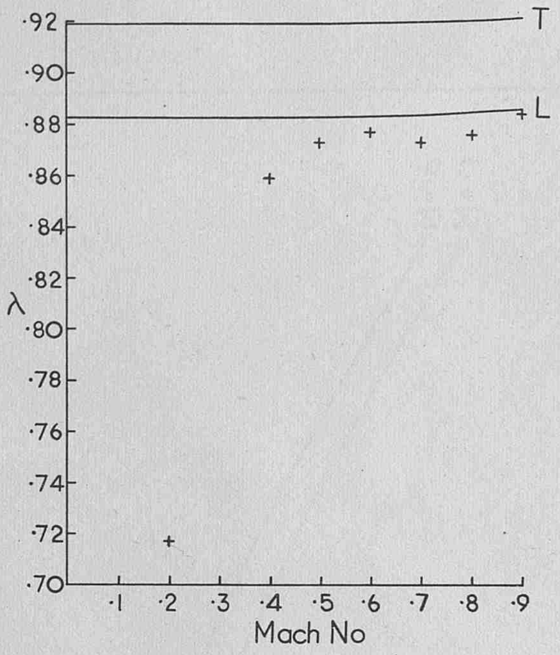

T : Calculated for turbulent boundary layer assuming no heat conduction along the surface
L : Ditto for laminar boundary layer

FIG. 5 Model I : λ against Reynolds No.

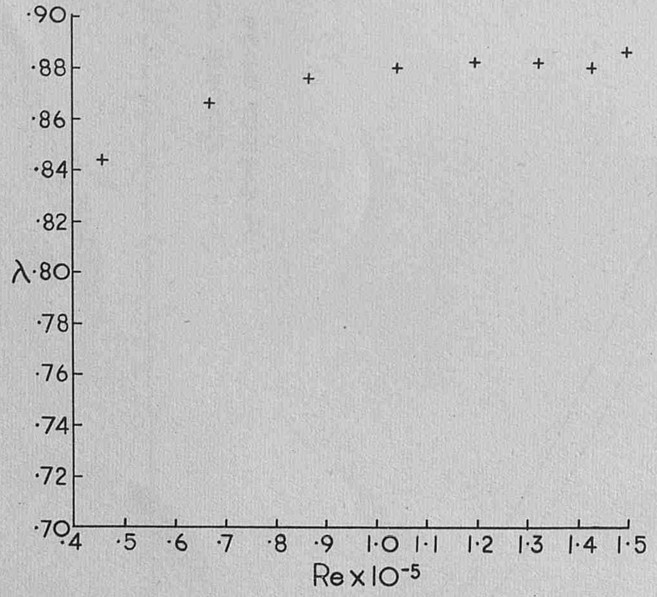

FIG. 6 Model II : λ against Reynolds No.

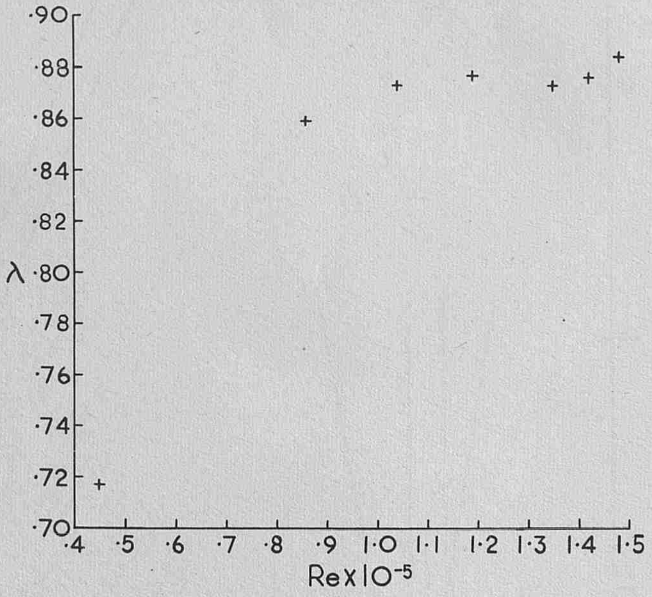

FIG. 7

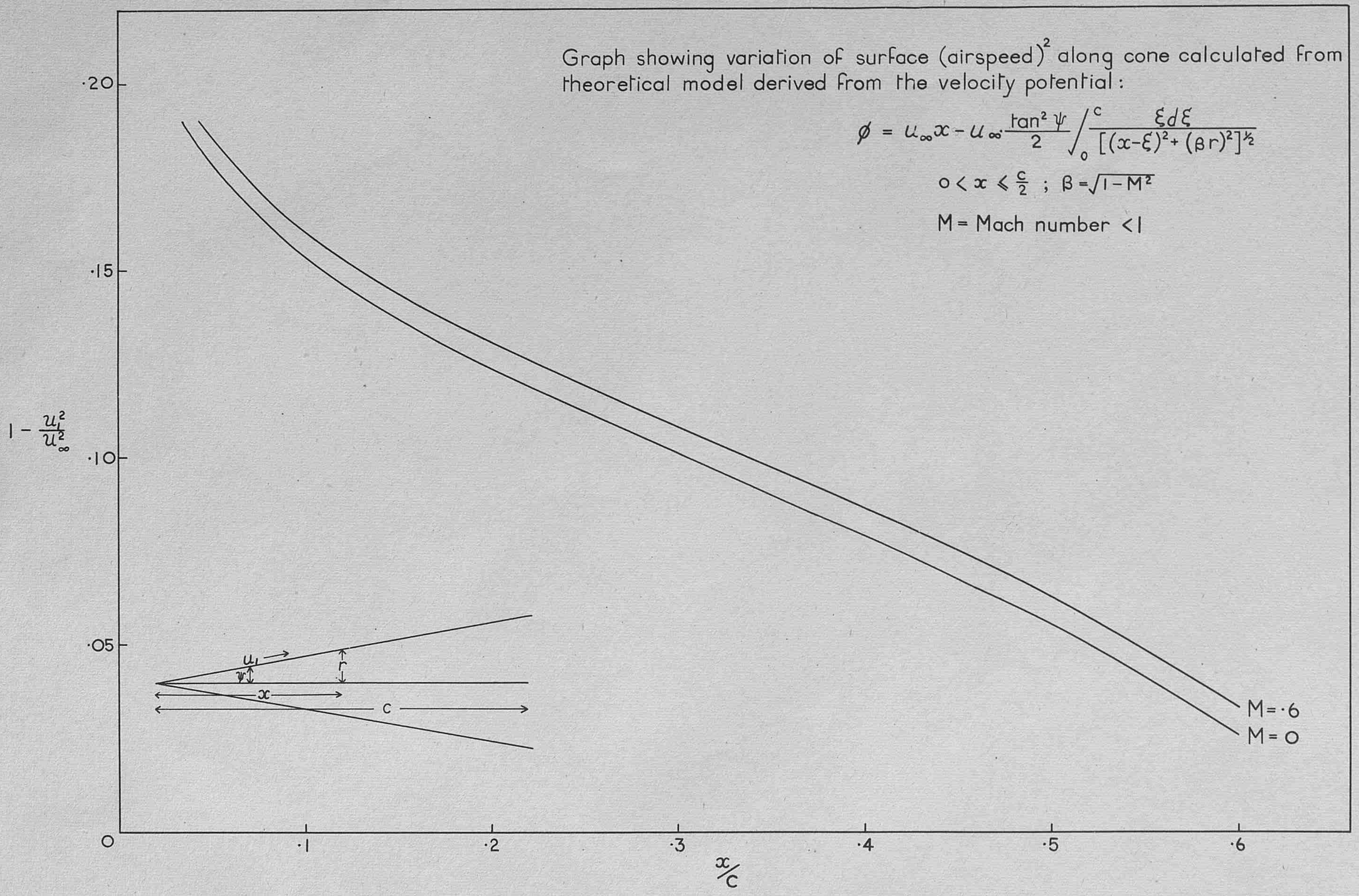

Graph showing variation of surface $(\text{airspeed})^2$ along cone calculated from theoretical model derived from the velocity potential:

$$\phi = u_\infty x - u_\infty \cdot \frac{\tan^2\psi}{2} \int_0^c \frac{\xi\, d\xi}{[(x-\xi)^2 + (\beta r)^2]^{1/2}}$$

$$0 < x \leqslant \frac{c}{2} \;;\; \beta = \sqrt{1-M^2}$$

M = Mach number <1

M.R.P. 961
S.C. 111/199
6th December, 1955

AD 223097

A technique for studying the local atmospheric diffusion of airborne material

by

J.S. Hay and F. Pasquill
(Meteorological Office)

AIR MINISTRY
METEOROLOGICAL RESEARCH COMMITTEE

At the time of issue this report has not been published. Any author desiring to quote this paper should refer to it as "A paper of the Meteorological Research Committee (London).
M.R.P. No. 961 by Mr. J.S. Hay and
Dr. F. Pasquill
A copy is available in the Library of the Meteorological Office."

M.R.P. 961
S.C.III/199
6th December, 1955

AIR MINISTRY

METEOROLOGICAL RESEARCH COMMITTEE

A technique for studying the local atmospheric diffusion of airborne material

by

J.S. Hay and F. Pasquill

Summary

A description is given of a technique for studying the atmospheric diffusion of particulate matter. Spores of Lycopodium released from a simple mechanical dispenser are collected on adhesive cylinders and subsequently counted under a microscope. The apparatus can be operated on captive balloon cables and used to investigate vertical diffusion at heights remote from the ground. The results of some preliminary experiments are discussed. The aim is to use diffusion measurements made by this technique in studying the relation between Lagrangian and Eulerian correlation coefficients in atmospheric flow.

Introduction

Much of the available knowledge of the processes of atmospheric diffusion has resulted from actual observations on the subsequent distribution in space of properties introduced naturally or deliberately into the air. In the particular case of airborne material these observations involve the collection and estimation of samples and, in experimental applications, the provision of a suitable source. These features present technical problems which increase in complexity as the region of the atmosphere to be studied becomes more remote from the laboratory and the ground, and as the number of samples required increases. The inevitable result has been that most data have so far been derived from relatively complex and cumbersome ground based arrangements for emission and sampling. Many ingenious techniques have been developed with one particular feature or another in mind, as for example in the ciné-photography of the horizontal spreading of a stream of bubbles released from a balloon-borne generator (Edinger, 1952), the use of fluorescent tracer material (Perkins et al, 1952) or the measurement of the local β-activity in a radioactive plume from a chimney (Stewart et al, 1954). However, if interest turns to a study of such diffusion processes without recourse to elaborate apparatus for sampling and estimation and without restriction to ground level operation there appears to be no well established technique.

In planning the observational aspects of a projected study of vertical diffusion in the first thousand feet or so of the atmosphere a promising basis for relatively simple measurements seemed to be provided by the impaction of airborne particles on cylindrical objects exposed to the airstream. A demonstration by this method of the turbulent diffusion in a wind tunnel airstream has already been provided by Gregory (1951) in his study of deposition of spores on cylinders and the method has also been used by Chamberlain (1953) in measuring airborne concentrations in some preliminary experiments on the deposition of particles on a natural surface. In the present case the interest lies in the

/application

application of this principle of impaction on cylinders to the examination of the vertical distribution shown by airborne particles after travelling some distance from a quasi-continuous point source operated at a considerable height above ground. The present note describes the equipment and technique as they have been developed so far and some of the experiences and results of preliminary experiments.

Equipment and Technique

Spores of Lycopodium appeared to be suitable particles for the present experiments. Their large size (30 μ diameter) facilitates examination of samples and their terminal velocity (1 - 2 cm./sec.) seems low enough not to affect their scattering in a turbulent atmosphere. The dispenser for producing the quasi-continuous emission consists of a hopper from which the spores are gravity fed on to a toothed wheel accommodated in a close fitting cavity in a perspex block. In the original version, the spores fell into a tube and were then blown out into the atmosphere by a current of air produced by a small air pump. In the latest version, shown in Figure 1, the spores fall from the toothed wheel through a vertical channel in the perspex block on to the blades of a small high speed fan operating in the free air immediately beneath the block. It had been previously demonstrated that the fan was effective in reducing the occurrence of aggregates of spores. The spores are emitted in discrete puffs but the speed of rotation of the wheel and the number of teeth are such that the interval between puffs is only 0.26 sec. From laboratory tests, the average rate of output is about 3 g./min.

The cylindrical surfaces used for sampling are simply 2" lengths of 0.25" external diameter glass tubing coated on the outside with a film of glycerine jelly similar to that described by Gregory (1951). Tubes of this size are convenient for handling and examination and their collection efficiency *, according to Gregory, exceeds 40 per cent in winds of more than 3.3 m./sec. In the present work, the tubes are exposed vertically on light metal vanes riding on small stops clamped to the cable of a Mark VI balloon, the vanes serving to keep the tubes upwind of the cable. The latest type of vane is shown in position on the cable in Figure 2. In practice a number of tubes is exposed at predetermined height intervals in order to explore the vertical distribution in a cloud of particles.

The general technique in the field operations is to position the Mark VI balloon at a suitable distance downwind of the dispenser, which can be set up either on the top of a tower or, for greater heights of operation, on the cable of another captive balloon. The dispenser is shown in Figure 3 mounted on the cable of a Mark X barrage balloon. Various aids to the positioning of the "sampling balloon" have been tried, such as a smoke candle or a small no-lift balloon tethered to a point near the dispenser. The latest method is to move the balloon into line with a pennant which is flown from the "source balloon" cable near the dispenser and which is observed in a horizontal mirror set up on the ground immediately below.

To estimate the deposit on the outer surface of a sampling tube, the tube is mounted on a horizontal spool attached to the stage of a microscope, the eyepiece of which is masked to give a field of view 0.11 cm. square. A section of tube 0.11 cm. long is then scanned by rotating the tube through 360

/degrees

---

* The collection efficiency is the number of particles impacting on the cylinder, expressed as a percentage of the number which would have passed through the same cross-sectional area if the cylinder had not been there. For a given particle size the collection efficiency depends on the type of adhesive used, the diameter of the cylinder and the speed of the air stream.

degrees and the number of spores which move across the field of view counted. This process is normally carried out at twenty points spaced 0.2 cm. apart along the tube and the mean number of spores taken as a measure of the deposit on the tube. If the efficiency of collection is the same for all tubes exposed in an experiment, the deposit can then be taken to be proportional to the concentration of spores in the air. The only systematic variation in efficiency which is known to occur is that due to the variation of wind speed with height above ground. As the experiments envisaged here involve sampling tubes spread out over a height range less than the height of the central tube, the variation in mean wind speed over the sampling positions will normally be within 15 per cent. For wind speeds of about 3 m./sec. the collection efficiencies (see Gregory (1951)) will vary only from 41 to 44 per cent. At higher wind speeds the variation will be less.

Lycopodium spores come from a type of moss which is usually found in mountainous districts. The spores are thus not commonly present in the atmosphere over Salisbury Plain, a fact confirmed by examination of tubes exposed while no emission was actually taking place. Their characteristic size, shape and yellow colour enable them to be distinguished from other particles collected on the sampling tubes. In the earlier stages of the work, however, positive identification was not always possible, for some particles were observed which were almost transparent but were similar in size and shape to Lycopodium spores. On investigation, these did in fact prove to be spores which were completely immersed in the jelly. With the incident light largely reflected at the surface of the jelly, they were subject to rather less illumination than those projecting from the jelly and showed up much fainter. This difficulty was overcome by using a more viscous jelly, obtained by doubling the proportion of gelatine recommended by Gregory. Tests showed that the majority of spores were then retained on the surface of the jelly and could be readily identified. As there was no apparent loss in efficiency, this form of jelly was adopted for all subsequent work. A further slight difference from the jelly used by Gregory is the inclusion of thymol instead of phenol.

Results of some preliminary experiments

The first few experiments were carried out with the dispenser operating for 15 minutes at a time on a tower 32.5 m. above the ground and the sampling tubes exposed on the Mark VI balloon cable 50 m. downwind. The tower was situated half way up the side of a ridge which rises a total of about 200 ft. in a distance of 1,000 yd. The vertical distributions obtained from four experiments on the same day are shown in Figure 4 where the mean number of spores per 0.11 cm. section of sampling tube is plotted against height above ground. The characteristic "cocked hat" shape of a cloud diffusing from a point source is clearly shown and the effect of atmospheric stability is demonstrated, the curves becoming narrower and the peaks greater with increasing stability. Atmospheric stability is here specified by the temperature difference between 23 and 4 ft. (23 - 4 in sign) measured on a tower approximately 2 miles away. It will also be noted that the positions of the peaks become progressively higher during the series of experiments and it will be seen later that this feature is associated with variations in the mean inclination of the wind.

Owing to movement of the "sampling balloon", there are fluctuations in the heights of the sampling tubes. The apparent spread of particles is thus a resultant of the true spread due to atmospheric diffusion and that due to the movement of the sampling tubes. No attempt has been made here to eliminate the latter component but theodolite observations showed that the standard deviation of the variation in height of the sampling tubes was approximately 0.5 m. in Experiments 3 and 4 and about 1 m. in the case of Experiment 1. These values are small in relation to the observed vertical spread of the spores. No theodolite measurements were made in the case of Experiment 2 but it seems reasonable to assume a variation of the same order.

During these experiments, readings were made at 5 second intervals of the

/inclination

inclination of the wind to the horizontal using a "V" hot wire anemometer of the type described by Simmons and Bailey (1927). This was positioned at the top of the tower a few feet away from the dispenser. The quantity measured is actually the instantaneous value of $\frac{w'}{u}$ where w' is the vertical component of velocity and u the horizontal component in the direction of the mean wind. Since the initial trajectories of the spores are determined by the local eddy velocities at the point of release their subsequent vertical distribution, when related to the elevations of the sampling positions with respect to the source, should at first approximate closely to the frequency distribution of the wind inclination. A test of this is given in Figure 5(a) for the case of Experiment 3 of Figure 4. The wind inclination was actually read to the nearest whole degree but in preparing the histogram, the observations were grouped in intervals of two degrees centred on even values, odd values being divided equally between adjacent intervals. The peak of the particle distribution curve was brought into correspondence with that of the wind distribution by suitable adjustment of scale. Bearing in mind the slight overestimation due to balloon movement the results indicate that the vertical spread of the spores for a time of travel of about 10 seconds is in close agreement with the wind inclination distribution at the point of release. A similar comparison has been made for Experiments 1, 2 and 4. In Nos. 1 and 2 a similar degree of agreement between the spread of the particles and the wind distribution is evident but in No. 4 the spread of particles appears to be wider than the corresponding wind distribution. The latter feature is rather difficult to understand and it is noteworthy at this point that of the four particle distributions No. 4 contains the greatest uncertainty as regards the peak value.

Turning now to the positions of the particle and wind distribution peaks, it is seen from Figure 5(a) that the former is 3 degrees below the latter. A similar difference (2 to 3 degrees) is also exhibited in the results of the other three experiments, though the effect is perhaps less convincing in No. 1 owing to a somewhat erratic wind distribution. Assuming a terminal velocity of the spores of 2 cm./sec., the relative displacement of the wind and particle distributions should be only about 0.25 degrees in the wind speeds of these experiments. The reasons for the much larger differences observed are not obvious and further investigation will be required. A further point of interest is that the systematic variation in peak position indicated in Figure 4 is apparently merely the result of a systematic variation in the mean inclination of the wind over a total range of about 6 degrees. It was noted during the experiments that the local wind direction changed and that the local ground slope in the direction of the mean wind was thereby increased by 2 degrees. This is insufficient to account for the total observed change in wind inclination and as yet no further explanation can be offered.

The experiments have recently been extended to greater heights with the dispenser mounted on the cable of a Mark X balloon and the sampling tubes on the cable of a Mark VI balloon as before. The maximum height attainable by the latter balloon is about 1,100 ft., so that at present the release of spores cannot be made above 1,000 ft. For measurement of the inclination of the wind, the "V" hot wire anemometer has been replaced by a vane instrument which is mounted on the cable in conjunction with the dispenser (see Figure 3). A sensitive vane responding to vertical air movement is held upwind of the cable by means of a bigger control vane, and the movements of the former vane recorded electrically on the ground. The details of this will be described elsewhere and it suffices here to note the principal feature, namely that the vane mounting is carried on a damped pendulum which automatically compensates for variations in the inclination of the balloon cable. There is in addition a variation in the height of the balloon, and hence of the vane support, which leads to a spurious component in the wind inclination record. In order that corrections may subsequently be made for this effect, the elevation of the vane support is observed at frequent intervals by a theodolite. Observations are similarly made on the central sampling tube since it may be necessary also to correct the apparent particle distribution for the vertical movement of both the source and the sampling apparatus.

The results of the only experiment of this series which have been analysed completely so far are displayed in Figure 5(b), which contains the distributions of particles and of 15 sec. mean values of wind inclination.* This experiment was carried out over relatively level terrain in unstable conditions with the source at a height of 500 ft. and the sampling tubes 100 m. downwind. An adjustment of the scales has been made to bring the central regions of the two distributions to the same value approximately. The distributions are very wide and agree roughly in width if not in detail. Once again the position of the particle distribution appears to be below the wind inclination distribution by a few degrees.

From the theodolite observations, which were made at half-minute intervals, it appears that the maximum vertical movement of the vane support between consecutive readings was 20 ft., which is equivalent to a wind inclination of 1.5 degrees. The height difference between the central sampling position and the source position 15 seconds earlier, this being the approximate time of travel of the particles, showed extreme variations of ± 16 ft. or 3^{0} in the scale of Figure 5(b). These figures again indicate that the spurious components due to balloon movement are small but it is evident that they might not be negligible in more critical examinations of the relation between diffusion and eddy fluctuations.

Concluding Remarks

From the early experiences described here it seems likely that the technique proposed could be of considerable value in studies of atmospheric diffusion. Further examination is undoubtedly required of the relation between the trajectory of the centre of gravity of the particles and the mode of the wind inclination. However, the first indication is that the vertical spread of particles after a short distance of travel is consistent with the frequency distribution of the vertical component of wind at the point of release, and this inspires confidence in the general reliability of the experimental techniques employed. Probably the greatest interest lies in the demonstrated feasibility of using the emitting and collecting devices at considerable heights above ground. At such heights not only is information on the diffusive properties greatly required, but it is likely that at times the turbulence there will approximate to the isotropic and steady conditions in which the predictions of statistical theories of turbulence can be tested. In the programme which is being followed here the main interest lies in the prospect of using diffusion measurements made by this technique in order effectively to specify the Lagrangian correlation coefficient and to make comparison with simultaneous measurements of the Eulerian correlation coefficient. Ø

Acknowledgements

Arrangements for balloon flying were made by Flt.Lt. F.H. Radford, R.A.F. The original version of the dispenser was designed by W.C. Prewett, Physics Section, Porton. Measurements of the inclination of the wind were made by J.I.P. Jones, Meteorology Section, Porton.

/REFERENCES

---

* The apparatus has a total response time of about 0.25 sec. and gives a continuous record of inclination.

Ø While preparing this note the writers have had their attention drawn to a current N.A.C.A. issue (Technical Note No. 3570, by W.R. Mickelson, October 1955) which describes an experimental comparison of the Lagrangian and Eulerian correlation coefficients in wind tunnel flow. In this case the Lagrangian coefficient was characterised by measurements of the distribution of helium downstream of a point source.

REFERENCES

Chamberlain, A.C.	1953	A.E.R.E. H.P./R.1261.
Edinger, J.G.	1952	M.I.T. Symposium, Geophysical Research Paper, No.19, Cambridge, Mass.
Gregory, P.H.	1951	Ann.App.Bio., 38, No.2, pp.357-376.
Perkins, W.A., Leighton, P.A., Grinnell, S.W. and Webster, F.X.	1952	Proc. 2nd National Air Pollution Symposium, U.S.A.
Simmons, L.F.G. and Bailey, A.	1927	Phil.Mag., Series 7, 3, p.81.
Stewart, N.G., Gale, H.J. and Crooks, R.N.	1954	A.E.R.E. H.P./R.1452.

FIGURE I. LATEST TYPE OF PARTICLE DISPENSER

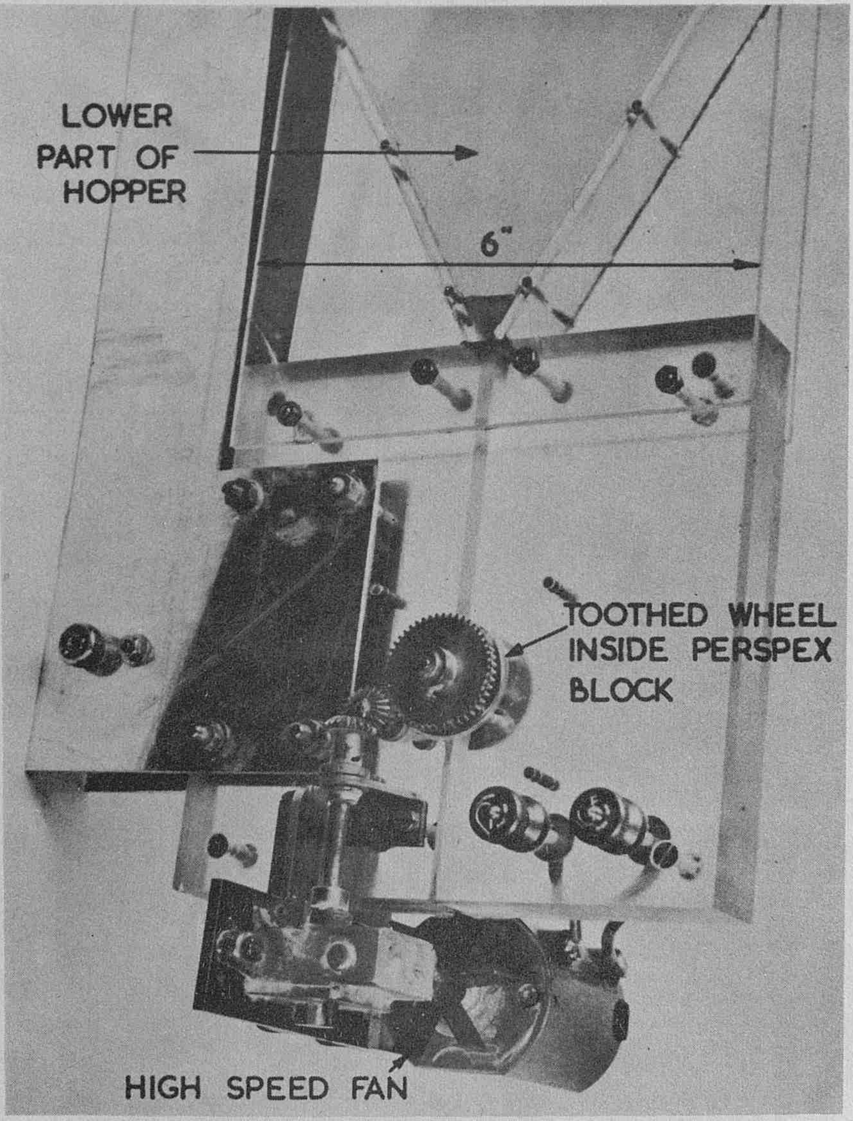
LOWER PART OF HOPPER
6"
TOOTHED WHEEL INSIDE PERSPEX BLOCK
HIGH SPEED FAN

T.1227/1.

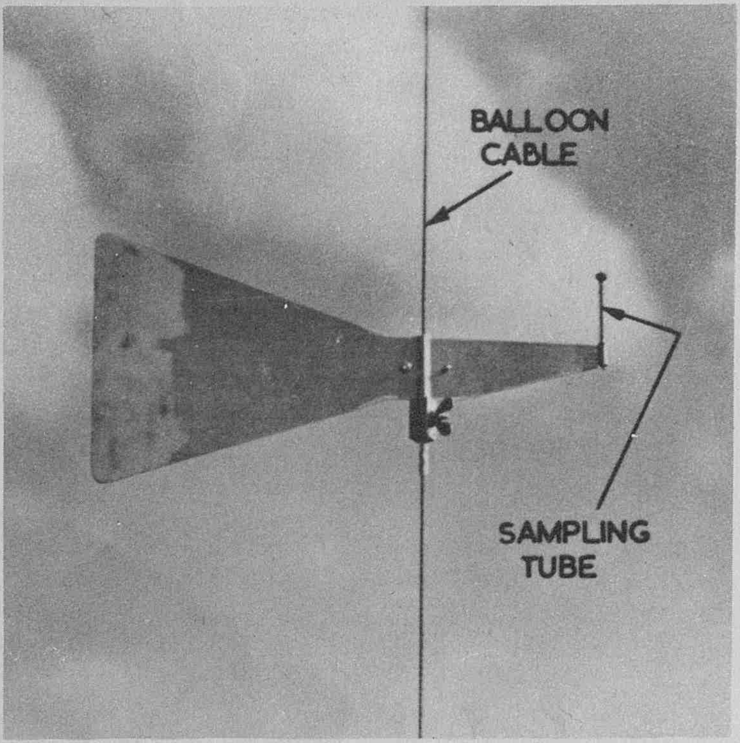
BALLOON CABLE
SAMPLING TUBE

FIGURE 2. VANE CARRYING SAMPLING TUBE

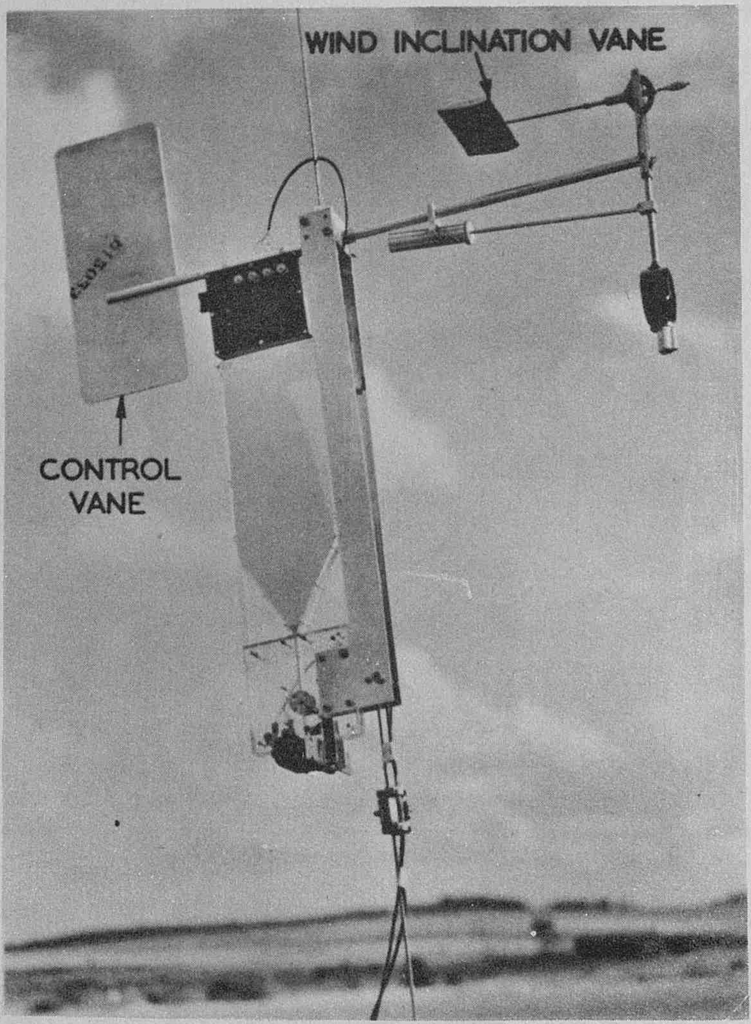
WIND INCLINATION VANE
CONTROL VANE

FIGURE 3. DISPENSER AND WIND INCLINATION INSTRUMENT ON BALLCON CABLE

T.1227/2.

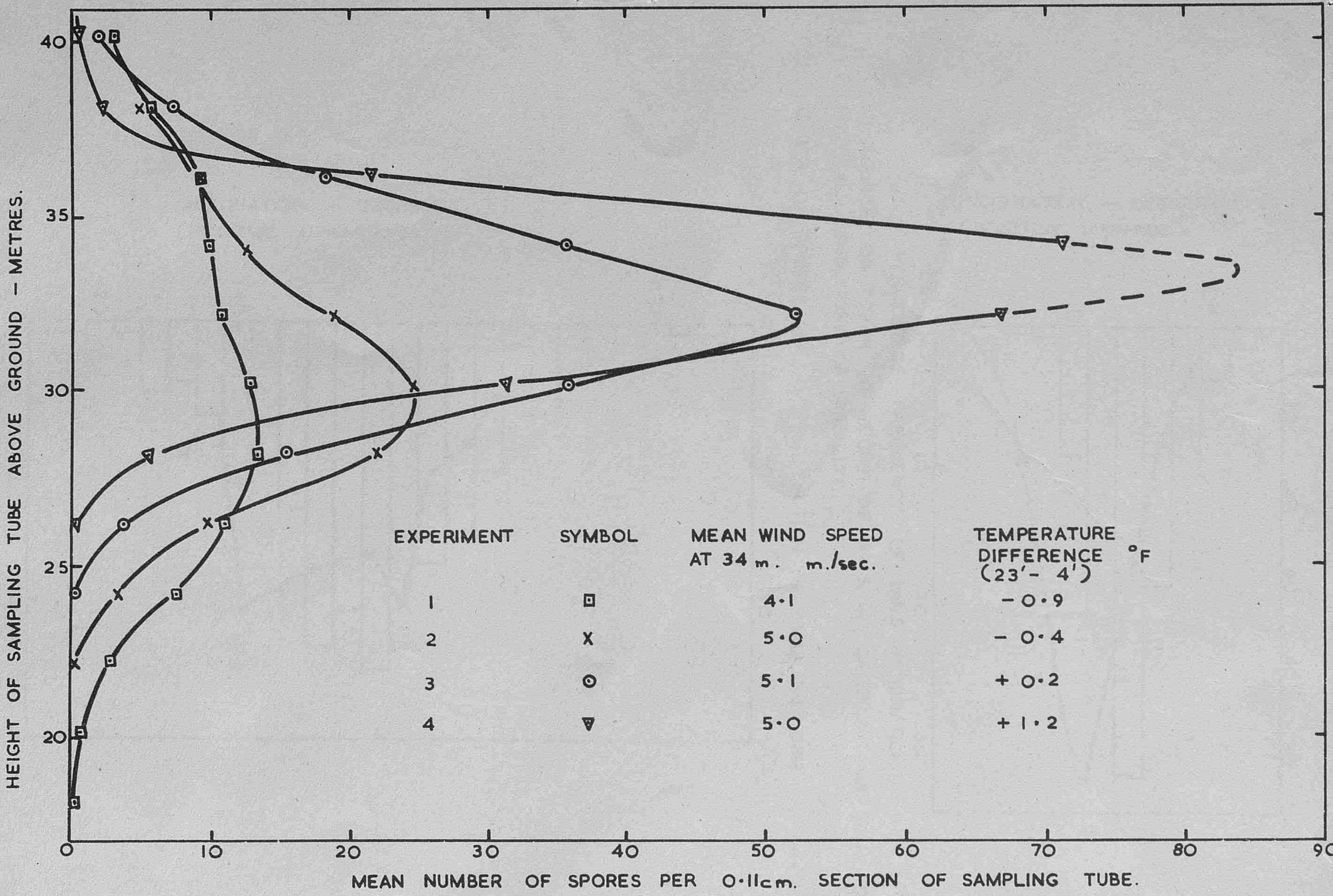

FIG. 4. VERTICAL DISTRIBUTION OF SPORES AT 50 m. DOWNWIND OF A POINT SOURCE OF DURATION 15 MINUTES AT 32·5 m. ABOVE GROUND LEVEL.

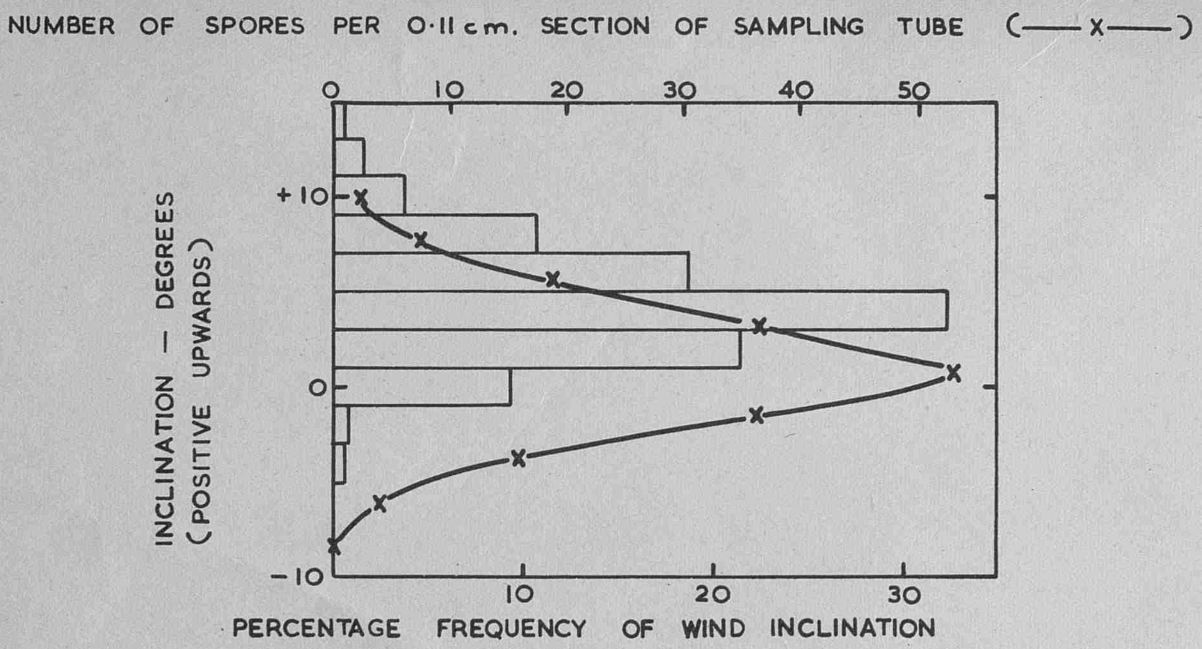

(a) SOURCE ON TOWER AT HEIGHT OF 32·5 m., SAMPLING AT 50 m. DOWNWIND, NEUTRAL CONDITIONS OF STABILITY.

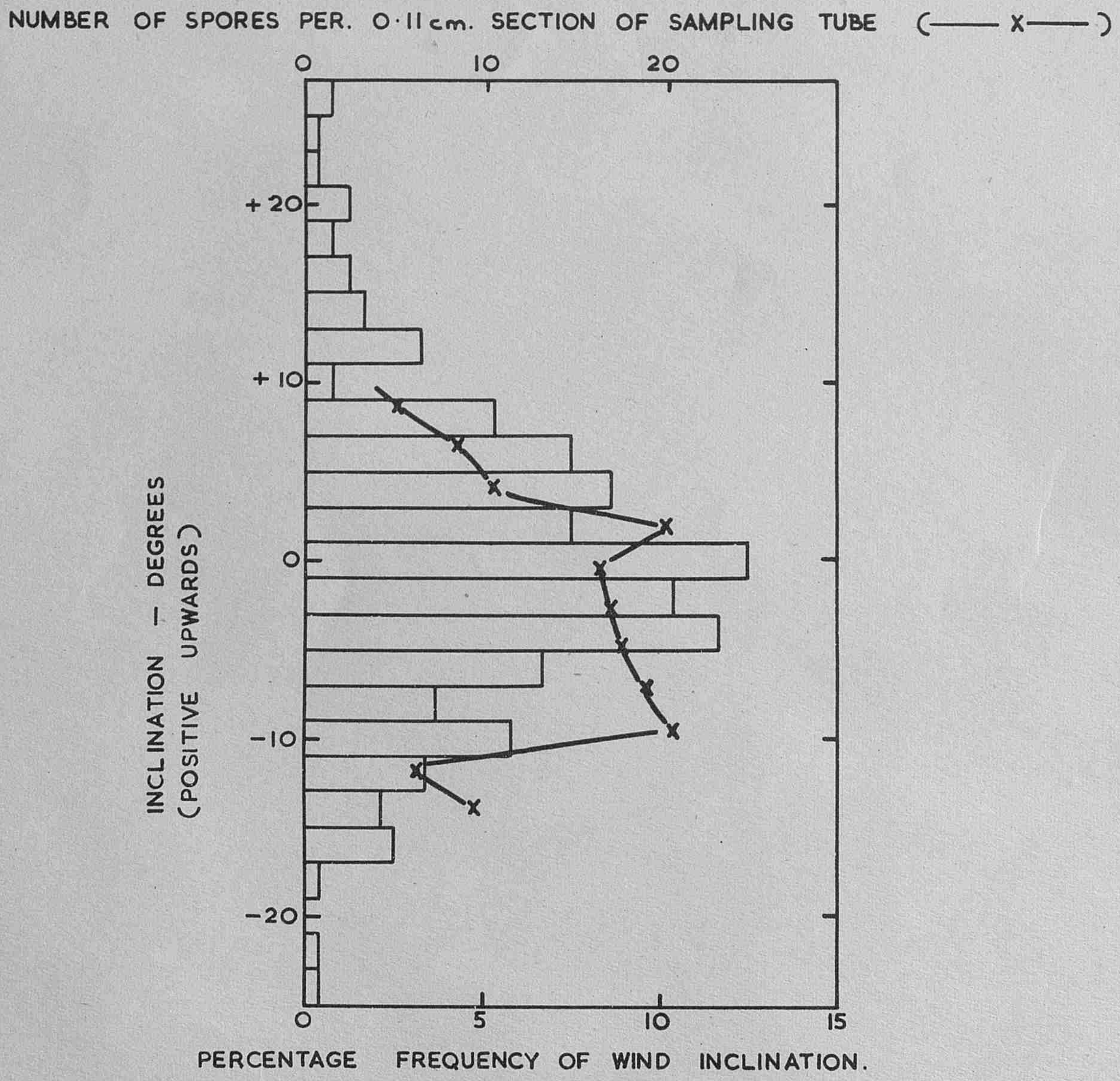

(b) SOURCE ON BALLOON CABLE AT HEIGHT OF 500 ft., SAMPLING AT 100 m. DOWNWIND, UNSTABLE CONDITIONS.

FIG. 5 DISTRIBUTIONS OF WIND INCLINATION AND SPORE DEPOSIT.

Mats (AWS)

M.R.P. 965
S.C. 11/207
31st March, 1956.

AD 223096

OBJECTIVE ANALYSIS

by

D.H. Johnson

(Meteorological Office)

AIR MINISTRY

METEOROLOGICAL RESEARCH COMMITTEE

56-1188

At the time of issue this report has not
been published. Any author desiring to
quote this paper should refer to it as "A
paper of the Meteorological Research
Committee (London).
M.R.P. No.965 by Mr. D.H. Johnson.
A copy is available in the Library of
the Meteorological Office".

M.R.P.965
S.C.II/207
31st March, 1956

AIR MINISTRY

METEOROLOGICAL RESEARCH COMMITTEE

Objective Analysis

by

D.H. Johnson (Meteorological Office)

1. Introduction

Techniques of numerical forecasting which are being developed in several countries, require the specification of the initial state in terms of the heights of isobaric surfaces and the thicknesses of isobaric layers at a network of points. For experimental numerical forecasts, produced in the Forecast Research Division (1), contour charts were constructed by the thickness technique and values of the contour height were read off from the charts, at the grid points, by interpolating between the isopleths. The time taken for the whole process, including plotting of observations, drawing of charts, interpolation and checking is to be measured in hours and exceeds the time taken by the faster electronic computers to produce a 24-hour forecast. If the initial processing of the data could be performed objectively, by numerical methods adapted for use with electronic machines, an appreciable economy in time might result.

Some elementary experiments in objective analysis are described in this paper. The computations were carried out on the Ferranti Mk. I machine at Manchester University by F.H. Bushby and V.M. Huckle, who also devised the programmes.

2. The problem

The Central Forecasting Office is concerned with a region, over different sectors of which the observations vary greatly in density, frequency, accuracy and homogeneity. A practical scheme of analysis requires a degree of flexibility sufficient to deal with these variations. The system of graphical analysis at present used in routine work enables the following factors to be considered in the construction of a contour chart for a given level:

(i) observations of height and wind for the synoptic hour to which the analysis relates - allowance is made for random errors, systematic errors affecting whole networks and mistakes due to coding, transmission, etc.;

(ii) continuity in time from previous analyses;

(iii) continuity in the vertical through the thickness technique, which not only maintains consistency between levels but also allows the upper air analysis to benefit from the more precise definition of the surface pattern.

In parts of the European network, for example over the British Isles, the observations are so close together that no attention need be paid to items (ii) and (iii) but elsewhere, particularly over the Atlantic, the latter factors are very important. It seems inevitable that a successful scheme of objective analysis must also take into account continuity in time and

/consistency

consistency in the vertical. As a first step, however, attention has been confined to the basic problem of interpolating within a two-dimensional network of observations, without regard to conditions at other levels or at other times.

3. Method of approach

One method of interpolating for the height of a contour surface at a given grid point is to represent the contour height over some area surrounding the grid point mathematically as a function of position, the function being chosen so as to give the appropriate values at the observing stations. By applying the geostrophic relation the conventional analyst is able to take the observed winds into account in spacing and aligning the isopleths of contour height, and it seems reasonable to use winds as well as contour heights to determine the required function.

An attempt was made to represent the contour height, H, as a quadratic function of suitable co-ordinates on the earth's surface. The co-ordinates chosen were those used for the numerical forecasts. They corresponded to rectangular Cartesian co-ordinates on a stereographic orthomorphic projection of the earth's surface from the south pole onto the tangent plane through the north pole. H was taken to be expressible in the form, $H = ax^2 + 2hxy + by^2 + 2gx + 2fy + c$ where a, h, b, g, f, c were constants to be determined from the observations. Because the observations contained errors, it was advisable not to fit them exactly but to introduce a degree of smoothing using the principle of least squares. A least-squares solution was obtained by choosing a, h, etc., so as to minimise the expression,

$$\sum_i (H - H_i)^2 + T^2 \sum_i (\mathbb{V} - \mathbb{V}_i)^2 \qquad \ldots\ldots (1)$$

where the H_i were the observed contour heights, the $\mathbb{V}_i$ were observed winds, $\mathbb{V}$ was the geostrophic wind, T was a weighting factor which decided the relative weight to be given to contour height and wind observations, and the summation was taken over i observing stations. Components of $\mathbb{V}$, V_x and V_y, were given by $-\frac{\beta g}{l}\frac{\partial H}{\partial y}$ and $\frac{\beta g}{l}\frac{\partial H}{\partial x}$ respectively, where g, l have their usual significance and β is a magnification factor arising from the choice of co-ordinates. The second term of (1) could be expanded as $T^2\left\{\sum_i (V-V_i)_x^2 + \sum_i (V-V_i)_y^2\right\}$, the subscripts denoting x and y components. Evidently, each wind observation gives two independent pieces of information regarding the contour gradient. Equation (1) was minimised when a, h, etc. satisfied the six simultaneous linear equations obtained by partial differentiation of expression (1) by a, h, b, g, f, and c, in turn.

4. Choice of weight

The weighting factor, T, which occurs in expression (1), holds a balance between contour heights and winds and depends, amongst other things, upon the units of H and $\mathbb{V}$. It allows the terms $\sum_i (H-H_i)^2$ and $T^2 \sum_i (\mathbb{V}-\mathbb{V}_i)^2$ to attain the same order of magnitude: if these terms differed greatly, the least squares process would ignore the smaller of the two. In the computations described below it was convenient to work with $\mathbb{V}$ in ft./sec. and H in ft. For the two terms of expression (1) to have equivalent dimensions, the units of T have been taken as seconds. The value of $\sum_i (H - H_i)^2$ depends on the random errors of observation of contour height and also upon a kind of topographical error which arises because quadratic surfaces comprise a restricted class of shapes: the true contour surface will not in general coincide with one of these shapes, although there may be a sufficient resemblance over a limited area. $\sum_i (\mathbb{V} - \mathbb{V}_i)^2$ contains ageostrophic effects as well as errors of observation and errors of a topographical character. The "topographical" errors will vary according to the function used to represent the contour surface, so T itself may require adjustment according to the function chosen.

Computation No. 1

To determine an optimum weighting factor, a quadratic surface was fitted, by the method outlined above, to 500 mb. heights and winds from six British stations, Aldergrove, Hemsby, Crawley, Leuchars, Camborne and Valentia, for 100 occasions selected from the first nine months of 1954. Computations were made in each case for the ten integral values of T from 0 to 9. Occasions were chosen when there were reports of contour height and wind from all six stations, but otherwise the cases were picked at random. To test the value of the quadratic surfaces for interpolation, the heights and geostrophic winds given by the surfaces for Liverpool were compared with those observed by the Liverpool upper air station. Figure 1 shows the disposition of the stations used for these and subsequent calculations. The root-mean-square differences between observed and computed contour heights and winds at Liverpool for the 100 cases, are shown graphically in Figure 2. Values for T = 0 were special since, if the winds are ignored, the six contour heights can be fitted exactly by a quadratic and there is no smoothing. The lowest interpolation errors apparently occurred in the range from T = 1 to T = 2, where the r.m.s. wind difference was 11.4 kt. and the height difference was 52 ft.

Figure 3 shows the variation with T of the r.m.s. height and wind differences when summed over the six stations to which surfaces were fitted and over the 100 cases. In the range T = 1 to T = 2 the r.m.s. height difference rose from 21 to 30 ft. whilst the r.m.s. wind difference fell from 15 to 12 kt. (25 to 20 ft./sec.). So the two terms of expression (1) did in practice attain the same order of magnitude:- at T = 1, $\sum (H - H_i)^2 = 400$ ft. while $T^2 \sum (\mathbb{V} - \mathbb{V}_i)^2 = 625$ ft.^{2}, T^2 having units of sec.^{2}; at T = 2, $\sum (H - H_i)^2 = 900$ ft.^{2} while $T^2 \sum (\mathbb{V} - \mathbb{V}_i)^2 = 1600$ ft^2.

Computation No. 2

It was remarked above that the results obtained for T = 0 in Computation No. 1 were special since the contour heights at the six stations were exactly fitted. The computations were repeated for 40 of the 100 cases using observations from Stornoway and Lerwick in addition to the six previously used. In this case, even at T = 0, there were more pieces of information than were required to determine the co-efficients of the quadratic uniquely.

In Figure 4 the r.m.s. height and wind differences at Liverpool for the eight station computations are compared with results for the same 40 cases from Computation No. 1. Except for the heights at T = 0, the Computation No. 2 differences exceed those of Computation No. 1. The inclusion of the two extra heights reduced the r.m.s. Liverpool height difference considerably. The improvement here was due entirely to the beneficial effect of smoothing out errors of observation, etc., since results for T = 1 to T = 9 suggest that it was generally undesirable to extend the area over which the quadratic was fitted beyond that covered in Computation No. 1. As in Computation No. 1, values of T in the range from T = 1 to T = 2 appeared to be satisfactory from the point of view of minimising the errors of representation. Neither the wind nor the height errors were very sensitive to variations in T.

Figure 5 gives the standard errors of fitting at the eight stations. These may be compared with the corresponding values for Computation No. 1 in Figure 3. Computation No. 1 values were smaller except for the winds at T = 0.

Computation No. 3

To examine whether a surface of greater complexity than the quadratic was of more value for interpolation, a cubic surface was fitted to the six stations used for Computation No. 1, in 38 cases. The method of obtaining the best-fitting surface was similar in principle to that outlined in Section 2 for the quadratic. Computations were made for six values of T: $T = 1, \sqrt{2}, 2, 2\sqrt{2}, 4$ and 6.

The r.m.s. differences between observed and interpolated heights and winds at Liverpool are given in Figure 6. Neither the height nor the wind differences showed much variation over the range of T explored, but such variations as there were followed a different pattern from the quadratic results of Computation No. 1. The lowest Liverpool wind difference occurred at about T = 4 whereas the height errors increased with T throughout the range examined. The cubic results are best compared with the quadratic six-station values given in Figure 4 which, with two exceptions, refer to the same occasions. The two exceptions do not materially affect the comparison. The cubic surfaces gave a slightly better fit than the quadratic at Liverpool.

Figure 7 gives the r.m.s. errors of representation at the six stations whose observations were used to obtain the cubics. The values are naturally lower than those obtained for the quadratic (Figure 3) since the cubics have a greater degree of freedom.

The cubic results show how the choice of weighting factor T may depend upon the purpose for which the interpolation is required. A preliminary to the preparation of a numerical forecast is the evaluation of the Laplacian derivative of the initial contour field. Normally, the Laplacian is derived from the set of interpolated contour heights by means of the finite difference approximation. If the contour field is represented by some mathematical function, it is possible to obtain the Laplacian in a second way, namely by direct differentiation of the function itself. For this latter purpose it is desirable that the function should not just give an accurate interpolation for height at the grid point, but should also approximate closely to the true contour surface over a certain area surrounding the grid point. In Computation No. 3 the contour height interpolation error was lowest at T = 1 (Figure 6), but Figure 7 shows that at T = 1 the heights at the six stations were fitted with an error of only 10 ft. This closeness of fit was unrealistic since the standard error of measurement of 500 mb. contour height at British stations is 30 ft. Furthermore the winds at the six stations were fitted at T = 1 with an error of about 10 kt., which is larger than the standard error, 3 kt., of British 500 mb. wind observations. At T = 4, on the other hand, the r.m.s. height error at the six stations was 30 ft. and the r.m.s. wind error was 5 kt. Thus, if a realistic fit is required over an area of 300 mi. or so centred upon Liverpool, a weighting factor T = 4 is to be preferred to T = 1.

According to Murray (2) the r.m.s. difference between observed winds and geostrophic winds measured from the C.F.O. working charts is 14 kt. at 500 mb. over the British Isles. It is interesting to note that the wind values interpolated from the cubic surfaces when compared with independent observed winds gave a r.m.s. difference of less than 10 kt. Murray shows that the 14 kt. can be broken down into the following components: 9 kt. due to the ageostrophic wind; 4 kt. due to turbulent wind fluctuations; 3 kt. due to errors in the observed wind; 9 kt. due to errors inherent in the graphical technique. The error of representation of the wind field given by the true contour pattern will contain the first three of these four components and should therefore have a root-mean-square value of about 10 kt. On this basis it appears that the 5 kt. error of representation at the six stations, given by the cubics for a weighting factor T = 4, is lower than is justified, but there is an advantage to be gained in fitting the winds more closely than seems proper on purely geostrophic grounds. Numerical forecasting requires the specification of the initial field of vorticity. The geostrophic vorticity, deduced from the contour pattern, is used as an approximation to the vorticity of the actual wind field. This approximation is believed to be responsible on occasions for sizeable errors in the forecasts. It may therefore be advantageous if the "geostrophic" wind field deduced from the objective analysis actually incorporates certain ageostrophic effects, and thus gives a closer approximation to the true wind field than the geostrophic wind field implied by the true contour pattern. Such a shrewd objective analysis is possible because the ageostrophic effects (apart from turbulence) are not distributed randomly, but form a sensible pattern of variation on the synoptic scale.

5. Various networks - Computation No. 4

The six-station network, centred upon Liverpool, was chosen somewhat arbitrarily as suitable for use in the above interpolation experiments. To examine the effect on the errors of representation of varying the distribution and quantity of data, quadratic surfaces were fitted to sixteen selections of data from the eight stations used in Computation No. 2. The computations were made with a weighting factor $T = \sqrt{2}$ for each of 40 occasions. The r.m.s. errors of representation at Liverpool and at stations used in the computations are given for each selection in Table 1, which also contains, for comparison, values previously obtained for corresponding occasions in the six-station and eight-station calculations (Computations Nos. 1 and 2).

The first six rows of Table 1 (series B, C, D, E, F and six-station) give information regarding the relative value of contour heights and winds. Comparing the Liverpool interpolation errors, series D, E and F, which contained more heights than winds, improved markedly upon series B and C in which winds preponderated.

Series M, K and I contained wind and contour height observations from five, four and three stations respectively, a compromise being made in the choice of stations between proximity to Liverpool and regularity of distribution. Each of these arrangements gave errors of interpolation similar to those of the six-station data, except that the three-station arrangement (series I) gave a slightly better fit to the Liverpool wind: Liverpool is not far from the centroid of the triangle formed by the three stations, Aldergrove, Hemsby and Camborne. When the size of the triangle was increased (series J and H), the interpolation errors were also increased.

Most of the above selections were chosen so as to have a reasonably symmetric distribution with respect to Liverpool, although comparison between series D and E shows how the disposition of the two winds materially affected the contour height errors. In series N, O and P the data were not symmetrically arranged about Liverpool, in fact for series O and P the problem was one of extrapolation rather than interpolation. In these last three cases the errors of representation were comparatively large.

6. Distance weighting - Computation No. 5

Since the correlation between the winds or contour heights at two places varies inversely with their distance apart, it may be possible to reduce the interpolation errors by weighting the observations according to their distance from the grid point. To examine this possibility a quadratic surface was fitted to the six stations of Computation No. 1 for 100 cases, each observation being weighted by a factor, p, which was a function of distance from Liverpool. The expression to be minimised, in place of expression (1) was,

$$\sum_i p_i (H - H_i)^2 + T^2 \sum_i p_i (\mathbb{V} - \mathbb{V}_i)^2$$

Two sets of distance weighting factors were tried. The first weight, p_α, was expressible as a function of distance, r, from Liverpool in the form $1/1+r^3$ and the second weight, p_β , as $1/1+r$. The unit of r was chosen so that for p_α , Valentia observations received about one half of the weight given to Aldergrove observations, and for p_β , Valentia observations received about three-quarters of the weight given to observations from Aldergrove. The weighting factors are shown graphically in Figure 8.

The interpolation errors are given in Table 2. The results were disappointing. Not only were the average errors practically unchanged by distance weighting, but the individual surfaces for the same occasions were nearly identical. Possibly the distance weights were not sufficiently discriminating, but it is more likely that the network of stations was unsuitable for distance weighting experiments, since four of the stations were bunched together on the distance scale (see Figure 8).

7. Oceanic networks

The foregoing experiments gave promising results, but the British network of upper air observations is probably the best in existence for accuracy and density of observations. The worst networks are found over the oceans. A difficulty which arises in experimenting with a weather ship network is that the reservation of one observation for verification purposes alone seriously depletes the network. The alternative to checking the objective interpolations against observations is to compare them with values read from a conventionally analysed chart. This latter practice may be unsound however, particularly for experiments in which "T" is varied, since the conventional analysis is subjective and itself depends upon the analyst's opinion regarding the relative weights to be given to wind and height observations. To avoid these difficulties the five stations, weather ships "I", "J" and "K", Crawley and Stornoway were chosen as being equivalent to a mid-ocean network. Valentia observations were used to test the accuracy of the interpolated values.

Computation No. 6

Quadratic surfaces were fitted to observations from the five stations for 100 occasions chosen from the year 1954. Computations were made for T-values of 1, 2 and 4. The errors of representation appear in Table 3. The interpolation errors considerably exceeded those obtained in previous computations.

Computation No. 7

Computation No. 6 was repeated, replacing the quadratic surfaces by cubics. Table 3 contains the results. The Valentia errors are slightly smaller for the cubics than for the quadratics.

8. Individual cases

On a few occasions the height contours given by the objective analyses have been drawn for visual comparison with the contours produced by analysts at the Central Forecasting Office for routine use. Figures 9 to 15 show the individual analyses. In scrutinising the objective analyses it should be borne in mind that the only stations taken into account in their computation were, Aldergrove, Hemsby, Leuchars, Crawley, Camborne and Valentia (not Liverpool). The objective analyses were not designed to give any sort of a fit outside of the area bounded by these stations.

Figures 9 to 13 contain quadratic analyses for three values of T. It is obvious that as T increased, the fit to the winds at the six stations was improved at the expense of the contour heights. Analyses for T = 0 take no account of the winds. In Figures 9(a), 12(a) and 13(a) the analyses for T = 0 are quite unrealistic and give high errors of interpolation at Liverpool. The quadratic contours are recognisable as families of conic sections: there is a slight distortion because the projection of the map on which they are drawn is conical, not stereographic.

In Figures 9, 14 and 15 quadratic analyses may be compared with cubic analyses for the same occasions.

9. Comparison with other work

Attempts to represent wind and contour fields by cubic polynomials have been made by Panofsky (3). Cubics were fitted over an area of the order of 10^6 square miles, which is about four times greater than the area considered for Computation No. 1. The intention was ultimately to construct an objective analysis by piecing together several such cubic surfaces. Calculations were not made electronically and few cubics were computed. Winds were weighted by a factor corresponding to T = 2. Visual comparison of the objective analyses with the corresponding subjective analyses showed that the two methods gave similar contour patterns, but the objective analyses were somewhat smoother. The Laplacian derivatives of the contour fields were also computed: here the agreement was "not good".

The last result might have been anticipated since the Laplacian of a cubic is a linear function and experience of vorticity fields computed from subjective analyses suggests that the true vorticity fields are very far from linear; in fact they are usually more complex than the contour patterns themselves. The implication of comparative simplicity of the vorticity field may be a considerable objection to the use of polynomials in representing contour patterns over large areas.

Gilchrist and Cressman (4) electronically computed objective analyses for a grid of 19 x 19 points covering most of North America and a part of the Atlantic. The method was very similar to that used for the computations described in Section 4: a quadratic surface was fitted to observations within a limited distance of a grid point to obtain an interpolated contour height. The process was repeated for each grid point. The computations were made for a single occasion and for a series of values of T. The interpolated heights were compared with the mean of three subjective analyses. The minimum height errors occurred with a wind weighting factor corresponding to T = 2. The finite difference Laplacians were computed for both objective and subjective analyses, the closest agreement being attained at T = 3. Numerical forecasts were made on the basis of both analyses. It is stated that neither forecast was observably superior to the other. The 24-hr. changes in 1000 mb. height, forecast by the two methods, were correlated and gave a correlation co-efficient of •96. The authors conclude that where a good data coverage is found, e.g., over North America, objective analyses are satisfactory for numerical prediction.

10. Future investigations

The experiments described in Sections 4 to 6 have shown that in a close network of observations, a reasonably accurate objective interpolation for contour height and wind can be made. Comparisons with the errors of representation of the conventional contour analysis, made in Section 4, suggest, as did the work of Gilchrist and Cressman, that in regions of good data coverage, objective analyses will probably be at least as satisfactory as conventional analyses for numerical prediction. However, it was pointed out in Section 2 that only in limited regions would an analysis, which took no account of continuity in time and in the vertical, give good results. Computations described in Section 7 for the ocean network confirmed this expectation.

/There

There is no difficulty in principle in introducing an element of continuity in time into the analysis, for forecast values of height and wind can be taken into account in the least squares process on the same basis as observations. The weight given to a forecast value would naturally be much less than the weight given to an observation.

The object of the present series of computations was to derive interpolated heights and winds for a single grid point. In extending the technique to get interpolations over a network of grid points one is led to consider whether it is better to represent the contour field over the whole network by a single function or whether a fresh function should be derived for each grid point. Gilchrist and Cressman (4) point out that the latter alternative agrees with synoptic practice in considering data only from the immediate vicinity of the grid point in question. For the former alternative, difficulties may arise due to the dependence of the expression for the contour height at a given grid point on data from distant regions. There is also the objection to the use of a single function for representation over a wide area mentioned in Section 9, namely that the degree of complexity of the implied geostrophic vorticity field may be over-restricted, although this objection would be less valid for harmonic functions, for example, than for polynomials. On balance, it seems that the method which treats each grid point independently is likely to prove the more flexible approach and at the present stage there seems no reason for adopting an alternative technique, although other approaches will require investigation in due course.

11. Conclusions

(1) In a close network of reliable observations, objective analyses are capable of representing the 500 mb. winds with a standard error of about 10 kt. This figure compares favourably with the errors of representation, about 14 kt., of the Central Forecasting Office routine analyses for the same area.

(2) In more open networks, such as are found over the Atlantic Ocean, providing that both winds and contour heights are available, winds can be interpolated with a standard error of about 16 or 17 kt. Errors of the conventional analysis are not known for such a region, but they are unlikely to be less than 16 or 17 kt., judging from the data available for the land area.

(3) The optimum weight to be given to wind observations as compared with contour heights varies according to the nature of the interpolation. When interpolating for wind or contour height using quadratic surfaces the weighting factor is best chosen so that a discrepancy of 30 ft. in contour height receives the same weight as a discrepancy of 10 - 15 kt. in wind. Using cubic surfaces, a similar weight gives good results in interpolation for contour height, but the optimum weight for wind interpolation equates a discrepancy of 30 ft. in contour height to a discrepancy of 5 kt. in wind.

(4) The errors of interpolation are not very sensitive either to small variations in the relative weights given to contour heights and winds or to small variations in the number and disposition of the observations.

(5) Tests to determine the effect of weighting observations according to their distance from the grid-point at which an interpolation is required are considered inconclusive and it is recommended that a further test be made with a less regular network of observations.

/(6)

(6) There is ample justification in results so far obtained for further work designed to produce interpolated contour heights at a network of points over the whole area from which the initial data must be taken for numerical forecasting. These experiments should include methods of maintaining continuity in time and consistency between levels.

12. References

(1) Bushby, F.H. and Hinds, M.K. 1954 Quart. J. R. Met. Soc., Vol. 80, p. 165.

(2) Murray, R. 1954 Met. Office, London, Professional Notes, Vol. 7, No. 110.

(3) Panofsky, H.A. 1949 J. Met., Vol. 6, p. 386.

(4) Gilchrist, B. and Cressman, G.P. 1954 Tellus, Vol. 6, p. 309.

Table 1. Computation No. 4. Errors of

Series	Selection											
	Heights								W			
	Ald.	Hem.	Leu.	Cra.	Cam.	Val.	Sto.	Ler.	Ald.	Hem.	Leu.	Cr
B	1								1	1	1	
C	1								1	1	1	1
D	1	1	1	1	1	1			1			
E	1	1	1	1	1	1			1	1		
F	1	1	1	1	1	1			1	1	1	1
6-station	1	1	1	1	1	1			1	1	1	1
8-station	1	1	1	1	1	1	1	1	1	1	1	1
M	1	1	1	1	1				1	1	1	1
L		1	1		1	1				1	1	
K	1	1	1		1				1	1	1	
J			1	1		1					1	1
I	1	1			1				1	1		
A	1	1			1				1	1		
H				1		1		1				1
N	1	1	1			1	1		1	1	1	
O	1		1		1	1	1		1		1	
P	1		1				1	1	1		1	

[illegible] kt. This figure compares favourably with the errors of representation, about 14 kt., of the Central Forecasting Office routine analyses for the same area.

(2) In more open networks, such as are found over the Atlantic Ocean, providing that both winds and contour heights are available, winds can be interpolated with a standard error of about 16 or 17 kt. Errors of the conventional analysis are not known for such a region, but they are unlikely to be less than 16 or 17 kt., judging from the data available for the land area.

(3) The optimum weight to be given to wind observations as compared with contour heights varies according to the nature of the interpolation. When interpolating for wind or contour height using quadratic surfaces the weighting factor is best chosen so that a discrepancy of 30 ft. in contour height receives the same weight as a discrepancy of 10 - 15 kt. in wind. Using cubic surfaces, a similar weight gives good results in interpolation for contour height, but the optimum weight for wind interpolation equates a discrepancy of 30 ft. in contour height to a discrepancy of 5 kt. in wind.

(4) The errors of interpolation are not very sensitive either to small variations in the relative weights given to contour heights and winds or to small variations in the number and disposition of the observations.

(5) Tests to determine the effect of weighting observations according to their distance from the grid-point at which an interpolation is required are considered inconclusive and it is recommended that a further test be made with a less regular network of observations.

/(6)

Table 1. Computation No. 4. Errors of representation for eighteen selections of data

Series	Selection																R.m.s. errors of representation			
	Heights								Winds								At Liverpool		At selected stations	
	Ald.	Hem.	Leu.	Cra.	Cam.	Val.	Sto.	Ler.	Ald.	Hem.	Leu.	Cra.	Cam.	Val.	Sto.	Ler.	Wind (kt.)	Height (ft.)	Wind (kt.)	Height (ft.)
B	1								1	1	1						14·0	74	4	0
C	1								1	1	1	1	1	1			14·5	76	9	0
D	1	1	1	1	1	1			1					1			11·2	64	12	20
E	1	1	1	1	1	1			1	1							11·5	53	13	19
F	1	1	1	1	1	1			1	1	1	1					11·5	53	12	21
6-station	1	1	1	1	1	1			1	1	1	1	1	1			11·5	50	14	25
8-station	1	1	1	1	1	1	1	1	1	1	1	1	1	1	1	1	12·8	64	14	30
M	1	1	1	1	1				1	1	1	1	1				11·4	54	12	18
L		1	1		1	1				1	1		1	1			11·9	58	14	14
K	1	1	1		1				1	1	1		1				11·4	55	12	13
J			1	1		1					1	1		1			12·8	69	11	9
I	1	1			1				1	1			1				10·1	52	9	10
A	1	1			1				1	1							10·4	51	8	6
H				1		1		1				1		1		1	14·4	81	14	8
N	1	1	1			1	1		1	1	1			1	1		12·3	62	14	18
O	1		1		1	1	1		1		1		1	1	1		13·6	75	13	19
P	1		1				1	1	1		1				1	1	20·6	67	10	17

Table 2. Computation No. 5

Errors of representation for a quadratic surface using distance weighting factors

Distance weighting factors	p_α			p_β			None		
Value of T sec.	1	$\sqrt{2}$	$2\sqrt{2}$	1	$\sqrt{2}$	$2\sqrt{2}$	1	$\sqrt{2}$ *	$2\sqrt{2}$ *
R.m.s. wind error at Liverpool (kt.)	11·3	11·3	11·8	11·3	11·3	11·8	11·3	?	11.8
R.m.s. height error at Liverpool (ft.)	51	51	51	52	51	52	52	52	53
R.m.s. wind error at the 6 stations (kt.)	15	14	11	15	14	11	15	14	11
R.m.s. height error at the 6 stations (ft.)	22	26	38	22	25	37	22	25	36

* Values interpolated from Figures 2 and 3. Interpolation doubtful for r.m.s. wind error at Liverpool at T = $\sqrt{2}$.

Table 3. Computations Nos. 6 and 7

Errors of representation for quadratic and cubic interpolation using an ocean-type network

Nature of surface	Quadratic (Comp. 6)			Cubic (Comp. 7)		
Values of T sec.	1	2	4	1	2	4
R.m.s. wind error at Valentia (kt.)	18	18	19	17	17	16
R.m.s. height error at Valentia (ft.)	96	94	94	92	92	92
R.m.s. wind error at the 5 stations (kt.)	25	23	21	16	14	11
R.m.s. height error at the 5 stations (ft.)	11	30	62	6	19	46

M.R.P. 965

Fig. 1
Key to stations used in the computations

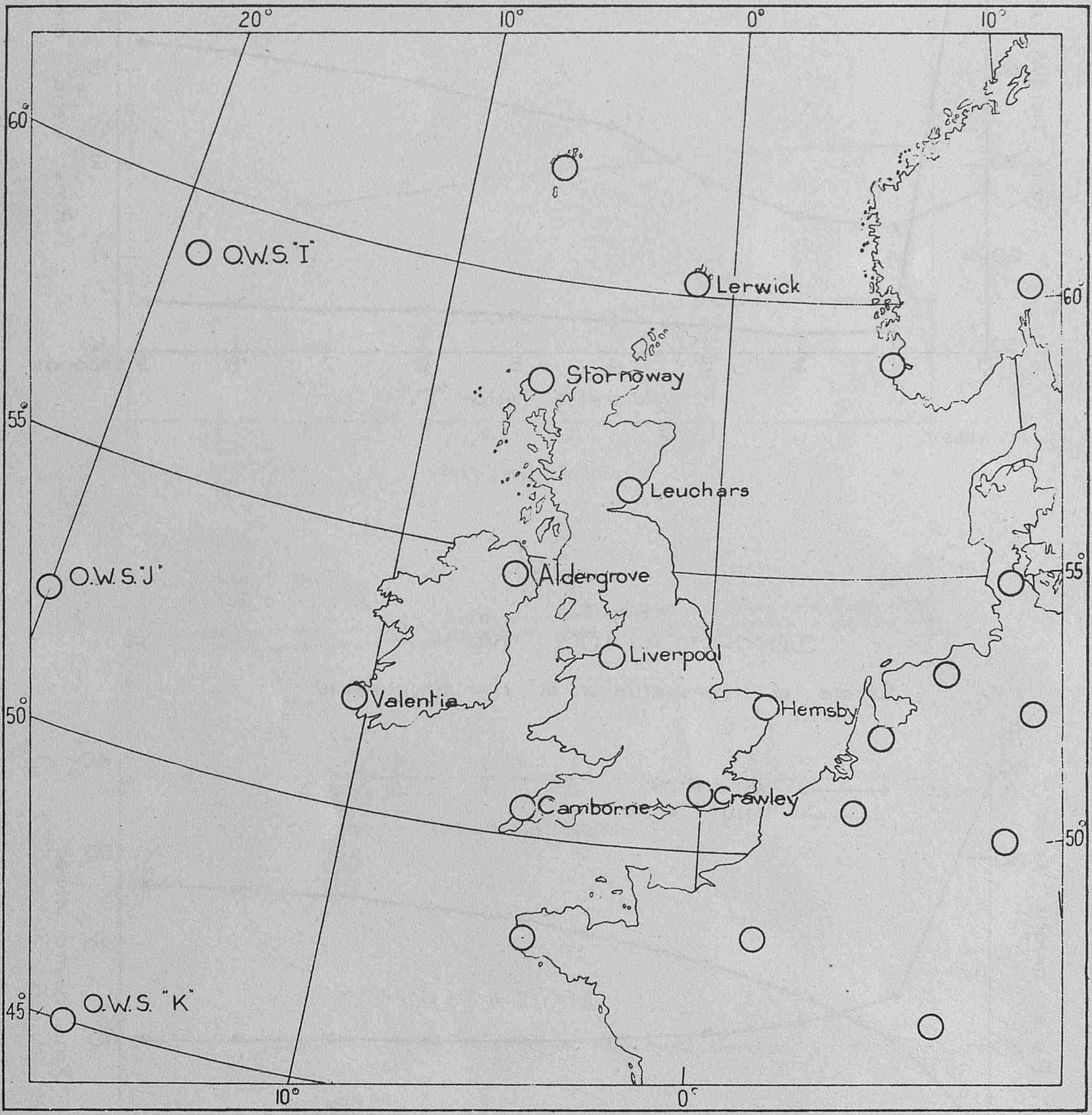
20°
10°
0°
10°
60°
55°
50°
45°
O.W.S. "I"
Lerwick
Stornoway
Leuchars
O.W.S. "J"
Aldergrove
Liverpool
Valentia
Hemsby
Camborne
Crawley
O.W.S. "K"
60°
55°
50°
10°
0°

Fig. 2

COMPUTATION No. 1

Errors of representation at Liverpool

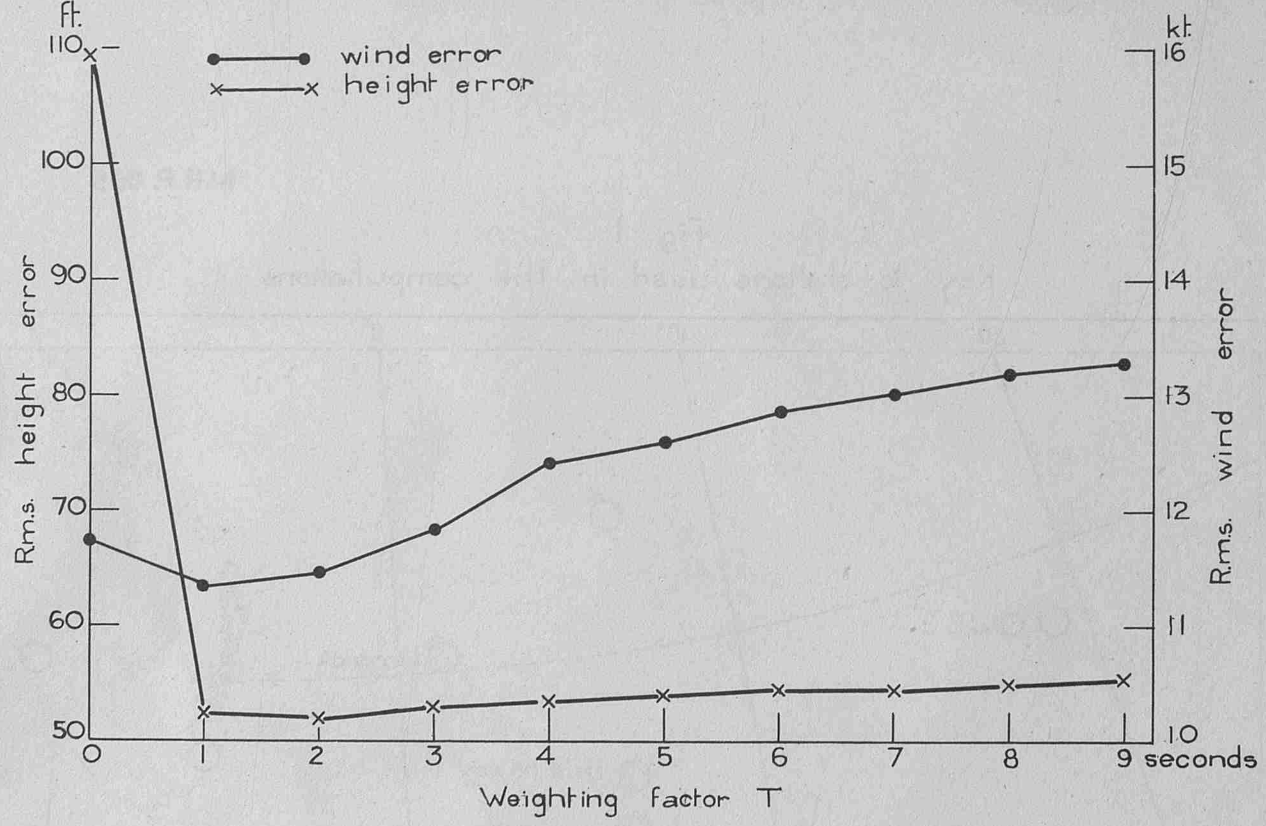

Fig. 3

COMPUTATION No. 1

Errors of representation at the six stations

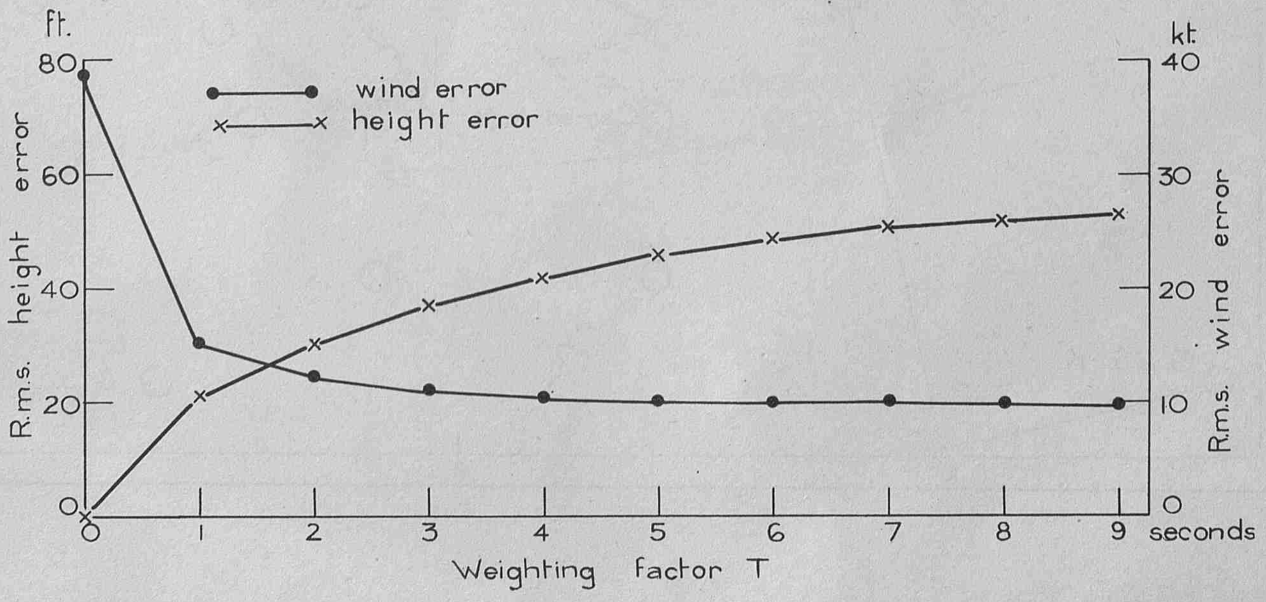

Fig. 4

COMPUTATION No. 2

Errors of representation at Liverpool

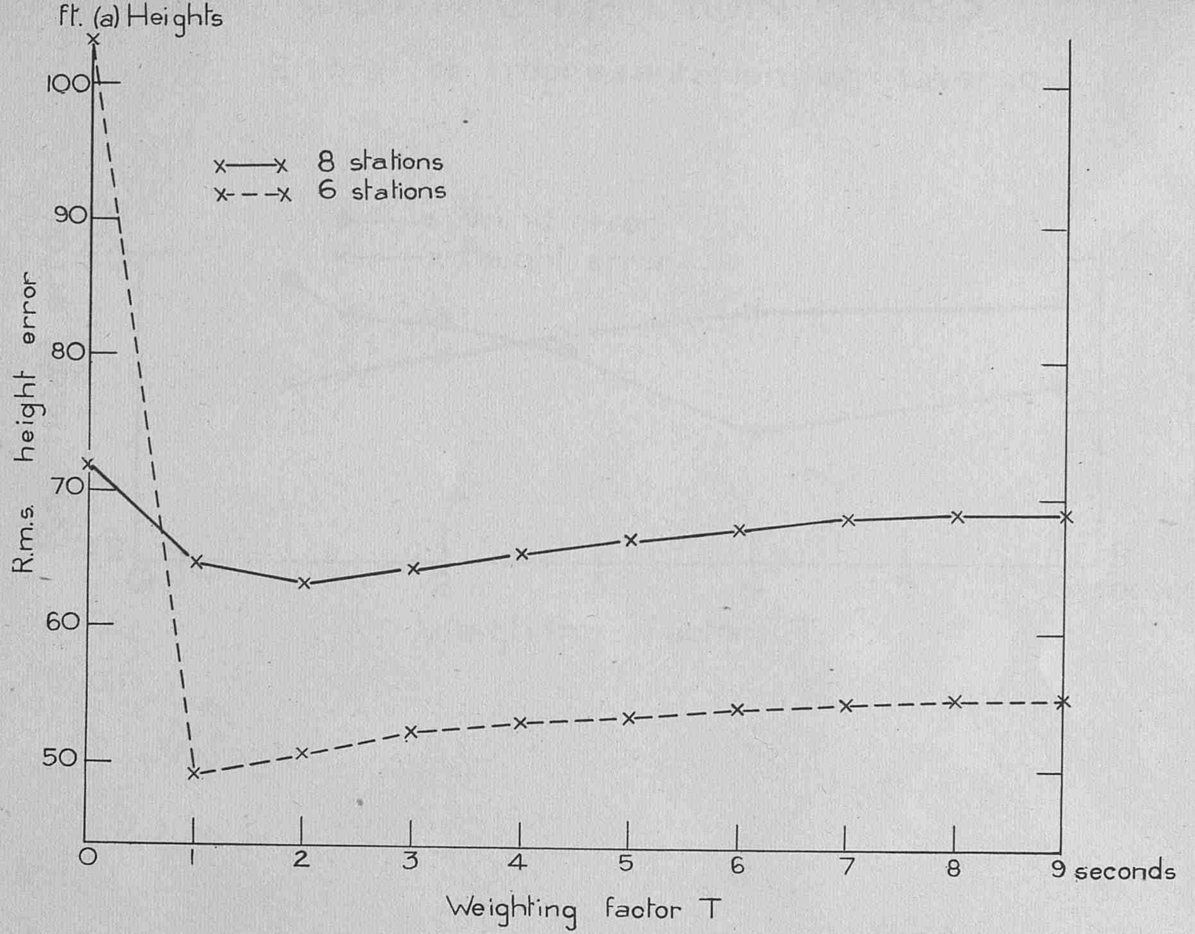

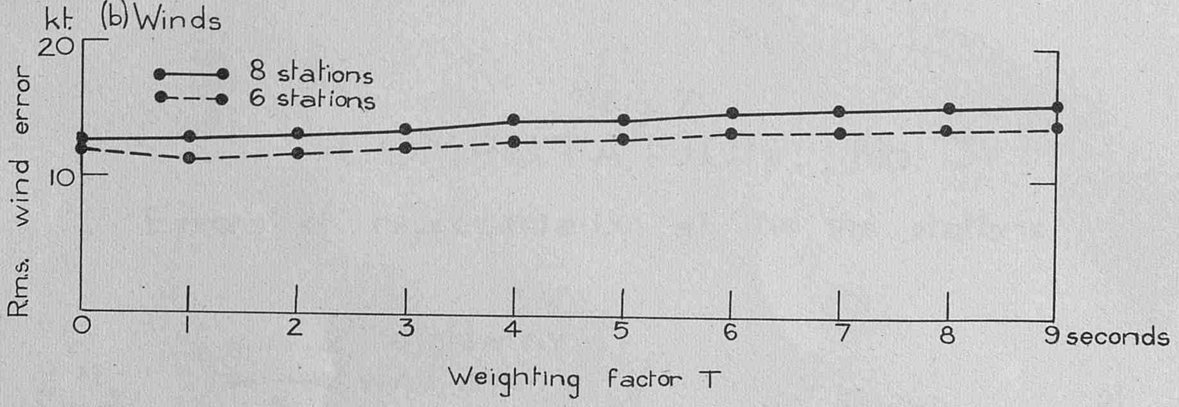

Fig. 5

COMPUTATION No. 2

Errors of representation at the eight stations

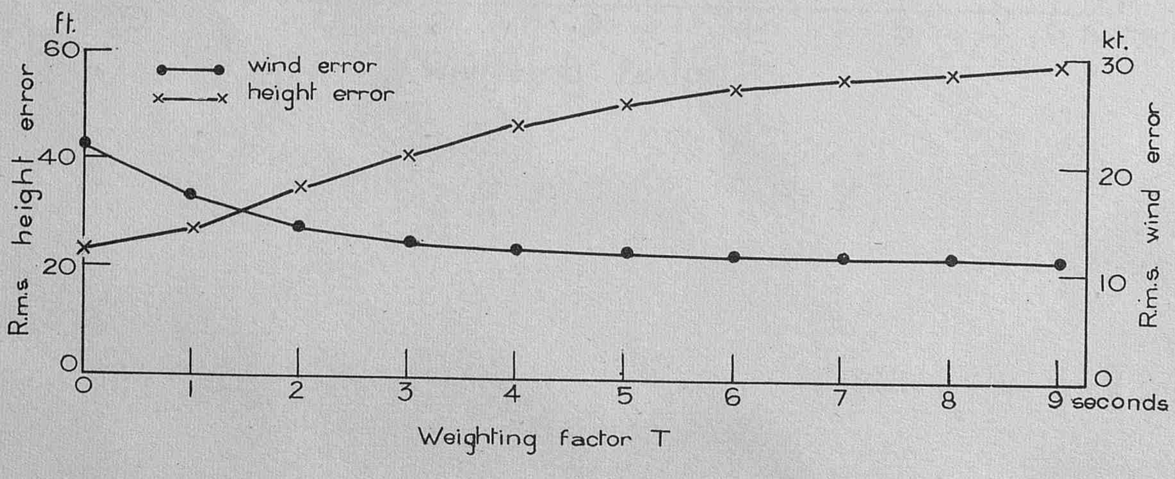

Fig. 6

COMPUTATION No. 3

Errors of representation at Liverpool

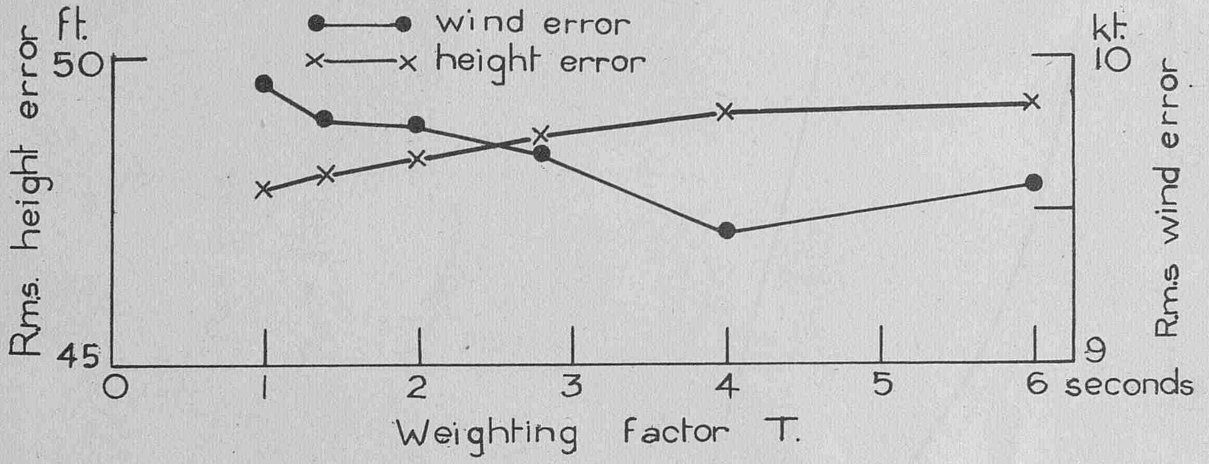

Fig. 7

COMPUTATION No. 3

Errors of representation at the six stations

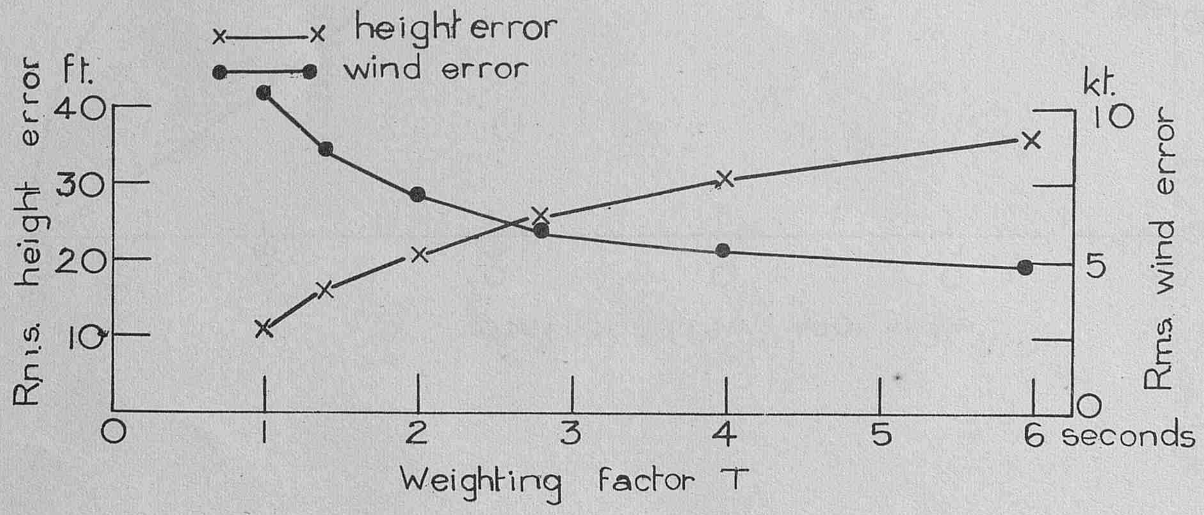

Fig. 8

COMPUTATION No. 5

Weighting factors

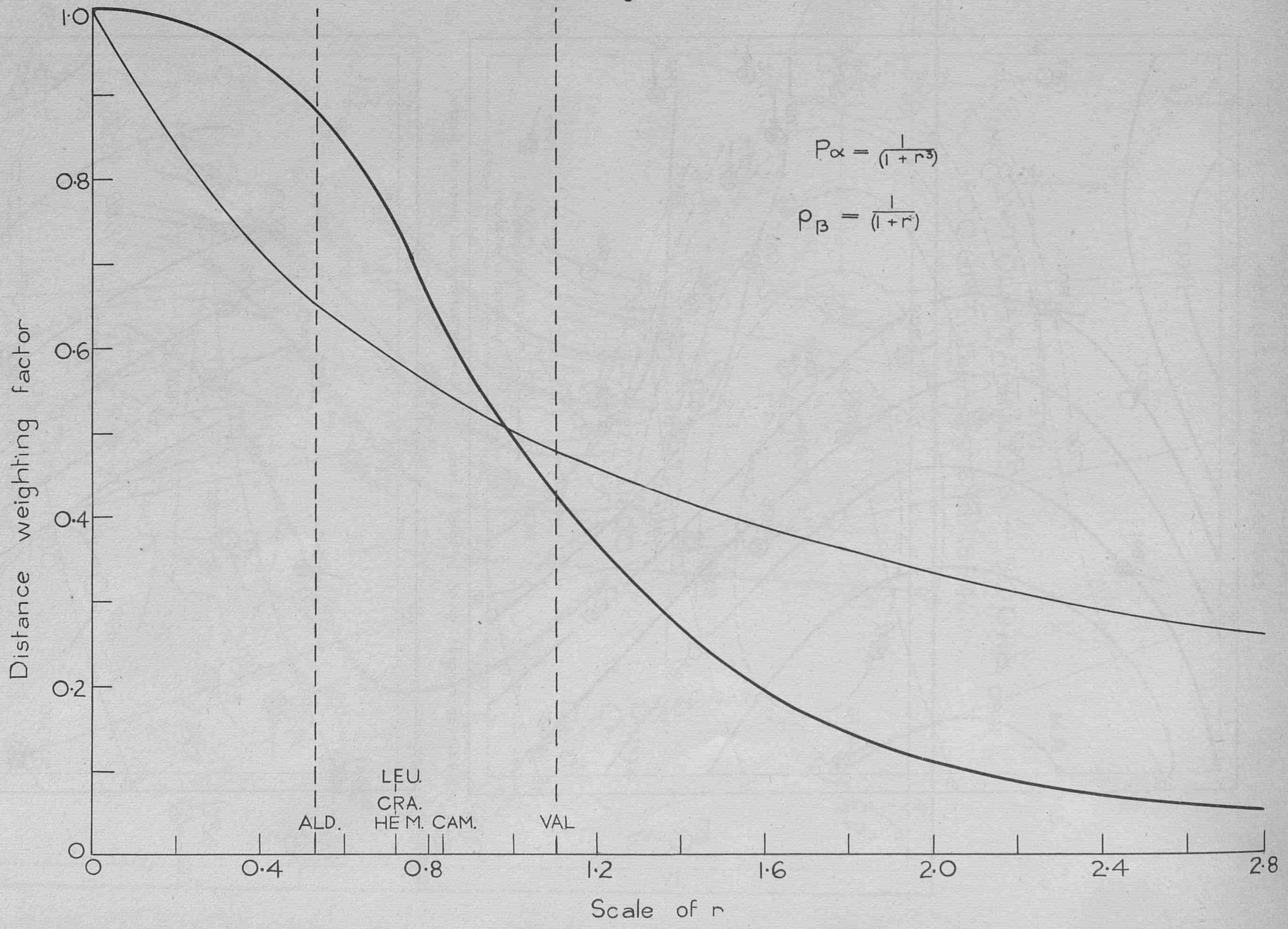

Fig. 9(a)

CONTOUR ANALYSIS — 500mb

1500 G.M.T. February 2nd 1954

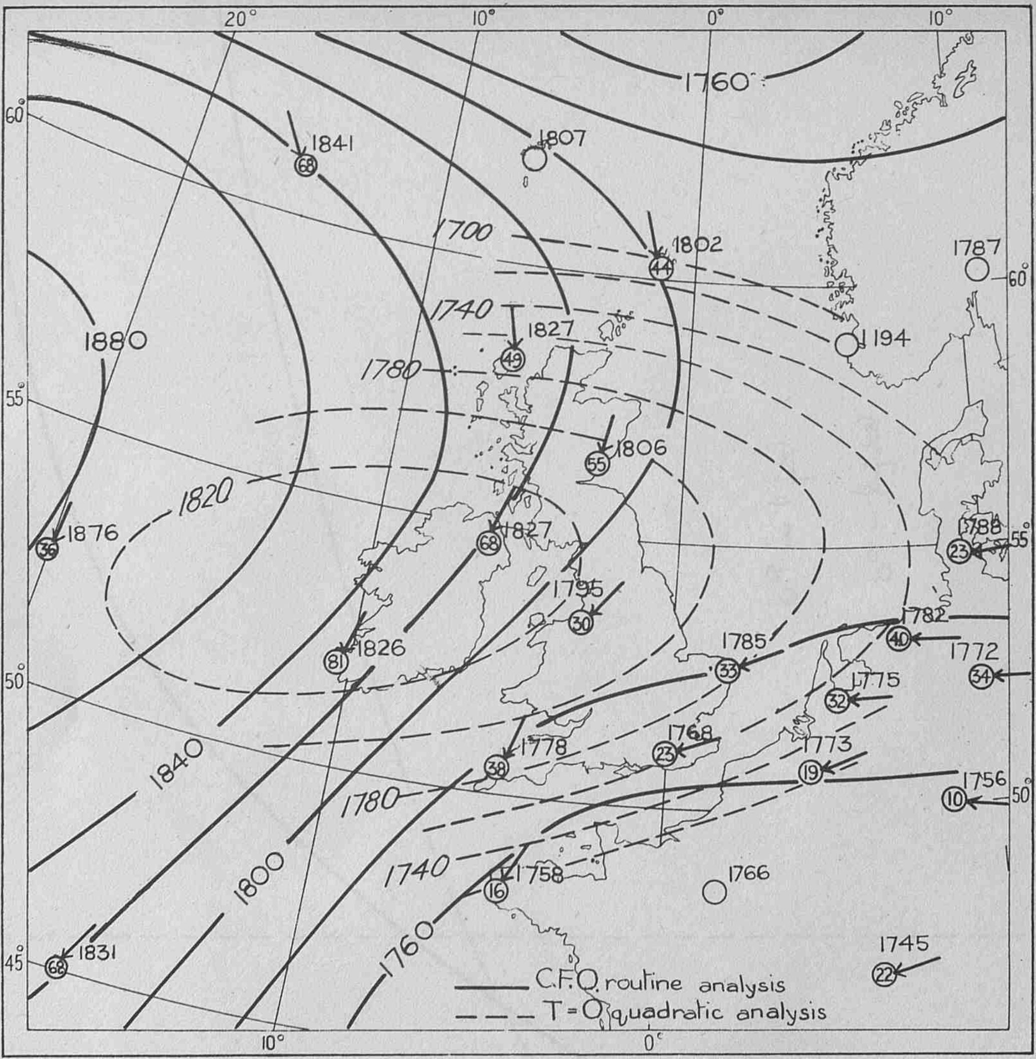
20°
10°
0°
10°
60°
55°
50°
45°
1760
1841
68
1807
1700
1802
44
1787
60°
1740
1827
49
1194
1780
1880
1806
55
1820
1876
36
1827
68
1788
23
55°
1795
30
1782
40
1772
34
1826
81
1785
33
1775
32
1840
1778
38
1768
23
1773
19
1756
10
50°
1780
1800
1740
1758
16
1766
1760
1831
68
1745
22
C.F.O. routine analysis
T=O quadratic analysis
10°
0°

Observed heights given in tens of feet. Observed wind speed given in knots.

Fig. 9 (b)

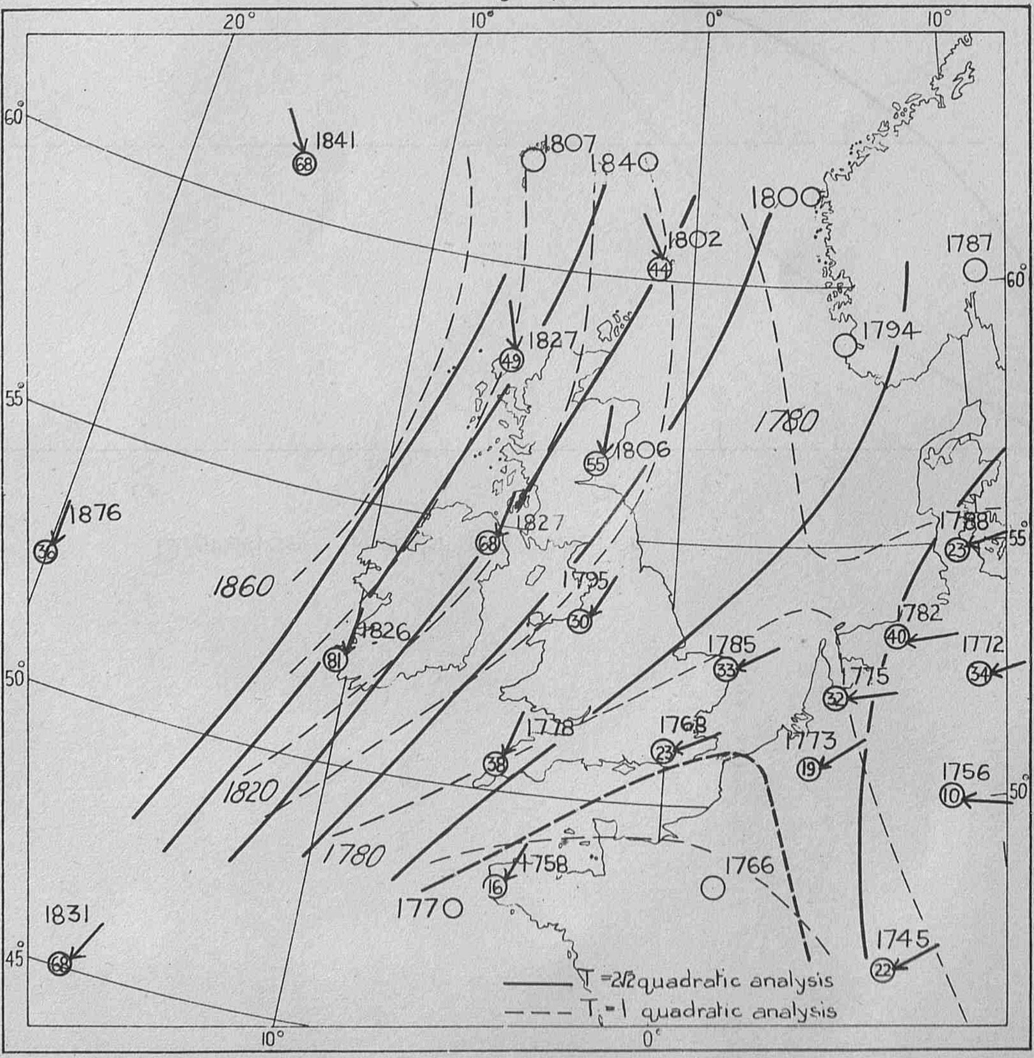
20°
10°
0°
10°
60°
55°
50°
45°
1841
68
1807
1840
1800
1802
44
1787
60°
1827
49
1794
1780
1806
55
1876
36
1827
68
1788
23
55°
1860
1795
30
1826
81
1782
40
1772
34
1785
33
1775
32
1778
38
1768
23
1773
19
1756
10
50°
1820
1780
1758
16
1766
1770
1831
68
1745
22
T=2½ quadratic analysis
T=1 quadratic analysis
10°
0°

Observed heights given in tens of feet. Observed wind speed given in knots.

Fig. 9 (c)

CONTOUR ANALYSIS — 500 mb.

1500 G.M.T. February 2nd. 1954

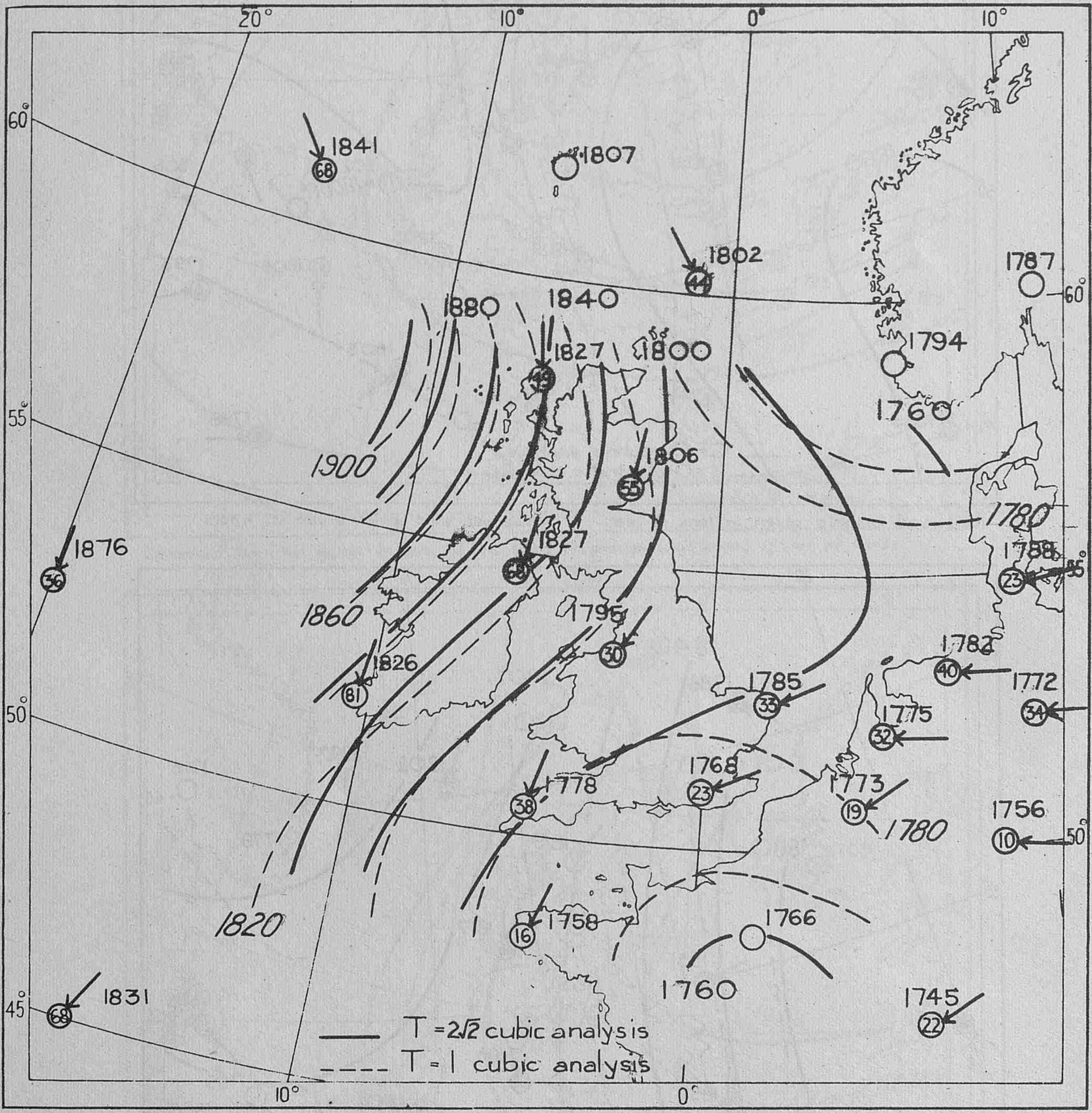
20°
10°
0°
10°
60°
55°
50°
45°
60°
55°
50°
1841
68
1807
1802
44
1880
1840
1827
49
1800
1787
1794
1760
1900
1806
55
1780
1876
36
1827
68
1788
23
1860
1795
30
1826
81
1782
40
1772
34
1785
33
1775
32
1768
23
1773
19
1778
38
1780
1756
10
1820
1758
16
1766
1760
1831
68
1745
22
T = 2√2 cubic analysis
T = 1 cubic analysis
10°
0°

Observed heights given in tens of feet. Observed wind speed given in knots.

Fig. 10 (a)

CONTOUR ANALYSIS - 500mb.

1500 G.M.T. February 15th 1954

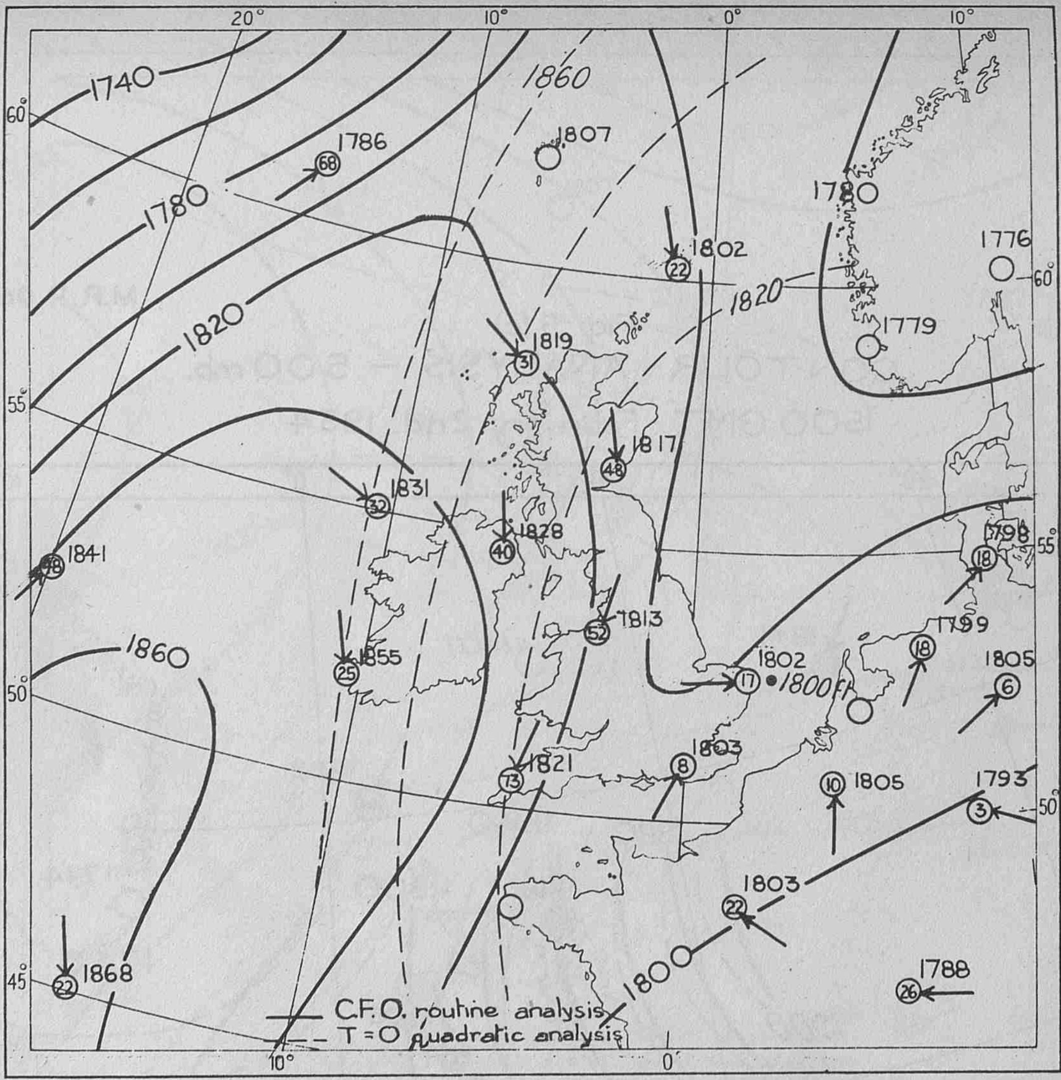
20°
10°
0°
10°
60°
55°
50°
45°
1740
1780
1820
1860
1786
68
1807
1780
1776
1802
22
1820
1779
1819
31
1817
48
1831
32
1828
40
1841
1798
18
1813
52
1799
18
1855
25
1802
17
•1800Ft
1805
6
1803
8
1821
73
1805
10
1793
3
1803
22
1800
1788
26
1868
22
C.F.O. routine analysis
T = O quadratic analysis

Observed heights given in tens of feet. Observed wind speed given in knots.

Fig. 10 (b)

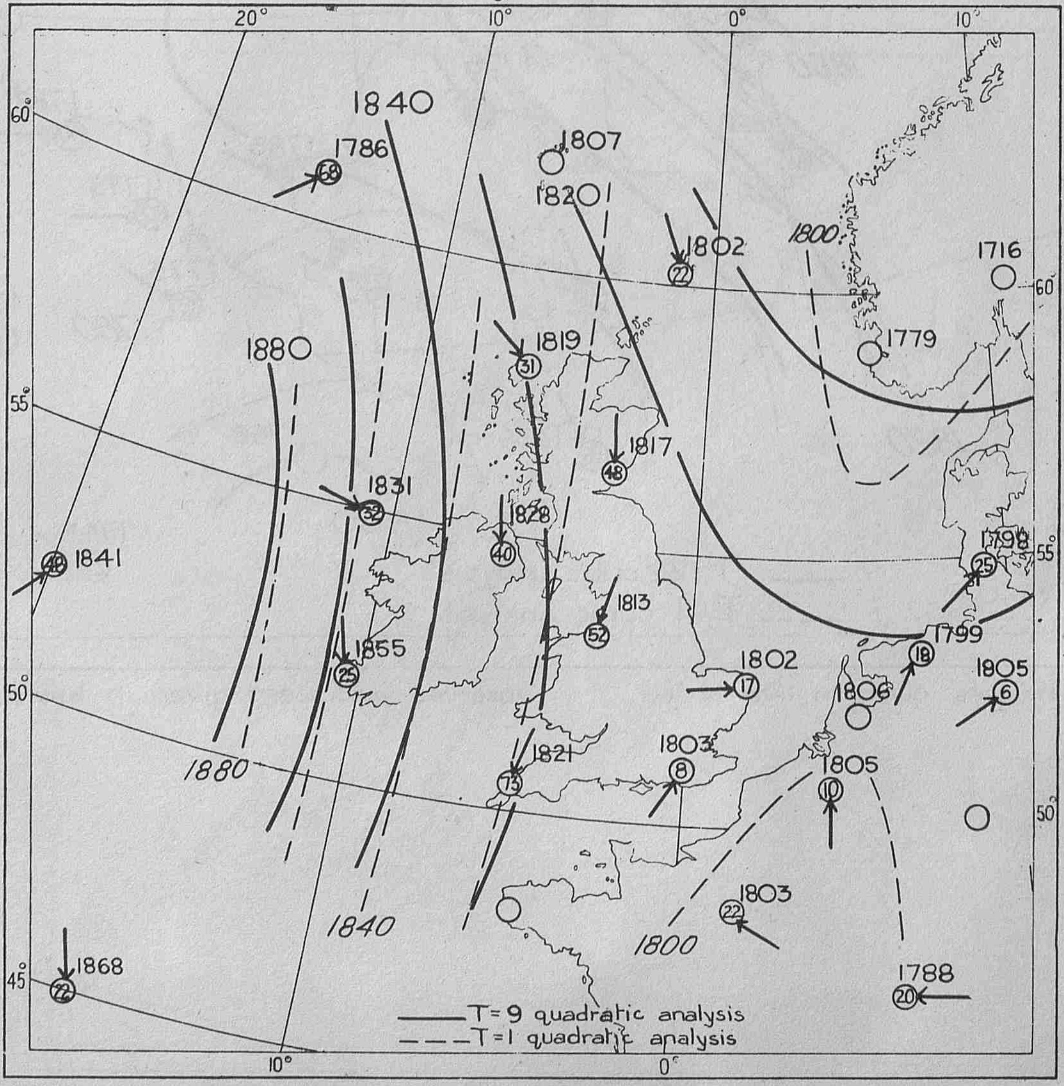
20°
10°
0°
10°
60°
55°
50°
45°
1840
1786
68
1807
1820
1802
22
1800
1716
1880
1819
31
1779
1817
48
1831
32
1828
40
1841
48
1798
25
1813
52
1799
18
1855
25
1802
17
1806
1805
6
1880
1803
8
1821
73
1805
10
1840
1803
22
1800
1868
72
1788
20
T = 9 quadratic analysis
T = 1 quadratic analysis

Observed heights given in tens of feet. Observed wind speed given in knots.

Fig. 11 (a)

CONTOUR ANALYSIS – 500mb.

1500mb. February 27th 1954

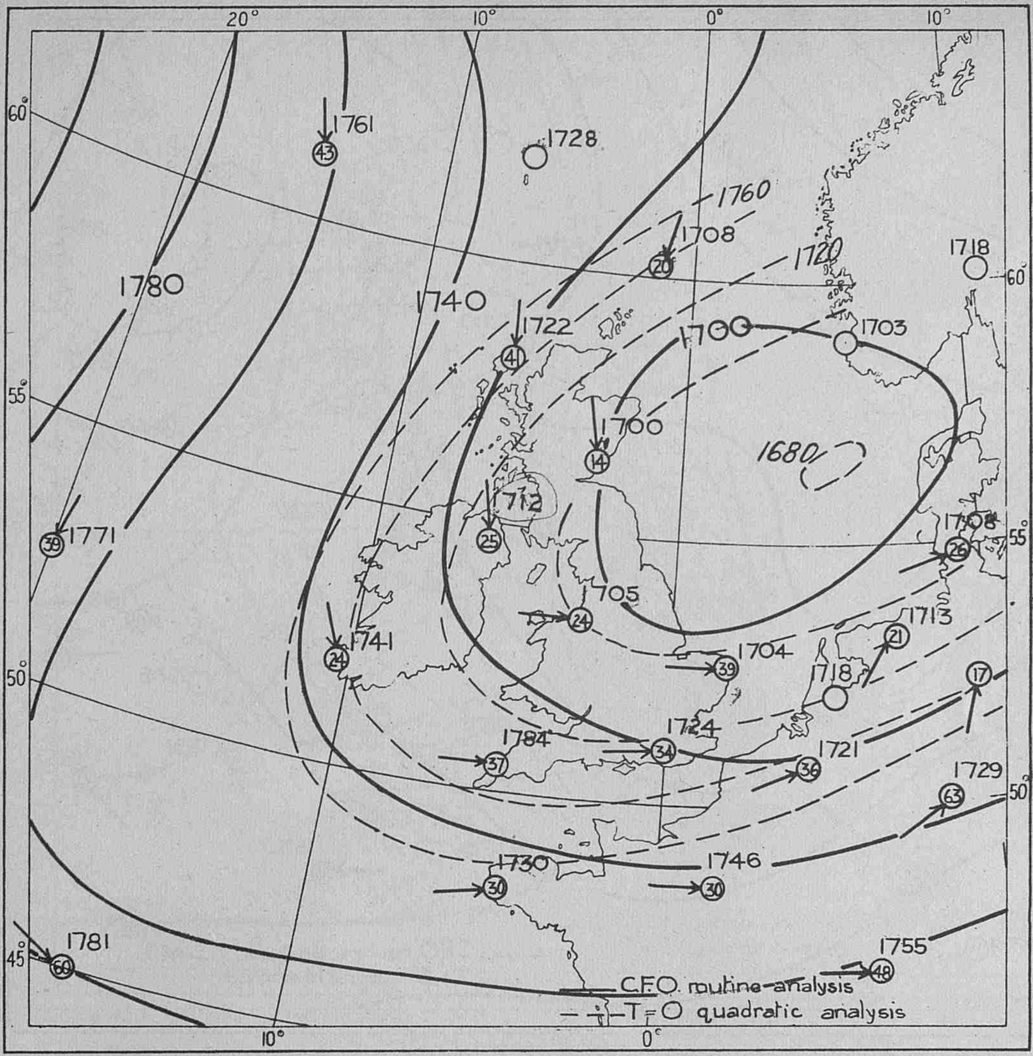
20°
10°
0°
10°
60°
55°
50°
45°
1761
43
1728
1760
1708
20
1720
1718
60°
1780
1740
1722
41
1700
1703
1700
14
1680
1712
25
1771
39
1708
26
55°
1705
24
1713
21
1741
24
1704
39
1718
17
1784
37
1724
34
1721
36
1729
63
50°
1730
30
1746
30
1781
60
1755
48
C.F.O. routine analysis
T=O quadratic analysis
10°
0°

Observed heights given in tens of feet. Observed wind speed given in knots.

Fig. 11(b)

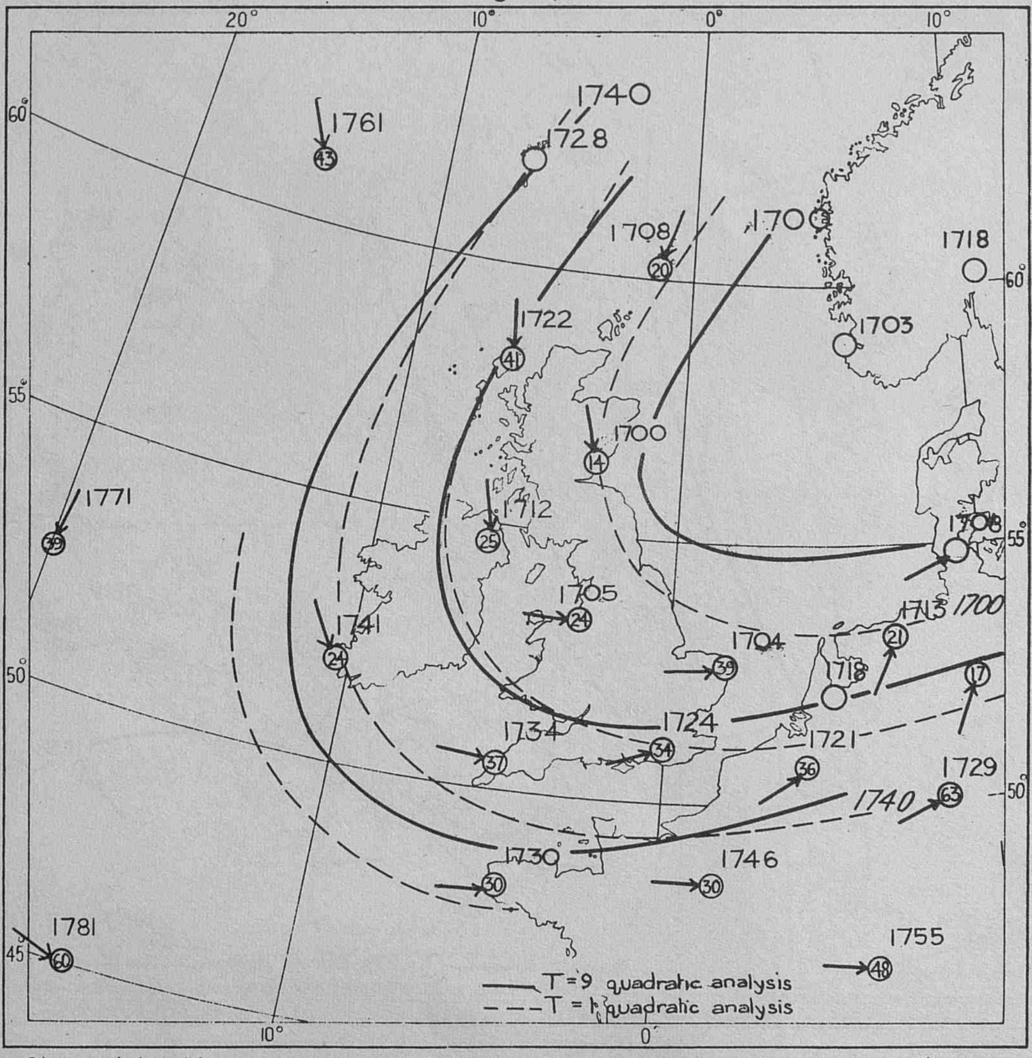
20°
10°
0°
10°
60°
55°
50°
45°
1740
1728
1761
43
1708
20
1700
1718
60°
1722
41
1703
1700
14
1771
39
1712
25
1708
55°
1705
24
1741
24
1713
1700
21
1704
39
1718
17
1734
1724
37
34
1721
1729
36
1740
63
50°
1730
30
1746
30
1781
60
1755
48
T=9 quadratic analysis
T = 1 quadratic analysis
10°
0°

Observed heights given in tens of feet. Observed wind speed given in knots.

Fig. 12 (a)

CONTOUR ANALYSIS—500 mb.

1500 G.M.T. March 19th 1954

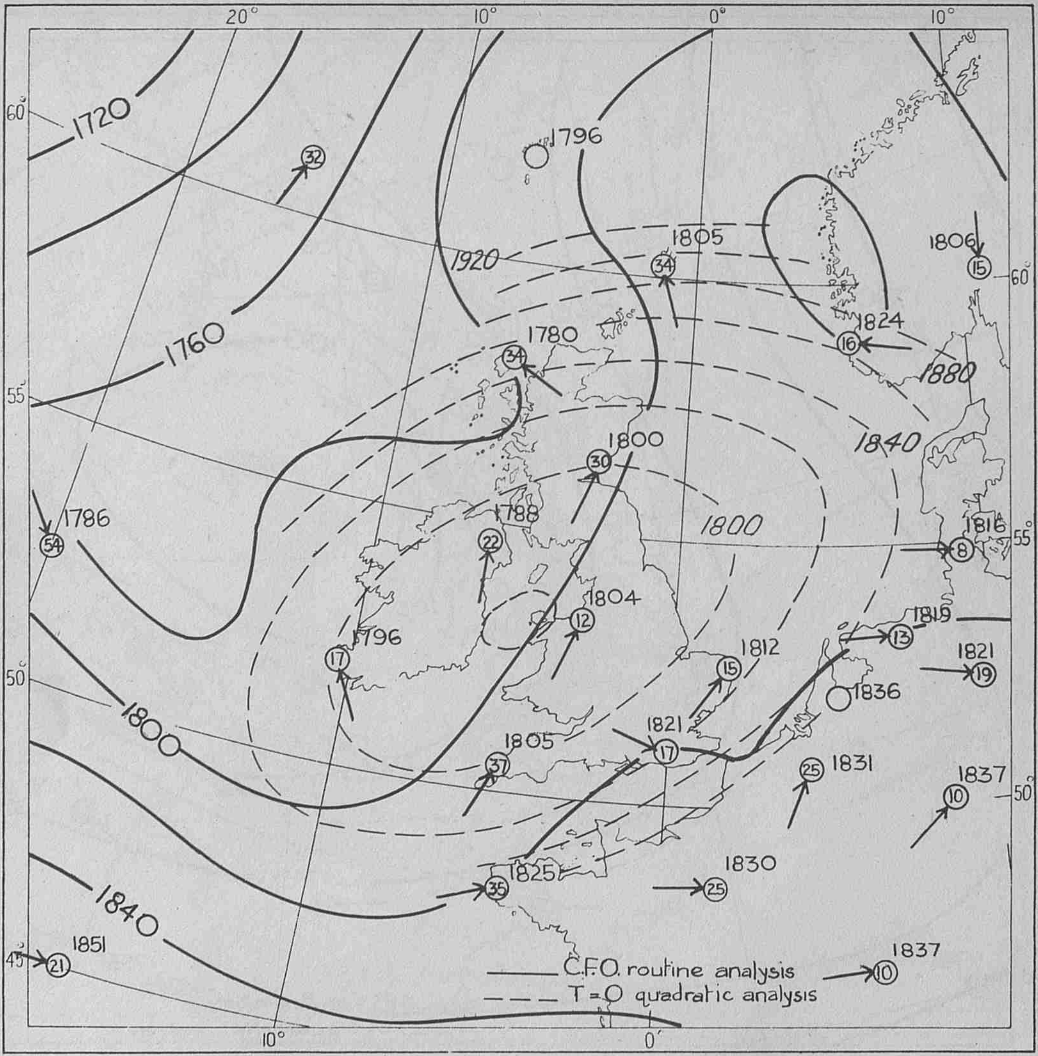
20°
10°
0°
10°
60°
55°
50°
45°
1720
1760
1800
1840
1920
1880
1840
1800
1796
32
1805
34
1806
15
1824
16
1780
34
1800
30
1786
54
1788
22
1816
8
1804
12
1819
13
1796
17
1812
15
1821
19
1836
1821
17
1805
37
1831
25
1837
10
1825
35
1830
25
1851
21
1837
10
C.F.O. routine analysis
T=0 quadratic analysis
10°
0°

Observed heights given in tens of feet. Observed wind speed given in knots.

Fig .12 (b)

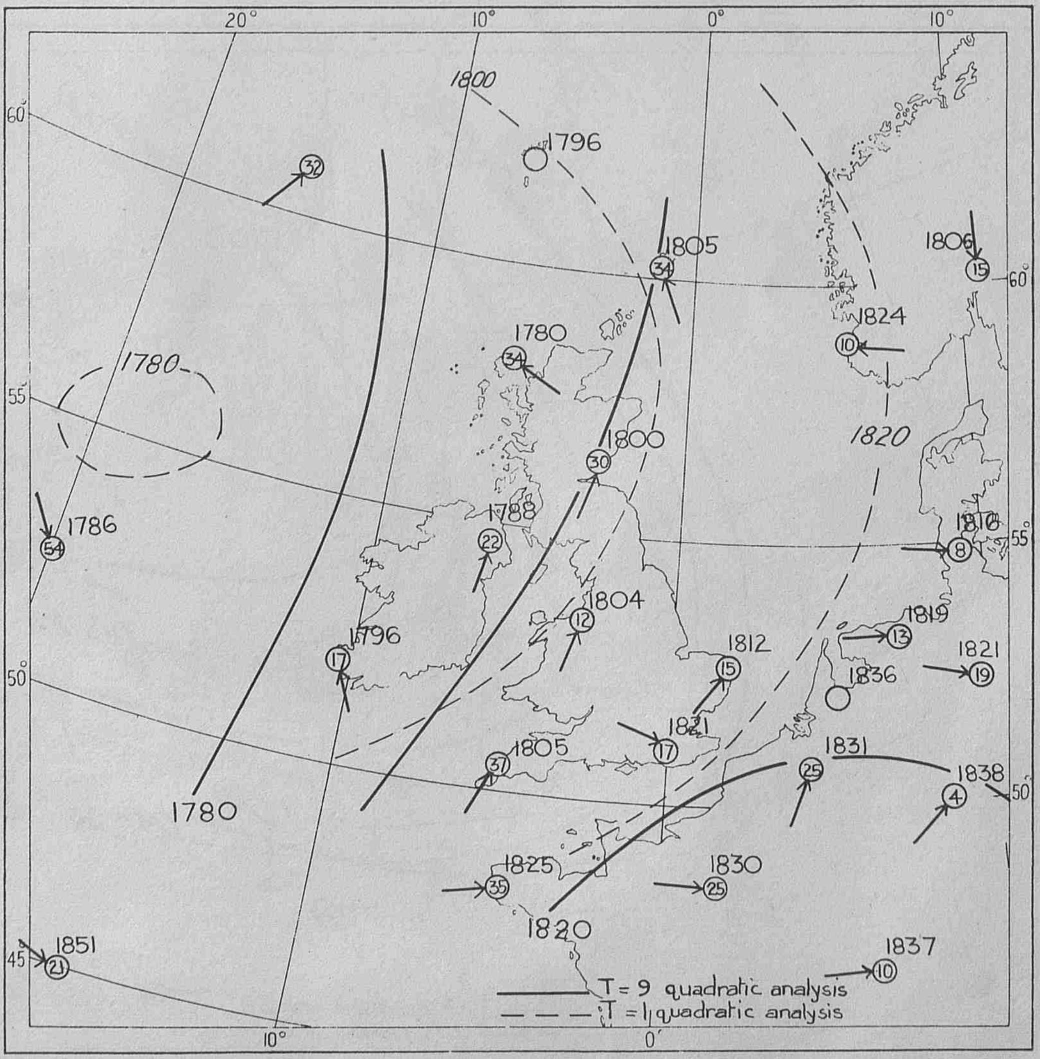
20°
10°
0°
10°
60°
55°
50°
45°
1800
1796
32
1805
34
1806
15
1824
10
1780
34
1780
1800
30
1820
1786
54
1788
22
1816
8
1804
12
1819
13
1796
17
1812
15
1821
19
1836
1821
17
1805
37
1831
25
1838
4
1780
1825
35
1830
25
1820
1851
21
1837
10
T = 9 quadratic analysis
T = 1 quadratic analysis
10°
0°

Observed heights given in tens of feet. Observed wind speed given in knots.

Fig. 13(a)

CONTOUR ANALYSIS — 500 mb

1500 G.M.T. May 28th. 1954

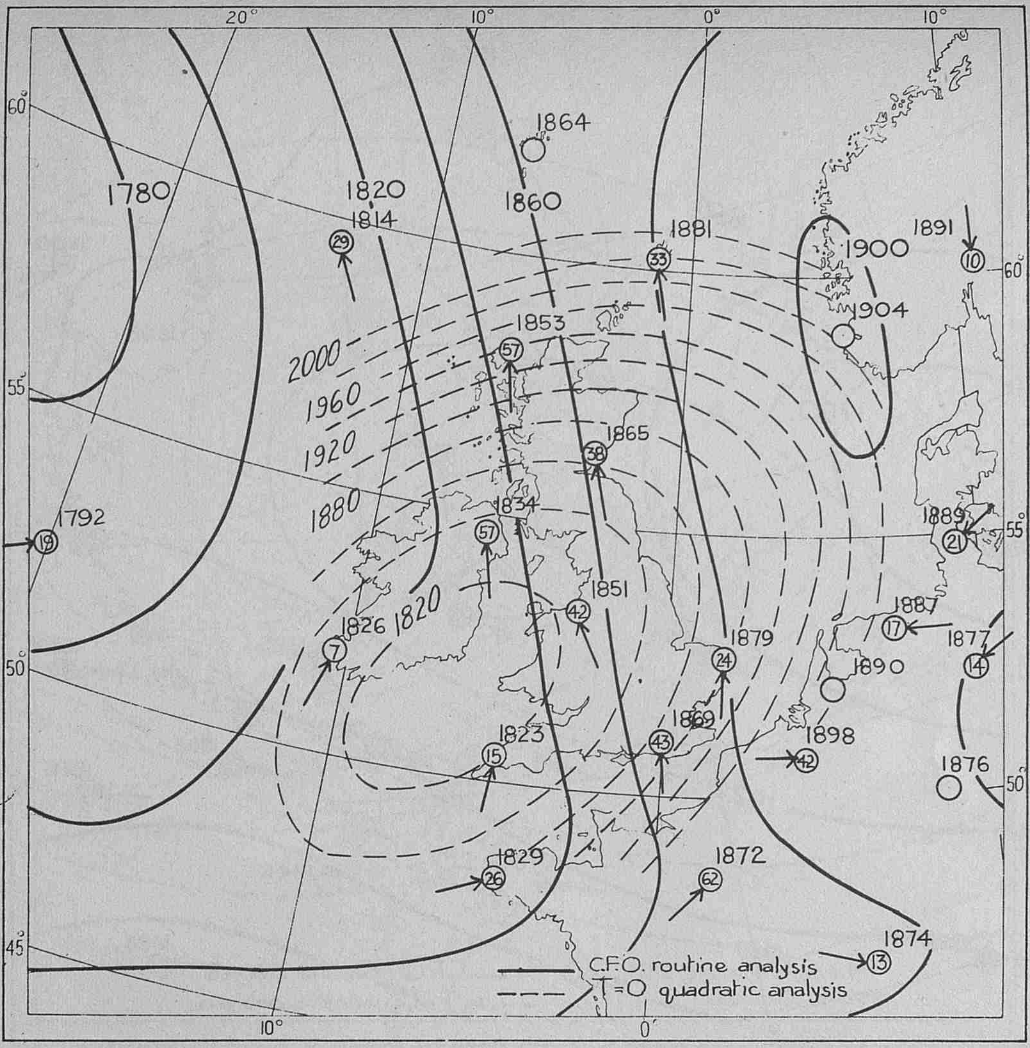
20°
10°
0°
10°
60°
55°
50°
45°
1780
1820
1814
29
1864
1860
1881
33
1891
10
1900
1904
2000
1960
1920
1880
1853
57
1865
38
1792
19
1834
57
1889
21
1820
1826
7
1851
42
1879
24
1887
17
1877
14
1890
1869
43
1823
15
1898
42
1876
1829
26
1872
62
1874
13
C.F.O. routine analysis
T=0 quadratic analysis
10°
0°

Observed heights given in tens of feet. Observed wind speed given in knots.

Fig 13(b)

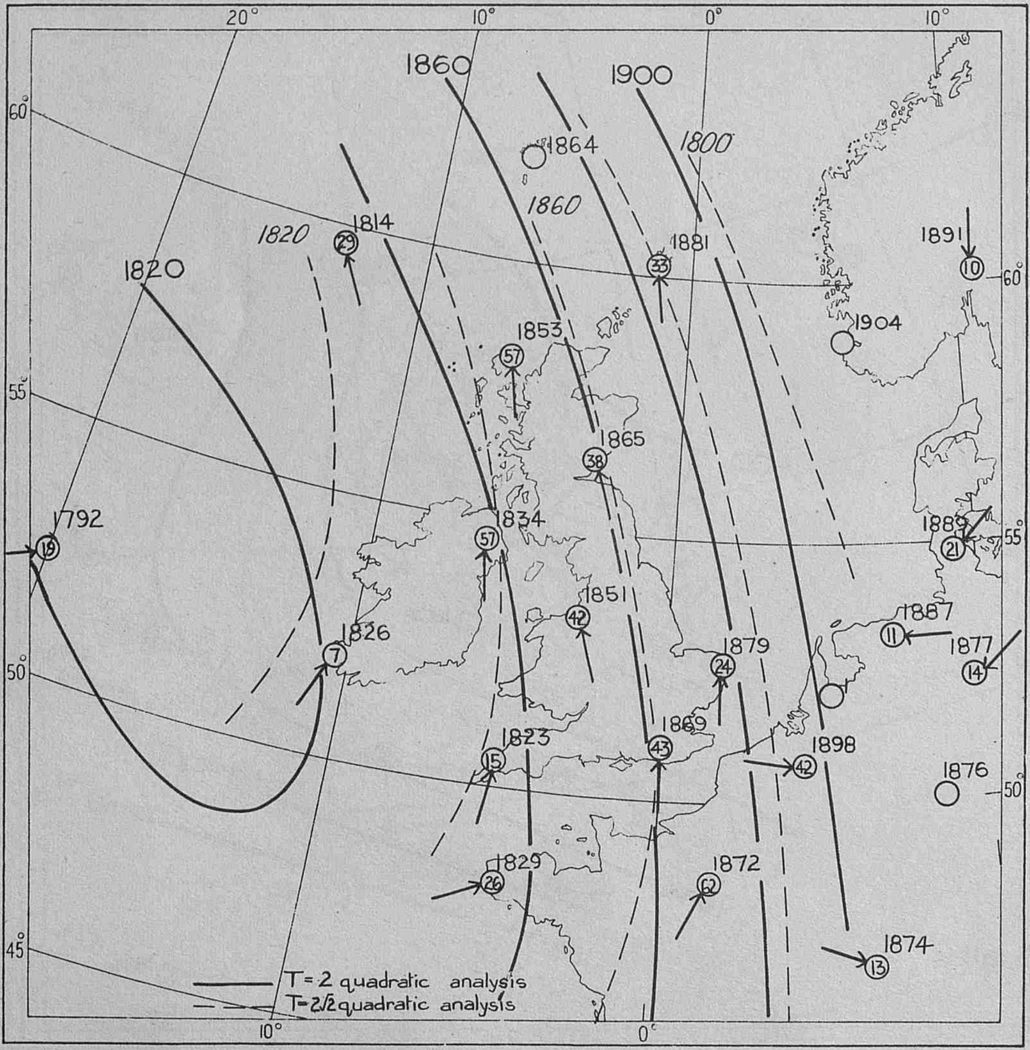
20°
10°
0°
10°
60°
55°
50°
45°
1860
1900
1800
1864
1860
1820
1814
29
1820
1881
33
1891
10
1853
57
1904
1865
38
1792
19
1834
57
1889
21
1851
42
1826
7
1887
11
1877
14
1879
24
1869
43
1823
15
1898
42
1876
1829
26
1872
62
1874
13
T=2 quadratic analysis
T=2½ quadratic analysis
10°
0°

Observed heights given in tens of feet. Observed wind speed given in knots.

Fig. 14 (a) M.R.P. 965

CONTOUR ANALYSIS — 500 mb.

1500 G.M.T. August 12th. 1954

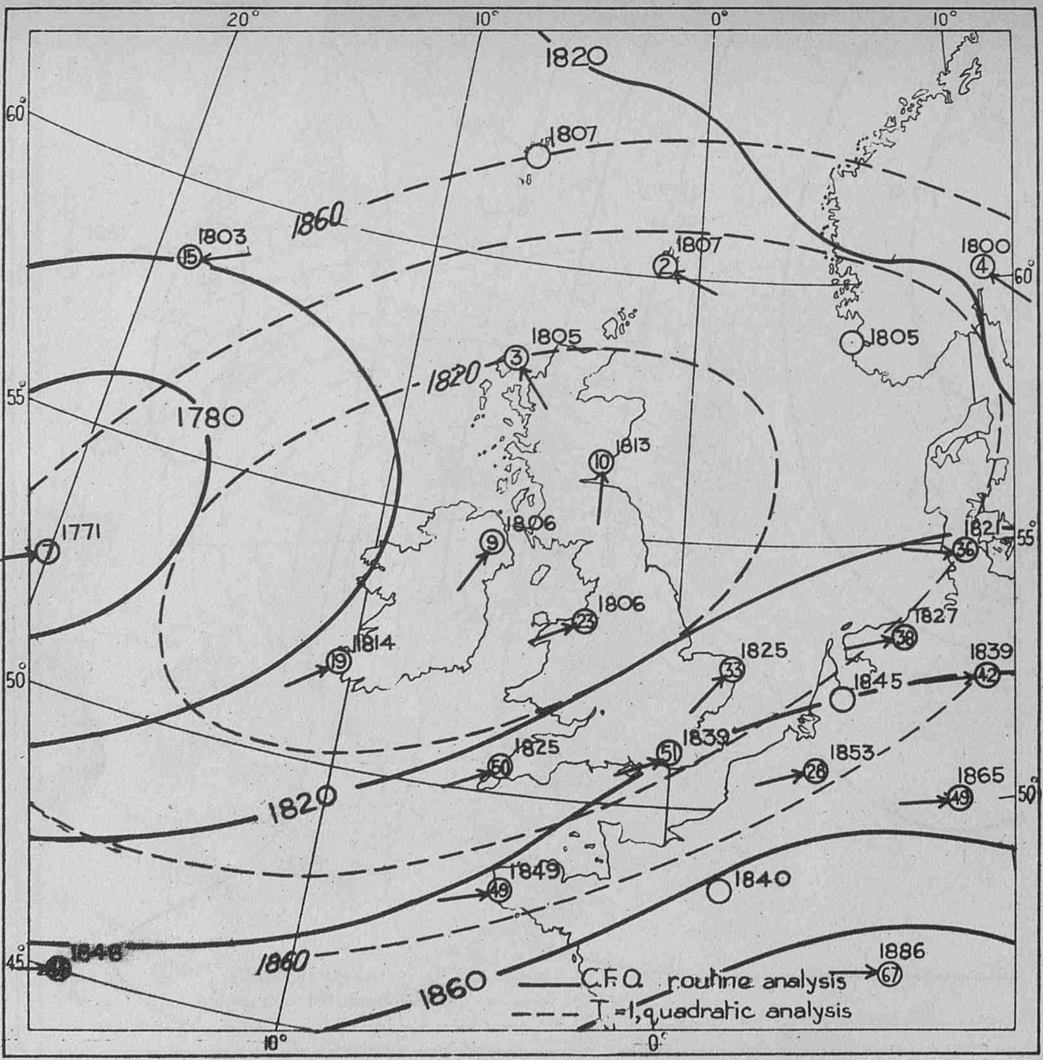
20°
10°
0°
10°
60°
55°
50°
45°
1820
1807
1860
1803
1800
1805
1780
1813
1771
1806
1821
1827
1814
1825
1839
1845
1853
1865
1849
1840
1848
1886
C.F.O. routine analysis
T=1, quadratic analysis

Observed heights given in tens of feet. Observed wind speed given in knots.

Fig. 14 (b)

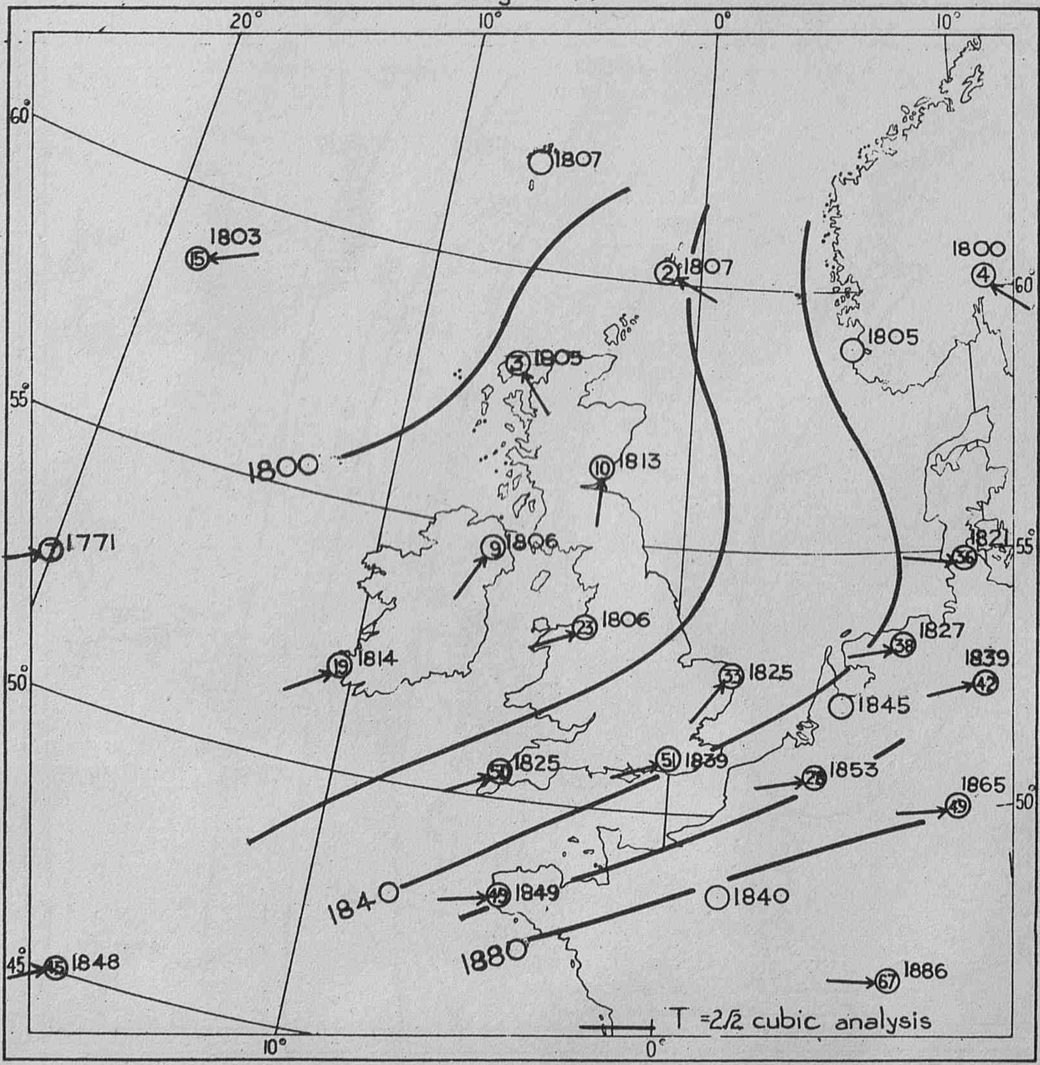
20°
10°
0°
10°
60°
55°
50°
45°
1807
1803
1800
1805
1813
1771
1806
1821
1827
1814
1825
1839
1845
1853
1865
1840
1849
1880
1848
1886
T = 2½ cubic analysis

Observed heights given in tens of feet. Observed wind speed given in knots.

Fig. 15 (a)

CONTOUR ANALYSIS — 500 mb.

1500 G.M.T. September 10th 1954

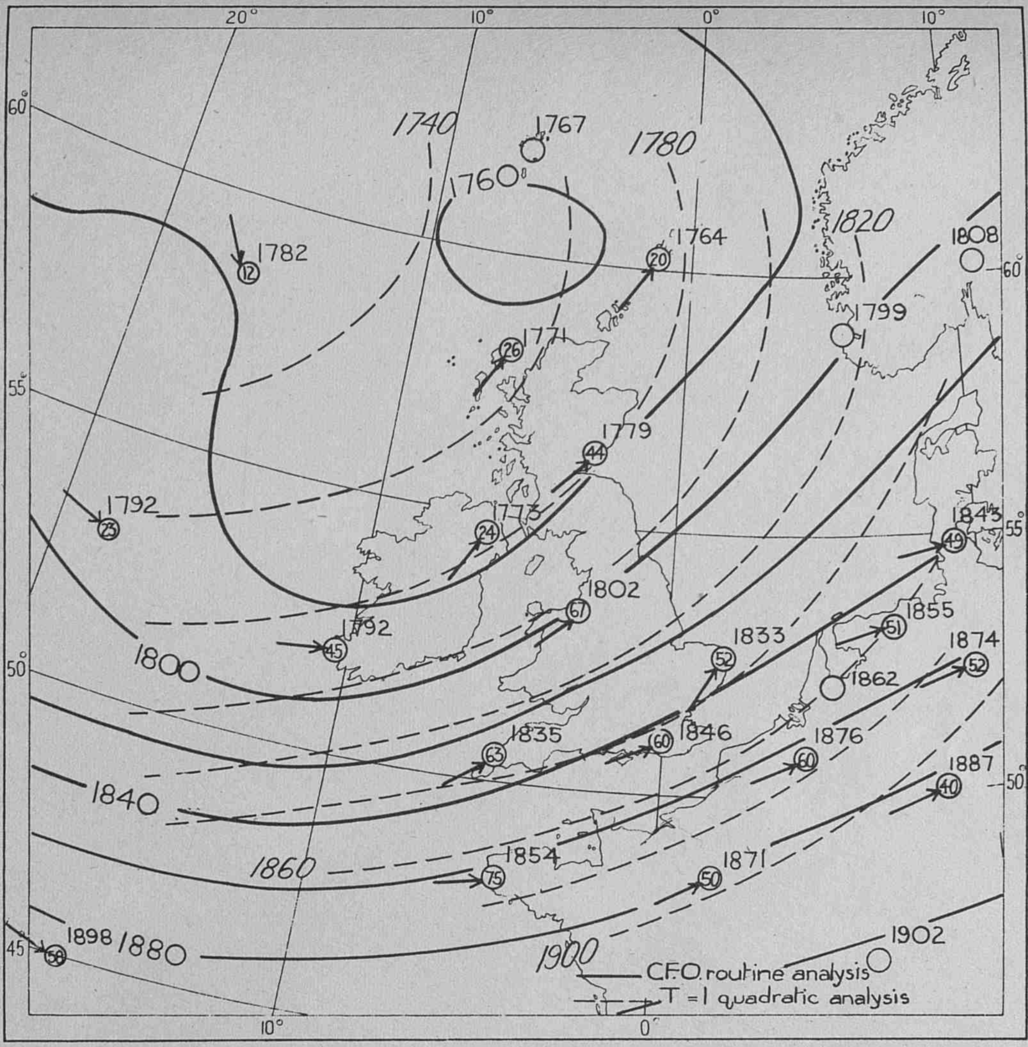
20°
10°
0°
10°
60°
55°
50°
45°
1740
1767
1780
1760
1764
1782
12
20
1820
1808
1799
1771
26
1779
44
1792
23
1773
24
1843
49
1802
67
1855
51
1792
45
1833
52
1874
52
1800
1862
1835
63
1846
60
1876
60
1840
1887
40
1860
1854
75
1871
50
1898
58
1880
1902
1900
C.F.O. routine analysis
T = 1 quadratic analysis

Observed heights given in tens of feet. Observed wind speed given in knots.

Fig. 15 (b)

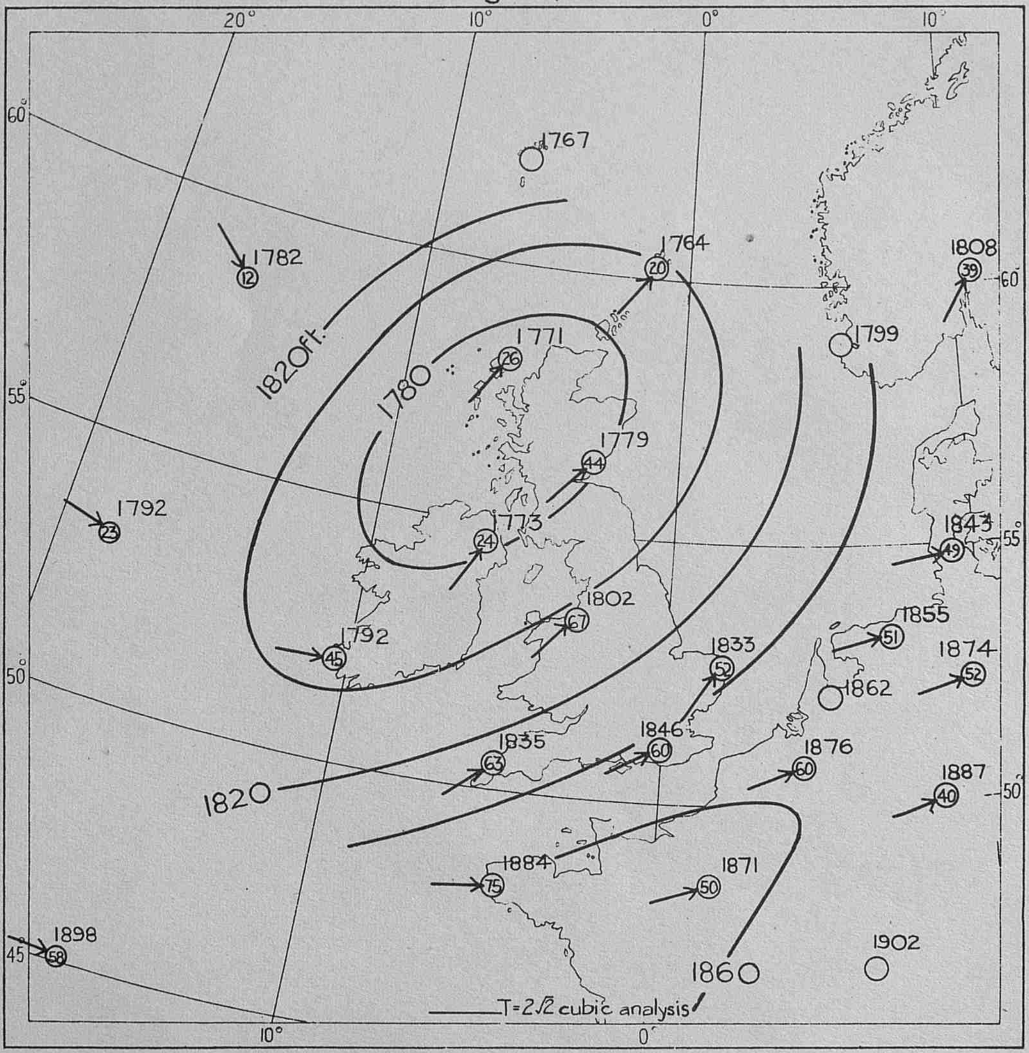
20°
10°
0°
10°
60°
55°
50°
45°
1767
1782
12
1764
20
1808
39
1820ft.
1780
1771
26
1799
1779
44
1792
23
1773
24
1843
49
1802
67
1855
51
1792
45
1833
52
1874
52
1862
1846
60
1835
63
1876
60
1820
1887
40
1884
75
1871
50
1898
58
1902
1860
T=2√2 cubic analysis

Observed heights given in tens of feet. Observed wind speed given in knots.

mats (AWS)

M.R.P. 970
S.C. 11/208
30th April, 1956.

AD 723095

The harmonic representation of the annual temperature variation in different parts of the British Isles.

by

J. M. Craddock.

(Meteorological Office)

AIR MINISTRY

METEOROLOGICAL RESEARCH COMMITTEE

56 - 1186

At the time of issue this report has not been published. Any author desiring to quote this paper should refer to it as "A paper of the Meteorological Research Committee (London). M.R.P. No.970 by Mr. J.M. Craddock. A copy is available in the Library of the Meteorological Office".

M.R.P.970
S.C.II/208
30th April, 1956

AIR MINISTRY

METEOROLOGICAL RESEARCH COMMITTEE

The harmonic representation of the annual temperature variation in different parts of the British Isles

by

J.M. Craddock (Meteorological Office)

1. This work forms part of the programme outlined in previous papers by Craddock (1955) (1) and (2) for providing reliable meteorological normals on the basis of the harmonic analysis of the annual variation. It presents temperature normals for all parts of the British Isles in a form from which it is easy to calculate the numerical value for any day of the year. It has been shown by Craddock (1) that over most parts of Europe the annual variation of the daily mean temperature can be represented for most purposes by the two term harmonic form

$$T = a_0 + a_1 \cos\theta + b_1 \sin\theta + a_2 \cos 2\theta + b_2 \sin 2\theta$$

or

$$T = a_0 + A_1 \cos(\theta - \phi_1) + A_2 \cos 2(\theta - \phi_2)$$

where θ is measured from zero at midnight on December 31 and $a_0\ a_1\ b_1\ a_2\ b_2$ are parameters which differ from one station to another. It also appears probable that in some areas there are some small deviations from the two term harmonic form associated with particular dates, which can be called singularities, of which magnitude (and permanence or otherwise) can only be established by much more elaborate investigation than has been possible up to date. The basic data on which the form (1) was justified consisted in 5-day mean temperatures for non overlapping periods covering the year, and the methods used are applicable only to the comparatively few stations for which these data are available.

However, if the principle is accepted that two harmonic terms are enough to give a very good approximation to the form of the annual temperature variation, then the form can be fitted to monthly mean temperatures. This has been done in a later paper (Craddock (1955) (2)) where results are given for a network of 305 stations spread over the Northern Hemisphere, and the large scale variation of the harmonic parameters over the Northern Hemisphere is discussed with illustrative charts. The harmonic parameters have also been used to provide by harmonic synthesis tables of the normal value of the air temperature at 5-day intervals throughout the year, and these form the basis of a study of the synoptic variations of large scale temperature anomalies, which is now being carried out in the Forecasting Research Division of the Meteorological Office.

2. The present paper follows the lines of the last, but is concerned only with the British Isles. Its main purpose is to provide a reliable means of estimating the normal temperature in all parts of the country at all times of the year, and for all purposes, including the estimation of the temperature

anomaly. It is also intended to throw light on the variation of the harmonic parameters with distance from the coast and, within the limits imposed by the rather low relief, with altitude. Most of the basic data were monthly mean temperatures for the new international period 1921-1950 taken from an official publication (3). 160 stations were chosen, including all for which the monthly means were based on data for the whole 30 years and about 45 others to cover gaps in the network. Most of the incomplete records covered 20 years or more.

These data provided a reasonably good cover over Great Britain. For Ireland 14 stations were used, for which most of the 30-year mean temperatures were calculated in the Forecasting Research Division. For stations in Eire the monthly mean temperatures were tabulated from the following sources:-

(a) for years up to 1940 from the Monthly Weather Reports of the British Meteorological Office,

(b) for 1940 to 1947 from values supplied by the courtesy of the Irish Meteorological Service, Dublin, and

(c) for years 1948 onwards, from the Monthly Weather Reports of the Irish Meteorological Service.

The harmonic parameters were calculated by the method already described (2) but for most stations the actual computation was done on the Manchester University electronic computer under the direction of Mr. F.H. Bushby. Full details of all the stations used are given in Table 1, and the values of the harmonic parameters are in Table 2. Figs. 1 to 6 show the more interesting features of the geographical distribution of these parameters.

3. (i) The annual mean temperature a_o

Fig. 1 shows the annual mean temperatures taken from Table 2 and reduced to mean sea level. It is included for comparison with similar maps based on earlier data, for example, that in the Climatic Atlas of the British Isles (4) which relates to the basic period 1901-30. Comparing 1901-30 with 1921-50 there seems to have been an increase of from half to one degree Fahrenheit in nearly all areas. Fig. 1, which shows the observations as well as the isopleths, shows several interesting local features of which a full discussion would run outside the scope of this paper.

(ii) The semi-amplitude of the first harmonic

Fig. 2 shows the semi-amplitude of the first harmonic. Over most of England the values are very uniform, ranging from about 11°F. to 12.5°F. but there is a rapid decrease near the coasts of Scotland, Wales and South West England. The mountain stations in Scotland seem to agree quite well with their lowland neighbours, though they may perhaps give a little support to the suggestion, based on data for German mountain stations (1) that the amplitude aloft is less than at neighbouring stations near sea level.

For Ireland the general picture is similar, with values of 9° to 10°F. over most of the country, including it seems much of the east coast, but with values about 7.5° to 8°F. on the south-west, west and north-west coasts.

(iii) The phase of the first harmonic

The phase of the first harmonic, ϕ_1 is given in Fig. 3 by the calendar date on which this harmonic attains its maximum. The date varies from the 23rd or 24th July inland over most of England and Ireland but is consistently later on the coasts, being latest of all in south-west England and Wales. The mountain stations can hardly be said to show any systematic difference from their lowland neighbours.

/(iv)

(iv) The semi-amplitude of the second harmonic

The semi-amplitude of the second harmonic is shown in Fig. 4, the values ranging from about 0.8° to 1.3°F. The general distribution seems to be that the higher values are inland, or on coasts facing east, while the lower values are on coasts facing west or south. There are, however, several stations facing south where the parameter exceeds 1°F. and an area in the English Midlands where it is less than 1°F. In Fig. 5 the amplitude of the second harmonic is given as a percentage of that of the first. The values range mostly from 10 to 14 per cent, but the variations do not show any obvious regularity.

(v) The phase of the second harmonic

If the phase of the second harmonic is represented in the way used for the first, the resulting chart shows dates varying from 30th July to the 20th August but not falling into any pattern capable of ready description. However, the second harmonic is of much smaller amplitude than the first, so that its importance really lies in the way in which it modifies the first. Fig. 5a has been drawn to illustrate the ways in which it can do so. On comparing the three curves, it is obvious that the effect of a second harmonic with date of maximum agreeing with that of the first harmonic is to sharpen the summer peak and to flatten the winter trough. That is, the annual cycle has a long, rather equable winter, and a short summer with a well marked maximum. If the maximum of the second harmonic is displaced day by day to fall after that of the first, up to 45 days, the combined peak becomes progressively later, the winter becomes shorter and sharper, while the autumn decline of temperature becomes more rapid than the spring rise. As the shift is increased past 45 days the curve comes to resemble the second one, only inverted, with a short winter and a long equable summer. If the maximum of the second harmonic is shifted backwards relative to the first the result is like the third curve laterally reversed.

With this illustration in mind, the phase of the second harmonic is shown in Fig. 6 by the number of days by which the maximum of the second harmonic falls after that of the first. The distribution is a simple one, with maxima of about 20 days inland and low values on coasts, especially in the south-west. The effect of this displacement is twofold: (1) in inland districts of the British Isles the autumn decline of temperature is appreciably more rapid than the spring rise, an effect which is much less marked, or altogether absent on the coasts, and (2) the probable date of the hottest day (i.e., the maximum of the combination of the first and second harmonics) shows less variation than is shown in Fig. 3 for the date of maximum of the first harmonic alone. The actual distribution cannot be shown without extra calculation, but probably in all parts the date with the highest average temperature lies within a day or two of the end of July.

References

(1) Craddock, 1955. Meteorological Research Papers, Air Ministry, London, No.915.

(2) Craddock, 1955. Meteorological Research Papers, Air Ministry, London, No.917.

(3) M.O.571, 1953. Averages of temperature for Great Britain and Northern Ireland.

(4) M.O.488, 1952. Climatological Atlas of the British Isles.

Table 1. The stations used

Station	Lat. °N.	Long.	Alt. (m)	Period
Aber	53°14'	4° 1'W	18.3	1925-50 *
Aberdeen	57°10'	2° 6'W	24.1	1921-47 *
Aberystwyth	52°25'	4° 4'W	137.2	1926-50 +
Achnashellac	57°29'	5°16'W	70.0	1923-50 *
Addington	51°22'	0° 4'W	143.3	1921-50
Aldergrove	54°39'	6°13'W	67.1	1927-50 *
Ampleforth	54°12'	1° 5'W	94.5	1921-50
Appleby	54°34'	2°30'W	134.1	1921-46 *
Arbroath	56°35'	2°35'W	28.3	1921-46 *
Ardtornish	56°34'	5°45'W	14.6	1921-45 *
Armagh	54°21'	6°39'W	62.0	1921-50
Balmoral	57° 2'	3°12'W	283.5	1921-50
Banff	57°40'	2°31'W	39.6	1926-50 *
Barnstaple	51° 5'	4° 3'W	7.6	1921-50
Beachy Head	50°44'	0°15'E	152.4	1925-50 *
Bellingham	55°13'	2°18'W	259.0	1921-50
Belper School	53° 1'	1°29'W	61.0	1921-50
Berwick	55°46'	2° 0'W	23.2	1924-50 *
Birmingham (Sparkhill)	52°27'	1°51'W	131.0	1921-50
Birr Castle	53° 5'	7°53'W	70.0	1921-50
Blacksod Point	54° 4'	10° 4'W	5.0	1926-50 +
Bognor Regis	50°47'	0°41'W	7.3	1921-50
Bolton	53°35'	2°27'W	103.6	1921-50
Bradford	53°49'	1°46'W	134.1	1921-50
Braemar	57° 0'	3°24'W	338.3	1921-50
Bude	50°50'	4°33'W	15.2	1926-50 *
Bungay	52°25'	1°23'E	24.1	1921-48 *
Burnley	53°48'	2°15'W	140.2	1921-50 *
Buxton	53°16'	1°55'W	307.8	1926-50 *
Cambridge (Botanic Gdn.)	52°12'	0° 8'E	12.5	1921-50
Camden Square	51°33'	0° 8'W	33.5	1921-50
Canterbury	51°17'	1° 5'E	39.6	1921-44 *
Cardiff	51°28'	3°10'W	61.0	1921-50
Cheltenham	51°54'	2° 3'W	64.0	1926-50 *
Chopwelwood	54°55'	1°47'W	137.2	1921-50
Colmonell	55° 8'	4°57'W	51.8	1921-50
Coventry	52°23'	1°29'W	73.1	1921-50
Craibstone	57°11'	2°12'W	91.4	1925-50 *
Cranwell	53° 2'	0°30'W	61.0	1921-50
Cromer	52°56'	1°17'E	54.9	1926-50 *
Croydon	51°21'	0° 7'W	67.1	1921-50
Cullompton	50°51'	3°23'W	61.0	1921-50
Cupar	56°19'	3° 1'W	64.0	1921-50
Dalwhinnie	56°56'	4°14'W	359.7	1931-50 +
Darwen	53°41'	2°28'W	219.5	1921-50
Donaghadee	54°38'	5°32'W	9.0	1921-42 +
Douglas	54°10'	4°28'W	85.3	1926-50 *
Dover	51° 7'	1°19'E	5.8	1926-50 *
Dublin (Phoenix Park)	53°22'	6°21'W	47.0	1921-50
Dumfries	55° 3'	3°36'W	42.7	1921-50
Dundee	56°28'	2°56'W	45.7	1921-50
Dungavel	55°37'	4° 8'W	243.8	1921-48 *
Dungeness	50°55'	0°58'E	6.1	1921-50
Durham	54°46'	1°35'W	103.6	1921-50
East Ham	51°32'	0° 4'E	4.6	1921-50
Edinburgh (Blackf'd Hill)	55°55'	3°11'W	134.1	1921-50
Eskdalemuir	55°19'	3°12'W	240.8	1921-50
Exmouth	50°36'	3°24'W	57.9	1921-50

/Falmouth

Station	Lat. °N.	Long.	Alt. (m)	Period
Falmouth	50° 9'	5° 5'W	51.8	1926-50 *
Felixstowe	51°57'	1°20'E	3.0	1921-50
Fort Augustus	57° 8'	4°40'W	20.7	1921-47 *
Fortrose	57°35'	4° 8'W	21.0	1921-50
Fort William	56°49'	5° 7'W	10.4	1932-50 +
Fowey	50°21'	4°38'W	15.2	1921-50
Foynes	52°37'	9° 7'W	15.0	1921-44 +
Frampton Cotterell	51°32'	2°29'W	48.8	1921-50
Garvagh	54°59'	6°36'W	36.6	1939-50 +
Glenbranter	56° 8'	5° 3'W	36.6	1926-50 *
Gordon Castle	57°37'	3° 5'W	30.5	1921-50
Gorleston	52°35'	1°43'E	1.5	1921-50
Greenock	55°56'	4°46'W	61.0	1921-50
Greenwich	51°29'	0° 0'	45.7	1921-50
Gulval	50° 8'	5°32'W	6.1	1925-50 *
Halstead	51°57'	0°38'E	42.7	1921-50
Hampstead	51°34'	0°11'W	137.2	1921-50
Haverfordwest	51°48'	4°58'W	39.6	1921-50
Hawarden Bridge	53°12'	3° 1'W	5.2	1921-50
Helensburgh	56° 1'	4°43'W	88.4	1921-50
Hereford	52° 5'	2°45'W	88.4	1921-50
Holyhead	53°19'	4°37'W	7.9	1921-50
Hoylake	53°23'	3°12'W	7.0	1921-50
Huddersfield (Ravensknowle)	53°38'	1°45'W	100.6	1921-50
Hull	53°45'	0°16'W	2.4	1921-50
Hunstanton	52°57'	0°29'E	30.5	1924-50 *
Hutton	53°44'	2°45'W	25.0	1921-50
Ilfracombe	51°12'	4° 8'W	7.6	1926-50 *
Ilkley	53°55'	1°50'W	94.5	1923-50 *
Inverness	57°26'	4°13'W	73.1	1926-50 *
Kelso	55°36'	2°25'W	57.9	1921-50
Kensington Palace	51°30'	0°10'W	24.4	1921-50
Keswick	54°36'	3° 9'W	76.2	1921-50
Kettins	56°32'	3°14'W	67.1	1921-50
Kew	51°28'	0°19'W	5.5	1921-50
Kilkenny	52°39'	7°14'W	55.0	1901-30
Kilmarnock	55°37'	4°29'W	39.6	1921-50
Kirkcaldy	56° 8'	3°10'W	42.7	1921-50
Larkhill	51°11'	1°48'W	131.1	1921-50
Lerwick	60° 8'	1°11'W	82.3	1921-50
Leuchars	56°23'	2°53'W	10.1	1921-50
Liverpool	53°24'	3° 4'W	61.0	1921-50
Long Ashton	51°26'	2°40'W	48.8	1921-50
Luton	51°54'	0°25'W	115.8	1921-50
Lympne	51° 5'	1° 1'E	103.6	1921-50
Macclesfield	53°16'	2° 8'W	152.4	1921-50
Malin Head	55°22'	7°20'W	26.0	1921-50
Malvern	52° 8'	2°18'W	115.8	1926-50 *
Manchester	53°28'	2°14'W	39.6	1921-50
Marchmont	55°44'	2°25'W	152.4	1921-50
Markree Castle	54°11'	8°27'W	37.0	1921-50
Marlborough	51°25'	1°44'W	128.0	1921-50
Morecambe	54° 4'	2°52'W	7.0	1926-50 *
Morpeth (Cockle Park)	55°13'	1°41'W	100.6	1921-50
Newport (Mon.)	51°35'	3° 0'W	82.3	1921-50
Newquay	50°25'	5° 4'W	54.9	1926-50 *
Newton Rigg	54°40'	2°47'W	170.7	1921-47 *
North Berwick	56° 3'	2°43'W	36.6	1923-50 *
Norwich	52°37'	1°17'E	33.5	1921-47 *
Nottingham Castle	52°57'	1° 9'W	57.9	1921-50

/Oxford

Station	Lat. °N.	Long.	Alt. (m)	Period
Oxford	51°46'	1°16'W	64.0	1921-50
Paisley	55°51'	4°26'W	33.5	1921-50
Perth	56°24'	3°27'W	23.5	1921-50
Plymouth (Mount Batten)	50°21'	4° 7'W	26.5	1921-50
Portland Bill	50°32'	2°27'W	9.7	1921-50
Porton	51° 7'	1°42'W	109.7	1921-50
Reading (Shinfield)	51°25'	0°57'W	61.0	1921-50
Reading University	51°27'	0°58'W	45.7	1921-50
Renfrew	55°52'	4°26'W	8.8	1921-50
Rhayader	52°18'	3°31'W	231.7	(1921-34 * (1936-50
Rhyl	53°19'	3°29'W	9.4	1926-50
Roches Point	51°48'	8°15'W	10.0	1921-50
Ross-on-Wye	51°55'	2°35'W	67.1	1921-50
Rothamsted	51°48'	0°22'W	128.0	1921-50
Rothesay	55°50'	5° 2'W	61.0	1921-50
Rothwell	55° 0'	3°26'W	20.4	1921-50
Ryde	50°44'	1°10'W	4.0	1921-50
St. Anne's Head	51°41'	5°10'W	42.7	1921-50
Sandown	50°39'	1° 9'W	4.0	1921-50
Scarborough	54°17'	0°24'W	36.6	1926-50 *
Scilly	49°56'	6°18'W	48.8	1921-50
Seskin (Carrick on Suir)	52°21'	7°24'W	165.0	1921-50
Shaftesbury	51° 1'	2°12'W	207.3	1921-50
Sheffield	53°23'	1°29'W	131.1	1921-50
Shoeburyness	51°32'	0°49'E	3.4	1921-50
Shrewsbury	52°43'	2°43'W	54.9	1931-50 +
Sidmouth	50°41'	3°14'W	7.6	1921-50
Skegness	53° 9'	0°21'E	4.6	1926-50 *
South Farnborough	51°17'	0°45'W	70.1	1921-50
Southampton	50°55'	1°24'W	19.8	1921-50
Southport	53°37'	3° 0'W	10.7	1921-50
Spurn Head	53°35'	0° 7'E	8.8	1921-50
Stirling	56° 7'	3°56'W	45.7	1921-50
Stonyhurst	53°51'	2°28'W	115.8	1921-50
Stornoway	58°13'	6°20'W	3.4	1921-50
Swansea	51°37'	3°55'W	9.8	1926-50 *
Tavistock	50°33'	4°10'W	140.2	1921-50
Tiree	56°30'	6°53'W	8.8	1927-50 +
Tunbridge Wells	51° 8'	0°16'E	106.7	1926-50 *
Turnberry	55°19'	4°50'W	19.2	1921-50
Tynemouth	55° 1'	1°25'W	33.5	1921-50
Ushaw	54°47'	1°39'W	179.8	1921-50
Valentia	51°56'	10°15'W	13.7	1921-50
Ventnor Hospital	50°36'	1°13'W	18.3	1921-50
Wakefield	53°40'	1°30'W	33.5	1921-50
Welshpool	52°39'	3° 8'W	76.2	1921-50
West Linton	55°45'	3°21'W	249.9	1921-50
Westminster	51°30'	0° 8'W	8.2	1921-50
Wick	58°27'	3° 5'W	36.6	1921-50
Wisley	51°17'	0°26'W	45.7	1921-50
Woburn	52° 1'	0°35'W	88.4	1921-50
Wolfelee	55°23'	2°39'W	164.6	1921-50
York	53°57'	1° 5'W	17.4	1921-50

* Less than 30 years data for means, but missing years are estimated by comparison with nearest complete station.

+ Less than 30 years data, with missing years not estimated. (See p.1 of M.O.571.)

Table 2

Harmonic parameters for stations in the British Isles

Station	a_0	a_1	b_1	a_2	b_2	A_1	ϕ_1	A_2	ϕ_2
Aber	50.55	- 8.09	-4.38	+0.40	+1.01	9.19	30/7	1.09	5/8
Aberdeen	47.00	- 8.44	-4.16	+0.62	+1.28	9.41	28/7	1.42	2/8
Aberystwyth	50.43	- 8.83	-4.69	+0.04	+0.82	10.00	30/7	0.82	16/8
Achnashellac	46.56	- 8.96	-3.52	+0.44	+0.97	9.63	23/7	1.06	4/8
Addington	49.45	-11.26	-4.62	+0.13	+1.17	12.17	24/7	1.18	13/8
Aldergrove	48.17	- 8.82	-3.80	+0.40	+1.08	9.60	25/7	1.15	6/8
Ampleforth	47.85	-10.50	-4.42	+0.24	+1.11	11.39	25/7	1.13	10/8
Appleby	46.74	-10.44	-3.80	+0.29	+0.97	11.11	22/7	1.01	8/8
Arbroath	47.04	- 9.00	-4.04	+0.19	+1.30	9.86	26/7	1.32	12/8
Ardtornish	47.60	- 8.75	-3.52	+0.50	+0.90	9.43	24/7	1.03	1/8
Armagh	48.79	- 9.07	-3.62	+0.51	+1.12	9.76	24/7	1.23	4/8
Balmoral	43.76	- 9.98	-4.04	+0.63	+1.18	10.76	24/7	1.34	1/8
Banff	47.24	- 8.97	-4.06	+0.25	+1.01	9.85	26/7	1.04	9/8
Barnstaple	51.07	- 8.52	-4.11	+0.34	+1.00	9.46	28/7	1.06	7/8
Beachy Head	49.24	- 9.39	-5.46	-0.11	+0.96	10.86	1/8	0.96	20/8
Bellingham	45.21	-10.30	-4.05	+0.38	+0.96	11.07	23/7	1.04	5/8
Belper School	48.73	-10.98	-4.23	+0.40	+1.10	11.76	23/7	1.17	6/8
Berwick	47.33	- 8.50	-4.30	+0.37	+1.27	9.53	29/7	1.32	8/8
Birmingham (Sparkhill)	49.33	-11.24	-4.32	+0.34	+1.15	12.04	23/7	1.20	8/8
Birr Castle	49.30	- 8.81	-3.54	+0.38	+1.26	9.49	24/7	1.32	7/8
Blacksod Point	50.38	- 6.78	-3.74	+0.06	+0.80	7.74	31/7	0.80	13/8
Bognor Regis	50.74	- 9.99	-5.09	+0.13	+1.03	11.21	29/7	1.04	13/8
Bolton	48.58	-10.44	-4.24	+0.30	+0.96	11.27	24/7	1.01	7/8
Bradford	47.95	-10.36	-4.49	+0.43	+1.06	11.29	25/7	1.15	5/8
Braemar	43.57	-10.05	-4.00	+0.72	+1.08	10.81	24/7	1.30	29/8
Bude	50.99	- 8.10	-4.47	+0.27	+0.93	9.25	31/7	0.97	8/8
Bungay	49.56	-11.65	-4.81	+0.01	+1.29	12.60	24/7	1.29	16/8
Burnley	47.53	-10.23	-4.36	+0.42	+1.05	11.12	25/7	1.13	5/8
Buxton	45.92	-10.17	-4.43	+0.46	+0.94	11.10	25/7	1.05	3/8
Cambridge (Botanic Gdn.)	49.73	-11.40	-4.41	+0.22	+1.29	12.22	23/7	1.31	11/8
Camden Square	51.72	-12.11	-4.48	+0.23	+1.11	12.91	22/7	1.13	10/8
Canterbury	50.60	-11.27	-4.67	+0.04	+1.24	12.19	24/7	1.24	15/8
Cardiff	50.25	-10.03	-4.32	+0.26	+0.97	10.92	25/7	1.01	8/8
Cheltenham	50.12	-11.13	-4.25	+0.40	+1.25	11.91	25/7	1.32	7/8
Chopwelwood	47.09	-10.01	-4.26	+0.36	+1.14	10.88	25/7	1.20	7/8
Colmonell	48.08	- 8.63	-3.95	+0.31	+0.88	9.49	26/7	0.93	6/8
Coventry	49.22	-11.31	-4.29	+0.31	+1.20	12.10	25/7	1.24	9/8
Craibstone	46.04	- 8.75	-4.29	+0.35	+1.05	9.74	28/7	1.11	7/8
Cranwell	48.79	-11.01	-4.55	+0.16	+1.31	11.92	24/7	1.32	12/8
Cromer	49.85	-10.49	-5.19	+0.06	+1.33	11.71	28/7	1.33	18/8
Croydon	50.61	-11.08	-4.56	+0.19	+1.22	11.98	24/7	1.24	12/8
Cullompton	50.61	-10.44	-3.97	+0.38	+1.09	11.17	23/7	1.15	6/8
Cupar	47.11	- 9.95	-3.92	+0.37	+1.38	10.70	23/7	1.43	9/8
Dalwhinnie	43.23	- 9.76	-4.25	+0.41	+1.08	10.65	25/7	1.15	6/8
Darwen	47.43	-10.48	-4.32	+0.53	+0.98	11.34	24/7	1.12	2/8
Donaghadee	48.90	- 7.29	-4.12	+0.37	+1.05	8.37	31/7	1.11	6/8
Douglas	48.81	- 7.82	-4.42	+0.49	+0.75	8.98	1/8	0.90	30/7
Dover	50.83	-10.16	-5.32	-0.10	+0.98	11.47	30/7	0.98	19/8
Dublin (Phoenix Park)	48.96	- 8.71	-3.92	+0.55	+1.31	9.55	26/7	1.42	4/8
Dumfries	47.69	- 9.77	-3.91	+0.45	+1.07	10.52	24/7	1.16	5/8
Dundee	47.23	- 9.89	-4.08	+0.46	+1.29	10.69	24/7	1.37	6/8
Dungavel	44.85	- 9.33	-3.90	+0.55	+0.95	10.12	25/7	1.10	1/8
Dungeness	50.33	- 9.84	-5.64	-0.11	+1.09	11.34	1/8	1.09	19/8
Durham	47.56	-10.01	-4.40	+0.39	+1.21	10.94	26/7	1.27	7/8
East Ham	51.16	-11.55	-4.68	+0.26	+1.25	12.47	24/7	1.27	10/8
Edinburgh (Blackf'd Hill)	47.44	- 9.09	-4.30	+0.61	+1.16	10.06	27/7	1.31	2/8
Eskdalemuir	44.65	- 9.59	-4.00	+0.63	+0.98	10.40	24/7	1.16	31/7
Exmouth	50.61	- 9.03	-4.56	+0.36	+1.09	10.11	29/7	1.15	7/8

/Falmouth

Station	a_0	a_1	b_1	a_2	b_2	A_1	ϕ_1	A_2	ϕ_2
Falmouth	52.14	- 8.10	-4.41	+0.26	+1.06	9.22	31/7	1.09	9/8
Felixstowe	50.38	-10.96	-5.66	+0.05	+1.26	12.33	29/7	1.26	15/8
Fort Augustus	46.76	- 9.25	-3.73	+0.44	+1.29	9.98	25/7	1.36	7/8
Fortrose	47.94	- 9.01	-3.72	+0.15	+0.86	9.74	24/7	0.87	11/8
Fort William	47.52	- 9.17	-3.76	+0.38	+1.17	9.91	24/7	1.23	7/8
Fowey	52.00	- 8.22	-4.34	+0.19	+1.00	9.30	30/7	1.02	11/8
Foynes	50.34	- 8.64	-3.53	+0.72	+1.15	9.33	24/7	1.36	31/7
Frampton Cotterell	49.92	-10.96	-4.05	+0.30	+1.12	11.69	25/7	1.16	8/8
Garvagh	48.05	- 9.30	-3.63	-0.17	+0.67	9.98	23/7	0.69	13/8
Glenbranter	47.03	- 9.26	-3.57	+0.43	+1.01	9.92	23/7	1.10	4/8
Gordon Castle	47.32	- 9.34	-3.85	+0.46	+1.26	10.10	24/7	1.34	6/8
Gorleston	49.86	-10.06	-5.56	-0.01	+1.31	11.49	31/7	1.31	16/8
Greenock	48.39	- 9.16	-3.98	+0.61	+0.88	9.99	25/7	1.07	30/7
Greenwich	50.63	-11.51	-4.54	+0.33	+1.38	12.37	23/7	1.42	9/8
Gulval	52.04	- 7.63	-4.28	+0.33	+0.96	8.75	31/7	1.01	6/8
Halstead	49.95	-11.76	-4.45	+0.04	+1.29	12.57	23/7	1.29	15/8
Hampstead	49.26	-11.55	-4.55	+0.13	+1.19	12.41	23/7	1.20	13/8
Haverfordwest	49.77	- 8.30	-4.29	+0.45	+0.97	9.34	29/7	1.07	3/8
Hawarden Bridge	50.05	-10.01	-4.18	+0.31	+1.12	10.85	24/7	1.16	8/8
Helensburgh	47.49	- 9.51	-3.96	+0.52	+0.92	10.30	24/7	1.06	1/8
Hereford	49.14	-10.65	-4.01	+0.43	+1.12	11.38	22/7	1.20	5/8
Holyhead	50.41	- 7.38	-4.70	+0.21	+0.84	8.78	1/8	0.87	9/8
Hoylake	49.90	- 9.79	-4.41	+0.36	+1.09	10.74	26/7	1.15	7/8
Huddersfield (Ravensknowle)	48.39	-10.64	-4.40	+0.57	+1.19	11.51	24/7	1.32	3/8
Hull	49.76	-10.70	-4.65	+0.25	+1.40	11.66	25/7	1.42	11/8
Hunstanton	49.84	-10.96	-4.91	-0.03	+1.26	12.01	26/7	1.26	20/8
Hutton	48.75	-10.09	-4.23	+0.20	+1.09	10.94	25/7	1.11	11/8
Ilfracombe	51.89	- 8.05	-4.82	+0.20	+0.95	9.38	2/8	0.98	10/8
Ilkley	47.94	-10.69	-4.33	+0.42	+1.11	11.53	24/7	1.18	6/8
Inverness	46.76	- 8.89	-3.86	+0.52	+1.23	9.70	25/7	1.33	5/8
Kelso	46.94	-10.17	-3.83	+0.37	+1.11	10.87	22/7	1.17	7/8
Kensington Palace	51.64	-11.56	-4.47	+0.20	+1.20	12.40	23/7	1.21	11/8
Keswick	48.49	- 9.41	-4.08	+0.57	+0.97	10.26	25/7	1.12	1/8
Kettins	46.38	-10.30	-3.77	+0.34	+1.27	10.97	22/7	1.31	8/8
Kew	50.76	-11.44	-4.36	+0.50	+1.21	12.24	23/7	1.31	6/8
Kilkenny	48.96	- 9.20	-3.51	+0.69	+1.23	9.85	23/7	1.41	1/8
Kilmarnock	48.13	- 9.82	-3.77	+0.36	+1.17	10.52	23/7	1.23	8/8
Kirkcaldy	47.69	- 9.75	-4.04	+0.39	+1.26	10.56	24/7	1.32	7/8
Larkhill	48.92	-10.68	-4.40	+0.17	+1.18	11.55	24/7	1.19	12/8
Lerwick	44.78	- 6.75	-4.19	+0.63	+1.03	7.94	4/8	1.21	31/7
Leuchars	47.36	- 9.33	-4.05	+0.29	+1.31	10.17	25/7	1.34	10/8
Liverpool	49.35	- 9.73	-4.31	+0.37	+0.91	10.64	26/7	0.98	5/8
Long Ashton	50.17	-10.25	-4.22	+0.31	+1.09	11.08	24/7	1.13	8/8
Luton	48.96	-11.17	-4.56	+0.24	+1.30	12.06	24/7	1.32	11/8
Lympne	49.37	-10.56	-5.06	-0.12	+1.19	11.71	27/7	1.19	19/8
Macclesfield	48.10	-10.88	-4.22	+0.34	+1.12	11.67	23/7	1.17	8/8
Malin Head	48.82	- 6.79	-4.03	+0.16	+1.00	7.90	2/8	1.01	11/8
Malvern	49.97	-11.04	-4.25	+0.26	+1.15	11.83	23/7	1.18	10/8
Manchester	49.81	-10.45	-4.09	+0.37	+1.08	11.22	23/7	1.14	7/8
Marchmont	46.42	- 9.86	-4.08	+0.45	+1.18	10.67	24/7	1.26	5/8
Markree Castle	48.69	- 8.39	-3.42	+0.27	+1.13	9.06	24/7	1.16	9/8
Marlborough	48.42	-10.59	-4.09	+0.35	+1.17	11.35	23/7	1.23	8/8
Morecambe	49.27	-10.27	-4.48	+0.34	+0.92	11.20	25/7	0.98	6/8
Morpeth (Cockle Park)	46.79	- 9.42	-4.34	+0.43	+1.23	10.37	27/7	1.30	6/8
Newport (Mon.)	50.37	-10.63	-4.14	+0.33	+0.98	11.41	24/7	1.04	7/8
Newquay	51.31	- 7.82	-4.46	+0.25	+1.03	9.00	1/8	1.06	9/8
Newton Rigg	46.88	-10.14	-3.91	+0.49	+0.99	10.87	23/7	1.10	3/8
North Berwick	47.70	- 9.21	-4.19	+0.28	+1.16	10.12	26/7	1.20	9/8
Norwich	49.79	-11.54	-4.69	+0.04	+1.29	12.46	24/7	1.29	15/8
Nottingham Castle	49.58	-11.00	-4.37	+0.31	+1.20	11.84	23/7	1.24	9/8

/Oxford

Station	a_0	a_1	b_1	a_2	b_2	A_1	ϕ_1	A_2	ϕ_2
Oxford	50.20	−11.18	−4.32	+0.22	+1.26	11.99	23/7	1.28	11/8
Paisley	48.68	− 9.87	−3.74	+0.55	+1.02	10.56	23/7	1.16	2/8
Perth	47.47	−10.55	−3.75	+0.40	+1.16	11.20	21/7	1.23	6/8
Plymouth (Mount Batten)	51.51	− 8.07	−4.51	+0.32	+0.90	9.24	31/7	0.95	6/8
Portland Bill	51.46	− 7.58	−5.63	+0.11	+0.83	9.44	8/8	0.84	12/8
Porton	48.81	−10.75	−4.35	+0.16	+1.19	11.59	24/7	1.20	12/8
Reading (Shinfield)	49.83	−11.28	−4.37	+0.25	+1.20	12.09	23/7	1.23	10/8
Reading University	50.63	−11.37	−4.24	+0.20	+1.16	12.14	22/7	1.18	11/8
Renfrew	47.69	− 9.63	−3.75	+0.42	+1.17	10.33	23/7	1.24	6/8
Rhyader	47.16	− 9.56	−4.20	+0.46	+1.03	10.44	26/7	1.13	4/8
Rhyl	50.13	− 8.98	−4.41	+0.33	+1.10	10.01	28/7	1.14	8/8
Roches Point	51.22	− 7.05	−3.98	+0.44	+1.07	8.09	31/7	1.16	5/8
Ross-on-Wye	50.00	−10.28	−4.11	+0.40	+1.12	11.07	24/7	1.19	6/8
Rothamsted	48.57	−11.21	−4.53	+0.14	+1.25	12.09	24/7	1.26	13/8
Rothesay	47.82	− 8.28	−3.88	+0.51	+0.81	9.14	27/7	0.96	31/7
Rothwell	47.60	−10.28	−3.92	+0.31	+1.06	11.00	23/7	1.10	8/8
Ryde	51.63	−10.24	−4.92	+0.26	+0.99	11.36	28/7	1.02	9/8
St. Anne's Head	50.68	− 7.01	−4.84	+0.35	+0.74	8.52	6/8	0.82	3/8
Sandown	51.55	− 9.80	−5.09	+0.22	+0.96	11.05	29/7	0.98	10/8
Scarborough	49.62	− 9.56	−4.72	+0.05	+1.37	10.66	28/7	1.37	15/8
Scilly	52.58	− 6.48	−4.45	+0.29	+1.10	7.86	5/8	1.14	9/8
Seskin (Carrick on Suir)	48.96	− 9.06	−3.68	+0.52	+1.17	9.78	24/7	1.28	3/8
Shaftesbury	48.81	−10.30	−4.48	+0.13	+1.07	11.23	25/7	1.08	13/8
Sheffield	49.22	−10.49	−4.51	+0.46	+1.10	11.42	25/7	1.19	5/8
Shoeburyness	50.47	−11.11	−5.22	+0.12	+1.42	12.28	27/7	1.43	14/8
Shrewsbury	49.46	−10.86	−4.24	+0.25	+1.01	11.66	23/7	1.04	9/8
Sidmouth	50.90	− 8.87	−4.65	+0.26	+1.07	10.02	30/7	1.10	7/8
Skegness	48.95	−10.37	−5.06	−0.01	+1.33	11.54	28/7	1.33	16/8
South Farnborough	50.01	−11.08	−4.34	+0.31	+1.24	11.90	23/7	1.28	9/8
Southampton	51.06	−10.76	−4.44	+0.18	+1.07	11.64	24/7	1.08	11/8
Southport	49.30	− 9.95	−4.35	+0.25	+1.05	10.86	26/7	1.08	9/8
Spurn Head	49.43	− 9.86	−5.43	+0.02	+1.24	11.25	31/7	1.24	16/8
Stirling	47.99	−10.09	−3.74	+0.46	+1.16	10.76	22/7	1.25	5/8
Stonyhurst	48.03	−10.20	−4.26	+0.43	+0.90	11.05	25/7	1.00	3/8
Stornoway	47.14	− 6.90	−3.74	+0.54	+1.07	7.85	30/7	1.20	3/8
Swansea	51.55	− 9.59	−4.54	+0.26	+0.87	10.61	27/7	0.91	8/8
Tavistock	50.12	− 9.00	−4.14	+0.26	+0.94	9.91	27/7	0.98	8/8
Tiree	48.62	− 6.82	−4.04	+0.18	+0.68	7.92	3/8	0.71	9/8
Tunbridge Wells	49.38	−11.44	−4.56	+0.09	+1.21	12.31	24/7	1.21	14/8
Turnberry	48.72	− 8.36	−4.07	+0.24	+0.82	9.29	28/7	0.85	8/8
Tynemouth	48.55	− 8.55	−4.72	+0.23	+1.30	9.77	31/7	1.32	11/8
Ushaw	47.22	−10.17	−4.37	+0.30	+1.21	11.07	25/7	1.25	7/8
Valentia	51.34	− 6.77	−3.57	+0.44	+1.00	7.65	30/7	1.09	4/8
Ventnor Hospital	51.98	− 9.43	−5.17	−0.04	+0.89	10.76	30/7	0.89	17/8
Wakefield	49.26	−10.94	−4.35	+0.28	+1.20	11.77	23/7	1.24	9/8
Welshpool	48.80	−10.20	−4.02	+0.45	+1.07	10.96	23/7	1.16	10/8
West Linton	44.79	− 9.71	−3.92	+0.57	+1.10	10.48	24/7	1.24	2/8
Westminster	51.98	−11.47	−4.51	+0.17	+1.16	12.32	23/7	1.18	12/8
Wick	46.01	− 6.94	−4.17	+0.31	+1.04	8.10	1/8	1.09	8/8
Wisley	50.26	−11.30	−4.30	+0.22	+1.26	12.09	23/7	1.28	11/8
Woburn	48.80	−11.08	−4.47	+0.25	+1.29	11.95	24/7	1.32	11/8
Wolfelee	45.49	− 9.99	−3.72	+0.52	+1.02	10.66	22/7	1.15	2/8
York	49.34	−10.85	−4.29	+0.34	+1.24	11.67	23/7	1.28	8/8

FIG1 ANNUAL MEAN TEMPERATURE 1921-1950 IN DEGREES FAHRENHEIT.

M.R.P. 970

TEMPERATURES CORRECTED TO MEAN SEA LEVEL

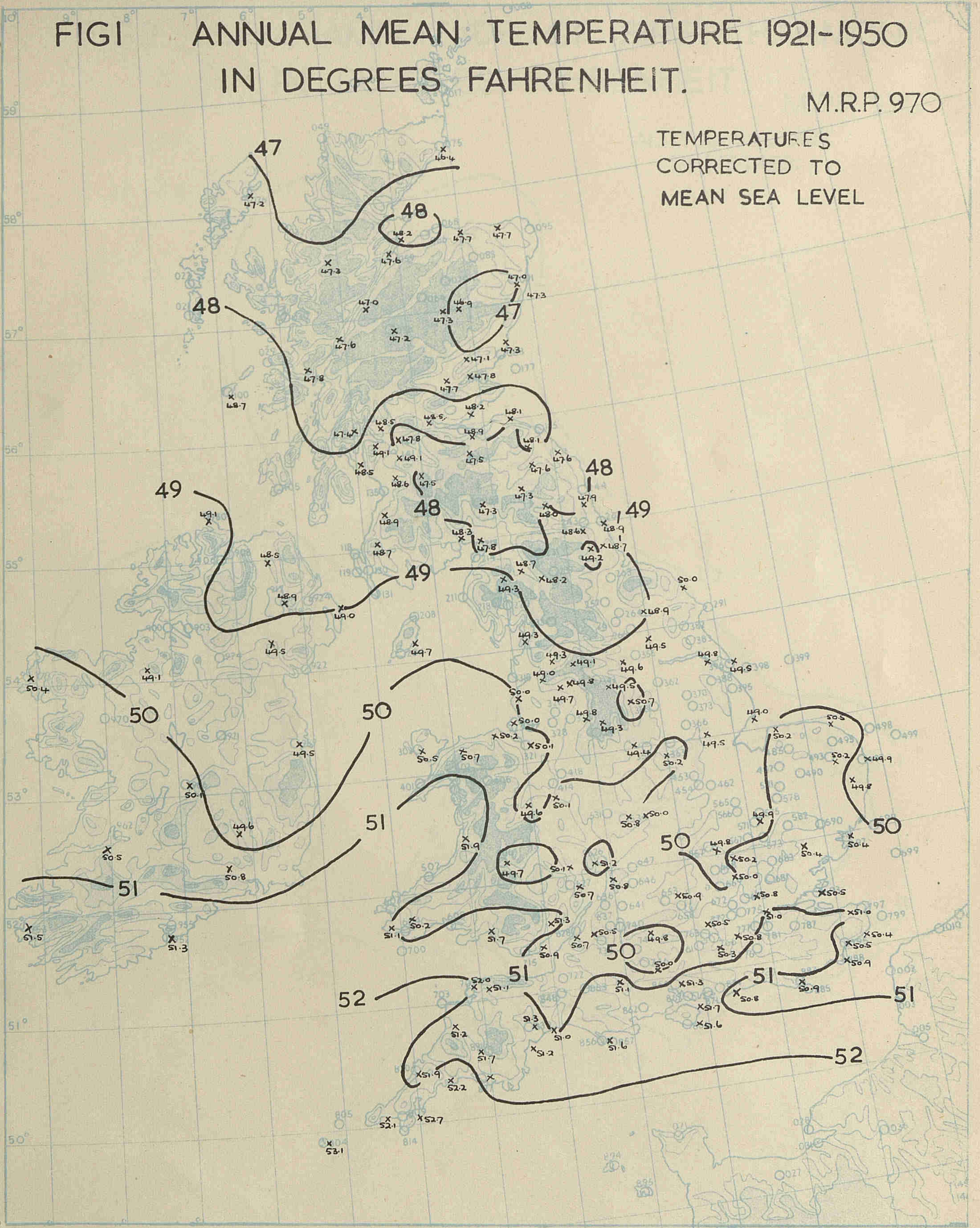

47
48
47
48
48
48
49
49
49
50
50
50
50
50
51
51
51
51
51
52
52

FIG 2. SEMI-AMPLITUDE OF FIRST HARMONIC IN DEGREES FAHRENHEIT.

M.R.P. 970

ALTITUDES GIVEN IN METRES.

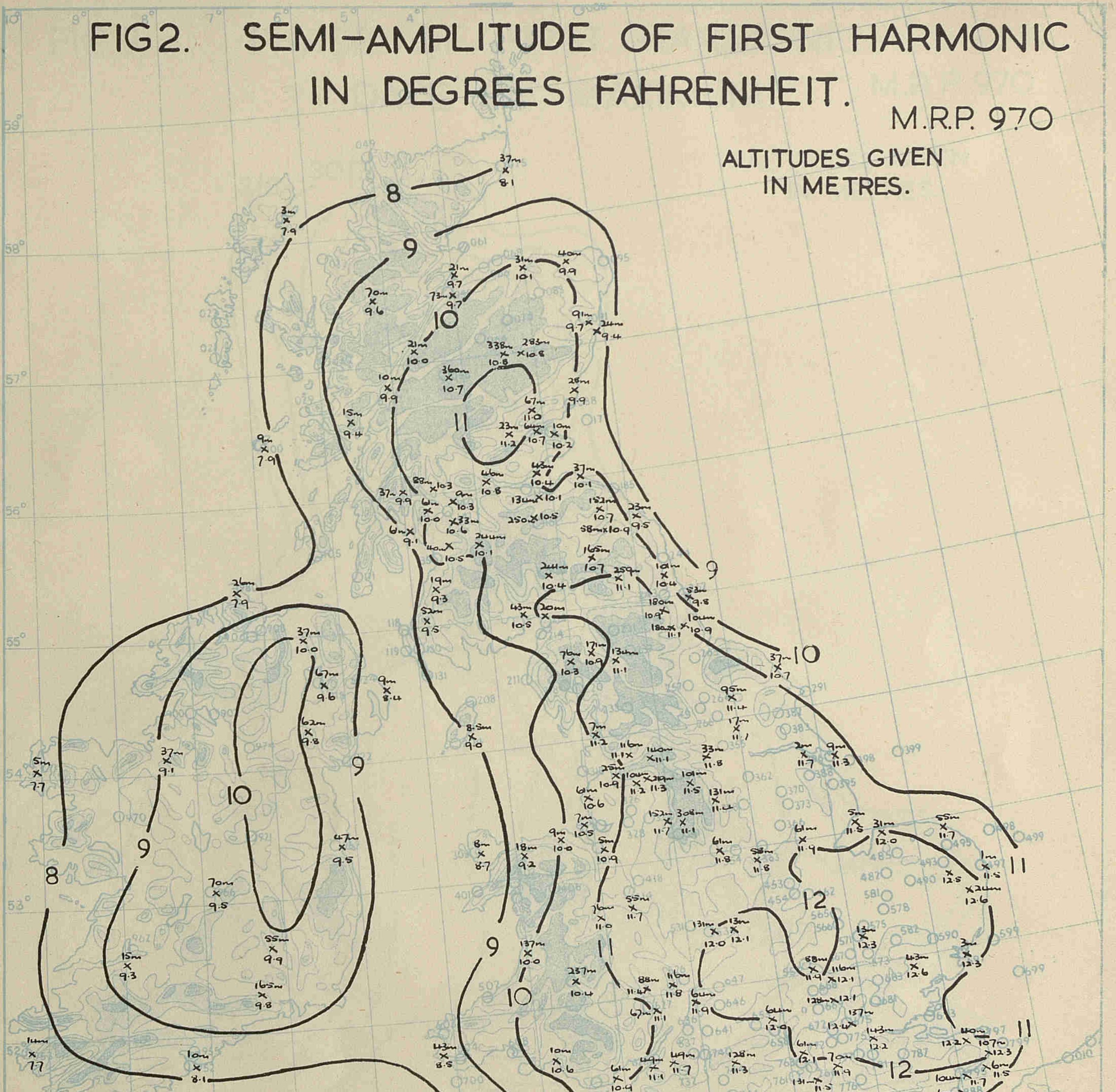

8
9
10
11
12
59°
58°
57°
56°
55°
54°
53°
52°
51°
50°
10°
9°
8°
7°
5°
4°
37m 8.1
3m 7.9
70m 9.6
21m 9.7
73m 9.7
31m 10.1
40m 9.9
91m 9.7
24m 9.4
21m 10.0
338m 10.8
283m 10.8
360m 10.7
10m 9.9
28m 9.9
67m 11.0
15m 9.4
23m 11.2
64m 10.7
10m 10.2
9m 7.9
88m 10.3
46m 10.8
43m 10.4
37m 10.1
37m 9.9
6m 10.0
9m 10.3
131m 10.1
152m 10.7
23m 9.5
6m 9.1
33m 10.6
250 10.5
58m 10.9
40m 10.5
244m 10.1
165m 10.7
26m 7.9
19m 9.3
241m 10.4
259m 11.1
101m 10.4
53m 9.8
52m 9.5
43m 10.5
20m
180m 10.9
10m 10.9
183m 11.1
37m 10.0
37m 10.7
67m 9.6
9m 8.4
76m 10.3
171m 10.9
134m 11.1
95m 11.4
62m 9.8
8.5m 9.0
7m 11.2
116m 11.1
140m 11.1
33m 11.8
17m 11.1
2m 11.7
9m 11.3
5m 7.7
37m 9.1
25m 10.9
10m 11.2
39m 11.3
101m 11.5
131m 11.4
6m 10.6
7m 10.5
152m 11.7
308m 11.1
5m 11.5
31m 12.0
55m 11.7
47m 9.5
9m 10.0
8m 8.7
18m 9.2
5m 10.9
61m 11.8
58m 11.8
61m 11.9
1m 11.5
12.5
24m 12.6
70m 9.5
55m 11.7
76m 11.0
131m 12.0
13m 12.1
13m 12.3
137m 10.0
3m 12.3
15m 9.3
55m 9.9
257m 10.4
88m 11.4
116m 11.8
6m 11.9
68m 11.9
116m 12.1
43m 12.6
165m 9.8
67m 11.1
61m 12.0
128m 12.1
137m
12.4
143m 12.2
110m 12.2
107m 12.3
1m 7.7
10m 8.1
43m 8.5
10m 10.6
61m 10.4
49m 11.1
49m 11.7
128m 11.3
61m 12.1
70m 11.9
131m 11.5
6m 11.5
10m 11.7
6m 11.3
2m
8m 9.5
201m 11.2
20m 11.6
7m 11.2
152m 10.9
15m 9.3
6m 11.2
8m 10.0
4m 11.4
4m 11.1
10m 9.4
140m 9.9
58m 10.1
85m 9.0
15m 9.3
27m
6m 8.7
52m 9.2
149m 7.4

FIG 3. PHASE OF FIRST HARMONIC DATE OF MAXIMUM.

M.R.P. 970

ALTITUDES GIVEN IN METRES.

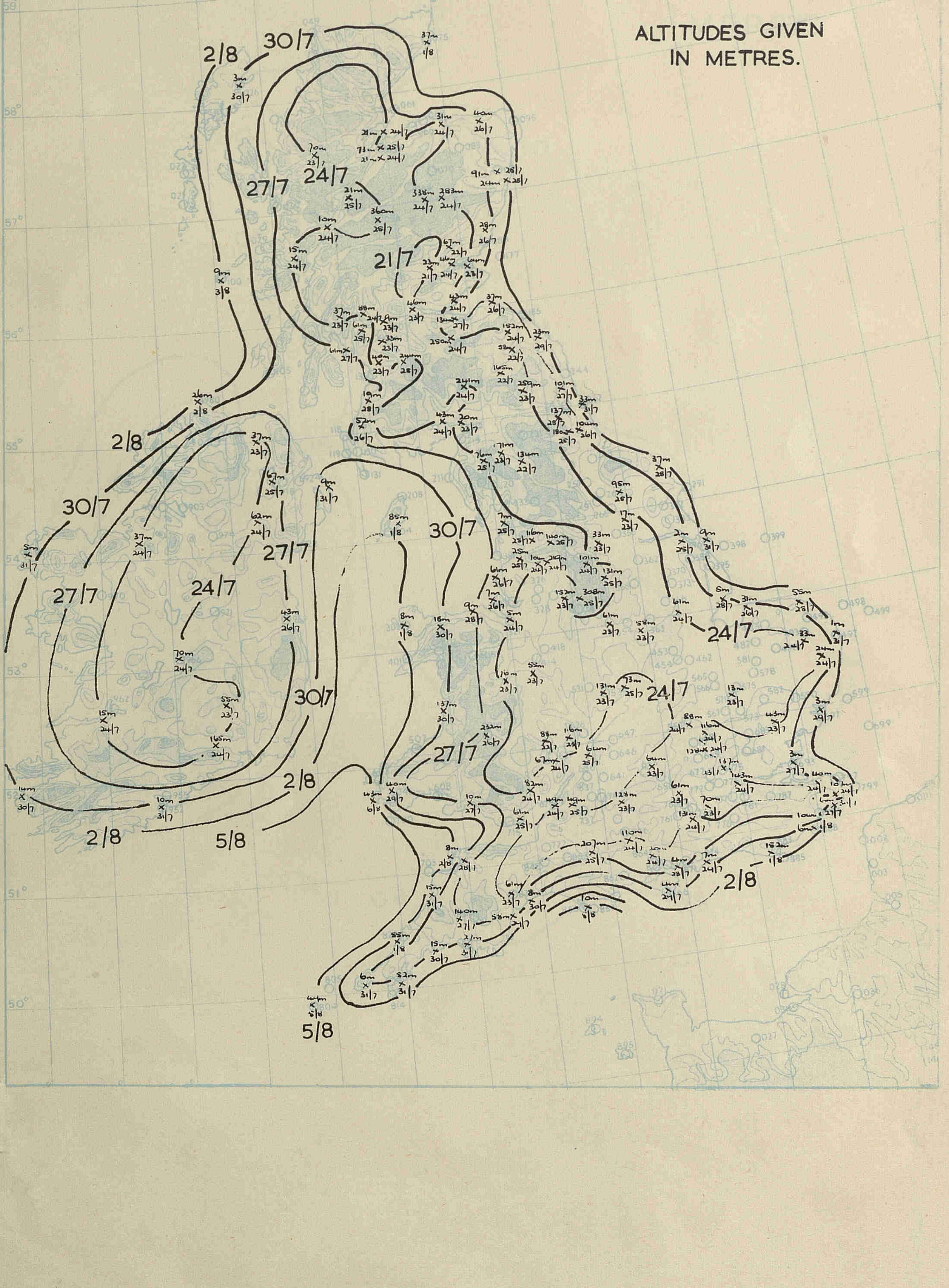

2/8
30/7
27/7
24/7
21/7
2/8
30/7
27/7
24/7
27/7
30/7
30/7
27/7
24/7
24/7
2/8
2/8
5/8
2/8
5/8

FIG 4. SEMI-AMPLITUDE OF SECOND HARMONIC IN DEGREES FAHRENHEIT.

M.R.P. 970

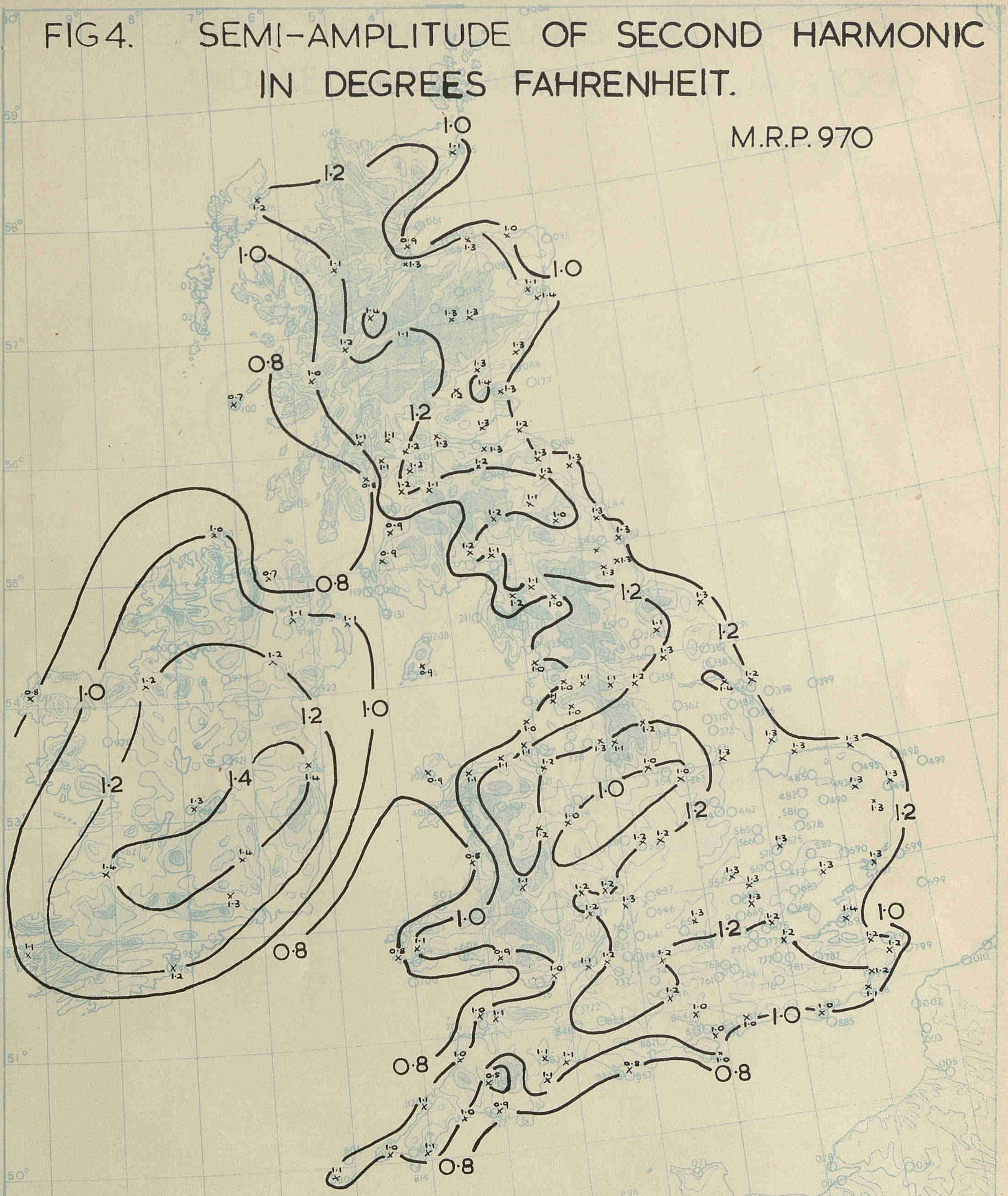

1·0
1·2
1·0
1·0
0·8
1·2
0·8
1·0
1·2
1·4
1·2
1·0
1·2
0·8
1·2
1·2
1·0
1·2
1·0
1·2
1·0
1·2
1·0
0·8
0·8
0·8

FIG 5. RATIO OF AMPLITUDES OF THE FIRST AND SECOND HARMONICS ($A_2/A_1 \times 100$)

M.R.P. 970

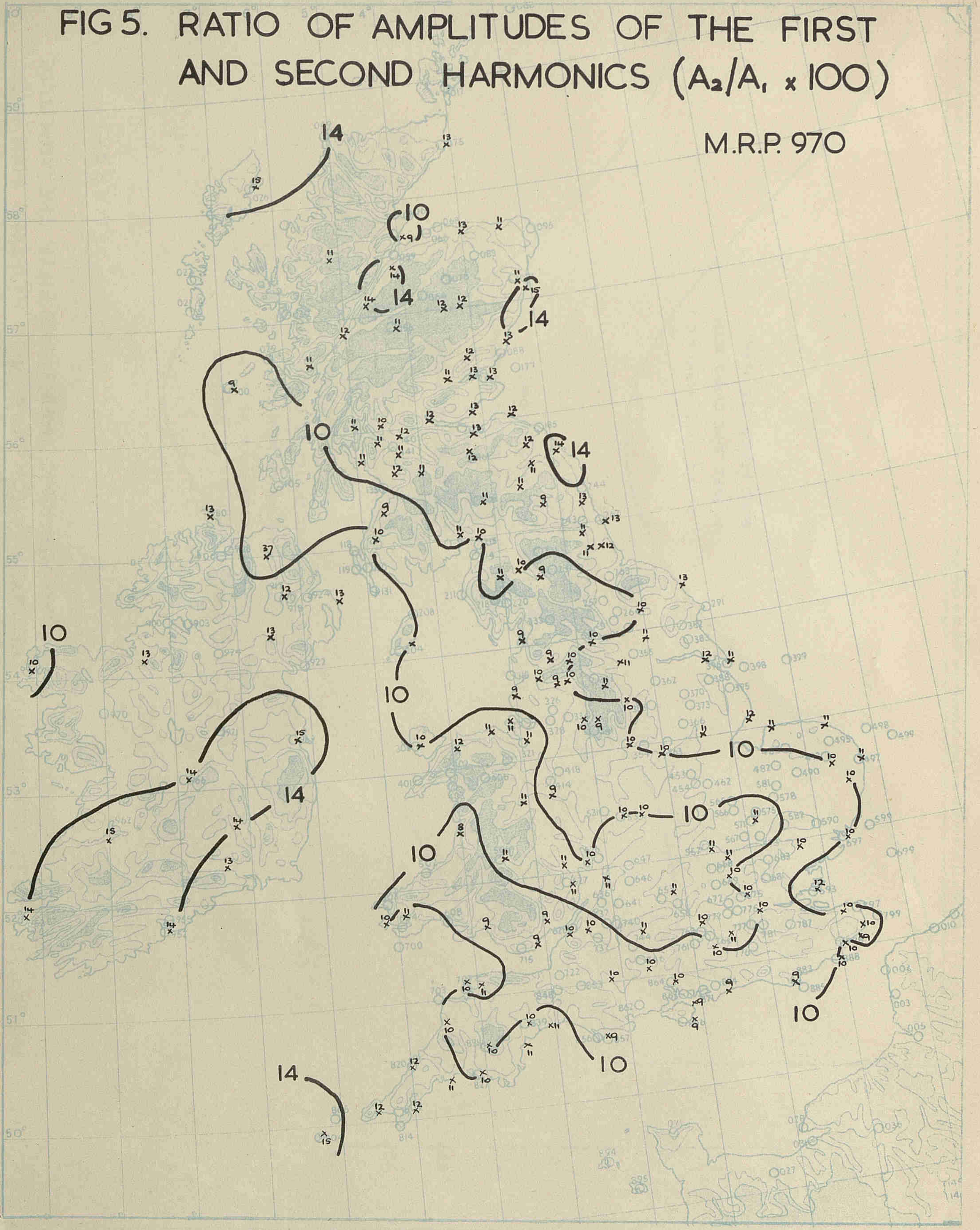

14
10
14
14
10
10
10
14
14
10
10
10
10
10
10
10
14

FIG 5A EXAMPLES ILLUSTRATING THE MODIFICATION OF A FIRST HARMONIC WITH BASIC PERIOD ONE YEAR BY A SECOND HARMONIC HAVING ONE FIFTH THE AMPLITUDE OF THE FIRST.

M.R.P. 970

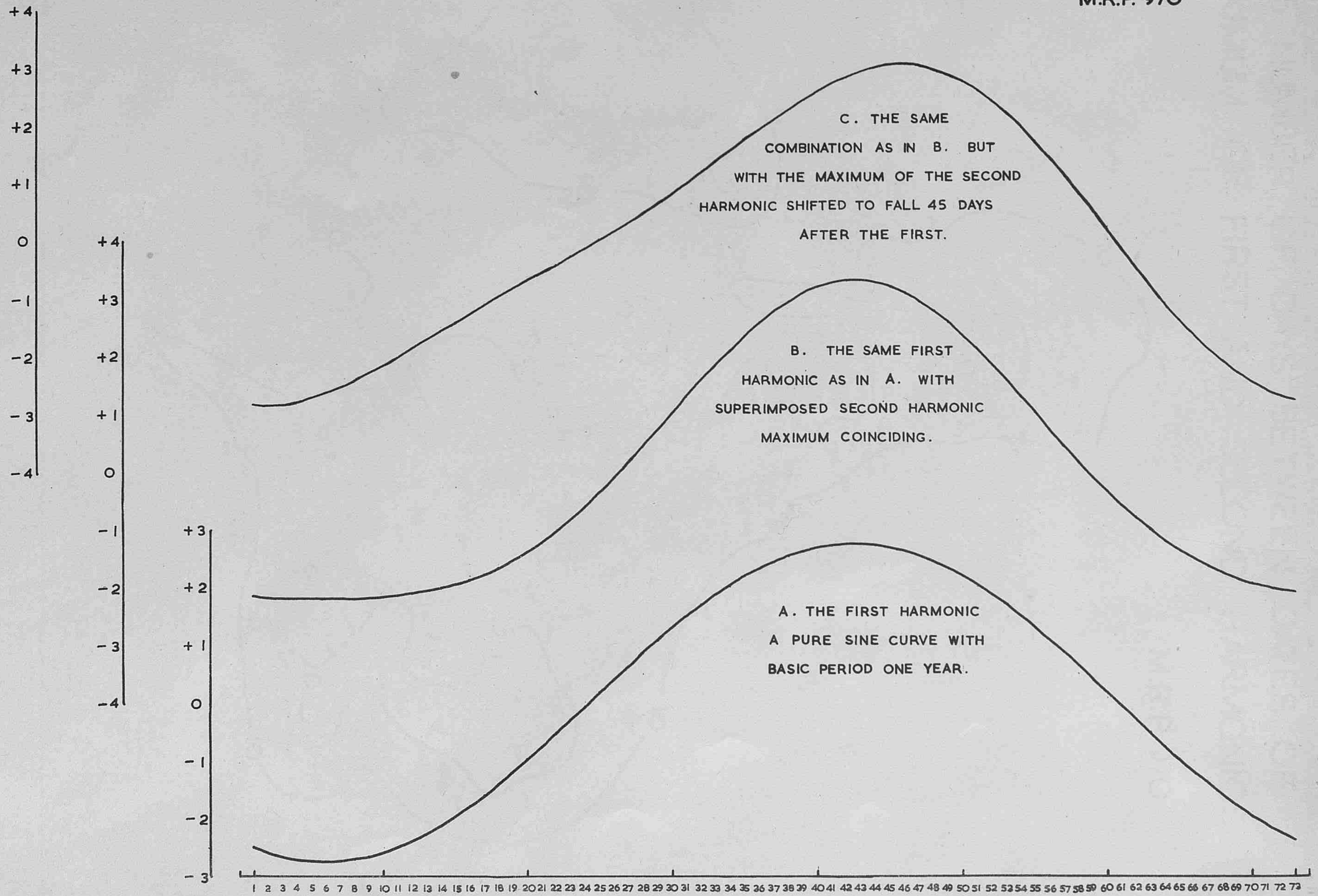

C. THE SAME COMBINATION AS IN B. BUT WITH THE MAXIMUM OF THE SECOND HARMONIC SHIFTED TO FALL 45 DAYS AFTER THE FIRST.

B. THE SAME FIRST HARMONIC AS IN A. WITH SUPERIMPOSED SECOND HARMONIC MAXIMUM COINCIDING.

A. THE FIRST HARMONIC A PURE SINE CURVE WITH BASIC PERIOD ONE YEAR.

FIG 6. NUMBER OF DAYS BETWEEN DATES OF MAXIMUM OF FIRST AND SECOND HARMONICS.

M.R.P. 970

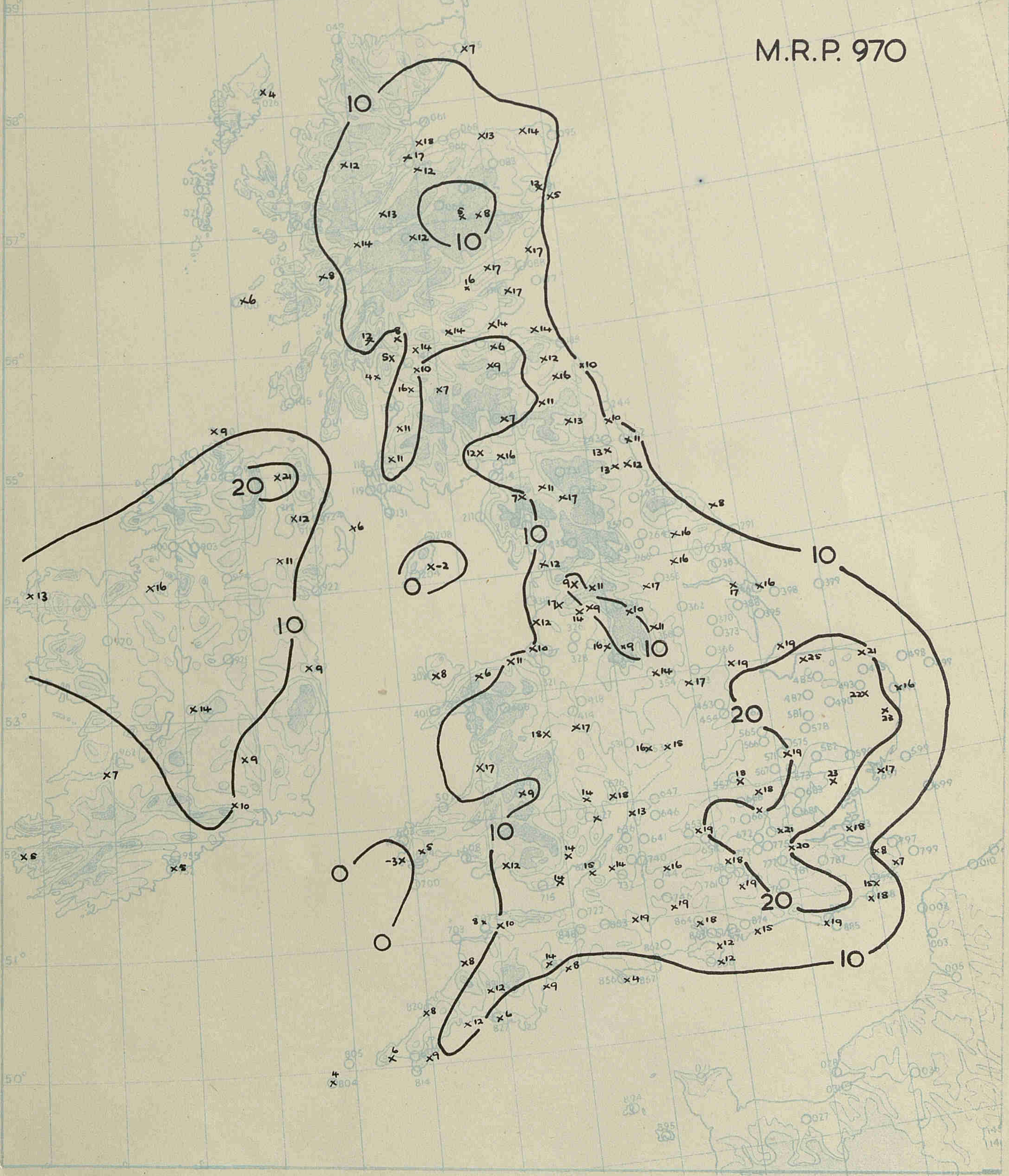
10
10
20
10
0
10
10
10
0
0
10
20
20
10

Mats (aws)

AD 139534

M.R.P. 971
S.C. 111/201
9th April, 1956

AD139534

Variation of visibility in fog at Exeter Airport, and the time of fog dispersal

by

W.E. Saunders
(Meteorological Office)

AIR MINISTRY
METEOROLOGICAL RESEARCH COMMITTEE

56- 1189

At the time of issue this report has not been published. Any author desiring to quote this paper should refer to it as "A paper of the Meteorological Research Committee (London).
M.R.P. No. 971 by Mr. W.E. Saunders
A copy is available in the Library of the Meteorological Office."

M.R.P. 971
S.C.III/201
9th April, 1956.

AIR MINISTRY

METEOROLOGICAL RESEARCH COMMITTEE

Variation of visibility in fog at Exeter Airport, and the time of fog dispersal

by

W.E. Saunders (Meteorological Office)

Summary

An account is given of the variation in visibility at Exeter Airport during periods of fog. Main features of interest are the rapidity with which visibility falls to lower values within the fog range once fog has formed, the effectiveness of cloud cover as a fog-clearing agency, and the comparatively regular intervals between times of clearance of fog during the morning, and times of sunrise.

The site and observational programme

The airfield lies in a shallow basin formed by the high ground of Dartmoor to the southwest and west, Exmoor to the north, and the Blackdown Hills to the east. There are no intervening hills between the airfield and the English Channel to the south and the Exe Estuary to the southwest.

The only significant source of local smoke is the city of Exeter, some three miles west of the airfield.

The situation of the airfield is shown in Fig. 1.

The normal hourly and special observations of a synoptic station were made at Exeter throughout the period from which data have been used in this study. Additional temperature readings, which have been included in the notes on clearance of fog beneath cloud, were as follows:-

(i) Hourly readings of the grass minimum thermometer used as an ordinary thermometer at grass level, and of a bent stem earth thermometer with the bulb at a depth of 2 in.

(ii) Twice-daily readings of a bent stem earth thermometer with the bulb at 8 in. These readings were made at 0900 and 2100 GMT.

Type of fog at Exeter

The fog was predominantly water fog as defined by Corby and Saunders (1); that is fog which did not form until after the relative humidity exceeded 95%. The investigation covers 145 cases (i.e., all the occasions of radiation fog) over the period September, 1953 to December, 1955. On only ten of these occasions did visibility enter the fog range with relative humidity less than 95%, the lowest being 93%. The results described therefore apply only to water fog. It is considered unlikely that they will apply to smoke fog, or to water fog containing a high smoke content. They may, however, be of interest to forecasters at other rurally placed stations, or to stations which experience "clean" fog when the airstream is moving from some known direction.

Time taken for visibility to fall below certain limits

The variation in visibility following the initial report of fog was studied in all cases (112 out of 145) in which fog-clearing agencies were not at work. The cases omitted were those in which there was freshening wind, cloud cover, frontal passage, or which occurred at the end of the night.

Variations in visibility were examined in terms of the time taken to fall to "550 yd. or below", and to "220 yd. or below". On some occasions fog-clearing influences became apparent soon after the 550 yd. stage was reached, but there were 92 occasions suitable for examination in regard to the 220 yd. limit.

The overall picture is given in Table I.

Table I - Time for visibility to fall below 550 or 220 yd.

	Hours, from initial report of fog					
	0 - 1	1 - 2	2 - 3	3 - 4	4 - 5	Not reached
For visibility to fall to 550 yd. or below	96	11	1	0	0	4
For visibility to fall to 220 yd. or below	47	21	6	6	1	11

Table I emphasises the rapid fall of visibility in water fog. On 95% of occasions visibility is 550 yd. or less within two hours of fog formation. The transition to dense fog is sometimes rather less rapid, but on 74% of occasions visibility is 220 yd. or below within two hours.

The rate of decrease of visibility was examined in relation to certain initial conditions which might have influenced the result. These were the initial fog point temperature and the rate of fall of temperature while the visibility was falling, the wind direction, the visibility preceding fog formation, and the state of ground. An account of these is given in the following paragraphs.

Variation with temperature

The rate of decrease of visibility was examined in conjunction with the fog point, i.e., the temperature at which water fog formed, and the results are given in Table II. This shows that the four cases included in Table I as failing to reach the 550 yd. limit were all on occasions when the initial fog point was below 40°F. Otherwise the table is not very conclusive. Dense fog may still be expected when the fog point is several degrees below freezing.

/Table II

Table II - Time taken for visibility in fog to fall below certain limits - variation with fog point temperature

Fog point °F.	Hours, from initial report of fog, for visibility to reach 550 yd. or less				Hours, from initial report of fog, for visibility to reach 220 yd. or less					
	0 - 1	1 - 2	2 - 3	Not reached	0 - 1	1 - 2	2 - 3	3 - 4	4 - 5	Not reached
60-64	3	1	-	-	2	1	1	-	-	-
55-59	5	-	1	-	3	-	--	2	-	-
50-54	21	2	-	-	11	3	1	1	-	2
45-49	27	2	-	-	9	10	2	1	-	2
40-44	19	3	-	-	11	4	1	-	-	3
35-39	11	2	-	2	6	1	1	-	1	2
30-34	7	1	-	1	4	2	-	-	-	1
25-29	3	-	-	1	1	-	-	2	-	1

Table III - Fall of temperature, from fog point, for visibility to reach certain limits

Fog Point °F.	Fall of temperature, from fog point, for visibility to reach 550 yd. or less, °F.						Fall of temperature, from fog point, for visibility to reach 220 yd. or less, °F.					
	0 - 1	1 - 2	2 - 3	3 - 4	4 - 5	5 - 6	0 - 1	1 - 2	2 - 3	3 - 4	4 - 5	5 - 6
60-64	2	1	1	-	-	-	1	-	1	2	-	-
55-59	3	1	-	2	-	-	1	1	-	2	1	-
50-54	16	3	1	2	1	-	8	3	1	3	1	-
45-49	24	1	1	-	1	2	11	1	4	1	1	4
40-44	16	4	1	-	1	-	6	7	3	-	-	-
35-39	8	2	2	1	-	-	5	1	1	-	2	-
30-34	7	1	-	-	-	-	4	1	1	-	-	-
25-29	2	1	-	-	-	-	2	-	-	1	-	-

Table III shows the further fall of temperature, once fog has formed, for visibility to reach 550 yd. or less, and 220 yd. or less. This shows that while, in general, only a slight fall of temperature amounting to a degree or so is required, there are a few occasions on which the fall is as much as five or six degrees. It might be expected on theoretical grounds that these would be the low temperature occasions, but this is not borne out by the table.

Variation with visibility before fog formation

In order to determine whether there was any connection between the rate of fall of visibility preceding fog and in the fog, the rate of decrease of visibility was compared with the visibility three hours before fog formation, and the results are given in Table IV.

Table IV - Time taken for visibility in fog to fall below certain limits - variation with visibility three hours before fog formation

Visibility 3 hours before fog formation	Hours, from initial report of fog, for visibility to reach 550 yd. or less				Hours, from initial report of fog, for visibility to reach 220 yd. or less					
	0 - 1	1 - 2	2 - 3	Not reached	0 - 1	1 - 2	2 - 3	3 - 4	4 - 5	Not reached
Over $6\frac{1}{4}$ mi.	27	2	-	1	15	7	1	-	-	3
$2\frac{1}{2}$ - $6\frac{1}{4}$ mi.	36	5	-	-	15	7	3	3	1	5
2200 yd.-$2\frac{1}{2}$ mi.	18	3	-	3	12	6	1	-	-	3
1100-2200 yd.	15	1	1	-	5	1	1	3	-	-

Table IV shows that there is some tendency for hazy initial conditions to be followed by a rather slower deterioration than when fog forms in clean air.

Variation with wind direction before fog formation

The time taken for visibility to fall to the prescribed limits was compared with the wind direction three hours before the time of fog formation, as shown in Table V.

/Table V

Table V - Time taken for visibility in fog to fall below certain limits - variation with wind direction three hours before fog formation

Wind direction 3 hours before fog formation (degrees)	Hours, from initial report of fog, for visibility to reach 550 yd. or less				Hours, from initial report of fog, for visibility to reach 220 yd. or less					
	0 - 1	1 - 2	2 - 3	Not reached	0 - 1	1 - 2	2 - 3	3 - 4	4 - 5	Not reached
001-030	4	1	-	1	1	2	-	-	-	1
031-060	4	3	-	-	2	2	-	1	1	1
061-090	2	-	1	-	1	1	-	1	-	-
091-120	6	-	-	-	2	1	-	1	-	1
121-150	7	-	-	-	5	-	-	-	-	-
151-180	11	2	-	-	8	3	1	-	-	-
181-210	2	-	-	-	2	-	-	-	-	-
211-240	4	-	-	-	2	1	-	-	-	-
241-270	3	-	-	-	2	-	1	-	-	-
271-300	2	-	-	-	-	1	-	-	-	1
301-330	9	1	-	-	2	1	2	-	-	1
331-360	1	-	-	2	-	-	-	-	-	2
Calm	41	4	-	1	20	9	2	3	-	4

The large proportion of "calms" renders analysis of Table V difficult, but perhaps some tentative conclusions may be drawn. The most significant feature seems to be the rapidity of decrease of visibility with wind direction bringing moist air from the English Channel and Exe Estuary. Thus, in all cases with wind direction between SE. and W. (through S.) the visibility was 550 yd. or less within two hours, and 220 yd. or less within three hours, of fog formation.

Variation with state of ground

The times for visibility to reach the agreed limits were compared with the reported state of ground before fog formation. The results, given in Table VI, show that in all cases of wet ground visibility fell to 550 yd. or less within two hours of fog formation, and that wet ground much reduces the chance of visibility 220 yd. or less not being reached.

Table VI - Time taken for visibility in fog to fall below certain limits - variation with state of ground before fog formation

State of ground before fog formation	Hours, from initial report of fog, for visibility to reach 550 yd. or less				Hours, from initial report of fog, for visibility to reach 220 yd. or less					
	0 - 1	1 - 2	2 - 3	Not reached	0 - 1	1 - 2	2 - 3	3 - 4	4 - 5	Not reached
Dry	50	2	1	4	23	11	4	3	-	9
Wet	46	9	-	-	24	10	2	3	1	2

/The

The effect of cloud cover on fog

The effect of cloud cover on existing fog was examined. The criteria adopted were that the cloud amount, excluding broken cirrus, should increase from four oktas or less to five oktas or more, or that an existing cloud sheet should lower significantly. The effect of cloud cover on the fog is shown in Table VII.

Table VII - The effect of cloud on fog

	Fog cleared. Time taken from increase in cloud for visibility to increase to 1100 yd. or more (hours)					Fog did not clear
0 - 1	1 - 2	2 - 3	3 - 4	4 - 5	5 - 6	
18	11	4	2	4	1	10
	(number of occasions)					

Table VII shows that to a marked extent water fog is dispersed by any appreciable cloud cover. This applied on 40 out of 50 occasions, and on nearly half the nights when fog cleared it did so within one hour of the cloud arriving or increasing.

The temperature distribution during the fog preceding the arrival or increase of cloud was always of the same type. The lowest temperature of those measured was at the grass level. Of the soil temperatures at -2 in. and -8 in. the latter was always the higher. The screen temperature was intermediate between the grass and -2 in. temperatures. After the arrival of cloud the most pronounced change was at grass level. This temperature always increased, in some cases by as much as 10 or 12°F. At both screen level and -2 in. changes were slight, often less than ±1°F. After clearance of the fog, readings of grass and screen temperatures were usually nearly the same, though sometimes there was still an inversion between them.

Example

					Temperatures			
Date	Time	Wind	Cloud	Visibility	Screen	Grass	-2 in.	-8 in.
18/11/53	2356	Calm	Nil	160 yd.	42.2	40.9	46.7	48.8°F.
19/11/53	0156	Calm	8/8 1800ft.	1800 yd.	44.9	44.3	47.2	-

The records of all the foggy nights affected by cloud were examined to see to what extent the result was affected by height of cloud. This showed that on all occasions when the cloud base was not above 2500 ft. the fog cleared. Most of these cases cleared within two hours of the arrival of cloud, but in one instance the process required 5-6 hours. The effects of medium and high cloud and of higher stratocumulus were much less regular. The records of cases in which fog failed to clear under cloud contained some suggestion of W. or NW.'ly drift at some stage in most of them; this might imply some smoke content from Exeter. The investigation leaves a strong impression that clean water fog is readily cleared by cloud, and that if the cloud is not above 2500 ft. the process is likely to be rapid.

/The

The time of clearance of fog

In the absence of other fog-clearing influences, such as freshening wind or increasing cloud cover, the time of clearance should be roughly determined by the amount of insolation, which varies with the date, and by the vertical thickness of the fog. In the absence of measurements of the depth of fog some guidance is given by the appearance of the fog from the ground, whether it is reported as "sky obscured" or "sky visible".

In Fig. 2, for which the period was extended to 1939-1955, the intervals between times of sunrise and of fog clearance have been plotted against the date, and separated according as the sky was or was not visible at 0600 GMT. This time was selected partly because it marks a stage at which, taking the year as a whole, cooling is practically completed, and partly because it is a convenient time in relation to the issue of short-term forecasts on which many day-time activities depend. Occasions when the fog formed after 0600 were plotted as "sky visible" regardless of whether it later became obscured. Occasions omitted were those in which cloud appeared to affect the result, or where there was freshening wind. The number of occasions was sufficient to draw the mean curves AA and BB with fair accuracy, except in mid-winter. The minimum time interval between sunrise and fog dispersal occurs in spring, and this is perhaps due to a somewhat lower water content in fogs at this season as compared with summer and autumn. A small number of "sky visible" cases was noted in January-March in which the original fog point was below 32°F. and the clearance time mostly before sunrise. The fog point temperature has been inserted against these cases in Fig. 2, and they have been disregarded in drawing BB. Presumably the fog clearance in these cases was due to deposition of the moisture as frost.

Fig. 2 shows that a substantial proportion of fogs cleared within one hour of the times indicated by AA and BB. It is not known how the scatter compares with accuracy at present attained by forecasters in forecasting fog clearance, but preparation of diagrams of this type for various sites may help to prevent large errors. Perhaps the real significance of Fig. 2 is that it shows that a quite marked separation can be obtained by use of a simple parameter to represent vertical thickness of fog. This suggests that if measurements of depth of fog were available it might be possible to replace AA and BB by a series of curves representing different thicknesses of fog, and so increase the usefulness of the diagram as a forecasting tool.

It is emphasised that the cases included must be regarded as water fog, and that for many sites it will be necessary to distinguish between clean and heavily polluted fog.

Acknowledgment

It is desired to record the excellent and very detailed observing work carried out by the staff at Exeter during 1953-1955, especially by Mr. J. Meadows and Mr. N. R. Broadbear.

Reference

1. CORBY, G. A. and SAUNDERS, W. E. Water Fog Point, a further test. Met. Mag., London, 81, 1952, p.225.

M.R.P. 971

Fig. 1

Location of Exeter Airport

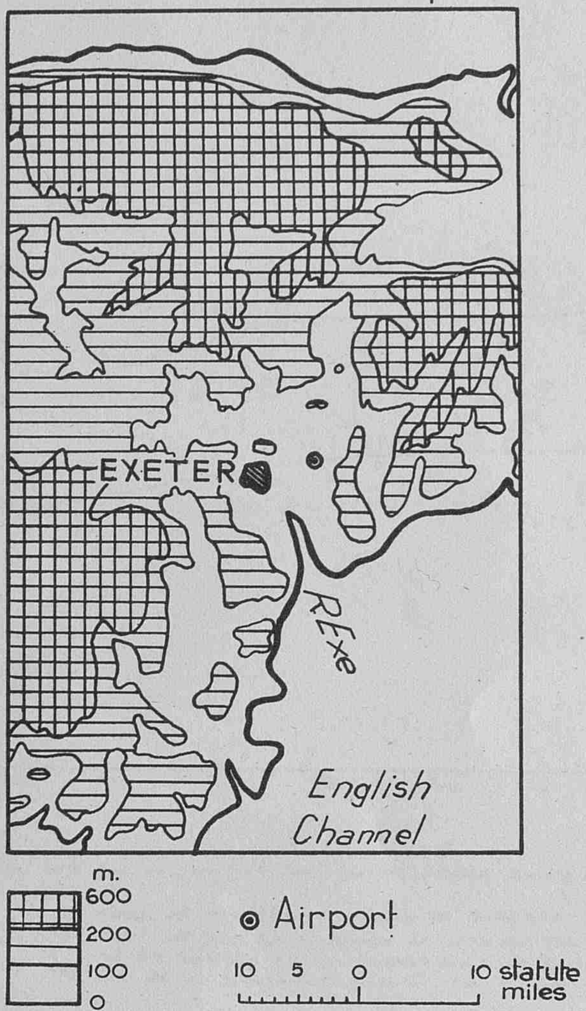
EXETER
R. Exe
English Channel
m.
600
200
100
0
Airport
10 5 0 10 statute miles

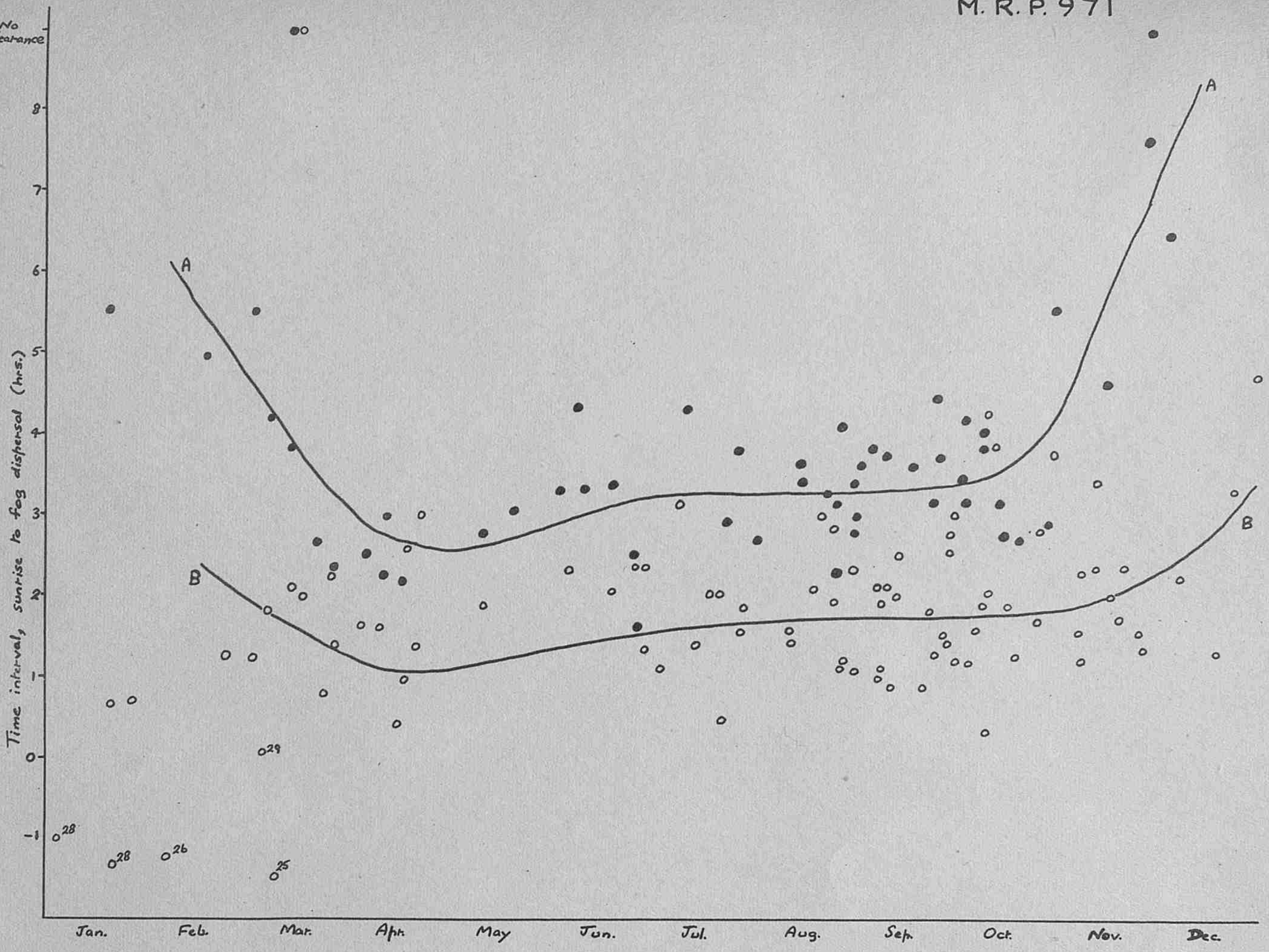

Fig. 2

Variation, with time of year, of time interval between sunrise and fog dispersal

● Cases of sky obscured reported at 0600 GMT
○ Cases of sky visible reported at 0600 GMT (the temperature of fog formation has been inserted beside the symbol if below 32°F)
AA and BB are curves drawn to fit cases ● and ○ respectively

mats (aws)

M.R.P. 972
S.C. 111/202
20th April, 1956.

AD 223109

Water loss from various cropped surfaces.

by

N. E. Rider.

(Meteorological Office)

AIR MINISTRY

METEOROLOGICAL RESEARCH COMMITTEE

56- 1185

At the time of issue this report has not been published. Any author desiring to quote this paper should refer to it as "A paper of the Meteorological Research Committee (London).
M.R.P. No. 972 by Mr. N.E. Rider
A copy is available in the Library of the Meteorological Office."

M.R.P. 972
S.C.III/202
20th April, 1956

AIR MINISTRY

METEOROLOGICAL RESEARCH COMMITTEE

Water loss from various cropped surfaces

by

N.E. Rider (Meteorological Office)

Summary

An account is given of some observations designed to evaluate the daily water losses from surfaces carrying crops of different size and shape which were transpiring at their potential rates. The familiar aerodynamic method is used and it is shown that considerable differences in water loss occur between fallow land, pasture, peas, and brussels sprouts, the differences being too large to be accounted for by possible errors in the observations or method employed.

Introduction

Penman's (1948) method for the calculation of evaporation from land surfaces has led to the adoption of a scheme for the computation of irrigation need which is gradually finding application in day to day farming practice (Pearl and others, 1954). In the present paper it is not proposed to discuss the basis of Penman's method for the calculation of the transpiration from a turf surface when the water supply is in no way limiting, that is the potential transpiration, by the substitution of readily available meteorological data in semi-empirical and empirical equations. This has already been done at some length by Pasquill (1950). Here we shall give the results of an experimental study of the variation in the rate of water loss from more or less adjacent areas carrying different crops. The investigation was undertaken in an attempt to test the adequacy of the assumption made in the general application of Penman's work that the potential transpiration from any normal cropped surface is the same as that from grass provided that the crop has the same colour as grass and completely covers the ground. The aim of irrigation is to add just sufficient water to the crop to maintain the actual transpiration rate at its potential value, which is controlled by the weather alone, since there is evidence that maximum growth takes place when this condition is satisfied. At present it is the practice to irrigate crops of very different size and character equally and this is a direct consequence of the assumption of equal potential transpiration. It is assumed in the last statement that the 'root constant' is identical for the crops under consideration. The root constant is the maximum soil moisture deficit (usually expressed in in. or cm.) that can be built up before the transpiration rate is checked. Irrigation is started when this deficit is reached.

In the work to be described the aerodynamic method is used to evaluate the daily water losses. This method has been under investigation at Cambridge for a number of years and the physics underlying it, together with the limitations and precautions that must be observed in its use, are now fairly well understood. It will be recalled that the validity of the Thornthwaite and Holzman (1939) equation, as modified by Pasquill (1949a),

/E =

$$E = \frac{\rho k^2(u_2 - u_1)(q_1 - q_2)}{\left[\ln \frac{z_2 - d}{z_1 - d}\right]^2} \quad \ldots\ldots 1$$

in which E is the rate of evaporation, k is von Karman's constant, ρ the air density, d the zero plane displacement and u_1, u_2, q_1 and q_2 are the wind speeds and specific humidities at the heights z_1 and z_2, has been demonstrated (Pasquill 1949a, 1950b, Rider 1954a) and that a summary of these investigations together with some discussion on the difficulties and accuracy to be expected in its application has been given by Rider (1954b).

Observational aspects

A site about 6 miles NW. of Cambridge was used. It was in level open country and throughout the period covered by the observations a pasture and a fallow field were generally available. At various times it was possible to expose apparatus in a pea field and in a field of fully grown brussels sprouts which were being allowed to run to seed. All these sites were within a circular area of some 500 m. diameter and therefore exposed to the same weather. The soil type of each was the same. The initial plan for the observations which had to be modified from day to day to meet ruling conditions was to undertake a series of six day runs, the first two and last two days of each series being occupied with control observations. It was hoped to get a number of such observations at intervals of about four weeks throughout the growing season but it proved impossible to maintain a strict schedule as this work had to be done in fine weather as well as give way to farming requirements. In the event three periods were covered. The first extended from 19 May to 7 June, the second from 16 to 24 June and the third from 7 to 14 July, 1955. There was also an initial day's observation on 9 to 10 May to test the apparatus, three sets of which were built for the investigation. The sites on which the apparatus was exposed during these periods can be seen by referring to Table I. Initially on 9 May the pasture had a grass length of about 15 cm. The grass grew steadily throughout the first period of observation until on 7 June it had reached a height of about 30 cm. Cattle were then sent into the field and when work recommenced on 18 June the grass had been reduced to a fairly uniform height of about 10 cm., after which it again grew steadily until the measurements finished. These changes in the length of the grass are reflected in the values of d given in Table I. The bare soil was harrowed before measurements started and occasionally during the observational period it was 'cultivated' to keep weeds down. The surface consisted of parallel ridges and troughs having an amplitude of about 20 cm. The brussels sprouts were fully grown plants about 1 m. high and when apparatus was placed over them they were on the point of flowering. Although the stems of these plants were fairly widely spaced the tops were bushy and formed a complete cover over the ground. The peas were just coming into flower on 18 June and had a height of about 60 cm. They covered the ground with a dense mat of green vegetation and when in pod in July this cover was even denser although there was no apparent increase in crop height.

The minimum requirements for the calculation of the rate of evaporation from Eq.1 are the measurement of humidity at two heights and the measurement of wind speed at three heights, the wind speed at the third height being required for the determination of d, since the latter can theoretically be obtained by the use of the equation

$$\frac{u_3 - u_2}{u_2 - u_1} = \frac{\ln(z_3 - d) - \ln(z_2 - d)}{\ln(z_2 - d) - \ln(z_1 - d)} \qquad \ldots\ldots 2$$

when neutral conditions of stability hold in the layer of air concerned. However, previous experience when working over an oat field (Rider, 1954c) has led to the conclusion that it is essential to have measurements of wind speed at more than three heights in order to arrive at reliable values of d as it is not possible to measure the wind speeds with sufficient precision for use in Eq.2, and a graphical method in which smoothing is possible has to be used. For this wind speeds at five or more heights are desirable, and in the majority of the observations this number of anemometers was exposed with each set of apparatus at heights up to 2.5 m. Fig.1 shows three sets of apparatus standing on the pasture on 10 May when only three anemometers per set were available. The anemometers were the sensitive cup type arranged to operate electromagnetic counters at some distance from the position of exposure. These counters were photographed every hour to provide a record of the runs of wind and hence of the mean hourly wind speeds. Each humidity mast carried two psychrometers, the psychrometers having dry and wet bulb thermo-electric thermometers which were aspirated at 3 m./sec. The thermometers were arranged in 'tandem' along the axis of a copper tube with the dry bulb in front of the wet bulb. The arrangement is shown in Fig.2. Outside the inner tube another copper tube was mounted co-axially with the first. In use air passed down the space between the two tubes at the same rate as over the thermometers. All metal surfaces were plated and the thermometers had a lag coefficient of about 75 sec. These housings were designed to overcome some undesirable features found in those used in previous work which were based on Pasquill's (1949b) design. In that design rectangular section tufnol tubes were used and it was found that when solar radiation falls on one side of this housing a difference of temperature of up to 0.5°F. can occur between two dry bulb thermometers mounted in it when the aspiration rate is as high as 3 m./sec. In the present housing the thermometer bulbs are mounted symmetrically with respect to the walls and the much higher conductivity of the copper tends to even up the temperature differences around the housing when sunshine is falling on one side. The one precaution to be taken is that the housing must not be directed at a low sun. No temperature differences have been detected between dry bulbs exposed in this housing in test runs and, further, the absolute temperature errors, although of secondary importance in this application, are considerably less than in the Pasquill type.

The housings are arranged to plug into tufnol collars which are attached to the mast. Each collar is provided with a butterfly valve which could be locked in position after being adjusted to provide the required rate of aspiration, the latter being arranged to be the same at each of the four mounting positions which were 25 cm. apart in height. The two positions not in use at any time were closed by corks, and the overall heights of the masts could be adjusted when necessary by lengthening the supports. The masts themselves were hollow, so providing the link between the aspiration fans and the psychrometers. The thermo-electric thermometers at the greater height were each provided with two thermo-junctions and one dry and one wet junction were used in conjunction with a standard junction kept in melting ice. The other two were connected in series with the corresponding junctions in the lower psychrometer. The details of the wiring and recorders have been given previously (Rider, 1954c, Fig.2). It is sufficient to recall here that two classes of recorder are used. The first is a comparatively insensitive type which is used to provide a record of the dry and wet bulb temperatures at the greater height (t_2 and t_2'), and the second is a sensitive photographic recorder which provides a record of the dry and wet bulb temperature differences between the two heights, $(t_1 - t_2)$ and $(t'_1 - t'_2)$. The temperatures are recorded to 0.1°F. and the temperature differences to 0.01°F. These limits of measurement enable the vapour pressure differences $(e_1 - e_2)$ to be obtained to 0.01 mb. The masts and recorders were calibrated as single units in the usual way and on the site the wind and temperature recorders associated with each of the three sets of apparatus were grouped together in a hut placed at one corner of the pasture. 200 m. lengths of cable enabled the apparatus to be moved from site to site as required. The main difficulties experienced in the observational work arose from,

(a) the lack of a mains power supply and the enforced reliance on motor generators and batteries

(b) the absence of a darkroom near the site

(c) the rather small areas of brussels sprouts and peas available for the observations. This made it necessary to site the apparatus near the downwind side of the fields to obtain an ample fetch over a uniform surface and changes in wind direction of more than about 45° made it necessary to abandon the run and resite the apparatus for **another** attempt, and

(d) the time taken to move the apparatus from site to site with the limited labour available.

Calculation of the water loss and discussion of the results

Eq.1 is strictly only valid in neutral conditions of atmospheric stability, its use in unstable and stable conditions leading to an underestimation and overestimation of the rates of evaporation respectively. However, since the degree of departure from neutral conditions is controlled by the vertical wind shear as well as by the departure from the adiabatic lapse rate it is possible to keep the systematic errors which arise from the neglect of the stability effect to a minimum by siting the psychrometers and anemometers at a low height above the vegetation (Pasquill 1949a, Rider 1954c). It has been estimated that above an oat field and a pasture, provided this precaution is taken, the underestimations in the daily totals of water loss will not exceed 15% and 10% respectively. Moreover in this instance we are endeavouring to compare the differences in water loss between surfaces which are exposed to the same weather and when an underestimate occurs for one site it will occur for another, but since the effective heights of exposure of the apparatus on the sites investigated was not always the same and there were differences in the micrometeorology from site to site the errors were somewhat different in magnitude. Other equations are available for the more precise evaluation of evaporation rate in non-neutral conditions but they contain parameters which are extremely difficult to determine with any confidence for a cropped surface.

From the records hourly mean values of the temperatures, temperature differences and wind speeds were easily obtained, and it only remained to obtain values for d before the rates of evaporation and hence the daily water losses could be calculated from Eq.1 which for practical use is conveniently written as

$$E = \frac{3\cdot46 \times 10^{-5}(e_1 - e_2)(u_2 - u_1)}{T\left[\ln \frac{z_2 - d}{z_1 - d}\right]^2}$$

in which e, the vapour pressure, is in mb., u is in cm./sec., z and d are in cm., T is the absolute temperature, and E is in g./cm.^{2}/sec. The method used for the determination of d was to select 'neutral' hours by referring to the records of $(t_1 - t_2)$ and to plot values of u_z against log $(z - d)$ using likely values of d. The best approach to a straight line indicated the required value of d. For this purpose neutral hours were considered to be those for which $(t_1 - t_2)$ did not exceed ±0.05°F.; the psychrometer heights z_1 and z_2 were always 25 cm. apart. When more than one hour on a particular day gave a different value from another, more weight was given to the hour with the higher wind speeds. When a number of suitable hours occurred a mean wind speed ratio plot was drawn. An example is given in Fig.3, in which the plots for a few single hours and the mean plots are given for the pea and grass surfaces. When working over a tall cereal Rider (1954c) found that the values of d obtained as outlined above showed a variation with wind speed, d increasing with increasing wind speed up to the maximum experienced (about 5 m./sec. at 2 m.). This was considered to be the result of the waving and bending of the crop and it added a complication to the computation of E. In the present observations stiff crops were deliberately chosen in the hope that this feature would not be found. This has proved to be the case, as while there is some variation in d from hour to hour there is no indication of a systematic change with wind speed. One value of d has therefore been used for each day of observation for each surface and these are set out in Table I together with the 24 hour water losses obtained from the computed values of E. In observations 1 to 4, 8, 9, 13, 14 and 19 the three sets of apparatus were exposed over either grass or bare soil and the 24 hour water losses were computed independently from the results provided by each set. It will be seen that these are in reasonable agreement except when the loss is very small. The worst case occurs in observation No. 8 when the gradients of dry and wet bulb temperature were small. The instrumental errors which arise in the main from stray e.m.f. in the thermo-electric circuits tend to produce absolute errors in the vapour pressure differences and hence in the values of E, and when the evaporation is small the relative errors are large. If it had been realised at the start that the evaporation from bare soil would be so small on many occasions compared with that from grass, more effort would have been made to restrict the control observations to the grass surface. Observation No.9 is of interest since although the psychrometers were exposed at different heights for each set, the 24 hour water losses are in reasonable agreement. Some details from one of the control runs are given in Fig.4. In this figure the mean hourly values of the dry and wet bulb temperature differences, $(t_1 - t_2)$ and $(t'_1 - t'_2)$, between the psychrometer heights z_1 and z_2 of 25 and 50 cm., and the values of $(e_{25} - e_{50})$ which were obtained from these differences and the observed values of t'_{50} are shown for observation No. 14. It will be seen that quite small differences in the values of $(t_{25} - t_{50})$ and $(t'_{25} - t'_{50})$ produce appreciable differences in the values of $(e_{25} - e_{50})$ which when multiplied by the wind speed differences etc. produce surprisingly large differences in the hourly values of E. The mean hourly wind speed differences do not themselves vary very much from set to set, nor do the values of t'_{50}. The variations in the dry and wet bulb temperature profiles are probably due in part to genuine point to point differences as well as to deficiencies in the apparatus. The whole range of control observations suggests that, except when the evaporation is small, the three sets give consistent results to within about 20% in the 24 hour water losses.

Turning now to those days on which the three sets of apparatus were exposed over different sites we see that the loss was greater from peas or brussels sprouts than from the pasture in every instance by a factor which varied from day to day and which reached a maximum of about an order of magnitude in observation No.10. Details of this observation have been plotted in Fig.5. A study of this figure shows that the elements follow the usual daily variation but the differences from site to site are considerable. In general the vapour pressure and wind speed gradients are larger over the peas than over the pasture and this, together with the differences in the effective heights of exposure of the anemometers and psychrometers, leads to the much higher values

/of

of E for the peas. An argument sometimes used to support the contention of equal potential transpiration from different surfaces is that the solar and sky energy available to each is the same. A glance at the dry bulb temperatures (t_2) given in Fig.5 shows that over the peas the air was colder than over the grass, and the air over the bare soil was hotter than that over either of the cropped surfaces. This remains true when a correction is applied on the basis of the measured temperature-height profiles to obtain the approximate temperatures at the same effective heights, that is the actual heights measured from the ground minus the appropriate zero plane displacements. It appears that more of the available energy is used in vaporizing water from the peas than from the grass. Similar features can be detected in the results for other days.

It is necessary to produce evidence that the crops were transpiring at their potential rates during the periods covered by these observations. Some support may be had here from calculations based on Penman's method for the computation of accumulated water deficit for a turf covered surface. The accumulated deficit is the excess of potential transpiration over rainfall and these figures for the dates of interest are set out in Table II. According to Pearl and others (1954)

TABLE II

Date 1955	Accumulated deficit (in.)
30/4	1.6
30/5	2.2
15/6	2.5
30/6	3.6
15/7	5.0
30/7	7.5

a deficit of 3 to 5 in. can occur under turf before the actual transpiration falls below its potential rate and for deeper rooted crops the deficit is larger when transpiration is checked. Thus it appears that up to and including observation No.13 on 24/6 we were definitely measuring potential transpiration from the grass surface and may have been doing so throughout the whole series, as the accumulated deficit did not reach 5 in. until after the last day of observation. The peas and brussels sprouts have a root constant which is probably at least equal to that of grass, and they too were probably transpiring at their potential rates. If their root constants are smaller then we must conclude from these results that a rate of transpiration less than the potential rate is greater than the potential rate from turf.

The greatest source of uncertainty in the results given in Table I arises from the lack of a precise knowledge of the values to be given to the zero plane displacements. It is safe to assume that the values used were reliable to the following limits,

grass and bare soil	± 2.5 cm.
peas	± 5 cm.
brussels sprouts	± 10 cm.,

these figures being suggested by the scatter in the individual determinations. Table III shows the changes in the 24 hour water losses which arise from this range of uncertainty in the values to be given to this displacement.

TABLE III

Observation No.	Apparatus Set No.	Surface	d cm.	Water loss mm.
5	1	grass	20	2.2 ∓ 0.3
	2	sprouts	60	3.6 ∓ 0.9
	3	soil	10	1.2 ∓ 0.2
10	1	grass	10	0.6 ∓ 0.1
	2	peas	25	7.4 ∓ 1.2
	3	soil	10	0.4 ∓ 0.1
15	1	peas	25	4.4 ∓ 0.8
	2	soil	10	1.9 ∓ 0.4
	3	grass	10	2.7 ∓ 0.6

It is apparent that any likely errors do not affect the general conclusion that must be drawn, namely that the potential transpiration is not the same for all crops which have roughly the same colour and completely cover the ground.

Another and disappointing feature of the results is that there is no steady relationship between the water losses from surface to surface. As far as bare soil is concerned this is easily explained, the rate of loss being controlled by the time that has elapsed since the last fall of rain as well as by the weather. For example during run No.17 there was a heavy thunderstorm from 1700 to 1730 on 11 July and the rate of evaporation on 12 July and 13 July was comparatively high while the soil surface remained wet. By 14 July the surface had dried out and the rate of water loss fell to near its value before the storm. The changes in the ratios of the daily losses of grass to peas or sprouts is not so easily explained. The ratios of the wind speed differences over the 25 cm. height intervals are reasonably constant but the vapour pressure profiles vary in an erratic way from site to site and hour to hour. The changes from lapse to inversion and vice versa in the dry and wet bulb temperature profiles do not occur at the same time over the different sites and it is even possible to have evaporation from one site and condensation on another at the same time. Fig. 5a shows that no inversion occurred over the bare soil during the last hours of 18 June, whereas over the other two surfaces one did occur and was much larger over the grass than over the peas. This type of variation from surface to surface was noted repeatedly and is thought to be a reflection of the role that soil heat plays in the control of microclimate. During the preceding daylight hours the soil temperatures under the bare surface reached much higher values than under the cropped surfaces and a relatively large reservoir of heat was available for liberation at night. This was released sufficiently quickly and proved large enough to offset the inversion which would have otherwise been present.

Conclusion

This report has been written to suggest that the concept of equal potential transpiration irrespective of crop size and character be approached with the utmost caution. It is readily admitted that the values of water loss given in Table I are liable to be in error but in the opinion of the writer no criticism whether from the standpoint of the validity of the aerodynamic formula, of the computations of the zero plane displacements, of the apparatus or method of observation can invalidate the conclusion that real differences exist from surface to surface. The work involved in collecting the observations and in computing the water losses is heavy and similar measurements are not likely to accumulate very quickly in the future. If it is thought worth while to continue this work in the hope that some relationship will be found between the losses from different surfaces in terms of some measurable characteristic of the surfaces then consideration must be given to the provision of power supplies on the site and to the design of an automatic temperature difference integrator.

/References

References

Pasquill, F.	1949a	Proc. Roy. Soc., 198, 116.
	1949b	Quart. J.R. Met. Soc., 75, 239.
	1950a	Meteorological Research Papers, Air Ministry, London, No. 579.
	1950b	Quart. J.R. Met. Soc., 76, 287.
Pearl, R.T. and others	1954	Tech. Bull. No. 4, Ministry of Agriculture and Fisheries
Penman, H.L.	1948	Proc. Roy. Soc., A. 193, 120.
Rider, N.E.	1954a	Phil. Trans., A. 246, 61.
	1954b	International Hydrology Association, Rome, I.U.G.G. Meeting (in the press).
	1954c	Quart. J.R. Met. Soc., 80, 198.
Thornthwaite, C.W. and Holzman, B.	1939	Monthly Weather Review, 67, 4.

Table I

Surfaces and periods of exposure, psychrometric heights, values of zero plane displacement and 24 hour water losses

Observation No.	Period 1955 24 hours commencing G.M.T.	Apparatus Set 1				Apparatus Set 2				Apparatus Set 3			
		Surface	Psychrometer heights (cm.)	d (cm.)	Water loss (mm.)	Surface	Psychrometer heights (cm.)	d (cm.)	Water loss (mm.)	Surface	Psychrometer heights (cm.)	d (cm.)	Water loss (mm.)
1	1400 9/5	Grass	25,50	10	2.0	Grass	25,50	10	2.3	Grass	25,50	10	2.2
2	1200 19/5	Grass	25,50	12	1.7	Grass	25,50	12	1.9	Grass	25,50	12	1.6
3	1700 20/5	Grass	25,50	-	-	Grass	25,50	12	1.9	Grass	25,50	12	2.1
4	1600 25/5	Grass	50,75	15	1.7	Grass	50,75	15	2.5	Grass	50,75	15	2.1
5	2000 26/5	Grass	50,75	20	2.2	Sprouts	125,150	60	3.6	Bare Soil	25,50	10	1.2
6	2300 27/5	Grass	50,75	20	0.7	Sprouts	125,150	60	1.2	Bare Soil	25,50	10	0.5
7	0900 6/6	Grass	50,75	20	2.3	Sprouts	125,150	60	4.3	Bare Soil	25,50	10	0.3
8	1200 16/6	Bare Soil	25,50	10	0.2	Bare Soil	25,50	10	0.3	Bare Soil	25,50	10	0.4
9	1400 17/6	Bare Soil	25,50	10	0.4	Bare Soil	75,100	10	0.5	Bare Soil	50,75	10	0.5
10	1600 18/6	Grass	25,50	5	0.6	Peas	75,100	25	7.4	Bare Soil	25,50	10	0.4
11	1100 21/6	Grass	25,50	5	1.1	Peas	75,100	25	2.3	Bare Soil	25,50	10	1.4
12	1200 22/6	Grass	25,50	10	1.2	Peas	75,100	25	5.0	Bare Soil	25,50	10	
13	1500 23/6	Bare Soil	25,50	10	0.3	Bare Soil	25,50	10	0.4	Bare Soil	25,50	10	0.6
14	1600 7/7	Grass	25,50	10	2.3	Grass	25,50	10	2.9	Grass	25,50	10	2.6
15	0900 9/7	Peas	75,100	25	4.4	Bare Soil	25,50	10	1.9	Grass	25,50	10	2.7
16	1000 10/7	Peas	75,100	25	3.3	Bare Soil	25,50	10	0.4	Grass	25,50	10	2.3
17	1100 11/7	Peas	75,100	25	2.6	Bare Soil	25,50	10	1.1	Grass	25,50	10	2.0
18	1200 12/7	Peas	75,100	25	2.9	Bare Soil	25,50	10	1.7	Grass	25,50	10	1.9
19	1500 13/7	Bare Soil	25,50	10	0.4	Bare Soil	25,50	10	0.6	Bare Soil	25,50	10	0.4

M.R.P. 972

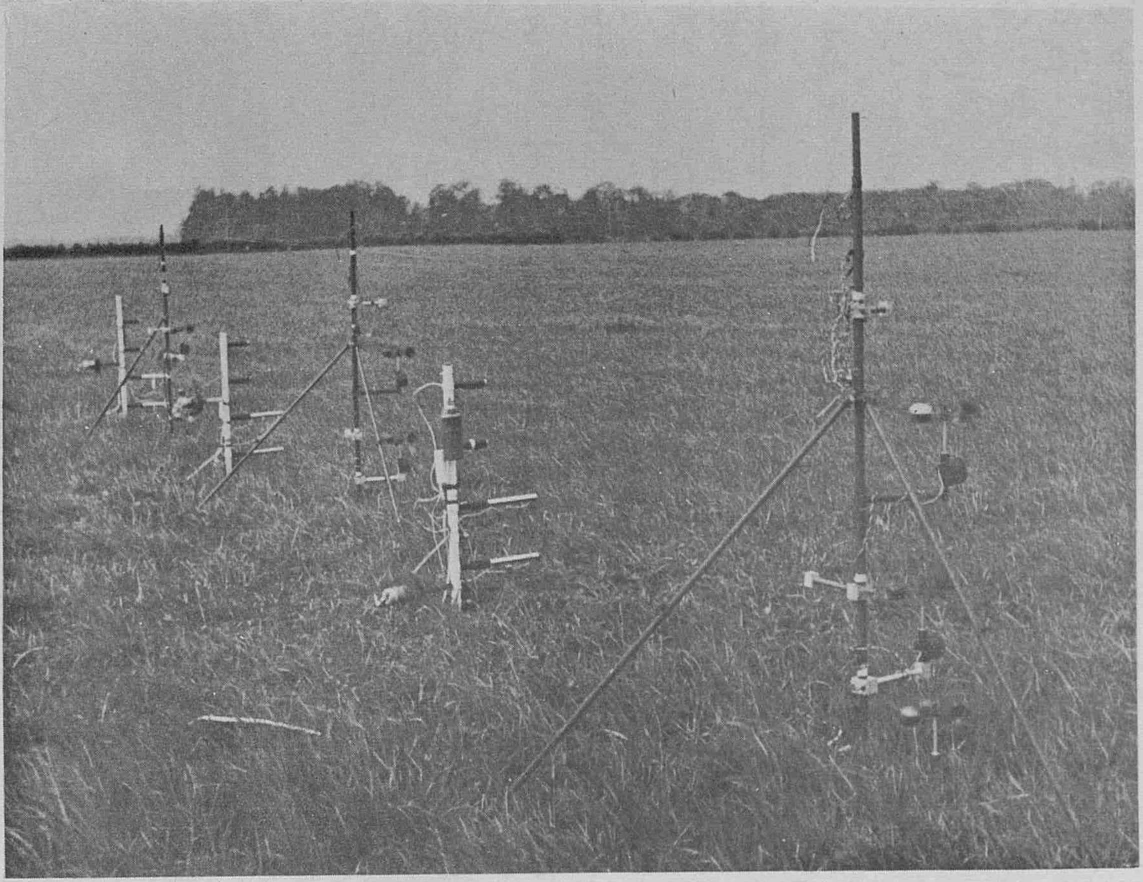

FIG. 1 THREE SETS OF APPARATUS EXPOSED ON THE PASTURE.

FIG. 2 SECTIONAL VIEWS OF THE PSYCHROMETER HOUSING

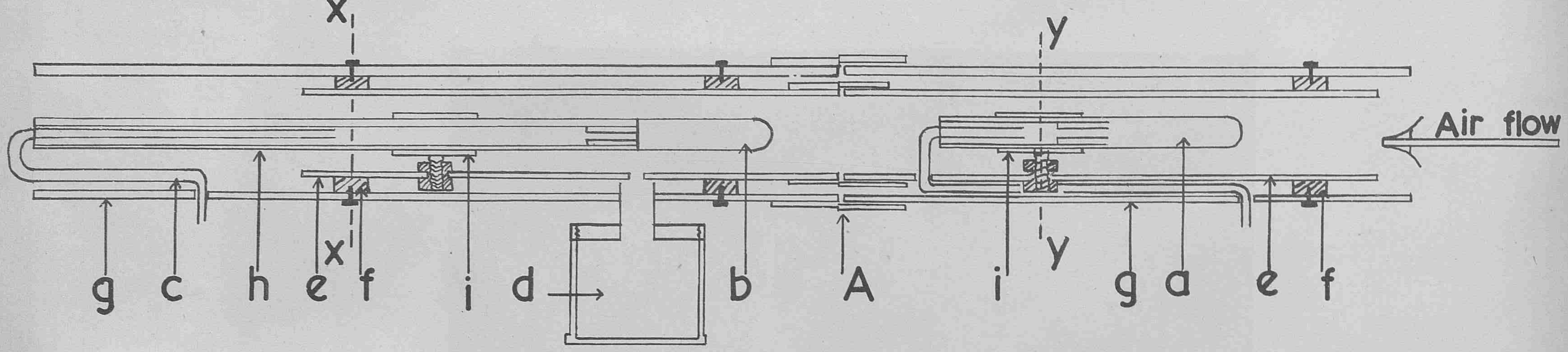

Vertical Section

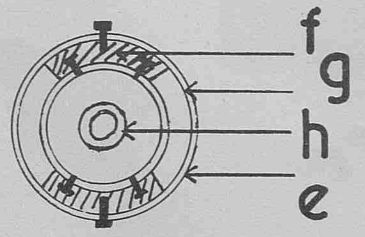

Section through x–x

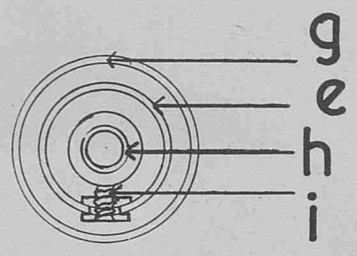

Section through y–y

Legend:-

(a) Dry bulb
(b) Wet bulb
(c) P.V.C. insulating thermo-couple wires
(d) Distilled water holder
(e) Inner copper tube
(f) Tufnol spacers
(g) Outer copper tube
(h) Paxolin tube
(j) Thermometer holders

Note; The housing can be parted at A. The 'dry' section is a tight push fit into the 'wet' section.

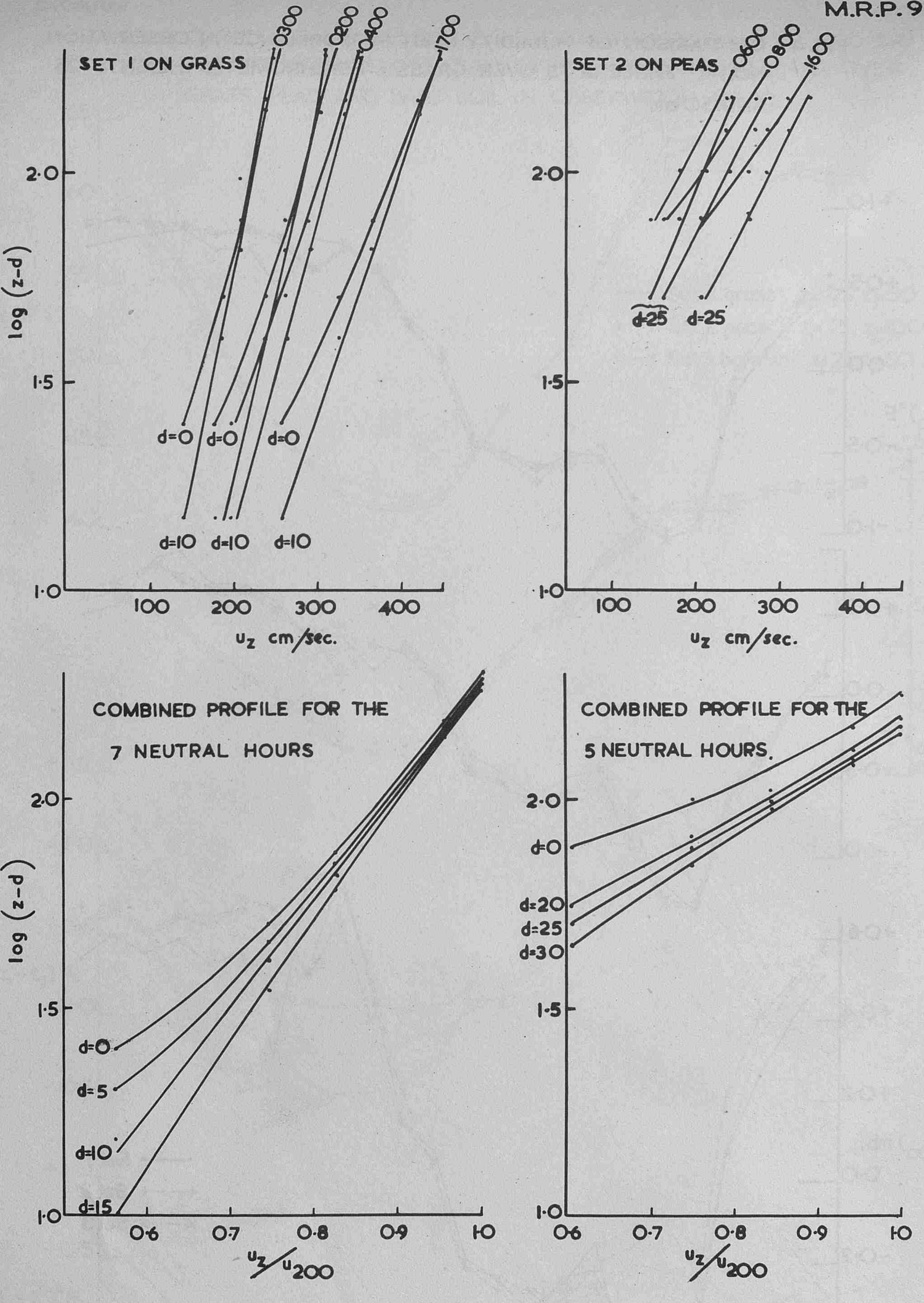

FIG. 3. DETERMINATION OF ZERO PLANE DISPLACEMENT OBSERVATION NO. 12. 22-23 JUNE 1955.

FIG. 4 COMPARISON OF HUMIDITY MAST PERFORMANCE IN OBSERVATION NO. 14. THREE SETS OVER GRASS. PSYCHROMETER HEIGHTS 25 AND 50 cm.

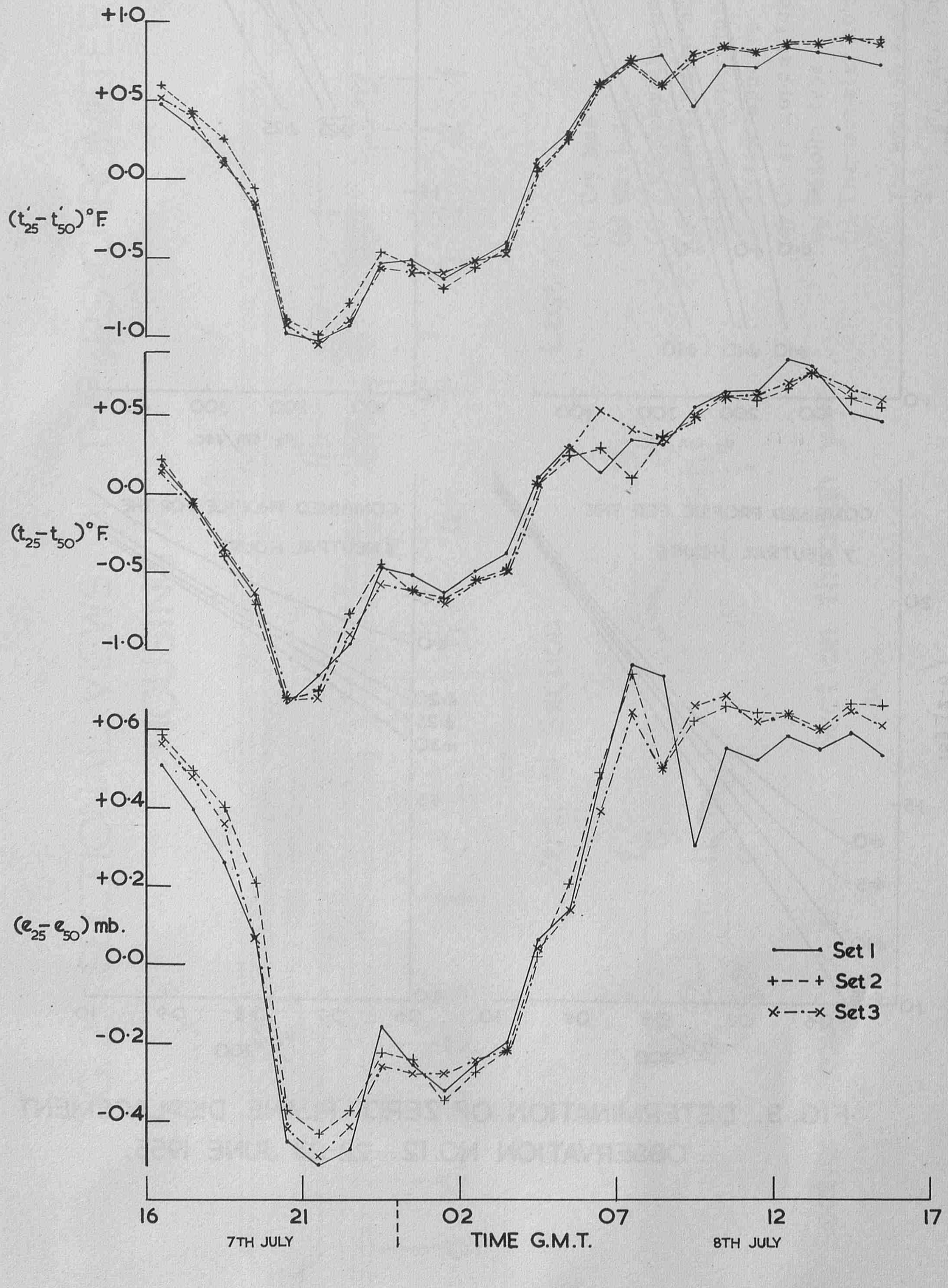

FIG. 5a CURVES OF DRY AND WET BULB TEMPERATURE (t and t') AND DRY AND WET BULB TEMPERATURE DIFFERENCE ($t_1 - t_2$) and ($t'_1 - t'_2$) OVER GRASS, PEAS AND BARE SOIL IN OBSERVATION NO. 10

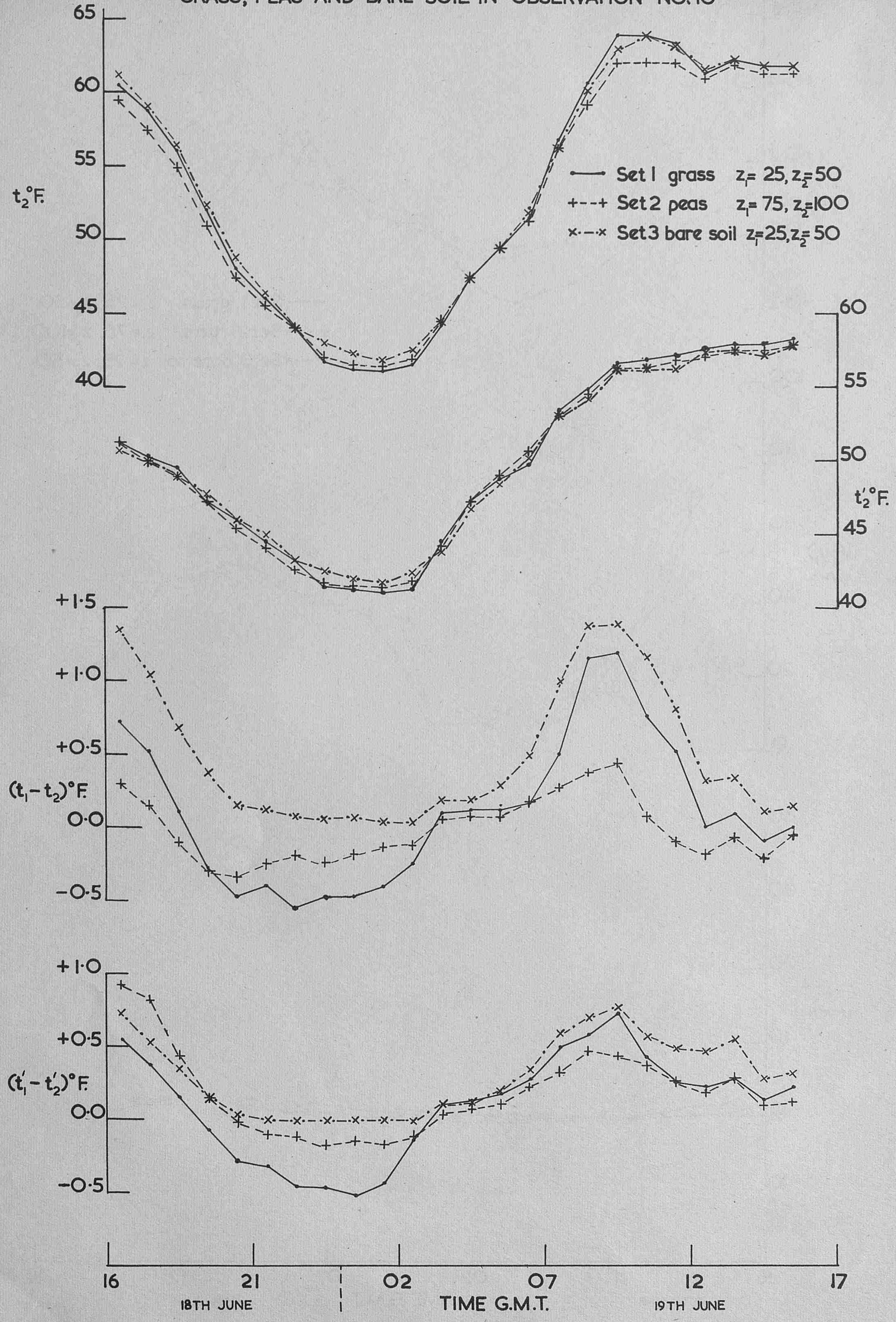

FIG. 5b CURVES OF VAPOUR PRESSURE DIFFERENCE $(e_1 - e_2)$, WIND SPEED DIFFERENCE $(u_1 - u_2)$ AND RATE OF EVAPORATION E OVER GRASS, PEAS AND BARE SOIL IN OBSERVATION NO. 10

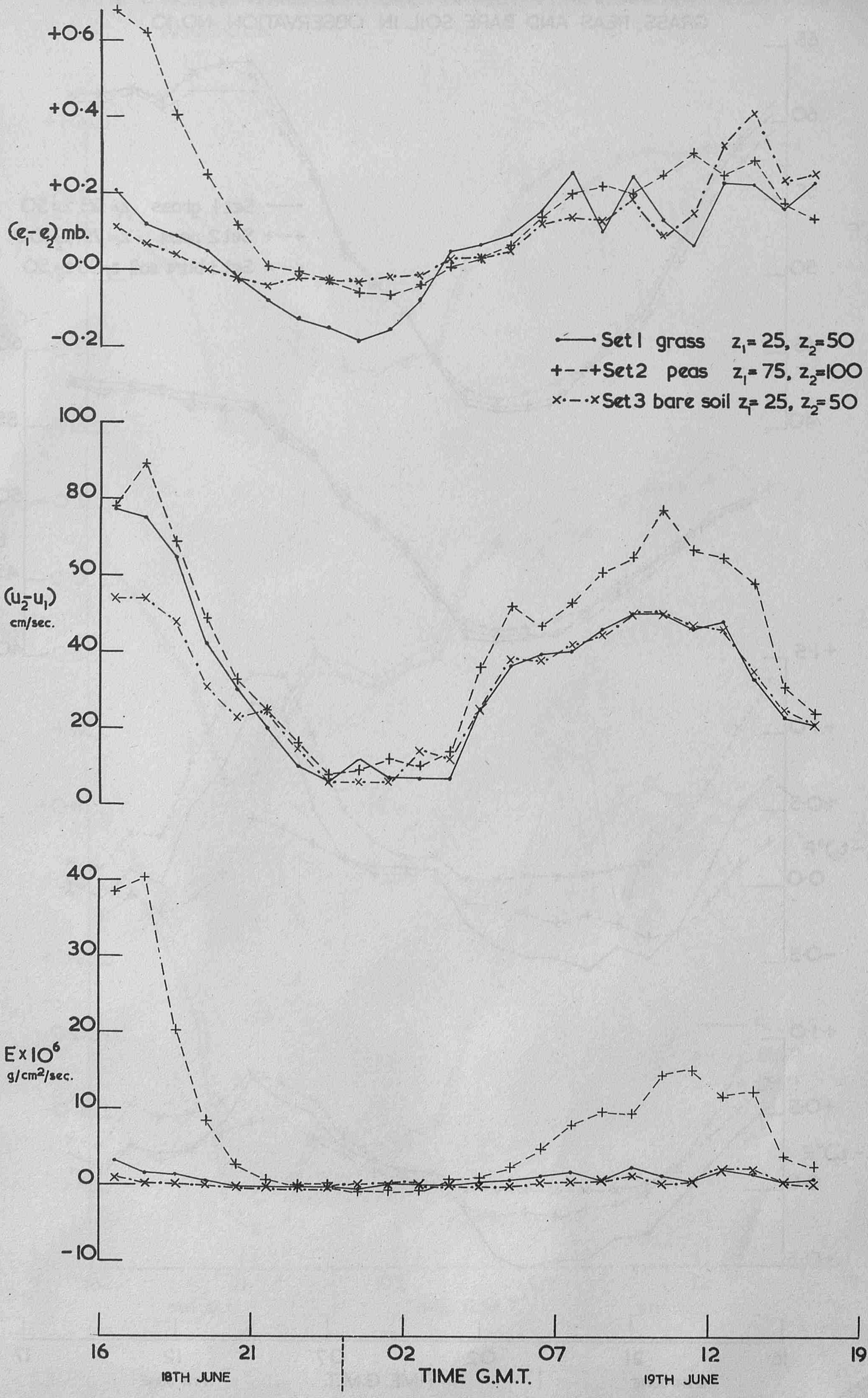

M.R.P. 973
S.C.111/203
24th January, 1956.

AD223108

Evaporation from a saturated rough surface into a turbulent air stream.

by

J. S. Hay.

(Meteorological Office)

AIR MINISTRY

METEOROLOGICAL RESEARCH COMMITTEE

At the time of issue this report has not been published. Any author desiring to quote this paper should refer to it as "A paper of the Meteorological Research Committee (London), M.R.P. No.973 by Mr. J.S. Hay.
A copy is available in the Library of the Meteorological Office."

M.R.P.973
S.C.III/203
24th January, 1956

AIR MINISTRY

METEOROLOGICAL RESEARCH COMMITTEE

Evaporation from a saturated rough surface into a turbulent air stream

by

J.S. Hay (Meteorological Office)

Summary

Wind tunnel measurements have been made of the rate of evaporation from saturated rough surfaces consisting of plaster casts in the form of rectangular ridges 0.3 cm. high or truncated cones 0.95 cm. high arrayed on a flat base of approximate dimensions 25 x 12 cm. For purposes of comparison, measurements were also made of the rate of evaporation from smooth surfaces of the same material. The vertical distribution of wind speed and of vapour concentration in the first few centimetres above the various surfaces were also studied, the former being used to confirm that the flow was aerodynamically rough or smooth according to the type of surface used and to compute the drag coefficient of the surface.

The variation of the rate of evaporation with wind speed was found to be similar, at least within a few per cent. for both smooth and rough surfaces over the range 1 to 9 m./sec. The absolute rate of evaporation from a smooth surface, however, was approximately half that from a rough surface of the same base area. Although the anticipated agreement between the drag and mass transfer coefficients in the case of a smooth surface was confirmed here, a pronounced discrepancy between the two was obtained in the case of the rough surfaces, the drag coefficient being 3 to 4 times the mass transfer coefficient. This lack of analogy between momentum and mass transfer processes over a rough surface is in keeping with a similar discrepancy between momentum and heat transfer observed elsewhere. The implied difference in mass and momentum coefficients for an array of cylinders is consistent with that observed directly for heat and momentum transfer.

Owing to the breakdown in the analogy between momentum and mass transfer near the boundary and to the fact that the vapour cloud did not extend substantially above the roughness elements, treatments of evaporation such as that developed by Calder (1949) cannot be expected to apply to the present cases.

1. Introduction

Much experimental study of evaporation from plane, free liquid surfaces has been carried out, notably by F. Pasquill (1942 and 1943), who attempted to relate evaporation to the aerodynamic conditions over the surface. He found the absolute rate of evaporation to be predicted satisfactorily by a theory due to O.G. Sutton (1943), apart from minor variations with the physical properties of the liquid. Pasquill suggested an empirical generalisation of Sutton's treatment, involving replacement of kinematic viscosity in the turbulent exchange coefficient by the appropriate molecular diffusion coefficient.

The aerodynamic conditions in Pasquill's experiments were of the so-called "aerodynamically smooth" type. In many practical problems of boundary layer flow however, especially in the lower atmosphere, the flow is of the "aerodynamically rough" type, resistance arising from pressure forces on the roughness elements and being independent of fluid viscosity.

The work described in the present paper is an extension to rough surfaces of the work previously done on smooth surfaces. It was commenced by S.G. Crawford (unpublished) who employed a surface which was saw-tooth in form and will be referred to as type RA. Finding the rate of evaporation to be lower than anticipated, Crawford turned his attention to a surface with parallel ridges but had to discontinue the research at this point. A surface of this type, designated type RB, and also one with small truncated cones as the roughness elements, type RC, both described in detail in the following section, were used by the author. Sections of these three types of surface are shown in figure 1. The measurements of evaporation were made using sections about 300 cm.^{2} in area and in wind speeds ranging from 1 to 9 m./sec.

2. Experimental details

The wind tunnel employed was that used and described by Pasquill (1942 and 1943). For present purposes, it is sufficient to note that the working section was 4 ft. long and 30 in. square but for fuller details, the reader is referred to the original papers. The modifications described therein were not however considered necessary in the present investigation for it was anticipated that the use of rough surfaces would ensure fully turbulent flow. The tunnel was thus restored to its original form, though without the gauze. Air was drawn in from outside the building and after passing through the working section was expelled from the building. By doing so, a build-up of vapour concentration within the room housing the wind tunnel was avoided.

A number of calestone (dental plaster) casts, prepared in tufnol moulds, were laid out on the floor of the working section to form the rough surfaces. Each cast consisted of a thin rectangular base with the roughness elements arrayed on it. The first rough surface used by the author, type RB, had small parallel ridges running across the working section of the wind tunnel. The second, type RC, had truncated cones spaced regularly in rows across the working section, the rows being staggered so that each cone was mid-way between two cones in the adjacent rows. Details are as follows:-

Type of surface	Dimensions of base	Description of roughness elements
RB	25.0 x 12.5 x 0.3 cm.	Ridges 0.3 cm. high, 0.15 cm. wide, spaced 2.5 cm. apart.
RC	23.9 x 12.1 x 0.4 cm.	Cones 0.95 cm. high, 0.2 cm. in diameter at top and 0.6 cm. at bottom, spaced 2 cm. apart in rows 1 cm. apart.

The evaporation plates were similar casts but with thinner bases attached to thin glass sheets of the same area, the total thickness being the same as that of an ordinary cast. The thinner bases meant an appreciable saving of liquid required for saturation. To prevent leakage, the edges of the plates were painted with shellac. The evaporation plate was positioned close to the downwind end of the working section with seven rows of ordinary casts, three in each row, upwind of it, one row downwind and a cast on either side. This ensured as deep a layer as possible of fully developed flow characteristic of the surface over the evaporation plate.

With the rough casts removed, experiments were also carried out with smooth evaporation plates, recessed into the floor of the working section at the position normally occupied by the rough evaporation plates. They were prepared in the same way and were equal in area to the bases of the rough plates. They will thus be referred to as smooth type SB and SC plates. A few observations were made using filter papers, almost equal in area to the type B plates, placed on a sheet of glass recessed into the floor at the same position.

The first evaporation plates were made of plaster of paris as they appeared to be more absorbent and so presumably more porous than calestone ones. Later it was found that absorbency varied considerably with the consistency of the mixture before it set and that calestone casts could be made just as absorbent as plaster of paris ones. Calestone was then preferred for it was stronger and the rather watery mixture took longer to set, allowing more time for pouring into the mould. Similar results were obtained with both materials and no further distinction need be made. The significance of absorbency will be discussed in Section 4.

Bromobenzene was chiefly employed as the evaporating liquid. The rate of evaporation E was determined gravimetrically using a balance positioned close to the working section. The balance scale was graduated in divisions of 0.1 g. and the readings estimated to 0.01 g. but tests showed it to be accurate to only 0.03 g. Other tests were carried out daily to estimate the loss of vapour during transfer of plate between balance and tunnel and a correction applied. Taking into account the reproducibility of the weighings and of the transfer correction, the weights of liquid evaporated during a single exposure in the tunnel are considered to be accurate to 0.1 g. As the exposures were long enough for 2 g. or more to be evaporated the errors in the rates of evaporation arising from the weighing measurements were within about 5 per cent.

The temperature T_a of the free air stream, indicated by a thermometer projecting through the roof of the working section, was noted at intervals and the mean during each exposure obtained. Practical difficulties precluded the direct measurement of surface temperature T_s. Subsidiary experiments with evaporation plates having several thermocouple junctions embedded in them were however carried out to determine the extent of surface cooling during evaporation.

The free air speed V during the period of exposure was measured by a Sheppard (1940) type anemometer positioned at the downwind end of the working section, and a little to one side, with its cups high above the floor, about 21 in., to avoid interference with the flow over the evaporation plate. The anemometer readings were related to the free air speed immediately above the plate by calibrating it against a small pitot-static tube, external diameter 0.3 cm. whose orifice was about 4 in. above one of the smooth plates. Observation showed that the wind speed distribution across the working section varied slightly with the ventilation conditions. Separate calibrations were accordingly carried out in the two sets of conditions employed.

Besides the main evaporation experiments, observations were made of the wind speed and vapour concentration profiles in the first few centimetres above the various surfaces. In the former case, the wind speed u at a number of heights and the corresponding free air speed V were measured by the small pitot-static tube and anemometer respectively. In the latter case, vapour samples were taken over type SB and RC plates saturated with methyl acetoacetate (MAA). The choice of MAA was governed by the fact that facilities for estimating the quantities of vapour absorbed, and hence the concentrations, by chemical methods were readily available.

3. Wind speed profiles

Two series of measurements, mostly in a free air stream of 5 m./sec., were made over each surface, with an interval of about two years between each. The measurements were first repeated over surface RC in an endeavour to find some explanation for an increase in the rate of evaporation which is discussed in the following section. When a change in this profile became apparent, the measurements were repeated over the other surfaces to see how well the previous results could be reproduced.

Within the boundary layer, the wind speed was not constant across the mouth of the pitot-static tube so that each value of u was appropriate not to the centre of the orifice but to a point slightly above it. To take this into account, a height correction of 0.048 cm. was applied, derived from a formula due to Young and Mass (1937). Corrected heights, referred to the base of the roughness elements, will be denoted by z. Fluctuations in the flow through the tunnel, due to gusts outside the building, may at times have given rise to errors of about 5 per cent in the values of u.

Over surface RB, the measurements in both series were made with the pitot-static tube in two positions, first with the orifice directly above a ridge and again mid-way between two ridges, at distances of 96.25 and 95 cm. respectively from the upwind edge of the surface. The wind speed ratios $\frac{u}{V}$ obtained in the second series of measurements have been plotted against $\log_{10} 10z$ in figure 2. The distribution obtained in the first series was similar in shape. It will be seen that close to the surface the profile varies with position, the wind speed at a given height being apparently greater between the ridges than above them, contrary to what might be expected. No great reliance however can be placed on the measurements in this region for the static holes were some 1.9 cm. behind the orifice of the tube. The Chattock-Fry manometer to which the pitot-static tube was connected thus recorded the difference between the dynamic plus static pressures at one point and the static pressure at another point. At the greater heights, above about 1.6 cm., the profile is clearly independent of position, indicating that the pitot-static tube is not subject to local effects and that the flow is characteristic of the surface.

Over surface RC, wind speeds in the first series were measured with the pitot-static tube in four different positions relative to the cones, the orifice being 92 cm. from the upwind edge of the surface in each case. The wind speed ratios did not appear to be dependent on position for heights above the top of the cones. The second series of measurements, with the tube employed in one position only, gave a similar distribution of wind speed ratios, shown in figure 2.

Laboratory studies (Nikuradse (1933) and Schlichting (1936)) have established that the wind speed distribution in aerodynamically rough flow, for which the parameter $\frac{u_* z_0}{\nu} > 2.5$, may be written in the form

$$\frac{u}{u_*} = 5.75 \log_{10} \frac{z}{z_0} \qquad (1)$$

where z_0 is the roughness parameter of the surface, ν is the kinematic viscosity of the fluid and $u_* = \sqrt{\tau_0 / \rho}$ is the shearing stress velocity, τ_0 being the shear stress per unit area and ρ the fluid density. The present results indicate in both cases a linear variation of $\frac{u}{V}$ with $\log_{10} 10z$, for heights above that at which local variations in flow die out. Thus, by deriving the lines of best fit, two of which are shown by full lines in figure 2, by means of the method of least squares and comparing with equation (1), appropriate values of z_0, u_* and $\frac{u_* z_0}{\nu}$ may be readily deduced*. The figures given in table 1 were obtained with V = 5 m./sec. and ν = 0.140 cm.^{2} sec.

/Table

---

* It may be recalled that Schlichting's measurements were made in the boundary layers developing over a number of flat plates covered with different types of roughness element. Denoting the distance from the leading edge of the plate to the point at which the measurements were made by x, equation (1) was verified explicitly for the range of conditions $2.6 \times 10^3 \leq \frac{x}{z_0} \leq 3.1 \times 10^5$. Although the range of $\frac{x}{z_0}$ 272 to 406, covered by the experiments reported here lay outside these limits, it was assumed that equation (1) was still valid. It certainly appeared to be of the correct functional form.

Table 1. Values of z_o, u_* and $\frac{u_* z_o}{\nu}$

	Smooth Surface		Surface RB		Surface RC	
	Series 1	Series 2	Series 1	Series 2	Series 1	Series 2
z_o cm.	-	-	0.247	0.235	0.266	0.338
u_* cm./sec.	22.7	23.1	63.6	64.8	61.7	69.6
$\frac{u_* z_o}{\nu}$	-	-	112	109	117	168

From the values of $\frac{u_* z_o}{\nu}$, it is quite obvious that the flow was aerodynamically rough in each case. The z_o value for surface RB derived from series 1 is in good agreement with that from series 2 but for surface RC there is a marked difference, z_o having increased in value by about 27 per cent from series 1 to series 2. Statistical analysis of the data showed that the values were accurate to about 15 per cent so the difference is significant. The reason for this is not clear.

Little reference has been made to the lower parts of the profiles for these are dependent on position and are not representative of the complete surface. In working with rough surfaces, it is frequently necessary to introduce a zero-plane displacement, a datum level a little way above the base of the roughness elements, above which active turbulent exchange commences. From the linearity of the profiles, this does not appear to be necessary with either of these rough surfaces.

Two series of measurements over a type SB plate were also made, the mouth of the pitot-static tube being 97.5 and 8.5 cm. from the upwind edges of the smooth surface and plate respectively. The distribution of wind speed ratios was similar for both series, that obtained in series 2 being shown in figure 2.

An approximately linear variation of $\frac{u}{V}$ with $\log_{10} 10z$ is evident at the greater and lower heights. An unexpected feature however is the change in slope, at about 0.9 cm., which may well be associated with a very slight difference in the natures of the plate and surrounding floor. During evaporation, the major part of the vapour cloud over the plate lies beneath this level so main interest centres on the lower section of the profile. The line of best fit relating $\frac{u}{V}$ and $\log_{10} 10z$ in the interval 0.3 to 0.8 cm. was determined for both series of observations, the appropriate one being shown by the full line in figure 2.

As the plate has been assumed to be smooth it should be possible to express the wind speed distribution, over this interval at least, in the familiar form

$$\frac{u}{u_*} = 5.5 + 5.75 \log_{10} \frac{u_* z}{\nu} \qquad (2)$$

where the various symbols are as already defined. To test this, the equation was solved using the wind speed derived from the lines of best fit for the logarithmic mean height of the above interval, taking V = 5 m./sec. The resulting values of u_* are included in table 1. With these values equation (2) was then employed to calculate wind speeds at the other heights. These were found to be, on the average, within about 1 per cent. of the observed speeds corrected slightly for deviations of V from 5 m./sec. In a few instances, the discrepancy was a little over 2 per cent. Applying equation (1) to both sets of observations and deriving values of z_o and $\frac{u_* z_o}{\nu}$, the greater value of the latter was found to be 0.71. It may be concluded then that the flow in the vicinity of the plate approximated closely to aerodynamically smooth flow.*

Some measurements in free air speeds of 3 and 7 m./sec. over each type of surface showed no systematic variation in wind speed ratios so the profiles are independent of speed, over this range at least. Comparative measurements over dry and saturated plates also showed the profiles to be unaffected by the steep temperature gradient established close to the surface during evaporation.

4. Absolute rate of evaporation in saturated conditions

Experimental studies of the drying of a saturated solid (see for example Sherwood (1936) and Calder (1938)) have shown that the rate of drying is initially independent of time and of liquid content ("constant rate period") but subsequently decreases ("falling rate period") as the content falls below some critical value. As the aim of the present investigation was to measure the rate of evaporation as a function of wind speed and length of surface, and to examine the results in terms of treatments of turbulent exchange over a rough surface, it was clear that it could be pursued most profitably in the so-called "constant rate period". It was thus necessary initially to establish the limits of liquid content over which the constancy could be assumed for the various plates used here.

The form of the drying curve for each type of plate was studied in an air stream of 5 m./sec. After soaking the evaporation plate with bromobenzene and draining off excess liquid, it was weighed and exposed in the wind tunnel. The weighing was repeated periodically and the mean rate of evaporation E g./min. and liquid content Q g. during each exposure determined. Following Pasquill (1942 and 1943), the observations were first reduced to the form $\frac{E}{p_a}$ g./min. mm. Hg., where p_a is the saturation vapour pressure at the temperature T_a of the free air stream. These values were then increased by 7 per cent to relate the rate of evaporation to the temperature T_s of the evaporating surface which was lower than T_a, since the latent heat of vaporisation was drawn from the plate. This correction was obtained from the subsidiary experiments previously referred to, which showed that T_s fell rapidly when evaporation commenced but after 2 minutes or so it steadied and thereafter the temperature difference $T_a - T_s$ changed little. In temperatures ranging from 40 to 58°F., the difference varied unsystematically from 1 to 2.5°F., the ratio $\frac{p_a}{p_s}$ where p_s is the saturation vapour pressure at temperature T_s, varying from 1.04 to 1.10. The average ratio was 1.07 so the temperature correction was taken to be 7 per cent. It appeared to be independent of air speed from 2 to 7 m./sec. The vapour pressure data used were those quoted by Pasquill. Small corrections for deviations of air speed from 5 m./sec. were applied using the law $\frac{E}{p_s} \propto V^a$ discussed in the following section, a varying with the type of surface.

Some of the results obtained are given in figure 3 where, to facilitate comparison, values $\frac{E}{p_s}$ have been plotted against percentage saturation $\frac{100\ Q}{Q_o}$, Q_o being the maximum amount of liquid absorbed. It will be seen that there are two distinct régimes, the first characterised by a slow decrease in $\frac{E}{p_s}$ which might be regarded as approximating to a "constant rate period". The slight departure from true constancy had however to be borne in mind in subsequent work. It was probably due to the underlying liquid requiring a finite time to diffuse through the plaster to replace that which had evaporated. At the lower liquid contents we have the familiar "falling rate period", probably associated with a progressive downwind drying out of the plate. The change from one régime to the other takes place at about 40 per cent. saturation in each case.

---

* On fitting a power law to the observations, it may be noted that the indices obtained were 0.132 and 0.141 for series 1 and 2 respectively, in good agreement with the well known $\frac{1}{7}$ value for a smooth surface.

A comparison of results from the various plates is not without interest. To eliminate the effects of varying diffusive properties of plaster, the comparison must be effected in saturated conditions. Appropriate values of $\frac{E}{p_s}$ were derived by inserting Q_o values in the regression equations of $\frac{E}{p_s}$ on Q obtained from the data at the higher liquid contents, where the variation is approximately linear. They are given in table 2. Appropriate equations are represented by the full lines in figure 3, the remainder of the curves being drawn by eye. Two series of data were obtained with type SB, RB and RC plates at times corresponding approximately to those of the wind speed profiles. The two results with the SB plates were almost identical, so only one has been quoted.

Table 2. Values of $\frac{E}{p_s}$ in saturated conditions

Type of plate	Area of plate cm.^{2}	Series	Q_o g.	$\frac{E}{p_s}$ g./min. mm. Hg.	$\frac{E \text{ rough}}{E \text{ smooth}}$
Filter paper	306	1	8	0.197 (±0.005)*	
SB	312	2	47	0.203 (±0.003)	
SC	289	1	45	0.188 (±0.006)	
RB	312	1	61	0.357 (±0.016)	1.76
RB	312	2	47	0.373 (±0.009)	1.84
RC	289	1	63	0.404 (±0.012)	2.15
RC	289	2	73	0.447 (±0.010)	2.38

* Standard error

The first feature to be noted from table 2 is that similar rates of evaporation are obtained from filter papers and smooth plaster plates, bearing in mind the differences in area. This had been observed earlier by Crawford and was taken to justify the use of plaster casts in this work. Secondly, the rate of evaporation has been enhanced by the roughening of the surface, the effect being greater with the RC surface. Crawford, with his type RA surface, found the rate of evaporation to be increased by a factor of 1.66. Thirdly, the rate of evaporation from the rough plates increased from series 1 to series 2, by a significant amount in the case of the RC surface. Various explanations for this were investigated but all had to be rejected, with the exception of a possible change in flow characteristics. When the wind profile measurements were repeated the surface roughness parameter z_o was in fact observed to have increased, as noted in the previous section, and it seems quite likely that this was associated with the increased value of $\frac{E}{p_s}$.

To demonstrate that the results given in table 2 were independent of the diffusive properties of the plaster, some data were obtained with a type RC plate of very low absorbency, and presumably low porosity. Defining absorbency as the maximum weight of bromobenzene absorbed per gram of plaster, the actual figure was 0.15, much below the range 0.55 to 0.95 covered by the other plates used in the investigation. A graph of $\frac{E}{p_s}$ against Q showed that the "falling rate period" extended up to the saturation level. At saturation however, $\frac{E}{p_s}$ was about 0.440 g./min. mm. Hg., agreeing well with the series 2 figure quoted for the RC plate in table 2.

/5.

5. Variation of the rate of evaporation with wind speed and downwind length of saturated surface

The variation with wind speed of the rate of evaporation from each type of plate was studied over the range 1 to about 9 m./sec. To minimise the effects of varying liquid content Q, the latter was maintained within certain limits and on the average was about 10 g. below the saturated value. It is estimated that variations in $\frac{E}{Ps}$ on this account were within 4 per cent. The measurements were made at about the time of the first series of wind profile observations.

To avoid the difficulty of handling longer plates, the effect of increasing the downwind length x_o of saturated surface was studied by placing one, two and then three saturated plates immediately upwind of the evaporation plate. Measurements were made with the latter alone, from which saturation values of $\frac{E}{Ps}$ from various sections of plates up to four times the normal length were inferred, and hence the total values by addition. Data were also obtained with plates on half the normal length. The measurements were restricted to the two rough surfaces and were made in an air stream of 5 m./sec., at about the time of the second series of wind profile observations.

Values of $\frac{E}{Ps}$ have been plotted against V and x_o in figures 4 and 5 respectively, the figures including the best fitting curves. Log-log plots of the data had been found to be linear so that the results could be expressed in the form $\frac{E}{Ps} \propto V^a x_o^b$. Values of the indices are given in table 3.

Table 3. Values of indices a and b

Type of surface	a	b
SC	0.782 (±0.014)*	-
RB	0.823 (±0.013)	0.940 (±0.004)
RC	0.762 (±0.009)	0.917 (±0.007)

* Standard error

The overall variation in a is about 8 per cent. so the rate of evaporation varies with wind speed in much the same manner for both rough and smooth surfaces. The standard errors do suggest however that the value of a for the RB surface may be significantly higher than the others. Similarly the values of b for the two rough surfaces only differ by about 2.5 per cent but the difference may again be significant.

As has already been indicated, the evaporation plates were never fully saturated during the determination of a. There is no reason to suppose however that values differing substantially from those quoted would have been obtained with the plates fully saturated at all times for the liquid deficiency, and hence the difference between observed values of $\frac{E}{Ps}$ and those obtaining at saturation, did not vary systematically with wind speed.

For consistency, the values of $\frac{E}{p_s}$ indicated by the curves in figure 4 at V = 5 m./sec. and in figure 5 at appropriate values of x_o should be comparable with those tabulated in the previous section. In the case of the RC plate, the value from figure 4 is about 9 per cent low, rather more than might reasonably be expected. The fact that the plate was never fully saturated would account for about half of the discrepancy but the explanation of the remainder is not clear.

/6.

6. The analogy between momentum and mass transfer

It will be of interest to consider the results in terms of the analogy between momentum and mass transfer similar to the Reynolds analogy between momentum and heat transfer. The drag coefficient f is conventionally defined by*

$$\frac{f}{2} = \frac{\tau_o}{\rho V^2} = \frac{u_*^2}{V^2}$$

Corresponding to $\frac{f}{2}$ we have the mass transfer coefficient m defined by

$$m = \frac{E}{\chi_s V} = \frac{E}{p_s} \quad \frac{RT_s}{MV}$$

where χ_s is the vapour concentration at the surface, M the molecular weight of the vapour, R the universal gas constant and T_s the absolute temperature of the surface. The value of $\frac{E}{p_s}$ here refers to unit area. In view of the different stages of development of the momentum and vapour boundary layers, we perhaps cannot expect equality of the coefficients. We may anticipate however that the effect of introducing the roughness elements would be shown by a similar variation in the coefficients. Values of $\frac{f}{2}$ and m derived from the figures in tables 1 and 2, after converting all units to the c.g.s. system are given in table 4, V being taken as 500 cm./sec. and T_s as 283°A. for all three surfaces. The type SB and SC plates were found to give identical values of m.

Table 4. Values of $\frac{f}{2}$ and m

	$\frac{f}{2}$			m		
Type of surface	Smooth	RB	RC	Smooth	RB	RC
Series 1 observations	0.00206	0.01618	0.01523	0.00243	0.00428	0.00523
" 2 "	0.00213	0.01681	0.01937	0.00243	0.00447	0.00578

It will be seen that the values of $\frac{f}{2}$ and m for the smooth plates are in fair agreement, but not for the rough plates. Furthermore, while the roughness elements have produced about an eightfold increase in $\frac{f}{2}$, m has only increased by a factor of about two. This is similar to the discrepancy between drag and heat transfer coefficients observed by W.F. Cope (1941) in experiments on the heating and cooling of water flowing through smooth and rough pipes. In his case, the drag coefficient of the roughest pipe was as much as six times that from a smooth pipe while the heat transfer coefficient was rather less than twice as much.

A circular cylinder placed transverse to the airstream may be regarded as an elementary form of roughness element. It is of interest then to refer to results obtained with such a body. A.P. Colburn (1933) has shown that there is in fact no analogy between momentum and heat transfer in this case, the drag coefficient being greater than the heat transfer coefficient. At low Reynolds numbers, when the flow is streamline, the difference is quite small, possibly associated with the difference in the molecular constants, kinematic viscosity and thermal diffusivity. With turbulent flow however, the difference increases with increasing Reynolds number, the factor becoming as large as 100 approximately. Colburn concluded that the transfer of heat to and from the cylinder was associated with skin friction alone, the process being independent of the form drag, the major component of the total resistance of a cylinder. The same conclusion must apply to the transfer of vapour from a cylindrical surface for T.H. Chilton and A.P. Colburn (1934) and R.W. Powell (1940) found good agreement between mass and heat transfer coefficients.

---

* There is no significance in the definition of $\frac{\tau_o}{\rho V^2}$ by $\frac{f}{2}$ instead of f, other than the fact that it is customary to do so.

Results quoted for a cylinder, or rather a bank of cylinders, may be compared in a general way with those obtained with a type RC plate, assuming the cones on the latter to be equivalent to small vertical cylinders of diameter 0.4 cm. Since the values of $\frac{f}{2}$ and m are in reasonable agreement for a smooth plate, and presumably also for the smooth interspaces of a rough surface, the discrepancy in the coefficients for a RC plate will arise mainly from the contributions of the cylinders. The present results suggest therefore that for such an assembly of cylinders, the ratio $\frac{f}{2m}$ will exceed 3. From the dimensions of the plate and the wind speed distribution in the vicinity of the cylinders, the appropriate Reynolds number will be about 400. At this Reynolds number, Chilton and Colburn's results give $\frac{f}{2m}$ equal to 11 which is reasonably consistent with the value estimated from the evaporation plate results.*

7. Theoretical considerations

K.L. Calder (1949) considered the problem of evaporation from a saturated strip of rough surface of infinite extent acrosswind and of finite length downwind. He developed expressions for the rate of evaporation E per unit width acrosswind and for the distribution of vapour concentration χ above and downwind of the strip, these being in terms of parameters deducible from the wind speed profiles and the constant, boundary value of concentration χ_o. From the nature of a rough surface, it is not clear what particular level constitutes the boundary, so that the appropriate value of χ_o is largely a matter of speculation. To avoid making any suppositions however, Calder suggested that χ_o might be obtained from the expression for χ and a measured value of concentration at one level. This could then be substituted in the expression for E and the rate of evaporation calculated.

To test this suggestion, measurements were made of the rate of evaporation of methyl acetoacetate and of the corresponding vapour concentrations at a height of 0.6 cm. above a type SB plate and at nine heights ranging from 0.6 to 3.4 cm. above a type RC plate, the vapour samples being taken close to the downwind edges of the plate. In the former case the value of $\frac{E}{p_s}$ computed in the above manner using the modified forms of Sutton's formulae (Pasquill 1942 and 1943) was 1.3 times the observed value. As the formula for the rate of evaporation had already been verified independently, it was assumed that this agreement demonstrated the sampling technique to be reasonably accurate. In the rough surface case, the computed values of $\frac{E}{P_s}$ varied systematically from 1.3 to 0.2 times the observed value according as the height of measurement of χ varied from 0.6 to 3.2 cm. In this instance then, the observed vertical distribution of vapour is quite different from that deduced from Calder's theory.

---

* The Chilton and Colburn results are expressed in the form of a mass transfer factor which, for the present case of a liquid with saturation vapour pressure small compared with atmospheric pressure, is equivalent to our mass transfer coefficient multiplied by $(\frac{\nu}{D})^{2/3}$ where D is the molecular diffusion coefficient. Allowance has been made for this in the above discussion.

Since the measurements showed that most of the vapour lay below 1.6 cm. and as the logarithmic wind speed profile only obtained above 1 cm., the disagreement is not perhaps surprising. It may be recalled that the underlying basis of Calder's treatment is firstly the assumption of equality of the eddy diffusivities of momentum and mass and secondly the calculation of the former diffusivity from the logarithmic relation for the wind profile over a surface. From the lack of analogy between momentum and mass transfer demonstrated in the previous section and the fact that the vapour cloud scarcely rose above the roughness elements into the region of logarithmic wind profile, these assumptions are obviously not applicable to the small surfaces used in these wind tunnel tests. The theory is more likely to apply to areas over which the vapour cloud is considerably deeper than the heights of the roughness elements. This is borne out in an examination by Calder of vapour concentrations observed over a strip of short grassland sprinkled with aniline. The grass was less than 1 in. high while the vapour cloud was at least 2 ft. deep at each of the sampling positions. Relating all observed and calculated concentrations to those at one level, to avoid the difficulties regarding χ_0, good agreement between observed and calculated ratios was obtained.

8. Acknowledgements

The author wishes to express his appreciation of the invaluable preliminary work carried out by Mr. S.G. Crawford. He is also indebted to Messrs. H. Scamell and R. Penny for their practical assistance, particularly in the construction of the moulds for making the plaster casts, and to Messrs. D. Thorp and B.J. Purser for analysing the vapour concentration samples.

References

Calder, K.L.	1938	Porton Report, No. 2036.
Calder, K.L.	1949	Quart.J.Mech.App.Math., 2,153.
Chilton, T.H. and Colburn, A.P.	1934	Ind.Eng.Chem., 26,1183.
Colburn, A.P.	1933	Trans.Am.Inst.Chem.Engrs., 29,174.
Cope, W.F.	1941	Proc.Inst.Mech.Eng., 145,99.
Nikuradse, J.	1933	Ver.Deutsch.Ing.Forsch., No.361.
Pasquill, F.	1942	Porton Report, No.2335.
Pasquill, F.	1943	Proc.Roy.Soc., A,182, 75.
Powell, R.W.	1940	Trans.Inst.Chem.Engrs., 18,36.
Schlichting, H.	1936	Ingen.Arch., 7, 1.
Sheppard, P.A.	1940	J.Sci.Instrum., 17,218.
Sherwood, T.K.	1936	Trans.Am.Inst.Chem.Engrs., 32,150.
Sutton, O.G.	1934	Proc.Roy.Soc., A, 146, 701.
Young, A.D. and Mass, J.N.	1937	Reports and Memoranda of the Aeronautical Research Committee No. 1770.

G.3223/PN/6/56/215

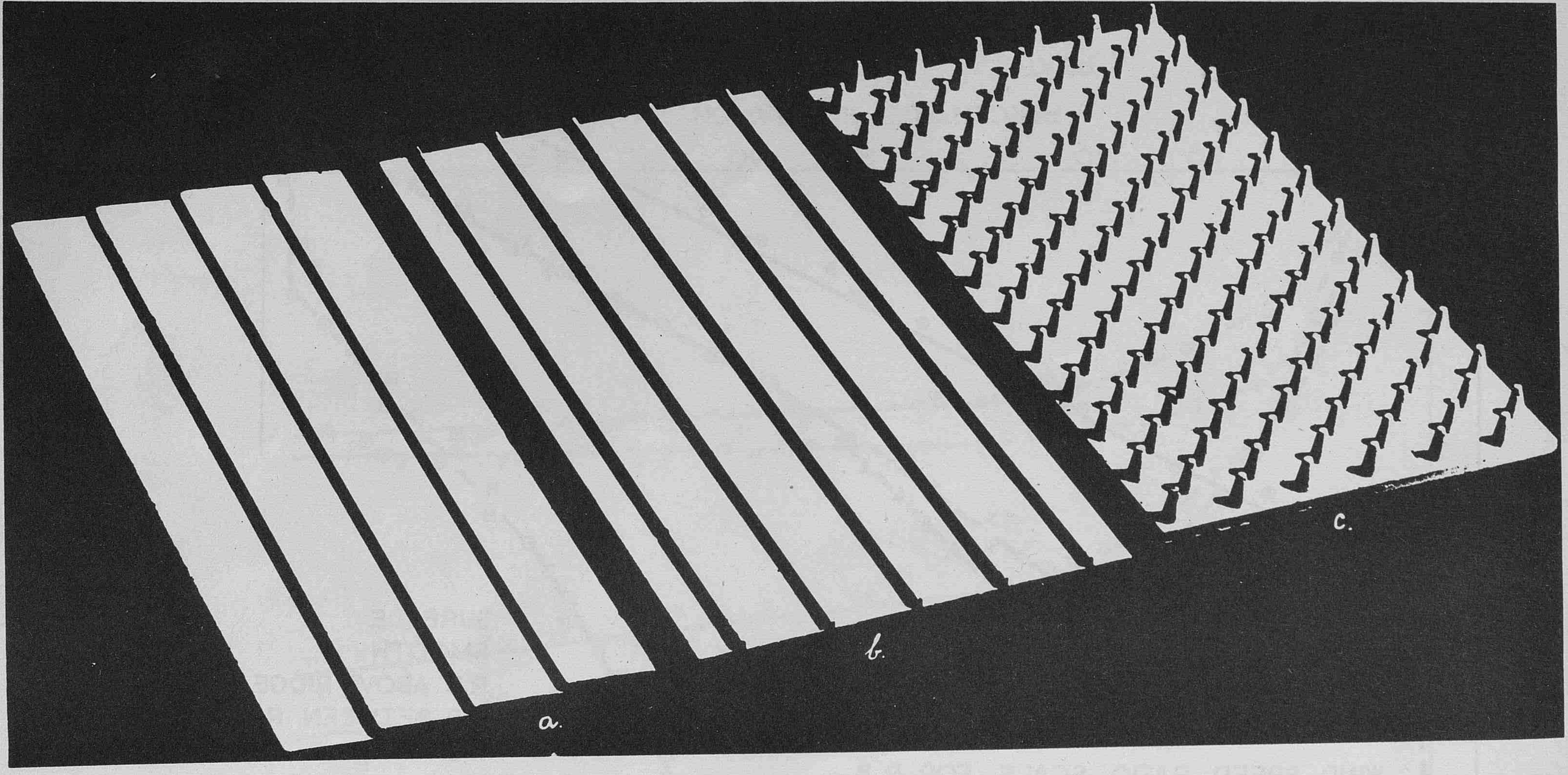

FIGURE I. THE ROUGH SURFACES

(a) RA (b) RB (c) RC

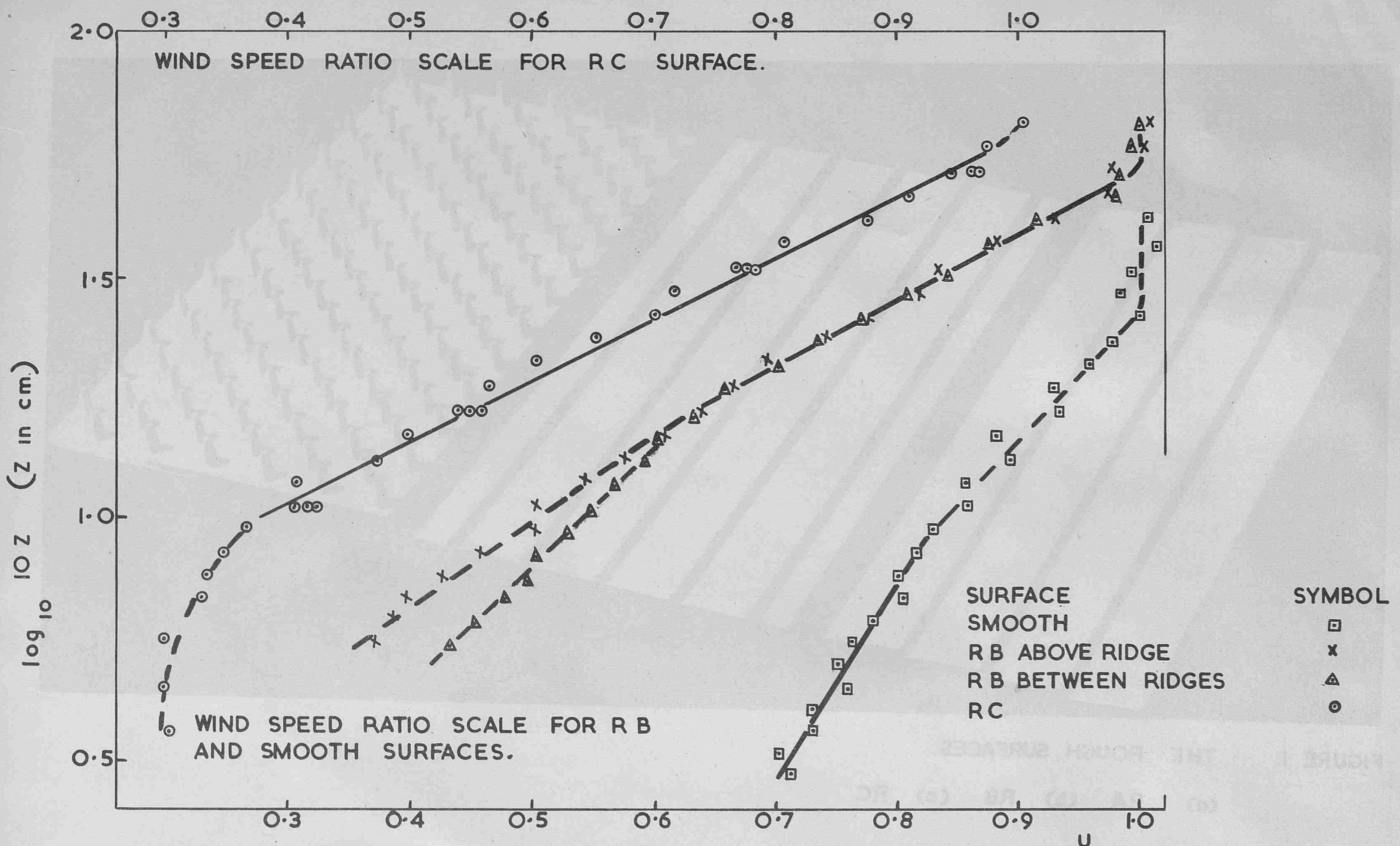

FIG.2. WIND SPEED PROFILES.

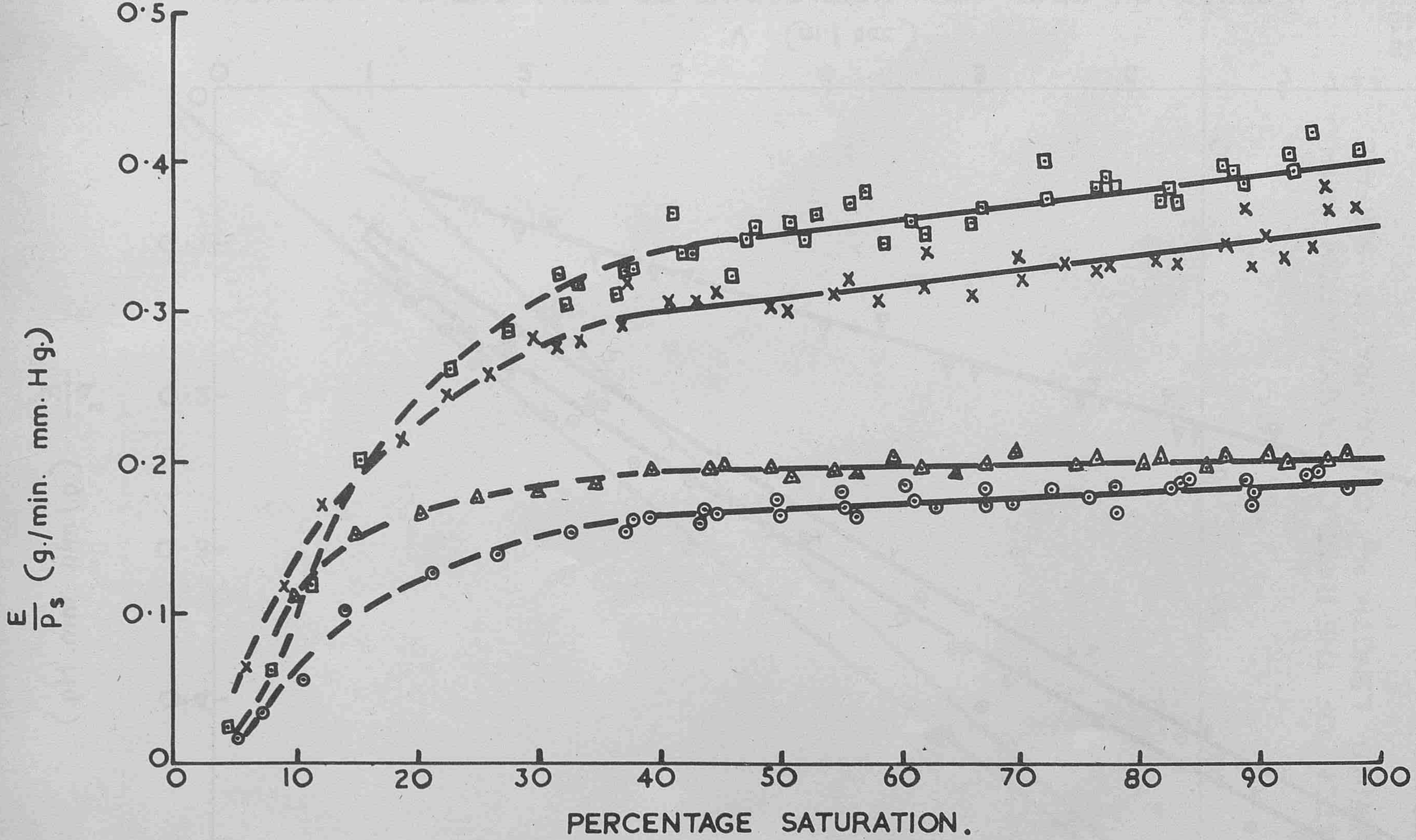

FIG. 3. THE DRYING CURVES.

PLATE	SYMBOL
SB	△
SC	⊙
RB	x
RC	⊡

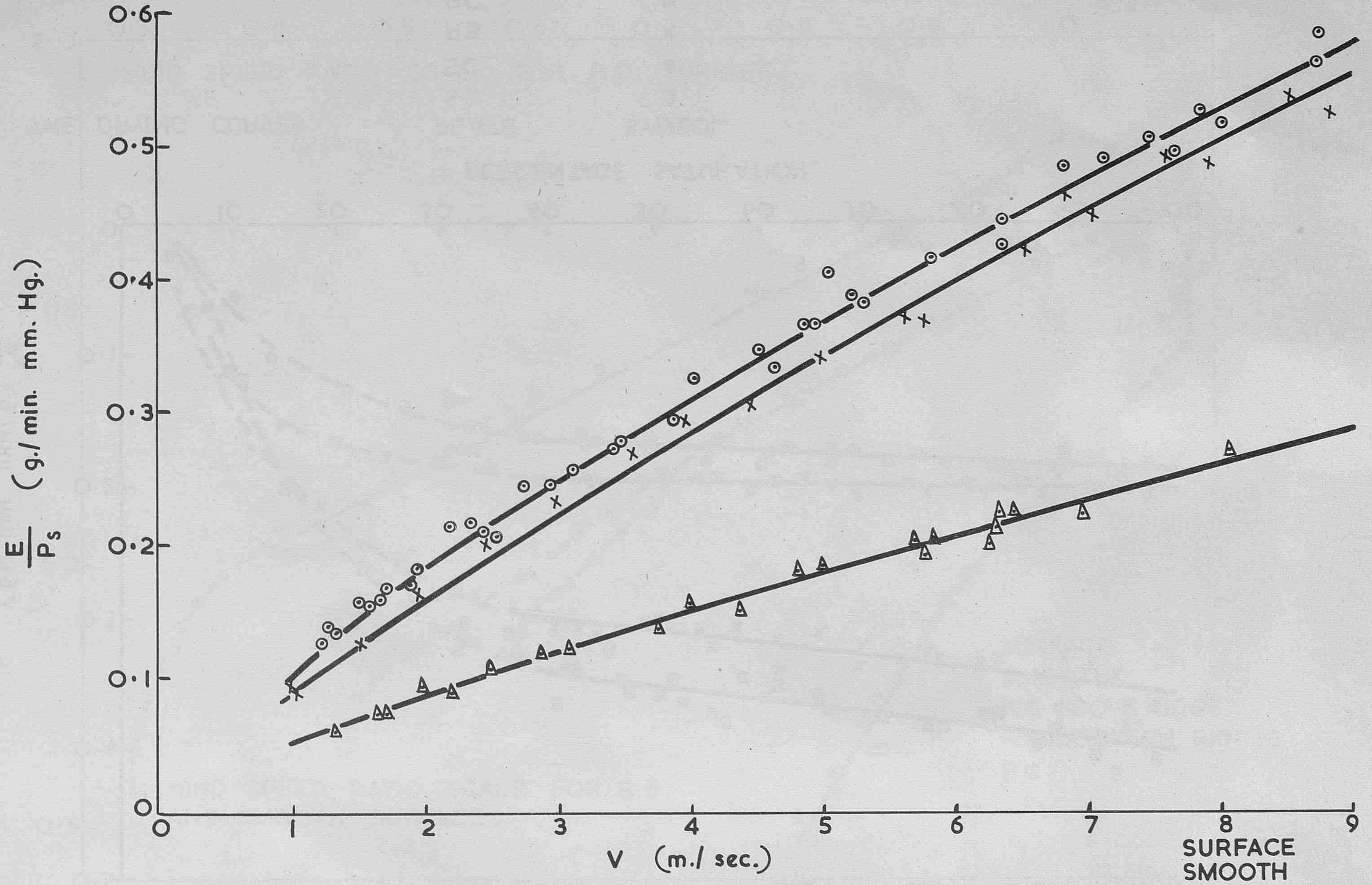

SURFACE	SYMBOL
SMOOTH	Δ
RB	x
RC	⊙

FIG. 4

VARIATION OF THE RATE OF EVAPORATION WITH FREE AIR SPEED V.

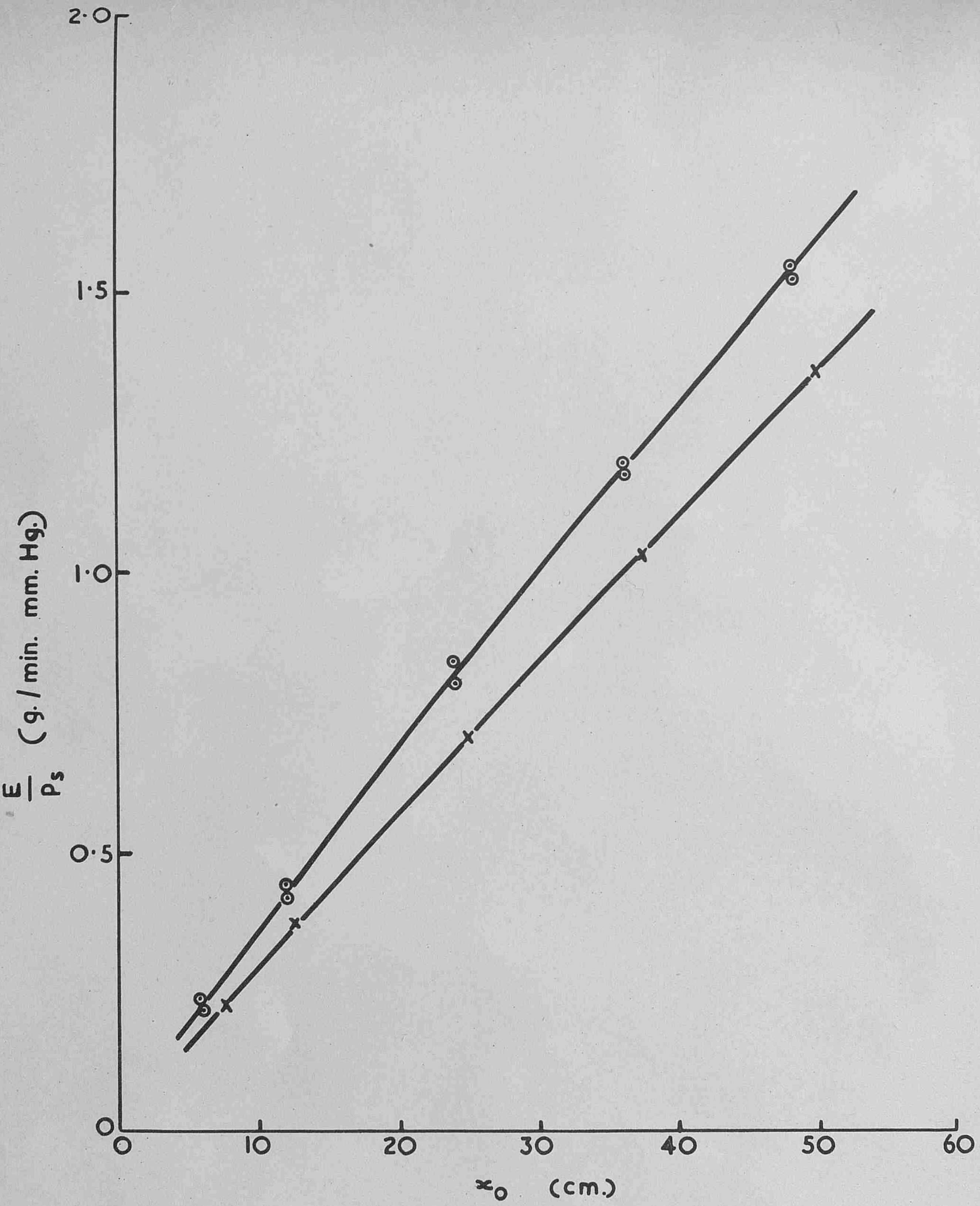

FIG. 5. VARIATION OF THE RATE OF EVAPORATION WITH DOWNWIND LENGTH x_0 OF SATURATED SURFACE.

SURFACE	SYMBOL
R B	x
R C	⊙

M.R.P. 974
S.C.1/113
28th February, 1956.

AD223107

A vertical gustiness recorder for use with a captive balloon.

by

J. I. P. Jones.

(Meteorological Office)

AIR MINISTRY

METEOROLOGICAL RESEARCH COMMITTEE

At the time of issue this report has not been published. Any author desiring to quote this paper should refer to it as "A paper of the Meteorological Research Committee (London), M.R.P. No. 974 by Mr. J.I.P. Jones. A copy is available in the Library of the Meteorological Office."

M.R.P. 974

S.C.I/113

28th February, 1956

AIR MINISTRY

METEOROLOGICAL RESEARCH COMMITTEE

A vertical gustiness recorder for use with a captive balloon

by

J.I.P. Jones (Meteorological Office)

Summary

A description is given of an instrument which has been designed and used to measure vertical gustiness in the form of inclination and mean speed of the wind, from a position on the cable of a captive balloon. A light wind vane and a 'windmill' anemometer were used as sensing heads with automatic partial compensation for balloon movements. The data and reference signals were relayed by electric cable to ground level and recorded on a single channel recorder. Some sample records taken at heights up to 4,000 ft. are presented.

Introduction

In connection with certain diffusion experiments a requirement arose for an instrument to measure vertical gustiness at heights beyond the reach of masts or towers. It was therefore necessary to design the instrument in a form suitable for suspension from a captive balloon. To use the near maximum operational height of the balloon, the weight of equipment together with any connecting electric cable had to be kept low compared with that of the tethering cable. The weight of the instrument could have been reduced by using a hot wire anemometer but this would have required heavy, low-resistance cables. Also a hot wire instrument is fragile, the output is nonlinear, and the calibration frequently unreliable. The use of radio for transmission of data was considered as a means of reducing the loading of the balloon, but was rejected because of the complexity of the equipment.

The requirement was met by the use of a light-weight vane responding to variations in wind inclination, its angular position being registered electrically. To eliminate the effect of the changing angle of the tethering cable, the instrument was effectively suspended, a principle previously used by J.H. Field and R. Warden* for a mechanical instrument used to investigate air currents in the lee of the Rock of Gibraltar. The instrument also incorporated a 'windmill' type anemometer for speed measurements and an arrangement for reference signals which served as a check on the functioning of the instrument and provided a calibration.

Instrumental Details

The inclination vane, A (Fig.1), was mounted to respond to vertical wind fluctuations and positioned the sliding contact, B (Fig.2), of a low friction potentiometer, C. This potentiometer formed two arms of a bridge network, (Fig.3), which gave an output voltage directly proportional to the vane inclination. The vane, and anemometer, D, were mounted at either end of an arm, E, which was maintained in the cross-wind vertical plane by suspension

/from

from the nose of the control vane arm, F. Freedom of the control arm to rotate axially through 40° ensured that the mounting of the sensing heads remained in the along-wind vertical plane when the balloon cable, G, moved out of this plane. Damping of any tendency to oscillatory motion of the arm, E, was effected in the along-wind plane by a balanced air piston-cylinder, H, and in the cross-wind plane by oil dampers, J.

The assembly, (Fig.1), including a box, K, containing circuit components and a 3 volt battery was mounted on the balloon cable by means of split bearings, L, and was free to turn into the mean wind direction (horizontal) under the action of the control vane, M.

The inclination vane, of aerofoil section (6 in. x 3 in.) was constructed of balsa wood and tissue paper, doped and waterproofed, and with the 6 in. long dowel support weight $\frac{1}{4}$ oz. This vane was balanced by a counterpoise weight, N, and electrical connection to the sliding contact was made via a hair spring, P. Response time (90%) when operating in a wind speed of 5 m./sec. was approximately 0.1 sec., increasing to approximately 0.3 sec. in a 3 m./sec. wind.

A step-cam operated switch, Q, built in at the rear centre of the anemometer was used to alternate the output voltage of the potentiometer with a reference voltage taken from a tapped resistor across the bridge, (Fig.3). This reference voltage was equivalent to an inclination of -20°. The cam was driven by the anemometer rotor through fine gears with a reduction ratio of 200:1 so that the switch was operated at every 100 metres of air flow for approximately 4 metres of air flow. The output from the bridge circuit thus indicates the wind inclination for 96% of the time and for the remainder gives pulses which calibrate for wind inclination and which enable the wind speed to be determined.

Ground Equipment

The instrument was connected to the recorder by 5000 ft. of light-weight cable (26 s.w.g. conductors, 0.2 in. outside diameter) via a low gain amplifier. The comparatively high input impedance of the amplifier, (Fig.4), enabled linearity of the bridge output voltage (directly proportional to inclination) to be maintained. The amplifier was balanced, with two directly coupled stages and with negative feedback (cathode of 6SN7 to screen of EF37). The feedback reduced the maximum voltage gain to 26db. but linearised the input/output characteristic and stabilised the gain.

As linearity was maintained throughout the measuring and recording systems and the 0° and -20° equivalent voltages (zero and reference pulse ht.) were known, subsequent calibration of the inclination vane was unnecessary. Sensitivity could be altered at will by adjustment of the 10,000 ohm variable resistor which interconnected amplifier and recorder, so that the reference pulse was of suitable height in relation to the scale of the chart. The value of this resistor was about 8,800 ohm for 20° = 1mA (recorder resistance $\doteq$ 2,400 ohm) and this maintained rapid response of the recorder where otherwise it would have been reduced considerably by the damping action (low impedance) of the cathode follower output stage. Drift within the amplifier was low, and, with the required degree of attenuation, caused negligible zero drift in the recorder.

The sample records shown in Fig.5 and 6 were taken with the 'Super-responsive' Everett Edgecumbe 'Inkwell' recorder, which had a range of 2.5 - 0 - 2.5 mA over a chart width of 10 cm. Measured response time (for 90% response) when used in conjunction with the above D.C. amplifier was 0.2 sec., with 50% attenuation at a frequency of 10 c/sec. Chart speeds of 1, 3 and 12 in./min. were available.

/Use

Use in the Field

The gustiness recorder has been used on diffusion experiments carried out over a period of two months. The captive balloon used for supporting the instrument was a Mark 10 kite balloon with a cable tension of 4-5 cwt. at low level. The maximum height quoted for this balloon, using standard tethering cable, and without any additional load, was 5,000 ft. The weight of the instrument was 7 lb. and the electric cable used weighed 15 lb. per 1,000 ft. Portability and operation of the instrument were satisfactory and no adjustment for drift or change of sensitivity was necessary after the initial warming up period (about 5 min.) of the amplifier. Compensation for changes in the angle of the tethering cable of the balloon was satisfactory but measurement of height variations was found to be necessary as this introduced a significant spurious component into the inclination record in strong gusty winds. These measurements were made by frequent observations on the instrument using a theodolite. An example of the vertical component due to balloon movement is shown plotted on the -30° line of Fig.6a. Fig.5a and b, and Fig.6b and c also contain some spurious component due to the vertical movement of the instrument but this was small due to the low wind speed (3-5m./sec.) in the case of Fig.5, when the tethering cable was near vertical, and due to the steady nature of the wind in the cases shown in Fig.6b and c.

The heights quoted on the sample records are length of cable paid out, actual heights above ground being lower by not more than 3% in these cases. Values of mean temperature difference ($\overline{\Delta T}$) are for 23 ft. - 4 ft. above ground level and also in Fig.6 for a 200 ft. interval about the point of gustiness measurement.

Reference

* Field, J.H. and Warden, R. 1933 Met.Office, G.M. 59.

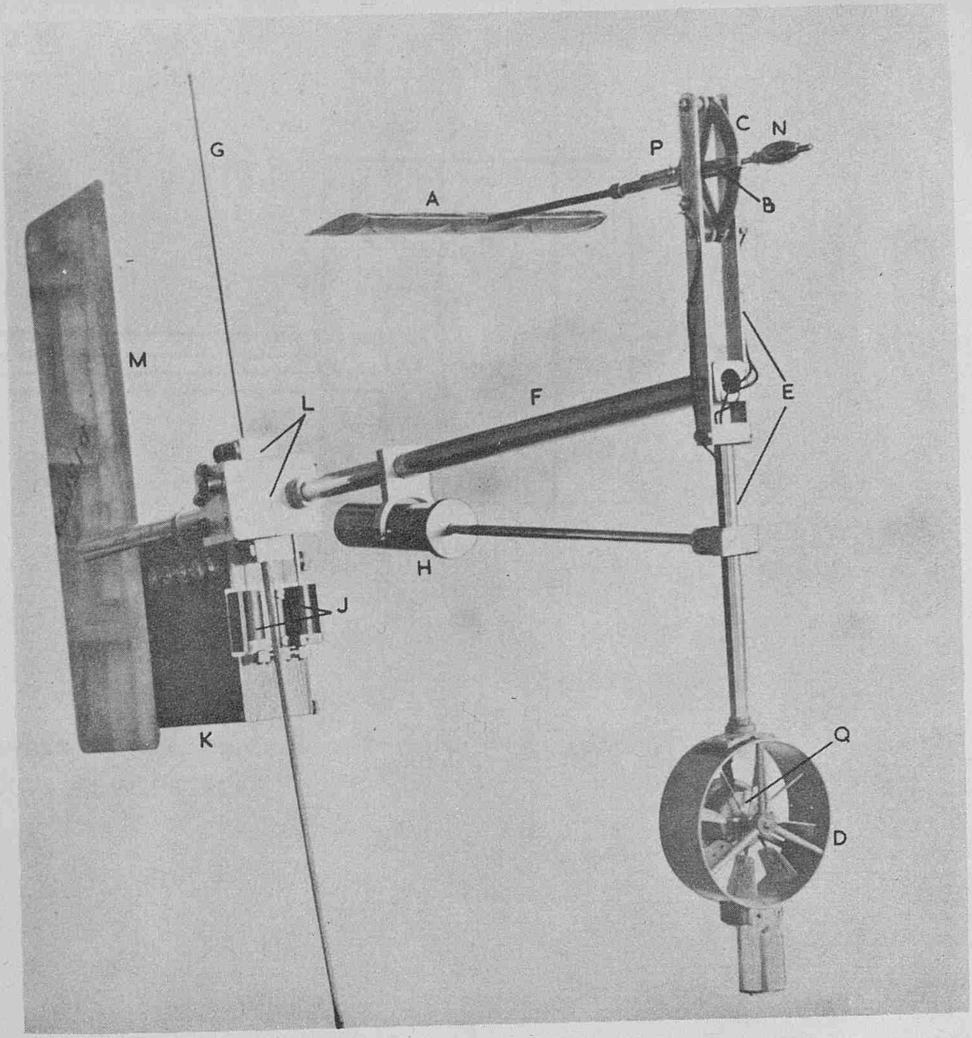
G
P
C
N
A
B
M
L
F
E
H
J
K
Q
D

FIG. 1.

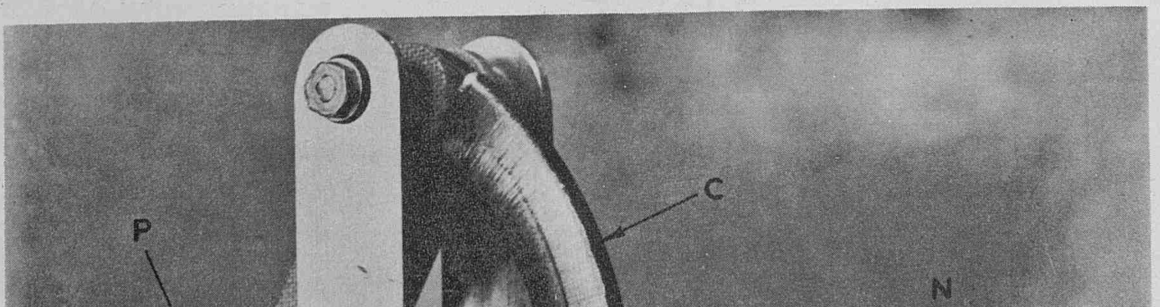

FIG. 2

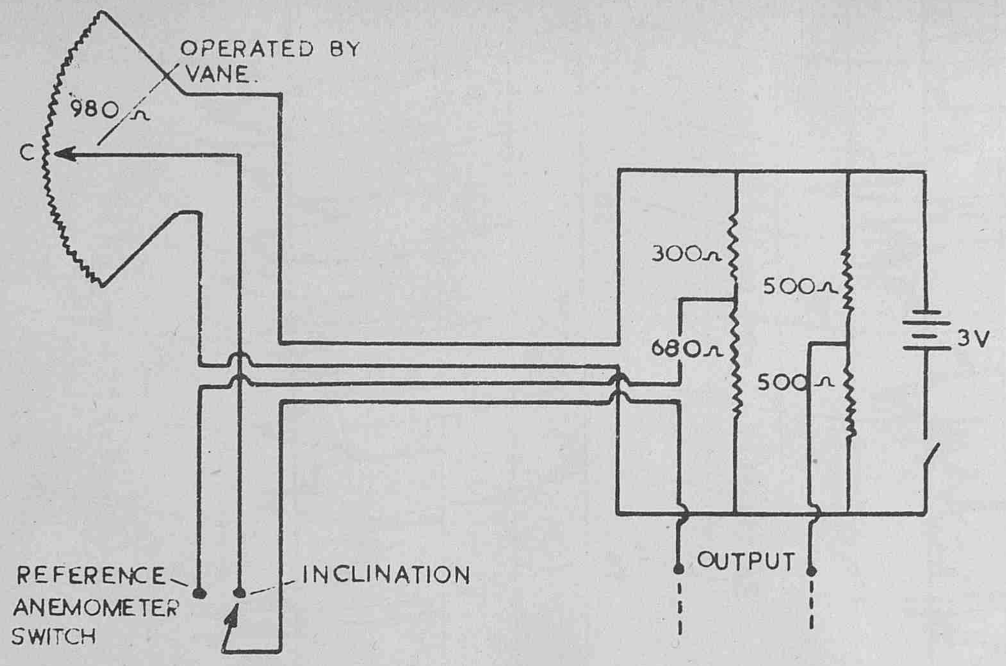
OPERATED BY VANE.
980 Ω
C
300 Ω
500 Ω
680 Ω
500 Ω
3V
OUTPUT
REFERENCE ANEMOMETER SWITCH
INCLINATION

FIG. 3. GUSTINESS METER CIRCUIT THE OUTPUT IS APPROXIMATELY 0.03 VOLTS PER DEGREE.

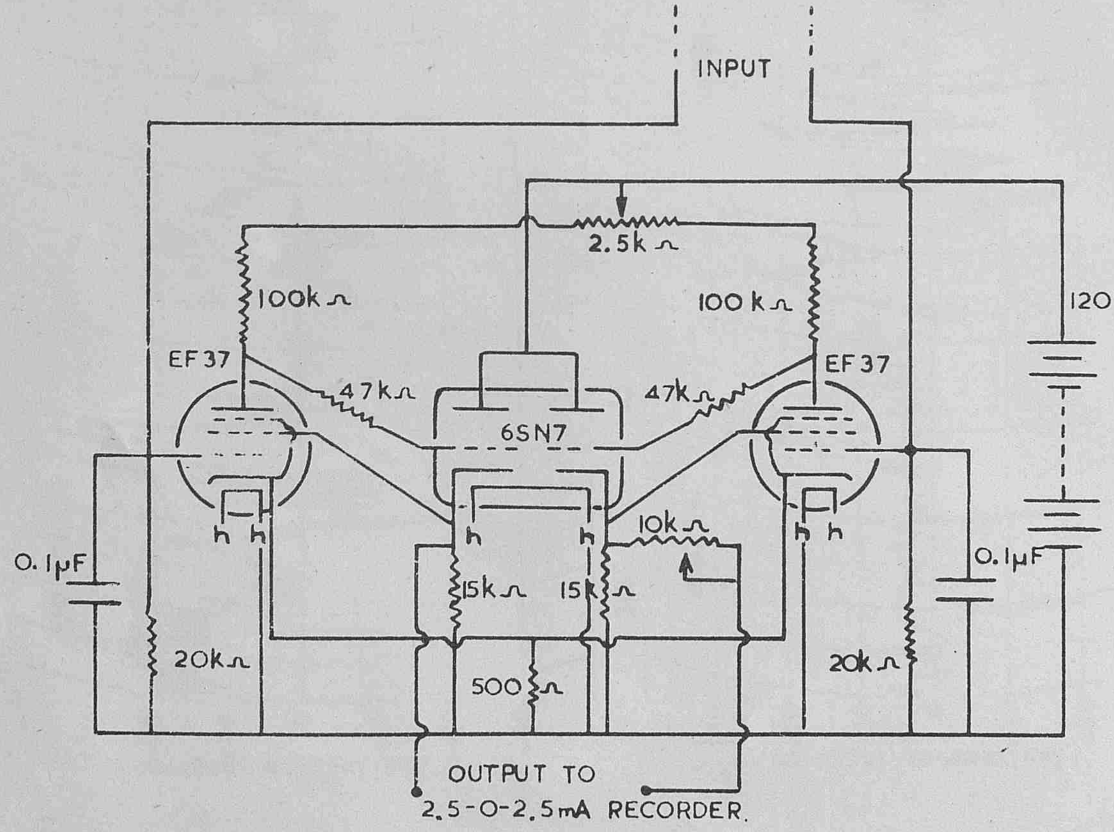
INPUT
2.5k Ω
100k Ω
100 k Ω
120V
EF 37
EF 37
47k Ω
47k Ω
6SN7
h h
h h
h h
10k Ω
0.1µF
0.1µF
15k Ω
15k Ω
20k Ω
20k Ω
500 Ω
OUTPUT TO 2.5-0-2.5mA RECORDER.

FIG. 4. CIRCUIT OF D.C. AMPLIFIER. VALVE HEATERS (h) ARE FED FROM A COMMON 6V ACCUMULATOR.

Figure 5 SAMPLE RECORDS AT 1000 ft. AND 2000 ft. ON 29 SEPT. 55.

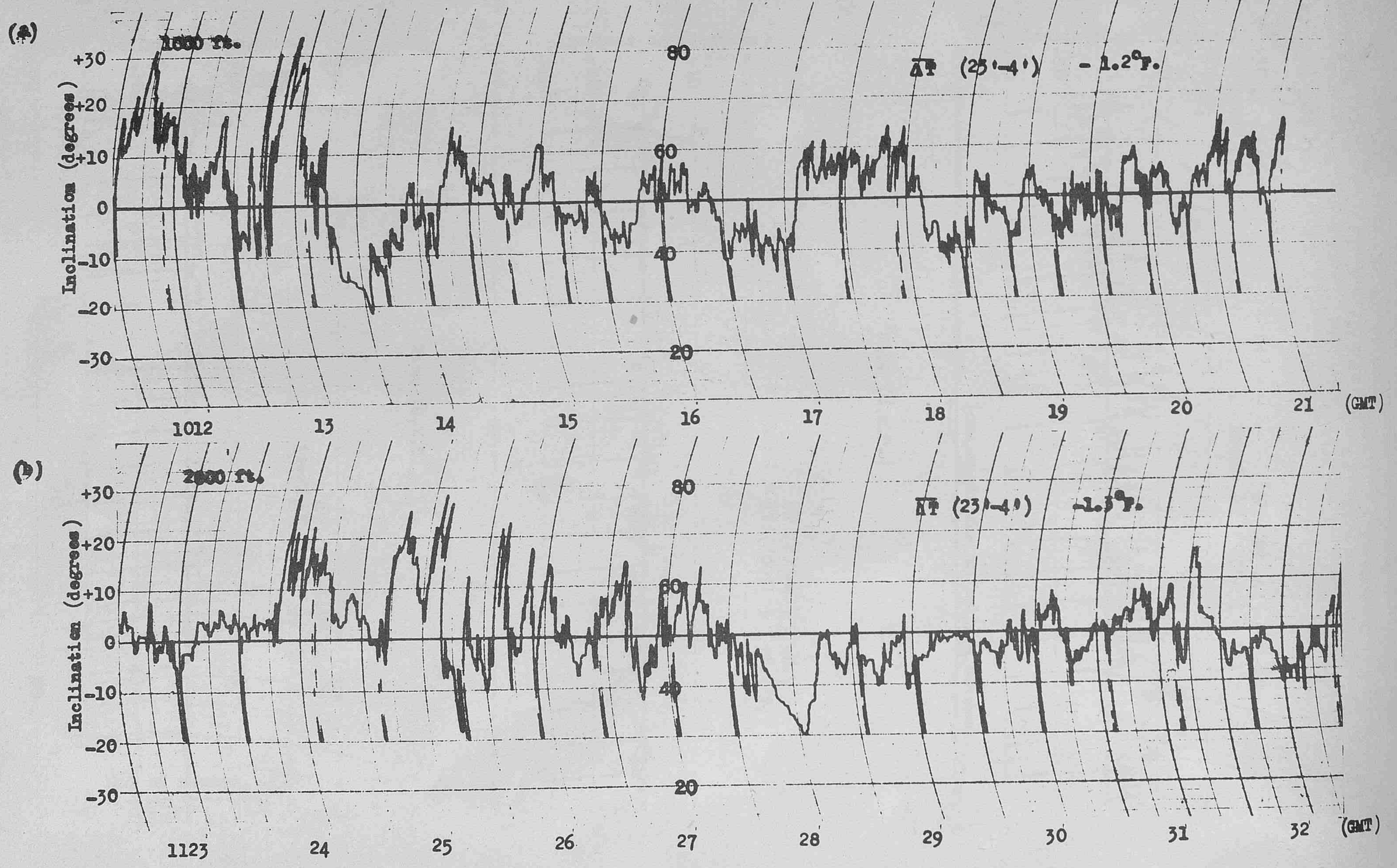

SAMPLE GUSTINESS RECORDS ON 13 OCT. 55.

Figure 6.

(a) 500 Ft.

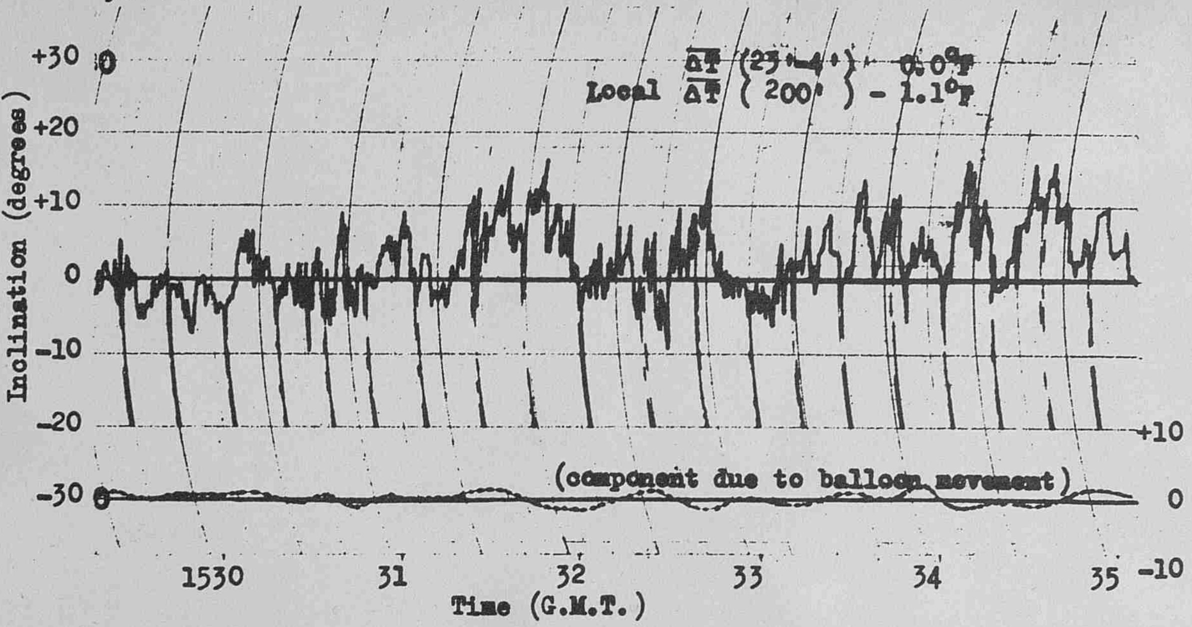

(b) 4000 Ft.

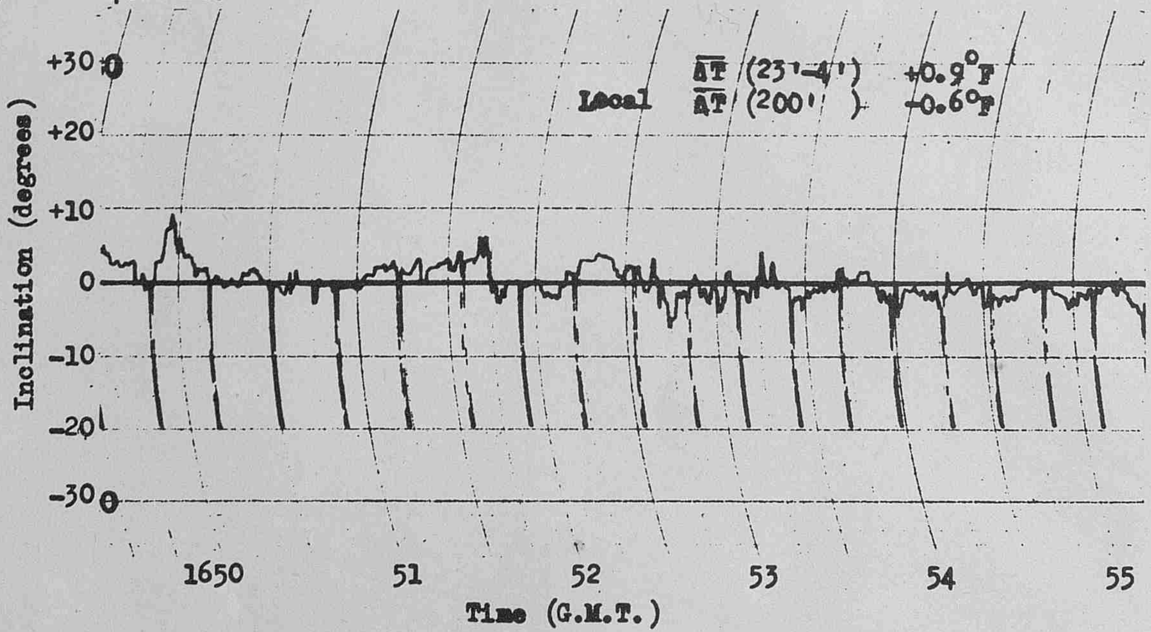

(c) 500 Ft.

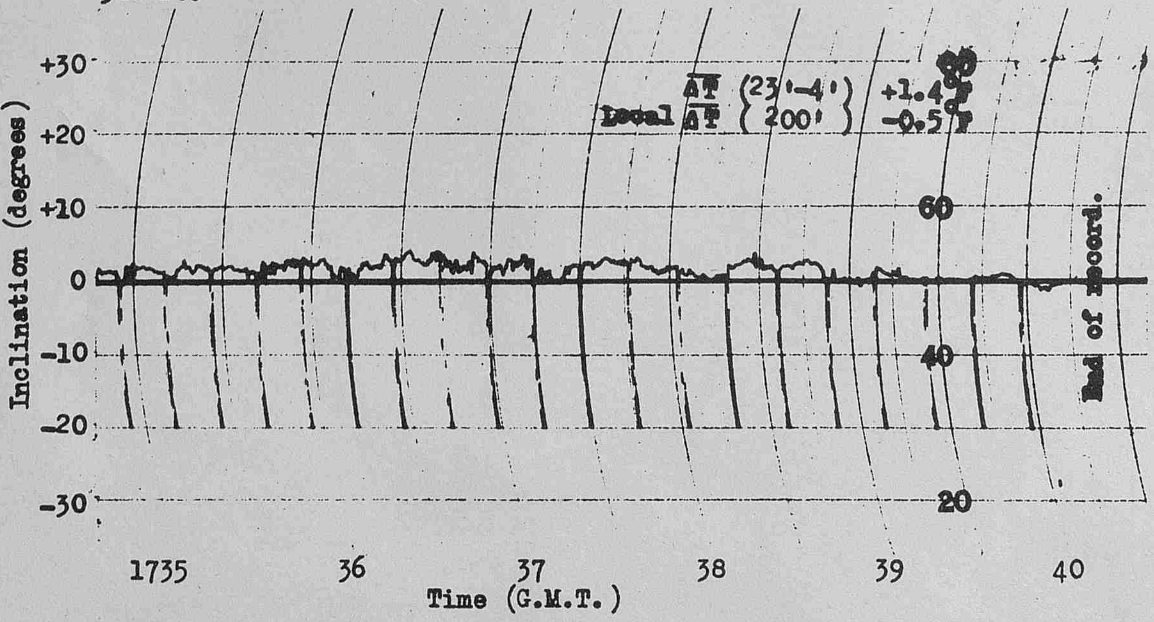

AIR WEATHER SERVICE
TECHNICAL FILES

M.R.P. 976
S.C.111/205
30th April, 1956.

Further observations of humidity up to 50,000 feet made from an aircraft of the Meteorological Research Flight in 1955.

by

N. C. Helliwell, J. K. Mackenzie
and
M. J. Kerley.
(Meteorological Office)

AWSSS
ROUTING SLIP

FILE	INFO	ACTION			
	1.1		DIRECTOR		
	1.2		DEP DIRECTOR		
	1		ASST TO DIRECTOR		
	2		CONSULTANTS		WS
	3		TRSD	CHF	
				TSS	LHC.
				RRB	Nils.
				EDB	VSH
				SEC	
	4		EDD	CHF	LDS
				✓ HLFB	
				✓ STB	
				S	
	5		TIPD	CHF	
				PUE	
				TECH INFO	
				SEC	

send to CL

AIR MINISTRY

METEOROLOGICAL RESEARCH COMMITTEE

At the time of issue this report has not been published. Any author desiring to quote this paper should refer to it as "A paper of the Meteorological Research Committee (London).
M.R.P. No. 976 by Messrs. N.C. Helliwell J.K. Mackenzie and M.J. Kerley.
A copy is available in the Library of the Meteorological Office."

M.R.P. 976
S.C.III/205
30th April, 1956

AIR MINISTRY

METEOROLOGICAL RESEARCH COMMITTEE

Further observations of humidity up to 50,000 feet made from aircraft of the Meteorological Research Flight in 1955

by

N.C. Helliwell, J.K. Mackenzie and M.J. Kerley (Meteorological Office)

Summary

The humidity of the air up to about 50,000 feet was measured on 46 occasions during 1955 using a pressurised Dobson-Brewer frost point hygrometer installed in the Canberra aircraft of the Meteorological Research Flight. The resulting observations are presented and a comparison and combination of them is made with the observations for 1954 described in (2) and (3).

Introduction

Measurements of humidity in the upper troposphere and lower stratosphere are discussed in (1) and (2). The Canberra aircraft was first used to obtain flights to about 50,000 feet in 1953. Regular observations began in 1954 and the results are discussed by Murgatroyd, Goldsmith and Hollings (3). The present report discusses measurements made in 1955 by similar methods.

Instrumentation

As stated in ref. (2), the pressurised Dobson-Brewer frost point hygrometer is installed on the starboard side of the Canberra aircraft and frost points were obtained using this instrument. At 50,000 feet the expected frost point is near -120°F. and glassy ice deposits which form at these temperatures are very difficult to see: but the observers (J.K. Mackenzie and M.J. Kerley) were able to make readings near this level with spans of only 8 to 12°F. between observations of deposit increasing and deposit decreasing. Only one or two frost points were obtained by the method described in ref. (5), using compressed air from the Avon engine of the Canberra aircraft, mainly because there was little difficulty in measuring them directly at the values encountered. Temperature was measured by a standard flat plate aircraft thermometer using a Balanced Bridge Mark II, and altitude and airspeed were taken from the aircraft instruments available on the navigator's console.

Observations

The 46 observations are shown in Table I and Fig.1 shows the arithmetic mean of the ascents taken only at levels where the number of observations was sufficient to justify the averaging process. These flights can be divided into two classes

(1) ascents made before 26 October, 1955

(2) ascents made after 26 October, 1955.

In the first class, the area covered by the ascents was considerable since in each flight lasting two hours the aircraft travelled about 1,000 miles and consecutive readings in the vertical were not over the same point on the ground. In the second class however the area covered by the aircraft was much reduced since an attempt was made to remain within a 30 mile radius of a radio-sonde station. In either class, of course, the individual values of frost point are means over some 20-30 miles, which is about the distance travelled by the aircraft while the observation is being made. The timing of these ascents was designed to coincide with the ascent of the radio-sonde balloon, and a comparison of the aircraft ascents and the balloon ascents will be the subject of a later report. I.C.A.N. heights measured by aircraft altimeter have a standard error of about 200 feet while the frost point is measured to within a standard error of 3°F. at maximum altitude and considerably better at lower levels. Air temperature is computed from the indicated temperature of the flat plate thermometer using a correction for airspeed and height. The speed correction coefficient is assumed constant at 1.76 and the temperature is estimated to be correct to 2°F. at 20,000 feet and 4°F. at 48,000 feet (standard errors) (4).

Discussion

Fig.2 shows the mean temperature and frost point referred to the tropopause level. "High tropopauses" are defined as in ref.(3) and are those at 36,000 feet and above. "Low tropopauses" are cases where the tropopause is 35,000 feet or below. 35,000 feet is very near the mean height of the tropopause for the ascents made in 1955. The mean frost points shown in Fig.2 decrease with height above the tropopause and at 15,000 feet above this level tend to reach a constant value: the lapse of frost point is 4.4°F. in the 1,000 feet above the tropopause but only .7°F. per thousand feet at 10,000 feet above a high tropopause, while at 10,000 feet above a low tropopause it is 2.6°F. per thousand feet.

In Fig.1 it can be seen that the mean frost point decreases almost linearly to 40,000 feet but changes its slope above this level so that at 50,000 feet the value of -117°F. is approached. The mean temperature shows an almost isothermal layer between 35,000 feet and 40,000 feet and then increases to another isothermal layer above 45,000 feet.

In Fig.2 the mean values show that for high tropopauses the frost points are generally lower than for a low tropopause.

The period of these ascents can be divided into two distinct seasons:-

(1) February and March -with late winter and early spring ascents.

(2) October and November -with early winter and late autumn ascents.

It is not therefore possible to claim that the observations are representative of conditions throughout the year, as in ref.(3) and it may be noted here that the mean temperature and mean frost point obtained and shown in Table II are several degrees below the comparable values for 1954 with the exception of the frost points at 44,000 and 48,000 feet (the latter exception is discussed below).

The high frost point measured on the 9th March 1955 is the subject of a separate article by Mr. J.K. Mackenzie (ref. (6)).

Fig.3 shows the variation of frost point at the tropopause and at 10,000 feet above the tropopause with season. This figure suggests that day to day variations of temperature, frost point and height of the tropopause are more significant than seasonal trends - a feature confirming the suggestions in ref.(2).

/Combination

Combination and comparison of observations for 1954 and 1955

Fig.4 shows mean curves of frost point and temperature at selected levels using observations for 1954 and 1955 combined. As stated in the foregoing discussion the 1955 observations were made in only restricted periods of the year but in 1954 observations were made in most months and were more uniformly spaced.

Table II

Mean values of temperature °F. and frost point for selected levels with standard deviations for 1954 and 1955

	Mean temperature °F.				Mean frost point °F.			
Height ft.	1954 & 1955	1955	1954	Standard deviation	1954 & 1955	1955	1954	Standard deviation
20,000	-14.4	-18.2	-7.7	10	-35	-38	-32	17
25,000	-35.2	-37.6	-30.2	8	-54	-56	-50	14
30,000	-53.3	-57	-48	7	-70	-74	-65	11
34,000	-66.9	-67.9	-64	7	-84	-86	-79	10
36,000	-68.9	-71.8	-64.5	10	-90	-92	-87	9
40,000	-67.4	-72.6	-60.8	15	-104	-105	-103	8
44,000	-64.2	-67.2	-60.3	9	-113	-112	-113	6
48,000	-63.5	-68.2	-58.4	9	-116	-115	-116	7

Table II compares mean values for selected levels for the two years. One interesting feature of Table II is that although there can be a spread of 10°F. in the mean at some levels the frost point at 48,000 feet and at 40,000 feet shows little variation in the mean from year to year. One disconcerting feature of these tables is the high standard deviation of frost point from the mean at 48,000 feet, and this deserves further discussion.

Fig.5 shows the total number of observations of frost point at 48,000 feet arranged in steps of 1°F. It will be seen that they are grouped fairly symmetrically about a temperature of -117°F., but that three observations, -102, -91, -89°F., appear to be anomalous. Two of these (-91 and -102°F.) occurred on consecutive days and Mackenzie (6) has suggested that they may be the effect of a nuclear explosion. If this view is accepted, and the three very high values are rejected as being due to unnatural causes, a mean frost point at 48,000 feet of -116.8°F. is obtained, with a standard deviation of 3.2°F.

A comparison of tropopause height with frost point at 48,000 feet has been made and Table III shows this comparison. The probability that the frost point is below the mean value for both years when the tropopause is high seems reasonably well established from this.

/Table III

Table III

Variation of frost point at 48,000 feet with tropopause height

	All frost points			Three high frost points omitted		
	Number of observations			Number of observations		
Tropopause	Above mean	Below mean	Total cases	Above mean	Below mean	Total cases
High	10	25	35	9	24	33
Low	12	14	26	11	14	25
	Probability		Total probability	Probability		Total probability
High	0.29	0.71	1	0.27	0.73	1
Low	0.46	0.54	1	0.44	0.56	1

Conclusion

These observations generally confirm the conclusions of ref.(2). There now seems little case for continuation of the humidity measurements to 50,000 feet over Southern England as a separate investigation although further data can be obtained incidentally during other investigations, e.g., measurements of ozone, radiation etc.

It is suggested that further work on humidity measurement at high levels should now be extended to other latitudes and greater heights. Only a small increase of the latter is possible with present aircraft and the acquisition of a suitable machine of greater performance is extremely desirable. It should however be possible to use facilities now available to R.A.E. at Farnborough to make measurements in other latitudes in the near future if this is considered worthwhile.

References

(1) Bannon, J.K., Frith, R. and Shellard, H.C. Geophysical Memoirs No.88, Air Ministry, London, 1952.

(2) Murgatroyd, R.J., Goldsmith, P. and Hollings, W.E.H. Meteorological Research Papers, Air Ministry, London, No.877, 1954.

(3) Murgatroyd, R.J., Goldsmith, P. and Hollings, W.E.H. Quart. Journal Royal Met.Soc., Volume 8, No.350, p.533, October, 1955.

(4) Durbin, W.G. Meteorological Research Papers, Air Ministry, London, No.930, 1955.

(5) Goldsmith, P. Meteorological Research Papers, Air Ministry, London, No.859, 1954.

(6) Mackenzie, J.K. Met. Mag., London, Vol. 86, No. 1010, 1956.

* Height of tropopause

Date		3 Feb.	4 Feb.	7 Feb.	p.m. 8 Feb	r.	10 Mar.	10 Mar.	11 Mar.	14 Mar.	15 Mar.
Time G.M.T.		1350	1220	1505	1410	5	1140	1620	1205	1150	1150
Height (ft.)	Mb.										
5,000	843	+24.3 (6000') (+08)	+28.7 (+16)	+37.4 (+33)		1					
7,000	782										
10,000	697	+7.8 (-23)	+11.9 (-17)	+23.8 (+06)	+15.7 (-33)	0					
15,000	572	-12.2 (-40)	-4.4 (-22)	+04.5 (-30)	+03.8 (-09)	7					
20,000	466	-33.2 (-60)	-23.7 (-37)	-07.7 (-17)		2	-22.3			-12.7	
25,000	376	-43.1 (-79)	-45.6 (-61)	-30.4 (-46)	-33. -(40)	4	-42.2		-36.4	-33.7	
26,000	360					5			-41.0	-40.3	
27,000	344					3			-46.1	-45.0	
28,000	329					7			-50.5	-49.5	-53.2 (-58)
29,000	315					4			-54.1		-53.5 (-62)
30,000	301	-55.0* (-94)	-61.6 (-82)	-52.3 (-66)	-52.4 (-68)	0 .0)	-62.8 (-70)		-60.5 (-70)	-59.0 (65)	-61.3 (-70)
31,000	287					2 0)	-66.6		-62.5 (-69)	-61.0	
32,000	274					5*)	-68.9		-68.4	-66.0 (-75)	-68.8 (-77)
33,000	262	-55.3					-71.5				
34,000	249.8				-68.7 (-77)	0)	-73.8		-75.1	-72.5 (-84)	-77.5 (-81)
35,000	238	-49.5 (-100)	-65.3* (-100)	-72.9* (-77)			-74.9 (-88)		-79.6		
36,000	227	-50.5 (-108)				5)	-77.6		-83.3 (-89)	-81.3 (-88)	-84.9 (-90)
37,000	216						-78.1*		-85.6*	-83.8	
38,000	206	-48.8 (-113)			-76.0 (-96)	3)	-74.7		-83.5	-89.8 (-100)	-88.2 (-94)
39,000	197						-76.2		-83.5		
40,000	187	-51.5 (-115)	-54.6 (-113)	-73.9	-72.0 (-112	7 0)	-75.9 (-98)	-76.6 (-99)	-85.8	-97.7* (-106)	-91.5* (-97)
41,000	179						-75.1		-84.2	-97.7	
42,000	170	-53.5	-59.3 (-117)		-66.9 (-11)		-70.4	-71.3 (-103)	-83.8	-93.7 (-108)	-85.5 (-112)
43,000	162								-78.2	-86.0	
44,000	155	-52.2	-57.5 (-116)		-66.0 (-117)	2	-73.6 (-106)	-70.9 (-108)	-74.4	-82.6 (-114)	
45,000	147						-68.8		-72.0	-80.2	
46,000	140	-55.8	-57.0 (-114)		-70.6 (-118)		-69.3	-70.7 (-111)	-70.0	-75.7 (-119)	
47,000	133						-66.9		-69.6		
48,000	127	-56.3	-55.6		-66.8 (-118)		-71.8 (-102)	-67.9 (-111)	-70.4 (-117)	-77.2 (-119)	
49,000	121										
50,000	116	-62.0	-58.1		-66.5 (-119						
tropopause height		30,000	35,000	35,000	38,000	00	37,000	–	37,000	40,000	40,000

G.58052/(a)/JEK/4/56/50

* Height of tropopause

Date		16 Mar.	18 Mar.	18 Mar.	2Oct.	31 Oct.	1 Nov.	8 Nov.	11 Nov.
Time G.M.T.		1525	1145	1605	45	1345	1350	1000	11130
Height (ft.)	Mb.								
5,000	843			+18.5 (+15)	+.0 ()	+29.5 (-20)	+32.7 (-22)	+41.3 (+33)	
7,000	782								
10,000	697			+13.3 (-11)	+.1 (4)	+20.1 (00)	+18.5 (-06)	+21.8 (+19)	+25.0
15,000	572		-4.0	-3.3 (-20)	.0 (6)	+1.5 (-16)	+02.1 (-12)	+04.9 (-12)	+7.2
20,000	466		-21.0	-23.5 (-53)	-.8 (3)	-15.1 (-27)	-19.1 (-27)	-16.3 (-54)	-12.5
25,000	376		-42.4	-43.6 (-67)	-.8 (6)	-36.9 (-54)	-41.0 (-54)	-40.5 (-51)	-33.0 (-43)
26,000	360		-46.9			-41.3	-45.1	-42.6	
27,000	344		-51.9			-45.6	-47.9 (-63)	-47.2 (-50)	
28,000	329		-55.8 (-68)			-51.3	-49.7	-51.5	
29,000	315	-57.8 (-56)	-60.2 (-72)			-54.1	-56.1	-54.5	-53.7 (-63)
30,000	301	-64.4 (-62)	-64.0 (-73)	-62.7 (-77)	-6.7 (-7)	-58.9 (-71)	-60.9 (-81)	-60.6 (-72)	
31,000	287	-66.0	-65.8 (-79)		.3*	-63.7	-64.9	-63.3	
32,000	274	-70.4	-69.2 (-85)	-70.0* (-83)	-6.0 (-3)	-67.0	-68.0	-66.8	
33,000	262	-75.2 (-82)			.3	-71.1 (-84)	-71.1	-70.7* (-74)	
34,000	249.8	-79.0 (-85)	-73.9 (-92)	-72.4 (-92)	-7.1 (-2)	-74.4	-72.0 (-85)	-70.4	
35,000	238		-75.4		.5	-78.9	-74.1*	-69.5	-82.3 (-86)
36,000	227	-85.0 (-91)	-78.7* (-95)	-78.0 (-95)	-7.1 (-5)	-82.5 (-90)	-74.2	-68.6 (-94)	-78.5 (-86)
37,000	216				.1	-84.5*	-72.4	-69.2	-86.9* (-88)
38,000	206	-89.8* (-93)	-76.2 (-101)	-75.4 (-99)	-7.9 (-01)	-84.8 (-90)	-70.7 (-103)	-66.4 (-101)	-77.8 (-95)
39,000	197		-73.9		.2	-78.4		-66.7	-73.5 (-104)
40,000	187	-89.1 (-97)	-71.8 (-109)	-80.3 (-103)	-6.7 (-05)	-82.9 (-101)		-65.7 (-107)	-66.4 (-106)
41,000	179								
42,000	170			-73.3 (-113)	-6.4 (-12)		-70.6 (-109)		
43,000	162					-72.9 (-113)		-63.9 (-112)	
44,000	155			-76.5 (-116)	-6.8 (-5)		-70.5 (-112)		
45,000	147								
46,000	140			-70.0 (-116)	-6.1 (-6)	-72.7 (-113)	-71.0 (-114)	-64.0 (-113)	
47,000	133								
48,000	127			-70.0 (-118)	-6.7 (-7)	-72.3 (-116)	-68.9 (-116)	-66.4 (-115)	
49,000	121								
50,000	116								
tropopause height		38,000	36,000	32,000	34,000	37,000	35,000	33,000	37,000

G.58052/(a)/JEK/4/56/50

Table I (contd.)

High level ascents 1955

Air temperature and frost point (in brackets)

Date		22 Nov.	28 Nov.	29 Nov.	1 Dec.
Time G.M.T.		1335	1335	1335	1125
Height (ft.)	Mb.				
5,000	843	+27.5		+38.4	
7,000	782				
10,000	697	+14.5 (-13)	+26.0	+24.8	
15,000	572	+04.2 (-46)	+07.9	+05.8	
20,000	466	-17.9 (-36)	-13.5	-13.6	-19.5
25,000	376	-33.0 (-59)	-34.7	-27.0	-42.0
26,000	360			-36.1 (-84)	
27,000	344			-46.9	
28,000	329		-50.8	-49.9 (-70)	-51.2 (-81)
29,000	315		-53.9	-48.7	-57.7 (-57)
30,000	301	-50.1 (-77)	-58.9	-49.7 (-82)	-55.6 (-88)
31,000	287	-53.0	-63.2	-54.8	
32,000	274	-57.2	-66.1	-58.2 (-88)	-60.0 (-88)
33,000	262	-59.8	-70.9 (-79)		-61.5* (-92)
34,000	249.8	-63.7		-64.1 (-90)	-60.8
35,000	238	-67.7 (-91)			-60.8
36,000	227	-72.8*	-79.6* (-85)	-77.3	-60.5 (-99)
37,000	216	-73.9	-79.6		-62.2
38,000	206	-74.2	-79.3	-71.7* (-95)	-61.2
39,000	197	-75.8	-79.0		-66.3
40,000	187	-75.4 (-103)	-78.6 (-99)	-83.4	-65.4 (-111)
41,000	179		-76.8		-64.4
42,000	170	-77.6	-75.5 (-110)	-74.1 (-112)	-65.4
43,000	162				-64.1
44,000	155	-77.4 (-112)		-73.7	-67.0 (-114)
45,000	147				-66.8
46,000	140	-78.8	-73.8 (-114)	-75.6 (-116)	-68.2
47,000	133				-68.3
48,000	127	-79.4 (-115)	-74.2 (-117)	-76.0 (-117)	-69.9 (-120)
49,000	121				
50,000	116				
tropopause height		36,000	36,000	38,000	33,000

*Height of tropopause

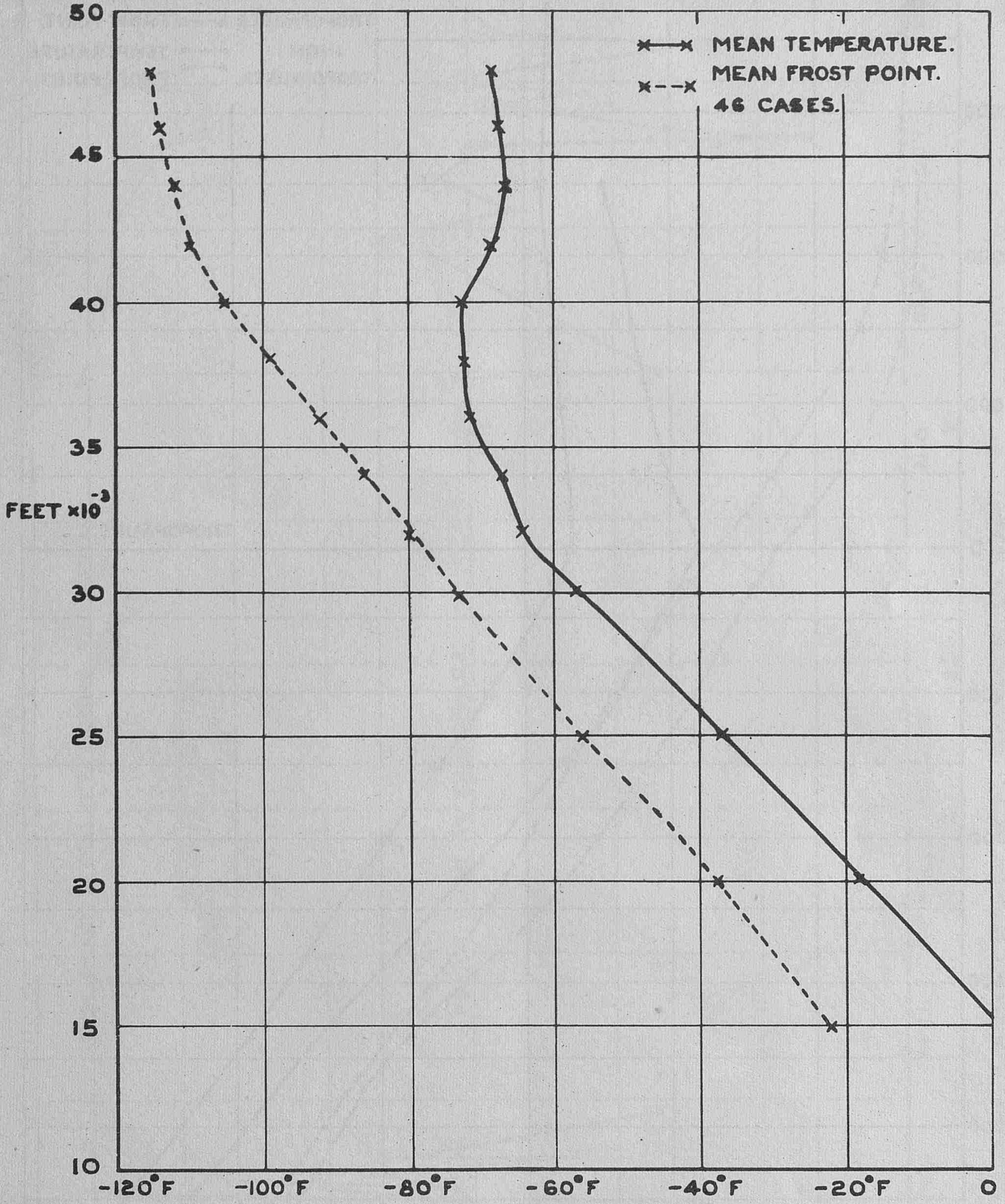

FIG. 1. MEAN TEMPERATURE AND FROST POINT 1955.

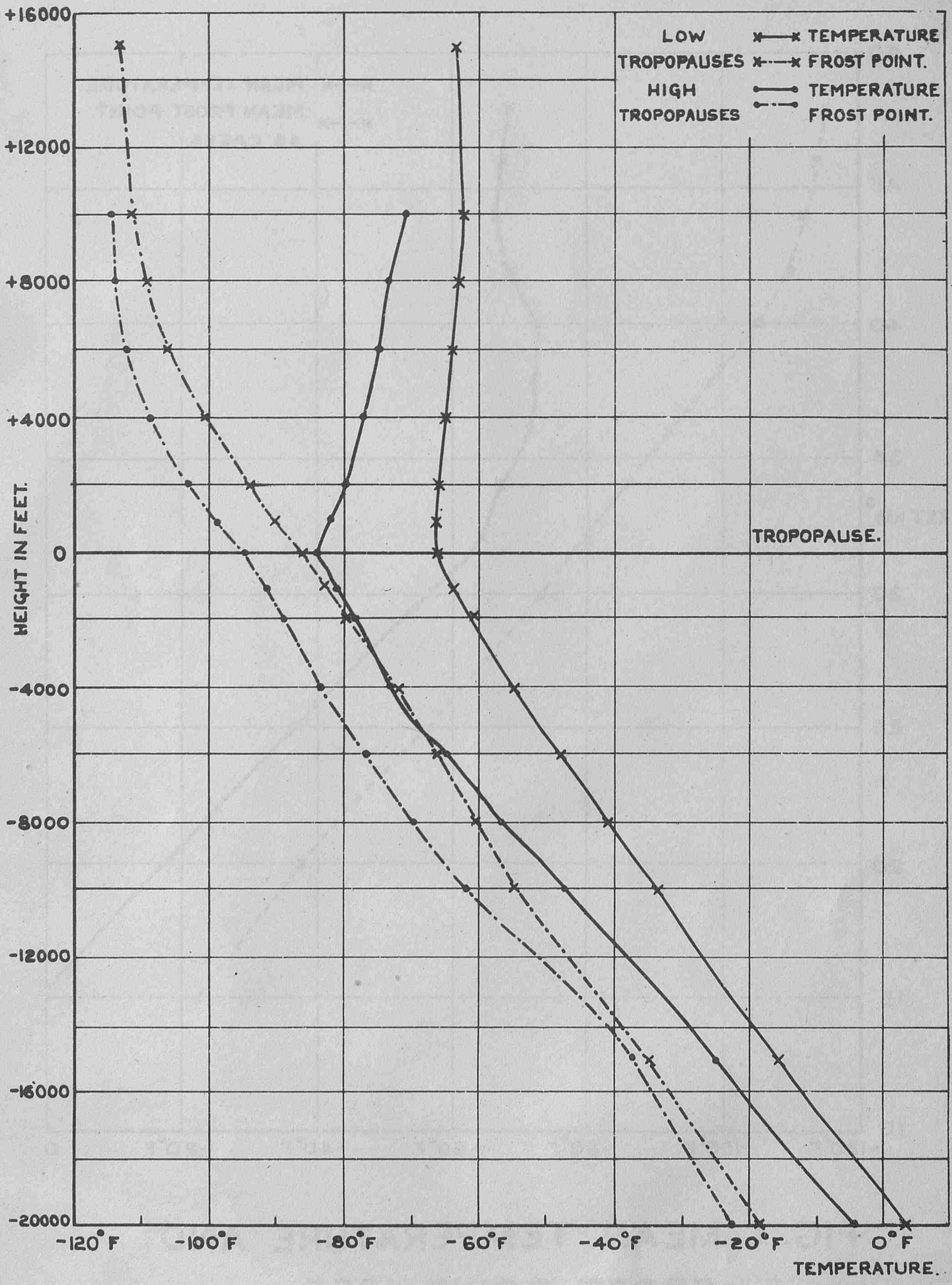

FIG. 2. MEAN TEMPERATURE AND FROST POINT REFERRED TO THE TROPOPAUSE.

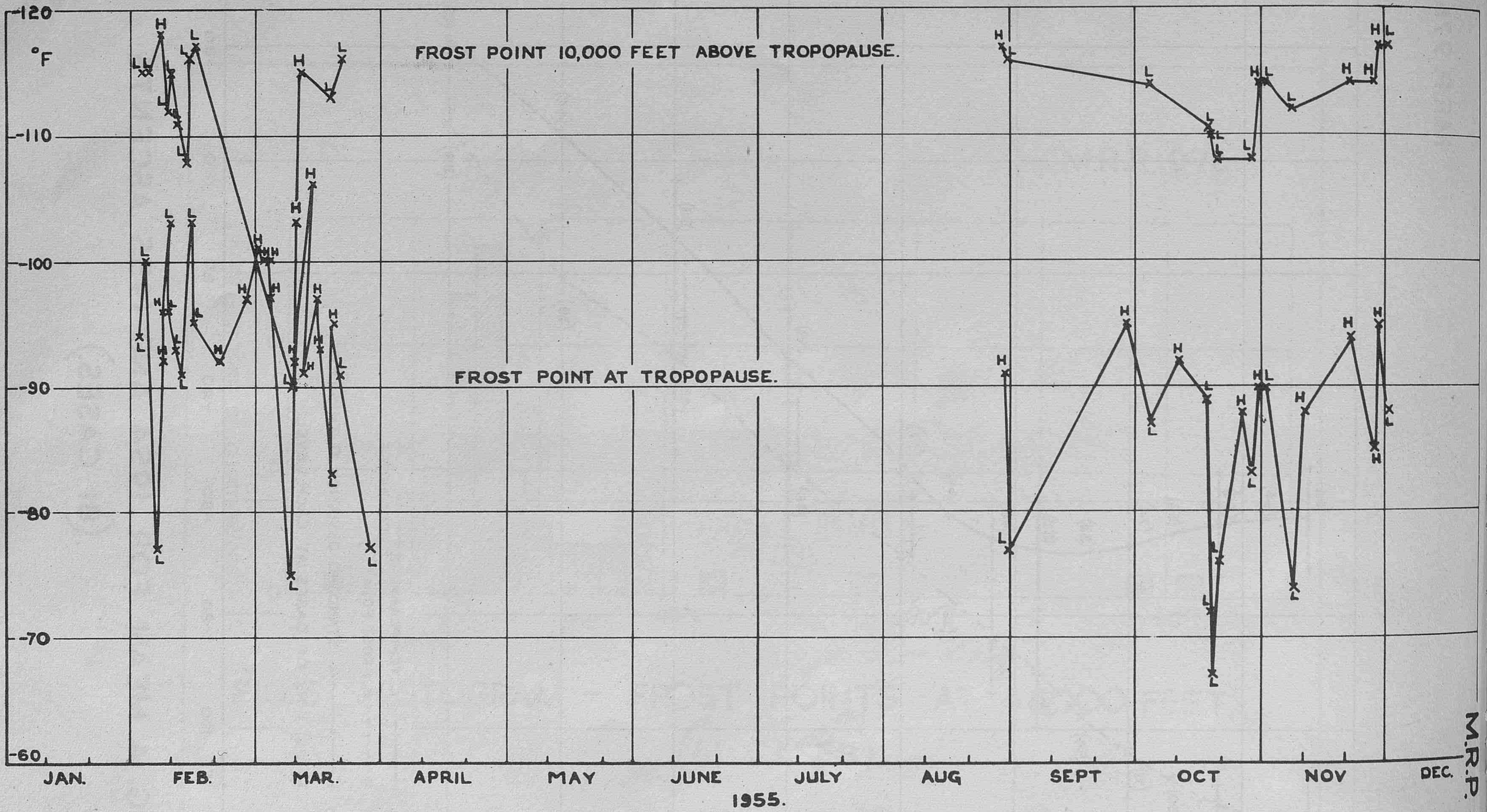

FIG. 3. DAY-TO-DAY VARIATIONS OF FROST POINT

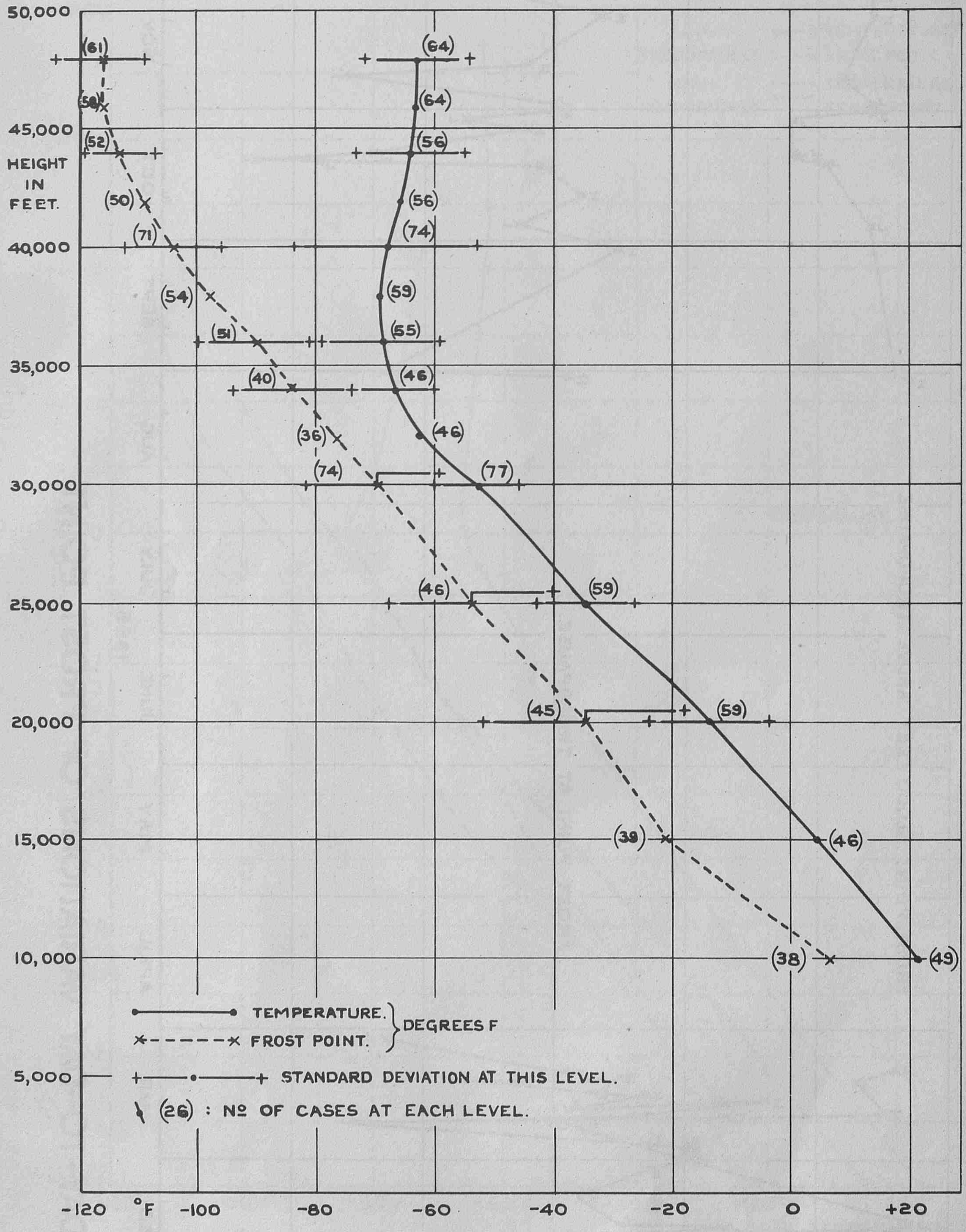

FIG. 4. MEAN FOR 1954 AND 1955 ASCENTS (81 CASES.)

M.R.P. 976.

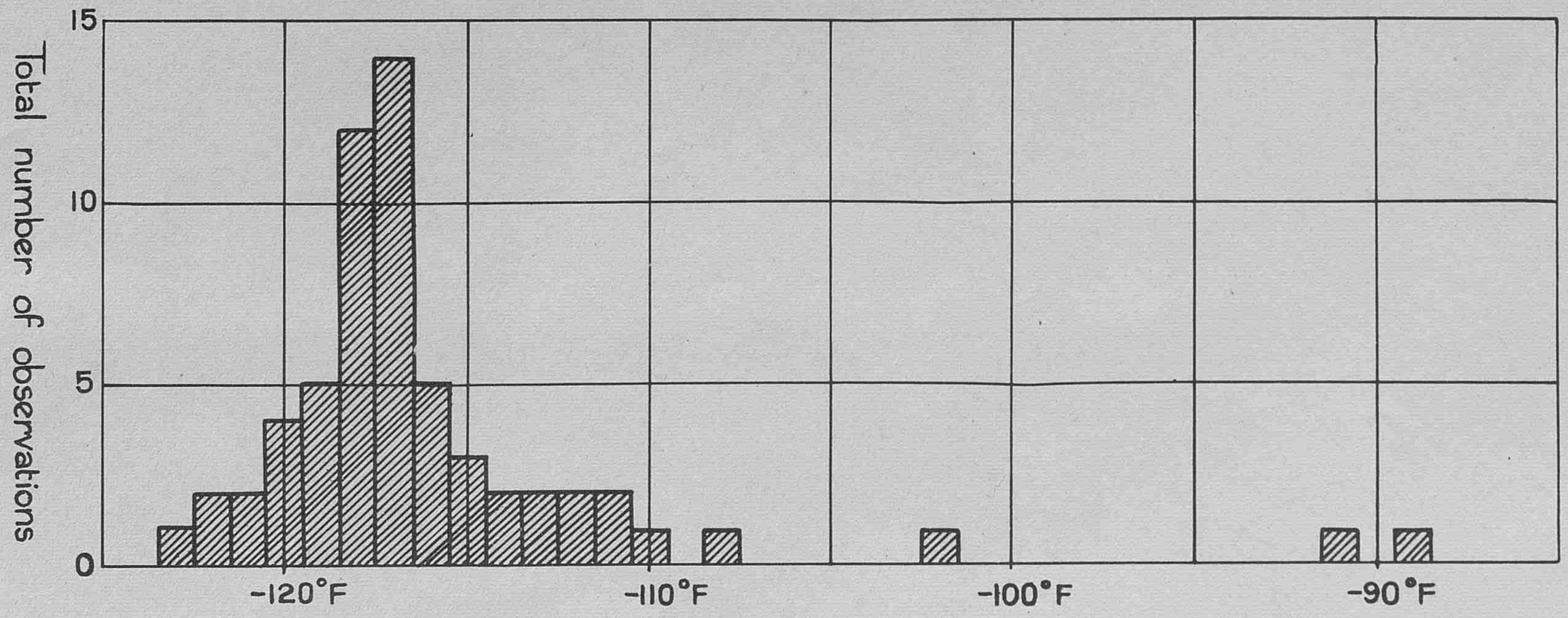

FIG. 5. HISTOGRAM – FROST POINTS AT 48,000 FEET.
(61 CASES)

M.R.P. 977
S.C. I/114
30th April, 1956.

AD223105

An electrical dewpoint hygrometer suitable for routine meteorological use.

by

J. MacDowall.

(Meteorological Office)

AIR MINISTRY

METEOROLOGICAL RESEARCH COMMITTEE

At the time of issue this report has not been published. Any author desiring to quote this paper should refer to it as "A paper of the Meteorological Research Committee (London)
M.R.P. No. 977 by Mr. J. MacDowall.
A copy is available in the library of the Meteorological Office."

M.R.P.977
S.C.I/114
30th April, 1956

AIR MINISTRY

METEOROLOGICAL RESEARCH COMMITTEE

An electrical dewpoint hygrometer suitable for routine meteorological use

by

J. MacDowall (Meteorological Office)

Introduction

The principle of this instrument was first described by W. Findeisen (1935), and consists of the determination of the dewpoint of a surface coated with a hygroscopic substance. The advantage of this method is that the dewpoint of such a surface is usually above air temperature so refrigeration is not required. This idea has been developed by the Foxboro Instrument Company in the U.S.A. in their Dewcel and first adapted for meteorological use by John H. Conover (1950) who found it accurate to ±3°F. of the dewpoint determined with an Assmann psychrometer. This paper describes a hygrometer similar to Conover's and comparisons with an Assmann psychrometer, twice a day (at about 0930 and 1700 local time) for six months. At the same time the dewpoint was measured with wet and dry bulb thermometers inside a large type of Stevenson screen.

2. Description of the instrument

(i) The hygrometer consists of a varnished brass tube 3 in. long, $\frac{1}{2}$ in. diameter covered with glass tape impregnated with lithium chloride on top of which are wound two parallel silver wires about 3/32 in. apart and insulated from each other at both ends. A supply of about 30 volts A.C. is connected to the two wires through a ballast resistance in the form of a 35v. 100w. lamp. The temperature of the hygrometer is measured with a mercury in glass thermometer with the bulb placed in the centre of the brass tube. A photograph of the element is shown in Fig.1 and the circuit in Fig.2.

(ii) The element and thermometer are mounted with the axis vertical at the centre of the double walled wind shield shown in Figs. 3 and 4. In operation the hygrometer is mainly between 30°F. and 70°F. above air temperature so an air circulation is set up inside the wind shield*.

3. Operation of the hygrometer

The temperature variation of the vapour pressure over a surface of water and a surface of a saturated lithium chloride solution is shown in Fig. 5. From this it can be seen that with the hygrometer at air temperature the lithium chloride will draw water from the atmosphere providing the R.H. is greater than about 10%. Consequently the electrical resistance between the two silver wires is very small (under 1 ohm) and a large current, limited by the ballast lamp, will flow between the two wires warming up the hygrometer. When the temperature of the hygrometer exceeds its equilibrium temperature (the dewpoint of lithium chloride) water will be evaporated from the glass tape, thus cutting off the current. Eventually the hygrometer will regulate itself at this equilibrium temperature. The dewpoint of the air surrounding the hygrometer is then determined from Fig.6. Clearly the instrument will not operate when the hygrometer temperature is below air temperature; the minimum measurable relative humidity is shown in Fig.7.

---

*Footnote. From Table 1, with an air temperature of 50°F. this corresponds to a R.H. of between 100% and 30%.

4. Comparison with an Assmann psychrometer

The instrument was first set up in September 1954 and has run without attention for over a year. From March to September 1955 simultaneous observations of dewpoint have been made with an Assmann psychrometer, the electrical hygrometer and the thermometers in a large Stevenson screen; wind and cloud cover were noted at the time of observation. The most notable operational features of this investigation were the great reliability of the electrical hygrometer and the simplicity of an observation below the freezing point. On these occasions it would take as much as half an hour to get a satisfactory reading of the screen ice bulb. No difficulty was experienced with the Assmann psychrometer in these conditions. During the period the screen muslin was changed weekly and the psychrometer observations were computed using a M.O. humidity slide rule. Hygrometer observations were converted to dewpoint using the curve shown in Fig.6, readings from which are tabulated in Table 1. Exposed stem corrections have been applied to all readings of the hygrometer. Fig.6 also shows the experimental result of Conover, a hygrometer calibration derived from the International Critical Tables and figures based on a determination of the vapour pressure over saturated lithium chloride by Wexler and Hasegawa (1954). The roof site at Harrow used for the experiment is shown in Fig.8.

Table 1

Hygrometer temperature °F.	52.5	66.0	79.5	92.9	106.0	119.8	133.9	148.5	163.8	179.8
Dewpoint °F.	0	10	20	30	40	50	60	70	80	90

5. Analysis and presentation of observations

The results are expressed as the difference between the hygrometer dewpoint and Assmann dewpoint, or the difference between the screen and Assmann psychrometer. The presentation used in Figs.9-14 is the integral distribution curve of the hygrometer and screen errors, the ordinate showing the percentage of observations whose error is less than or equal to the value of the abscissa. The mean of the errors considered is marked on these graphs.

In addition to the overall behaviour of the instruments shown in Fig.9 the observations are split into the groups shown in Table 2 to examine the effects of radiation, wind and relative humidity.

/Table 2

Table 2

Effect	Groups compared	No. of obs.	Fig.
(i) Radiation	Days with $\geq$ 6/8 Cloud Days with $\leq$ 2/8 Cloud	130 50	10,11
(ii) Wind	Wind $\leq$ 5 kt. 5 $<$ Wind $\leq$ 10 kt. Wind $>$ 10 kt.	40 50 40	12,13
(iii) Relative humidity	50° $\leq$ (Hygrometer-Air) $<$ 60°F. 60° $\leq$ (Hygrometer-Air) $<$ 70°F.	40 60	14

We will now consider the significance of these curves.

(i) All observations

In Fig.9, the electrical hygrometer can be seen to have an overall scatter similar to the screen, but the scatter of negative errors is greater than for the screen, which shows a fairly sharp cut off. A surprising feature of the screen observations is the mean error of + 1.0°F. which could be due to an error in the psychrometer constants used. This error has been investigated by four stations, two in the south of England and two in Scotland, and shows that the error and scatter are in some way connected with poor exposure.

(ii) Effect of radiation

This is the most serious effect on the instrument, the difference between the means of cloudy and clear days being 1.4°F. compared with 0.4°F. for the screen. As no attempt has been made to protect the wind shield from radiation it should be possible to reduce this error to about 0.5°F.

(iii) Effect of wind

The deterioration in the performance of a screen due to insufficient ventilation can be seen in Fig.13 but no systematic change in the performance of the hygrometer with wind speed, measured about 30 ft. above the screen, can be detected in Fig.12. On the other hand an unshielded instrument shows a marked variation in calibration with wind speed. This effect has been examined in a wind tunnel for transverse air flow over the hygrometer and the results are presented in Fig.15.

(iv) Variation with relative humidity

This is due to the changes in the rate of loss in heat caused by variations in the difference between the hygrometer temperature and air temperature. The magnitude of the effect is small but clearly detectable in Fig.14*.

A similar effect must exist in a screen due to the exposed stem and conduction errors but is partially compensated by the value used for the psychrometric constant.

6. Conclusions

This electrical hygrometer has been shown to be capable of a higher accuracy in the measurement of dewpoint than the ±3°F. claimed by Conover. The errors have been examined to show up the effect of radiation, relative humidity and wind. Radiation is shown to have an effect on the reading. As no attempt has been made to protect the shield against radiation a significant reduction in this error should be possible.

---

*An electrical hygrometer temperature - air temperature difference of 70°F. corresponds to a relative humidity of about 100%; and 50°F. to about 50% R.H., at an air temperature of about 70°F.

The electrical hygrometer is ideally suited for the continuous recording of dewpoint. Air temperature and dewpoint can be recorded on the same scale with similar thermometers, providing the hygrometer thermometer is fitted with fixed shunt and series resistors. Using a platinum resistance thermometer this device may be used over a range of dewpoints from -20°F. to +70°F. with a maximum correction of about 2°F.

REFERENCES

Conover, John H. Tests and adaptation of the Foxboro Dew Point Recorder for Weather Observatory use. Bull.Amer.Met.Soc., Milton, Mass., Vol.31, No.1, pp.13-21. (Jan. 1950).

Findeisen,W. Uber ein neues elektrisches Feuchtigkeitmessverfahren. Erfahrb. D. Flugw. Sonderbd.4, pp.49-61. (1935).

Wexler, A. and Hasegawa, S. Relative humidity temperature relationship of some saturated salt solutions. Jour. Res. N.B.S., Vol. 53, No.1, pp.19-25. (July 1954).

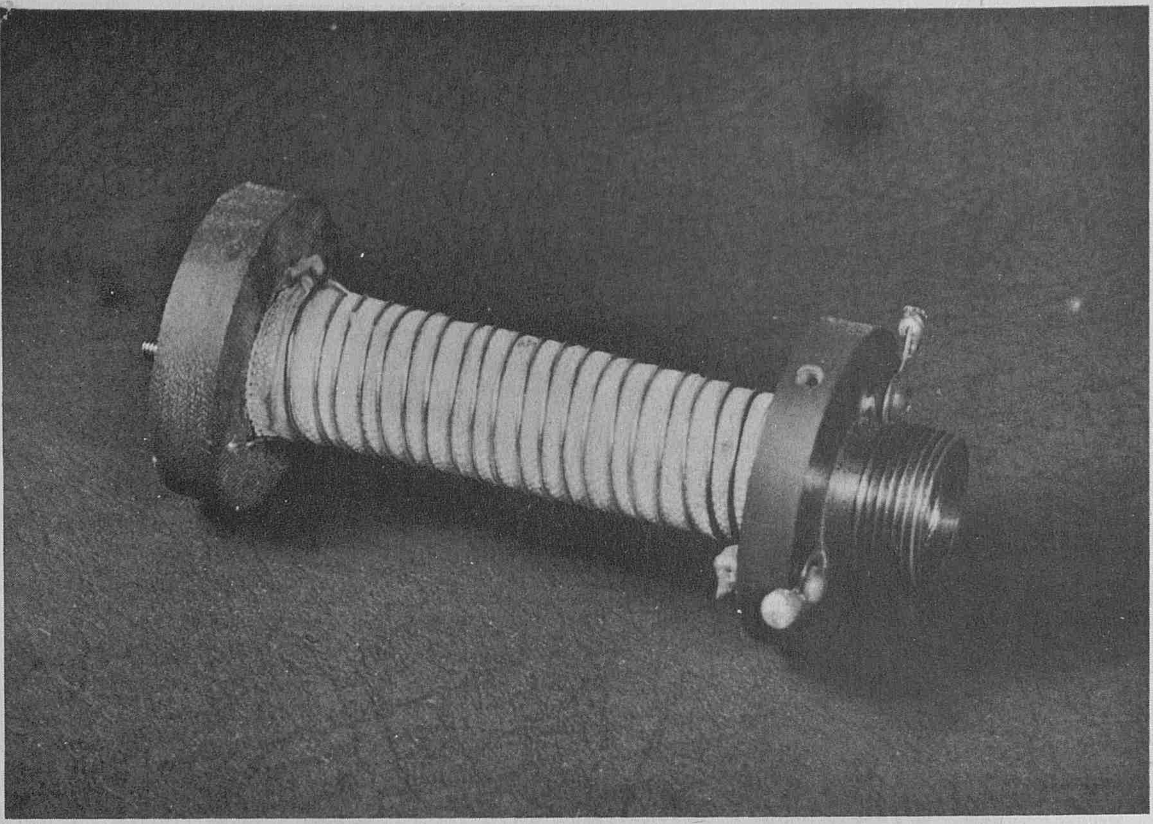

Fig. 1. THE HYGROMETER ELEMENT.

ELECTRICAL HYGROMETER CIRCUIT

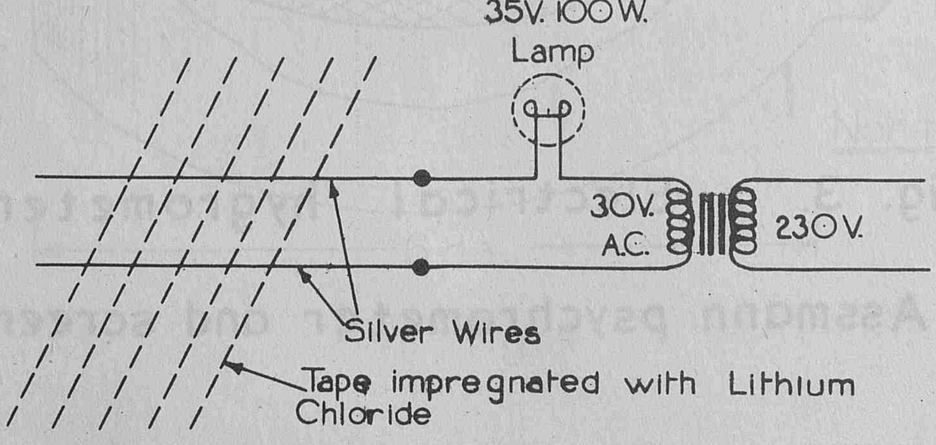
35V. 100 W.
Lamp
30V.
A.C.
230 V.
Silver Wires
Tape impregnated with Lithium Chloride

Fig. 2.

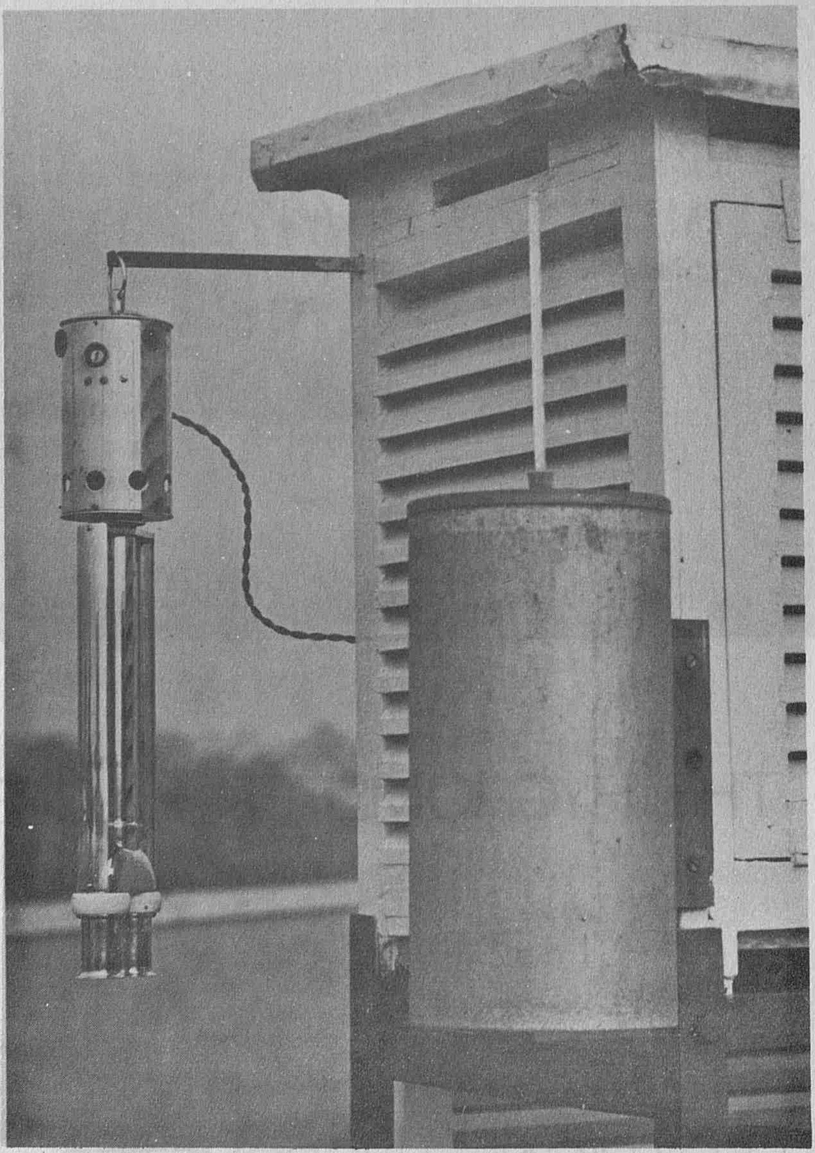

Fig. 3. Electrical hygrometer, Assmann psychrometer and screen.

THE HYGROMETER SHIELD

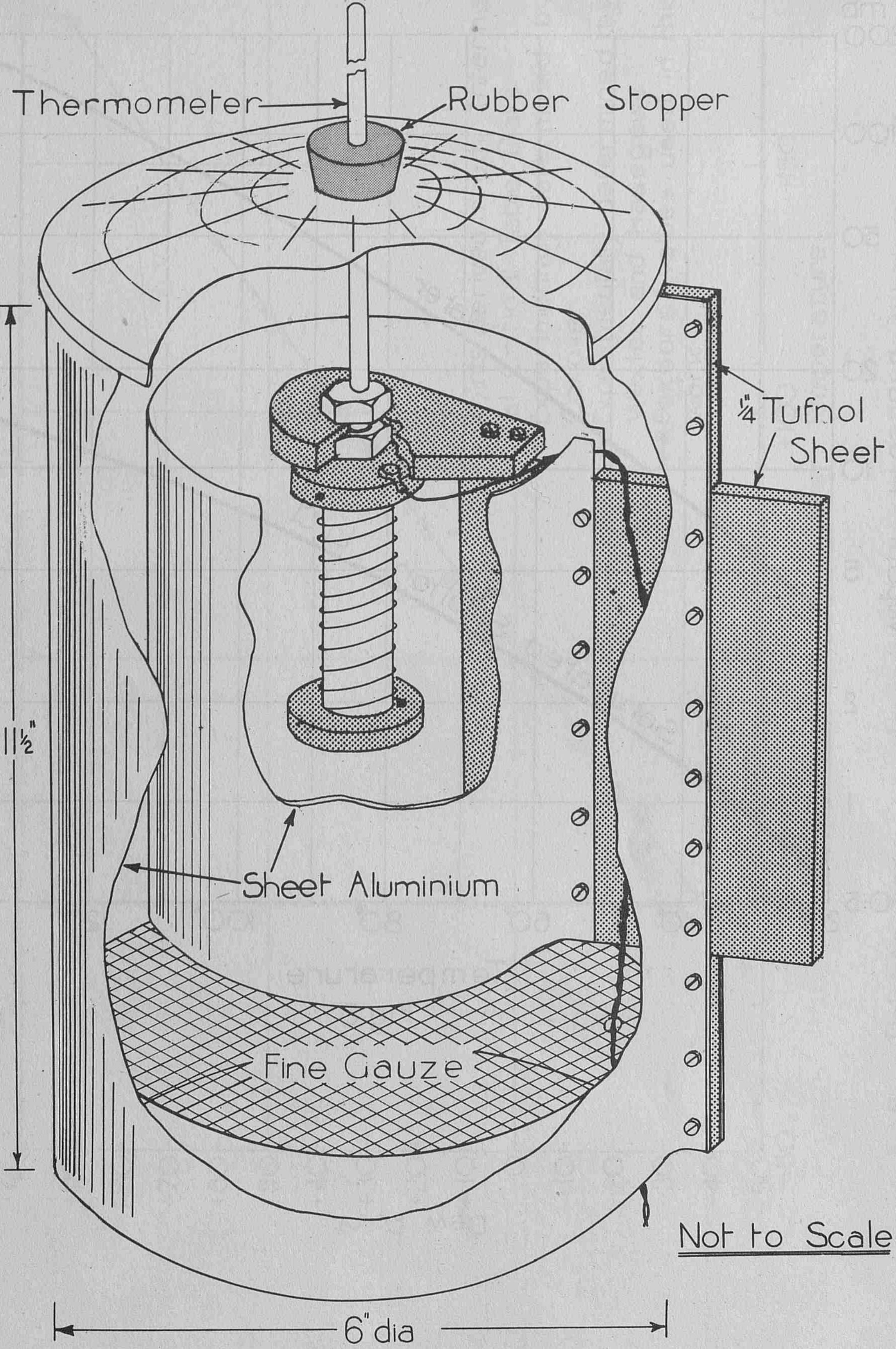
Thermometer
Rubber Stopper
¼" Tufnol Sheet
11½"
Sheet Aluminium
Fine Gauze
Not to Scale
6" dia

Fig 4

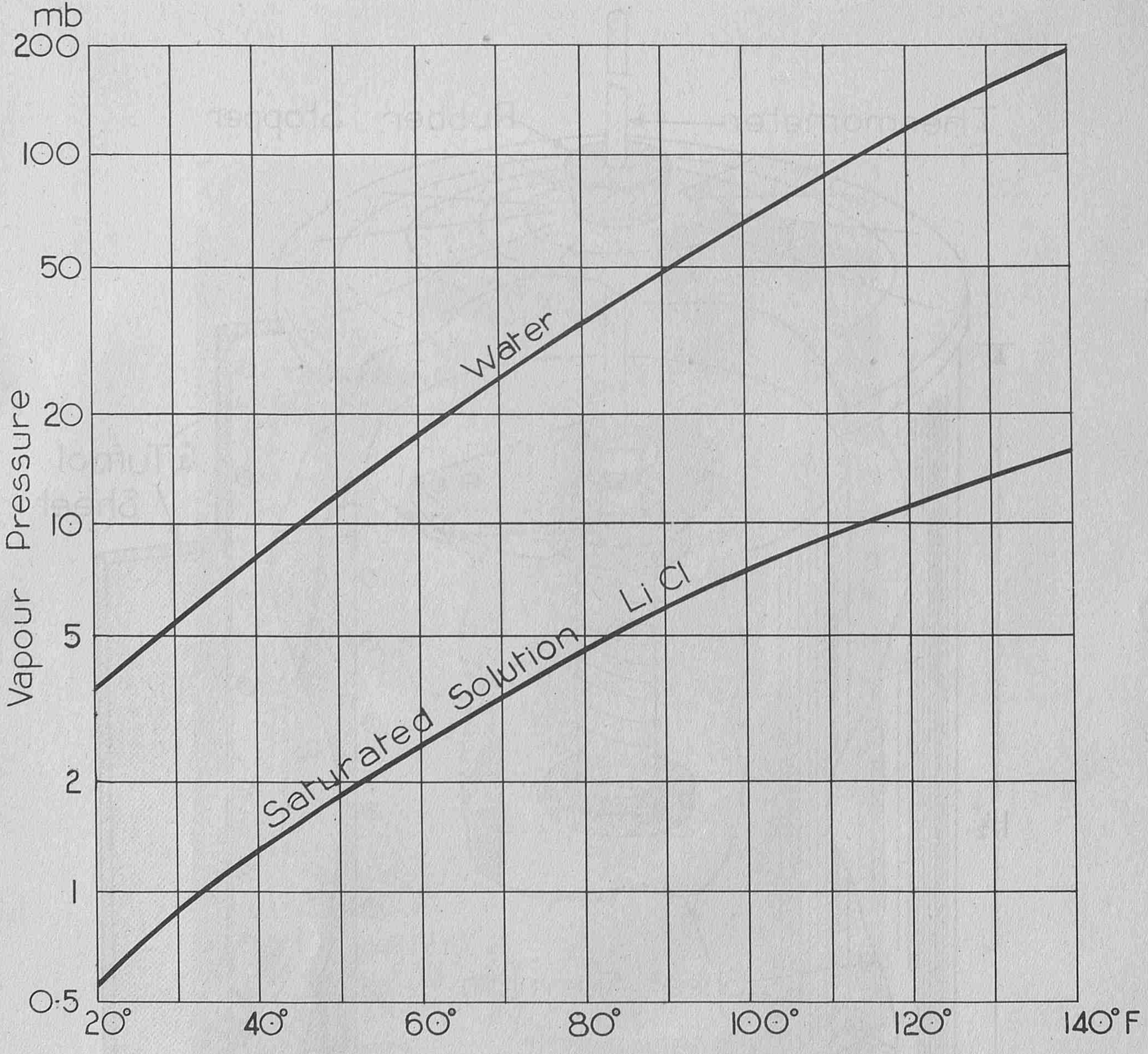
mb
200
100
50
20
10
5
2
1
0·5
Vapour Pressure
Water
Saturated Solution Li Cl
20°
40°
60°
80°
100°
120°
140°F
Temperature

Fig 5

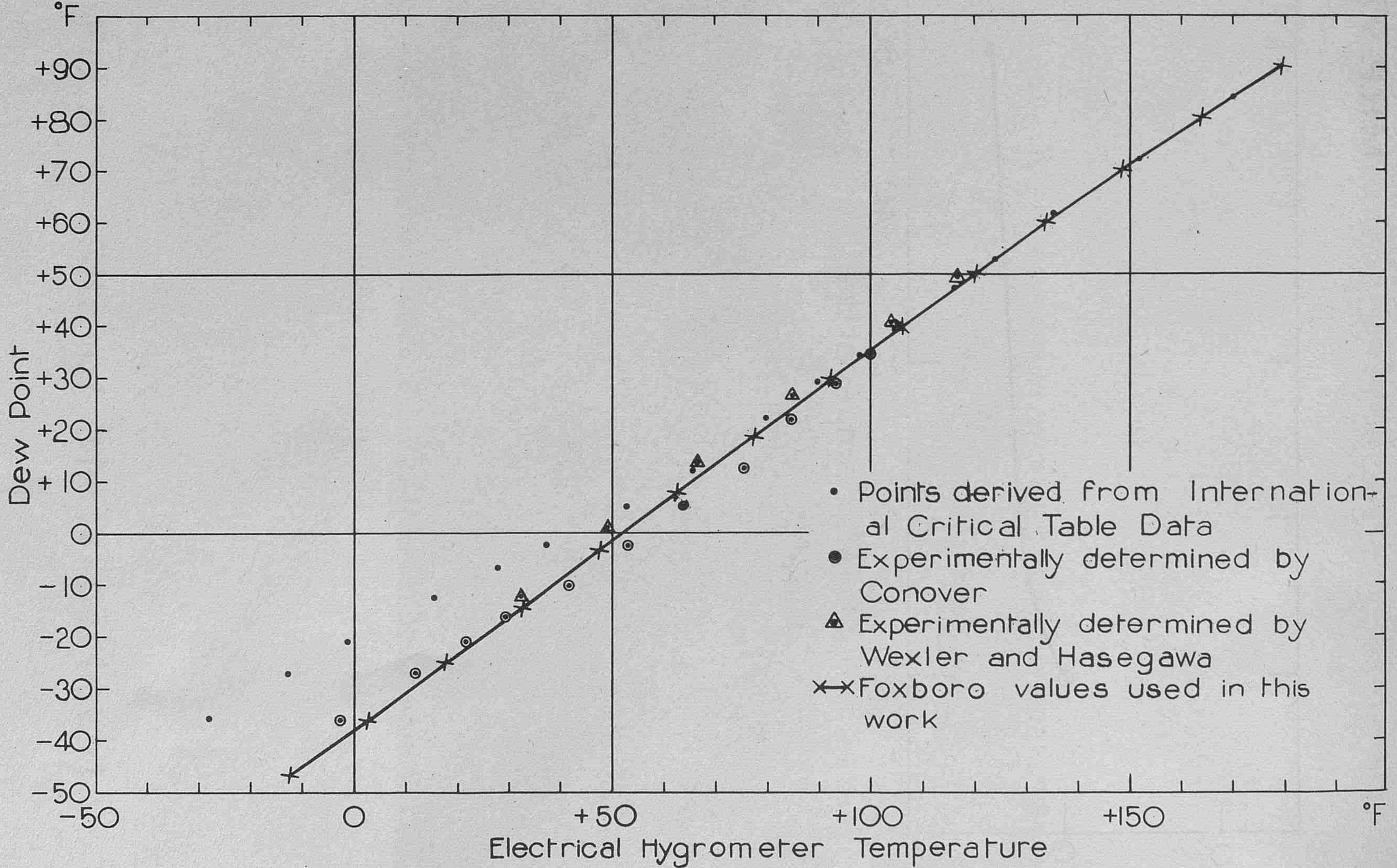

Fig 6 Relation between electrical hygrometer equilibrium temperature and dew point of surrounding air

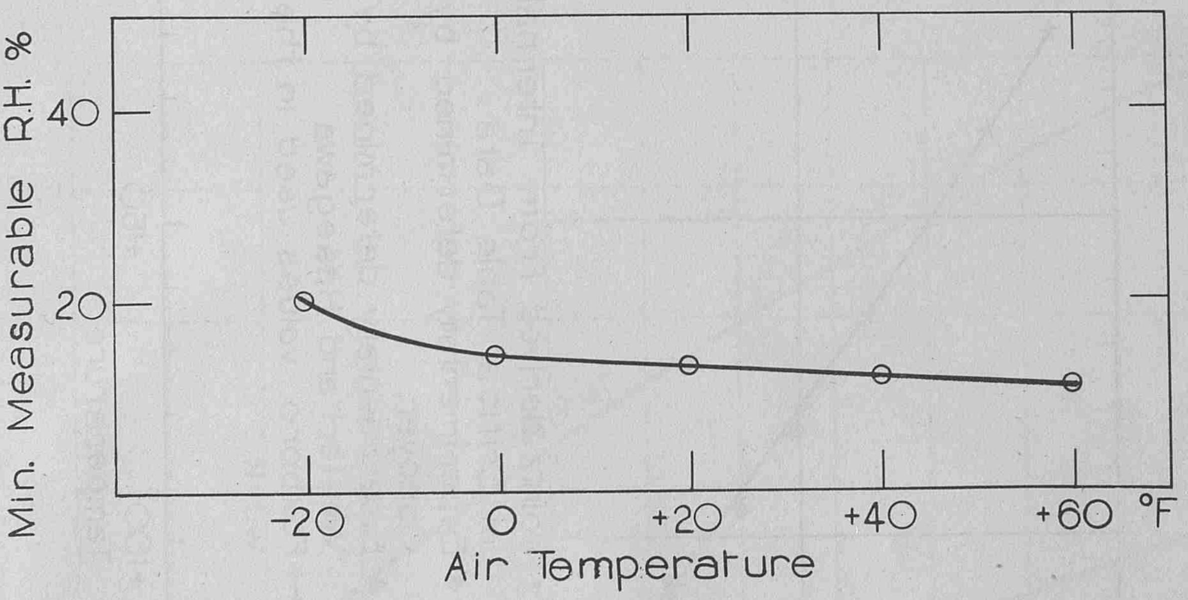

Fig 7.

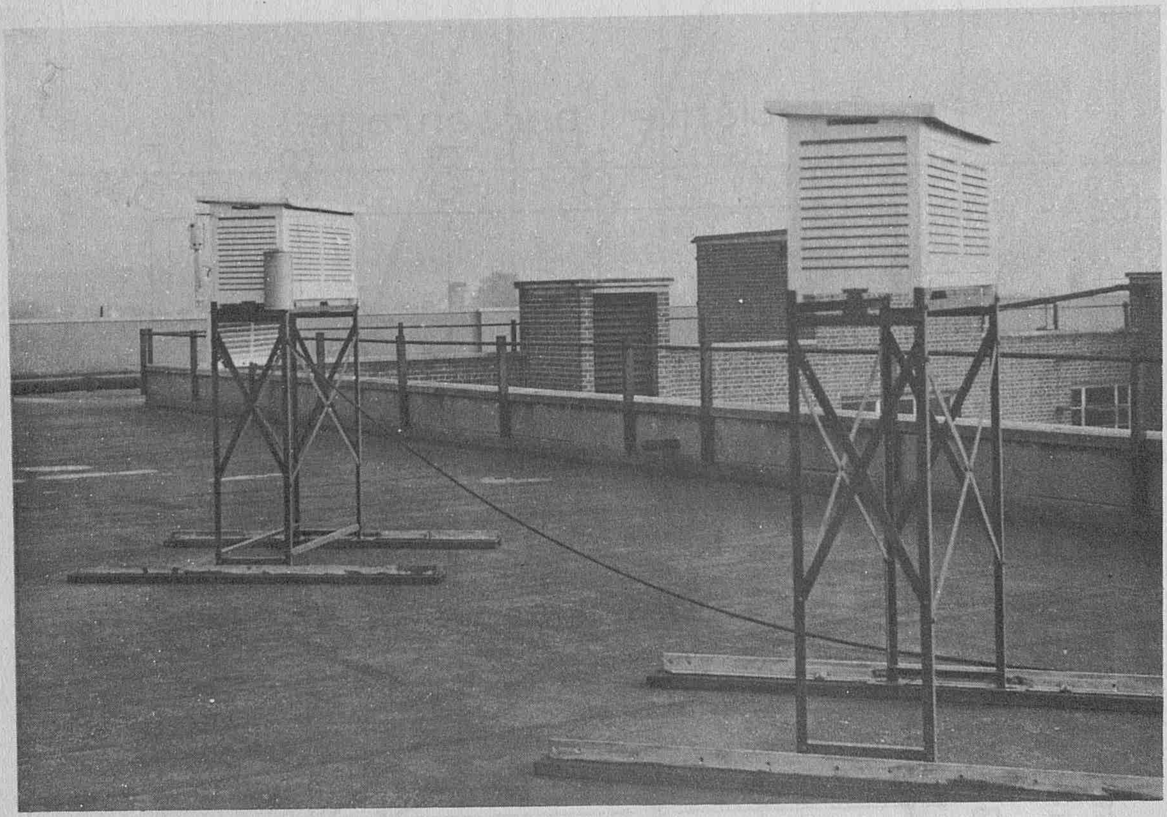

Fig. 8 Site of the experiment.

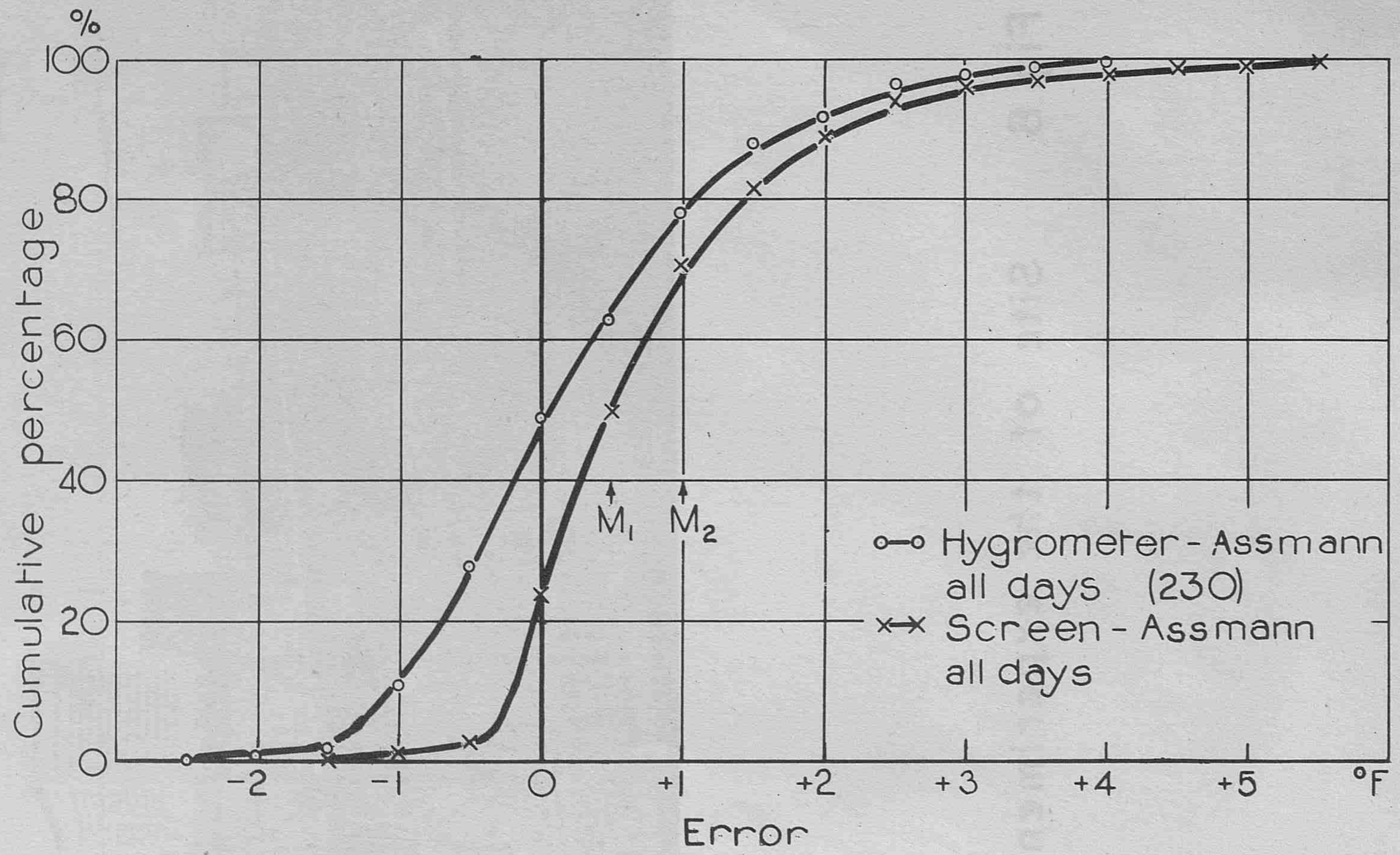

Means: Hygrometer - Assmann = M_1 = +0·5 °F
Screen - Assmann = M_2 = +1·0°F

Fig 9

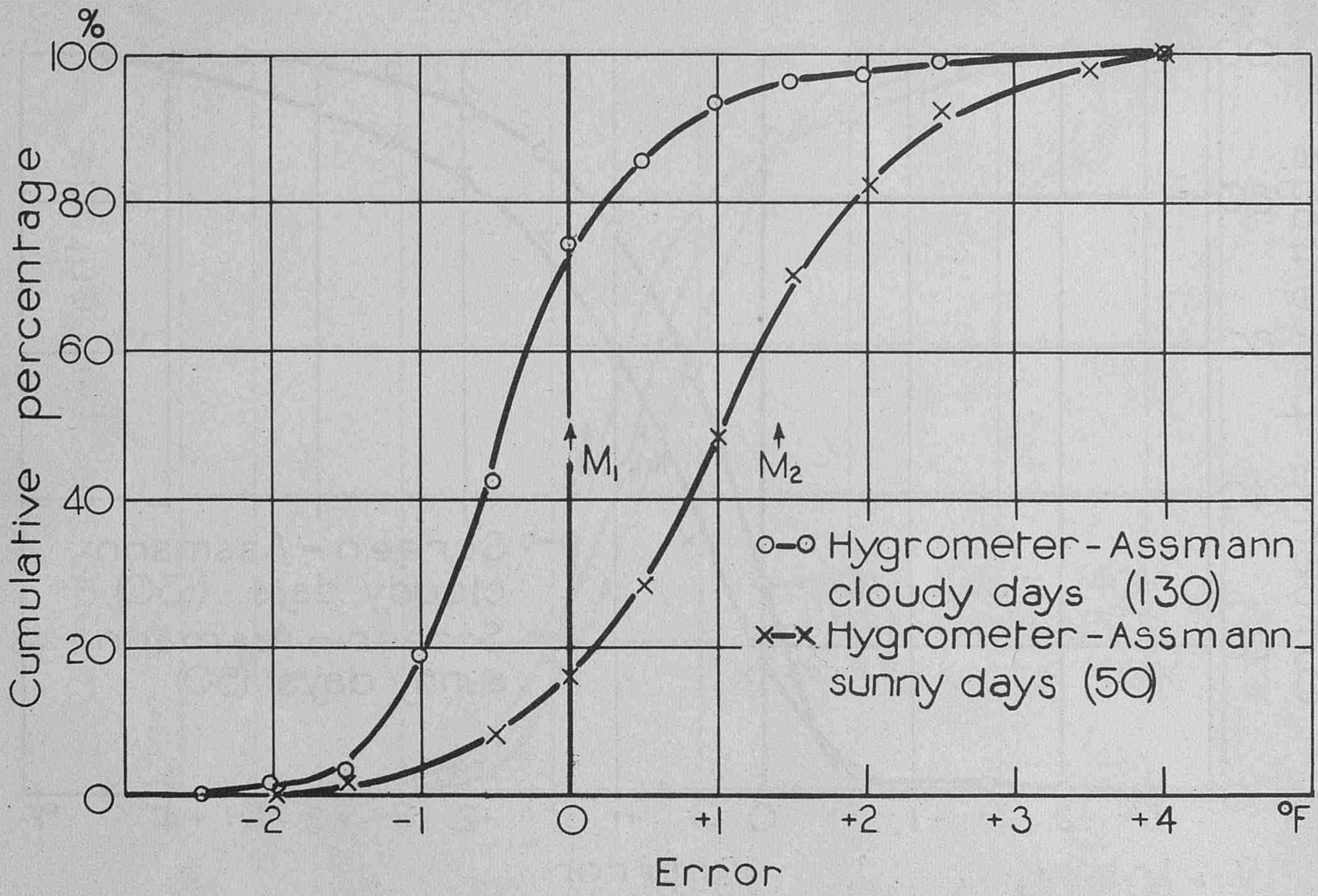

Means: Cloudy days = M_1 = + 0·0 °F
Sunny days = M_2 = + 1·4 °F

Fig 10

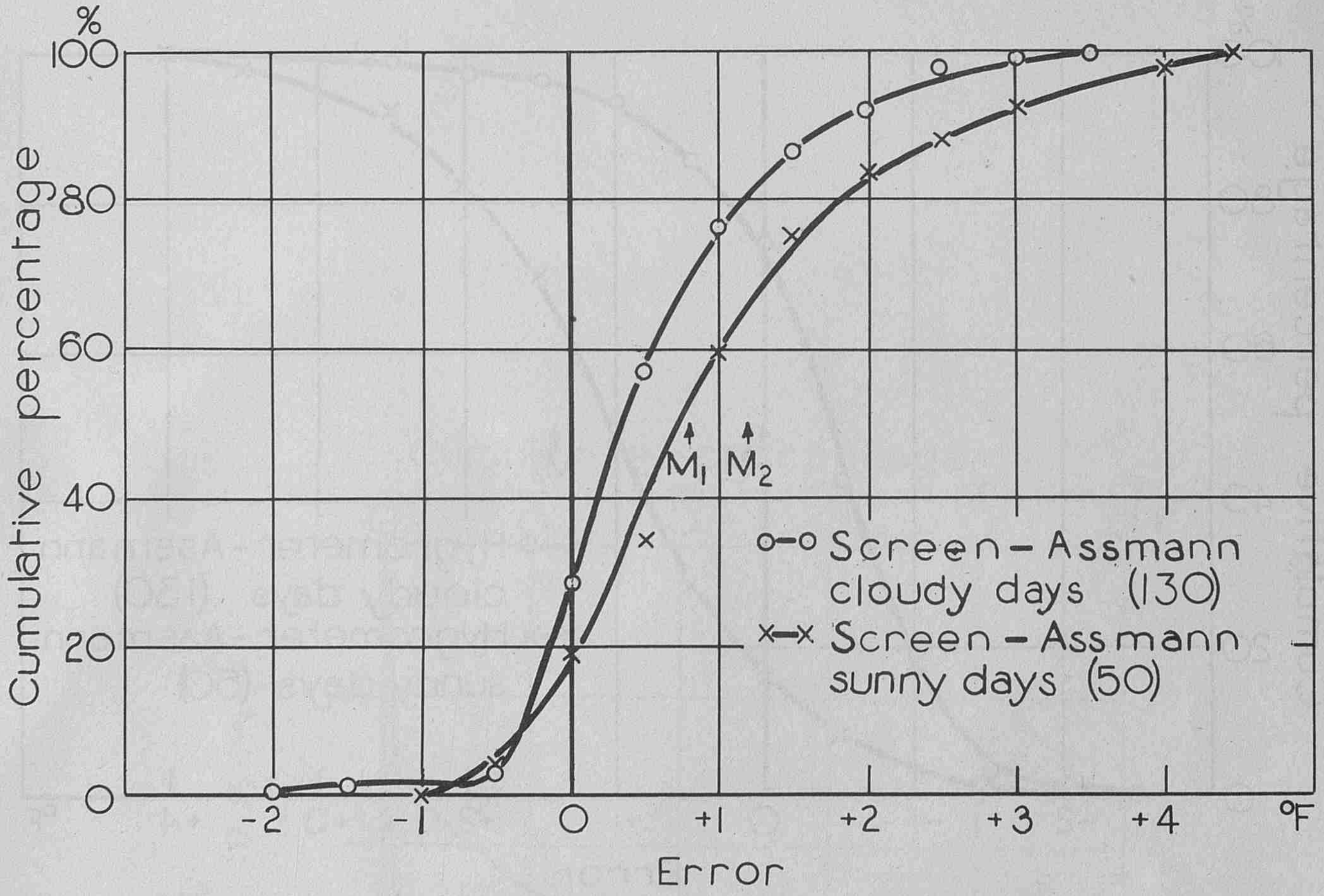

Means: Cloudy days = M_1 = + 0·8 °F
Sunny days = M_2 = +1·2 °F

Fig 11

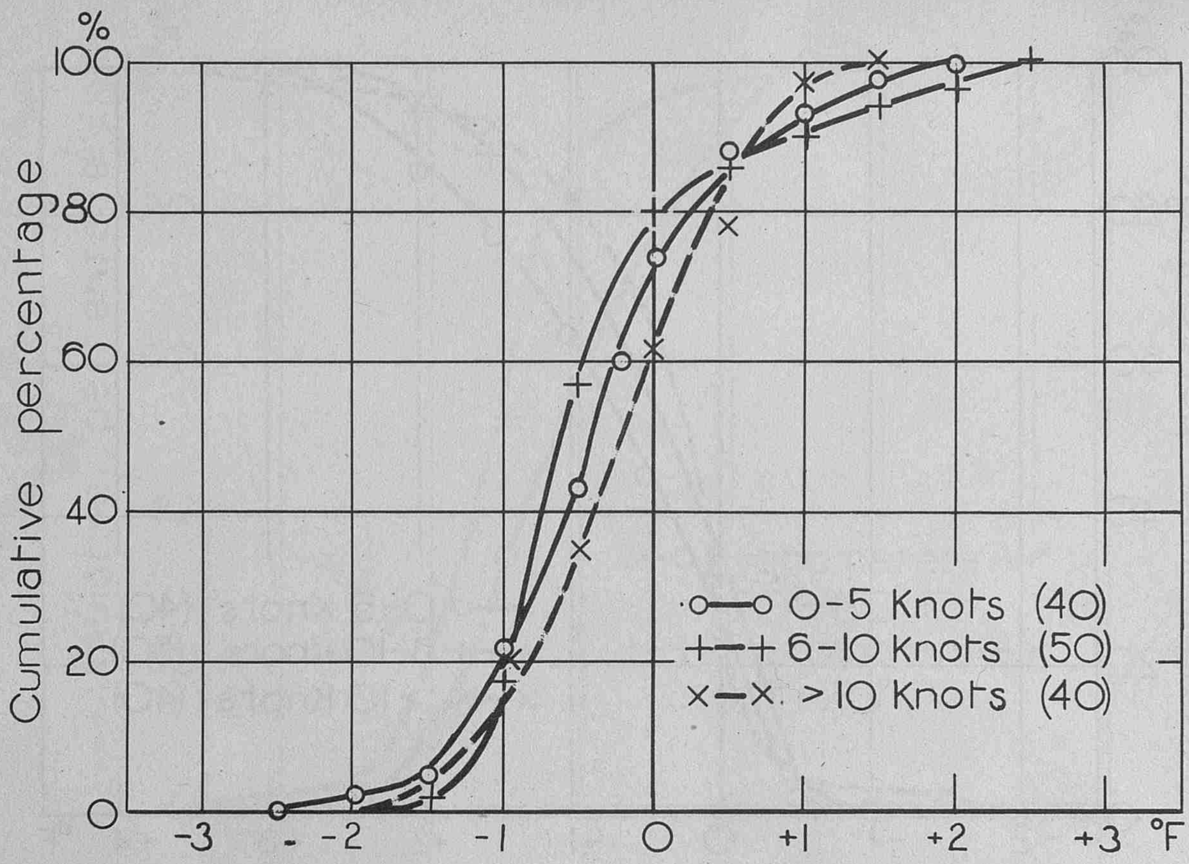

Error
Hygrometer v Assmann
Cloudy days

Fig 12

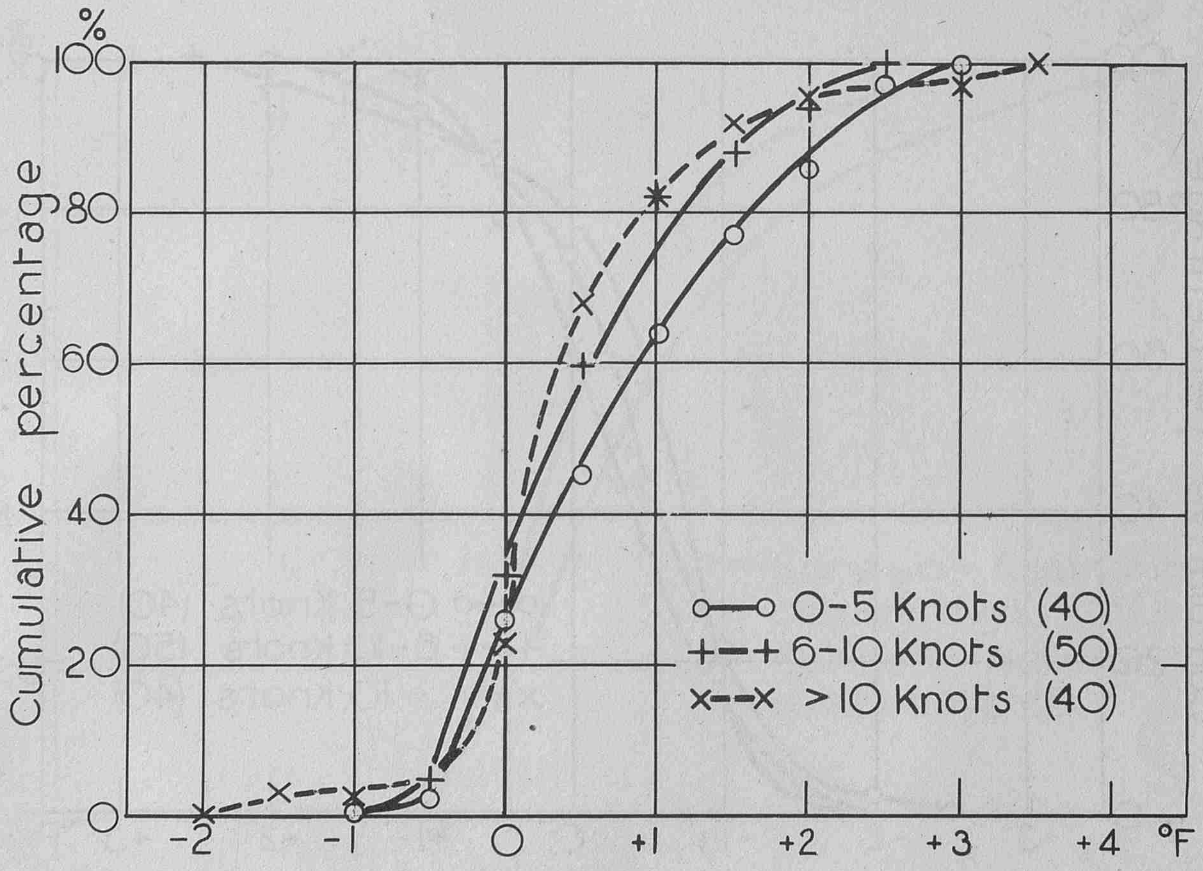

Error
Screen v Assmann
Cloudy days

Fig 13

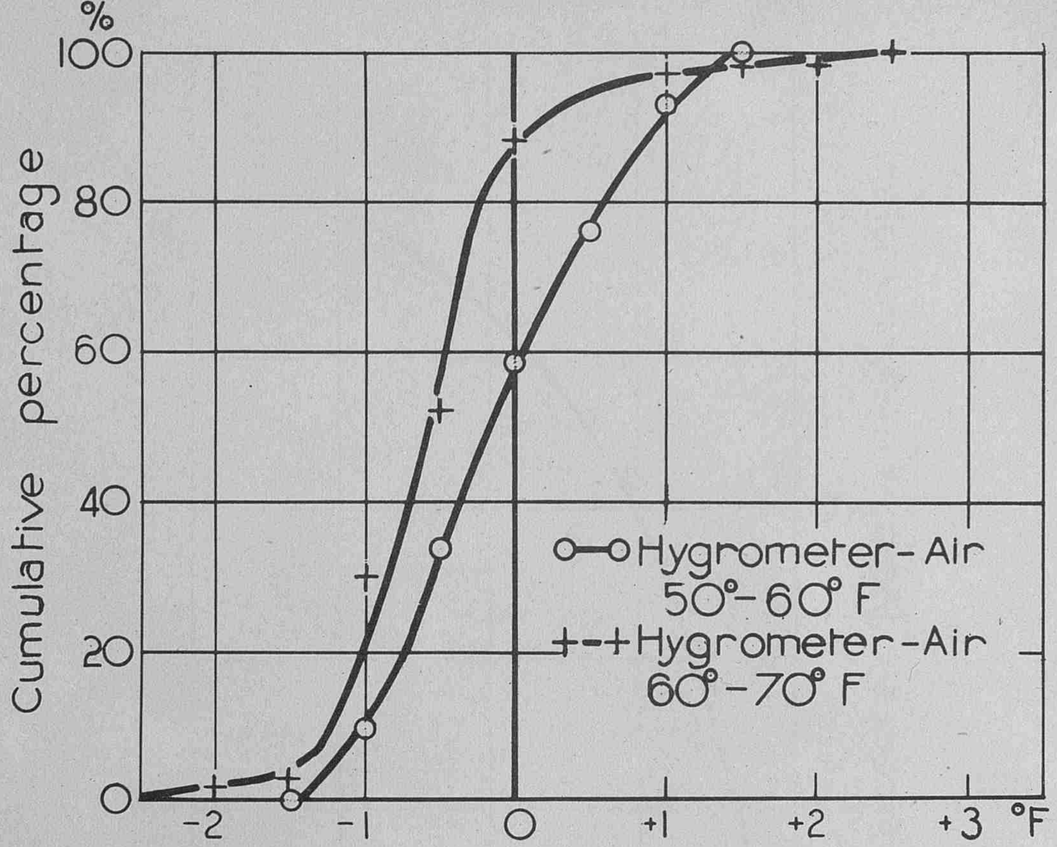

Error

Cloudy days

Fig 14

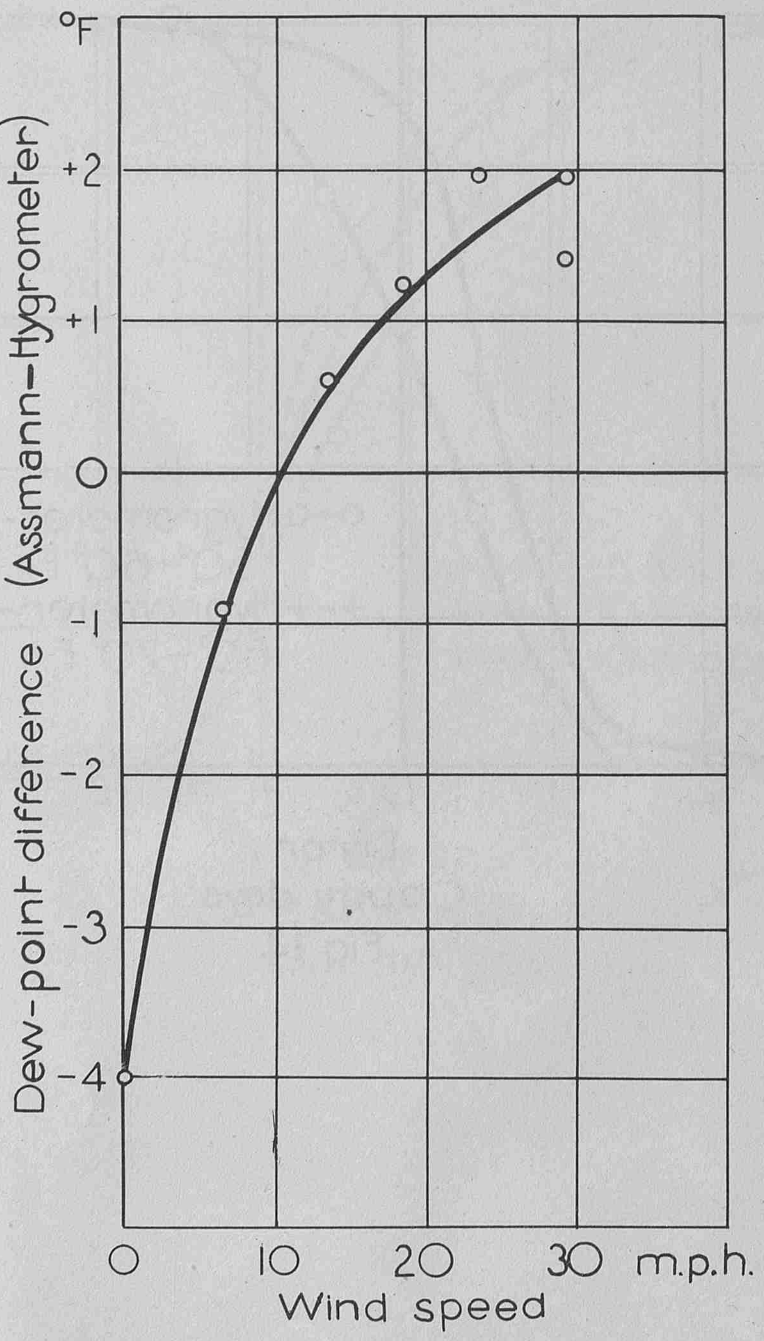

Fig 15. Effect of a steady wind on the Electrical Hygrometer.

AIR WEATHER SERVICE
TECHNICAL [illegible] FILES

M.R.P. 978
S.C. 11/209
30th April, 1956.

AD 223126

Long-period averages for the upper air.

by

J. K. Bannon.

(Meteorological Office)

AWSSS
ROUTING SLIP

FILE	INFO	ACTION				
			DIRECTOR			
			DEP DIRECTOR			
	1		ASST TO DIRECTOR			
	2		CONSULTANTS			
	4		TRSD			
				✓	SS R.	LHC. ean
				✓	RRB Mits JBA	
				✓	TDB VSB	
					SEC	
	3		FDO		IF	
					LFB	AK
					STB SJK R	
					STB	
					CU	
					SEC	
	5		TIPD		CHF	
					PUE	
					TECH INFO	
					SEC	

send to CL

AIR MINISTRY

METEOROLOGICAL RESEARCH COMMITTEE

At the time of issue this report has not been published. Any author desiring to quote this paper should refer to it as "A paper of the Meteorological Research Committee (London).
M.R.P. 978 by Mr. J.K. Bannon.
A copy is available in the Library of the Meteorological Office".

M.R.P.978
S.C.II/209
30th April, 1956

AIR MINISTRY

METEOROLOGICAL RESEARCH COMMITTEE

Long-period averages for the upper air

by

J.K. Bannon (Meteorological Office)

Summary

Average monthly pressures of the tropopause at Larkhill and Lerwick for 1942-1953 show an erratic variation from month to month, anomalous values occurring in months when the average sea-level pressures differ from the averages for the period 1900-1939. The average tropopause pressures are adjusted, by a simple regression method, to be in keeping with the average sea-level pressures for 1900-1939 and the upper air temperatures are also adjusted correspondingly. The resulting figures have a more regular variation through the year than the averages for 1942-1953.

1. Introduction

This study stems from an attempt to discover the seasonal variation of the tropopause over the British Isles. For this purpose the average pressure of the tropopause was computed for each month of the year for Larkhill and Lerwick for the 12-year period 1942-1953 inclusive. These are shown in Figure 1, together with the greatest and least monthly means observed in the period. It is seen from this Figure that the variation from month to month is irregular, especially in spring, and this suggested that the period of observations was not sufficiently long to yield reliable averages. The annual variation of the average monthly tropopause pressure in Canada (1,2) appears to be more regular though Moore's figures for Hanover (1) for the period 1948-1952 also show irregularities in the spring.

There is a rough relation between the height (or pressure) of the tropopause and the general character of the weather. The pressure of the tropopause is high in unsettled weather with low surface pressure and low temperatures in the troposphere and vice versa in anti-cyclonic weather (3).

The average monthly sea-level pressures for the points 60°N., 0°W., 50°N., 0°W. (as representing Lerwick and Larkhill respectively) for the period 1942-1953 were therefore compared with similar values for the period 1900-1939(4). To do this daily values for these two points were extracted from the Daily Weather Report for the years 1942-1948*. For the remaining years 1949-1953 the values were taken from Die Grosswetterlagen Mitteleuropas(5). The comparison is shown in Table I and it is seen that the average pressures for some months for the 12-year period differ considerably from those for the longer period and further that the months which show abnormally high pressure at the tropopause at Lerwick (Figure 1) also show a low surface pressure compared with the long-term values, and vice versa; this feature is not so well marked for Larkhill. It seems clear therefore that some or perhaps all of the irregularities in the average curves in Figure 1 are not representative of true long-term mean effects but arise because the period of observation is comparatively short.

/Adjustments

---

* Daily values were also extracted for other points at 60°N., and 50°N. at 10-degree intervals from 10°E. to 80°W. inclusive, for the same period.

Adjustments are therefore here suggested to the average monthly pressures of the tropopause at Larkhill and Lerwick so that these pressures are more in keeping with the corresponding average surface pressures for the period 1900-1939. Adjustments are also suggested to the average monthly temperatures at the tropopause and at standard levels, so that they are in keeping with these amended tropopause pressures.

2. Adjusted monthly averages of tropopause pressure

Dines (3) has shown that the height of the tropopause and surface pressure are related, correlation coefficient 0.68. This result was obtained by analysing ballon-sonde data from many stations in Europe for all seasons. The relation between monthly mean values of sea-level pressure and tropopause pressure at Larkhill and Lerwick is slightly closer. The Table II gives values of the correlation coefficients between these two variables for the mid-season months evaluated from the data for 1942-1953. The mean sea-level pressures at 50°N., 0°W., and 60°N., 0°W., were used for the mean pressures at Larkhill (51°N., 2°W.), and Lerwick (60°N., 1°W.) respectively. Each coefficient in Table II was evaluated from only twelve pairs of values and there does not appear to be any significant seasonal variation in the coefficients since the extremes at the two stations occur in different months. Accordingly the mean values of the coefficients were used in the following computations.

The average tropopause pressures were adjusted to correspond to the average sea-level pressures for the period 1900-1939 by simple regression equations using the data for 1942-1953 to evaluate the standard deviations and taking the mean values of the correlation coefficients (Table II) as described above. It was found that the standard deviation of mean tropopause pressure, as computed, varied erratically from month to month, a result which was to be expected as the number of observations from which each standard deviation was computed was small (12). These standard deviations were therefore smoothed graphically, conforming to a regular variation from a maximum in the late winter or early spring to a minimum in mid-summer, as indicated by the crude values. The amount of smoothing is shown in Figure 2. The standard deviations of monthly sea-level pressures did not vary in so erratic a manner as those for tropopause pressure and the crude values were used.

The adjusted average monthly pressures and the averages for 1942-1953 are given in Tables III and IV and are also shown in Figures 3 and 4. The other figures in these tables will now be described.

3. Adjusted monthly averages of temperature

The pressure of the tropopause and the temperatures in the troposphere and lower stratosphere are related (3,6). The monthly means of the same quantities are also related and the mean temperature at the tropopause and the mean pressure of the tropopause are also associated. Table V shows average values of the correlation coefficients for Larkhill and Lerwick evaluated from the data for 1942-1953. As with the association between mean surface pressures and mean tropopause pressures there did not appear to be a significant seasonal variation in the coefficients and average values were used.

By means of simple regression equations the average temperatures at the levels 100, 200, 300, 500 mb. and the tropopause were adjusted to be in keeping with the adjusted tropopause pressures described in Section 2. Adjustments for the level 150 mb. were also made by direct interpolation. Since mean lapse rates in the troposphere are remarkably constant the same adjustments were made to the temperatures for 700 mb. as for 500 mb. The results are given in Tables III and IV, together with the averages for the period 1942-1953; some of the results are also shown in Figures 3 and 4. The adjusted values are given to the nearest degree Fahrenheit. The averages for the period 1942-1953 are given to the nearest 0.1°F. Radiation and lag corrections were not applied to the observations from which both these sets of averages were computed and the average temperatures at 100 mb. are therefore too high by amounts varying between about 2° and 3°F. depending on the season (7). Errors at lower levels are smaller.

It may be argued that the "corrected" long period average temperatures in Tables III and IV should have been computed directly from the relation between mean temperature and mean sea-level pressure. It was felt however that the method of computation described above produces a more consistent set of temperatures. The main connection between surface pressure and the tropopause is the association of low surface pressure with subsidence at tropopause level and vice versa. Having found the "correction" for the tropopause it seemed best to apply a similar type of correction to the temperatures at the other levels. Test computations of "corrections" to the temperature at 100 mb. directly from the sea-level mean pressures gave for Larkhill larger differences than shown by A-B in Table III (about double) so that the resulting average temperatures after "correction" appear irregular. Similar computations for Lerwick were impossible for winter and some spring months as the correlation coefficients between monthly mean temperatures at 100 mb. and monthly mean sea-level pressures were then very small.

4. Conclusions

The differences A-B in Tables III and IV are not large. Figures 3 and 4 show however that the estimated average values for the period 1900-1939 vary from month to month in a more regular manner than the averages for the period 1942-1953; this is more noticeable at Lerwick than at Larkhill. The method of estimating the averages for the long period is perhaps open to criticism, as any such estimation must be; however the self-consistency of the results gives some confidence in their reality.

If these results are accepted they demonstrate that upper air data for a few years are inadequate to provide a representative average. This is well known for meteorological data for the earth's surface. The results also show that in climatological studies of average values of upper air parameters it is advisable to analyse all the data for the same definite period of years; data for one short period of years may not be comparable with data for a different period.

REFERENCES

1. Moore, J.G. Average pressure and temperature of the tropopause. Meteorological Research Papers, Air Ministry, London, No. 874, 1954.

2. Kochanski, A. Cross-sections of the mean zonal flow and temperature along 80°W. J. of Met., 12, 1955, p.95.

3. Dines, W.H. The characteristics of the free atmosphere. Geophys. Mem., Met. Off., 2, No.13, 1919.

4. Normalwerte des Luftdruckes auf der Nordhemisphäre für die Periode 1900-1939. Inst. für Met. und Geophysik der Frein Un. Berlin, Met. Abhand., Band III, Heft. 1, 1953.

5. Die Grosswetterlagen Mitteleuropas. Deutscher Wetterdienst, Bad Kissingen.

6. Bannon, J.K. and Gilchrist, A. Variation of temperature in the troposphere and lower stratosphere. Quart. J. Roy. Met. Soc., 82, 1956, p.58.

7. Scrase, F.J. Radiation and lag errors of the Meteorological Office radio sonde and the diurnal variation of upper air temperature. Quart. J. Roy. Met. Soc., 80, 1954, p.565.

Table I

Mean sea-level pressures: (mb.-1000)

Period	Jan.	Feb.	March	April	May	June	July	Aug.	Sept.	Oct.	Nov.	Dec.
					50°N. 0°W.							
1942-53	16	18	18	16	16	17	17	15	16	17	15	16
1900-39	17	16	14	13	16	17	16	16	18	14	14	14
					60°N. 0°W.							
1942-53	7	9	14	8	16	12	12	10	9	11	8	6
1900-39	7	8	9	11	13	14	12	11	12	9	8	7

Table II

Correlation coefficients between monthly mean values of sea-level pressure and tropopause pressure. (From data for 1942-53)

	January	April	July	October	Mean
Larkhill	-0.91	-0.88	-0.63	-0.71	-0.78
Lerwick	-0.75	-0.59	-0.80	-0.88	-0.75

Table V

Average correlation coefficients between mean monthly values of pressure at the tropopause and temperature at

	100 mb.	200 mb.	tropopause	300 mb.	500 mb.
Larkhill	0.60	0.80	0.70	-0.70	-0.80
Lerwick	0.75	0.80	0.75	-0.60	-0.75

(computed from data for 1942-53)

Table III

Monthly average temperatures in the upper air and average tropopause pressures: observed 1942-53 (A) and estimated 1900-39(B). Larkhill

		Jan.	Feb.	March	April	May	June	July	Aug.	Sept.	Oct.	Nov.	Dec.
							°F.						
100 mb.	A	-71.4	-71.4	-69.0	-65.8	-60.7	-59.8	-59.5	-59.4	-66.1	-71.8	-75.4	-73.6
	B	-72	-71	-67	-64	-61	-60	-59	-60	-67	-71	-75	-73
150 mb.	A	-69.9	-69.7	-68.7	-63.8	-61.0	-60.3	-59.6	-60.0	-66.6	-71.0	-72.8	-70.9
	B	-70	-69	-67	-62	-61	-60	-59	-61	-68	-69	-72	-70
200 mb.	A	-72.3	-72.5	-73.9	-67.7	-64.7	-62.8	-60.6	-59.8	-64.2	-68.3	-70.9	-72.8
	B	-73	-71	-72	-66	-65	-63	-60	-61	-65	-66	-70	-72
Tropopause Pressure (mb.)	A	237	239	227	240	241	229	224	227	221	222	231	236
	B	235	243	236	249	241	229	228	224	215	231	234	240
Tropopause Temperature	A	-75.8	-76.1	-76.9	-72.3	-69.1	-67.1	-64.6	-64.0	-68.2	-71.2	-73.7	-75.6
	B	-76	-75	-75	-71	-69	-67	-64	-65	-69	-70	-73	-75
300 mb.	A	-56.4	-57.6	-55.8	-52.2	-50.1	-44.3	-40.5	-41.3	-42.4	-46.8	-51.5	-55.7
	B	-56	-58	-57	-53	-50	-44	-41	-41	-42	-47	-52	-56
500 mb.	A	-12.5	-12.8	- 8.6	- 7.3	- 4.0	2.3	6.5	5.9	4.2	- 0.3	- 6.2	-10.3
	B	-12	-13	-10	- 9	- 4	2	6	6	5	- 1	- 7	-11
700 mb.	A	16.5	16.4	20.3	21.7	25.7	30.5	34.0	33.0	31.7	28.3	22.0	18.8
	B	17	16	19	20	26	31	33	33	33	27	22	18

A Averages for the period 1942-53.

B Estimated averages for the period 1900-39.

G.57955/JIJ/4/56/50.

Table IV

Monthly average temperatures in the upper air and average tropopause pressures: observed 1942-53 (A) and estimated 1900-39 (B). Lerwick

		Jan.	Feb.	March	April	May	June	July	Aug.	Sept.	Oct.	Nov.	Dec.
						°F.							
100 mb.	A	-73.8	-72.4	-69.2	-59.7	-56.2	-51.2	-50.4	-51.6	-58.3	-67.0	-72.7	-73.4
	B	-74	-72	-66	-61	-55	-52	-50	-52	-59	-66	-73	-73
150 mb.	A	-70.4	-69.6	-67.5	-57.9	-56.3	-51.0	-50.7	-52.9	-58.2	-66.2	-68.9	-70.0
	B	-70	-69	-64	-60	-54	-52	-51	-54	-60	-65	-69	-70
200 mb.	A	-72.0	-71.6	-70.7	-60.6	-61.1	-53.0	-52.8	-55.6	-58.5	-65.9	-67.8	-70.8
	B	-72	-71	-67	-63	-59	-54	-53	-56	-60	-65	-68	-70
Tropopause Pressure (mb.)	A	255	254	248	271	253	260	249	242	246	239	253	255
	B	255	256	262	261	263	254	249	239	238	244	253	253
Tropopause Temperature	A	-75.7	-76.4	-75.5	-66.9	-67.5	-61.0	-62.0	-63.9	-64.1	-69.7	-71.0	-74.5
	B	-76	-76	-73	-69	-66	-60	-62	-64	-66	-69	-71	-74
300 mb.	A	-61.5	-61.9	-59.6	-55.1	-51.9	-47.2	-45.5	-45.8	-46.9	-50.6	-56.3	-59.2
	B	-61	-62	-61	-54	-53	-46	-45	-46	-46	-51	-56	-59
500 mb.	A	-19.2	-19.8	-16.3	-14.8	- 7.3	- 3.5	- 0.7	- 0.9	- 3.1	- 5.7	-13.2	-16.5
	B	-19	-20	-19	-13	- 9	- 3	- 1	0	- 2	- 6	-13	-17
700 mb.	A	10.1	9.6	12.4	14.0	20.8	24.4	28.4	28.7	24.6	22.3	15.1	13.2
	B	10	9	10	16	19	25	28	29	26	22	15	13

A Averages for the period 1942-53.

B Estimated averages for the period 1900-39.

G.57955/JIJ/4/56/50.

Fig. 1

MEAN MONTHLY RRESSURE OF TROPOPAUSE (1942-53)

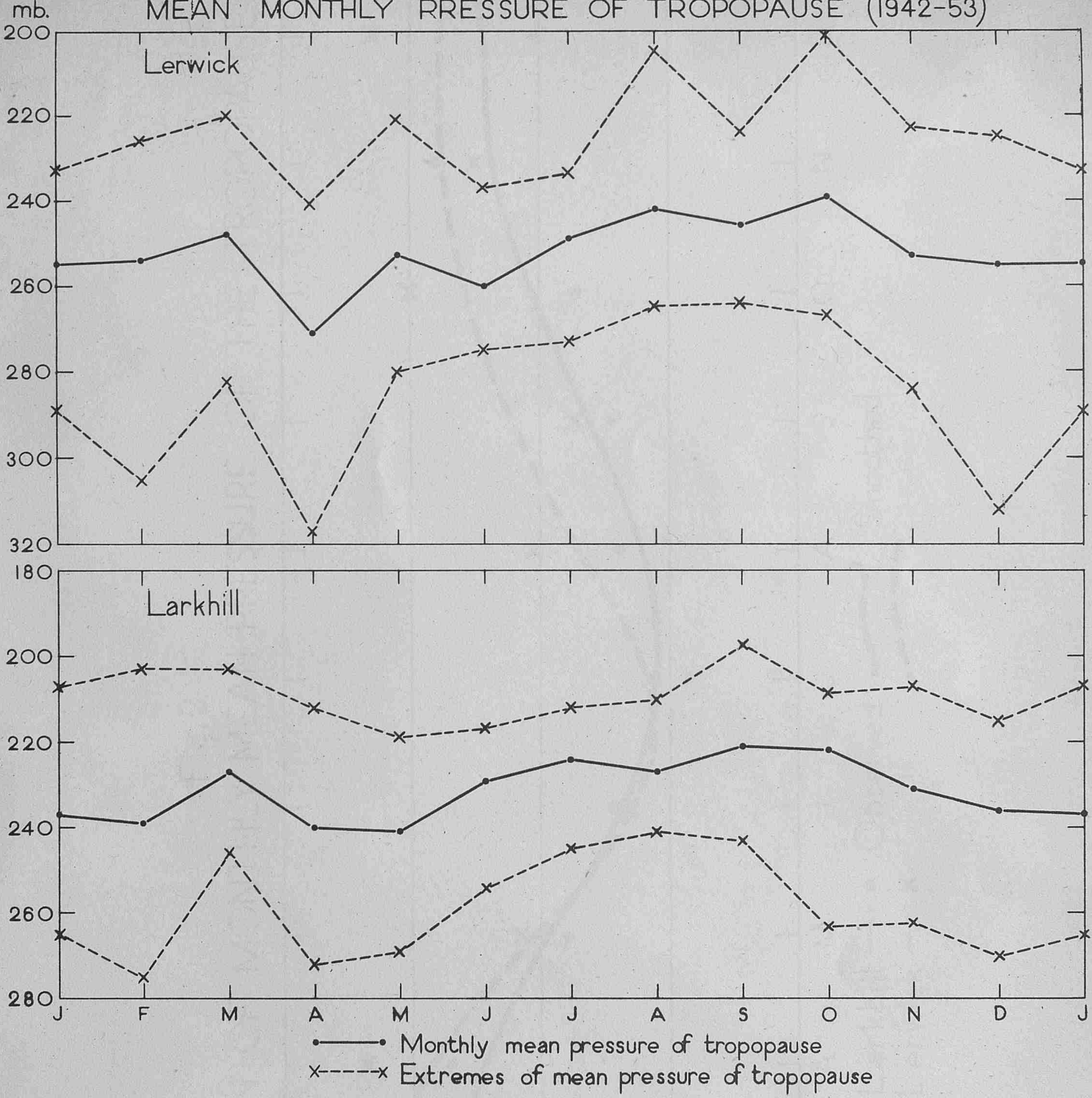

Fig. 2

STANDARD DEVIATION OF MONTHLY MEAN PRESSURE OF THE TROPOPAUSE

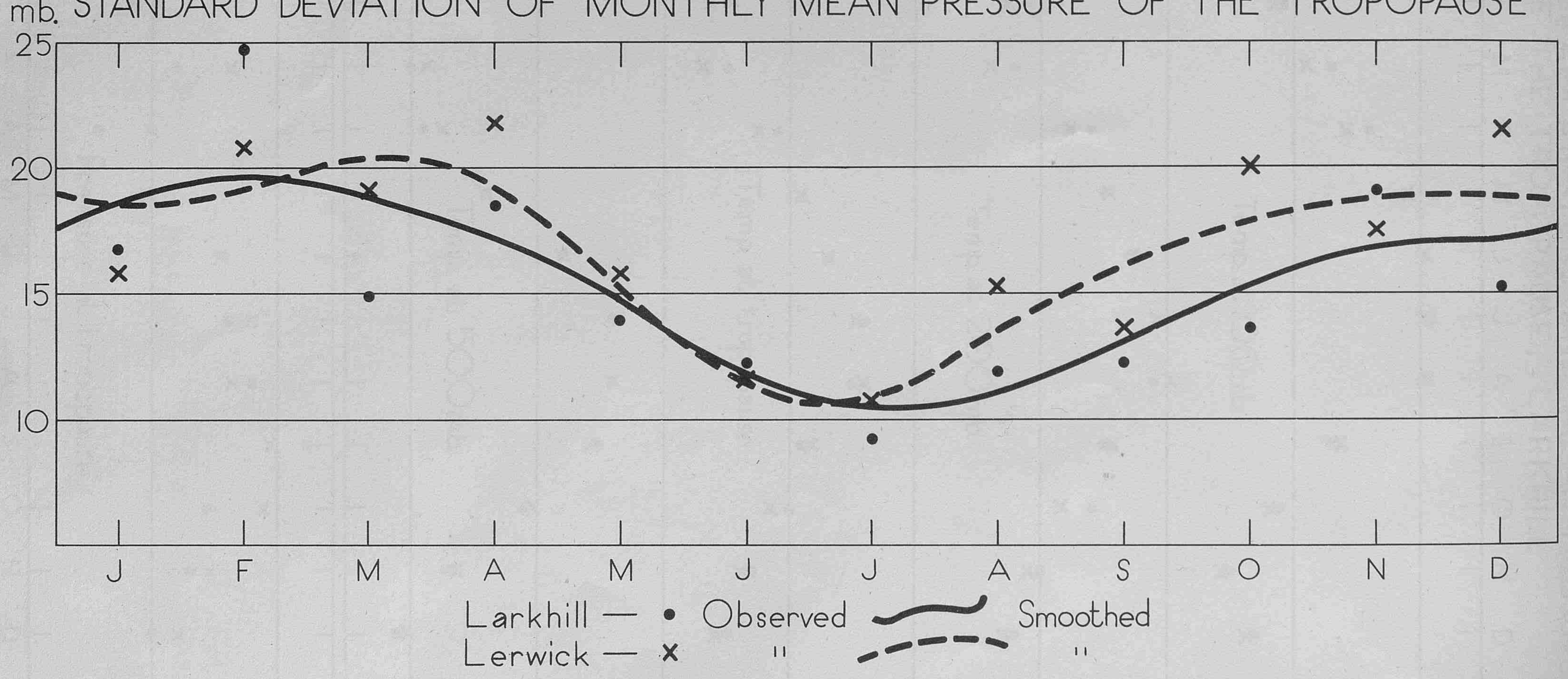

Fig. 3

MEAN TEMPERATURE AND MEAN PRESSURE OF THE TROPOPAUSE, LARKHILL

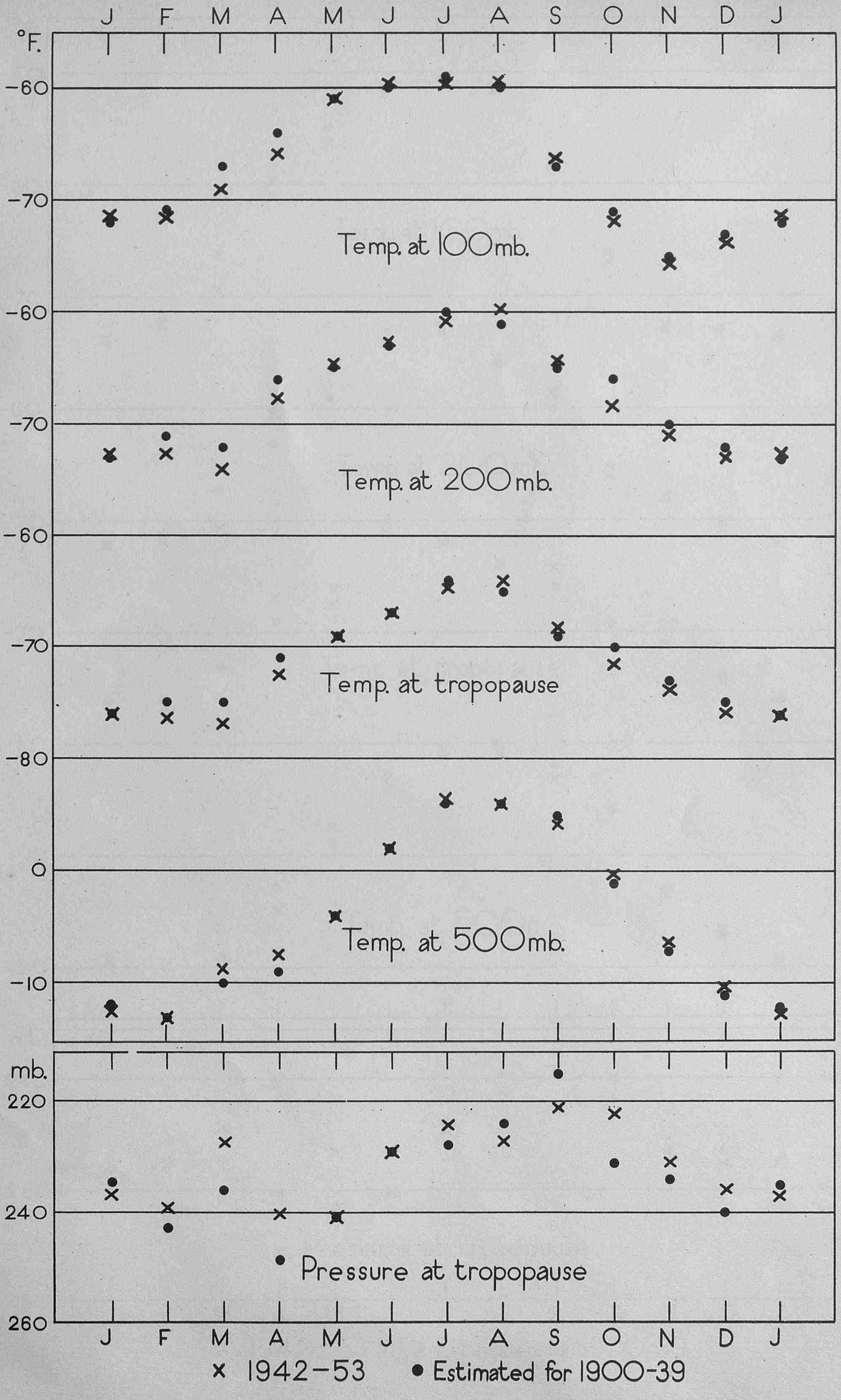

Fig. 4

M.R.P. 978

MEAN TEMPERATURE AND MEAN PRESSURE OF THE TROPOPAUSE, LERWICK

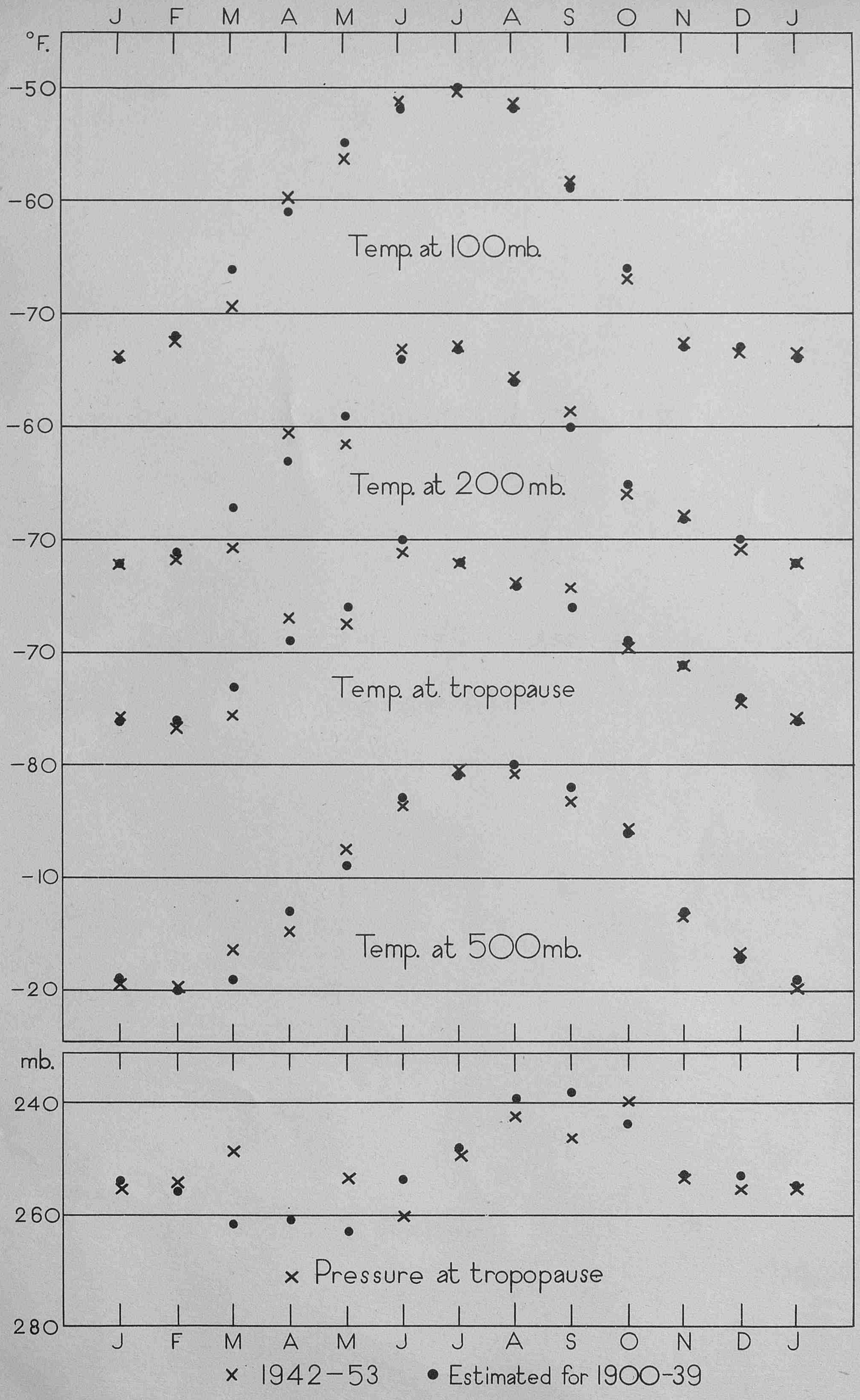

M.R.P. 979
S.C.111/206
27th June, 1956.

AD131894

Further observation of condensation trails

by

N. C. Helliwell and J. K. Mackenzie

(Meteorological Office)

AIR MINISTRY

METEOROLOGICAL RESEARCH COMMITTEE

M.O.15/31

P.979

To all recipients of M.R.P.979

Will you please amend your copy of M.R.P.979 as follows:-

Table I, 11/11/55 (4th line from end of table):

Delete	37,700	209	- 62.2	- 69.4	36.0
Replace by	40,000	187	- 55	- 76.6	5.1

Will you also please replace Figures 1 and 7 by the revised diagrams attached.

Hwl Absalom
Secretary
Meteorological Research Committee

Meteorological Office (M.O.15),
Air Ministry,
London, W.C.2
28th February, 1957

G.5525/AP/2/57/270

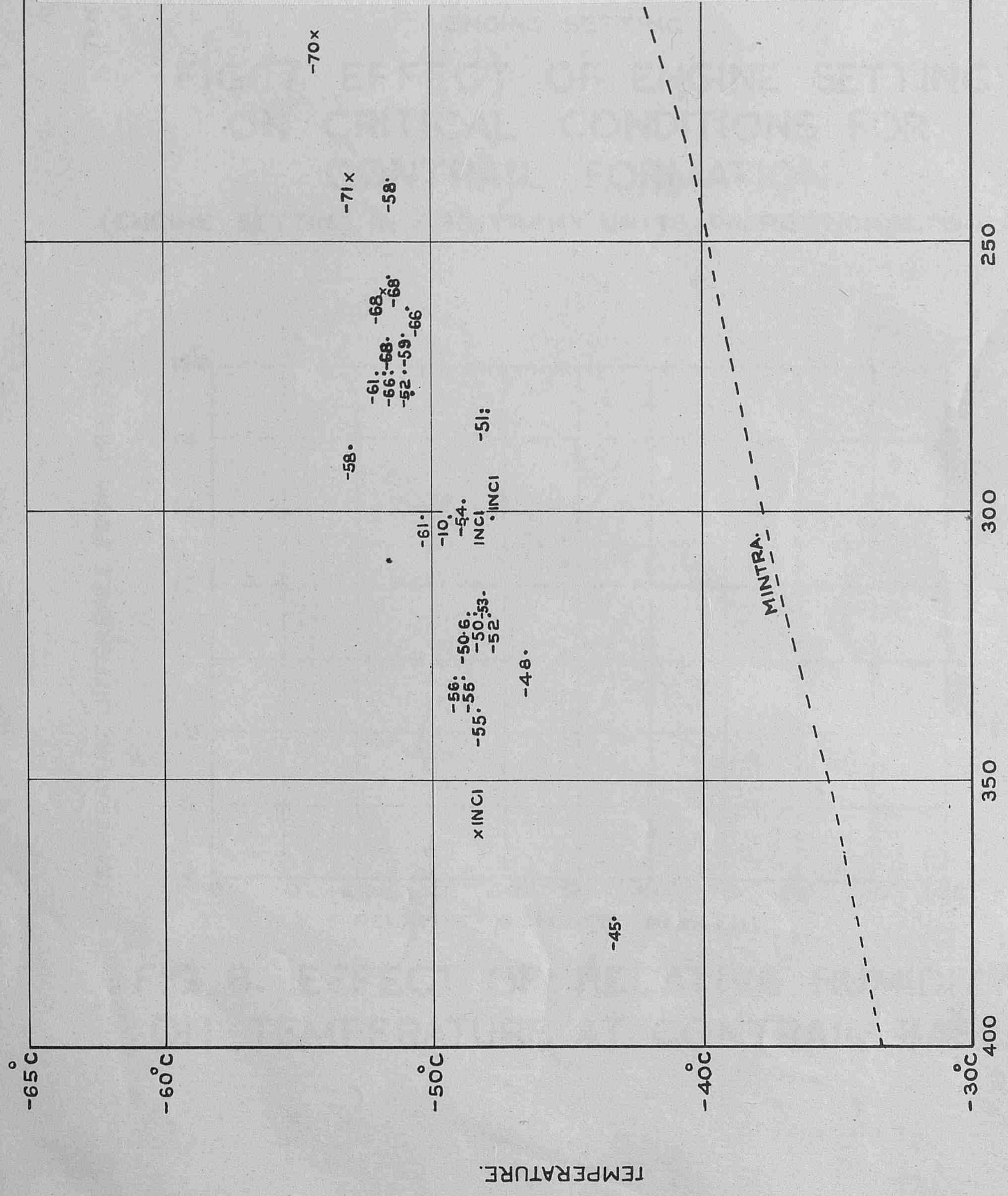

FIG. I.

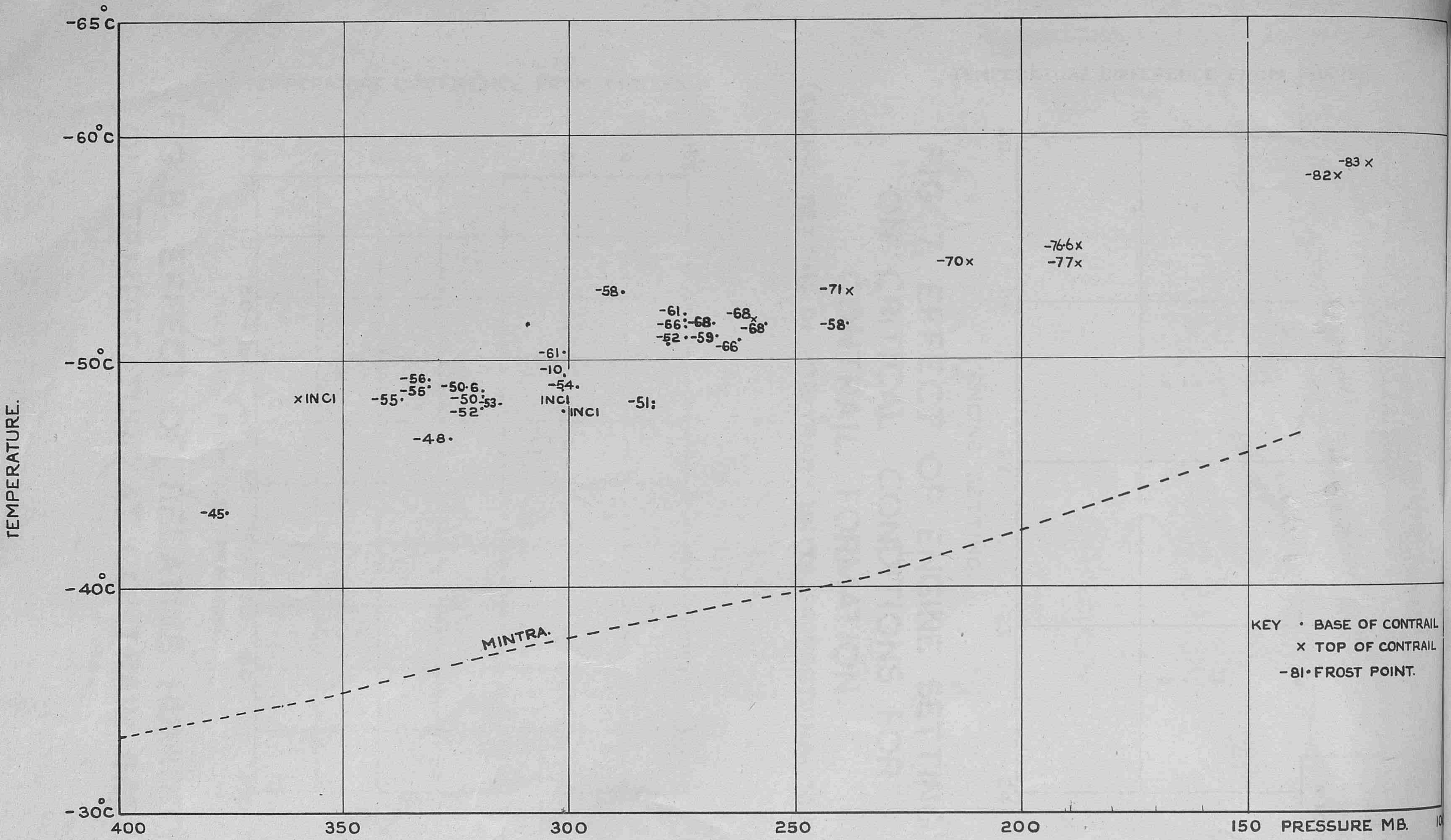
-65°C
-60°C
-50°C
-40°C
-30°C
TEMPERATURE.
400
350
300
250
200
150
PRESSURE MB.
-83 ×
-82×
-76·6×
-77×
-70×
-71×
-58·
-58·
-61·
-66·
-68·
-68×
-68·
-52·
-59·
-66·
-61·
-10·
-54·
INCI
INCI
-51:
-56:
-56·
-55·
-50·6·
-50·
-53·
-52·
×INCI
-48·
-45·
MINTRA.
KEY · BASE OF CONTRAIL
× TOP OF CONTRAIL
-81· FROST POINT.

FIG. 1.

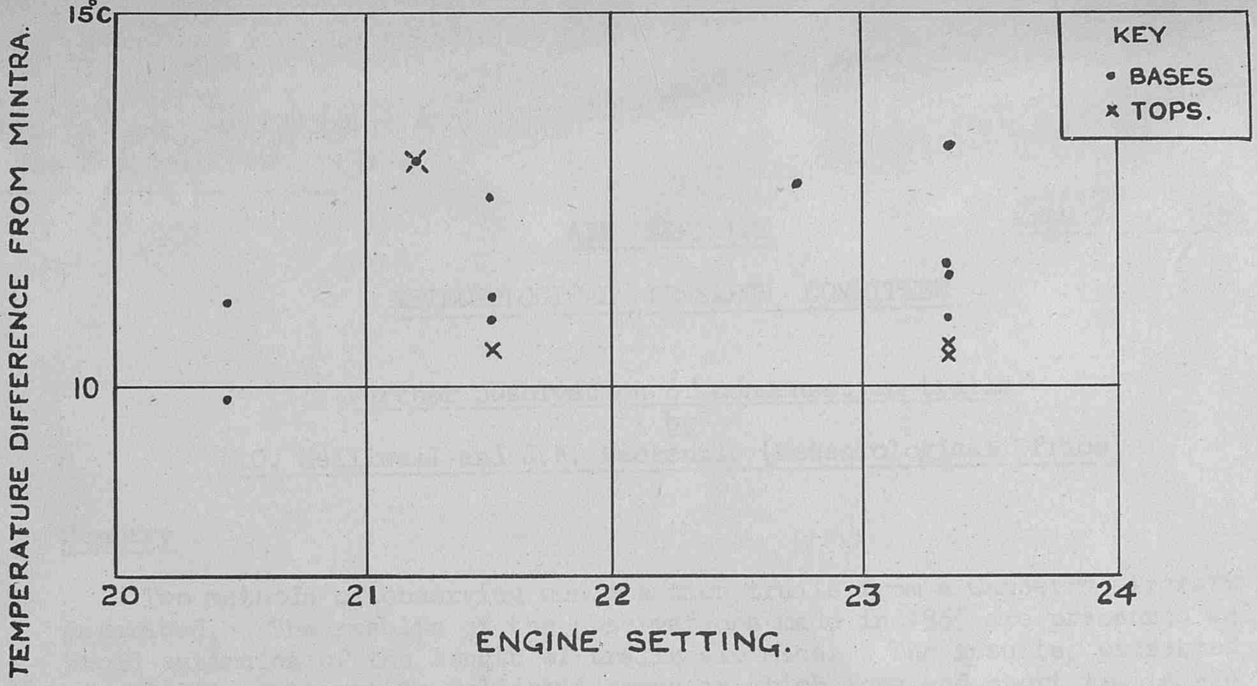

FIG. 7. EFFECT OF ENGINE SETTING ON CRITICAL CONDITIONS FOR CONTRAIL FORMATION.

(ENGINE SETTING IN ARBITRARY UNITS, PROPORTIONAL TO R.P.M.)

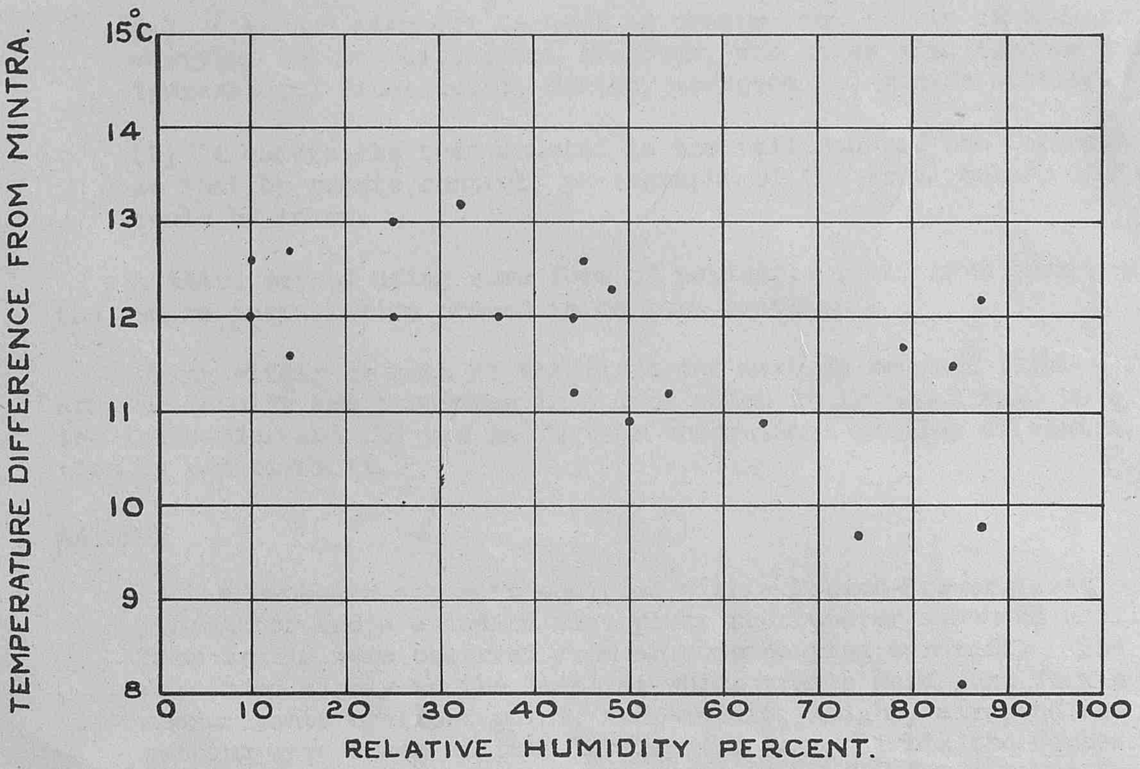

FIG. 8. EFFECT OF RELATIVE HUMIDITY ON TEMPERATURE AT CONTRAIL BASE.

At the time of issue this report has not been published. Any author desiring to quote this paper should refer to it as "A paper of the Meteorological Research Committee (London).
M.R.P. No.979 by Messrs. N.C. Helliwell and J.K. Mackenzie
A copy is available in the Library of the Meteorological Office."

M.R.P. 979
S.C.III/206
27th June, 1956

AIR MINISTRY

METEOROLOGICAL RESEARCH COMMITTEE

Further observation of condensation trails

by

N.C. Helliwell and J.K. Mackenzie (Meteorological Office)

Summary

Two methods of observing condensation trails from a Canberra aircraft are described. The results of the observations made in 1955 are presented and broad estimates of the length of trails are made. The results, presented graphically, attempt to delineate zones in which long and short trails are formed. An empirical forecasting procedure applicable to Canberra aircraft, and based on these data, is suggested.

Introduction

During 1955 several flights were made in a Canberra aircraft of the Meteorological Research Flight to examine the physical conditions governing the formation of condensation trails. Since the crew in this aircraft are so positioned that they cannot look backwards and see the trail it makes, two indirect methods have been used for observing the trail:-

(a) A second aircraft is used to observe the trails of the aircraft carrying the meteorological observer, who takes simultaneous readings of temperature, frost point, height, airspeed and engine setting.

(b) A camera has been mounted in the tail cone of the Canberra aircraft so that by remote control, photographs of the trail behind the aircraft could be taken.

A third method using some form of periscope could have been employed but the camera installation proved to be more practical.

Using either or both of the first two methods several flights were made and the results are presented in a form which it is hoped will be of value to the forecaster and for use in further theoretical studies of contrail formation by jet aircraft.

Methods

(1) A Canberra aircraft equipped with a Dobson-Brewer frost point hygrometer and a standard flat plate thermometer ascended until condensation trails were observed from an accompanying aircraft. The Canberra descended slowly to the level at which trails were just forming and measurements of frost point, temperature, height, airspeed and engine setting were taken at this level. In some flights the Canberra descended a further 1,000 ft. and a further set of readings was taken in conditions of no contrails. The aircraft then climbed slowly on a different engine setting and the observations were repeated at the level at which trails just formed. The aircraft ascended 1,000 ft. above this second level and the observations were repeated. On some occasions observations were made at 1,000 ft. intervals from base of trails to top of trails and then a further set of readings was taken 1,000 ft. above this. Photographs were taken whenever possible by the observer in the accompanying aircraft and it was hoped that the length of trails could be derived from these photographs. One or two were successful but generally the results do not justify inclusion at the present stage and it has been decided to

classify the trails as long, medium and short as described below.

(2) In the second method a camera, mounted in the tail cone and facing backwards, was electrically operated from the pressure cabin by a push button as required. To obviate fogging, the end of the tail cone was fitted with a heated glass window, and to prevent the camera freezing or failing to obtain photographs on account of ice formation on the lens, a special heater muff was designed and fitted.

Whenever a high-level ascent was made to measure humidity, or on the occasions when the aircraft was used to observe contrails by Method (1), photographs were taken at 500 ft. intervals during the ascent and at one minute intervals in level flight. During the high-level ascents temperature was measured on most occasions at intervals of 1,000 ft. and frost points were obtained at 2,000 to 4,000 ft. intervals. The pilot had previously been asked to bank the aircraft at certain specified heights so that when the photographs were developed it would be easier to check the heights at which individual photographs were taken against the log of the observer.

Accuracies

Temperature, height, airspeed and frost point were measured to the accuracy quoted in M.R.P.877 (1) and M.R.P.930 (2) , the standard errors being 2°C., 200 ft., 10 knots, and 3°C. respectively. In Method (1) the pressure-height of formation can be found to 50 ft. In Method (2) the heights of the first and last photographs on which trails were just visible were taken to be the lowest and greatest heights at which contrails formed.

Results

Table I and Fig.1 give the basic data for the occurrence of the contrail bases (29 cases) and tops (8 cases). The MINTRA line printed on M.O. Form 2810A (1949 Edition) is shown for comparison on Fig. 1. The data from Method (1) correspond with the observer's log and the data from Method (2) refer to the photograph on which trails were first visible.

Figs.2, 3 and 4 show the results of three typical ascents in which observations were made by Method (2) and illustrate respectively

(1) a case with a well-defined layer in which contrails formed,

(2) a case in which the aircraft had not ceased to make trails at 48,000 ft. and

(3) a marginal case in which trails barely formed.

In each case photographs were taken at 500 ft. intervals as described above and a selection of photographs is shown for various heights.

Fig.2 shows the results of an ascent on 8th November, 1955 in which contrails formed in a band from 29,000 ft. to 40,000 ft. A layer of thin cirrus at 344 mb. (28,000 ft.) can be seen on photograph (a) and this has become a more distinct band on (b). The contrails are only just visible on (b) and this suggests that they were short and very faint. On photograph (c) the trails are more dense and probably of medium length. The change from white trails to grey or black trails is due to the different angle of illumination by the sun. This effect can be used as an additional check on the height at which photographs were taken if the heading is known. Contrails are easily visible to 40,000 ft. (photographs (d) to (f)). They then become short and dense (photograph (g)) and at 40,500 ft. no trails are visible (photograph (h)). At 47,000 ft. (photograph (i)) there are similarly no trails visible.

Fig.3 is an ascent to 48,000 ft. on 28th November, 1955. A band of thin cirrus from 27,000 ft. to 33,000 ft. was noted by the observer and long trails were first visible at 29,500 ft. (photograph (b)). The records show that trails were still forming up to the maximum height of the ascent, 48,000 ft. (photographs (c) to (h)).

On 1st December, 1955 both methods were employed to find the base and top of condensation trails. A band of dense cirrus was present to 27,000 ft. being continuous from an altostratus layer below. In the accompanying aircraft the observer saw long dense trails at 28,000 ft. on the ascent but these ceased at 28,200 ft. and reappeared at 32,000 ft. in a narrow band. No further trails were observed during the ascent to 48,000 ft. The photographs shown in Fig.4 were taken during the descent which took place in a different area from the ascent. No trails formed between 48,000 ft. and 36,000 ft. A narrow band of trails is just visible on photographs (h) to (j) (34,000 to 35,000 ft.) although these are short and faint and yet another layer is shown on photographs (b) to (d) (25,500 to 26,500 ft.). The trails forming in the cirrus cloud appeared from the other aircraft to be very persistent and long.

The photographic records were examined for lengths by a subjective method. The geometry of the camera optics was used to define three types of trail (1) long, (2) medium and (3) short. It is not easy to be sure that the trails put in any particular classification definitely belong to that class but, in the main, there is little difficulty in distinguishing long and short trails from these photographs. On all occasions temperatures and frost points were available corresponding to certain levels within and along the boundary of the band of contrails and all photographs of trails obtained by Method (2) within this band were classified as above, i.e., intermediate observations as well as those of tops and bases.

Fig.5 shows the depression of the temperature from the MINTRA value at the pressure level corresponding to any photograph plotted against the depression of the frost point from ambient temperature at that level. Long trails are marked by a triangle, medium trails by a dot and short trails by a cross, while cases of no contrail are marked by a square. If an observation was available at the tropopause it is marked T and a circle is drawn round observations taken in the stratosphere. Zones of short and long contrails in the troposphere and stratosphere have been sketched in from the data. From this diagram it is possible to forecast the length of the contrail which will be formed by a Canberra aircraft at any height where the temperature and frost point are known or can be estimated.

Figs.6(a) & 6(b) are frequency diagrams for long, medium and short trails showing the number of observations in 2°C. bands of depression of temperature below MINTRA and 2°C. bands of depression of frost point below ambient temperature. For comparison the measurements of temperature and frost point made 500 ft. and 1,000 ft. below the base and above the top of the layer of contrails are shown as "cases of no contrails". The diagrams 6(a) show that, subjective though the criteria of lengths were, a short contrail may be expected to form at a higher temperature than a long trail. This is not surprising in itself but since the humidity diagrams 6(b) show little variation of length with depression of frost point, the inference can be drawn that the length of the trail is dependent principally on the temperature. It is interesting to note that trails in the stratosphere can be long if the temperature is sufficiently low and the depression of the frost point is not too great.

Fig.7 shows the few observations of engine setting plotted against temperature difference from MINTRA at the height at which trails first form. All these settings are for Canberra aircraft and the results show no connexion between the height at which trails first form and engine power.

Type of engine may cause some variation in the level at which contrails first form. An example of this effect occurred on 27th October, 1955. A Canberra aircraft first made contrails at 31,500 ft. and ceased to make trails at 35,000 ft., but an observing Javelin aircraft did not make trails until 31,700 ft. and ceased to make trails at 34,000 ft. Presumably the difference is due to the different engines in the two aircraft, an Avon engine in the Canberra and a Sapphire engine in the Javelin. It was found by A.M. Young (unpublished) that the temperature at which trails are first formed by a Venom aircraft was one or two degrees centigrade below that at which trails are formed by a Canberra.

The effect of relative humidity on the height of the contrail base was also examined and the results are shown in Fig.8. Although there is a slight increase of the temperature at which trails form with increasing humidity, this effect does not seem to be a principal factor in contrail formation but rather a subsidiary controlling factor. This agrees with the results of Murgatroyd (unpublished) as regards contrail formation by Mosquito piston-engined aircraft, and the theoretical results of Appleman (5).

The results of this series of experiments are therefore summarised:-

(1) Temperature is the most important variable in the physical state required for contrails both as regards height of formation and length when formed.

(2) Relative humidity has only secondary effects.

(3) The length of the trail is a complex function of temperature and humidity. A method of estimating the lengths of trails is suggested, based on the experimental data.

(4) Engine setting and type of engine must have some effect on the formation of contrails, but insufficient evidence is at present available to enable any conclusions to be drawn.

Forecasting contrails for Canberra aircraft in southern England

In order to forecast contrails in practice by the use of Fig.5 it is first necessary to estimate the temperature and frost point at a given height. Data on the former are always available from routine radio-sonde ascents. Ref.(6) gives a statistical method of estimating frost point up to 40,000 ft. if the temperature of the tropopause is known, but an alternative method of estimation, using synoptic and statistical data, is given below and is applicable up to 50,000 ft.

Fig.9 is a graph showing the results of 81 high level ascents by aircraft of the Meteorological Research Flight in 1954 and 1955 to measure the humidity of the upper atmosphere. As presented here, all observations above 25,000 ft. were used to derive a relationship between ambient temperature and frost point depression. On this graph are drawn various MINTRA temperatures for selected pressure levels so that frost point depression can be estimated in the form of a band width. Standard deviations of depression of frost point at selected levels are shown in Table II and this combined with Fig.9 will give a first estimate of the frost point depression over southern England at any level for a given ambient temperature. Use can also be made of Ref.(9) which describes the humidity structure of the atmosphere associated with cirrus cloud observations. From this information a good estimate of the humidity structure on any day can be derived.

A forecasting procedure based on these ideas would therefore be

(1) Find the temperatures at levels in the atmosphere for which contrail information is required. Read off the isobaric depression of this temperature from the MINTRA line using the Form 2810A on which the appropriate radio-sonde ascent is plotted.

(2) Use Fig.9, Table II and any synoptic data on high cloud to get an estimate of the frost point depression.

/(3)

(3) Use Fig.5 to find the expected length of the contrail.for the values of depression of temperature and depression of frost point obtained in (1) and (2) above.

Conclusion

Although these data are comparatively few, the results as regards levels of formation are in agreement with those previously presented from several sources, e.g., Murgatroyd, Young, and the calculations of Appleman (5) and Godson (10). It is known that in a few cases there have been reports at lower levels and higher temperatures than any observed by the Meteorological Research Flight but it is considered that these are exceptional.

References

(1) Murgatroyd, Goldsmith and Hollings 1954 Meteorological Research Papers, Air Ministry, London, No.877.

(2) Durbin, W.G. 1955 Meteorological Research Papers, Air Ministry, London, No.930.

(3) Murgatroyd, Goldsmith and Hollings Oct.1954 Q.J.R.Met.Soc., Vol.8, No.350, p.533.

(4) Brewer, A.W. Weather, June, 1946.

(5) Air Weather Service Technical Report, pp.105-112 1953.

(6) Bannon, Frith and Shellard 1952 Geophysical Memoirs, Air Ministry, London, No.88, pp.16-22.

(7) Goldie, A.H.R. 1953 Meteorological Research Papers, Air Ministry, London, No.805.

(8) Murgatroyd and Goldsmith 1953 Meteorological Research Papers, Air Ministry, London, No.832.

(9) Murgatroyd and Goldsmith 1953 Meteorological Research Papers, Air Ministry, London, No.833.

(10) Met. Division of Transport, Canada 1954 C.I.R.Tech. 178.

AIR WEATHER SERVICE

M.O.15/31

To all recipients of M.R.P.979

Will you please amend your copy of M.R.P.979 as follows:-

Table I, 11/11/55 (4th line from end of table):

Delete	37,700	209	- 62.2	- 69.4	36.0
Replace by	40,000	187	- 55	- 76.6	5.1

Will you also please replace Figures 1 and 7 by the revised diagrams attached.

Hwl Absalom
Secretary
Meteorological Research Committee

Meteorological Office (M.O.15),
Air Ministry,
London, W.C.2
28th February, 1957

G.5525/AP/2/57/270

AFOIN-1B4

8/11/55	1345	2	Base	29,000	315	-48.1	[illegible]	[illegible]
11/11/55	1130	1 & 2	Base	31,000	287	-53.1	-57.7	58
14/11/55	1410	1 & 2	Base	30,400	298	-48.9	-53.9	54
15/11/55	1155	1 & 2	Base	31,700	278	-50.8	-	-
21/11/55	1115	1 & 2	Base	32,100	272	-51.9	-	-
"	"	"	"	32,000	274	-51.6	-66.1	14
22/11/55	1340	2	Base	33,000	262	-51.0	-65.8	14
28/11/55	1330	2	Base	29,500	308	-48.9	in Cirrus	-
29/11/55	1410	2	Base	32,500	267	-51.1	-58.9	36
1/12/55	1125	1 & 2	Base	28,200	326	-46.6	-47.8	87
"	"	"	"	32,500	267	-51.7	-68.3	10
"	"	"	"	33,500	256	-51.7	-68.3	10
"	"	"	"	25,500	368	-47.7	-	-
4/ 3/55	1125	1	Top	47,500	130	-58.2	-82.2	03.2
14/ 3/55	1140	1	Top	48,700	123	-58.8	-83.3	02.7
4/10/55	0800	2	Top	37,500	211	-54.4	-70.0	11.5
8/11/55	1345	2	Top	40,000	187	-54.3	-77.2	04.0
11/11/55	1130	1 & 2	Top	37,700	209	-62.2	-69.4	36.0
1/12/55	1125	1 & 2	Top	33,000	262	-51.9	-68.2	10.1
"	"	"	"	35,000	238	-53.1	-71.1	08.3
"	"	"	"	26,000	360	-48.2	-	-

Relative humidity with respect to ice

Table II. Mean temperature and mean depression of frost point

Height ft.	Mean Temperature °C.	Mean Frost Point Depression °C.	S.d ⁎
25,000	-37.3	10.4	8.9
30,000	-47.4	9.3	7.2
34,000	-54.9	9.5	6.8
36,000	-56.1	11.7	7.5
40,000	-55.2	20.3	9.4
44,000	-53.4	27.1	6.0
48,000	-53.1	29.2	6.3

⁎ Standard deviation of depression of frost point.

RECEIVED
20 MAR 1957
DIR/INT
HQ USAF

Date	Time	Method	Base or	I.C.A.N.	Pressure	Temp.	Frost	R.H.

Table I. Observations of

Date	Time GMT.	Method	Base or Top	I.C.A.N. ht. in ft.	Pressure in mb.	Temp. in °C.	Frost Point °C.	R.H. %
4/3/55	1125	1	Base	28,800	319	-48.7	-50.6	79
14/3/55	1140	1	Base	28,700	320	-48.5	-50.0	84
15/3/55	1150	1	Base	28,700	320	-47.9	-51.7	64
16/3/55	1530	1	Base	29,400	309	-51.7	-	-
18/3/55	1605	1	Base	27,900	331	-49.2	-55.6	45
28/3/55	1500	1	Base	27,900	331	-48.9	-55.0	48
"	"	"	"	27,500	337	-48.3	-55.0	44
"	"	"	Layer	25,100	375	-43.3	-45.0	85
29/ 9/55	1445	2	Base	35,000	238	-51.7	-58.1	44
4/10/55	0800	2	Base	32,000	274	-52.1	-61.1	32
12/10/55	1435	2	Base	31,500	281	-48.2	-50.7	74
17/10/55	1045	2	Base	30,000	301	-47.8	in Cirrus	-
26/10/55	1530	2	Base	32,000	274	-51.1	-52.2	87
27/10/55	1555	2	Base	31,500	281	-48.2	-	-
28/10/55	1345	2	Base	29,500	308	-49.4	-60.3	25
1/11/55	1345	2	Base	29,500	308	-50.4	-61.1	25
8/11/55	1345	2	Base	29,000	315	-48.1	-53.6	50
11/11/55	1130	1 & 2	Base	31,000	287	-53.1	-57.7	58
14/11/55	1410	1 & 2	Base	30,400	298	-48.9	-53.9	54
15/11/55	1155	1 & 2	Base	31,700	278	-50.8	-	-
21/11/55	1115	1 & 2	Base	32,100	272	-51.9	-	-
"	"	"	"	32,000	274	-51.6	-66.1	14
22/11/55	1340	2	Base	33,000	262	-51.0	-65.8	14
28/11/55	1330	2	Base	29,500	308	-48.9	in Cirrus	-
29/11/55	1410	2	Base	32,500	267	-51.1	-58.9	36
1/12/55	1125	1 & 2	Base	28,200	326	-46.6	-47.8	87
"	"	"	"	32,500	267	-51.7	-68.3	10
"	"	"	"	33,500	256	-51.7	-68.3	10
"	"	"	"	25,500	368	-47.7	-	-
4/ 3/55	1125	1	Top	47,500	130	-58.2	-82.2	03.2
14/ 3/55	1140	1	Top	48,700	123	-58.8	-83.3	02.7
4/10/55	0800	2	Top	37,500	211	-54.4	-70.0	11.5
8/11/55	1345	2	Top	40,000	187	-54.3	-77.2	04.0
11/11/55	1130	1 & 2	Top	37,700	209	-62.2	-69.4	36.0
1/12/55	1125	1 & 2	Top	33,000	262	-51.9	-68.2	10.1
"	"	"	"	35,000	238	-53.1	-71.1	08.3
"	"	"	"	26,000	360	-48.2	-	-

Relative humidity with respect to ice

Table II. Mean temperature and mean depression of frost point

Height ft.	Mean Temperature °C.	Mean Frost Point Depression °C.	S.d [*]
25,000	-37.3	10.4	8.9
30,000	-47.4	9.3	7.2
34,000	-54.9	9.5	6.8
36,000	-56.1	11.7	7.5
40,000	-55.2	20.3	9.4
44,000	-53.4	27.1	6.0
48,000	-53.1	29.2	6.3

[*] Standard deviation of depression of frost point.

G.58043(a)/MFW/4/56/50

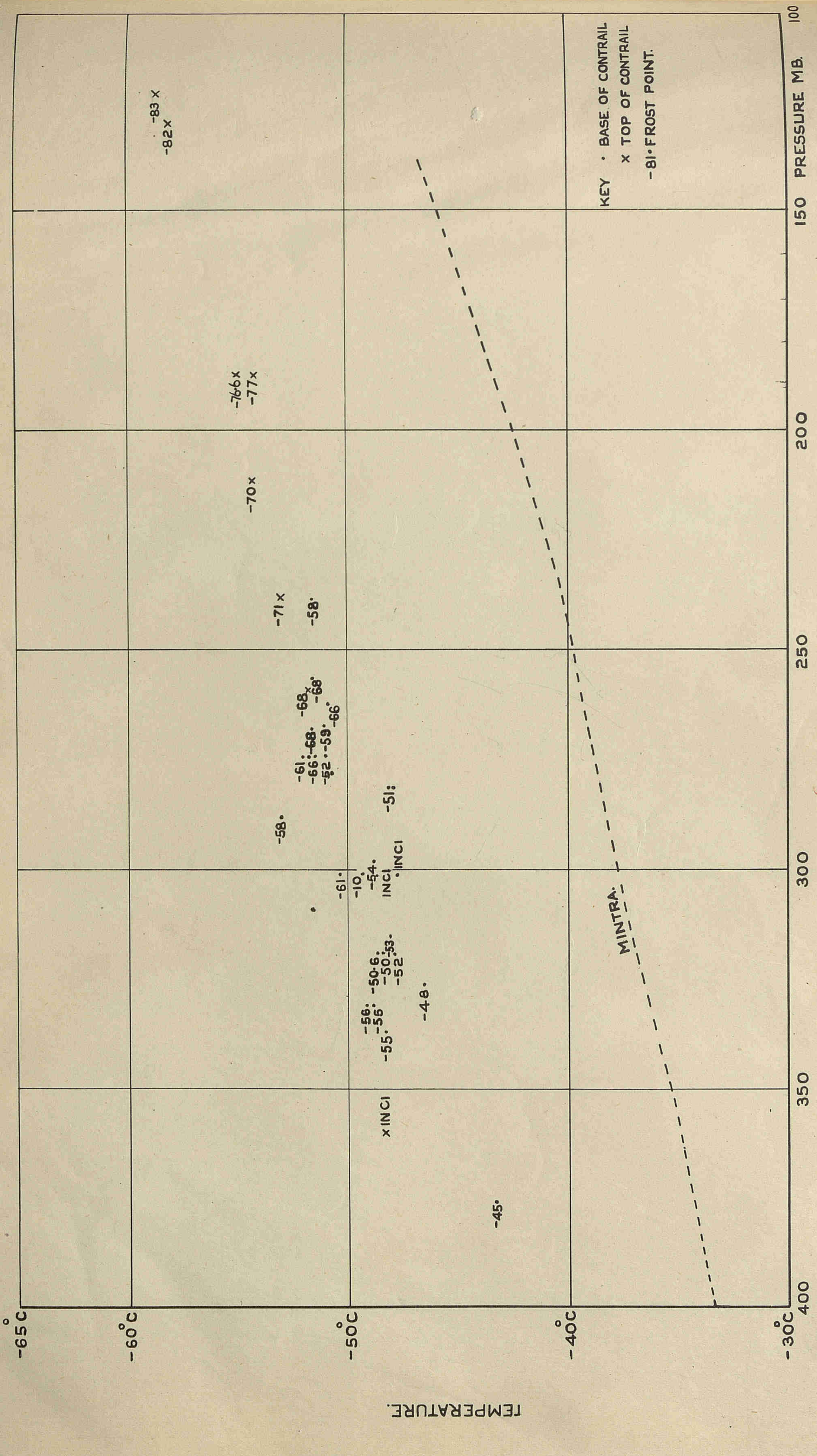

(Corrected)

FIG. I.

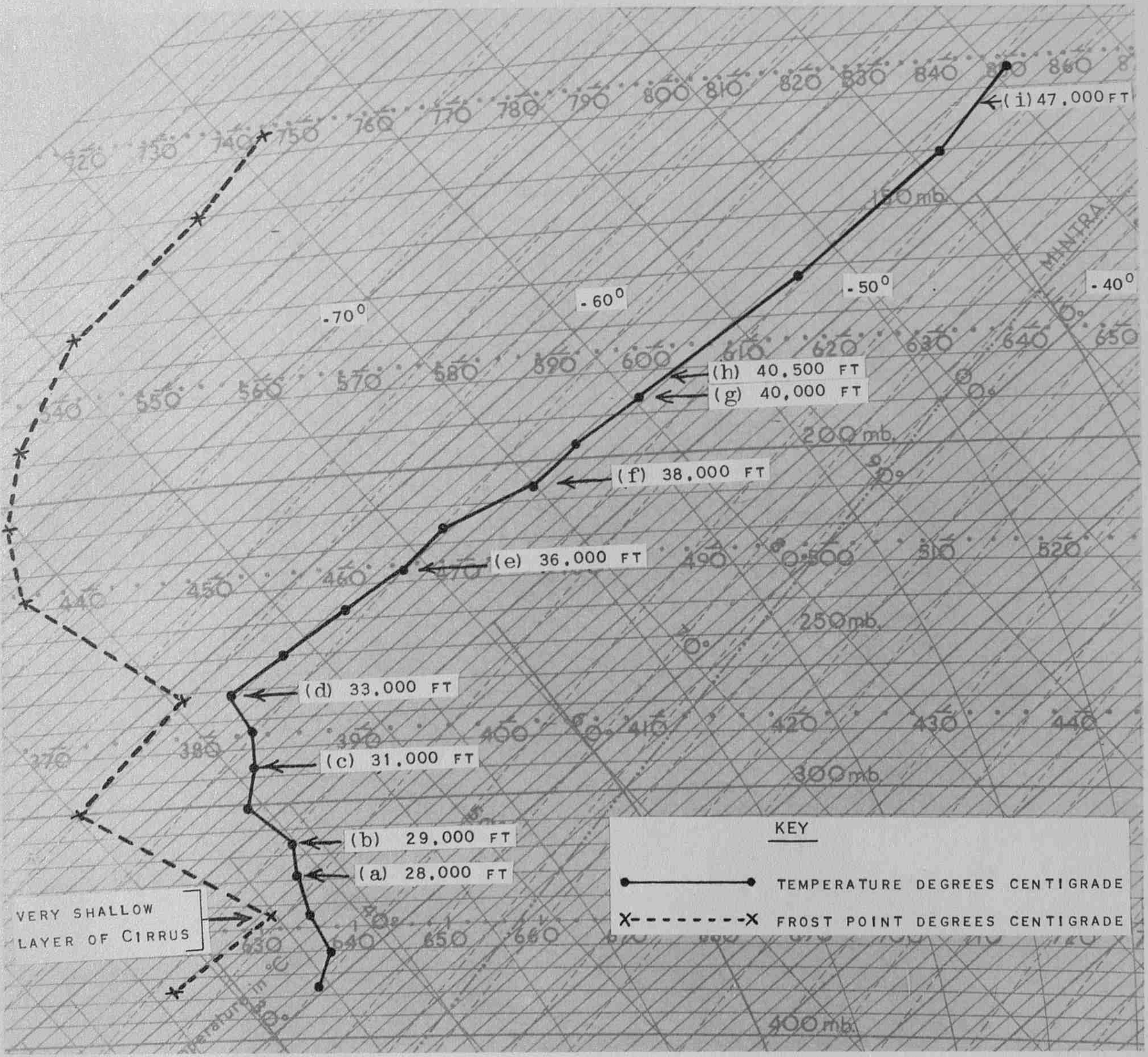

PART OF AIRCRAFT ASCENT ON 8TH NOVEMBER, 1955, TO 48,000 FT. OVER CRAWLEY. ON THIS OCCASION CONTRAILS WERE OBSERVED IN A BAND FROM 29,000 FT. TO 40,000 FT. (I.C.A.O.)

THE CONTRAIL PHOTOGRAPHS ON THE FACING PAGE WERE TAKEN AT THE LEVELS INDICATED BY ARROWS ON THE TEPHIGRAM ABOVE.

FIG.2a

R.A.E. 124601 56

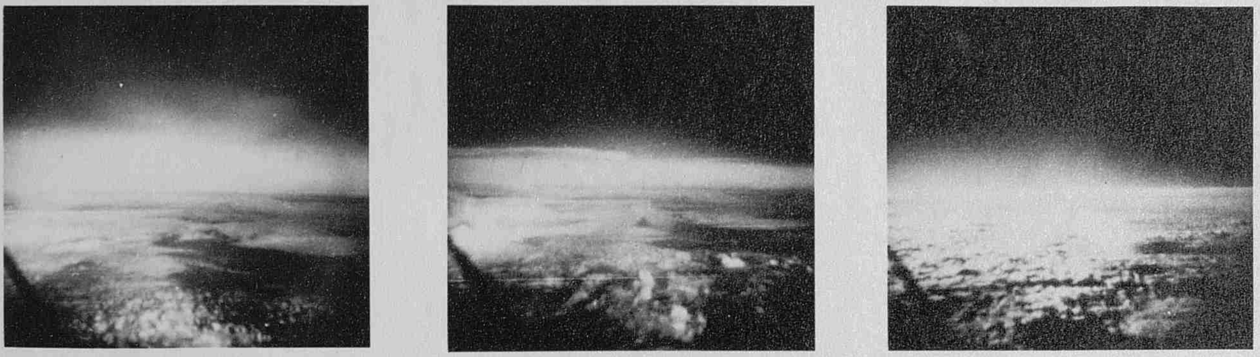

a
28,000 FEET. NO TRAILS

b
29,000 FEET. TRAILS SHORT AND FAINT.

c
31,000 FEET. TRAILS MEDIUM.

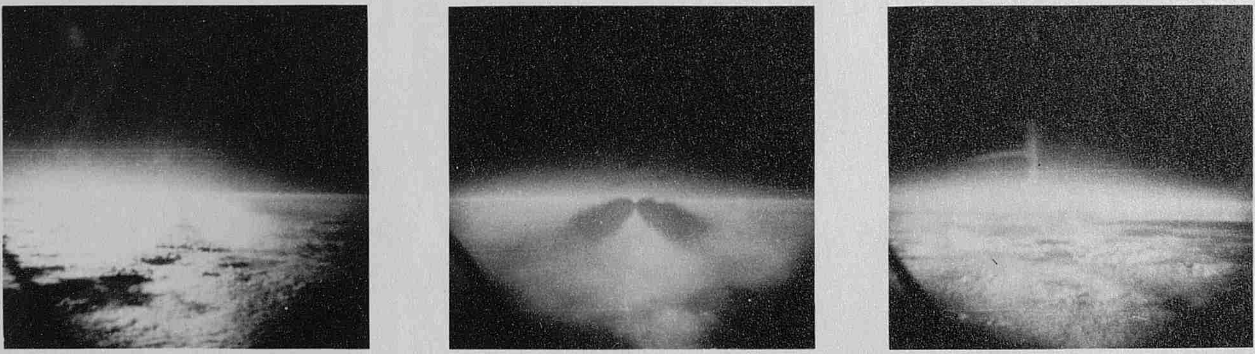

d
33,000 FEET. TRAILS LONG.

e
36,000 FEET. TRAILS MEDIUM.

f
38,000 FEET. TRAILS SHORT.

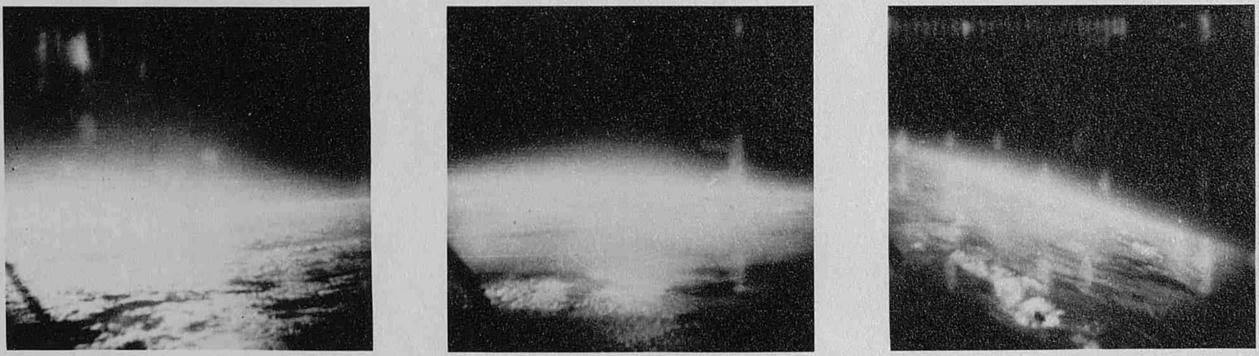

g
40,000 FEET. TRAILS SHORT AND FAINT.

h
40,500 FEET. NO TRAILS.

i
47,000 FEET. NO TRAILS.

FIG.2b

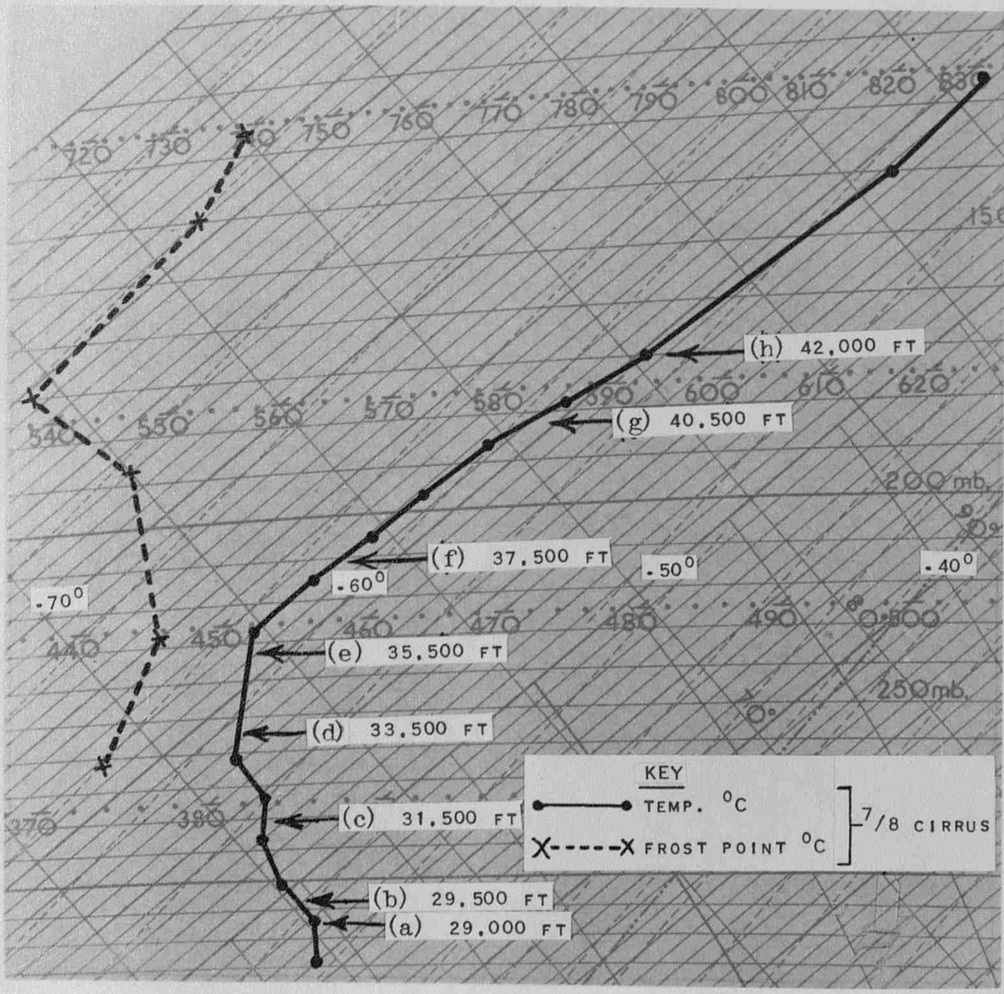

PART OF AIRCRAFT ASCENT ON 28TH NOVEMBER, 1955, TO 48,000 FT. OVER CRAWLEY. ON THIS OCCASION CONTRAILS WERE OBSERVED EVERY 500 FT. FROM 29,500 TO 48,000 FT. (I.C.A.O.) NO TRAILS WERE OBSERVED AT 28,000 TO 29,000 FT.

THE CONTRAIL PHOTOGRAPHS ON THE FACING PAGE WERE TAKEN AT THE LEVELS INDICATED BY ARROWS ON THE TEPHIGRAM ABOVE.

FIG.3a

R.A.E. "124603 56

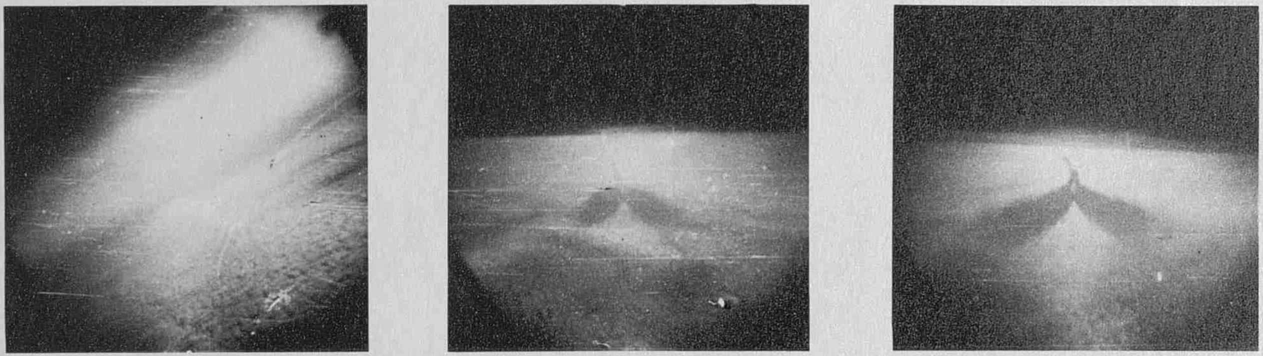

a
29,000 FEET. NO TRAILS.

b
29,500 FEET. TRAILS LONG.

c
31,500 FEET. TRAILS LONG.

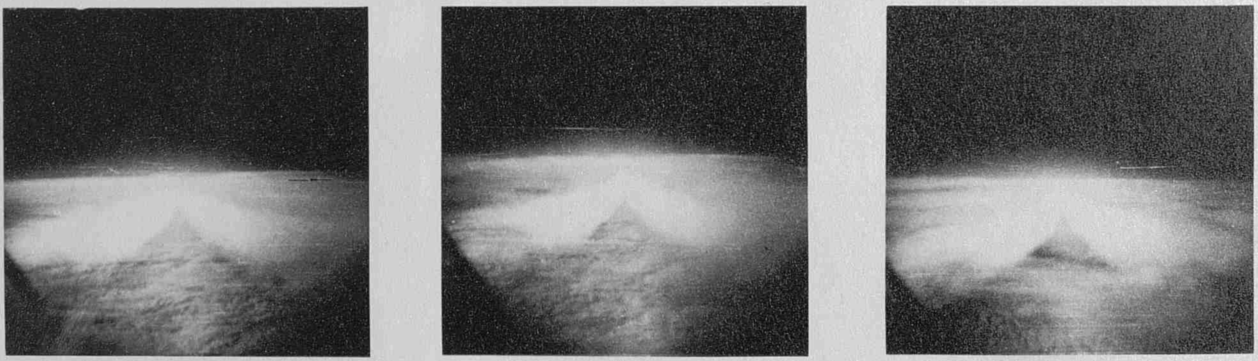

d
33,500 FEET. TRAILS LONG.

e
35,500 FEET. TRAILS MEDIUM.

f
37,500 FEET. TRAILS LONG.

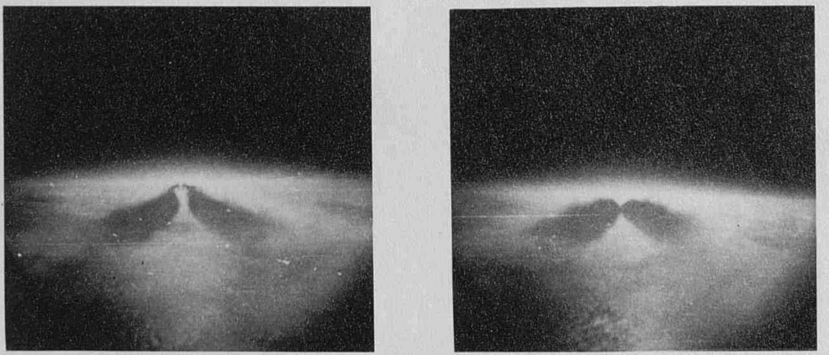

g
40,500 FEET. TRAILS MEDIUM.

h
42,000 FEET. TRAILS SHORT.

FIG.3b

R.A.E. 124604 56

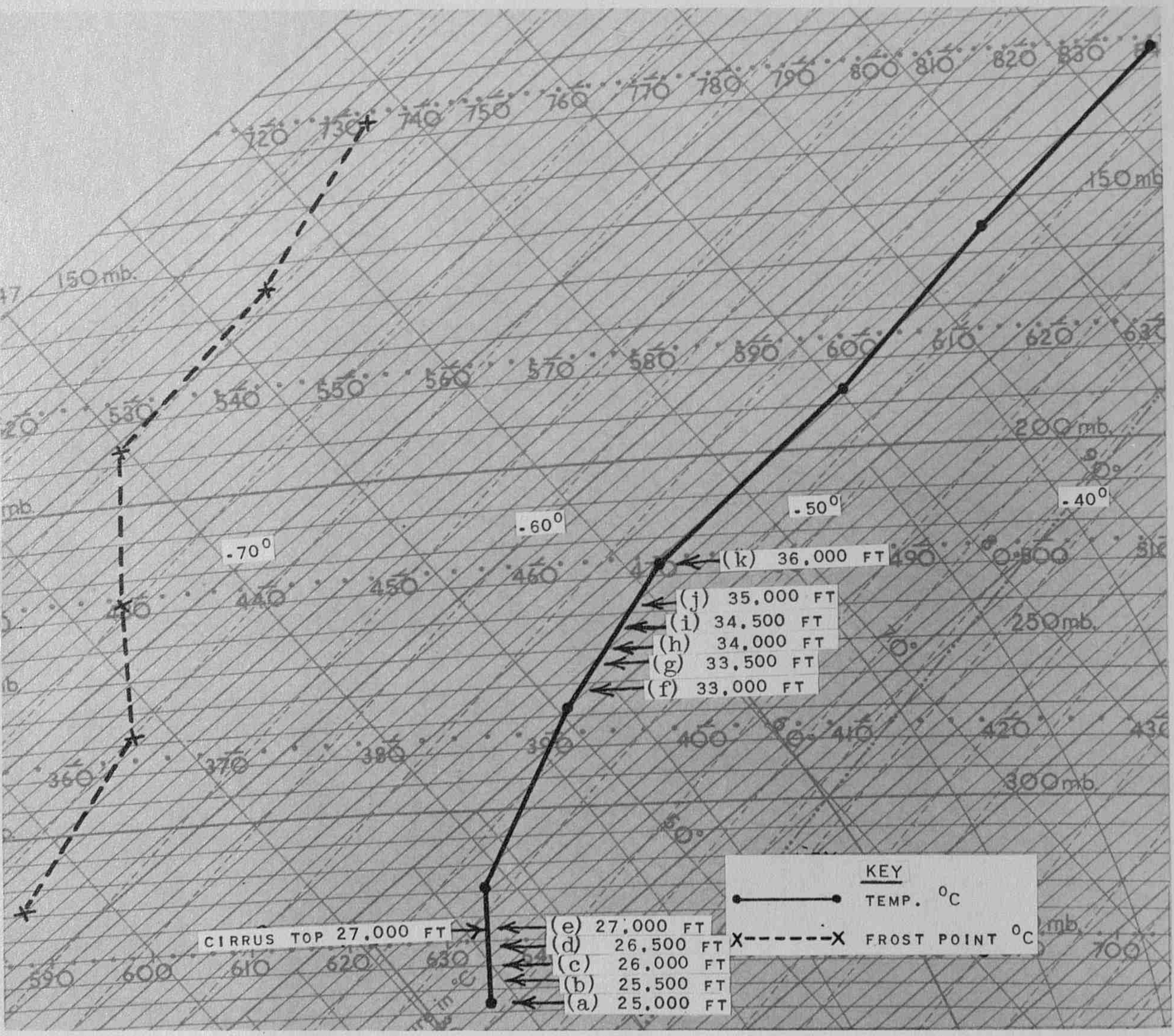

PART OF AIRCRAFT ASCENT ON 1ST DECEMBER, 1955, TO 48,000 FT. OVER CREWE TO HARTLAND POINT. ON THIS OCCASION TRAILS WERE OBSERVED FROM 25,500 FEET TO 26,500 FEET AND FROM 34,000 FEET, 35,000 FEET ONLY. NO OTHER TRAILS WERE NOTED BY ANOTHER AIRCRAFT FLYING IN FORMATION.

THE CONTRAIL PHOTOGRAPHS ON THE FACING PAGE WERE TAKEN AT THE LEVELS INDICATED BY ARROWS ON THE TEPHIGRAM ABOVE.

FIG.4a

R.A.E. 124605 56

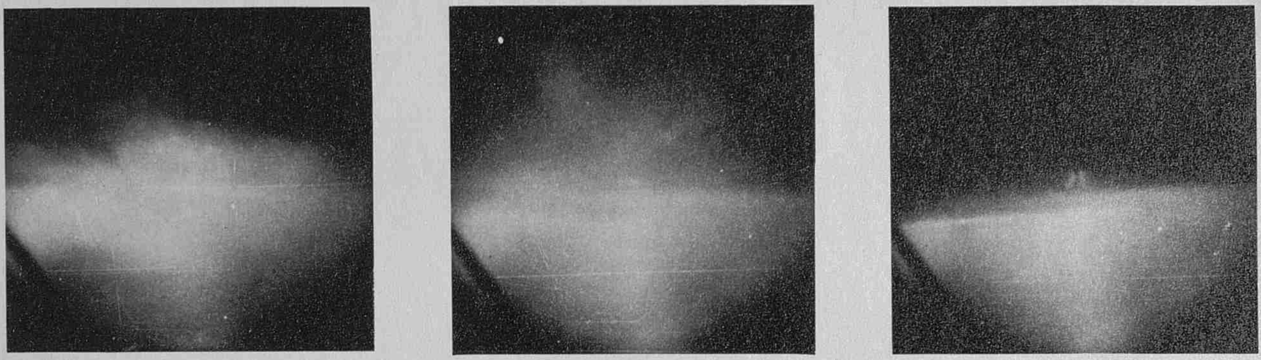

a
25,000 FEET. NO TRAILS VISIBLE IN CLOUD.

b
25,500 FEET. TRAILS JUST VISIBLE AS TWO DOTS IN CLOUD.

c
26,000 FEET. TRAILS VISIBLE IN CLOUD.

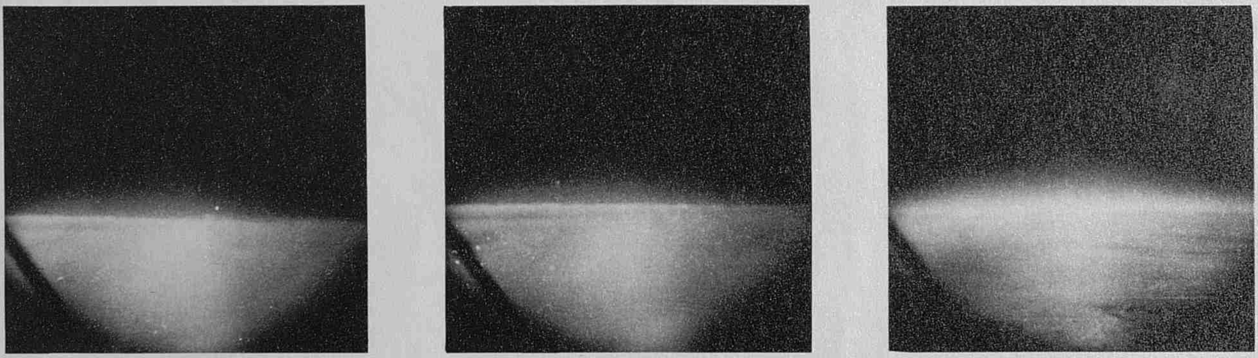

d
26,500 FEET. TRAILS JUST VISIBLE IN CLOUD.

e
27,000 FEET. NO TRAILS.

f
33,000 FEET. NO TRAILS.

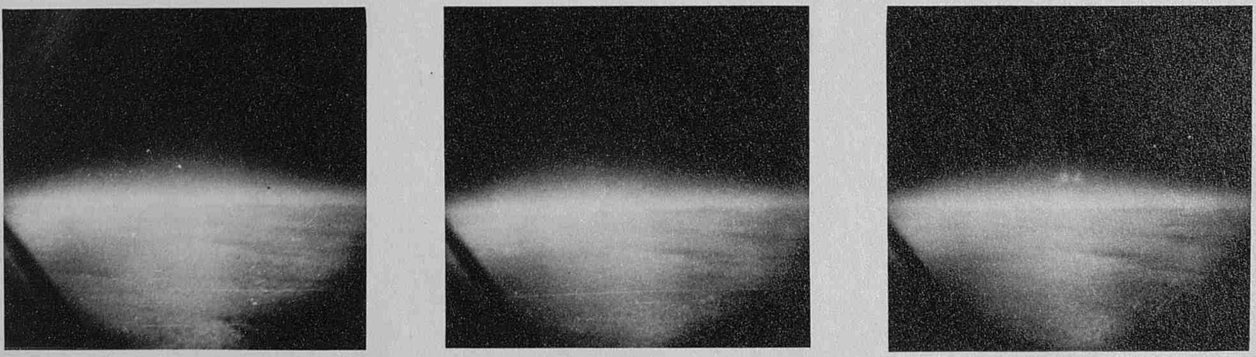

g
33,500 FEET. NO TRAILS.

h
34,000 FEET. TRAILS JUST VISIBLE.

i
34,500 FEET. TRAILS VISIBLE.

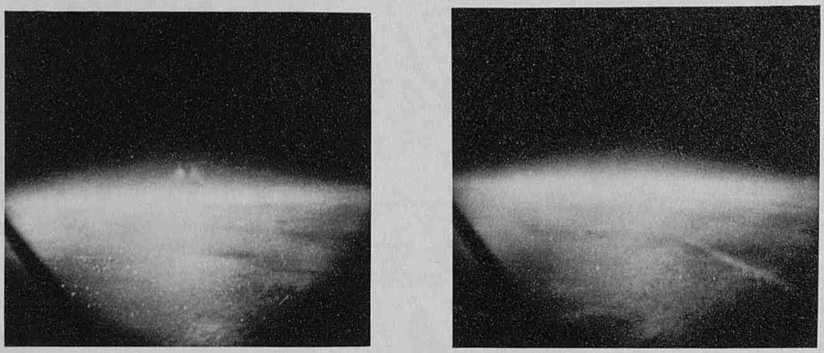

j
35,000 FEET. TRAILS JUST VISIBLE.

k
36,000 FEET. NO TRAILS.

FIG.4b

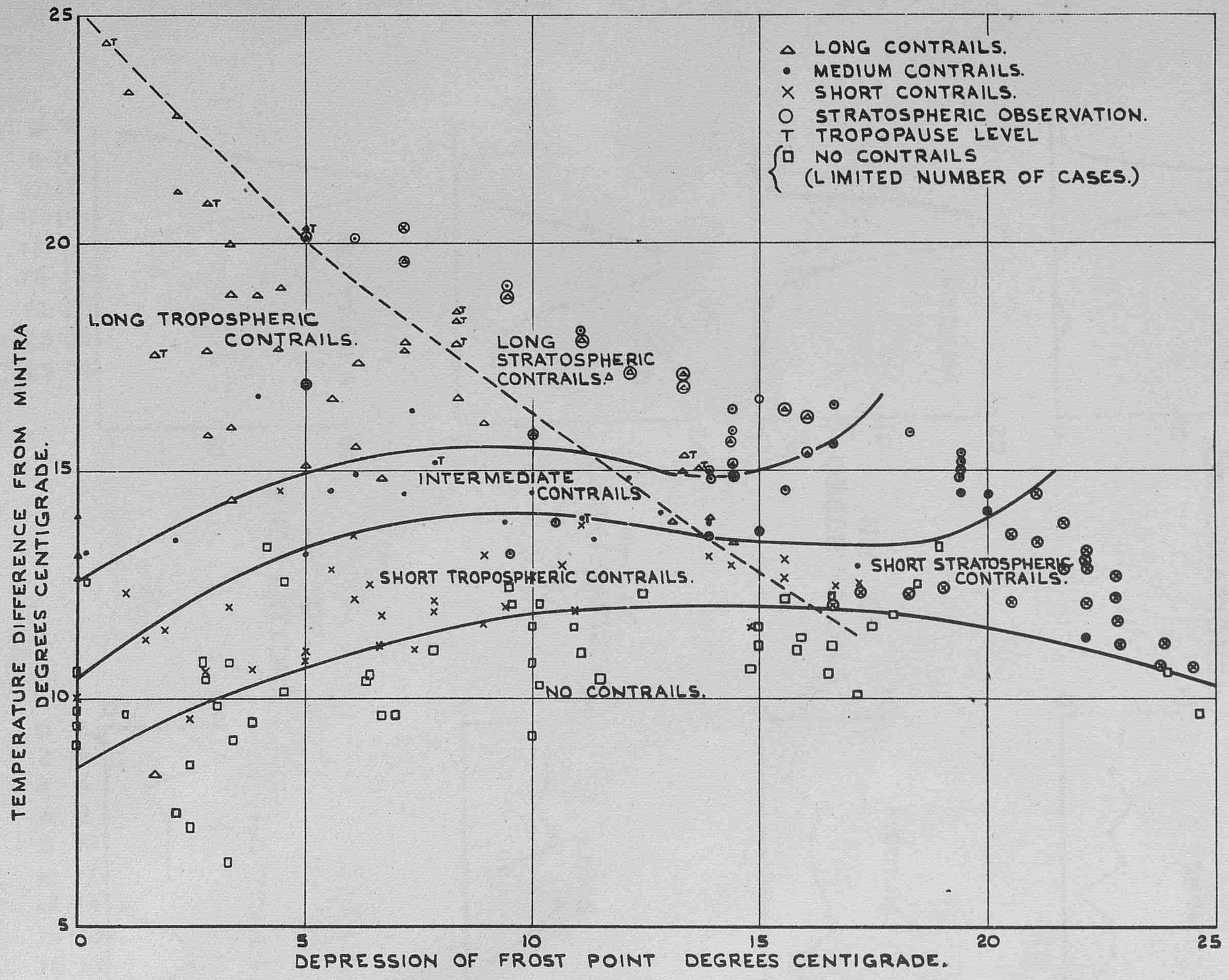

FIG: 5. LENGTH OF CANBERRA CONTRAILS FOR VARYING TEMPERATURE AND HUMIDITY.

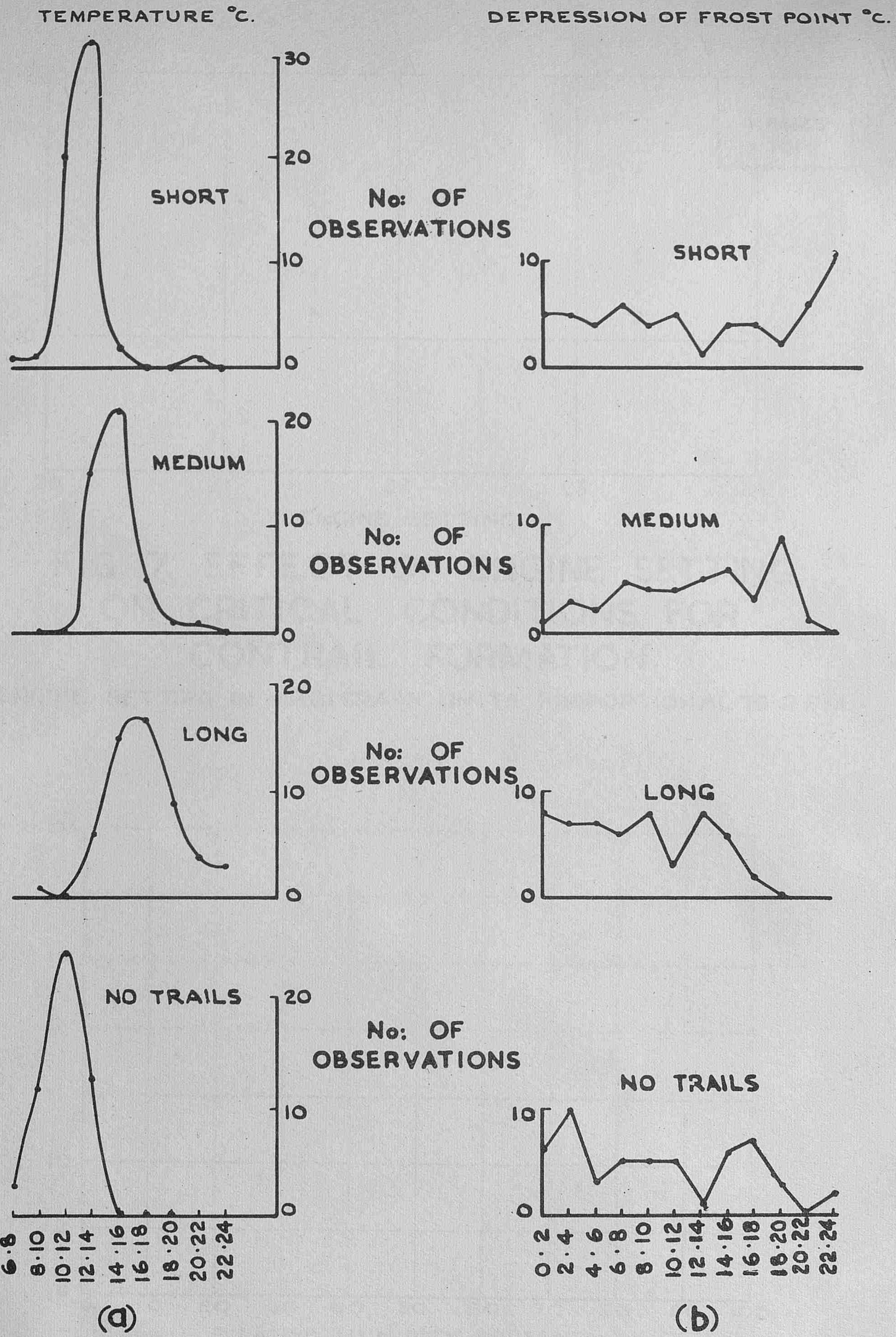

FIG: 6a & b. FREQUENCY DISTRIBUTION CURVES. OF CONDENSATION TRAILS FROM 1000 FEET BELOW THE BASE TO 1000 FEET ABOVE THE TOP WITH RESPECT TO (a) TEMPERATURE DEPRESSION BELOW MINTRA AND (b) DEPRESSION OF FROST POINT.

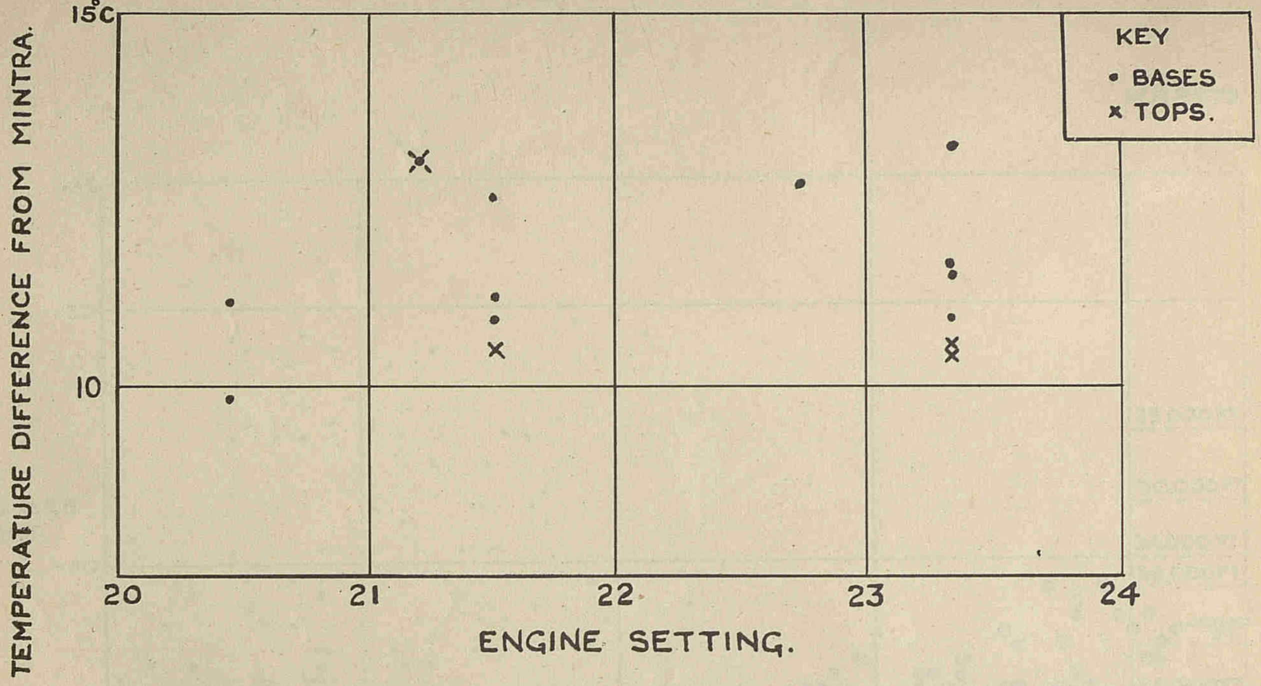

FIG. 7. EFFECT OF ENGINE SETTING ON CRITICAL CONDITIONS FOR CONTRAIL FORMATION.

(ENGINE SETTING IN ARBITRARY UNITS, PROPORTIONAL TO R.P.M.)

(Corrected sheet)

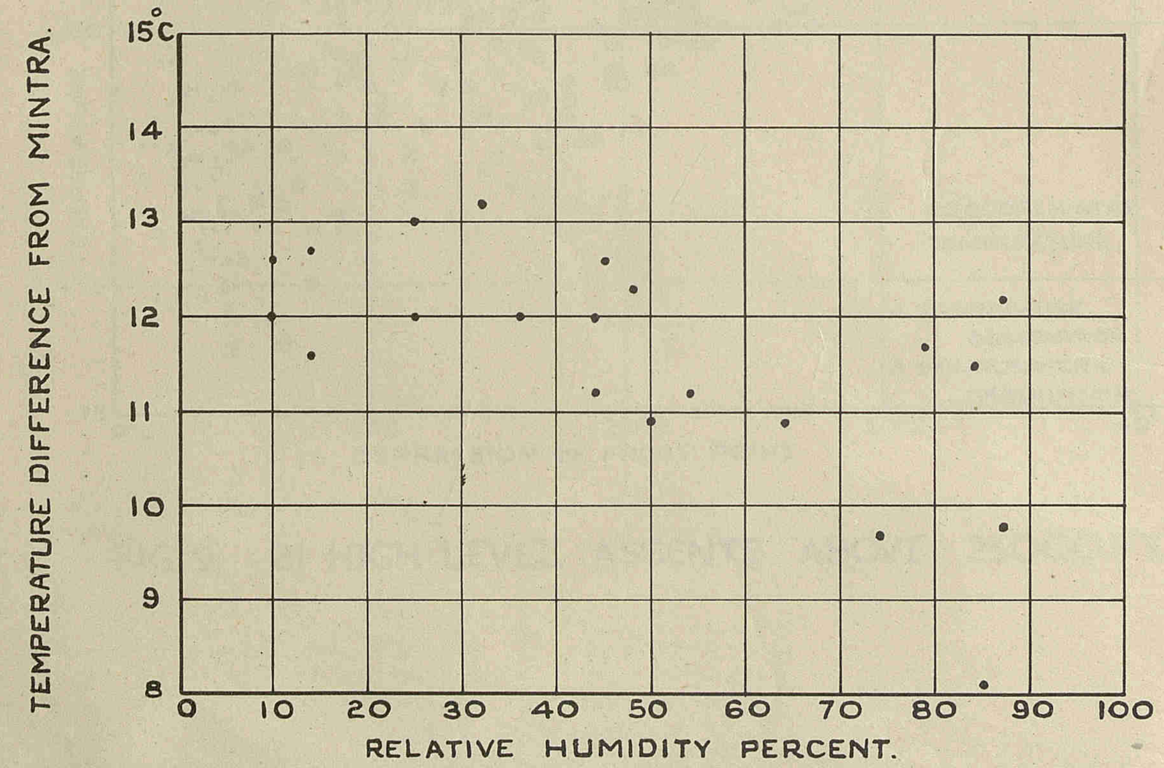

FIG. 8. EFFECT OF RELATIVE HUMIDITY ON TEMPERATURE AT CONTRAIL BASE.

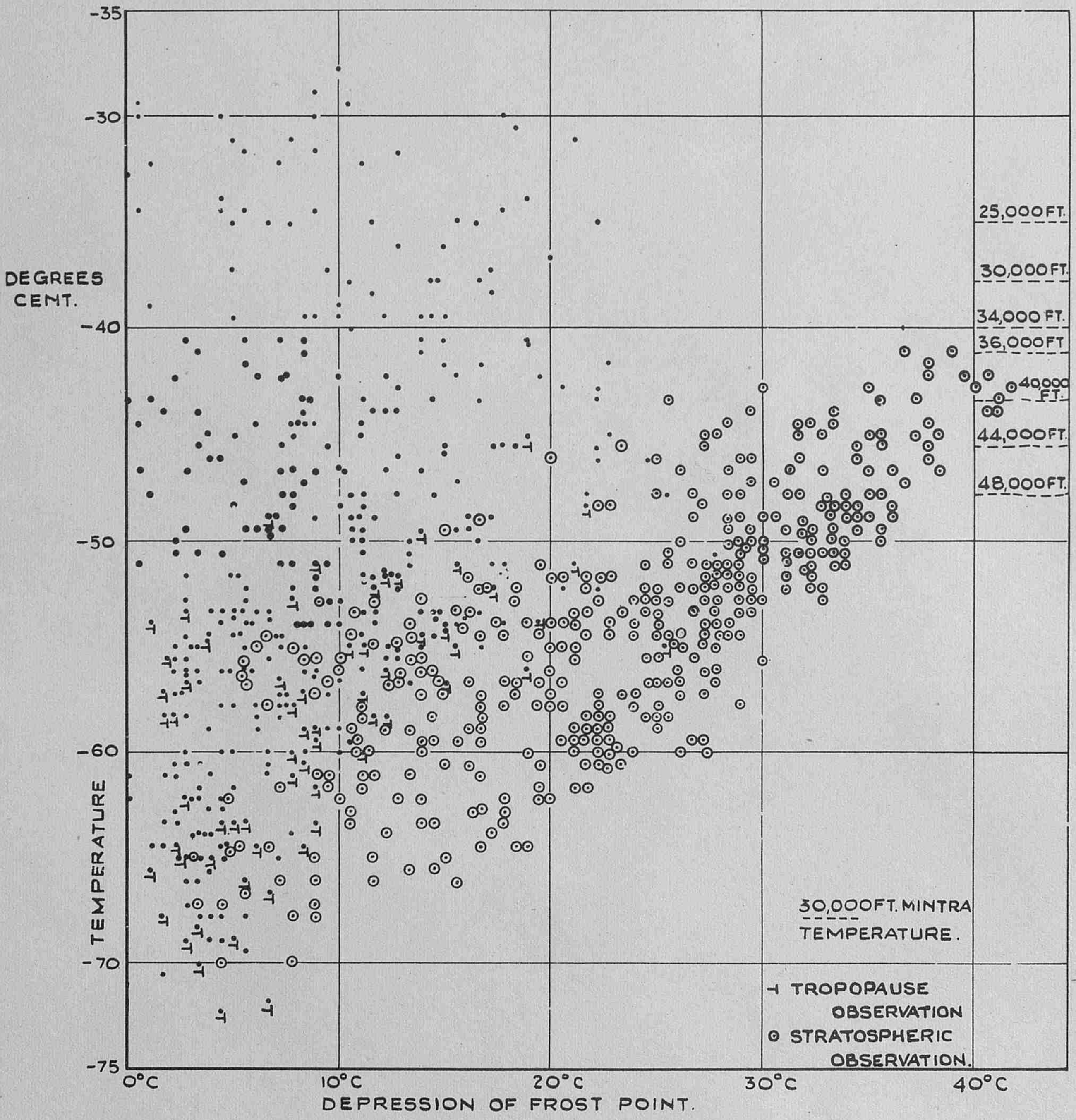

FIG. 9. 81 HIGH LEVEL ASCENTS ABOVE 25000 FT.

M.R.P. 980
S.C.III/207
30th April, 1956.

AD223122

Further observations of large cumuliform clouds by the Meteorological Research Flight.

by

G. J. Day.

(Meteorological Office)

AIR MINISTRY

METEOROLOGICAL RESEARCH COMMITTEE

At the time of issue this report has not been published. Any author desiring to quote this paper should refer to it as "A paper of the Meteorological Research Committee (London), M.R.P. No. 980 by Mr. G. J. Day. A copy is available in the Library of the Meteorological Office."

M.R.P. 980
S.C.III/207
30th April, 1956

AIR MINISTRY

METEOROLOGICAL RESEARCH COMMITTEE

Further observations of large cumuliform clouds by the Meteorological Research Flight

by

G.J. Day (Meteorological Office)

1. Summary

The results of nine flights made to investigate the structure of selected cumuliform clouds are discussed. These flights were designed to provide information on the variation of cloud parameters with time and space separately as distinct from the simultaneous variation characteristic of the flights reported in (1).

It is tentatively concluded that water contents of the order of 5.0 gm.m^{-3} exist in limited regions in the large convective clouds of temperate latitudes and that droplet coalescence plays an important part in the mechanism of shower production. Some support is found for the "bubble" theory of convective cloud structure.

2. Introduction

Since the life of the average cumulus cell is about 30 min. and a horizontal traverse of the cloud by an aircraft occupies about 5 min. it is not possible to obtain detailed information of the development of the whole cell with one aircraft. It therefore becomes necessary to restrict the investigation to one level and ultimately to combine the results of several series of investigations each restricted to a particular region of the cloud.

In this series, therefore, each flight was concerned with a particular level within the top third of an initially well developed cumulus cloud. In some cases radar echoes from the cloud were photographed by the East Hill Weather Radar station (near Dunstable, Beds.).

Since the data accumulated in this study are very extensive it has not been possible to discuss them in detail in this paper which should be regarded as a preliminary summary of the main findings. It is hoped in the future to supplement this paper with a series of supporting papers each dealing with one of the main aspects of the work in greater detail than is here possible, and drawing on the further results of the continuing investigation.

3. Aircraft instrumentation

This was in the main similar to that discussed in (1) i.e., measurements were made of temperature, humidity, height, airspeed, vertical acceleration, water content, rate of icing, size and nature of particles. There were certain improvements in technique:-

(i) Except for the size and nature of particles and vertical acceleration all the quantities measured were displayed on an automatic observer panel and photographed at 5 sec. intervals throughout the traverse.

/(ii)

(ii) Humidity of the environment was measured with an automatic frost-point hygrometer of the type described in (2), as well as with the manual frost-point hygrometer.

(iii) Vertical motion of the aircraft was obtained in some cases by integration of the accelerometer trace and in the remainder by a modification of the method used in (3). This matter is discussed further below.

(iv) Temperature measurements were made with an axial vortex thermometer of the type described in (4). This instrument has limitations when used in cloud, particularly in icing conditions, but its use represents an advance on that of the flat plate type. There is further discussion of this aspect below.

(v) After several tests in flight and in the wind tunnel it was decided to use oil as the sampling medium in droplet-impactors rather than magnesium oxide since oil permits the sampling of considerably larger droplets and also avoids the necessity for an empirical relationship between size of crater and size of droplet. The system at present in use still has a number of defects which are discussed further below.

4. Operational procedure

It was customary for the aircraft to climb from base towards East Hill, observations being made of temperature and frost-point at 500 ft. vertical intervals throughout the layer affected by convection. Visual observations of cloud were made as appropriate.

In the vicinity of East Hill a cumulus cloud approaching maturity and reasonably isolated from its neighbours was selected and identified by the East Hill radar. Traverses through cloud were made as far as possible between the same two air positions and at a constant nominal height which was chosen so that a representative range of temperature should be covered in the series of investigations. Traverses were commenced about 5 min. after the cloud had appeared at the height of the traverse and continued until the cloud could no longer be positively identified or until it had passed through at least one cycle of growth and decay. During each traverse observations were commenced 1 to 2 min. before cloud was entered and continued for a similar period after it had been left; photographs were taken of the cloud as it was approached.

During the traverses East Hill radar maintained a watch on the cloud under investigation and Farnborough long range radar maintained a safety watch on the aircraft.

5. Treatment of results

Each flight has been analysed separately and in considerable detail but it is obviously not possible to present the separate analyses in a paper of this type. For the purpose of this preliminary report it has been considered more suitable to summarise the measurements in tables of mean and extreme values of the more important parameters. These tables, numbered 1 to 9, are given in an appendix.

In subsequent sections the individual analyses have been considered as a whole and the data discussed with particular reference to the following topics:-

a. General - including structure, life cycle, heights of base and top of the clouds examined and their relation to relevant soundings

b. Composition

/c.

c. Vertical motions and turbulence

d. Water content and icing

e. Temperature

f. Additional information

the interpretation of the observed facts being a provisional one. Each of these sections is now considered in detail:-

General

(i) Structure. The clouds investigated usually consisted of a cloudy region of small water content, small and randomly distributed vertical motions, and low droplet concentrations, in which was set an actively developing entity of higher water content and organized vertical motion. These active regions, which are sharply defined, are termed cells.

Usually only one cell was encountered during a traverse, the diameter of which was so large in comparison with the diameter of the cloud as to make it evident that there was in fact only one cell present. On two occasions, however, the aircraft passed through two separate cells, and it is impossible to be certain that these were the only ones in the cloud.

Cells usually had a horizontal dimension of 2 to 3 mi. but exceptionally they were as large as 5 mi. or as small as 1 mi. Where there was more than one cell, they were never more than 2.5 mi. across.

The cloudy region around the cell was of varying horizontal dimension and the cell was usually asymmetrically situated in it. The general trend with time was for the cloud to be identical with the cell at first and for the surrounding cloudy region to grow with time during the development of the cloud. Generally the cloudy region was much narrower on one side of the cell than the other.

Horizontal dimensions of the cloudy regions were usually 0.5 to 1 mi. on the narrow side, and 2 to 5 mi. on the wide side, though on occasions the wide region was between 4 and 7 mi. across.

(ii) Life cycle. The usual life cycle of the cell appears to be between 20 and 25 min. rising occasionally to 30 to 35 min. In the case of the cell of small horizontal dimension the life may be between 10 and 15 min. This is consistent with the erosion process proposed in (5).

(iii) Bases and tops. The cloud observations made are summarised in Table 10 together with the base and top levels calculated by the "parcel method". The height of base was obtained from the temperature and humidity observed at the nearest synoptic station, while the height of the tops was deduced entirely from the temperatures at the base of the cloud and above, as observed from the aircraft. The calculated heights of base were in error by between 200 and 1,700 ft. in either direction, the most frequent errors being about 550 ft. above the observed level and about 1,100 ft. below.

Determinations of the level of tops can often be made very accurately when one allows for the fact that quite small variations in the stability of the environment are often sufficient to stop the vertical development, but when the parcel method is applied strictly errors of several thousand feet may easily be made. The conclusion is that the excess of virtual temperature suggested by the parcel method is not realised throughout the entire cloud and that near the top the cloud is of considerably lower buoyancy than might be expected. In such conditions small stabilisations of the temperature-lapse would be sufficient to retard development.

On several occasions the atmosphere became very dry above 10,000 ft. but this does not seem to have retarded development. It appears from this that entrainment into the upper portion of a cloud is not a significant feature in vertical development and, therefore, that it is of small magnitude.

(iv) Other clouds. On most occasions thin layers of stratocumulus and altocumulus lay around the cumulus. These layers were invariably to be found at the base of a shallow region of stabilisation of the temperature-lapse revealed by the aircraft sounding though not shown in the routine radio-sonde sounding. On a few occasions a very thin layer of cirrostratus was observed at the level of the highest tops and this again was usually to be found in such a region of greater stability.

On a very few occasions there was a shear in the vertical of the horizontal wind field some 50 mb. below the stratocumulus layer.

Observations of layer cloud are summarised in Table 11.

The findings above, though more detailed, agree broadly with those of (1). There is a divergence on the accuracy of the forecasts of base and tops though this may be ascribed to small personal errors in the application of the parcel method, emphasising the large subjective element in its application.

Composition

(i) Certain comments are necessary in respect of the sampling of cloud-particles:-

Tests in the wind tunnel of all the types of impactor used by M.R.F. during the past four years suggest that these instruments are affected by splash to some extent, particularly in clouds of high water content and when the period of exposure is long.

A further defect arises when ice crystal or mixed water droplet and ice crystal clouds are sampled, since, unless precautions are taken to maintain the sampling oil at a temperature below 32°F. until the sample has been photographed, many of the ice crystals melt and spurious distributions of droplet diameter result (6).

Both defects lead to distributions falsely biased toward the larger droplet diameters. Improvements subsequent to this work have largely eliminated errors arising from splash, and development of the microphotographic equipment by Abel (6) has shown how the melting of sampled ice crystals may be avoided.

In the examination, therefore, of droplet samples care has been taken to reject all those which may have been affected by splash or by the melting of crystals. As a result droplet information is biased toward pure droplet cloud and clouds of low water content and generalisation from this evidence is difficult.

Some representative drop-size spectra are shown in Fig.3 and a brief statement of the distribution of droplet diameters as observed in each flight is given in Tables 1 to 9.

Within the limitations of the sampling system, and those imposed by the considerable scatter of the results, it appears that, in the top third of the clouds examined and between the temperatures 0° and 18°F., droplets were most numerous and most uniform in size in the body of the cloud early in development. In the later stages the droplet-size spectra became "stepped" - suggestive of coalescence - and the concentration of droplets less, the largest droplets then being observed in updraught regions. At the edges of the cloud droplet spectra were usually not stepped and concentrations and diameters much less than in the body of the cloud. Variations in both diameter and concentration were often very great over distances of the order of 500 ft.

Maximum droplet diameters in the body of these clouds were about 40 μ at first and became 60 to 80 μ about five min. after the cloud had appeared at the height of traverse; 5 min. later droplet diameters of 60 to 80 μ were common and those of 90 to 120 μ were often observed, this latter range of sizes becoming common a further 5 min. later. Diameters of 120 μ were rarely exceeded but observations of droplet diameters of up to 350 μ have been made.

(ii) The technique at present in use at M.R.F. for the sampling of ice crystals is the "replica" technique due to Schaefer (7). As used at M.R.F. it is thought that the crystals are damaged in the sampling process and that the strength of the sampling solution used had been incorrectly chosen. Information provided by crystal sampling in these flights therefore, is limited to occurrence and probable size. Within the temperature range concerned in these flights crystals rarely appeared less than 10 min. after appearance of the cloud at the height of the traverse but usually grew rapidly thereafter, often reaching overall diameters of 50 μ in periods of the order of 5 min. The subsequent aggregation of simple crystals into snow appeared to take much longer.

Crystals were rarely observed at temperatures above 10°F.; when they were, it was late in the life of the cloud when degeneration was advanced. At temperatures below 10°F. crystals were numerous and appeared early in the life of the cloud, though Flight 4 was anomalous in that no crystals were observed although the temperatures observed were between 5 and 9°F. This must presumably be ascribed to a lack of freezing nuclei on this occasion. These observations agree well with those of (8a).

(iii) In general it is probable that the usual rain-producing mechanism in these convective clouds was a combination of the Bergeron and coalescence mechanisms. The usual process appears to have been the rapid growth of cloud droplets by coalescence to about 100 μ diameter in 8 to 10 min. after the appearance of the cloud at the height of the traverse, and the onset of crystallization at temperatures below 10°F. thereafter. The aggregation of simple crystals in the development of the snow stage and subsequent production of rain seemed to take about 15 to 20 min. after the initial appearance of droplets of 100 μ diameter. Where coalescence alone operated the mechanism usually took about 15 to 20 min. to produce rain at the height of the traverse.

Droplet-diameters of 100 μ appeared to be critical in rain production where the Bergeron mechanism operated; it is suggested that this diameter is associated with the probability of nucleation at the temperatures commonly associated with shower production (8b).

Summarising then, the Bergeron mechanism appeared to operate at temperatures below 10°F. and through the intermediate formation of droplets of about 100 μ diameter by the coalescence process, the whole process taking about 30 min. At temperatures higher than 20°F., production of rain seemed to be by the coalescence mechanism alone and the process took about 20 min. Between 10° and 20°F. the coalescence process predominated in the production of rain and the Bergeron mechanism commenced late in the life of the cloud and tended to assist in its dissipation.

/A

A similar conclusion reached by Murgatroyd (9) was based on the fact that mean temperatures of crystallisation of cumuliform clouds are in the range 0° to 10°F. whereas according to the data in (10) the mean temperature in the tops of cumuliform clouds which produce rainfall is of the order of 20°F.

Vertical motions and turbulence

The problem of obtaining information about the field of vertical motion through which an aircraft passes is of extreme difficulty. It was customary earlier (1) to obtain vertical velocity from the record of the aircraft's height and airspeed, thus following the procedure used in Project Thunderstorm (3) but this is a rather crude method and at best yields values of vertical velocity averaged over 5 sec. intervals.

Two methods of computing vertical velocity have been used in this series of flights. In the first, vertical velocities have been derived from height and airspeed variations, but with allowance made for changes in aircraft attitude in the pitching plane by reference to the results of a secondary experiment. In this latter experiment the change in airspeed after various intervals consequent on a sudden change of attitude was determined in nominally still air. Again the information is coarse and rather inaccurate but all observations are used whereas in (1) those in which airspeed varied were rejected.

The second method was used for those flights for which accelerometer traces were available. If it is assumed that an aircraft responds instantaneously and accurately to the vertical velocity field through which it moves, and further that an accelerometer mounted at the centre of gravity of the aircraft responds similarly to consequent vertical accelerations of the aircraft, then the vertical velocity field may be obtained by simple integration of the accelerometer trace. This is the method adopted; a similar one was used by R.F. Jones (11).

In fact the response of an aeroplane to a gust of the simplest form is extremely complicated and the response of available accelerometers to a series of accelerations is far from accurate. The present position is that even were an ideal accelerometer and the complete range of aerodynamic constants for the aircraft used, and the variations of aircraft speed and attitude known, the field of vertical motion could still not be computed, even at considerable expenditure of effort, because of other uncertain factors arising from aircraft structural response. The problem has been reviewed recently in (12) and (13).

Since no better method at present exists we have assumed in the present series of flights that the velocity can be obtained by simple integration of recorded acceleration. Although the procedure is at best inaccurate, it appears that the inaccuracies are likely to be smaller than those inherent in the first method and that, in particular, the fine structure of the field of vertical velocity will be more accurately given. The conservative nature of the form of the integral trace in some of the flights is taken to support this view.

Within these limitations, then:-

(i) The maximum updraught observed was about 32 ft. sec.$^{-1}$ and the maximum downdraught about 40 ft. sec.$^{-1}$. The average maximum strengths were 23 ft. sec.$^{-1}$ upwards and 21 ft. sec.$^{-1}$ downwards. Mean vertical motions over the whole cloud width ranged from about 1 ft. sec.$^{-1}$ in both senses in advanced decay to about 10 ft. sec.$^{-1}$ in both senses at the peak of development. Motions were usually clearly defined in growth but weak and randomly distributed in decay, save where there was precipitation when downwards motions were well organized. At the onset of decay there was often a very rapid change from predominantly upward to predominantly downward motion.

On most occasions significant vertical motions were confined to cloud and they were of similar strength and horizontal extent irrespective of sense. On a few occasions there were vertical motions outside the cloud which were of comparable strength and horizontal extent to those within. These were apparently associated with the cloud, since they occurred only in air fairly close to it, and were usually encountered during the decay of the cloud. Some clouds were composed of a well defined draught and had weak compensating motions around them. These were the cases where a sudden change in the sense of motion occurred at the onset of decay and the clouds were invariably single celled.

In some cases, then, there appeared to be little interaction between the cloud and its environment in the region of the investigation - the upper third of the cloud; in a few cases there was an interaction and these were usually multi-celled clouds.

In general the draught had a horizontal dimension of about 1 to 2 mi. with fine structure on the scale of 500 to 1,000 ft., many features of which were conserved from one traverse to the next. It seems reasonable to regard the draught as defining the cloud cell and to attribute the fine structure to the presence of convection bubbles constituting the cell.

There is some evidence to suggest that fresh development was usually on the upshear side of the cloud.

(ii) Turbulence was invariably greatest in the cloud; vertical accelerations rarely exceeded 0.5g. (at 170 kt.) and were usually about 0.2g. The maximum value observed was 0.7g. These accelerations were almost invariably associated with regions of high horizontal gradient of vertical velocity and therefore with multi-celled clouds or single-celled clouds near maturity.

These conclusions are in agreement with those of (1) though more detailed. They appear to accord well with (5) though the difficulty of measuring vertical motion in cloud is reflected in the imprecision of most of the conclusions.

Water content and icing

(i) The maximum water content of clouds which could be measured by M.R.F. at this time was about 2gm.m.$^{-3}$ with the rotating disc icing meter and about 1.8gm.m.$^{-3}$ with the heated cylinder instrument. The maximum theoretical water content which is to be expected in convective clouds of temperate latitudes is of the order of 5 gm.m.$^{-3}$ but such values should be fairly limited in space and probably time, and the available instruments have sufficient capacity for the great majority of encounters.

For the flights of this series each observation of water content or icing rate has been reduced to a percentage of the maximum theoretical amount to be expected on the occasion, and its position given as a percentage of the cloud width and depth. On the basis of these figures a smooth non-dimensional model has been constructed and from it computed the distribution of water content to be expected in a convective cloud having its base at 900 mb. and a temperature of 60°F. and its top at 400 mb.; these models are given in Figs. 1 and 2 respectively, and have previously been discussed by Murgatroyd (9). The water content contours shown are similar to these given by Zaitsev (14).

From Fig. 2 it is seen that water contents of the order of 5 gm.m.$^{-3}$ might be expected in a central region of such a cloud at a height of about 75% of the cloud depth (about 16,000 ft.) and extending over about 25% of cloud width (about 1 mi.). A fairly uniform gradient of water content is found over the greater portion of the cloud but greatly increased gradients are found in the outer regions. At the vertical edges and at the base the increased gradients extend over a thickness of about 8%, whilst at the top the gradient in the uppermost 25% is notably greater than elsewhere in the cloud, again increasing markedly in the uppermost 4% of cloud depth.

These findings are somewhat similar to those of (1), but of more exact form. It seems likely that there is support here for (5) and that the outermost regions of high gradient of water content may be ascribed to those in which the purely aerodynamic erosion forces operate, the thinner uppermost surface being consistent with the continual renewal of this region from within the cell. It seems possible that the slacker internal gradients may be ascribed to diffusion of the modified boundary air into the main body of the cloud.

Detailed examination of the individual flights shows that water contents approaching the maximum theoretical amount may be encountered more than once during the life of a particular cloud; in Flight 7, such values were found for almost the whole life -about 20 min.- of the cloud, which produced a shower by the coalescence mechanism.

It must be mentioned that the later conclusions above are dependent on the assumption that all flights passed through the central region of the cloud: any transverse displacement of the flight path introduces an uncertainty. Such a shift of flight path undoubtedly occurs in some instances though it is not felt that the general conclusions are invalidated in any way. When more flights of this type have been made a non-dimensional approach to the time variation such as that applied to the space variation will be possible.

(ii) Airframe icing was encountered at temperatures between 28° and 7°F. (no flights were made at temperatures below the latter value). Icing was encountered during the greater part of the life of the convective cell and it appeared, therefore, that material advance of glaciation normally heralded a rapid decay. A noteworthy observation was that of heavy icing over a period of about 57 min. at a temperature of about 7°F. during Flight 4; this period is much in excess of those normally observed by M.R.F. and must presumably be associated with a deficiency of freezing nuclei.

It seems, then, that in cumulus such as those investigated the probability of icing is high during the greater part of their lives, but becomes small when decay commences. Whilst ice accretion will normally be small due to the small horizontal extent of the cloud it may on occasions be large where extremely high values of water-content are encountered.

Temperature

It seems likely that in droplet cloud above freezing point a vortex thermometer of the type used consistently under-reads by a small amount but that in icing conditions its behaviour is not straightforward. In the flights of this series icing conditions were common and excesses over environment temperature consistent with parcel method calculations were observed. The temperature traces show peaks which are roughly symmetrical with respect to the cell which suggests that any reduction in amount of correction due to the partial blocking of the entry by ice did not contribute to the apparent temperature rise in cloud, i.e. it must to a certain extent have been real. It seems reasonable, then, to accept the indicated cloud temperatures as minima accurate to at least 1 or 2°F.

In general it appeared that in the earliest stages of growth there was invariably a good agreement between the strength and direction of vertical motions and the excess or deficit of cloud-temperature over environment-temperature. Where the structure of the cloud was simple the agreement became less good as maturity was approached and weakly negative as decay became established.

Where the cloud structure was complicated the agreement very rapidly ceased to be good and there then appeared to be no relation between temperature contrasts and the vertical motion.

A typical variation of temperature excess appeared to be a steady increase from 0.3° to 2.5°F. during growth, (the corresponding excess to be expected from calculation by the parcel method being about 5°F.) and a fairly rapid decrease to about -1.5°F. in decay, the whole process taking about 25 min. Updraughts were warmer than the rest of the cloud which was usually warmer than the environment by a similar amount so that the excess of temperature in the updraught was probably about the value to be expected from the parcel method except near the top of the cloud.

An attempt was made by Murgatroyd (9), on the basis of the observations of this series of flights, to obtain a relationship between the vertical velocity, w ft.sec.$^{-1}$, and the excess of virtual temperature, Δ T°F. - corrected for the weight of suspended water -, and a relationship

$$w = 14\sqrt{\Delta T}$$

was suggested. There was a large scatter of the observations due to their small number but it seems that this will be a profitable avenue of enquiry when more observations with better instruments are available.

Other observations

(i) The clouds investigated were of a simpler structure generally than those reported in (1) and electrical activity was small. Precipitation static was reported early in Flights 2, 3 and 9, which were made through multi-celled clouds in which droplets of about 100 μ diameter or larger co-existed with crystals about 50 μ in diameter or larger. These observations are consistent with the hypothesis that electrical activity is characteristic of clouds in which the Bergeron and the coalescence mechanism of rain production are both operating, as suggested by workers at the New Mexico School of Mines (19) and others.

(ii) Radar echoes were observed from the cloud of Flight 2 alone. This contained snow for a considerable period but other clouds not giving an echo also had a snow stage though not so marked. The cloud of Flight 2 is distinguished from the others of the series in that it contained an appreciable fraction of droplets of diameter between 100 and 200 μ .

(iii) Visibility in cloud was usually estimated to be 5 to 20 yd. in periods of growth and rose to 100 to 300 yd. in decay. The smallest visibilities were observed where there was a large number of the very small droplets.

Tests of Trabert's formula, as modified by Best (18), using measured water contents and droplet diameters and estimated visibilities, when these were obtained simultaneously, suggested that the calculated visibilities were probably too great by a factor of about three. Visibilities used were those less than the semi-span of the aircraft and the estimates should be reasonably accurate. The number of these observations is rather small at present and they are biased towards small visibilities so that a definite statement on this matter is not justified.

/7.

7. Discussion

As was stated in (1) the object of this work is to obtain a knowledge of the various cloud parameters and the manner in which they develop during the life of the cloud.

Since the work reported in (1) the technique of investigation has been improved though it is still inadequate. It is obvious that several more such series of flights will be necessary, each devoted to a particular region of the cloud, in order that the generalisations made above may be extended from the upper portion of the cloud to the whole structure. Without a very large aircraft commitment and a complex organization of research it is inevitable that information will remain largely statistical and indeed this seems desirable as the considerable differences between clouds prevent progress by the complete investigation of a very few clouds. An investigation blending the type of observation described in (1) and those described above will obviously be ultimately necessary.

In the instrumental field it has become obvious that considerable difficulties exist particularly in the measurement of temperature and vertical motion and the sampling of ice crystals. Although in the flights reported above the measurement of water content was satisfactory it has recently been improved considerably at M.R.F. by the introduction of a heated wire water content meter and a refrigerated rotating disc icing meter. Moderately detailed observations of liquid water content up to 5.0 $gm.m.^{-3}$ are now possible and amounts up to 2.5 $gm.m.^{-3}$ may now be measured on the scale of about 800 ft.

Sampling of cloud droplets and raindrops has been refined considerably since this series of flights but that of ice crystals is still not satisfactory. Although no progress is expected immediately in the measurement of temperature and vertical motion it is hoped that methods currently being explored will prove profitable.

8. Conclusions

The more important features of the large convective cloud over southern England suggested by these flights appear to be:-

a. The importance of the coalescence mechanism in advance of the Bergeron mechanism in shower production and the possibility that on occasions the coalescence mechanism alone may operate at the higher temperatures in these latitudes.

b. The probability that water contents approaching 5.0 $gm.m.^{-3}$ exist in these clouds over a small region in time and space. This has since been directly confirmed by the author (17).

c. The association of turbulence in cloud with strong gradients of vertical motion and hence with multi-celled clouds or simple clouds entering the precipitation stage.

d. Support, from measurements of vertical motion and of water content, for the structure of convective cloud in accord with the "bubble" theory.

e. The absence of marked vertical motions outside cloud and the balance of vertical motions within the cloud, suggesting a rather weak interaction of the cloud with its environment, that is, small entrainment and detrainment motions. There is some support for this contention from radar observations.

f. The dependence of electrical activity on the co-existence of large droplets and large crystals in the cloud.

These conclusions are in general agreement with those of (1) and it is hoped that they will be examined in the future at greater length together with data from further flights of this nature in a series of supplementary papers.

9. Acknowledgments

Acknowledgment is due to those members of M.R.F. who assisted in the basic analysis of the formidable body of data accumulated and in particular to Mr. R.J. Murgatroyd, S. Met. O., M.R.F., who made several of the suggestions on which this work is based and who participated in the detailed analysis.

10. References

1. Day, G.J. and Murgatroyd, R.J. 1953 Meteorological Research Papers, Air Ministry, London, No. 826.

2. Palmer, H.P. 1952 Meteorological Research Papers, Air Ministry, London, No. 774.

3. Weather Bureau, Washington, D.C. 1949 The Thunderstorm.

4. a. Ruskin, R.E. Schechter, R.M., Dinger, J.E. 1952 N.R.L. Report 4008.

   b. Murgatroyd, R.J. 1955 (unpublished).

5. Ludlam, F.H. and Scorer, R.S. 1953 Q.J. Roy. Met. Soc., 79, 341, p.317.

6. Abel, G.C. 1954 AAEE/Res./278.

7. Schaefer, V.J. 1949 Chem. Res., Baltimore, 44, p.291.

8. a. Day, G.J. 1954 Meteorological Magazine, 83, 986, p.230.

   b. Bigg, E.K. 1953 Proc. Phys. Soc., 66, B, p.688.

9. Murgatroyd, R.J. 1954 Meteorological Magazine, 83, 985, p.208.

10. Petterssen, S., Knighting, E., James, R.W., Herlofson, N. 1946 Geofys. Publ., Oslo, 16, No.10.

11. Jones, R.F. 1955 Quart. J. Roy. Met. Soc., 80, p.377.

12. Hollings, W.E.H. 1955 Quart. J. Roy. Met. Soc., 81, 347, p.121.

13. Malkus, J.S. 1955 Quart. J. Roy. Met. Soc., 81, 347, p.122.

14. Zaitsev, V.A. 1953 Tech. Trans., N.R.C.C., Ottawa, No. TT - 395.

    Original in Russian 1949 Trud. glad. geofiz. Obs., Moskva, 81, p.122.

15. Scorer, R.S. and Ludlam, F.H. 1953 Quart. J. Roy. Met. Soc., 79, 339, p.96.

16. aufm Kampe, H.J. and Weickmann, H.K. 1952 J. Met., 9, 3.

17. Day, G.J. 1955 Meteorological Research Papers, Air Ministry, London, No. 916.

18. Best, A.C. 1953 J. Met., 10, 3.

19. Thunderstorm Final Report, Appendix D, (New Mexico School of Mines Research and Development Division, 1951).

Table 1

10/6/53

Main features of cloud investigated in Flight 1

Run	1	2	3	4	5	6
Maximum water content, gm. m.$^{-3}$	1.06	> 1.8	> 1.8	> 1.8	> 1.8	> 1.8
Mean water content, gm. m.$^{-3}$	0.30	0.37	0.64	0.59	0.60	0.33
Icing, Yes or No	Yes	Yes	Yes, 1/16in. clear on airframe	Yes, on airframe	Yes, clear airframe, windscreen	Yes, windscreen
Mean height, ft. (ICAN)	13,870	13,640	13,537	13,544	12,965	12,446
Height variation, ft.	+20 -30	+120 -130	+113 -77	+206 -64	+685 -435	+124 -166
Mean airspeed, kt.	182	174	181	172	180	179
Airspeed variation, kt.	+3 -2	+8 -4	+5 -7	+10 -14	+10 -10	+6 -4
Mean temperature, °F.	+18.1	+18.2	+19.3	+18.1	+16.5	+16.1
Temperature variation, °F.	+1.8 -1.2	+0.9 -1.4	+1.7 -2.6	+0.6 -1.0	+2.5 -2.3	+1.5 -1.3
Maximum excess temperature in cloud, °F.	1.4	1.0	In updraught 2.8 In downdraught -1.5	In updraught 0.9 In downdraught -0.5	In updraught 2.2 In downdraught -2.1	In updraught 1.4 In downdraught -1.5
Average turbulence in cloud, 'g'	0.1-0.2	Not observed		0.1-0.2	0.1-0.2	0.1-0.2

/Precipitation

Run		1	2	3	4	5	6
Precipitation static, Yes or No		No	No	No	No	No	No
Vertical velocity strength. ft.sec.$^{-1}$ Peak:-		(+3 (-4	+25 - 8	+14 -13	+31 -38	+27 -22	+5 -6
Average:-		($+1\frac{1}{2}$ ($-2\frac{1}{2}$	+7 -5	+ 8 - 7	+12 -10	+11 - 9	$+2\frac{1}{4}$ $-3\frac{1}{2}$
(+ve. sign indicates updraught) (-ve. sign indicates downdraught)		Up on west side Down on east.	Mostly up	Whole cloud descending, save for narrow central core 2.5 mi. across	Mostly descending, narrow central core 0.8 mi. across	Generally down, a wide, new ascending cell	Small but mainly down
Crystals. Yes, No		Not observed	Not observed	Not observed	Not observed	Not observed	Not observed
Other observations		-	-	Cloud rising fast	-	Whole cloud rising	Visibility 5yd.
Time, hr.		1616	1619	1624	1629	1632	1638
Extent, mi.		1.8	4.9	2.6 -0.6 Very tenuous to east	2.4 -0.8 Very tenuous to east	8.0 1.5 old cloud, 3.0 new cloud, rest wispy	10.4 2.0 old cloud, 1.0 new cloud, rest wispy
Droplet diameter μ — Volume median:-	at edge	50		20	30	12	
Volume maximum:-	at edge	100		200	100	100	
Distribution stepped at:-	at edge			80%, 40-150 μ		20%,80 μ	
Volume median:-	at centre	30		250	150	130	
Volume maximum:-	at centre	300		300	200	200	
Distribution stepped at:-	at centre	30%, 80-120 μ		30%,80-230 μ	40%,80-140 μ	40%,50-120 μ	

Table 2

8/7/53

Main features of cloud investigated in Flight 2

Run	3	4	5	6	7	8
Maximum water content, gm. m.$^{-3}$	Highest to west 1.37	Highest to east 1.7	Highest to east 0.78	Highest to east > 1.8	Highest to west > 1.8	Highest to east 0.92
Mean water content, gm. m.$^{-3}$	0.75	0.58	0.32	0.46	0.61	0.51
Icing. Yes or No	Yes, clear airframe and windscreen	Yes, heavy clear windscreen and airframe	Yes, heavy on airframe	Yes, rough white on airframe	No	Yes, slight on airframe
Mean height, ft. (ICAN)	10,332	10,110	10,210	10,234	10,147	10,137
Height variation, ft.	+138 -132	+160 -135	+120 -160	+166 -84	+73 -67	+33 -17
Mean airspeed, kt.	173	175	182	173	179	175
Airspeed variation, kt.	+ 7 - 8	+ 10 - 8	+ 6 - 5	+10 - 3	+ 7 - 6	+ 5 - 3
Mean temperature, °F.	21.4	20.8	19.8	19.8	20.6	20.5
Temperature variation, °F.	+1.8 -1.6	+1.1 -1.0	+0.7 -1.3	+0.7 -0.6	+1.9 -1.4	- -
Maximum excess temperature in cloud, °F.	1.2 -0.7 in down-draught	0.3 -0.7 in down-draught	0.1 -0.3 in down-draught	0.4	-	-

Runs 1 and 2 lost through faulty recording gear

/Precipitation

Run	3	4	5	6	7	8
Precipitation static, Yes or No	Yes, intermittent	Yes, intermittent	Yes, continuous	Yes, continuous	No	No
Vertical velocity strength. Peak:- ft. sec.$^{-1}$	(+12.8 (- 5.3	+7.2 -13.1	+7.9 -4.1	+12.0 - 2.4	+5.0 -6.0	- -
(+ve. sign denotes updraught) Average:- (-ve. sign denotes downdraught)	(+ 6.4 (- 2.6	+3.4 -7.2	+3.3 -1.8	+ 4.8 - 1.2	+2.1 -3.6	- -
Average over run:-	3.8 up	3.1 down	2.6 up	3.6 up	1.0 down	-
Crystals. Yes or No	Not observed	Not observed	Yes	Yes	Yes	Yes
Other observations	Vis. 20 yd.	Vis. 50 yd.	Vis. 100 yd.		Vis. 300 yd.	Vis. > 200 yd.
Time, hr.	1600	1607	1615	1622	1631	1637
Extent, mi.	4.5	> 5.0	> 7.8	> 7.8	> 7.6	-
Droplet diameter μ Volume median:- maximum:-) at centre	40-45 60-100	20-150 200-300	20-25 60-100	50 occ. 240	20-30 120	
Droplet diameter μ Volume median:- maximum:-) at edge	20			26 40-60		
Remarks	Radar echoes, pptn. static coincides with snow region	Radar echoes, pptn. static coincides with snow region. Cloud very thin at edge	Radar echoes, pptn. static much stronger, cloud fibrous and decaying	Radar echoes, pptn. static much stronger, cloud very fibrous	No echo. Cloud fibrous and decaying markedly	Cloud degenerated

Table 3 14/7/53

Main features of cloud investigated in Flight 3

Run	1	2	3	4
Maximum water content, gm.m.$^{-3}$	1.50	1.25	1.36	1.15
Mean water content, gm.m.$^{-3}$	0.77	0.42	0.33	0.58
Icing. Yes or No	No	Yes	No	Yes
Mean height, ft. (ICAN)	15028	15339	15430	15520
Height variation, ft.	+ 97 -103	+61 -69	+130 -100	+260 -180
Mean airspeed, kt.	173	173	171	171
Airspeed variation, kt.	+ 7 - 9	+ 5 - 5	+ 9 -10	+ 4 - 5
Mean temperature, °F.	10.0	6.7	7.6	4.2
Temperature variation, °F.	+1.7 -2.1	+2.0 -1.0	+4.9 -1.2	+0.7 -0.7
Maximum excess temp. in cloud, °F	+3.7	+2.1	+6.1	+2.0
Average turbulence in cloud, 'g'	0.2-0.4	0.2-0.3	0.2-0.6	0.2-0.5
Precipitation static. Yes or No	No	No	Yes	No
Vertical velocity strength. Peak:- ft.sec.$^{-1}$	+12 -15	+17 -9.5	+ 9 -10	+ 9 - 5
Average:- Cell (a)	+5.4 -6.2	+9 -5.1	+3.2 -4.1	+4 -2.5
Cell (b)	+4 -1.8			
Crystals. Yes or No	Yes	Yes	Yes	Yes
Other observations	Vis. 20 yd. Freezing rain	Ice 1/8 in. rough white	-	Ice 1/8 in. rough white, small hail
Time, hr.	1651	1657	1701	1709
Extent, mi.	4.6	3.0	5.2	1.6
Droplet diameter μ Volume median:- at centre of cell	75	65	75	85
maximum:- at centre of cell	120	110	130 (occ.220)	110
Distribution stepped at:- at centre of cell			40%, 50 μ	
Volume median:- at edge		23	20	23
maximum:- at edge		35	50	110

Table 4(a) 14/4/53

Main features of cloud investigated in Flight 4

Run	Cell	1	2	3	4	5
Maximum water content, gm. m.$^{-3}$	1	> 1.7	1.06	> 1.8	> 1.8	1.36
	2	0.64	0.39			
Mean water content, gm. m.$^{-3}$	1	0.20	0.12	0.75	0.64	0.40
	2	0.62	0.32			
Icing. Yes or No (both cells)		Yes, heavy	Yes, heavy	Yes, heavy	Yes, heavy	Yes, heavy
Mean height, ft. (ICAN)	1	8999	8946	9162	9204	8998
	2	9048	8978			
Height variation, ft.	1	+202	+ 32	+ 58	+16	+52
	1	− 68	− 28	−112	−14	−18
	2	+ 21	+ 4			
	2	− 19	− 6			
Mean airspeed, kt.	1	179	172	182	184	179
	2	170	171			
Airspeed variation, kt.	1	+ 10	+ 4	+ 8	+ 8	+ 9
	1	− 4	− 4	− 5	− 8	− 4
	2	+ 1	+ 8			
	2	− 1	− 5			
Mean temperature, °F.	1	+8.3	+5.0	+6.8	+7.3	+7.7
	2	+4.4	+7.5			
Temperature variation, °F.	1	+4.0	+2.5	+2.7	+2.1	+2.3
	1	−3.2	−0.9	−3.6	−2.5	−2.7
	2	+3.2	+2.0			
	2	−1.0	−0.8			

/Maximum

G. 58108(d)/PN/4/56/50

Run	Cell	1	2	3	4	5
Maximum excess temperature in cloud, $^{\circ}F$.	Both	1.8 in updraught -2.0 in downdraught	3.0 in updraught -2.4 in downdraught	+2.0 in downdraught	4.7 in updraught -0.8 in downdraught	3.5 in updraught
Average turbulence in cloud, 'g'	Both	0.1 - 0.2, occasionally 0.3	0.1 - 0.2, occasionally 0.3	0.1, occasionally 0.2 - 0.3	0.1, occasionally 0.2 - 0.3	0.1, occasionally 0.2 - 0.3
Precipitation static. Yes or No	Both	No	No	No	No	No
Vertical velocity strength. Peak:-	(1	+ 10	+ 2	+ 32	+ 6	+ 10
ft. sec.$^{-1}$	(1	- 40	- 2	- 20	- 2	- 4
(+ ve. sign denotes updraught)	(2	0	+ 8			
(- ve. sign denotes downdraught)	(2	- 4	- 2			
Average:-	(1	+ 3	+ 1	+ 11	+ 2	+ 3
	(1	- 3	- ½	- 5½	- 1	- 2
	(2	0	+ 4			
	(2	- 2½	- 1½			
Crystals. Yes or No	Both	Not observed	Not observed	Not observed	Not observed	Not observed
Other observations		-	Freezing rain, 3/32 in. ice on props. and wings	-	-	Small hail, 1/16 in. rime and glazed ice
Time, hr.	Both	1147	1153	1200	1205	1212
Extent, mi.	1 2	3.1 2.0	2.6 2.1	4.0	2.8	3.5

/Droplet

Run			Cell	1	2	3	4	5
Droplet diameter	Volume median:-	at centre	1		135	105		310
μ			2			27		30
	maximum:-		1		150	220		340
			2			70		70
	Distribution stepped at:-		1		30%,50-130 μ	50%,110-180 μ		35%,180-300μ
			2					
	Volume median:-	at edge	1			23		
			2					
	maximum:-		1			70		
			2					
	Distribution stepped at:-		1			75%,35-50 μ		
			2					

Table 4(b)

14/4/53

Main features of cloud investigated in Flight 4

Run	Cell	6	7	8	9	10
Maximum water content gm. m.$^{-3}$	1 2	1.8	1.8	1.8	1.36 1.30	0.92
Mean water content gm. m.$^{-3}$	1 2	0.75	0.77 0.85	0.80 0.59	0.40 0.71	0.43
Icing. Yes or No	Both	Yes, heavy	Yes, heavy	Yes, heavy	Yes, heavy	Yes, light
Mean height, ft. (ICAN)	1 2	9213	9013 9000	8999 9016	8995 8998	9004
Height variation, ft.	1 1	+ 7 - 3	+ 6 - 5	+ 5 - 14	+ 7 - 14	+ 2 - 5
	2 2	+ 8 - 13	+ 5 - 3	+ 5 - 3		
Mean airspeed, kt.	1 2	181	182 179	185 183	184 190	181
Airspeed variation, kt.	1 1	+ 4 - 2	+ 3 - 8	+ 5 - 4	+ 6 - 6	+ 9 - 7
	2 2		+ 14 - 13	+ 4 - 3	+ 4 - 3	
Mean temperature, °F.	1 2	+7.0	+7.8 +6.6	+6.8 +8.5	+9.1 +7.3	+8.1

/Temperature

Run	Cell	6	7	8	9	10
Temperature variation, ^{o}F.	1	+1.2	+2.4	+2.0	+1.2	+1.5
	1	-2.4	-5.1	-2.4	-3.0	-2.1
	2		+3.3	+1.7	+1.3	
	2		-3.6	-2.8	-1.1	
Maximum excess temperature in cloud, ^{o}F.	Both	4.2 in up-draught	1.3 in up-draught	4.6 in up-draught -1.2 in downdraught	4.6 in up-draught	3.6 in up-draught
Average turbulence in cloud, 'g'	Both	0.1 - 0.2, occasionally 0.3	0.2 - 0.3	0.1 - 0.2, occasionally 0.3	0.1 - 0.2	0.1 - 0.2, occasionally 0.3
Precipitation static. Yes or No	Both	No	No	No	No	No
Vertical velocity strength. Peak:- ft. sec.$^{-1}$	(1	+ 2	0	+ 2	0	+ 2
	(1	- 4	- 8	- 2	- 6	- 12
	(2	+ 16	+ 10	+ 1		
	(2	- 12	0	- 2		
Average:- (+ ve. sign denotes updraught) (- ve. sign denotes downdraught)	(1	$+\frac{1}{2}$	0	+ 2	0	$+\frac{1}{2}$
	(1	- 2	- 3	$-\frac{1}{2}$	- 5	- 4
	(2		$+4\frac{1}{2}$	+ 3	$+\frac{1}{2}$	
	(2		- 4	0	- 1	
Crystals. Yes or No	Both	Not observed	Not observed	Not observed	Not observed	Not observed

/Other

Run			Cell	6	7	8	9	10
Other observations					1/8 in. ice. Vis. 10 yd. Freezing rain	3/4 in. ice on leading edge. New cloud top developing	Freezing rain. 1 in. ice, rough	$1\frac{1}{2}$ in. ice
Time, hr.				1220	1230	1235	1244	1252
Extent, mi.			1	2.8	3.7	3.0	3.1	3.6
			2		5.5	2.8	4.1	
Droplet diameter μ	Volume median:-	at centre	1		160			
			2		30		15	
	maximum:-		1		180			
			2		70		35	
	Distribution stepped at:-		1		12%,50-150 μ			
			2					
	Volume median:-	at edge	1					
			2				20	
	maximum:-		1					
			2				25	
	Distribution stepped at:-		1					
			2					

Table 5(a) 13/4/53

Main features of cloud investigated in Flight 5

Run	1	2	3	4	5
Maximum water content gm.m.$^{-3}$	1.36	> 1.7	1.06	1.06	0.78
Mean water content gm.m.$^{-3}$	0.40	0.98	0.48	0.47	0.24
Icing. Yes or No		Yes	Yes	Yes	Yes
Mean height, ft. (ICAN)	7746	7767	7740	7757	7746
Height variation, ft.	+ 4 - 6	+133 - 27	0 0	+ 23 - 7	+ 4 - 6
Mean airspeed, kt.	181	184	186	184	183
Airspeed variation, kt.	+ 6 - 10	+ 8 - 12	+ 4 - 6	+ 5 - 3	+ 7 - 2
Mean temperature, °F.	+16.0	+16.5	+17.8	+17.0	+18.2
Temperature variation, °F.	+1.2 -0.7	+0.6 -1.4	+2.0 -1.8	+0.7 -0.5	+1.4 -1.5
Maximum excess temperature in cloud, °F.	1.0	1.0	2.4		1.6
Average turbulence in cloud, 'g'	0.1	0.1	0.1	0.1	0.2
Precipitation static. Yes or No	No	No	No	No	No
Vertical velocity strength. ft. sec.$^{-1}$ Peak:-	(+ 10 (- 14	+ 26 - 8	+ 10 - 11	+ 11 - 5	+ 8 - 10
Average:-	(+3.0 (-3.5	+5.5 -3.5	+4.5 -4.0	+4.5 -2.5	+3.0 -4.0

/Crystals

Run		1	2	3	4	5
Crystals. Yes or No		Not observed	Not observed	Not observed	Not observed	Not observed
Other observations				Mixed, 3/32 in. thick. Rime and clear	Rime and clear ice mixed, 1/16 in. thick. Vis. 5 yd.	Clear ice 1/32 in. thick. Vis. 50 yd.
Time, min. from appearance of cloud at traverse height (1130Z)		0+5	0+12	0+19	0+27	0+34
Extent, mi.		6.0	7.4	2.8	2.6	2.3
Droplet diameter µ	Edge	Largest 50, most 20 or smaller	Mostly 20-10	Largest 50, most 10		
	Centre		Largest 85, mostly 20		Largest 80 most 35 or less	Largest 180 but occ. 320. Most 40-20

Table 5(b)

13/4/53

Main features of cloud investigated in Flight 5

Run	6	7	8	9
Maximum water content, gm.m.$^{-3}$	1.20	> 1.8	> 1.8	1.06
Mean water content, gm.m.$^{-3}$	0.74	0.66	0.75	0.36
Icing. Yes or No	Yes	Yes	Yes	Yes
Mean height, ft. (ICAN)	7743	7745	7748	7764
Height variation, ft.	+ 7 − 3	+ 5 − 5	+ 2 − 8	+ 96 −124
Mean airspeed, kt.	178	176	178	184
Airspeed variation, kt.	+ 4 − 8	+ 5 − 5	+ 4 − 4	+ 3 − 4
Mean temperature, °F.	+18.5	+17.1	+17.3	+18.5
Temperature variation, °F.	+0.6 −1.6	+1.1 −1.2	+0.6 −0.7	−0.7 −1.0
Maximum excess temperature in cloud, °F.	2.0	2.0	2.0	1.8
Average turbulence in cloud, 'g'	0.2	0.2	0.1	0.1
Precipitation static. Yes or No	No	No	No	No
Vertical velocity strength. ft. sec.$^{-1}$ Peak:-	+ 11 − 18	+ 6 − 5	+ 10 − 6	+ 11 − 20
Average:- (+ ve. sign denotes updraught) (− ve. sign denotes downdraught)	+4.5 −4.5	+4.0 −3.5	+4.0 −2.5	+3.5 −6.5

/Crystals

Run		6	7	8	9
Crystals. Yes or No		Not observed	Not observed	Not observed	Not observed
Other observations		Vis. 5 yd.	1/8 in. glazed ice. Vis. 5 yd.	Vis. 5 yd. 3/32 in. ice. Freezing rain	
Time, min. from appearance of cell at traverse height (1130Z)		0+43	0+50	0+56	0+62
Extent, mi.		2.0	2.7	3.0	2.3
Remarks		Tops flattening out.	Tops flattening, anvil to south		Tops fibrous
Droplet diameter μ	Edge		30 - 20	Largest 70, most 20	Largest 50, most 20 or less
	Centre	Largest 80, most 20-30	Largest 50, most 30-20	Largest 120, most 30-20	Largest 120 but occ. 260. Most 20 or less

Table 6

Main features of cloud investigated in Flight 6

Run	1	2	3	4	5	6	7	8
Maximum water content, $gm.m.^{-3}$	1.20	1.20	1.20	1.20		0.28	1.36	1.36
Mean water content, $gm.m.^{-3}$	0.45	0.45	0.72	0.52	Recorder film fogged, record lost	0.09	0.34	0.52
Icing. Yes or No	Yes	Yes	Yes, slight	Yes, slight		Yes, very light	Yes	Yes, slight
Mean height, ft. (ICAN)	10248	10725	10883	10901		10724	10829	10746
Height variation, ft.	+ 52 - 28	+ 55 - 45	+ 57 - 43	+ 89 -101		+ 36 - 94	+ 91 - 98	+ 54 - 66
Mean airspeed, kt.	181	179	179	175		180	178	181
Airspeed variation, kt.	+ 5 - 3	+ 2 - 4	+ 3 - 2	+ 7 - 5		+ 3 - 3	+ 4 - 8	+ 1 - 2
Mean temperature, °F.	+15.4	+14.9	+15.5	+14.7		+16.6	+16.7	+16.7
Temperature variation, °F.	+0.6 -0.8	+0.4 -0.3	+1.0 -0.8	+0.6 -1.1		+0.4 -1.2	+0.9 -0.5	+0.7 -0.7
Maximum excess temperature in cloud, °F.	1.1 in up-draught		1.3 in up-draught				1.3 in up-draught	1.4 in downdraught
Average turbulence in cloud, 'g'	0.2	0.1	0.1	0.2 - 0.3		0.1	0.1	0.1
Precipitation static. Yes or No	No	No	No	No		No	No	No

/Vertical

Run	1	2	3	4	5	6	7	8
Vertical velocity strength. ft. sec.$^{-1}$ Peak:-	(+ 10 (- 3	+ 4 - 8	+ 14 - 4	+ 12 - 8		+ 3 - 8	+ 10 - 2	+ 9 - 7
Average:- (+ ve. sign denotes updraught) (- ve. sign denotes downdraught)	(+ 6 (- 2	+ 2 - 4	+ 8 - 2	+ 8 - 4		+ 2 - $3\frac{1}{2}$	+ 5 - $1\frac{1}{2}$	+ 3 - 4
Crystals. Yes or No	No	No	No	No		No	No	No
Other observations		Vis. 5 yd.	Vis. 5 yd., slight air-frame icing	Vis. 5 yd.			Vis. less than 2 yd., windscreen icing	Vis. 5 yd., 2 yd. in places
Time, hr.	1645	1650	1654	1700		1709	1712	1717
Extent, mi.	3.8	2.0	2.0	1.5		3.2	3.0	1.8
Remarks					Film Fogged			
Droplet diameter μ Edge	Largest 30, most 20	Largest 40, most 20	Largest 40, most 20					
Centre	Largest 90, occ. 150-250. Most 20-40.	Largest 200, most 20-40	Largest 100, occ. 490. Most 30-40					

Table 7

23/7/53

Main features of cloud investigated in Flight 7

Run	1	2	3	4	5
Maximum water content, gm.m.$^{-3}$	0.92	> 1.8	> 1.8	> 1.8	
Mean water content, gm.m.$^{-3}$	0.35	0.93	1.03	1.56	
Icing. Yes or No	No	No	No	No	
Mean height, ft. (ICAN)	10146	10306	10160	10184	
Height variation, ft.	+ 29 - 26	+ 94 -166	+ 80 - 95	+ 71 - 84	
Mean airspeed, kt.	177	172	178	175	
Airspeed variation, kt.	+ 1 - 3	+ 4 - 4	+ 7 - 7	+ 6 - 7	
Mean temperature, °F.	27	27	27	27	
Temperature variation, °F.					
Maximum excess temperature in cloud, °F.					
Average turbulence in cloud, 'g'	0.2 - 0.3	0.3 - 0.4	0.3 - 0.4	0.3 - 0.4	
Precipitation static. Yes or No	No	No	No	No	No
Vertical velocity strength. ft. sec.$^{-1}$ Peak:-	(+ 9 (- 3	+ 17 0	+ 25 - 6½	+ 3 - 18	
Average:- (+ ve. sign denotes updraught) (- ve. sign denotes downdraught)	(+ 5 (- 2	+ 9 0	+ 10 - 3	+ 2 - 9	

/Crystals.

Run	1	2	3	4	5
Crystals. Yes or No	No	No	No	No	No
Other observations	Vis. 20 yd.	Vis. 5 yd. at times	Vis. 5 yd.	Cloud building vigorously in north	Vis. 10 yd.
Time, hr.	1206	1216	1220	1225	1230
Extent, mi.	1.2	1.9	3.0	4.4	
Remarks				Heavy rain in cloud. Vis. 5 yd.	Cloud decaying in south. Film fogged.

Table 8

17/9/53

Main features of cloud investigated in Flight 8

Run	1	2	3	4	5	6	7	8
Maximum water content, gm.m.$^{-3}$	> 1.8	1.8	> 1.8	1.2	Film fogged, record lost	0.92	> 1.8	> 1.8
Mean water content, gm.m.$^{-3}$	0.84	0.86	0.98	0.72		0.61	0.84	1.14
Icing	Slight on windscreen	Moderate on windscreen	Slight on windscreen	Slight on windscreen		Slight on windscreen	Slight on windscreen	Moderate on windscreen
Mean height, ft. (ICAN)	12120	11963	11998	11906		11914	11962	11890
Height variation, ft.	+410 -155	+117 -148	+ 87 - 98	+ 34 - 41		+ 21 - 39	+ 83 - 62	+ 80 -210
Mean airspeed, kt.	176	183	184	188		182	186	189
Airspeed variation, kt.	+ 6 - 6	+ 12 - 6	+ 10 - 8	+ 6 - 6		+ 10 - 10	+ 6 - 7	+ 7 - 8
Mean temperature, °F.	Thermometer unserviceable							
Temperature variation, °F.	Thermometer unserviceable							
Maximum excess temperature in cloud, °F.	Thermometer unserviceable							
Average turbulence in cloud, 'g'	0.1	0.2	0.2 - 0.3	0.2 - 0.3		0.2	0.2 - 0.3	0.3
Precipitation static. Yes or No	No	No	No	No	No	No	No	No

/Vertical

Run	1	2	3	4	5	6	7	8
Vertical velocity strength. ft. sec.$^{-1}$ Peak:-	+ 6 -6.5	+ 6 - 7	+ 9 - 8	+ 5 - 6		+6.5 -6.0	+8.0 -9.5	+7.5 -5.5
Average:- (+ ve. sign denotes updraught) (- ve. sign denotes downdraught)	+3.3 -5.1	+2.8 -2.4	+3.8 -5.2	+1.5 -2.3		+2.0 -1.6	+3.5 -3.2	+2.7 -1.7
Overall average:-	+0.9	-0.9	+0.7	-0.5		+0.3	-0.5	+0.6
Crystals. Yes or No	Possibly on western edge	Possibly at western edge	No	No		No	No	No
Other observations		Cloud not very dense	Vis. 20 yd.	Vis. 40 yd.			Vis. 100 yd.	Very bumpy
Time, hr.	1148	1154	1203	1208		1218	1225	1231
Extent, mi.	4.0	4.0	4.0	4.0		3.0	3.5	4.5
Remarks		Cloud rather tenuous			Cassette exhausted. No record for Run 5			
Droplet diameter μ At centre	Largest 320, most 80	Largest 250, most 50	Largest 200, most 40	Largest 320				

Table 9

9/7/53

Main features of cloud investigated in Flight 9

Run	Cell	1	2	3	4	5	6
Maximum water content, gm.m.$^{-3}$	1 2	0	0.32	0.03 0.03	1.80	2.0	1.7 } From icing rates
Mean water content, gm.m.$^{-3}$	1 2	0	0.04	0.02 0.01	1.00	0.66	0.66)
Icing. Yes or No	Both	No	Yes, slight	Yes, slight	Yes, heavy	Yes, heavy	Yes, heavy
Mean height, ft. (ICAN)	1 2	15076	15201	15027 15052	15060	15247	15274
Height variation, ft.	1 1 2 2	+ 34 - 56	+ 39 - 61	+ 8 - 2 + 3 - 7	+ 20 - 30	+ 93 - 97	+156 - 64
Mean airspeed, kt.	1 2	179	179	180 180	179	177	171
Airspeed variation, kt.	1 1 2 2	+ 2 - 5	+ 2 - 6	0 - 1 + 1 - 1	+ 1 - 1	+ 7 - 4	+ 12 - 5
Mean temperature, °F.	1 2	+10.8	+11.5	+10.4 +10.7	+6.9	+7.6	+11.4
Temperature variation, °F.	1 1 2 2	+0.9 -1.1	+3.0 -2.2	+0.9 -0.5 +0.6 -0.1	+0.9 -0.6	+2.2 -3.5	+4.9 -2.6

/Maximum

Run	Cell	1	2	3	4	5	6
Maximum excess temperature in cloud, °F.	Both	1.2 -1.3 in downdraught	2.8 -2.6 in downdraught		+1.4 in downdraught	5.6 in updraught	6.8 in updraught
Average turbulence in cloud, 'g'	Both	0.1 - 0.2	0.1 rising to 0.3 occasionally	0.1 - 0.2	0.1 - 0.2	0.2 - 0.4	0.2 - 0.5
Precipitation static. Yes or No	Both	No	No	No	No	No	No
Vertical velocity strength. ft. sec.$^{-1}$ Peak:-	1	+ 8	+ 8	0	0	+ 18	+ 1
	1	- 6	- 10	- 2	- 12	- 6	- 14
	2			+ 8			
	2			0			
Average:-	1	+ 4	+ 3	0	0	+ 11	+ 5
	1	- $2\frac{1}{2}$	- $4\frac{1}{2}$	- 1	- 7	- $3\frac{1}{2}$	- $5\frac{1}{2}$
(+ ve. sign denotes updraught)	2			+ 4			
(- ve. sign denotes downdraught)	2			0			
Crystals. Yes or No	Both	Yes	Yes	Yes	No	Few	Few
Other observations		Cloud thin and fibrous		Cloud degenerating	Cloud degenerating	Cloud wispy	New cell, remainder of cloud dropping
Time, hr.	Both	1602	1610	1615	1624	1635	1641
Extent, mi.	1	4.0	6.0	1.7	1.2	2.9	4.5
	2			1.0			
Droplet diameter μ Centre			Largest 120, occ. 280. Mainly 40-60	Largest 140, occ. 350. Mainly 40-60	Largest 140, mainly 30-40	Largest 200, mainly 60-100	Largest 40, mainly 30
Edge				Largest 80, mainly 20		Largest 40, occ. 80. Mainly 30	

Table 10

Summary of observed and forecast cumulus clouds

Flight, date and time	Observed levels, ft. (ICAN)		Levels forecast by parcel method, ft. (ICAN)	
	Base	Top	Base	Top
1 10/6/53 1628 G.M.T.	3500	14500	1800	9800 generally 14500 occasionally
2 8/7/53 1615 G.M.T.	2000	12000	2200	11800 generally 14000 occasionally
3 14/7/53 1700 G.M.T.	3200	17000 generally 22-23000 occasionally	1800	10500 generally 24000 occasionally
4 14/4/53 1215 G.M.T.	4000	12000	4200	11500 generally 16000 occasionally
5 13/4/53 1200 G.M.T.	3000	9500	3600	7500 to 8500 generally 16000 occasionally
6 4/6/53 1700 G.M.T.	4000	12000	3300	10000 generally 15000 very occasionally
7 23/7/53 1218 G.M.T.	4200	12000	3500	12500 to 13500 very occasionally 15000
8 17/9/53 1209 G.M.T.	1800	14000	2800	10000 generally 17500 occasionally
9 9/7/53 1621 G.M.T.	3000	22000	3700	Very many to 7500, a few to 22000.

G.58108(m)/PN/4/56/50

Table 11

Observed clouds other than cumulus

Flight, date and approx. time	Height and type of cloud (height ICAN)	Remarks
1 10/6/53 1630 Z	Ac. 9500 ft.	At base of stabilisation of temperature lapse and 50 mb. above a marked wind shear
2 8/7/53 1620 Z	Ac. 10500 ft.	At base of small temperature "stop", no wind shear
3 14/7/53 1700 Z	None	
4 14/4/53 1215 Z	None	
5 13/4/53 1200 Z	Sc. 7000 ft.	At base of small temperature "stop", no wind shear
6 4/6/53 1700 Z	Ac. 9500 ft.	At base of small temperature "stop", no wind shear
7 23/7/53 1220 Z	Sc. 7000 ft.	At base of very small temperature "stop", no wind shear
8 17/9/53 1210 Z	Sc. 4000 ft. Sc. 7500 ft. Ac. 9300 ft. Ac. 10500 ft. Ac. 11000 ft.	All at bases of very small temperature "stops," no wind shear
9 9/7/53 1620 Z	Ac. 9700 ft. Cs. 22000 ft.	Both at bases of small temperature "stops"

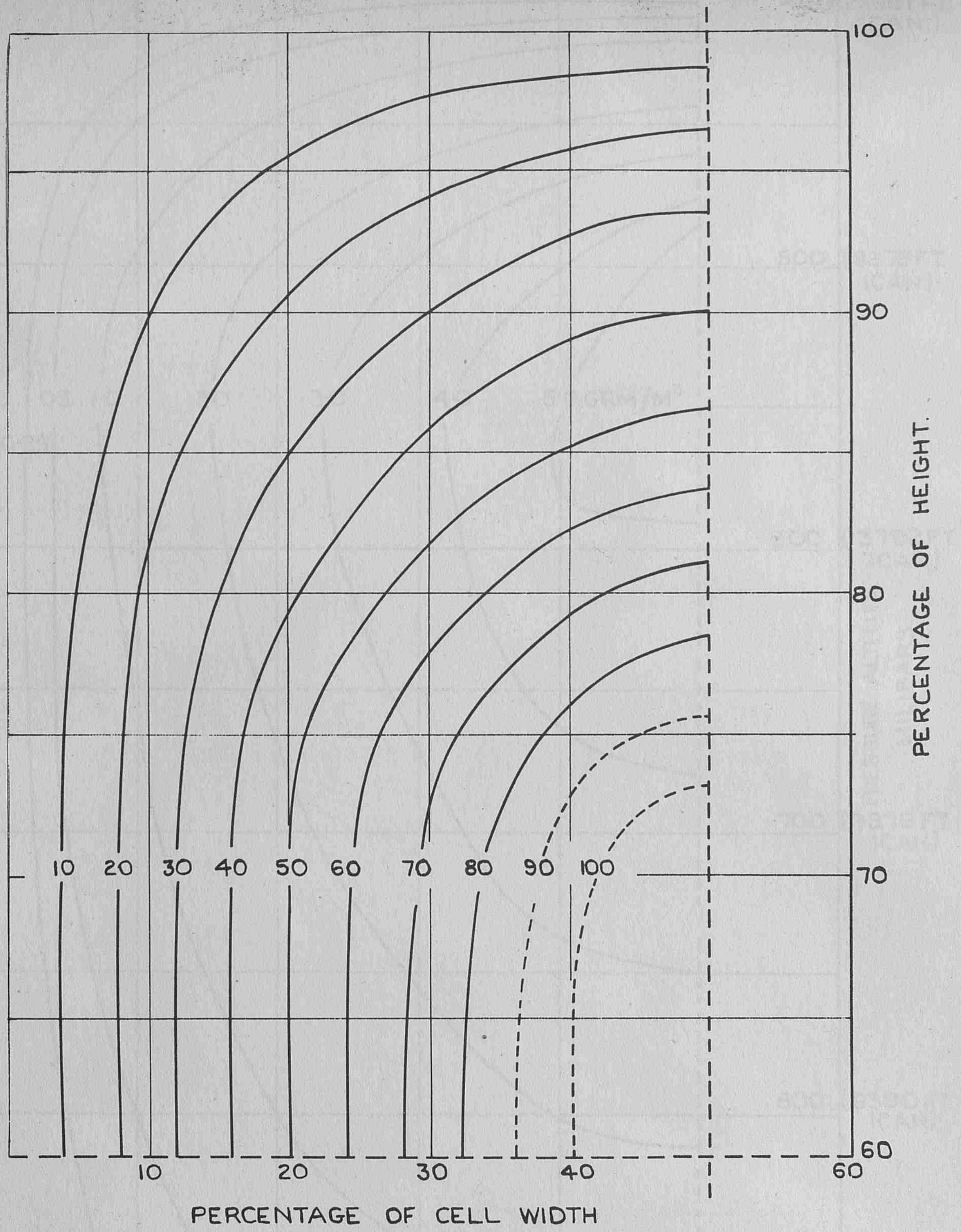

FIG 1. IDEALISED DISTRIBUTION OF WATER-CONTENT IN A CUMULUS CLOUD EXPRESSED AS A PERCENTAGE OF MAXIMUM REALISABLE WATER-CONTENT ON THE ASSUMPTION OF ADIABATIC LIFTING.

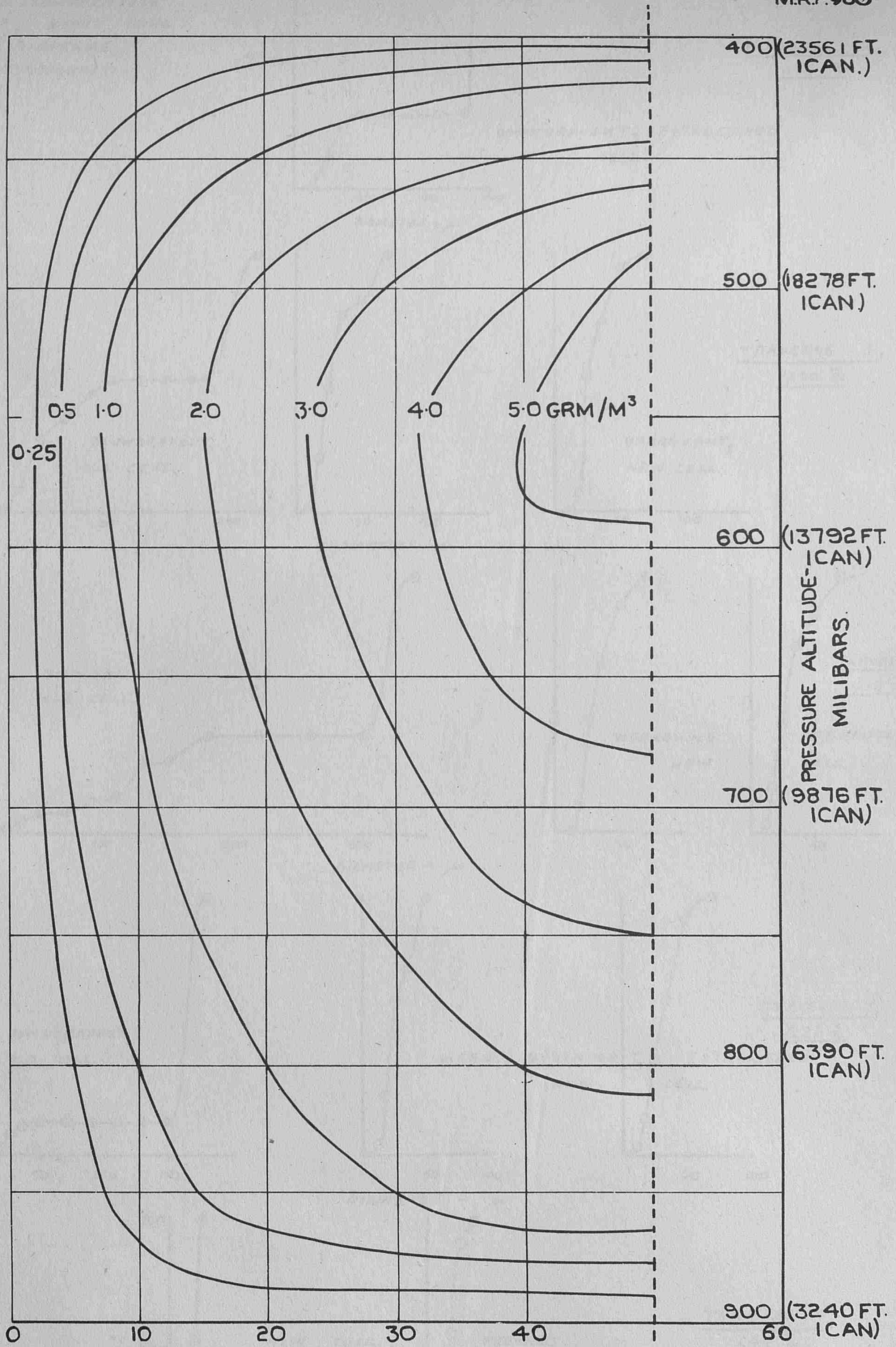

FIG. 2. DISTRIBUTION OF WATER-CONTENT TO BE EXPECTED IN TYPICAL CUMULUS CLOUD HAVING BASE AT A HEIGHT OF 900MB. (3240 FT.) AND A TEMPERATURE OF 60°F AND HAVING TOP AT 400 MB. (23561 FT.)

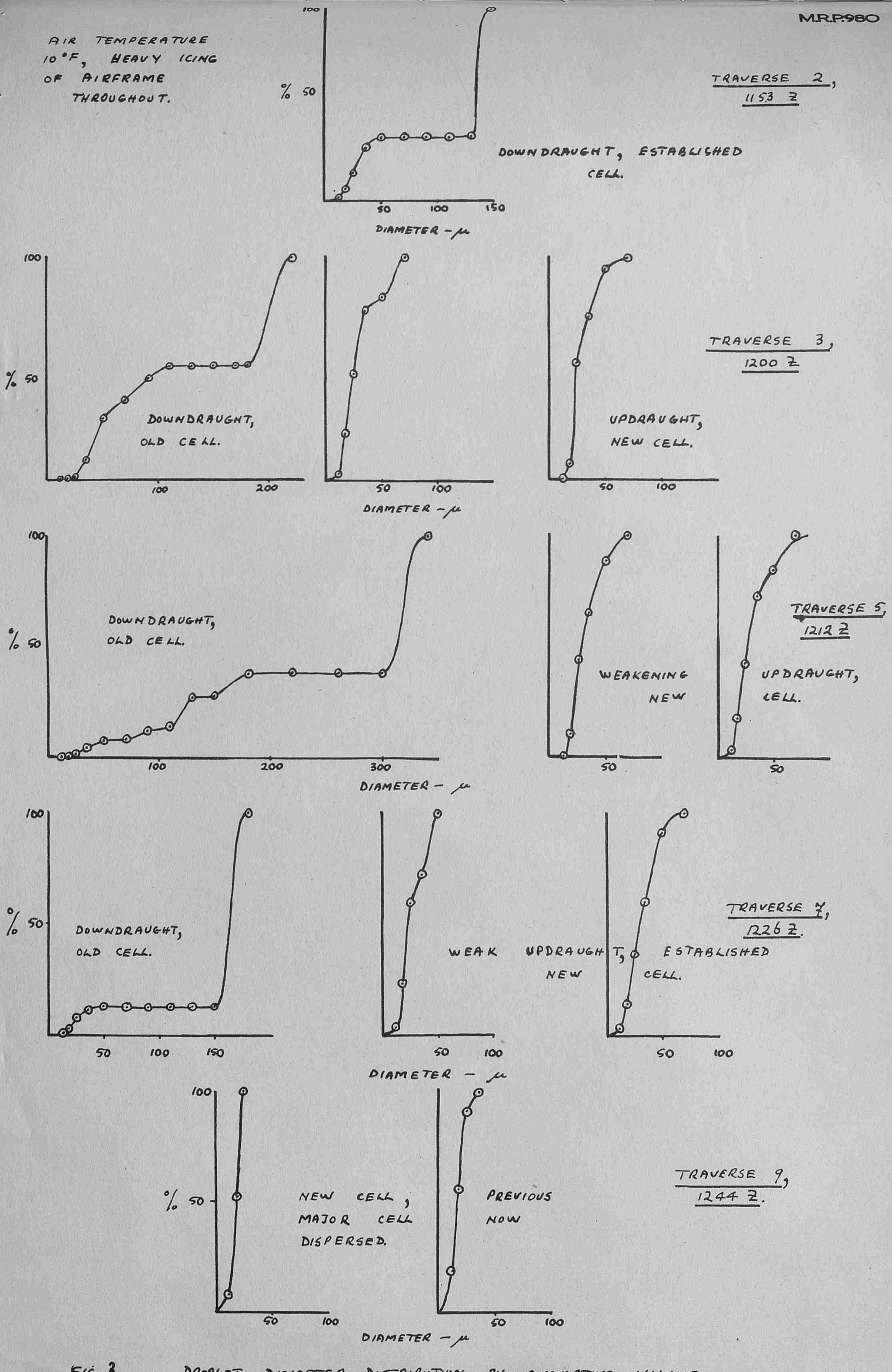

AIR TEMPERATURE 10°F, HEAVY ICING OF AIRFRAME THROUGHOUT.

FIG. 3 DROPLET DIAMETER DISTRIBUTION BY CUMULATIVE VOLUME, LARGE CUMULUS CLOUD OF 14.4.53

AIR WEATHER SERVICE
TECHNICAL FILES

M.R.P. 981
S.C. 11/210
30th April, 1956.

AD 208840

Average height of the standard isobaric surfaces over the area from the North Pole to 55°N in July.

by

H. Heastie.

(Meteorological Office)

AWSSS
ROUTING SLIP

FILE	INFO	ACTION				
	1.2		DIRECTOR			
	1.1		DEP DIRECTOR			
	1		ASST TO DIRECTOR			
	2		CONSULTANTS			WS
	4		TRSD		CHF	
				✓	TSS	LHC.
				✓	RRB	
				✓	CDB	
					SEC	
	3		EDD		CHF	
					LFB	DK
					STB	
					SPFB	GK
					CU	
					SEC	
	5		TIPD		CHF	
					PUE	
					TECH INFO	
					SEC	

send to CL

AIR MINISTRY

METEOROLOGICAL RESEARCH COMMITTEE

At the time of issue this report has not been published. Any author desiring to quote this paper should refer to it as "A paper of the Meteorological Research Committee (London).
M.R.P. No.981 by Mr. H. Heastie.
A copy is available in the Library of the Meteorological Office".

M.R.P.981
S.C.II/210
30th April, 1956

AIR MINISTRY

METEOROLOGICAL RESEARCH COMMITTEE

Average height of the standard isobaric surfaces over the area from the North Pole to 55°N in July

by

H. Heastie (Meteorological Office)

1. Introduction

This paper is essentially a continuation of M.R.P. 918(1). In the latter paper the decision to start the revision of Geophysical Memoir 85 - Upper Winds over the World - by constructing circumpolar charts of the standard isobaric surfaces, was explained and the charts for January were presented. The present paper shows a similar set of average contour and thickness charts for July.

2. The data

Data for the same fixed period, 1949-53, were used and the sources are listed in the earlier paper. The labour of extraction was eased by the receipt of further micro-film data for Norwegian stations from Det Norske Meteorologiske Institutt, Oslo and of manuscript data for Alaska and the Aleutians from U.S. Weather Bureau.

3. Method of constructing the charts

(1) General. The method employed was the same as that used in the construction of the January charts, although there was one slight complication over Siberia. In general, the data available from the U.S.S.R. were even scantier than in January and for July, 1949 there were no data at all from Siberia. For this month the monthly mean 500 mb. contour chart published in the monthly supplement to the German Daily Weather Report (2) was accepted over Siberia and the 700-500 mb. thickness chart constructed over this area by correlating the 700-500 mb. thickness with the 500 mb. contour height along the meridians 20°E, 40°E, ... 180°E for the four years 1950-53. As the grid values obtained fitted in reasonably well with the rest of the chart drawn from data and as the nine values obtained for the pole lay within a ten metre range the method was regarded as satisfactory. The 500-300 mb. thickness chart and the 300 mb. temperature chart were similarly computed by correlating the 500-300 mb. thickness with the 700-500 mb. thickness and the 300 mb. temperature with the 500-300 mb. thickness. A further check on the drawing over the U.S.S.R. was obtained by comparing the average 300 mb. temperature chart with that in the memoir on upper air temperature (3).

(2) Effect of solar radiation. For a large part of the area covered by the chart no night time ascents were available and the effect of solar radiation on the various types of radiosondes used by the different countries had to be considered. It has not proved possible to avoid this difficulty completely. With one exception, noted below, 0300 G.M.T.

/data

data were used since, in most areas, these were the only data readily available. For the U.S.S.R. the 0300 G.M.T. ascents are made in daylight and unfortunately very little, if anything, is known about the characteristics of the Russian instrument. Russian data were available up to 300 mb. only and at this level there was some indication that the temperature reading was 1-2°C. too high. Above 300 mb., temperature lapse rates from the memoir on upper air temperature were used and these again may be subject to error for similar reasons. Data from U.S.W.B. stations and the joint U.S.-Canadian stations in northern Canada are corrected (from March, 1950) for the effect of solar radiation and the 0300 G.M.T. data were accepted. No radiation correction is made at Canadian stations, at some of which a U.S. type of radiosonde is used and at others a Canadian instrument. The data from the latter group of stations were modified in the light of a paper by Henry (4) who estimated corrections to obtain agreement between Canadian-instrument stations and American-instrument stations corrected for radiation. Of the Canadian stations using the U.S. type of radiosonde the majority are in darkness at 0300 G.M.T. The data from those in daylight at 0300 G.M.T. were corrected approximately by reference to the U.S.W.B. publication (5) on the subject. The weather ships A, B, C, I and J and the British stations, with the partial exception of Lerwick, are in darkness at 0300 G.M.T. The ascents from the Scandinavian stations on the other hand were made in daylight. The Danish and Finnish data are corrected while the Norwegian and Swedish are not. No attempt was made to apply any systematic correction to the latter. At a small group of stations in the Aleutians no radiation correction is applied and for these stations only 1500 G.M.T. data were used.

4. The charts

The July contour charts show some marked differences from those for January. In January there is mainly westerly flow in the troposphere with considerable asymmetry about the pole. The very cold arctic winter stratosphere leads to a thermal pattern which reinforces this flow so that the January charts present a picture of mainly westerly flow increasing with height and becoming almost symmetric about the pole at the 100 mb. level. In July there is again mainly westerly, though much weaker, flow in the troposphere (Figs. 1, 2 and 3). The 700-500 mb. and 500-300 mb. thickness charts (Figs. 7 and 8) both show centres of low thickness over northern Canada and the main axis of the tropospheric flow is tilted southwards with height along the 90°W meridian. The 300-200 mb. thickness chart (Fig.9) where the layer is partly in the troposphere and partly in the stratosphere shows a rather confused pattern. In the region considered the tropopause is everywhere below the 200 mb. surface and the very warm arctic summer stratosphere is reflected in the 200-150 mb. and 150-100 mb. thickness charts (Figs.10 and 11) which both show an easterly thermal centred on the pole. The resulting contour charts show a mainly westerly flow over Eurasia at all levels, increasing up to 200 mb. (Fig.4) decreasing again at 150 mb. (Fig.5) and at 100 mb. (Fig.6) and spreading across the pole to give an easterly flow over extreme northern Canada and Greenland. Over the Canadian sector of the chart the centre of low contour height is transferred southwards from about 87°N at 700 mb. to about 68°N at 100 mb. and lies between the 70°W and 90°W meridians. The flow round this low centre increases generally up to 300 mb. and above 200 mb. decreases again to less than 15 kt. everywhere. Hence, up to 100 mb., where the January charts show increasing symmetry with height, the July charts become more asymmetric with height. Temperature lapses 100-25 mb. shown on the Air Weather Service charts (6) suggest that from about 25 mb. upwards the circulation is again tending towards symmetry round the pole with a contour high moving northwards over central Siberia towards the pole and the Canadian low centre moving southwards and being absorbed.

One interesting feature arising out of the symmetry of the thickness pattern and the asymmetry of the contour pattern in the stratosphere may be mentioned here. Over a large area of the chart north of the Arctic Circle the flow in the stratosphere (Figs.4, 5 and 6) is directly across the thickness pattern (Figs.10 and 11). Neither the flow in the troposphere (Figs.2 and 3) nor the tropopause pressure chart (3) suggests any appreciable vertical motion of the atmosphere in this area and the implied temperature changes are presumably due to radiative effects. For both the layers 200-150 mb. and 150-100 mb. the heating of the air moving poleward from 70-75°N appears to be of the order of 0.5°C./day over 2-4 days. The stratosphere over this area is in continuous sunlight during the whole of July, but no attempt has been made to estimate whether variation in solar altitude or in ozone concentration could account for this heating.

It may be argued that average contour lines crossing average thickness lines do not necessarily imply flow across the thickness lines on any single occasion. Indeed, it is possible to construct a series of wind and temperature systems, such that for each system separately, the flow is along the thickness lines, while the mean flow is across the mean thickness lines. However, to produce this anomaly, too many systems which violate the Dines relationships between troposphere and stratosphere have to be used, and it is known that these relationships hold for arctic regions in July (7).

References

(1) Heastie, H. Average height of the standard isobaric surfaces over the area from the North Pole to 55°N in January. Meteorological Research Papers, Air Ministry, London, No. 918, 1955.

(2) Die Grosswetterlagen Mitteleuropas. Deutsche Wetterdienst, Bad Kissingen, Germany.

(3) Goldie, N., Moore, J.G. and Austin, E.E. Upper air temperatures over the world. Geophys. Mem., London (in the press).

(4) Henry, T.J.G. A comparison of mean temperatures obtained with Canadian and American types of radiosonde. Department of Transport, Meteorological Division, Toronto, Circular 2041, 1951.

(5) Washington, U.S. Weather Bureau. Manual of Radiosonde Observations, Circular P (Addendum), 1950.

(6) Washington, U.S. Air Weather Service. Mean monthly maps of 300, 200, 100, 50 and 25 mb. surfaces over North America. Technical Report No.105-107, Washington, 1953.

(7) Bannon, J.K. and Gilchrist, A. Variation of temperature in the troposphere and lower stratosphere. Quart. J.R. Met. Soc., 82, p.58, 1956.

AVERAGE 700 mb. CONTOURS

M.R.P. 981

JULY 1949-1953

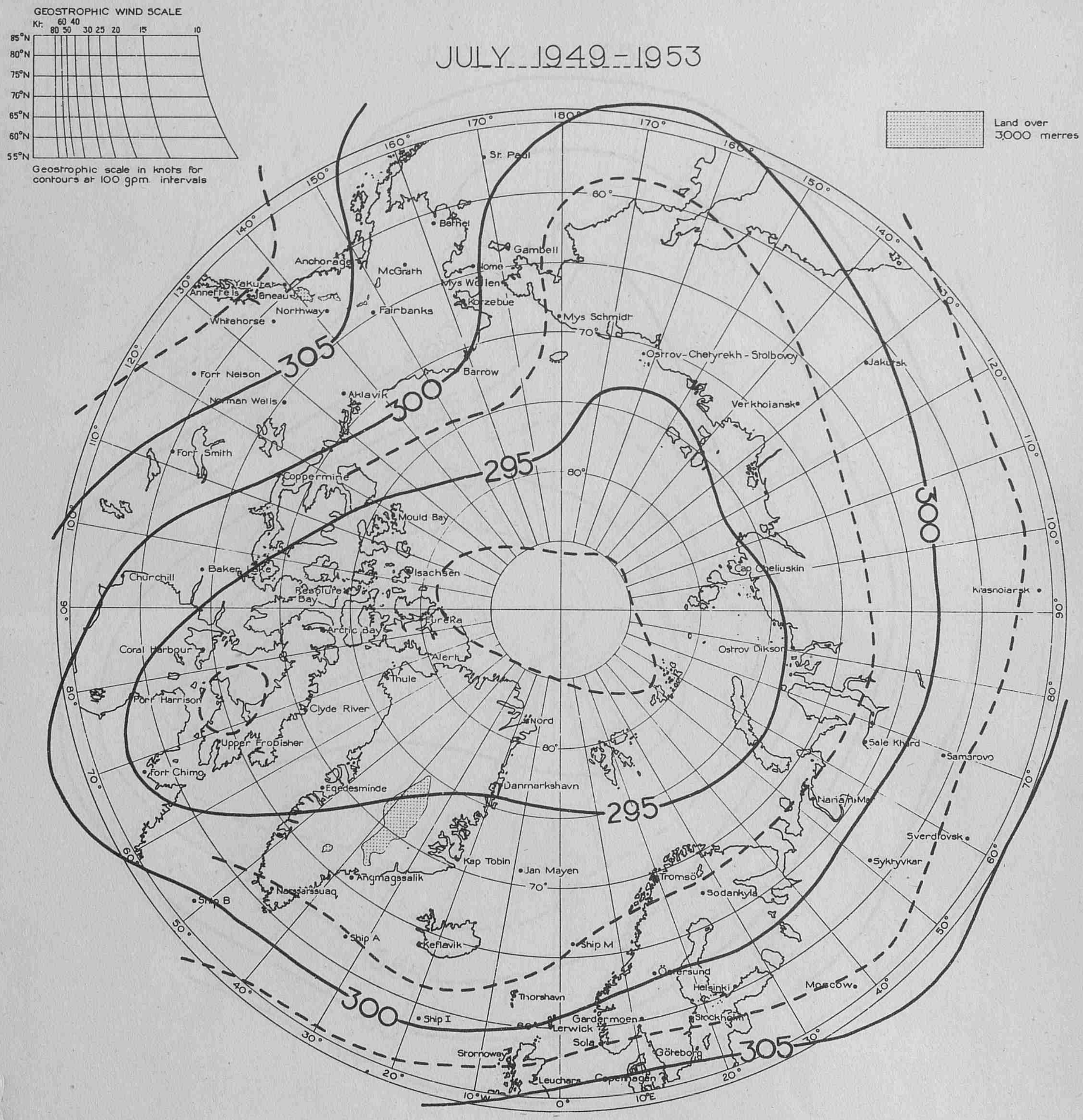
GEOSTROPHIC WIND SCALE
Kt. 80 60 50 40 30 25 20 15 10
85°N
80°N
75°N
70°N
65°N
60°N
55°N
Geostrophic scale in knots for contours at 100 gpm. intervals
Land over 3,000 metres
305
300
295
295
300
300
305
60°
70°
80°
80°
70°
180°
170°
170°
160°
160°
150°
150°
140°
140°
130°
130°
120°
120°
110°
110°
100°
100°
90°
90°
80°
80°
70°
70°
60°
60°
50°
50°
40°
40°
30°
30°
20°
20°
10°W
0°
10°E
St. Paul
Bethel
Gambell
Nome
McGrath
Mys Wellen
Kotzebue
Anchorage
Yakutat
Annette Is.
Juneau
Northway
Fairbanks
Whitehorse
Mys Schmidt
Ostrov-Chetyrekh-Stolbovoy
Jakutsk
Verkhoiansk
Barrow
Fort Nelson
Norman Wells
Aklavik
Fort Smith
Coppermine
Mould Bay
Isachsen
Baker Lake
Churchill
Resolute Bay
Eureka
Arctic Bay
Alert
Coral Harbour
Thule
Port Harrison
Clyde River
Upper Frobisher
Fort Chimo
Egedesminde
Nord
Danmarkshavn
Cap Cheliuskin
Krasnoiarsk
Ostrov Dikson
Sale Khard
Samarovo
Narian Mar
Sverdlovsk
Sykhyvkar
Kap Tobin
Jan Mayen
Angmagssalik
Narssarssuaq
Ship B
Ship A
Keflavik
Ship M
Tromsö
Sodankyla
Östersund
Helsinki
Moscow
Thorshavn
Ship I
Gardermoen
Lerwick
Sola
Stockholm
Stornoway
Göteborg
Leuchars
Copenhagen

Height in dekametres

Fig. 1

Upper Air Branch (M.O.23)

AVERAGE 500 mb. CONTOURS

M.R.P. 981

JULY 1949-1953

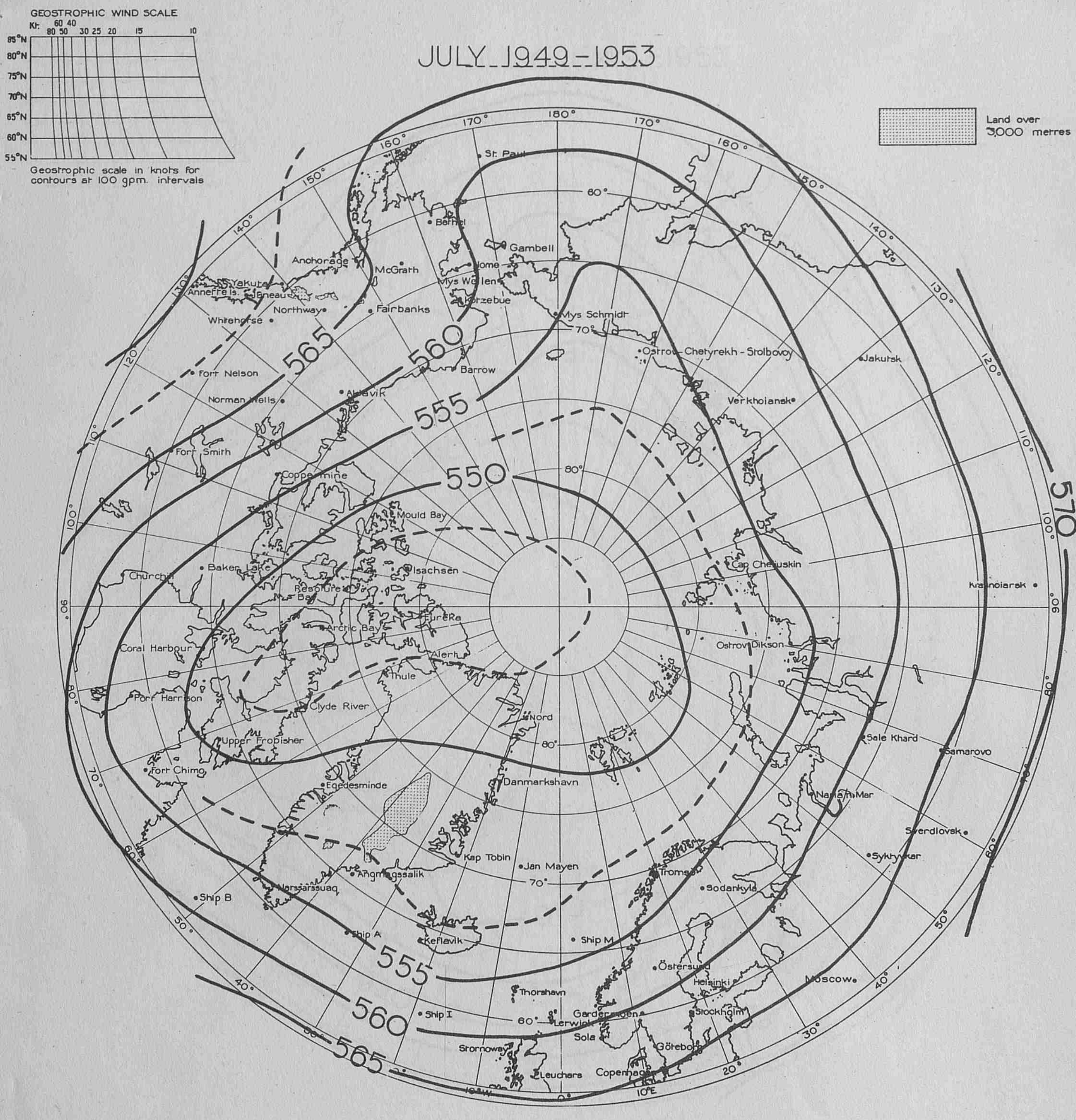
GEOSTROPHIC WIND SCALE
Kt. 60 40 80 50 30 25 20 15 10
85°N
80°N
75°N
70°N
65°N
60°N
55°N
Geostrophic scale in knots for contours at 100 gpm. intervals
Land over 3,000 metres
570
565
560
555
550
180°
170°
160°
150°
140°
130°
120°
110°
100°
90°
80°
70°
60°
50°
40°
30°
20°
10°E
0°
10°W
St. Paul
Bethel
Gambell
Nome
Mys Wellen
Kotzebue
McGrath
Anchorage
Fairbanks
Yakutat
Annette Is.
Juneau
Northway
Whitehorse
Mys Schmidt
Ostrov-Chetyrekh-Stolbovoy
Jakutsk
Verkhoiansk
Barrow
Aklavik
Fort Nelson
Norman Wells
Fort Smith
Coppermine
Mould Bay
Isachsen
Eureka
Baker Lake
Churchill
Resolute Bay
Arctic Bay
Alert
Thule
Coral Harbour
Port Harrison
Clyde River
Upper Frobisher
Fort Chimo
Egedesminde
Nord
Danmarkshavn
Cap Chelyuskin
Krasnoiarsk
Ostrov Dikson
Sale Khard
Samarovo
Nar'yan Mar
Sverdlovsk
Sykyvkar
Kap Tobin
Angmagssalik
Narssarssuaq
Jan Mayen
Tromsø
Sodankyla
Ship B
Ship A
Keflavik
Ship M
Östersund
Helsinki
Moscow
Thorshavn
Ship I
Lerwick
Gardermoen
Stockholm
Sola
Stornoway
Göteborg
Leuchars
Copenhagen

Height in dekametres

Fig. 2

Upper Air Branch (M.O.23)

AVERAGE 300 mb. CONTOURS M.R.P. 981

JULY 1949-1953

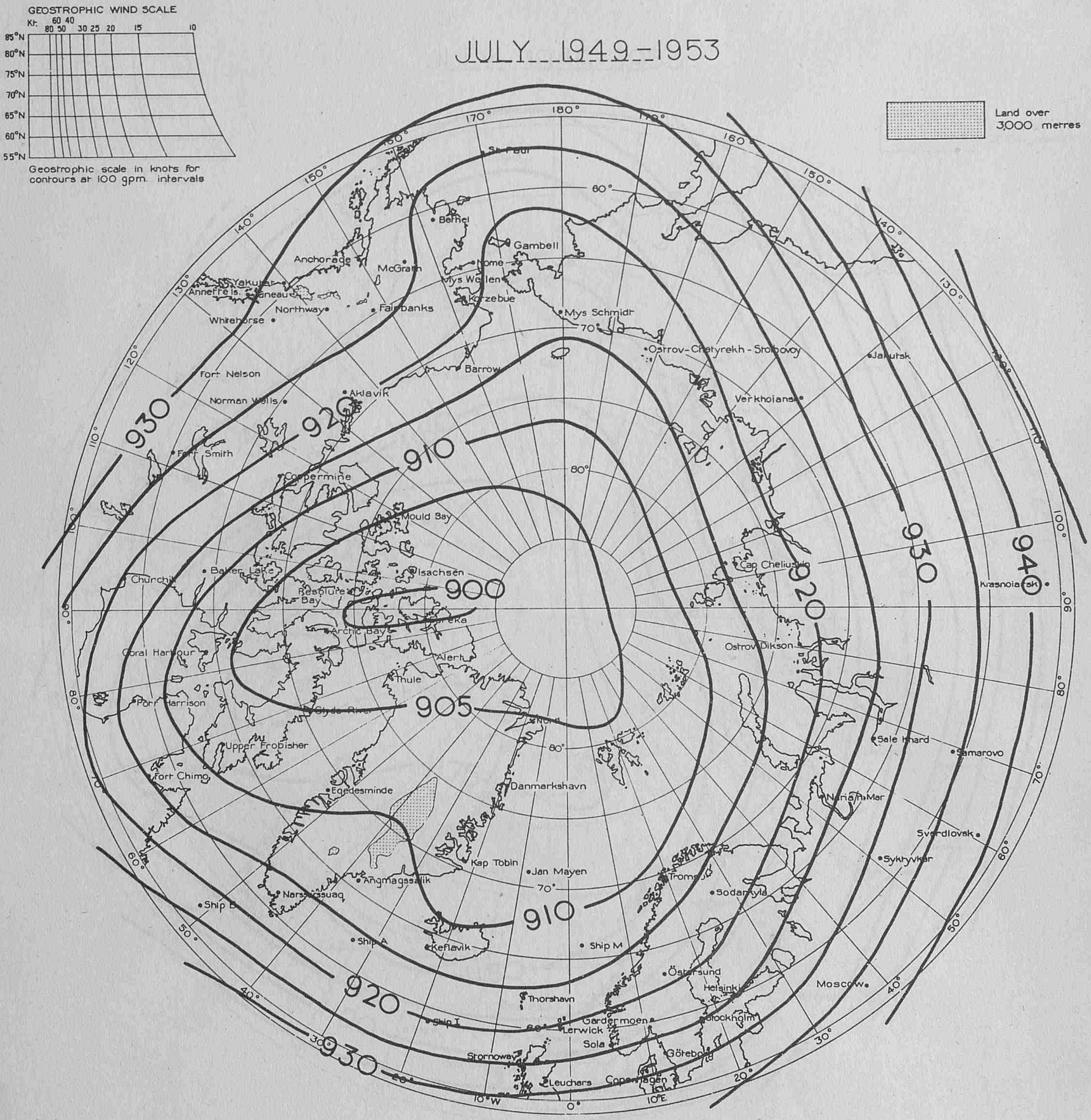
GEOSTROPHIC WIND SCALE
Kt. 80 60 50 40 30 25 20 15 10
85°N
80°N
75°N
70°N
65°N
60°N
55°N
Geostrophic scale in knots for contours at 100 gpm. intervals
Land over 3,000 metres
900
905
910
920
930
940
St. Paul
Bethel
Gambell
Anchorage
McGrath
Nome
Mys Wellen
Yakutat
Annette Is.
Juneau
Kotzebue
Northway
Fairbanks
Whitehorse
Mys Schmidt
Ostrov-Chetyrekh-Stolbovoy
Jakutsk
Barrow
Fort Nelson
Aklavik
Norman Wells
Verkhoiansk
Fort Smith
Coppermine
Mould Bay
Isachsen
Baker Lake
Cap Cheliuskin
Churchill
Resolute Bay
Eureka
Krasnoiarsk
Arctic Bay
Alert
Ostrov Dikson
Coral Harbour
Thule
Port Harrison
Clyde River
Nord
Sale Khard
Samarovo
Upper Frobisher
Danmarkshavn
Fort Chimo
Egedesminde
Narian Mar
Sverdlovsk
Sykyvkar
Kap Tobin
Jan Mayen
Angmagssalik
Tromsø
Narssarssuaq
Sodankyla
Ship B
Ship A
Keflavik
Ship M
Östersund
Helsinki
Moscow
Thorshavn
Ship I
Gardermoen
Lerwick
Stockholm
Sola
Stornoway
Göteborg
Leuchars
Copenhagen
180°
170°
160°
150°
140°
130°
120°
110°
100°
90°
80°
70°
60°
50°
40°
30°
20°
10°W
0°
10°E
60°
70°
80°

Height in dekametres

Fig. 3

Upper Air Branch (M.O.23)

AVERAGE 200 mb. CONTOURS

M.R.P. 981

JULY 1949-1953

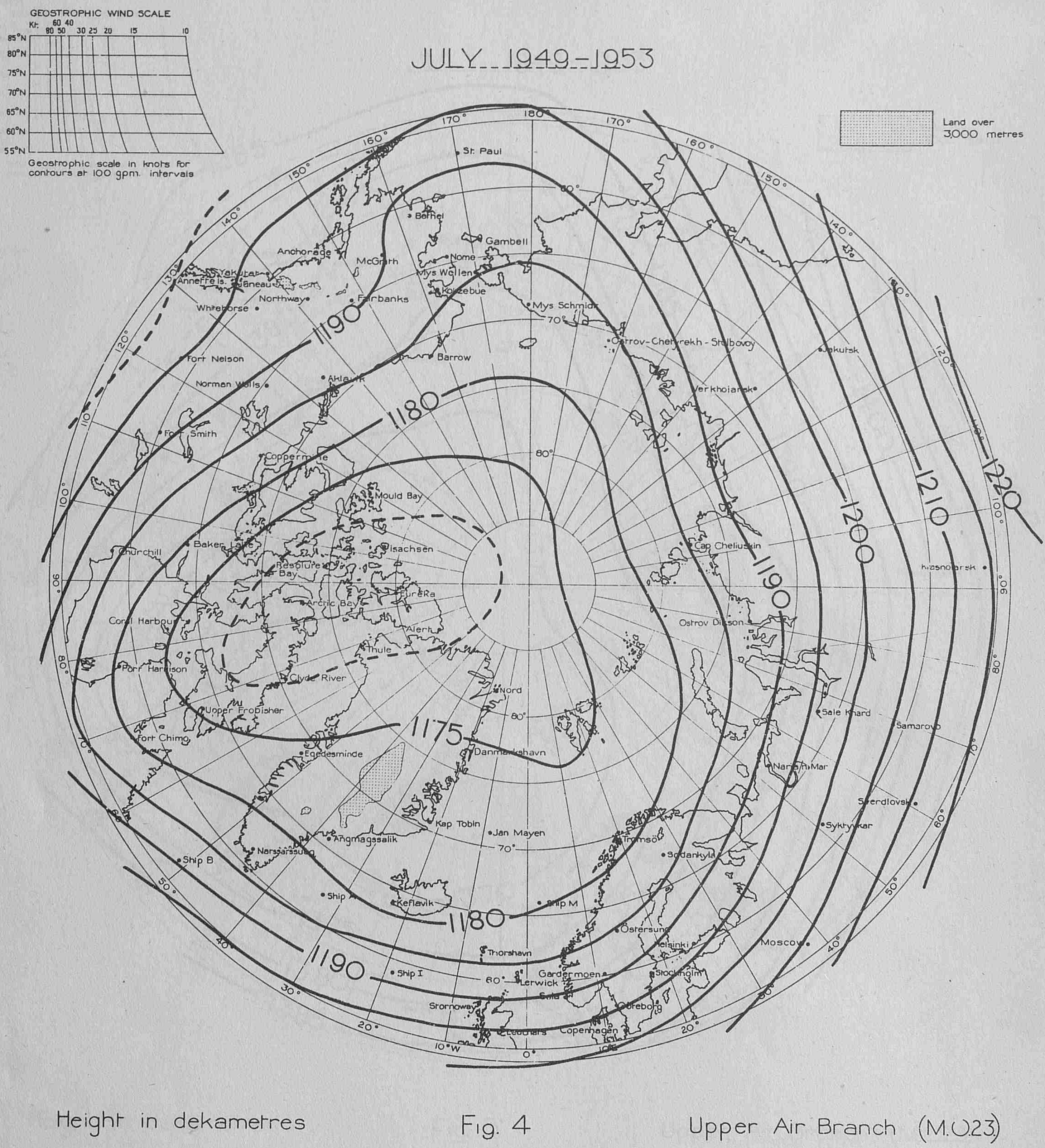
GEOSTROPHIC WIND SCALE
Kt. 80 60 50 40 30 25 20 15 10
85°N
80°N
75°N
70°N
65°N
60°N
55°N
Geostrophic scale in knots for contours at 100 gpm. intervals
Land over 3,000 metres
1175
1180
1180
1180
1190
1190
1190
1200
1210
1220
180°
170°
170°
160°
160°
150°
150°
140°
140°
130°
130°
120°
120°
110°
110°
100°
100°
90°
90°
80°
80°
70°
70°
60°
60°
50°
50°
40°
40°
30°
30°
20°
20°
10°W
0°
10°E
80°
80°
70°
70°
60°
60°
St. Paul
Bethel
Gambell
Nome
Mys Wellen
Kotzebue
Anchorage
McGrath
Yakutat
Annette Is.
Juneau
Northway
Fairbanks
Whitehorse
Mys Schmidt
Ostrov-Chetyrekh-Stolbovoy
Jakutsk
Barrow
Aklavik
Fort Nelson
Norman Wells
Verkhoiansk
Fort Smith
Coppermine
Mould Bay
Baker Lake
Churchill
Isachsen
Resolute Bay
Cap Cheliuskin
Krasnoiarsk
Eureka
Arctic Bay
Alert
Coral Harbour
Thule
Ostrov Dikson
Port Harrison
Clyde River
Nord
Upper Frobisher
Sale Khard
Samarovo
Fort Chimo
Egedesminde
Danmarkshavn
Narjan Mar
Sverdlovsk
Syktyvkar
Kap Tobin
Jan Mayen
Angmagssalik
Tromsö
Narssarssuaq
Sodankyla
Ship B
Ship A
Keflavik
Ship M
Östersund
Helsinki
Moscow
Thorshavn
Ship I
Gardermoen
Stockholm
Lerwick
Sola
Stornoway
Orebro
Leuchars
Copenhagen

Height in dekametres

Fig. 4

Upper Air Branch (M.O.23)

AVERAGE 150 mb. CONTOURS

M.R.P. 981

JULY 1949-1953

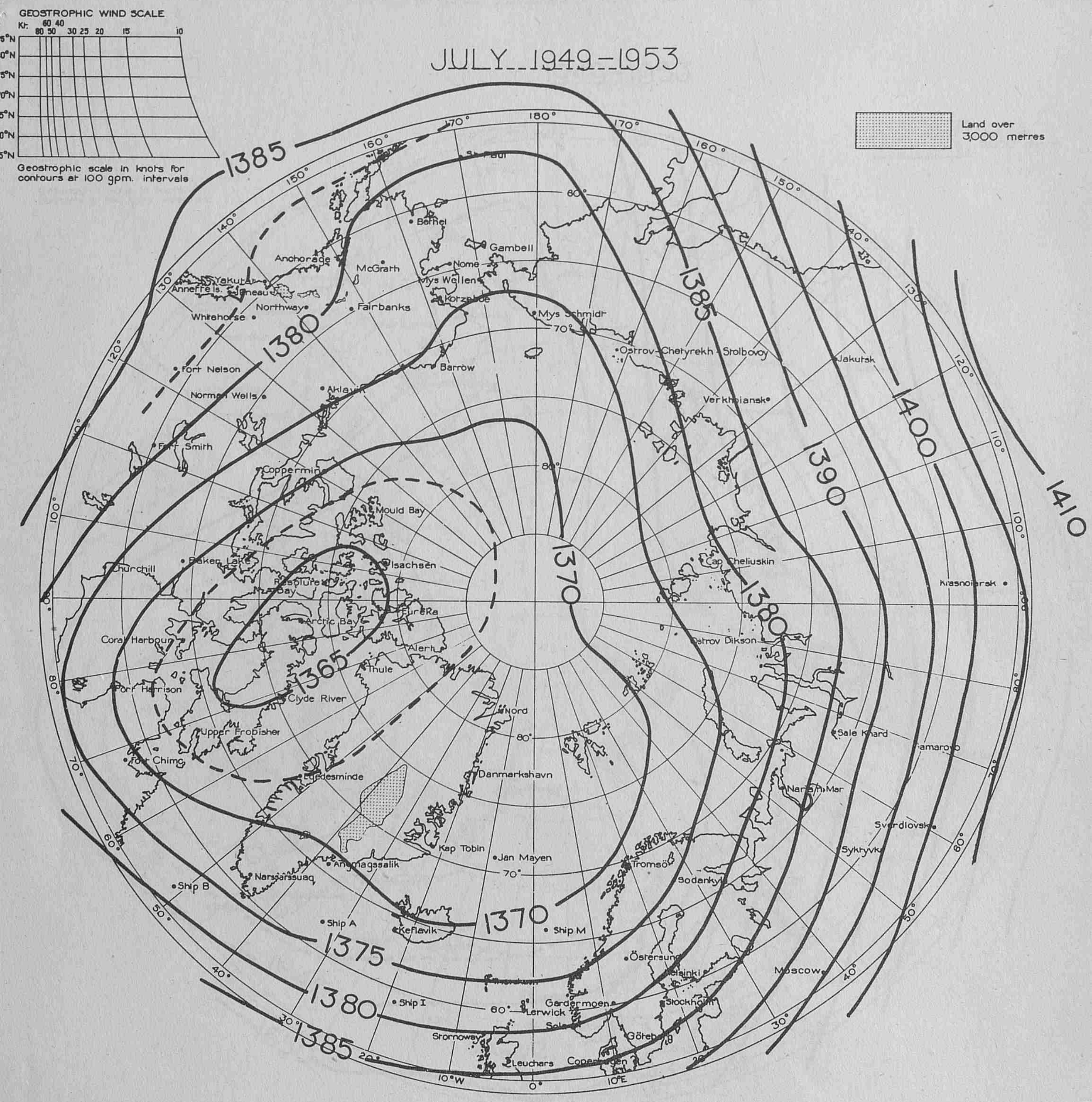
GEOSTROPHIC WIND SCALE
Kt: 60 40
80 50 30 25 20 15 10
Geostrophic scale in knots for contours at 100 gpm. intervals
Land over 3,000 metres
1385
1380
1365
1370
1375
1390
1400
1410
180°
170°
160°
150°
140°
130°
120°
110°
100°
80°
70°
60°
50°
40°
30°
20°
10°W
0°
10°E
St. Paul
Bethel
Gambell
Nome
Mys Wellen
Korzebue
Anchorage
McGrath
Yakutat
Annette Is.
Juneau
Northway
Whitehorse
Fairbanks
Mys Schmidt
Ostrov-Chetyrekh-Stolbovoy
Barrow
Jakutsk
Verkhoiansk
Fort Nelson
Norman Wells
Aklavik
Fort Smith
Coppermine
Mould Bay
Isachsen
Baker Lake
Churchill
Resolute Bay
Eureka
Arctic Bay
Cap Cheliuskin
Krasnoiarsk
Coral Harbour
Alert
Thule
Ostrov Dikson
Port Harrison
Clyde River
Nord
Sale Khard
Upper Frobisher
Fort Chimo
Egedesminde
Danmarkshavn
amarovo
Narian Mar
Sverdlovsk
Kap Tobin
Jan Mayen
Angmagssalik
Tromsö
Sykryvkar
Narssarssuaq
Ship B
Sodankyla
Ship A
Keflavik
Ship M
Östersund
Helsinki
Moscow
Ship I
Gardermoen
Lerwick
Stockholm
Sola
Stornoway
Göteborg
Leuchars
Copenhagen

Height in dekametres

Fig. 5

Upper Air Branch (M.O.23)

AVERAGE 100 mb. CONTOURS

M.R.P. 981

JULY 1949-1953

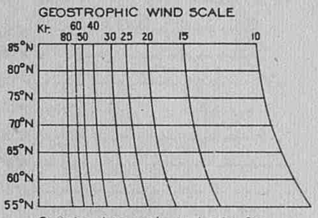

Geostrophic scale in knots for contours at 100 gpm. intervals

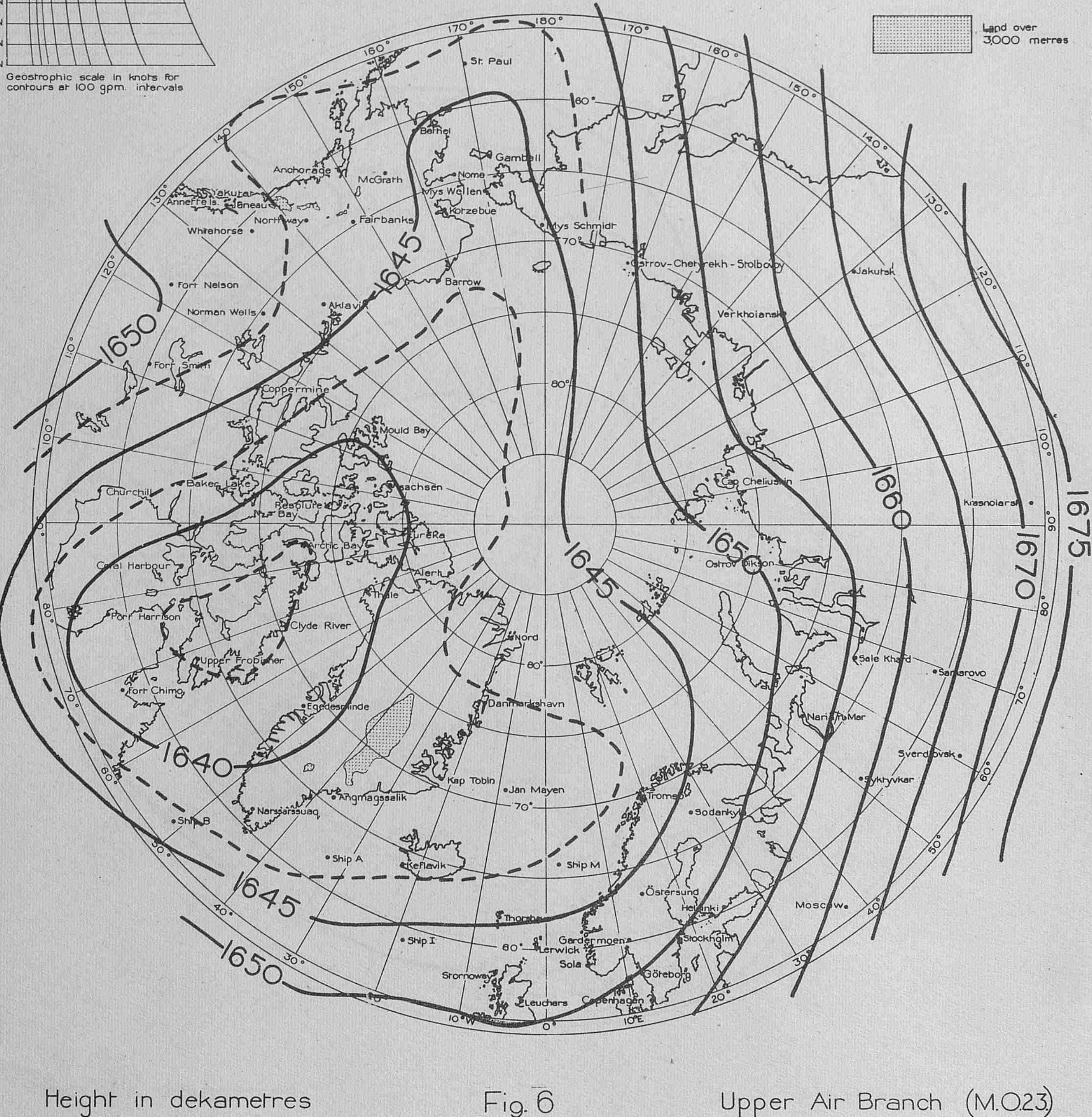
Land over 3,000 metres
1640
1645
1650
1660
1665
1670
1675
180°
170°
160°
150°
140°
130°
120°
110°
100°
90°
80°
70°
60°
50°
40°
30°
20°
10°E
0°
10°W
St. Paul
Bethel
Gambell
Nome
Mys Wellen
Kotzebue
Anchorage
McGrath
Fairbanks
Yakutat
Annette Is.
Juneau
Northway
Whitehorse
Fort Nelson
Norman Wells
Fort Smith
Aklavik
Barrow
Mys Schmidt
Ostrov-Chetyrekh-Stolbovoy
Jakutsk
Verkhoiansk
Coppermine
Mould Bay
Isachsen
Baker Lake
Churchill
Resolute Bay
Eureka
Arctic Bay
Alert
Thule
Coral Harbour
Port Harrison
Clyde River
Upper Frobisher
Fort Chimo
Egedesminde
Nord
Danmarkshavn
Cap Cheliuskin
Ostrov Dikson
Krasnoiarsk
Sale Khard
Samarovo
Narian Mar
Sverdlovsk
Sykhyvkar
Kap Tobin
Jan Mayen
Angmagssalik
Narssarssuaq
Ship B
Ship A
Keflavik
Ship M
Tromsø
Sodankylä
Östersund
Helsinki
Moscow
Stockholm
Thorshavn
Ship I
Gardermoen
Lerwick
Sola
Göteborg
Stornoway
Leuchars
Copenhagen

Height in dekametres

Fig. 6

Upper Air Branch (M.O.23)

AVERAGE 700-500 mb. THICKNESS

M.R.P. 981

JULY 1949-1953

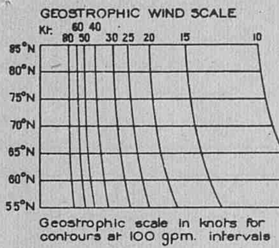

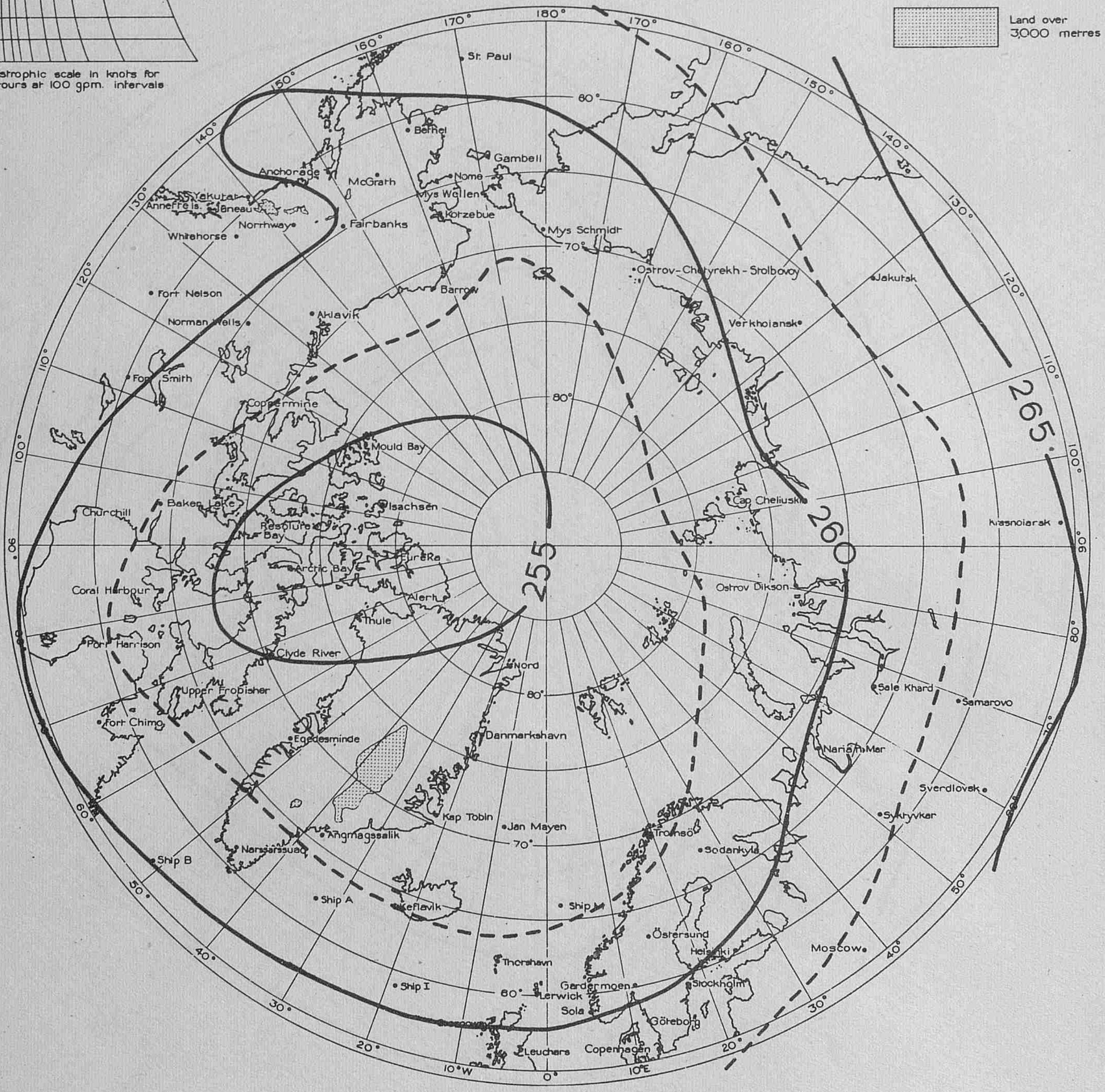
▨ Land over 3,000 metres
255
260
265
180°
170°
160°
150°
140°
130°
120°
110°
100°
90°
80°
70°
60°
50°
40°
30°
20°
10°W
0°
10°E
St. Paul
Bethel
Gambell
Nome
Mys Wellen
Kotzebue
McGrath
Anchorage
Fairbanks
Yakutat
Annette Is.
Juneau
Northway
Whitehorse
Fort Nelson
Norman Wells
Aklavik
Barrow
Mys Schmidt
Ostrov-Chetyrekh-Stolbovoy
Jakutsk
Verkhoiansk
Fort Smith
Coppermine
Mould Bay
Isachsen
Baker Lake
Resolute Bay
Churchill
Eureka
Arctic Bay
Alert
Thule
Coral Harbour
Port Harrison
Clyde River
Nord
Upper Frobisher
Fort Chimo
Egedesminde
Danmarkshavn
Kap Tobin
Jan Mayen
Angmagssalik
Narssarssuaq
Ship B
Ship A
Keflavik
Ship M
Tromsö
Sodankylä
Cap Cheliuskin
Ostrov Dikson
Krasnoiarsk
Sale Khard
Samarovo
Narian Mar
Sverdlovsk
Syktyvkar
Östersund
Helsinki
Moscow
Stockholm
Göteborg
Copenhagen
Gardermoen
Sola
Lerwick
Thorshavn
Ship I
Leuchars
Stornoway
60°
70°
80°

Height in dekametres

Fig. 7

Upper Air Branch (M.O.23)

AVERAGE 500-300 mb. THICKNESS

M.R.P. 981

JULY 1949-1953

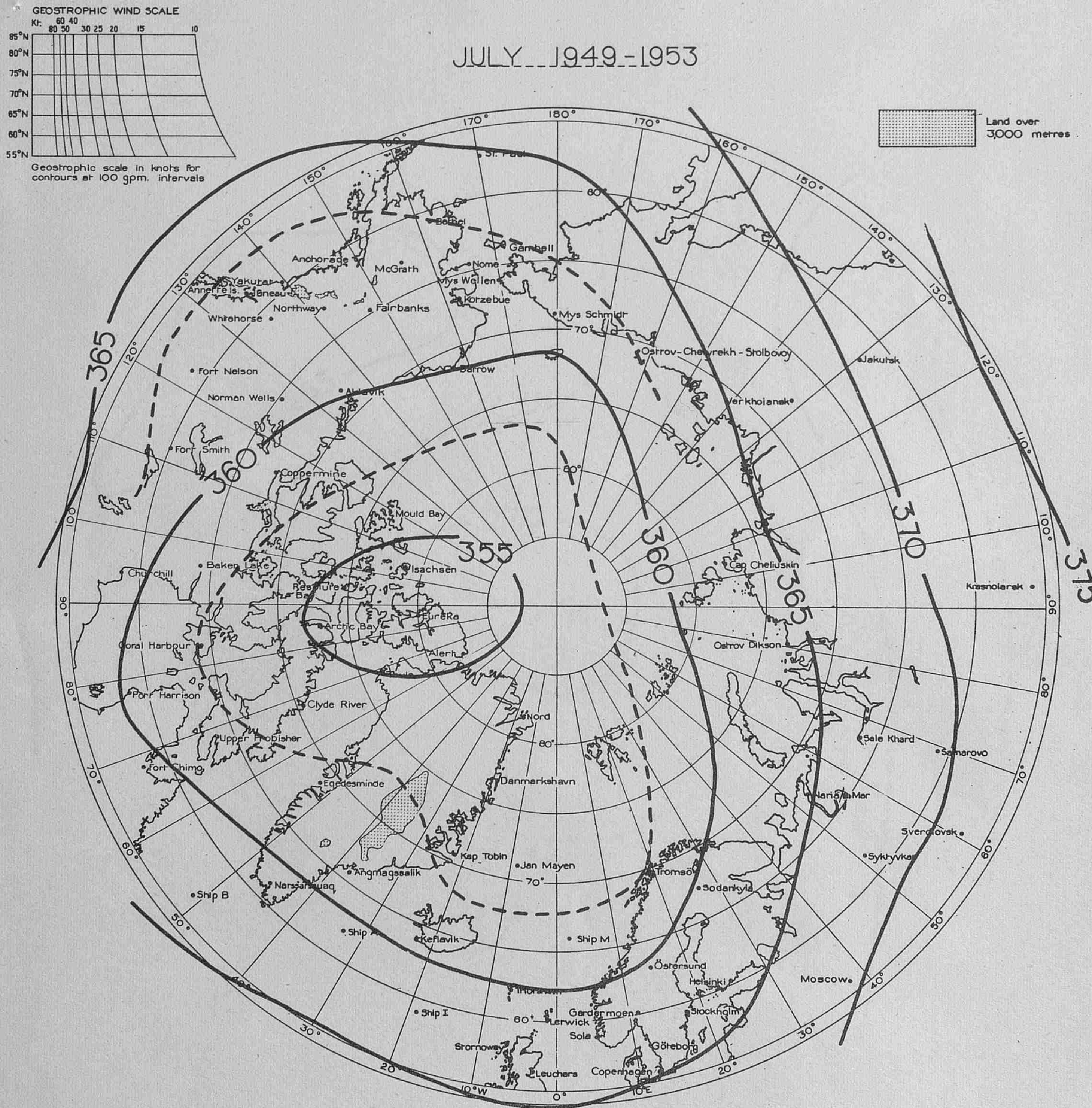
GEOSTROPHIC WIND SCALE
Kt. 80 60 50 40 30 25 20 15 10
85°N
80°N
75°N
70°N
65°N
60°N
55°N
Geostrophic scale in knots for contours at 100 gpm. intervals
Land over 3,000 metres
355
360
360
365
365
370
375
180°
170°
170°
160°
160°
150°
150°
140°
140°
130°
130°
120°
120°
110°
110°
100°
100°
90°
90°
80°
80°
70°
70°
60°
60°
50°
50°
40°
30°
30°
20°
20°
10°W
0°
10°E
80°
80°
80°
70°
70°
70°
60°
St. Paul
Bethel
Gambell
Nome
Mys Wellen
Kotzebue
McGrath
Anchorage
Yakutat
Annette Is.
Juneau
Northway
Fairbanks
Whitehorse
Mys Schmidt
Ostrov-Chetyrekh-Stolbovoy
Jakutsk
Verkhoiansk
Barrow
Fort Nelson
Norman Wells
Aklavik
Fort Smith
Coppermine
Mould Bay
Isachsen
Baker Lake
Churchill
Resolute Bay
Arctic Bay
Eureka
Alert
Cap Cheliuskin
Krasnoiarsk
Ostrov Dikson
Coral Harbour
Port Harrison
Clyde River
Nord
Upper Frobisher
Fort Chimo
Egedesminde
Danmarkshavn
Sale Khard
Samarovo
Narian Mar
Sverdlovsk
Sykhyvkar
Kap Tobin
Jan Mayen
Angmagssalik
Narsarssuaq
Ship B
Tromsö
Sodankyla
Ship A
Keflavik
Ship M
Östersund
Helsinki
Moscow
Thorshavn
Ship I
Gardermoen
Lerwick
Stockholm
Sola
Göteborg
Stornoway
Leuchars
Copenhagen

Height in dekametres

Fig. 8

Upper Air Branch (M.O.23)

AVERAGE 300-200 mb. THICKNESS

M.R.P. 981

JULY 1949-1953

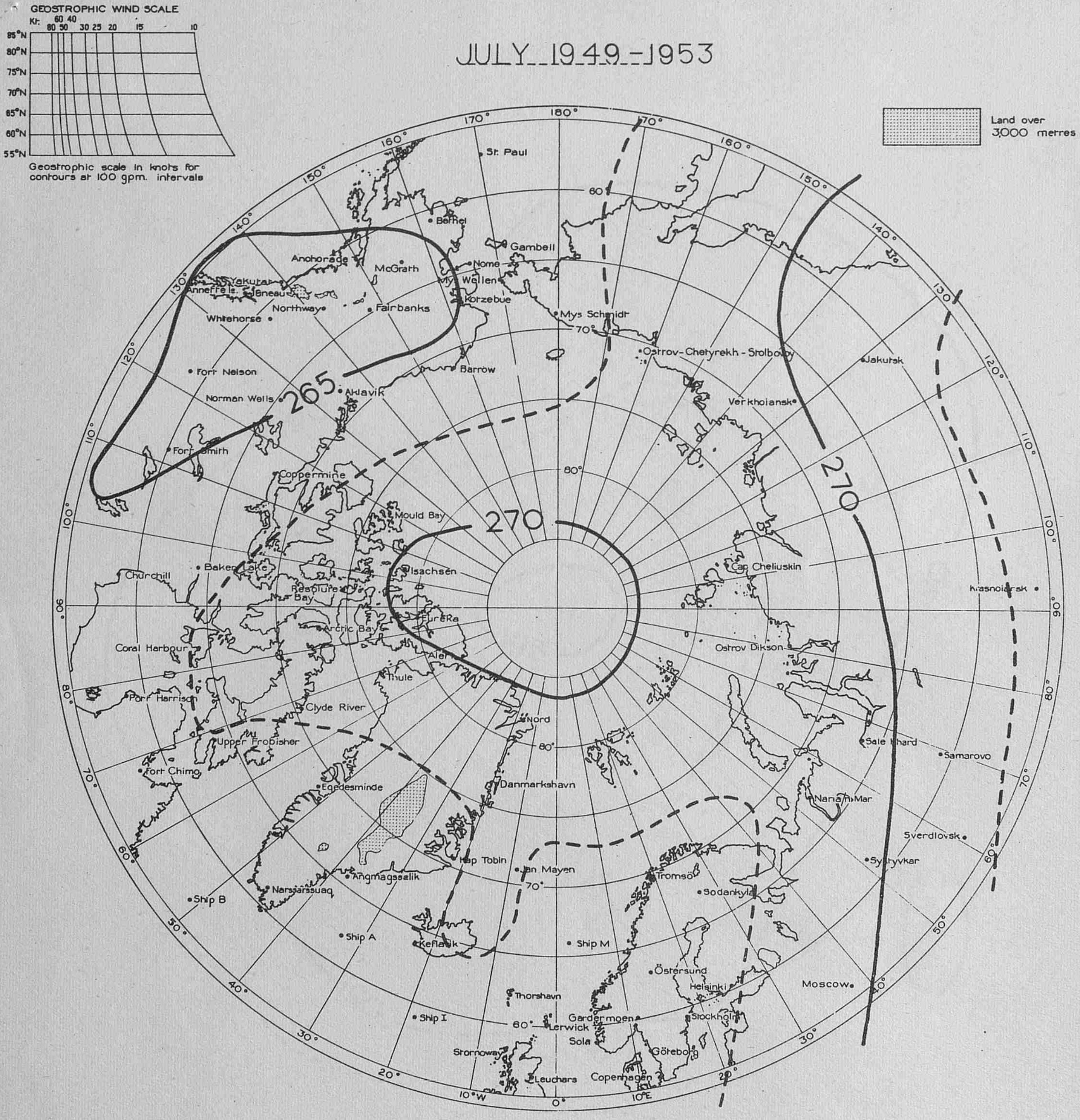
GEOSTROPHIC WIND SCALE
Kt. 80 60 50 40 30 25 20 15 10
85°N
80°N
75°N
70°N
65°N
60°N
55°N
Geostrophic scale in knots for contours at 100 gpm. intervals
Land over 3,000 metres
265
270
270
270
180°
170°
160°
150°
140°
130°
120°
110°
100°
90°
80°
70°
60°
50°
40°
30°
20°
10°W
0°
10°E
60°
70°
80°
St. Paul
Bethel
Gambell
Nome
Wellen
Kotzebue
McGrath
Anchorage
Yakutat
Annette Is.
Juneau
Northway
Fairbanks
Whitehorse
Mys Schmidt
Ostrov-Chetyrekh-Stolbovoy
Barrow
Fort Nelson
Norman Wells
Aklavik
Fort Smith
Coppermine
Mould Bay
Isachsen
Eureka
Alert
Thule
Jakutsk
Verkhoiansk
Cap Cheliuskin
Krasnoiarsk
Ostrov Dikson
Sale Khard
Samarovo
Narian Mar
Sverdlovsk
Syktyvkar
Baker Lake
Churchill
Resolute Bay
Arctic Bay
Coral Harbour
Port Harrison
Clyde River
Nord
Upper Frobisher
Fort Chimo
Egedesminde
Danmarkshavn
Kap Tobin
Jan Mayen
Angmagssalik
Narssarssuaq
Ship B
Ship A
Keflavik
Ship M
Tromsö
Sodankylä
Östersund
Helsinki
Moscow
Thorshavn
Ship I
Lerwick
Gardermoen
Stockholm
Sola
Stornoway
Göteborg
Leuchars
Copenhagen

Height in dekametres

Fig. 9

Upper Air Branch (M.O.23)

AVERAGE 200-150 mb. THICKNESS

M.R.P. 981

JULY 1949-1953

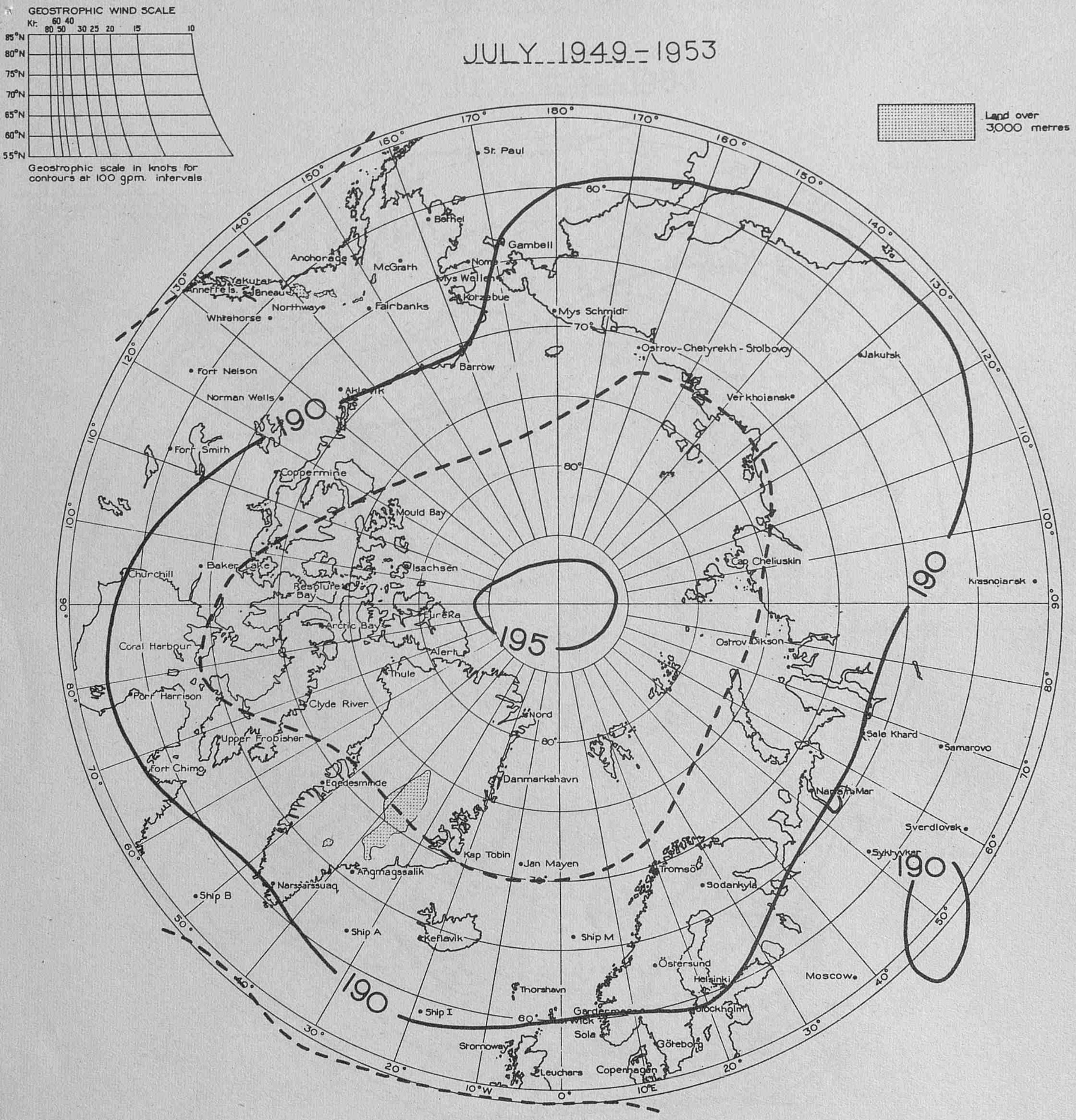
GEOSTROPHIC WIND SCALE
Kt. 60 40
80 50 30 25 20 15 10
85°N
80°N
75°N
70°N
65°N
60°N
55°N
Geostrophic scale in knots for contours at 100 gpm. intervals
Land over 3,000 metres
180°
170°
160°
150°
140°
130°
120°
110°
100°
90°
80°
70°
60°
50°
40°
30°
20°
10°W
0°
10°E
St. Paul
Bethel
Gambell
Nome
Mys Wellen
Kotzebue
McGrath
Anchorage
Yakutat
Annette Is.
Juneau
Northway
Fairbanks
Whitehorse
Mys Schmidt
Barrow
Ostrov-Chetyrekh-Stolbovoy
Jakutsk
Verkhoiansk
Fort Nelson
Norman Wells
Aklavik
Fort Smith
Coppermine
Mould Bay
Isachsen
Cap Cheliuskin
Krasnoiarsk
Churchill
Baker Lake
Resolute Bay
Eureka
Arctic Bay
Alert
Thule
Ostrov Dikson
Coral Harbour
Port Harrison
Clyde River
Nord
Sale Khard
Samarovo
Upper Frobisher
Fort Chimo
Egedesminde
Danmarkshavn
Narian Mar
Sverdlovsk
Syktyvkar
Kap Tobin
Jan Mayen
Tromsö
Sodankyla
Angmagssalik
Narssarssuaq
Ship B
Ship A
Keflavik
Ship M
Östersund
Helsinki
Moscow
Thorshavn
Ship I
Gardermoen
Wick
Sola
Stockholm
Stornoway
Göteborg
Leuchars
Copenhagen
190
190
190
190
195
80°
70°
60°
80°
60°

Height in dekametres

Fig 10

Upper Air Branch (M.O.23)

AVERAGE 150-100 mb. THICKNESS

M.R.P. 981

JULY 1949-1953

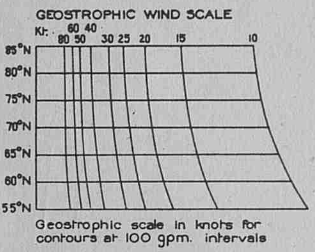

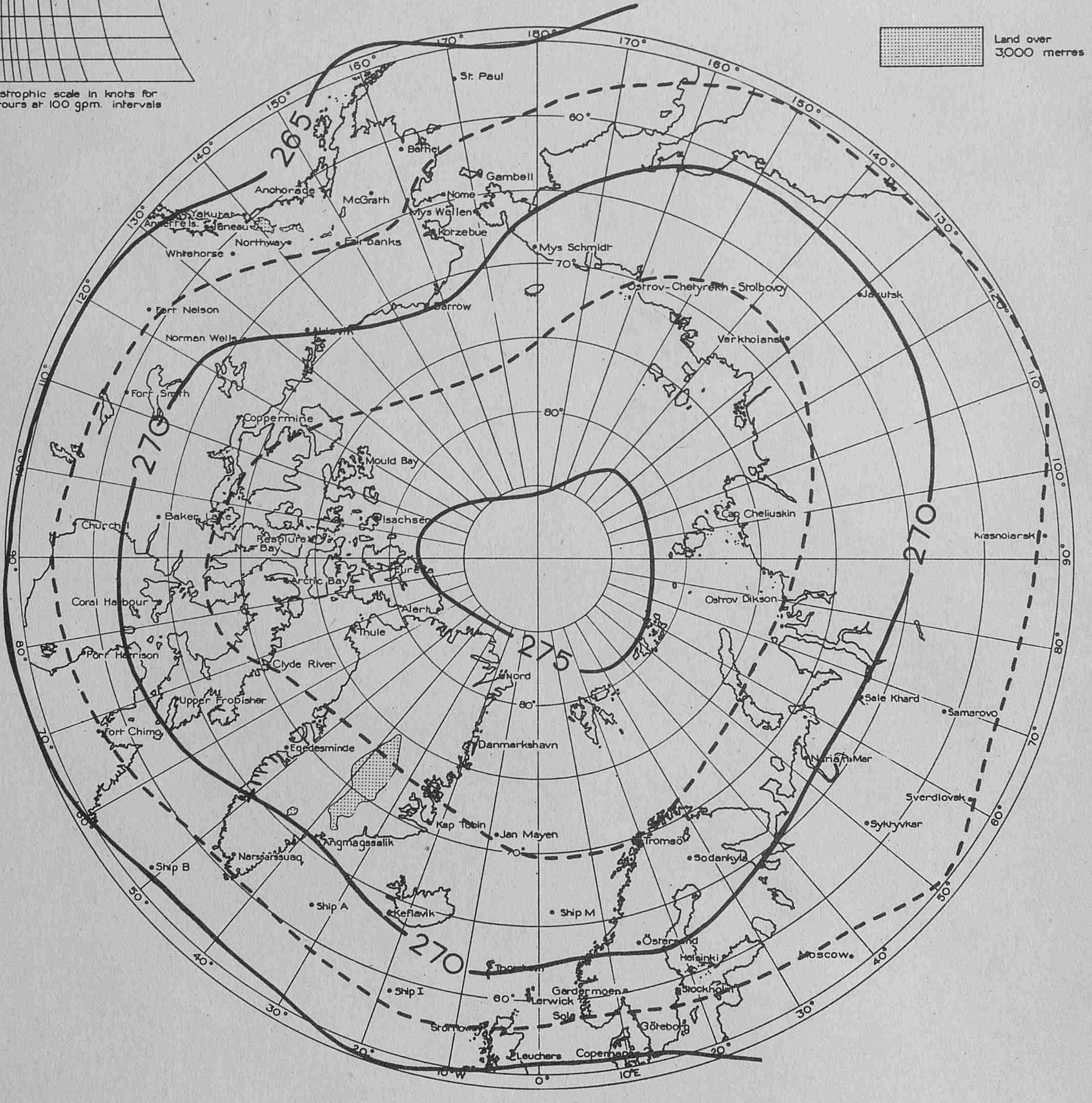
Land over 3,000 metres
265
270
275
270
270
180°
170°
160°
150°
140°
130°
120°
110°
100°
90°
80°
70°
60°
50°
40°
30°
20°
10°W
0°
10°E
60°
70°
80°
St. Paul
Bethel
Gambell
Nome
Mys Wellen
Kotzebue
McGrath
Anchorage
Yakutat
Annette Is.
Juneau
Northway
Fairbanks
Whitehorse
Mys Schmidt
Barrow
Ostrov-Chetyrekh-Stolbovoy
Jakutsk
Verkhoiansk
Fort Nelson
Norman Wells
Aklavik
Fort Smith
Coppermine
Mould Bay
Isachsen
Baker Lake
Resolute Bay
Churchill
Arctic Bay
Eureka
Alert
Coral Harbour
Thule
Cap Cheliuskin
Krasnoiarsk
Ostrov Dikson
Nord
Port Harrison
Clyde River
Upper Frobisher
Fort Chimo
Egedesminde
Danmarkshavn
Sale Khard
Samarovo
Narjan Mar
Sverdlovsk
Sykryvkar
Kap Tobin
Jan Mayen
Tromsö
Sodankyla
Angmagssalik
Narssarssuaq
Ship B
Ship A
Keflavik
Ship M
Östersund
Helsinki
Moscow
Thorshavn
Ship I
Gardermoen
Lerwick
Sola
Stockholm
Stornoway
Göteborg
Leuchars
Copenhagen

Height in dekametres

Fig. 11

Upper Air Branch (M.O.23)

M.R.P. 983
S.C. I/115
14th May, 1956.

AD 223123

R-22745

The measurement of humidity at Britannia Sø 1952-53.

by

R. A. Hamilton.

(Meteorological Office)

AIR MINISTRY

METEOROLOGICAL RESEARCH COMMITTEE

At the time of issue this report has not been published. Any author desiring to quote this paper should refer to it as "A paper of the Meteorological Research Committee (London).
M.R.P. No. 983 by Mr. R. A. Hamilton.
A copy is available in the Library of the Meteorological Office."

M.R.P.983
S.C.I/115
14th May, 1956

AIR MINISTRY

METEOROLOGICAL RESEARCH COMMITTEE

The measurement of humidity at Britannia Sø 1952-53

by

R. A. Hamilton (Meteorological Office)

Introduction

The object of this note is to describe and discuss the method used in determining the values of relative humidity, vapour pressure etc. which will be published in the meteorological tables for Britannia Sø, the main base of the British North Greenland Expedition in Dronning Louise Land (77°09'N, 23°36'W, altitude 231 m.).

The annual range of temperature was from around - 40°C to about +16°C. The lowest temperatures occurred during calm periods during the winter when hoar frost deposits indicated that the relative humidity was high. The hoar frost deposits were usually light, rarely heavy, and fog occurred only once during the two winter periods. During the winter the calm clear periods alternated with windy periods during which dry air poured downwards from the inland-ice to the coast, with a low relative humidity and dew point.

The difficulties experienced arose through the lack of an absolute instrument for measuring humidities at low temperatures. The Dobson-Brewer frost point hygrometer which had been used by the Norwegian-British-Swedish Antarctic expedition had given trouble and could not be modified in time to be taken by B.N.G.E. The modifications were carried out and the instrument was dropped by parachute to the expedition in 1953 but was damaged and could not be repaired.

Instruments in use

The instruments used were:-

(a) Dry-and wet-bulb hygrometer. This will be referred to as D.W.B. even when an ice-bulb was used. Normally a whirling psychrometer was used, but in the spring when temperatures were higher the normal dry- and ice-bulb thermometers in the screen were used when there was appreciable wind. The bulb was painted with ice half an hour or so before reading.

The D.W.B. is of little use at temperatures below -15°C, as the depression of the ice-bulb is so small that it cannot be read with any degree of accuracy on the small thermometers in use. In the conditions which frequently occurred, viz. strong katabatic winds of low relative humidity and temperatures above -15°C, a determination of relative humidity could be made which was probably correct to 5% - assuming, that is, that the tables used for determining the water vapour pressure from readings of the ice-bulb were correct. The tables used are from the 1951 edition of Smithsonian Meteorological Tables, Table 98. Values of saturation vapour pressure over water and over ice are derived from Tables 94 and 96 of this volume.

(b) Hair hygrograph. This was a normal M.O. pattern. The trace shows that it responds well to change of humidity, but it cannot, of course, be regarded as an absolute instrument. The intention was to calibrate the hygrograph so that the relative humidity at the standard hours could be deduced from the trace and the calibration - which might vary from month to month.

/(c)

(c) Lithium chloride hygrometer. This will be referred to as the L.C.H. This instrument was made by the Meteorological Office, but is commercially made under the name "Dewcel" and is patented. Two coils are wound close to one another, without making contact, on a thermometer bulb and the whole is painted with lithium chloride, a hygroscopic substance. When the lithium chloride is wet, it conducts and a current can be passed between the two coils. This current heats the thermometer and lithium chloride coating and the temperature rises until the lithium chloride becomes dry and ceases to conduct. The temperature at which this occurs, is that at which the vapour pressure of the lithium chloride is equal to the ambient atmospheric water vapour pressure, and is measured by the thermometer. A calibration curve (experimentally determined at Blue Hill) was provided but it was not suggested that it was absolutely correct and the intention was not as much to regard the L.C.H. as an instrument of precision but one which was to be studied and perhaps calibrated. Subsequently a second calibration curve has been supplied by Messrs Foxbro Yoxall, the manufacturers of the "Dewcel", which differs appreciably from the original calibration curve.

Comparison of hair hygrograph with D.W.B.

The instruments were installed in the Stevenson screen late in October. The hair hygrograph had been set in the normal way, viz. the hairs were wetted indoors and the pen set to read 95%. During the period Nov.-Dec. 1952 measurements were made with the D.W.B. whenever possible. These are set out in Table 1 with the computed values of vapour pressure, relative humidity and dew point. The computed values of the relative humidity, R, are compared with the hygrograph readings, H, in Table 2. Bearing in mind the small depressions of the ice-bulb and the consequent rather large error in the determination of R, the agreement can be seen to be fairly good with no apparent zero error of the hygrograph. There is some uncertainty in the value of the constant used in the computations of humidity from ice-bulbs but if the one which was used is correct, then it appears that the hygrograph, if set up in the normal manner at room temperature, will read correctly at temperatures down to -10°C to -15°C.

During these two months, November and December 1952, during calm clear weather when hoar frost was deposited (fairly lightly) on the roof of the screen the hair hygrograph recorded values mainly in the range 90 to 96% (see Table 3). It has frequently been stated that at temperatures below 0° the hair hygrometer measures humidities relative to water vapour, and in the belief that during these calm periods with hoar frost depositing on the screen, the relative humidity relative to ice must be approaching 100%, a zero adjustment was made (in two stages) so as to give a hygrograph reading more closely in accord with the presumed relative humidity relative to water. At -30°C the R.H. relative to water is 75% when relative to ice it is 100%.

This, unfortunately, began a series of adjustments to the hygrograph in an effort to agree with the presumed high humidity value, the D.W.B. and the L.C.H. which continued until temperatures above 0°F were experienced in May. Thereafter no more zero adjustments were made. The hygrograph readings in May agreed well with the D.W.B. and by that time the sum of the zero adjustments amounted to only 1% - a fortuitously good agreement as the adjustment had not always been made in steady conditions and the error in measuring and adjustment must have been as much as 1%. The dates and magnitudes of the zero adjustments together with the accepted scale correction for each period between adjustments is shown in Table 4.

/Table 1

Table 1 Dry- and ice-bulb hygrometer measurements

GMT/Date	Dry t°C	Wet t'°C	t-t'	Δe 1000 mb. Tab 98	p mb.	Δe mb.	e' mb. Tab 96	e mb.	Sat. e water mb. Tab 94	R.H. water %	D.P. °C Tab 94
Nov. 1952											
1200/16	-5.9	-7.8	1.8	1.18	994	1.17	3.15	1.98	3.92	51	-14.6
1140/17	-6.9	-9.2	2.2	1.48	983	1.45	2.79	1.34	3.63	37	-19.2
1200/17	-7.2	-9.4	2.2	1.48	983	1.45	2.73	1.28	3.56	36	-19.8
1300/17	-6.1	-8.1	1.9	1.27	983	1.25	3.08	1.83	3.87	47	-15.5
1500/17	-5.0	-6.7	1.7	1.09	982	1.07	3.48	2.41	4.21	57	-12.2
2100/17	-5.0	-7.8	2.8	1.82	982	1.78	3.16	1.38	4.21	33	-18.9
0930/18	-10.0	-11.9	1.9	1.26	990	1.25	2.18	0.93	2.86	33	-23.4
1730/18	-11.1	-12.5	1.4	0.90	992	0.90	2.08	1.18	2.62	45	-20.7
1800/18	-10.3	-11.7	1.4	0.94	992	0.93	2.23	1.30	2.80	46	-19.6
1030/19	-7.1	-8.8	1.7	1.09	989	1.08	2.89	1.81	3.59	50	-15.7
1300/20	-4.2	-7.2	3.1	1.99	981	1.95	3.31	1.36	4.49	30	-19.1
1600/20	-5.8	-8.1	2.2	1.44	980	1.41	3.08	1.67	3.95	42	-16.6
1340/24	-12.8	-13.9	1.1	0.72	985	0.71	1.83	1.12	2.29	49	-21.3
1300/25	-11.1	-12.7	1.6	1.02	990	1.01	2.04	1.03	2.62	39	-22.3
1400/27	-13.3	-14.4	1.1	0.72	990	0.71	1.74	1.03	2.19	47	-22.3
Dec. 1952											
1140/1	-10.3	-12.2	1.9	1.26	980	1.24	2.13	0.89	2.80	32	-23.9
1200/10	-12.8	-13.9	1.1	0.72	991	0.71	1.83	1.12	2.29	49	-21.3
1300/30	-9.4	-11.1	1.7	1.09	1000	1.09	2.35	1.26	2.99	42	-19.9
Jan. 1953											
1130/2	-2.8	-5.8	3.1	1.99	980	1.95	3.74	1.79	4.98	36	-15.8
1200/9	-8.9	-10.6	1.7	1.09	982	1.07	2.47	1.40	3.12	45	-18.7
1400/27	-7.0	-7.7	0.7	0.44	975	0.43	3.19	2.76	3.62	76	-10.5
1300/29	-13.3	-13.9	0.6	0.36	984	0.35	1.83	1.48	2.19	68	-18.1
April 1953											
1220/2	-9.4	-11.4	1.9	1.26	999	1.26	2.29	1.03	2.99	34	-22.3
1140/6	-10.0	-11.4	1.4	0.91	990	0.90	2.29	1.39	2.86	49	-18.8
1740/22	-2.8	-5.3	2.5	1.63	1000	1.63	3.92	2.29	4.98	46	-12.8
1140/23	-1.4	-2.8	1.4	0.91	1002	0.91	4.84	3.93	5.52	71	-5.9
1440/23	-0.6	-1.7	1.1	0.73	1002	0.73	5.32	4.59	5.86	78	-3.9
1730/26	-2.2	-4.4	2.2	1.46	1004	1.46	4.20	2.74	5.19	53	-10.6
2120/26	-4.2	-5.4	1.4	0.91	1004	0.91	3.86	2.95	4.49	66	-9.6
1140/27	-1.4	-4.4	3.1	2.00	1002	2.00	4.20	2.20	5.51	40	-13.3
1830/29	-6.4	-7.7	1.3	0.84	995	0.84	3.19	2.35	3.79	62	-12.5
1200/30	-8.1	-8.9	0.8	0.51	995	0.51	2.86	2.35	3.32	71	-12.5
1730/30	-8.2	-8.9	0.8	0.51	993	0.51	2.85	2.34	3.30	71	-12.5
May 1953											
1140/1	-4.2	-4.4	0.3	0.19	989	0.19	4.20	4.01	4.49	89	-5.7
1740/1	-1.2	-1.8	0.6	0.37	989	0.37	5.27	4.90	5.58	88	-3.0
2100/1	-1.2	-2.2	1.0	0.66	989	0.65	5.08	4.43	5.58	79	-4.4
0540/2	-0.4	-1.4	0.9	0.62	988	0.61	5.44	4.83	5.92	82	-3.2
1740/2	+0.1	-1.0	1.1	0.73	988	0.72	5.62	4.90	6.15	80	-3.0
2100/2	-1.2	-2.2	1.0	0.66	988	0.65	5.08	4.43	5.58	79	-4.3
1140/3	-2.0	-3.4	1.4	0.94	988	0.93	4.58	3.65	5.28	69	-6.9
1740/3	-1.8	-3.1	1.3	0.85	988	0.84	4.74	3.90	5.36	73	-6.0
1140/4	-3.1	-5.0	1.9	1.25	990	1.24	4.01	2.77	4.86	57	-10.4

Note $$\Delta e = \frac{p}{1000} \Delta e_{1000}$$

$$e = e' - \Delta e$$

/Table 2

Table 2

Comparison of hair hygrograph readings (corrected) with determinations of relative humidity by the dry-and-ice-bulb hygrometer

R = Relative humidity from Table 1.
H = Hygrograph reading corrected for zero error.

GMT/Date	R	H	R-H	GMT/Date	R	H	R-H	GMT/Date	R	H	R-H
1952	%	%	%	1952	%	%	%	1953	%	%	%
November				December				April			
1140/17	37	38	-1	1140/1	32	40	-8	2120/26	66	72	-6
1200/17	36	37	-1	1200/10	49	51	-2	1140/27	40	36	4
1300/17	47	36	11	1300/30	42	54	-12	1200/30	71	74	-3
1500/17	57	34	23					1730/30	71	69	2
2100/17	33	33	0	1953							
0930/18	33	27	6	April				May			
1030/19	50	38	12	1220/2	34	34	0	1140/1	89	83	6
1300/20	30	32	-2	1140/6	49	52	-3	1740/1	88	77	11
1600/20	42	41	1	1740/22	46	48	-2	0540/2	82	83	-1
1340/24	49	44	5	1140/23	71	47	24	1740/2	80	76	4
1300/25	39	44	-5	1440/23	78	49	29	2100/2	79	76	3
1400/27	47	50	-3	1730/26	53	57	-4	1740/3	73	76	-3

N.B. A few cases have been omitted, when the hygrograph indicated that the humidity was changing rapidly.

The disagreement at 1300/17 and 1500/17 is probably due to evaporating of the ice-bulb, a source of error which was watched in later measurements.

Comparison of hair hygrograph readings (corrected) with determinations of relative humidity by the dry-and-wet-bulb hygrometer

R = Relative humidity determined by dry-and-wet-bulb hygrometer.
H = Hygrograph reading corrected for zero error.

GMT/Date	R	H	R-H	GMT/Date	R	H	R-H	GMT/Date	R	H	R-H
1953	%	%	%	1953	%	%	%	1953	%	%	%
May				July				August			
1800/6	40	36	0	1200/20	32	36	-4	0530/5	41	35	6
2100/6	66	65	1	1800/20	29	30	-1	1200/6	51	51	0
0600/7	40	37	3	2100/20	30	32	-2	1800/8	69	71	-2
0900/7	58	68	-10	2300/20	31	31	0	1130/13	39	39	0
1200/7	59	63	-4	0600/21	26	27	-1	1130/14	40	36	4
1300/7	62	63	-1	1800/21	38	33	4	1130/16	35	36	-1
1500/7	55	58	-3	2300/21	52	43	9	1730/18	32	34	-2
1800/7	62	64	-2	1800/22	58	61	-3	1730/19	72	72	0
1200/25	39	41	-2	2100/22	65	65	0	1730/22	56	55	1
1500/25	39	39	0	1200/23	52	45	7	1130/27	28	31	-3
1800/25	34	37	-3	2300/23	39	38	1	0900/28	31	39	-8
0900/26	68	59	9	1200/24	33	27	6	0900/29	44	48	-4
1200/26	76	62	14	1200/25	40	37	3	0600/30	63	71	-8
1800/29	19	18	1	2300/25	37	39	-2	1730/31	51	47	4
				0600/26	42	41	1				
July				1200/28	49	51	-2	September			
2300/14	33	32	1	1800/29	69	71	-2	1730/1	39	43	-4
1800/15	25	23	2	1800/30	45	42	3	1130/2	54	55	-1
0600/16	74	81	-9	1800/31	40	39	1	0530/4	44	37	7
								1730/4	47	37	10

/Table 3

Table 3

Steady hair hygrograph readings (corrected) at high humidities

1952 GMT/Date	Hoar frost	t °C	H %
November			
0600/2		−19	88
0540/10	x_o	−24	91
0540/11	x_o	−24	91
0540/13	x_o	−24	90
0540/17		−18	86
0540/29	x_o	−23	98
0900/30	x_o	−26	96
December			
0900/8	x_o	−24	89
0900/9	x	−22	90
0540/14	x	−25	89
0540/15	x	−27	89
0540/21	x	−27	95
0540/22	x	−27	96
0540/23	x	−28	96
0540/24	x	−30	96
0540/25	x	−29	96
0540/26	x	−28	96
0540/29	x	−25	97

1953 GMT/Date	Hoar frost	t °C	H %
January			
1740/8	x_o	−21	99
0540/12	x	−29	94
0540/13	x	−30	93
0540/14	x	−31	93
0540/15	x	−30	93
0540/22	x	−28	92
0540/23	x	−29	91
0540/24	x_o	−28	91
1200/25	x	−29	94
February			
0540/1	x	−36	88
0540/2	x	−35	89
March			
0540/6		−29	80
0540/7		−29	79
0540/8		−31	78
0540/9	x_o	−31	82
0540/10	x_o	−28	82
0540/14	x_o	−38	83
0540/22	x_o	−31	86
April			
0540/11		−24	96
0540/27		−9	95

In all cases cloud amount $< 3/8$, wind speed < 3 kt.

At $t = -35°$: if D.P. $= -36°$ R.H. $= 91\%$; if D.P. $= -36.5$ R.H. $= 86\%$

At $t = -25°$: if D.P. $= -26°$ R.H. $= 91\%$; if D.P. $= -26.5$ R.H. $= 87\%$

At $t = -15°$: if D.P. $= -16°$ R.H. $= 92\%$; if D.P. $= -16.5$ R.H. $= 88\%$

The following values of H were recorded on occasions during October, 1953:-

0900/4 H = 93 at −18°C with slight hoar frost
2100/12 H = 88 at −6°C during long period of snow
1200/23 H = 96 at −11°C during blizzard with 80 m. visibility
0530/26 H = 97 at −8°C during blizzard with 100 m. visibility
0900/29 H = 96 at −13°C in fog with hoar frost.

Table 4

Table 4

Hygrograph resettings

		Change	Net change from Oct '52	Accepted scale correction
Initial setting in Oct. 1952		0	0	0
1830/30 Dec.	lower	8	-8	+8
1230/9 Jan.	lower	12	-20	+20
1800/2 Feb.	lower	18	-38	+38
1800/3 Feb.	raise	10	-28	+28
2100/4 Feb.	raise	7	-21	+21
1740/4 Mar.	raise	18	-3	+3
1030/10 Mar.	lower	15	-18	+17
1815/30 Apr.	raise	7	-11	+10
1800/2 May	raise	15	+4	-5
2100/3 May	lower	5	-1	0

The values of H given in Tables 2 and 3 have been corrected for zero adjustment according to the accepted scale correction shown in Table 4. During May, August and September, 1953 the accepted correction was zero, in July a correction of +3 has been added. This gives the best agreement with the D.W.B. but it is felt the amount is too small to be significant. It will be seen from Table 2 that the hygrograph, corrected for zero error, gives good agreement with relative humidity determined by the D.W.B., with no appreciable temperature coefficient, down to temperatures of around -15°C and dew points down to -22°C.

The hair hygrograph in conditions of high relative humidity

An experiment carried out by M.O.16 at Harrow (private communication) on a sample of hair showed that "Down to temperatures of -30°C the hair was found to follow the room temperature calibrations remarkably well if one assumes that the hair responds to R.H. with respect to water with a negligible temperature effect. The effect of temperature on a M.O. type of hygrograph has also been shown to be the same as that of the brass frame used in this experiment".

If then it is accepted that the hair hygrograph measures humidity correctly relative to water, the implication of the B.N.G.E. measurements is that in the free atmosphere hoar frost is not deposited until the air is super-saturated with respect to ice. The assumption that is now made is that hoar frost is deposited when the air is saturated with respect to water.

In order to obtain an approximate measurement of the temperature of the air in contact with surfaces on which hoar frost was being deposited a thermometer was exposed on top of the screen and the temperature of this was measured when a deposit of hoar frost had deposited on it. This temperature, t_o, is given in Table 5,

/Table 5

Table 5

Date 1952	Hoar frost	t	D.P.(W) t_o	e	D.P.(F)
20/12	x	-27.8	-29.0*	0.42	-32.0
21/12	x	-26.9	-28.1	0.46	-31.1
29/12	x	-24.4	-25.5*	0.60	-28.2
1953					
11/1	x	-27.5	-28.9	0.43	-31.8
22/1	x	-28.4	-29.5	0.40	-32.5
31/1	x	-34.4	-36.7	0.19	-40.2
9/3	x_o	-30.0	-31.5	0.32	-34.8

*Estimated

together with the air temperature t. It will be seen that normally $t-t_o$ is between 1.0 and 1.5, and such a difference has been assumed in the two cases when t_o was not measured. If it is assumed that frost is deposited when the air is saturated with respect to water, then t_o is the dew point D.P.(W). If on the other hand t_o is taken as the frost point, then e is the water vapour pressure and D.P.(F) is the corresponding dew point.

The note below Table 3 indicates that when the depression of the dew point is 1 C° to 1.5 C° below the air temperature the relative humidity is 92% to 86%. If, therefore, the assumption that hoar frost is deposited at the dew point is correct, and if the hair hygrograph reads relative humidity relative to water, then the hygrograph should read about 92% for a normal hoar frost deposit, and about 85% for a light deposit. That this is so in the main is shown by the figures in Table 3.

The hygrograph readings during October 1953 on occasions when the relative humidity can be expected to be high are shown at the foot of Table 3. Again the figures are reasonable. The fog on October 29th was the only fog which occurred during the winter half of the year.

The lithium chloride hygrometer

Though the L.C.H. was set up in November 1952 and measurements with it were made at once, it was some time before the initial difficulties were overcome. The commutator did not alternate for equal periods in each direction and it was soon found that the L.C.H. reading oscillated in apparently steady meteorological conditions. Perhaps this would not have occurred if the L.C.H. had been left running continuously, but this was not possible, firstly because its relays interfered with the radio research, secondly because there was a shortage of power after the breakdown of the main generator, and thirdly because the bottle of lithium chloride had been lost in transit and there was no means of recoating the element. It seemed wise, therefore, to keep it at air temperature so as to minimise the rate of sublimation, and to use the L.C.H. only when humidity could be measured concurrently by some other means.

The relays were adjusted on Decmber 19th so that an A.C. ammeter kicked equally for each of the alternate impulses in opposite directions. A long run was made 21/12/52 and Fig. 1 illustrates the behaviour of the L.C.H. whose temperature is plotted against time for a period of about 4½ hours. It will be seen that the period of the oscillation is about half-an-hour, and twice the amplitude of the oscillation of the L.C.H. temperature is about 15 F°, corresponding to a variation of dew point determination of about 5 C°.

Subsequent runs showed that the period was usually 20 to 40 minutes, but at higher dew points the amplitude was much less.

In making L.C.H. observations the L.C.H. was run for an hour or two, and then readings were taken every 5 or 10 minutes for an hour or so, so that one or two complete cycles were completed. The L.C.H. temperatures were then plotted against time and the value which appeared to represent best the mean of the L.C.H. readings was taken as the L.C.H. temperature: this could be estimated to within about 1 F° corresponding to 0.3 C° in dew point determination.

There is a close relation between the ammeter readings and the L.C.H. temperature. It was found that when the current through the L.C.H. was plotted on the same time scale as the L.C.H. temperatures it too varied in a manner similar to the temperature, the latter reaching its maximum and minimum values soon after those of the former. In unpleasant weather the observer sometimes plotted the ammeter reading indoors and only went outside to read the L.C.H. temperatures when the current had just passed through its extreme values.

That the L.C.H. temperatures oscillated is not surprising as the system of automatic cutting off the heating when the lithium chloride was dry and restarting the current when it became wet is intrinsically oscillatory as is a thermostat. At low temperatures and light winds the oscillation was marked, as is to be expected for at temperatures and dew points around -30°C the L.C.H. temperature is around -15°C. The L.C.H. will, therefore, cool quite quickly when the current ceases and with the water vapour pressure as low as 0.5 mb. it will take some time for enough moisture to be taken up by the lithium chloride to enable it to conduct. At higher temperatures the amplitude of oscillation was much smaller amounting to only about 1 F° at temperatures around freezing point.

Table 6 gives the L.C.H. temperature reading on all occasions, after the commutator adjustment on December 19th, on which a measurement of the dew point was made by another method. The L.C.H. temperature is plotted against the dew point measurement in Fig. 2. The circles are dew points determined by D.W.B., the crosses determinations by hair hygrograph, but excluding cases when the humidity was high, i.e. in cases of cold calm weather. The estimates of dew point in cases of cold calm weather with hoar frost depositing are also shown: the squares are the estimated dew points on the assumption that hoar frost is deposited at the dew point, the triangles are the estimated dew points on the assumption that hoar frost is deposited at the frost point.

In the figure are also plotted other calibration curves (1) that determined experimentally at Blue Hill, (2) that provided by Messrs Foxbro Yoxall and (3) the theoretical curve from the International Critical Tables. It will be seen that the points do not lie around any of these three calibration curves, at higher dew points the plotted points lie close to the theoretical curve and at low dew points they lie closer to it than do either of the other calibration curves. Moreover the squares, the estimated dew points on the assumption that hoar frost is deposited at the dew point, lie well on the best curve drawn through the D.W.B. and the hair hygrograph determinations. That the hair hygrograph points fit with the D.W.B. points is not surprising as it has already been shown that the two sets of determinations were in reasonable agreement, but it must be borne in mind that most of the hair hygrograph determinations were made at temperatures well below -15°C, the lowest temperature at which appreciable depressions of the ice-bulb are experienced. It is satisfactory, therefore, to find these points fitting well with the estimated dew points in cases of high relative humidity, though of course that is no proof that the underlying assumptions are correct, viz. that hoar frost is deposited at the dew point, and that the hair hygrograph has a negligible temperature coefficient.

For the purpose of determining the humidities, vapour pressures etc. given in the meteorological summaries of Britannia Sø the dotted line (B.N.G.E.) in Fig. 2 has been accepted as correct. The implication of this assumption is that:-

(1) In the clear Arctic atmosphere hoar frost is deposited at the dew point.

(2) The constants for computing humidities from ice-bulbs as given in the Smithsonian Tables are correct.

(3) The hair hygrograph functions down to temperatures of -35°C with no appreciable temperature coefficient. (This is confirmed by laboratory experiment).

The value of relative humidity at the synoptic hours is therefore the hygrograph reading, corrected for zero error.

Estimate of the standard error in determining relative humidities

The values of the dew point determined by the L.C.H. according to the accepted calibration curve are shown in the last column of Table 6, headed D.P.(L). These values can readily be compared with the determinations by other methods.

If the calibration is accepted as correct, the standard error of the determinations of dew point by the other methods are:-

By hair hygrograph	1.6 C°
By D.W.B.	1.1 C°
By hoar frost deposit	1.0 C°

The mean value of hygrograph reading H when hoar frost is being deposited (at temperatures around -30°C) was 93% with a standard deviation of 2.8%. For light hoar frost deposit the corresponding figure (at a slightly lower temperature) was 90% with a standard deviation of 5.6%.

At -35°C a standard error of 1.6°C in the dew point involves a standard error of 0.05 mb. in the water vapour pressure. At 40% relative humidity the corresponding standard error in measuring relative humidity is about 6%. At -15°C the corresponding standard errors are 0.24 mb. and 5%.

Thus the standard error in measuring the relative humidity by the hair hygrograph when the dew point is below -10°C is around 5%. When monthly means are calculated the standard error is less than one fifth of the standard error of each observation and is inappreciable. These are random errors. If the accepted calibration of the L.C.H. is in error then the random error is superimposed on a constant error. The appropriate magnitude of the constant error can be estimated as follows.

It must be assumed that the other three calibrations are equally likely to be correct. The standard error of the dew point measurement by the accepted calibration curve is then:-

(a) 2.0 C° when the dew point is -5°C when $e = 4.2$ mb.
The corresponding error in water vapour pressure Δe is 0.64 mb., introducing an error of $\Delta R = 15\%$ in the relative humidity.

(b) 2.8 C° at -15°C when $e = 1.91$ $\Delta e = 0.44$ $\Delta R = 23\%$

(c) 3.3 C° at -25°C when $e = 0.80$ $\Delta e = 0.25$ $\Delta R = 31\%$

(d) 3.9 C° at -35°C when $e = 0.31$ $\Delta e = 0.08$ $\Delta R = 25\%$

It will be seen that the random error is small compared with these, so the standard error of the observations arises solely through error in the calibration of the L.C.H. and amounts to 2 to 4 C° in the dew point, and 15 to 30% in the relative humidity. In view of the fact that the accepted calibration lies between the other calibrations and the theoretical curve, it seems likely that the errors are appreciably lower than the estimated standard error quoted above.

/Table 6

Table 6

Lithium chloride hygrometer calibration

Key:-
t = air temperature in C°
H = corrected hair hygrograph reading
Sat. e = Saturated water vapour pressure with respect to water at t°C, in mb.
e(H) = Water vapour pressure as measured by hair hygrograph
D.P.(H) = Dew point measured by hair hygrograph, in C°
D.P.(D.W.) = Dew point measured by D.W.B.
D.P.(W) = Estimated dew point assuming hoar frost is deposited at dew point
D.P.(F) = Estimated dew point assuming hoar frost is deposited at frost point
L = L.C.H. reading in F°
D.R.(L) = Dew point measured by L.C.H. according to accepted calibration.

GMT/Date 1952	t °C	H %	Sat. e water mb.	e(H) mb.	D.P.(H) °C	D.P.(D.W.) °C	D.P.(W) °C	D.P.(F) °C	L °F	D.P.(L) °C
December										
1400/19	-27.2	99	0.66	0.65	-27.3				13.5	-29.1
1500/20	-27.8	95	0.62	0.59	-28.3		-29.0	-32.0	18.0	-27.5
1200/21	-26.9	92	0.68	0.62	-27.9		-28.1	-31.1	16.0	-28.2
1300/29	-24.4	100	0.85	0.85	-24.4		-25.5	-28.2	23.0	-25.1
1300/30	-9.4	54	3.00	1.62	-17.0	-19.9			35.0	-20.8
Jan. 1953										
1130/2	-2.8	50	4.97	2.49	-11.8	-15.8			44.5	-17.5
1200/9	-8.9	54	3.12	1.68	-16.6	-18.7			48.0	-16.5
1200/11	-27.5	93	0.64	0.60	-28.3		-28.9	-31.8	14.7	-28.7
1200/22	-28.4	91	0.59	0.54	-29.4		-29.5	-32.5	12.0	-29.9
1400/27	-7.0					-10.5			67.5	-9.6
1300/29	-13.3	89	2.20	1.95	-14.8	-18.1			46.0	-17.0
1200/31	-34.4	89	0.33	0.30	-35.6		-36.7	-40.2	-1.0	-35.1
February										
1100/17	-22.3	60	1.03	0.61	-28.0				16.0	-28.2
1140/20	-22.2	52	1.04	0.54	-29.4				12.5	-29.5
2100/26	-17.8	32	1.51	0.48	-30.5				10.0	-30.6
1500/27	-21.1	50	1.14	0.57	-28.8				16.5	-27.8
March										
1740/8	-30.0	81	0.51	0.41	-32.3				5.0	-32.6
1600/9	-30.0	80	0.51	0.41	-32.3		-31.5	-34.8	4.0	-33.0
1100/10	-26.1	79	0.73	0.58	-28.6				13.3	-29.2
1100/12	-27.8	75	0.62	0.47	-30.9				3.7	-33.2
1330/13	-32.8	77	0.39	0.30	-35.5				-0.5	-35.0
1200/14	-35.3	79	0.30	0.24	-37.6				-10.3	-39.0
1530/15	-27.2	70	0.66	0.46	-31.0				3.1	-33.4
1600/16	-15.6	56	1.82	1.02	-22.4				26.5	-24.0
2200/18	-12.5	52	2.34	1.22	-20.3				38.5	-19.6
1400/21	-20.0	52	1.25	0.65	-27.4				13.0	-29.4
1200/26	-23.9	51	0.89	0.45	-31.3				6.0	-32.2
1500/29	-17.5	54	1.55	0.84	-24.6				21.7	-25.7
April										
1200/12	-9.4	35	3.00	1.05	-22.0	-22.3			28.0	-23.5
1140/6	-10.0	51	2.86	1.46	-18.2	-18.8			42.0	-18.5
1500/13	-11.7	37	2.50	0.93	-23.4				25.4	-24.3
1330/21	-11.7	68	2.50	1.70	-16.4				47.5	-16.5
1440/23	-0.6	49	5.85	2.86	-10.0				64.5	-10.5
1830/29	-6.4	63	3.79	2.38	-12.3	-12.5			59.5	-12.3
May										
1620/6	+8.0	33	10.7	3.55	-7.2	-7.2			77.0	-6.1

Fig. 1

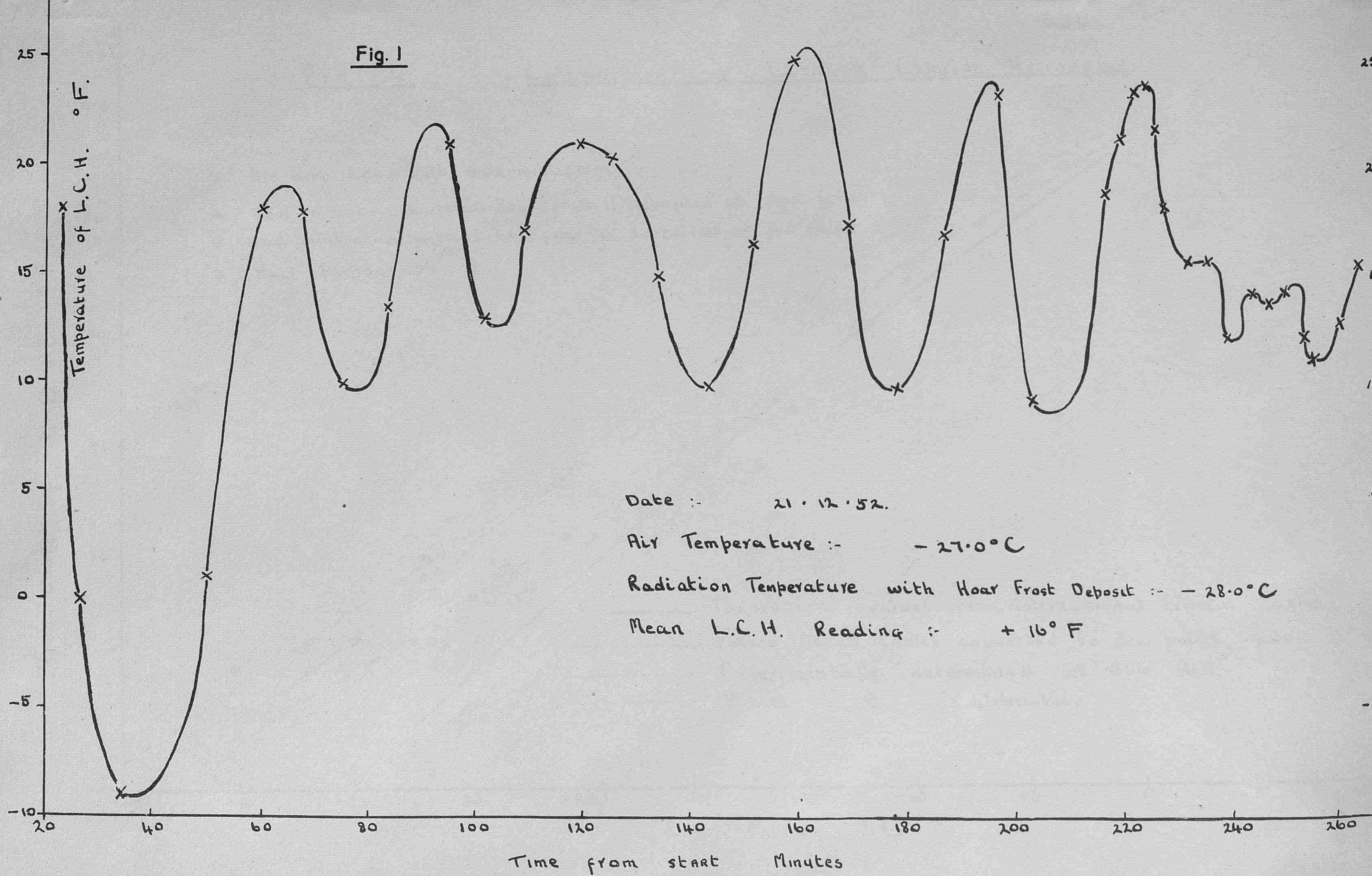

Date :- 21 · 12 · 52.

Air Temperature :- − 27·0°C

Radiation Temperature with Hoar Frost Deposit :- − 28·0°C

Mean L.C.H. Reading :- + 16° F

Fig. 2 Calibration of Lithium Chloride Hygrometer.

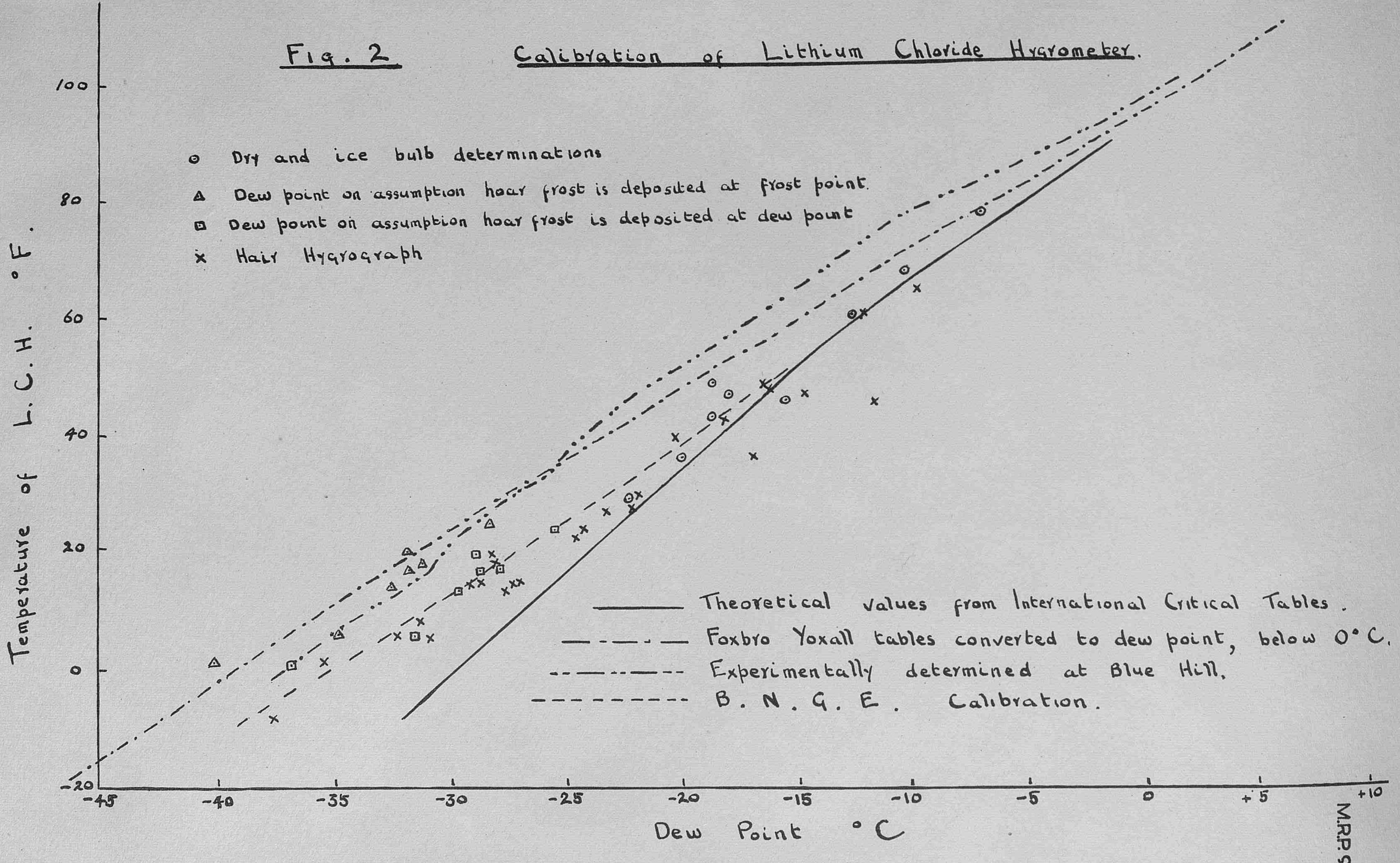

M.R.P. 984
S.C.111/209
23rd May, 1956.

AD 223124

Variation with height of rainfall below the melting level.

by

W. G. Harper.

(Meteorological Office)

AIR MINISTRY

METEOROLOGICAL RESEARCH COMMITTEE

At the time of issue this report has not
been published. Any author desiring to
quote this paper should refer to it as "A
paper of the Meteorological Research
Committee (London),
M.R.P. No. 984 by Mr. W. G. Harper.
A copy is available in the Library
of the Meteorological Office."

M.R.P. 984
S.C.III/209
23rd May, 1956

AIR MINISTRY
METEOROLOGICAL RESEARCH COMMITTEE

Variation with height of rainfall below the melting level

by

W. G. Harper (Meteorological Office)

Summary

3-cm radar intensity measurements, made at a range of heights up to 6,000 ft on three days with widespread moderate rain, suggest that there was considerable uniformity of drop-size distribution with height once melting of snowflakes was complete and terminal velocity was achieved, and that all significant growth of precipitation was taking place at and above the melting level.

The measurements suggest that the cloud-water content below the melting level was low, and this may prove to be typical of warm-front precipitation in those parts of the British Isles in which orographic effects are unimportant.

The contribution to signal intensity due to the coalescence of drops (as distinct from the coalescence of droplets as a growth-initiation mechanism), which has been computed by Mason and Ramanadham (1) to be 0.8 db/km for closely similar conditions to ours, could not be detected.

Rates of rainfall calculated from the radar equation agree reasonably well with measured values if a factor F of value 0.15 is inserted in the equation. This is in close agreement with the value 0.2 obtained in America by Austin and Williams (2), who have made a particularly extensive series of measurements using pulse integration methods.

---

1. Introduction

It must be admitted that the quantitative use of radar in the study of rainfall has made relatively little progress. There has for example been doubt as to whether radar signals which are received from precipitation above the ground can be immediately related to rainfall measurements or drop-size distributions taken at ground level.

Mason and Ramanadham (1) have made a positive contribution to this by making computations of accretion effects and collision processes below the melting level. They found that after a fall of only 1 km in layer cloud conditions the smaller drops should be seriously depleted and the larger ones increased.

Confirmation of these effects is desirable but is hard to come by. Reliable measurement of raindrops from aircraft has not yet been achieved. Balloon-borne measuring instruments have been developed in Australia (Adderley (3)) but are attended with great difficulty and have given some unexplained results. In radar however we have a method of measurement which is particularly sensitive to changes in drop-size distribution. Radar echo intensity from rain is proportional to $\sum d^6$, where d is the drop diameter, the summation being taken over all the drops in unit volume. It is evident that small drops and cloud droplets, although occurring in larger numbers than big drops, provide a negligible contribution to the received echo, and that the echo intensity will attain large values when large drops are present.

Mason and Ramanadham also computed theoretical radar echo intensitites, and concluded that growth of drops by collision and accretion should, in the steady rainfall conditions they assumed, be detectable by radar if the fall path is greater than about 1 km. The present paper reports measurements made in such conditions.

2. Radar measurements

There is considerable advantage to radar in studying 'steady state' rain in widespread rain conditions. There is then no doubt that the radar beam is being filled by the precipitation, and it is advantageous to scan in elevation at a fixed range and azimuth which have previously been checked as being free from unwanted permanent echoes from ground targets. Wexler and Austin (4) and Boucher et al (5) have made intensity studies of this type, but have concentrated their attention on the variations of intensity in the melting level and in the snow above, and have not reported any detailed measurements below the melting level. Their working range was 11 mi, and they scanned in steps of 1 or 2° in elevation, i.e. steps of 1,000 or 2,000 ft in height.

It might be thought that use of a vertically-looking radar would be preferable to scanning in elevation because of the short ranges which would then be involved. A great disadvantage of this method is that, when a single aerial has to be used for both transmitting and receiving, the receiver suffers from paralysis for the duration of the transmitted pulse, and with our equipment no signals are received from the lowest 2,000 ft. It was therefore decided to scan in elevation at a range of about 3 mi. This made it possible to study in detail the lowest 6,000 ft in steps of 250 or 500 ft. Reliable measurements could not be made below 500 ft because of obstructions in the path of the beam. Results obtained on three days with widespread continuous moderate rain are presented. On each occasion there is independent radar evidence that the rain was reasonably uniform over an area of several hundred square miles.

3. Radar theory

The signals from a calibrated radar can be interpreted in terms of rate of rainfall if drop-size distribution is known. For precipitation uniformly filling the beam at range r the received power averaged over many pulses P_r is given by

$$P_r = \frac{P_o h A_e}{8 \pi r^2} \Sigma \sigma \qquad \text{........ (1)}$$

P_o	peak output power
h	pulse length
A_e	effective area of antenna
$\Sigma\sigma$	scattering cross-section of the precipitation per unit volume.

A_e usually has a value between 0.5 and 0.85 of the actual area A of the antenna, and is constant for any one antenna. The reduction factor is caused by the non-uniformity of the radiation across the transmitted beam.

The scattering cross-section of a single drop which is small in relation to the wavelength has been evaluated by Ryde (6) as

$$\sigma = 4 \pi a^2 \left(\frac{2 \pi a}{\lambda} \right)^4 \left| \frac{\epsilon - 1}{\epsilon + 2} \right|^2 \qquad \text{........(2)}$$

a	radius of drop
λ	wavelength of radar
ϵ	dielectric constant

The dependence of σ on λ is seen to be a form of Rayleigh scattering. (2) simplifies to

$$\sigma = \frac{\pi^5 d^6 |K|^2}{\lambda^4} \qquad \text{........(3)}$$

where $K = \epsilon - 1/\epsilon + 2$, d diameter of drop.
Inserting in (1) we have

$$P_r = \frac{P_0 h A_e \pi^4 |K|^2 Z}{8 \lambda^4 r^2} \qquad \text{........(4)}$$

$$\text{where} \quad Z = \sum d^6 \qquad \text{........(5)}$$

the summation being taken over all the drops in unit volume.

Numerous studies of drop-size distribution at the ground have been made, both in Europe and America. A valuable summary of this work was undertaken by Best (7). He found a relationship of the form $Z = a R^b$; where R is rate of rainfall and a and b are constants. a and b showed some variability, but mean values gave

$$Z = 346\ R^{1.54} \qquad (Z\ \text{mm}^6\text{m}^{-3},\ \ R\ \text{mm hr}^{-1}).$$

Inserting in (4) we have

$$P_r = 4{\cdot}33 \times 10^{-11} \pi^4 P_0 h A_e |K|^2 \lambda^{-4} R^{1.54} r^{-2} \qquad \text{........(6)}$$

(R mm hr^{-1}, all other quantities in cgs units).

This is a very convenient form for interpretation of radar echo intensities in terms of rate of rainfall.

4. Scanning technique

The radar measurements were made on the amplitude display of the range-height radar AN/TPS-10. This is American equipment, designed to scan in elevation from 0 to 22° on any chosen bearing. The beam width (to half-power points) of 0.7° in the vertical samples a layer 200 ft deep at the selected working range of 15,000 ft, while its 2° beam in azimuth is 500 ft wide at this range. The signal appearing at any point in the display is that from a range interval equal to half the pulse length, in this case 500 ft. The measurements were thus made along a column 500 ft square in cross-section. The use of a constant slant range meant that the highest measurements were on a sample displaced 1,200 ft from the lowest sample. This slanting column is quite acceptable for steady rain scans, and makes range correction of individual readings unnecessary. In any case the wind drift of precipitation through the column in the 2 to 5 min taken to complete a scan is usually much more than 1,200 ft, and cannot readily be allowed for.

The effect of attenuation of the 3 cm beam by the intervening rain can be safely neglected for this short double path-length of 6 mi and the steady rain intensities involved. It would amount to less than 1 db, and being very closely the same for the constant slant range and the scanning elevation involved, would not affect comparisons in elevation.

/5.

5. Absolute intensity measurements

Radar signals can be compared by direct measurement on an amplitude display, but they cannot in this way be related to an absolute level. A signal generator test set TS-263 was therefore used to calibrate the gain dial of the radar in decibels (db) before and after each set of intensity measurements, and this calibration was normally found to be stable within 1 db. To convert these signal generator db values to dbm (decibels below the level of 1 milliwatt), a factor of +45 db is applied. The various contributions to this factor are listed in Table 1.

Table 1. Factors to be applied to signal generator readings to relate to level below 1 milliwatt

Cause	Factor db	Notes
Insertion loss of directional coupler	+37	Makers' calibration 37 db ± ½ db.
Loss in concentric cable between directional coupler and signal generator	+2	Makers' calibration
Attenuation in waveguide between horn and directional coupler	-1	Affects received signals only. TPS-10 handbook
Difference in saturation levels of the displays used for calibration and for precipitation scanning	+2	Measured on gain dial
Difference between signal generator pulse level and precipitation setting level	+5	See footnote [*]
Total factor	+45	

The following quantities are known or can be measured:-

P_o	peak power output measured on test set
h	pulse length 1μ sec (3×10^4 cm)
$\|K\|^2$	0.93 for water, practically independent of temperature
A_e	effective area of antenna. This is obtained from the known aerial gain G, 18,000. The gain of a given aerial over an isotropic radiator is given by $G = \frac{4\pi A_e}{\lambda^2}$ from which we obtain A_e 15,600 cm^2.

Footnote [*] This combines two corrections. Precipitation echoes, which result from incoherent scattering, give a rapidly beating signal of the same nature as receiver noise. It is surprisingly difficult to bring the peaks of a beating signal accurately up to saturation level on an amplitude display. It proved more satisfactory to make measurements by increasing the gain until the 15,000 ft range marker shape could just be detected at the saturation level. This required a slightly higher gain setting than for measurement on the peaks.

The peak amplitude of a randomly beating signal is greater than its rms value. From gain dial settings in steady precipitation it was concluded that the range marker level was nearly twice the rms amplitude i.e. peak intensity between 3 and 4 times the rms intensity.

The signal generator output on the other hand, although pulsed, is long compared with precipitation echo peaks, and it is more appropriate to compare this with the rms value of a beating echo. This factor 3 to 4 leads to the correction 5 db.

We can now interpret variations of signal intensity with height in equation (6) in terms of rate of rainfall, for comparison with raingauge values. The nearest recording raingauge was at Dunstable, 4 mi west of the scanning site.

6. 5th September 1955

Continuous moderate rain associated with a well-defined trough fell at East Hill from 0830 to 0945 GMT. The 10 cm plan-position photograph (Fig.2) taken at 0929 shows a belt of precipitation 20 to 30 mi wide lying over the station. The rainfall recorder at Dunstable, which is only 2 mi south-west of East Hill (though 4 mi from the scanning site) shows particularly steady rain from 0910 to 0940 of 2.7 mm hr^{-1}. In all 7.4 mm fell in the period 0800 to 1400.

The 10 cm range-height photograph (Fig.1) taken at 0845 looking along the belt of precipitation shows echo to 20,000 ft. The steadily falling echo top out to a range of 35 mi is an effect of the increasing range, but its evenness is a clear indication of the steadiness of the precipitation. As uniform an echo as this is quite unusual. A further reliable guide to the steadiness of the precipitation is the reduced gain photograph (Fig.3) taken at 0943 using an extended range scale. This shows an unusually uniform echo in the melting level at about 8,500 ft. A full description of the bright band at the melting level has been given by Browne, Palmer and Wormell (8) and will not be repeated here. It will be noticed that there is practically no echo within 5 mi of the station in Fig.3. This is not due to weaker rain, but is a 'swept gain' effect built into the receiver where strong echoes from ground targets are a permanent feature of the display with the wider angle beams of the 10 cm equipment (it is only by careful selection of azimuth and because of the much narrower beam of the 3 cm radar that these effects can be avoided when scanning at a range of 3 mi).

The normal range photograph (Fig.4) taken at 0945 shows that a cellular structure had developed beyond 25 mi by 0945, with almost vertical columns of heavier precipitation imbedded in lighter precipitation. It must be remembered that the height scale on this display is nearly five times as open as the range scale so that an echo column which appears twice as tall as it is wide is actually coming from a precipitation column twice as wide as it is tall.

Four complete scans were made with the 3 cm range-height radar in the period 0916 to 0932, with measurements at each degree step in elevation. Each scan took about four minutes. The results plotted as signal intensity against height (Fig.5) show that rainfall was heaviest at 0916. The unsteady and generally low signal intensities of the scan made at 1000 were in much weaker rainfall, and operations had to be discontinued. In fact rain ceased at East Hill at 1003 and at Dunstable at 1000.

A logarithmic scale of rate of rainfall has been added from equation (6) based on the rate of fall of 2.7 mm hr^{-1} at Dunstable. This scale has been added to give more meaning to the signal intensity values. It should not be regarded as a strictly absolute scale, though internal evidence for its approximate validity will be brought forward in para.9.

The top of the scan at 5,600 ft was well below the melting level, and it is clear that the radar measurements were not affected by the melting process. Discussion of the results is reserved for para.11.

7. 19th October 1955

A deep and slow-moving depression centred over Ireland (pressure at centre 976 mb) gave 21.1 mm of rain at Dunstable in the 24 hours ending 0900/20 but the continuous moderate to heavy rain from 1010 to 1150 on the 19th, when 8 mm of this fell, seems to have been associated with the rapid eastward movement across Southern England of a narrow warm sector. The plan-position photograph (Fig.8) taken at 1020 in the middle of the intensity measurements shows extremely uniform echo extending between 20 and 50 mi in all directions (the lack of brightness in this picture is not caused by weakness of echo but by a slight photographic fault).

The extended scale range-height photographs taken at 1005 (Figs.6 and 7) show uniform echo out to 20 mi and an extremely uniform bright band at the melting level at 5,000 ft. There is an indication of stronger precipitation at 22½ mi, and this is again shown in the normal range photograph taken at 1021 (Fig.9).

Thirteen scans were made with the 3 cm range-height radar in the period 0955 to 1025 GMT. This was only possible by taking intensity measurements in 4 deg. steps in elevation, each scan then taking about 2 min. The scans are numbered consecutively on the signal intensity-height plots (Fig.10) which for clarity are plotted on two graphs. The rain was clearly very variable for scans 1 and 2. Scan 3 at 1005 is much steadier, but shows no sign of the strong echoes to be expected from the melting band, the base of which must have been above 5,600 ft at this time.

Scans 4 to 11 between 1010 and 1022 show a very definite melting band effect at 5,600 ft and relatively uniform intensity below 5,000 ft. The scale of rate of rainfall is based on the 3.5 mm hr^{-1} recorded at Dunstable for this period.

Scan 13 at 1024 was in heavier precipitation, but both 12 and 13 seem to indicate a further slight lowering of the base of the melting layer. This may however have been due to a deepening of the layer by cooling by the melting snow rather than to a lowered freezing level. For discussion of the intensity measurements see para.10.

8. 20th October 1955

By 1200 GMT 20th October the depression which was over Ireland on the 19th had filled to 984 mb and was moving up the Norwegian coast. A cold northerly airstream had spread to most parts of the British Isles, but a wave had developed on the cold front of the depression, and a period of continuous rain was experienced in the Dunstable area during its passage. The Dunstable rain recorder collected 5 mm of rain in the 24 hours ending 0900/21, and 4 mm of this fell in the period 0900 to 1230 on the 20th. Measurements were made in two periods and it is convenient to treat them separately.

(a) 0955-1025 GMT

The 10 cm plan-position photograph taken at 1015 (Fig.13) shows clearly the uniform echo from this rain area. It extends to ranges of 30 to 60 mi from East Hill. The range-height photographs at 0932 and 1035 (Figs.11 and 14) show the echo tops as 20,000 ft close to the station, while the reduced gain picture at 0933 (Fig.12) again shows a uniform bright band as on 19th but now down to 4,000 ft.

The first 3 scans in the period 0955 to 1005 were made only on the rain below the bright band in 2 deg steps from 16 down to 2 deg. As the rain showed no sign of abating, scans 4 to 9 investigated in addition the bright band in some detail, in 1 deg steps from 22 to 14 deg and then 2 deg steps as before. The results, plotted in Fig.15, are of particular interest. The top of the melting level is particularly well-defined in all the scans, and shows remarkably little variation in height. The melting process and the acceleration of the resulting raindrops to terminal velocity appears to be complete in a layer only a little over 1,000 ft deep, for below this there is relatively little change in intensity, and hence in rate of rainfall, down to ground level.

There would seem to be definite evidence of a deepening of the melting layer by lowering of its base by perhaps 500 ft in 15 min in this series of observations. This is probably due to cooling by the melting snow, but advection of colder air may be a contributory cause.

The rain was clearly heaviest at the beginning and end of the period. It was steady throughout scans 4 to 7 (1014 to 1017) but the logarithmic scale of rate of rainfall is based on the average rate of fall at Dunstable for the 8 scans in the period 1158 to 1228 GMT.

/(b)

(b) 1158-1228 GMT

Dunstable recorded steady rainfall of 1.2 mm hr^{-1} in this period, and a further series of 8 scans was made at the same range 15,000 ft and with the same technique i.e. 1 deg steps through the bright band and 2 deg steps beneath.

The short range plan-position photograph (Fig.16) taken at 1156 shows the uniform precipitation echo on which the measurements were made. It is especially uniform from SE to SW of the station. The medium range picture taken immediately after completion of the series at 1230 (Fig.18) shows the same rain area almost past East Hill, but still uniform to the SE, the direction in which the scans were made. The 10 cm range-height photograph taken at 1212 (Fig.17) shows uniform echo in the first 20 mi with echo top 11,000 ft close to East Hill. The small patch of echo at 15,000 ft at range 13 mi is evidence however that there was still some precipitation at higher levels but that it was not as widespread or intense as it had been two hours earlier. The final range-height photograph (Fig.19) was taken at 1246 looking northeast through the rain, which had by then cleared East Hill.

The results are again plotted on two intensity-height graphs (Fig.20). All but one scan again show a well-defined top to the melting layer at 5,000 ft (these heights are above station level; 400 ft must be added to reduce to msl). The reason for the lower top on scan 5 is not clear. The bottom of the bright band was exceptionally uniform for the last three scans. As for series (a) the bright band was again only a little over 1,000 ft thick.

The temperature scales which have been added at the right-hand edge of each intensity-height plot are based on the 1400 GMT ascents at Hemsby, 100 mi northeast of East Hill. It will be noticed that the maximum of intensity in the bright band at the melting level on this day lies on the average 1,500 ft below the freezing level found at Hemsby. It is usually closer to the freezing level than this, and the results found by Hooper and Kippax (9) are thought to be typical. They made radar observations of the bright band at a radiosonde station simultaneously with the radiosonde ascents, ten determinations giving a difference of 440 ft between the two levels with a probable error of ± 150 ft. The present large difference is due to a near-isothermal layer between 4,000 and 6,000 ft which can be seen reflected in the temperature scale; the layer from 0 to 2.5°C is almost 3,000 ft deep while that from 2.5 to 5°C is barely 1,000 ft deep. This layer is probably due to prolonged cooling by melting snow.

A scale of rate of rainfall has again been added to the intensity plots based on the steady fall measured at Dunstable in the period of these scans.

9. Calculated rates of rainfall

The mean value of signal intensity in the rain below the bright band in each of these series has been inserted in Equation (6) and a calculated rate of rainfall obtained. These values are given in col.4 of Table 2, and are seen to be in every case much lower than the measured rates of fall. This has been the

Table 2. Calculated and measured rates of rainfall

Date	Time GMT	No. of scans	R mm hr^{-1} Radar	R mm hr^{-1} Raingauge	F
5. 9.55	0916-0932	4	0.74	2.7	0.14
19.10.55	1010-1022	8	1.25	3.5	0.21
"	1022-1025	2	1.96	5.7	0.19
"	Max. at 1024	1	2.28	-	-
20.10.55	1006-1016	4	0.09	1.4	0.01
"	1158-1228	8	0.33	1.2	0.14
"	1220-1227	3	0.41	-	-

experience of most workers in this subject. Almost invariably a marked discrepancy has been found between theory and measurement. Austin and Williams (2) have probably made the most extended investigation, using pulse integration methods. They found it necessary to insert a factor F of value 0.2 in the numerator of equation (6) to make rainfall from radar and gauge agree i.e. the intensity of the signal received from precipitation was only one fifth that which theory indicated.

Values found for this factor by various workers are given in Table 3. The extremely high value derived from the measurements of Hooper and Kippax (9) calls for some comment. Their measurements on rainfall (0.5 - 10 mm hr^{-1}) gave signal intensities averaging 1 db above the theoretical relationship, giving F 1.25. Mr. Hooper has confirmed however that no allowance was made for the difference in the criteria used in making amplitude measurements of the precipitation echoes and the signal generator pulse (see para.5). Robinson (10), working more recently at Malvern, and making similar amplitude measurements allowed 4.8 db for this, in close agreement with the 5 db we derived independently. 4.8 db applied to Hooper and Kippax's data would give F 0.4.

Table 3. Values for the factor F which have been found by various workers (measurements on rain unless otherwise stated)

	F	λ cm	Notes
Austin & Williams	0.2	10	Pulse integration methods
Hood	0.4	10	
Langille & Thain	0.6	3	
Hooper & Kippax	1.25	3	
Hood	0.1	3	
Kodaira	0.13	3	
Robinson	0.8	0.8	
Donaldson	0.1		Measurements on fog at millimetric wavelength

It must be remembered too that all these assessments of F depend on the drop-size relationship which has been assumed. Hooper, Kippax and Robinson, for example, accepted Ryde's theoretical relationship which was based on the drop-size distribution studies of Laws and Parsons in America. Best has shown that these can be represented by $Z = 317 R^{1.46}$. If Best's relationship $Z = 346 R^{1.54}$ had been assumed the values of F would have been further reduced to 0.3 (Hooper and Kippax) and 0.6 (Robinson).

A value of F has been calculated for each period of uniform rain of Table 2 for which a reliable raingauge value is available. These are given at col.6. The comparative uniformity of four out of five of the values is confirmation of the uniformity of the rain in space and time. The weighted mean of these 26 scans gives F 0.15. This is sufficiently close to the 0.2 found by Austin and Williams (2) to justify applying this value in calculation of rates of rainfall. This has been done in Table 4. The agreement is seen to be good in four cases out of five.

The necessity for introducing a factor F remains obscure. By careful calibration and the use of a standard metal sphere Austin and Williams have shown that it is not instrumental in origin, nor is it due to the non-uniform distribution of radiation across the radar beam. It would seem to be inherent in the nature of the beating signal back-scattered from precipitation. Marshall, Hitschfeld and Gunn (11) suggest that it may prove to be related to an unusual finding of Dr. W.E. Gordon of Cornell who has found in the course of radio propagation studies that the energy received is not proportional to A_e when the antenna dimensions are greater than the 'correlation distance', i.e. the distance between two points for which the received signals have zero correlation. This work is at present unpublished, and it is perhaps premature to refer to it here.

/Table 4.

Table 4. Comparison of measured and calculated rates of rainfall assuming F has the value 0.2

Date	Time GMT	R mm hr^{-1} Measured	R mm hr^{-1} Calculated
5. 9.55	0917-0930	2.7	2.1
19.10.55	1010-1022	3.5	3.5
"	1022-1025	5.7	5.6
20.10.55	1006-1016	1.4	0.3
"	1158-1228	1.2	0.9

10. Errors in calculating rainfall

The values of Table 4 should be considered in relation to the possible errors. Comparison of measured and calculated rainfall may be in error due to three main causes:-

(a) radar calibration errors

(b) drop-size distributions not conforming to the relationship $Z = 346 R^{1.54}$

(c) raingauge measurements not being made on the actual echoing rain.

None of these factors can be easily assessed

(a) The signal generator calibration readings have a standard deviation of about 1 db from the mean. This is probably due to slight instability in the receiver. We can expect that the gain dial setting error is of the same order. In addition it is probable that the transmitted power cannot be measured with our present equipment to better than 10% accuracy. When these effects are combined and interpreted in terms of rate of rainfall we obtain the probable error of a single calculation of rainfall as 35%. The scatter of the points in a single scan in the nominally steady rain below the bright band is seen to be of this order.

(b) Farnsworth (12) has found that even an accurately calibrated radar can indicate rainfall rates in error by a factor of two due to variability of drop-size distribution. His measurements however included a wide range of rates of rainfall, and smaller errors may be expected when measurements are limited to conditions of continuous moderate rain from layer cloud.

(c) It is clearly desirable in future measurements to scan directly above a raingauge or raingauge network.

11. Discussion of results

If the 3 scans made in extremely unsteady rain are excluded we can find 5 of the remaining 32 scans which show a slight tendency to increase of signal intensity towards the ground, averaging 2.6 db/km. 3 others however show an almost equal tendency to decrease, average 2.0 db/km. The remaining 24 cases show no obvious trend towards increase or decrease of rainfall with height, and it is not unreasonable to conclude that the variation in the 8 cases was due to slightly heavier or lighter rain drifting into the beam in the course of the scan. Mean values of signal intensity for the whole 32 scans have been plotted (Fig.21, full curve). There is seen to be remarkably little change of intensity with height below the freezing level.

Detailed records of cloud and humidity are not available for the observing site; the nearest hourly weather reports are those from Cranfield,

/12 mi

12 mi northwest of East Hill (Table 5). Complete coincidence in the occurrence of the steady rain cannot be expected at stations 12 mi apart, but these reports suggest very similar cloud conditions in each of the periods, with variable amounts of thin fractostratus, base 500 to 1,000 ft, and a main overcast cloud layer close to 2,000 ft in the steady rain. It will be seen that whenever the rain was continuous the relative humidity recorded lay between 93 and 99%. This suggests that evaporation of drops below cloud base was negligible, and could not mask any measurable coalescence effect. Indeed the upper air soundings at both Hemsby and Crawley were close to the saturated adiabatic, with humidities very close to saturation, to great heights.

Table 5. Hourly observations at Cranfield, 12 mi northwest of East Hill

Date	Time GMT	Cloud amounts and bases (ft) Scud	Main layer	R.H. %	Weather
5. 9.55	1000 1100	5/8 St 500 3/8 Fs 800	8/8 Ns 4000 8/8 Sc 1500	95 95	cr_or_o cir_o
19.10.55	1000 1100	3/8 Sc 1200 7/8 Fs 800	8/8 Ns 5000 8/8 Ns 1500	88 99	øcir_o crr
20.10.55	1000 1100 1200 1300	3/8 Fs 800 2/8 Fs 1000 4/8 Fs 900 3/8 Fs 1100	8/8 Sc 2000 8/8 Sc 2000 8/8 Sc 2200 8/8 Sc 2000	95 95 93 94	cir_o crr crr cr_or_o

ø Rain very light at Cranfield until 1006.

It is of interest to compare this measured signal intensity curve (Fig. 21) with that derived from the step-by-step computation of accretion and coalescence effects by Mason and Ramanadham, which was for very similar conditions. The rainfall in our observations averaged 2.7 mm hr^{-1}, while they assumed a steady rate of rainfall at the melting level of 3 mm hr^{-1}, a 1 km fall through cloud of cloud-water content 0.2 gm m^{-3}, and a cloud base 1 km above the ground. They computed that the radar echo intensities just below the melting level, at the cloud base, and at the ground would be in the ratios 1 : 1.86 : 2.2. In this computation 70% of the increase of intensity in cloud (1.9 db/km) was contributed by the accretion of cloud droplets, 30% (0.8 db/km) by the coalescence of drops. This rate of growth, applied at point A just below the melting level in Fig. 21 is represented by the broken line. It represents growth by accretion of cloud droplets and by coalescence of drops above cloud base, and by coalescence of drops alone below cloud base with negligible evaporation, for which there is strong support from the Cranfield observations of Table 5.

Very similar calculations have been made by Rigby, Marshall and Hitschfeld (13). For a slightly higher rainfall of 4.5 mm hr^{-1} and an assumed cloud-water content 0.4 gm m^{-3} they computed a rate of increase of intensity of 2.4 db/km due to accretion of droplets, and 0.8 db/km due to coalescence of drops. The rather small difference from Mason and Ramanadham's result despite the greater cloud density assumed is due to their taking a somewhat different initial distribution of drop sizes at the melting level.

There is seen to be a clear separation between the computed and measured growth curves in Fig. 21. The relative constancy of the measured signal intensity with height suggests that there was considerable uniformity in drop-size distribution once melting was complete and terminal velocities had been achieved, and that all significant growth of precipitation was occurring at and above the melting level. It seems that in these conditions the radar measurements at say 2,000 ft are an accurate measure of the rainfall at the ground assuming, as we think is reasonable, that no significant change occurs in the lowest 500 ft, which could not be investigated by radar.

Our failure to find any measurable increase of intensity which could be

/attributed

attributed to accretion growth suggests that the cloud-water content below the freezing level was much lower than 0.2 gm m^{-3}. It may well be that the initial rain at a warm front washes out most of the cloud droplets below the melting level, and that, unless there is some cloud renewal mechanism at these low levels, e.g., orographic or frontal uplift, the cloud-water content thereafter remains low. One would then be forced to assume that the cloud at around 2,000 ft was merely a second layer of thin turbulence cloud of negligible water content. This could probably only be reliably confirmed by coincident aircraft investigations, but it may prove to be typical of warm-front precipitation in those parts of the British Isles in which orographic effects are unimportant.

The computed increase of 0.8 db/km due to coalescence of drops is necessarily more difficult to confirm experimentally. It was not in fact detected, and the measured values of Fig. 21 are so nearly constant below the melting level as to provide some evidence that the contribution to growth from such collisions does at least not exceed the computed values.

12. References

1. Mason, B.J. and Ramanadham, R. "Modification of the size distribution of falling raindrops by coalescence". Q.J., 80, 1954, 388.

2. Austin, P.M. and Williams, E.L. "Comparison of radar signal intensity with precipitation rate." M.I.T., Dept. of Met., Tech. Rep. No.14, 1951.

3. Adderley, E.E. "The growth of raindrops in cloud." Q.J., 79, 1953, 380.

4. Wexler, R. and Austin, P.M. "Radar signal intensity from different levels in steady snow." M.I.T., Dept. of Met., Res. Rep. No.23, 1954.

5. Boucher, R.J. et al. "Synoptic investigation of the rainstorms of November 23 and 25, 1953." Harvard, Blue Hill Met. Obsy., Met. Radar Studies No.1, 1955.

6. Ryde, J.W. "Echo intensities and attenuation due to clouds, rain, hail, sand and dust storms at centimetre wavelengths." G.E.C. Rep. No. 7831, 1941.

7. Best, A.C. "The size distribution of raindrops". Q.J., 76, 1950, 16.

8. Browne, I.C., Palmer, H.P. and Wormell, T.W. "The physics of rain-clouds". Q.J., 80, 1954, 291.

9. Hooper, J.E.N. and Kippax, A.A. "Radar echoes from meteorological precipitation". Proc. I.E.E., 97, Pt. 1, 1950, 89.

10. Robinson, N.P. "Measurement of the effect of rain, snow and fogs on 8.6 mm radar echoes". Proc. I.E.E., 102B, 1955, 709.

11. Marshall, J.S., Hitschfeld, W. and Gunn, K.L.S. "Advances in weather radar". Advances in Geophysics, 2, 1955, 1.

12. Farnsworth, G. "Quantitative radar-rainfall problems." Proc. Conf. Water Resources, Illinois State Water Survey, Bull. No.41, 1951, 235.

13. Rigby, E.C., Marshall, J.S. and Hitschfeld, W. "The development of the size distribution of raindrops during their fall". J. Met., 11, 1954, 362.

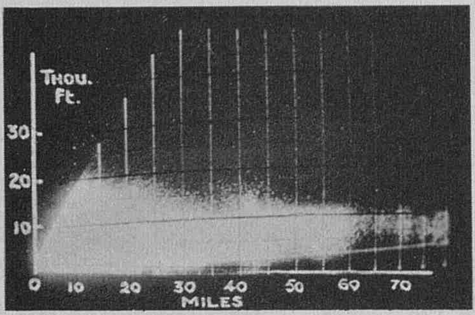

Fig. 1 0845 GMT 5th September 1955. Range-height photograph looking along the belt of precipitation. Unusually uniform echo.

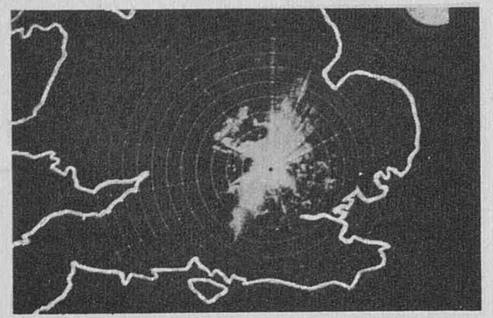

Fig. 2 0929 GMT 5th September 1955. Plan-position photograph on 120 mi. range (range circles in 10 mi steps) shows belt of precipitation over the station 20 to 40 mi in width.

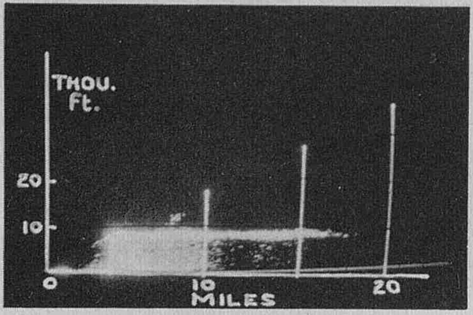

Fig. 3 0943 GMT 5th September 1955. Reduced gain photograph showing the melting level at 8,500 ft.

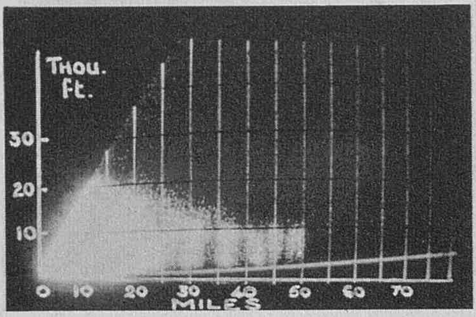

Fig. 4 0945 GMT 5th September 1955. Cellular structure has developed. Compare with much more uniform echo of fig. 1 .

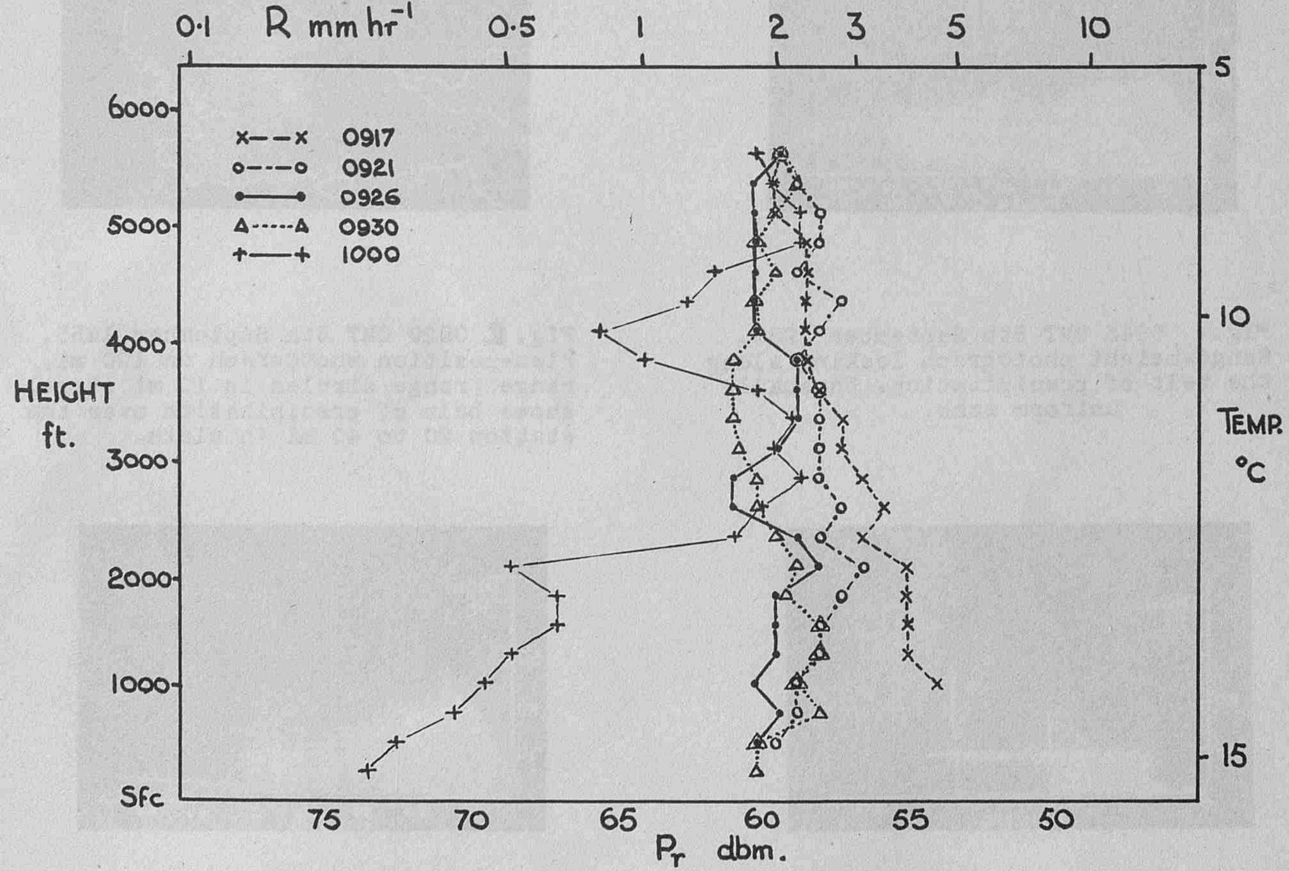

FIG. 5. SIGNAL INTENSITY MEASUREMENTS IN dbm (DECIBELS BELOW 1 MILLIWATT) ON 5TH SEPTEMBER 1955. RAIN UNSTEADY FOR LAST SCAN, AND HAD ALMOST CEASED AT LOWEST ELEVATIONS.

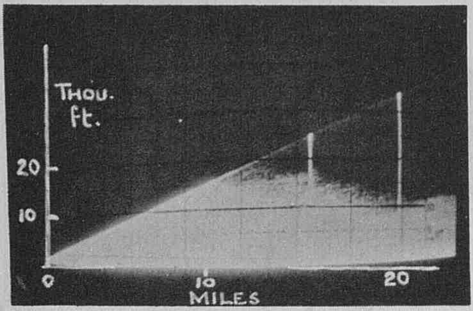

Fig. 6 1005 GMT 19th October 1955.
An open scale range-height photograph of the precipitation within 20 mi. Very uniform echo.

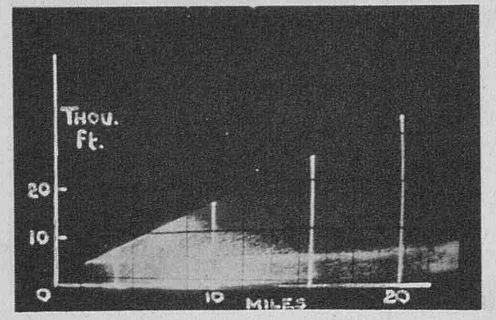

Fig.**7** 1005 GMT 19th October 1955.
Reduced gain photograph showing the bright band at the melting level at 5,000 ft.

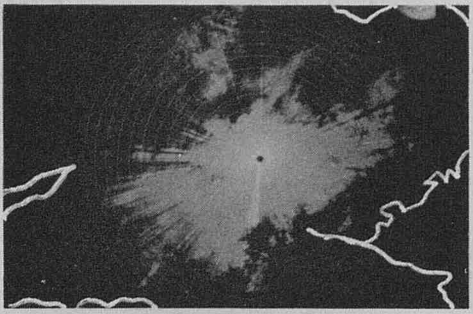

Fig.**8** 1020 GMT 19th October 1955.
Plan-position photograph on 60 mi range. (range circles in 5 mi steps). The lack of brightness is not caused by weakness of echo, but by a slight photographic fault.

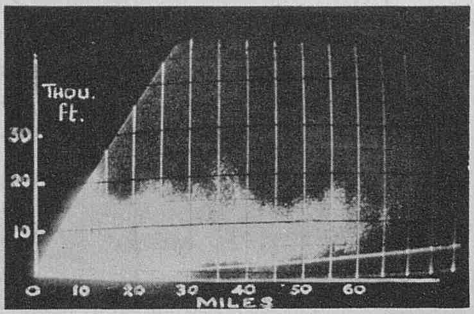

Fig.*9* 1021 GMT 19th October 1955.
Range-height photograph. Precipitation is probably more variable beyond 20 mi as evidenced by uneven tops.

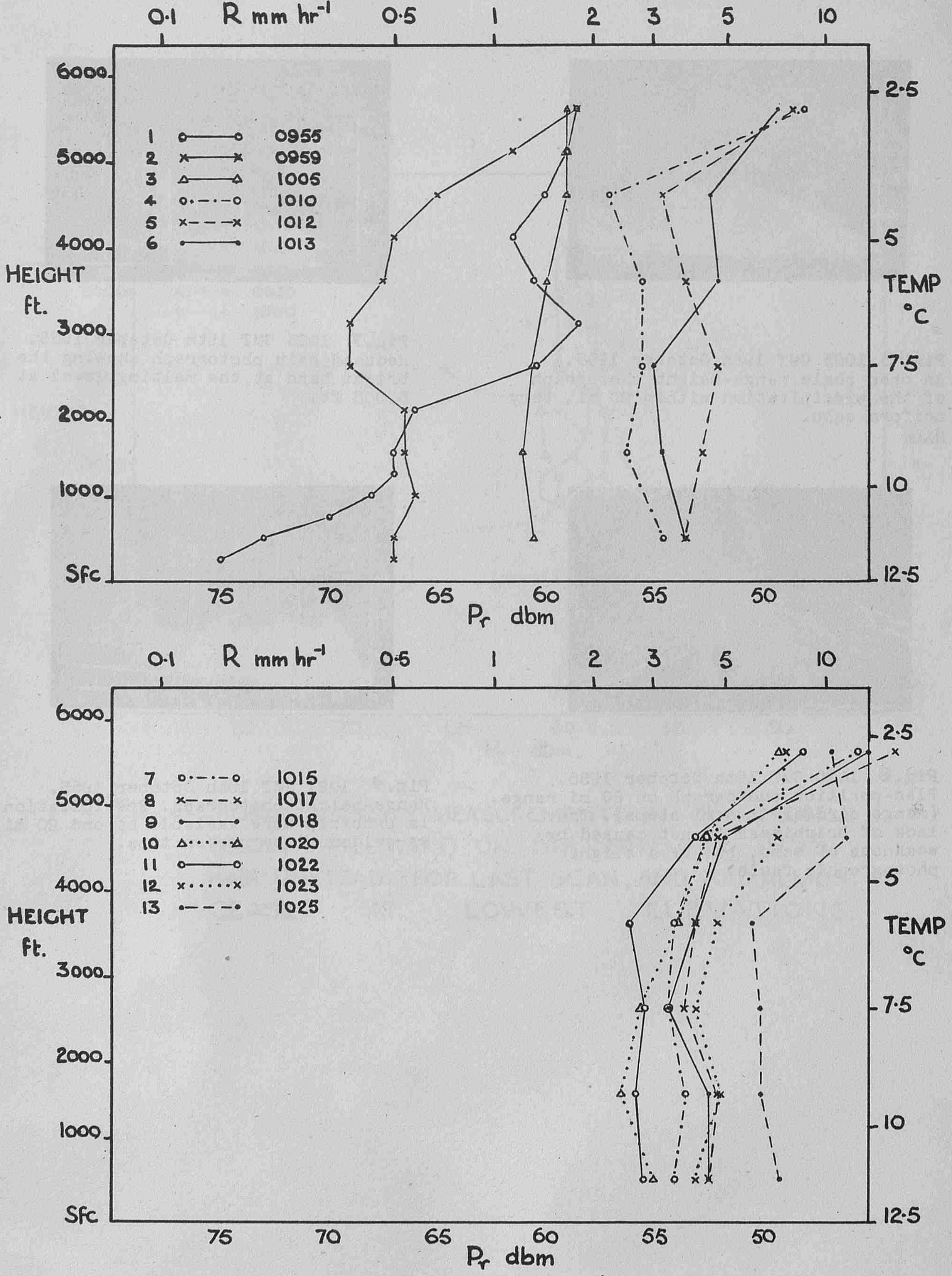

FIG. 10. SIGNAL INTENSITY MEASUREMENTS ON 19TH OCTOBER 1955. RAIN LIGHT AND VARIABLE UNTIL 1005. THE SCALE OF RATE OF RAINFALL APPLIES ONLY TO THE RAIN BELOW THE MELTING LAYER.

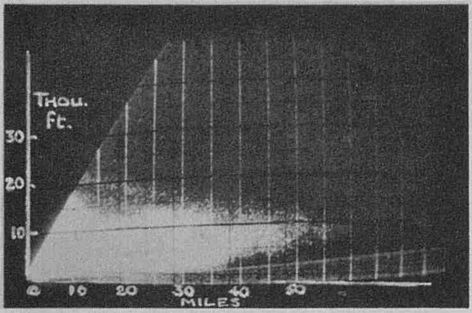
THOU.
Ft.
30
20
10
0
10
20
30
40
50
MILES

Fig. 11 0932 GMT 20th October 1955.
Range-height photograph showing fairly uniform echo out to 60 mi, subject to range attenuation. The faint echo at 20,000 ft suggests ice crystal echo.

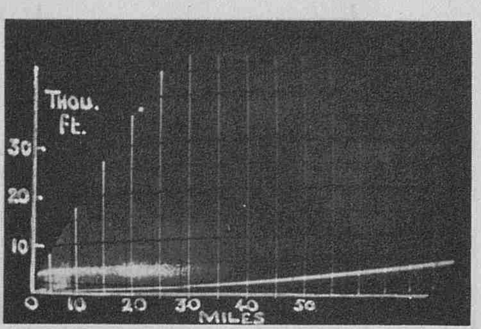
THOU.
Ft.
30
20
10
0
10
20
30
40
50
MILES

Fig. 12 0933 GMT 20th October 1955.
Reduced gain photograph of the same precipitation showing uniform bright band at the melting level at 4,000 ft.

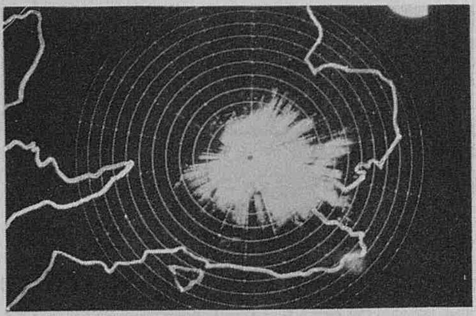

Fig. 13 1015 GMT 20th October 1955.
Plan-position photograph on 120 mi range (range circles in 10 mi steps). Uniform echo to 30-60 mi.

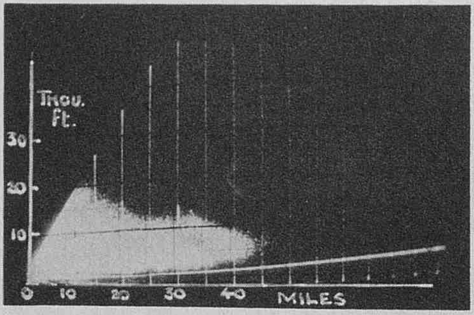
THOU.
Ft.
30
20
10
0
10
20
30
40
MILES

Fig. 14 1035 GMT 20th October 1955.
Echo still uniform out to 45 mi.

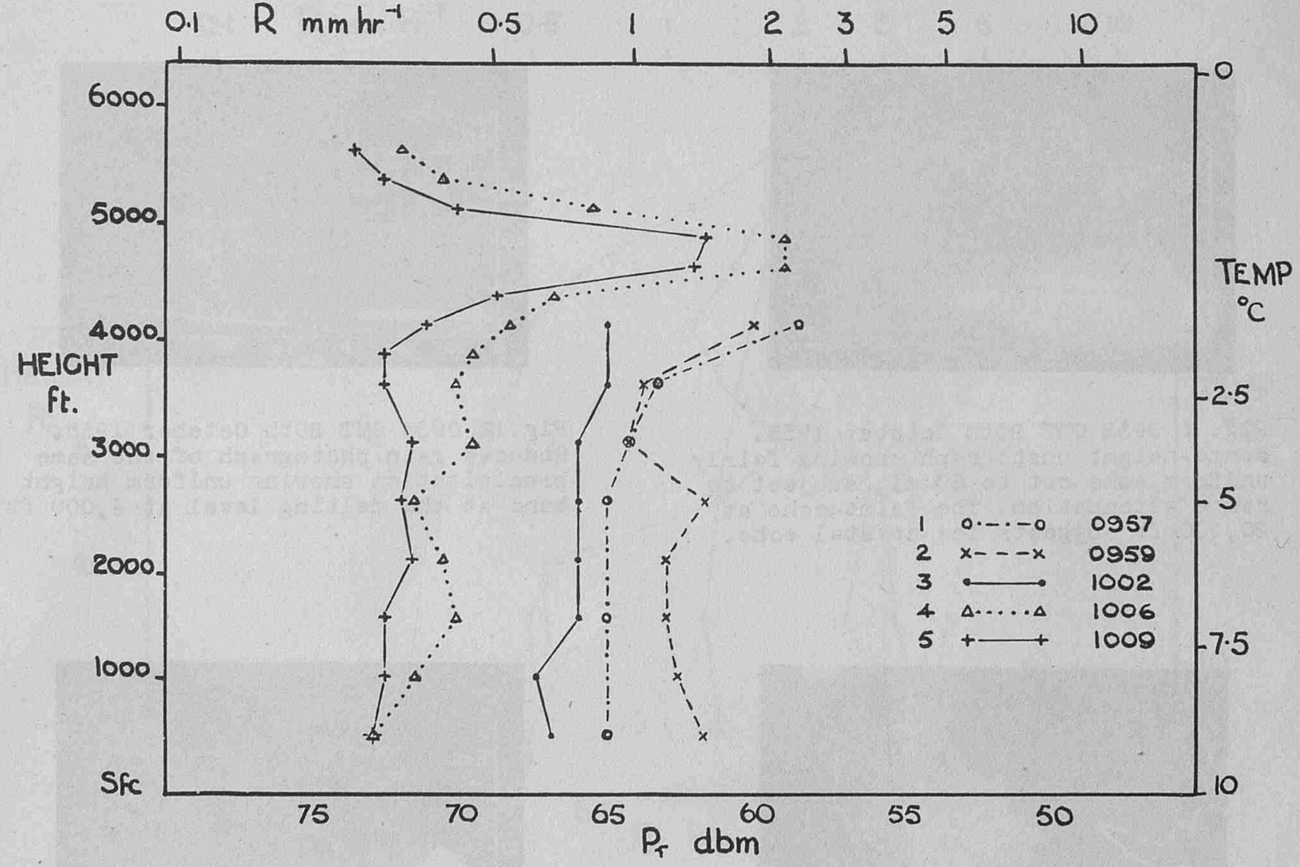

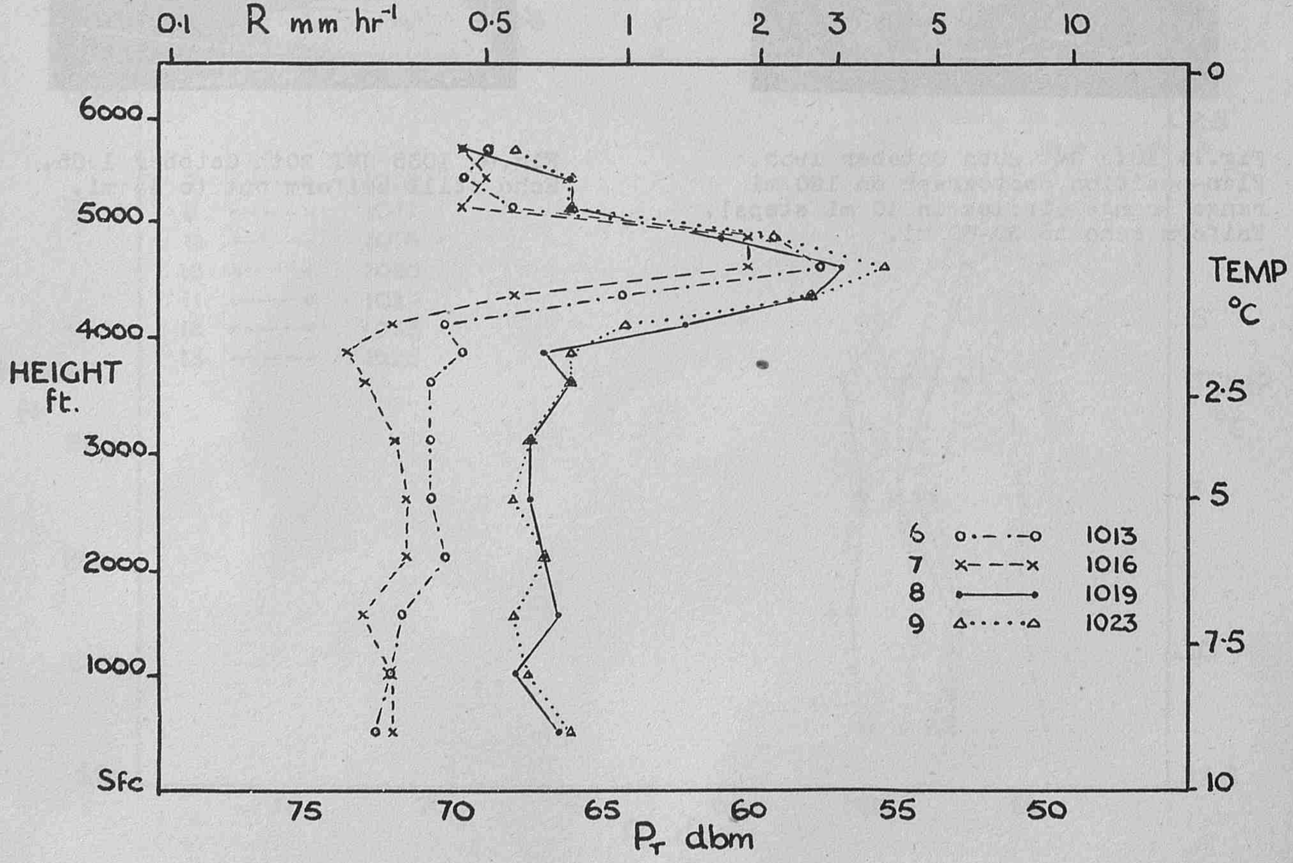

FIG. 15 SIGNAL INTENSITY MEASUREMENTS ON 20TH OCTOBER 1955. THE SCALE OF RATE OF RAINFALL APPLIES ONLY TO THE RAIN BELOW THE MELTING LAYER.

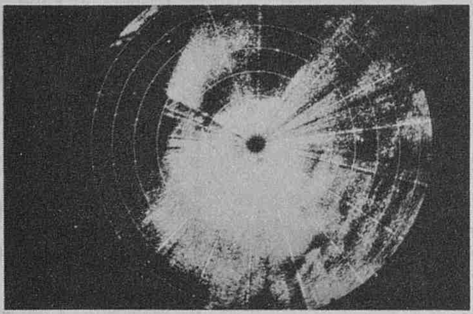

Fig.16 1156 GMT 20th October 1955. Plan-position photograph on 35 mi range (range circles in 5 mi steps) showing uniform precipitation over and to the South of East Hill.

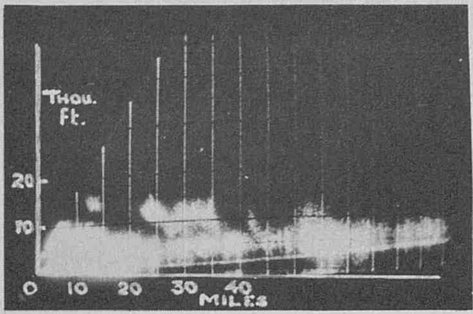

Fig.17 1212 GMT 20th October 1955. Range-height photograph looking SE showing uniform echo attenuating with range out to 20 mi, but much more variable beyond.

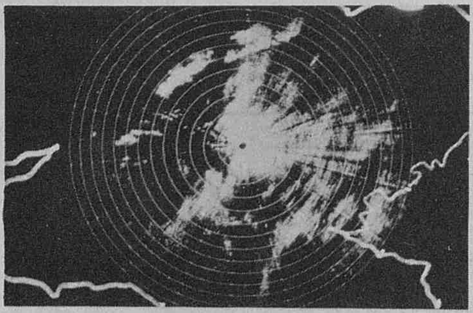

Fig.18 1230 GMT 20th October 1955. Plan-position photograph on 70 mi range (range circles in 5 mi steps) showing rain area of fig.16 almost past East Hill.

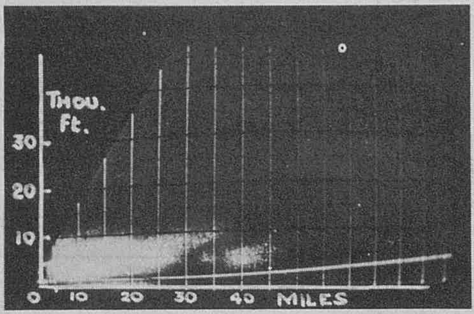

Fig.19 1246 GMT 20th October 1955. Range-height photograph looking NE through the rain, which had by then cleared East Hill.

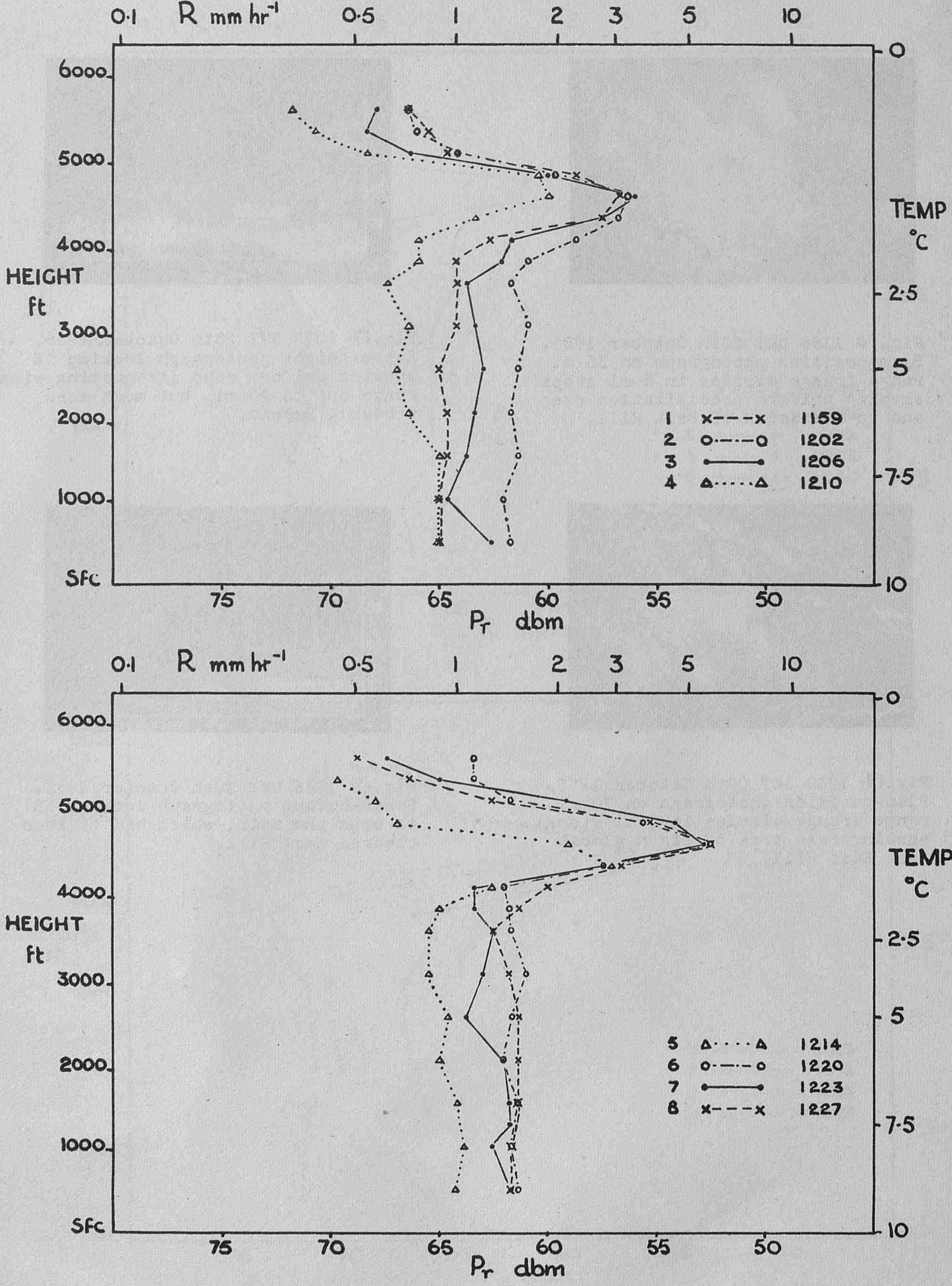

FIG. 20 SIGNAL INTENSITY MEASUREMENTS ON 20TH OCTOBER 1955. THE SCALE OF RATE OF RAINFALL APPLIES ONLY TO THE RAIN BELOW THE MELTING LAYER.

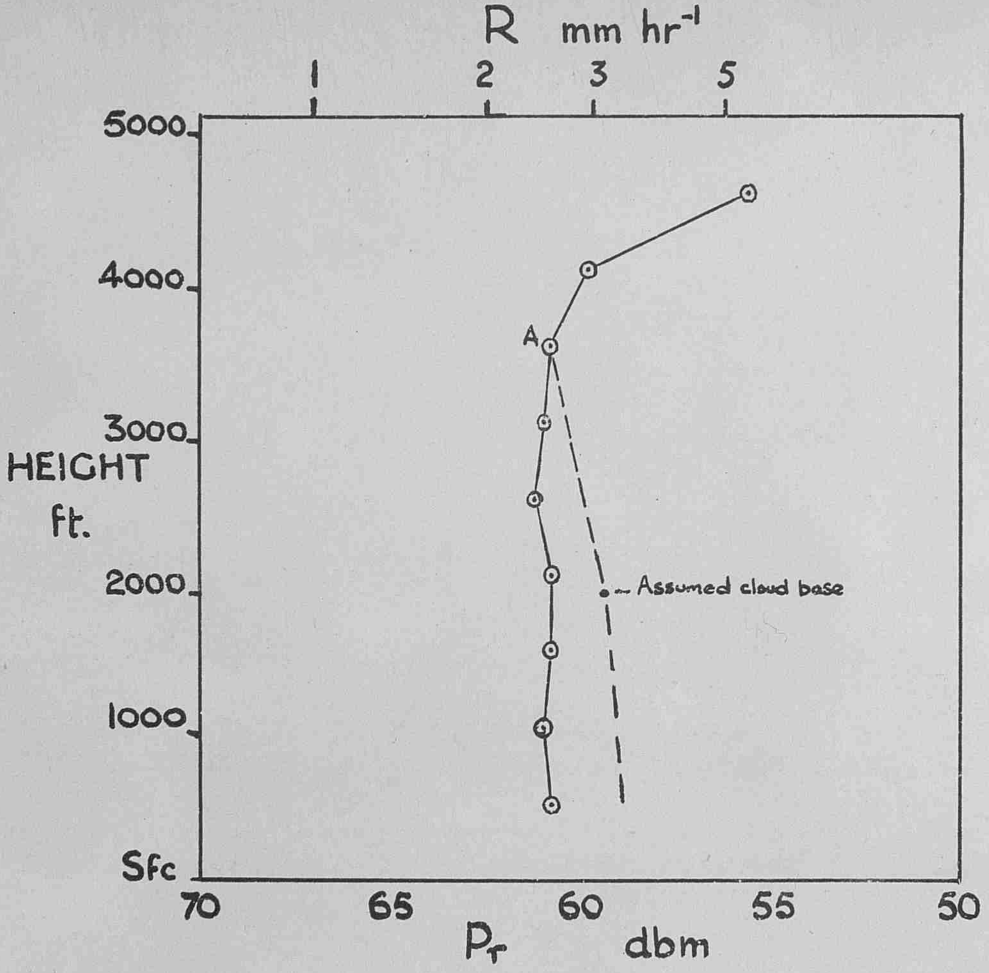

FIG.21 Mean signal intensity from 32 scans in steady rain. There is complete absence of any evidence of growth of drops below the melting layer. The broken line is a computed growth curve due to Mason and Ramanadham applied to the fall from the level marked A.

AD 139535

M.R.P. 985
S.C.11/211
24th May, 1956.

AD 139535

A preliminary study of atmospheric waves using radiosonde data.

by

G. A. Corby.

(Meteorological Office)

AIR MINISTRY

METEOROLOGICAL RESEARCH COMMITTEE

At the time of issue this report has not been published. Any author desiring to quote this paper should refer to it as "A paper of the Meteorological Research Committee (London), M.R.P. No. 985 by Mr. G.A. Corby A copy is available in the Library of the Meteorological Office."

M.R.P. 985
S.C.II/211
24th May, 1956

AIR MINISTRY
METEOROLOGICAL RESEARCH COMMITTEE

A preliminary study of atmospheric waves using radiosonde data

by
G.A. Corby (Meteorological Office)

Introduction

Most of the observational evidence of mountain airflow effects in general, and of lee waves in particular, has come from the pilots of gliders and aircraft. Although such observations have contributed greatly to our understanding of the problem of mountain airflow, their application is nevertheless limited. Furthermore, field investigation of the problem using gliders or aircraft presents formidable difficulties, apart from being extremely expensive. It is natural to enquire, therefore, to what extent the data from routine radiosonde ascents can be used to study atmospheric waves. This paper is concerned with a trial determination and analysis of the vertical air currents revealed by six months radiosonde data from four British upper air stations.

1. The data and their treatment

The data used were from the stations Leuchars, Stornoway, Aldergrove and Liverpool for the six months period November 1953 to April 1954. Both the 0200 and 1400 G.M.T. soundings were used, making a total of about 1440 soundings in all.

The so-called Vaisala diagram which is plotted at British radiosonde stations includes a plot of pressure against time during the ascent. If the rate of ascent of the balloon varies substantially and systematically with height, it is easy to recognise this visually from the pressure-time plot, and an examination of these curves was found to be adequate for the purpose of selecting the cases worth studying in greater detail. In this way, 61 occasions were selected when the rate of ascent of the balloon varied by approximately ± 300 ft./min. or more; consideration of the errors of estimating vertical currents from radiosonde data indicated that it would not be profitable to study evidence of smaller vertical currents.

Readings of the audio-frequency of the note controlled by the pressure element of the sonde are plotted against time by the operator at intervals of about 1/3 min., the exact interval depending on the rate of revolution of the sonde's "windmill". From these curves the mean rate of change of pressure-cycles, dc/dt, was evaluated over each minute of each sounding, up to 30 min., using a protractor and a conversion table. In similar fashion, the corresponding rates of change of pressure with pressure-cycles, dp/dc, were evaluated from the calibration curves. Multiplication of these two quantities gave the mean rate at which the balloon crossed the isobaric surfaces, dp/dt, over each minute. Values of dp/dt were converted to the vertical velocities, dh/dt, by multiplying by the values of dh/dp appropriate to the mean pressure and temperature over each minute.

The above procedure for the evaluation of the rates of ascent is one of several alternative methods. It was adopted as the best compromise between convenience and accuracy. As would be expected, as the radiosonde is not

/designed

designed to measure vertical air currents, the currents which can be detected are limited by errors of technique and measurement. An assessment of the errors is made in the Appendix, where it is concluded that up to the 30th minute of a sounding, vertical air currents exceeding about 120 ft./min. can be detected. (At higher levels the errors of the procedure would increase rapidly).

An attempt was made to seek independent confirmation of the results from the radar data, which comprise readings of range, elevation and azimuth every minute. The Appendix also contains an estimate of the errors in vertical air currents deduced from these data. The errors depend greatly on range and to a lesser extent on elevation, and although accurate vertical velocities can be determined in the first few thousand feet, the errors rapidly increase upwards (e.g., about 600 ft./min., at a range of 30,000 yd.).

Graphs of the rate of ascent against height of balloon were plotted and a mean rate of ascent was inserted by eye in each case. The graphs were then re-plotted in terms of departures from the mean rate of ascent, i.e., vertical air currents. Most of the cases showed evidence, often striking, of vertical currents which were periodic along the path of the balloon and in some cases of substantial magnitude. These were strongly suggestive of gravity waves, presumably of orographic origin, but it must be realised that other factors could give rise to such variations, for example: convective cloud, intermittent icing, or precipitation. Cases when factors of this sort might conceivably have caused the observed variations in the rate of ascent were rejected on the basis of a study of the synoptic charts. There remained after this sifting process 48 cases in which the deduced vertical air motions could be regarded with considerable confidence as being manifestations of gravity waves.

2. Examples of wave motions, and general comments

In Figs.1 to 12 we give some examples of the graphs of vertical velocity of the air plotted against height of balloon. Each graph comprises two curves, the thick curve being that deduced from the pressure observations of the radiosonde and the thin curve that from the radar data. The areas between the lines AB, CD for the pressure curves and between OX, OY for the radar curves, define the zones in which individual values of vertical velocity are not significant, on the basis of the assessment of errors given in the Appendix. Within these zones the curves are in dashed form. As already indicated, the radar data are more sensitive to vertical currents in about the first five thousand feet, but above this level the pressure data are much more reliable for the purpose in hand. Where a number of successive values are consistently of the same sign they may be significant even if within the "zone of no significance" because the latter zone applies strictly to individual values. In Figs. 4 and 5, the asterisk (*) after the time indicates that the radar data were derived from a separate sounding launched an hour or so later than that from which the pressure data were obtained.

The examples, which are typical of the 48 occasions found, show clear evidence of vertical currents which, as measured by the balloon during its oblique ascent, were periodic in the vertical. Much of the curves obtained from the pressure data is outside the zone of no significance and even where the curves lie within the zone there is in general a good measure of consistency with the remainder of the pattern. Furthermore, the corresponding curves from radar data confirm to a convincing degree the pattern of vertical motion in the lower troposphere, at least as regards the general form if not always the magnitude. It may also be mentioned that on about half the 48 occasions there was confirmation in the form of aircraft reports of waves viz., the reports collected at Northolt Airport for the same period and used by Pilsbury (1955) in an analysis of aircraft reports of waves. There is, therefore, no reason to doubt the reality of the waves deduced here from radiosonde data.

In the majority of cases, the amplitude of the vertical velocity perturbation attains a pronounced maximum in the lower troposphere (usually from 5,000 - 10,000 ft. above the ground) and decreases sharply above. Sometimes, however, the amplitude is maintained to considerable heights, as for example in

Figs. 7 and 11. In no case was there convincing evidence of the amplitude increasing with height in the upper troposphere.

In some cases waves were present on two or more successive ascents, e.g., in Figs. 4 and 5, and also at more than one upper air station, showing that at least sometimes waves have a fair degree of persistence in space and time. It is interesting to note, too, the agreement on Fig. 5 between the radar and pressure data which were not in this case simultaneous. On the other hand, Fig. 4, for which the two sets of data were also not simultaneous, shows differences between the heights of the crests and troughs; such differences could easily be explained in terms of small changes in wavelength affecting the location of crests and troughs relative to the point of release of the balloon.

The case which gave rise to the largest amplitude waves (with vertical velocities of about 1,000 ft./min.) is included in these examples, viz., Fig. 8, referring to 15th April 1954. For two or three days about this time waves were widespread and were the subject of many aircraft reports, one of which refers to vertical currents of 1,900 ft./min. in the region of Edinburgh (see Pilsbury, 1955). In addition, it may be noted that the violent turbulence encountered by a Canberra at 40,000 ft. near Edinburgh and described by D.C.E. Jones (1955) occurred on the evening of 14th April 1954. Strong waves were evident from the Leuchars sounding nearest in time (1400 G.M.T., 14th April 1954) although not as large in amplitude as those on Fig. 8.

3. Some statistical results

(a) Distribution amongst stations

The 48 cases were divided amongst the stations as follows:-

Station	No. of cases
Leuchars	27
Liverpool	14
Stornoway	4
Aldergrove	3

We should expect the frequency of detectable waves to be closely dependent on the character of the topography upwind of the stations in the direction of the prevailing wind and this no doubt accounts for the wide variation in the frequency of waves at the four stations.

(b) Distribution of maximum vertical currents

The frequency distribution of the maximum vertical currents, based on the pressure frequency data, is illustrated by the histogram at Fig. 13(a). As expected, the distribution is J-shaped indicating increasing rarity the larger the vertical current.

The distribution of the heights at which the balloon encountered the maximum vertical current is given in Fig. 13(b). The main feature is the pronounced maximum in the layer 5,000 to 10,000 ft. Generally speaking, the theory of mountain airflow leads us to expect the amplitude of lee waves to increase upwards to some level in the lower troposphere and to decrease at higher levels. This picture is supported by the present data. It is not thought that the minor secondary maximum from 20,000 to 25,000 ft. is significant.

(c) Seasonal and synoptic variations

The occasions of waves were distributed amongst the six months as follows:-

Month	No. of cases
November 1953	10
December 1953	2
January 1954	14
February 1954	4
March 1954	10
April 1954	8

We know that the winter produces more situations favourable for waves than other times of the year because of the greater frequency in winter of strong winds and high static stability in the lower troposphere. However, the only significance to be attached in the above table to the low frequency of waves in December 1953 and February 1954 probably arises from the variability of the British climate. These particular two months were on the whole much quieter and less windy than usual over Britain.

The theoretical condition for lee waves deduced by Scorer (1949) is not one which can be applied with precision in practice and it is well known that the condition can be satisfied in a wide variety of synoptic situations. However, in a high proportion of the present cases, viz. 30 out of 48, the radiosonde station was near a front - sometimes ahead of a warm front or near an occlusion, but more commonly to the rear of a cold front. Such a location generally provides the stability in the lower troposphere and the increasing winds with height, both of which tend to favour waves. Furthermore, it was clear from the time sequence of the occasions of waves at the different upper air stations that the region relative to the front where waves occurred tended to be advected with the front and to be maintained with it during the passage of the front across the British Isles. The remaining cases mostly occurred in warm sectors or anticyclonic westerlies both of which are characterised by low level stability and increasing winds with height.

(d) Diurnal variations

It has been suggested on theoretical grounds (see Scorer, 1953) that lee waves should be more common by night than by day, the reason being the greater tendency at night for high static stability and laminar flow in the low levels. In the present examples, however, the reverse occurred, 34 cases being from 1400 G.M.T. soundings and only 14 from the 0200 G.M.T. ascents. This apparent discrepancy probably arises because the theoretical conclusion is concerned only with the occurrence of waves irrespective of their amplitude. In a discussion of the amplitude of lee waves, Corby and Wallington (1955) indicated that a falling off of surface wind such as occurs at night should be accompanied by a reduction in the amplitude of any lee waves, although it might also result in waves when these were not previously operating. Thus waves of unspecified amplitude may well be more common by night than by day, but in the present study waves of small amplitude were necessarily excluded.

(e) Wind speed and direction

In Figs.14(a) and (b) are given in the form of polar diagrams the 900 mb. wind speeds and directions at Leuchars and Liverpool for the wave cases. The mean 900 mb. wind speed was 32.1 kt. at Leuchars and 28.4 kt. at Liverpool; these appear to be a little above normal for the winter months, although not greatly so.

As regards wind direction, all the Leuchars cases except two occurred with winds between N and S through W, i.e., directions with high ground upwind. In one case which might appear suspicious, viz., that with a NE wind, the wind below 900 mb. was well backed and was sharply anticyclonic with Westerlies in extreme N. Scotland; the low-level flow had, thus, a predominantly land track. The largest amplitude waves were concentrated in the NW'ly quadrant where the highest mountains, upwind from Leuchars, exist.

The wind directions at Liverpool, Fig.14(b), were much more varied, as might be expected in view of the local topography. We will refrain from speculating as to whether waves with NW'ly winds owed their origin to the effect of the Isle of Man or to the hills of Northern Ireland, but will remark that lenticular clouds have been observed from the Lancashire coast stretching across the Irish Sea.

Of the 48 cases as a whole, the change in wind direction from 900 to

500 mb. was less than 20 deg. in 36 cases and in only 2 did it exceed 30 deg. This confirms the well-established conclusion that relative constancy of wind direction with height is required for well developed lee waves.

The four cases at Stornoway all occurred with strong SSW'ly winds; the airflow would thus have passed over the high ground in the SSW of the island of Lewis itself. The Aldergrove examples were all with NW'ly winds.

(f) The wavelength

In many of the graphs of vertical motion against height of balloon, of which Figs. 1-12 are examples, a dominant wavelength stands out unmistakably. In fact, it was found possible in 26 cases to obtain a good estimate of the dominant wavelength, as the average of about 5 or 6 assessments over different portions of the curve, assuming vertical wave fronts. The average wavelength for the 26 cases was 6-7 mi. (S.D. 3 mi.), the extreme values being 2.6 mi. and 14.4 mi. These values are consistent with observational evidence and with the order expected from theoretical considerations.

Perturbation theory enables us to set down equations which formally determine the wavelength, but a general analytical solution is not possible owing to the complex way in which variations of static stability and wind in the vertical are involved. However, it seems clear that generally speaking the wavelength should increase with the mean wind speed through the troposphere. This conclusion is strikingly borne out by Fig. 15 which is a plot of the wavelengths in the 26 cases against the corresponding wind speed meaned over the layers contributing to the wavelength assessments. The correlation coefficient is 0.91 which is sufficiently high to justify estimates of wavelength from mean tropospheric wind speed alone.

In Fig. 16 is plotted the maximum vertical component of wind in the Leuchars examples against the wavelength, when an estimate of wavelength was possible. Clearly there is no linear relation; indeed there are signs of a peak maximum vertical velocity for a wavelength of about 8 mi. with smaller vertical velocities for both shorter and longer wavelengths, and a rough curve has been drawn by eye expressing this trend. This appears to offer some support for the conclusion reached by Corby and Wallington (1955) viz., that a kind of resonance effect would be expected to occur when the natural wavelength of the airstream matched the dominant wavelength component of the topography. Admittedly the points on Fig. 16 represent a variety of wind directions and therefore the support is by no means conclusive; sufficient data to enable such graphs to be plotted for distinct wind directions should throw more light on this aspect.

4. Apparent distortion of temperature structure

It was pointed out by Scorer (1953) that if a radiosonde balloon passes through waves, the temperature structure measured by the sonde will differ from that of the undisturbed stream and, indeed, that spurious inversions might appear on this account. If static stability is expressed, in the usual way, as $\theta^{-1}\,\partial\theta/\partial z$ where θ is potential temperature, and we neglect perturbations of horizontal velocity, then it may readily be shown that the apparent stability will be $W/(W + w)$ times the true stability, where W is the rate of ascent of the balloon relative to the air and w is the vertical component of wind. Thus in an ascending current stability will appear to be reduced and vice versa. In the extreme case of a descending current which brought the balloon to rest (in the vertical), the sonde would indicate an ideally sharp inversion whatever the undisturbed lapse rate.

The above remarks prompt us to enquire to what extent the temperature structure measured by a radiosonde passing through waves is in fact distorted in such ways.

If we represent the displacement of a streamline from its undisturbed level by

$$\zeta = a \sin \frac{2\pi}{L}(x+\epsilon) \qquad (1)$$

where a = semi-amplitude

L = wavelength

and ϵ is a phase angle

then $$\frac{\partial \zeta}{\partial x} = \frac{w}{U} = \frac{2\pi}{L} a \cos \frac{2\pi}{L}(x+\epsilon) \qquad (2)$$

and $$\left[w\right]_{max} = \frac{2\pi U a}{L} \qquad (3)$$

In a number of cases an estimate of the wavelength, L, was made, values of $[w]$ max. were read from curves such as Figs. 1 to 12, and thus from Eq. (3) the semi-amplitude, a, was obtained at several levels. The value of a at other levels was obtained by interpolation and the displacement at any level deduced from Eqs. (1) and (2). This provides a basis for correcting the temperature structure, subject to the important assumption that the centre line of the wave form at any level is the same as the corresponding undisturbed level upstream. Several tephigrams were corrected in this way and three examples are given in Figs. 17 to 19. In these diagrams the temperature structure as measured by the sonde is plotted as a full line and the corrected version is left dashed. Layers of steep lapse rate are not, of course, much affected but layers of marked stability and in particular inversions may be modified considerably. If a layer containing an inversion in the undisturbed stream is subjected to a maximum vertical current in the wave system as the balloon passes through it, the intensity of the inversion will be modified; if the balloon passes through such a layer in the crest of a wave there will be little effect on intensity but the temperature level will appear to be lower, whilst if measured in a wave trough the temperature will be higher. There is evidence of all these effects in the examples of Figs. 17-19, but it is emphasised that the precise effect in any given case must be almost fortuitous; release of the balloon a mile or two up- or downstream would change the measured temperature structure.

In no case examined in this way did it appear that any of the substantial inversions, which are commonly found when lee waves occur, were completely spurious. The main effect seems to be to change the intensity or level of strong inversions. The dew point curves are modified in a similar fashion.

Conclusions

Where upper air stations are to the lee of hills or mountains, the routine radiosonde data can provide a valuable means of studying orographic lee waves, and of building up background statistics of such phenomena. In the present preliminary study, support was found for several conclusions which have been deduced from perturbation theory. The results obtained here suggest that profitable work might be done by using a mobile radiosonde station amongst mountains. Furthermore, useful indications of the occurrence of waves could be given from existing radiosonde stations on a current basis; at present little or no observational data on waves reaches aviation forecasters, and radiosondes could be exploited to help fill this gap.

/References

References

Corby, G.A. and Wallington, C.E. 1955 "Airflow over mountains - the lee wave amplitude". Meteorological Research Papers, Air Ministry, London, No. 939.

Jones, D.C.E. 1955 "Exceptionally severe clear-air turbulence and other phenomena 14th April, 1954". Met. Mag., 84, p.107.

Pilsbury, R.K. 1955 "Standing-wave reports received at Northolt during the winter of 1953-54". Met. Mag., 84, p.313.

Scorer, R.S. 1953 "Theory of airflow over mountains: II - the flow over a ridge". Quart. J.R. Met. Soc., 79, p.70.

Values of the pressure-cycles, c, are plotted to the nearest $\frac{1}{2}$ cycle and this is understood to be well justified by the stability of the pressure element. Thus the maximum error in a single reading is $\frac{1}{4}$ cycle. The error in placing the curve in the vicinity of an individual point is, however, less than this because neighbouring points have an influence. It seems appropriate to take the maximum error in a single value read from the curve as $1/4\sqrt{2}$ cycles. If the slope of the curve of pressure frequency is measured over a one-minute interval, the maximum error in dc/dt will therefore be $1/2\sqrt{2}$ cycles/minute. Hence the maximum percentage error in dc/dt due to errors in the values of c will be $\frac{100}{2\sqrt{2}\, dc/dt}$ %.

There is also an error due to the uncertainty of timing. Readings are plotted to the nearest 1/20 min., so that the maximum error of an individual reading is 1/40 min. Hence on the same basis as above, the maximum % error in dc/dt due to timing errors will be $100/20\sqrt{2}$%.

There remains the error in the measurements by protractor. Assessed as in (i) above this leads to a range of values for the maximum error in dc/dt of 2.4 to 2.9% and we shall use 3% throughout.

(iii) Total error of the combined procedure

We take the square root of the sum of the squares of the component errors to obtain as the total error of the combined procedure:-

$$\left\{(2)^2 + \left(\frac{100}{2\sqrt{2}\, dc/dt}\right)^2 + \left(\frac{100}{20\sqrt{2}}\right)^2 + (3)^2\right\}^{1/2} \quad \%$$

maximum vertical current in the wave system as the balloon passes through it, the intensity of the inversion will be modified; if the balloon passes through such a layer in the crest of a wave there will be little effect on intensity but the temperature level will appear to be lower, whilst if measured in a wave trough the temperature will be higher. There is evidence of all these effects in the examples of Figs. 17-19, but it is emphasised that the precise effect in any given case must be almost fortuitous; release of the balloon a mile or two up- or downstream would change the measured temperature structure.

In no case examined in this way did it appear that any of the substantial inversions, which are commonly found when lee waves occur, were completely spurious. The main effect seems to be to change the intensity or level of strong inversions. The dew point curves are modified in a similar fashion.

Conclusions

Where upper air stations are to the lee of hills or mountains, the routine radiosonde data can provide a valuable means of studying orographic lee waves, and of building up background statistics of such phenomena. In the present preliminary study, support was found for several conclusions which have been deduced from perturbation theory. The results obtained here suggest that profitable work might be done by using a mobile radiosonde station amongst mountains. Furthermore, useful indications of the occurrence of waves could be given from existing radiosonde stations on a current basis; at present little or no observational data on waves reaches aviation forecasters, and radiosondes could be exploited to help fill this gap.

/References

Appendix

Assessment of errors in the evaluation of rates of ascent from radiosonde records

1. Method using pressure data

In assessing the errors of our procedure we are not concerned with the errors in the measurement of pressure from one sonde to another, that is with the absolute accuracy of pressure readings, but with the effect of random errors between successive readings during a single ascent.

Let p = pressure
c = corresponding pressure-cycles
t = time
h = height
T = temperature.

Our procedure is to evaluate dp/dc from the calibration curve and multiply this by the corresponding value of dc/dt from the plot of pressure-frequency against time. The result is dp/dt which is converted to dh/dt using a table giving dh/dp in terms of p and T. We ignore the very small systematic error due to the temperature correction to the calibration of the pressure element.

(i) Error in dp/dc

Denoting the slope of the calibration curve by θ so that $dp/dc = k \tan \theta$ then if θ is measured by protractor to the nearest degree, the maximum error in θ will be $\frac{1}{2}$ deg. or, say, 1/100 radian. Then maximum error in $dp/dc = \frac{1}{100} \times k \sec^2 \theta$ and maximum percentage error in $dp/dc = 2 \operatorname{cosec} 2\theta$ %.

Now, typical values of θ are about 55 deg. at release decreasing upwards to about 35 deg. by the 30th minute. Thus the maximum % error in dp/dc over the first 30 minutes of a sounding varies in the range 2.0 to 2.1% and for our present purpose we shall use 2% throughout.

(ii) Error in dc/dt

Values of the pressure-cycles, c, are plotted to the nearest $\frac{1}{2}$ cycle and this is understood to be well justified by the stability of the pressure element. Thus the maximum error in a single reading is $\frac{1}{4}$ cycle. The error in placing the curve in the vicinity of an individual point is, however, less than this because neighbouring points have an influence. It seems appropriate to take the maximum error in a single value read from the curve as $1/4\sqrt{2}$ cycles. If the slope of the curve of pressure frequency is measured over a one-minute interval, the maximum error in dc/dt will therefore be $1/2\sqrt{2}$ cycles/minute. Hence the maximum percentage error in dc/dt due to errors in the values of c will be $\frac{100}{2\sqrt{2}\, dc/dt}$ %.

There is also an error due to the uncertainty of timing. Readings are plotted to the nearest 1/20 min., so that the maximum error of an individual reading is 1/40 min. Hence on the same basis as above, the maximum % error in dc/dt due to timing errors will be $100/20\sqrt{2}$%.

There remains the error in the measurements by protractor. Assessed as in (i) above this leads to a range of values for the maximum error in dc/dt of 2.4 to 2.9% and we shall use 3% throughout.

(iii) Total error of the combined procedure

We take the square root of the sum of the squares of the component errors to obtain as the total error of the combined procedure:-

$$\left\{ (2)^2 + \left(\frac{100}{2\sqrt{2}\, dc/dt}\right)^2 + \left(\frac{100}{20\sqrt{2}}\right)^2 + (3)^2 \right\}^{1/2} \quad \%$$

Now, dc/dt has typical values as follows:-

From release to 15 min.	5.0 cycles/min.
From 16 " 20 "	4.7 " "
From 21 " 25 "	4.2 " "
From 26 " 30 "	4.0 " "

Thus, departures from the mean rate of ascent having percentage values less than the following could arise due to errors of measurement and of the method:-

From release to 15 min.	8.7%
From 16 " 20 "	9.1%
From 21 " 25 "	9.8%
From 26 " 30 "	10.2%

Departures from the mean rate of ascent exceeding these percentage values should have real significance. This, of course, relates to a single value for the rate of ascent evaluated over a 1 minute interval. If n successive departures had the same sign, their mean would be significant if it exceeded the above values divided by $\sqrt{n}$.

2. Method using radar data

Let R = true range and
E = true elevation.

Then true height $h = R \sin E$.

The measured height $(h + \delta h) = (R + \delta R) \sin (E + \delta E)$

where δR, δE are the errors in range and elevation and δh is the corresponding height error.

Thus the height error of a single observation

$$= (R + \delta R) \sin (E + \delta E) - R \sin E$$

$$\simeq \delta R \sin E + R\, \delta E \cos E$$

$$\simeq R\, \delta E \cos E$$ since this term will dominate.

Hence the probable error in the difference between successive readings is $\sqrt{2}.R\, \delta E \cos E$ where δE is now the probable error in the elevation of a single observation.

Now $\delta E = 0.1$ deg. $\simeq 1/600$ radians (A.P. Taylor, unpublished).

The radar observations are made at 1 min. intervals and thus rates of ascent calculated from successive radar readings will be significantly different from the mean rate of ascent (at the 5% level) if the difference from the mean exceeds $\frac{\sqrt{2}}{200} R \cos E$.

Typical vertical air currents detectable from radar heights will thus be of the following order:-

Radar	30,000 yd.	- 600 ft./min.
	60,000 yd.	- 1200 ft./min.
Range	90,000 yd.	- 1800 ft./min.

The variation from sounding to sounding is, however, quite wide and actual values of R and E were used in the paper to assign the limits OX, OY on Figs. 1 to 12.

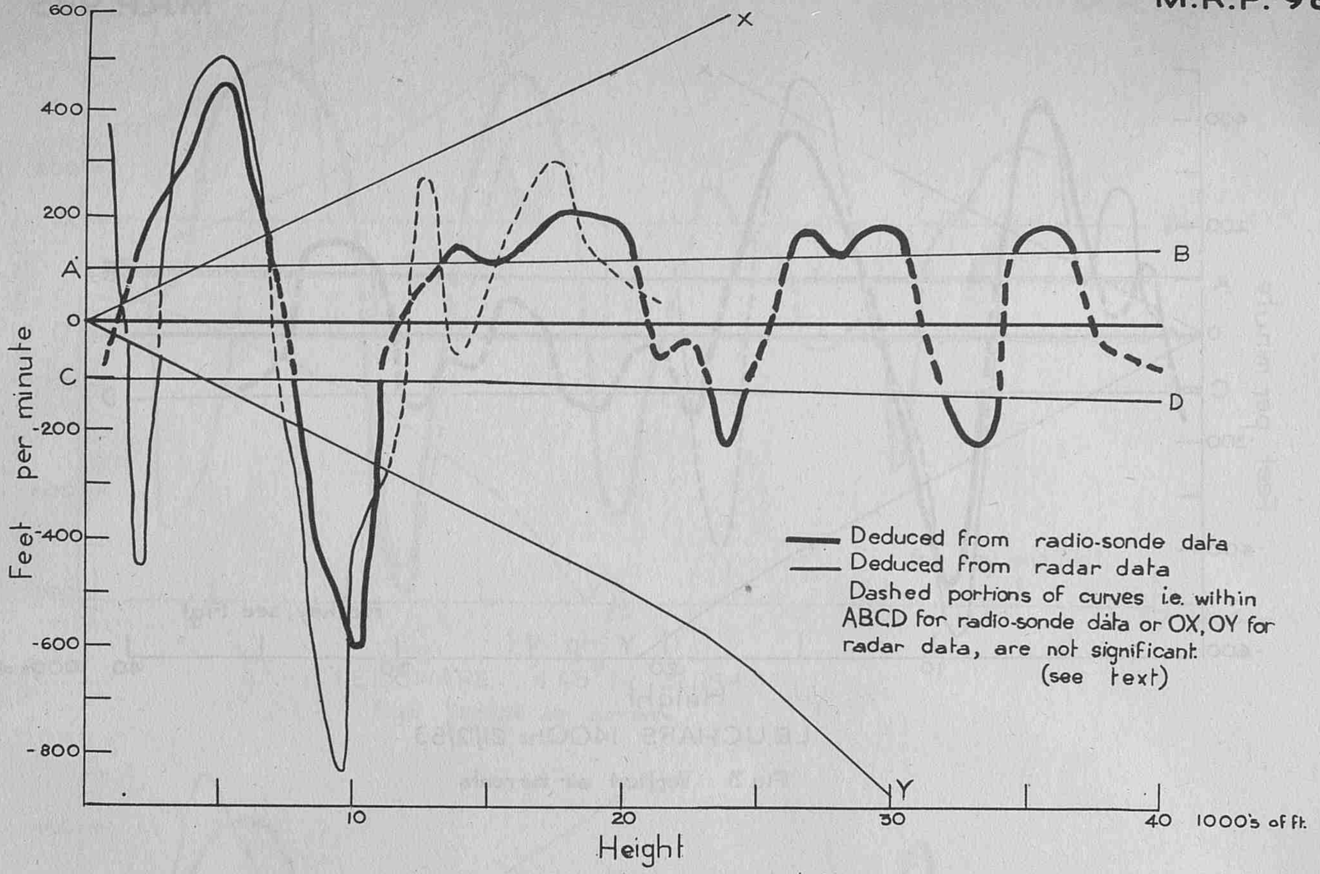

LEUCHARS 1400hr. 4/11/53

Fig.1 Vertical air currents

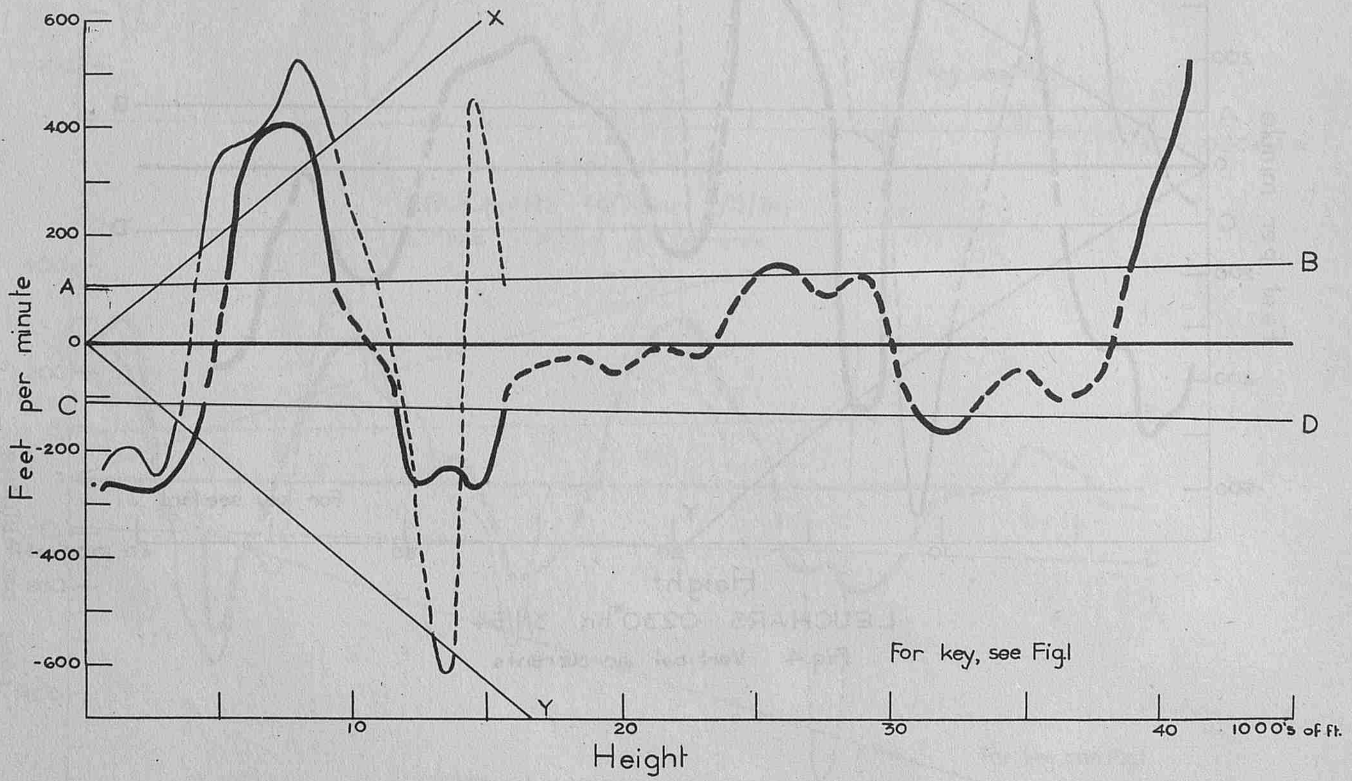

LEUCHARS 0200hr. 30/11/53

Fig.2 Vertical air currents

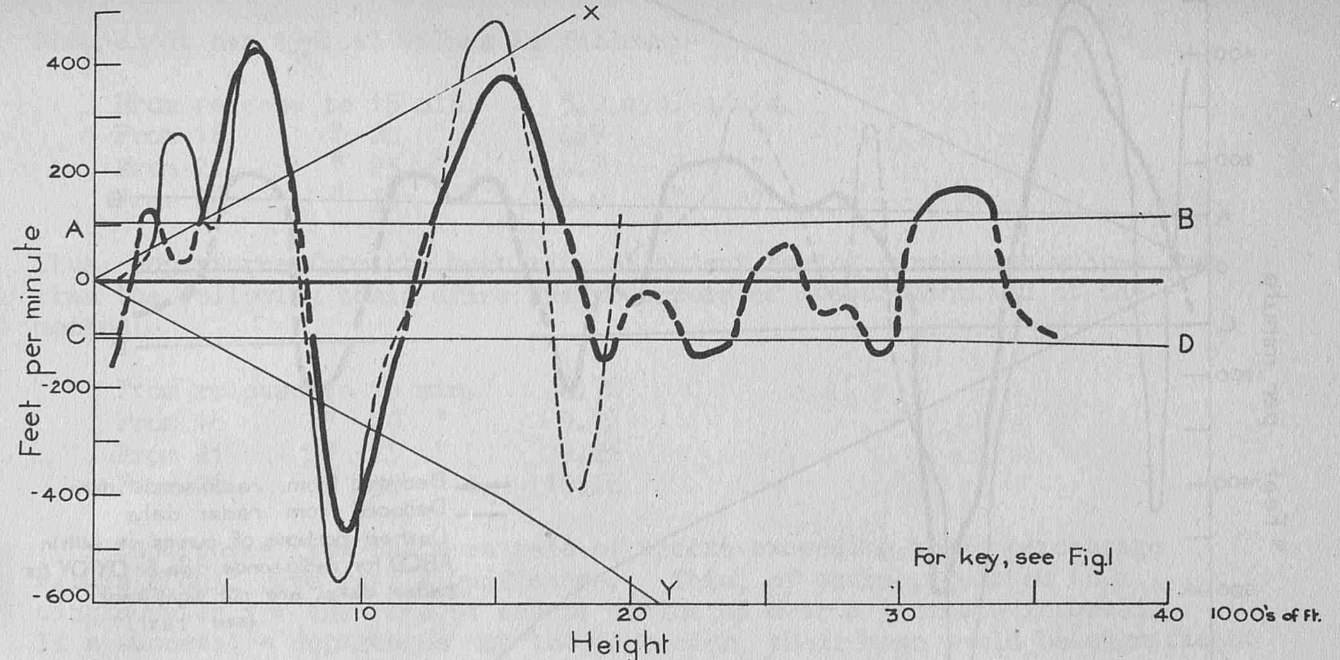

LEUCHARS 1400hr. 21/12/53

Fig. 3 Vertical air currents

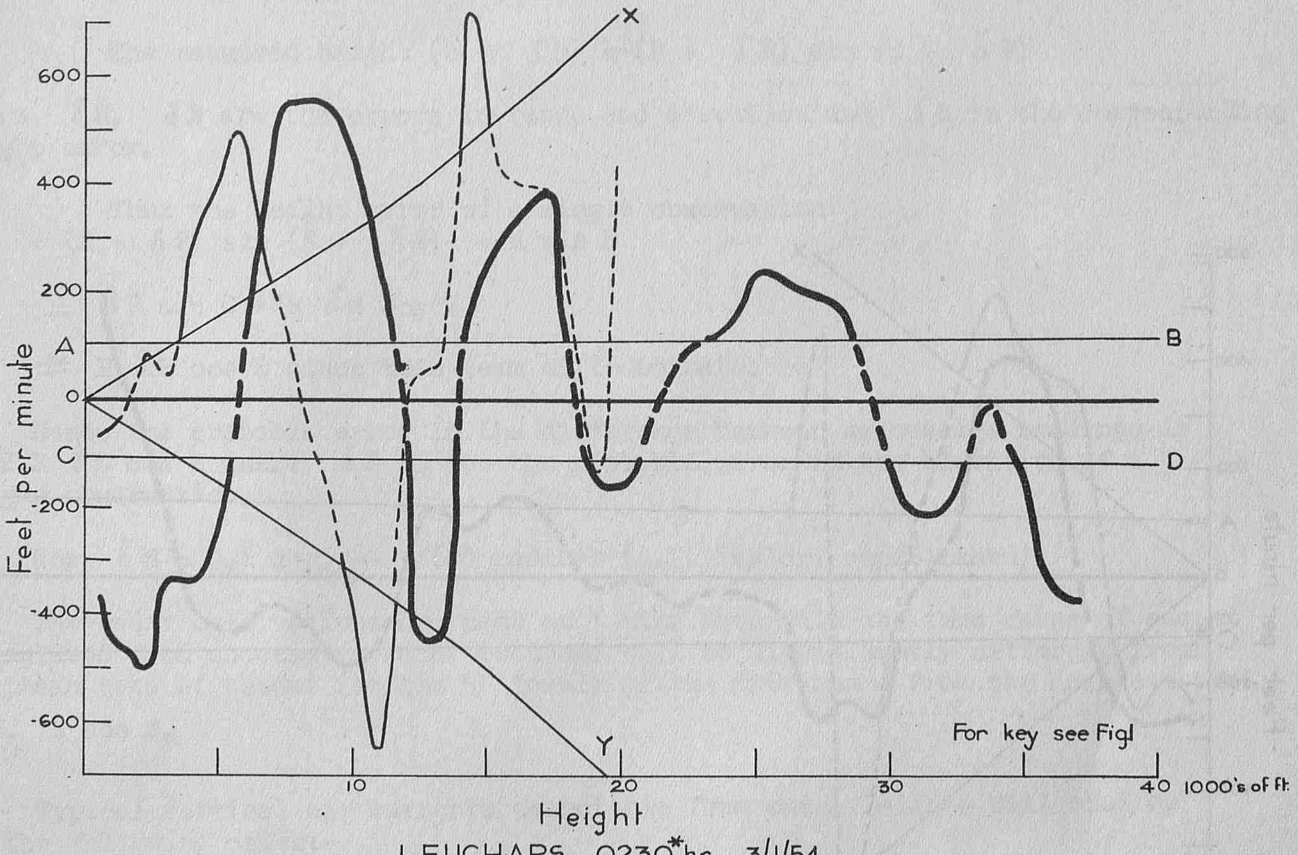

LEUCHARS 0230*hr. 3/1/54

Fig. 4 Vertical air currents

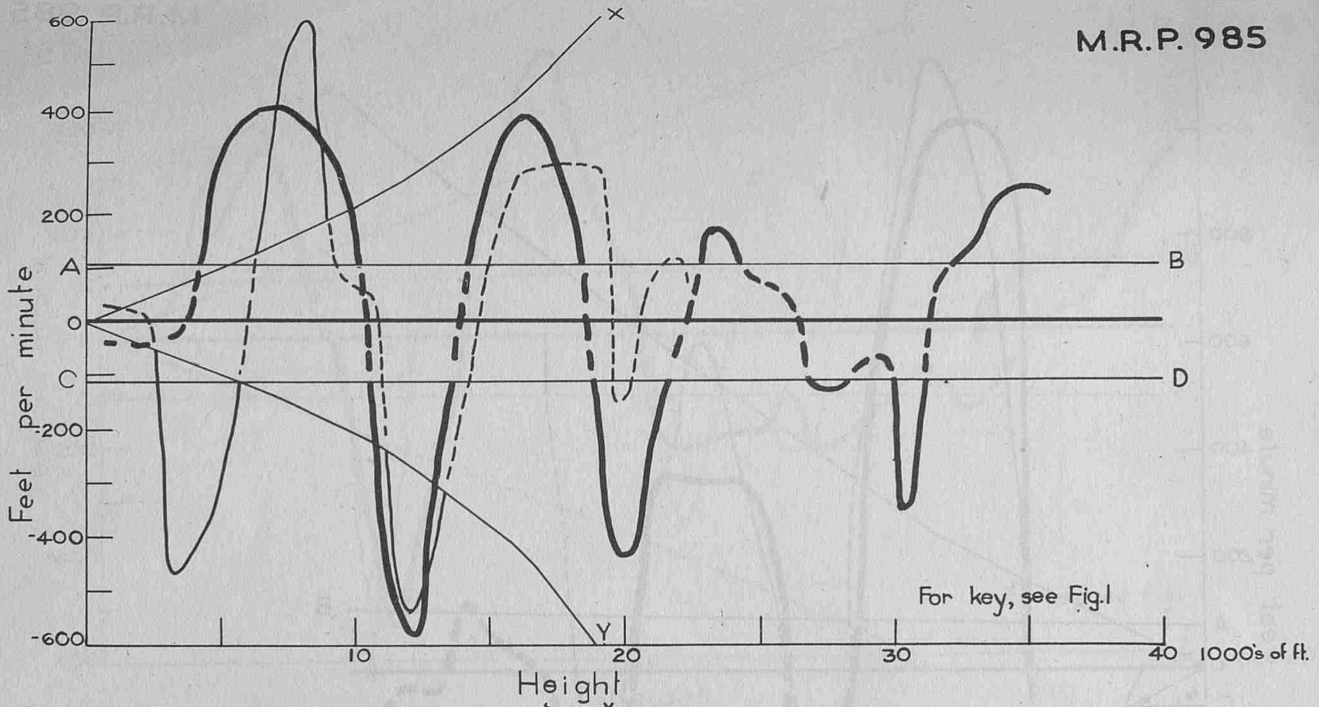

For key, see Fig.1

LEUCHARS 1445* hr. 3/1/54

Fig.5 Vertical air currents

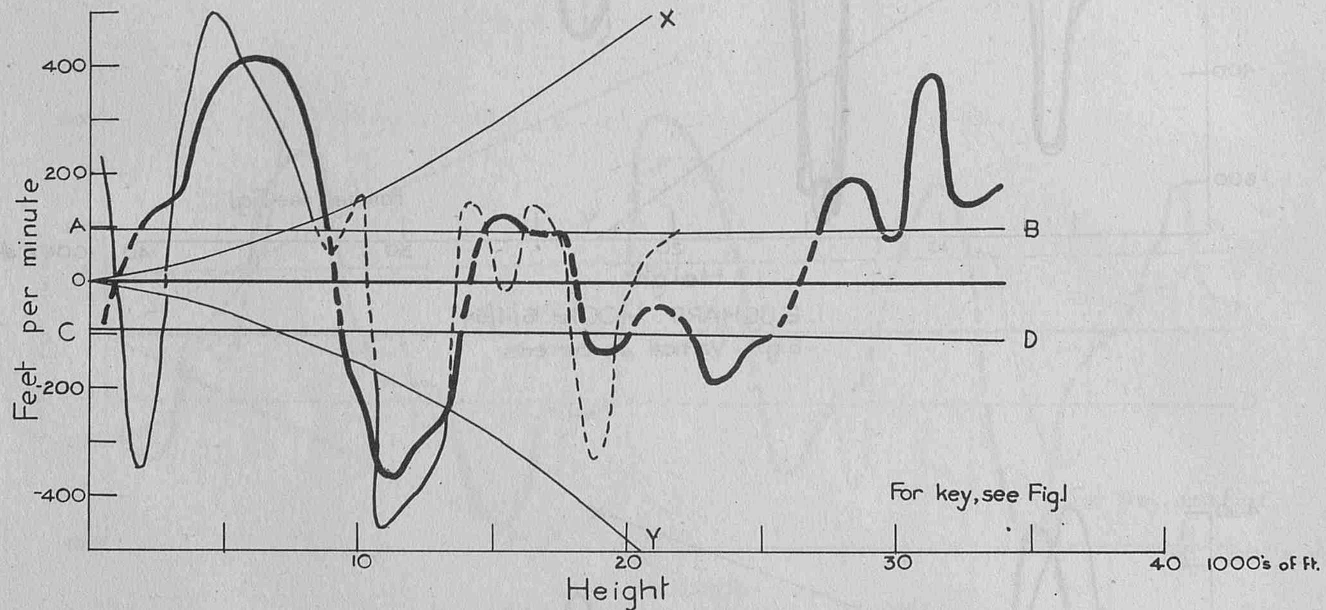

For key, see Fig.1

LEUCHARS 1400hr. 5/3/54

Fig.6 Vertical air currents

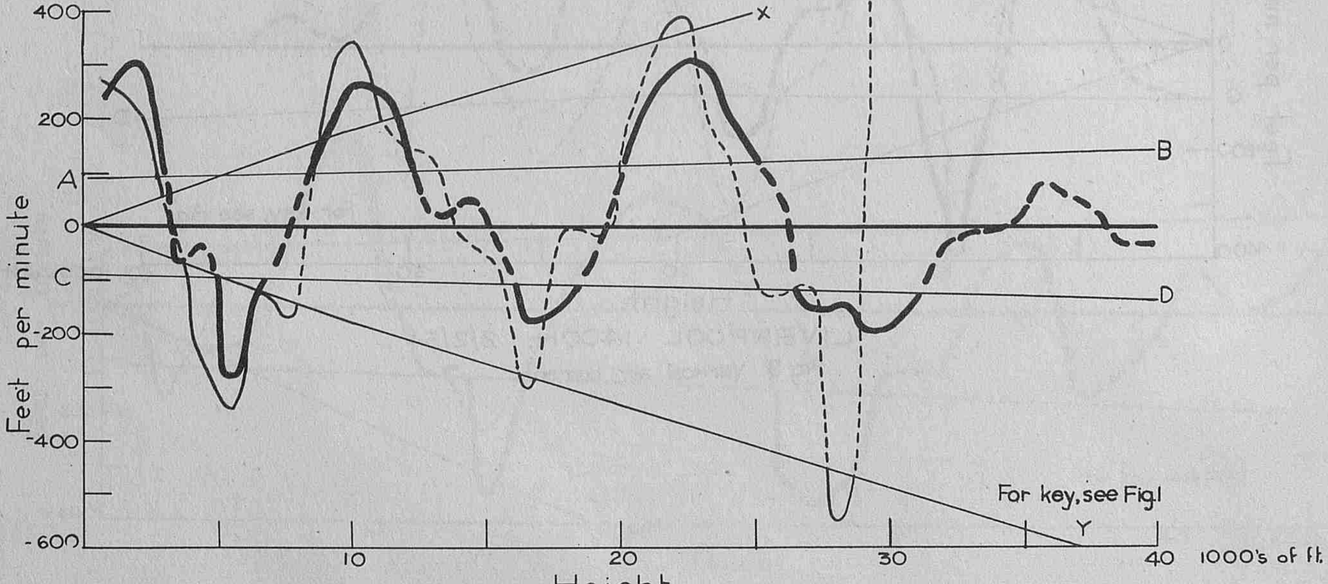

For key, see Fig.1

LEUCHARS 1400hr. 11/4/54

Fig.7 Vertical air currents

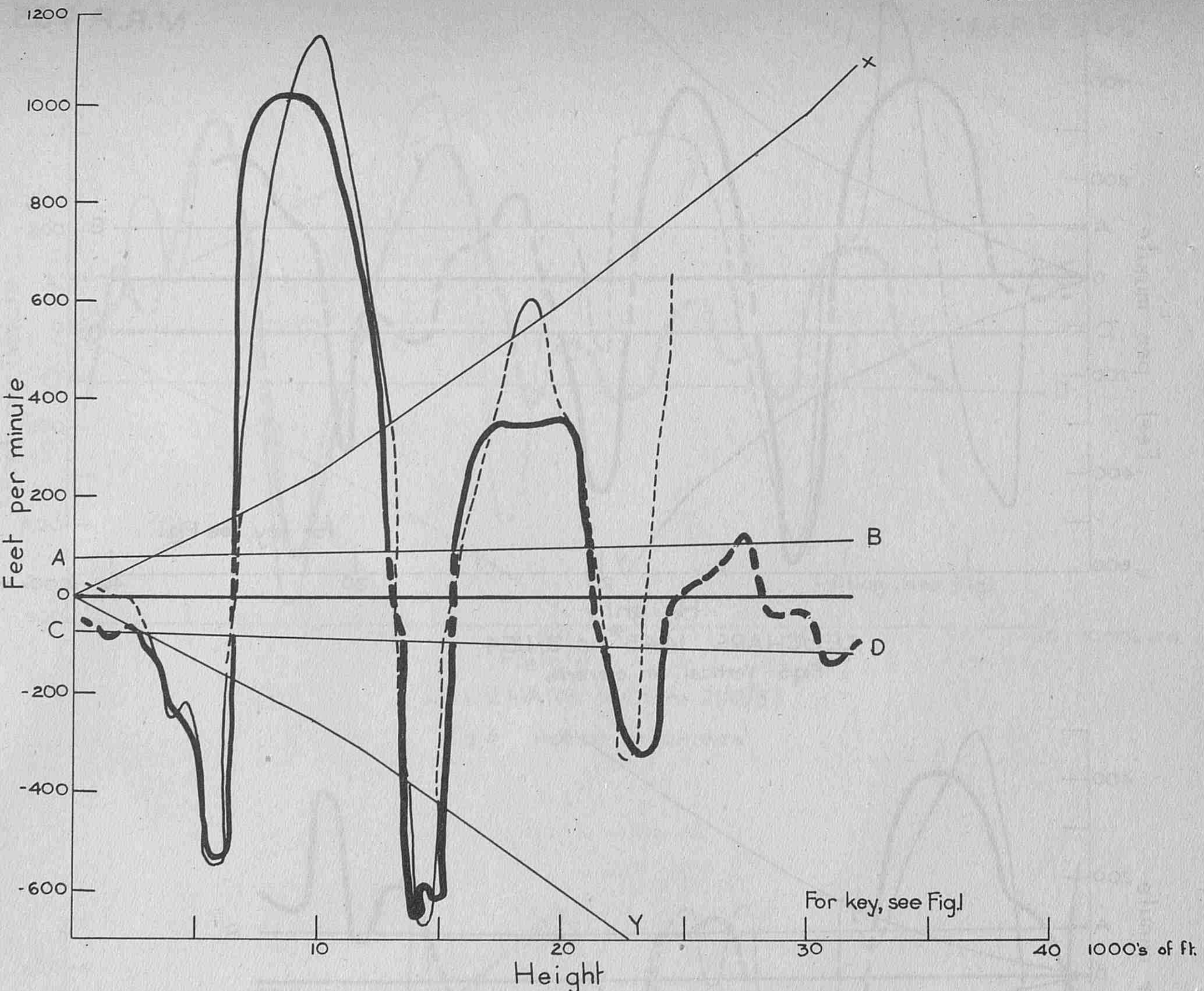

LEUCHARS 1400hr. 15/4/54

Fig.8 Vertical air currents

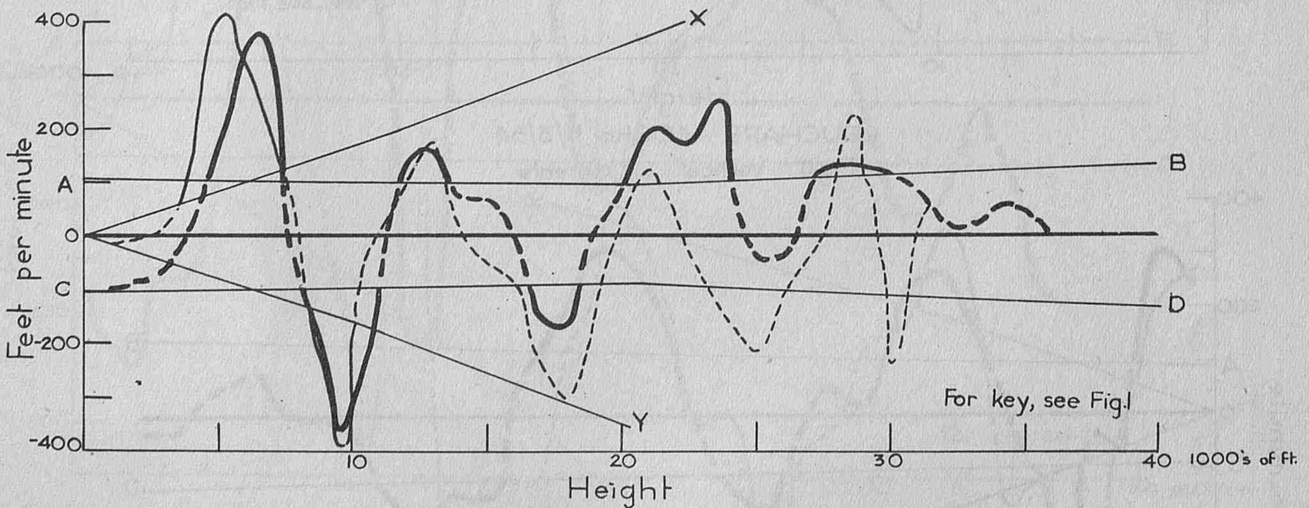

LIVERPOOL 1400hr. 2/2/54

Fig.9 Vertical air currents

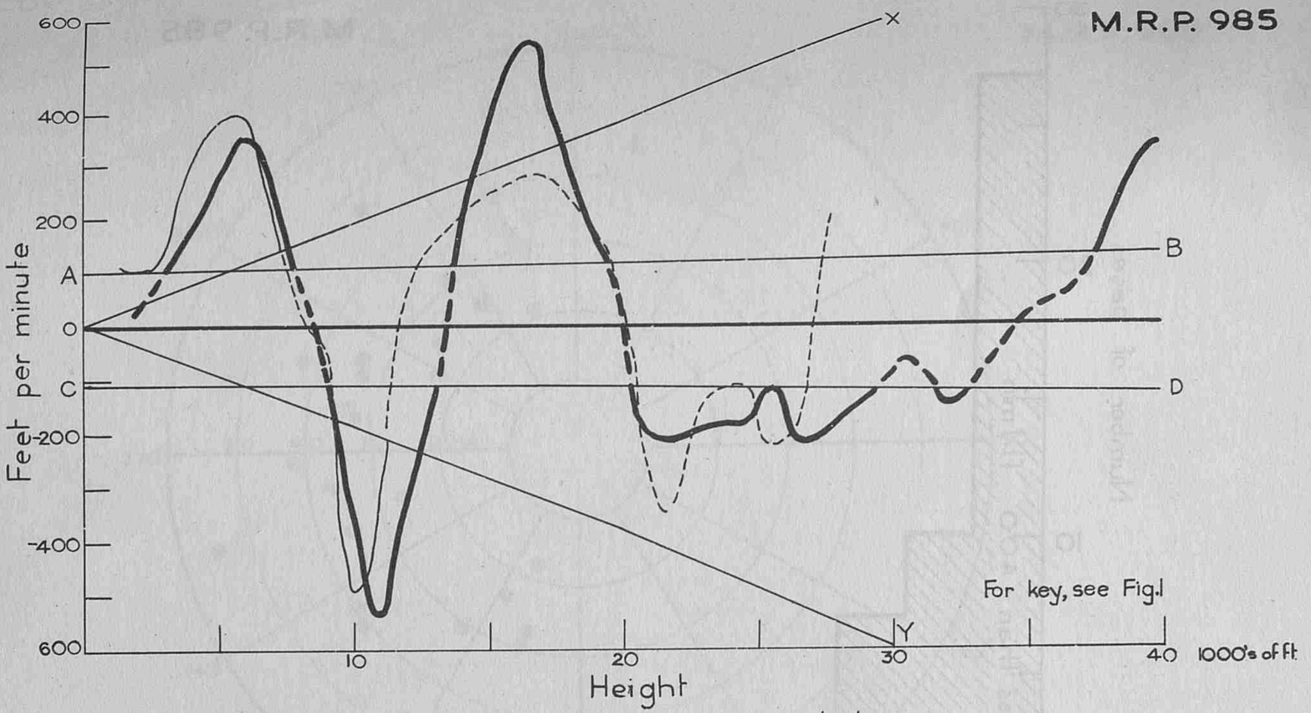

LIVERPOOL 1400 hr. 21/3/54

Fig.10 Vertical air currents

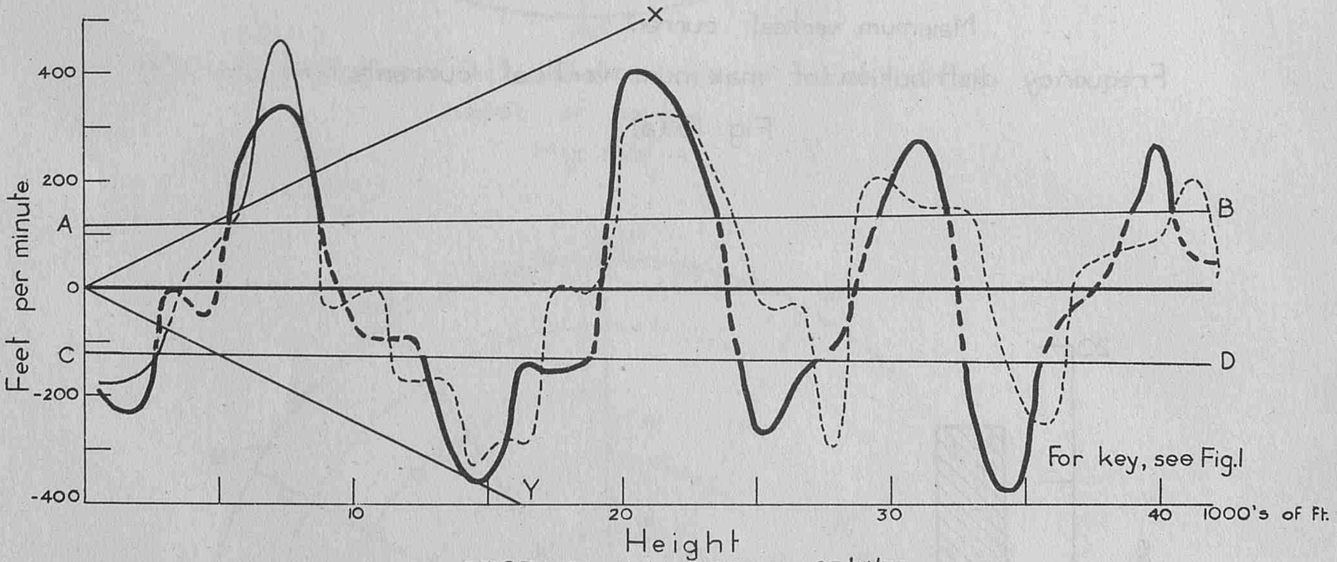

STORNOWAY 0200 hr. 23/11/53

Fig.11 Vertical air currents

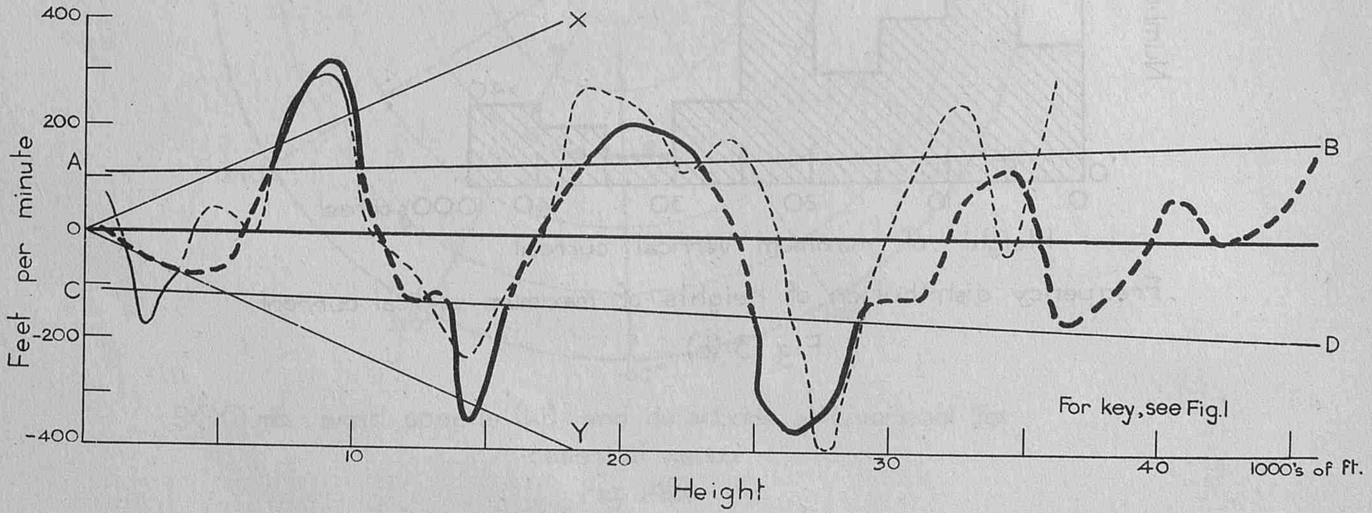

ALDERGROVE 0200 hr. 15/4/54

Fig 12. Vertical air currents

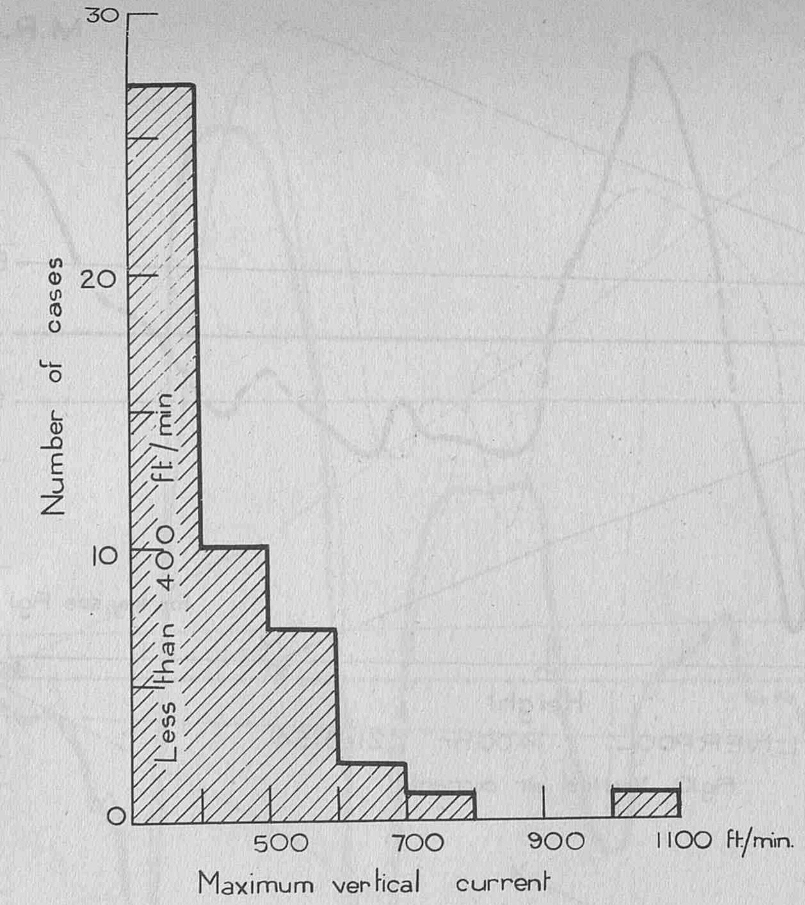

Frequency distribution of maximum vertical currents

Fig. 13 (a)

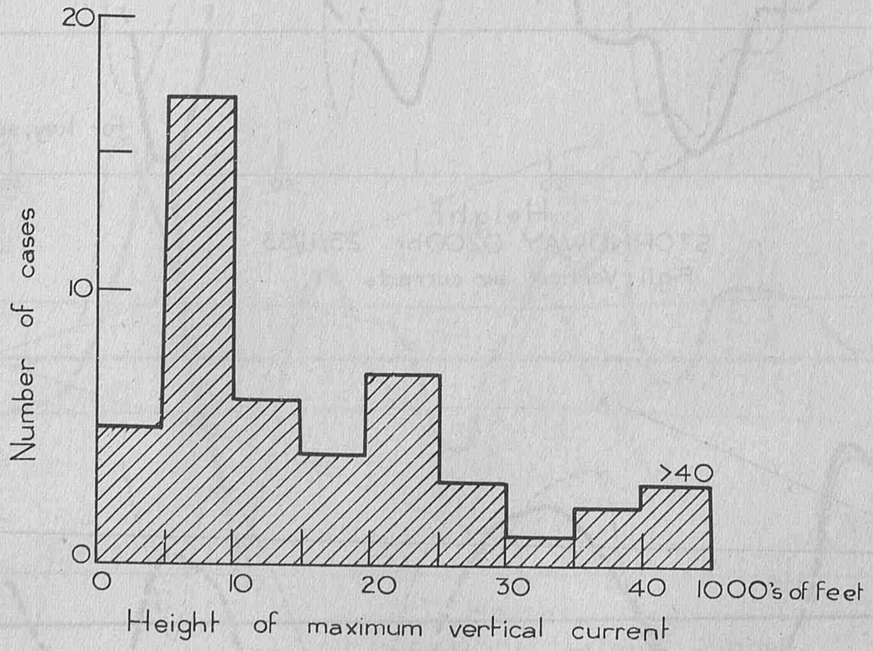

Frequency distribution of heights of maximum vertical current

Fig. 13 (b)

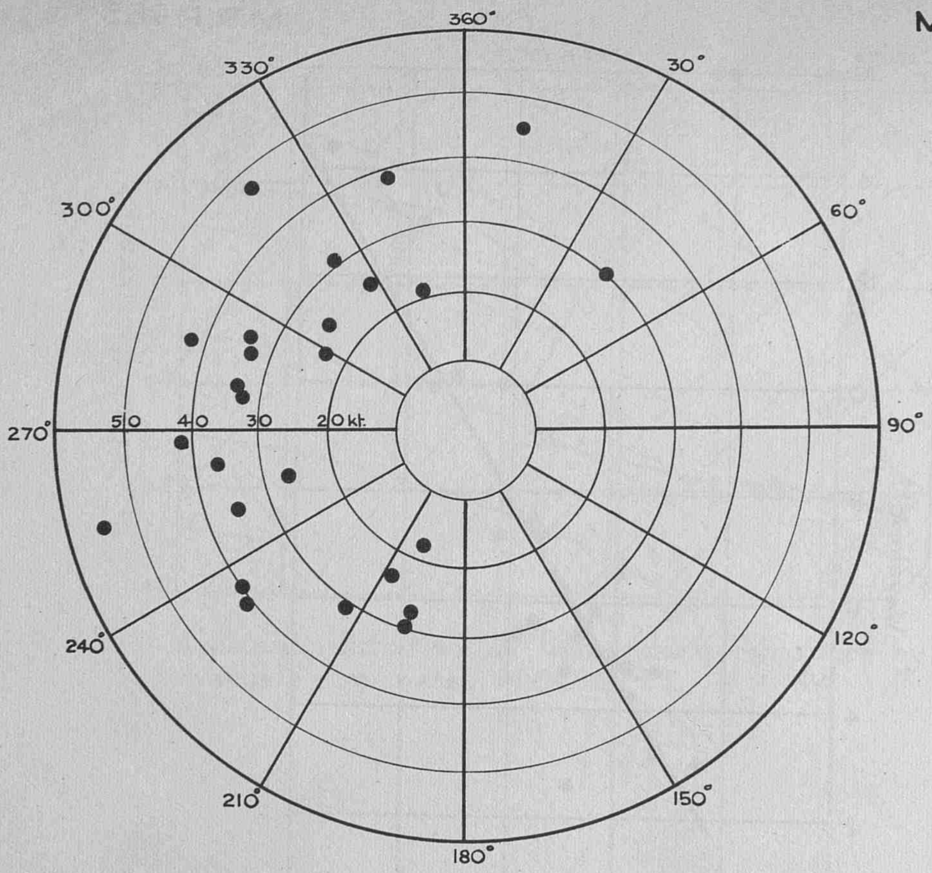

900 mb. wind speeds (kt.) and directions at Leuchars for cases of waves
Fig. 14(a)

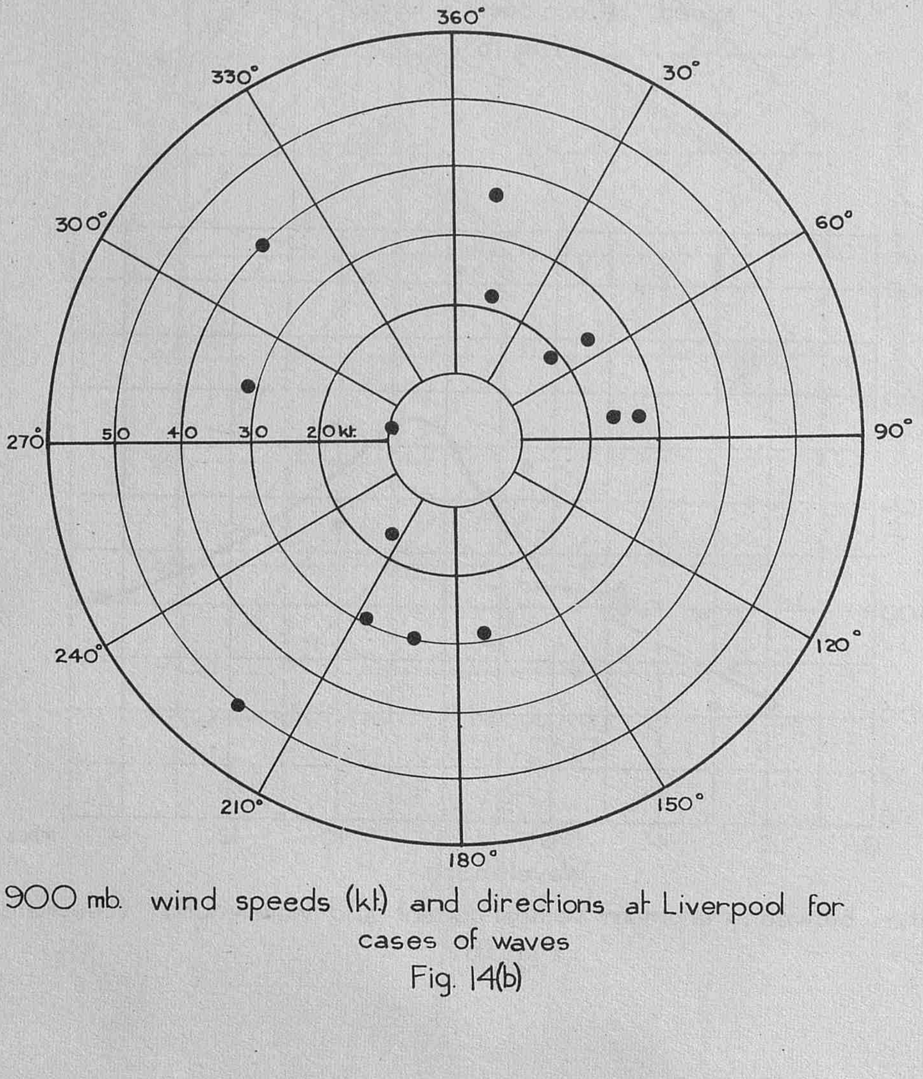

900 mb. wind speeds (kt.) and directions at Liverpool for cases of waves
Fig. 14(b)

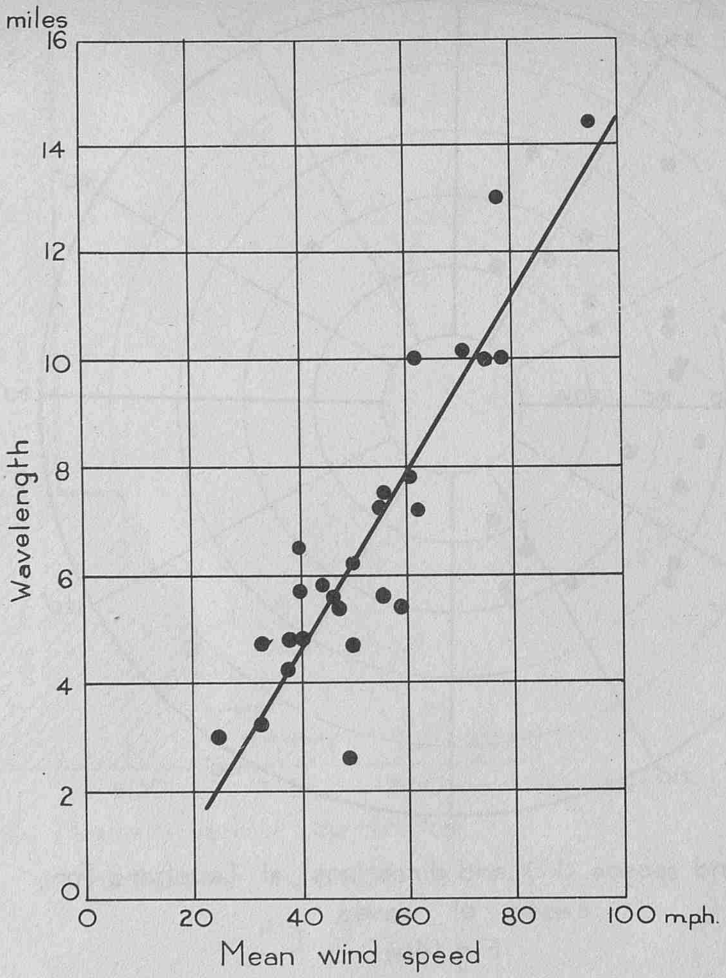

Relation between wavelength and mean wind speed. (Corr. coeff. = 0·91)
Fig. 15

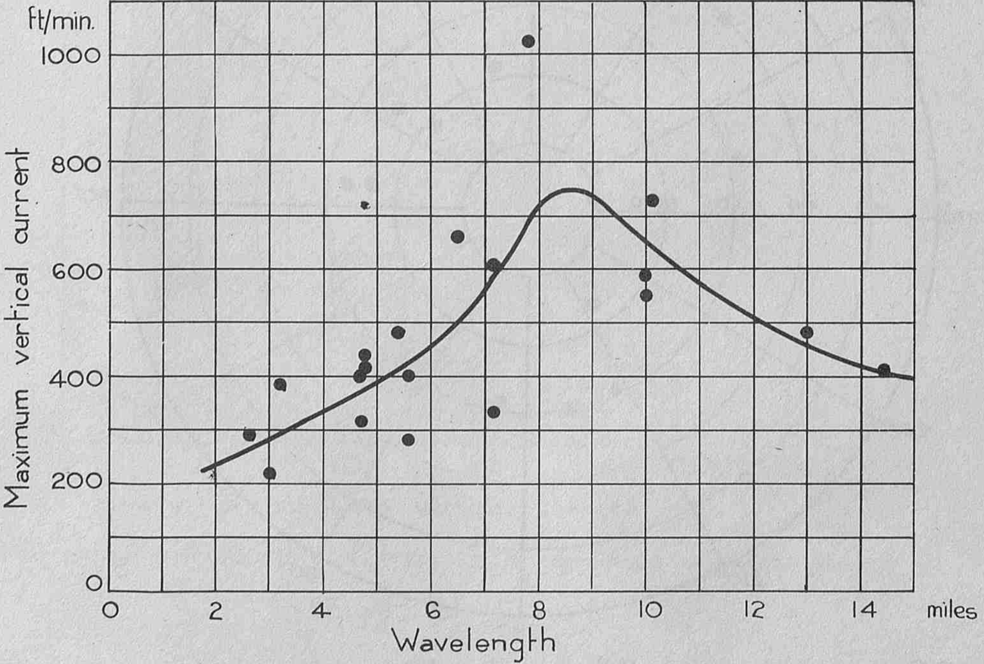

Relation between maximum vertical current and wavelength (Leuchars)
Fig. 16

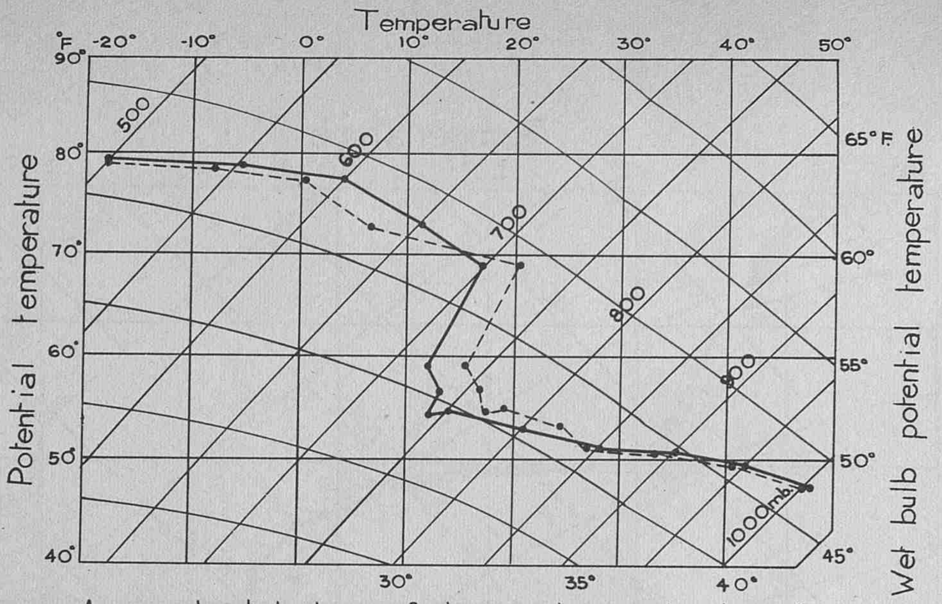

Apparent distortion of temperature structure by waves, Leuchars, 1400 G.M.T., 4:11:54

Fig. 17

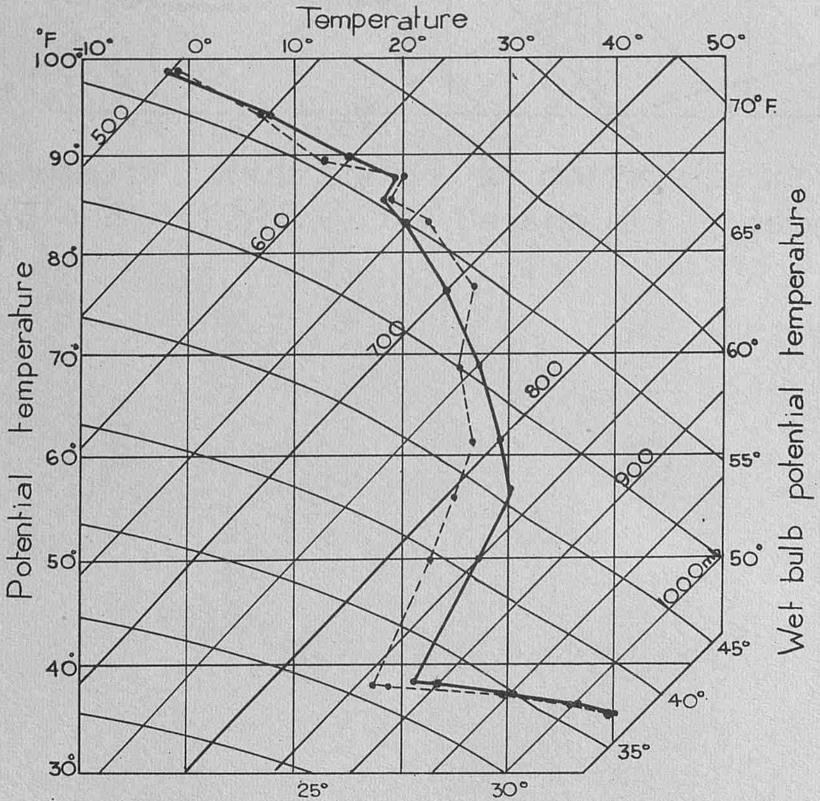

Apparent distortion of temperature structure by waves, Leuchars 0200 G.M.T. 3:1:54

Fig. 18

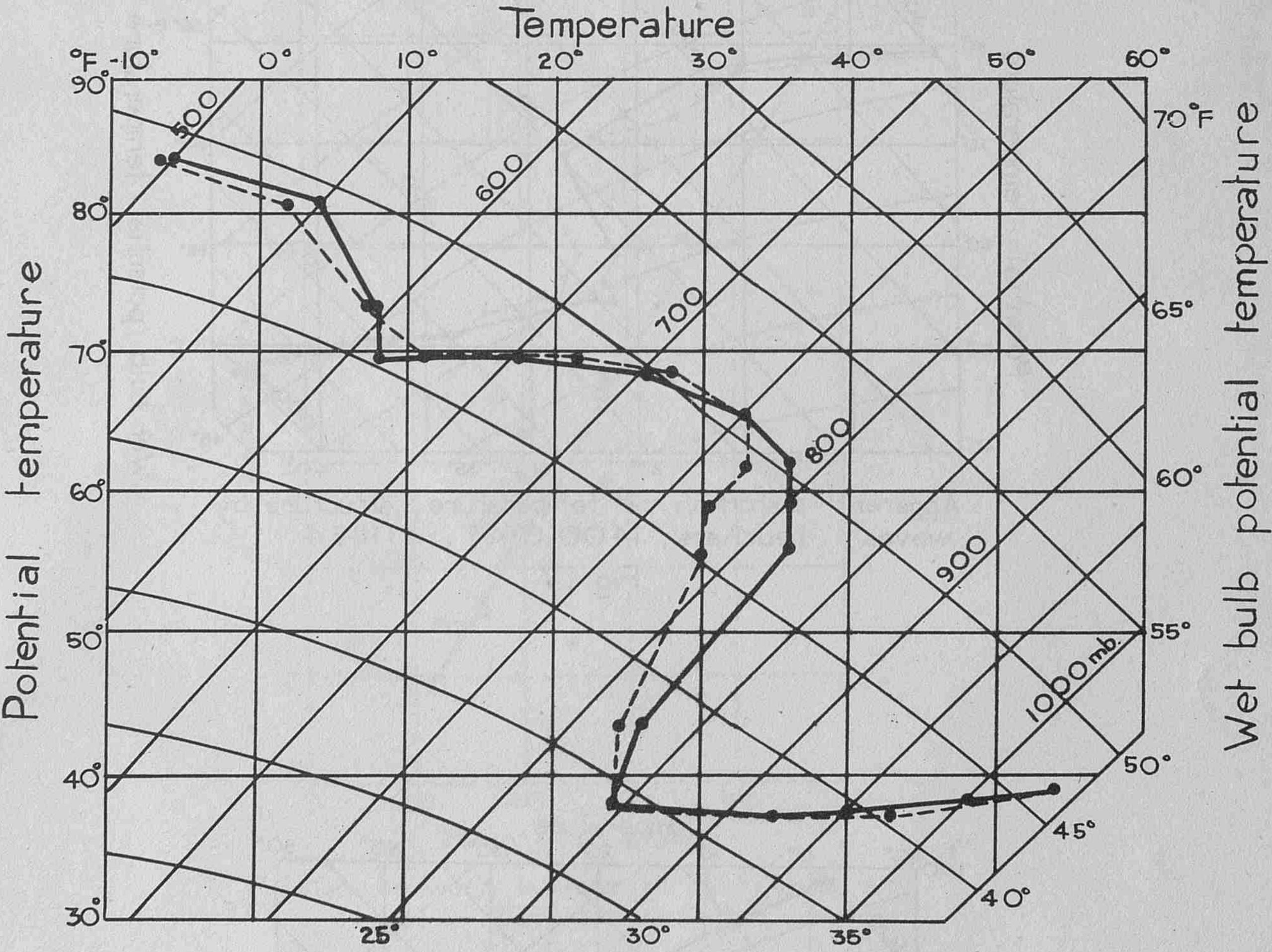

Apparent distortion of temperature structure by waves, Leuchars, 1400 G.M.T 15:4:54

Fig. 19.

M.R.P. 986
S.C.11/212
25th May, 1956.

A D 147514

The objective analysis of some 500 mb. charts.

by

F. H. Bushby

(Meteorological Office)

AIR MINISTRY

METEOROLOGICAL RESEARCH COMMITTEE

At the time of issue this report has not been published. Any author desiring to quote this paper should refer to it as "A paper of the Meteorological Research Committee (London),
M.R.P. No. 986 by Mr. F.H. Bushby
A copy is available in the Library of the Meteorological Office."

M.R.P. 986
S.C. II/212
25th May, 1956

AIR MINISTRY

METEOROLOGICAL RESEARCH COMMITTEE

The objective analysis of some 500 mb. charts

by

F.H. Bushby (Meteorological Office)

1. Introduction

The recent results obtained from the production of prognostic charts by numerical integration of systems of equations relating to various models of the atmosphere have been very encouraging. Indeed, in America and Sweden forecast charts are already being produced on a routine basis under operational conditions. This has only been made possible by the use of electronic computing machines, and it is natural to consider whether or not it is desirable to use these machines for any of the preliminary work prior to the actual integration calculation.

At present, most if not all of the integration procedures make use of the calculus of finite differences, and it is necessary to know the initial fields of the basic variables at mesh points of a horizontal grid. This is normally done by plotting observations on a map and then drawing isopleths of the required variable. A grid is then superimposed on the map and the initial values of the variable (such as 500 mb. height) are read off from the map at grid points by interpolation by eye from the isopleths. This is a subjective process and Gilchrist and Cressman (1954) and Bergthorrson and Döös (1955) have suggested how this can be done objectively by computation. The advantages of this technique of analysis are that it is objective, and that it is time-saving when fast electronic computing machines are available. A possible disadvantage is that the conventional analyst often puts into his analysis something as a result of his experience (especially where observations are scanty), and it is difficult for an objective technique to make use of this kind of experience.

It was therefore decided to analyse objectively a few 500 mb. charts in order to ascertain whether or not a satisfactory technique could be evolved which would not necessarily be dependent upon a dense network of observations. This report describes the method used and the results of these computations.

2. The method

The technique used by Bergthorrson and Döös (1955) for obtaining contour heights at grid points was essentially an empirical modification of a weighted mean of forecast and climatological data by the observations. That proposed by Gilchrist and Cressman (1954) was the finding of the best quadratic surface to fit the observations over a limited area. In each case the geostrophic approximation was used to enable wind observations to be taken into account.

The method of computing the 500 mb. contour heights which was tested at Dunstable is one which has something in common with both of these techniques. Each grid point is dealt with individually and essentially the method consists of finding, by the method of least squares, the quadratic or cubic surface which best fits the observed 500 mb. contour heights and winds and the forecast 500 mb. contour heights. Different weights are given to observed heights and winds and to forecast heights. The method differs from that of Gilchrist and Cressman in that it makes use of forecast values and it differs from the method of Bergthorrson and Döös in that a best fitting surface is found.

We denote by H_s the height of the surface (quadratic or cubic) which best fits the observations and forecasts over a limited area of the chart where

$$H_s = F(x, y) \qquad \ldots. \quad (1)$$

F being a quadratic or cubic function of x and y. Then the expression E which we minimise in order to obtain our best fitting surface is given by

$$E = \sum_1^m \left\{ p(H_s - H_o)^2 \right\}_r + T^2 \sum_1^n \left\{ p(\underline{V_s} - \underline{V_o})^2 \right\}_r + \sum_1^l \left\{ q(H_s - H_F)^2 \right\}_r \quad \ldots. \quad (2)$$

where H_o and V_o represent the observed 500 mb. contour height and wind respectively, H_F represents a forecast 500 mb. height, V_s is the geostrophic wind obtained from the surface represented by Eq. (1), p and q are weighting factors depending upon the distance of the observation or forecast from the grid point for which interpolation is being made, T^2 is a weighting factor relating the fitting of the wind observations to the fitting of the height observations and m, n and l denote the number of height observations, wind observations and forecast heights used to determine F.

One of the main purposes of the work described in this paper was to decide which values of p, q and T^2 gave the best results and whether the use of a cubic form of F gave any improvement over a quadratic form. If we represent the polynomial $F(x, y)$ by

$$F = \sum \alpha_{jK} x^j y^K \qquad \ldots. \quad (3)$$

where $0 \leq j \leq 2$ and $0 \leq K \leq 2$ in the quadratic case and $0 \leq j \leq 3$ and $0 \leq K \leq 3$ in the cubic case, we determine α_{jK} by solving the set of simultaneous equations

$$\frac{\partial E}{\partial \alpha_{jK}} = 0 \qquad \ldots. \quad (4)$$

In order to determine the 500 mb. height at each grid point, the data were searched and the six nearest observing stations, at which either a 500 mb. height or wind or both were reported, were found. Only those stations within a radius of 1000 miles of the grid point were used, and sometimes the number of stations chosen was less than six; indeed on rare occasions there could be no stations available. The information available from these stations therefore consisted of m contour heights and n winds where m and n are both integers and $0 \leq m \leq 6$ and $0 \leq n \leq 6$. When m or n is equal to zero then the appropriate summation term in Eq. (1) is of course zero.

The forecast heights used in this experiment were read from the forecast 500 mb. charts prepared by the Forecast Division at Dunstable, and they were 21 hour forecasts issued for a time three hours previous to the time for which the objective analysis was made. No correction was made for this discrepancy. If this technique was being applied on a routine basis twice daily then numerical forecasts would be available for this purpose and would be based on information only 12 hours old. For the purpose of evaluating the final term in Eq. (2) we took $\ell = 9$, i.e. the summation was effected over the nine nearest grid points to the grid point in question. Thus in the quadratic case we have enough information to determine F at a grid point even if no observations are available. This is not so in the cubic case, and in these circumstances we simply make $H_S = H_F$ at the grid point.

The values of p and T^2 were chosen as a result of some work by Johnson (1956). Two expressions for p were used, and these are shown in Fig. 1 as functions of the distance from the grid point at which interpolation was being carried out. In the first trials a value of T^2 equal to 2 sec.^{2} was used for the quadratic surface and a value of T^2 equal to 16 sec.^{2} was used for the cubic surface. Later, $T^2 = 16$ sec.^{2} was used for the quadratic surface. Two expressions for q were tried; $q = p / 4$ and $q = p / 16$. On the Ferranti Mark I machine at Manchester University the computation took 40 sec. per point for the quadratic case and 60 sec. per point for the cubic case.

3. The experiment

The three situations used for the experiment were those for 1500 G.M.T. on the 12th September, 1955, 15th October, 1955 and 31st October, 1955. These situations were chosen because the 500 mb. prontours for 1200 G.M.T. on those days were substantially in error over some part of the area. They were not chosen as being typical of everyday differences between forecast and actual charts, but in this experiment it was necessary that there should be differences between the forecast and the actual observations in order to assess the effect that each was having on the objective analysis.

The objective analyses were made for the 18 x 14 grid used for previous work at Dunstable, but the computations were done firstly for the European half of the grid and secondly for the Atlantic half. This allowed the technique to be tried first for the European network of stations, which is very much denser than the Atlantic network. In order that the reader may assess the smoothness of the results for himself, the results for each grid point have been plotted on the diagrams to the nearest ten feet with the ten thousand figure omitted.

Since the effect of varying the parameters was very similar in each case, only one case is described in detail (Figs. 2a-2h) but the results for the best values of the parameters for the quadratic surface and the results for the cubic surface are given in each case. The observations used in the computations are shown in Figs. 2a, 3a and 4a, together with the analysis of the Forecast Division at Dunstable*. Figs. 2b, 3b, and 4b show the forecast charts which were also used in the experiments.

The first objectively analysed chart (1500 G.M.T. 12th September, 1955) which was computed using this technique is shown in Fig. 2c. T^2 was taken equal to 2 sec.^{2}, $p = p_1 = 2^7(1 + 2^{-29} . 10^8 r^4)^{-1}$
where r is the distance in grid lengths of the reporting station from the

---

* Certain observations outside the area covered by the background map were also used.

grid point and $q = q_1 = p_1 / 4$. From this and similar computations using the other two sets of data it was obvious that the forecast heights were being given too much weight in all areas except where the network of reporting stations was dense. The objective analyses were therefore repeated using $q = q_2 = p_1 / 16$ and the result of this computation for 1500 G.M.T. 12th September, 1955 is shown in Fig. 2d. In general there was some improvement over Europe in areas of few reporting stations where the forecast was different from the observations. In the analyses for 1500 G.M.T. 12th September, 1955 this improvement is confined to the Mediterranean where the cut-off low is further west in Fig. 2d than in Fig. 2c, which is more in accordance with the observations (Fig. 2a) than the forecast position (Fig. 2b). Over the Atlantic there is also a change away from the forecast values towards the conventional analysis. However, it is easy to see from Fig. 2d that the objective analysis still leaves a lot to be desired over the Atlantic. The main cause of the unsatisfactory nature of these objective analyses over the Atlantic is the introduction of short wavelength features to accommodate isolated observations which are different from the smooth forecast values. The remainder of the experiment was therefore devoted to endeavouring to find ways of removing these short wavelength features from the analyses.

The first step was to repeat the computations using $p = p_2 = 2^7(1 + 2^{-33}.10^8 r^4)^{-1}$. p_2 represents a weighting factor which decreases less rapidly with distance than p_1, and thus each observation has an influence over a greater area than when p_1 was used. The results are shown in Fig. 2e for 12th September, 1955, and the appearance of this chart is typical of the results obtained from the other two situations. Over Europe, only very slight changes occurred and in this area the analyses are as good as can be expected. Over the Atlantic, Fig. 2e shows a marked improvement over Fig. 2d, but there is still some distortion of the main flow in the vicinity of the ship observations. The computations over the Atlantic were repeated taking $T^2 = 16$ sec.^{2} which has the effect of increasing the weight of the wind observations relative to the observed and forecast height. Fig. 2g is typical of the other two computations and it is evident by inspection that this does give a smooth pattern over the Atlantic. Computations were also made in which no forecast heights were used at all (Fig. 2f) but the results were not as good as those obtained in Fig. 2g. At one or two points south of the Azones it was not possible to solve Eqs. (4), due to lack of sufficient data.

One set of computations for each of the three situations was completed using a cubic rather than a quadratic surface, $T^2 = 16$ sec.^{2}, $p = p_2$ and $q = q_2$. The results are shown in Figs. 2h, 3d and 4d, but it does not appear that any significant improvements have been achieved over Figs. 2g (and European half of 2e), 3c and 4c, which represent the best results achieved with the quadratic surface.

4. Conclusion

As a result of this experiment it is evident that for the three situations which were considered, the best objective analysis using a quadratic surface can be obtained when $T^2 = 16$ sec.^{2}, $p = p_2$ and $q = q_2$, although over Europe $T^2 = 2$ sec.^{2} is satisfactory. There does not appear to be any advantage in increasing the length and complexity of the computations in order to use a cubic surface. Indeed, in one or two areas it appears that the quadratic surface probably gives a better answer than the cubic surface as it introduces a greater measure of smoothing. The cubic surface with its extra degrees of freedom is able to fit more closely both the observations and forecast values, and this is not necessarily a good thing in regions not near a reporting station.

It must be remembered that the comparison between analyses has been subjective in this experiment, but an inspection of the actual results plotted on the diagrams indicates that the contour lines could hardly have been drawn

/differently

differently. Whether the objective analysis technique suggested in this report can produce charts sufficiently smooth and accurate to be used as initial data for time integrations remains to be tested, but visual inspection of the charts suggests that this will be possible. It is certain that this technique used on an operational basis with a Ferranti Mark II computer would enable the initial data for a time integration to be available inside the machine considerably sooner than if the data had first to be plotted, the chart analysed, values read off at grid points, and these values punched on to paper tape.

5. Acknowledgement

I wish to acknowledge the fact that Miss Huckle was responsible for a large part of the programming of the computations connected with this work.

References

B. Gilchrist and C.P. Cressman	Tellus, Vol. 6, No. 4, 1954, p.309.
P. Bergthorrson and B. Döös	Tellus, Vol. 7, No. 3, 1955, p.329.
D.H. Johnson	Meteorological Research Papers, Air Ministry, London, No. 965, 1956.

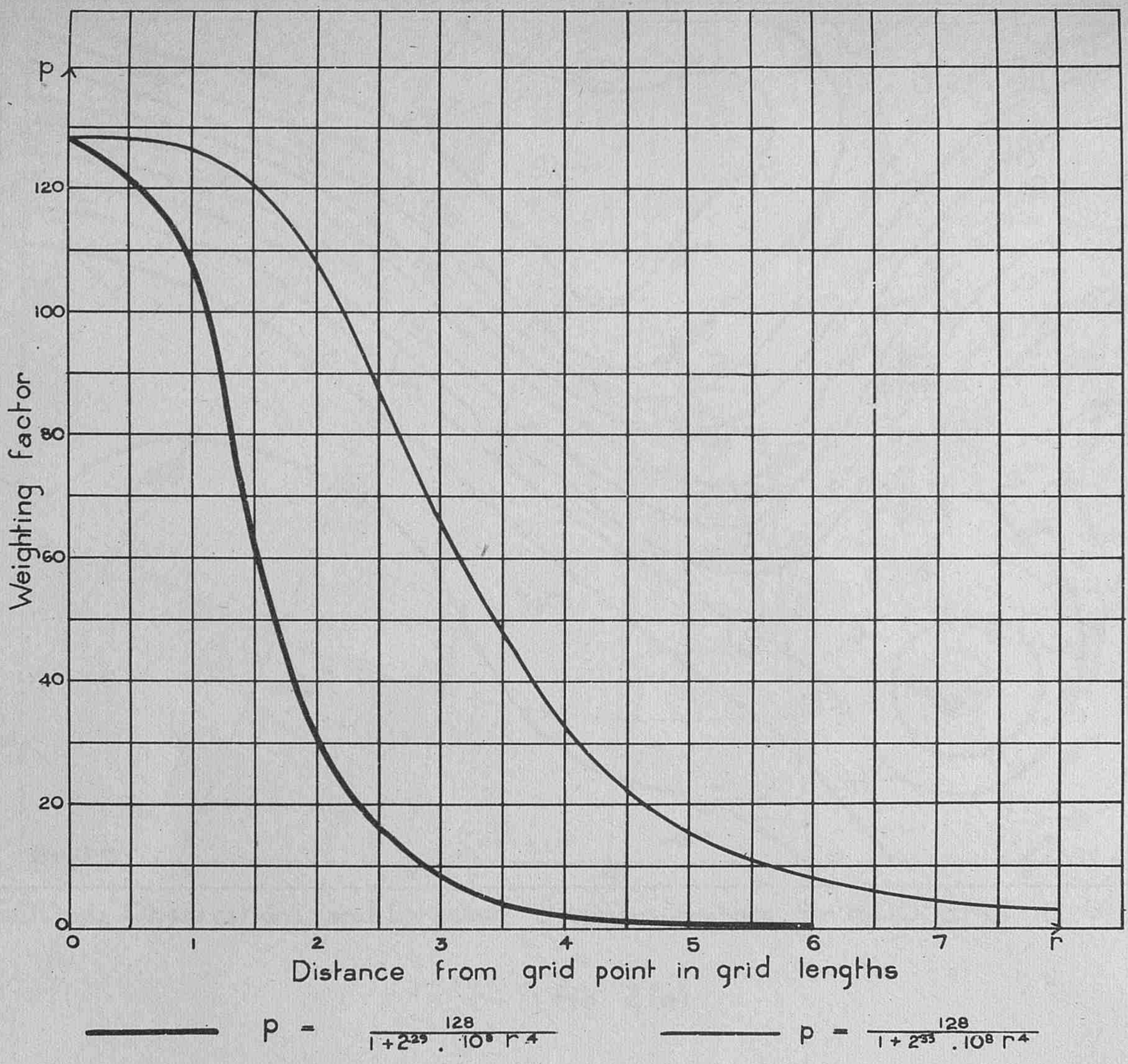

$p = \frac{128}{1 + 2^{29} \, . \, 10^{8} \, r^{4}}$ $\qquad$ $p = \frac{128}{1 + 2^{33} \, . \, 10^{8} \, r^{4}}$

Distance weighting factors

Fig. 1

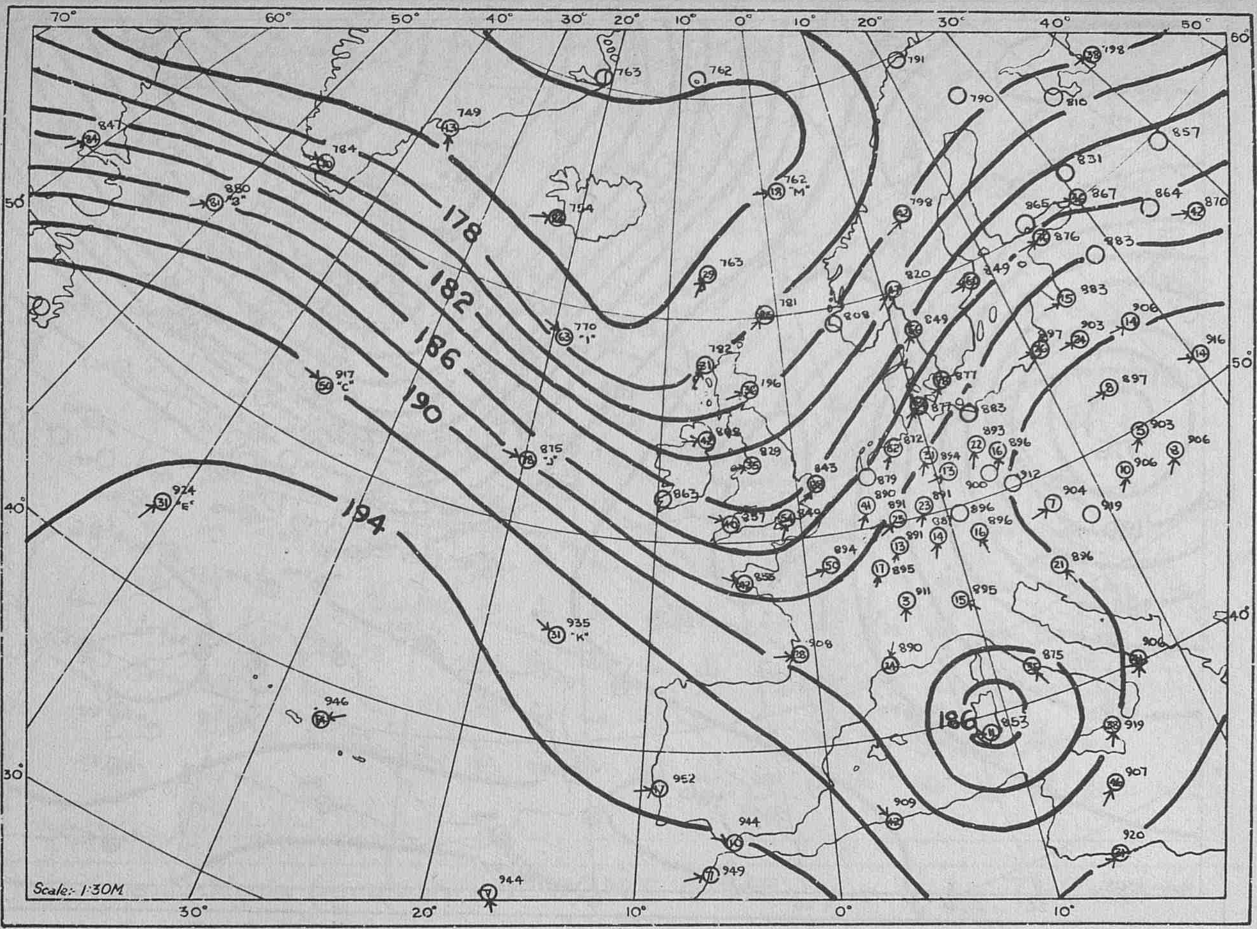
70°
60°
50°
40°
30°
20°
10°
0°
10°
20°
30°
40°
50°
60°
50°
40°
30°
178
182
186
190
194
186
"B"
"C"
"E"
"I"
"J"
"K"
"M"
Scale:- 1:30M
30°
20°
10°
0°
10°

500mb. Observations and forecast division analysis for 1500 G.M.T. 12: 9: 55

Fig. 2(a)

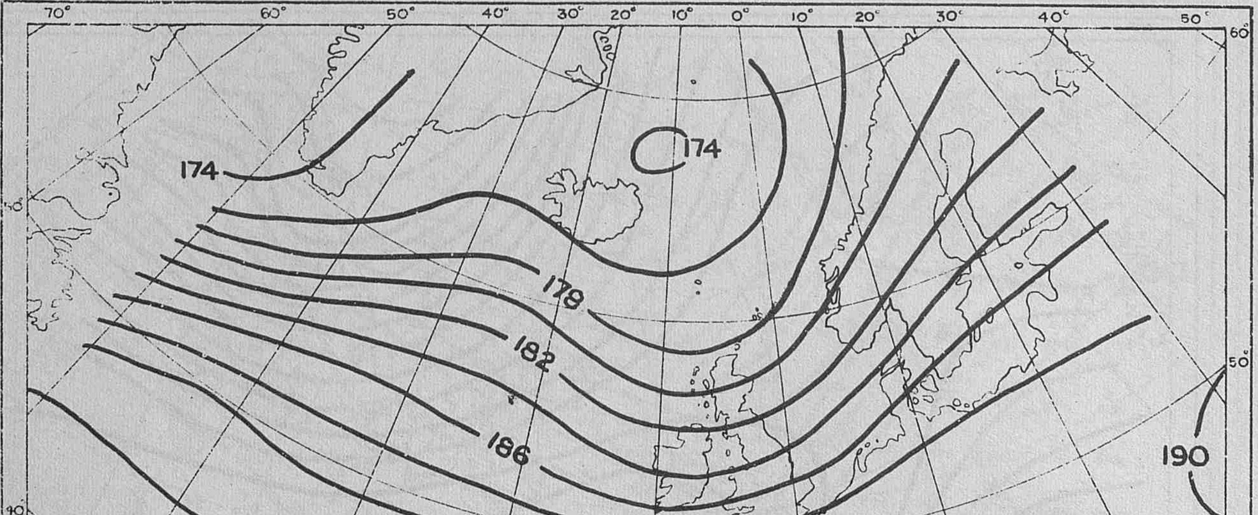
70°
60°
50°
40°
30°
20°
10°
0°
10°
20°
30°
40°
50°
60°
50°
40°
30°
174
174
178
182
186
190
190
190
192
194
Scale 1:30M
30°
20°
10°
0°

500 mb prontour 1500 G.M.T. 12·9·55

Fig 2 (b)

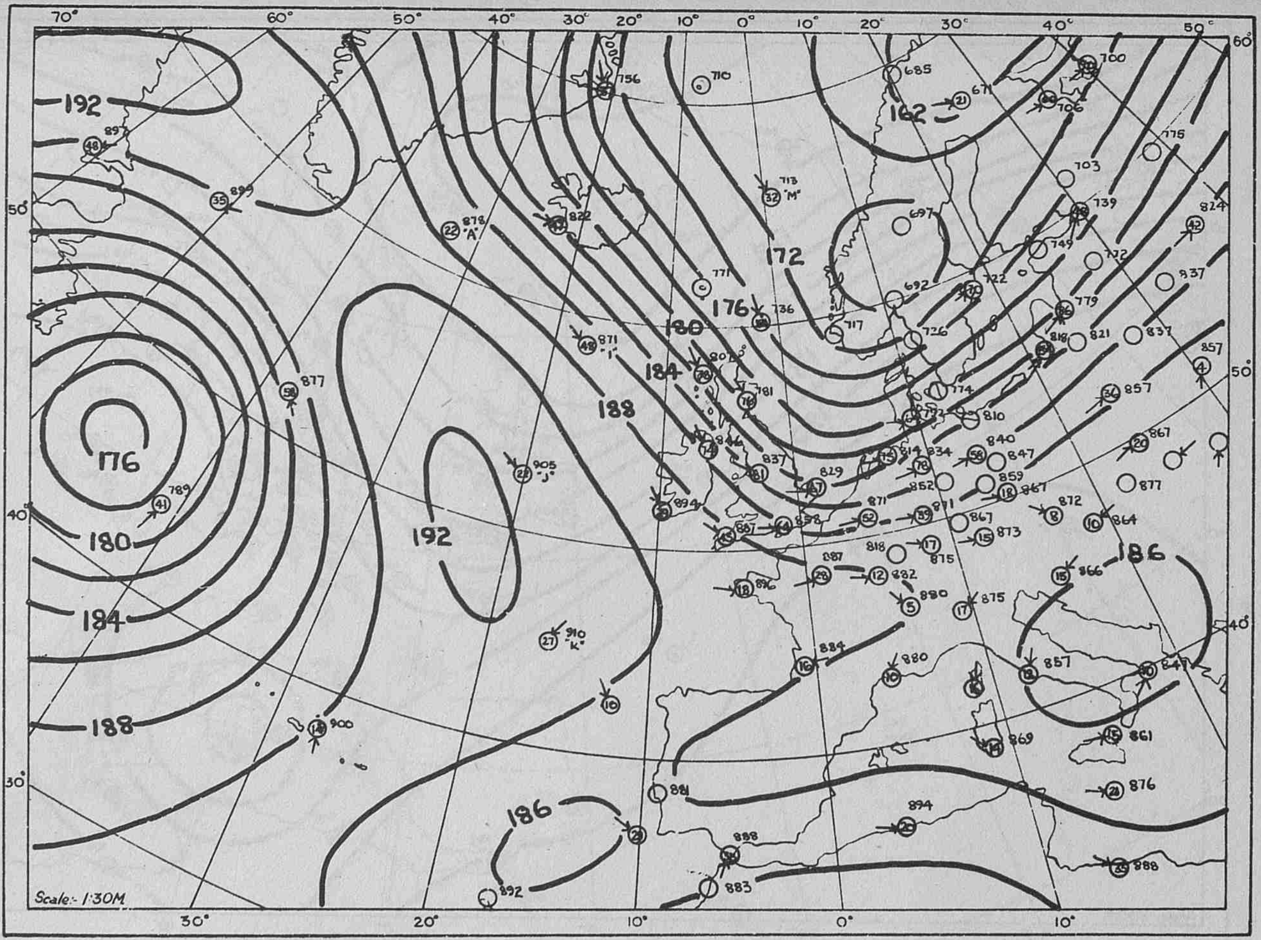
70°
60°
50°
40°
30°
20°
10°
0°
10°
20°
30°
40°
50°
192
176
180
184
188
192
188
184
180
176
172
162
186
186
Scale:- 1:30M
30°
20°
10°
0°
10°

500mb. Observations and forecast division analysis 1500 G.M.T. 15:10:55

Fig 3(a)

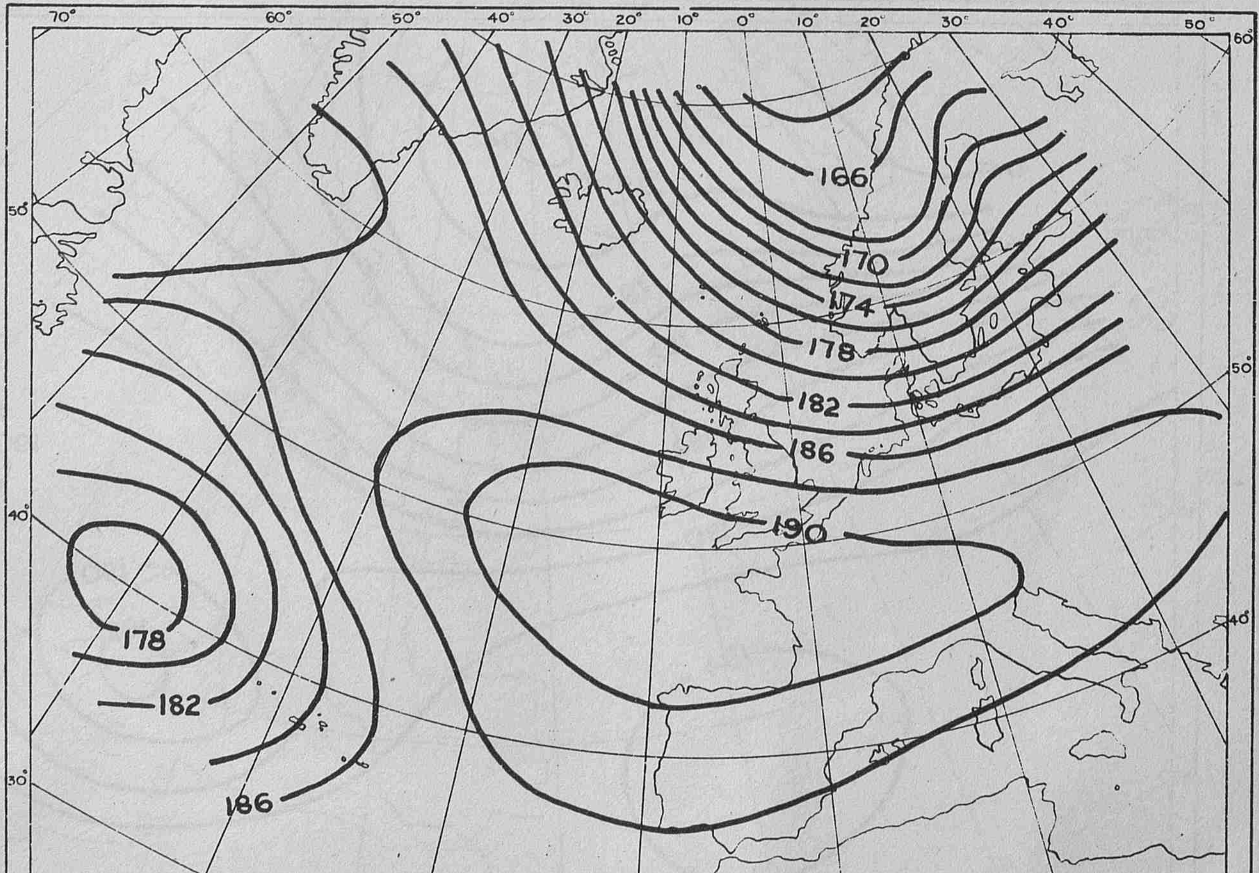
70°
60°
50°
40°
30°
20°
10°
0°
10°
20°
30°
40°
50°
166
170
174
178
182
186
190
178
182
186
Scale:- 1:30M
30°
20°
10°
0°
10°

500 mb prontour, 1200 G.M.T. 15:10:55

Fig. 3(b)

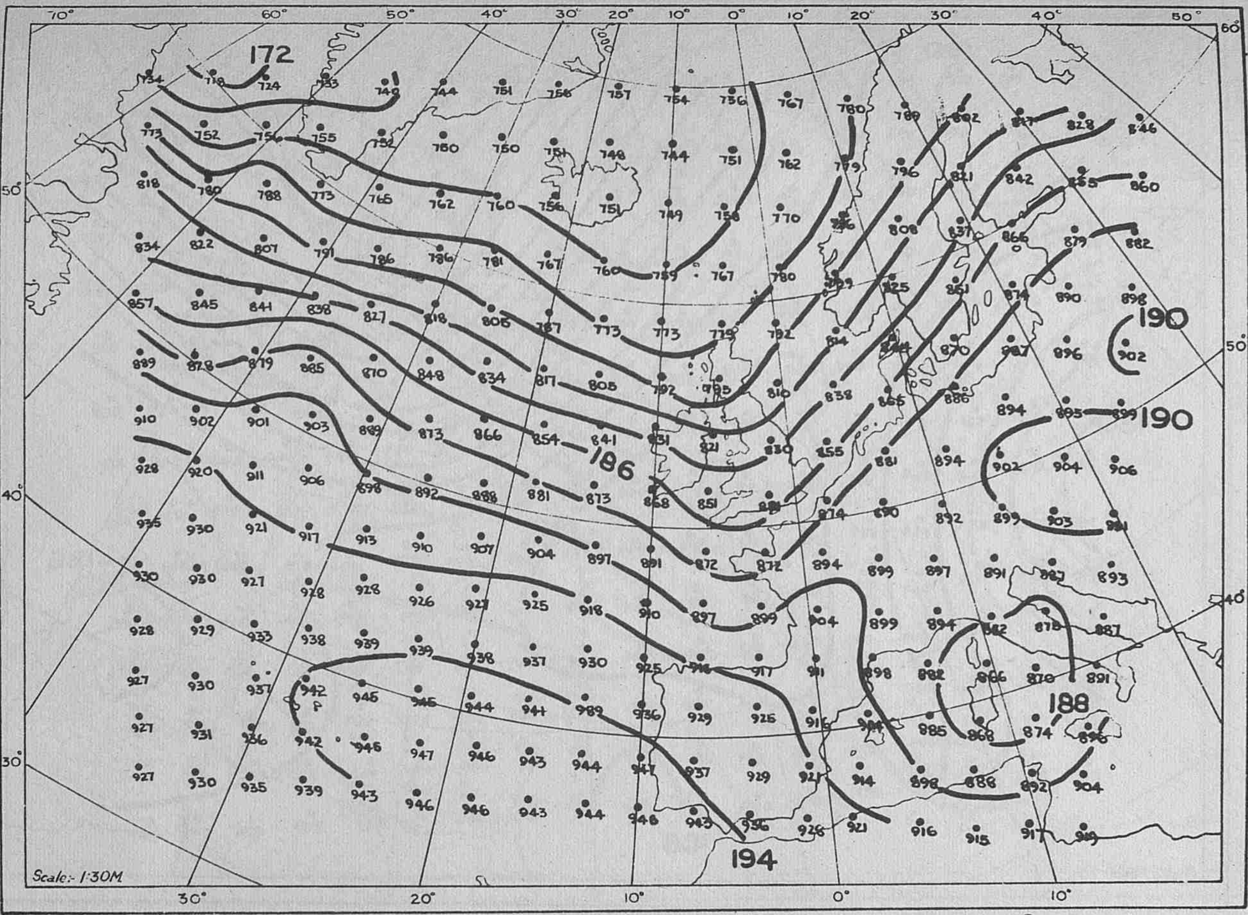
172
186
190
190
188
194
70°
60°
50°
40°
30°
20°
10°
0°
10°
20°
30°
40°
50°
60°
50°
40°
30°
50°
40°
30°
20°
10°
0°
10°
Scale:- 1:30M

Objective analysis (quadratic) 1500 G.M.T. 12·9·55 $p = p_1$ $q = \frac{1}{4}p_1$ $T^2 = 2\ \text{sec}^2$

Fig. 2 (c)

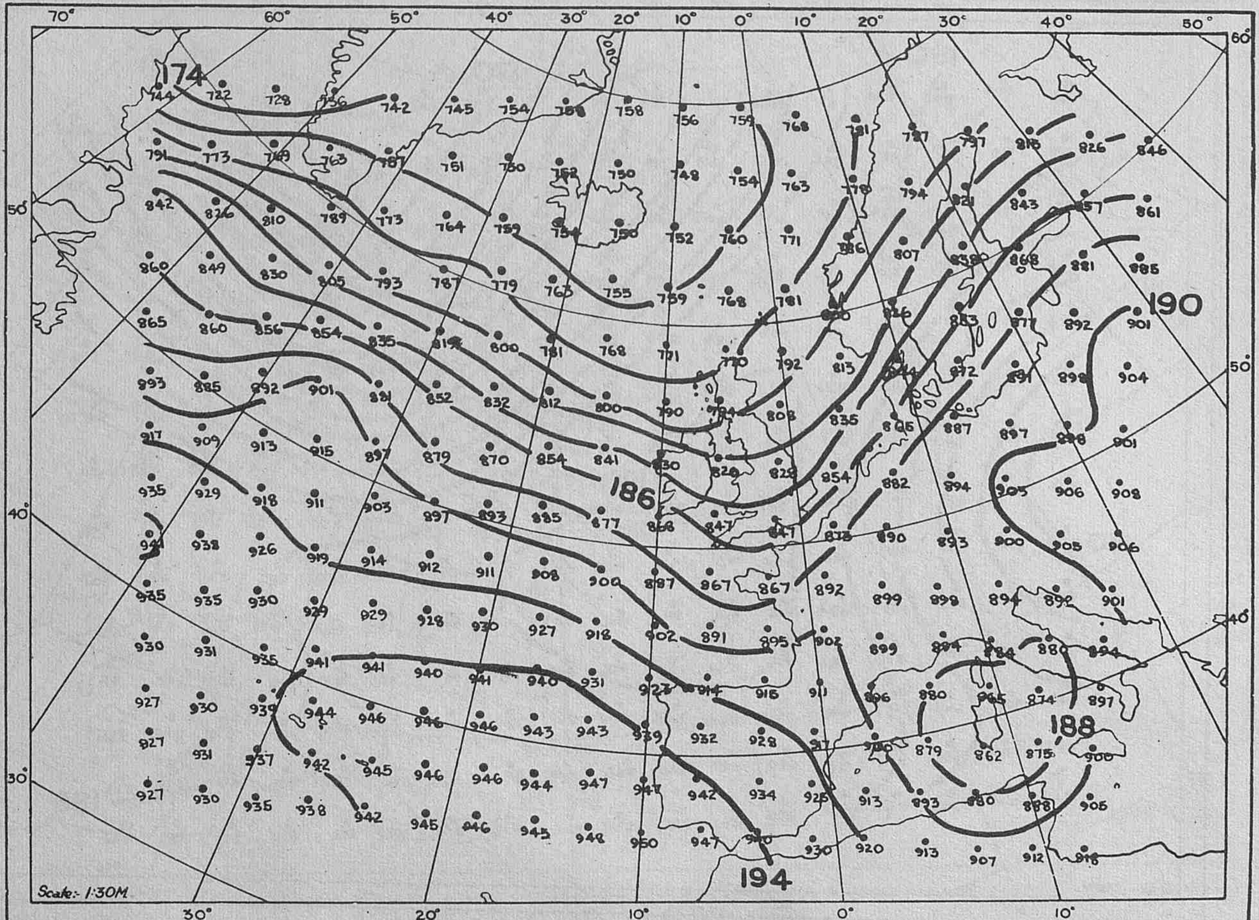
174
186
190
188
194
70°
60°
50°
40°
30°
20°
10°
0°
10°
20°
30°
40°
50°
60°
50°
40°
30°
50°
40°
30°
20°
10°
0°
10°
Scale:- 1:30M

Objective analysis (quadratic) 1500 G.M.T. 12·9·55

$p = p_1$ $q = \frac{1}{16}p$ $T^2 = 2\ \text{sec}^2$

Fig. 2 (d)

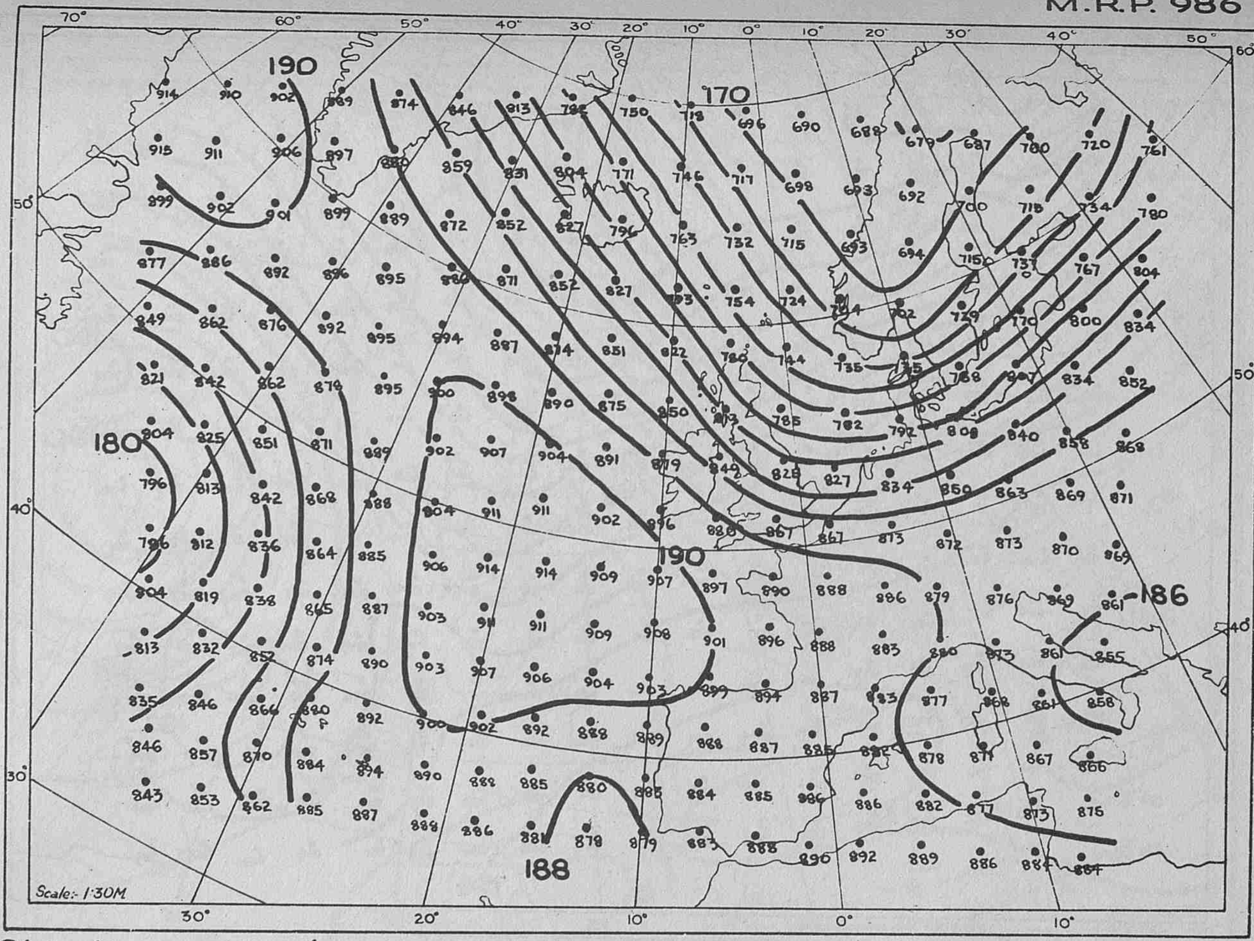
70°
60°
50°
40°
30°
20°
10°
0°
10°
20°
30°
40°
50°
60°
50°
40°
30°
190
170
180
190
186
188
30°
20°
10°
0°
10°
Scale:- 1:30M.

Objective analysis (quadratic) 1500 GMT. 15:10:55

$P = P_2$ $\quad q = \frac{1}{16}P_2$ $\quad T^2 = 2\ \text{sec}^2$ (Europe) $\quad T^2 = 16\ \text{sec}^2$ (Atlantic)

Fig. 3(c)

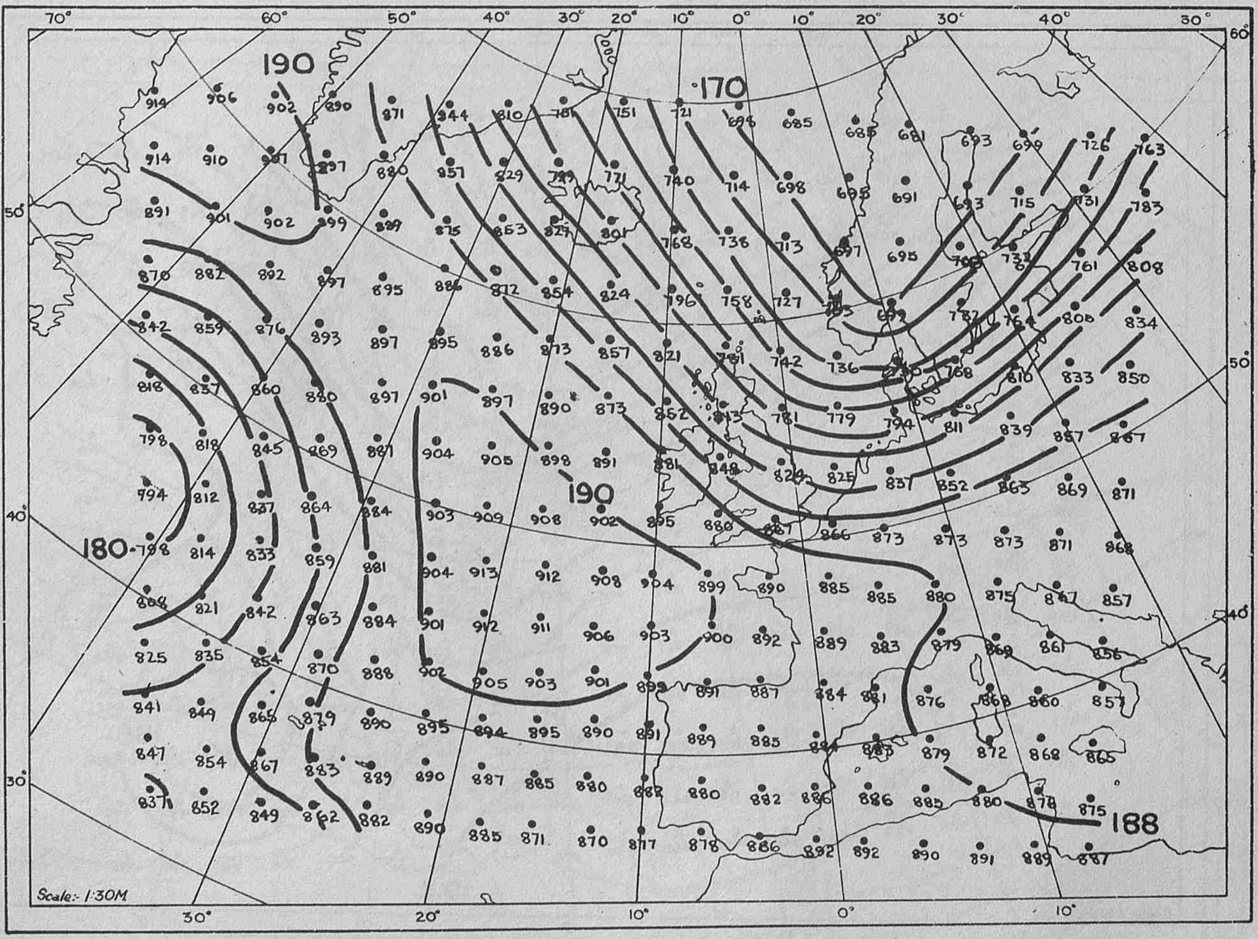
70°
60°
50°
40°
30°
20°
10°
0°
10°
20°
30°
40°
30°
60°
50°
40°
30°
190
170
180
190
188
30°
20°
10°
0°
10°
Scale:- 1:30M.

Objective analysis (cubic) 1500 GMT. 15:10:55

$P = P_2$ $\quad q = \frac{1}{16}P_2$ $\quad T^2 = 16\ \text{sec}^2$

Fig. 3(d)

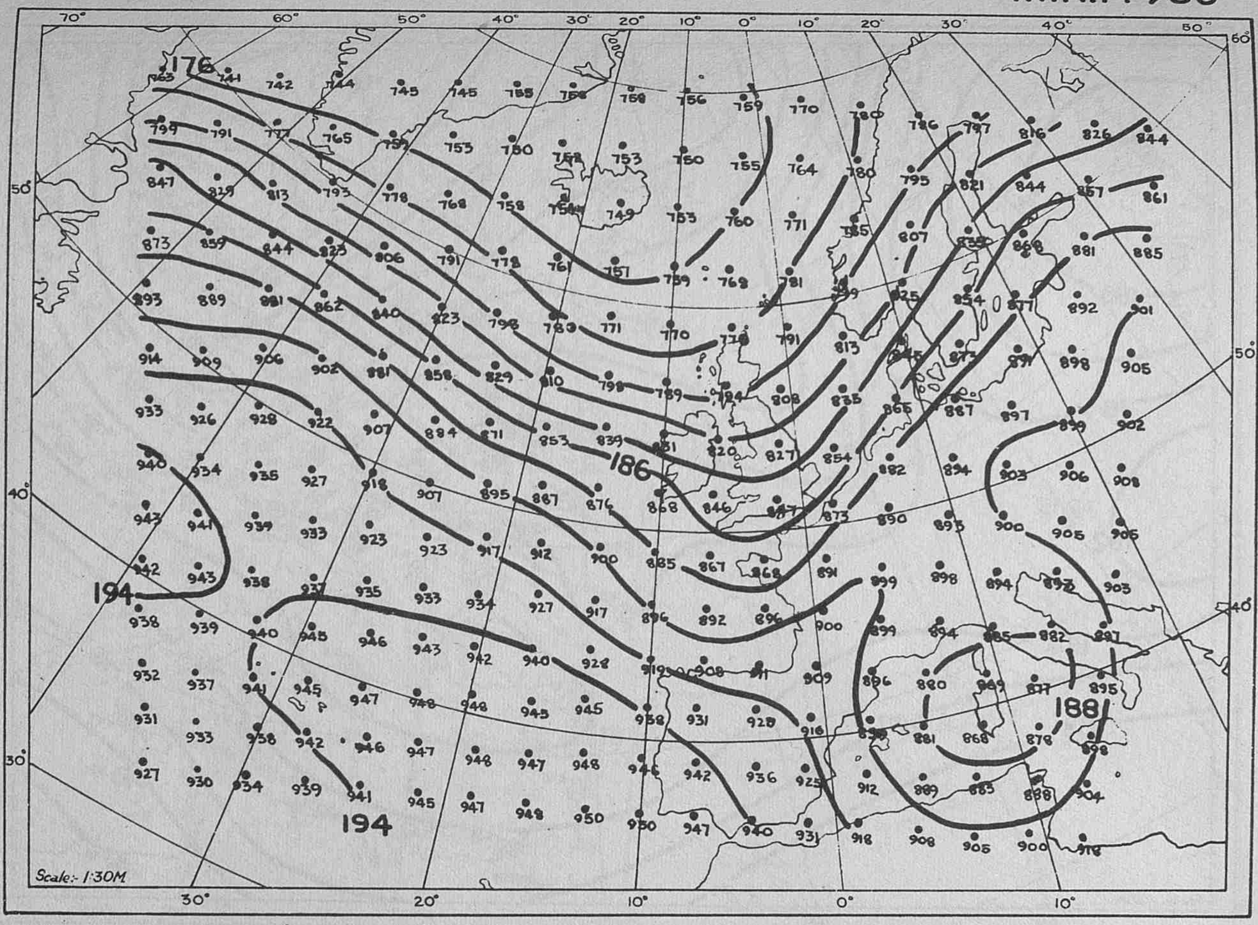
176
186
188
194
194
70°
60°
50°
40°
30°
20°
10°
0°
10°
20°
30°
40°
50°
60°
50°
40°
30°
30°
20°
10°
0°
10°
Scale:- 1:30M

Objective analysis (quadratic) 1500 G.M.T. 12:9:55

$p = P_2$ $q = \frac{1}{16}P_2$ $T^2 = 2\,\mathrm{sec}^2$

Fig. 2 (e)

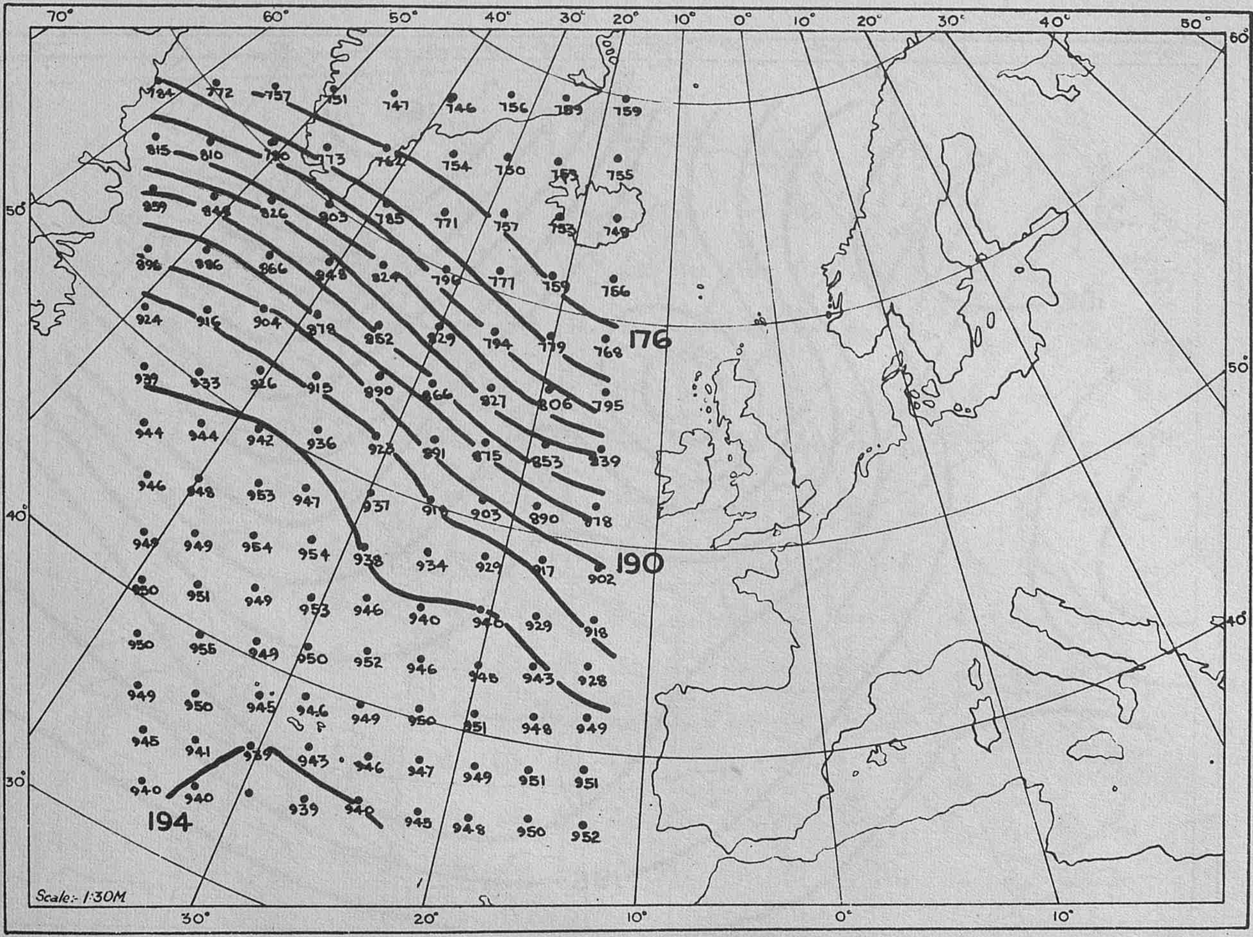
176
190
194
70°
60°
50°
40°
30°
20°
10°
0°
10°
20°
30°
40°
50°
60°
50°
40°
30°
30°
20°
10°
0°
10°
Scale:- 1:30M

Objective analysis (quadratic) 1500 G.M.T. 12:9:55

$p = P_2$ $q = 0$ $T^2 = 2\,\mathrm{sec}^2$

Fig 2 (f)

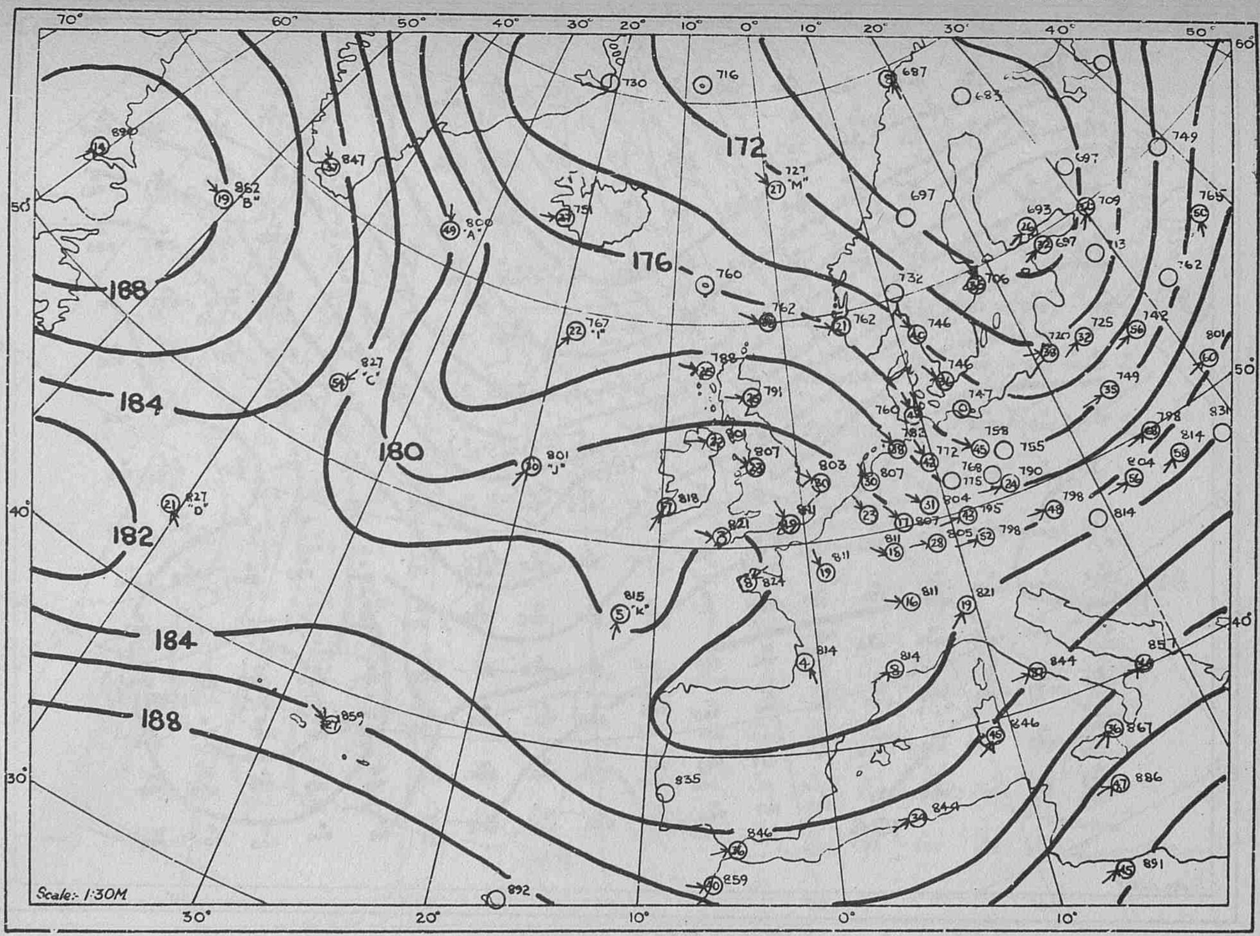
70°
60°
50°
40°
30°
20°
10°
0°
10°
20°
30°
40°
50°
60°
50°
40°
30°
172
176
180
184
188
182
"A"
"B"
"C"
"D"
"I"
"J"
"K"
"M"
Scale:- 1:30M
30°
20°
10°
0°
10°

500 mb Observations and forecast division analysis 1500 G.M.T. 31:10:55

Fig 4(a)

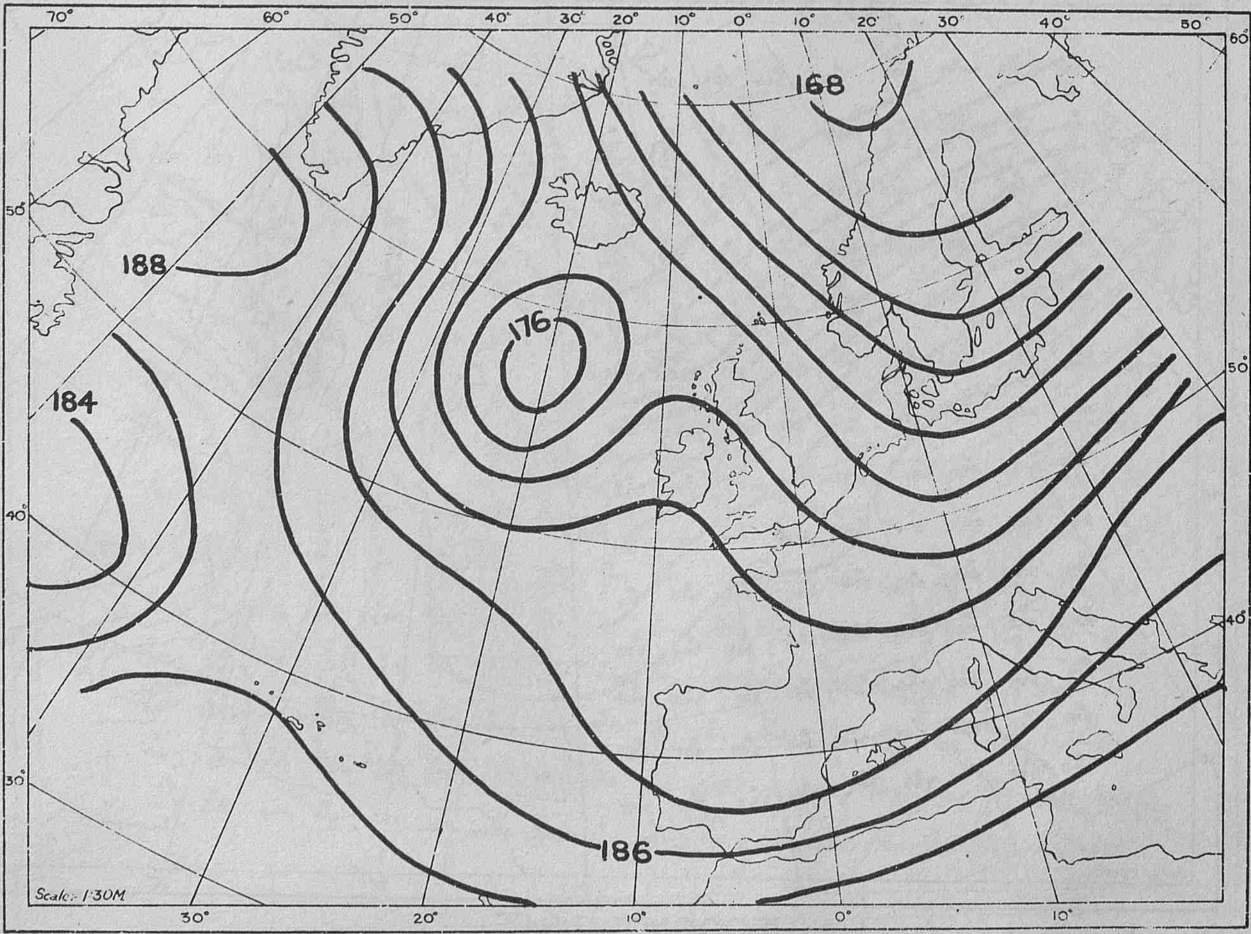
70°
60°
50°
40°
30°
20°
10°
0°
10°
20°
30°
40°
50°
60°
50°
40°
30°
168
176
184
186
188
Scale:- 1:30M
30°
20°
10°
0°
10°

500 mb. prontour 1200 G.M.T. 31:10:55

Fig. 4 (b)

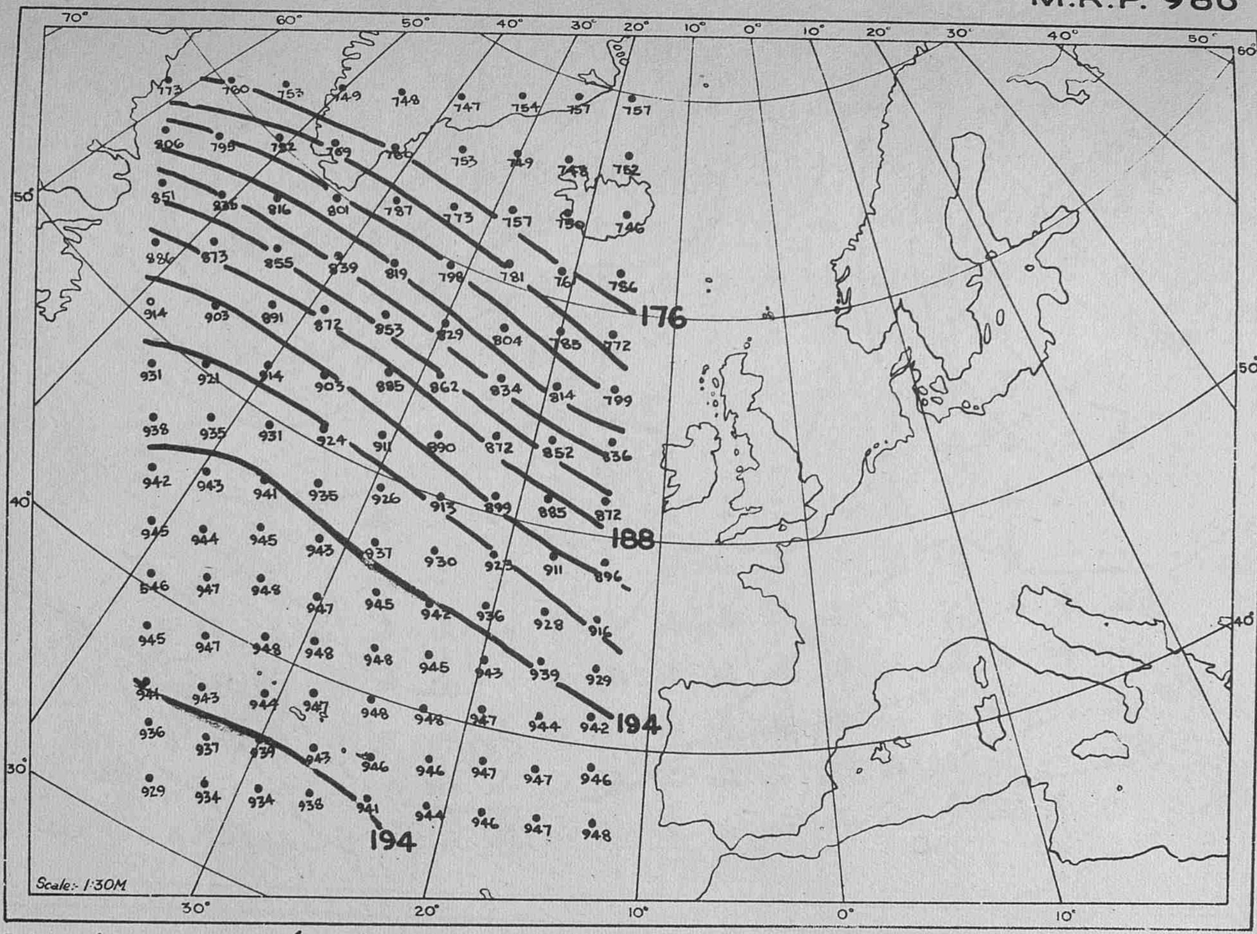
176
188
194
194
Scale:- 1:30M
70°
60°
50°
40°
30°
20°
10°
0°
10°
20°
30°
40°
50°

Objective analysis (quadratic) 1500 G.M.T. 12:9:55

$p = P_2 \quad q = \frac{1}{16} P_2 \quad T^2 = 16\,\text{sec}^2$

Fig. 2 (g)

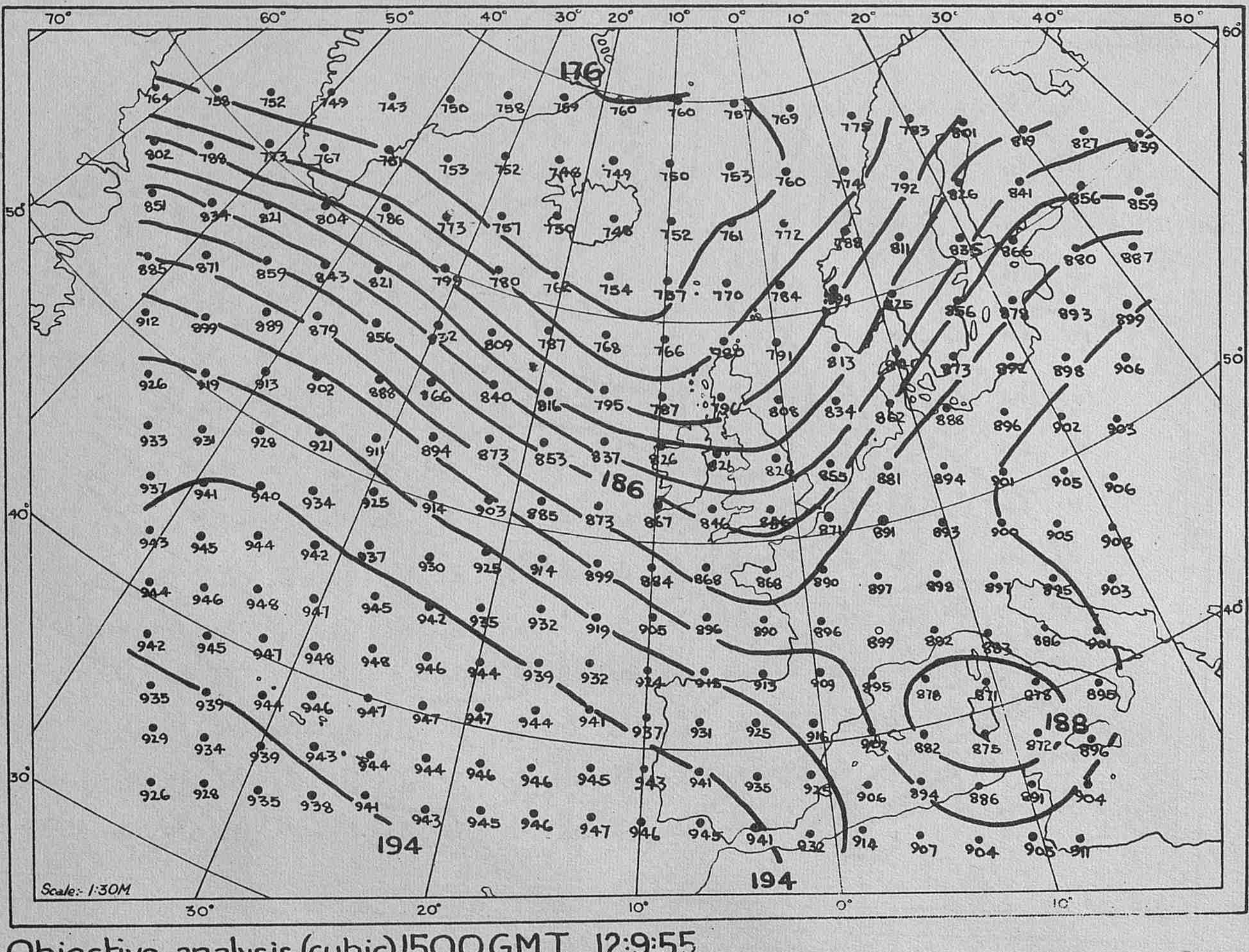
176
186
188
194
194
Scale:- 1:30M
70°
60°
50°
40°
30°
20°
10°
0°
10°
20°
30°
40°
50°

Objective analysis (cubic) 1500 G.M.T. 12:9:55

$p = P_2 \quad q = \frac{1}{16} P_2 \quad T^2 = 16\,\text{sec}^2$

Fig. 2 (h)

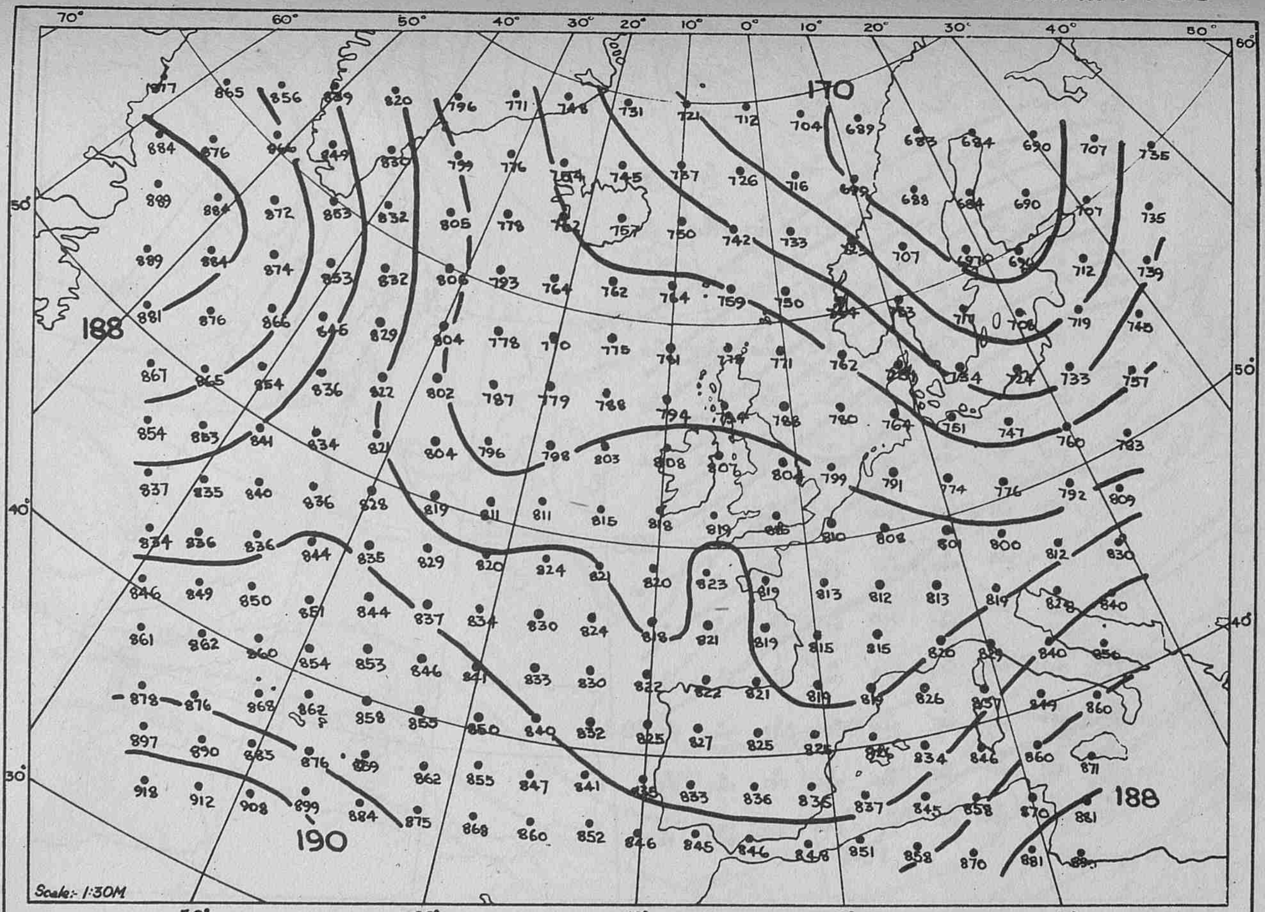
170
188
190
188
70°
60°
50°
40°
30°
20°
10°
0°
10°
20°
30°
40°
50°
60°
50°
40°
30°
Scale:- 1:30M

Objective analysis (quadratic) 1500 G.M.T. 31:10:55

$p = p_2$ $q = \frac{1}{16} p_2$ $T^2 = 2 \sec^2$ (Europe) $T^2 = 16 \sec^2$ (Atlantic)

Fig. 4 (c)

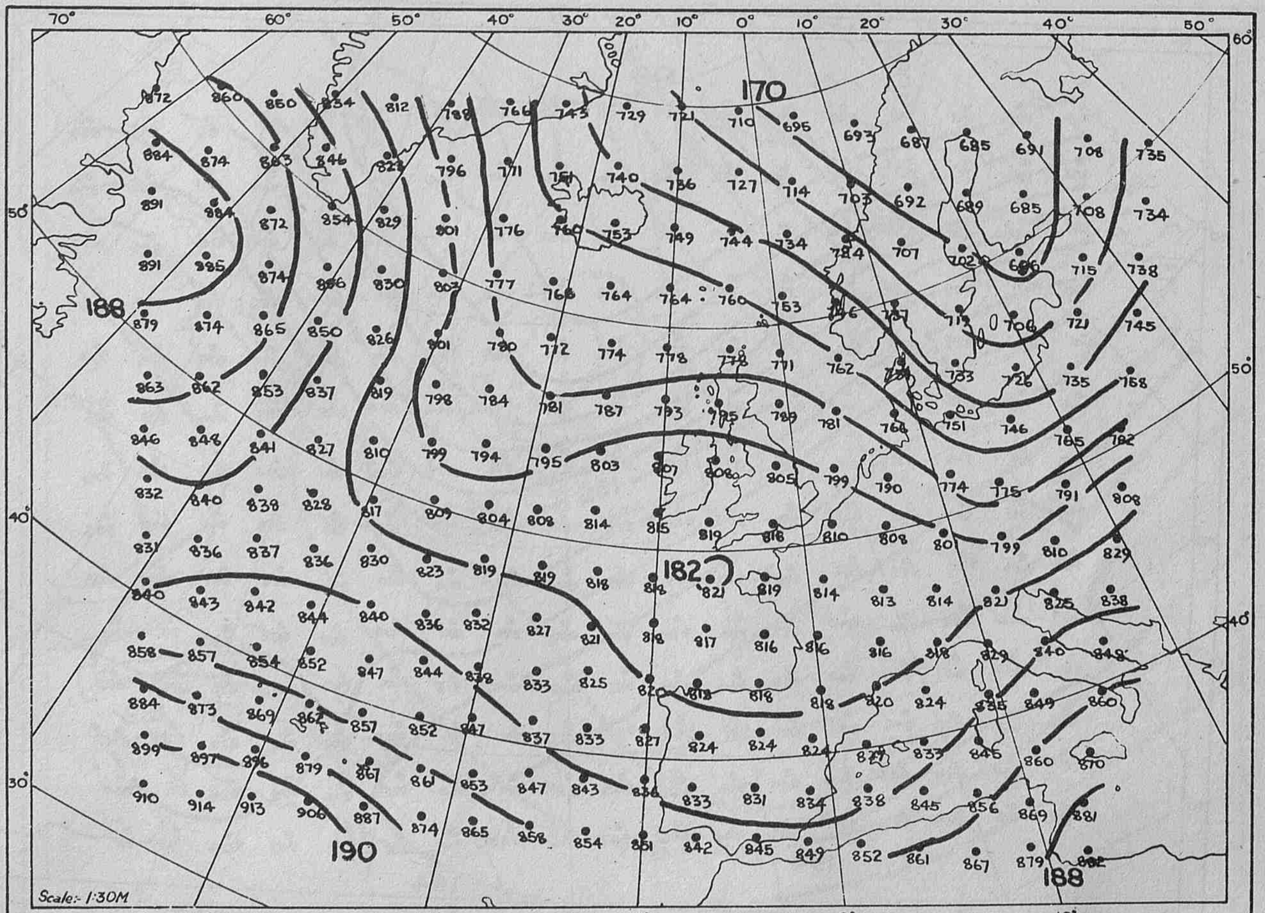
170
188
182
190
188
70°
60°
50°
40°
30°
20°
10°
0°
10°
20°
30°
40°
50°
60°
50°
40°
30°
Scale:- 1:30M

Objective analysis (cubic) 1500 G.M.T. 31:10:55

$p = p_2$ $q = \frac{1}{16} p_2$ $T^2 = 16 \sec^2$

Fig. 4 (d)

AD 139536

M.R.P. 987
S.C.11/213
22nd June, 1956.

AD 139536

Equivalent head-wind statistics for variable tracks.

by

P. Graystone.

(Meteorological Office)

AIR MINISTRY

METEOROLOGICAL RESEARCH COMMITTEE

At the time of issue this report has not been published. Any author desiring to quote this paper should refer to it as "A paper of the Meteorological Research Committee (London),
M.R.P. No. 987 by Mr. P. Graystone
A copy is available in the Library of the Meteorological Office."

M.R.P. 987
S.C.II/213
22nd June, 1956

AIR MINISTRY

METEOROLOGICAL RESEARCH COMMITTEE

Equivalent head-wind statistics for variable tracks

by
P. Graystone (Meteorological Office)

Summary

The frequency distribution of equivalent head-winds over an air route may be computed by statistical methods, using certain assumptions, from mean upper wind charts. For any given air route, however, economy of fuel may be achieved by flying the most favourable, from a wind point of view, of several fixed tracks. The statistical technique is extended to illustrate how the resulting frequency distribution of equivalent head-winds may be computed, and the relative merits of the different tracks assessed. Illustrations are given for the London-New York route, using two or three alternative tracks.

Introduction

The theory of equivalent head-winds has been outlined by Sawyer[1] and Crossley[2]. On the premise that seasonal upper winds at a point possess a normal, circular distribution, and that the form of correlation of wind with distance is known, they have shown that the frequency distribution of route equivalent head-winds can readily be computed from charts of mean vector wind and standard vector deviation.

Over long-distance routes, a considerable time-saving may be effected by flying the minimal flight path. For operational and other reasons, however, this is generally impracticable and a compromise method is to fly the most favourable of several fixed tracks. For planning purposes, the resulting frequency distribution of flight durations requires lengthy tabulations. For instance, an aircraft operator planning a new route has to make a detailed analysis of upper-air contour charts over the route in question over a period, preferably, of several years.

A statistical method is given below, enabling a fairly rapid computation to be made of the frequency distribution of equivalent head-winds, using the variable track technique. Though the theory is applicable to any number of tracks, it is too cumbersome to apply when more than three are considered. The basic assumptions made are largely the same as those which are at present used in computing equivalent head-wind statistics for single tracks and which have proved sufficiently accurate in practice.

Correlation of route winds

Durst[3] has found that the correlation of point winds with distance is largely independent of height, but varies to some extent with latitude and direction. In this paper, the form of correlation with distance is assumed constant, and the values used are applicable to temperate latitudes. Statistics of wind over single tracks computed in the Meteorological Office likewise assume constant correlation, but use separate curves for temperate and tropical regions.

The correlation of mean equivalent head-winds over two different routes can now be derived as follows:-

Consider two parallel routes (Fig. 1) each of length S, and distance apart h. Let u(m) and v(n) be the departures of the equivalent head-winds from their long-period means at any points m and n, along the first and second routes respectively.

The departures, U and V, of the route mean equivalent head-winds from their long-period means are:

$$U = \frac{1}{S}\int_0^S u(m)\,dm \; ; \qquad V = \frac{1}{S}\int_0^S v(n)\,dn \qquad \ldots\ldots (1)$$

Let σ_T be the standard deviation of the route equivalent head-winds (for simplicity assumed the same for both routes).

Following Sawyer, we take σ^2, the variance of the point equivalent head-winds, to be constant, and equal to its mean value for the route. Sawyer has shown that:

$$\sigma_T^2 = \frac{2\sigma^2}{S^2}\int_0^S\int_0^s R(t)\,dt\,ds \qquad \ldots\ldots (2)$$

where R(t) is the correlation coefficient between winds at points distant t apart.

We require the correlation coefficient ρ between the mean winds on the two routes:

Now
$$\rho = \frac{\overline{UV}}{\sigma_T^2} \qquad \ldots\ldots (3)$$

and from (1).
$$UV = \frac{1}{S^2}\int_0^S\int_0^S u(m)\,v(n)\,dm\,dn$$

Hence, from (2) and (3)
$$\rho = \frac{\int_0^S\int_0^S \overline{u(m)\,v(n)}\,dm\,dn}{2\sigma^2\int_0^S\int_0^s R(t)\,dt\,ds}$$

But
$$\overline{u(m)\,v(n)} = \sigma^2 R(p)$$

where
$p^2 = h^2 + (m-n)^2$ as shown in fig. 1.

Hence
$$\rho = \frac{\int_0^S\int_0^S R(p)\,dm\,dn}{2\int_0^S\int_0^s R(t)\,dt\,ds} \qquad \ldots\ldots (4)$$

Integrating,
$$\int\left[\int_0^t R(t)\,dt\right]dt = t\int_0^t R(t)\,dt - \int t\,R(t)\,dt$$

whence
$$\int_0^S\int_0^s R(t)\,dt\,ds = \int_0^S (S-t)\,R(t)\,dt$$

Also it is easily seen that

$$\int_0^S \int_0^S R(p)\, dm\, dn = 2\int_0^S (S-t)\, R(p)\, dt$$

where, now, $p^2 = h^2 + t^2$

Equation (4) therefore reduces to

$$\rho = \frac{\int_0^S (S-t)\, R(p)\, dt}{\int_0^S (S-t)\, R(t)\, dt}$$

where ρ is the correlation coefficient between the mean equivalent head-winds over two parallel routes, length S, separation h; R(t) is the correlation coefficient between winds at points distant t apart, and $p^2 = h^2 + t^2$.

Variation of route wind correlation

From the observed form of variation of R(t) with distance, it is clear that ρ will increase with S, becoming almost constant for route lengths greater than about 1,500 miles. An exponential decrease of point wind correlation with distance is probably the best assumption that can at present be made, and the curve of best fit to those given by Durst is

$$R(t) = \exp(-0.2\, t)$$

in temperate latitudes, where t is measured in hundreds of nautical miles.

The integral

$$\int_0^S \exp\left(-0.2\sqrt{h^2+t^2}\right) dt$$

has been tabulated for different values of h and S, and the following are corresponding values of ρ.

Table 1. Correlation coefficients between mean equivalent head-winds over two parallel routes, length S, separation h

	Values of h (nautical miles)			
S(n.m.)	200	400	600	800
0	0.67	0.45	0.30	0.20
500	0.80	0.56	0.38	0.26
1000	0.83	0.61	0.43	0.30
2000	0.85	0.64	0.47	0.34
3000	0.86	0.66	0.49	0.36
4000	0.87	0.67	0.50	0.36

In the practical case, the mean distance apart of two non-parallel routes is used to obtain an approximation to ρ, the route lengths being approximately equal.

Wind distribution for two tracks

Let x and y be equivalent head-winds on the shorter and longer of two fixed tracks respectively, means $\bar{x}$, $\bar{y}$ and standard deviations σ_1, σ_2. Let a be the value by which the equivalent head-wind on the shorter route must exceed that on the longer for the flight durations to be equal, i.e. the longer route is flown only if $y < x - a$. a is a function of the route-lengths, aircraft's still air speed and wind velocity. Provided the aircraft's speed greatly exceeds that of the wind, the variation in a will be small. In the examples below, a has been taken as constant, though its exact value could be used if required.

We want the distribution of r, where r is the lesser of the two winds x and y + a, and is a 'compensated' equivalent head-wind, referring always to the shorter route length, whichever track is flown.

r will lie between r and r + dr if either

A) $r < x < r + dr$ and $r - a < y$

or B) $r - a < y < r - a + dr$ and $r < x$

i.e. P (r lies between r and r + dr) = P(A) + P(B)
where P denotes probability.

The bivariate normal frequency distribution of x, y, as given in most text-books is:

$$\phi(x,y) = \frac{1}{2\pi\sigma_1\sigma_2\sqrt{1-\rho^2}} \exp\left[-\frac{1}{2(1-\rho^2)}\left(\frac{(x-\bar{x})^2}{\sigma_1^2} + \frac{(y-\bar{y})^2}{\sigma_2^2} - 2\rho\frac{(x-\bar{x})(y-\bar{y})}{\sigma_1\sigma_2}\right)\right]$$

and

$$P(A) = dr\int_{r-a}^{\infty}\phi(r,y)\,dy$$

$$P(B) = dr\int_{r}^{\infty}\phi(x,r-a)\,dx$$

Simplifying

$$P(A) = \frac{1}{\pi\sigma_1\sqrt{2}}\exp\left(-\frac{(r-\bar{x})^2}{2\sigma_1^2}\right)dr\int_{q_1}^{\infty}\exp(-z^2)\,dz$$

and

$$P(B) = \frac{1}{\pi\sigma_2\sqrt{2}}\exp\left(-\frac{(r-a-\bar{y})^2}{2\sigma_2^2}\right)dr\int_{q_2}^{\infty}\exp(-z^2)\,dz$$

where

$$q_1 = \frac{1}{\sqrt{2}\sqrt{1-\rho^2}}\left(\frac{r-a-\bar{y}}{\sigma_2} - \frac{\rho(r-\bar{x})}{\sigma_1}\right)$$

$$q_2 = \frac{1}{\sqrt{2}\sqrt{1-\rho^2}}\left(\frac{r-\bar{x}}{\sigma_1} - \frac{\rho(r-a-\bar{y})}{\sigma_2}\right)$$

The distribution may be computed by evaluating P(A) and P(B) for, say, 5-knot intervals, using tabulations of the normal error function.

London- New York route - two tracks

The distribution has been computed for the London - New York route using the following two tracks: (Fig. 2)

1. London - Fastnet - Torbay - New York (3008 nautical miles)

2. London - Malin - Goose Bay - New York (3055 nautical miles).

The great circle track was used for each leg.

For the winter season, Dec.-Feb. at 300 mb., the following values were computed from charts of mean vector wind and standard vector deviation:

$$\bar{x} = 58 \text{ kt.}, \ \sigma_1 = 18.1; \ \bar{y} = 45, \ \sigma_2 = 17.4$$

Also a = 4 kt. approximately, and for h = 300 n.m., $\rho = 0.76$, from Table 1.

Table 2 gives the computed values of P(A) + P(B) for different values of r.

Table 2

r (kt.)	P(A) + P(B)	r	P(A) + P(B)	r	P(A) + P(B)
0	.00051 dr	35	.01798	70	.00969
5	.00109	40	.02134	75	.00628
10	.00215	45	.02320	80	.00375
15	.00386	50	.02320	85	.00202
20	.00648	55	.02121	90	.00101
25	.00989	60	.01782	95	.00046
30	.01392	65	.01375	100	.00019

Table 3 shows the percentage frequencies with which equivalent head-winds will be exceeded in winter at 300 mb. (a) on the shorter route only, (b) on the alternative route only, (c) using the most favourable of the two. 'Compensated' values are given in (b) and (c), so that all the winds refer to a route length of 3008 nautical miles.

Table 3

	a	b	c
100 kt.	1%	0.2%	0%
90	4	0.9	0.5
80	11	4	3
70	25	11	9
60	46	26	23
50	67	48	44
40	84	70	67
30	94	86	85
20	98	95	95
10	99.5	99	99
0	100	100	100

The frequency with which each route is the more favourable is obtained by summing the values of P(A) and P(B) separately. In this case, the alternative route is preferable on 77%, and the shorter route on 23% of occasions.

/Extension

Extension to three routes

Let x, y, z be equivalent head-winds on three tracks, means $\bar{x}$, $\bar{y}$, $\bar{z}$ and standard deviations $\sigma_1\ \sigma_2\ \sigma_3$. $\rho_{12}\ \rho_{13}\ \rho_{23}$ are the total correlations between the mean equivalent head-winds on the three routes. Then the normal trivariate distribution of x, y, z as given in standard text-books (see e.g. Aitken[4]) is

$$\phi(x,y,z) = \frac{1}{(2\pi)^{3/2}\Delta^{1/2}\sigma_1\sigma_2\sigma_3}\exp\left[-\frac{Q}{2\Delta}\right]$$

where $\Delta = 1 + 2\rho_{12}\rho_{13}\rho_{23} - \rho_{12}^2 - \rho_{13}^2 - \rho_{23}^2$

and
$$Q = \frac{(x-\bar{x})^2}{\sigma_1^2}(1-\rho_{23}^2) + \frac{(y-\bar{y})^2}{\sigma_2^2}(1-\rho_{13}^2) + \frac{(z-\bar{z})^2}{\sigma_3^2}(1-\rho_{12}^2)$$
$$- \frac{2(\rho_{12}-\rho_{13}\rho_{23})(x-\bar{x})(y-\bar{y})}{\sigma_1\sigma_2} - \frac{2(\rho_{13}-\rho_{12}\rho_{23})(x-\bar{x})(z-\bar{z})}{\sigma_1\sigma_3}$$
$$- \frac{2(\rho_{23}-\rho_{12}\rho_{13})(y-\bar{y})(z-\bar{z})}{\sigma_2\sigma_3}$$

Let b and c be the reduction in equivalent head-wind necessary on the second and third routes to compensate for their additional length. Then r will lie in the range (r, r + dr) if any of the following applies:

A) $r < x < r + dr$ and $r - a < y,\ r - b < z$
B) $r - a < y < r - a + dr$ and $r < x,\ r - b < z$
C) $r - b < z < r - b + dr$ and $r < x,\ r - a < y$

Then $P(A) = dr\int_{r-b}^{\infty}\int_{r-a}^{\infty}\phi(r,y,z)\,dy\,dz$

$P(B) = dr\int_{r-b}^{\infty}\int_{r}^{\infty}\phi(x,r-a,z)\,dx\,dz$

$P(C) = dr\int_{r-a}^{\infty}\int_{r}^{\infty}\phi(x,y,r-b)\,dx\,dy$

Simplifying,

$$P(A) = \frac{dr}{\sigma_1\sqrt{2\pi}}\exp\left[-\frac{(r-\bar{x})^2}{2\sigma_1^2}\right]\int_{q_1}^{\infty}\int_{q_2}^{\infty}f(y,z,R_1)\,dy\,dz$$

$$P(B) = \frac{dr}{\sigma_2\sqrt{2\pi}}\exp\left[-\frac{(r-a-\bar{y})^2}{2\sigma_2^2}\right]\int_{q_3}^{\infty}\int_{q_4}^{\infty}f(x,z,R_2)\,dx\,dz$$

$$P(C) = \frac{dr}{\sigma_3\sqrt{2\pi}}\exp\left[-\frac{(r-b-\bar{z})^2}{2\sigma_3^2}\right]\int_{q_5}^{\infty}\int_{q_6}^{\infty}f(x,y,R_3)\,dx\,dy$$

where $$f(x, y, R) = \frac{1}{2\pi\sqrt{1-R^2}} \exp\left[-\frac{1}{2(1-R^2)}\left(x^2+y^2-2Rxy\right)\right],$$

$$R_1 = \frac{\rho_{23}-\rho_{12}\rho_{13}}{\sqrt{(1-\rho_{12}^2)(1-\rho_{13}^2)}}, \quad R_2 = \frac{\rho_{13}-\rho_{12}\rho_{23}}{\sqrt{(1-\rho_{12}^2)(1-\rho_{23}^2)}}, \quad R_3 = \frac{\rho_{12}-\rho_{13}\rho_{23}}{\sqrt{(1-\rho_{13}^2)(1-\rho_{23}^2)}}$$

and the limits of integration q are as follows:

$$q_1 = (1-\rho_{13}^2)^{-\frac{1}{2}}\left(\frac{r-b-\bar{z}}{\sigma_3} - \rho_{13}\frac{r-\bar{x}}{\sigma_1}\right); \quad q_2 = (1-\rho_{12}^2)^{-\frac{1}{2}}\left(\frac{r-a-\bar{y}}{\sigma_2} - \rho_{12}\frac{r-\bar{x}}{\sigma_1}\right)$$

$$q_3 = (1-\rho_{23}^2)^{-\frac{1}{2}}\left(\frac{r-b-\bar{z}}{\sigma_3} - \rho_{23}\frac{r-a-\bar{y}}{\sigma_2}\right); \quad q_4 = (1-\rho_{12}^2)^{-\frac{1}{2}}\left(\frac{r-\bar{x}}{\sigma_1} - \rho_{12}\frac{r-a-\bar{y}}{\sigma_2}\right)$$

$$q_5 = (1-\rho_{23}^2)^{-\frac{1}{2}}\left(\frac{r-a-\bar{y}}{\sigma_2} - \rho_{23}\frac{r-b-\bar{z}}{\sigma_3}\right); \quad q_6 = (1-\rho_{13}^2)^{-\frac{1}{2}}\left(\frac{r-\bar{x}}{\sigma_1} - \rho_{13}\frac{r-b-\bar{z}}{\sigma_3}\right)$$

Integrals of the bivariate normal distribution $\int_y^\infty \int_x^\infty f(x, y, R)\, dxdy$ have been tabulated by Pearson[5] for values of R at intervals of .05, and hence the probability that r lies in the range (r, r+dr), which equals P(A)+P(B)+P(C), can be computed for appropriate values of r.

London - New York route

The distribution of r has been computed for October at 300 mb. on the London - New York route, using the two previous tracks, and one further north. The three tracks are: (Fig. 2)

1. London - Fastnet - Torbay - New York (3008 nautical miles)
2. London - Malin - Goose Bay - New York (3055 nautical miles)
3. London - Prestwick - 60½ N 50 W - New York (3198 nautical miles).

As before, great circle routes are used on each individual leg. From seasonal charts

$$\bar{x} = 44, \quad \sigma_1 = 17.3; \quad \bar{y} = 35, \quad \sigma_2 = 17.2; \quad \bar{z} = 29, \quad \sigma_3 = 15.9$$

these corresponding to routes 1, 2, and 3 respectively.

Taking the separation 1 to 2 as 300 n.m., 2 to 3 as 150 and 1 to 3 as 450,

$$\rho_{12} = 0.76, \quad \rho_{23} = 0.87, \quad \rho_{13} = 0.60.$$

For ease in computation these values have been very slightly adjusted, and give $R_1 = +0.80$, $R_2 = -0.20$, $R_3 = +0.60$. Also the winds to compensate for the additional route lengths are

$$a = 4 \text{ kt.}, \qquad b = 16 \text{ kt.}$$

Table 4 gives computed values of P(A) + P(B) + P(C) for different values of r.

/Table 4

Table 4

r (kt.)	P(A)+P(B)+P(C)	r	P(A)+P(B)+P(C)	r	P(A)+P(B)+P(C)	r	P(A)+P(B)+P(C)
-20	.00008 dr	10	.00715	40	.02388	70	.00242
-15	.00021	15	.01101	45	.02095	75	.00116
-10	.00052	20	.01549	50	.01667	80	.00050
-5	.00115	25	.01987	55	.01197	85	.00019
0	.00230	30	.02320	60	.00784	90	.00007
5	.00425	35	.02468	65	.00459	95	.00002

Table 5 gives the percentage frequencies with which winds at 300 mb. in October would be exceeded on tracks 1, 2 and 3 alone, and on the most favourable of the three, all winds referring to a route length of 3008 n.m.

Table 5

r (kt.)	Track 1	Track 2	Track 3	Most favourable
100	0.1%	0%	0%	0%
90	0.4	0.2	0.2	0
80	2	1	1	0.2
70	7	4	6	1.5
60	18	11	17	6
50	36	26	38	18
40	59	48	62	39
30	79	70	83	63
20	92	87	94	83
10	98	95	99	94
0	99.5	99	99.8	98
-10	99.9	99.8	100	99.7
-20	100	100	100	100

When the most favourable route is chosen, track 1 would be flown on 31% of occasions, track 2 on 50%, and track 3 on 19%.

Conclusion

Using assumptions similar to those at present made in computing statistics of equivalent head-wind over single tracks, the corresponding frequency distribution when the most favourable of two or three tracks is flown may be obtained. The examples illustrate the order of magnitude of reduction in head-wind that may be achieved. For three routes whose mean compensated equivalent head-wind is similar, the reduction is considerable, especially at the higher velocities. The variable track technique requires, of course, accurate wind prediction; errors in the latter have not been considered in this paper.

References

1. Sawyer, J.S. - Application of upper-wind statistics to air route planning - M.O. 535a, 1950.
2. Crossley, A.F. - Equivalent head-winds on air routes - J.Inst.Nav., 2, 1949, pp. 195-207.
3. Durst, C.S. - Variation of wind with time and distance - G.M. No. 93 - 1954.
4. Aitken, A.C. - Statistical Mathematics - Oliver & Boyd, 1947.
5. Pearson, K. - Tables for Statisticians and Biometricians, Part II - 1931.

M.R.P. 987

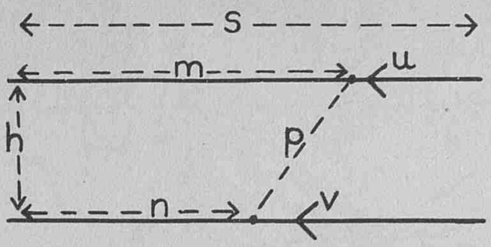

Figure 1.

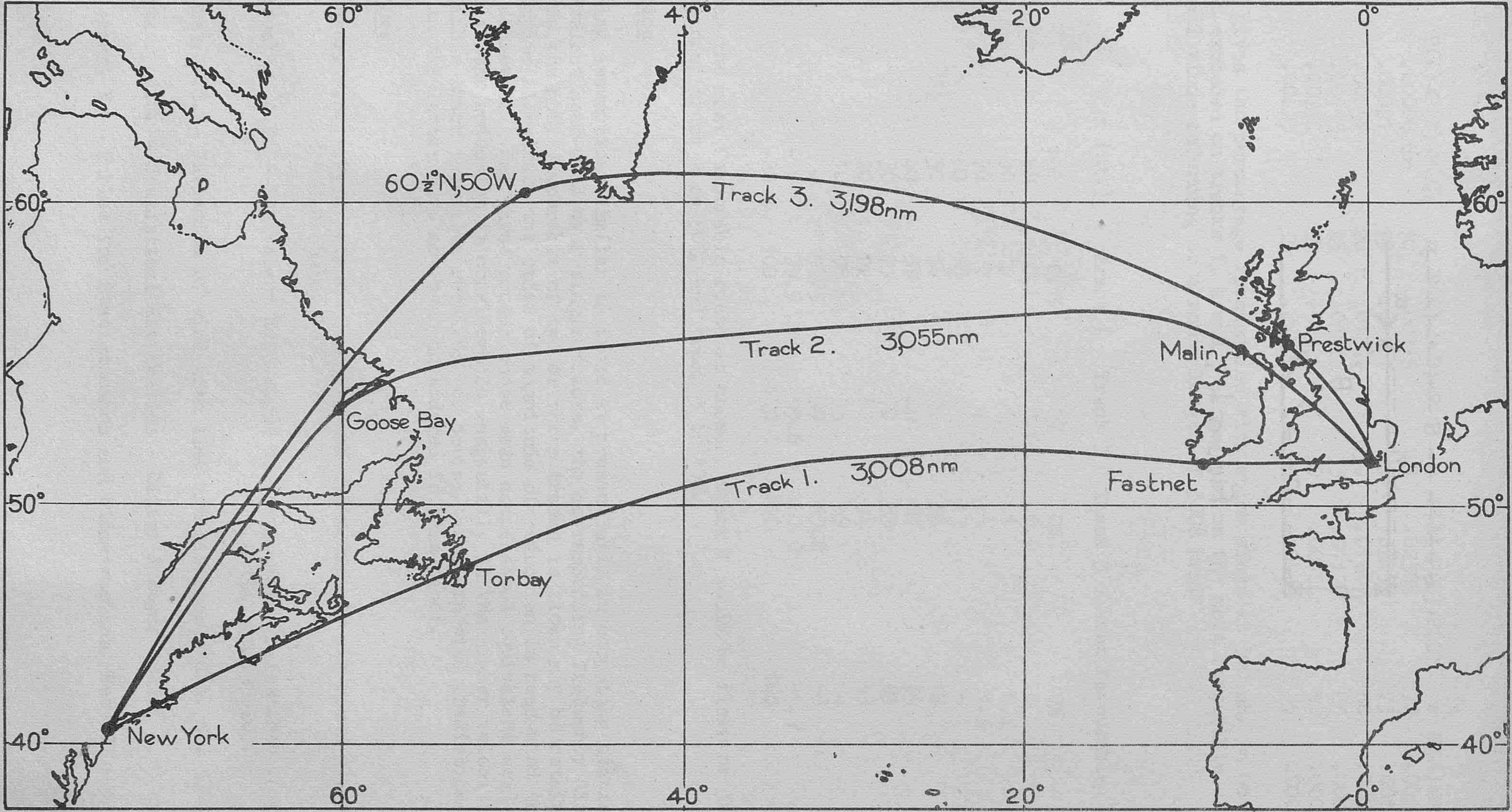
60°
40°
20°
0°
60°
50°
40°
60½°N,50°W
Track 3. 3,198nm
Track 2. 3,055nm
Track 1. 3,008nm
Prestwick
Malin
Fastnet
London
Goose Bay
Torbay
New York

Figure 2.

M.R.P. 988
S.C. I/116
1st June, 1956.

AD147513

On the development of an improved daylight illumination recorder.

by

M. J. Blackwell and D. B. B. Powell.

(Meteorological Office)

AIR MINISTRY

METEOROLOGICAL RESEARCH COMMITTEE

At the time of issue this report has not been published. Any author desiring to quote this paper should refer to it as "A paper of the Meteorological Research Committee (London)
M.R.P. No. 988 by Messrs. M.J. Blackwell and D.B.B. Powell.
A copy is available in the Library of the Meteorological Office"

M.R.P. 988
S.C.I/116
1st June, 1956

AIR MINISTRY

METEOROLOGICAL RESEARCH COMMITTEE

On the development of an improved daylight illumination recorder

by

M.J. Blackwell and D.B.B. Powell (Meteorological Office)

Summary

The imperfections of the present daylight recorder, in use at Kew Observatory and Victory House, are briefly reviewed and a critical analysis is made of existing calibration techniques.

The development of the improved instrument is shown to follow logically from considerations of ease of maintenance and calibration, and from the requirement that its indicated readings should not need to be adjusted retrospectively.

Some evidence as to the accuracy of the Kew daylight measurements is discussed. Finally, the first available comparisons of readings from the two instruments are given for various meteorological conditions.

1. Introduction

It may be convenient first to restate the problem. The quantity to be measured is the brightness of daylight in the ordinary sense of the words - that is, as perceived by the human eye. The sensitivity of the eye varies greatly with the wave-length of the incident light, so that any instrument used to measure illumination must have a response which varies in the same way. This can be achieved by using a photo-electric cell in combination with a suitable optical filter. In the Kew instrument the daylight is first received on a horizontal disc of translucent material, and the filter-photocell combination is exposed only to the light from under the surface of this disc. The instrument is not an absolute one, but must be calibrated by exposing it to a known artificial illumination.

In a previous report by Blackwell (1953), an attempt was made to eliminate the systematic errors inherent in measurements made with this instrument, by computing the necessary corrections and applying them retrospectively to the tabulations.

During the development of the improved instrument described below, a further source of systematic error became apparent. This error, which is considered in section 3(b), arises during calibration from the fact that the opal glass or plastic discs used do not act as perfectly diffusing layers. The existence of some such error was foreshadowed in a report by Blackwell, Eldridge and Robinson (1954) in which the mutual consistency of radiation and illumination measurements at Kew Observatory was examined. Estimates of this error, derived experimentally and deduced analytically, will be shown to be in fair agreement.

The final results obtained with the present (Mark II) recorder, corrected for all known systematic errors, will be compared with those from the improved (Mark III) instrument for various meteorological conditions.

/2.

2. Imperfections of the Mark II instrument

(a) Temperature coefficient of the photocell and filter

This was determined accurately, as described by Blackwell (1953), and found to be - 0.3% per 1°C. at normal ambient temperatures.

(b) Cosine law response of receiver

The largest single source of error results from the markedly imperfect cosine law response of the receiving unit (diffusing plate + protecting hemispherical glass dome). The overall response was therefore redetermined, using a lamp at about two metres distance and measuring the photocell output with a precision potentiometer and galvanometer of high sensitivity. The final curve was indistinguishable from that given by Blackwell (1953).

It is of interest to note here an essential difference between a blackened thermopile and a photometer of the present type, even though both have perfectly matt receiving surfaces (as viewed from above). The former has a cosine law response, whereas the latter shows a marked departure from such a law. Some insight into this difference may be gained by considering the analogous case of a thick stratified cloud. Mr. D.B. Lake, in an unpublished paper, has deduced theoretically that in such a case the total transmitted light, $T(\theta)$, depends on the angle of incidence, θ, of the light falling on the top of the cloud, in the following way:

$$T(\theta) \propto \cos\theta\,(1 + k\cos\theta)$$

where k is probably close to the value 2. Fig. 1 shows the experimentally determined response lying between the curves for $\cos\theta$ and $\cos\theta\,(1+2\cos\theta)$. One reason why the actual response is better than that predicted may be due to the fact that the diameter of the diffusing plate is of comparable size to that of the dome. Indeed, this is one method by which some degree of cosine-correction may be effected, since more of the light, falling on the disc, strikes the dome nearly perpendicularly at low elevations, than at higher elevations.

It is therefore necessary, with photometers of this type, to devise such means of cosine-correction as will raise the response curve to approximate coincidence with that of a perfect receiver (i.e. one obeying the cosine law).

(c) Spectral sensitivity

Allowance is made for the difference in colour-temperature of natural daylight (6000°K) and the calibrating lamps (2500°K) as described by Blackwell (1953). The spectral sensitivity data supplied by the N.P.L. are obtained from the transmission characteristics of the filter and the response of the photocell as determined by a monochromator. There is thus a small uncertainty due to the fact that the spectral response of the cells used may be slightly different for the higher values of illuminance when normally exposed from the response at the extremely low intensities obtained with a monochromator.* It is thought, however, that the error involved is small.

---

* An effect pointed out by Dr. J.S. Preston of the N.P.L.

---

3. Calibration errors

The instrumental response to light at any given angle is related to that for normal incidence by the empirically determined response of the receiver. The photometric measurements are therefore based on the routine calibrations which are carried out at normal incidence. The standard lamps used in the laboratory have remained unchanged within the limits of accuracy of the N.P.L. calibrations (± 2%). It is in the method of their use that a further source of error has become apparent (see section 3(b)).

The lamps produce an illumination which is known at points on the optical axis at distances considerably greater than the dimensions of the filament. Hitherto, a two-stage calibration technique has been used to overcome the difficulty of producing in the laboratory a known illumination comparable in intensity with natural daylight. A non-standard 100 watt lamp is first used to establish the variation of cell output with intensity, using the cell + filter unit alone and invoking the inverse-square law. In this way, the full working range (for the unit, when mounted in its normal position inside the recorder) is covered, up to effective intensities of about 200 kilolux (outside the recorder).

To minimise casual errors of calibration in the future, the corrections for non-linearity for each month have been embodied in a table based on a large number of such calibrations (Fig. 2). The percentage differences, between the values of cell sensitivity derived from the tangents at the origin and the best straight lines, drawn for the appropriate ranges of intensity for each month, lie between 0% and 3% as follows:

Table I - Non-linearity corrections

Month	J	F	M	A	M	J	J	A	S	O	N	D
Percentage	0	½	1	1¾	2½	3	2½	1¾	1	½	0	0

The stability of the class of cells used is such that the general form of the curves appears to remain unchanged while the sensitivity undergoes a smooth and gradual decrease. The use of Table I can therefore replace the first stage of the calibrations.

The second stage would ideally consist of producing a known high illumination on the complete assembled recorder, using a parallel light beam. It has been the practice to set up the standard lamp at about 25 cm. from the diffusing plate in order to produce an illumination of some 40 kilolux. The problem remained to deduce the instrumental factor (microamps per kilolux) from such an arrangement. Two aspects of the optical system must be considered: the illumination of the diffusing plate, and the transmission characteristics of the pot-opal glass, bearing in mind any effects which might be introduced by the use of a non-parallel light beam.

(a) Illumination of the diffusing plate

The intensity of illumination over the receiving area falls away from the central point toward the edges for the following reasons:

(i) because of the greater distances from the lamp to off-centre points on the opal disc

(ii) because of the cosine effect at the opal disc for off-axis rays

(iii) because of the polar diagram of the emitted light from the lamp.

In slight opposition to these factors is the effect of reflection at the glass dome, which is less for an off-axis ray (to a given point on the opal disc) than for a ray which is parallel to the optical axis.

The variation of illumination over the opal disc was previously determined (with some difficulty owing to lack of sufficiently sensitive apparatus) in the following manner. A probe, consisting of a photocell masked down to a 5 mm. square, was moved from side to side of the illuminated area immediately behind the diffusing plate. A difference of 2% was found between the illumination at the centre and at the edge of the effective area (defined by a diaphragm of 2in. diameter behind the diffusing surface). An allowance of 1% was made for the average effect.*

---

* Strictly, this should have been about 1½% after weighting the larger areas near the edge of the disc.

In the present investigation, this experiment was repeated by using the actual photocell in the recorder and moving a 4 mm. square aperture across the front surface of the opal disc (Fig. 3a) with the lamp at the normal calibration distance of 25 cm. The very small output from the photocell was amplified by a D.C. galvanometer-amplifier to give what we shall call "curve 1". This represents the combined effect of instrumental response plus the required variation of illumination on the opal disc. The instrumental response behind the diffusing surface is affected by:

(i) the polar diagram of the diffuse transmitted light

(ii) the varying distance from the parts of the opal disc to the photocell + filter unit

(iii) the cosine effect at the photocell for rays not at normal incidence.

Secondly, the 4 mm. aperture was again moved across the diffusing plate, but this time the lamp was given equal displacements in the same sense, so that the instrumental response alone was determined (Fig. 3b). The resulting response, "curve 2", was then subtracted algebraically from "curve 1" to give the same 2% variation previously found.

(b) Transmission characteristics of the pot-opal glass

During the development of the new instrument, it was decided to determine the instrumental factor by means of an extrapolation technique. This was done by plotting the uncorrected factor (in microamps per kilolux) against distance of the lamp, on the assumption that the illumination at the opal disc was uniform. By extrapolating to get the value at infinity (i.e. for a parallel beam of light), it was found, unexpectedly, that this value was considerably higher than the uncorrected value corresponding to a distance of 25 cm. (Fig. 4). The extrapolation method was therefore repeated with the old instrument and a difference (in the same sense) of about 7½% was found, instead of the 1½% expected.

Since this work was done, our attention has been drawn * to an earlier paper by Poole and Atkins (1935) in which they make the following comments:

> "With most cells, the agreement with the inverse square law is not so good, the results at 10 cm. being generally too small by some 5-10% compared with the values found at 40 or 50 cm., even when the calculated correction has been made for the sizes of the source and window. Several suggestions may be offered ..... If the diffusing power of the opal glass were inadequate it would not be correct to take the distance from the filament to the glass as the effective distance, but rather something greater, as the cell is behind the glass."

These authors did not, however, come to any definite conclusions on the matter.

---

* By Mr. H. Hack of the Glasshouse Crops Research Institute, Littlehampton.

The assumption that the opal glass acted as a perfect diffusing layer was therefore investigated. Reverting to the analogous case of a layer of dense cloud, we should expect a certain polar diagram (such as the zenith light being three times the light from the horizon), which would remain unchanged whatever the directive qualities of the light incident on the top of the cloud.

In order to test the transmission characteristics of the pot-opal glass, an experiment was devised (Fig. 5a) as follows. A $\frac{1}{2}$ in. square aperture was moved across the front surface of the opal glass between two alternative positions at opposite ends of a horizontal diameter of the circular plate. The lamp was placed at about $1\frac{1}{2}$ metres from the recorder which was mounted normal to the beam. In order to eliminate any errors caused by misalignment, the ratio of the photocell outputs was noted for the two positions of the aperture.

The recorder was then pivoted on a turn-table about a vertical axis until the diffusing plate was offset 15° from the normal position (Fig. 5b). The geometry of the experiment was such that no allowance was required for the polar diagram of the lamp, and only a negligible correction for the difference in reflection at the two positions. When allowance had been made for the cosine effect at the two positions and for the difference in distance from the lamp, the ratio previously noted above was found to have changed by about 2%; this can only be attributed to the spatial shift of the polar diagram of the transmitted light. The magnitude of the effect is not known with sufficient accuracy to apply a quantitative correction to the calibration results at 25 cm; it is only necessary to realise the source of error and to modify the experimental technique of future calibrations accordingly, i.e. by using the extrapolation method described earlier in this section.

One remaining geometrical factor should be mentioned as it may contribute to the difference between the instrumental factors at 25 cm. and at infinity. A glass sheet interposed between the lamp and the diffusing plate would cause an 8% reduction in intensity due to reflection losses. It was noticed that the hemispherical dome caused a reduction of only 2%. The pattern of inter-reflections, between the diffusing surface and the dome, which produces this effect might well be significantly modified by close proximity of the lamp.

4. Development of the Mark III recorder

The present prototype model overcomes the imperfections of the Mark II instrument insofar as it faithfully records the physical quantity to be investigated, without the need for a system of retrospective corrections. Attention has also been given to facility of maintenance, reduction in size and weight, simplification of construction and ease of calibration.

Owing to the excessive size of certain component parts, there is still room for further improvement of design but we are more concerned here with the physical performance of the instrument. As foreshadowed earlier (Blackwell 1953), the main modifications are concerned with elimination of temperature effects and cosine law imperfections.

(a) Temperature effects

To achieve the highly desirable result of an instrument registering directly in photometric units, it was decided not merely to arrange to record the working temperature of the photocell but to control this thermostatically at a single practicable value. The difficulty arises that this temperature must be higher than any value which might be reached under natural conditions, and yet be below the danger limit where destructive absorption of infra-red radiation by the selenium barrier-layer photocell becomes of importance.

Previously, the Mark II instrument had been sited on the main roof of Kew Observatory, which is covered with lead. On days of strong insolation, the working temperature of the cell rose as much as 30°F. above screen temperature, aided no doubt by the enhanced radiation for the roof. As reported by Blackwell (1954), the site of the horizontal surface instruments at Kew has now been transferred to a circular platform above the Observatory dome. One useful result of this, not considered at the time, is that the reflected radiation is much reduced and that the average temperature at this greater height is several degrees lower. A controlled temperature of 100°F. was therefore chosen to ensure efficient thermostatic operation, and this value is about 20°F. below the danger limit usually quoted in the literature.

To achieve this control of temperature, the cell and filter are mounted in an inner chamber which is sealed with a clear glass lid and retaining ring immediately above the filter (Fig. 6). The cylindrical chamber is heated by a glass-insulated coil of resistance wire, connected in series with a cartridge thermostat which is screwed into the cavity below the photocell mounting. The resistance element and thermostat are connected to the mains supply via a ballast lamp of suitable wattage which also acts as a visual monitor on the functioning of the thermostat.

During the initial testing period, a recording thermocouple was placed on the photocell mounting. Observations of the amplitude of the temperature cycles showed that this could be minimised by selecting ballast lamps of suitable wattage according to season. The extremes of working temperature recorded are 98°F. and 102°F. In setting up the instrument, the adjustable cartridge thermostat is fitted with an extension rod which can be rotated by means of a divided wheel, readily accessible below the instrument.

When a calibration has to be done in the laboratory (it is not intended that this should be done more than once a year in future), the instrument can be disconnected from the mains supply at the site and reconnected in the laboratory with little loss of time. The temperature does not change appreciably in this short interval and the calibration can be started immediately. At these occasional times when a check of the degree of non-linearity of the recorder is required, the inner chamber is mounted on the optical bench and the inverse square law can still be invoked in spite of the intervening clear glass cover. The temperature-controlled chamber is rigidly attached to the main base of the instrument through which pass the leads to the mains supply, the output leads from the photocell, and the thermocouple leads to potentiometer or recording galvanometer.

(b) Cosine law correcting-device

Many methods of obtaining improved responses (more in keeping with the cosine law) from receiving surfaces of photometers have been tried. The best results which can be achieved by the various methods are very similar. Among the more common of these devices may be mentioned:

(i) roughened upper surfaces of the diffusing material chosen

(ii) convex domes which are not hemispherical

(iii) roughened inner surfaces of hemispherical domes

(iv) setting the disc of diffusing material with its upper surface slightly above the level of the surrounding metal cover so that it receives some of the incident light on its edge.

Method (i), which was used in the Mark II recorder, is not sufficiently effective by itself (see section 2(b)), nor is method (ii). Methods (i) and (iii) require grinding or sand-blasting (techniques which must be carefully controlled if consistent results are to be obtained), and suffer from the drawback that the response characteristics change irreversibly if the surfaces get clogged with dirt or grease. Method (iv) has been tried successfully by Pleijel and Longmore (1952) in conjunction with method (i), but the instrument was intended as a non-weatherproof, portable probe for indoor determinations of daylight factors. It has also been tried alone by Foster (1951) with good results. Neither of these instruments has a protecting dome, the pot-opal receiving surface of the latter model having to be carefully sealed to prevent ingress of moisture. In addition, its bevelled housing allows light to be received from below the horizon.

After careful consideration of all known methods and their respective advantages, it was decided:

(i) to use the "edge-effect" compensating-device of method (iv)

(ii) to use a clear glass hemispherical dome, mounted above a circular diffusing disc of diameter comparable with that of the dome

(iii) to dispense with all roughened surfaces, whether of the diffusing material or of the dome.

By this choice of design details, the construction is simplified as much as possible, sealing of the instrument is made straightforward and the cleaning of component parts can be carried out without affecting the response characteristics. After some initial experiments with pot-opal glass discs, it was soon realised that closer tolerances could be obtained by machining diffusing opal plastic, which also has non-selective transmission over the visible range.

The total transmission through the opal plastic, being much higher than that of the pot-opal glass, enables most of the underneath surface to be masked out with a centrally placed opaque diaphragm. This, in turn, increases the correcting power of the edge-effect relative to the response of the polished flat receiving surface. The amount by which the plastic disc must finally be set up, above the level of the surrounding metal cover, is nevertheless fairly critical. A micrometer adjusting ring with a 1 mm. screw thread is used to support the diffusing plate. The ring has a circular scale, divided into fortieths of a revolution, which permits rapid adjustments of height to be made to one thousandth of an inch.

The glass dome protects the receiving surface; and the air space between them, though isolated from the rest of the instrumental cavity, is connected to two small tubes at either side (Fig. 6). These can be used in conjunction with a dry-air pump to remove condensation in a matter of seconds. The whole unit is mounted on the outer case of the recorder which protects the heating element round the inner chamber. The interspace does not have to be sealed from the outside atmosphere, but the air in the temperature-controlled chamber is connected to a drier-bulb containing silica-gel.

Initial tests on the cosine law characteristics of the light collector showed that, to obtain a gradually changing family of response curves, it was essential that the diffusing material be worked to a close running fit with the surrounding mounting. This requirement led to the use of a diffusing opal plastic (Perspex No. 040, made by Imperial Chemical Industries Ltd., was the eventual choice), which could be accurately turned to the correct size.

To show in detail how the present cosine-correcting device can produce an almost theoretically perfect response with polished opal perspex, two typical curves are plotted in Fig. 7a. The response at any given angle of elevation is expressed as a percentage of that for a perfect receiver. For comparison, the response curve of the Mark II recorder is also plotted, and shows the inadequacy of the method of roughening the upper surface of the diffusing material as a means of cosine correction.

It is not sufficient to choose the response characteristic which appears to be the best in Fig. 7a. We are concerned with the total luminous flux on a horizontal surface and must weight the instrumental response according to the contribution, to that total flux, of each zone of the sky. As a first step in this assessment, the curves are redrawn in Fig. 7b, which shows the calculated response of these different receiving surfaces in the ideal case of light coming from a uniformly illuminated hemisphere of sky. The response to the light from that part of the sky lying between zenith angles of θ and $\theta + d\theta$ will be proportional to $E_\theta . \sin \theta . \cos \theta . d\theta$, where E_θ is the efficiency of the receiving surface, i.e. the ratio of actual response to light from direction θ to the corresponding response of a perfect receiver. In Fig. 7b, the value of $E_\theta . \sin \theta . \cos \theta$ is plotted against θ for a perfect receiver ($E_\theta = 1$) and for both the Mark II and the finally selected Mark III instruments. It is at once evident how much closer the Mark III instrument is to the perfect receiver.

As reported by Blackwell (1953), the Mark II instrument registered only 89% of the natural diffuse sky light, and would have recorded 87% of the light from a uniform diffuse hemisphere. By means of the relatively simple correcting-device just described, the Mark III recorder is made to register 100% of the luminous flux from the same ideal hemisphere.

Fortunately, the selected response curve which gives this result is also one which departs but little from the true curve between angles of incidence from 0° to 80°. Beyond this point, contributions from the sky light are energetically of little importance, nor is the effect of the direct solar beam of great significance. At higher solar altitudes, when the direct component is dominant, the accuracy is of the order of ± 2%. To maintain this degree of accuracy, the levelling of the receiving surface must be periodically checked by reference to the circular spirit-level attached to the side of the outer case.

(c) Routine use and standardisation

The air space under the dome may require to be connected to a dry air pump at infrequent intervals in order to remove condensation. The silica-gel drier will need to be renewed every month or two, since excessive moisture will permanently affect the photocell sensitivity. The ballast lamp in the heating circuit should be noted as "on" or "off" at suitable intervals and a permanent record kept in order to check the functioning of the thermostat.

About once a year, it will be advisable to check the degree of non-linearity of the photocell response, as described in section 3. At other times, a portable sub-standard of essentially the same design will be set up alongside the continuously recording instrument and its output recorded on the same thread-recorder. The same portable instrument could also be used to standardise the daylight recorders at other stations.

Calibration of the portable sub-standard will be carried out in the laboratory, using standard lamps at about two metres from the receiving surface. It has been found that the uncorrected instrumental factors reach a steady value at this distance and that the photocell output is still large enough to be measured accurately with a precision potentiometer and galvanometer of high sensitivity. A typical curve, obtained by the extrapolation method, is given in Fig. 4.

5. Accuracy of the Kew standard of photometry

Blackwell (1953) estimated that the means of large numbers of observations quoted by Blackwell (1953) should be correct to within ± 5%. In a report by Blackwell, Eldridge and Robinson (1954), it was found that mutual consistency of the radiation and illumination measurements (made at Kew) could only be obtained on the assumption that the latter data were about 5% too high.

The radiation measurements consisted of total and diffuse radiation on a horizontal surface and the intensity of the direct solar beam for the whole spectrum and for two spectral regions. These, and measurements of the total illumination of a horizontal surface, were compared with the results to be expected from an extraterrestrial distribution of solar radiation proposed by Nicolet (1951a, 1951b) and the predicted attenuation by a model atmosphere. Similar estimates of the additional attenuation by the actual atmosphere were obtained by several methods, involving the use of different combinations of the available data. Anomalous results, however, occurred in the method involving the illumination record, and it was here that mutual consistency could only be regained by reducing the daylight measurements by 5%.

There is little external material with which to compare the Kew values, but those results found in cloudless conditions by Lopukhin (1953) at Tashkent (a locality probably less subject to smoke but more subject to dust haze than Kew) are some 5-10% less. The values of luminous efficiency of daylight computed by Blackwell (1953, 1954) are also somewhat higher than those usually seen in the literature.

It is of interest that this later work, described above in section 3(b), suggests that the previously quoted results should be reduced by about 6%. We therefore believe that the present standard of photometry (now embodied in the measurements made at Kew with the Mark III recorder) is a close approximation to the photometric standard as defined internationally.

6. Comparison of results from old and new instruments

It is not intended to make an exhaustive comparison of the performance of the two instruments, because the scheme of corrections applicable to readings of the Mark II instrument was intended only for means of large numbers of observations. In addition to this limitation, these corrections have been partially invalidated by subsequent changes in the local operating conditions, among which are:

(i) the repainting of the Observatory dome in a much brighter cream than before

(ii) the installation of central heating in the building

(iii) departures in the day to day climate from the averages on which the original corrections were based

(iv) the different sites of the two instruments.

The effect of item (i) is to increase the back-reflection from the dome onto the old instrument. It was previously estimated that this just about counter-balanced the loss due to obstruction. Now it may overcompensate by some 1-2% on sunny days, especially when there is little cloud. Item (iv) relates to the fact that the new recorder is mounted above the dome, receives no reflected light and, in addition, loses some 1-2% because of obstruction by the anemometer mast.

In item (ii), the presence of central heating in the laboratory tends to raise the calibration temperatures above those on which the old corrections were based, particularly in winter. Since the temperature coefficient of the photocell is negative, the present readings of the Mark II recorder will therefore be about 1-2% lower than previous readings in winter, the effect acting in opposition to the earlier ones.

Apart from these largely random errors, and those arising inevitably from item (iii), the Mark II data have been processed according to the scheme of corrections described by Blackwell (1953). In addition, allowance has now been made for the newly discovered lack of diffusing power of the opal glass, the values being reduced by 6% on this account. The Mark III data have not been processed in any way, since the calibrations of this instrument have always been based on the extrapolation method.

Comparisons were made of the records obtained under cloudless and overcast skies (selected by the same criteria as those described by Blackwell, 1953) during the period July - September, 1955. The results are shown in Fig. 8, and broadly confirm the predictions made above.

7. Conclusions

It may be helpful at this stage to bring together the essential points which have been raised in the foregoing discussion. The new photometer includes thermostatic control, to remove temperature effects; its receiving surface is cosine-corrected to an accuracy of ± 2%; other features of the design facilitate calibration and maintenance. Experience has shown that corrections for non-linearity can be embodied in a simple table, the contents of which require only infrequent laboratory checks, while routine calibrations can conveniently be carried out in situ against a portable sub-standard instrument.

With regard to the accuracy of the standard of photometry, it was discovered that the opal glass used in the Mark II instrument did not act as a perfectly diffusing material, and this effect was then shown qualitatively by a suitably devised experiment. The extrapolation technique of calibration shows that a difference of 6% is involved. To ensure continuity of the Kew daylight record, simultaneous operation of the two instruments was started which, though not an entirely rigorous check, does substantiate the difference of 6% found in the laboratory. Certain other external evidence, which has also been reviewed, had previously suggested the existence of a systematic error of this sign and order of magnitude.

The design of the new instrument had developed largely from physical considerations of how best to bring the standard of natural daylight recording into line with the better established field of solar radiation recording. As well as providing qualitative data of general use to workers in many applied fields - biophysicists, agriculturists, electricity supply engineers, architects, paint and textile manufacturers, etc., - we are now in a position to use quantitative knowledge of a well-defined spectral component of the solar radiation. This can provide important contributions to the study of atmospheric absorption and scattering and to the wider problem of the planetary albedo.

8. Acknowledgments

We wish to express our thanks to Dr. G. D. Robinson for his help and encouragement throughout this work. Thanks are also due to Mr. H. D. Henley, who constructed and reconstructed the instrument several times, and to Mr. H. Heath, who completed the comparisons given in section 6 after our departure from Kew.

References

Blackwell, M.J.	1953	Meteorological Research Papers, Air Ministry, London, No. 831.
Blackwell, M.J.	1954	Meteorological Research Papers, Air Ministry, London, No. 895.
Blackwell, M.J., Eldridge, R.H. and Robinson, G.D.	1954	Meteorological Research Papers, Air Ministry, London, No. 894.
Foster, N.B.	1951	Illum. Eng., Vol. 46, No. 2, p.59.
Lopukhin, E.A.	1953	Isvest. Akad. Nauk. U.S.S.R. Ser. Geophys., Vol. 5, p.469.
Nicolet, M.	1951a	Arch. Met. Geophys. Biokl., B. Vol. 3, p.209.
	1951b	Annales d' Astrophys., Vol. 14, No. 3, p.249.
Pleijel, G. and Longmore, J.	1952	J. Sci. Inst., Vol. 29, No. 5, p.137.
Poole, H.H. and Atkins, W.R.G.	1935	Phil. Trans., A. Vol. 235, p.18.

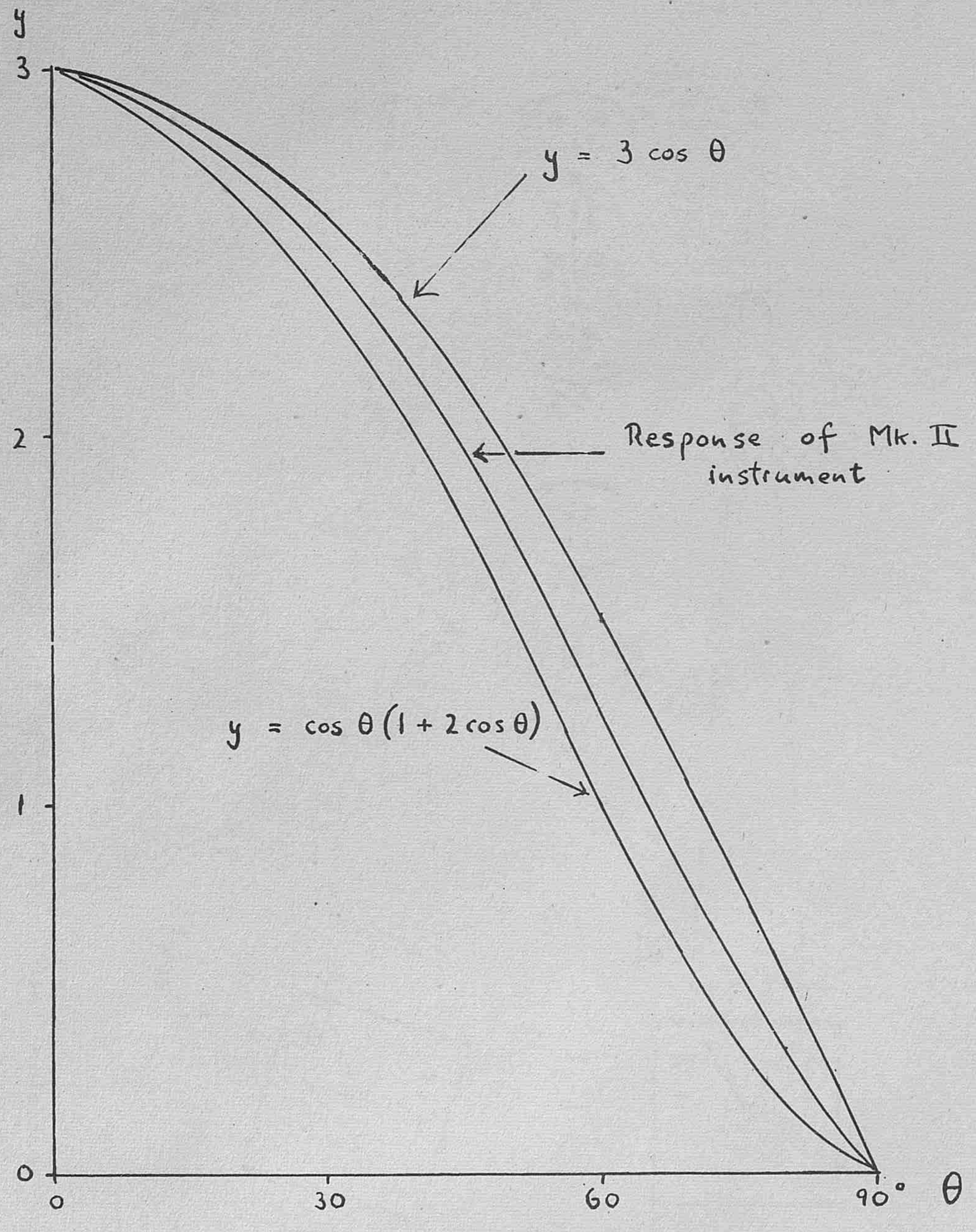

Fig. 1 - Response of Mk. II instrument.

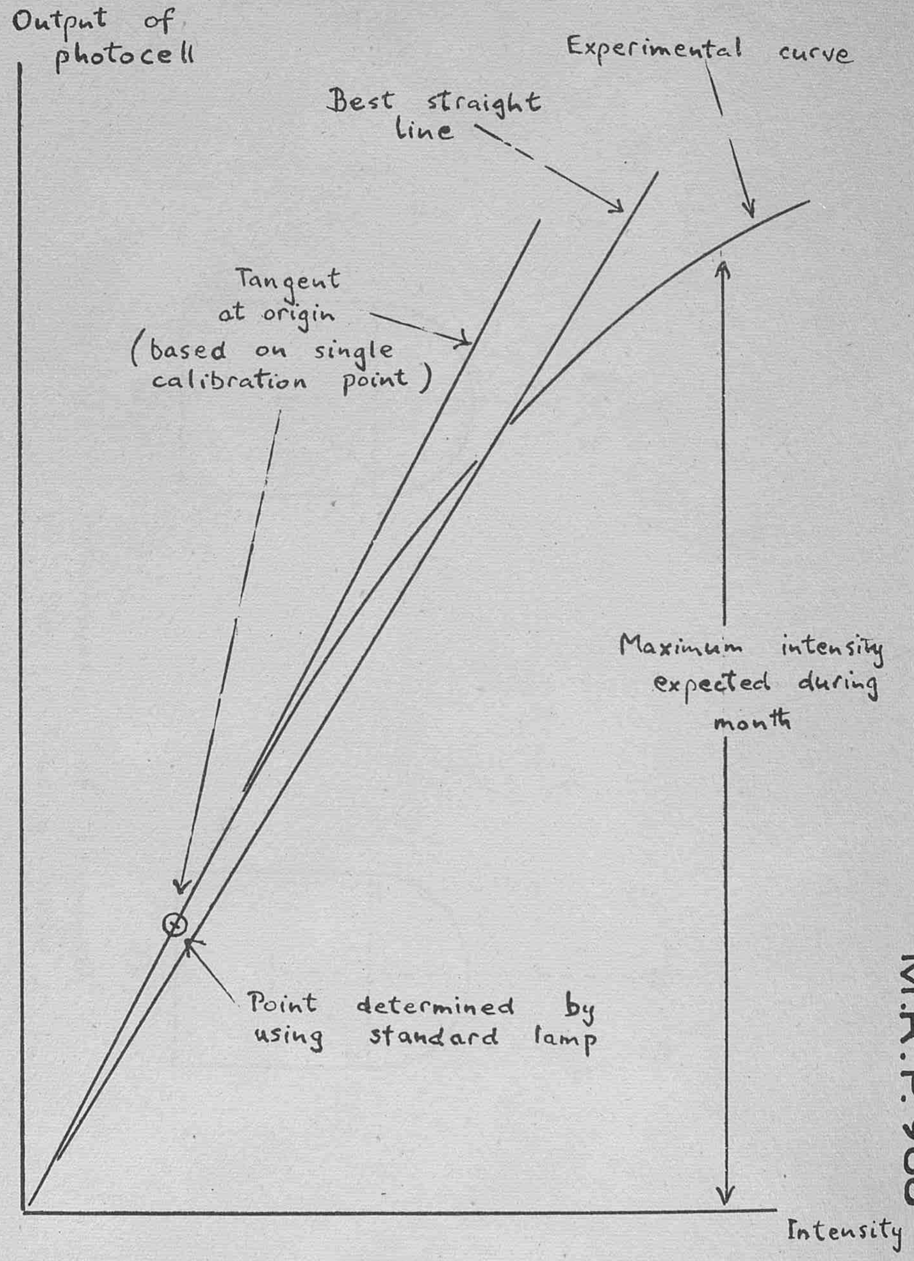
Output of photocell
Intensity
Experimental curve
Best straight line
Tangent at origin (based on single calibration point)
Maximum intensity expected during month
Point determined by using standard lamp

Fig. 2 - Correction for non-linearity.

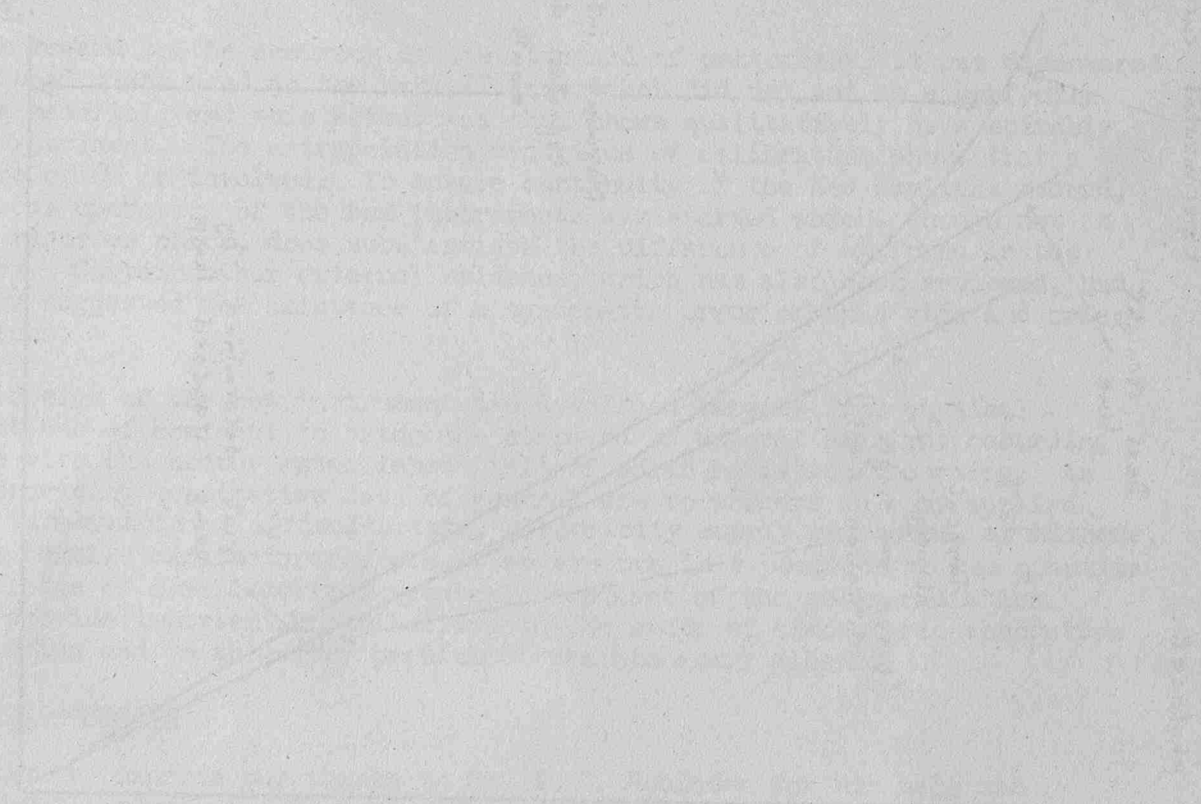

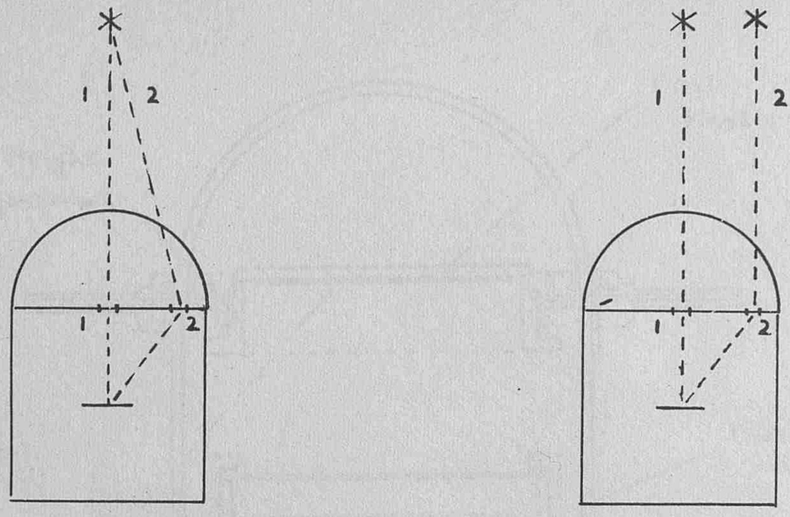

(a) (b)

Fig. 3 - Determination of illumination of the diffusing plate.

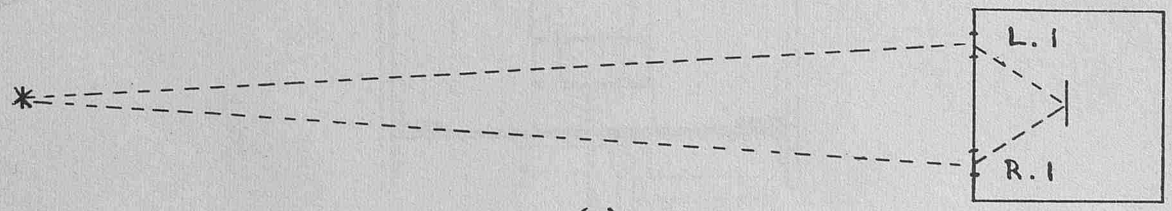

(a)

$$\left(\frac{R.2}{L.2}\times\frac{\cos\theta_L}{\cos\theta_R}\times\frac{d_R^{2}}{d_L^{2}}\right)\% - \left(\frac{R.1}{L.1}\right)\% \simeq 2\%$$

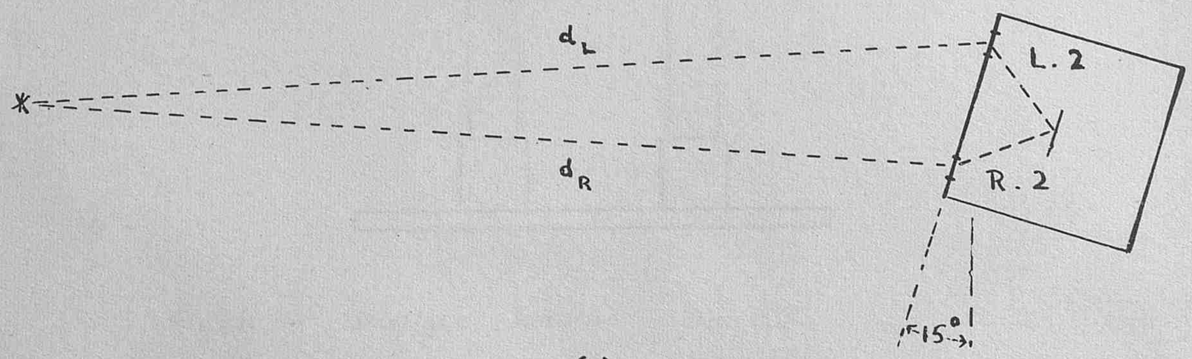
d_L
d_R
L.2
R.2
15°

(b)

Fig. 5 - Test of diffusing properties of opal glass.

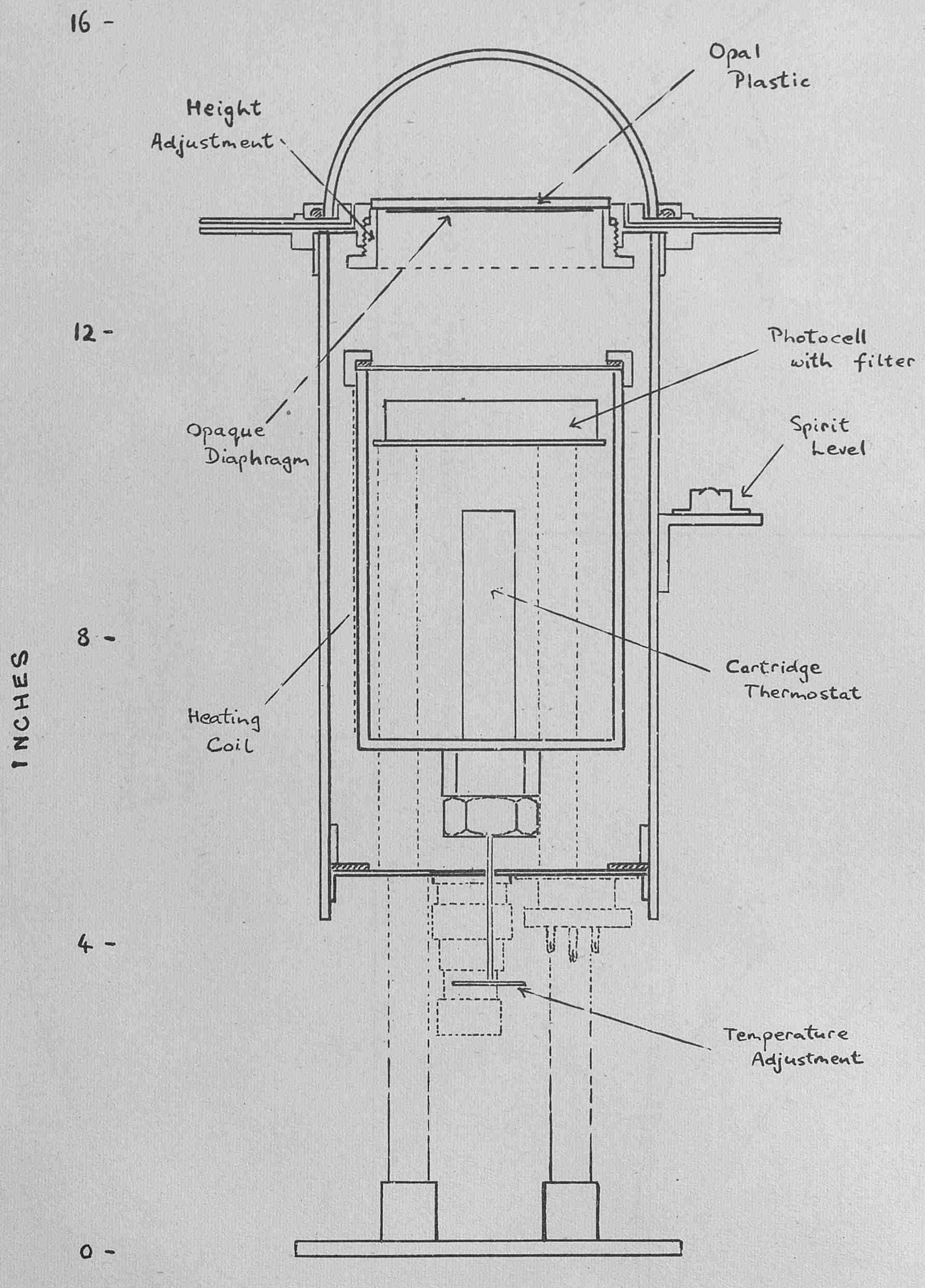
16 -
12 -
8 -
4 -
0 -
INCHES
Opal Plastic
Height Adjustment
Photocell with filter
Spirit Level
Opaque Diaphragm
Cartridge Thermostat
Heating Coil
Temperature Adjustment

Fig. 6 - Daylight Recorder Mk. III.

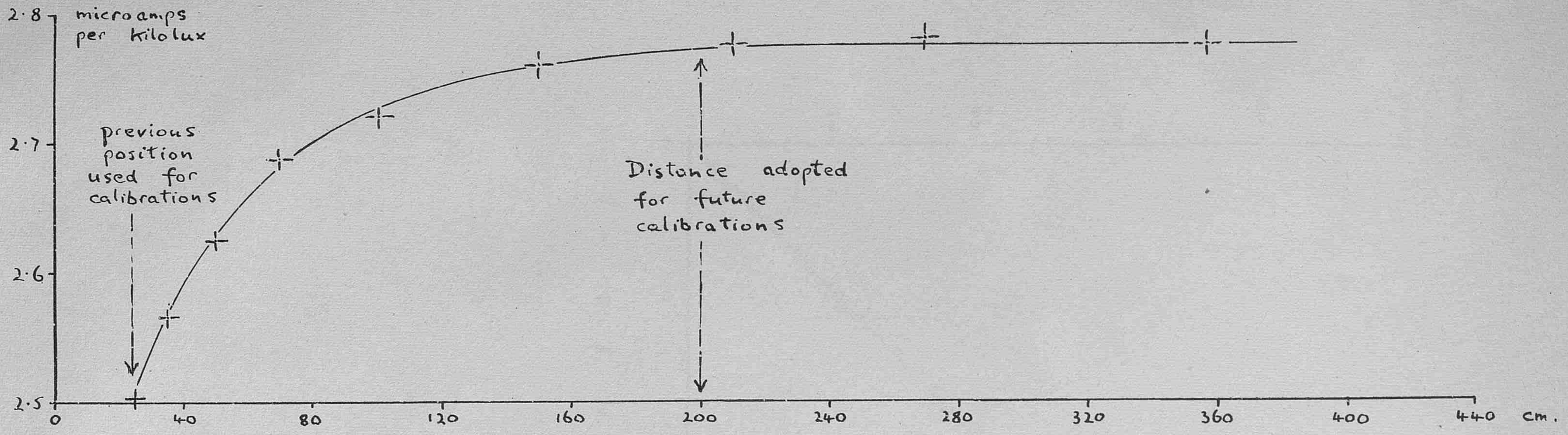

Fig. 4 - Calibration by the extrapolation method.

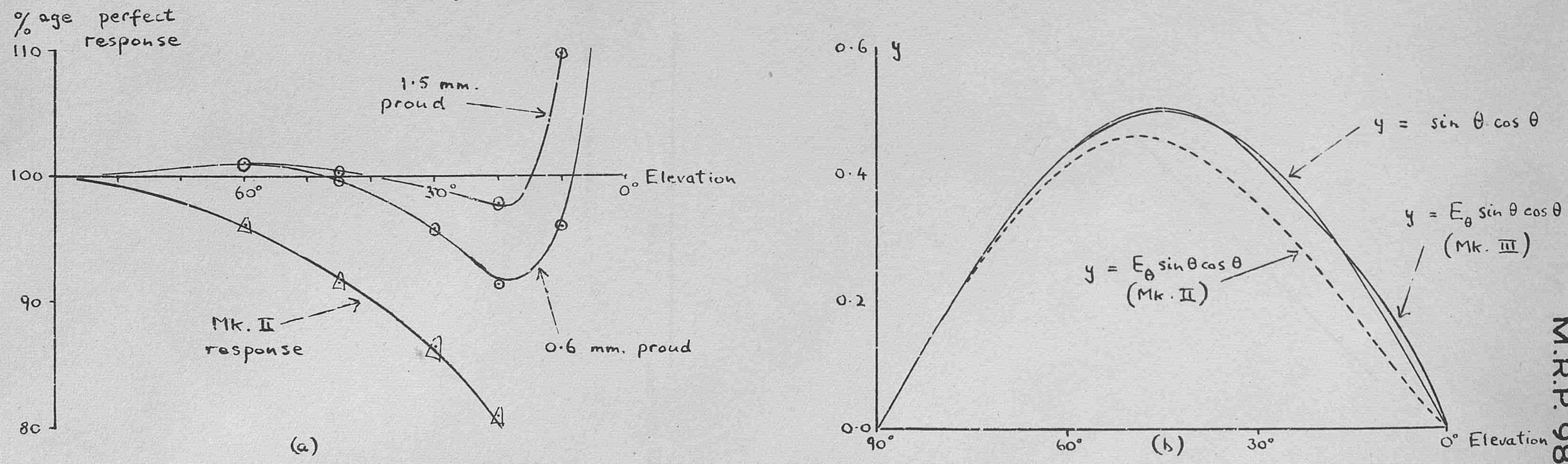

Fig 7 - Effect of Mk. III cosine-correcting device.

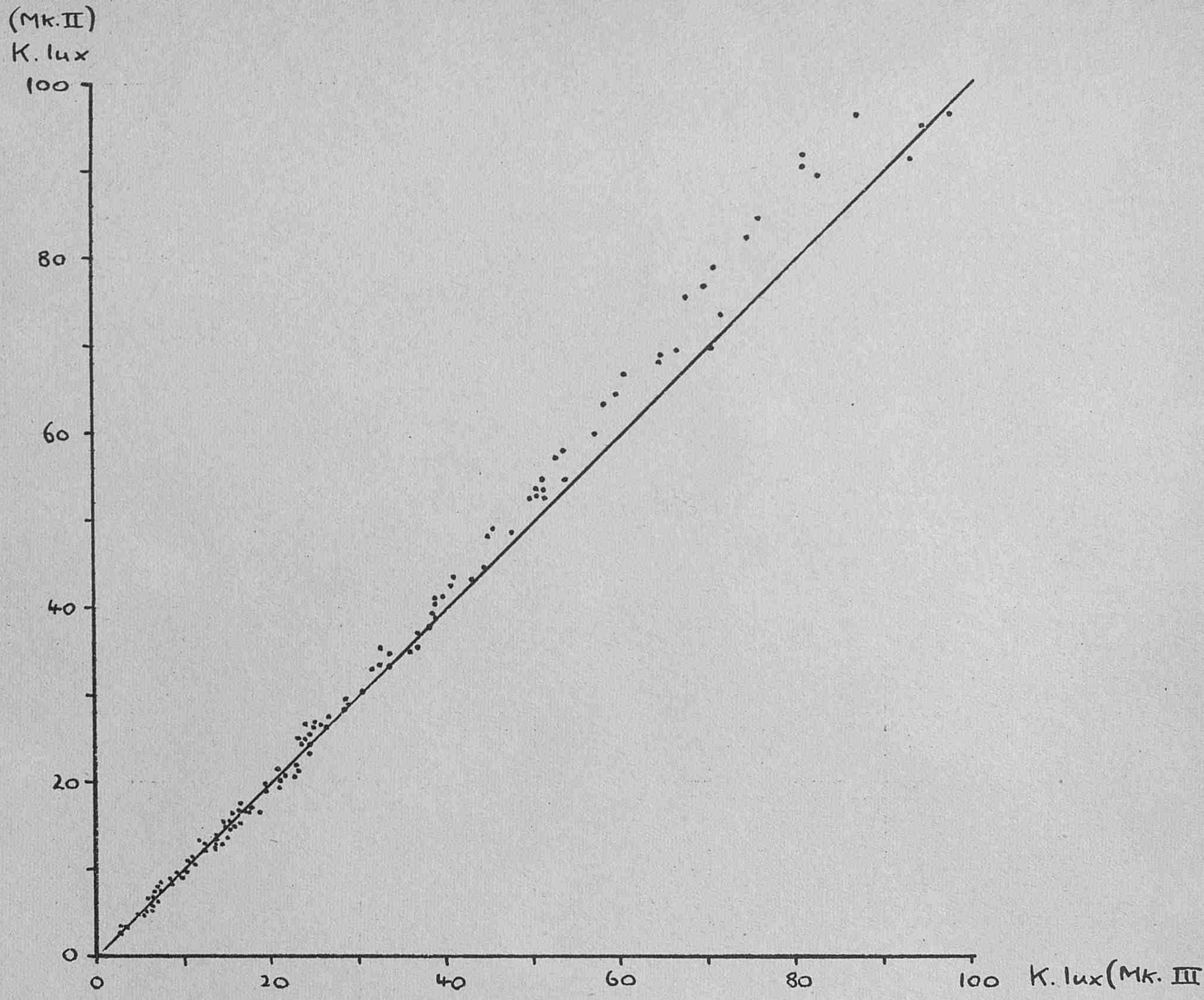

Fig. 8 - Mk. II v. Mk. III comparisons.

M.R.P. 989

S.C. I/117

1st June, 1956

AD 223125

The measurement of surface wind

by

R. Frith

(Meteorological Office)

AIR MINISTRY

METEOROLOGICAL RESEARCH COMMITTEE

At the time of issue this report has not been published. Any author desiring to quote this paper should refer to it as "A paper of the Meteorological Research Committee (London), M.R.P. No. 989 by Dr. R. Frith
A copy is available in the library of the Meteorological Office."

M.R.P. 989
S.C. I/117
1st June, 1956

AIR MINISTRY

METEOROLOGICAL RESEARCH COMMITTEE

The measurement of surface wind

by

R. Frith (Meteorological Office)

Introduction

There is a twofold demand for accurate surface wind data. On the one hand, Aerodrome Control Officers and air crew wish to know, at all times, what the wind is on the runway. On the other hand a variety of users (architects, agriculturists etc.) wish to be provided with accurate information about wind régimes over more or less extensive areas and periods.

These two demands pose rather different problems. On an airfield the problem is to assess the wind (speed, direction, gustiness) on the runway from readings of a nearby anemometer exposed as may be. The World Meteorological Organisation's definition of 'surface wind' is the wind at a height of 10 m. in an open situation. Since the vicinity of a runway is an open situation, and since 10 m. seems to have become the accepted height of measurement for aviation purposes, the problem reduces to obtaining the 'surface wind', as defined by W.M.O., from the readings of a nearby anemometer which is perhaps not exposed in an open situation, and is perhaps not exposed at a height of 10 m.

For other purposes the problem is this:-

(i) What is the best definition of the concept of a 'representative wind' and how should this be derived from instruments exposed as may be?

(ii) Given, by observation or interpolation, a 'representative wind' for a locality, how can we best estimate the actual wind at any place or height taking account of terrain and obstacles?

The W.M.O. definition of a 'surface wind' can perhaps be accepted as the 'representative wind'. It would probably be unreasonable to attempt to make the measurement more 'representative' by removing from it any component due, for example, to local topography or to a sea breeze.

We have, therefore to consider:-

(a) how to assess the 'surface wind' (i.e., the wind at 10 m. in an open situation) from an anemometer exposed as may be; and

(b) how, from assessments at a network of stations, we can best estimate the actual wind at any place or height taking account of terrain and obstacles.

If an anemometer is exposed at a height of 10 m. in an open situation, then it measures, directly, the surface wind as defined by W.M.O. If it is exposed at a height different from 10 m., or if the site is not open, then the reading may have to be reduced in some way in order to obtain an accurate assessment of the 'surface wind'.

/Height

Height of exposure

A good deal of field work has been done on the variation of wind with height under various conditions of stability, wind speed and surface roughness. Deacon (1) and Giblett (2) quote results which indicate that the Hellmann formula, which is used in the Meteorological Office for the reduction of anemometer readings, may give results which are in error by as much as 20 per cent. It has been suggested that an observational accuracy, after reduction to the standard height of 10 m., of ± 5 per cent. or one knot, whichever is the greater, in speed (both mean speed and gust speed) and ± 5 degrees in direction is desirable.

Probably enough is now known to enable corrections for height to be made with this accuracy up to a height of, perhaps, 70 feet. It is doubtful whether readings from anemometers exposed at heights above 70 feet could be reduced with the required accuracy except when the wind is strong.

The effect of poor exposure

Where an exposure is poor it is usually due to the presence near the anemometer of obstacles, such as buildings and trees*.

The effect of isolated obstacles has received a certain amount of qualitative study both in wind tunnels and in the field, the latter mostly in connection with wind breaks. It is fairly well established, for example, that at a height of about three times the height of an isolated bluff obstacle the wind characteristics are practically unchanged by the obstacle; but there seems to be little precise information about the effect inside the disturbed air flow.

Where an instrument has a poor exposure an appropriate reduction formula can best be determined by an on-site investigation; by erecting an anemometer at 10 m. on a nearby open site and comparing the readings over a long period.

It is desirable, however, that there should be some fairly simple rule of thumb which would indicate whether any particular exposure, or proposed exposure, is:-

(a) good (i.e., no corrections or reductions needed);

(b) poor (i.e., acceptable but reductions or corrections needed);

(c) not acceptable (i.e., such that no practicable reduction or correction formulae could be found to obtain wind speed, direction and gustiness with the required accuracy).

A large number of comparisons at existing sites would probably enable such a rule to be formulated; but it might be useful to carry out a special and detailed field investigation into the effect of a single obstacle. This would be simpler to carry out, and would be more revealing, than a wind tunnel experiment.

---

*The present method of dealing with a poor exposure is for some inspector to form an estimate of an 'effective height'. This 'effective height' is defined as "the height at which a properly exposed anemometer would register a mean wind equal to that recorded by the anomometer in question". It might be better if the anemometer reading were corrected to indicate the undisturbed wind at the height of the anomometer, and this corrected reading reduced to 10 m.

/Summary

Summary and proposed investigations

An observational accuracy, after reduction to the standard height of 10 m., of ± 5 per cent in speed, and of ± 5 degrees in direction, cannot be achieved until more is known about the effect of local obstacles. Nor can it be achieved using our present universal reduction formula. It is proposed that:-

(i) on-site investigations be carried out at a number of stations where the exposure of the anomometer is not good;

(ii) a study of the literature be made to assess the accuracy with which reductions to a standard height can be made under various conditions of surface roughness, wind speed and stability;

(iii) a field investigation be carried out into the effect of a single obstacle to determine:

(a) at what height, and how far away, the flow is unaffected by the obstacle:

(b) to what extent it is possible to correct for the presence of the obstacle.

References:

(1)	Deacon, E.L.	1949	Q.J. Roy.Met.Soc., 75
(2)	Giblett, M.A.	1932	Geophys. Mem. Met.Off. London, No. 54

Appendix on the problem of interpolation in the horizontal

By definition the 'surface wind' is the wind at 10 m. in an open situation. If an anemometer can be exposed at 10 m. in an open situation then the 'surface wind' can be measured with high accuracy. In other circumstances it is necessary to 'reduce' the readings to allow for the effects of exposure at heights differing from 10 m. and exposure in non-open situations. The preceding sections have discussed the problems involved in this reduction.

High accuracy in measurement and in reduction is, however, of little value unless interpolation can be carried out with comparable accuracy. In the absence of topographical effects and provided there are no variations in surface roughness, there is no obvious reason why interpolation (of statistics, or of means over not too short a period) should not give results with an accuracy comparable with that of the basic data. The results of the interpolation would, of course, refer to the standard height of 10 metres and extrapolation to other heights would have to be made with care. In particular, extrapolation to heights above 25 metres could probably only be made with precision when the wind was strong.

Where there are variations of surface roughness this would have to be taken into account. In assessing the surface roughness, the nature of the actual surface (short grass, long grass, bare soil, snow, crops, water, etc.) must be considered and also the absence or presence of fences or walls, trees, houses, etc. Results quoted by Deacon suggest that with a long fetch over short grass, the wind at 10 metres would be 5 - 10% greater than over long grass, and 5 - 10% less than over snow.

Where marked topographical effects exist, interpolation to the accuracy specified must frequently be impossible. There is, nevertheless, a growing interest, particularly among agriculturists, in the variations of the surface winds in hilly country, and some sort of pilot experiment might be worth while. It would be preferable that any such experiment should be designed and carried out by someone directly concerned - perhaps an agricultural meteorologist.

M.R.P. 990
S.C.111/210
30th June, 1956.

AD 131893

The exhaust trail from jet engines

by

R.F. Jones

(Meteorological Office)

AIR MINISTRY

METEOROLOGICAL RESEARCH COMMITTEE

At the time of issue this report has not been published. Any author desiring to quote this paper should refer to it as "A paper of the Meteorological Research Committee (London), M.R.P. No.990 by Mr. R.F. Jones
A copy is available in the Library of the Meteorological Office."

M.R.P. 990
S.C.III/210
30th June, 1956

AIR MINISTRY

METEOROLOGICAL RESEARCH COMMITTEE

The exhaust trail from jet engines

by

R.F. Jones (Meteorological Office)

1. Introduction

The "Mintra" line shown on the Meteorological Office Tephigram (Form 2810A) gives for any given height an indication of the temperatures above which contrails are unlikely to form. The theory leading to the determination of these temperatures is given in M.O.479(1). For many purposes it is more desirable, if possible, to forecast the temperatures below which contrails are likely to form. Using the Mintra temperatures for this purpose is unsatisfactory and a body of evidence has accumulated which suggests that, at least for jet engines, the Mintra temperature is too high for practical forecasting purposes, i.e. forecasts of the likelihood of contrails if the temperature falls below the Mintra value are not sufficiently precise and the majority of trails form first several degrees Centigrade below the Mintra value.

In this paper a somewhat different approach from that of M.O.479(1) is used. It assumes that for jet engines the temperature and issuing speed of the exhaust gases together with fuel consumption and mass flow through the engine are known, or can be determined, for various engines under different operating conditions.

2. Theory

The increased water content in the exhaust trail above that of the ambient air is produced by the burning of the fuel in the jet engine. For the kerosene fuel at present used 1 gm of such fuel when burnt yields 1.3 gm of water vapour. Knowing the rate of burning of the fuel and the mass flow of air through the engine it is possible, assuming all the fuel is burnt and all the water vapour produced is taken up by the air flowing through, to calculate the humidity mixing ratio of the exhaust air at the point where it is about to leave the jet pipe. Both the assumptions made above are reasonable since the oxygen supplied by the air flowing through the engine is very greatly in excess of that required for complete combustion of the fuel and the temperatures are such that it is impossible to visualise any loss of water vapour by condensation or other means.

If the mass flow of air through the engine is M lb/sec and the fuel consumed is F lb/sec the water vapour produced by the burning of the fuel will be WF lb/sec where W is the mass of water vapour produced by burning unit mass of fuel (W = 1.3 for kerosene). This water vapour will be included in the (M + F) lb/sec of exhaust gases along with the original water content of the M lb/sec of air. If x g/Kg is the mixing ratio of the ambient air, the mixing ratio x_e of the exhaust air will then be given by:-

$$x_e = \frac{1000\left(WF + \frac{Mx}{1000 + x}\right)}{(M + F) - \left(WF + \frac{Mx}{1000 + x}\right)} \text{ g/Kg}$$

$$= \frac{1000\left(WF + \frac{Mx}{1000 + x}\right)}{M\left(\frac{1000}{1000 + x}\right) - F(W - 1)} \text{ g/Kg} \qquad (1)$$

Because of the action of the compressors and the burning of the fuel the exhaust gas will arrive at the jet outlet at a temperature T and pressure P (different from the ambient temperature and pressure) and speed V and will immediately suffer adiabatic expansion to ambient pressure P_o. This will result in a cooling of the exhaust gas to a temperature T_1 given by:

$$T_1 = T\left(\frac{P_o}{P}\right)^{\frac{\gamma-1}{\gamma}} \qquad (2)$$

where γ is the ratio of the specific heats at constant pressure and constant volume for the mixture of gases comprising the exhaust gas.

This adiabatic cooling will leave the mixing ratio of the exhaust gas unchanged so that immediately after leaving the exhaust the gas is at a temperature T_1 given by equation (2) with a mixing ratio x_e given by equation (1). Further cooling of the air without condensation or mixing with the ambient air would leave the mixing ratio unchanged so that if mixing did not take place the exhaust air would become saturated when cooled to a temperature having a saturation mixing ratio of x_e.

The exhaust gases, however, leave the exhaust at a high speed v (of the order of 1,500 ft/sec relative to the aircraft and perhaps 800 ft/sec relative to the ambient air) and it is certain that considerable mixing with the ambient air will take place into such a jet.

As well as possessing thermal energy corresponding to the temperature T_1 the exhaust gases will also possess kinetic energy which will ultimately be given up to the trail in the form of heat as the speed of the exhaust jet is reduced by mixing with ambient air.

If 1 gm of exhaust gas moving with a speed v_1 cm/sec relative to the ambient air ($v_1 = v - V$, where V is the forward speed of the aircraft) is mixed with m gm of ambient air then considerations of momentum show that the speed v' of the (1 + m) gm of mixture will be given by

$$v' = \frac{v_1}{1 + m} \text{ cm/sec .}$$

The initial kinetic energy of 1 gm of exhaust gas is $\frac{1}{2}v_1{}^2$ erg and the final kinetic energy after mixing with m gm of ambient air is

$$\tfrac{1}{2}(1 + m)(v')^2 = \frac{v_1^2}{2(1 + m)} \text{ erg .}$$

The loss of kinetic energy on mixing therefore, which appears in the mixture in the form of heat, is

$$\tfrac{1}{2}\,v_1^{\,2}\left(1 - \frac{1}{1 + m}\right) = \frac{m\,v_1^{\,2}}{2(1 + m)}\ \text{erg}\,.$$

The heat given to the (1 + m) gm of mixture is therefore $\dfrac{m\,v_1^{\,2}}{2J(1 + m)}$ cal where J is the mechanical equivalent of heat ($= 4.18 \times 10^7$ erg/cal).

If c_p is the specific heat at constant pressure of the mixture of exhaust gas and ambient air the temperature increase of the mixture due to conversion of kinetic energy into heat will be

$$\tfrac{1}{2}\cdot\frac{v_1^{\,2}}{J.c_p}\cdot\frac{m}{(1 + m)^2}\ {}^{\circ}\text{C}\,.$$

In practice, since the mass flow of air through the jet engine is likely to be very much greater than the fuel consumption and since at heights important in the contrail problem the water content of the ambient air will be small, negligible error would be involved in taking the specific heat at constant pressure (c_p) of the mixture of exhaust gas and ambient air as identical with that of dry air (0.24 cal/gm/°C).

Considering now the thermal energies of the exhaust gas and ambient air we know that if 1 gm of gas of temperature T_1 °K is mixed at constant pressure with m gm of the same gas at temperature T_2 °K the temperature of the mixture will be $\dfrac{T_1 + mT_2}{1 + m}$ °K (see ref.(2), p.48).

Since, as we have seen above, the specific heats at constant pressure of exhaust gas and ambient air are unlikely to differ significantly from that of dry air the exhaust gas and ambient air can be considered to be of the same constitution for this purpose and the temperature of the mixture will be $\dfrac{T_1 + mT_2}{1 + m}$ °K where T_2°K is the temperature of the ambient air, when thermal energies alone are considered.

Taking conversion of kinetic energy also into account we find that the temperature T_m of the mixture of 1 gm of exhaust gas with m gm of ambient air will be given by:

$$T_m = \frac{T_1 + mT_2}{1 + m} + \tfrac{1}{2}\cdot\frac{v_1^{\,2}}{Jc_p}\cdot\frac{m}{(1 + m)^2} \qquad (3)$$

The mixing ratio, x_m, of the mixture of 1 gm of exhaust gas (mixing ratio x_e) with m gm of ambient air (mixing ratio x) will be:

$$x_m = \frac{1000\phi}{1 + m - \phi}\ \text{g/Kg}$$

$$\text{where}\ \phi = \frac{x_e}{1000 + x_e} + \frac{mx}{1000 + x}$$

Using equation (1) it can be shown that

$$x_m = \frac{1000\{1000WF + x[(1 + m)M + (W + m)F]\}}{1000(1 + m)(M + F) - F[1000W + x(W - 1)]} \qquad (4)$$

Now x in the contrail problem is unlikely greatly to exceed 1g/Kg and W (water vapour produced by burning 1 gm of fuel) is of the order of 1.3 so that x(W-1) in the denominator of (4) is small compared with 1000W and without important error we can write:-

$$x_m = \frac{1000WF + x[(1 + m)M + (W + m)F]}{(1 + m)(M + F) - WF}$$

$$= \frac{1000WF}{(1 + m)(M + F) - WF} + x\left[1 + \frac{F(2W - 1)}{(1 + m)(M + F) - FW}\right]$$

$$= 1000W\beta + x\left[1 + (2W - 1)\beta\right] \quad \text{where } \beta = \frac{F}{(1 + m)(M + F) - WF}$$

$$= \beta\left[1000W + (2W - 1)x\right] + x \qquad (5)$$

and since $(2W-1)x$ is also small compared with 1000W and β itself is usually small especially when m (the degree of mixing) becomes large it is often legitimate to make the further approximation

$$x_m = 1000W\beta + x \qquad (6)$$

For constant m, β is a function only of the engine performance and W depends only on the type of fuel used so that the expression (6) conveniently separates the effects of engine performance and fuel type from the properties of the ambient air.

Equations (3) and (6) (or more strictly (4)), therefore, give the temperature and mixing ratio respectively of the gases in the exhaust trail as long as the air remains unsaturated. Thus, knowing the engine performance details, it is possible to obtain values of T_m, x_m for various conditions of ambient temperature and mixing ratio and different degrees of mixing with the ambient air. The values of T_m can conveniently be converted by means of meteorological tables into values of the mixing ratio for which at the ambient pressure concerned the air would be saturated with respect to ice (or water). Two sets of curves can then be drawn on the same diagram showing the variation with m of saturation mixing ratio in the trail and x_m for various values of the ambient temperature and mixing ratio. Where the curves intersect will give the degree of mixing which needs to be achieved before the exhaust trail becomes saturated and the saturation mixing ratio within the trail at which this occurs. In particular if the ambient air is saturated with respect to ice (or water) critical temperatures will be defined above which saturation in the trail with respect to ice (or water) can never be achieved. These temperatures would define the "Mintra" temperature for the level concerned. Similarly if the ambient air is completely dry (x = o) "Drytra" temperatures would also be defined.

As an example of the use of such a diagram let us assume reasonable values for the various parameters involved for a jet engine operating at an ambient pressure of 200 mb.

Such values may be: $T_1 = 600°A$, $v_1 = 2.5 \times 10^4$ cm/sec, $W = 1.3$, $F = 0.5$, $M = 32.5$ together with known values of J and c_p ($J = 4.18 \times 10^7$ erg/cal, $c_p = 0.24$ cal gm^{-1} °C^{-1}).

It can then be shown using equations (3) and (6) (in accurate computations equation (4) can be used) that T_m, x_m are given by:

$$T_m = \frac{600 + 631\,m}{(1 + m)^2} + T_2 \left[1 - \frac{1}{1 + m} \right]$$

$$x_m = \frac{650}{33m + 32{\cdot}35} + x$$

where T_2 and x are the temperature and mixing ratio respectively of the ambient air.

Values of T_m for various values of T_2 and m and of x_m for various values of m assuming $x = 0$ (completely dry ambient air) are shown in Table I. Also shown are saturation mixing ratios over ice and water, x_i, x_w corresponding to T_m at a pressure of 200 mb; for convenience in the use of the Meteorological Tables(3) degrees Centigrade + 273 have been used in preference to °K.

TABLE I

Temperature T_m and mixing ratio x_m in the exhaust trail for various degrees of mixing with completely dry ambient air at temperature T_2. (x_i is the saturation mixing ratio over ice at 200 mb corresponding to T_m, x_w that over water)

m	9	19	29	39	49	59	99	199	499	999
					T_2 = 210 °A					
T_m	251.8	231.0	224.0	220.5	218.4	217.0	214.2	212.1	210.8	210.4
x_i	2.87	0.318	0.138	0.089	0.069	0.057	0.040	0.030	0.025	0.024
x_w	3.54	0.478	0.222							
					T_2 = 220°A					
T_m	260.8	240.5	233.7	230.3	228.2	226.8	224.1	222.1	220.8	220.4
x_i	6.68	0.912	0.434	0.294	0.230	0.195	0.140	0.109	0.092	0.088
x_w	7.57	1.251	0.634	0.444	0.354	0.304	0.225	0.178		
					T_2 = 225°A					
T_m	265.3	245.2	238.5	235.1	233.1	231.8	229.1	227.0	225.8	225.4
x_i	10.02	1.489	0.736	0.506	0.405	0.349	0.255	0.199	0.173	0.165
x_w	10.86	1.953	1.028	0.732	0.595	0.520	0.390	0.310	0.272	0.260
					T_2 = 230°A					
T_m	269.8	250.0	243.3	240.0	238.0	236.7	234.0	232.0	230.8	230.4
x_i	14.8	2.406	1.220	0.864	0.696	0.604	0.448	0.357	0.311	0.298
x_w	15.4	3.019	1.635	1.191	0.979	0.861	0.653	0.531	0.469	0.449
					T_2 = 240°A					
T_m	278.8	259.5	253.0	249.8	247.8	246.5	243.9	241.9	240.8	240.4
x_i	30.1	5.95	3.224	2.361	1.935	1.699	1.300	1.056	0.941	0.902
x_w	30.1	6.81	3.929	2.970	2.482	2.202	1.729	1.431	1.288	1.239
x_m	1.973	0.986	0.657	0.493	0.394	0.328	0.197	0.099	0.039	0.020

These values are shown plotted in Fig. 1. Curves allowing for the mixing ratio, x, of the ambient air can readily be plotted since all that is required (equation (6)) is to add the value of x at each stage to the corresponding value for a completely dry atmosphere. Two such curves are plotted in Fig. 1 corresponding to values of x representing saturation of the ambient air at temperatures of 230°A and 240°A (x = 0.284 and 0.864 g/Kg respectively).

If the assumed values of the parameters were accurate values for a particular jet engine then for this engine the following deductions could be made from Fig. 1 for the pressure level of 200 mb:

(i) If the ambient air is completely dry saturation of the exhaust trail with respect to ice would just be achieved if the ambient temperature was 225°A but for ambient temperatures higher than this value saturation would never be achieved. 225°A would, therefore, be the "Drytra" temperature for this engine at a pressure of 200 mb. If saturation with respect to water is required the corresponding "Drytra" temperature would be about 221°A.

(ii) At an ambient temperature of 225°A saturation of the exhaust trail with respect to ice is just achieved after mixing with 39 times its own weight of completely dry ambient air and, by reference to Table I, at a temperature of the trail of 235.1°A.

(iii) At an ambient temperature of 220°A saturation of the trail with respect to ice would be achieved after mixing with about 19 times its own weight of dry ambient air and saturation would be maintained until mixed with about 160 times its own weight of ambient air. The maximum free ice content of the air would be about 0.22 g/Kg when mixed with about 29 times its own weight of dry ambient air. The trail would become unsaturated again at a temperature still some 3°C higher than that of the ambient air.

(iv) If the ambient air is saturated with respect to ice at 230°A the trail will also become saturated with respect to ice after mixing with about 50 times its own weight of ambient air and thereafter remain saturated but if the ambient air is saturated at 240°A the trail will never become saturated. The "Mintra" temperature for this engine at 200 mb pressure lies therefore between 230°A and 240°A and its accurate value can readily be determined.

(v) Similar deductions can be made for varying values of humidity of the ambient air by suitable adjustment of the curves for the appropriate values of x.

(vi) For low ambient temperatures (e.g. below 210°A) a saturated trail is likely to be attained with a low degree of mixing whatever the ambient humidity and the trail will remain saturated until very greatly mixed with ambient air. The effect of ambient humidity is likely therefore to become less marked as the ambient temperature decreases.

3. The effect of release of latent heat of condensation or sublimation

The argument of Section 2 is valid as long as the gases in the exhaust trail remain unsaturated but as soon as saturation of the trail is achieved a further source of heat becomes operative, namely the release of the latent heat of condensation or sublimation once water drops or ice crystals begin to form in the trail. There is some evidence to support the belief that even at temperatures well below the freezing point direct sublimation from the vapour in the form of ice crystals does not take place as soon as supersaturation with respect to ice is achieved but that saturation with respect to water must first be achieved and the initial deposition of surplus water vapour is in the form of supercooled water droplets. At very low temperatures such as commonly occur in contrail formation, of the order of 230°K and below, subsequent freezing of these droplets is likely to be very rapid.

Suppose condensation in the liquid form has occurred at a temperature, T_m, of about 230°K until 0.01 g/Kg of liquid water has been condensed. The condensation of this quantity of liquid from the vapour will release 0.01 x 620 cal/Kg sufficient to raise the temperature of the air by $\frac{0.01 \times 620}{0.24 \times 1000} = 0.03°C$, assuming the specific heat of the exhaust gases to be the same as that of dry air. If we suppose that this water now freezes the latent heat liberated (0.01 x 56 cal/Kg) will have an insignificant effect on the temperature but, with ice crystals now present, direct sublimation from the vapour onto the ice crystals will proceed rapidly until the vapour content is reduced to that corresponding to saturation with respect to ice. Since the difference in saturation mixing ratios with respect to water and ice at about 230°K is about 0.15 g/Kg this amount of water vapour must be converted directly into ice releasing 0.15 x 676 cal/Kg.

If x_i is the saturation mixing ratio with respect to ice, at temperature T_m, therefore, the total latent heat contributed to the trail would be $(x_m - x_i) \times 676$ cal/Kg which in the case discussed would be sufficient to raise the temperature of the gas by about 0.5°C. This full rise of temperature will not be achieved since as the temperature rises the saturation mixing ratio will also rise (by about 0.02 g/Kg for a temperature rise of 0.5°C from about 234°K) so that a balance is finally achieved whereby the final temperature rise due to release of latent heat is about 0.4°C and the final solid ice content in the trail is somewhat less than $(x_m - x_i)$g/Kg. As mixing with the ambient air proceeds a stage will be reached when the solid ice content $(x_m - x_i)$ in the trail will reach a maximum and the temperature increase due to latent heat will also be a maximum. Thereafter $(x_m - x_i)$ will decrease as some of the solid content is evaporated in order to bring the entrained air up to saturation with respect to ice at the temperature of the trail. The gain of latent heat in the early stages of mixing will then be balanced in the later stages by loss of heat to evaporate the ice until when all the ice has been evaporated the temperature T_m and mixing ratio x_m will again be those determined by equations (3) and (4). Thus, in the stage when the exhaust trail contains ice crystals the temperature T_m will be greater than that given by equation (3) by an amount given approximately by $(x_m - x_i) \times \frac{676}{240}$°C and the true ice content will be slightly less than that deduced using x_m from equation (4).

Instead of making corrections to T_m and $(x_m - x_i)$ it is more convenient to deal with T_m and x_m as determined by equations (3) and (4) and refer to $(x_m - x_i)$ as the "effective ice content" regarding a small proportion of $(x_m - x_i)$ as being earmarked to provide the water vapour required to maintain saturation as T_m rises on account of the release of latent heat of sublimation of the remainder of $(x_m - x_i)$.

4. The visible exhaust trail (contrail)

The argument of Section 2 enables a deduction to be made of when, if at all, the exhaust trail is saturated with respect to ice or water. Saturation alone, however, is not sufficient to make the trail visible, there must be condensation to liquid water or sublimation to ice to such an extent that the number and size of particles render the trail visible. What this number and size must be has never been clearly demonstrated and in any case must depend on the conditions of viewing, e.g., the distance away and contrast with the background as well as the acuity of the observer's eye.

Appelman(4) has considered as necessary a minimum water (or ice) content of 0.004 g/m^3 for a faint trail and 0.01 g/m^3 for a distinct trail but recognises that these definitions are quite arbitrary.

From observations of the level of first formations of contrails from an instrumented aircraft having engines of known characteristics it is possible by the use of a diagram such as Fig.1 to make a close estimation of the excess ice crystal content in the trail. For example, if an aircraft using the hypothetical engine discussed in Section 2 first made a visible trail at 200 mb when the ambient temperature was 220°A and the mixing ratio 0.01 g/Kg (equivalent to a relative humidity with respect to ice of 12%) Fig.1 would show the maximum effective ice crystal content of the trail to be 0.21 g/Kg. Since the temperature in the trail at this point would be 233.7°A (Table I) the maximum effective ice crystal content would be $\frac{0.21}{0.298}$ g/m^3 = 0.07 g/m^3, the density of air at 233.7°A and 200 mb pressure being 0.298 Kg/m^3. Observations such as this have suggested that the minimum effective ice crystal content necessary to make the trail visible is much in excess of the value of 0.004 g/m^3 quoted by Appelman. It is worth noting, however, that if it is considered that condensation to water droplets is first necessary in the trail followed by rapid freezing of these droplets then the ice crystal content of the trail, when freezing and reduction of the mixing ratio to saturation with respect to ice has been completed, will certainly be greater than the Appelman criterion. Fig.1 shows that in the example considered saturation with respect to water is achieved for the same degree of mixing as gives the maximum ice crystal content, so that the requirement for saturation with respect to water automatically leads to a maximum effective ice crystal content in the trail of 0.07 g/m^3. If, however, the minimum ice crystal content to make the trail visible is in excess of 0.07 g/m^3 the critical temperature for visible trail formation becomes less than that given for saturation with respect to water. If, for example, the minimum effective ice crystal content is 0.1 g/m^3 (equivalent to about 0.33 g/Kg at the probable trail temperature at 200 mb pressure) Fig.1 shows that for completely dry ambient air the critical temperature for visible trail formation is about 218°A compared with 221°A if saturation with respect to water is used as the criterion and 225°A for saturation with respect to ice. It is therefore clearly desirable to determine as accurately as possible the minimum ice crystal content necessary to make the trail visible and any variation with height. Having determined this value it is a simple matter to adjust the ambient mixing ratio curves of diagrams like Fig.1, taking account of the variation of density with temperatures in the trail for various ambient temperatures, to ensure that the minimum visibility criterion is met, leading to new values of "Mintra" and "Drytra" temperatures. These new values will not differ from those determined assuming initial saturation of the trail with respect to water unless (a) the trail remains as a water cloud for an appreciable time after formation, or (b) if freezing of the water droplets in the trail is rapid, the minimum ice crystal content necessary to make the trail visible is greater than would result from the change from saturation with respect to water to saturation with respect to ice. A further point requiring examination, therefore, is how quickly the change of state within the trail takes place.

5. The persistence of contrails

The persistence of a trail once visible must clearly depend on the degree of mixing with the ambient air before the minimum ice crystal content for visibility is again reached and the time taken for this mixing to be achieved. Observations of the lengths of trails from an instrumented aircraft having engines of known characteristics can again be used in association with diagrams of the form of Fig.1 to assist in the forecasting of the length of the visible trail. For example, using Fig.1, we see that saturation with respect to water is achieved at an ambient air temperature of 220°A if the air is completely dry after mixing corresponding to $m = 25$ and saturation is again reached for $m = 71$; if freezing has taken place there will be an ice crystal content in the exhaust trail until saturation with respect to ice is once more achieved at $m = 166$. The visible trail will certainly vanish therefore before $m = 166$ and according to the value of minimum ice content necessary for visibility a value of m can be found which will mark the beginning and end of the visible trail. Aircraft observations of the distances from the aircraft of commencement and cessation of trails will therefore give, by use of diagrams such as Fig.1, a mean value for the way m varies with distance, making possible an assessment of the length of trails for that particular aircraft for any occasion when the ambient temperature and humidity are known. It is clear from the form of the curves in Fig.1 that the effect of ambient humidity may be considerable on the length of a trail, e.g., if the ambient air is saturated at 220°A (mixing ratio 0.084 gm/Kg) saturation with respect to ice is not reached again until m exceeds 1000.

By determining a minimum value of m corresponding to "persistent" trails it becomes possible to forecast for a particular aircraft whose engine characteristics are known temperatures at a certain level analogous to "Drytra" and "Mintra" temperatures below which and above which persistent trails are likely and not likely to form respectively.

6. The diameter of the exhaust trail

Suppose the exhaust gas immediately before leaving the exhaust pipe is at temperature T, pressure P and moving at speed v relative to the ambient air. After adiabatic expansion to ambient pressure P_o, reducing T to T_1, and mixing with m times its own weight of ambient air of temperature T_2, it will have a temperature of T_m, pressure P_o and speed v_m where

$$v_m = \frac{v}{1 + m}$$

and

$$T_m = \frac{T_1 + mT_2}{1 + m} + \frac{1}{2}\,\frac{v^2}{Jc_p}\,\frac{m}{(1 + m)^2} \qquad \text{(equation 3)}$$

The total transfer of mass per second across the whole cross-section of the trail is constant so that if ρ, ρ_m are the densities of the exhaust gas before and after mixing, A the cross-sectional area of the jet pipe and A_m the cross-sectional area of the trail after mixing

$$\rho . A . v = \rho_m . A_m . v_m$$

$$= \rho_m . A_m . \frac{v}{1 + m} \quad \text{i.e. } \rho . A = \frac{1}{1 + m} . \rho_m . A_m .$$

$$\text{Now } \rho = \frac{P}{RT}, \quad \rho_m = \frac{P_o}{RT_m}$$

$$\text{so that } \frac{P}{RT} . A = \frac{1}{1 + m} . \frac{P_o}{RT_m} . A_m$$

$$\text{giving } \frac{A_m}{A} = (1 + m) . \frac{T_m}{T} . \frac{P}{P_o}$$

Since T_1 is the temperature of the exhaust gas after adiabatic expansion from pressure P to pressure P_o we have $\frac{P}{P_o} = \left(\frac{T}{T_1}\right)^{\frac{\gamma}{\gamma-1}}$ and substituting for T_m and $\frac{P}{P_o}$ we have

$$\frac{A_m}{A} = \left\{T_1 + mT_2 + \tfrac{1}{2} \cdot \frac{v^2}{J.c_p} \cdot \frac{m}{1+m}\right\} \left(\frac{T}{T_1^{\gamma}}\right)^{\frac{1}{\gamma-1}}.$$

For the hypothetical engine discussed in Section 2 we then have, assuming $T = 700°K$,

$$\frac{A_m}{A} = 0{\cdot}0026 \left\{600 + mT_2 + \frac{31m}{1+m}\right\}$$

$$\doteq 1{\cdot}64 + {\cdot}0026mT_2 \quad \text{since} \quad \frac{m}{1+m} \doteq 1$$

for all but small values of m.

If D_m is the diameter of the cross-section of the trail and D the diameter of the jet pipe exit, both assumed circular, we have

$$\frac{D_m}{D} = \sqrt{\frac{A_m}{A}}$$

$$= \sqrt{1{\cdot}64 + {\cdot}0026\, mT_2}$$

Values of $\frac{D_m}{D}$ for various values of m at an ambient temperature of 200°K are shown in Table II.

Table II

Change in trail diameter with varying entrainment of ambient air at a temperature 200°K

m	D_m/D
10	2.61
20	3.47
30	4.15
40	4.74
50	5.26
60	5.73
80	6.58
100	7.32
1000	22.8

It is clear from the form of Fig.1 that saturation of the exhaust trail will never be achieved until mixing of the order of m = 10 or more has been achieved so that on first becoming visible the contrail diameter is likely to be about 3 times the diameter of the jet orifice. The diameter of the trail will increase thereafter as the mixing with the ambient air proceeds but, unless the mixing is very rapid, the rate of change of diameter will be small. The observations suggested in Section 5 will give the variation of m with distance for a particular aircraft but it may be noted that observations from the ground of persistent trails suggest usually a small rate of growth of the diameter of the trail with distance although the trail starts quite close to the aircraft. This suggests an initial high rate of entrainment into the exhaust trail followed by relatively slow entrainment. This is shown also by the type of persistent trail formed by an aircraft having four jet engines. It is seen that the four trails from the engines very quickly merge into two as the trails from neighbouring engines on each side of the aircraft amalgamate. The distance between neighbouring jet pipes on the same side of the aircraft is small and, as Table II suggests, each trail will very quickly grow to more than three times the diameter of the jet pipe so that amalgamation of neighbouring trails is likely to be rapid. The distance apart of the pairs of engines, however, separated as they are by the fuselage, will be many diameters of the jet pipe and Table II suggests that the two remaining trails are unlikely to merge into one until m exceeds perhaps 100 or more. The very great distance behind the aircraft at which the two trails merge into one indicates that although mixing corresponding to $m = 10$ is very rapid that corresponding to $m = 100$ may not take place until the trail is several miles long.

Summary

Knowing certain performance data of a jet engine it is possible by a simple mixing theory to deduce the temperatures and humidity mixing ratio distribution in the exhaust trail. In particular "Mintra" and "Drytra" temperatures can be determined. By comparison with contrail observations from an instrumented aircraft having engines of known characteristics it will be possible to determine the minimum water or ice content in the trail necessary to make the trail visible, leading to the possibility of forecasting the length, diameter and persistence of visible trails.

References

(1) Meteorological Office: Condensation trails from aircraft. M.O.479, 2nd Edition, 1952.

(2) Brunt, D: Physical and Dynamical Meteorology. 2nd Edn., Cambridge University Press, 1941.

(3) Smithsonian Meteorological Tables, Smithsonian Institute, Washington, 1951.

(4) Appelman, H: The formation of exhaust condensation trails by jet aircraft. Bull. Amer. Met. Soc., Vol.34, p.14, 1953.

will increase thereafter as the mixing with the ambient air proceeds but, unless the mixing is very rapid, the rate of change of diameter will be small. The observations suggested in Section 5 will give the variation of width with distance for a particular aircraft but it may be noted that observations from the ground of persistent trails suggest usually a small rate of growth of the diameter of the trail with distance although the trail starts quite close to the aircraft. This suggests an initial high rate of entrainment into the exhaust trail followed by relatively slow entrainment. This is shown also by the type of persistent trail formed by an aircraft having four jet engines. It is seen that the four trails from the engines very quickly merge into two as the trails from neighbouring engines on each side of the aircraft amalgamate. The distance between neighbouring jet pipes on the same side of the aircraft is small and, as Table II suggests, each trail will very quickly grow to more than three times the diameter of the jet pipe so that amalgamation of neighbouring trails is likely to be rapid. The distance apart of the pairs of engines, however, separated as they are by the fuselage, will be many diameters of the jet pipe and Table II suggests that the two remaining trails are unlikely to merge into one until n exceeds perhaps 100 or more. The very great distance behind the aircraft at which the two trails merge into one indicates that although mixing corresponding to n = 10 is very rapid that corresponding to n = 100 may not take place until the trail is several miles long.

Summary

Knowing certain performance data of a jet engine it is possible by a simple mixing theory to deduce the temperature and humidity pattern in the distribution of the exhaust trail. In particular "Mixing" and "Drying" temperatures can be determined. By comparison with detailed observations from an instrumented aircraft having engines of known characteristics it will be possible to determine the minimum water or ice content in the trail necessary to make the trail visible, leading to the possibility of forecasting the length, diameter and persistence of visible trails.

References

(1) Meteorological Office: Condensation trails from aircraft. M.O.479, 2nd Edition, 1951.

(2) Brunt, D: Physical and Dynamical Meteorology. 2nd Edn., Cambridge University Press, 1944.

(3) Smithsonian Meteorological Tables, Smithsonian Institute, Washington, 1951.

(4) Appleman, H: The formation of exhaust condensation trails by jet aircraft. Bull. Amer. Met. Soc., Vol.34, p.14, 1953.

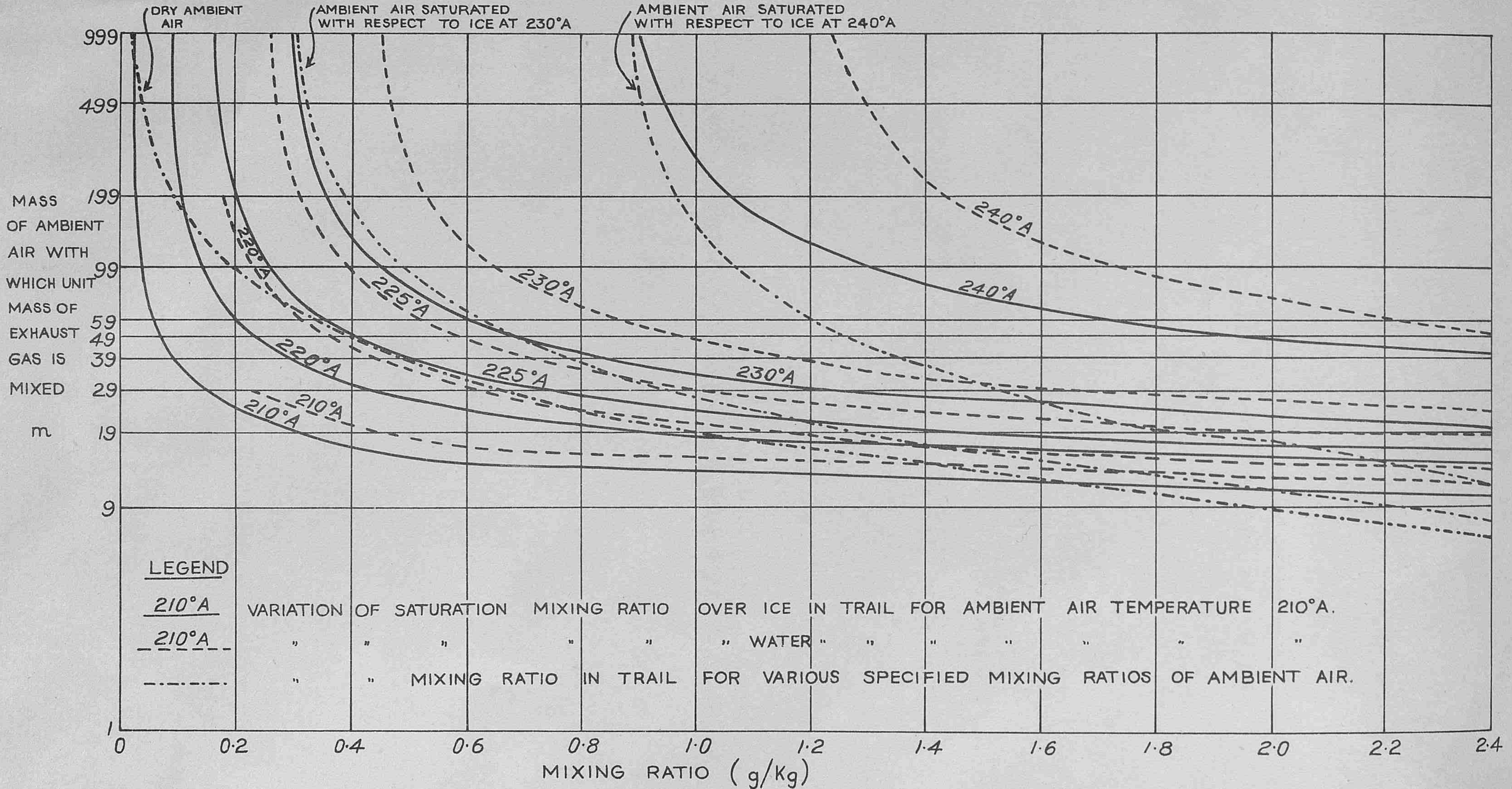

FIG. I. CONDITION IN EXHAUST TRAIL AT 200mb.

M.R.P. 991
S.C.111/211
14th June, 1956.

AD 147512

Droplet sampling in cumulus clouds.

by

AD147512

W. G. Durbin.

(Meteorological Office)

AIR MINISTRY

METEOROLOGICAL RESEARCH COMMITTEE

At the time of issue this report has not been published. Any author desiring to quote this paper should refer to it as "A paper of the Meteorological Research Committee (London) M.R.P. No. 991 by Mr. W.G. Durbin. A copy is available in the Library of the Meteorological Office."

M.R.P.991
S.C.III/211
14th June, 1956

AIR MINISTRY

METEOROLOGICAL RESEARCH COMMITTEE

Droplet sampling in cumulus clouds

by
W. G. Durbin (Meteorological Office)

Summary

An analysis is made of 150 impactions of cloud droplet samples made in cumulus clouds varying in vertical depth from 750 to 7,000 ft.

From a consideration of the spectra (meaned for each cloud) relating droplet number with droplet diameter, a mode diameter of about 8 microns is found. A secondary mode diameter of about 15 microns is in evidence in some clouds and this is considered to be associated with cloud development. Numbers of droplets per cm.^{3} are in the main between 100 and 300 though extreme values of 19 and 976 occur.

Spectra relating water content with droplet diameter show that in clouds between about 750 and 2,500 ft. thick the bulk of the liquid water is contained in droplets of about 8 microns diameter whereas in clouds between about 4,000 and 7,000 ft. thick the mode diameter is about 18 microns. The highest value of water content found is 4.97 gm.m^{-3}.

Evidence is found that mean volume diameter and water content tend to increase with height and that high values of water content are due to larger droplets rather than to greater numbers of droplets per cm.^{3}.

A droplet distribution formula given by Best is examined and the constants involved are found to depend on the largest size of droplet present.

Contents

1. Introduction

2. Experimental technique

3. Observations

4. Results

4.1. Variation between samples

4.1.1. Variation with regard to droplet size and number between the different samples on one selected flight (no. 7)

4.1.2. Consideration of the droplet diameters above which 10% of the droplets, obtained as averages for each flight, remain

4.1.3. Discussion of the spectra relating droplet diameter and droplet number

(a) for the individual clouds
(b) for two groups of clouds, 750-2,500 and 3,850-7,000 ft. thick respectively.

/4.1.4.

4.1.4. Variation with regard to water content between different samples on one selected flight (no. 7)

4.1.5. Consideration of the droplet diameters below which and above which 10% of the liquid water, obtained as averages for each flight, is contained

4.1.6. Discussion of the spectra relating droplet diameter and water content

(a) for the individual clouds

(b) for two groups of clouds 750-2,500 and 3,850-7,000 ft. thick respectively.

4.2. Variation of parameters

4.2.1. Variation of mean volume diameter with height

4.2.1.1. For clouds 6,000 - 7,000 ft. thick

4.2.1.2. For clouds 4,000 - 5,000 ft. thick

4.2.1.3. For clouds less than 2,500 ft. thick

4.2.1.4. Development of a cumulus cloud with time

4.2.2. Variation of water content with height

4.2.2.1. For clouds 6,000 - 7,000 ft. thick

4.2.2.2. For clouds 4,000 - 5,000 ft. thick

4.2.2.3. For clouds less than 2,500 ft. thick

4.2.2.4. Comparison of theoretically computed values of water contents with observed values

4.2.3. Variation of number of droplets per cm.^{3} with height

4.2.4. Variation of water content with mean volume diameter for different values of the number of droplets per cm.^{3}

4.3. Consideration of the applicability of a formula given by Best relating diameter of droplets and the quantities of water contained by them

5. Discussion

6. Acknowledgments

7. References

1. Introduction

On eight days between June and September 1951 ten flights were made in a Hastings aircraft of the Meteorological Research Flight for the purpose of taking samples of cloud droplets in cumulus clouds. In this paper the results of the flights are examined, summarized and compared with the results of other workers.

2. Experimental technique

The method of sampling was similar to that described by Mazur (1) and an account of its use in stratocumulus clouds has been given by Frith (2).

The aircraft impactor shown in fig.1 contains a slot into which a glass slide can be fitted and a shutter mechanism which can expose the slide for a certain time interval (in this case 1/75th sec.). The impactor was pushed through a hole in the window near the second pilot's seat and, when flying in a suitable cloud, operation of the shutter would expose the slide to the cloud droplets. The slides had previously been coated with a layer of magnesium oxide and the effect of droplets striking this layer was to give rise to small pits. After each flight the slides were microphotographed and a count made of the number of pits with diameters falling within certain specified limits.

It has been estimated(3) that a pit of diameter "a" is due to a droplet of diameter ".713a".

The flights were made in cumulus clouds varying from about 1,000 to 7,000 ft. in vertical extent. In the thicker clouds samples were generally taken at height intervals of 1,000 ft. whereas in the thinner clouds samples were generally taken at intervals of about 100 ft., and several samples were taken at the same height. In all 150 samples were taken during the ten flights.

The camera used to photograph the slides consisted in part of a microscope and a graticule on which were a number of circles of decreasing diameter. These diameters were related by $D = D_o.2^{N/2}$ where D is the diameter of the circle and N = 0, 1, 2, 3 etc. From this expression it will be seen that the areas of the circles are in geometric progression of common ratio 2. A photograph of the graticule was superimposed on each droplet sample, the actual diameters of the graticule circles being a function of the focal length of the microscope objective lens. The droplet diameters corresponding with the series of graticule circles were 5.28, 7.48, 10.41, 14.95, 21.39, 29.95, 42.10, 59.90, 84.0 and 119.0 microns after making allowance for the factor 0.713 mentioned above.

The first step in analysing the photographs of the samples of cloud droplets was to count the numbers of droplets of different sizes. The counts were made by assessing the numbers of droplets within categories which, as far as could be judged by eye, had approximately the same diameters as the graticule circles and assuming that the graticule diameters were the mean diameters within those categories. The series of diameters given above should cover the following ranges.

TABLE 1

Size category	Diameter of graticule circle x.713 (microns)	Spread of diameters (microns)	True range within the category (microns)	Mid point of range (microns)
0	0	0-2.64	2.64	1.32
1	5.28	2.64-6.38	3.74	4.51
2	7.48	6.38-8.95	2.57	7.67
3	10.41	8.95-12.68	3.73	10.81
4	14.95	12.68-18.17	5.49	15.43
5	21.39	18.17-25.67	7.50	21.92
6	29.95	25.67-36.02	10.35	30.85
7	42.10	36.02-52.0	15.98	44.01
8	59.9	52.0-72.0	20.00	62.0
9	84.0	72.0-101.5	29.50	86.7
10	119.0	101.5-146.5	45.00	124.0

It will be seen from the second and last columns of Table 1 that the sizes used are smaller than the mid-values of the ranges they actually cover (except in the case of the smallest sizes 0 and 5.28). The reason for the differences of course lies in the form of the microscope graticule which does not provide for an arithmetical progression of diameters. Mean diameters, mean volume diameters and water contents are therefore biased towards lower values by using the graticule diameters as mean diameters. This is, however, a bias in the right direction since the average cloud droplet sample is one in which there are more smaller droplets than bigger droplets and the mean diameter of a number of droplets having diameters lying between certain limits should, on the average, be less than the mean of the limits. The assumption made that the graticule diameters could be taken as the mean diameters is therefore felt to be justified, within the accuracy of the size estimations.

3. Observations

The summary of the information available is given in Table 2. This shows the numbers of samples taken together with the lowest and highest levels of sampling, the object being to obtain samples throughout the depth of cloud on each flight. In addition a column is given listing the numbers of samples containing a minimum of 200 droplets, a value considered adequate for statistical purposes. The last column lists the number of samples in which no cloud droplets having diameters greater than 80 microns were found, this value being infrequently exceeded.

TABLE 2

Flight no. and date	Sampling levels		Sampling depth ft.	Numbers of samples		
	Lowest ft.	Highest ft.		Total taken	Containing at least 200 droplets	Containing no droplets having diameters $> 80\ \mu$
1 19/6/51	3,900	10,020	6,120	9	9	9
2 26/6/51	5,000	12,000	7,000	7	7	7
3 17/7/51	3,300	4,050	750	16	14	16
4 24/7/51	3,450	5,400	1,950	10	9	10
5 25/7/51	3,200	5,460	2,260	14	14	14
6 17/9/51	5,200	6,150	950	21	19	19
7 24/9/51	2,950	6,800	3,850	22	10	22
8 26/9/51	2,050	4,560	2,510	17	13	17
9 26/9/51	3,460	8,450	4,990	12	7	6
10 26/9/51	3,980	8,850	4,950	22	20	16
			Total	150	122	136

All the detailed data are listed in Table 4 which gives for each flight

(a) Height and temperature at which the sample was taken.

(b) The percentage number of droplets in each of the categories 1 to 10 in Table 1. To avoid the effect of varying airspeed these have been expressed in each case as a percentage of the total number of droplets on the sample rather than actual numbers counted.

(c) Derived data including mean diameter, mean volume diameter, number of droplets per cm.^3 of air and cloud water content. In the calculation of these values the collection efficiency of the impactor was assumed to be unity.

(d) The constants "a" and "n" in a formula given by A.C. Best(4) for typical droplet distributions. Their derivation is discussed more fully below.

(e) Observations noted at the time the sample was taken. These include estimations of the position of sampling in the cloud, visibility and the intensity of precipitation. The absence of a report of precipitation means that no precipitation occurred but the absence of any other remark is due to the observation not having been made.

4. Results

The results are treated in three main sections

/(1)

(1) A general statistical analysis and discussion of the droplet number and water content distributions obtained as averages during each flight.

(2) The variation with height of the droplet diameters, numbers of droplets and water contents in each cloud.

(3) The applicability of a formula given by A.C. Best to the size distributions obtained.

4.1 Variation between samples

4.1.1. It is immediately obvious from Table 4 that there is little consistency between different samples. For example in flight 7, most samples contain droplets in category 6 (29.95 microns), only 7 contain droplets in category 7 (42.10 microns) and only one contains droplets in category 8 (59.9 microns). On the other hand one sample taken on this flight, no. 78, contains no droplets having diameters bigger than 10.41 microns. Furthermore, there is no consistency between the corresponding figures for samples taken at or within 100 ft. or so of the same height. Considered as a whole, the droplet distributions show how greatly the droplet content of a cumuliform cloud differs from point to point in both the horizontal and vertical.

4.1.2. Table 3 shows the droplet sizes below which are contained 10% and 90% of the total number of droplets. The flights are arranged in order of sampling thickness.

TABLE 3

Droplet sizes below which are contained 10% and 90% of total number of droplets

Flight	3	6	4	5	8	7	10	9	1	2
Sampling thickness ft.	750	950	1,950	2,260	2,510	3,850	4,950	4,990	6,120	7,000
					Microns					
10%	4.0	4.7	4.0	3.4	4.0	4.8	5.3	3.9	6.0	5.7
90%	11.0	17.0	9.3	16.3	18.3	15.0	21.0	28.0	17.6	14.5

These figures show the range of sizes in which are contained 80% of the total number of droplets. It will be seen that 10% of the droplets are of sizes less than 3-6 microns, but 10% are also comprised of droplets greater than between about 9 and 28 microns. It must be borne in mind however that the sampling efficiency of the impactor has been considered to be unity whereas in fact, its efficiency of catch for droplets smaller than about 3 microns is very low.

4.1.3. To examine the mean droplet spectra of these clouds it was first necessary to make the ranges appropriate to each size equal. This was done by dividing the mean percentages in each category, given in Table 4, by the appropriate range of diameters. The figures obtained are given below in Table 5, the flights being arranged in order of sampling depth, and are also plotted in fig. 2(a). The areas under the curves of fig. 2(a) are therefore equal, and correspond numerically to 100 droplets.

/TABLE 5

TABLE 5

Mean percentage numbers of droplets per unit range

Category

Flight no.	No. of samples	Sampling depth ft.	1	2	3	4 (size)	5	6	7	8	9	10
			5.28	7.48	10.41	14.95	21.39	29.9	42.1	59.9	84.0	119.0
3	16	750	5.52	12.43	7.80	3.28	0.04	.001	.0006	.0005		
6	21	950	3.22	7.49	5.96	5.50	1.51	0.34	.066	.0015	.0017	
4	10	1,950	7.45	13.86	8.55	0.81	0.01					
5	14	2,260	5.71	7.77	5.63	4.45	1.42	0.20	.0257	.0025		
8	17	2,510	5.67	14.58	5.05	3.19	0.56	0.06	.006			
7	22	3,850	5.32	7.70	4.47	3.55	2.34	0.04	.0025	.0005		
10	22	4,950	2.54	6.09	4.29	5.70	2.51	0.54	0.110	.047	0.0085	.0002
9	12	4,990	4.63	6.50	3.43	3.77	2.04	0.84	0.200	0.200	.037	.0022
1	9	6,120	1.30	9.09	7.07	4.48	2.34	0.29	0.010			
2	7	7,000	1.64	8.34	9.10	5.35	1.18	0.23				

It appears that there is a wide variation of mean distributions between the different clouds sampled. Considering the shapes of the mean spectra in fig.2(a), it is seen that they generally have a single maximum and a variable amount of positive skew, while some have, or tend to have, a secondary maximum at a diameter greater than that of the primary one.

The peaks of these curves are given below in Table 6 in which the flights are arranged in order of increasing thickness of clouds sampled.

TABLE 6

Most common droplet sizes for each of the ten flights

Flight	3	6	4	5	8	7	10	9	1	2
Sampling depth (ft.)	750	950	1,950	2,260	2,510	3,850	4,950	4,990	6,120	7,000
Size (microns)										
Primary maxima	8	8½	8	7½	7½	7½	8	7½	7½	9
Secondary maxima							15	15		

It will be seen from Table 6 that each of the curves of fig.2(a) has its primary mode at about 8 microns, irrespective of cloud depth. In two cases secondary maxima occur at about 15 microns. It should be noted that although the secondary maxima tend to be more evident in the clouds of greatest depth this is not always so and presumably other factors as well as depth contribute to the nature of these spectra.

On the whole there is a tendency for the curves for the thinner clouds to be narrower and to have higher peaks than those for the thicker clouds and it seems that the smallest droplet sizes are more frequent in the thinner clouds. This can be better illustrated by combining the flights into two groups.

(a) Flights 3, 6, 4, 5 and 8 which have sampling depths between about 750 and 2,500 ft. and

(b) Flights 7, 10, 9, 1 and 2 which have sampling depths between 3,850 and 7,000 ft.

The average distribution in these two groups is given in Table 7 and is plotted in fig.3(a).

/TABLE 7

TABLE 7

Weighted mean of figures shown in Table 4 for two ranges of cloud thickness

Clouds with sampling depths between	Category 1	2	3	4	5	6	7	8	9	10
(a) 750 and 2,500 ft.	5.21	10.91	6.41	3.75	0.79	0.14	0.024	0.0045	0.0003	
(b) 3,850 and 7,000 ft.	3.49	7.24	5.02	4.53	2.29	0.48	0.069	0.047	0.0084	0.0004

In the above table the figures for categories 7 to 10 have been taken to 3 and 4 decimal places simply to facilitate comparison of the corresponding figures in the two groups. From fig.3(a) it will be seen that the mode diameter is about the same for the two groups of clouds, being about 8 microns. It is of interest to note that significant numbers of droplets of at least 60 microns diameter can exist on occasion in even the thinnest clouds, about 0.1% of the droplets having diameters greater than 60 microns in clouds of 750 to 2,500 ft. thickness. When the cloud depth increases to between about 4,000 and 7,000 ft. the proportion of these large droplets also increases, about 1% having diameters greater than 60 microns.

4.1.4. The next step in the analysis was to calculate the percentage volume of water in the different size ranges. To avoid presenting another large table of the size of Table 4, a typical result, for one flight only (Flight 7, which contains a large number of samples) is given in Table 8. This shows the percentage of water in the different range categories. There is a tendency for samples taken in the lower part of the cloud to have higher percentages of water content composed of small droplets and lower percentages composed of large droplets than in the upper part of the cloud.

TABLE 8 (From the results of Flight 7)

Percentages of water contents in the different size ranges

Sample no.	Height ft.	Category 1	2	3	4	5	6	7	8	9
78	2,950	28.0	56.5	15.5						
79	3,100	1.7	7.0	15.7	42.3	24.9	8.4			
80	3,400	0.3	5.7	17.1	40.0	27.5	9.4			
81	3,400	12.8	25.0	16.7	34.4	11.1				
82	3,900	0.5	3.9	13.9	25.1	28.0	10.9	0.0	17.7	
83	4,000	1.2	5.1	14.7	30.0	38.2	10.8			
84	4,500	1.3	3.2	15.0	35.6	35.9	9.0			
85	4,500	0.04	0.3	1.5	9.1	45.2	43.8			
86	4,600	0.5	1.7	7.3	23.3	54.7	12.5			
87	4,600	3.1	4.6	3.9	12.5	50.6	25.3			
88	5,000	0.9	1.4	3.7	20.2	59.0	14.8			
89	5,100	0.01	0.4	1.2	10.9	47.0	30.9	9.6		
90	5,200	0.9	1.8	3.2	8.6	50.1	24.2	11.2		
91	5,550	1.8	2.7	4.6	23.3	45.9	21.7			
92	5,650	0.3	0.4	1.7	16.4	44.3	22.7	14.2		
93	5,950	0.9	2.7	9.0	14.1	36.1	29.1	8.1		
94	6,050	0.1	1.1	2.0	13.8	44.4	38.6			
95	6,200	0.3	0.9	1.4	11.2	62.7	23.5			
96	6,200	2.3	3.1	6.3	20.6	44.7	23.0			
97	6,700	0.0	0.3	1.3	3.5	27.0	48.6	19.3		
98	6,700	0.1	0.6	0.9	11.0	48.0	29.2	10.2		
99	6,800	0.4	2.8	6.0	14.7	25.6	31.7	18.8		
Means		2.61	5.96	7.39	19.12	38.68	21.28	4.15	0.80	

/4.1.5.

4.1.5. In the same way as for the size-number analysis, cumulative mean water content curves were plotted. These are not reproduced but the droplet diameters below which are contained 10% and 90% of the total water are listed below in Table 9, the flights again being arranged in order of increasing sampling thickness.

TABLE 9

Droplet sizes below which are contained 10% and 90% of the total water content

Flight	3	6	4	5	8	7	10	9	1	2
Sampling thickness ft.	750	950	1,950	2,260	2,510	3,850	4,950	4,990	6,120	7,000
					Microns					
10%	5.5	9.0	4.0	8.0	5.5	8.0	11.5	15.5	8.0	8.0
90%	14.0	47.0	11.0	17.5	19.0	25.5	48.0	73.0	24.0	18.0

These figures, which are given to the nearest 0.5 micron, show the range of sizes in which is contained 80% of the total water content. It will be seen that 10% of the water is composed of droplets having diameters less than a value lying between 4 and 16 microns and 10% is composed of droplets having diameters greater than a value between 11 and 73 microns. In the case of water content the effect of assuming that the efficiency of catch of the impactor is urity does not give rise to appreciable inaccuracy in the figures quoted in the 10% row of Table 9, because the quantity of water contained in droplets which the impactor will not collect is a very small percentage of the total water content.

4.1.6. In order to examine the mean spectra of water content in the different size ranges for the various flights, Table 10 and fig.2(b) have been prepared. In a similar manner to Table 5, Table 10 is in terms of mean percentage water content per unit diameter range to allow comparison of water contents at different diameters.

TABLE 10

Mean percentages of water content per unit diameter range for each of the ten flights

Flight no.	Sampling depth (ft.)	Category 1	2	3	4	5	6	7	8	9	10
3	750	1.69	8.33	7.55	6.51	0.55	0.03	0.12	0.09		
6	950	0.36	2.14	2.43	4.95	3.09	1.43	0.57	0.29	0.13	
4	1,950	4.62	10.83	10.57	2.65	0.13					
5	2,260	0.50	1.91	3.39	5.68	3.78	1.30	0.37	0.08		
8	2,510	2.49	12.05	4.94	4.40	1.29	2.06	0.19			
7	3,850	0.70	2.32	1.98	3.48	5.16	1.51	0.26	0.004		
10	4,950	0.12	0.70	1.28	4.94	3.64	2.10	0.74	0.38	0.15	0.03
9	4,990	0.05	0.20	0.32	1.29	2.13	1.18	0.67	1.10	0.51	0.19
1	6,120	0.10	2.65	4.76	4.69	4.55	0.20	0.17			
2	7,000	0.11	2.13	6.90	7.04	3.67					

Compared with fig.2(a), fig.2(b) exaggerates the effect of the large droplets compared to the small since the ordinate is proportional to the cube of the diameter. Plotted in this way the droplet diameter corresponding to maximum water content does not always have a well defined mode. Diameters corresponding to peak water contents are listed in Table 11.

TABLE 11

Flight no.	3	6	4	5	8	7	10	9	1	2
Sampling thickness ft.	750	950	1,950	2,260	2,510	3,850	4,950	4,990	6,120	7,000
Diameter for peak water content (microns)	8	15	7½	15	7½	21	15	23	10	13

These values are in general considerably larger than the mode diameters for the number distributions. A comparison of the flights made in clouds with depths of 750 - 2,500 ft. and 3,850 - 7,000 ft. has been made for water content distribution with diameter in the same way as for the droplet number distributions above.

The average distribution in these two groups is given in Table 12 and is plotted in fig.3(b).

TABLE 12

Weighted mean of figures shown in Table 10 for two ranges of cloud thickness

Clouds with sampling depths between	Category 1	2	3	4	5	6	7	8	9	10
(a) 750 and 2,500 ft.	1.67	6.64	5.27	4.99	1.92	0.71	0.29	0.11	0.03	
(b) 3,850 and 7,000 ft.	0.91	1.49	2.32	3.92	3.97	1.61	0.41	0.31	0.13	0.03

The results in fig.3(b) show that as the sampling depth is increased, the water content spectrum as a whole moves towards the larger droplet diameters, maxima occurring respectively at about 8 microns and 18 microns. The water contained in droplets of diameter greater than 60 microns is similarly about 3.2% and 11.4% (corresponding to 0.1% and 1.0% in the number distributions.)

4.2. Variation of parameters

Another method of investigating the variations of droplet size and number in clouds is by computing the following parameters:-

(a) Mean droplet diameter (microns)

(b) Mean volume diameter (microns)

(c) No. of droplets per cm.^{3}

(d) Water content (gm.m^{-3})

and considering the variations in these for each cloud.

(The mean volume diameter of a sample is defined to be the diameter of a droplet which contains the mean of the total volume of water in the sample.) The water content was computed from a knowledge of the area of the sample, the airspeed and the time of exposure.

These parameters were computed for all the samples and the values are given in Table 4. The first part of the subsequent analysis is devoted to a consideration of the variation of these parameters with height. The variations of mean diameter and mean volume diameter are clearly in the same direction and differ only in magnitude. A detailed analysis of the two parameters separately is therefore unnecessary and in what follows only the variations with height of the mean volume diameters are considered. Apart from numerical values the conclusions from this analysis may be considered to apply to both parameters.

4.2.1. Variation of mean volume diameters with height

Fig.4 shows graphs of mean volume diameter against height of sample for the ten flights. It is pointed out that it would only be possible to obtain a true indication of the vertical variation of any one of the above parameters if there were no variation in the horizontal or with time. It is largely a matter of chance whether a particular sample be taken in a thin or dense region of the cloud so that to obtain a representative indication of the variation with height it would be necessary to take a large number of samples at each level. This would enable mean values to be calculated for each level but the procedure is still not entirely satisfactory unless several aircraft make simultaneous measurements at different heights. Also, one must be certain that one has taken all the samples in the same cloud. It is often possible with isolated large cumulus clouds to confine sampling to one cloud but not, as a rule, with small clouds. Furthermore, if the tops of the cumulus clouds vary, samples taken at the same level are possibly associated with cells in different stages of development. The sampling in any one cloud took about 30 min. so that the curves cannot be regarded as representative of a particular stage of development.

4.2.1.1. The data here available do not meet the above requirements, and in particular fewer samples were taken in the two largest clouds than in the smaller ones. In fact, on those flights (1 and 2) for which the cloud depths were about 6,000 and 7,000 ft. respectively, only 9 and 7 samples were taken. These however are plotted in figs. 4(a) and 4(b) and from the curves (which were drawn by eye) there appears to be a definite tendency for the mean volume diameter to increase with height. Values near the base of the cloud are about 10 microns and they increase to about 17-20 microns near the top of the cloud.

4.2.1.2. Figs.4(g), (j) and (k) show the results for cumulus clouds between about 4,000 and 5,000 ft. thick. The 22 values plotted in fig.4(g) again display a definite tendency for mean volume diameters to increase with height. The 11 values plotted in fig.4(j) show no such tendency however, though the tendency is again perceptible in fig.4(k). The overall variation of mean volume diameter with height in these clouds is from 7 - 13 microns at the base to 23 - 27 microns at the top so that on the whole it seems from these data that droplet size does increase with height. However, it can be seen that although the average values in these clouds did not exceed about 30 microns, some much larger values of mean volume diameter were found on Flights 9 and 10 and precipitation was reported in the cloud on both of these flights. Fig.7 shows a photograph of the sample in Flight 10 in which the mean volume diameter was 40.34 microns.

4.2.1.3. Figs.4(c), (d), (e), (f) and (h) show the plots of mean volume diameters against height for small cumulus clouds of less than 2,500 ft. thickness. The evidence of an increase of mean volume diameter with height is not as pronounced as with the thicker clouds but is nevertheless there in all cases except fig. 4(f) where, probably due to the shallowness of the sampled layer, the results merely portray a large scatter. The overall variation is between about 5 and 20 microns though fig.4(d) contains none greater than about 11 microns and fig.4(f) contains two values of about 25 and 27 microns.

4.2.1.4. Figs.4(h), (j) and (k) represent plots of the values of samples taken in the same area and general synoptic conditions, those of 4(h) and 4(j) in the morning with a time interval of about 1½ hours and 4(k) in the afternoon another 3 hours later. These three flights therefore give some indication of the development of the droplet sizes throughout a summer day with the cloud depth increasing from about 2,500 ft. to 5,000 ft. and producing precipitation. Cloud top temperature in the case of Flight 10 was 29°F. and it seems likely that only the coalescence and not the Bergeron mechanism was operating to produce the rainfall.

4.2.1.5. In all these clouds values of mean volume diameter similar to those found near the top of the cloud can exist in the lower regions. Furthermore, due presumably to factors of change with time and space and the general inhomogeneity of the cloud, there is a large scatter from any mean curves drawn through the values.

4.2.2. Variation of water content with height

The same considerations as outlined for the analysis of mean volume diameters apply to water contents, the results of which are plotted in fig.5.

4.2.2.1. Figs.5(a) and 5(b) show the results for the two flights made in cumulus clouds 6,000 and 7,000 ft. thick. Fig.5(b) shows some slight evidence of a systematic increase with height but fig.5(a) does not. In both cases, however, the largest values are found in the upper regions of the cloud. In the main, water contents varied between 0.25 and 0.62 $gm.m^{-3}$ in fig.5(a) and between 0.17 and 0.28 $gm.m^{-3}$ in fig.5(b). However, a value of 1.07 $gm.m^{-3}$ occurred near the top of the cloud in fig.5(a) and values of 0.55 and 0.71 $gm.m^{-3}$ were found near the top of the cloud in fig.5(b). Summarising, the water contents in these two clouds of 6,000-7,000 ft. thickness largely lay between 0.2 and 0.6 $gm.m^{-3}$, but 1.1 $gm.m^{-3}$ was found on occasion. It must be remembered, however, that these results were obtained from only two flights in which only 16 samples were taken.

4.2.2.2. The results for medium sized cumulus cloud (4,500 - 5,000 ft. thick) are plotted in figs.5(g), (j) and (k). Fig.5(g) shows some tendency for water content to increase with height though the scatter is large. The overall variation is from about 0.025 to about 0.35 $gm.m^{-3}$ but the highest value of 0.55 $gm.m^{-3}$ occurs near the top of the cloud. For the 12 results plotted in fig.5(j), no really satisfactory curve can be drawn. Five of the results point to a slight increase with height while the other seven indicate local high values at all levels of the cloud. However the highest values are again found near the top of the cloud. Of the 22 samples plotted in fig.5(k), 19 lie between about 0.05 and 1.1 $gm.m^{-3}$ while the remaining three show very much larger values. Of these three, the value of 4.97 $gm.m^{-3}$, which is the highest value of water content found in M.R.F. by the method of cloud droplet sampling, again occurs near the top of the cloud which was precipitating at the time. On the whole in these four clouds the water content varied between about 0.1 and 1 $gm.m^{-3}$ with local extreme values, one of which reached almost 5 $gm.m^{-3}$. The overall variation of water content in these cumulus clouds was significantly different from one cloud to another. Where the variation throughout the greater part of the cloud was large, the local extreme values were also large.

4.2.2.3. The results for small cumulus clouds, considered as being less than 2,500 ft. thick, are plotted in figs. 5(c), (d), (e), (f) and (h). There is little, if any, indication of an increase in the values of water content with height but in view of the scatter obtained in thicker clouds this is hardly surprising. An interesting feature of fig.5(f) is that the average values of water content are fairly high although the cloud is only about 1,000 ft. thick.

It is concluded from the results for the small cumulus clouds that the variation of water content within different clouds is different from cloud to cloud and, from fig.5(f), that comparatively large values can occur in thin clouds. In the main values of water content varied between about 0.01 and 0.5 gm.m^{-3} but values up to 1.4 gm.m^{-3} also occurred.

4.2.2.4. In order to see how the observed values of water content compared with the theoretical adiabatic values, the latter were computed using cloud base temperatures from the flight data (where given) or from the relevant Te-Phi-gram and the values are plotted as full line curves in fig.5. It will be seen that on the whole computed values of water content are greater than the observed values but this is not always the case. For example, some of the observed values on flights 9 and 10 were greater than the calculated values but this could be explained by the fact that it was raining in these clouds. On the other hand although no rain was reported in the cloud sampled on flight 6 (which was only 1,000 ft. thick) a large number of values of water content greater than the theoretical adiabatic values were observed in the lowest 500 feet.

Adiabatic values of water content necessarily increase uniformly from zero at the cloud base to a maximum value at the cloud top and would strictly be found only in those regions of the cloud in which no entrainment, mixing or precipitation occurs.

Mixing and entrainment will cause the actual values to be less than those calculated from adiabatic ascent in which there is no interchange of air between the rising cloud mass and the environment, and therefore lower values of water content would suggest some interchange. As most of the values observed are lower it seems likely that this interchange in fact occurs over most of the cloud, although not necessarily everywhere within it. On the other precipitation would normally result in some increase of the values lower down at the expense of the higher regions. The extent of any mixing and precipitation obviously depends on many factors such as speed of updraughts, state of development and age of the cloud so that all that can be concluded safely from these results is that the application of calculated water contents to given clouds is at the best a rough process and in the main except where there is precipitation will usually lead to over estimates.

4.2.3. Variation of the number of droplets per cm.^{3} with height

Graphs showing the variation of numbers of droplets per cm.^{3} with height are shown plotted in fig.6. There was nowhere any evidence of a systematic variation with height and in the main there were between 100 and 300 droplets per cm.^{3} in any of the clouds. However, local extreme values, as high as 976 cm.$^{-3}$ and as low as 19 cm.$^{-3}$ occurred and there was a tendency for higher values to be found near the base of the cloud.

4.2.4. Variation of water content with mean volume diameter and number of droplets per cm.^{3}

The relationship between mean volume diameter "D", and water content "W" and number of droplets per cm.^{3} "N" is evidently

$$W = \frac{\pi}{6} N D^3$$

Curves of W against D for different values of N are shown superimposed on the plotted points for the 150 samples in fig.8 giving an overall presentation. A mean curve, shown dotted, has been drawn through the points. It will be seen that the mean curve differs very little from the curve corresponding to N = 150 for mean volume diameters greater than about 20 microns and that all but 4 of the 150 samples lie between the curves for N = 25 and N = 500. The mean curve shows that the tendency is for higher values of water content to be due to higher values of mean volume diameter rather than higher values of number of droplets per cm.^{3}.

4.3. An examination of Best's equation for the droplet distribution in clouds

An equation suggested by Best(4) which is frequently used to relate

/quantities

quantities of water and droplet size within a cloud is

$$1-F = e^{-\left(\frac{d}{a}\right)^n}$$

where F is the fraction of liquid water comprised of droplets with diameters less than "d" and where "a" and "n" are constants. The equation can be rewritten in the form

$$\log_{10} \log_{10} \frac{1}{1-F} = n\log_{10} d - (n\log_{10} a + 0.3617)$$

which represents a straight line of slope n. The constant "a" is easily seen to be the value of d for which $\log_{10} \log_{10} \frac{1}{1-F} = -0.3617$ (or $\bar{1}.6383$).

To find values of the constants "a" and "n" values of $\log_{10} \log_{10} \frac{1}{1-F}$ were plotted against $\log_{10} d$ (d having the values 6.38, 8.95, 12.68 etc. as given in Table 1 for the upper limits of the ranges covered by the graticule circles) for all the samples.

For many of the samples the relationship between $\log_{10} \log_{10} \frac{1}{1-F}$ and $\log_{10} d$ was not that of a straight line but a curve. For most of the samples however, the curvature was not very great and it was possible to draw the best straight lines through the points fairly accurately by eye. (It was not considered worthwhile to undertake the task of computing the best straight lines by the method of least squares.) Fig.9 shows plots of $\log_{10} \log_{10} \frac{1}{1-F}$ against $\log_{10} d$ for the 9 samples of Flight 1.

For the largest droplet size present, F = 1 and $\log_{10} \log_{10} \frac{1}{1-F}$ = infinity. If F be taken as 0.99 the value of $\log_{10} \log_{10} \frac{1}{1-F}$ drops to 0.301.

Hence, for values of F approximately equal to 1, a very small change in F makes a significant difference to the nature of the curve. For this reason it was decided that the point corresponding to the largest droplet size present was unrepresentative and was not used in assessing the best straight lines. The percentage of water considered was therefore that for values of $\log_{10} \log_{10} \frac{1}{1-F}$ up to the greatest but one size.

Within the above restrictions it was possible to obtain values of "a" and "n" for 108 of the 150 samples. For the remaining 42 samples the curvature was considered too great to merit drawing straight lines. The main reason for this appears to be because the largest droplets of some samples, while being small in number, have a large size range. Deviations from a straight line will, however, always occur to some extent.

The 108 values of "a" and "n" are listed in Table 4. Mean values are also given for all the samples in each flight and the mean values for all the 108 samples were "a" = 23.0 and "n" = 5.1.

In an attempt to correlate the values of the two constants with other parameters graphs were plotted of the constants against (1) water content, (2) number of droplets per cm.^{3} and (3) maximum diameters. It was found that

(1) "a" increased in a fairly regular manner and "n" decreased in a most irregular manner with increasing water content,

(2) "a" and "n" did not show any regular variation with number of droplets per cm.^{3},

(3) "a" increased almost linearly and "n" decreased rather irregularly with increasing maximum droplet diameter.

/Graph

Graphs showing the variations of "a" and "n" with maximum droplet diameter and water content are reproduced in fig.10. The most useful of the four curves (which were drawn by eye) is that shown in fig.10(a) from which it will be seen that the points lie fairly close to a straight line of slope $3/2$ which passes through the origin. It therefore seems that in practice a good approximation to the value of the constant "a" is about $2/3$ of the diameter of the largest droplet present. By way of confirmation, the 108 values of "a" have been listed, regardless of flight, under the representative diameters used, viz. 10.41, 14.95, 21.39 microns etc. The table obtained showed a scatter which was to be expected due to the representative diameters not being the true diameters as discussed in para. 2 and to different samples having different numbers of droplets at the maximum size. The complete table is not reproduced but the mean values are shown below in Table 13.

TABLE 13

Mean values of Best's constant "a" for different maximum droplet sizes

Maximum diameter (microns)	10.41	14.95	21.39	29.95	42.1	59.9	84	119
No. of samples	7	12	22	32	22	7	2	4
Mean "a" (microns)	7.3	12.05	14.45	22.0	25.42	43.4	52.5	70.7
Ratio $\frac{a}{D_{max.}}$	0.70	0.81	0.67	0.73	0.60	0.72	0.63	0.59

The weighted mean value of the ratio $\frac{a}{D_{max.}}$ by this method is 0.68 which agrees well with the value quoted above.

Compared with the variation of "a" with maximum droplet diameter, that of "n" is not as clearly defined. However it seems that a reasonable approximation to "n" can be obtained from fig.10(b).

It is possible to carry out a considerable amount of further statistical research on the variations of "a" and "n" with different parameters but there seems little to be gained by such an undertaking.

5. Discussion

Impactor techniques for cloud droplet sampling have been used by other workers (Mazur 1943(1), Diem 1948(5), Squires and Gillespie 1952(6)). The work of Squires and Gillespie in Australia was largely devoted to the presentation of a new type of cloud droplet impactor (which also used magnesium oxide coated slides) and results were given for only nine impactions taken at one level on one flight through a cumulus cloud from which precipitation fell. The highest value of water content found was 1.6 $gm.m^{-3}$ which is not in disagreement with values published in this report. However the largest value of the number of droplets per $cm.^3$ found was 93 and this seems rather small. The data given by Diem and Mazur have been analysed by Best(7). Mazur gives results from 11 flights in cumulus clouds but the greatest number of samples taken on any flight was only six. The largest mean water content he found was 0.49 $gm.m^{-3}$ and the largest mean value of the mean volume diameter was 17.3 microns. Diem's results which were obtained using an oil technique include only two flights in cumulus clouds with maximum values of water content and mean volume diameter of 0.21 $gm.m^{-3}$ and 17.1 microns respectively. The results of the present paper are not in disagreement with the results of these workers but, in virtue of the much greater number of samples examined, present a fuller picture of the processes.

The manner in which water is distributed in droplet form throughout a cumulus cloud depends primarily on the life and extent of the cloud. An exact analysis requires knowledge of the positions in the cloud at which the samples were taken and further requires that all samples be taken at the same time. The best that can be done to satisfy the first requirement is to state roughly the location within the cloud at which the sample was taken though this is not always obvious. The second requirement cannot be fulfilled at all and in consequence results which have been obtained using a single shot impactor must be treated with reserve especially when several samples are grouped together to obtain mean values which are considered to be representative of the cloud. It should also be remembered that impactors of the type used for this work and in quoted references tend to underestimate the numbers of very small droplets. This will affect droplet number distributions more than water content distributions.

However with these reservations in mind the following conclusions may be drawn from this report.

1. Mean spectra of droplet diameter against droplet number have a mode at about 8 microns. A secondary maximum at about 15 microns was partly in evidence in some clouds and fully evident in others.

The primary mode at 8 microns could suggest that condensation nuclei produce droplets which soon grow to this size though the reason why this should represent a preferred state is not clear. It is thought that the establishment of the secondary mode is associated with development within the cloud and occurs at the expense of the 8-micron diameter droplets by coalescence. In clouds of greater thickness than those examined it is possible that the secondary mode will be displaced towards larger droplet diameters.

2. If mean droplet diameter is plotted against water content it is found that for clouds between about 750 and 2,500 ft. thick the mode is at about 8 microns but for clouds between about 4,000 and 7,000 ft. thick the mode is at about 18 microns.

This increase of the mode diameter represents another aspect of development from a small cloud to a bigger one. Larger clouds have higher water contents and the bulk of the water is contained in larger droplets.

3. In clouds between 1,000 and 2,500 ft. thick about one droplet in 1,000 has a diameter larger than 60 microns and these large droplets account for about 3.2% of the liquid water. In clouds between about 4,000 and 7,000 ft. thick about one droplet in 100 has a diameter larger than 60 microns and accounts for about 11.4% of the liquid water.

4. Mean droplet diameters and mean volume diameters tend to increase with height, the latter having values of about 5-10 microns near cloud bases and 20-25 microns near cloud tops. Higher values occur locally within the cloud and values of about 45 microns have been noted in clouds between 4,000 and 5,000 ft. thick which were precipitating.

5. Water content tends to increase with height and to have larger values in thicker clouds. In the main, values are up to about 0.5 $gm.m^{-3}$ in clouds up to about 2,500 ft. thick and up to about 1.0 $gm.m^{-3}$ in clouds of up to about 7,000 ft. thick. Higher values occur locally however and a value of almost 5 $gm.m^{-3}$ has been observed in cloud between 4,000 and 5,000 ft. thick which was precipitating.

On the whole observed values of water content are less than adiabatic values and this is doubtless due to dilution. However, higher-than-adiabatic values occur and while in some cases this may be due to modification caused by precipitation within a cloud this is not always so. In general it seems that adiabatic values are an unreliable guide to the disposition of water within a cloud.

/6.

6. The number of droplets per cm.^{3} is in the main between 100 and 300 in most parts of cumulus clouds but there is a trend towards higher values near cloud bases.

7. Higher water contents in cumulus cloud appear to be due to larger droplets rather than to greater number of droplets per cm.^{3}.

8. The formula relating quantities of water and droplet diameter given by Best over-estimates the importance of the larger droplets in relation to the smaller droplets to such an extent that it was possible to obtain values of the parameters "a" and "n" for only about 70% of the samples. However it appears that the value of "a" is governed by the largest size of droplet on the sample and a good approximation to it may be taken as 2/3 of the diameter of the largest droplet. Similarly a reasonable estimation of the value of "n" can be obtained from its variation with maximum droplet diameter (fig.10(b)) though the nature of the variation is not as well defined as in the case of "a".

An examination of Best's formula has been made in a somewhat different manner by Boucher and Bartnoff (8). They found, considering the results of Diem, that on the whole both Best's formula and another derived by Atlas and Bartnoff(8) were valid. For large droplet diameters the contribution of the theoretical distribution function F given by Best was greater than for the observed distributions. This is in agreement with what has been stated above.

9. Future work in the field of cloud droplet distribution can more usefully be undertaken using a technique which allows continuous sampling during a traverse through a cloud. Neglecting the time taken for the aircraft to traverse the cloud, this will enable reasonably accurate investigations of the droplet distribution at a given level to be made and successive traverses at the same level would provide valuable information on cloud development. In particular such an instrument would be capable of checking the theory of Ludlam (9) which requires small numbers of large droplets (of order 40-60 microns diameter) in the base of a cloud to initiate precipitation. It is strongly recommended that time and effort be expended in the pursuit of such an instrument, possibly along the lines of an instrument described by Hacker (10). The possibility is being studied in M.R.F. but instrumentation and analysis involved in this project would be formidable.

6. Acknowledgments

The author wishes to acknowledge the help given by Messrs. M.J. Kerley and G.D. White in the arduous tasks of computation and preparation of tables.

7. References

1. Mazur, J. 1943 An investigation of the number and size distributions of water particles in natural clouds. Meteorological Research Papers, Air Ministry, London, No.109.

2. Frith, R. 1951 The size of cloud particles in stratocumulus cloud. Q.J. R.Met.Soc., Vol.77, No.333.

3. Levine, J. and Kleinknecht, K.S. 1951 Adaptation of a cascade impactor to flight measurements of droplet size in clouds. N.A.C.A. R.M. E51G05.

4. Best, A.C. 1951 Drop-size distribution in cloud and fog. Q.J. R.Met.Soc., Vol. 77.

5. Diem, M. 1948 Messing der Grosse von Wolken elementen II. Meteor. Rundschau, No.9/10.

/6.

6. Squires, P. and Gillespie, G.A. 1952 A cloud droplet sampler for use on aircraft. Q.J. R.Met.Soc., Vol.78, No.337.

7. Best, A.C. 1946 The size distribution of cloud particles. Meteorological Research Papers, Air Ministry, London, No.309.

8. Boucher, R.J. and Bartnoff, S. 1955 A comparison of theoretically derived and observed drop-size distributions in clouds and rain. Scientific Report No.4, Research Laboratory of Physical Electronics, Dept. of Physics, Tufts University.

9. Ludlam, F.H. 1951 The production of showers by the coalescence of cloud droplets. Q.J. R.Met.Soc., Vol.77.

10. Hacker, P.T. 1956 An oil-stream photomicrographic aeroscope for obtaining cloud liquid water content and droplet size distributions in flight. N.A.C.A. Tech. Note 3592.

Details of height, numbe

remarks for individ

Item no.			
1.	Sample No.	1.	2.
2.	Sampling height, ft.	3,900	4,300
3.	Temperature	-	-
4.	Total no. of drops	2,034	833
5.	Percentage no. of droplets in:-		
	Category 1. (5.28 microns)	-	1.80
6.	Category 2. (7.48 microns)	35.00	21.36
7.	Category 3. (10.41 microns)	55.06	54.26
8.	Category 4. (14.95 microns)	9.68	20.64
9.	Category 5. (21.39 microns)	0.24	1.92
10.	Category 6. (29.95 microns)	-	-
11.	Category 7. (42.10 microns)	-	-
12.	Category 8. (59.9 microns)	-	-
13.	Category 9. (84.0 microns)	-	-
14.	Category 10. (119.0 microns)	-	-
15.	No. of droplets cm.$^{-3}$	976	397
16.	Mean diameter (microns)	9.90	10.88
17.	Mean volume diameter (microns)	9.90	11.62
18.	Water content (gm. m.$^{-3}$)	0.50	0.33
19.	Best's constant "a"	13.8	-
20.	Best's constant "n"	3.7	-
	Remarks		
21.	Approximate position of sample	-	-
22.	Precipitation reported	-	-
23.	Estimated visibility (yd.)	-	-
24.	Additional remarks	-	-

at the same level would provide valuable information on cloud development. In particular such an instrument would be capable of checking the theory of Ludlam (9) which requires small numbers of large droplets (of order 40-60 microns diameter) in the base of a cloud to initiate precipitation. It is strongly recommended that time and effort be expended in the pursuit of such an instrument, possibly along the lines of an instrument described by Hacker (10). The possibility is being studied in M.R.F. but instrumentation and analysis involved in this project would be formidable.

6. Acknowledgments

The author wishes to acknowledge the help given by Messrs. M.J. Kerley and G.D. White in the arduous tasks of computation and preparation of tables.

7. References

1. Mazur, J. 1943 An investigation of the number and size distributions of water particles in natural clouds. Meteorological Research Papers, Air Ministry, London, No.109.
2. Frith, R. 1951 The size of cloud particles in stratocumulus cloud. Q.J. R.Met.Soc., Vol.77, No.333.
3. Levine, J. and Kleinknecht, K.S. 1951 Adaptation of a cascade impactor to flight measurements of droplet size in clouds. N.A.C.A. R.M. E51G05.
4. Best, A.C. 1951 Drop-size distribution in cloud and fog. Q.J. R.Met.Soc., Vol. 77.
5. Diem, M. 1948 Messing der Grosse von Wolken elementen II. Meteor. Rundschau, No.9/10.

TABLE 4

Details of height, number, size, water content, temperature and remarks for individual samples. Flight 1. 19/6/51

Item no.											Mean values
1.	Sample No.	1.	2.	3.	4.	5.	6.	7.	8.	9.	
2.	Sampling height, ft.	3,900	4,300	5,000	6,000	7,000	8,000	8,900	9,000	10,020	-
3.	Temperature	-	-	-	-	-	-	-	-	-	-
4.	Total no. of drops	2,034	833	335	899	449	538	400	489	528	-
5.	Percentage no. of droplets in:-										
	Category 1. (5.28 microns)	-	1.80	-	1.66	2.00	16.17	0.75	1.02	20.26	4.85
6.	Category 2. (7.48 microns)	35.00	21.36	8.95	43.15	24.72	22.11	5.50	18.40	31.06	23.36
7.	Category 3. (10.41 microns)	55.06	54.26	20.89	28.58	33.40	16.35	8.25	17.38	3.40	26.39
8.	Category 4. (14.95 microns)	9.68	20.64	24.47	22.24	35.41	28.25	40.75	38.24	1.89	24.61
9.	Category 5. (21.39 microns)	0.24	1.92	42.38	3.67	4.00	16.17	42.75	23.72	23.48	17.59
10.	Category 6. (29.95 microns)	-	-	2.98	0.44	0.44	0.55	2.00	1.22	19.31	2.99
11.	Category 7. (42.10 microns)	-	-	0.29	0.22	-	0.37	-	-	0.56	0.16
12.	Category 8. (59.9 microns)	-	-	-	-	-	-	-	-	-	-
13.	Category 9. (84.0 microns)	-	-	-	-	-	-	-	-	-	-
14.	Category 10. (119.0 microns)	-	-	-	-	-	-	-	-	-	-
15.	No. of droplets cm.$^{-3}$	976	397	160	427	214	248	191	233	252	344
16.	Mean diameter (microns)	9.90	10.88	16.6	10.64	11.76	12.23	17.20	14.45	15.10	13.19
17.	Mean volume diameter (microns)	9.90	11.62	18.4	12.35	12.93	14.80	18.35	16.04	20.10	14.94
18.	Water content (gm. m.$^{-3}$)	0.50	0.33	0.52	0.43	0.25	0.44	0.62	0.51	1.07	0.52
19.	Best's constant "a"	13.8	-	22.9	-	17.4	21.9	-	21.9	-	19.6
20.	Best's constant "n"	3.7	-	5.6	-	5.7	4.9	-	5.3	-	5.0
	Remarks										
21.	Approximate position of sample	-	-	-	-	-	-	-	-	-	-
22.	Precipitation reported	-	-	-	-	-	-	-	-	-	-
23.	Estimated visibility (yd.)	-	-	-	-	-	-	-	-	-	-
24.	Additional remarks	-	-	-	-	-	-	-	-	-	-

Table 4 (contd.)

Flight 2. 26/6/51

Item no.								
1.	10.	11.	12.	13.	14.	15.	16.	Mean values
2.	5,000	7,000	8,000	9,000	10,000	11,000	12,000	-
3.	-	-	-	-	-	-	-	-
4.	507	742	446	597	636	628	537	-
5.	6.31	-	4.48	27.13	1.25	1.43	2.23	6.12
6.	39.64	18.59	23.09	31.65	21.22	7.80	8.00	21.43
7.	33.53	80.86	37.21	15.41	40.56	12.73	17.31	33.94
8.	20.11	0.53	24.21	17.08	36.79	55.57	51.21	29.36
9.	0.39	-	10.76	8.37	0.15	21.65	20.85	8.88
10.	-	-	0.22	0.33	-	0.79	0.37	0.24
11.	-	-	-	-	-	-	-	-
12.	-	-	-	-	-	-	-	-
13.	-	-	-	-	-	-	-	-
14.	-	-	-	-	-	-	-	-
15.	242	354	212	284	293	299	255	277
16.	9.75	9.97	11.88	9.93	11.43	14.30	14.86	11.73
17.	10.75	10.00	13.48	12.72	11.82	16.50	16.07	13.05
18.	0.17	0.19	0.27	0.27	0.28	0.71	0.55	0.35
19.	14.1	10.7	19.1	19.9	14.8	21.4	20.4	17.1
20.	6.9	14.3	4.0	3.6	8.0	5.9	6.1	7.0
21.	-	-	-	-	-	-	Top	
22.	-	-	-	-	-	-	-	
23.	-	-	-	< 20	< 20	<10	<10	
24.	-	-	Hail at higher level	-	-	Icing	Icing	

Flight 3. 17/7/51

Item no.								
1.	17.	18.	19.	20.	21.	22.	23.	24.
2.	3,300	3,400	3,400	3,450	3,700	3,750	3,900	3,950
3.	-	-	-	-	-	-	-	-
4.	439	580	452	309	548	497	407	141
5.	12.30	39.65	3.09	79.61	46.71	8.24	23.83	32.62
6.	34.16	44.31	31.41	20.06	41.24	24.54	34.88	18.43
7.	41.00	15.17	49.11	-	10.03	62.77	27.02	29.78
8.	12.30	0.68	16.15	0.32	1.82	4.42	13.51	17.73
9.	-	0.17	-	-	0.18	-	0.73	1.41
10.	0.22	-	-	-	-	-	-	-
11.	-	-	-	-	-	-	-	-
12.	-	-	0.22	-	-	-	-	-
13.	-	-	-	-	-	-	-	-
14.	-	-	-	-	-	-	-	-
15.	211	277	214	139	255	248	179	70
16.	9.44	7.10	10.10	5.75	6.92	9.57	8.92	9.20
17.	10.27	7.64	11.97	5.78	7.48	9.88	10.00	10.58
18.	0.12	0.07	0.19	0.01	0.06	0.13	0.09	0.04
19.	-	-	-	6.8	-	12.3	13.2	15.1
20.	-	-	-	3.7	-	6.7	5.4	5.0
21.	-	-	-	-	-	-	-	-
22.	-	-	-	-	-	-	-	-
23.	-	-	-	-	-	-	-	-
24.	-	-	-	-	-	-	-	-

Table 4

Flight 3(contd.)

Item no.									Mean values
1.	25.	26.	27.	28.	29.	30.	31.	32.	
2.	3,950	4,000	4,000	4,000	4,050	4,050	4,050	4,050	-
3.	-	-	-	-	-	-	-	-	-
4.	291	434	142	422	527	598	236	476	-
5.	5.84	40.32	7.04	12.79	4.11	0.66	8.89	4.62	20.66
6.	29.89	50.23	14.78	83.17	15.86	22.57	18.22	27.31	31.94
7.	59.45	9.21	20.42	4.02	37.72	44.81	16.94	37.81	29.08
8.	4.81	-	57.74	-	42.30	31.93	55.08	29.41	18.01
9.	-	-	-	-	-	-	0.84	0.84	0.26
10.	-	-	-	-	-	-	-	-	0.01
11.	-	0.22	-	-	-	-	-	-	0.01
12.	-	-	-	-	-	-	-	-	0.01
13.	-	-	-	-	-	-	-	-	-
14.	-	-	-	-	-	-	-	-	-
15.	139	216	66	208	389	298	113	222	184
16.	9.49	6.97	12.30	7.37	13.68	11.20	12.06	10.80	9.10
17.	9.84	8.10	12.15	7.45	14.36	13.33	13.00	11.70	10.05
18.	0.07	0.06	0.08	0.05	0.38	0.26	0.13	0.19	0.12
19.	12.0	-	17.8	8.5	17.4	14.1	14.8	-	13.2
20.	8.3	-	5.4	12.5	10.5	7.4	6.0	-	7.1
21.	-	-	-	-	-	-	-	-	-
22.	-	-	-	-	-	-	-	-	-
23.	-	-	-	-	-	-	-	-	-
24.	-	-	-	-	-	-	-	-	-

Flight 4. 24/7/51

Item no.						
1.	33.	34.	35.	36.	37.	38.
2.	3,450	3,650	4,000	4,500	4,500	4,500
3.	-	-	-	-	-	-
4.	546	227	339	673	372	221
5.	96.33	14.53	21.23	9.80	55.64	66.51
6.	3.66	62.55	45.72	32.98	43.01	33.03
7.	-	21.58	32.15	50.66	1.34	0.45
8.	-	1.32	0.58	6.53	-	-
9.	-	-	0.29	-	-	-
10.	-	-	-	-	-	-
11.	-	-	-	-	-	-
12.	-	-	-	-	-	-
13.	-	-	-	-	-	-
14.	-	-	-	-	-	-
15.	272	110	173	324	180	107
16.	5.37	7.90	8.04	9.25	6.28	6.04
17.	5.39	8.30	8.57	9.81	6.52	6.23
18.	0.02	0.03	0.06	0.16	0.03	0.01
19.	-	11.0	12.6	12.3	7.4	7.1
20.	-	6.3	4.1	6.5	6.1	6.3
21.	base	-	-	just above base	-	-
22.	-	-	-	-	-	-
23.	-	-	-	-	-	-
24.	wispy	-	-	-	-	-

Table 4
Flight 4 (contd.)

Item no.					Mean values
1.	39.	40.	41.	42.	
2.	5,000	5,000	5,000	5,400	–
3.	–	–	–	–	–
4.	306	644	715	62	–
5.	3.26	4.50	7.41	–	27.92
6.	10.13	25.77	46.01	53.22	35.61
7.	78.75	64.59	40.41	29.03	31.90
8.	7.51	4.96	6.01	17.74	4.46
9.	0.32	0.15	0.13	–	0.09
10.	–	–	–	–	–
11.	–	–	–	–	–
12.	–	–	–	–	–
13.	–	–	–	–	–
14.	–	–	–	–	–
15.	143	311	338	31	199
16.	10.32	9.68	8.99	9.54	8.14
17.	10.69	10.09	9.57	10.45	8.56
18.	0.09	0.16	0.15	0.02	0.07
19.	13.5	13.2	12.9	14.8	11.6
20.	8.0	6.9	6.3	3.1	5.9
21.	–	edge	–	tops	–
22.	–	–	–	–	–
23.	–	–	100	–	–
24.	–	wispy	quite dense	–	–

Flight 5. 25/7/51

Item no.												
1.	43.	44.	45.	46.	47.	48.	49.	50.	51.	52.	53.	54.
2.	3,200	3,200	3,500	3,500	3,800	3,800	4,200	4,200	4,500	4,800	4,800	5,100
3.	–	–	–	–	–	–	–	–	–	–	–	–
4.	639	823	417	455	996	352	497	919	237	226	469	328
5.	19.40	37.30	6.23	52.96	49.59	3.12	35.41	11.20	3.79	17.25	29.63	12.80
6.	30.98	28.91	16.06	21.31	31.22	14.48	20.32	15.56	18.98	18.58	15.99	28.35
7.	30.04	19.68	22.06	6.81	10.34	23.01	10.46	25.68	16.87	42.03	14.49	38.41
8.	17.05	12.63	35.97	4.83	7.02	46.02	19.31	32.10	35.02	22.12	19.61	17.68
9.	2.50	1.21	17.50	5.05	1.40	11.93	11.46	13.16	23.62	–	14.92	2.74
10.	–	0.24	2.15	4.61	0.40	1.42	2.61	2.06	1.68	–	4.47	–
11.	–	–	–	3.73	–	–	0.40	0.21	–	–	0.85	–
12.	–	–	–	0.65	–	–	–	–	–	–	–	–
13.	–	–	–	–	–	–	–	–	–	–	–	–
14.	–	–	–	–	–	–	–	–	–	–	–	–
15.	296	364	193	214	448	156	247	406	101	113	233	149
16.	9.58	8.40	13.60	10.22	8.98	13.50	10.76	12.75	18.78	10.00	12.10	10.03
17.	10.94	10.02	15.62	18.36	9.28	15.05	14.46	15.12	16.14	10.94	16.18	10.60
18.	0.20	0.19	0.38	0.70	0.19	0.28	0.41	0.78	0.22	0.08	0.52	0.09
19.	15.5	17.0	22.4	36.3	17.8	19.9	19.5	24.0	22.9	14.8	30.2	14.1
20.	4.8	3.2	4.9	2.6	2.0	6.3	4.2	3.9	4.9	5.0	2.6	5.4
21.	–	–	–	–	–	–	–	–	–	–	–	–
22.	–	–	–	–	–	–	–	–	–	–	–	–
23.	–	–	–	–	–	–	–	–	–	–	–	–
24.	–	–	–	–	–	–	–	–	–	–	–	–

Table 4

Flight 5 (contd.)

Item no.			Mean values
1.	55.	56.	
2.	5,350	5,400	-
3.	-	-	-
4.	415	1,068	-
5.	16.38	4.11	21.37
6.	9.15	9.73	19.97
7.	17.34	16.57	20.98
8.	35.90	37.17	24.46
9.	15.90	27.99	10.67
10.	4.81	4.40	2.06
11.	0.48	-	0.41
12.	-	-	0.05
13.	-	-	-
14.	-	-	-
15.	193	514	259
16.	13.40	15.50	11.97
17.	14.84	17.54	13.93
18.	0.33	1.45	0.42
19.	29.5	25.1	22.1
20.	3.2	6.3	4.2
21.	tops	tops	-
22.	-	-	-
23.	-	-	-
24.	-	-	-

Flight 6. 17/9/51

Item no.												
1.	57.	58.	59.	60.	61.	62.	63.	64.	65.	66.	67.	68.
2.	5,200	5,200	5,300	5,400	5,400	5,450	5,500	5,500	5,500	5,750	5,750	5,750
3.	33.2	33.3	33.7	33.0	33.0	33.1	32.9	33.1	32.7	32.8	32.2	31.8
4.	366	344	416	316	476	304	292	458	327	305	326	662
5.	16.66	24.70	3.12	3.48	5.25	14.47	1.36	15.28	7.33	26.88	10.12	42.29
6.	15.84	18.60	6.49	8.54	12.60	20.72	5.13	14.41	11.92	36.72	17.17	48.48
7.	22.95	23.54	11.53	21.51	18.69	14.47	14.38	18.99	22.62	25.90	18.09	6.79
8.	32.24	24.70	44.47	46.20	49.36	18.42	36.30	29.03	43.73	8.85	19.63	1.96
9.	9.28	7.26	33.41	18.35	12.60	8.55	21.91	10.91	9.48	0.65	28.22	0.30
10.	2.18	1.16	0.96	1.89	1.26	13.48	11.98	8.07	3.97	0.32	5.52	-
11.	0.27	-	-	-	0.21	6.25	7.19	3.05	0.91	0.32	0.61	0.15
12.	0.54	-	-	-	-	2.96	1.71	0.21	-	-	0.61	-
13.	-	-	-	-	-	0.65	-	-	-	0.32	-	-
14.	-	-	-	-	-	-	-	-	-	-	-	-
15.	168	188	188	152	218	139	150	218	152	227	141	306
16.	12.35	10.72	15.92	14.48	13.70	17.40	19.68	14.33	13.78	8.85	15.00	6.98
17.	16.26	13.06	17.30	16.06	15.40	27.20	25.06	19.34	16.46	14.62	19.06	8.18
18.	0.38	0.22	0.51	0.33	0.42	1.47	1.25	0.81	0.35	0.37	0.51	0.09
19.	-	20.9	21.9	21.9	-	61.7	-	-	-	-	-	-
20.	-	3.6	6.1	5.9	-	2.7	-	-	-	-	-	-
21.	-	-	-	-	-	-	-	-	-	-	-	-
22.	-	-	-	-	-	-	-	-	-	-	-	-
23.	-	100	100	50	50	50	50	50	50	-	-	-
24.	-	-	-	-	-	-	-	-	-	-	-	-

Table 4
Flight 6 (contd.)

Item no.										Mean values
1.	69.	70.	71.	72.	73.	74.	75.	76.	77.	
2.	5,750	5,750	5,750	5,750	5,750	5,800	6,100	6,150	6,150	-
3.	32.0	32.0	31.7	31.3	31.4	31.6	30.6	32.1	31.9	-
4.	135	183	379	356	219	580	366	447	340	-
5.	4.44	1.63	35.35	3.37	9.13	2.75	7.65	11.40	6.17	12.04
6.	22.96	14.20	49.07	20.50	26.94	7.58	18.85	18.56	9.11	19.25
7.	27.40	15.84	13.98	30.61	22.37	51.20	27.86	28.85	29.41	22.24
8.	26.66	36.61	1.58	40.44	31.96	37.41	37.15	28.18	39.41	30.20
9.	15.55	20.21	-	4.77	7.30	1.03	5.73	9.84	12.64	11.33
10.	2.96	9.83	-	0.28	2.28	-	2.45	2.46	2.64	3.51
11.	-	1.63	-	-	-	-	0.27	0.67	0.29	1.04
12.	-	-	-	-	-	-	-	-	0.29	0.30
13.	-	-	-	-	-	-	-	-	-	0.05
14.	-	-	-	-	-	-	-	-	-	-
15.	62	84	173	200	91	272	168	212	153	173
16.	13.00	16.27	7.24	12.05	11.82	11.83	12.32	12.33	13.75	13.04
17.	15.48	19.40	7.76	13.26	14.04	12.54	14.52	15.18	16.50	15.79
18.	0.12	0.32	0.04	0.27	0.15	0.28	0.27	0.39	0.36	0.42
19.	-	-	-	-	-	15.9	-	-	-	28.4
20.	-	-	-	-	-	7.10	-	-	-	5.1
21.	-	-	-	-	-	-	tops	tops	tops	-
22.	-	-	-	-	-	-	-	-	-	-
23.	-	-	100	-	-	-	-	-	-	-
24.	-	-	-	-	-	-	-	-	-	-

Flight 7. 24/9/51

Item no.						
1.	78.	79.	80.	81.	82.	83.
2.	2,950	3,100	3,400	3,400	3,900	4,000
3.	-	50.0	47.5	47.3	45.7	45.0
4.	469	183	131	304	442	347
5.	56.07	20.21	4.58	50.32	9.72	17.57
6.	39.87	29.86	29.77	34.53	26.01	25.93
7.	4.05	24.04	32.82	8.55	34.16	27.95
8.	-	21.85	25.95	5.92	20.81	19.30
9.	-	4.37	6.10	0.65	7.91	8.35
10.	-	0.54	0.76	-	1.13	0.86
11.	-	-	-	-	-	-
12.	-	-	-	-	0.22	-
13.	-	-	-	-	-	-
14.	-	-	-	-	-	-
15.	207	77	64	145	197	173
16.	6.52	10.10	11.32	7.18	11.28	10.72
17.	6.66	11.98	12.96	8.32	14.04	12.90
18.	0.03	0.07	0.07	0.04	0.28	0.18
19.	6.61	19.5	-	13.8	-	20.9
20.	10.0	3.8	-	2.7	-	3.6
21.	-	base	-	-	-	-
22.	slight	-	-	-	-	heavy
23.	-	-	-	-	-	100
24.	-	-	-	-	wispy	-

Table 4
Flight 7 (contd.)

Item no.																Mean values
1.	84.	85.	86.	87.	88.	89.	90.	91.	92.	93.	94.	95.	96.	97.	98.	99.	
2.	4,500	4,500	4,600	4,600	5,000	5,100	5,200	5,550	5,650	5,950	6,050	6,200	6,200	6,700	6,700	6,800	-
3.	43.5	43.5	43.0	43.0	42.0	42.1	41.0	40.0	40.0	38.0	39.0	38.5	39.0	37.5	38.0	39.5	-
4.	133	42	58	195	46	178	296	217	162	274	76	374	282	91	92	273	-
5.	19.54	2.38	12.06	46.66	23.91	0.56	28.71	34.56	14.81	20.43	6.57	11.76	38.65	-	7.60	10.98	19.89
6.	17.29	7.14	15.51	24.10	13.04	8.42	19.59	18.34	6.79	21.53	17.10	12.56	18.79	9.89	10.86	29.30	19.79
7.	30.07	11.90	24.13	7.69	13.04	8.98	12.50	11.52	9.87	27.37	11.84	7.75	13.82	15.38	6.52	23.07	16.68
8.	24.06	23.80	25.86	8.20	23.91	28.65	11.48	19.81	32.09	14.23	26.31	21.39	15.24	13.18	26.08	19.04	19.42
9.	8.27	40.47	20.68	11.28	23.91	42.13	22.97	13.36	29.62	12.40	28.94	40.90	11.34	35.16	39.13	11.35	19.06
10.	0.75	14.28	1.72	2.05	2.17	10.11	4.05	2.30	5.15	3.64	9.21	5.61	2.12	23.07	8.69	5.12	4.72
11.	-	-	-	-	-	1.12	0.67	-	1.23	0.36	-	-	-	3.29	1.08	1.09	0.40
12.	-	-	-	-	-	-	-	-	-	-	-	-	-	-	-	-	0.01
13.	-	-	-	-	-	-	-	-	-	-	-	-	-	-	-	-	-
14.	-	-	-	-	-	-	-	-	-	-	-	-	-	-	-	-	-
15.	62	19	29	89	20	75	130	101	71	127	36	178	136	41	39	129	97
16.	11.04	18.18	13.13	9.09	12.95	18.40	12.40	11.00	15.60	11.55	15.78	15.95	10.22	20.13	17.20	10.50	12.67
17.	13.10	20.60	15.48	12.98	15.82	20.60	16.48	14.16	18.72	14.98	18.54	18.54	13.54	23.36	21.05	16.32	15.45
18.	0.07	0.09	0.05	0.11	0.05	0.37	0.31	0.15	0.26	0.23	0.12	0.59	0.17	0.27	0.17	0.29	0.18
19.	20.9	27.5	22.9	-	24.0	29.5	28.8	24.5	25.7	26.9	26.9	26.9	24.0	33.9	29.5	-	24.1
20.	3.6	5.5	4.2	-	3.7	4.4	3.4	3.2	5.0	3.3	4.9	4.4	3.17	4.5	4.4	-	4.3
21.	-	-	-	-	-	-	-	-	-	edge	edge	-	-	-	top edge	top centre	-
22.	moderate	-	slight	slight	-	-	-	-	moderate	moderate	moderate	-	-	-	-	-	-
23.	-	-	200	200	-	200	200	-	200	-	100	100	100	-	-	-	-
24.	wispy	wispy	-	-	wispy	-	-	thick	-	-	-	-	-	wispy	-	-	-

Table 4
Flight 8. 26/9/51

Item no.

1.	100.	101.	102.	103.	104.	105.	106.	107.	108.	109.	110.	111.	112.	113.	114.	115.	116.	Mean values
2.	2,050	2,050	2,310	2,310	2,320	2,340	2,350	2,790	2,790	2,800	2,800	3,300	3,300	3,320	3,320	4,530	4,560	-
3.	52.0	51.0	49.6	49.8	50.0	49.4	49.4	47.5	47.9	47.8	48.8	46.3	45.6	46.3	45.6	44.6	43.3	-
4.	453	332	603	483	293	1,261	190	569	638	152	582	65	493	584	90	373	364	-
5.	42.38	53.61	37.98	83.64	26.96	14.90	34.21	3.16	2.03	10.52	17.52	4.16	3.85	-	11.11	3.75	10.44	21.22
6.	53.42	44.57	58.54	16.14	42.66	79.06	65.26	35.32	13.63	55.26	69.75	16.92	19.47	4.62	25.55	8.31	28.57	37.47
7.	3.31	1.50	3.48	0.20	21.84	5.94	0.53	59.57	27.11	28.28	11.85	38.46	18.66	8.56	56.66	18.76	15.93	18.86
8.	0.66	0.30	-	-	8.19	0.07	-	1.75	53.13	5.26	0.68	38.46	34.68	66.09	6.67	45.84	35.71	17.50
9.	0.22	-	-	-	0.34	-	-	0.17	3.91	-	0.17	-	17.64	20.20	-	19.30	9.06	4.18
10.	-	-	-	-	-	-	-	-	0.15	-	-	1.53	5.07	0.51	-	3.48	0.27	0.65
11.	-	-	-	-	-	-	-	-	-	0.65	-	-	0.60	-	-	0.53	-	0.10
12.	-	-	-	-	-	-	-	-	-	-	-	-	-	-	-	-	-	-
13.	-	-	-	-	-	-	-	-	-	-	-	-	-	-	-	-	-	-
14.	-	-	-	-	-	-	-	-	-	-	-	-	-	-	-	-	-	-
15.	203	159	292	236	137	590	93	273	307	74	285	30	229	281	43	178	165	243
16.	6.72	6.37	6.75	5.65	8.19	7.33	6.74	9.31	6.85	8.70	7.52	11.72	14.34	15.59	13.38	15.03	11.71	10.75
17.	7.16	6.64	6.98	5.78	9.18	7.51	6.91	9.66	13.70	9.06	7.89	13.03	17.10	16.44	14.23	17.11	13.52	11.28
18.	0.04	0.02	0.05	0.02	0.05	0.13	0.02	0.13	0.41	0.03	0.07	0.03	0.60	0.65	0.07	0.47	0.21	0.20
19.	10.7	8.5	7.9	6.3	11.7	9.5	7.2	11.7	18.2	-	11.0	15.9	26.9	27.5	17.4	25.7	16.2	14.3
20.	3.1	5.6	7.1	7.7	4.9	3.7	14.3	7.4	5.3	-	5.4	6.1	2.7	4.9	6.5	4.7	5.4	6.0
21.	-	base	centre	edge	centre	centre	edge	centre	edge	edge	centre	top	centre	top edge	edge	edge	centre	-
22.	-	-	-	-	-	-	-	-	-	-	-	-	-	-	-	-	slight	-
23.	-	-	-	-	-	100	-	100	100	-	100	-	-	-	-	100	20	-
24.	wispy	-	-	-	-	-	-	-	-	-	-	wispy	-	-	-	-	-	-

Table 4
Flight 9. 24/9/51

Item no.													Mean
1.	117.	118.	119.	120.	121.	122.	123.	124.	125.	126.	127.	128.	values
2.	3,460	4,450	4,580	5,450	5,500	6,400	7,420	7,460	7,470	8,430	8,430	8,450	-
3.	-	-	-	-	-	-	-	-	-	-	-	-	-
4.	431	213	305	143	289	175	192	89	242	303	253	195	-
5.	5.8	14.0	19.3	20.3	34.6	21.7	4.7	14.6	19.0	14.8	28.5	10.2	17.3
6.	10.6	22.5	28.9	21.0	20.1	13.7	9.4	16.8	13.2	18.5	15.4	10.3	16.7
7.	16.2	26.8	12.2	8.4	9.3	12.6	7.3	11.2	13.2	14.5	11.1	11.3	12.8
8.	44.0	14.1	18.4	18.9	14.9	26.9	43.2	9.0	9.5	11.5	8.7	29.7	20.7
9.	17.4	9.4	5.6	21.7	4.8	18.3	26.0	29.2	16.5	7.6	5.5	21.5	15.3
10.	3.9	4.7	2.3	9.1	2.4	6.9	8.9	15.7	23.1	5.6	5.9	15.9	8.7
11.	0.7	6.6	3.9	0.7	5.2	-	-	2.2	3.7	8.6	5.5	1.0	3.2
12.	0.2	1.9	7.8	-	6.6	-	0.5	1.1	0.8	14.5	14.6	-	4.0
13.	0.5	-	1.3	-	1.7	-	-	-	0.8	4.3	4.7	-	1.1
14.	0.2	-	0.3	-	0.4	-	-	-	-	-	-	-	0.1
15.	198	99	140	64	129	80	91	41	121	142	118	95	110
16.	15.39	14.63	16.93	13.99	16.27	13.46	16.70	17.12	11.82	24.62	23.14	16.73	16.73
17.	22.98	22.88	32.72	18.10	32.96	16.82	18.67	22.68	26.16	40.34	40.41	20.26	24.88
18.	1.26	0.62	2.57	0.20	2.40	0.20	0.36	0.25	1.22	4.86	4.08	0.41	1.54
19.	-	50.1	85.1	29.5	100.0	26.3	27.5	38.0	52.5	-	-	29.5	48.7
20.	-	2.6	2.8	4.2	2.38	3.7	5.0	3.39	3.2	-	-	4.3	3.5
21.	edge	centre	centre	centre	centre	edge	centre	edge	centre	centre	centre	top edge	-
22.	heavy	slight	mod.	mod.	mod.	mod.	mod.	-	heavy	mod.	mod.	-	-
23.	100	100	300	50	-	-	20	100	150	100	100	100	-
24.	-	thin	thin	-	-	-	-	wispy	-	-	-	-	-

Flight 10. 26/9/51

Item no.			
1.	129.	130.	131.
2.	3,900	3,950	3,970
3.	46.0	46.0	47.0
4.	235	454	773
5.	2.1	3.3	1.5
6.	18.7	10.1	3.2
7.	18.7	29.5	8.5
8.	48.5	52.6	69.2
9.	12.0	4.4	15.9
10.	-	-	1.4
11.	-	-	0.1
12.	-	-	-
13.	-	-	-
14.	-	-	-
15.	106	205	404
16.	13.26	12.82	15.44
17.	14.55	13.15	16.47
18.	0.17	0.24	0.94
19.	17.8	22.9	22.9
20.	6.7	5.3	3.5
21.	-	-	base
22.	-	-	-
23.	100	200	-
24.	wispy	wispy	wispy

Table 4
Flight 10 (contd.)

Item no.																	
1.	132.	133.	134.	135.	136.	137.	138.	139.	140.	141.	142.	143.	144.	145.	146.	147.	148.
2.	4,850	4,850	4,900	5,900	5,900	5,900	5,900	6,600	6,800	6,850	6,900	6,900	6,900	7,800	7,800	8,750	8,800
3.	43.0	43.0	44.0	40.0	39.0	41.0	38.0	35.0	35.0	35.0	35.0	36.0	33.0	33.0	32.0	29.0	29.0
4.	542	409	145	817	582	237	510	423	372	420	463	188	587	205	452	461	272
5.	6.8	2.2	15.8	0.4	0.7	-	17.2	6.1	10.7	14.0	2.2	34.0	8.6	12.2	8.2	32.1	14.0
6.	12.4	5.1	34.5	3.9	7.2	16.4	32.0	13.9	13.4	26.2	7.5	31.9	8.4	15.6	20.0	36.5	11.0
7.	23.2	8.8	18.0	47.3	7.0	20.2	11.2	9.2	13.2	12.6	16.2	22.3	7.7	9.3	31.8	11.0	15.8
8.	27.2	31.8	21.4	45.7	17.5	27.5	19.2	40.2	30.1	32.6	37.1	6.9	50.9	7.8	32.0	10.2	30.5
9.	16.8	18.4	5.5	0.6	52.0	31.6	10.2	28.4	22.3	10.2	30.7	4.8	23.2	10.2	6.2	3.7	14.7
10.	11.8	27.2	3.4	1.6	10.3	3.4	7.8	1.2	6.7	3.2	3.9	-	1.2	13.2	0.9	3.2	9.9
11.	1.5	5.9	1.4	0.5	3.4	0.8	2.2	0.9	2.7	1.2	2.1	-	-	10.7	0.4	1.5	2.9
12.	0.2	0.4	-	-	1.5	-	0.2	-	0.5	-	0.2	-	-	15.1	0.2	1.5	0.7
13.	-	-	-	-	0.2	-	-	-	0.3	-	-	-	-	4.4	0.2	-	0.4
14.	-	0.2	-	-	-	-	-	-	-	-	-	-	-	1.5	-	-	-
15.	258	195	70	414	285	106	225	196	182	204	233	86	285	99	219	235	119
16.	15.65	21.27	11.27	12.79	20.67	15.57	12.89	15.16	15.91	12.51	16.68	8.56	14.81	29.08	12.13	10.43	15.88
17.	19.61	25.25	15.30	14.19	24.90	18.01	18.23	15.99	21.51	15.16	19.64	10.43	16.42	45.77	16.49	18.45	24.42
18.	1.02	1.64	0.13	0.62	2.30	0.33	0.71	0.55	0.95	0.43	0.92	0.06	0.66	4.98	0.51	0.77	0.70
19.	40.7	36.3	-	-	-	28.8	40.7	28.8	-	25.7	-	17.8	19.9	61.7	-	70.8	-
20.	3.2	3.8	-	-	-	3.6	2.8	4.6	-	3.8	-	2.9	5.7	3.3	-	1.8	-
21.	edge	centre	centre	centre	centre	edge	centre	edge	edge	edge	-	edge	edge	centre	edge	edge	centre
22.	-	-	-	-	-	-	-	slight	-	slight	-	-	-	-	-	-	-
23.	-	5	50	5	100	100	50	100	200	20	300	10	50	5	50	500	10
24.	wispy	-	-	-	dense	-	-	-	-	-	wispy	-	-	-	-	-	-

Table 4
Flight 10 (contd.)

Item no.			Mean values
1.	149.	150.	
2.	8,800	8,850	-
3.	30.0	29.0	-
4.	377	485	-
5.	14.6	2.1	9.49
6.	10.9	5.2	15.64
7.	7.9	3.9	16.01
8.	26.5	23.3	31.30
9.	38.5	54.1	18.84
10.	1.6	10.7	5.57
11.	-	0.6	1.76
12.	-	-	0.93
13.	-	-	0.25
14.	-	-	0.01
15.	173	217	205
16.	15.08	19.46	18.81
17.	17.36	21.09	19.19
18.	0.47	1.08	0.81
19.	36.3	19.1	32.0
20.	3.3	6.1	4.1
21.	edge	centre	-
22.	-	-	-
23.	10	10	-
24.	-	-	-

A note on M.R.P. 991
by
B.C.V. Oddie (Meteorological Office)

The relationship between drop-size distribution and visibility

The visibility can be calculated from a known droplet-size distribution by means of the equation

$$\frac{15.6}{\pi V} = \sum_i K_i n_i d_i^2$$

where V is the visibility, and n_i is the number of droplets of diameter d_i per unit volume. The value of K_i is somewhat uncertain: it is believed to vary between 1 and 2, and is here taken to be 2: but there is some reason to think that a variable and somewhat lower value might be appropriate (see e.g. Johnson 'Physical Meteorology' pp. 81-83).

The visibility has been calculated in this way from all those measurements of drop-size distribution in M.R.P.991 for which estimates of visibility were made. The results are shown in Table I. On an average of 59 cases, the calculated visibility was 98 yd., the measured visibility 96 yd. This very close agreement is undoubtedly to some extent fortuitous: but it confirms, in a general way, that the sampling technique is sound - that no class of drop which is significant in the visibility problem is escaping detection, and that the drop-sizes are fairly accurately estimated.

It follows that the estimates of water content must be fairly reliable: for if this sampling technique misses any class of drops, it must be the smallest ones. If the effect of the missed drops on visibility is, as we have seen, not very great, the effect on water content must be even less, since the former is proportional to $\Sigma n_i d_i^2$, the latter to $\Sigma n_i d_i^3$.

When one comes to examine the individual observations, the agreement is much less good. This was to be expected. In the first place, estimates of visibility made from an aircraft in cloud are highly subjective, since the most distant object which can be seen is the wing-tip, 50 feet or so away. Again the almost instantaneous sample of droplets is not necessarily a representative one; this is especially true in cumulus cloud which is always patchy.

Apart from the wide general scatter, the most striking and consistent feature of Table I is that at very low observed visibilities (25 yd. or less) the calculated visibility is always greater than the observed, by a factor of about 5. This ratio is relatively constant: except for one case, (where the value is 60) all the values lie between 3 and 7.2.

A discrepancy at these low visibilities is the more remarkable because it is precisely in this range that the direct observations of visibility should be most reliable. No satisfactory explanation can be offered.

It is suggested that work on the relationship between visibility and drop-size distribution in cloud should continue in an attempt to trace the reason for the discrepancies in Table I. The great disadvantage of the sampling technique is the enormous labour of counting and sizing droplets: but so long as our interest is limited to visibility, neither operation is necessary - we merely need to know the total area covered by the droplets on each slide, and it should be possible to estimate or measure this by a single operation. An accurate means of measuring visibility is also necessary.

Table I

Visibilities calculated from the measured drop-size distribution of M.R.P.991 compared with estimated visibilities

Observation number	Estimated visibility (yd.)	Calculated visibility (yd.)
13	< 20	78
14	< 20	68
15	< 10	36
16	< 10	45
41	100	88
58	100	103
59	100	52
60	50	59
61	50	58
62	50	40
63	50	36
64	50	45
65	50	79
71	100	290
83	100	112
86	200	450
87	200	270
89	200	97
90	200	98
92	200	130
94	100	250
95	100	49
96	100	140
105	100	83
107	100	101
108	100	51
110	100	160
115	100	60
116	20	104
117	100	43
118	100	79
119	300	42
120	50	160
123	20	92
124	100	170
125	150	47
126	100	17
127	100	20
128	100	82
129	100	130
130	200	76
133	5	26
134	50	220
135	5	36
136	100	19
137	100	92
138	50	48
139	100	52
140	200	49
141	20	66
142	300	36
143	10	600
144	50	39
145	5	19
146	50	67
147	500	61
148	10	64
149	10	59
150	10	30
Mean	96	98

FIG. I. PHOTOGRAPHS OF CLOUD DROPLET SAMPLER.

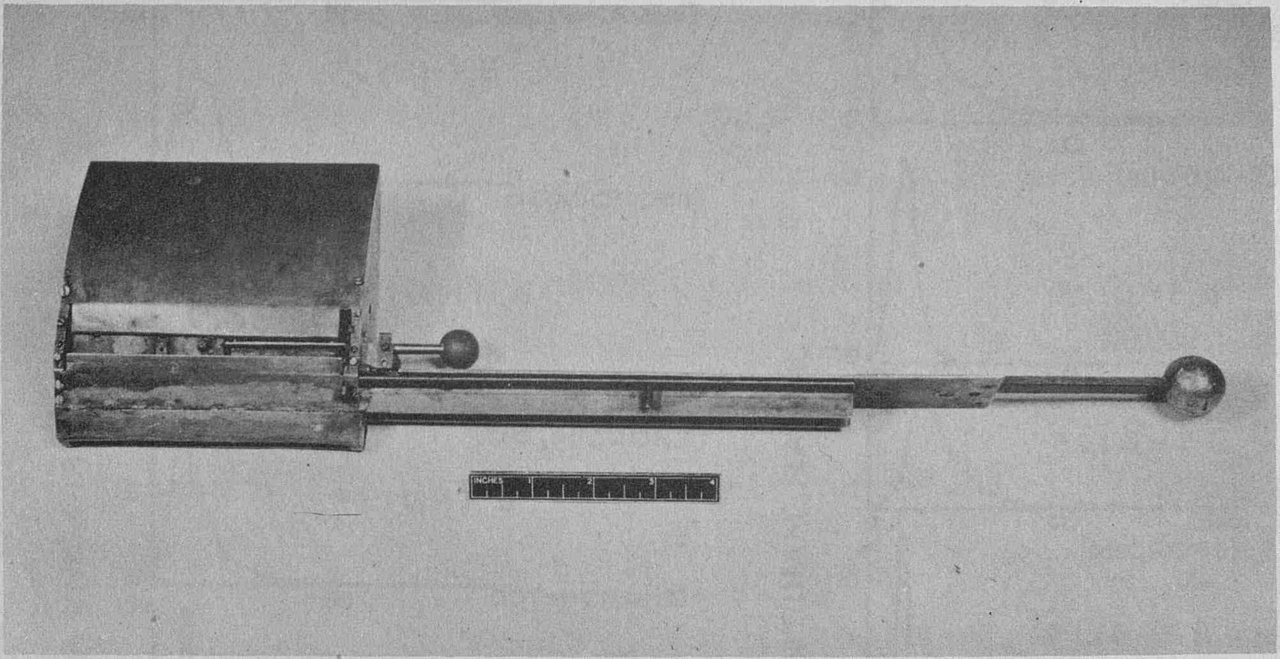
INCHES
1
2
3
4

(a) View of complete instrument.

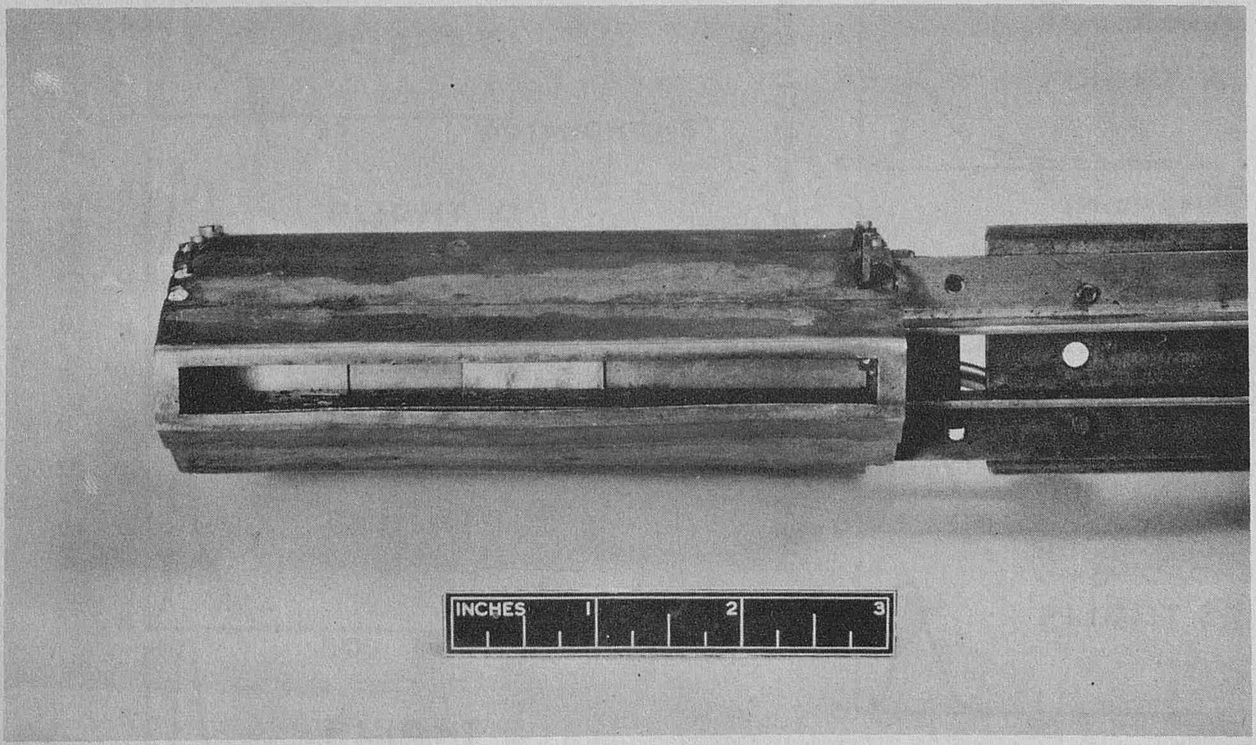

(b) Close-up view of shutter arrangement.

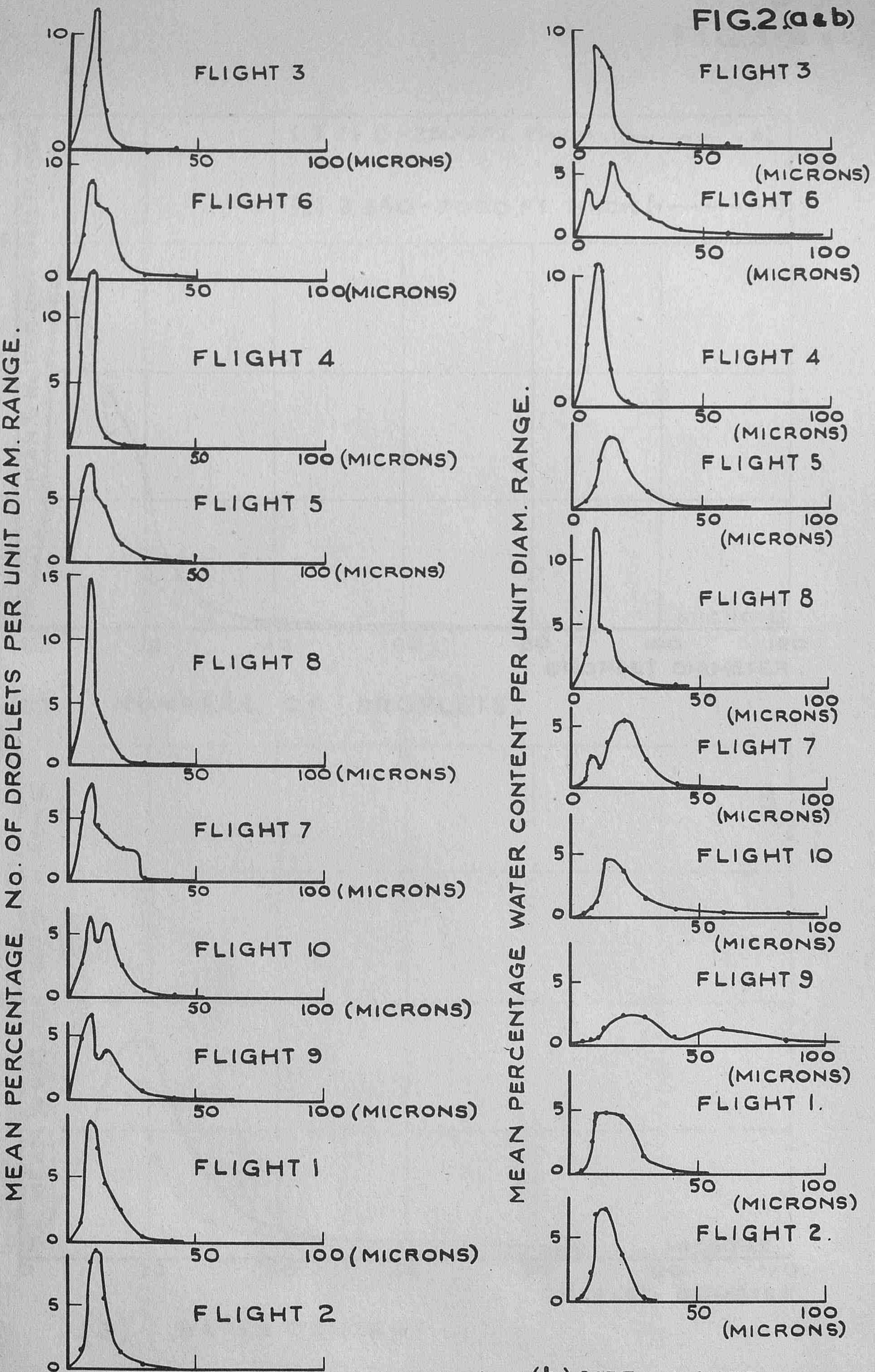

(a) SIZE - NUMBER SPECTRA.

(b) SIZE - WATER CONTENT SPECTRA.

FIG. 2. (a & b)

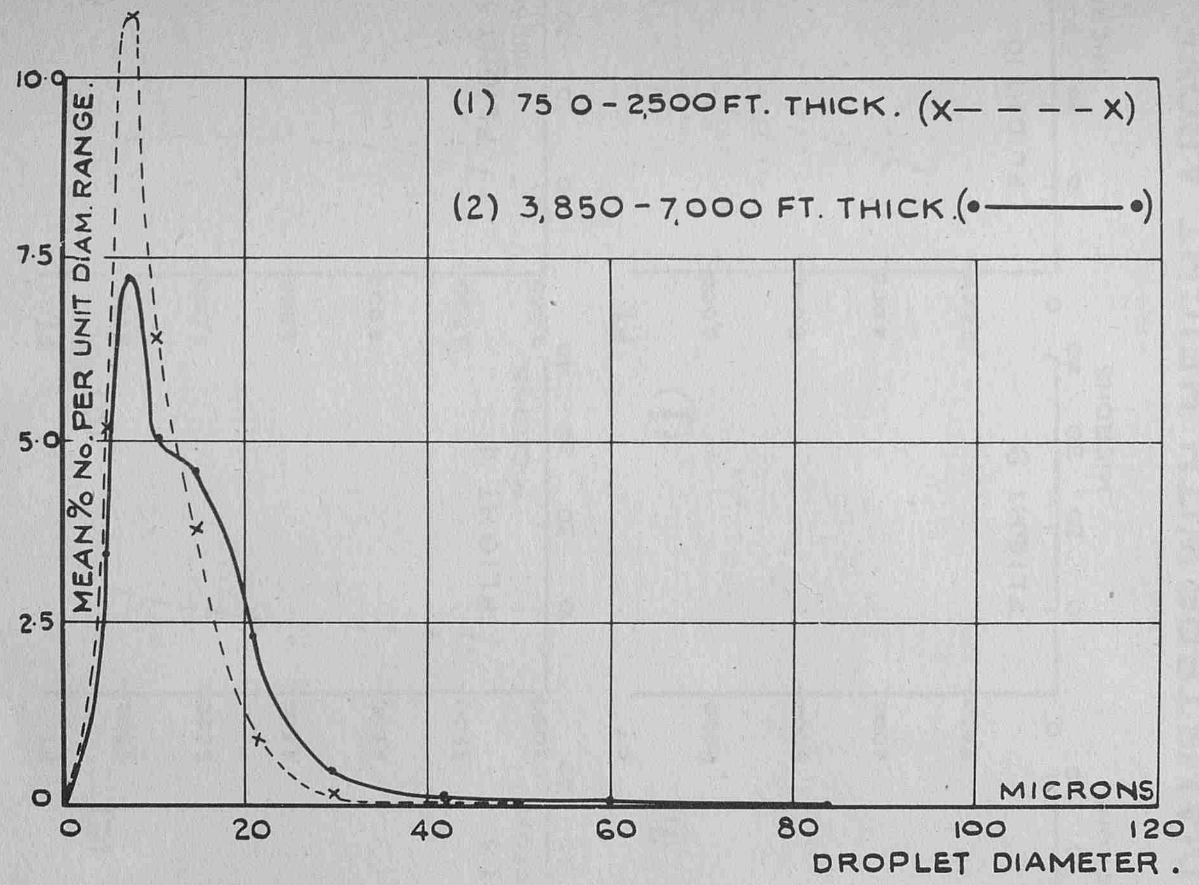

(a) NUMBERS OF DROPLETS.

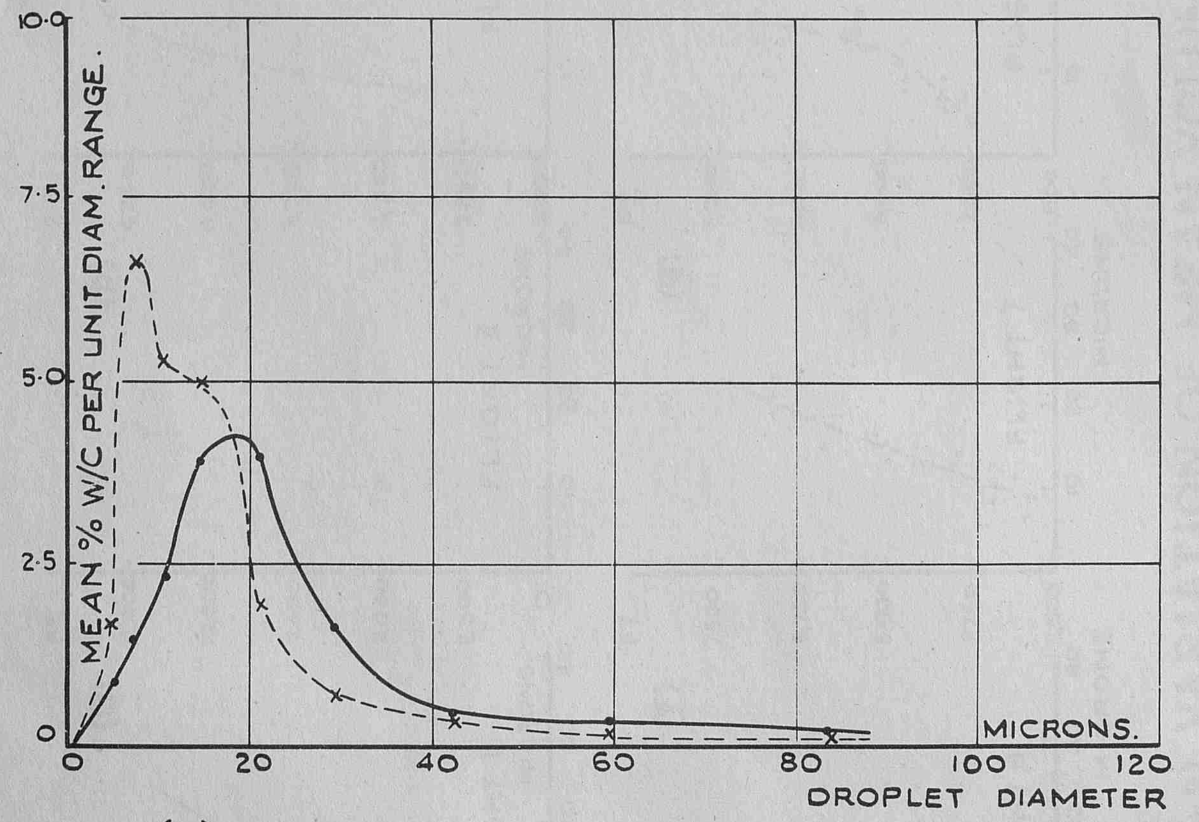

(b) WATER CONTENT.

FIG. 3. (a & b) COMPARISON OF WEIGHTED MEANS BETWEEN TWO GROUPS OF FIVE CUMULUS CLOUDS.

M.R.P. 991
FIG.4(a-k)

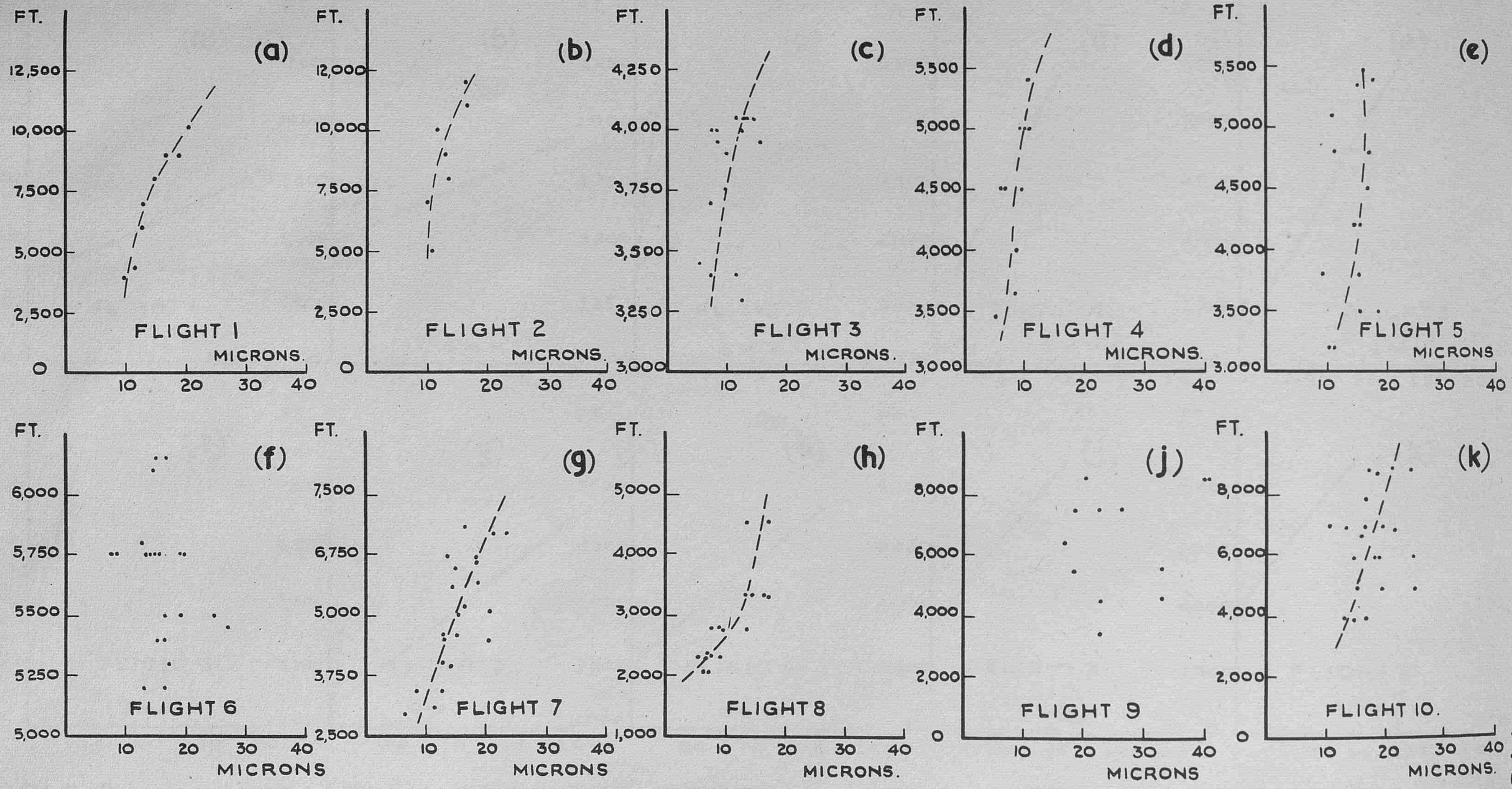

FIG.4(a-k) VARIATION OF MEAN VOLUME DIAMETERS WITH HEIGHT ABOVE GROUND.

M.R.P. 991
FIG.5 (a - k)

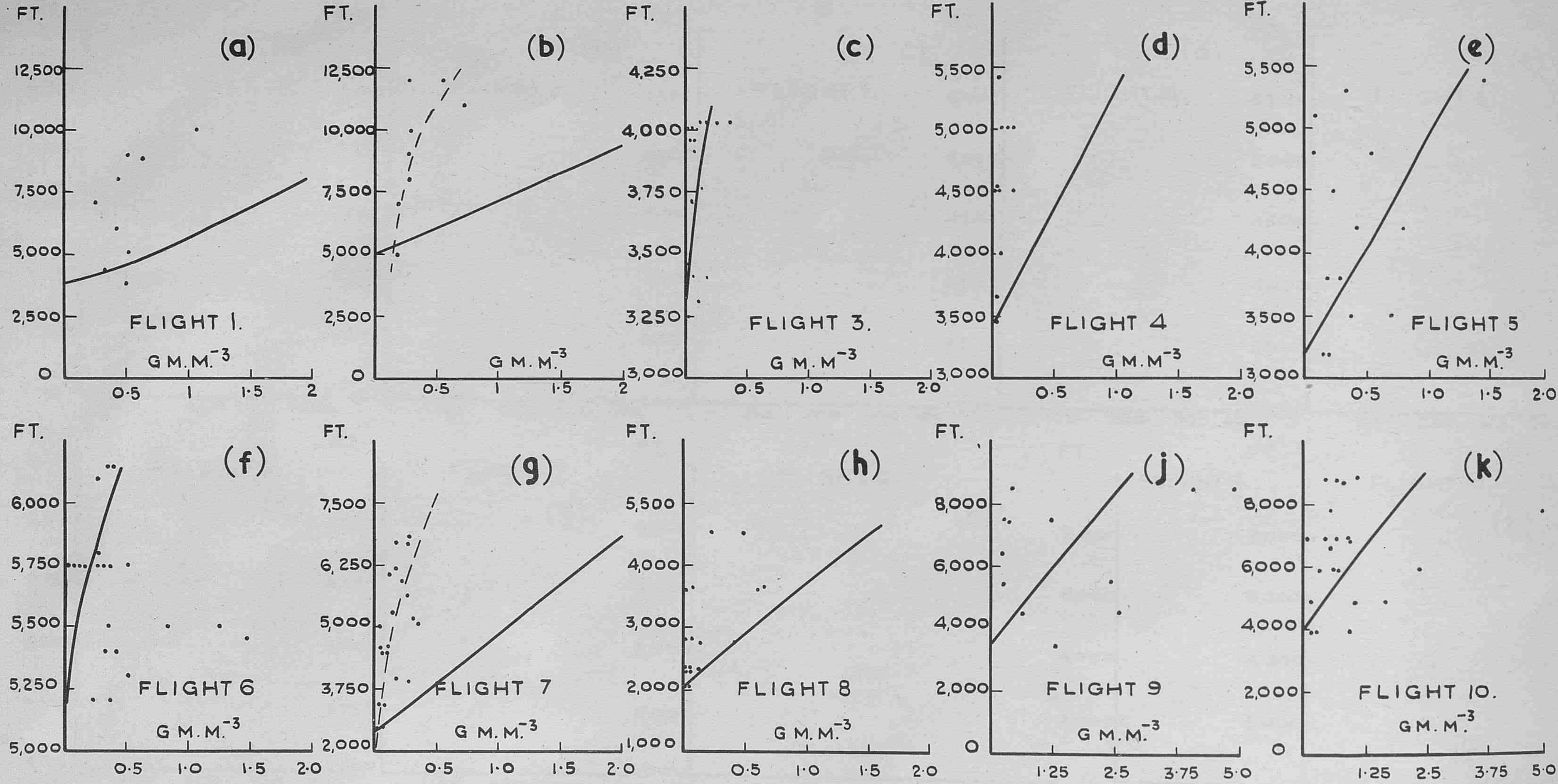

FIG.5(a - k) VARIATION OF WATER CONTENT WITH HEIGHT ABOVE GROUND.

(THE FULL LINE CURVES REPRESENT THEORETICALLY COMPUTED ADIABATIC VALUES.)

M.R.P. 991
FIG.6(a-k)

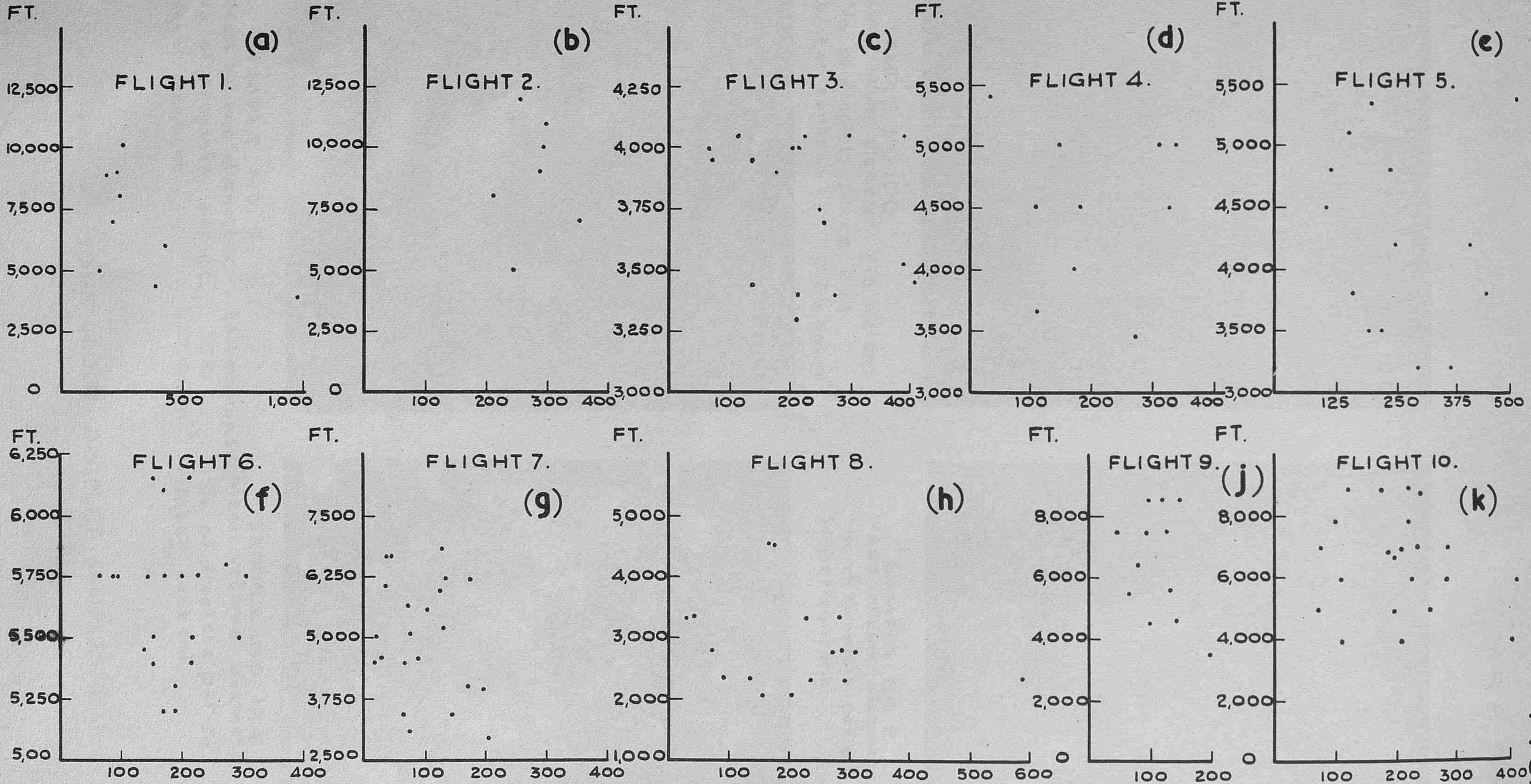

FIG.6 (a-k) VARIATION OF NUMBER OF DROPLETS PER C.C. WITH HEIGHT ABOVE GROUND.

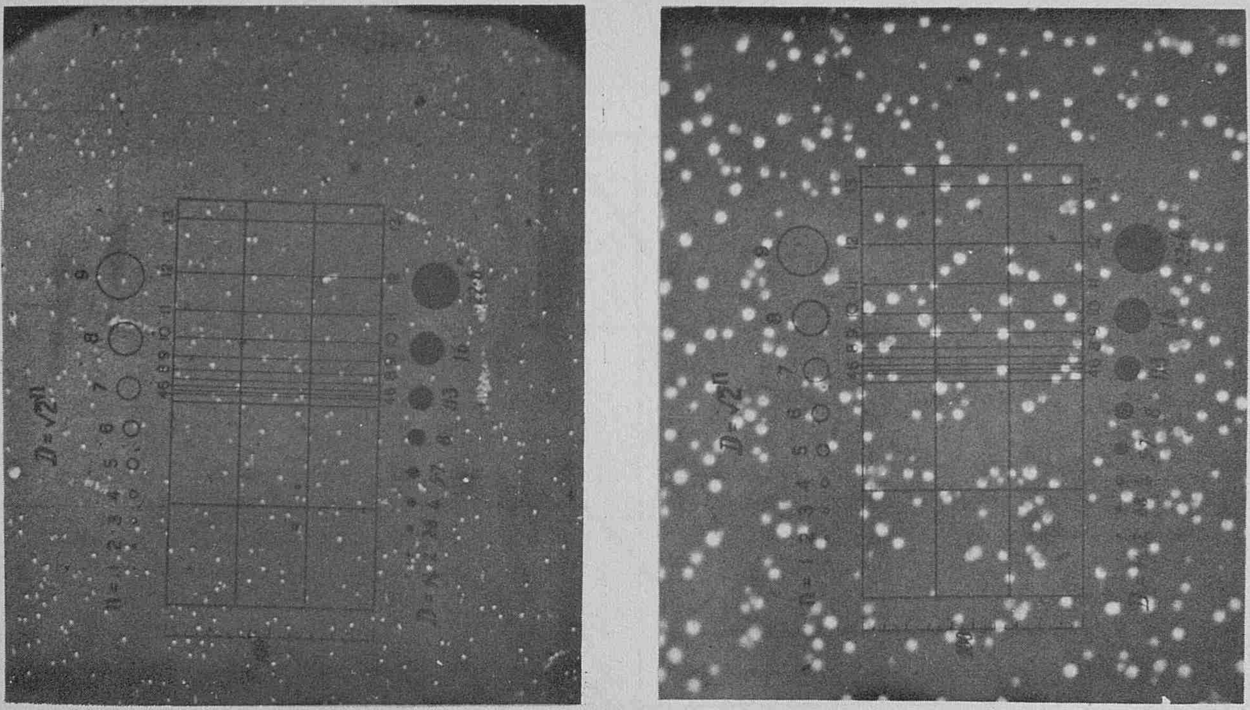

SAMPLE NO. 100.
Mean volume diameter 7·16 microns
No of droplets per c.c. 203
Water content 0.04 gm.m^{-3}

SAMPLE NO. 2.
Mean volume diameter 11.62 microns
No. of droplets per c.c. 397
Water content 0.33 gm. m^{-3}

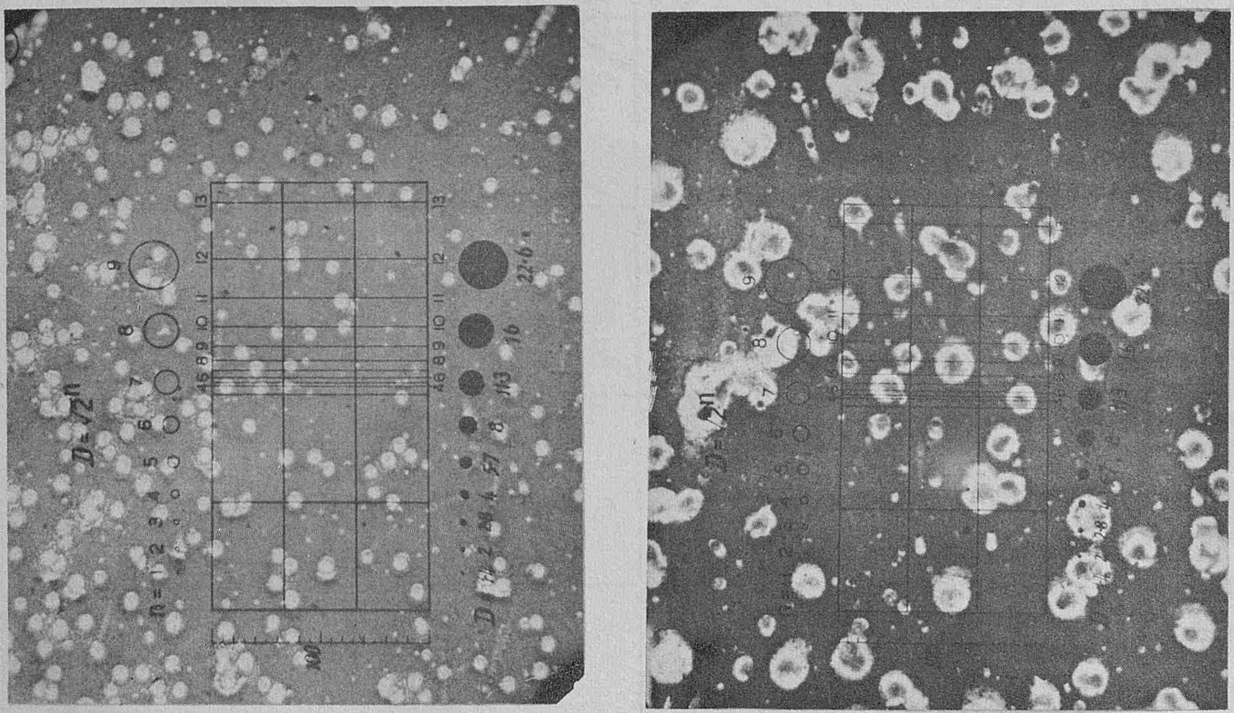

SAMPLE NO. 9
Mean volume diameter 20.1 microns
No. of droplets per c.c. 252
Water content 1.07 gm. m^{-3}

SAMPLE NO. 126
Mean volume diameter 40.34 microns
No. of droplets per c.c. 142
Water content 4.86 gm.m^{-3}

FIG. 7. SOME CLOUD DROPLET SAMPLES.

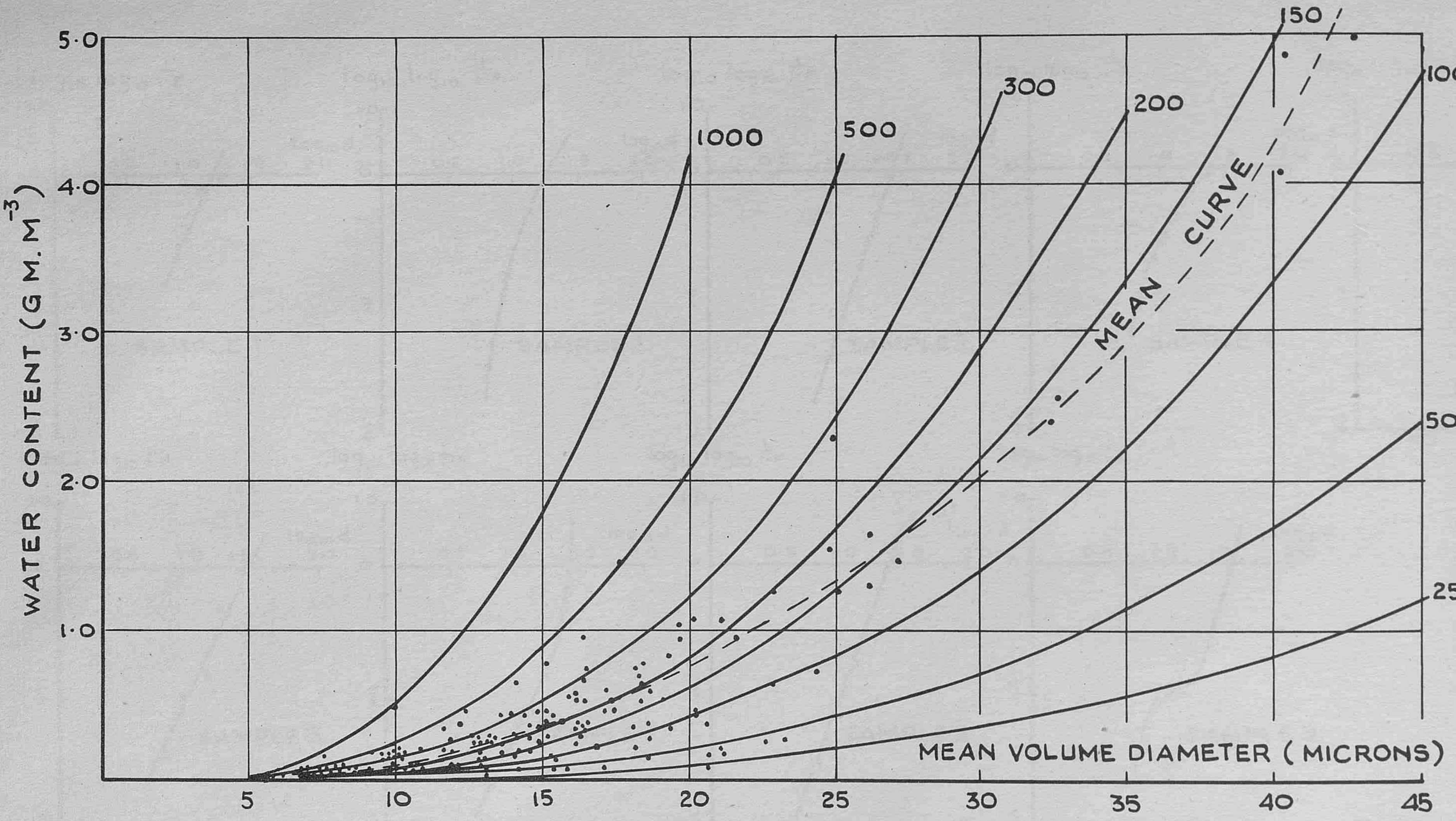

FIG.8. RELATIONSHIP BETWEEN WATER CONTENT, MEAN VOLUME DIAMETER & NUMBER OF DROPLETS PER C.C.

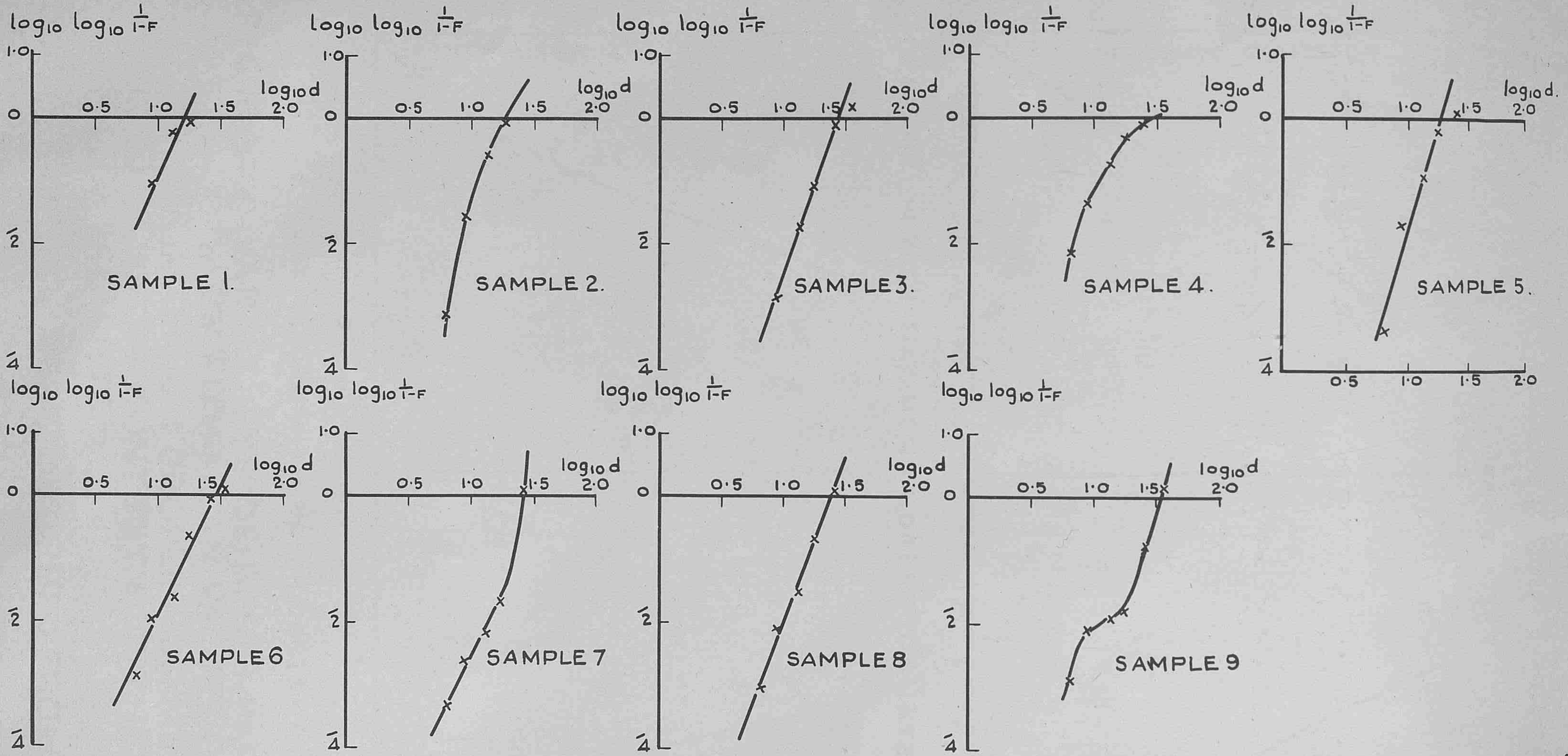

FIG. 9. GRAPHICAL ILLUSTRATION OF THE NUMBER-DISTRIBUTION FORMULA $1-F=e^{-(d/a)^n}$ USING THE SAMPLES TAKEN ON FLIGHT 1.

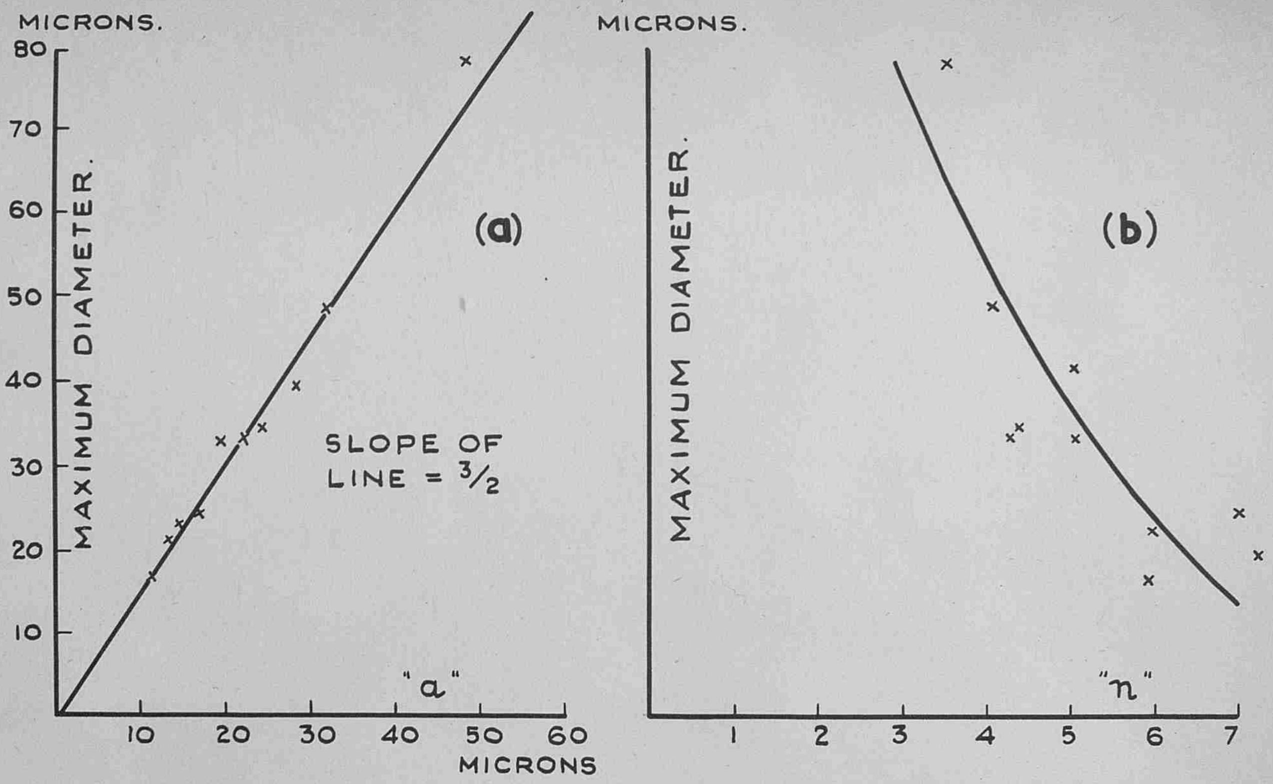

VARIATION WITH MAXIMUM DROPLET DIAMETER.

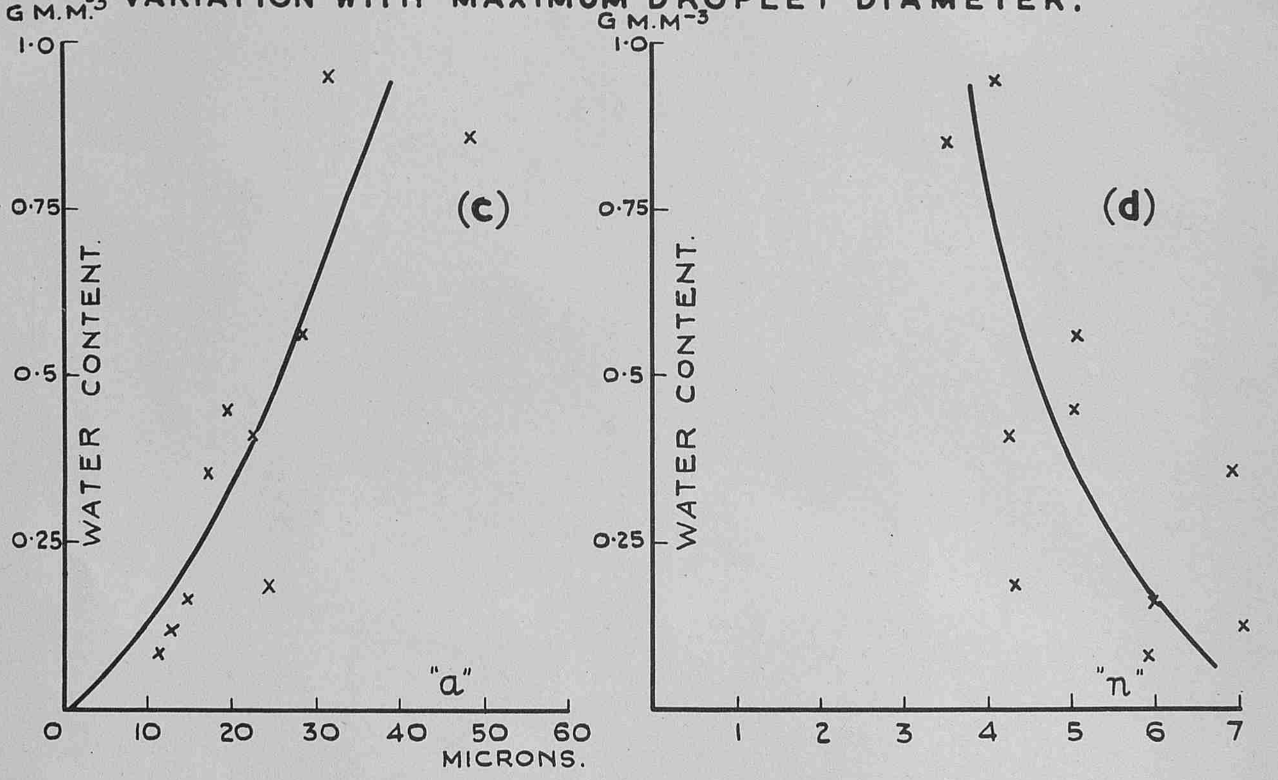

VARIATIONS WITH WATER CONTENT.

FIG.10(a – d) VARIATIONS OF BEST'S PARAMETERS "a" & "n" WITH MEAN VALUES OF MAXIMUM DROPLET DIAMETER & WATER CONTENT FOR THE TEN FLIGHTS.

(VALUES OF "a" & "n" WERE OBTAINED FROM 108 SAMPLES.)

M.R.P. 994
S.C.11/214
12th July, 1956.

AD 147511

A Synoptic Study of Anomalies of Surface Air Temperature over the Atlantic half of the Northern Hemisphere

by

J.M. Craddock and C.A.S. Lowndes

(Meteorological Office)

AIR MINISTRY

METEOROLOGICAL RESEARCH COMMITTEE

At the time of issue this report has not been published. Any author desiring to quote this paper should refer to it as "A paper of the Meteorological Research Committee (London). M.R.P. No.994 by Messrs. J.M. Craddock and C.A.S. Lowndes
A copy is available in the Library of the Meteorological Office."

M.R.P. 994
S.C.II/214
12th July, 1956

AIR MINISTRY

METEOROLOGICAL RESEARCH COMMITTEE

A Synoptic Study of Anomalies of Surface Air Temperature over the Atlantic half of the Northern Hemisphere

by

J.M. Craddock and C.A.S. Lowndes
(Meteorological Office)

Summary

The preparation is described of a series of charts covering the Atlantic half of the Northern Hemisphere giving the 5-day mean temperature anomaly for 73 non-overlapping periods covering the year 1st May, 1955 to 30th April, 1956. The more important features seen during the year are described, and their relationship to the patterns found on contemporaneous series of 5-day mean charts of pressure at mean sea level and of daily charts of the 1000-500 mb thickness.

The possible application of the temperature anomaly charts in long-range forecasting is discussed.

1. Introduction

A good deal is known about the yearly variation of air temperature at the ground surface over the world, while the diurnal temperature variation has also been studied extensively. The present work deals with temperature variations on an intermediate time scale. The effect of the diurnal variation and any other short-period fluctuation has been eliminated by averaging the observations over periods of five days, while annual variations have been removed by subtracting from the observed 5-day mean values the appropriate normal value. Thus the charts discussed here distinguish the geographical areas which are unseasonably warm from those which are unseasonably cold.

Before the temperature anomaly charts could be produced, the normal air temperature had to be estimated for each of a network of stations covering the Northern Hemisphere for each of the 73 non-overlapping 5-day periods which cover the year. This ground-work has been described by Craddock (1955) (1) and (2), the essential feature being that for every station the annual temperature variation is represented by the best fitting two-term harmonic form.

The actual 5-day mean temperatures were found for a network of about 240 stations covering the Atlantic sector of the Northern Hemisphere. Values observed twice daily were copied from the reports of synoptic broadcasts received at the Central Forecasting Office and were averaged. From each 5-day mean value the corresponding normal was subtracted to give the anomaly.

The work of finding a suitable method for estimating the 5-day temperature normals and carrying out the actual estimations on a hemisphere-wide scale was carried out during 1954. The normals were mostly derived from data for the period 1921-40, that being the latest for which adequate data were available (mostly in the Smithsonian World Weather Records), but it is intended that as the network of normals is amplified, as will certainly be necessary, data for the full international period 1921-1950 should be used wherever possible. A programme of synoptic study, involving charting (a) the normal temperature for each 5-day period, (b) the actual mean temperature for the same period, (c)

/the

the temperature anomaly and (d) the total rainfall in that period, was started from the 1st May, 1955, the first 5-day period being the 1st-5th May, and since then has been carried on currently, so that the series up to date covers more than a year. These charts are discussed weekly at the Central Forecasting Office, Dunstable, together with charts showing once daily the distribution over the Northern Hemisphere of the surface pressure, the height of the 500 mb surface and the 1000-500 mb thickness.

The next section describes the main changes in the surface temperature anomaly patterns during the year May, 1955 to April, 1956. The area studied always included Europe and the eastern Atlantic, and by July, 1955 was extended to cover the whole North Atlantic, North America east of the Rocky Mountains, and western Siberia. The description deals mainly with about ten major anomalous areas, each of which dominated the pattern over much of the region. These areas can be followed without much difficulty from chart to chart, and most of them lasted more than a month.

Charts of the 5-day mean air pressure are published monthly by the German Weather Service (3). These charts cover an area extending from Labrador to European Russia and unlike our temperature anomaly charts cover overlapping 5-day periods centred on each calendar day. They are not received at Dunstable early enough to be used at the weekly discussions, but it is interesting to see how far the significant features of the temperature anomaly pattern can be explained in arrear in terms of the 5-day mean pressure field.

2. The sequence of anomaly patterns during the year May, 1955 to April, 1956

The first temperature anomaly charts to be drawn showed several striking and rather surprising features. The patterns were not only unexpectedly simple and well defined but were on a very large scale. The charts were clearly divided into regions of positive and negative anomaly which individually covered large areas. The size of these areas in general ranged from that of the British Isles to that of the continent of Europe. The chart for the 21st-25th May (Fig.1) illustrates in a striking manner the large scale of the patterns.

The very large anomalies recorded at the centres of many of the warm and cold areas were a further unexpected feature. The cold area over Europe in Fig. 1 had a maximum value of -9°C.

On the temperature anomaly charts, odd value isopleths are drawn at intervals of 2°C and zero isopleths are shown as pecked lines. The maximum value at the centre of each area is shown to the nearest whole degree.

(a) European cold area* (6th May - 4th July)

The charts for May were dominated by a cold area which first appeared near Iceland. It extended southwards across the British Isles and then moved east, expanding and intensifying until by the end of May its eastern boundary had reached the Urals.

This anomaly appears from the pressure charts to have been associated with persistent northerly advection behind a centre of low pressure which appeared off the Norwegian coast by the 9th of May and later drifted eastward to north Russia and there intensified. This low decayed on the 28th May, but another lasted over north Russia from the 7th to the 22nd June. The cold anomaly, however, extended over a much larger area than that affected by northerly advection and lasted for about a fortnight after the advection had ceased.

---

* A large-scale pattern such as this which persisted for several weeks and which moved with some degree of continuity seemed worthy of further study. An investigation was made to determine whether any such cold areas had affected Europe in previous years. Data for Kew and Potsdam suggested that between 1901 and 1940 there were two years, 1923 and 1928, in which a similar cold area affected Europe in May. In both these years the cold May at Kew was followed by a cool June and a warm July. It was later found that the same sequence occurred in 1955.

In early June, this cold area covered most of Europe, though a warm area persisted over southwest Europe with little interruption from the 1st May to the 9th July. Towards the end of June an extension of the European cold area from Scandinavia to Greenland became a persistent feature whilst the original cold area weakened and dispersed in early July.

(b) Greenland cold area (25th June - 23rd August)

The cold area over Greenland continued throughout July and the first half of August. The chart for the 10th-14th July (Fig. 2) gives a good indication of its size and shape.

This Greenland cold area shows no obvious connection with the 5-day mean pressure gradient which during late June and early July was mostly weak easterly or southerly, or else indefinite.

(c) Trans-Atlantic warm area (10th July - 7th September)

By the 10th-14th July (see Fig. 2) a large warm area had formed extending from east America across the Atlantic to Scandinavia. This area persisted as a major feature for nearly two months. It was disrupted by cold areas in only three periods, twice south of Greenland and once in the longitude of the British Isles. The chart for the 19th-23rd August (Fig. 3) shows the warm area stretching from the west coast of America to the Urals.

This warm anomaly was associated with a well-developed Azores high. Moving anticyclones crossed the British Isles into Scandinavia, and by late July the 5-day mean high, still with its main centre northwest of the Azores, had an extension northeastwards across the British Isles to Finland. This extension was broken on the 6th and 7th August, and the warm anomaly also broke down over Europe in the period from the 4th-8th August. The high over Scandinavia and the warm anomaly over Europe then became established again; the warm anomaly disappeared over America early in September and the Scandinavian high declined about the same time but the warm anomaly over Europe persisted subject to gradual encroachments until late October.

(d) Mediterranean cold area (30th July - 17th October)

At the beginning of August a cold area formed over southern Europe and moved slowly southwards to the Mediterranean by the middle of the month. Although not very intense, it appeared on every chart for the next 2½ months with some variation in size and position. The chart for the 19th-23rd August (Fig. 3) shows the cold area centred over southern Italy. This cold anomaly is not readily explicable in terms of the 5-day mean pressure charts, which during most of the period showed only indefinite gradients over the area.

During September, a cold area formed over America disrupting the western end of the trans-Atlantic warm area. Over America and Russia there were rapid changes in pattern from one period to the next, intense warm areas being replaced by cold and vice versa. At the same time a warm area persisted over the Atlantic. The chart for the 23rd-27th September (Fig. 4) illustrates this phase. The cold area over Russia had replaced a warm area of comparable size on the preceding chart.

(e) Canadian warm area (3rd-27th October)

The patterns over America became more stable during October, a warm area covering most of Canada and the northern part of the U.S.A.

The central Atlantic continued warm whilst a cold area persisted near Iceland. The chart for the 13th-17th October (Fig. 5) shows these features and also the Mediterranean cold area just before dispersal.

During early November the patterns became unstable over the Atlantic, Europe and Russia. In the American sector the warm area persisted over eastern Canada whilst cold areas appeared over the Rockies.

(f) Rockies cold area (12th November - 21st December)

About mid-November an intense cold area suddenly formed over the Rockies with a maximum anomaly of -21°C (see Fig. 6). This feature dominated the American sector for over a month extending southeast at times to the east coast and beyond.

(g) Russian cold area* (17th November - 31st December)

At about the same time a cold area formed over Russia and became a persistent feature until the end of December. During this period the maximum anomaly increased from -8°C to -20°C and the area extended westward at times to Greenland and the British Isles. At the same time there was a marked tendency for a warm area to persist in the region of Hudson Bay and over the Atlantic. The chart for the 17th-21st December (Fig. 7) shows the Rockies and Russian cold areas at their maximum eastward and westward extension respectively.

The Russian cold area is only rudimentary on the chart for the 12th-16th November whereas on that for the 17th-21st November negative anomalies cover nearly all Europe During the period of change a high was centred over the British Isles and the extension of the cold anomaly over western Europe may have been partly due to advection on the periphery.

The cold area broke down over western Europe towards the end of December as a result of westerly advection associated with intense cyclonic activity near Iceland.

(h) Nova Scotia warm area (6th-30th January, 1956)

Early in January a warm area formed over Nova Scotia and persisted to the end of the month. The chart for 11th-15th January (Fig. 8) shows this feature and also a cold area near Iceland which was associated with it for most of the period. This anomaly seems to have been due to persistent advection across Labrador of relatively warm air from the open sea. The patterns over Europe were rather unstable at this time.

(i) European cold area (21st January - 1st March)

During the last week in January an intense cold area with a maximum anomaly of -18°C developed over northeast Europe and spread rapidly westwards to cover the continent. The chart for the 10th-14th February (Fig. 9) shows this feature and also a warm area over Spitzbergen which persisted over much the same period. Violent fluctuations were taking place over America. The development of the European cold area seems to have started with a northerly outburst behind a low centred over Scandinavia about 20th January, but by the 24th this had declined and had been replaced by a high which persisted with variations until mid-February. The cold anomaly lasted until the end of February, but early in March was broken down for five days only by advection of warm air from the west.

/(j)

---

* The Russian cold area was not, as might be supposed, mainly associated with anticyclonic conditions. It developed as a result of intense cyclonic activity near the Russian Arctic coast which brought down cold air from the polar regions. Except for the period 17th-21st December the area continued mainly cyclonic.
The Rockies cold area was, on the other hand, associated with anticyclones during most of its lifetime.

(j) European cold area (7th March - 30th April)

By the 7th March a less intense cold area had established itself over most of Europe. The new cold area intensified and retreated to eastern Europe by the end of the month. The chart for the 12th-16th March (Fig. 10) shows this feature and also a warm area over the Barents Sea which persisted over much the same period. The resurgence of the European cold area and the warm area further north seems to have been due to advection round an anticyclone over south Scandinavia. The patterns over America continued to fluctuate widely.

Early in April the cold area returned to western Europe. The chart for the 21st-25th April (Fig. 11) shows the elongated shape of the area during the latter half of the month. Over America, a warm area persisted in the region of Hudson Bay for the first three weeks of the month.

(k) This completes an outline of most of the salient features of the temperature anomaly charts covering the year.

There is evidently a relation between the patterns on these charts and the character of the general circulation, though the nature of the association varies with place and time of year. For example, a large negative surface temperature anomaly is generally associated with a persistent trough or cold pool in the 1000-500 mb thickness pattern, while in winter over the continents a positive temperature anomaly is usually associated with the persistent advection of air from the direction of the open sea and a negative temperature anomaly with stagnant air, or air which has had a long land track. With more experience we should be able to describe these relations more fully.

It is, however, obvious that the relationship between the temperature anomaly patterns and the daily surface pressure patterns is quite loose and changeable.

The bigger anomalies usually occur over the continents rather than over coastal or sea areas.

(l) Finally, a general comparison was made between the series of temperature anomaly charts and a series of 5-day mean pressure charts for the same non-overlapping periods. The latter series was obtained from the German series covering overlapping periods by masking the charts centred on intermediate days. When this was done it appeared that the patterns on the temperature charts show a good deal more persistence than those on the pressure charts. Often a new temperature pattern would be accompanied by advection in the right direction on the pressure chart, but the temperature pattern would persist after the pattern on the pressure chart had become something quite different. Occasionally, too, a temperature pattern would occur first, and advective flow to maintain it would develop later.

3. Discussion

The outstanding impression of the year's charts, which the preceding section tries to convey, is that the patterns of temperature anomaly are large, slow moving and long lived, with a good deal more stability than might have been expected. There are two possibilities for using them as a tool in long-range forecasting.

For the inside of a large area of positive or negative anomaly, a "persistence" forecast that the present anomaly will continue for several days to come must have quite a high expectation of success. Such forecasts may be useful for continental areas especially when the anomaly is big enough to make it the most important feature of the local weather, but are likely to be less useful over the British Isles, since the country is often near the boundary of two large areas of opposite temperature anomaly, so that a small change in the boundary may alter the British weather from warm to cold, or vice versa.

/A

A more attractive possibility is to use the temperature anomaly pattern as an indicator of the state of the general atmospheric circulation. If we are justified in doing this, and the experience of the past year suggests that we are, then we may be able to apply arguments concerning the general circulation to data for years before the era of upper air analysis. For example, we may try, on the basis of temperature anomaly patterns to select previous years in which the character of the general circulation resembles that of the present year, in the hope of being able to forecast future changes by analogy. This has been attempted for several months, with an encouraging degree of success.

4. References

1. Craddock, J. M. 1955 Meteorological Research Papers, Air Ministry, London, No. 915. "The representation of the annual temperature variation over Central and Northern Europe by a two term harmonic form."

2. Craddock, J. M. 1955 Meteorological Research Papers, Air Ministry, London, No. 917. "The variation of the normal air temperature over the Northern Hemisphere during the year."

3. Deutscher Wetterdienst, Seewetteramt, Hamburg, Luftdruck - Pentaden - Karten.

FIG I TEMPERATURE ANOMALY °C. 21-25 MAY 1955. MRP 994.

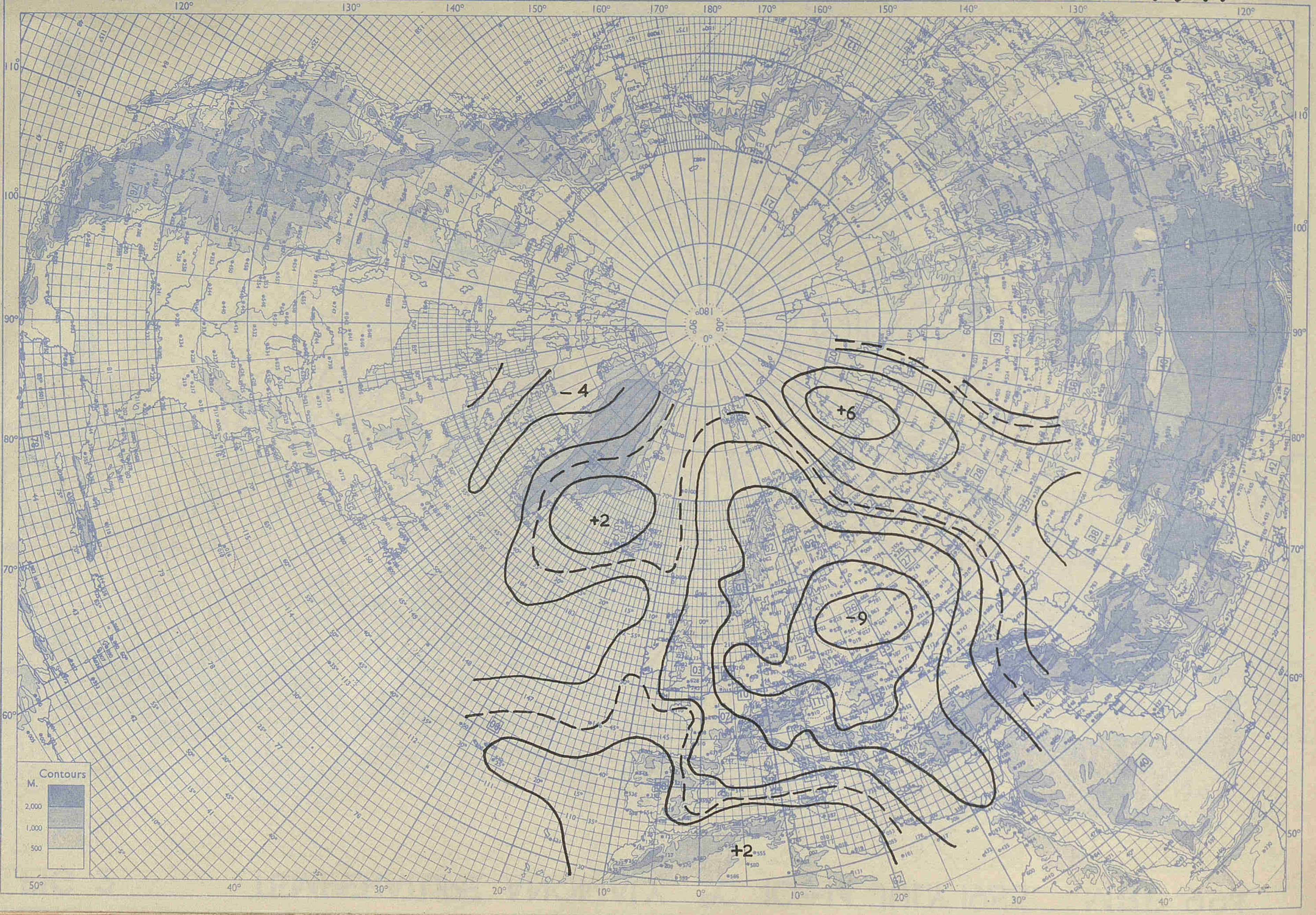
-4
+2
+6
-9
+2
Contours
M.
2,000
1,000
500

FIG 2 TEMPERATURE ANOMALY °C 10–14 JULY 1955. MRP 994.

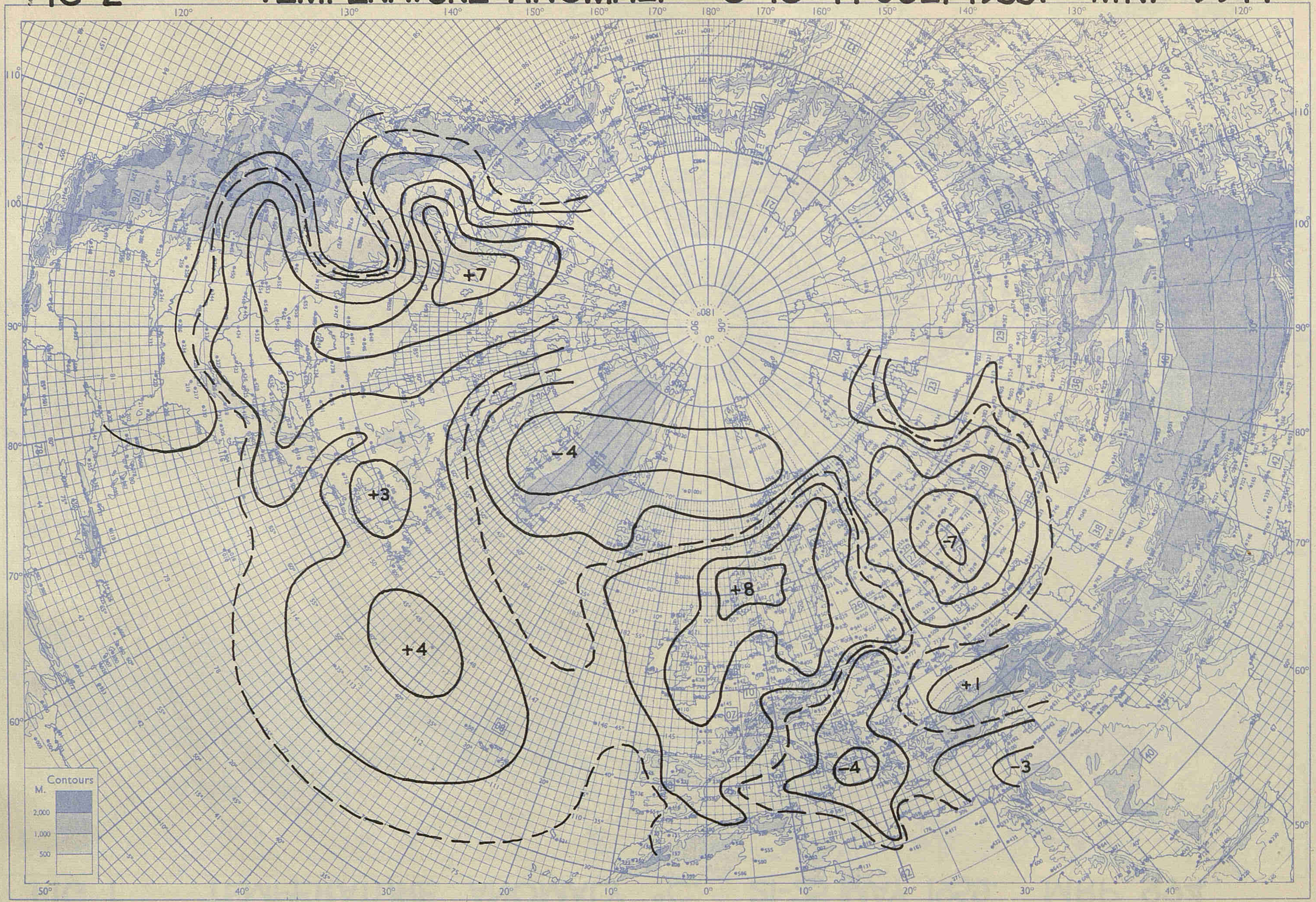
+7
+3
+4
−4
+8
−7
+1
−4
−3
Contours
M.
2,000
1,000
500
120°
130°
140°
150°
160°
170°
180°
110°
100°
90°
80°
70°
60°
50°
40°
30°
20°
10°
0°

FIG 3 TEMPERATURE ANOMALY °C 19-23 AUG. 1955. MRP 994.

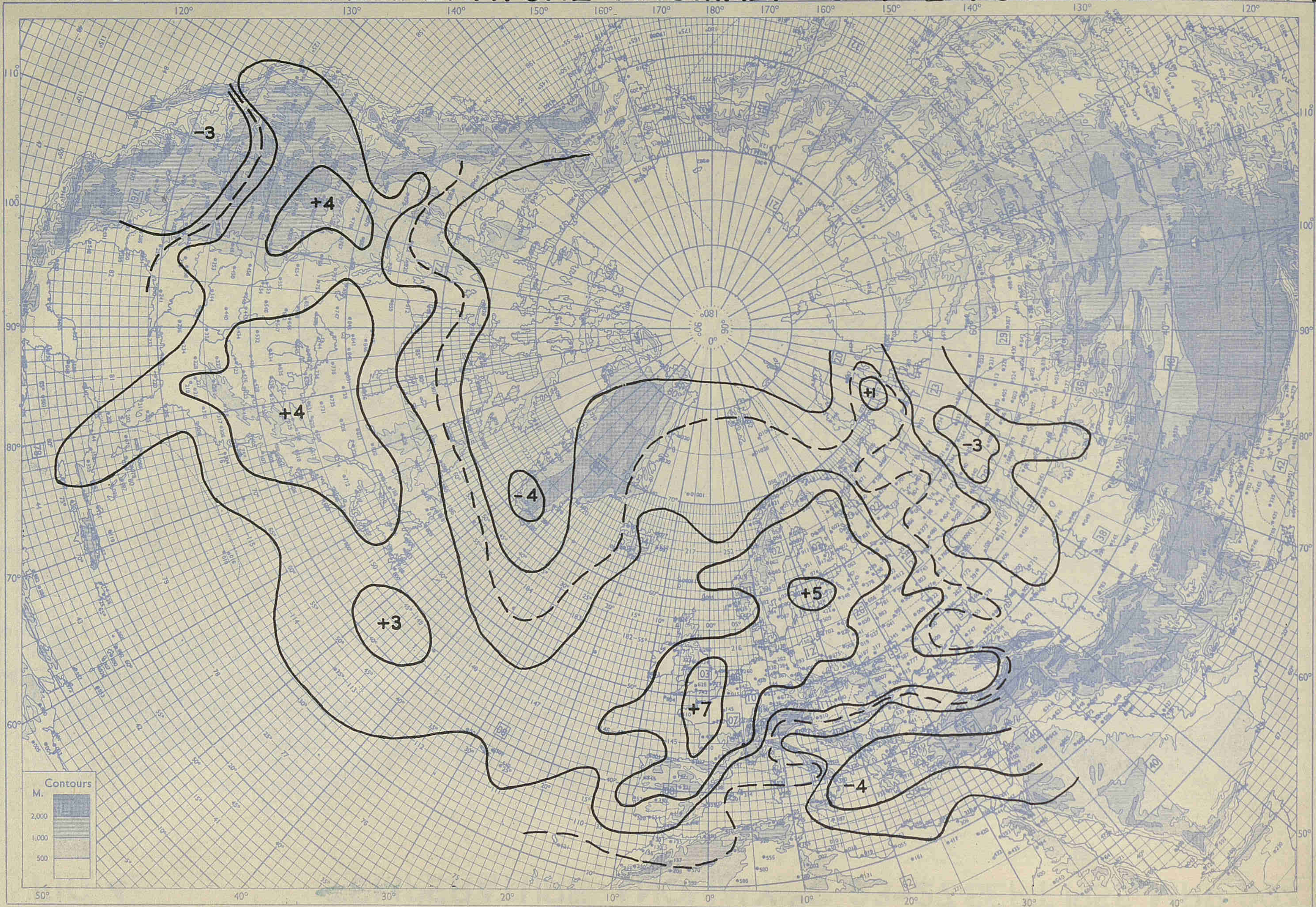

-3
+4
+4
-4
+3
+7
+5
+1
-3
-4
Contours
M.
2,000
1,000
500

FIG 4. TEMPERATURE ANOMALY °C 23–27 SEPT. 1955. MRP 994

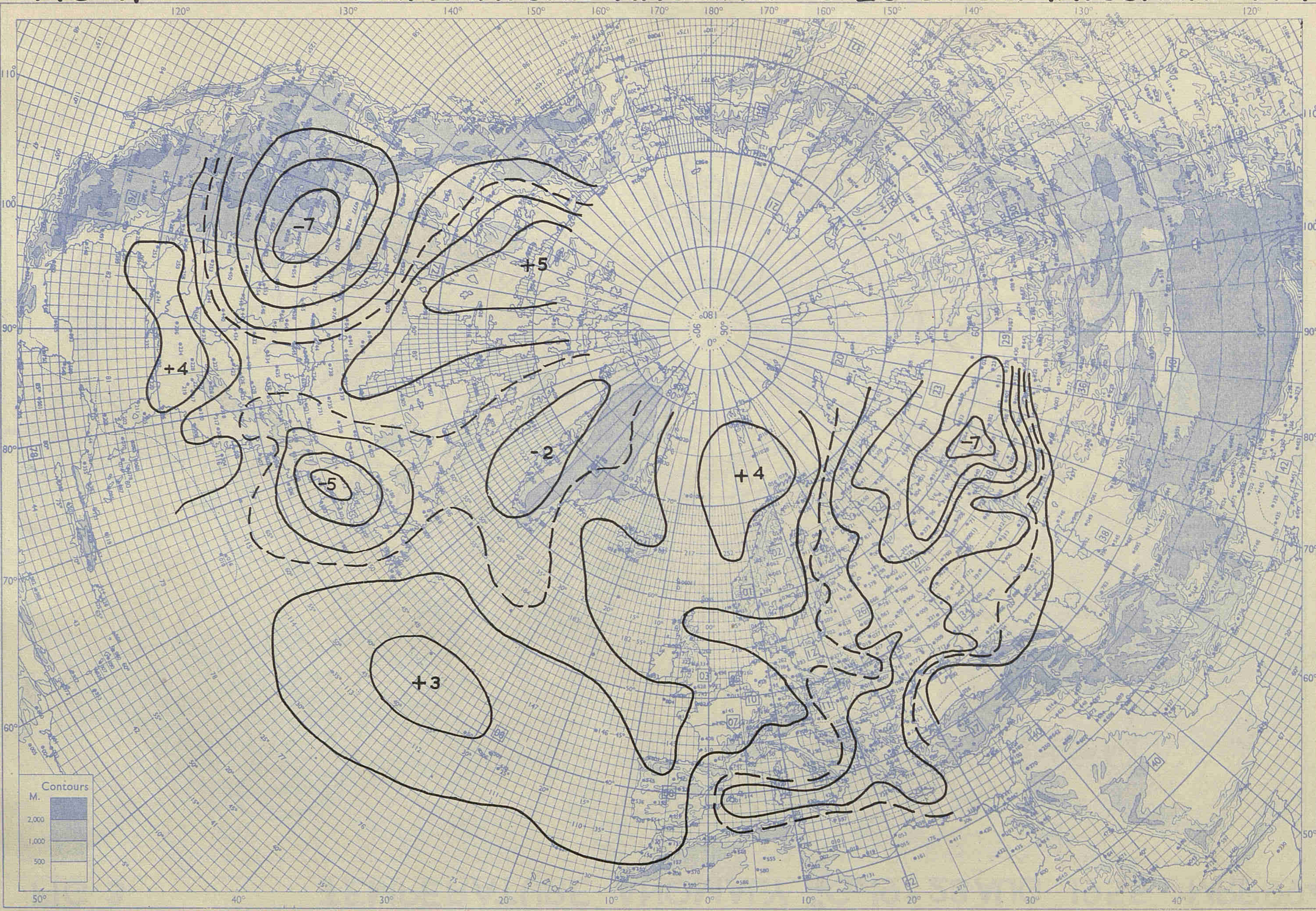
-7
+5
+4
-5
-2
+3
+4
-7
Contours
M.
2,000
1,000
500
120°
130°
140°
150°
160°
170°
180°
110°
100°
90°
80°
70°
60°
50°
40°
30°
20°
10°
0°

FIG 6 TEMPERATURE ANOMALY °C 12-16 NOV. 1955. MRP 994.

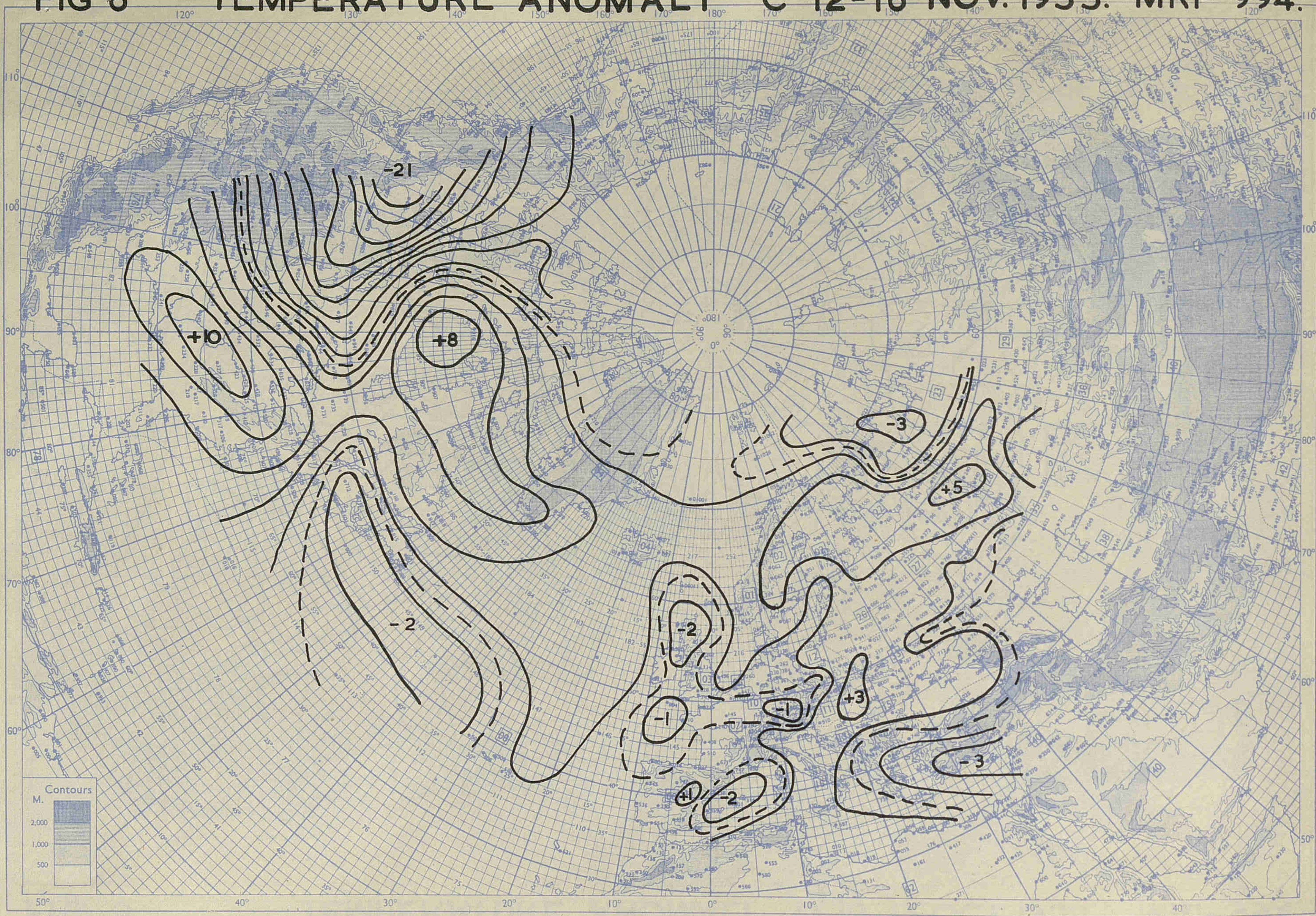
-21
+10
+8
-2
-3
+5
-2
-1
-1
+3
-3
+1
-2
Contours
M.
2,000
1,000
500

FIG 5 TEMPERATURE ANOMALY °C 13–17 OCT. 1955. MRP 994.

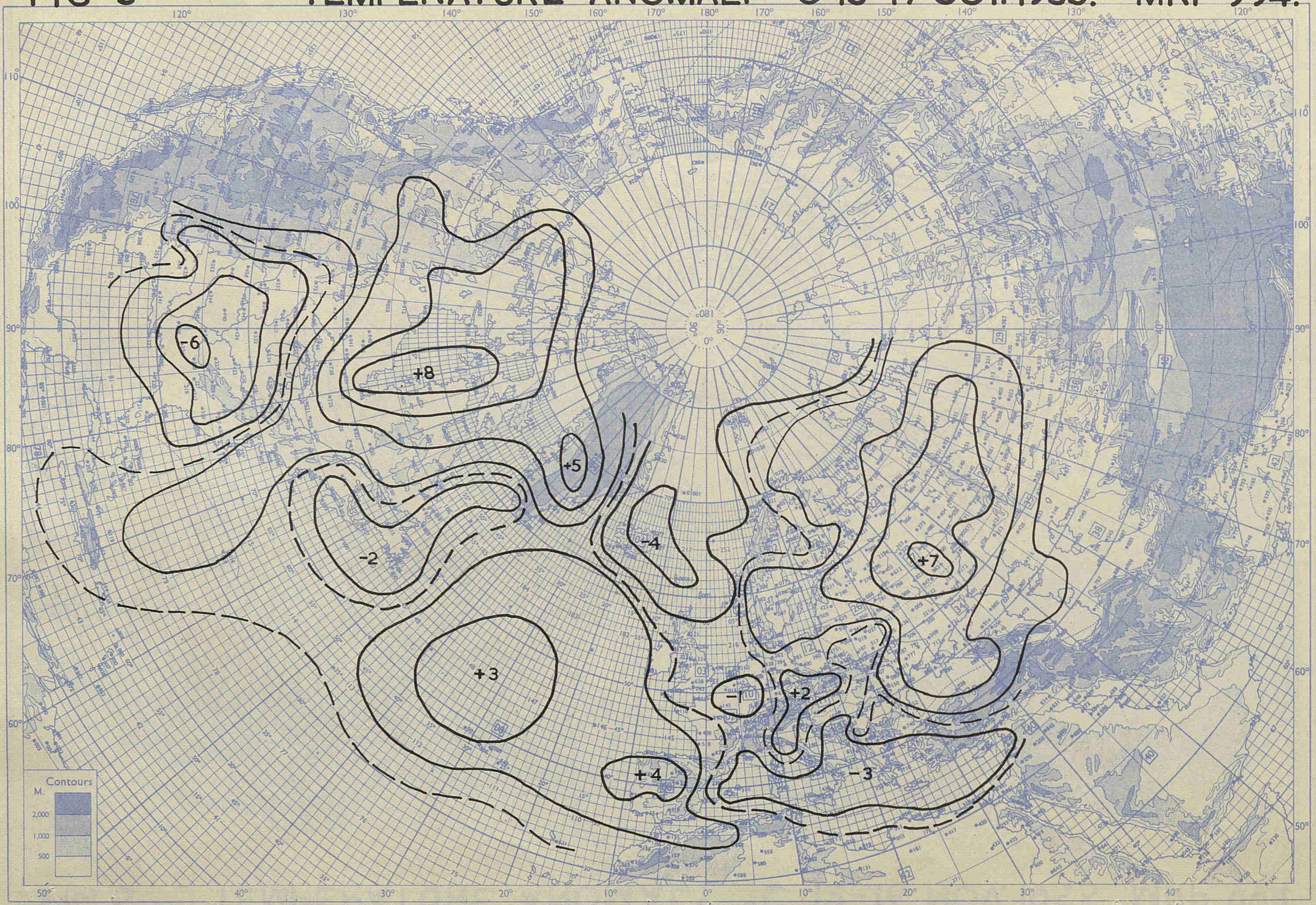
-6
+8
+5
-2
-4
+3
+4
-1
+2
-3
+7
Contours
M.
2,000
1,000
500

FIG 7 TEMPERATURE ANOMALY °C 17-21 DEC. 1955. MRP 994.

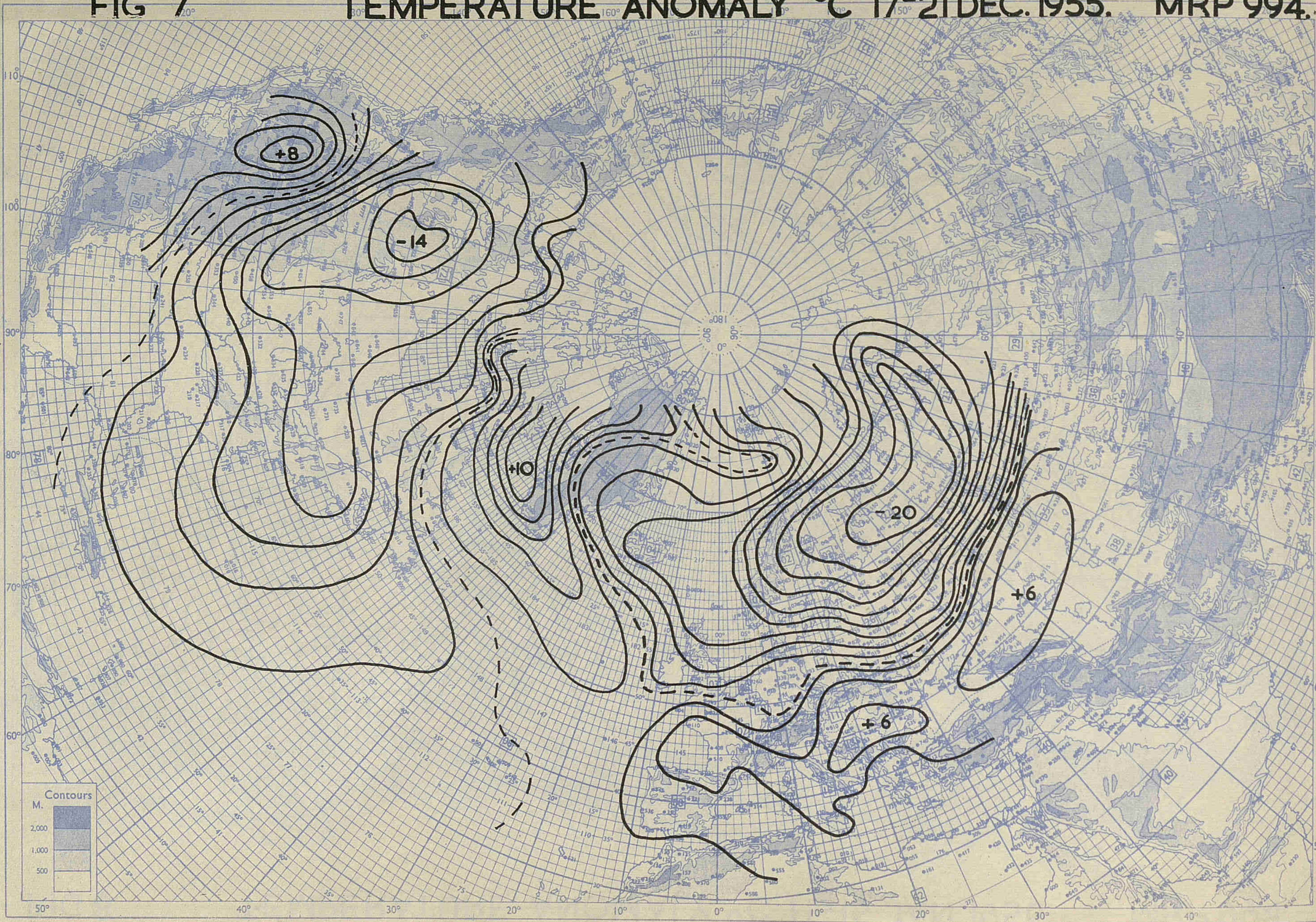

+8
-14
+10
-20
+6
+6
Contours
M.
2,000
1,000
500
110°
100°
90°
80°
70°
60°
50°
40°
30°
20°
10°
0°
180°

FIG 8. TEMPERATURE ANOMALY °C 11–15 JAN. 1956. MRP 994.

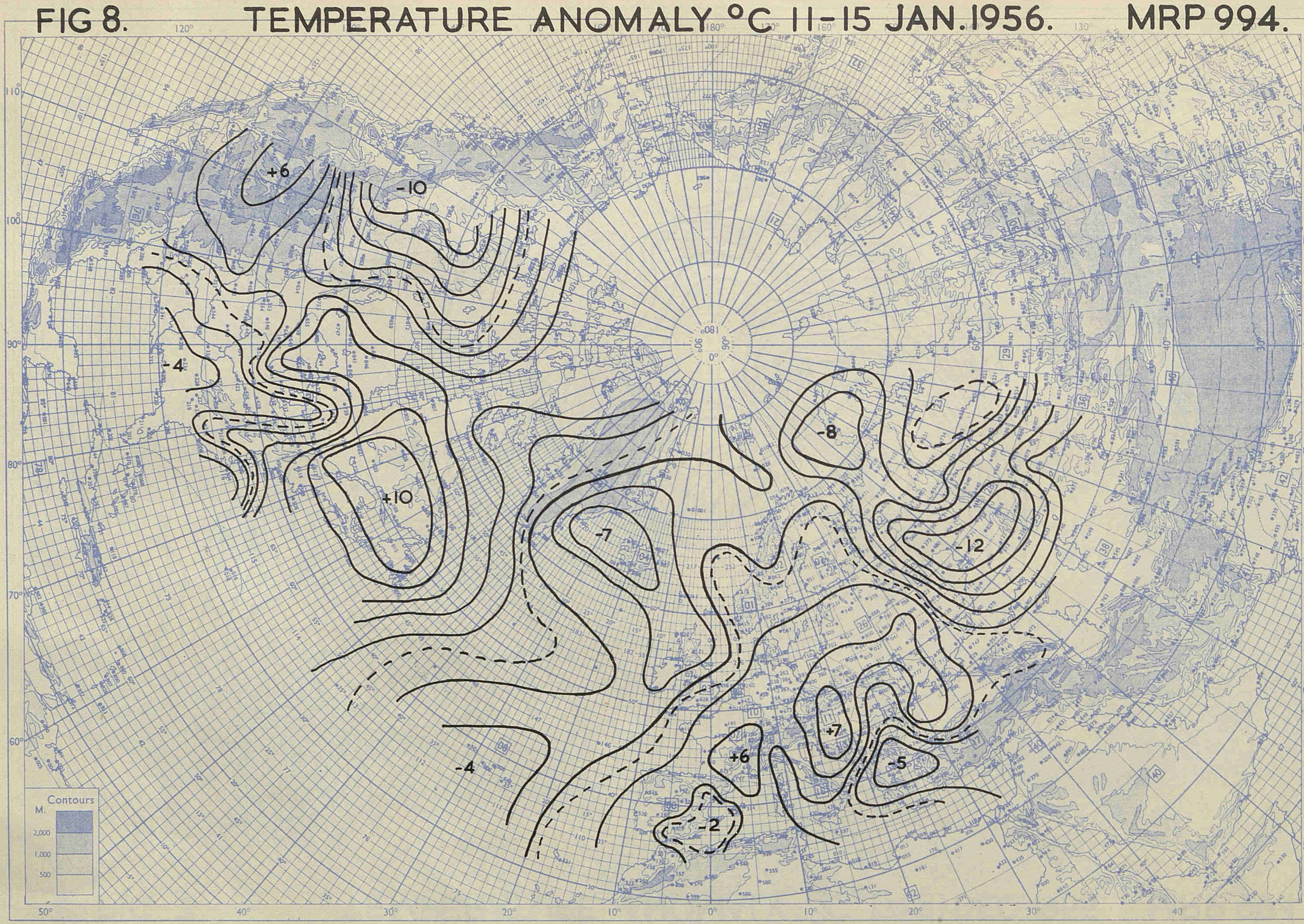
+6
-10
-4
+10
-7
-8
-12
-4
+6
+7
-5
-2
Contours
M.
2,000
1,000
500
120°
180°
160°
130°
110°
100°
90°
80°
70°
60°
50°
50°
40°
30°
20°
10°
0°
10°
20°
30°
40°

FIG 9. TEMPERATURE ANOMALY °C 10-14 FEB. 1956. MRP 994.

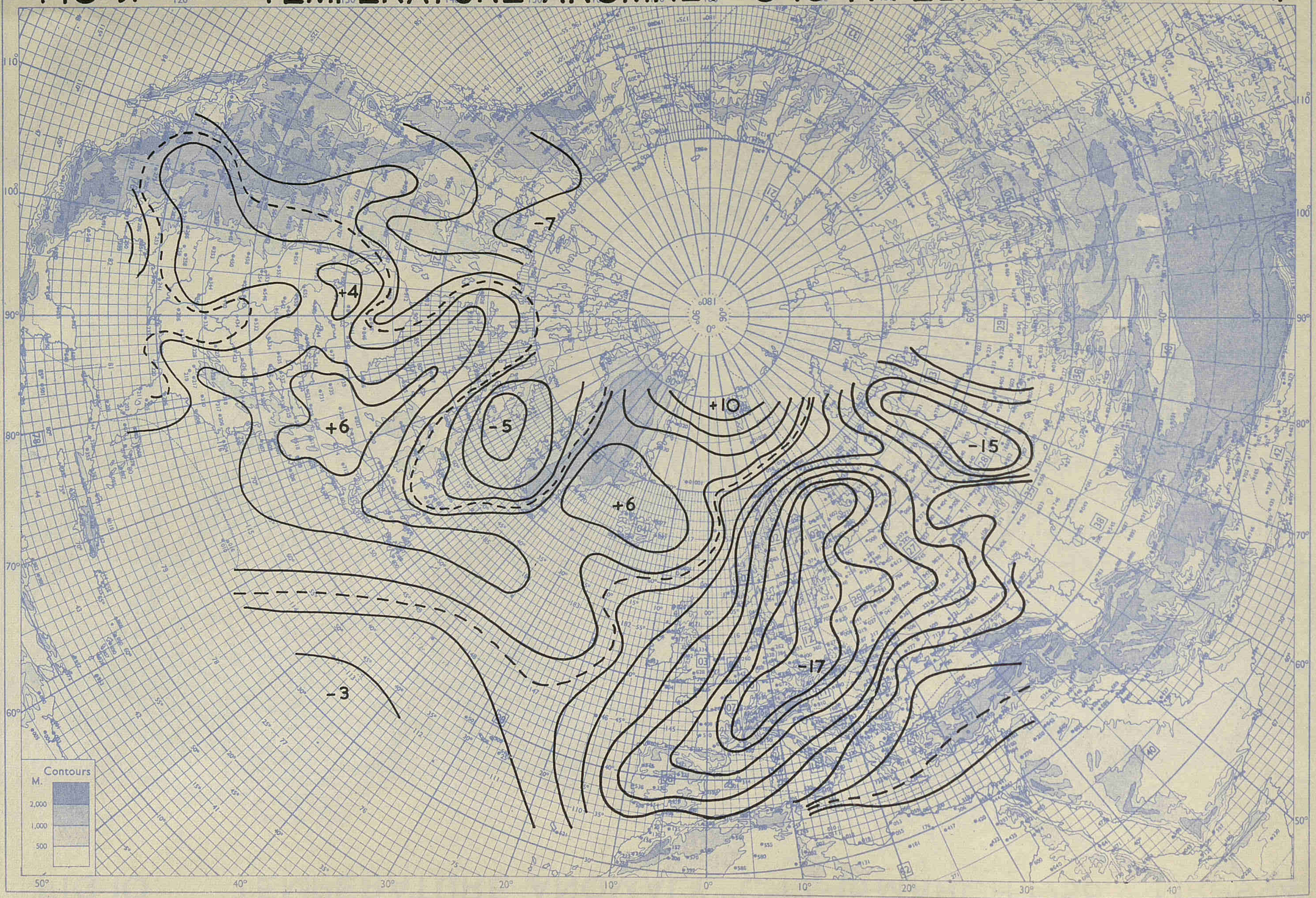

-7
+4
+6
-5
+10
+6
-15
-17
-3
Contours
M.
2,000
1,000
500

FIG 10. TEMPERATURE ANOMALY °C 12-16 MARCH 1956. MRP994.

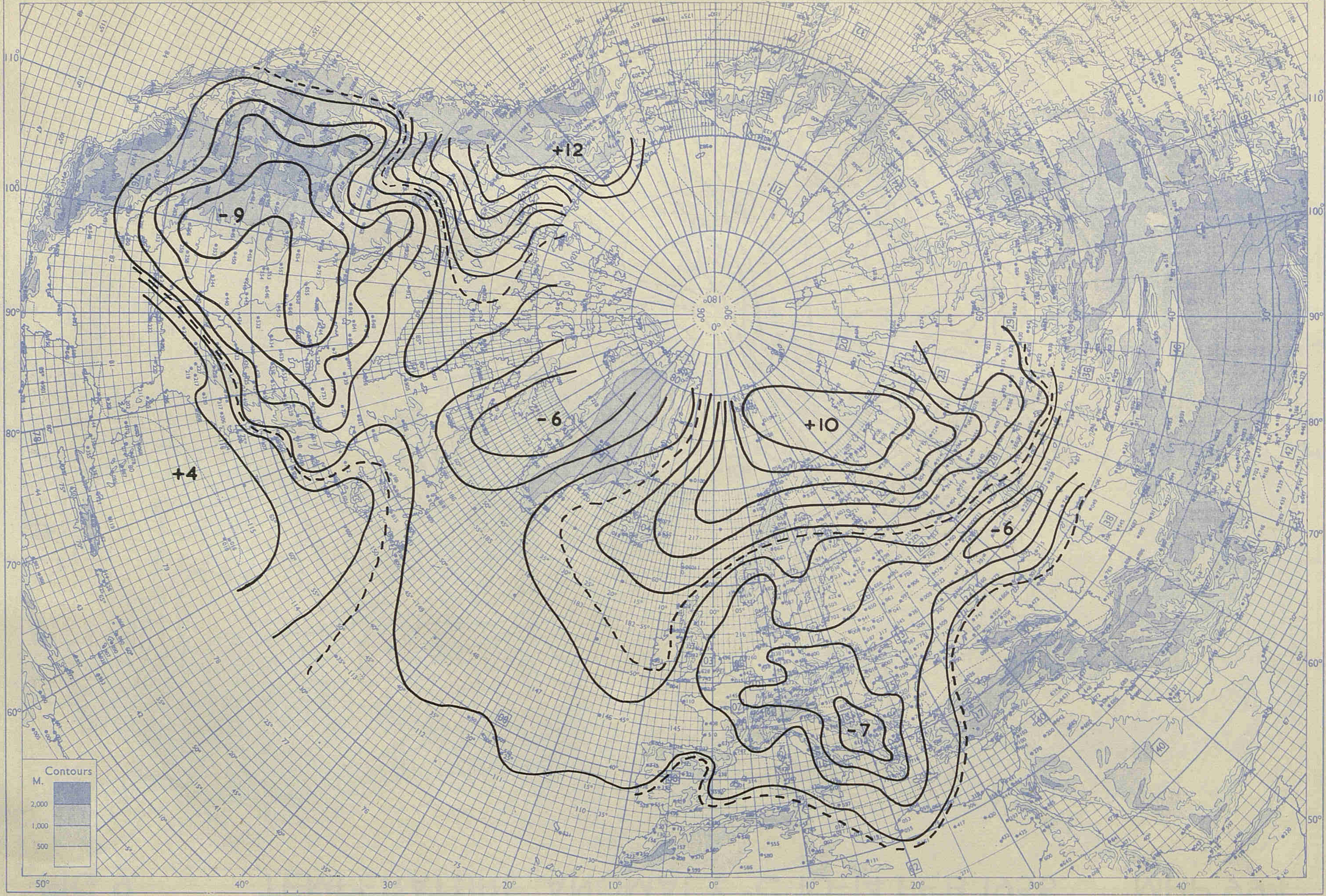
+12
-9
-6
+10
-6
-7
+4
Contours
M.
2,000
1,000
500
50°
40°
30°
20°
10°
0°
10°
20°
30°
40°
60°
70°
80°
90°
100°
110°
120°

FIG 11. TEMPERATURE ANOMALY 21-25 APRIL 1956. MRP 994.

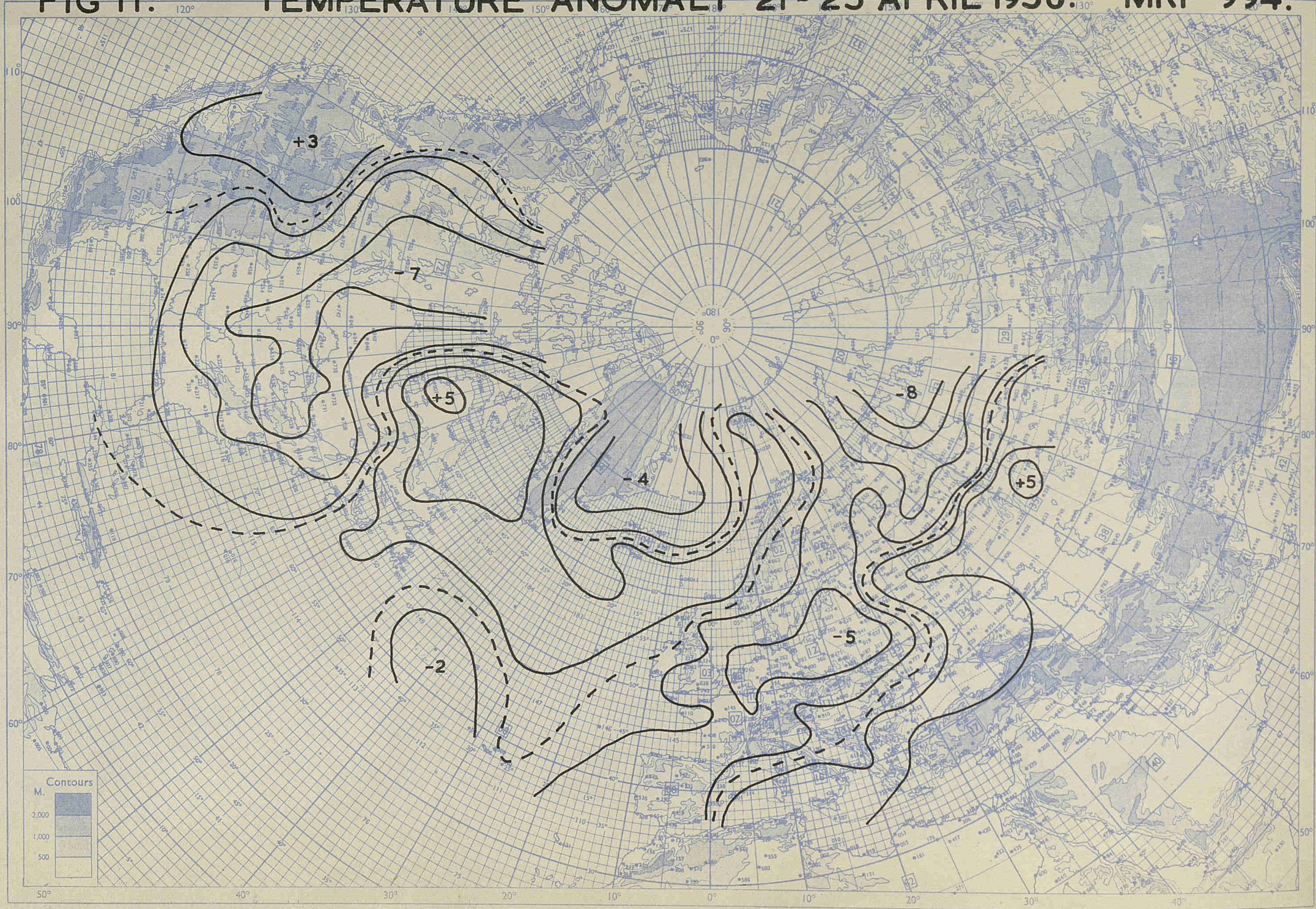
+3
-7
+5
-4
-8
+5
-5
-2
Contours
M.
2,000
1,000
500
50°
40°
30°
20°
10°
0°
10°
20°
30°
40°
110°
100°
90°
80°
70°
60°

M.R.P. 995

31st July, 1956.

AD 147510

METEOROLOGICAL RESEARCH IN AIRCRAFT.

by

R. J. Murgatroyd.

(Meteorological Office)

AIR MINISTRY

METEOROLOGICAL RESEARCH COMMITTEE

At the time of issue this report has not been published. Any author desiring to quote this paper should refer to it as "A paper of the Meteorological Research Committee (London), M.R.P. No.995 by Mr. R.J. Murgatroyd. A copy is available in the Library of the Meteorological Office."

FOREWORD

Meteorology, the science of the atmosphere, has a long history with important applications to many sides of human activity, but nowhere has the application been more direct or more vital than in aviation. In the design of aircraft, for the long-term planning of civil air-routes or military operations, and for the safe, efficient and effective execution of day-to-day operations in peace and war, the advice of the meteorologist has been and continues to be essential and often critical: the debt which aviation owes to meteorology is immeasurable. But the account has never been one-sided and the contributions to meteorological knowledge provided by the observer in the aircraft began with the earliest days of flying and continue to grow in scope and importance as new aircraft are developed, and new instrumentation in the hands of expert meteorologists is carried wherever the aircraft will reach.

The account here presented describes the work of the Meteorological Research Flight, an integral part of the research organization of the Meteorological Office, with aircraft instrumented and manned by scientific staff directing their whole time to the solution of problems for which the aircraft is an eminently suitable and, in many respects, an irreplaceable tool. The author has been for some years the Senior Meteorological Officer of the Flight and has been personally responsible for the design and installation of much of the technical equipment as well as for supervising the execution of the research itself. There could be no-one better fitted to prepare such a report and it is believed that it will be of wide interest and value.

Few, if any, other meteorological organizations in the world have hitherto been so fortunately placed with aircraft continuously and exclusively provided for meteorological research. The present account indicates the wealth of information which these facilities bring within the reach of the meteorologist and should be an encouragement to other services which may be contemplating similar establishments.

(SGD.) R.C. SUTCLIFFE

Deputy Director
(Research)

Meteorological Office,
Air Ministry,
London.

G.3868/PN/7/56/500

At the time of issue this report has not been published. Any author desiring to quote this paper should refer to it as "A paper of the Meteorological Research Committee (London), M.R.P. No.995 by Mr. R.J. Murgatroyd. A copy is available in the Library of the Meteorological Office."

M.R.P. 995
31st July, 1956

AIR MINISTRY

METEOROLOGICAL RESEARCH COMMITTEE

METEOROLOGICAL RESEARCH IN AIRCRAFT

by

R.J. Murgatroyd (Meteorological Office)

1. Introduction

Although the use of aircraft for routine observations of wind, temperature, and humidity in the upper air has almost everywhere given way to that of radio and radar-sonde balloons, the aircraft has several unique advantages as a tool for special observations needed for research purposes. These derive mainly from its ability to travel at will to selected positions and to carry a number of observers and complicated apparatus. With modern aircraft and specialised instrumentation the field of meteorological measurements at altitudes up to 50,000 feet is very wide, and includes all types of nuclei and dust particles, the chemical constituents of the atmosphere, the composition and structure of clouds, rainfall mechanisms, electrical phenomena, radiation measurements, turbulence and diffusion recordings and detailed studies of large weather systems made in conjunction with large-scale synoptic observations. The difficulties in operating an organisation to do this work are, however, considerable and for economic reasons the organisation must be able to utilise fully the aircraft allocated to it. Aircraft are expensive. Research flights of many types can not be made in areas where there are civil airways or military restrictions. The instrumentation must be such that accurate measurements are obtained at high speeds and in bumpy conditions and the mounting and location of instruments on the aircraft must be such that the readings are representative of conditions in air undisturbed by the presence of the aircraft. The data obtained on a single flight may result in weeks of analysis and study before they can be fully assimilated. A considerable backing of scientific and technical manpower is therefore needed both to devise the instrumentation and digest the results obtained.

During the second World War 1939-45 the Meteorological Office operated aircraft as part of the High Altitude Flight at Boscombe Down to make specialised measurements and at the end of the war formed the Meteorological Research Flight at R.A.E. Farnborough. At present this is believed to be the only institution in the world equipped on a regular basis to deal with all types of meteorological measurements. It is the purpose of this article to describe some of the results obtained up to date and outline the work now being carried out and its prospects for the future. Most of the space will be devoted to methods of measurement and it will only be possible to indicate very briefly in a short article of this type how the results of the measurements are being utilised.

2. Measurements at high altitudes

For high-level and high-speed work, a Canberra aircraft is used with a ceiling of about 50,000 ft. and the chief measurements made at present with this machine are summarised in the next paragraph.

/2.1.

2.1. Temperature

Owing to kinetic and friction effects the indicated temperature of a thermometer in a moving airstream of true air-speed V is greater than the air temperature by an amount KV^2, where, under given conditions, K is a constant. The term KV^2 may be about 40°F when V is 500 kt. and hence small variations of K due to the thermometer's design and position on the aircraft structure will produce important errors in the measured temperature. Studies of this latter effect and improvements in aircraft thermometers, made in collaboration with the Meteorological Office at Harrow, have resulted in various electrical resistance thermometers for use in aircraft, which are shown in Fig.1. A comparatively recent American suggestion (Refs.1 and 2) for eliminating the effect of aircraft-speed has been to mount the thermometer element at the centre of a vortex, where it will undergo cooling which can be adjusted to offset the heating induced by kinetic effects. Models of these vortex thermometers of both the tangential type, and the axial flow type shown in Fig.1, have been tested in flight up to 40,000 ft. and shown to be efficient in clear air. In cloudy air the performance of all conventional thermometers is affected by partial evaporation of the water deposited, or the ice formed, on their surfaces and it has not yet proved possible to obtain reliable temperature readings in cloud. The accuracy required here is about ±1°F, for use in calculations of buoyancy in the development of cumulus clouds for example. It may be that it will prove impossible to design simple thermometers which will give readings of this accuracy in cloud, and that more complicated instruments such as sonic or radiation thermometers will have to be developed for this purpose. This problem is discussed in more detail below.

2.2. Humidity

The difficulty in measuring humidity at high levels, particularly in the stratosphere, arises from the minute quantity of water there. The instrument in use at present (which was designed for this work) is the Dobson-Brewer hygrometer (Ref.3) which consists essentially of a cooled surface whose temperature can be controlled and measured. The temperature at which a frost deposit first appears when air is passed over it is the frost point of the air. In an automatic version of this instrument the surface is viewed by a photo-electric cell whose output controls the surface temperature at the frost point through suitable electronic circuits. For high-altitude work the instrument has to be pressurised so that it can be operated with outside air while it is within the pressure cabin. It is also advantageous at high levels to compress the air to a high pressure before reading its frost point and in a recent adaptation the air is passed through the compressor of the jet aircraft in which the measurement is made before its humidity is measured (Ref.4).

The results of this work (Refs.5 and 6) show that the stratosphere over England is very dry and that the frost point at 50,000 ft. is usually about -115°F (Fig.2). The most likely explanation of these low frost points is that air in the lower stratosphere over temperate latitudes must recently have passed through the equatorial tropopause (Ref.7). It has been planned to extend these humidity measurements, together with those of ozone, to other latitudes to obtain more information on the way they vary, and hence on the general changes of circulation at high levels, as well as to utilise them in more obvious ways for forecasting high cloud and condensation trails and as data in radiation studies.

The most commonly occurring condensation trails are formed at high altitudes and arise from the addition of exhaust water vapour to the air behind the aircraft. The study of this process, and of the effects of exhaust heat and the mixing of the exhaust gases with the air at high altitudes, involves a knowledge of the aircraft-engine performance as well as the meteorological factors involved (Ref.8). Fig.4 shows photographs of contrails taken during some of these studies. The conditions for the formation of high cloud are at present not well understood but a great deal of data on its occurrence, temperature, height and extent have been collected (Fig.3 and Ref.9). Studies of radiation are discussed further below.

/2.3.

2.3. Ozone

Another parameter of importance in the study of circulation and radiative equilibrium in the upper troposphere and lower stratosphere is the amount of ozone in the atmosphere at these levels. The apparatus shown in Fig.5 is an adaptation, by the Meteorological Department of the Clarendon Laboratory, Oxford University and the Meteorological Research Flight, of a system due to Ehmert (Ref.10) of determining chemically the ozone-content of air, and has been used in the stratosphere in jet aircraft. Each of the test tubes is arranged by remote control to have 5 litres of air passed through it at chosen levels up to 50,000 ft. They all contain solutions of sodium thiosulphate in an excess of potassium iodide. The effect of ozone passing through this solution is to liberate free iodine from the potassium iodide. This iodine then reacts with some of the sodium thiosulphate and a subsequent electrometrical titration, made on the ground, is directed towards determining the remaining amount of sodium thiosulphate and hence the amount of ozone originally sampled. The chemical equations for this process are:

$$O_3 + 2\,KI + H_2O = 2\,KOH + O_2 + I_2$$

$$2\,Na_2S_2O_3 + I_2 = 2\,NaI + Na_2S_4O_6$$

The results in the troposphere in England are in agreement with previous work (Ref.11) and show small amounts, considerable variability and little change with height. Measurements of ozone-content in the stratosphere so far have not been consistent enough to reveal any well-marked features and further measurements are to be made in the near future. In England (latitude 50°N) the measurements up to date have not shown any marked increase at the tropopause but rather a tendency for the increase with height to become more evident at about 50,000 ft. Some preliminary measurements made by Dr. A.W. Brewer of the Clarendon Laboratory, Oxford University, using this apparatus in Norway (latitude 70°N) have, however, shown significant increases just above the tropopause between 30,000 and 35,000 ft.

2.4. Winds and turbulence

The measurement of wind from aircraft is usually accomplished by comparing its ground-movement with its air-movement over a given time interval. The accuracy depends entirely on the accuracy of the airspeed indicator and of the ground navigation system. At present the measurements are rather crude compared with those that can be achieved by radar-wind methods using balloons, but they have the advantage that variation in space and time can be measured successfully. Other methods of using an aircraft for special wind measurements, e.g. over short periods and short distances, involve the firing of smoke puffs over a camera obscura on the ground, the discharge of smoke trails or the dropping of "window", the movement of which can be tracked by a ground radar station. The latter, together with the camera obscura, is located at the Meteorological Office's radar station at East Hill near Dunstable. Studies of this type provide valuable information on the variability of wind and on turbulence-parameters at high levels (Ref.12).

The occurrence of clear-air turbulence at high levels is a problem of considerable interest to airline operators and aircraft designers. The main difficulty of investigating this phenomenon is to locate it. An aircraft may be flying at a fairly high altitude, say 30,000 ft., in clear smooth air and suddenly enter a region of rough bumpy air which may persist for a hundred miles or so or may be only a few miles in extent. Similarly it is frequently only a few thousand feet in thickness and may be avoided by a slight change of height. The characteristic frequencies of the bumpiness can be examined by means of accelerometers carried on the aircraft. Attempts have been made with some success (Ref.13) to relate its occurrence to large wind shears in the vertical or horizontal or to unstable lapse rates - a frequent location being on the cold side of the jet stream. It is also a possibility that the turbulence is produced up to very high altitudes, under certain conditions, by the degeneration of wave motion set off by mountains. A very large effort has been put into the study of clear air turbulence by several agencies, but it is clear that considerably more research will be necessary before it is thoroughly understood.

In connection with investigations of large-scale meteorological systems, such as the jet stream, the Meteorological Research Flight works in conjunction with the Forecasting Research Division at Dunstable. The system is for the aircraft to fly accurate courses making as many instrumental and visual observations as possible, and for the Forecast Division to attempt to relate these to data obtained from synoptic weather-reporting and radio-sonde stations. It is possible in this way to obtain information on the characteristics of these systems which cannot be obtained in any other manner, e.g. the distribution of humidity, cloud and turbulence round a jet stream has been investigated. (Ref.14). A typical cross-section of a jet stream built up from both aircraft and other measurements is shown in Fig.6. Measurements of this type have helped to explain the circulation and vertical motions associated with the jet stream, the high humidity and cloud being almost always located on its warm side.

The above selection of high level investigations is not exhaustive. It is of course possible to sample aerosols of all types at high levels, catch samples of ice crystals in high clouds, and make radiation measurements, for example. Further details of some of these techniques are given below in the section on measurements at lower altitudes.

3. Lower altitudes

3.1. General facilities

At lower altitudes the scope of the work is considerably greater. A large transport aircraft, a Hastings (Figs.7 and 8) which has an effective ceiling of about 25,000 ft., has been transformed into a flying laboratory for this purpose. Whereas the Canberra can carry only one meteorological observer, who works in a cramped position in a pressurised cabin and operates many of his instruments by remote control, six or more observers can work together as a team in the Hastings, sitting at benches with different apparatus and supplied with a variety of power supplies transformed from the aircraft's electrical system. In its early stages of development an instrument may be adjusted and read directly, and later its dial may be photographed or continuous traces of several instruments can be recorded on a multichannel galvanometer.

The design and production of each instrument for measurement of meteorological parameters in the air raises special difficulties of its own. Usually the aircraft is travelling at about 3 miles a minute, so that for most applications an instrumental lag of more than a few seconds is unacceptable, whilst for some a few milliseconds only is allowable. Moreover aspects of strength, stressing and wind loads have to be carefully considered so that the experimental equipment will not constitute a danger to the aircraft's safety. Factors of this type often impose severe limitations on the exposure that can be given to the various probes although it is always the aim to ensure that the measurements made are representative of the actual conditions in the air without the interference of the aircraft.

A summary of the instrumentation available, and some results, will be given below for the main fields of investigation - cloud physics and cloud modification, atmospheric nuclei, radiation and general investigations. The latter includes studies of large scale phenomena, e.g. fronts, wave motions and stratocumulus formation, in conjunction with the Forecast Research Division at Dunstable, and diffusion studies, in conjunction with the Meteorological Section at C.D.E.E. Porton.

Some of the work does not involve the use of a large amount of special instrumentation and for this a Varsity aircraft which is less well equipped is used.

3.2. Cloud physics

Cloud physics is a very large subject which involves all aspects of the micro- and macrophysics of clouds and includes the study of precipitation-mechanisms and of the environmental conditions in which the clouds develop. A review of some aspects of this work has been given (Ref.15) but for completeness the short description below of the instrumentation will include these as well as other instruments not previously described.

3.2.1. Particle-sampling

3.2.1.1. Cloud droplets

Cloud droplets have diameters ranging from a few microns to about 100μ in most clouds, the smaller sizes being most common in fair-weather cumulus and stratocumulus, and the larger sizes in cumulus congestus and cumulonimbus clouds. Their sampling is accomplished either by direct capture in oil or by measuring the craters they make on impact with a slide covered with a coating of soot or magnesium oxide. Their number is usually of the order of a few hundreds per cubic centimetre and it follows from this that, generally, the impactor used must be capable of exposing the slide for about $\frac{1}{20}-\frac{1}{50}$th of a second. If the interval can be timed and the collection-efficiency of the sampler is nearly unity this method also provides a measurement of the water-content of the air. The sampler-head must be designed to minimize the effects of splash, and in the case of the oil-sampling method the whole operation, including the photography of the sample, must be accomplished very rapidly to avoid coalescence or partial evaporation of the droplets in the oil. Fig.9 shows different types of cloud droplet and raindrop samplers, Fig.10 shows the present arrangement in the aircraft for rapid photography of the droplet-samples immediately after they are taken, and Fig.11 shows typical photographs of samples. Some results of this work are shown in Fig.12, which shows some curves for droplet-concentrations in cumulus clouds in England.

3.2.1.2. Raindrops

Until recently the problem of sampling raindrops in the atmosphere had not received much attention. It is however of great practical importance because of the severe damage which heavy rain and hail can inflict on a high-speed aircraft even in a very short space of time. In physical meteorology, moreover, an understanding of the history of raindrops during their growth and descent is necessary in order to relate the distribution of drop-sizes observed on the ground to the process by which the drops are formed. Direct measurements of falling raindrops are also necessary in certain studies of radar echoes from precipitation. The relatively large size of the raindrop, which is a difficulty in making measurements by oil or similar techniques, can be utilized in systems based on impact with the collecting surface. For small raindrops and intensities a sooted slide or gauze can be used successfully. Fig.9 includes the type of impactor used for this purpose, the time of exposure being about 1 second for a reasonable sample. Fig.13 shows typical results and it can be seen that even snow-flakes can be sampled by this method. A recent development due to Mr. F.J. Bigg and his colleagues of the M.E. Dept. R.A.E. makes use of the deformation of thin foil by impact with the drop, a method which improves with larger droplets and high aircraft speeds. Fig.14 shows an impactor for continuous recording made by the Meteorological Research Flight to utilise this method. An aluminium foil is exposed for a short time in front of a gauze backing and continuous recording is obtained by driving the rotating drum at an appropriate speed.

/3.2.1.3.

3.2.1.3. Ice crystals, snow and hail

Samples of ice crystals in cloud were taken successfully in aircraft up to cirrus levels as long ago as 1943 (Ref.16). In this work an evaporating lacquer on which crystal replicas were imprinted was used. An alternative method (Ref.17) utilising Formvar in an evaporating solvent, such as ethylene dichloride or chloroform, which is in common use for ice-crystal sampling in cloud chambers, has also been adapted for aircraft work. The development of modern high-speed aircraft has however introduced difficulties in obtaining ice-crystal samples unbroken, and special arrangements are necessary when working from a pressurized cabin.

Imprints of small snow-flakes can be obtained in sooted gauzes (Fig.13) and crystals can also be caught in oil and photographed with special precautions.

Hail-sampling has not yet been attempted from aircraft. There are many cases of structural damage produced by hail, and a device based on the force of an impact could almost certainly be made if a sufficiently urgent need arose for it.

3.2.2. Water content

In addition to data on the size and number of the particles constituting cloud, information is required both for cloud-physics studies and practical applications, such as aircraft deicing, of the amount of free water contained in clouds - usually expressed in gm./$m.^3$. The upper limit of this may be in the region of 10 gm./$m.^3$ and values of about 1 gm./$m.^3$ are usual. Difficulties arise in the design of an instrument for this work owing to the great difference in size between the cloud droplets (a few microns diameter) and the larger raindrops (a few millimetres diameter), and to the different phases of the water sampled (ice, supercooled water, water above freezing). In addition to covering a range up to about 10 g./$m.^3$ a successful instrument must have a very small time-lag (preferably less than a second to measure the rapid changes in a cumuliform cloud), have a high collection efficiency for all particle-sizes, and be robust enough to work on an aircraft. No instrument has yet been devised which will satisfy all these requirements, although several types are in use giving results within their various limitations (Ref.18). The calibration of water-content meters also presents problems as it is not easy to reproduce the actual working conditions in the laboratory. The principal types are:-

3.2.2.1. Forward facing scoops. For these to be effective isokinetic sampling must be achieved (i.e. with a 100% collection efficiency), icing difficulties have to be overcome and a sufficiently large volume of air drawn in to make the accurate measurement of the water it contains a feasible proposition. Some success has however been achieved in America with a capillary collection device. Similar considerations apply to systems in which the air is drawn in, heated to evaporate the water it contains and then passed through a humidity-measuring device. At aircraft speeds the time required to evaporate a cloud droplet (which is usually about one-tenth of a second) becomes important, and for a satisfactory measurement of free water with this method, cloud temperature and relative humidity must also be known accurately. Probably, it is sufficient to assume 100% for the latter but the former is not usually known to within ±2°F.

Under this heading may also be included systems of catching a sample of particles in a given volume, finding their sizes and integrating their volumes. Practical considerations of collection efficiency and counting, apart from the prohibitive amount of labour involved, make this method impractical for general use.

3.2.2.2. Conductivity type of measurement. A very successful method at temperatures above the freezing-point is to allow the water to wet a surface for a given time and then to measure the electrical resistance between two contacts resting on the surface. The Commonwealth Scientific and Industrial Research Organisation, Australia, have produced an instrument in which paper is used as the surface and continuous records obtained. (Ref.19). The method however fails at temperatures below the freezing-point (as do all other methods based on the absorption of water into a surface).

3.2.2.3. Hot wire instruments. If the cloud droplets impinge on a hot wire and evaporate, the resulting change of electrical resistance of the wire will be a measure of the power supplied for evaporation, and several instruments have been built to utilise this effect for measurement purposes. The process is complicated, as the wire temperature depends on the temperature and speed of the air stream as well as on its water-content. Moreover, the ability of the wire to evaporate the droplets sufficiently rapidly varies with the wire temperature. When this is low, evaporation will be very slow. On the other hand, at very high wire temperatures, a barrier of steam appears to form on the wire which has the effect of preventing the oncoming droplets from impinging on it. Furthermore ice crystals also do not appear to remain on the wire sufficiently long to be evaporated completely. However, within the design limitations imposed by these effects some success has been achieved by the method.

3.2.2.4. Icing meters. Another system utilises the fact that supercooled droplets on striking a surface will adhere to it in the form of ice (aircraft icing). In one method a cylinder with its axis normal to the airstream is rotated until it acquires a uniform coating of ice. The thickness of ice deposited in a given time or, alternatively, the amount of water when it is melted, is a measure of the water-content of the amount of air swept through in that time. A development of this method uses a rotating disc in which the thickness of ice acquired per revolution is measured by an electrical transducer. Still another method uses pitot pressure to switch on a heater cyclically as soon as icing blocks up the air holes leading into the pitot tube.

All of these devices work only when supercooled droplets are present, i.e. when the air temperature is below freezing, and moreover they fail at very high values of water-content because the latent heat released on the phase change from water to ice finally raises the instrument-temperature to a point where a considerable proportion of the oncoming water will flow off it rather than freeze. Some success has been achieved in overcoming these difficulties by refrigerating the collection head of the instrument (Ref.20). Fig.16 shows a rotating disc instrument on which this has been done.

3.2.2.5. Results of water-content measurements. The present position is that the general features of water-content distribution in clouds are fairly well known, e.g. it is almost always less than 2 g./m.^{3} in stratiform clouds and does not vary much in time and space. In the centre of cumuliform clouds it may rise to considerably higher values in small areas usually less than a mile across. Within these areas the theoretical maximum value expected from a consideration of the rise of air from cloud base at say 2,000 ft. is about 5 g./m.^{3} at 15,000 ft. in temperate latitudes and 7 g./m.^{3} in the tropics - and present evidence is that these values do in fact occur although the mean over the whole cross-section of the cloud may be only 1-2 g./m.^{3}. When there is sedimentation and heavy rain these concentrations are considerably exceeded in very local areas. However, the data obtained so far are rather sparse and poorly substantiated, and further work is required.

Fig.15 shows some typical results recently obtained in cumuliform and layer clouds with conductivity and heated wire instruments.

3.2.3. Vertical currents and turbulence

Vertical currents in layer-type clouds are seldom more than a few cm. per second and any attempt to measure these by means of the aircraft's motion will fail owing to the comparatively large variations caused by small deviations in attitude, aircraft weight, etc. In cumuliform clouds however the prospect is better as vertical motions of 20 or perhaps 30 m./sec. may be found over flight paths of the order of a mile. Thus estimates may be obtained by using the altimeter and airspeed records during a cloud traverse or, alternatively, by integrating a record of the aircraft's vertical acceleration obtained by means of an accelerometer. (Refs.21 and 22). Fig.17 shows a good case from Ref.21.

Many uncertainties may arise due to the effect of the aircraft pitching and assuming a climbing attitude during the traverse but, nevertheless, by examination of these records a good deal of information has been accumulated on the sizes, shapes and magnitudes of up and down currents in these clouds.

Cumuliform clouds are also associated with the most severe turbulence (or bumpiness) encountered by aircraft. The accelerometer records only the aircraft movement at the accelerometer-mounting and the records have to be corrected, where possible, for the lag in the aircraft taking up the air movement and for the elasticity of the aircraft structure. The problem is important in obtaining data for structural design.

3.2.4. Other cloud parameters

Apart from types and sizes of particles, water-content and vertical currents, other parameters, such as the environmental temperatures and humidities, cloud temperatures, concentrations of condensation and freezing nuclei and electrical effects, are important in cloud-physics studies. In addition aircraft observations are also useful in the interpretation of radar reflections from cloud and precipitation and the relation of cloud parameters to the broad synoptic picture, e.g. frontal conditions (Ref.23). Notes on these are now given:

3.2.4.1. Environmental conditions

Mean temperatures can be found simply with any of the aircraft thermometers described above. For fine structure of the thermals rising below cumulus clouds, however, it is often necessary to measure the temperature change in less than 100 feet of aircraft track. A thermometer capable of doing this utilising very fine platinum wires (50 s.w.g.) on an aircraft is available (Ref.24 and Fig.18). Hot wire anemometers can also be used to measure the vertical speed of thermals. From studies with these instruments it has been found that well below clouds thermals are normally a few hundred metres across and rise, in an environment with a dry adiabatic lapse rate, at 1 - 3 m./sec.

Near the cloud base, however, the lapse rate stabilises and the rising air appears to reorganise itself into the larger scale motions found in the clouds. Around cumuliform clouds the atmosphere is characterised by rather smooth flying conditions. There appears to be very little lateral mixing between the cloud and its environment, except perhaps very near the base, and relative humidity is frequently low in the environment.

The cloud-air will tend to rise as long as its buoyancy exceeds that of the environment. If we compute the buoyancy of the air in the cloud on the assumption that the suspended water at a given level is supported by the surrounding air it appears that for typical cumulus clouds in these latitudes:-

(a) The cloud-air will often have positive buoyancy up to heights of about 10,000 feet, even if the cloud-air temperature does not materially exceed the environmental temperature. If the humidity of the environment is very low near cloud base it may even be possible for the cloud temperature to be less than the temperature of the surrounding clear air and positive buoyancy still to exist.

/(b)

(b) At high levels, say 20,000 to 30,000 feet, the effect of the suspended water in concentrations of about 4 or 5 g./m.^{3} becomes very important. The cloud temperature will have then to exceed the environment temperature by 3 or 4°F to maintain positive buoyancy. When a level is reached where the cloud temperature excess is not sufficient to do this the updraughts begin to decelerate and finally the cloud top will occur when friction forces bring the vertical currents to a standstill. There are several theories concerning the nature of the processes of updraughts and the heights reached by the tops of cumulus clouds, and these could be improved if accurate data on cloud temperatures were available.

3.2.4.2. The measurement of cloud temperature

In general aircraft thermometers will record temperatures in cloud which are low compared to those recorded outside the cloud. This is because of the evaporation, due to kinetic heating, of water collected on their surfaces, the magnitude of the effect being governed by the proportion of the thermometer surface which becomes wet. If ice forms on the surface of the element the release of latent heat of sublimation will also affect the readings and tend to make them too high. In all but the worst conditions, however, experience has shown that the flat plate type of element is not affected to a great extent by icing effects and also that its readings, corrected empirically for the wetting of the element at temperatures above freezing, will only be a few degrees in error. This error, although not appreciable for many applications, may be serious when the buoyancy of a cloud mass has to be estimated and efforts have been made to improve the accuracy by shielding the element from wetting and particularly from the effects of icing. Unfortunately, although this does bring about some improvement the shield itself will normally tend to become wet and air in contact with it cooled by evaporation, so that it is likely that the thermometer will still read low. Whether or not this is the true explanation, practical tests with vortex thermometers have given low readings even when it appeared that there was little chance of the element itself becoming wet. Alternative explanations, based on the idea that droplets evaporate in the air and thereby cool it as they approach an obstacle, hardly seem feasible in view of the comparatively large time needed to evaporate a droplet compared with the time it is in the vicinity of the thermometer element. At the present time the vortex thermometer probably gives the most reliable readings in cloud, although other types are available in which the element is shielded. At temperatures above freezing point a wet-bulb thermometer may be used: its advantage is that, as the whole bulb is covered with water, the effect of evaporation is less variable than in the case of a thermometer which is only incidentally wetted by its passage through the cloud. Some success has been achieved in this way in studies of cumulus clouds in trade winds (Ref.25).

3.2.4.3. The use of radar for cloud physics studies

In this country the Meteorological Office operates a ground radar station at East Hill, near Dunstable, and aircraft in radio communication with this station have been directed into regions giving radar echoes from cloud and precipitation, with the object of linking the radar reflection with the size and nature of the cloud particles and other cloud parameters. Studies of this type present many operational difficulties in this country as the height, position and course of the aircraft are severely limited by Air Traffic Regulations. A series of results linking radar and aircraft observations has been produced by Jones (Ref.26) and it is likely, with the improved methods of particle sampling recently developed, that it will be possible to extend this work considerably.

An alternative method, already used in America and Australia, and also for icing research in this country, is for the aircraft to carry radar equipment in its nose and for radar observations of the cloud to be taken while the cloud is being approached before a traverse. This has the advantage that the observations can be co-ordinated more readily and also that the state of the cloud as regards precipitation can be estimated without actually traversing it.

On the other hand, the instrumental equipment of an aircraft engaged in cloud physics work is already very large without the complication of the airborne radar equipment, the inclusion of which adds considerably to the technological problems of the operator.

3.3. Cooperation with other meteorological research sections

It is, of course, not difficult to combine the research effort of a meteorological flight with that of other research sections both as regards the macroscopic aspects of cloud studies and other phenomena. In this connection, apart from the work on jet streams mentioned above, studies of lee waves from mountains and of the conditions for dissipation of stratocumulus cloud are in hand at present. Other fields in which this type of cooperation is carried out include studies of radiation and diffusion discussed below and, in collaboration with the Forecast Research Division at Dunstable, of the structure of frontal cloud systems. Fig.19 shows a typical section of a frontal surface obtained during this work.

3.4. Atmospheric nuclei

One of the most active fields of research, in which considerable progress has been made over the last two decades, is the study of nuclei in the atmosphere. Such nuclei effectively range in diameter from about 10^{-7} to 10 microns in cloud physics studies, and their investigation requires the measurement of their sizes, shape and chemical composition as well as of their ability to act as condensation or freezing nuclei. Information of their distribution in time and space (particularly altitude) is also required. Recent studies using aircraft for some of these purposes in this country are outlined below:

3.4.1. Condensation nuclei

For many years the study of condensation nuclei on the ground has been carried out using the Aitken nucleus counter or some variant of it. This instrument has also been used in aircraft in America but it was found at the Meteorological Research Flight that the instrument designed by Pollak (Ref.27) was more suitable for aircraft use. (Fig.20). The results of flights with this instrument have been presented by G.J. Day (Ref.28). It was found in flights over the sea that clean maritime air contains in the order of 10^2 to 10^3 condensation nuclei per cc., but that over the land the concentration is usually about an order more and, near to certain industrial sources, considerably higher. In general, concentration fell off considerably with height, the vertical distribution being dependent on the atmospheric stability. Concentration varied considerably with location, as illustrated in Fig.22 which shows the measurements taken in a flight round England.

3.4.2. Freezing nuclei

The concentration of freezing nuclei in the atmosphere can be determined by means of the "cold box" and work using this apparatus has been described by E.J. Smith and K.J. Heffernan of the Commonwealth Scientific and Industrial Research Organisation, Australia (Ref.29). A similar installation is in use in the Meteorological Research Flight (Fig.21). A cylindrical chamber of about 60 litres capacity is cooled by pumping methylated spirits round a circuit which includes pipes wound round the cylinder and a copper spiral immersed in solid carbon dioxide. Steam is introduced into the chamber by means of a small boiler, the chamber is strongly illuminated and the light beam viewed at right angles. The water droplets appear as a dull opaque fog but any ice crystals which appear sparkle and glisten. The estimation of the number of ice crystals is subjective, but by measuring the temperature at which they appear in recognisable quantities, some idea can be formed of the temperature at which any freezing nuclei present become active. It is found that in general the ice crystals are very few down to -20°C or so when the number usually increases markedly. Even so, the concentration is only of the order of 10 to 10^4 per litre, which is small compared to the number of condensation nuclei at low levels. It appears on the whole that ice nuclei do not decrease in numbers with increasing height in the same manner as condensation nuclei and it may be that they are of extra-terrestrial origin. Fig.23 shows some recent results of the variation of freezing nuclei concentrations from day to day in January, 1956.

3.4.3. Salt nuclei and the determination of the chemical constitution of nuclei

Various techniques exist for the sampling of salt nuclei and their chemical determination. Both in Australia and the U.S.A. particles have been captured on hydrophobic surfaces and examined microscopically under conditions of varying humidity (Refs.30 and 31). Their distribution in relation to the wind and to the distance from the sea allows an estimate to be made of the possible concentrations of these particles available for initiating the coalescence mechanism of rainfall in different localities. It has been found, for instance, that over the sea rather small clouds with tops well below the freezing level will produce rain, while much larger clouds in the centre of land masses fail to do so, and one possible explanation of this is the relative availability of large hygroscopic nuclei.

Chemical determinations of nuclei can be made by the Liesegang ring or similar techniques (Ref.32). An impactor of the type designed for the diffusion studies described below may be used to project an airstream on to a specially prepared surface consisting of a gelatine impregnated with a soluble salt chosen to give a suitable reaction with the radical to be sampled. An impinging nucleus will react to produce an insoluble characteristic deposit which may be examined under a microscope at leisure. For instance, when one is attempting to sample chloride the agent may be a soluble silver salt, and the deposit to be examined will be the insoluble silver chloride, which can also be reduced to metallic silver.

Other techniques for sampling small particles are available, and it is probable that this aspect of the work will receive more and more attention as the subject develops. One application of small-particle sampling which has recently been used in the U.S.A. and in this country (Refs.33 and 34) is concerned with the study of medium- and long-range diffusion of particles.

3.4.4. Diffusion studies and their application to rain-making experiments

It is important for some purposes to be able to predict the concentrations at given heights and distances downwind of particles released from a ground source, and data of this type are also required for fundamental studies of diffusion processes. An obvious practical application is the release of silver iodide particles from surface generators in the hope that they will be carried up into the air and act as freezing nuclei, thereby modifying the composition of clouds and perhaps producing greater rainfall. The physical processes involved are not at present thoroughly understood so that work is being carried out both on the fundamental physics of rain-producing processes and practically, by a series of experiments involving large scale release of silver iodide into cloud systems, followed by a statistical analysis of the rainfall downwind compared with that falling in nearby control areas. An obvious prerequisite of the process is that the silver iodide particles reach a height at which they can be effective within a reasonable time. Unfortunately it is difficult to sample silver iodide particles in the air, and detailed work from aircraft both in this country and the U.S.A. has usually been carried out with zinc sulphide particles of sizes 0.5μ to 3μ diameter. These particles fluoresce characteristically when illuminated by ultra-violet light and hence can easily be counted once they are sampled by an impactor in the aircraft. Fig.24 shows the type of impactor used. Air is sucked through the nozzle on to a suitably prepared surface of a drum. The drum is rotated in three-degree steps by an actuator, so that 120 samples can be obtained on it, each for example corresponding to one minute, or say, 3 miles of flight. Course, height, direction and location are also noted for each sample and it is possible to relate concentrations in the plume of material to other factors such as lapse rate, wind speed, etc.

The preliminary results of this work show that the plume, up to any level, normally travels at the speed and in the direction of the mean wind from the surface to that level and also that the particles do not penetrate through sizeable inversions. Mean plume widths are variable and rapidly exceed their heights. They may subtend an angle at the release point of as much as 40° at distances of 5 miles or so from the source but only about 20° at 40 miles from it. The distribution has much the same form at all heights.

Because of the variability of the results and the many conditions in which the information is needed, considerably more data are required before reliable empirical formulae for concentrations at any point can be derived or a worthwhile agreement with theory obtained. In particular it is hoped to extend the sampling work to frontal-cloud conditions. Modifications of the impactor system are being devised to allow sampling to be carried out in clouds and rain.

3.5. Other aspects of cloud modification

Apart from cooperation in experiments on large-scale rain-making, aircraft have been used in many countries in small-scale trials for modifying cloud. Either a nucleating agent such as silver iodide is used, or, more commonly, solid carbon dioxide is dropped into super-cooled clouds with the object of converting the droplets into ice crystals. Work of this type on cumuliform clouds is often not very satisfactory, as this type of cloud changes so rapidly that it is not always possible to ascertain whether the cloud has in fact been modified by the operation. For successful scientific experiments of this type observations other than those of a single aircraft, e.g. radar photographs of the cloud, a second observing aircraft and ground observers, are necessary before it can be stated with any authority that the subsequent changes in the cloud have been induced by the seeding. Even when these are available it is not always possible to be sure. Similar remarks also apply when attempts are made to induce precipitation by the coalescence mechanism by introducing water drops or salt nuclei into the base of a cumulus cloud.

Supercooled layer clouds however can be modified with certainty and the process of modification followed and examined. Figs.25 and 26 show pictures taken during experiments of this type carried out on 9.1.56 and 23.1.56 respectively. Other similar work by the Meteorological Research Flight has been described in Refs.35 and 36. The plan of these experiments was to make measurements in the layer to be seeded, e.g. water content, drop size, etc., when possible, and lapse rates of temperature above and below the cloud, and then to drop about 100 lb. of dry ice in the form of small pellets into the cloud at the rate of 3 to 10 lb./mile of flight. The presence of water cloud was revealed either by icing of the aircraft when flying in it or by the presence of a "glory" around the shadow of the aircraft on the cloud when flying above it. After seeding, the aircraft usually ascended a few thousand feet above the cloud to a convenient height from which to take photographs. For a cloud several thousand feet thick about 15-20 minutes elapse before anything is seen. Then the seeded area takes on a characteristic opaque appearance and precipitation patterns of a similar shape may be observed on the screen of a ground radar station. A little later the cloud in the seeded area disperses, leaving a hole which slowly enlarges. Sun pillars may appear, formed by reflection of the sun's rays from ice crystals at the edges of the surrounding cloud. There may also be slight cumuliform growth around the edge of the hole, which is reflected in a local increase in water content if measurements are made during an aircraft traverse across it.

The practical value of these experiments is however limited. In favourable conditions, areas of perhaps 10 to 15 square miles in a cloud 2,000 feet thick may be cleared by using about 100 lb. of dry ice. However the whole process takes between 40 minutes and an hour, and during that time the seeded area may drift 20 or 30 miles, so that any operational work based on it would be difficult to plan. Moreover, the occasions when these experiments can be carried out in the United Kingdom are few. In Southern England large areas of supercooled stratocumulus usually only occur during the winter months during periods of easterly winds.

3.6. Radiation measurements from aircraft

Many of the current uncertainties in our knowledge of solar and terrestrial radiation can be resolved by carrying suitable instruments on aircraft. Attempts have been made to carry out infra-red spectroscopy in the stratosphere, since most of the absorption is in the lower troposphere (Ref.37) and this work is continuing. Extensive aircraft observations are required of the albedo of clouds and haze as well as that of different land and sea surfaces before the total albedo of the earth can be estimated. In conjunction with Kew Observatory a start has been made on some of these aspects by carrying two solarimeters, one below and the other on top of the main fuselage of the aircraft. Preliminary results for these measurements give values of 0.06 to 0.07 for the albedo of sea surfaces and 0.1 to 0.3 for land (0.8 when snow covered). For water clouds the values are extremely variable, depending on depth, water content and possibly particle size, while thin ice clouds show little more effect than would be anticipated from their saturated water vapour content. Absorption by water cloud usually appears to be in the region 10 - 20% although theoretical studies suggest rather smaller values. Fig.27 shows a typical result from this type of flight (Ref.38).

A parallel series of experiments has been made measuring infra-red radiation at night using instruments (Fig.28) described by J.T. Houghton and A.W. Brewer in Ref.39. A typical result from these flights is shown in Fig.29 in which simultaneously measured temperatures, frost points, and incoming and outgoing radiation values are compared. Using these data Houghton (Ref.40) has been able to check the results of computations made by means of radiation charts of the upward and downward flux of radiation at high levels as well as to provide information on the emissivity of various surfaces and specified clouds. The value of this work for measurements in the stratosphere is at present limited by the range to which the instruments can extend into the infra-red region. As further improvements are made in instruments of this type, however, it should be possible to accumulate more data on radiation in the stratosphere.

4. Concluding remarks

Although the review above has covered somewhat sketchily a large variety of subjects which are of particular interest at present to the Meteorological Research Flight it has by no means exhausted the applications of aircraft to investigations of atmospheric phenomena. Notable omissions include electrical and magnetic measurements, especially such interesting features as charge distribution in thunderstorms, conductivity and ion content of the air, etc., and investigations of radio-activity which, although perhaps not pure meteorological research, are allied subjects.

The multiplicity of the problems, their separate difficulties of instrumentation, observation and, in particular, reduction of the data, create serious problems of subject priority and allocation of manpower for those directing the use of the aircraft resources. Once aircraft become allocated for general research work they must, for economic reasons, be used as far as possible to the limit of their flying capacity and this must be also an extremely important factor in determining the particular fields to be investigated. It also means that there is often room for University staffs to make use of the flying facilities in allied researches provided their experiments can be satisfactorily combined in the flying programme of the official organisation. It is certainly advantageous, in a subject such as meteorology where there is so much to investigate, to have the aircraft always available for many purposes rather than to

/obtain

obtain them specially for a limited research on a particular subject, and there are signs that other countries are now contemplating setting up similar organisations.

As regards the future, the tendency will be for the aircraft to be flown to greater altitudes and at greater speeds, and for the observations to be extended to other latitudes. At the same time, methods will become more refined and involve more advanced technology. At the highest altitudes we may expect the techniques of measurement to be intermediate between those used in present-day aircraft and those used in rockets for research in the upper atmosphere, with a greater emphasis on remotely controlled and automatically recorded measurements. Near the surface the emphasis will probably change gradually towards measurement of smaller-scale phenomena, with concentration on small lag and greater rapidity in measurement and recording, and the improvement of the experimental procedure as a whole to a standard comparable with that attainable on the ground.

References

1. Vonnegut, B. 1949. Vortex thermometer for measuring true air temperature and true air speeds in flight. Rep. Gen. Elec. Res. Lab. Schenectady N.Y., No. RL-247.

2. Ruskin, R.E., Schecter, R.M., Dinger, J.E. and Merrill, R.D. 1952. Development of the N.R.L. axial-flow vortex thermometer. Rep. Nav. Res. Lab. Washington D.C., No.4008.

3. Dobson, G.M.B. with Brewer, A.W. and Cwilong, B.M. Bakerian lecture: Meteorology of the lower stratosphere. Proc. Roy. Soc., London, A, 185, 1946.p.144.

4. Goldsmith, P. 1955. A method of increasing the range of the Dobson-Brewer frost-point hygrometer in jet aircraft. Quart.J.R.Met.Soc. London. 81 350. p.607.

5. Bannon, J.K., Frith, R. and Shellard, H.C. 1952. Humidity of the Upper Troposphere and Lower Stratosphere over Southern England. Meteorological Office, Air Ministry, London. Geophysical Memoirs No.88.

6. Murgatroyd, R.J., Goldsmith, P. and Hollings, W.E.H. 1955. Some recent measurements of humidity from aircraft up to heights of about 50,000 ft. over Southern England. Quart.J.R.Met.Soc., London. 81. 350. p.533.

7. Brewer, A.W. 1949. Evidence for a world circulation provided by the measurements of helium and water vapour distribution in the stratosphere. Quart.J.R.Met.Soc., London, 75. 326. p.351.

8. Condensation Trails from Aircraft. 2nd Edition. 1952. M.O.479. Meteorological Office, Air Ministry, London.

9. Murgatroyd, R.J. and Goldsmith, P. 1953. Meteorological Research Papers, Air Ministry, London. No. 833.

10. Ehmert, A. 1951. Ein einfaches Verfahren zur absoluten Messung des Ozongehaltes von Luft. Met. Rundschau, 4, (1951) 3/4, 64-68.

11. Kay, R.H. 1953. An interim report on the measurement of the vertical distribution of atmospheric ozone by a chemical method, to heights of 12 Km., from aircraft. Meteorological Research Papers, Air Ministry, London. No.817.

12. Jones, R.F. 1953. Observations of smoke puffs at heights up to 40,000 ft. Meteorological Research Papers, Air Ministry, London. No.784.

13. Bannon, J.K. 1951. Meteorological aspects of turbulence affecting aircraft at high altitude. Prof. Note No.104, Air Ministry, London.

14. Murray, R. 1953. The upper troposphere and lower stratosphere near Jet Streams. Meteorological Research Papers, Air Ministry, London. No.813.

15. Murgatroyd, R.J. 1955. Cloud-physics at the Meteorological Research Flight. Archiv für Meteorologie, Geophysik and Bioklimatologie. Serie.A. Band 8, 3 Heft.

16. Weickmann, H. 1947. Die Eisphase in der Atmosphäre. Volkenrode R. and T. No.716.

17. Schaefer, V.J. 1949. The formation of ice crystals in the laboratory and the atmosphere. Chem. Rev., Baltimore, 44., 291.

18. Murgatroyd, R.J. 1952. Meteorological Research Papers, Air Ministry, London. No. 737.

19. Warner, J. and Newnham, T.D. 1952. A new method of measurement of cloud-water content. Quart.J.R.Met.Soc. 78. 335. p.46.

/20.

20. Day, G.J. 1955. A refrigerated disc icing meter. Meteorological Research Papers, Air Ministry, London, No.916.

21. Jones, R.F. 1954. Five flights through a thunderstorm belt. Quart. J.R.Met.Soc. 80. 345. p.377.

22. Bunker, A.F. 1955. Turbulence and shearing stresses measured over the North Atlantic Ocean by an airplane acceleration technique. J.Met. Vol. 12. pp.445-455.

23. Sawyer, J.S. 1955. The free atmosphere in the vicinity of fronts. Analysis of the observations by the Meteorological Research Flight, 1950-52. Meteorological Office, Air Ministry, London. Geophysical Memoirs No.96.

24. Grant, D.R. 1950. Meteorological Research Papers, Air Ministry, London, No.542.

25. Malkus, J.S. 1952. Recent advances in the study of convective clouds and their interaction with the environment. Tellus. 4. 2.

26. Jones, R.F. 1954. Radar echoes from and turbulence within cumulus and cumulonimbus clouds. Meteorological Office, Air Ministry, London. Professional Notes No.109.

27. Pollak, L.W. and Murphy, T. 1953. Archiv für Meteorologie, Geophysik und Bioklimatologie, Serie A., p.101.

28. Day, G.J. 1955. Some airborne observations of condensation nucleus concentration. Geofisica Pura e Applicata. Milano. 31. pp.169-181.

29. Smith E.J., and Heffernan, K.J. 1954. Airborne measurements of the concentration of natural and artificial freezing nuclei. Quart.J.R.Met. Soc. 80. 344. p.182.

30. Twomey, S. 1955. The distribution of sea salt nuclei in air over land J.Met. 12. 1.

31. Reitan, C.H. and Braham, R.R. 1954. Observations of salt nuclei over the midwestern United States. J.Met. 11.6.

32. Fedele, D. and Vittori, A. Determinazone delle particelle di cloruro nell'atmosfera e metodi di misura. Revista di meteorologia aeronautica, 13, (1953) 4, pp.9-13.

33. Crozier, W.D. and Seely, Ben. K. 1949. Some techniques for sampling and identifying particulate matter in the air. Proceedings of the First National Air Pollution Symposium, Stanford Research Institute.

34. Pasquill, F. 1955. Preliminary studies of the distribution of particles at medium range from a ground level point source. Quart.J.R. Met.Soc. 81. 350. p.636.

35. Frith, R. 1951. Wind shear revealed by artificial nucleation. Quart.J.R. Met.Soc. 77. 331. p.131.

36. Shellard, H.C. and Grant, D.R. 1951. Results of an artificial nucleation experiment. Met.Mag. 80. p.253.

37. Yarnell, J. and Goody, R.M. 1952. Infra-red solar spectroscopy in a high altitude aircraft. J.Sc.Inst., 29, p.352.

38. Day, G.J. 1956. Meteorological Office Discussion. Met.Mag. April 1956. Vol.85.

39. Houghton, J.T. and Brewer, A.W. 1954. A new radiometer. J. Sc.Inst., 31, p.184.

40. Houghton, J.T. and Brewer, A.W. 1955. Measurements of the flux of long wave radiation in the upper air. 1953-54. Meteorological Research Papers, Air Ministry, London. No.914.

M.R.P. 995

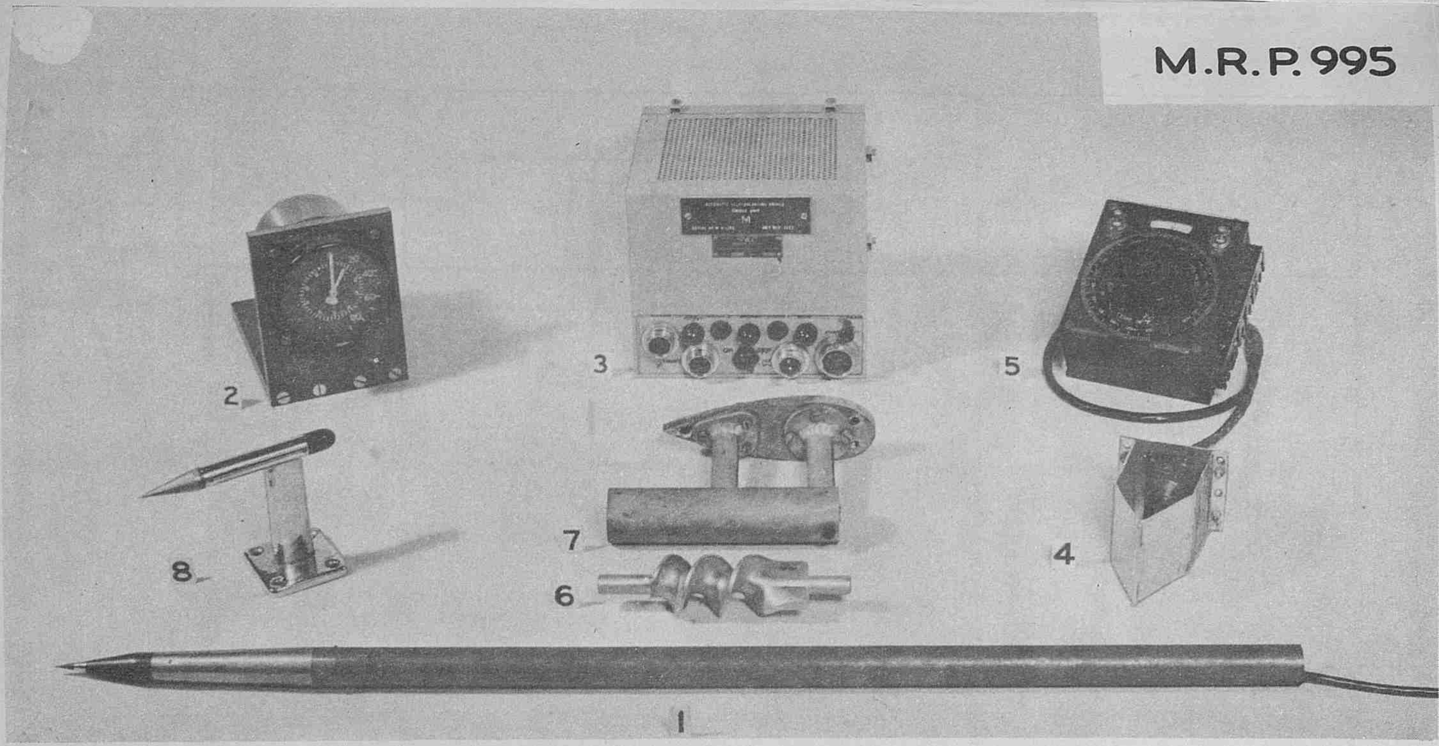

FIG. I AIRCRAFT THERMOMETERS

(1) Experimental Conical Head type (Meteorological Office, Harrow). This is mounted ahead of a wing tip or fuselage nose. The element is a platinum resistance in the cone.

(2) Dial for (1) operated through (3).

(3) Self balancing resistance bridge controlled by (1) with output presentation on (2).

(4) Meteorological Office Flat Plate Aircraft Thermometer.

(5) Hand operated bridge, reading temperature when balanced to resistance of (4).

(6) Internal spiral to transform linear airflow into Vortex in the Axial type of Vortex Thermometer.

(7) External view of Vortex Thermometer.

(8) M.R.F. Conical Type Aircraft Thermometer for under wing or under fuselage mounting.

FIG. 1. AIRCRAFT THERMOMETERS

(1) Impregnated Optical Head type (Meteorological Office, Harrow) This is mounted ahead of a wing tip or fuselage nose. The element is a platinum resistance in the cone.

(2) Dial for (1) operated through (3).

(3) Self balancing resistance bridge controlled by (1) with output presentation on (2).

(4) Meteorological Office Flat Plate Aircraft Thermometer.

(5) Dial operated bridge reading temperature when connected to resistance of (4).

(6) Internal sketch to [illegible] into Vortex in the axial tube of Vortex Thermometer.

(7) External view of Vortex Thermometer.

(8) N.A.E. [illegible] Thermometer for under wing or under fuselage mounting.

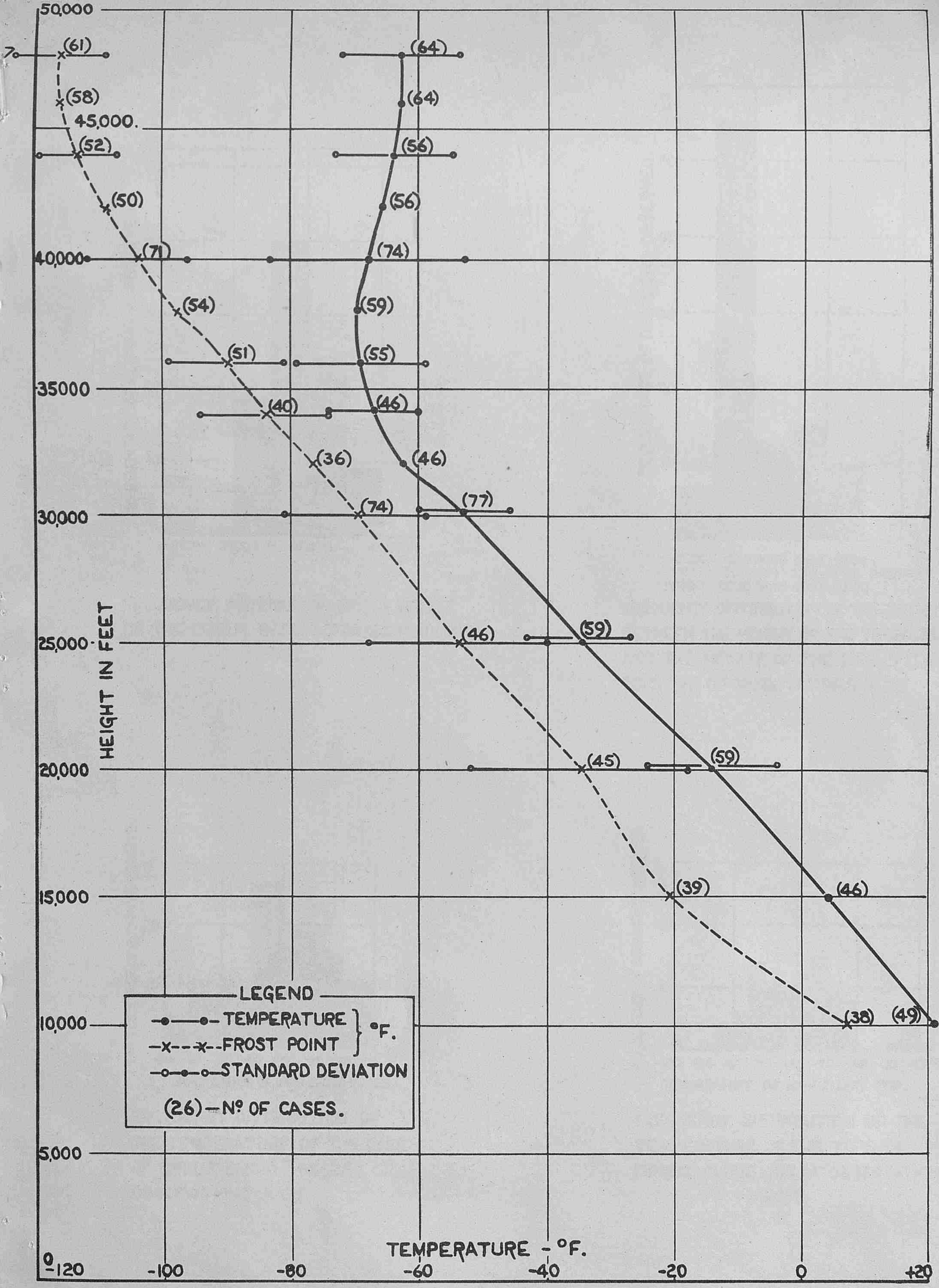

FIG.2. TEMPERATURE AND FROST POINT OVER SOUTHERN ENGLAND (81 ASCENTS FOR 1954 AND 1955.)

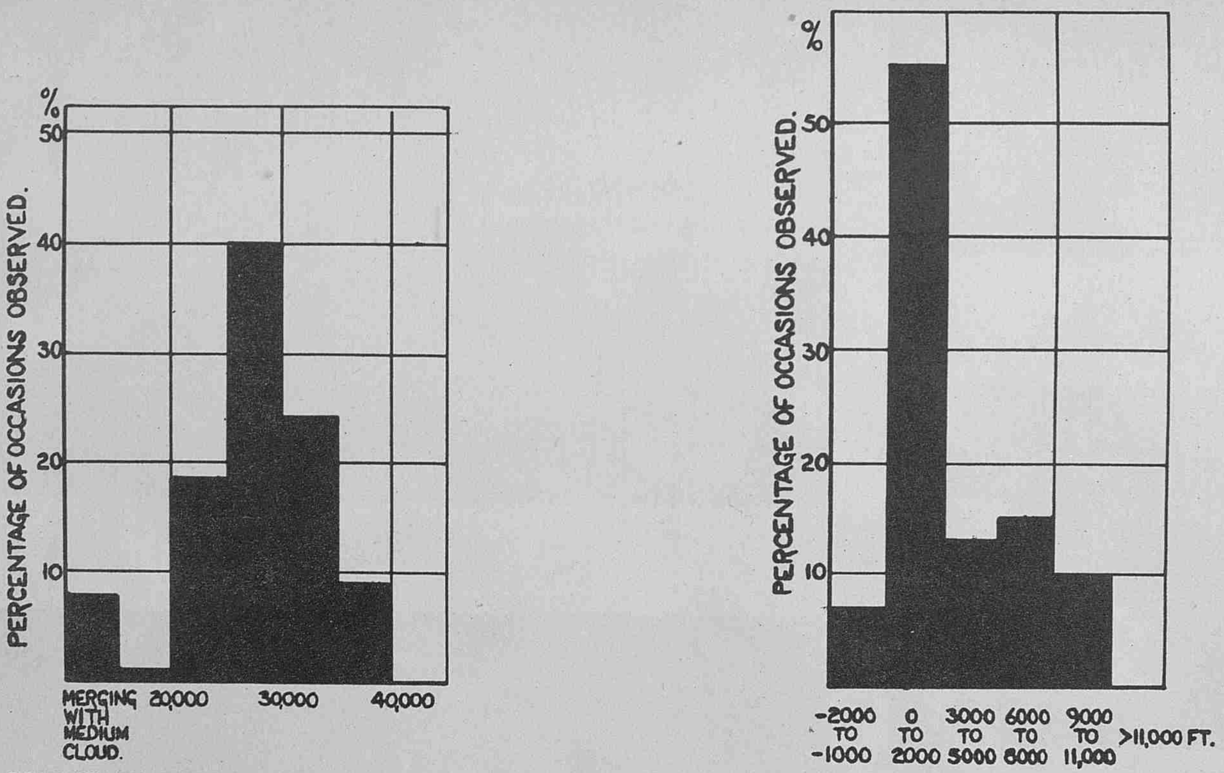

FREQUENCY DISTRIBUTION OF THE HEIGHT OF THE CIRRUS BASE. Nº OF OBSERVATIONS = 63.

FREQUENCY DISTRIBUTION OF THE DIFFERENCE BETWEEN THE HEIGHT OF THE TROPOPAUSE AND THE HEIGHT OF THE CIRRUS CLOUD TOPS. Nº OF OBSERVATIONS = 78.

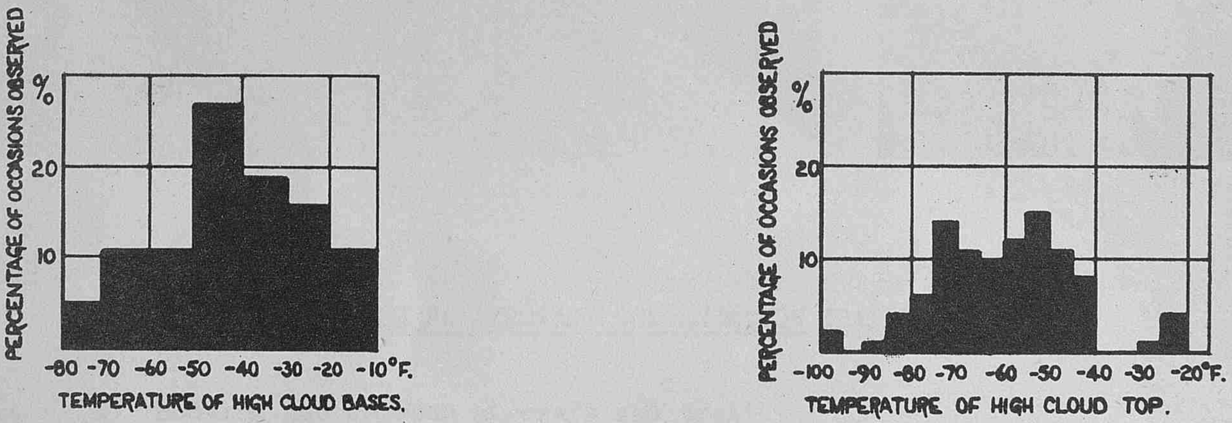

FREQUENCY DISTRIBUTION OF THE TEMPERATURE OF THE BASE OF CIRRUS CLOUD. Nº OF OBSERVATIONS = 63.

FREQUENCY DISTRIBUTION OF THE TEMPERATURE OF THE TOPS OF CIRRUS CLOUD. Nº OF OBSERVATIONS = 81.

FIG.3 OCCURRENCE OF HIGH CLOUD OVER SOUTHERN ENGLAND.

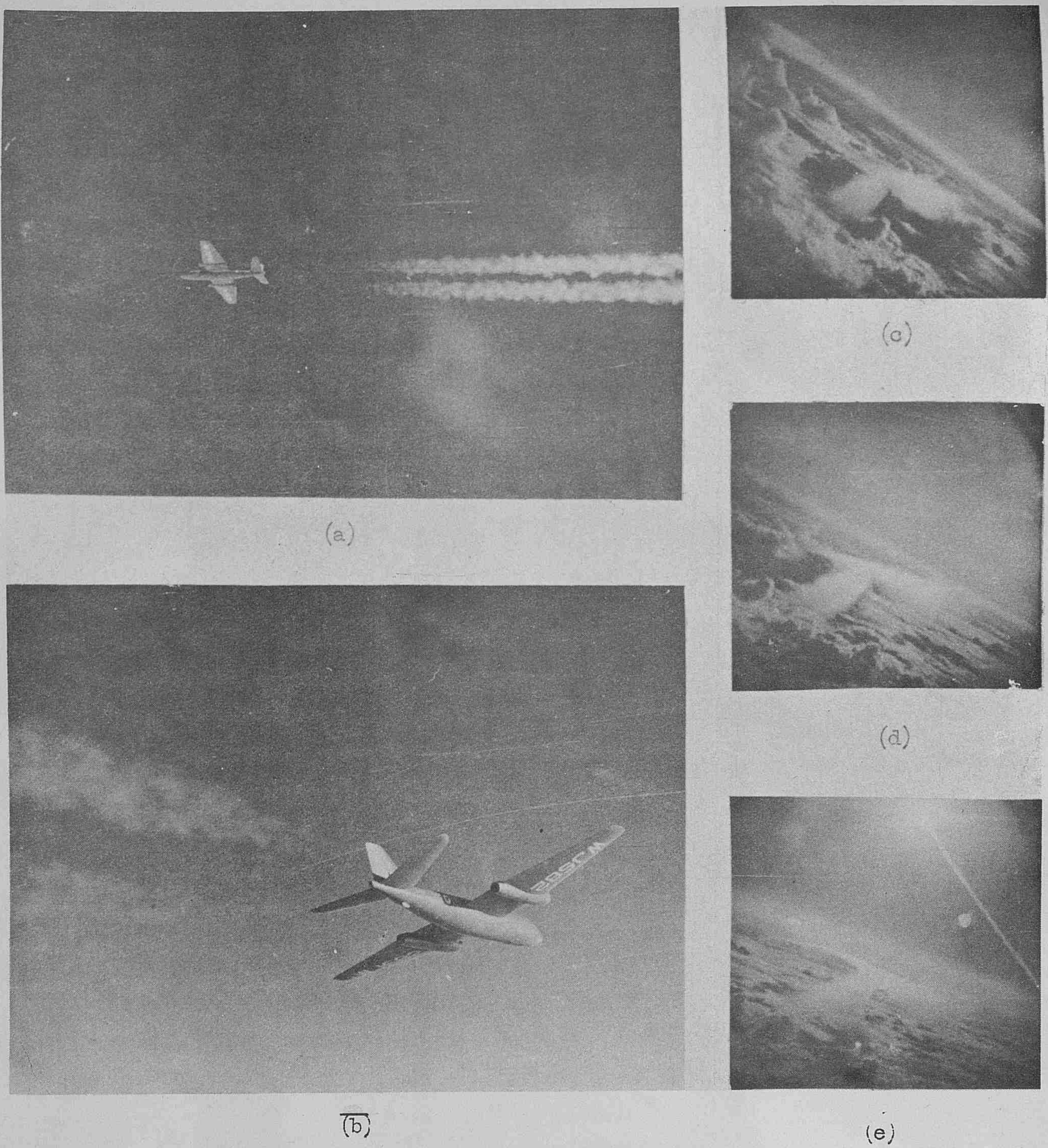

(a)

(b)

(c)

(d)

(e)

FIG.4 CANBERRA AIRCRAFT CONDENSATION TRAILS

(a) Showing gap between aircraft and trail.

(b) Close-up.

(c),(d),(e) Photographs taken with camera looking backwards from the aircraft tail, showing trails from each engine merging in the distance.

(c) and (d) Short trails above large cumuliform clouds.

(e) Long persistent trail.

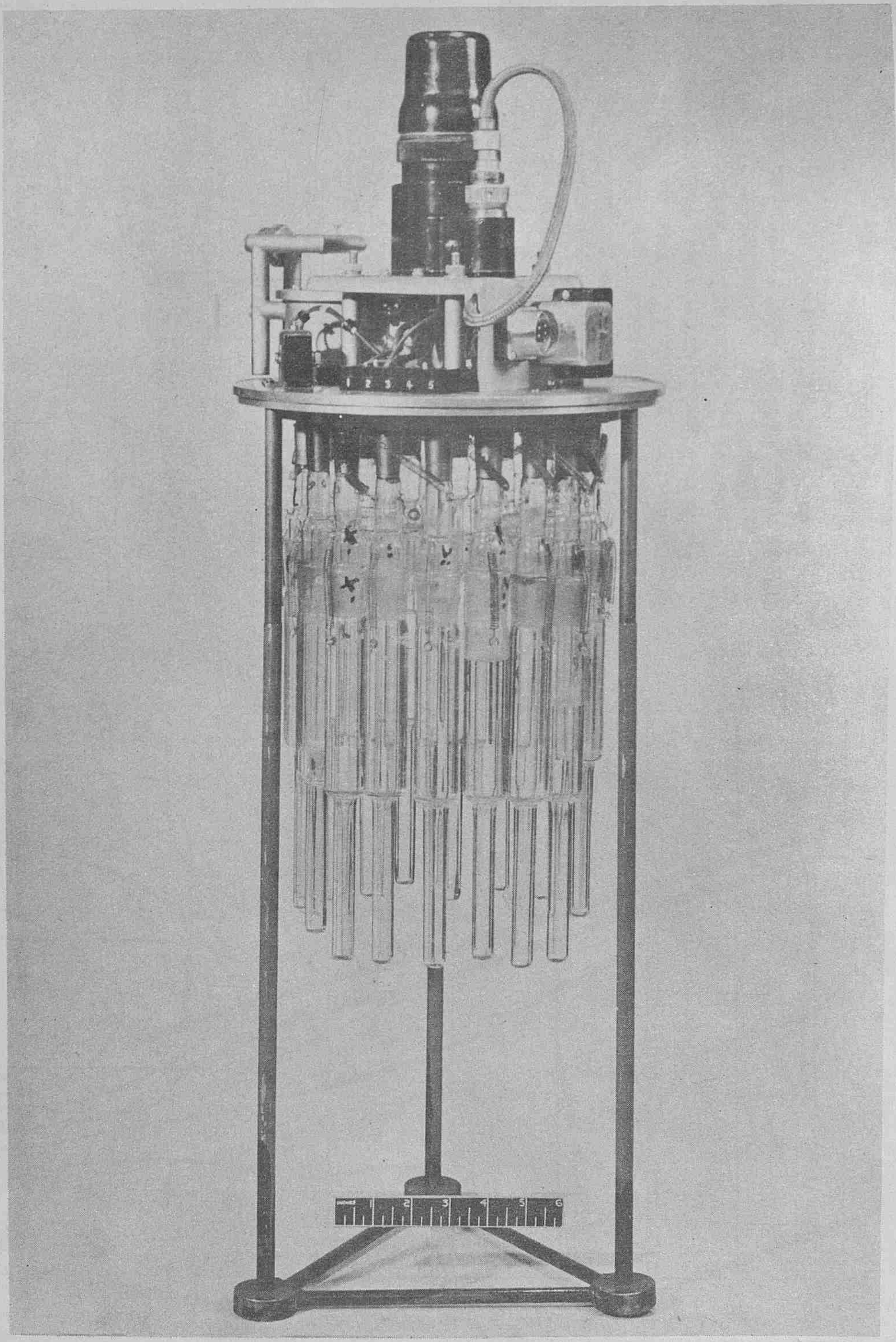

FIG.5 AIRBORNE OZONE SAMPLING APPARATUS

After going through a control valve the air is passed through a selected test tube. Selection of the test tubes is controlled electrically from the observer's seat by means of the actuator mounted above the tubes. This part of the apparatus is located in the bomb bay and the test tubes are loaded before each flight and withdrawn afterwards for analysis.

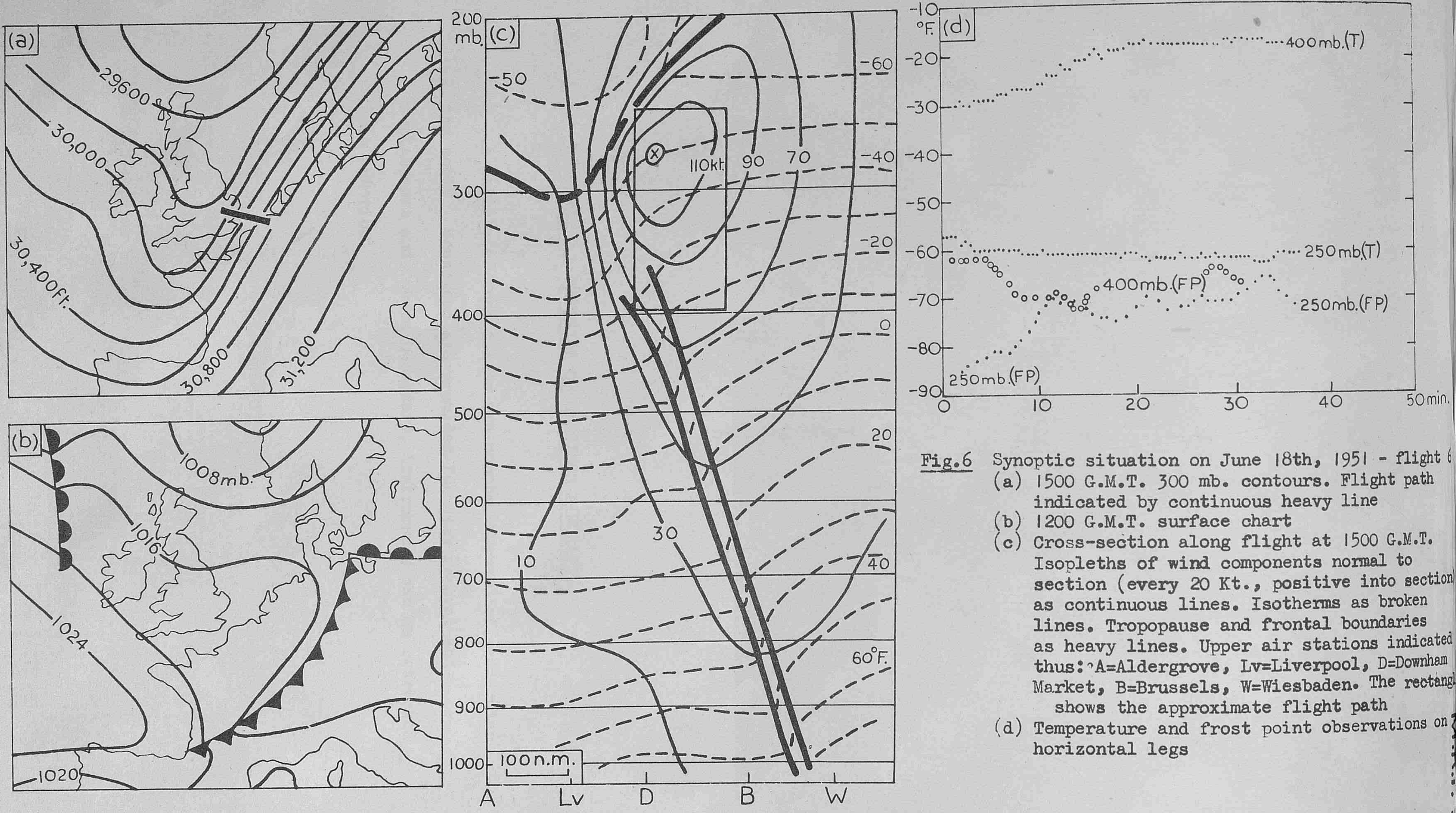

Fig.6 Synoptic situation on June 18th, 1951 - flight 6

(a) 1500 G.M.T. 300 mb. contours. Flight path indicated by continuous heavy line

(b) 1200 G.M.T. surface chart

(c) Cross-section along flight at 1500 G.M.T. Isopleths of wind components normal to section (every 20 Kt., positive into section) as continuous lines. Isotherms as broken lines. Tropopause and frontal boundaries as heavy lines. Upper air stations indicated thus: A=Aldergrove, Lv=Liverpool, D=Downham Market, B=Brussels, W=Wiesbaden. The rectangle shows the approximate flight path

(d) Temperature and frost point observations on horizontal legs

RESULTS OF A JET STREAM INVESTIGATION

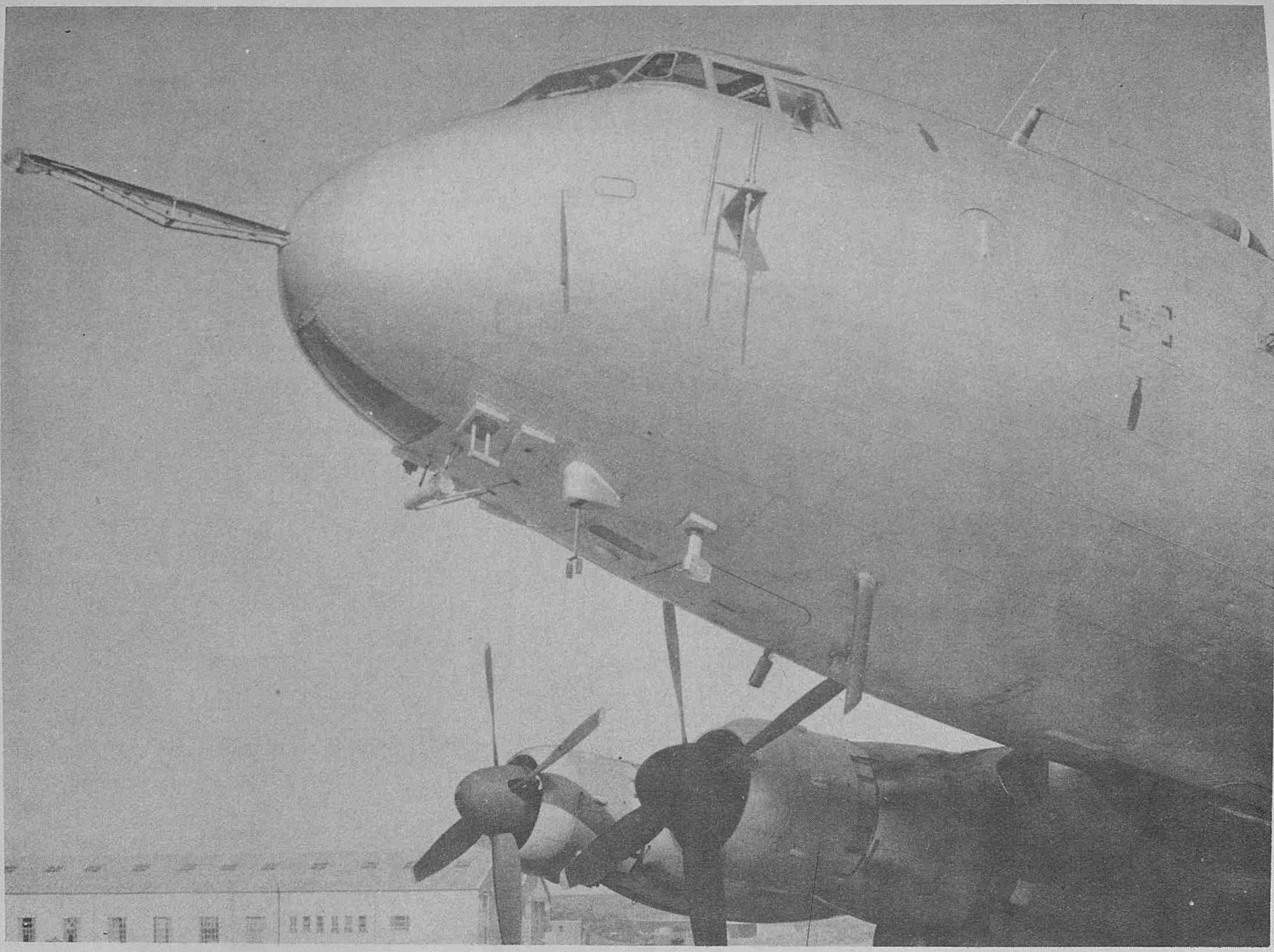

FIG.7 EXTERIOR OF HASTINGS AIRCRAFT

A variety of instruments are mounted forward of, and under the nose. Mountings are provided for easy removal and replacement and, where necessary, instruments can be retracted into interior.

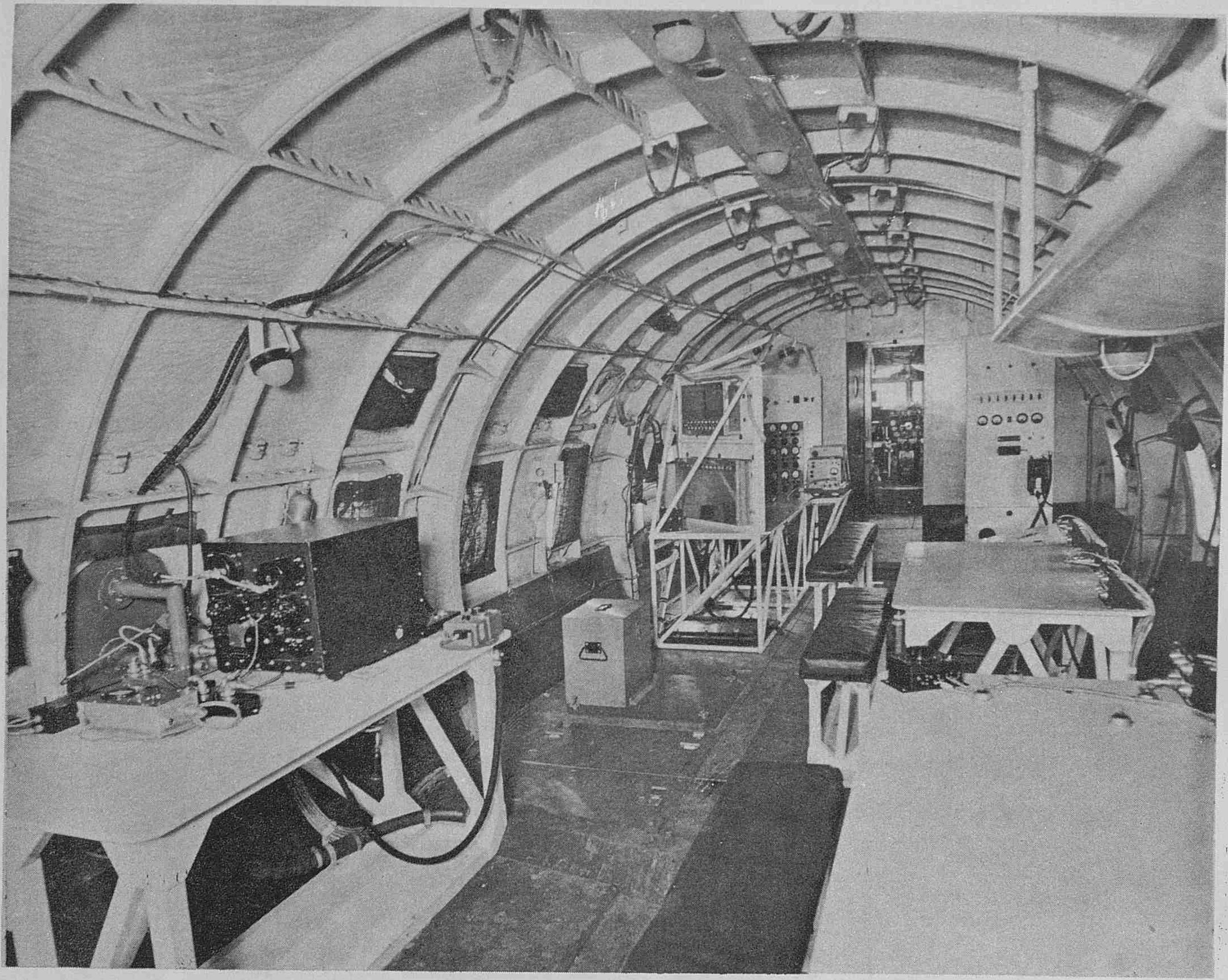

FIG.8 INTERIOR OF HASTINGS AIRCRAFT

This has been rebuilt to provide laboratory conditions of work as far as possible.

Each bench is provided with several plug positions for different power supplies and connections to instrument heads.

In Left Foreground is an Automatic Observer.

Left Rear is the multichannel galvanometer equipment.

Right Rear is the power board for the experimental equipment.

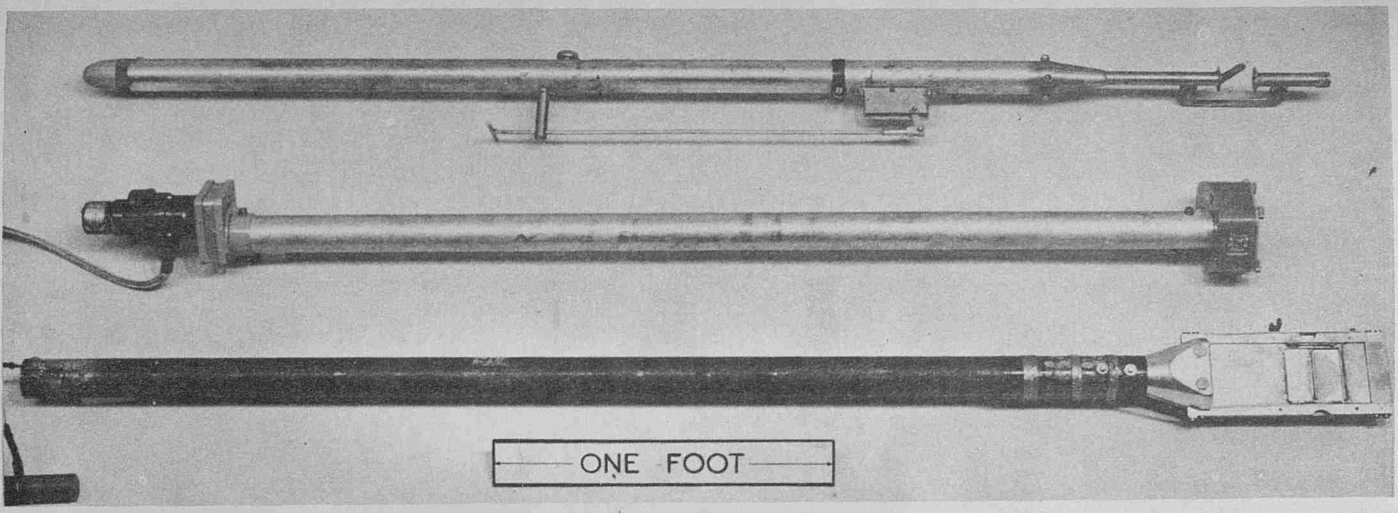

FIG.9 PARTICLE SAMPLERS

TOP: CLOUD DROPLET TYPE. Slide is oiled and placed in holder between bell mouths. (So shaped to avoid splash effect on the slide.) Slide is fired across the gap by means of trigger arrangement below, immediately the sampler is pushed out of the aircraft.

(This impactor was adapted from a design by D. Napier & Sons Ltd.)

CENTRE: RAINDROP SAMPLER. Small electric motor on the left drives drums in the head on the right. Tinfoil strip is run at about 4 inches per second, under the opening in the head, and suffers indentations by oncoming raindrops, thus producing a continuous record of raindrop size.

BOTTOM: RAINDROP SAMPLER USING SOOTED GAUZE METHOD. Gauze is placed in the holder on the right and is exposed by manually operating a shutter from the left.

All these samplers are exposed by mounting on a ramp and pushing through a hole in the aircraft skin, as shown in FIG.10.

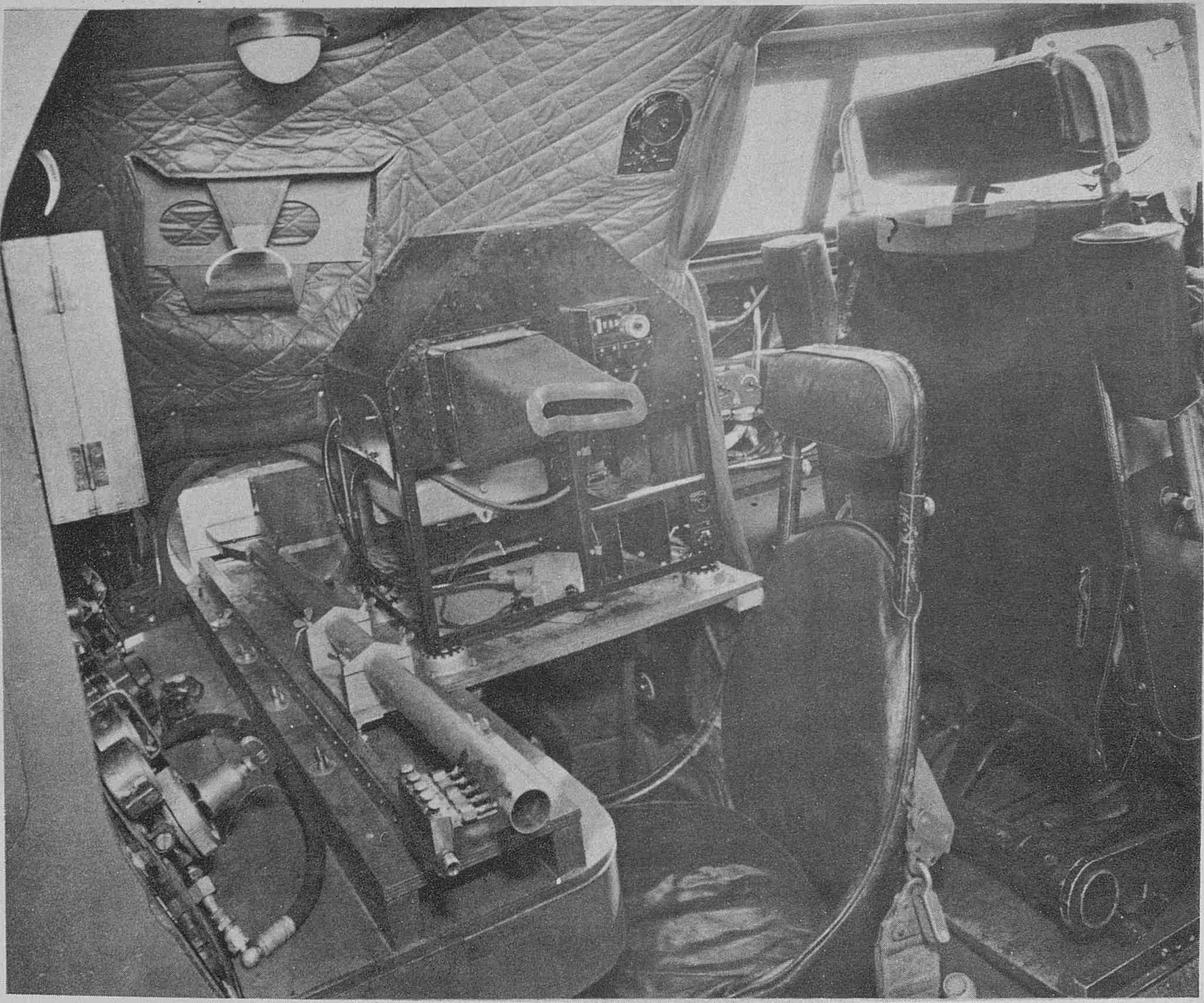

FIG.10

Illustrates method of exposing samples through aircraft skin by means of sliding ramp.

Droplet samples are photographed immediately, in the micro-camera to the right of the operator's seat.

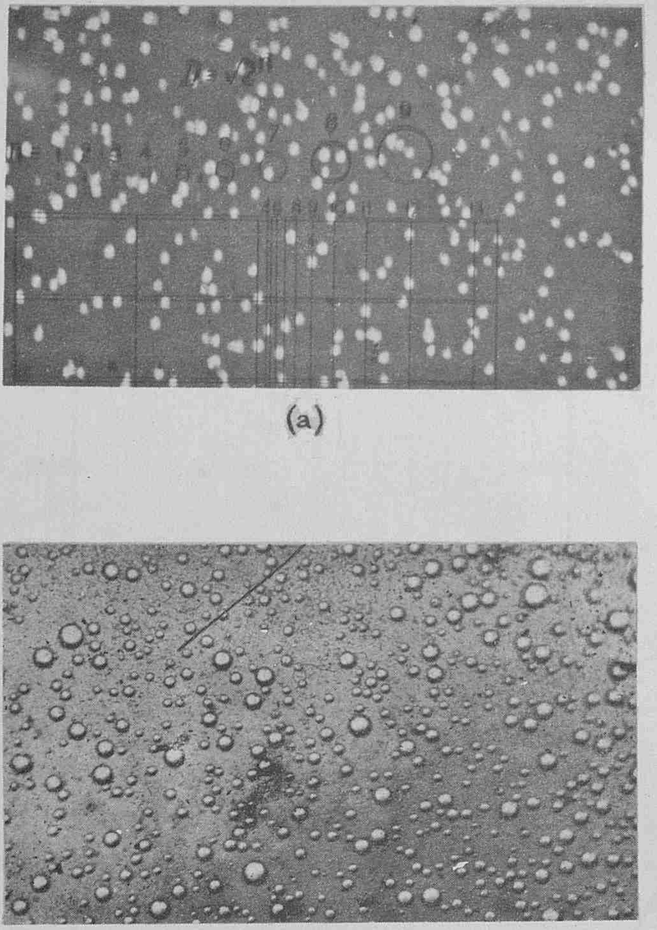

(a)

(b)

FIG. 11 TYPICAL CLOUD DROPLET SAMPLES

(Mean diameter approximately 20 microns)

(a) Craters in coating of Magnesium Oxide.

(b) Droplets captured in oil.

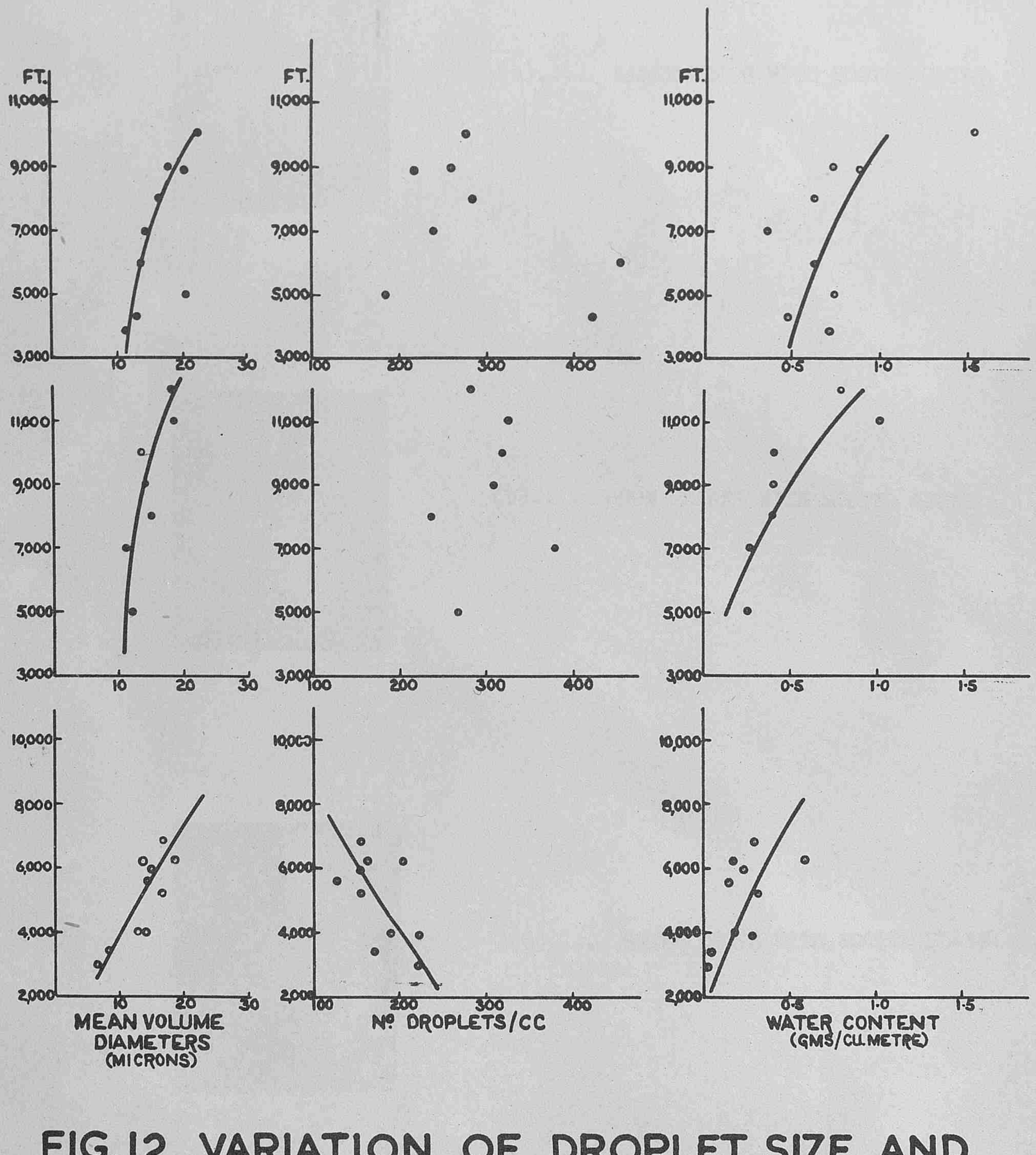

FIG. 12. VARIATION OF DROPLET SIZE AND CONCENTRATION IN CUMULUS CLOUDS. (THREE SEPARATE FLIGHTS).

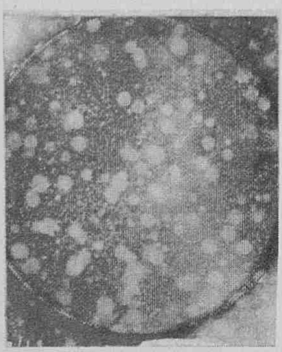

(a).... LARGE DROPS WITH SOOTED GAUZE.

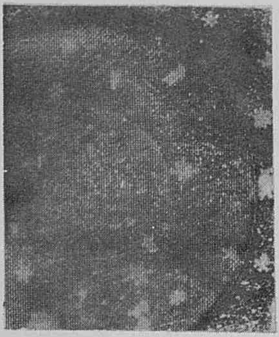

(b).... SNOW FLAKES WITH SOOTED GAUZE.

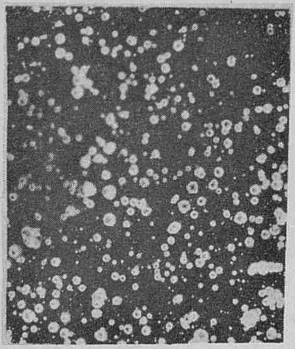

(c).... SMALL DROPS WITH SOOTED PLATE.

FIG. 13 RAINDROP AND SNOWFLAKE SAMPLING WITH SOOTED SLIDES
(Approximately original size)

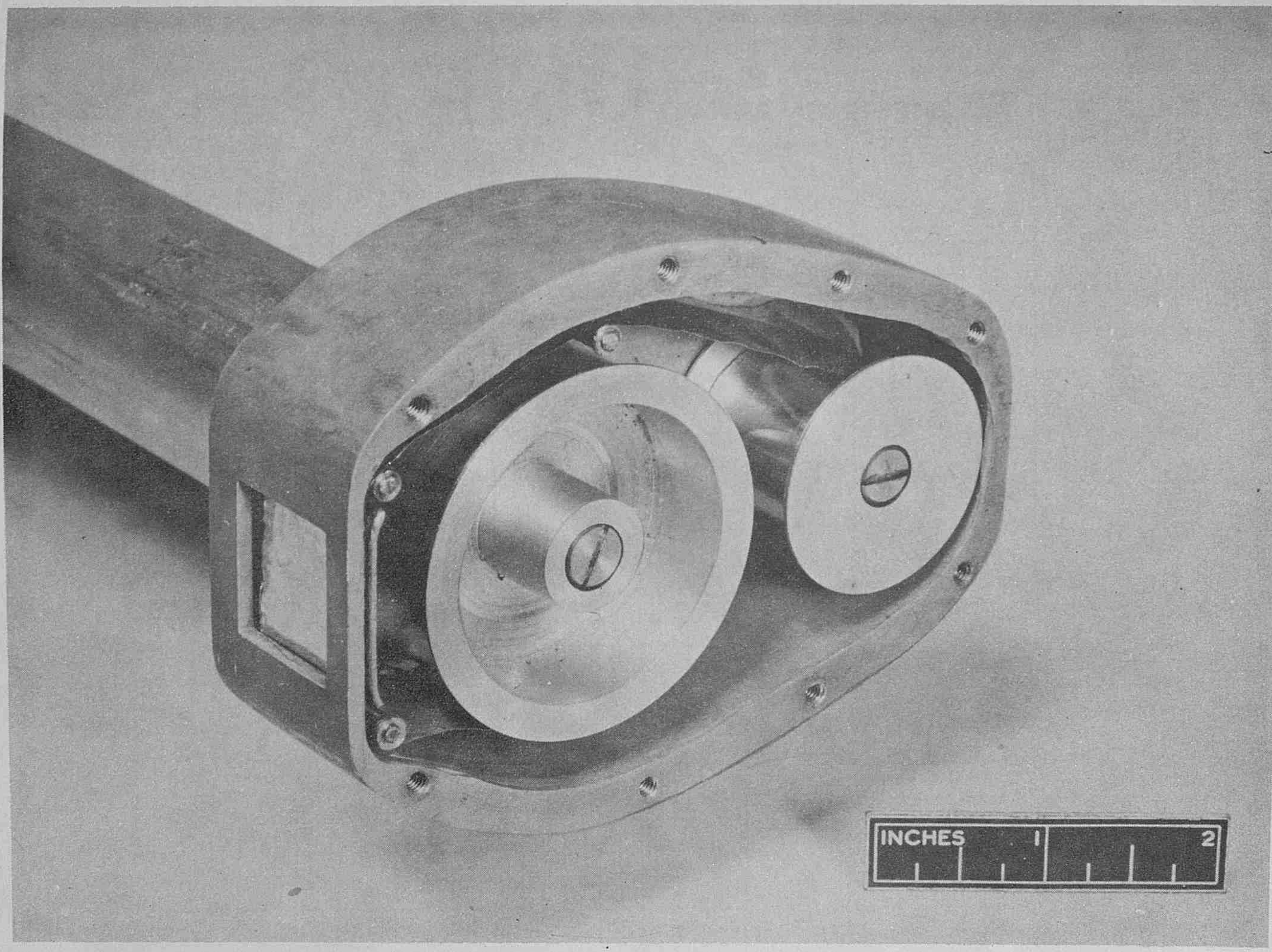

FIG. 14 HEAD OF IMPACTOR FOR MEASURING RAINDROP SIZE

(end cover removed)

This instrument is exposed on the end of a pole through the aircraft skin and the take-up drum rotated electrically.

Raindrops produce indentations in the foil which can be counted and sized, thus obtaining a continuous record of the raindrop spectrum.

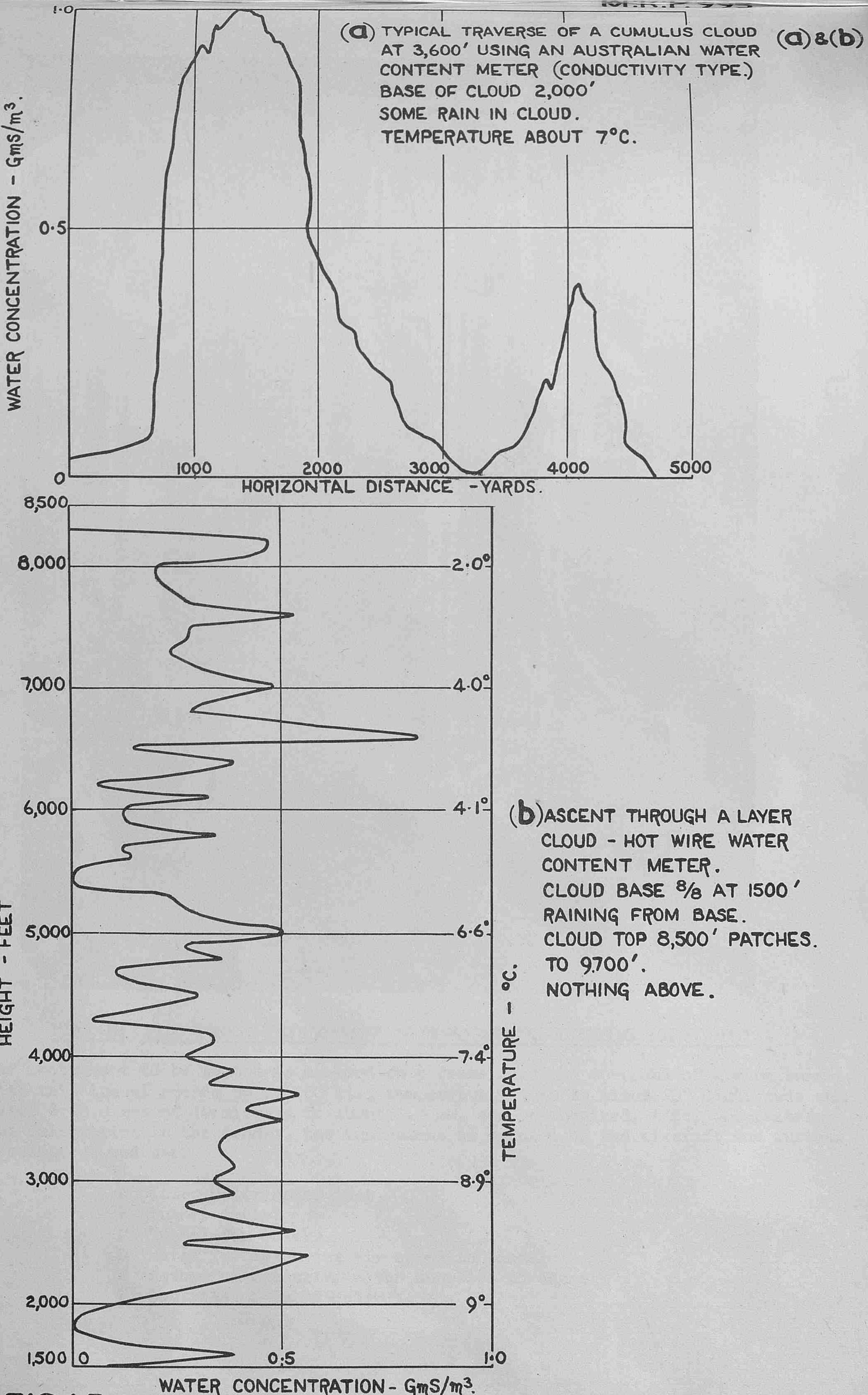

(a) TYPICAL TRAVERSE OF A CUMULUS CLOUD AT 3,600′ USING AN AUSTRALIAN WATER CONTENT METER (CONDUCTIVITY TYPE.)
BASE OF CLOUD 2,000′
SOME RAIN IN CLOUD.
TEMPERATURE ABOUT 7°C.

(b) ASCENT THROUGH A LAYER CLOUD - HOT WIRE WATER CONTENT METER.
CLOUD BASE 8/8 AT 1500′
RAINING FROM BASE.
CLOUD TOP 8,500′ PATCHES. TO 9700′.
NOTHING ABOVE.

FIG.15.
(a) & (b) CLOUD WATER CONTENT MEASUREMENT.

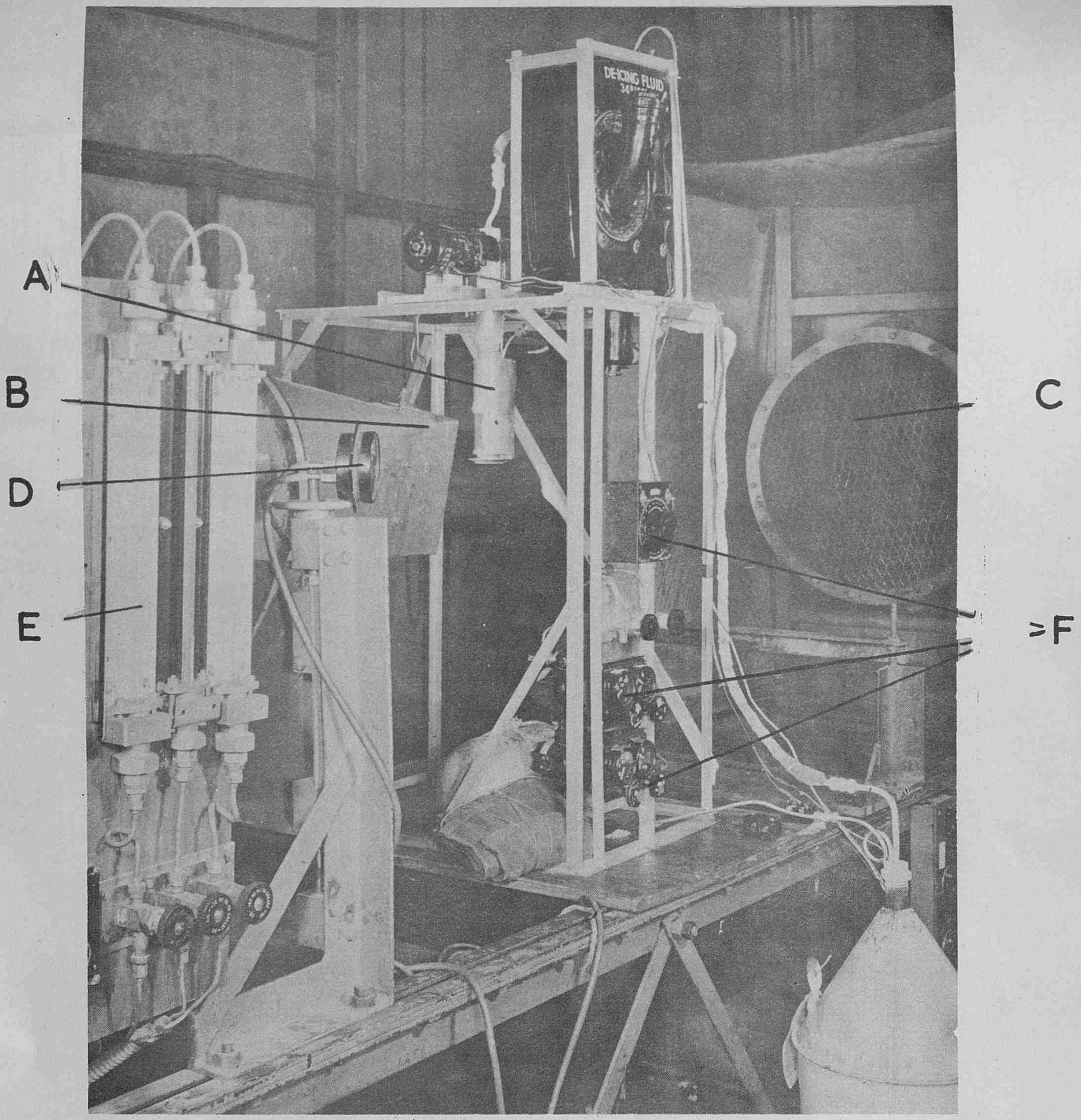

Fig. 16 WIND TUNNEL DEVELOPMENT OF REFRIGERATED ROTATING ICING DISC

The instrument to be tested is mounted on a frame near the open end of a wind tunnel. With this tunnel speeds up to 150 Kt., temperatures down to minus 20° Centigrade and water drop sizes of 10 microns to about 0.5 mm. can be obtained. After observation and calibration in the tunnel, the instrument is mounted on the aircraft for further development and use.

A	Icing Meter under test
B	Tunnel outlet
C	Tunnel-fan intake
D	Meter for measuring air-speed in tunnel
E	Meter for measuring water supplied to tunnel
F	Controls of Icing Meter

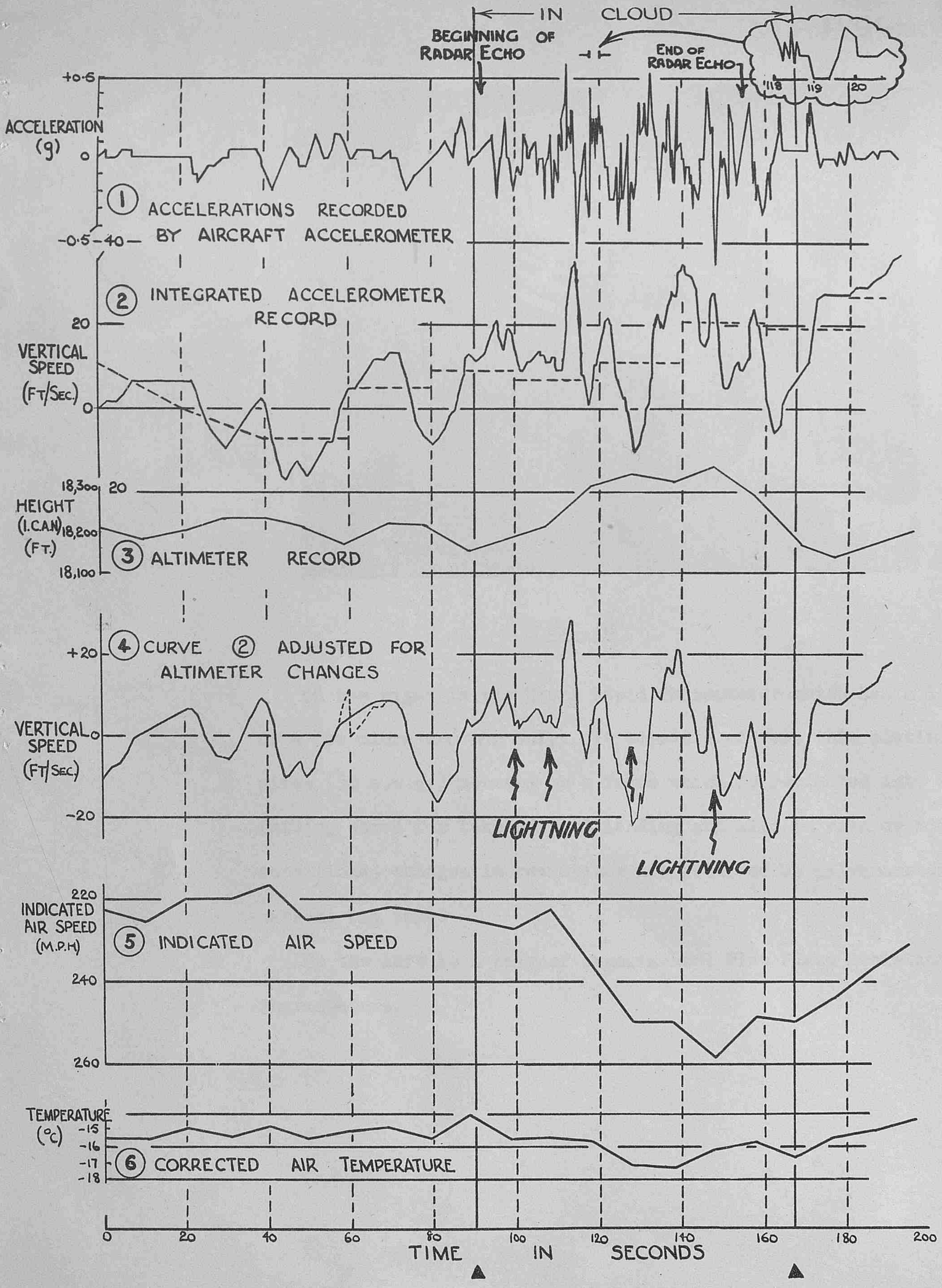

CUMULONIMBUS INVESTIGATION - 13TH JUNE 1952 - RUN 5 - 18,200′

FIG. 17

The graphs show the variations in height, airspeed and acceleration (bumpiness) as an aircraft traversed a large cumulonimbus cloud. Positions of radar echoes and lightning are also shown. By integrating the acceleration curve, the distribution of vertical up- and down-draughts (curve 4) was obtained.

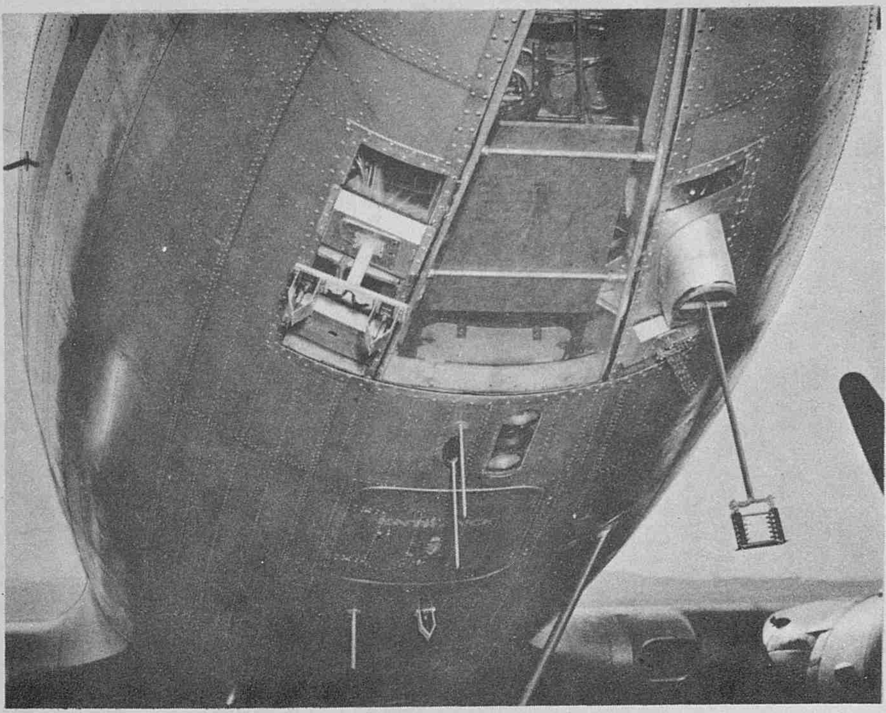

FIG. 18

On the right is the Ultra Rapid Thermometer which has a lag of a few micro-seconds only. It consists of very thin platinum wires (50 s.w.g.) mounted on a frame which is retracted into the fairing above for take off and landing and also in rain or icing conditions; changes in resistance are recorded by galvanometer or cathode ray tube.

On the left is a pair of experimental Flat Plate Resistance Thermometers.

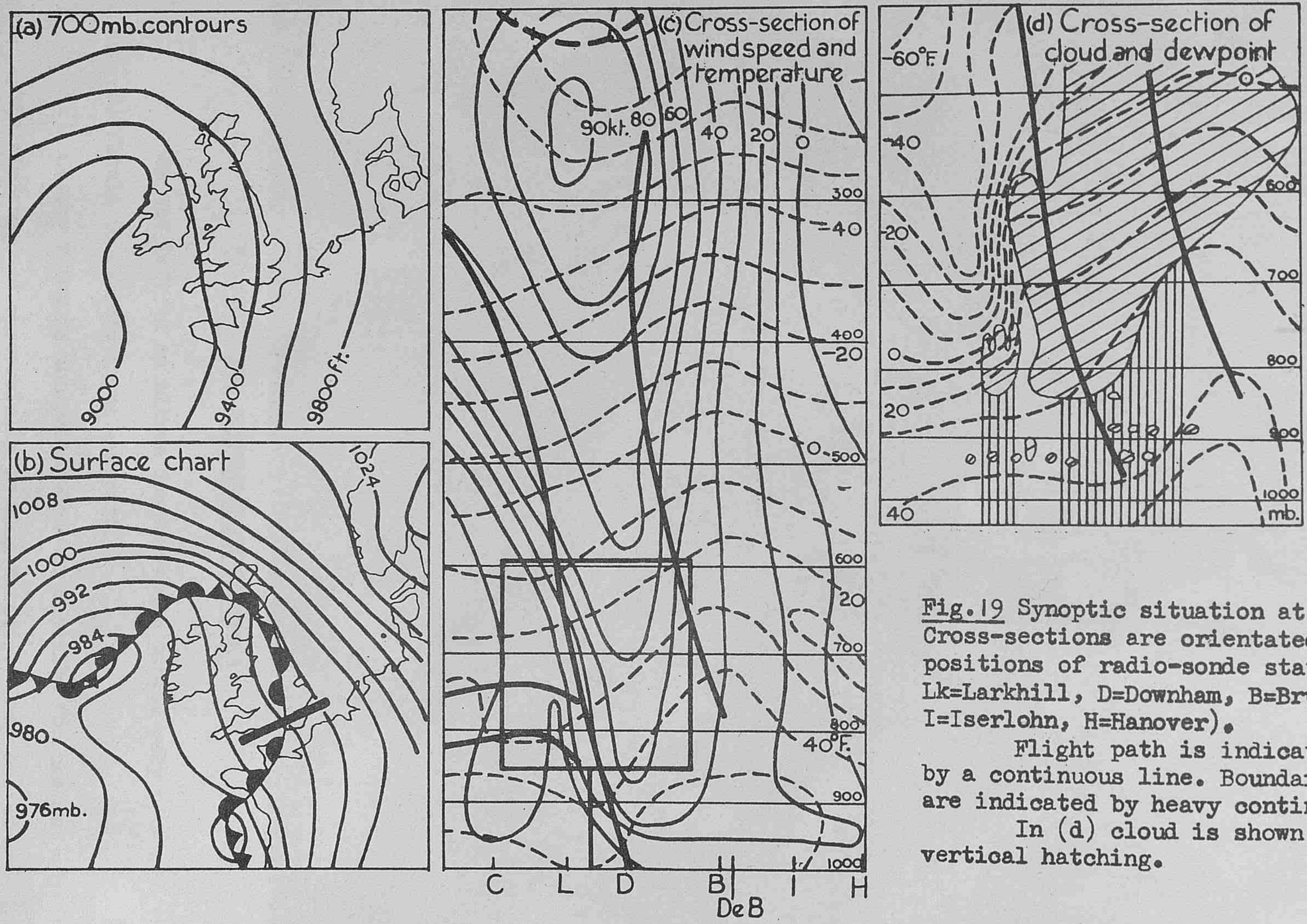

Fig.19 Synoptic situation at 1500 G.M.T. 5.11.51. Cross-sections are orientated east-west with approximate positions of radio-sonde stations indicated(C=Camborne, Lk=Larkhill, D=Downham, B=Brussels, DeB=De Bilt, I=Iserlohn, H=Hanover).

Flight path is indicated on diagrams (b) and (c) by a continuous line. Boundaries of the frontal zone are indicated by heavy continuous lines.

In (d) cloud is shown by diagonal, and rain by vertical hatching.

FIG.19 CROSS-SECTION THROUGH A FRONTAL SURFACE

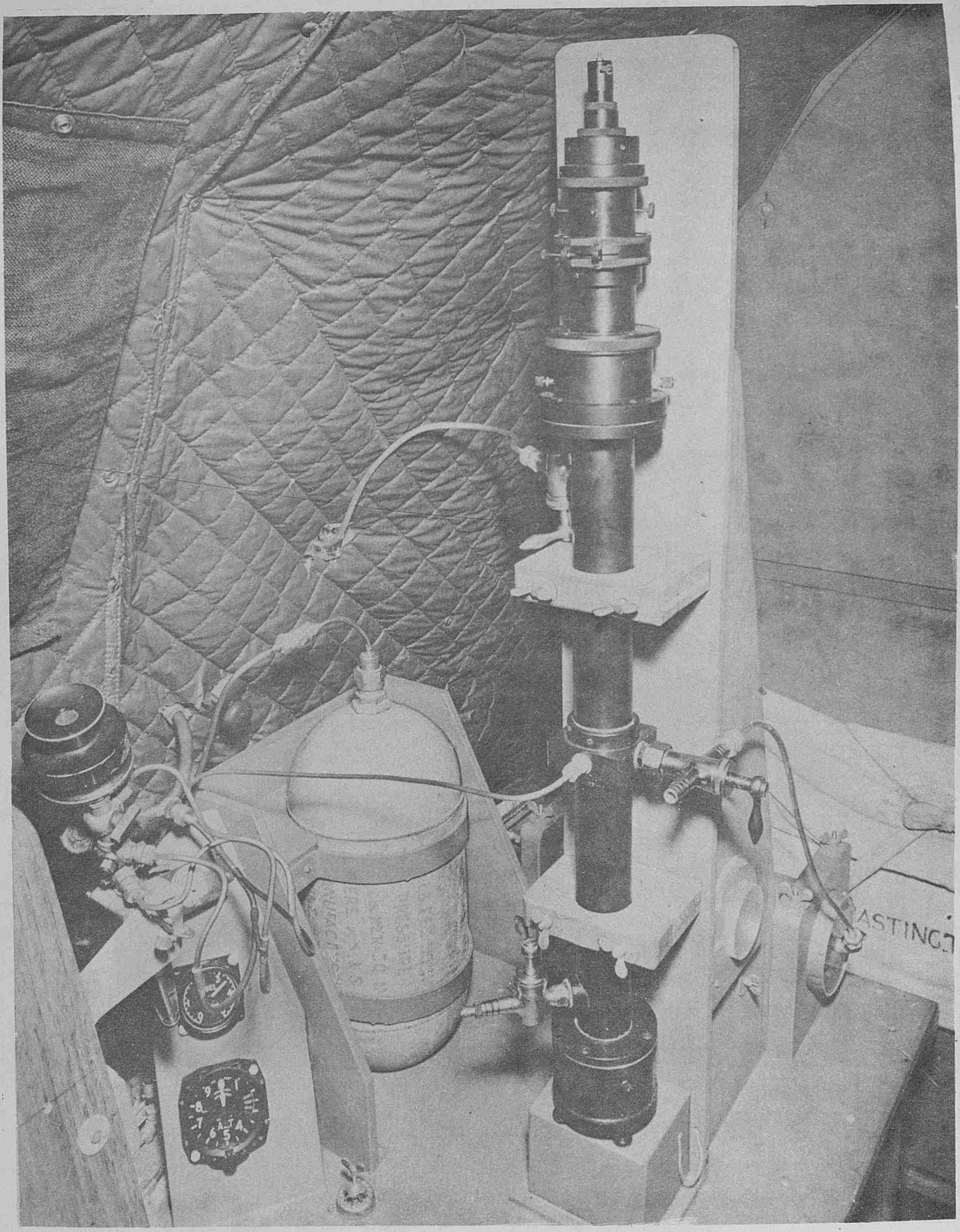

FIG.20 TWO CONDENSATION COUNTERS

On the left is an Aitken Counter which proved very difficult to operate in an aircraft.

On the right is the Pollak Counter modified for use in the air and used successfully on many flights. Air expanded in the main body of the instrument obscures light passing from the top to a photocell at the bottom. The density of the cloud is a measure of the number of nuclei present.

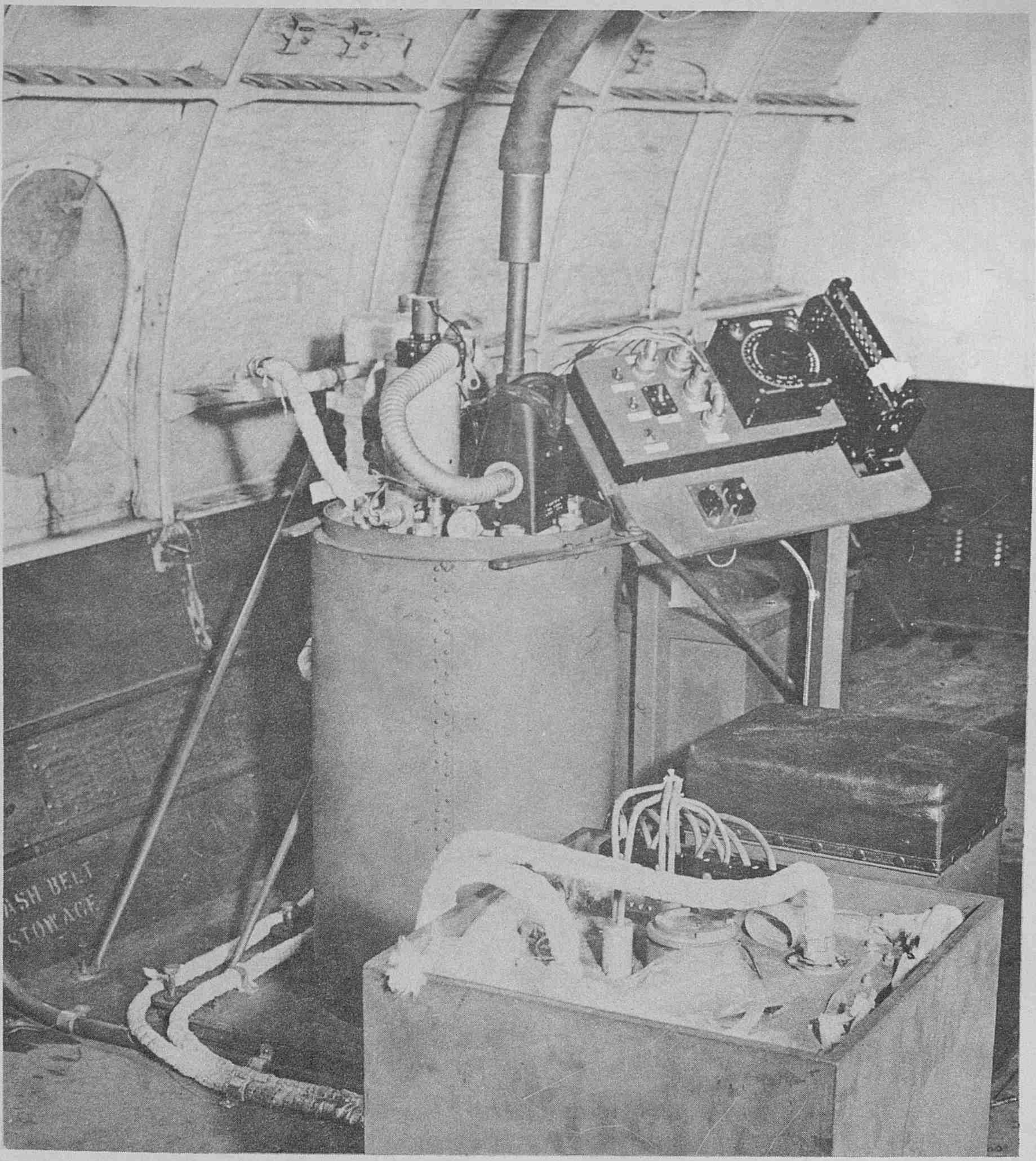

FIG.21 FREEZING NUCLEUS COUNTER

Air is inducted into the cylindrical chamber which is cooled by passing methylated spirits through pipes around it and a spiral immersed in solid carbon dioxide.

A small boiler provides steam inside the chamber which is also brightly illuminated by a beam of light from a high power lamp.

The observer, looking in the chamber, observes and estimates the number of ice crystals he can see at various temperatures. Ice crystals sparkle and glisten, whereas water droplets appear dull and opaque.

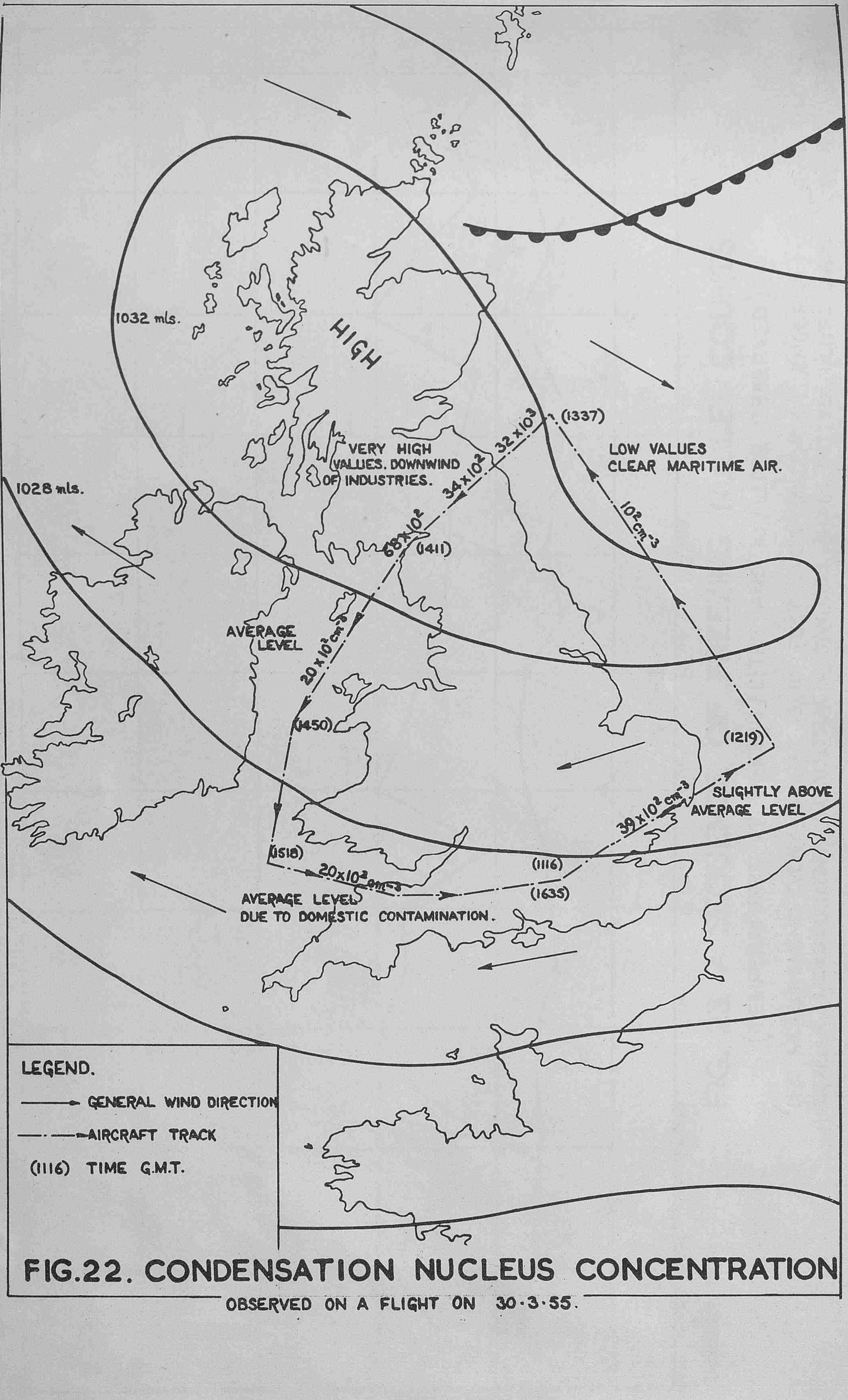
HIGH
1032 mls.
1028 mls.
VERY HIGH
VALUES. DOWNWIND
OF INDUSTRIES.
(1337)
32 x 10^3
34 x 10^2
68 x 10^2
(1411)
LOW VALUES
CLEAR MARITIME AIR.
10^2 cm^{-3}
AVERAGE
LEVEL
20 x 10^2 cm^{-3}
(1450)
(1219)
SLIGHTLY ABOVE
AVERAGE LEVEL
39 x 10^2 cm^{-3}
(1518)
20x10^2 cm^{-3}
(1116)
(1635)
AVERAGE LEVEL
DUE TO DOMESTIC CONTAMINATION.
LEGEND.
GENERAL WIND DIRECTION
AIRCRAFT TRACK
(1116) TIME G.M.T.

FIG.22. CONDENSATION NUCLEUS CONCENTRATION

OBSERVED ON A FLIGHT ON 30·3·55.

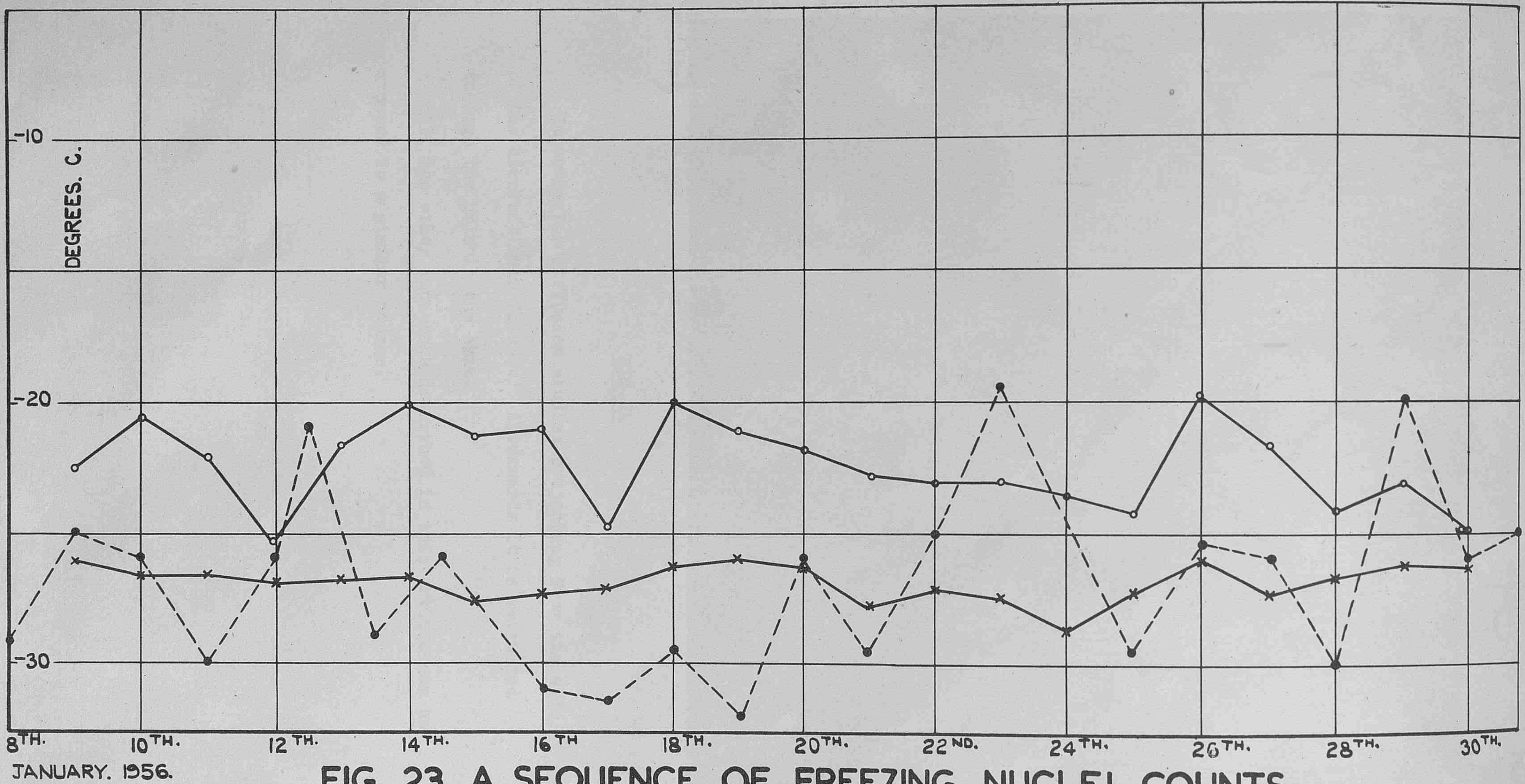

FIG. 23. A SEQUENCE OF FREEZING NUCLEI COUNTS.

(TEMPERATURES AT WHICH 1/LITRE AND 10^4/LITRE OBSERVED.)

(ONE MEASUREMENT EVERY DAY AT 10,000 FEET OVER SOUTHERN ENGLAND)
SIMILAR MEASUREMENT IN AUSTRALIA JAN. 1955. SHOWN DOTTED, 1/LITRE ONLY.

o—o 1/LITRE.
x—x 10^4/LITRE.

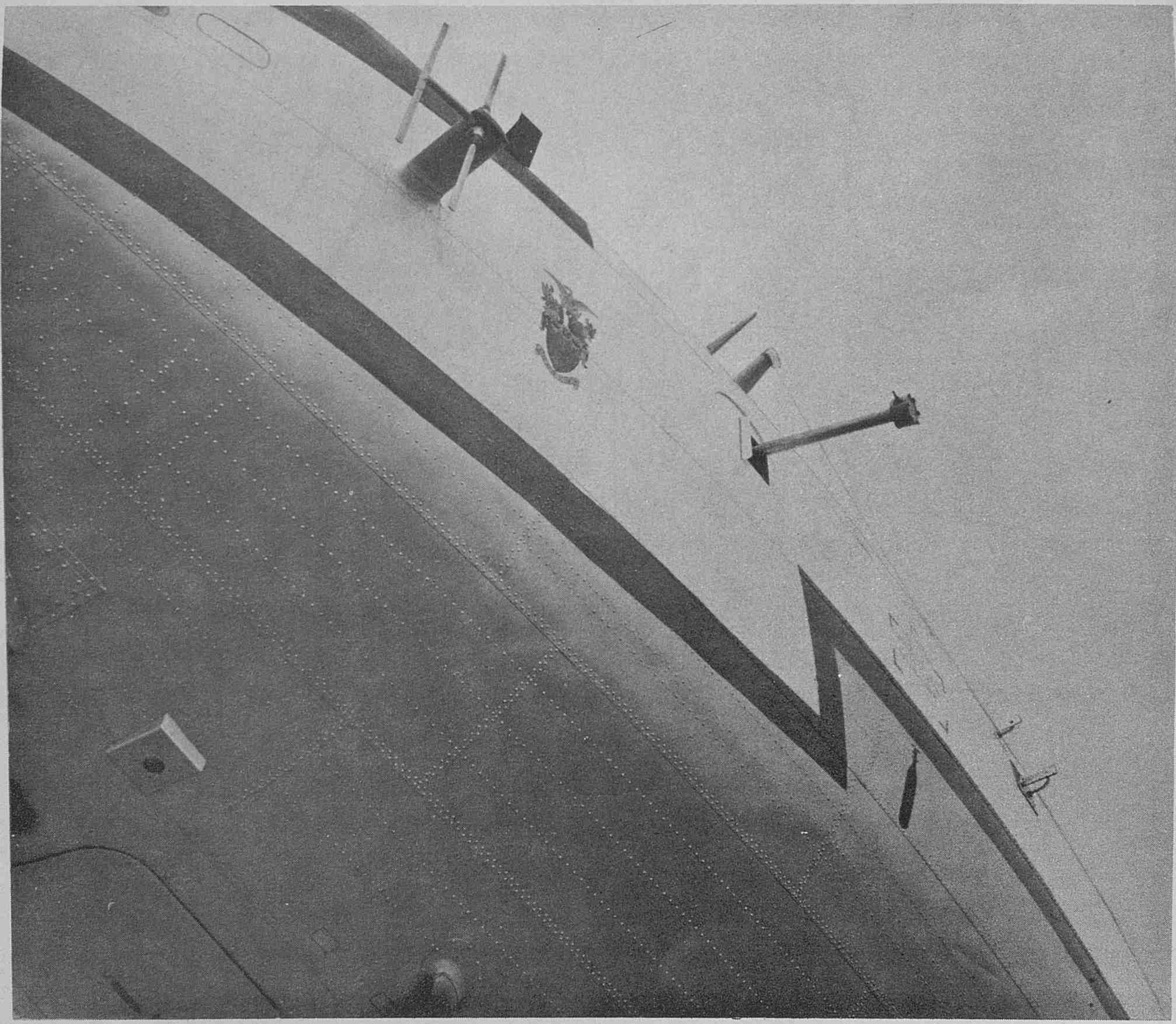

FIG.24

Impactor for diffusion studies projecting from the side of the aircraft when in use. Afterwards it is retracted through the hole in the skin.

All the other impactors described in this article can be exposed in a similar manner.

SEEDING EXPERIMENT 9.1.56 at 1100 HRS.

STRATOCUMULUS LAYER, BASE 2,200 FT. AT +27.5°F., TOP 4,500 FT. AT +21.0°F

AIRCRAFT FLEW AN 'S' CURVE 100 FT. ABOVE TOPS. DRY ICE SEEDING 70 LBS.

IN 3½ MINUTES (6LBS. PER MILE APPROX.)

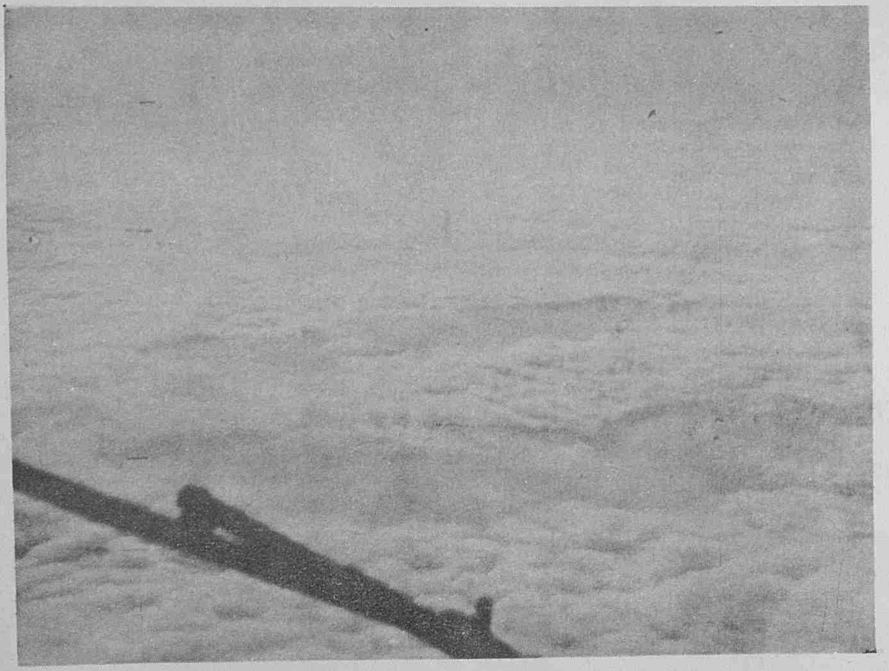

14 MINS. AFTER SEEDING.
FIBROUS LANES APPEAR
IN CLOUD TOPS.

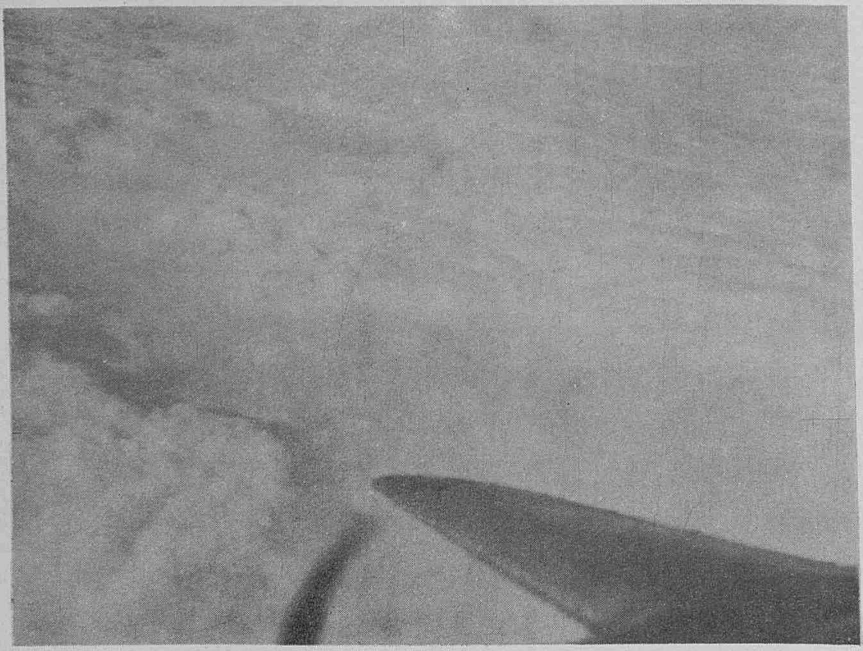

22 MINS. AFTER SEEDING.
CLOSE UP OF SEEDED AREA
SHOWING 'S' SHAPE.

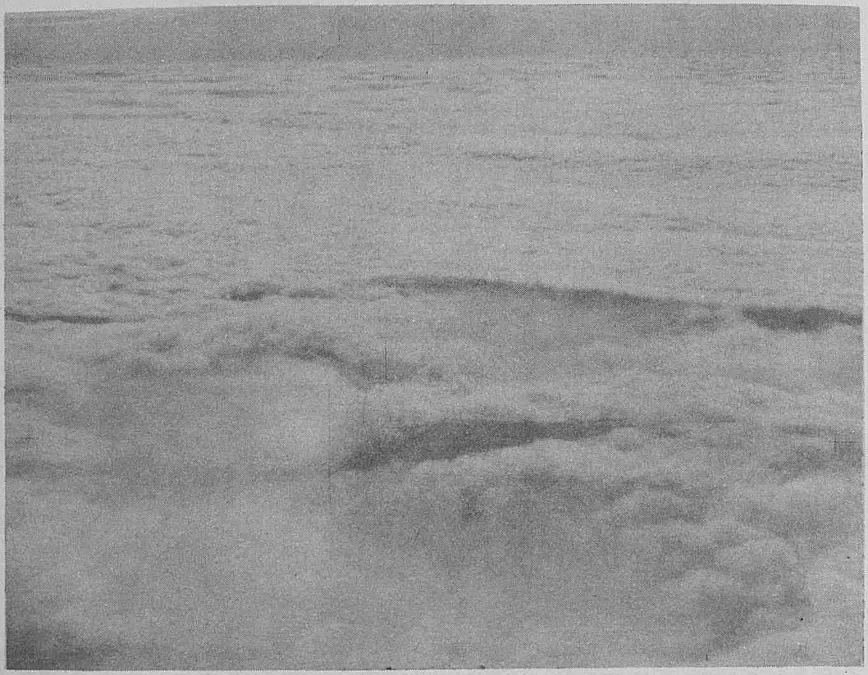

28 MINS. AFTER SEEDING.
SUN PILLAR REFLECTION;
DISTORTION OF 'S' SHAPE
WITH SHARP EDGE TO
SEEDED AREA.

FIG. 25

SEEDING EXPERIMENT 9.1.56 at 1100 HRS

STRATOCUMULUS LAYER, BASE 2,200 FT. AT +27.5°F., TOP 4,500 FT. AT +21.0°F.
AIRCRAFT FLEW AN 'S' CURVE 100 FT. ABOVE TOPS. DRY ICE SEEDING 70 LBS.
IN 3½ MINUTES (6 LBS PER MILE APPROX.)

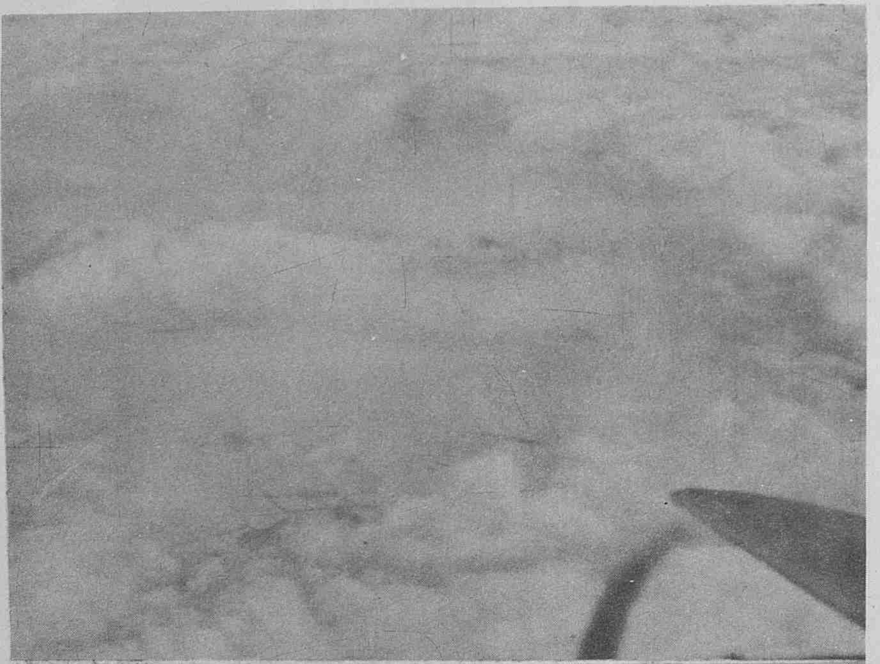

37 MINS. AFTER SEEDING,
GROUND FIRST SEEN.

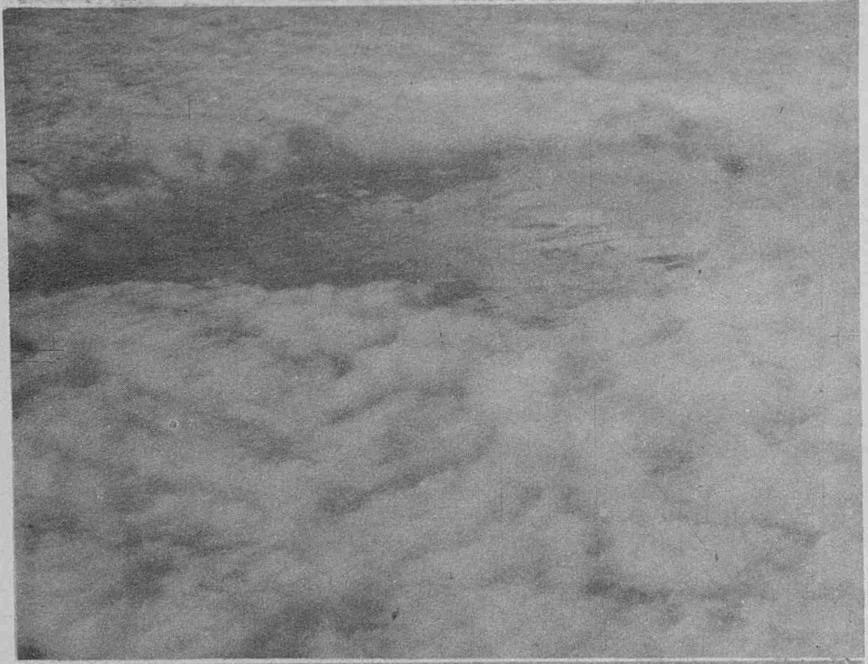

48½ MINS. AFTER SEEDING,
GROUND CLEARLY VISIBLE
HOLE PROBABLY 5 MI. ACROSS.

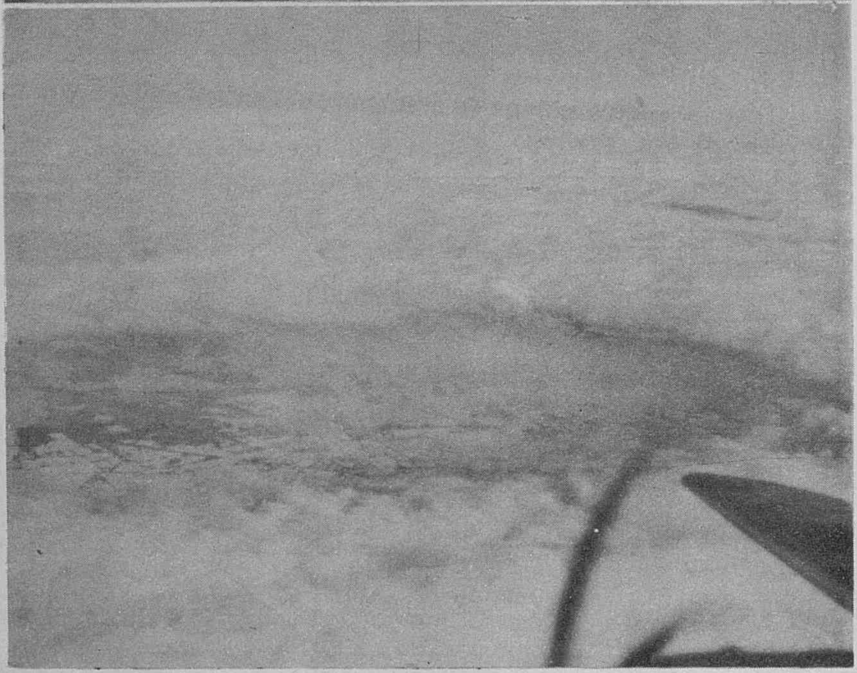

50½ MINS. AFTER SEEDING.
END OF EXPERIMENT. HOLE
NOW ABOUT 30 MI. DOWN-
WIND OF ORIGINAL SEEDED
LOCATION.

FIG.25 (CONT.)

RADAR P.P.I. PHOTOGRAPHS DURING SEEDING EXPERIMENT OF 23.1.52

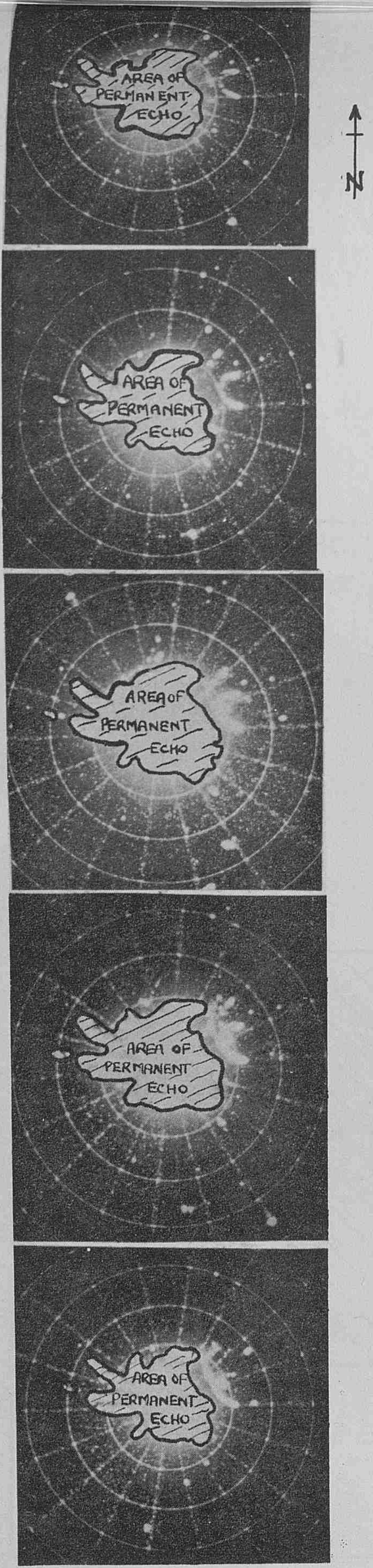
N
AREA OF PERMANENT ECHO
AREA OF PERMANENT ECHO
AREA OF PERMANENT ECHO
AREA OF PERMANENT ECHO
AREA OF PERMANENT ECHO

(a)... First semicircle forming.
23 minutes after seeding.

(b)... First semicircle well marked.
25m. 50 sec. after seeding.

(c)... Signs of second semicircle.
31m. 20 sec. after seeding.

(d)... Second semicircle also well marked.
34m. 20 sec. after seeding.

(e)... Semicircles drifting apart.
35m. 03 sec. after seeding.

FIG.26. The aircraft dropped dry ice in a semicircle through two layers of supercooled stratocumulus cloud.

Seeding commenced at 1522 hours. Area of permanent echo is enclosed. P.P.I. range markers are at five mile intervals. Cloud reflections are in northeast quadrant.

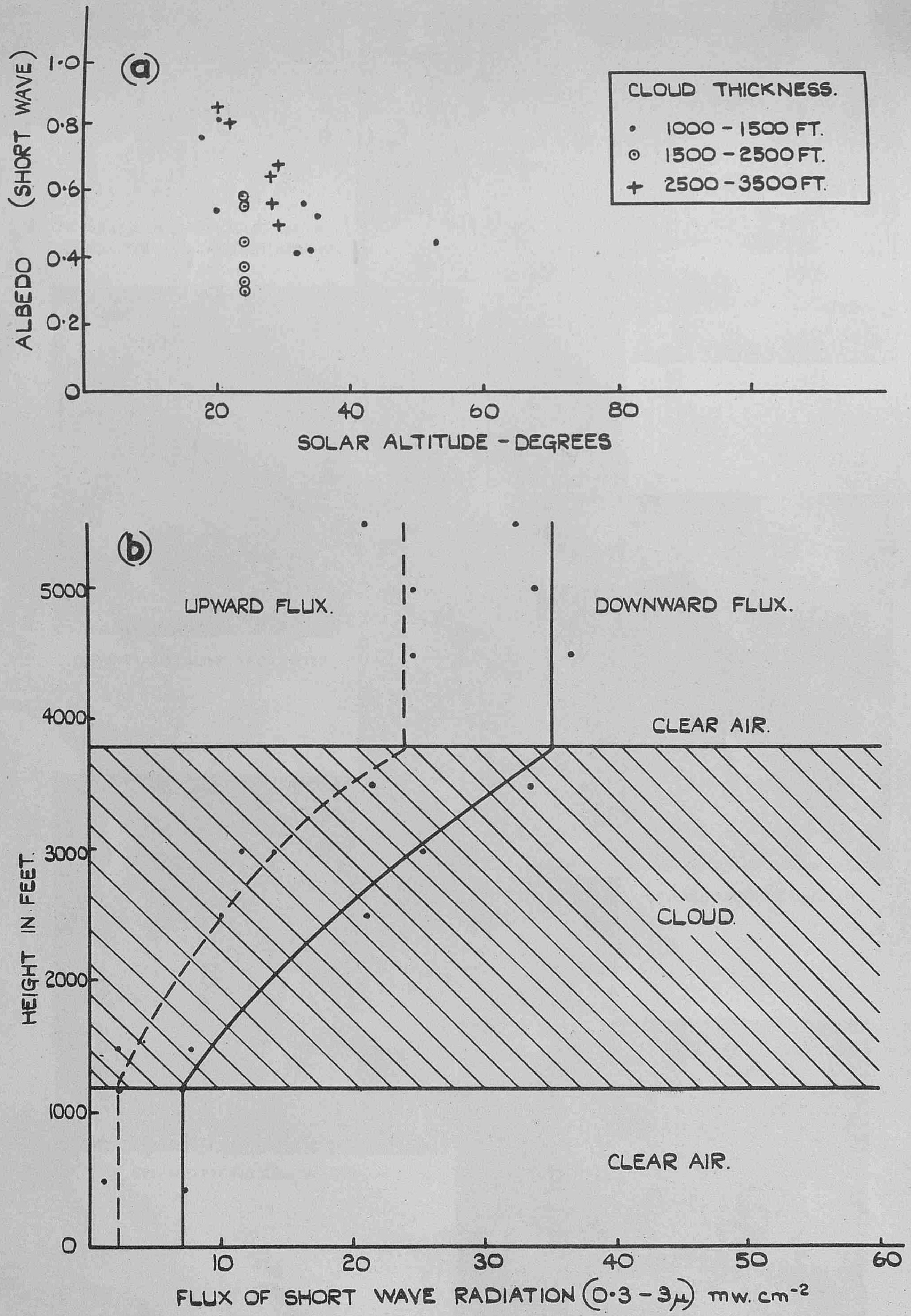

FIG. 27

ALBEDO MEASUREMENTS FROM AIRCRAFT.

(a) FLIGHT RESULTS ABOVE SUNLIT STRATOCUMULUS.

(b) TYPICAL VARIATION THROUGH A CLOUD LAYER.

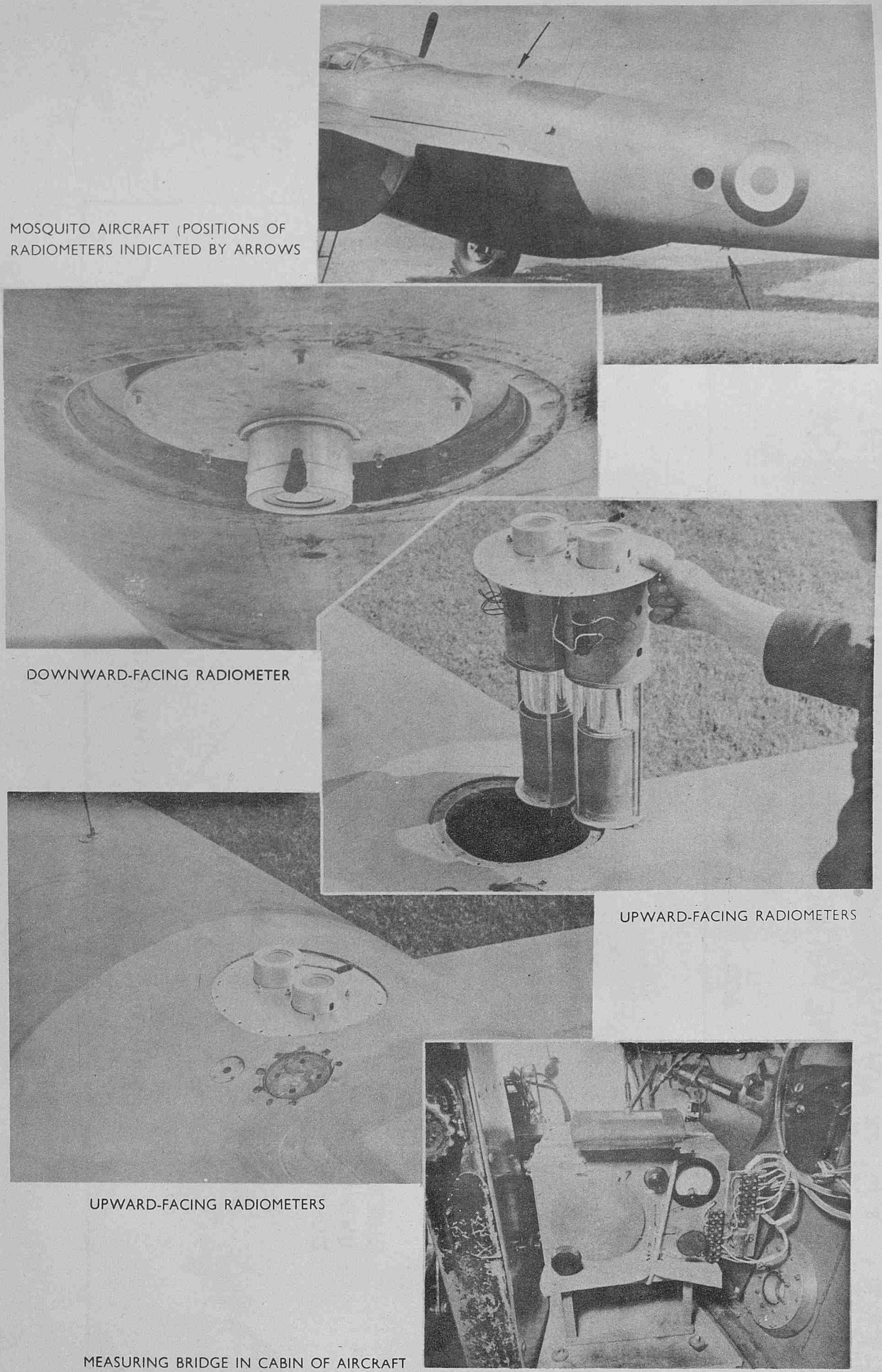

MOSQUITO AIRCRAFT (POSITIONS OF RADIOMETERS INDICATED BY ARROWS

DOWNWARD-FACING RADIOMETER

UPWARD-FACING RADIOMETERS

UPWARD-FACING RADIOMETERS

MEASURING BRIDGE IN CABIN OF AIRCRAFT

FIG. 28

THE USE OF RADIOMETERS FOR MEASUREMENT OF LONG WAVE RADIATION USING A MOSQUITO AIRCRAFT OF THE METEOROLOGICAL RESEARCH FLIGHT

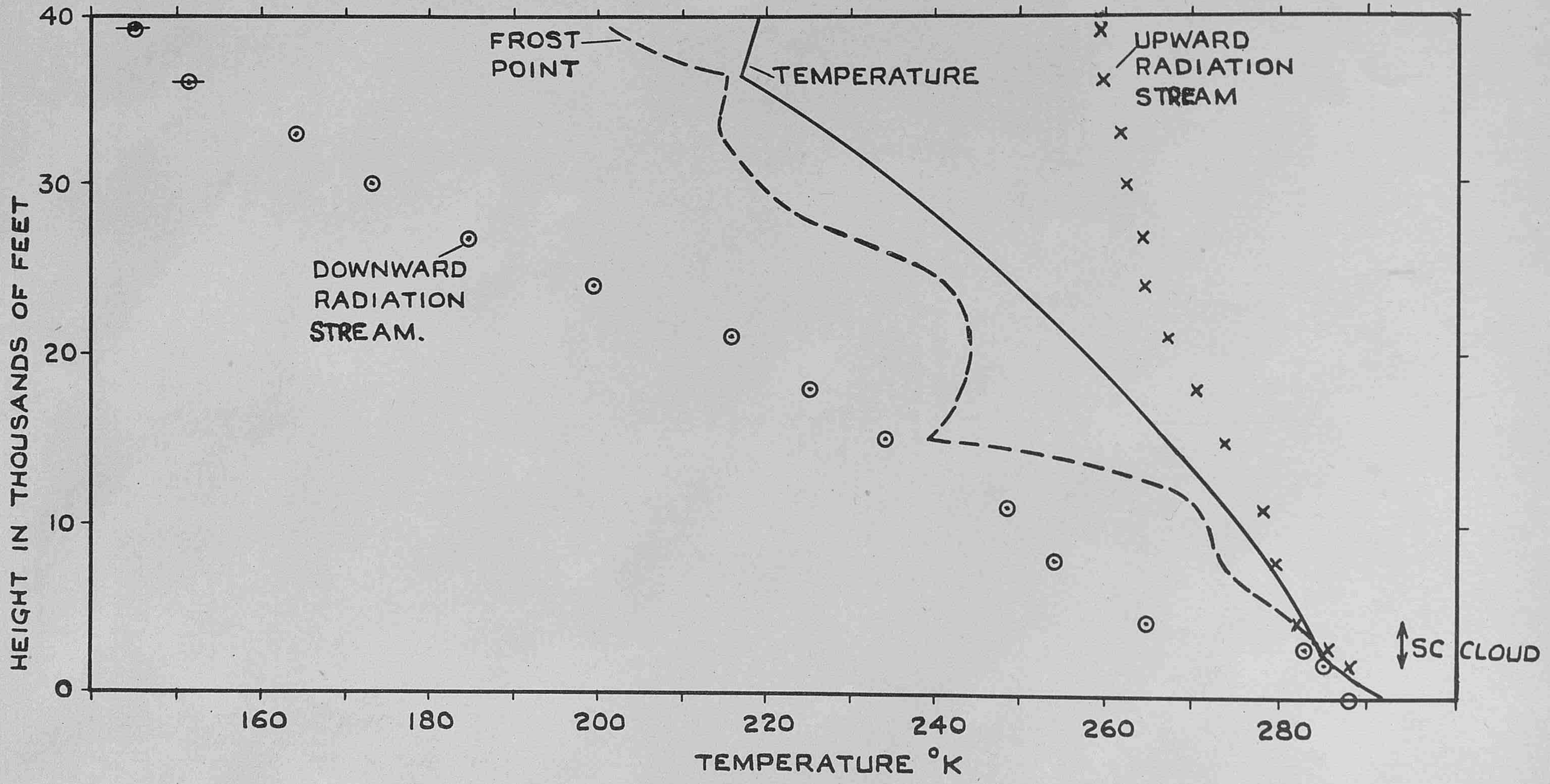

FIG. 29. TYPICAL MEASUREMENT OF UPWARD & DOWNWARD LONG WAVE (4-50 μ) RADIATION AT NIGHT. (Expressed as equivalent black-body temperature)

mate

M.R.P. 996
S.C.111/214
20th July, 1956.

AD 139537

Condensation Trails formed by Jet Aircraft

by

J. Briggs.

(Meteorological Office)

AIR MINISTRY

METEOROLOGICAL RESEARCH COMMITTEE

57-77

At the time of issue this report has not been published. Any author desiring to quote this paper should refer to it as "A paper of the Meteorological Research Committee (London),
M.R.P. No. 996 by Mr. J. Briggs
A copy is available in the Library of the Meteorological Office."

M.R.P.996
S.C.III/214
20th July, 1956

AIR MINISTRY

METEOROLOGICAL RESEARCH COMMITTEE

Condensation Trails formed by Jet Aircraft

by

J. Briggs (Meteorological Office)

1. At present, methods of forecasting the height of likely condensation trail formation are based on the 'Mintra' line and tropopause height. These methods do not give satisfactory results when applied to jet aircraft. In particular it is known that trails frequently continue well into the stratosphere. An attempt is made here to determine forecasting criteria for use with jet aircraft, and persistence of trails is considered.

Symbols used are:-

Velocity of aircraft relative to air = V cm/sec
Rate of fuel consumption = M gm/sec
Amount of heat added to air by combustion of 1 gm of fuel = F calories
Amount of water vapour added to air by combustion of 1 gm of fuel = w gm
Area of cross-section swept out by aircraft = A sq.cm
Relative humidity of air with respect to ice = U
Temperature of air = T °A
Atmospheric pressure = p mb
Saturation water vapour pressure with respect to ice = e mb
Amount of water condensed in air immediately behind aircraft = X gm/sec
Latent heat of sublimation of ice = L cal/gm
Specific heat of air at constant pressure = c_p cal/gm/degree A.
Specific gravity of water vapour with respect to air = E
Density of air = ρ gm/c.c.
Joule constant for mechanical equivalent of heat = $J = 4.18 \times 10^7$ ergs/cal
Gas constant for dry air = $R = 2.87 \times 10^6$ ergs/gm

2. Initial formation of trails

It is assumed that the heat and water vapour supplied by the aircraft engine is mixed thoroughly with the air in the first few yards of wake. It is then possible to accept the area swept out by the aircraft as small; Bannon (1) estimates that A is of the order of 6×10^5 at a distance 20 to 50 yards behind the aircraft.

Using the First Law of Thermodynamics we have

$$FM + LX = c_p . A \rho V . \delta T \qquad 2.1.$$

/Also,

G.3655/FN/7/56/50

Also, since water vapour is not destroyed,

$$wM + \frac{Ee}{p}\cdot\frac{U}{100}\cdot A\rho V = X + \frac{E(e+\delta e)}{p}\cdot A\rho V$$

which, using the Clausius Clapeyron equation $\frac{de}{dT} = \frac{JeEL}{RT^2}$, becomes

$$wM + \frac{Ee}{p}\cdot\frac{U}{100}\cdot A\rho V = X + \frac{Ee}{p}\left(1+\frac{JEL\,\delta T}{RT^2}\right)\cdot A\rho V \qquad 2.2.$$

Eliminating δT between 2.1. and 2.2. we have

$$X = \frac{wM - \frac{Ee}{p}\left(1-\frac{U}{100}\right)A\rho V - \frac{E^2eJLFM}{Rpc_pT^2}}{1 + \frac{E^2eJL^2}{Rpc_pT^2}} \qquad 2.3.$$

Now if the air is near saturation then $1 - U/100$ approaches zero and it is possible to ignore the middle term in the numerator since A is also relatively small near the aircraft and we can write

$$X = \frac{wM - \frac{E^2eJLFM}{Rpc_pT^2}}{1 + \frac{E^2eJL^2}{Rpc_pT^2}} \qquad 2.4.$$

Saturation is reached when X=0 but trails are unlikely to become visible until X exceeds a certain critical value. From 2.4. it can be shown that

$$\frac{dX}{dT} = \frac{E^2eJLpc_pM(F+wL)(2TR-EJL)}{(Rpc_pT^2 + E^2eJL^2)^2}$$

and since, for all normal atmospheric temperatures, $2TR \ll EJL$ then dX/dT is negative.

Putting $X = 0$, we get as the criterion for trails to be just possible in a near-saturated atmosphere

$$T = \left(\frac{E^2eJLF}{Rpc_pw}\right)^{1/2} \qquad 2.5.$$

If T exceeds this value then X is negative.

This critical value is independent of M, the rate of fuel consumption, and is determinate if F and w are known.

For jet aircraft, using paraffin, we have w = 1.3 gm and F = 10^4 calories (assuming all the heat of the combustion is available to heat the air just behind the aircraft).

If saturation with respect to ice is the critical state then the trail forms as ice particles. It is possible that trail formation may be delayed until saturation with respect to water is reached but to determine the absolute threshold of trail formation it is necessary to use the value of L for ice, i.e., $L = 677$ cal/gm.

2.5. then reduces to

$$T = 11060\left(\frac{e}{p}\right)^{1/2} \qquad 2.6.$$

Brunt (Physical and Dynamical Meteorology-p.405) gives data showing the variation of e. Using these data 2.6. can be solved for T, given p, and yields:-

Table I

Variation of critical temperature, for initial trail formation, with pressure

Pressure (mb)	Corresponding critical temperature (°C)
150	-45.4
200	-43.0
250	-41.1
300	-39.5
350	-38.0
400	-36.6
450	-35.3
500	-34.0

The figures of Table I correspond to the Mintra values for piston-type aircraft and serve as a criterion of the possible initial formation of condensation trails. If the air is not near saturation then it is reasonable to suppose that the critical temperature will be somewhat lower than that shown by Table I. Bannon (3) suggests that the humidity has little effect on the initial formation of trails.

3. Persistency of trails

Frost (4) has suggested that the diffusion of particles (or droplets) formed immediately behind the aircraft can be treated as a continuous point source problem with the indicated air speed of the aircraft replacing the mean wind of the point source problem. It is unlikely that the actual diffusion will correspond with that in conditions in which the mean wind is as high as the speed of a jet aircraft.

It seems more reasonable to assume that the mixing is complete at a very short distance behind the aircraft and that thereafter any particles or droplets formed are diffused normally. In view of the high speed of jet aircraft it is suggested that the problem should be treated as one of diffusion of droplets produced almost instantaneously along a line (the line of flight of the aircraft).

Sutton (5), considering diffusion from an instantaneous point source, has obtained the expression

$$\chi(x,y,z,t) = \frac{\chi_{0'}}{\pi^{3/2} C_x C_y C_z (\bar{u}t)^{\frac{3}{2}m}} \exp\left[-(\bar{u}t)^{-m}\left(\frac{x^2}{C_x^2} + \frac{y^2}{C_y^2} + \frac{z^2}{C_z^2}\right)\right] \qquad 3.1.$$

where X is the amount of matter instantaneously produced at time $t = 0$ and $\chi(x,y,z,t)$ represents the concentration at a point (x,y,z) at time t. (x,y,z) is measured from an origin moving with the cloud at constant speed $\bar{u}$ (the mean wind speed). C_x, C_y, C_z are coefficients of diffusion in directions parallel to the co-ordinate axes. Sutton shows that $m = 7/4$ gives reasonably accurate results over distances varying from metres to hundreds of kilometres. Using 3.1. and taking axes moving with the mean wind speed and the x axis parallel to the line of flight of the aircraft we have:-

amount of condensed water vapour at (x,y,z) at time t due to original condensed water vapour at $(x',0,0)$ is

$$\frac{(X/V)\,dx'}{\pi^{\frac{3}{2}} C_x C_y C_z (\bar{u}t)^{\frac{3}{2}m}} \exp\left[-(\bar{u}t)^{-m}\left(\frac{(x-x')^2}{C_x^2} + \frac{y^2}{C_y^2} + \frac{z^2}{C_z^2}\right)\right] \qquad 3.2.$$

since the amount of condensed water vapour in unit length of the original trail is X/V.

The line source is assumed infinite and then from 3.2. the total amount of condensed water vapour at (x,y,z) and at time t is

$$\frac{X/V}{\pi^{\frac{3}{2}} C_x C_y C_z (\bar{u}t)^{\frac{3}{2}m}} \int_{-\infty}^{+\infty} \exp\left[-\frac{\frac{(x-x')^2}{C_x^2} + \frac{y^2}{C_y^2} + \frac{z^2}{C_z^2}}{(\bar{u}t)^m}\right] dx'$$

$$= \frac{X/V}{\pi C_y C_z (\bar{u}t)^m} \exp -\left\{\frac{\frac{y^2}{C_y^2} + \frac{z^2}{C_z^2}}{(\bar{u}t)^m}\right\} \qquad 3.3.$$

If the particles originally formed are spherical and of uniform radius r_0 we have

$X = \frac{4}{3}\pi r_0^3 \rho_i N$ where ρ_i = density of ice

N = no. of particles formed per second and using 3.3. the number of particles at (x,y,z) at time t is

$$\frac{N/V}{\pi C_y C_z (\bar{u}t)^m} \exp -\left\{\frac{\frac{y^2}{C_y^2} + \frac{z^2}{C_z^2}}{(\bar{u}t)^m}\right\} \qquad 3.4.$$

Due to evaporation the particle will now have a radius r_t where r_t is connected with r_0 by the relation (cf. Frost (4))

$$r_t^2 = r_0^2 - \frac{2Dt}{\rho_i}(\rho_s - \rho_a) \qquad 3.5.$$

in which
D = coefficient of diffusion of water vapour in air
ρ_s = vapour density at surface of particle
ρ_a = vapour density in free air.

From 3.4. the number of particles in a section of the trail at a fixed distance z from the axis at time t is

$$\frac{N/V}{\pi C_y^2 C_z^2 (\bar{u}t)^m} \exp\{-z^2/(C_z^2(\bar{u}t)^m\} \int_{-\infty}^{+\infty} \exp\{-y^2/C_y^2(\bar{u}t)^m \, dy$$

$$= \frac{N/V}{\pi^{\frac{1}{2}} C_z (\bar{u}t)^{m/2}} \exp\{-z^2/C_z^2(\bar{u}t)^m\} \qquad 3.6.$$

The trail is visible when the illumination from the particles is sufficient to obscure the background. The scattering produced by any single particle is proportional to the cross-section of the drop and hence proportional to the square of the radius. Therefore the scattering of incident sunlight by all the particles in the section (of 3.6.) is

$$\frac{k(N/V) r_t^2}{\pi^{\frac{1}{2}} C_z (\bar{u}t)^{m/2}} \exp\{-z^2/C_z(\bar{u}t)^m \qquad 3.7.$$

in which k is a constant.

If the amount of scattered light required to obscure the background of the sky is P then from 3.7. the radius of the visible trail is given by

$$P = \frac{k(N/V) r_t^2}{\pi^{\frac{1}{2}} C_z (\bar{u}t)^{m/2}} \exp\{-R^2/C_z^2(\bar{u}t)^m\} \qquad 3.8.$$

Figure 1 shows a cross-section of the trail. The shaded circle represents the visible part of the trail whilst the outer circle represents the whole spread of particles. The observer sees only the shaded portion since in any cross-section for which z exceeds R, the visible radius, the light scattered by the particles in the cross-section is not sufficient to obscure the background.

The trail vanishes when the visible radius $R = 0$ or, from 3.8, when

$$P = \frac{k(N/V) r_{t_c}^2}{\pi^{\frac{1}{2}} C_z (\bar{u}t_c)^{m/2}} \qquad 3.9.$$

where t_c is the time during which the trail persists.

If L = length of visible trail we may write, taking axes with the origin moving with the aircraft, $x = Vt$ and $L = Vt_c$.

Elimination of P between 3.8.and 3.9.gives

$$\frac{r_t^2}{(t)^{m/2}} \exp\{-R^2/C_z^2(\bar{u}t)^m\} = \frac{r_{t_c}^2}{(t_c)^{m/2}}$$

or neglecting evaporation so that $r_t = r_{t_c} = r_0$ we have

$$\frac{\exp\left\{-R^2/C_z^2(\bar{u}x/V)^m\right\}}{(\bar{u}x/V)^{m/2}} = \frac{1}{(\bar{u}L/V)^{m/2}}$$

or $$\exp\left\{R^2/C_z^2(\bar{u}x/V)^m\right\} = (L/x)^{m/2}$$

i.e., $$R^2 = C_z^2\left(\frac{\bar{u}}{V}\right)^m \cdot \frac{m}{2}\, x^m \log_e \frac{L}{x}$$

and putting y for R, the equation of the outline of the visible trail can be written in the form

$$y^2 = A x^m \log_e L/x \qquad 3.10.$$

where $$A = C_z^2\left(\frac{\bar{u}}{V}\right)^m \cdot \frac{m}{2}$$

This equation agrees with that given by Frost (4) in his equation 3.08. if $\bar{u} = V$ as Frost, in effect, assumes.

Figure 2 illustrates successive cross-sections of the trail and shows the continuous spread of particles together with a growth then diminution of the visible trail. The outline of the trail which is obtained by joining the successive shaded portions of Figure 2 can be compared with photographs of trails (cf. Figure 1 in Frost's paper (4)).

Returning to equation 3.9. and substituting for N and r_t we have

$$\frac{X}{\frac{4}{3}\pi r_0^3 \rho_i} = \frac{P}{k} \cdot \frac{\pi^{\frac{1}{2}} C_z (\bar{u}t_c)^{m/2} V}{r_0^2 - \dfrac{2Dt_c(\rho_s - \rho_a)}{\rho_i}}$$

so that the condition for the trail to remain visible for a minimum time t_c is given by

$$X = \frac{P}{k} \frac{\frac{4}{3}\pi^{3/2} \rho_i r_0^3 C_z (\bar{u}t_c)^{m/2} V}{r_0^2 - \dfrac{2Dt_c(\rho_s - \rho_a)}{\rho_i}} \qquad 3.11.$$

or

$$X = \frac{K_1 \bar{u}^{m/2} r_0 V}{1 - \dfrac{K_2(\rho_s - \rho_a)}{r_0^2}} \qquad 3.12.$$

where $K_1 = \frac{4}{3}\frac{P}{k}\pi^{3/2}\rho_i t_c^{m/2} C_z$ and is approximately constant,

and $K_2 = 2Dt_c / \rho_i$.

For near saturated air $(\rho_s - \rho_a)$ approximates to zero and it is then possible to combine 2.4. and 3.12. to give

$$\omega M - \frac{E^2 eJLFM}{Rpc_pT^2} = \left\{1 + \frac{E^2 eJL^2}{Rpc_pT^2}\right\} K_1 \bar{u}^{m/2} r_0 V \qquad 3.13.$$

This equation indicates the conditions under which a visible trail will persist for a minimum time t_c in near-saturated air.

Trail persistency depends therefore on a number of factors (including air temperature, humidity, rate of fuel consumption, indicated airspeed, mean wind speed, and radius of particles condensed immediately behind aircraft). It is possible to say that, for any particular aircraft, persistent trails are more likely the higher the humidity, the lower the temperature and the lower the mean wind.

The complexity of equation 3.13. suggests that simple forecasting criteria can hardly be expected to indicate more than broad average conditions. By assuming reasonable values it may however be possible to check the equation.

The equation can be rewritten in the form

$$\frac{T^2}{e} = \frac{E^2 JLF}{Rpc_p\omega} \cdot \frac{1 + K_1 u^{m/2} r_0 L (V/M)(1/F)}{1 - K_1 u^{m/2} r_0 (V/M)(1/\omega)}$$

$$= \frac{T_i^2}{e_i} \cdot \frac{1 + K_1 u^{m/2} r_0 L (V/M)(1/F)}{1 - K_1 u^{m/2} r_0 (V/M)(1/\omega)} \qquad 3.14.$$

where T_i, e_i are values corresponding to initial trail formation and satisfy equation 2.5.

Experimental values suggest r_0 of the order of 15μ (cf. Mason (6)) whilst Frost, considering a trail against the blue sky with the sun in the zenith, reaches a value which is equivalent to $P/k = 8.5 \times 10^{-4}$. Also, from values reached by various experimenters, Frost takes $C_z = 0.30$ cm and $m = 7/4$.

Since $t_c = 10$ sec corresponds to a trail length of one mile or more it is considered that this is a reasonable value to take.
We have then

$$K_1 = \frac{4}{3}\frac{P}{k}\pi^{3/2}\rho_i t_c^{m/2} C_z$$

$$= 1{\cdot}3 \times 10^{-2} \text{ approx.}$$

whilst performance figures for Sabre aircraft suggest V/M is approximately constant at 50 cm/gm.

In equation 3.14. it is necessary that

$$1 > K_1 u^{m/2} r_0 (V/M)(1/w) \quad \text{since} \quad T^2/e > 0$$

Hence $$K_1 u^{m/2} r_0 (V/M)(L/F) \ll 1 \quad \text{since} \quad wL/F \ll 1$$

and therefore

$$\frac{T^2}{e} \simeq \frac{T_i^2}{e_i} \frac{1}{1 - K_1 u^{m/2} r_0 \frac{V}{M} \frac{1}{w}} \qquad 3.15.$$

or, with the constants assumed, we have that trails can only persist for 10 seconds if

$$u^{7/8} < 1333$$

i.e., $u < 3726$ cm/sec

or $u < 75$ knots (approx).

The critical temperature is now given by

$$\frac{T^2}{e} = \frac{T_i^2}{e_i} \frac{1}{1 - 7.5 \times 10^{-4} u^{7/8}}$$

Substituting for u we obtain Table II.

Table II

Theoretical critical temperatures required for visible trails to persist at least 10 seconds under varying winds and pressures and in near-saturated air. (Figures in degrees C)

Pressure in mb	Wind in knots 60	50	40	30
150	-58	-55	-53	-51
200	-56	-53	-51	-49
250	-55	-52	-49	-47
300	-54	-51	-47	-45
350	-53	-50	-46	-44
400	-52.5	-48	-45	-43
450	-52	-47	-44	-42
500	-51	-46	-43	-40.5

4. Comparison with actual results

Some 94 aircraft reports of condensation trails were forwarded by outstations to Watnall during the months of October, November and December, 1954. In these reports were given the aircrew estimates of the height of formation of trails, both persistent and non-persistent, and the meteorological officer's estimates of temperatures at the heights, places and times concerned.

These estimates of temperatures at the base, or tops, of reported persistent trails were regarded as being the critical temperatures for formation of persistent trails under the conditions prevailing. A total of 96 values was obtained and was expressed in a contingency table as follows.

/Table III

Table III

Reported height for base (or tops) of a persistent trail and corresponding critical temperature (estimated from relevant tephigrams)

Temperature (°A)

Height (feet)	207	210	213	216	219	222	225	228	231	234	237	240	Total
20000													
22000									½				½
24000							1	0	1½	½			3
26000					1	1	1	0	2	0			5
28000					1	2¼	1¾	2½	4	½	1½		13½
30000					1½	2½	3	1½	1				9½
32000			¼	1½	2½	2½	2¾	1½	½				11½
34000			¼	3	4¾	4	2						14
36000		1	½	2½	2¼	3¼							9½
38000	¼	1¾	1	1½	1								5½
40000	1½	4¼	2¾	1½	1½	½							12
42000	1¼	3½	2¼	2½	1								10½
44000		½	0	½	½								1½
Total	3	11	7	13	17	16	11½	5½	9½	1	1½		96

The table yields a correlation between the height H and the critical temperature of -0.8. The corresponding lines of regression are:-

$$T = 256.7 - 0.001052\,H \quad \ldots \quad \ldots \qquad 4.1.$$

$$H = 171500 - 623.7\,T \quad \ldots \quad \ldots \qquad 4.2.$$

H in feet, T in degrees Absolute.

No attempt was made to alter aircrew estimates of persistency in the above analysis except that two cases reported as semi-persistent were clsssified as persistent. The good correlation between T and H therefore indicates that temperature alone could be used as a good guide to forecasting the height at which aircrew would begin to estimate trail formation as persistent. Equation 4.1. yields the following figures for critical temperature:-

at 150 mb	-63°C	at 350 mb	-44°C	4.3.
200 mb	-57°C	400 mb	-41°C	
250 mb	-52°C	450 mb	-38°C	
300 mb	-48°C	500 mb	-36°C	

The theoretical values shown in Table II above are in reasonable agreement with 4.3. and indeed if comparison is limited to the range 250 to 350 mb, i.e., the zone in which more than two-thirds of the reported cases occurred, then 4.3. agrees very closely indeed with the values corresponding to a mean wind of 40 knots. No actual wind observations were available but 40 knots is a reasonable mean value for winds over England between 250 and 350 mb in autumn. (The mean wind at 300 mb over Larkhill in November was 37 knots for the years 1946-50.)

5. Conclusions

It is suggested that aircrew may usefully be told:-

a. the height above which trails are likely
b. the zone in which trails are likely to persist.

/(a)

(a) could be based on Table I which would replace the existing Mintra values. Section 3 shows the complicated problem involved in (b) but Section 4 suggests that empirical values on the lines of equation 4.1. could be used: the values probably differing slightly for each type of aircraft. Alternatively (b) could be based on a combination of wind and temperature, provided the air is near saturation, by using the figures of Table II. Similar tables could be constructed for different persistence times.

References

1. J.K. Bannon - Meteorological Research Papers, Air Ministry, London, No. 489.
2. W.L. Godson - Paper issued by Met. Division, Dept. of Transport, Canada.
3. J.K. Bannon - Meteorological Research Papers, Air Ministry, London, No. 476.
4. R. Frost - Meteorological Research Papers, Air Ministry, London, No. 830.
5. O.G. Sutton - Micrometeorology.
6. B.J. Mason - Q.J.R.M.S., 79, p.104.

FIGURE 1

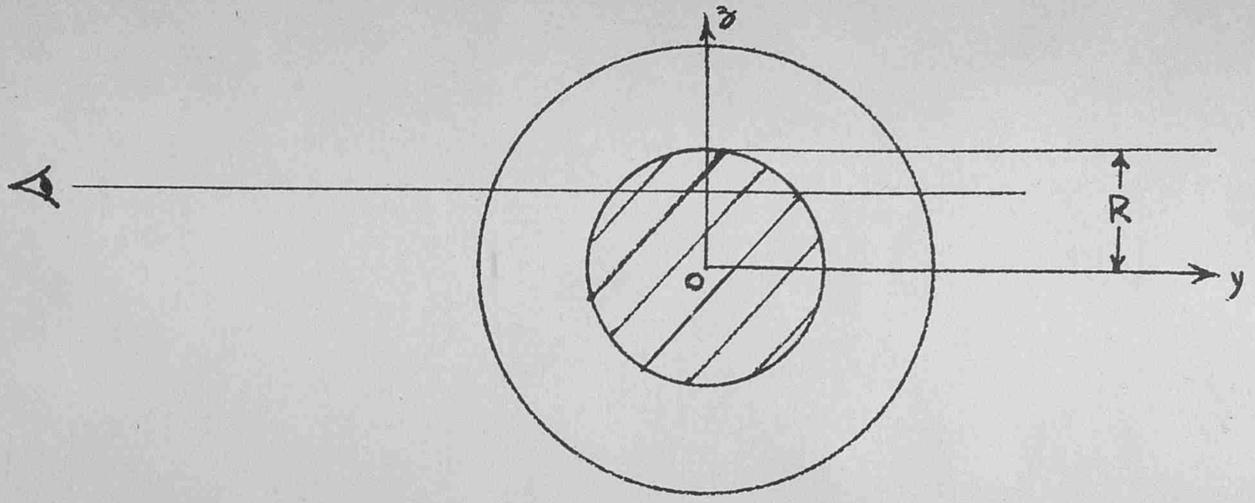

FIGURE 2

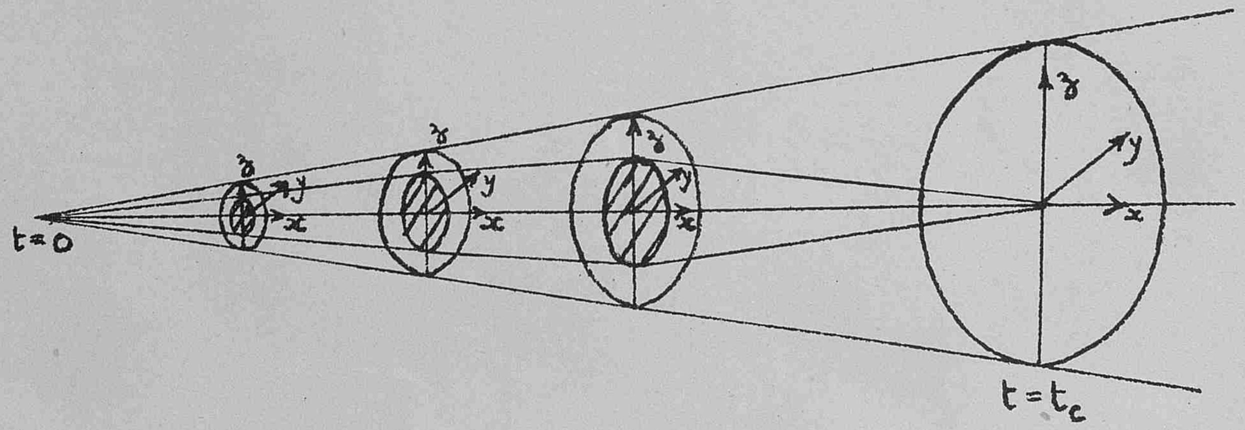
t=0
z
y
x
z
y
x
z
y
x
z
y
x
t=t_c

CONDENSATION TRAILS FORMED BY JET AIRCRAFT

M.R.P. 997
S.C.I/118
14th August, 1956.

AD 223117

A simple method for measuring atmospheric attenuation of light ("meteorological optical range" or visibility) at night.

by

K.H. Stewart.

(Meteorological Office)

AIR MINISTRY

METEOROLOGICAL RESEARCH COMMITTEE

At the time of issue this report has not been published. Any author desiring to quote this paper should refer to it as "A paper of the Meteorological Research Committee (London), M.R.P. No. 997 by Mr. K.H. Stewart. A copy is available in the Library of the Meteorological Office".

M.R.P. 997
S.C.I/118
14th August, 1956

AIR MINISTRY

METEOROLOGICAL RESEARCH COMMITTEE

A simple method for measuring atmospheric attenuation of light ("meteorological optical range" or visibility) at night

by

K.H. Stewart (Meteorological Office)

1. Introduction

The standard British instrument for measuring visibility at night is the "Night Visibility Meter (Mk.II)". This is basically the instrument devised by Gold(1939) with modifications described by Bibby (1947). The more elaborate "Photoelectric Visibility Meter (Mk.II)" is used at a few stations to give continuous records, and the very simple and direct method of counting the number of lights visible is used on the runways of important airports to give precise local estimates of "runway visual range". The method to be described is put forward as an alternative to the Gold meter method; it would not give the specialized information required for runway visual range reports or the continuous records provided by the photoelectric meter. Its great advantage over the Gold meter is that it uses a "matching" rather than an "extinction" method for estimating the illumination from a distant lamp.

2. Outline of method

The method requires two lights and a small convex mirror. One light is set up at a distance comparable with the visibilities to be measured and is viewed directly. The other light is carried on the observer's head and is viewed by reflection in the mirror, which is fixed on a stand at eye level a few yards from the observer (see Fig. 1). The observer moves until the distant light comes nearly into line with the reflection of his own light and then moves backwards or forwards until the two lights appear equally bright. The exact theory is given in the appendix, but it is easy to see that if the distance from observer to mirror is small compared with that of the distant light and large compared with the focal length of the mirror, then the apparent intensity of the distant light will vary little as the observer moves, while that of the reflection will vary roughly inversely as the fourth power of his distance from the mirror. The distance from observer to mirror thus gives a measure of the apparent intensity of the distant lamp, and if the measurement is made first on a clear night then on one of poor visibility, the ratio of the matching distances in the two cases is a measure of the attenuation of the rays from the distant lamp, independent of the relative power of the two lamps and of the reflectivity of the mirror, provided these remain constant. The distance of the distant light being known, the attenuation per unit distance can be calculated and hence, by well-known formulae, the "visibility" or "meteorological optical range".

/3.

3. Practical trial

The method has been tried at Kew Observatory on a number of occasions in the past two winters. A street lamp of about 100 c.p. 700 m away was used as the distant light and a 60 watt bulb was carried by the observer on simple headgear. The convex mirror was back-silvered, of "school" quality, 5 cm aperture and 10 cm focal length. In clear conditions matching occurred at about 5 m from the mirror, so that by walking backwards to 20 m from the mirror the observer could reduce the reflected intensity about 250 times. The mirror was supported on a single thin pillar so that by moving his head the observer could view the distant light either to left or right of the reflected one. Distance from the mirror was measured by reference to pegs in the ground at 1 m intervals, the observer's eyes being assumed to be vertically above his toes. Readings were estimated to 0.1 m.

Eight different observers tried the method. Most had little confidence in their matching ability at first, but were soon able to obtain reproducible readings (the accuracy is assessed quantitatively in the next section). One observer (with poor eyesight) obtained very discordant results, which were not used. The main difficulty in matching was caused by slight differences in the appearance of the two lights. The reflected image always appeared effectively a point source, but the distant street lamp sometimes seemed to have a perceptible angular size (the bulb of the lamp was small enough to appear as a point source, but parts of the reflector and cover glass may have reflected light to the observer and increased the size of the source). In hazy weather the distant lamp sometimes appeared considerably redder than the near one. The consequent difficulty in matching can easily be overcome by viewing both lights through a roughly monochromatic filter, but in practice this seemed unnecessary because it was found surprisingly easy to ignore the colour difference and match the lights for brightness alone.

4. Accuracy

Systematic errors may occur through ageing of one or other of the lamps, fluctuations of one supply voltage (ideally the two lamps would be run from the same supply) or deterioration of the mirror. These errors have not been investigated experimentally, but, with reasonable precautions, they seem likely to be small in comparison with the random errors of the matching procedure. These random errors were studied in two series of trials. In the first trials one observer matched the reflection to the distant light five or more times in quick succession, noting the matching distance (x) each time. This was repeated on many different nights, in visibilities ranging from twenty miles to less than half a mile. In the second series of trials two observers made the observations in succession, each usually taking three readings. In both series of trials Gold meter observations, on the same distant light, were made just before or after the mirror observations.

From the first series of trials we can estimate the variability of readings by a single observer. This is best expressed in terms of the variability of the attenuation represented by the readings. The difference in attenuation corresponding to readings x and $\bar{x}$ is $(x/\bar{x})^4$ or $40 \log_{10}(x/\bar{x})$ decibels. The departure of each individual reading (x) from the mean of its set ($\bar{x}$) was expressed in decibels in this way and a histogram of the departures is shown in Fig. 2(a). The standard deviation of individual observations (the square root of the average variance) is 0.4 db.

The Gold meter method measures attenuation-differences directly in "nebules", and from their respective definitions, 1 nebule = 0.3 decibels. The departure of each reading from the mean of its set was found and the departures are plotted in Fig. 2(b). The standard deviation is 1.1 db.

It is clear that, at any rate with this observer, the mirror method gives much smaller random errors than the Gold meter. The second series of trials measured the variability of readings between different observers. For each occasion the difference in the readings (usually the means of three observations) by the two observers was expressed in decibels, as before, and the standard deviation of these differences was calculated. With the mirror method the mean difference between any two observers should be zero, so the standard deviation from zero was calculated, but with the Gold meter there will be a difference between observers with different eyesight (a difference that can be allowed for, if constant, by calibration of individual observers) so the standard deviation from the mean was calculated. Only one pair of observers made enough observations to give a reliable mean difference of Gold meter readings, so the estimate of standard deviation of Gold meter observations is restricted to this pair. The results were:

Standard deviation of differences between
Gold meter observations by one pair of observers = 3.8 db
(eight pairs of observations).

Standard deviation of differences between
mirror observations by the same pair of observers = 1.4 db
(eight pairs of observations).

Standard deviation of differences between
mirror observations by various other pairs of observers = 1.3 db
(eight pairs of observations).

These deviations are about three times as large as would be expected from the scatter of readings obtained by a single observer on any one occasion, as measured in the first series of trials. Presumably changes in the criteria for matching (with the mirror method) and extinction (with the Gold meter method) occur from one occasion to another and increase the difference between the results of two observers when observations are made on a number of different occasions. This might be expected with the Gold meter because the sensitivity of the eye is known to vary with health, fatigue, diet and so forth, but it is rather surprising to find it occurring with the matching process. It may be that the changes in colour and shape of the distant lamp noted earlier affect different observers differently and that their elimination would improve the agreement between observers. Even without this possible improvement, however, the mirror method clearly gives much better agreement between different observers than the Gold meter method, with the additional advantage that no individual calibration is needed. The possibility that the rather large standard deviation of differences between Gold meter observations was caused by inability of one or other of the observers to use the instrument properly was checked by finding the standard deviations of the differences between each observer's mirror and Gold meter observations. These were 3.1 and 3.9 db, implying no great difference between the observers. (They may, of course, both have been insufficiently practised in the use of the instrument, but this seems unlikely.)

The relation between Gold meter and mirror estimates of attenuation is shown in Fig. 3. The points show considerable scatter, as would be expected from the figures given above, but the general agreement between the two methods seems satisfactory.

Accuracy has been discussed so far in terms of the measurement of attenuation. If the result of the measurement is expressed as a visibility (V) the accuracy will depend on the ratio of the visibility to the path length over which it is measured (i.e., the distance (y) of the distant light), as well as on the accuracy of the actual measurement. If there is an error of B decibels in the attenuation it can be shown that the corresponding percentage error in visibility is

$$\frac{100 \log_{10} e}{3.91 \times 10} \frac{V}{y} B = 5.75 \frac{V}{y} B.$$

The standard deviation of 1.4 db found between two observers' estimates by the mirror method would thus correspond to a deviation of about 32 per cent. in visibility, if the visibility was four times the path length. For smaller visibilities the accuracy would be greater, but the method becomes unusable when the visibility is much smaller than the path length, because the distant light is invisible. A set of lights at different distances would therefore be required to measure a wide range of visibilities with tolerable accuracy.

5. Discussion

The mirror method was designed as a simple way of using the matching principle to compare two point sources. It has been shown that it is simple to use and gives reasonably accurate results. The reproducibility of readings on a single occasion, in fact, is as good as that reported by Collier (1938) for the laboratory comparison of point sources. The main practical disadvantage of the mirror method is that it requires a 20-25 yd pathway for the observer, level and in line with the distant light, and is therefore almost inevitably an outdoor measurement, which may be difficult and uncomfortable (and so, probably, inaccurate) in bad weather. The importance of this disadvantage and the general value and practicability of the method could only be found by several months' trial in routine working conditions. A hand-held "artificial star" type of instrument would preserve the advantage of the matching principle and might prove more convenient in use, though it would probably be more expensive.

References

Collier, L.J. 1938 Trans. Ill. Eng. Soc., 3, 141.

Gold, E. 1939 Q.J.R. Met. Soc., 65, 139.

Bibby, J.R. 1947 Met. Mag., 76, 130.

Appendix. Calculation of matching distance

The system is sketched in Fig. 1. The observer's eye, E, and the light he carries, P, (of candlepower P) are at a distance x from the surface of the mirror M, of semi-aperture a, radius of curvature r and reflectivity ρ. A light of candlepower Q is at a distance y from the mirror. We assume the attenuation coefficient for visible light, σ, to be uniform between P and Q. Then illumination produced by Q at E,

$$I_Q = \frac{Q}{(x+y)^2} e^{-\sigma(x+y)} \qquad \text{lumens/unit area}$$

Also, light flux from P falling on M is

$$L = \frac{\pi a^2 P}{x^2} e^{-\sigma x} \qquad \text{lumens}$$

This flux forms an image at a distance z behind M, given by

$$\frac{1}{z} = \frac{2}{r} - \frac{1}{x}$$
$$\doteq \frac{2}{r} \quad \text{if } x \gg r$$

and the reflected flux is therefore distributed over a solid angle of

$$\frac{\pi a^2}{z^2} = \frac{4\pi a^2}{r^2} \text{ steradians} \quad (a \ll z)$$

/The

The illumination (flux per unit area) at E due to the light from P reflected in M is thus

$$I_P = \frac{\pi a^2 P}{x^2} e^{-\sigma x} \frac{r^2}{4\pi a^2 x^2} \rho e^{-\sigma x}$$

$$= \frac{P r^2 \rho}{4 x^4} e^{-2\sigma x} \qquad \text{lumens/unit area}$$

Matching of Q to the image of P in M occurs when

$$I_P = I_Q$$

$$\text{or } e^{-\sigma(y-x)} = \frac{1}{x^4} \frac{P r^2 \rho (x+y)^2}{4Q} \qquad (1)$$

In most applications $x \ll y$ and we can write, for matching,

$$e^{-\sigma y} = \frac{1}{x^4} \frac{P r^2 \rho y^2}{4Q}$$

If x_o is the matching distance in very clear conditions ($\sigma = 0$) we have

$$x_o^4 = \frac{P r^2 \rho y^2}{4Q}$$

and the equation for matching in other conditions is simply

$$e^{-\sigma y} = \left(\frac{x_o}{x}\right)^4 \qquad (2)$$

$$\sigma = \frac{4}{y} \log_e \frac{x}{x_o}$$

The visibility, V, is given by Koschmieder's equation

$$V = \frac{3.91}{\sigma}$$

so that we can write, with very little error,

$$V = \frac{y}{\log_e (x/x_o)} \qquad (3)$$

To show the relation between V and x the table below has been calculated for a system with the following values:

P = 50 c.p. ρ = 0.70 r = 20 cm

Q = 10 c.p. at 100 m, 50 c.p. at 400 m and 250 c.p. at 1600 m

(i.e., using a set of three distant lights to cover a range of visibilities). Table 1 has been calculated from the more exact equation (1); a few values calculated (with the same value of x_o) from the approximate equation (2) are given in brackets.

/Table 1

Table 1

Visibility (metres) for matching distance x

x metres	y = 100 m	y = 400 m	y = 1600 m
4.4	∞	-	-
5.8	-	∞	-
7.7	-	-	∞
5	770	-	-
6	308	9,900	-
7	204	2,020	-
8	156	1,180	41,000
9	129	870	10,500
10	111 (122)	700 (712)	5,970 (5,970)
12	89	524	3,510
14	76	430	2,600
16	66	372	2,120
18	60	333	1,830
20	54 (66)	303 (315)	1,630 (1,640)
22	50	281	1,480
24	47	261	1,370

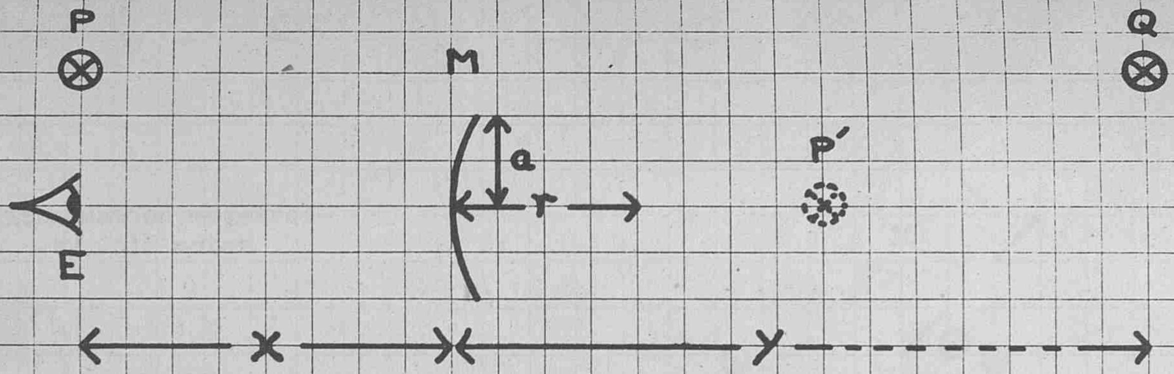

Fig. 1 Arrangement of lights and mirror (not to scale) .

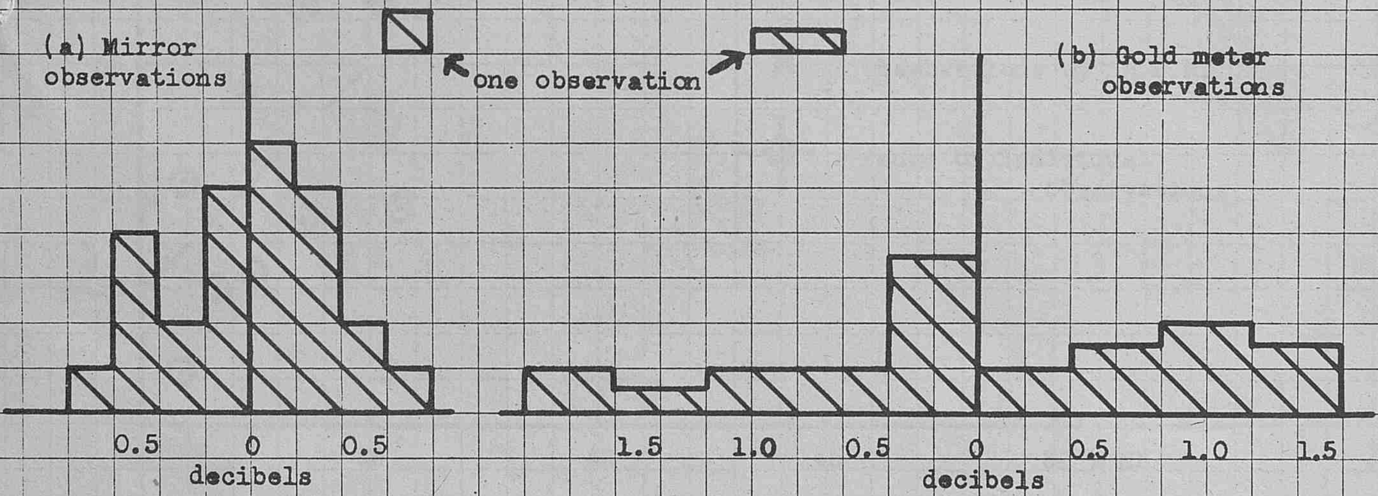

Fig. 2 Departures of individual observations from mean of their set.

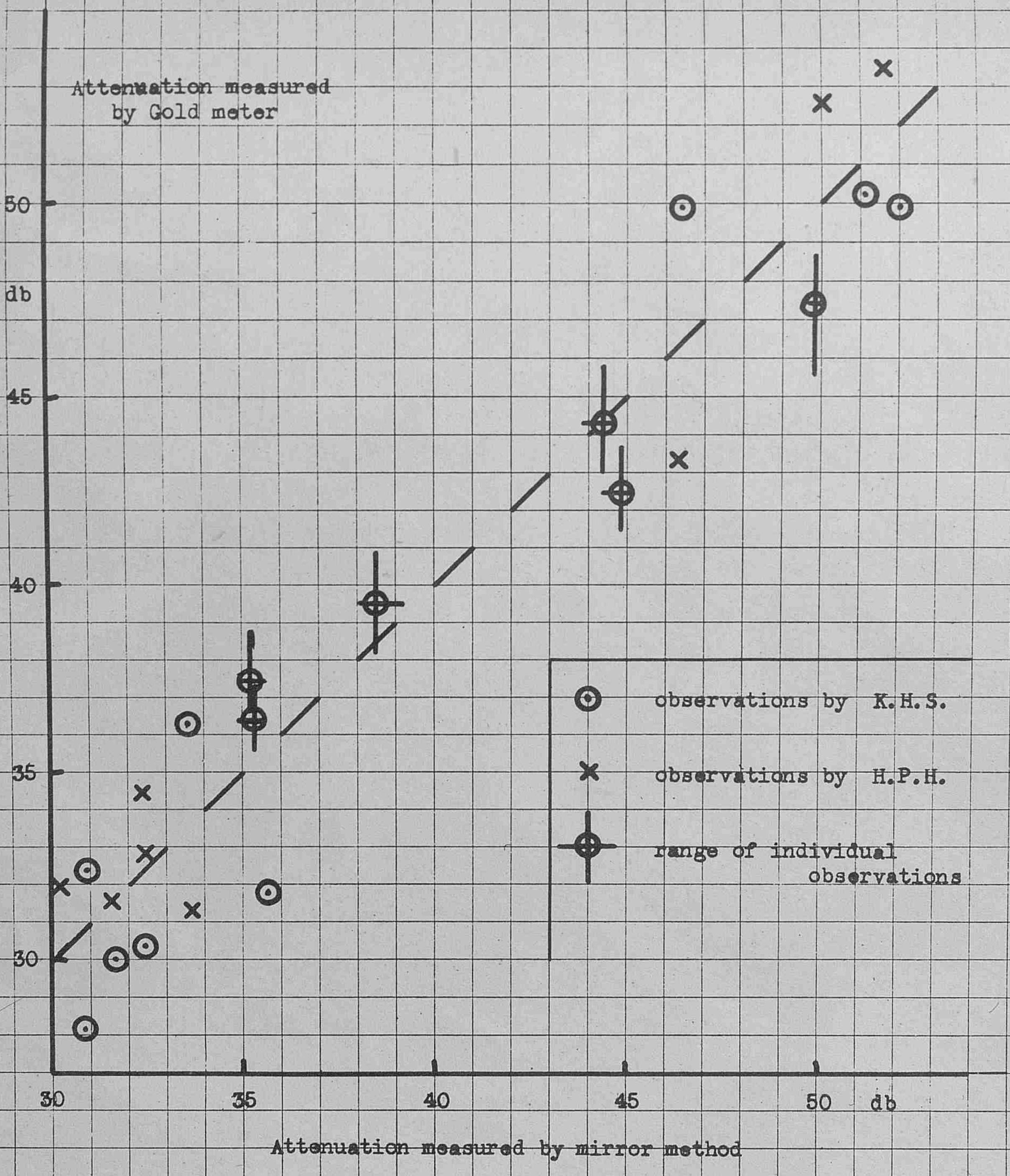

Fig. 3 Comparison of mirror and Gold meter observations (arbitrary zero)

M.R.P. 998
S.C.111/215
23rd August, 1956.

AD223119

The Measurements of Natural Freezing Nuclei made by the Meteorological Research Flight during January, 1956.

by

R. J. Murgatroyd. and. M. P. Garrod.

(Meteorological Office)

AIR MINISTRY

METEOROLOGICAL RESEARCH COMMITTEE

At the time of issue this report has not been published. Any author desiring to quote this paper should refer to it as "A paper of the Meteorological Research Committee(London).
M.R.P. No.998 by Messrs. R.J. Murgatroyd and M.P. Garrod
A copy is available in the Library of the Meteorological Office."

M.R.P. 998
S.C.III/215
23rd August, 1956

AIR MINISTRY

METEOROLOGICAL RESEARCH COMMITTEE

The Measurements of Natural Freezing Nuclei made by the Meteorological Research Flight during January, 1956

by

R.J. Murgatroyd and M.P. Garrod (Meteorological Office)

1. Introduction

As part of the investigation of the rainfall mechanism by the Bergeron process, and of the possibility of modifying rainfall over England by injecting artificial freezing nuclei into supercooled clouds, it was decided in 1954 that counts of natural freezing nuclei in the free atmosphere should be made by the Meteorological Research Flight. Measurements on the ground have been described by several authors (Ref. 1, 2, 3) but the only previous airborne measurements in this country were a few by Palmer made in aircraft of the Meteorological Research Flight in 1950 (Ref.4). More extensive work in aircraft by E.J. Smith and K.J. Heffernan of C.S.I.R.O., Australia is described in Ref.5.

After preliminary experiments in the laboratory in which both expansion chambers and cold chambers were tested, it was decided that the latter was more convenient for work in aircraft. Accordingly a cold chamber was constructed very similar to that described by Smith and Heffernan and, after some preliminary flight-tests in the summer of 1955, the techniques outlined in their article were adopted and have since been followed rather closely. This apparatus, although the most convenient at present, has severe limitations and some of them are mentioned below.

Dr. E.G. Bowen of C.S.I.R.O. suggested that flights should be made with this apparatus on as many days as possible during January, 1956, in order to provide data bearing on his hypothesis (Ref.6) that the variations of rainfall are related to the occurrence of meteor showers, and to afford a comparison with a similar series of observations to be made by Smith and his colleagues in Australia. It proved possible to make measurements on 25 days of this month in M.R.F.'s Hastings aircraft and to combine them with other work, e.g., simultaneous measurements of condensation nuclei, temperature, humidity, and cloud structure. In addition several samples were taken during other flights in a beam of silver iodide particles emitted from C.D.E.E., Porton and the results will be presented in another report. The present paper describes the results of the sampling of natural freezing nuclei with particular reference to Dr. Bowen's hypothesis. Some of the measurements of condensation nuclei will be included, but a more complete discussion of these will be given later in a separate paper.

2. Instrumentation

2.1. The cloud chamber consisted of a cylindrical tank 55 cm high and 30 cm diameter, its volume being about 40 litres. It was lagged externally and cooled or heated by circulating methylated spirits in copper pipes brazed round its periphery and in a spiral under its base. The methylated spirits could be pumped electrically either through a spiral immersed in solid carbon dioxide for cooling purposes or through another spiral in a water tank containing a 1 kw immersion heater for heating purposes, before circulating round the cloud chamber. The illumination was provided by a beam of light, at an angle of 45° to the horizontal, from a 250 kw lamp and the inside of the chamber was painted a matt black. Steam was produced by switching on a small immersion heater in a vacuum flask containing distilled water, placed at the bottom of the chamber. The cloud of water droplets or ice crystals produced was viewed through a visor, the illuminated observed volume being about 0.5 litres. Temperature was measured at 10 cm from the bottom and also at 10 cm from the top of the chamber by small 50-gauge platinum-wire resistances connected to M.O. bridges. Essentially the apparatus is similar to that described by Smith and Heffernan but rather smaller. Fig.1 shows its arrangement in the Hastings aircraft. It was located near the tail and air was supplied to it through a copper pipe, 10 cm in diameter, extending from an intake ahead of the propellers. Air passed along this pipe at a speed almost equal to that of the aircraft and consequently the rate of flushing was very high. When a sample had been taken the air supply was shut off and the chamber was sealed, all inlets being airtight and the removable top of the chamber being clamped down on a rubber washer.

2.2. In flight the chamber was flushed for at least a minute before the sample was taken with the chamber at a temperature well above freezing point to avoid any immediate deposition of hoar frost on the walls. The chamber was then cooled continuously at the maximum rate, which was about 5°C/min at 0°C falling off to about 0.5°C/min at -30°C. Details of cooling rate are given in each of the quoted results. If a cumulus cloud is ascending at 20 ft/sec with a lapse rate of 3°F/1000 ft, a particle in it will be cooled at about 2°C/min so that the conditions in the chamber were in this respect somewhat similar to those in a large cumulus cloud. While the temperature was falling, a cloud was maintained in the chamber by switching the boiler on and off at intervals, the cloud being kept at a sufficient density to allow the ice crystals to grow rapidly, but not so thick as to impede visibility. Estimations of crystal concentrations were then made in the range from 0°C to about -30°C. To prepare for a new experiment, the chamber was heated up again by switching the methylated spirits through the heater tank circuit and by flushing out the chamber. As the air passed through the long pipe its temperature increased considerably and there appeared to be no difficulty in taking samples in cloud. No effects of any possible icing at the inlet have yet been noticed. The time between the commencement of successive samples was usually about 30 minutes.

2.3. It is easy to see the crystals in the chamber as they sparkle, in contrast with the dull opaque background of the droplet clouds. The estimation of their concentration however is essentially a subjective one and to ensure as high an internal consistency as possible all the observations quoted throughout this series were taken by one of us (M.P. Garrod).

(a) When there were enough crystals in the chamber a visual estimation of their apparent spacing allowed an estimate of their number per litre to be made. Spacing estimates varied between 20 cm and 0.25 cm.

(b) At very low concentrations the number of crystals seen in the beam during a given period was counted. When the number exceeded about 8 in 30 sec the observer was able to relate this to a spacing: e.g., 8 in 30 sec was equivalent to a spacing of 1 particle per 20 cm. It was then assumed that lower numbers could be linearly related to equivalent spacings from this relationship. The figures obtained in this manner for low concentrations (0.1/litre or less) must be treated with reserve.

There are of course many objections to this procedure. Estimates of spacing, made, as described in para. 2.3.(a), by different observers may differ by as much as a factor three although agreement improves with experience. Any improvement on (b), e.g., by postulating that any crystals seen in the beam must have been produced in the volume of the cloud chamber immediately above the beam requires a knowledge of the fall-velocities of the crystals and of the movements of the air within the chamber.

/A

A purely objective system is difficult to design. For example, any system of photographing the particles requires the use of a microscopic system of small focal depth, which limits the volume that can be photographed. Another system which was tried was to have a disc covered with Formvar rotating under a slot at the bottom of the chamber. Any crystals falling into the slot formed replicas on the disc, and a complete record was obtained for the period when the crystal-concentration was large. However, this method gives no information for very small crystal-concentrations.

3. Limitations of the equipment

3.1. The apparatus is clumsy and more than half an hour is needed to take and examine a sample. By careful design and by the use of large rates of cooling Smith and Heffernan obtained samples in 10 minutes or so. For the sampling of natural nuclei, however, this is a doubtful procedure as there may be a delay before nuclei become active at a given temperature. Even with samples every 10 minutes the scope of the measurements achieved in a given flight is undesirably small. The bulk of this particular apparatus moreover confines its use to large aircraft.

3.2. The subjective nature of the estimations of the concentration of ice crystals has been discussed above. There may also be variations in the rate of production of steam, and hence in the rate of growth of the ice crystals, particularly as the rate of boiling is a function of altitude.

3.3. The visible concentration at a given instant is affected by the following:-

(a) There is a constant depletion of concentration as crystals fall out to the bottom of the chamber. The rate at which they do this depends on their size which is affected by the rate of supply of steam from the boiler.

(b) There is an increase of concentration as more nuclei become activated with time at a given temperature.

Hence there will generally be an uncertainty in evaluating total concentrations due to these two opposing effects, and the best that can be done for natural nuclei is to observe the apparent concentration at given temperatures. Smith and Heffernan have produced conversion factors which take these effects into account when the effective nuclei are silver iodide, by comparing the observed concentration at given times with the total number of crystals falling on to the bottom of the chamber at fixed temperatures. This factor varies linearly from about 30 at -10°C to 2 at -30°C and it is therefore most important at the higher temperatures. Although the few laboratory tests made by M.R.F. showed that a factor of comparable magnitude should be used for natural nuclei, it cannot be applied with any confidence in practice as it may vary from experiment to experiment. The results given below do not include any conversion factor, but this is not thought to affect the validity of comparison between measurements on different days.

3.4. The measurement of the temperature in the chamber presents some difficulties as there is a difference of about 2°C between the top and bottom thermometers at -10°C and 4°C at -30°C. Moreover the temperature is lowered continuously which means that thermometer lags are important. The illuminated area does not include the bottom of the chamber and in the results given below the temperature at the centre of the chamber is quoted. In fact, due to turbulence, ice crystals which are formed in the lower temperature region at the bottom of the chamber may be transported upwards in the beam, and other investigators have given a temperature measured nearer the bottom as that corresponding to a given concentration. The thermometer lag was found by a subsidiary experiment and the correction applied to the indicated readings was obtained from the following expression which gives the reading of a thermometer with lag in an environment whose temperature is changing

$$T_{r+1} - \theta_{r+1} = \frac{\theta_{r+1} - \theta_r}{k\Delta t} \qquad (1)$$

where k is the thermometer lag coefficient (= 0.7 in this case), θ_r, θ_{r+1} are the indicated temperatures at time t, $t+\Delta t$ respectively, and T_{r+1} is the true air temperature at time $t + \Delta t$.

The crystals themselves take some time to grow to a visible size which results in a lower temperature being assigned to their formation. If the time is 30 sec the error is 1 to 2°C.

3.5. As the chamber capacity is about 40 litres and the illuminated area is approximately 0.5 litres the observations are not well based for concentrations less than about 1/litre (Smith and Heffernan consider that the threshold of detection with their 100 litre chamber is 0.1/litre). There is some evidence that smaller concentrations may be significant in rainfall production by the Bergeron process.

Although there is little doubt that the readings are significant at concentrations of 1/litre and above, an observation of a single flashing particle in the beam may be suspect if any dust particle gets into the chamber.

It should also be noted that, in connection with its application to rainfall production, the apparatus does not make any count of small pure ice particles which may be floating in the atmosphere, as they will be melted before the measurement begins. On the other hand there is a danger at the lower temperatures that any hoar frost on the walls of the chamber may fall off and act as a freezing agent.

3.6. Although the limitations of this type of instrument are considerable and the objections to any quantitative results based on its use may be formidable, nevertheless it does give results which are generally reproducible and it determines in a semi-quantitative way the freezing nucleus spectrum for crystal concentrations of 1/litre to about 10^4/litre with indications of the temperature of lower concentrations.

4. Flight details

4.1. During January, 1956 samples were taken on 25 days between 11 a.m. and 3 p.m. at 10,000 ft over Southern England within a 50 mile radius of Farnborough. Temperatures, humidities, and numbers of condensation nuclei were also measured at this level and at different levels on the ascent and descent. These measurements are shown in Fig.2. In connection with other work, raindrop sampling and cloud water content measurement was also carried out whenever possible. On a few flights data on the variation of freezing nucleus counts in the vertical and in the horizontal were obtained. Table 1 lists the detailed observations of ice crystals observed during each experiment.

5. Application of the results to Bowen's hypothesis

5.1. Fig. 3 shows a plot of the temperature at which observed concentrations of 1/litre to 10^4/litre occurred from the 2nd to 30th of January, 1956. The temperatures at which the first crystal was observed in each case are also shown. Included for comparison is a copy of Smith's results giving temperatures at which 1/litre occurred in January, 1955 in Sydney, Australia. Similar curves for Sydney in 1954 and Arizona 1955 are given in Ref.7 in which it is pointed out that in the main they tend to exhibit peaks around the 13th, 23rd and 31st of the month which coincide roughly with the dates of abnormal rainfall in Sydney given by Bowen in Ref.6.

The Meteorological Research Flight results however do not exhibit any well marked peaks and the temperature for the 1/litre concentration is always between -20 and -25°C while the day to day variation at the 10^2, 10^3 and 10^4/litre level is no more than would be expected from random errors of measurement. No conclusions have been drawn from the temperatures at which the first crystal was seen, these being regarded as very doubtful observations. At the 0.1/litre level there was probably a peak on the 28th only.

The mean temperature for the Meteorological Research Flight readings is several °C higher than that of the Australian measurements. It is thought that this can be accounted for by differences in chamber design and reading technique - e.g., rates of cooling and position in the chamber at which the temperature measurement was taken. Considering the spectrum as a whole the day of maximum concentrations was the 4th January although of course it is possible that there may have been a peak during the period from the 5th to the 8th when no flying was possible.

5.2. It appears therefore that this set of measurements give no support to the hypothesis of Bowen, i.e., they do not show any correlation with an expected increase of freezing nuclei concentration on dates falling about 30 days after the occurrence of meteor showers. In a private communication (Ref. 8) Smith informed us that his flight results for 1956 in Sydney also exhibited no well-marked peaks. On the other hand K. Bigg working with a cold box in Carnarvon, Western Australia, on the coast with on-shore winds and virtually no clouds obtained concentrations of 1/litre at about -10°C on 13th, 21st, 23rd and 1st February compared to a general level of about -20°C for the rest of the month.

5.3. It should be noted that whereas the recent Meteorological Research Flight results, and those given in Ref.7, exhibit nucleation temperatures at the 1/litre level which vary from a minimum of -25°C to -30°C to a maximum of -16°C to -20°C, Bigg's results give maxima of -10°C. This point appears to be important as it is fairly well established (e.g., in Ref. 9 and 10) that natural clouds usually glaciate between about -10°C and -15°C. Thus it appears that there is a temperature gap of about 10°C between the temperature at which the clouds glaciate and at which nuclei appear, in concentrations of 1/litre and above, in the cloud chamber experiments. This difference, which has also been noted by previous workers with cloud chambers, makes dubious the support given to Bowen's hypothesis by the results in Ref. 7. Palmer (Ref. 4) has interpreted the difference as "a shortage of freezing nuclei" and has suggested that the discrepancy might be made up by a splintering process from rapidly growing crystals particularly in the dendritic stage at about -15°C.

5.4. It seems likely therefore that the temperature range of most interest for counts of freezing nuclei is between 0 and -20°C. The concentrations here however are frequently as low as $1/m^3$ and can therefore only be investigated with a chamber having a volume of at least $1m^3$. The installation of so large a chamber, together with its heating and cooling system, in an aircraft, would present a serious engineering problem. The present chamber however seems to be adequate for other purposes, e.g., determining concentrations of silver iodide relatively near to a generating source.

5.5. It should be added that although these results do not support Bowen's hypothesis they do not of course disprove it. All that can be said is that the variations of nucleation-temperature, at levels of 1/litre or higher, are small and show no singularities corresponding with those predicted by Bowen's hypothesis. Owing to the limitations of the equipment, one cannot attach very much weight to the observations at lower concentrations, but, such as they are, they likewise fail to support Bowen's hypothesis.

6. Comparison with other cloud chamber results

6.1. It has been pointed out by Findeisen and Schulz, followed later by Palmer and then by Smith and Heffernan, that the earlier results from expansion chambers indicating a "threshold temperature" for the activation of freezing nuclei were explicable in terms of a spectrum of freezing nuclei. Typical spectra obtained in these flights are shown in Fig.4. The results below the 0.1/litre level are very questionable but there seems to be little doubt that the temperature, at which the main increase of concentration begins, varies from sample to sample. The curve for 4/1/56, for instance, clearly shows considerable increase in activation at about -19°C whereas that of 30/1/56 requires -25°C for the same type of increase. The mean curve for the series is shown in Fig.5 and this is compared with a diagram from Ref.2 from which it appears that the type of curve is rather similar to that observed by other workers.

6.2. The typical shape of the curve in Fig.5 suggests that there may be different types of freezing agents active at temperatures roughly above and below -20°C. The former, in the mean, were not observed above about -8°C and remained at concentrations of less than 0.1/litre between -10°C and -18°C - the range of temperatures in which clouds commonly glaciate. The latter type of nucleus evidently becomes active in greatly increasing numbers as the temperature is lowered. Counts were rarely taken below -30°C in this work.

6.3. In Ref.11 E.K. Bigg has attempted to predict the number of crystals which will occur in a cloud chamber at temperatures below about -25°C when the water content and the rate of cooling are known. He assumes that at these lower temperatures freezing can be regarded as an event whose probability depends on the size of the droplets and the time they are held at given temperatures. His results, which were compared with Smith and Heffernan's mean freezing spectrum from 155 measurements, were considered to justify the application of his laboratory results (obtained by freezing drops suspended in an insoluble liquid) to calculations of the freezing temperature of airborne droplets.

Bigg's results for water contents of 0.3 and 3 gm/m^3 are plotted on Fig.5 using the mean rate of cooling of the Meteorological Research Flight apparatus of 1.3°C/min at -25°C to -30°C. The arithmetic mean of the Smith and Heffernan 155 results is also included in this diagram. Their agreement with the mean spectrum of the Meteorological Research Flight results is not thought to be good, the slope of the curve of the M.R.F. spectrum being considerably greater. This may be partly due to the subjective estimation of the crystal concentration, but may also indicate that between -20° and -30°C freezing nuclei may still be playing a decisive role in the freezing processes.

The day to day variations of concentrations of freezing nuclei were also examined with respect to rate of cooling of the chamber at -20°C and no correlation was found.

7. Sources of freezing nuclei

7.1. Although the variability of the counts was small, it seemed worth while to attempt to find a relationship between freezing nucleus concentrations and other factors such as air mass, wind direction, and vertical stability using Fig.2 and the data in Table 2, which includes information on weather and air mass. In the last column of this table an opinion is given on the likelihood that the nuclei could have been transported upwards from the earth's surface, based on consideration of the lapse rate and the counts of condensation nuclei. Table 3 gives a summary based on these opinions.

/Table 3

Table 3

Number of cases of high, moderate and low concentrations of freezing nuclei at -20°C and -25°C in which transport upwards from the earth's surface was likely

	Freezing nucleus concentration					
Transported upwards from earth's surface	at -20°C			at -25°C		
	High > 1/litre	Moderate 0.1-1.0/litre	Low < 0.1/litre	High >100/litre	Moderate 10-100/litre	Low < 10/litre
likely	1	4	9	2	3	9
unlikely	2	4	4	1	3	6

In general there is no evidence from this table that the higher concentrations were produced by transport of nuclei upwards from the earth's surface but rather the reverse is suggested, i.e., in unstable conditions the counts tended to be low.

7.2. A few flights have been made giving data directly on variation of freezing nuclei in the vertical and the results of these are shown in Fig.6, 7 and 8.

(a) On 19.1.56 counts were made at 2,000 ft and 10,000 ft with an inversion at 4,000 ft ahead of a warm front. The freezing nucleus concentrations were generally higher above the inversion (Fig.6).

(b) On 6.3.56 samples were taken at 1,500 ft and at 5,000 ft with an inversion at 3,000 ft ahead of a warm front. In this case there was very little change with height (Fig.7).

(c) On 30.1.56 counts were made at 10,000 ft, 15,000 ft and 20,000 ft. The lapse rate was unstable throughout and there was considerable cloud and rain ahead of a small wave depression. At concentrations greater than 1/litre the temperature of activation appeared to increase with height. At lower concentrations however the reverse appeared to be the case although of course this is the region where the measurements are doubtful.

7.3. Although the major part of the evidence suggests that most of the condensation nuclei in the free atmosphere up to 10,000 ft at least are produced at the surface and decrease upwards there is not a direct correspondence between the counts of condensation nuclei and vertical stability (Fig.2). Presumably other factors such as the source of the nuclei and the previous trajectory of the air are important. The possibility that condensation nuclei and freezing nuclei arise from the same source was examined with Fig.9 and Fig. 10 which show at the various dates the concentrations of condensation nuclei and of freezing nuclei at -20°C and -25°C respectively. There is no correlation at -20°C but some signs of correspondence between high and low counts of condensation nuclei, and of freezing nuclei at -25°C, can be detected.

The majority of dust and soil substances appear to have activation temperatures lower than -20°C so that any agreement between counts of freezing and condensation nuclei might be expected to be better at the lower temperatures, whereas nuclei active at higher temperatures might, as suggested by Bowen, originate at greater altitudes. Smith and Heffernan found higher activation temperatures for a concentration of 1/litre above inversions than below inversions but otherwise no correlation between the concentration of freezing nuclei and altitude. Palmer on the other hand, detecting concentrations of probably no more than 10/litre, found a "threshold temperature" of -32°C near the surface and -41°C at higher altitudes.

In general therefore the evidence up to date supports the view that the small concentrations of freezing nuclei active at temperatures higher than -20°C are not usually produced at the earth's surface. Those active at -25°C and below may originate there, but in assessing their numbers other factors as well as stability on the day of measurement are probably important. Clearly further measurements are required before any further conclusions can be drawn.

7.4. The question of the variation with wind direction was studied by means of Table 4.

Table 4

Number of cases of high, moderate and low counts of freezing nuclei at -20°C and -25°C in various wind directions

	Freezing nucleus concentration					
	at -20°C			at -25°C		
Wind direction at 10,000 ft	High >1/litre	Moderate 0.1-1.0/litre	Low < 0.1/litre	High >100/litre	Moderate 10-100/litre	Low <10/litre
Northerly			2			2
NW	1	2	2		1	4
W	1	4	7	1	4	7
SW		2	2	1	1	2
S	1			1		

There were no data from the easterly sectors.

No obvious tendency is revealed by this table nor did there appear to be any tendency for large concentrations to be associated with a given air mass.

7.5. Two flights have been made up to date in which variation in the horizontal was examined, and these have shown changes within 100 miles or so as large as the day to day variations at 10,000 ft plotted in Fig.3. This further work also does not support Bowen's hypothesis which presumably requires similar freezing nucleus spectra over considerably greater areas.

The spectra obtained on these two flights are shown in Fig.11 and Fig.12 which both include small synoptic charts.

(a) On 25.1.56 during a flight at 10,000 ft from Farnborough to Aldergrove samples were taken near Stratford-on-Avon and also over the Irish Sea. At concentrations greater than 1/litre the nucleation temperature over the latter place was consistently about 2°C warmer than over the former, for the same concentration. The second sample was taken somewhat nearer to an incoming warm front and in light southerly winds whereas the first was taken in the ridge ahead with light winds and a stable lapse rate. No measurement was made of the lapse rate over the Irish Sea but it was probably stable there also.

(b) On 5.3.56 during a similar flight counts were made over Warwick, Blackpool and Belfast - the last somewhat later in time and at a lower altitude. The W to WNW airstream was stabilising from the west during the period but all counts were made below the inversion. At concentrations of 1/litre and above there appeared to be a significant decrease in counts from south to north.

The two sets of results appear to have little in common except to show that variations in the horizontal exist. It is not thought that the magnitudes of the variations can be accounted for by instrumental uncertainties.

Finally an attempt was made to compare counts with the incidence of rainfall which occurred on 10th-12th, 14th, 19th-21st, 23rd, 26th, and 28th-30th. On 23rd and 30th the samples were actually taken in rain and cloud. From an examination of the temperatures for 1/litre concentrations of freezing nuclei on these days it appears that they were days of rather low temperature of activation.

8. Conclusions

8.1. The general results of this series of measurements were as follows:-

(a) No support was provided for Bowen's hypothesis, as freezing nucleus concentrations of 1/litre and above did not vary significantly from day to day and did not exhibit peaks on or near the predicted dates.

(b) Concentrations of 1/litre and above did not usually appear until the temperature had fallen to -20°C or below. This is almost 10°C lower than the temperature at which clouds commonly glaciate and further explanation of this is required.

(c) There was little evidence to suggest that freezing nuclei active at -20°C or above usually originate at the earth's surface.

(d) No correlation of freezing nuclei counts with wind direction, weather or air mass was found although significant changes in concentration were found within horizontal distances of 100 miles or so.

(e) As regards further work it appears that

(i) Apparatus is required capable of counting freezing nuclei in concentrations down to $1/m^3$ in the 0°C to -20°C range.

(ii) A flight programme aimed specifically at finding the origin of freezing nuclei in the free atmosphere is desirable.

(iii) Further efforts should be made to produce a more objective method of making counts.

9. References

1. Findeisen, W. and Schulz, G. 1944 Forsch. u. Erfahrb. Reichs. Wetterdienst, Berlin, A., No.27.
2. Aufm Kampe, H.J. and Weickmann, H.K. 1951 J.Met., 8, p.282.
3. Schaefer, V.J. 1948 Project Cirrus. Occasional Report No.9. G.E. Res. Lab.
4. Palmer, H.P. 1949 Q.J.R.Met.Soc., 75, 323.
5. Smith, E.J. and Heffernan, K.J. 1954 Q.J.R.Met.Soc., 80, 344.
6. Bowen, E.G. 1953 Aust. J. Phys., 6.
7. Smith, E.J., Kassander, A.R. and Twomey, S. 1956 Nature, 177, 14.1.56.
8. Smith, E.J. Private communication.
9. Peppler, W. 1940 Forsch. und Erfahrb. Reichs. Wetterdienst, Berlin, B. No.1.
10. Day, G.J. 1954 Met.Mag., 83, 230.
11. Bigg, E.K. 1955 Q.J.R.Met. Soc., 81, 349.

Table 1

Daily counts of freezing nuclei (ice crystals observed)

2. 1.56			3. 1.56		
Time	Temp. °C	Instantaneous number per litre	Time	Temp. °C	Instantaneous number per litre
15.00	-6.7	2x10^{-2}	11.17	-12.7	2x10^{-2}
	-7.0	2x10^{-2}	11.18	-13.5	2x10^{-2}
	-9.8	2x10^{-2}	11.19	-15.3	2x10^{-2}
	-10.7	2x10^{-2}	11.20	-15.8	2x10^{-2}
15.03	-13.2	3x10^{-2}	11.20$\frac{1}{4}$	-16.5	3x10^{-2}
	-15.7	Nil	11.21$\frac{1}{2}$	-18.9	-
	-16.5	2x10^{-2}	11.22$\frac{1}{4}$	-20.1	2x10^{-2}
	-16.7	2x10^{-2}	11.23	-20.8	5x10^{-2}
	-17.7	Nil	11.24	-21.4	2x10^{-2}
	-19.0	3x10^{-2}	11.24$\frac{1}{2}$	-21.8	2x10^{-2}
	-20.2	3x10^{-2}	11.26	-22.9	5x10^{-2}
15.08	-21.8	6x10^{-2}	11.27$\frac{1}{4}$	-23.3	3x10^{-2}
15.10	-24.0	1x10^{0}	11.28$\frac{1}{2}$	-24.6	3x10^{-2}
15.11	-25.5	1x10^{0}	11.29$\frac{1}{2}$	-25.4	1x10^{0}
15.15	-28.5	8x10^{3}	11.30$\frac{3}{4}$	-27.0	8x10^{3}
4. 1.56			9. 1. 56		
11.17$\frac{1}{2}$	-7.9	2x10^{-2}	11.34	-4.2	3x10^{-2}
11.18	-9.7	2x10^{-2}		-5.3	2x10^{-2}
11.19$\frac{1}{2}$	-12.1	2x10^{-2}	11.36	-9.3	Nil
11.22	-14.4	Nil	11.37$\frac{1}{2}$	-12.6	Nil
11.25	-17.8	Nil	11.38	-13.9	Nil
11.27	-19.7	3.7x10	11.42	-16.9	Nil
	-21.0	1.3x10^{2}		-18.5	3x10^{-2}
11.28	-21.8	1x10^{3}		-20.0	2x10^{-2}
11.28$\frac{1}{2}$	-25.1	2.4x10^{3}	11.43$\frac{1}{2}$	-22.3	2x10^{-2}
	-26.6	8x10^{3}	11.44	-23.6	8x10^{0}
11.30	-27.9	6.4x10^{4}	11.44$\frac{1}{2}$	-24.9	3.7x10
				-25.1	1.3x10^{2}
			11.45$\frac{1}{2}$	-25.3	1x10^{3}
				-25.7	2.4x10^{3}
			11.46	-26.1	8x10^{3}
			11.47	-27.0	8x10^{3}
			11.48$\frac{1}{2}$	-28.1	6.4x10^{4}

Table 1 (continued)

9. 1. 56			10. 1.56		
Time	Temp. °C	Instantaneous number per litre	Time	Temp. °C	Instantaneous number per litre
12.08	-4.0	2x10^{-2}	11.43½	-15.3	2x10^{-2}
12.09¾	-7.8	Nil	11.45	-18.7	Nil
12.11	-10.1	2x10^{-2}	11.45¼	-19.6	2x10^{-2}
12.12	-11.9	Nil	11.45¾	-20.6	1x10^{0}
12.13	-13.4	Nil	11.46½	-21.9	8x10^{0}
12.14	-15.3	Nil	11.47¾	-22.6	1x10^{0}
12.15	-17.6	Nil	11.50	-24.6	8x10^{0}
12.16	-18.9	2x10^{-2}	11.50½	-25.2	1.3x10^{2}
12.16¼	-19.5	2x10^{-2}	11.51	-25.7	1x10^{3}
12.18	-22.1	8x10^{0}		-26.0	2.4x10^{3}
12.18½	-24.2	1x10^{3}	11.52	-26.5	8x10^{3}
12.18¾	-24.9	8x10^{3}	11.52¾	-27.4	6.4x10^{4}
12.19¼	-25.8	6.4x10^{4}			

11. 1. 56			12. 1. 56		
11.13½	-12.8	2x10^{-2}		-8.4	2x10^{-2}
11.16	-17.7	2x10^{-2}	12.17½	-12.6	Nil
11.17	-22.2	1x10^{0}		-12.9	2x10^{-2}
11.17½	-22.4	1x10^{0}	12.19	-14.8	2x10^{-2}
11.18½	-22.7	8x10^{0}	12.21	-18.0	Nil
11.19½	-23.8	8x10^{0}	12.22	-19.7	3x10^{-2}
11.20	-24.5	1.3x10^{2}	12.23	-20.1	2x10^{-2}
11.20½	-25.1	1x10^{3}	12.24	-21.4	3x10^{-2}
11.21½	-25.8	1x10^{3}		-23.1	6x10^{-2}
11.21¾	-26.1	8x10^{3}	12.27	-24.8	1.3x10^{-1}
11.22	-26.6	8x10^{3}		-26.0	8x10^{0}
11.22½	-27.2	6.4x10^{4}		-26.5	1.3x10^{2}
				-26.6	1x10^{3}
			12.28	-26.7	2.4x10^{3}
				-26.8	8x10^{3}
			12.30	-27.2	6.4x10^{4}

Table 1 (continued)

13. 1.56

Time	Temp. °C	Instantaneous number per litre
11.24	-9.3	2×10^{-2}
11.33	-17.9	2×10^{-2}
11.34	-21.7	1×10^{0}
11.35	-23.2	1×10^{0}
11.36	-23.8	2.9×10^{0}
11.37½	-25.0	8×10^{0}
11.38	-25.5	1.3×10^{2}
11.38¾	-26.4	1×10^{3}
11.39	-26.7	8×10^{3}
11.40	-27.3	6.4×10^{4}

15. 1.56

Time	Temp. °C	Instantaneous number per litre
11.12	-5.6	2×10^{-2}
11.15¼	-10.3	2×10^{-2}
11.16¼	-11.0	2×10^{-2}
11.17½	-12.4	2×10^{-2}
11.20½	-16.9	2×10^{-2}
11.21	-18.3	2×10^{-2}
11.21¾	-18.6	2×10^{-2}
11.22	-19.9	3×10^{-2}
11.22½	-21.3	1×10^{0}
11.23½	-22.5	1×10^{0}
11.24¾	-23.1	8×10^{0}
11.26	-24.5	2.9×10^{0}
11.27½	-25.4	2.9×10^{0}
11.27¾	-25.6	1.3×10^{2}
11.28¼	-26.4	8×10^{3}
11.29	-27.6	8×10^{3}
11.30	-27.7	6.4×10^{4}

14. 1.56

Time	Temp. °C	Instantaneous number per litre
11.21½	-11.7	2×10^{-2}
11.22½	-12.4	2×10^{-2}
11.24½	-15.0	3×10^{-2}
11.25½	-16.2	2×10^{-2}
11.26	-16.7	5×10^{-2}
11.28½	-18.9	5×10^{-2}
11.29	-20.2	1×10^{0}
11.30	-22.2	2×10^{0}
11.31	-23.6	2.9×10^{0}
11.32	-25.2	1×10^{0}
11.32½	-25.7	1×10^{3}
11.33	-26.1	2.4×10^{3}
11.33¼	-26.6	8×10^{3}
11.33¾	-27.2	6.4×10^{4}

16. 1.56

Time	Temp. °C	Instantaneous number per litre
11.25	-6.7	2×10^{-2}
11.26	-8.1	2×10^{-2}
11.26½	-8.2	3×10^{-2}
11.29	-12.4	2×10^{-2}
11.33	-17.3	3×10^{-2}
11.34	-19.7	8×10^{-2}
11.35	-20.6	3×10^{-1}
11.35½	-21.8	8×10^{0}
11.36	-22.9	8×10^{0}
11.38	-24.2	3×10^{-1}
11.38¾	-25.3	8×10^{0}
11.39	-26.0	3.7×10
11.39¼	-26.1	1×10^{3}
11.39½	-26.7	2.4×10^{3}
11.39¾	-27.3	8×10^{3}
11.40	-27.4	6.4×10^{4}

Table 1 (continued)

17. 1.56

Time	Temp. °C	Instantaneous number per litre
11.23	-5.6	$2x10^{-2}$
11.25	-10.1	$2x10^{-2}$
11.26½	-12.1	$2x10^{-2}$
11.28	-13.4	$2x10^{-2}$
11.31	-17.4	$2x10^{-2}$
11.32	-19.1	$3x10^{-1}$
11.33¾	-19.9	$3x10^{-1}$
11.35	-21.0	$2x10^{-2}$
11.36¾	-21.9	$8x10^{-2}$
11.38	-22.8	$9x10^{-2}$
11.40	-23.3	$5x10^{-2}$
11.41½	-24.8	$1x10^{0}$
11.42	-25.5	$8x10^{0}$
11.42¼	-26.1	$1x10^{3}$
11.42½	-26.3	$2.4x10^{3}$
11.42¾	-27.1	$8x10^{3}$
11.43¼	-28.1	$6.4x10^{4}$

19. 1.56

Time	Temp. °C	Instantaneous number per litre
13.30	-4.2	$2x10^{-2}$
13.33½	-12.4	$2x10^{-2}$
13.35	-14.0	$5x10^{-2}$
13.36	-14.5	$3x10^{-2}$
13.37	-14.6	$3x10^{-2}$
13.39	-16.6	$3x10^{-2}$
13.40	-18.9	$8x10^{-2}$
13.41	-20.6	$3x10^{-1}$
13.42	-21.7	$2.9x10^{0}$
13.42¾	-23.1	$8x10^{0}$
13.43½	-24.2	1.6x10
13.43¾	-24.8	3.7x10
13.44¼	-25.6	$1x10^{3}$
13.44½	-25.9	$8x10^{3}$
13.44¾	-26.1	$6.4x10^{4}$

18. 1.56

Time	Temp. °C	Instantaneous number per litre
11.11½	-7.4	$2x10^{-2}$
11.15	-10.8	$2x10^{-2}$
11.20	-17.6	$2x10^{-2}$
11.20¼	-19.0	$6x10^{-2}$
11.21	-20.0	$1x10^{0}$
11.22	-21.8	$2x10^{0}$
11.23	-23.0	$1x10^{0}$
11.24	-24.6	$1x10^{0}$
11.24½	-25.0	$8x10^{0}$
11.25	-25.4	1.6x10
11.25¼	-25.6	$1.3x10^{2}$
11.25½	-25.9	$1x10^{3}$
11.26	-26.2	$8x10^{3}$
11.26¾	-26.8	$6.4x10^{4}$

20. 1.56

Time	Temp. °C	Instantaneous number per litre
13.12	-4.0	$2x10^{-2}$
13.13	-5.0	$2x10^{-2}$
13.16	-7.4	$3x10^{-2}$
13.20	-9.6	$3x10^{-2}$
13.21½	-15.3	$3x10^{-2}$
13.23½	-17.7	$3x10^{-2}$
13.24½	-19.3	$5x10^{-2}$
13.25	-20.0	$5x10^{-2}$
13.27	-20.7	$5x10^{-2}$
13.29	-21.1	$3x10^{-2}$
13.29½	-21.9	$1x10^{0}$
13.31	-22.8	$2.9x10^{0}$
13.33	-23.8	$3x10^{-1}$
13.36½	-25.5	$1x10^{0}$
13.37	-26.2	$8x10^{3}$
13.38	-27.6	$6.4x10^{4}$

Table 1 (continued)

21. 1.56			22. 1.56		
Time	Temp. °C	Instantaneous number per litre	Time	Temp. °C	Instantaneou number per litre
11.36	-16.9	3×10^{-2}	11.35½	-22.3	2×10^{-2}
11.38	-17.6	2×10^{-2}	11.36	-22.6	3×10^{-2}
11.40	-18.7	3×10^{-2}	11.36¼	-23.2	1×10^{0}
11.41	-19.8	3×10^{-2}	11.36½	-23.7	8×10^{0}
11.42	-20.7	5×10^{-2}	11.37	-24.3	1.6×10
11.43½	-20.7	5×10^{-2}	11.37½	-24.9	3.7×10
11.45	-21.7	3×10^{-1}	11.38½	-25.8	1.3×10^{2}
11.47	-22.3	9×10^{-2}	11.39	-26.6	1×10^{3}
11.48	-22.9	1×10^{0}	11.39½	-26.7	2.4×10^{3}
11.49	-23.4	1×10^{0}	11.39¾	-27.0	8×10^{3}
11.52	-24.6	1.3×10^{-1}	11.41½	-28.6	6.4×10^{4}
11.52½	-25.6	1×10^{0}		24. 1.56	
11.52¾	-26.1	8×10^{0}	11.15½	-6.6	3×10^{-2}
11.53	-26.3	1.3×10^{2}	11.16½	-7.4	2×10^{-2}
11.53½	-26.6	1×10^{3}	11.18	-7.9	2×10^{-2}
11.54	-27.4	2.4×10^{3}	11.21	-10.3	2×10^{-2}
11.54¼	-27.6	8×10^{3}	11.22½	-13.3	3×10^{-2}
11.55	-29.0	6.4×10^{4}	11.30½	-18.3	3×10^{-2}
	23. 1.56		11.34	-20.0	5×10^{-2}
10.48½	-16.1	2×10^{-2}	11.35½	-21.1	5×10^{-2}
10.54½	-22.0	5×10^{-2}	11.36½	-21.8	1.3×10^{-1}
10.55	-22.6	3×10^{-1}	11.38	-22.9	5×10^{-2}
10.55½	-23.1	1×10^{0}	11.39	-23.3	3×10^{-1}
10.56½	-23.7	3×10^{-1}	11.40	-23.8	2×10^{0}
10.57½	-24.6	1×10^{0}	11.41½	-25.3	8×10^{0}
10.58¾	-25.0	8×10^{0}	11.43	-26.1	1.6×10
11.02	-25.9	1.3×10^{2}	11.44½	-26.7	1.3×10^{2}
11.04	-26.6	1×10^{3}	11.46½	-27.6	1×10^{3}
11.04½	-27.4	8×10^{3}	11.50	-28.1	2.4×10^{3}
11.05	-27.9	6.4×10^{4}	11.50½	-28.6	8×10^{3}
			11.51½	-29.1	6.4×10^{4}

Table 1 (continued)

25. 1.56

Time	Temp. °C	Instantaneous number per litre
11.15	-6.0	3x10^{-2}
11.15½	-6.1	2x10^{-2}
11.16½	-6.7	2x10^{-2}
11.20½	-10.3	3x10^{-2}
11.22	-14.0	3x10^{-2}
11.23	-15.1	2x10^{-2}
11.29	-20.1	2x10^{-2}
11.31½	-21.3	3x10^{-2}
11.33	-23.5	1.3x10^{-1}
11.33½	-24.0	3x10^{-1}
11.33¾	-24.3	1x10^{0}
11.34	-24.6	2x10^{0}
11.35	-25.2	8x10^{0}
11.36	-25.6	1.6x10
11.36½	-25.8	3.7x10
11.37	-26.1	1.3x10^{2}
11.38	-26.6	3x10^{2}
11.38½	-26.9	1x10^{3}
11.39½	-27.2	8x10^{3}
11.40	-27.8	6.4x10^{4}

27. 1.56

Time	Temp. °C	Instantaneous number per litre
12.58	-10.2	3x10^{-2}
12.59	-11.5	6x10^{-2}
13.00	-12.7	3x10^{-2}
13.03	-15.6	5x10^{-2}
13.05½	-17.3	3x10^{-2}
13.06½	-18.7	3x10^{-2}
13.07½	-19.9	1.3x10^{-1}

26. 1.56

Time	Temp. °C	Instantaneous number per litre
11.43	-8.4	2x10^{-2}
11.44½	-10.9	3x10^{-2}
11.45½	-12.4	3x10^{-2}
11.46	-14.2	5x10^{-2}
11.47½	-15.3	6x10^{-2}
11.49	-17.5	6x10^{-2}
11.50½	-19.9	1x10^{0}
11.51½	-21.5	2.9x10^{0}
11.53	-23.1	4.6x10^{0}
11.53½	-23.9	8x10^{0}
11.54	-25.0	1.3x10^{2}
11.54¼	-25.2	1x10^{3}
11.54½	-25.8	8x10^{3}
11.55	-26.6	6.4x10^{4}

27. 1.56 (continued)

Time	Temp. °C	Instantaneous number per litre
13.09	-20.8	3x10^{-1}
13.09¾	-21.3	1.3x10^{-1}
13.10	-21.7	1x10^{0}
13.11½	-23.3	1x10^{0}
13.12	-24.4	2.9x10^{0}
13.12½	-24.7	1.6x10
13.13	-25.5	3.7x10
13.13½	-26.1	1x10^{3}
13.14	-27.2	8x10^{3}
13.15	-27.8	6.4x10^{4}

Table 1 (continued)

28. 1.56

Time	Temp. °C	Instantaneous number per litre
11.37	-7.6	1.1x10^{-1}
11.37½	-8.0	5x10^{-2}
11.38¼	-8.8	8x10^{-2}
11.38¾	-10.0	1.1x10^{-1}
11.40¾	-11.5	5x10^{-2}
11.41½	-13.5	8x10^{-2}
11.43	-16.0	2x10^{-2}
11.44½	-17.6	3x10^{-2}
11.45½	-19.1	3x10^{-2}
11.46½	-20.1	9x10^{-2}
11.48	-21.3	3x10^{-2}
11.49	-22.9	1.3x10^{-1}
11.50	-24.0	3x10^{-1}
11.50¼	-24.7	8x10^{0}
11.51	-25.4	1.6x10
11.51¼	-25.6	1.3x10^{2}
11.52½	-25.8	1x10^{3}
11.53½	-26.4	2.4x10^{3}
11.53¾	-26.6	8x10^{3}
11.54½	-27.2	6.4x10^{4}
	29. 1.56	
11.30½	-9.4	2x10^{-2}
11.33½	-11.9	3x10^{-2}
11.34½	-13.3	2x10^{-2}
11.37	-17.1	2x10^{-2}
11.38	-18.1	2x10^{-2}
11.39	-20.2	1.1x10^{-1}
11.40	-21.5	9x10^{-2}
11.40½	-22.2	3x10^{-1}
11.42	-23.1	1x10^{0}
11.43½	-24.4	3x10^{-1}
11.44	-25.3	1x10^{0}
11.44¼	-25.5	8x10^{0}
11.44½	-26.1	8x10^{3}
11.45	-26.6	6.4x10^{4}

30. 1.56

Time	Temp. °C	Instantaneous number per litre
11.03½	-6.7	5x10^{-2}
11.05	-10.1	5x10^{-2}
11.06½	-11.2	3x10^{-2}
11.09½	-13.1	5x10^{-2}
11.11	-16.2	3x10^{-2}
11.12½	-17.5	2x10^{-2}
11.13	-18.5	2x10^{-2}
11.14	-19.2	2x10^{-2}
11.15½	-20.3	2x10^{-2}
11.15¾	-20.5	1.3x10^{-1}
11.17	-22.6	1.3x10^{-1}
11.18	-23.4	1.3x10^{-1}
11.19½	-23.6	3x10^{-2}
11.20½	-24.6	1.3x10^{-1}
11.20¾	-24.9	1x10^{0}
11.21	-25.4	8x10^{0}
11.21¼	-25.6	1x10^{3}
11.22	-26.2	8x10^{3}
11.22½	-26.7	6.4x10^{4}

Table 2

Comparison of freezing nuclei counts with other observations

Date Wind at 10,000 ft Air mass	Vertical ascent	Cloud and weather	Condensation nuclei	Freezing nuclei per litre		Remarks on freezing nuclei
				at -20°C	at -25°C	
2. 1.56 Northerly Cold Polar	Inversion at 4,000 ft. Subsidence, dry above	Small Cu. only	Decrease above inversion. Number average	$3\text{x}10^{-2}$ Low	$1\text{x}10^{0}$ Low	Little chance of supply from ground
3. 1.56 NE'ly ahead of weak warm front	Inversion at 4,000 ft probable subsidence	8/8 Sc. topped by inversion	Decrease above inversion. Number below average	$1.7\text{x}10^{-2}$ Low	$1.3\text{x}10^{-1}$ Low	Number very low
4. 1.56 Light S'ly Anticyclonic	Inversion near surface	No cloud. Haze top 2,000 ft. Also haze above 7,500 ft	Very low throughout	$4.6\text{x}10$ High	$2.4\text{x}10^{3}$ High	Freezing nuclei counts high. No correlation with condensation nuclei and little transport from surface. Origin could have been extra-terrestrial
No observations 5. 1.56 - 8. 1.56 inclusive						
9. 1.56 W'ly ahead of ridge or High	Inversion at 4,000 ft	8/8 Sc. topped by inversion. Some light snow	Considerable decrease to low values above inversion. Readings variable	$1.7\text{x}10^{-2}$ Low	$7\text{x}10$ Moderate	Doubtful whether supply could have come from below
10. 1.56 SW'ly Post cold front	Unstable	Cu. and Cb. to 20,000 ft. Some rain	Low counts	$9\text{x}10^{-2}$ Moderate	$4\text{x}10$ Moderate	Supply could have been from below, although condensation nuclei counts low

Table 2 (continued)

Date Wind at 10,000 ft Air mass	Vertical ascent	Cloud and weather	Condensation nuclei	Freezing nuclei per litre		Remarks on freezing nuclei
				at -20°C	at -25°C	
11.1.56 WSW'ly	Rather unstable	Cb. locally. Also thin Sc. layers. Showers	Low counts	1.7×10^{-2} Low	8×10^{2} High	Supply could have been from below, although condensation nuclei counts low
12.1.56 W'ly Post-wave	Rather unstable	Sc. layer 5,000 to 10,000 ft. Rain	Below average	1.7×10^{-2} Low	2.5×10^{-1} Low	Supply could have been from below, although condensation nuclei counts low
13.1.56 W'ly Ridge of high pressure	Fairly stable	No cloud. Haze top 4,000 ft. Very dry	Below average	1.7×10^{-2} Low	8×10^{0} Low	Supply could have been from below, although condensation nuclei counts low
14.1.56 SW'ly	Unstable	Layered cloud to 10,000 ft and above	Below average decreasing with height	5×10^{-1} Moderate	1.2×10^{0} Low	Doubtful if supply came from below - some decrease with height of condensation nuclei
15.1.56 W'ly airstream	Fairly stable	4/8 Sc. at 2,500 ft. Rather dry above	Moderate and variable. Constant with height	3.3×10^{-2} Low	2.9×10^{0} Low	Could have come from below
16.1.56 WNW airstream	Unstable to 7,000 ft. Small inversion	1/8 Sc. at 5,000 ft	Rather small-decreasing with height	1×10^{-1} Moderate	1.5×10^{0} Low	Doubtful if supply could have come from below
17.1.56 W'ly airstream	Inversion at 4,000 ft	St. near surface otherwise dry	Rather large decreasing with height	3×10^{1} Moderate	1.5×10^{0} Low	Possible transport from below in spite of inversion
18.1.56 NW'ly Post cold front	Small inversion at 4,000 ft	1/8 Cu. dry above	Below average decreasing with height	1×10^{0} High	8×10^{0} Low	Doubtful if transport possible from below

Table 2 (continued)

Date Wind at 10,000 ft Air mass	Vertical ascent	Cloud and weather	Condensation nuclei	Freezing nuclei per litre		Remarks on freezing nuclei
				at -20°C	at -25°C	
19.1.56 WNW'ly Pre warm front	Stable. Inversion at 4,000 ft	Cu. 3,000 to 3,500 ft. Ac.As. 7,500 to 8,500 ft and also above 9,700 ft	Above average	1.5x10^{-1} Moderate	6x10 Moderate	Transport from below unlikely
20.1.56 W'ly Warm sector	Unstable to 5,000 ft. Inversion above	8/8 Sc. 3,000 to 5,500 ft. Very dry above. Slight rain	Below average. Decrease above inversion	5x10^{-2} Low	7x10^{-1} Low	Transport from below unlikely
21.1.56 W'ly Pre warm front	Rather unstable	No low cloud. 8/8 Ac.As. Rain later	Below average	3.3x10^{-2} Low	2.6x10^{-1} Low	Transport from below possible
22.1.56 W'ly Post cold front	Fairly stable	8/8 Ac.As. above 7,000 ft	Rather high	Nil	4x10 Moderate	Some transport from below possible
23.1.56 NW'ly Cold frontal	Unstable	Cloud layers 1,800 to 3,500 ft, 4,500 to 8,000 ft. More above. Rain	Very high	Nil	8x10^{0} Low	Transport could definitely have come from below
24.1.56 NW'ly	Unstable	No cloud	High	5x10^{-2} Low	6.3x10^{0} Low	Transport could have come from below
25.1.56 NW'ly Ridge of high pressure	Stable inversion at 6,000 ft	No cloud	High	1.7x10^{-2} Low	5.1x10^{0} Low	Transport from below doubtful in spite of high condensation nuclei counts

Table 2 (continued)

Date Wind at 10,000 ft Air mass	Vertical ascent	Cloud and weather	Condensation nuclei	Freezing nuclei per litre		Remarks on freezing nuclei
				at $-20^{\circ}C$	at $-25^{\circ}C$	
26.1.56 W'ly Warm sector	Rather unstable	8/8 St. 1,000 to 7,500 ft. Slight rain	No data	$1x10^{0}$ High	$1.2x10^{2}$ High	Transport could probably have come from below
27.1.56 W'ly Weak occlusion	Rather unstable	Local Cu., tops 7,000 ft	Very high	$1.3x10^{-1}$ Moderate	2.2x10 Moderate	Transport could have been from below
28.1.56 W'ly Warm front	Fairly stable	Layers 500 to 1,500 ft, 2,500 to 4,000 ft, 7,500 to 8,000 ft. Slight rain	Generally low	$1x10^{-1}$ Moderate	1.1x10 Moderate	Transport from below unlikely
29.1.56 W'ly Cold frontal	Unstable	8/8 Nb. St. 800 to 10,000 ft. Rain	No data	$1x10^{-1}$ Moderate	$6.3x10^{-1}$ Low	Transport from below unlikely
30.1.56 Light SW'ly Secondary depression	Unstable	Layers 800 to 1,200 ft, 3,200 to 5,400 ft, 7,200 to above 20,000 ft. Rain	High. Decrease with height	$1.7x10^{-2}$ Low	$1.4x10^{0}$ Low	Transport from below possible

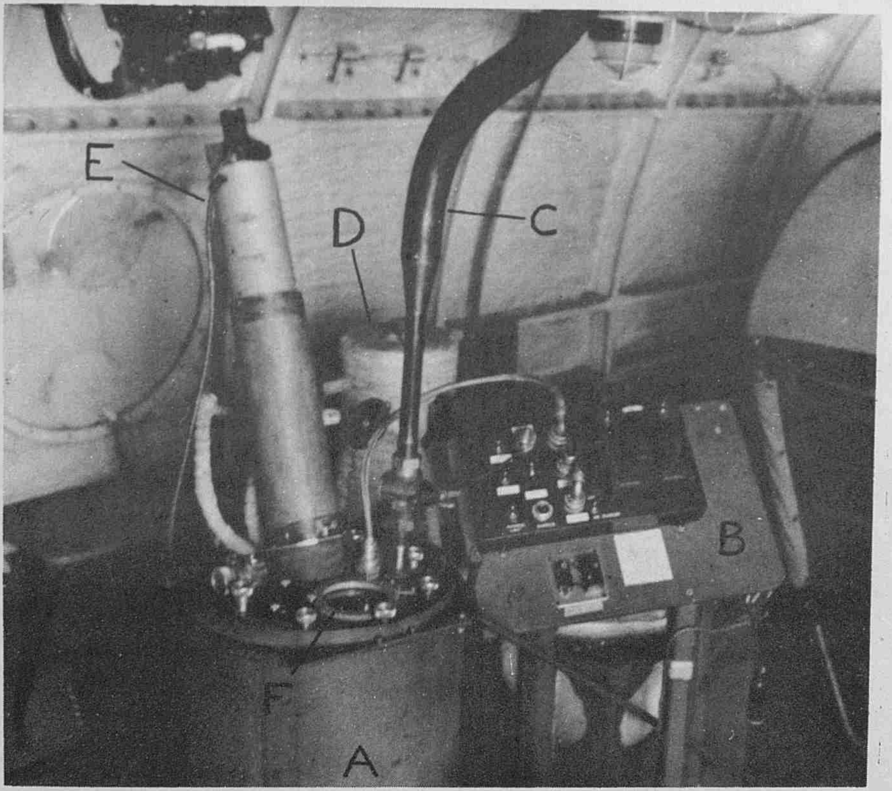

FIG. 1

EXTERNAL ARRANGEMENT OF THE CLOUD CHAMBER

A. 40 LITRE CHAMBER

B. CONTROL PANEL (SOLID CO_2 CONTAINER BENEATH)

C. AIR INTAKE PIPE

D. ELECTRIC PUMP - COOLING CIRCUIT

E. INTERNAL ILLUMINATION UNIT

F. VIEWING PANEL

NOTE: HEATING UNIT NOT ILLUSTRATED

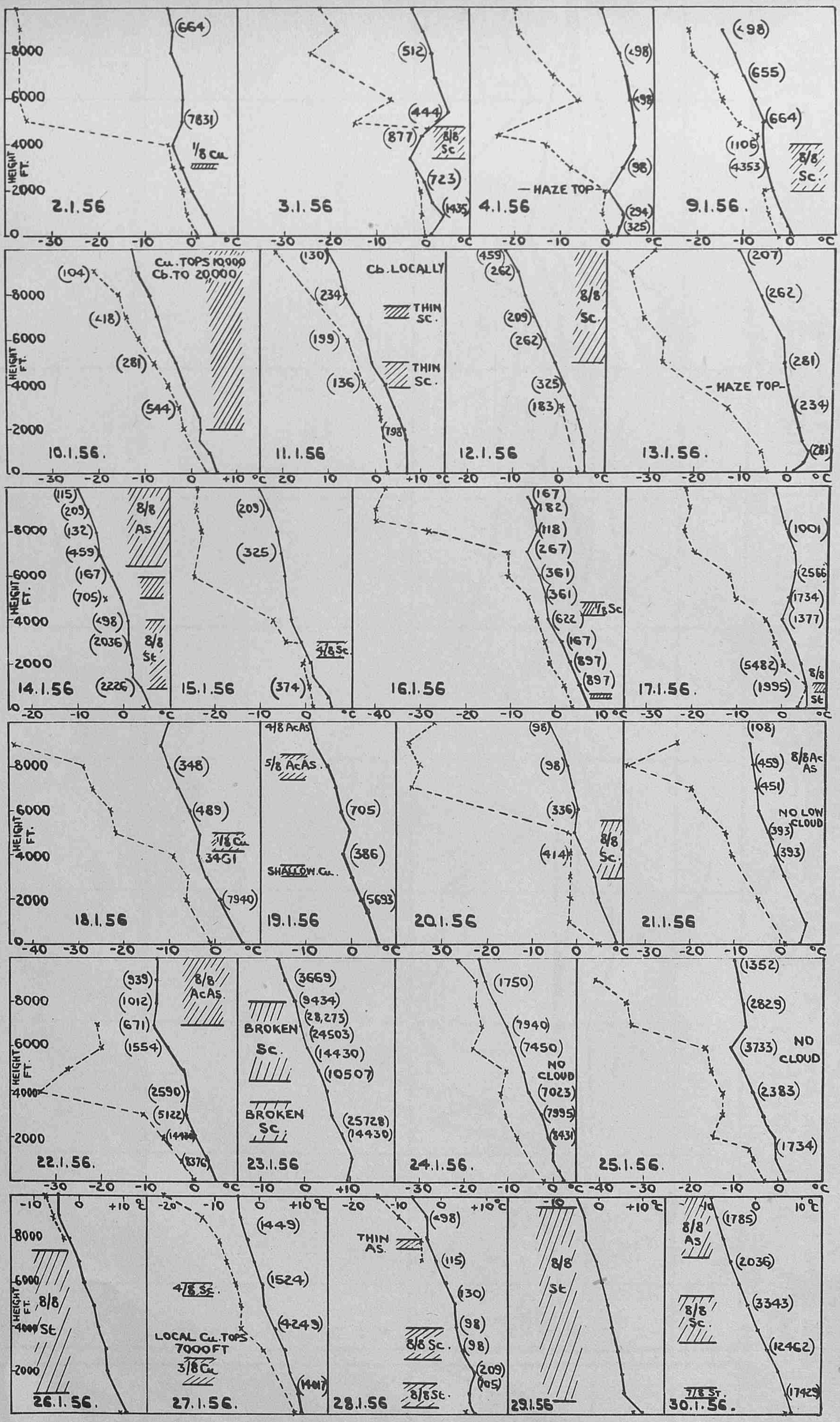

—•— TEMPERATURE °C.
×--× FROST POINT °C.
( ) CONDENSATION NUCLEI/CC.
▨ CLOUD.

FIG. 2 DAILY AIRCRAFT ASCENTS

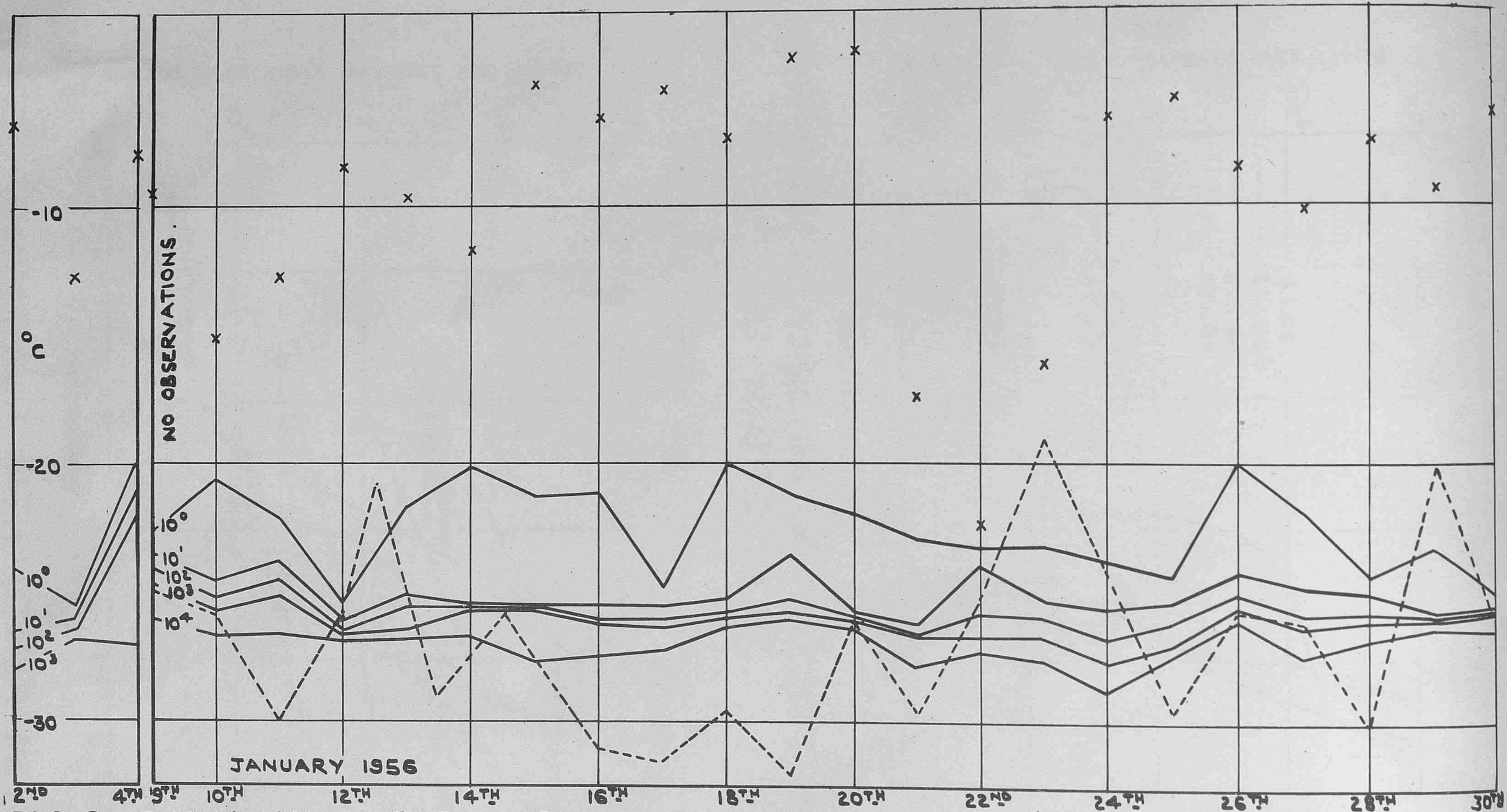

FIG. 3 DAILY VARIATION OF FREEZING NUCLEI. (10^0, 10^1, 10^2, 10^3 & 10^4/LITRE)
ONE SAMPLE EVERY DAY AT 10,000 FT. OVER SOUTHERN ENGLAND. (●——●)
SIMILAR MEASUREMENTS IN AUSTRALIA. JAN. 1955. OF 1/LITRE ONLY. (●- - - -●)
TEMPERATURE AT WHICH ICE CRYSTALS WERE FIRST OBSERVED. (X)

M.R.P. 998

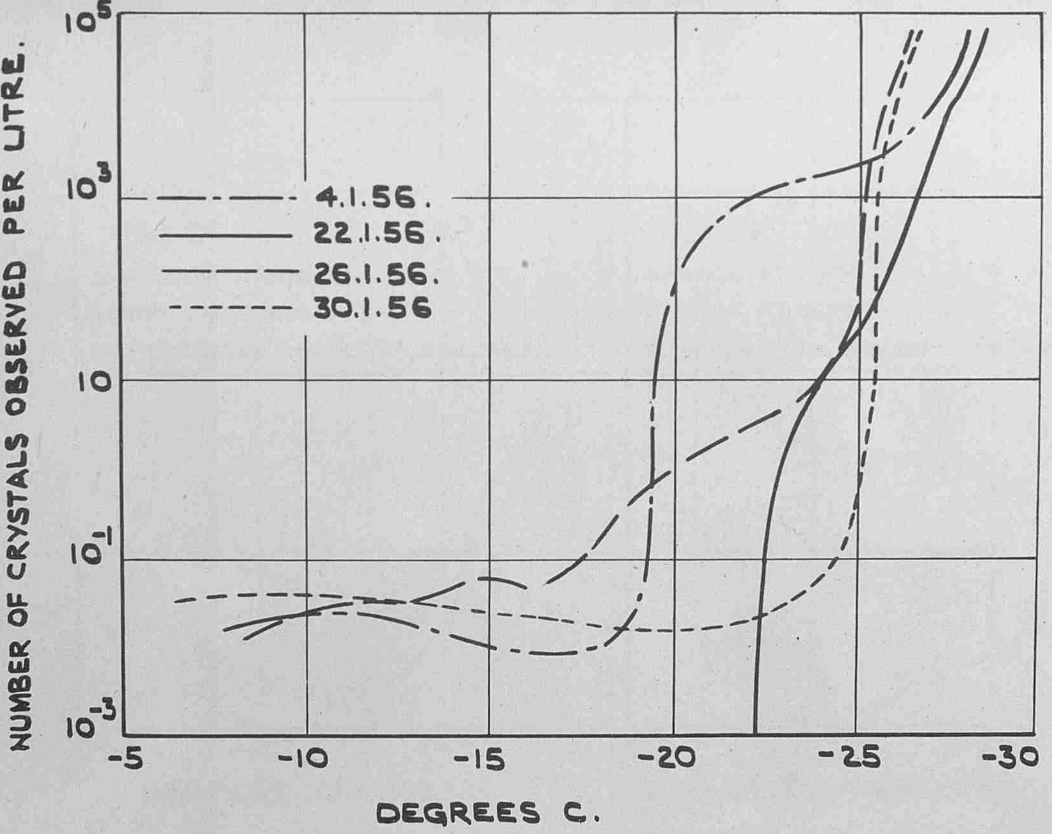

FIG.4 TYPICAL SPECTRA OF FREEZING NUCLEI AT 10,000 FEET.

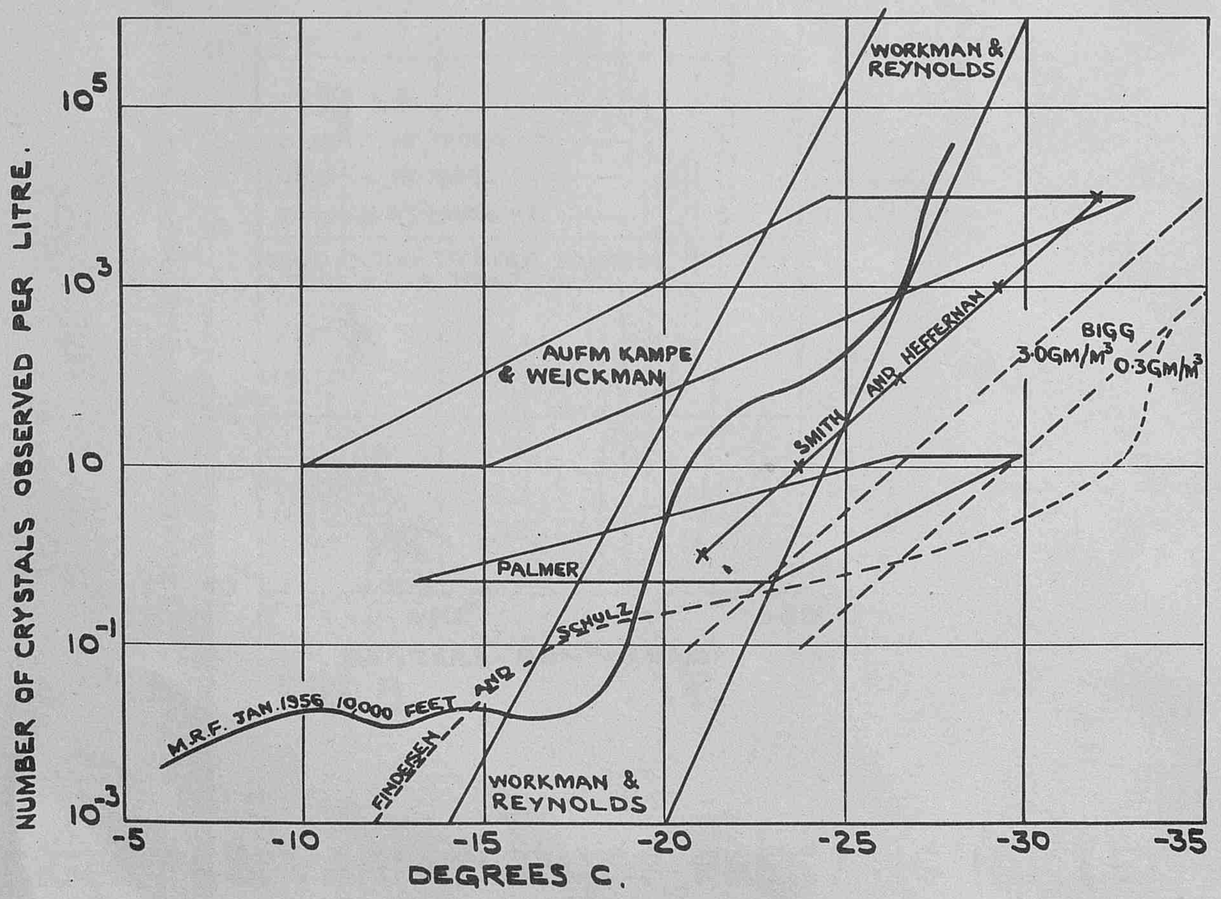

FIG.5 COMPARISON WITH OTHER RESULTS.

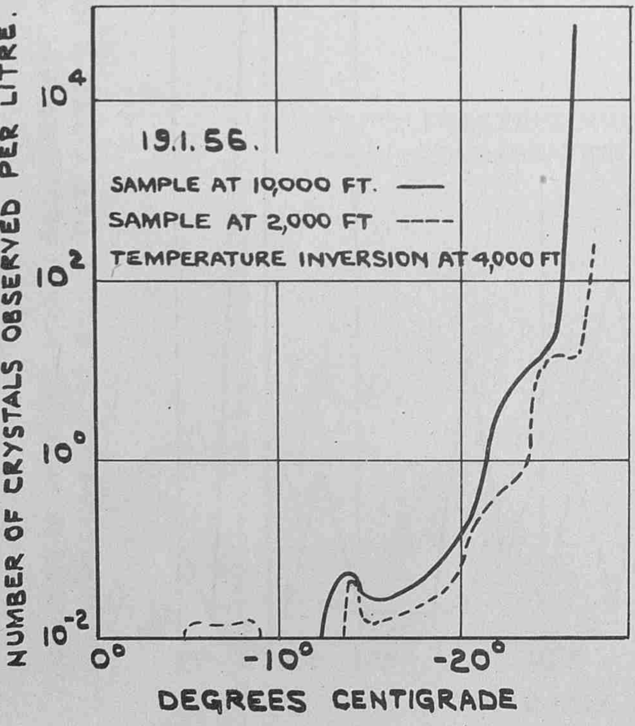

FIG. 6

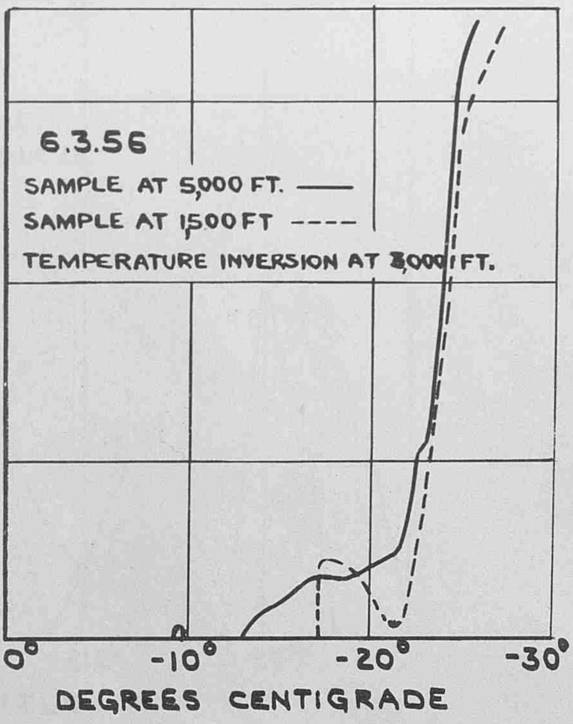

FIG. 7

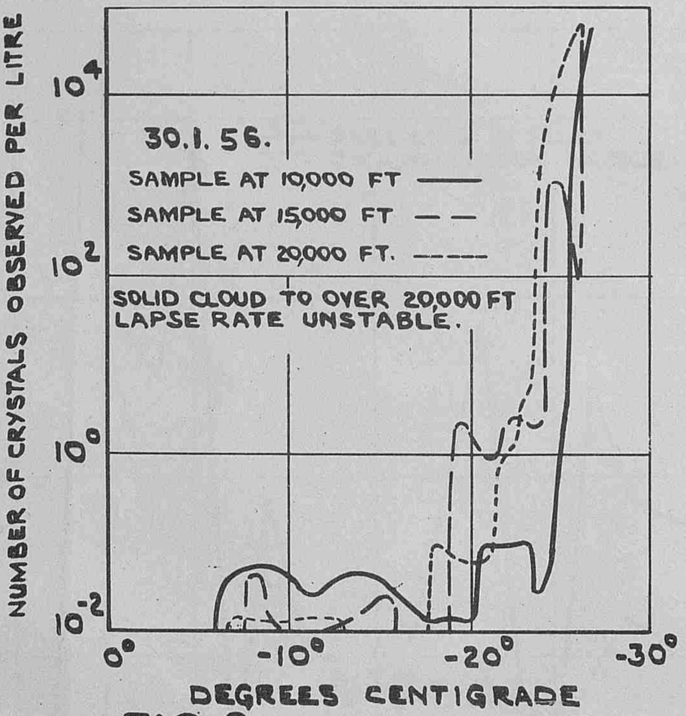

FIG. 8

FIG. 6,7 & 8 VARIATION OF FREEZING NUCLEI WITH HEIGHT.

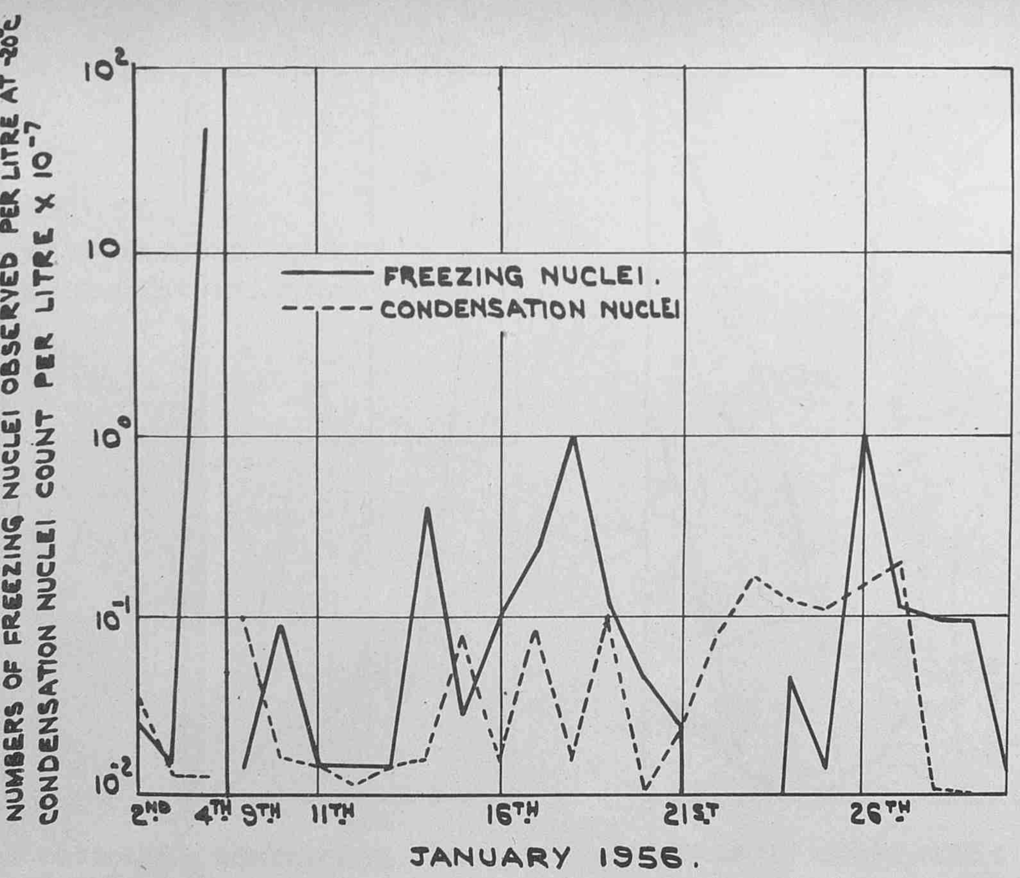

FIG. 9 COMPARISON OF FREEZING NUCLEI ACTIVE AT - 20°C. WITH CONDENSATION NUCLEI. 10,000 FT.

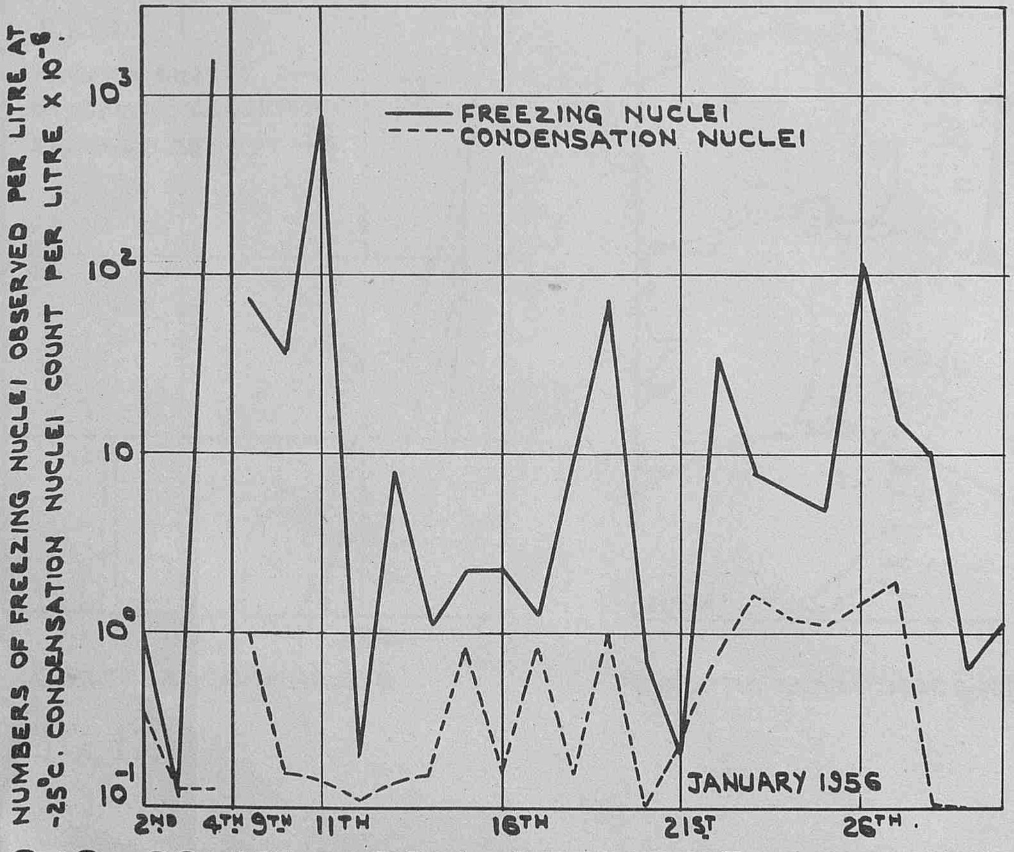

FIG. 10 COMPARISON OF FREEZING NUCLEI ACTIVE AT - 25° C. WITH CONDENSATION NUCLEI. 10,000 FT.

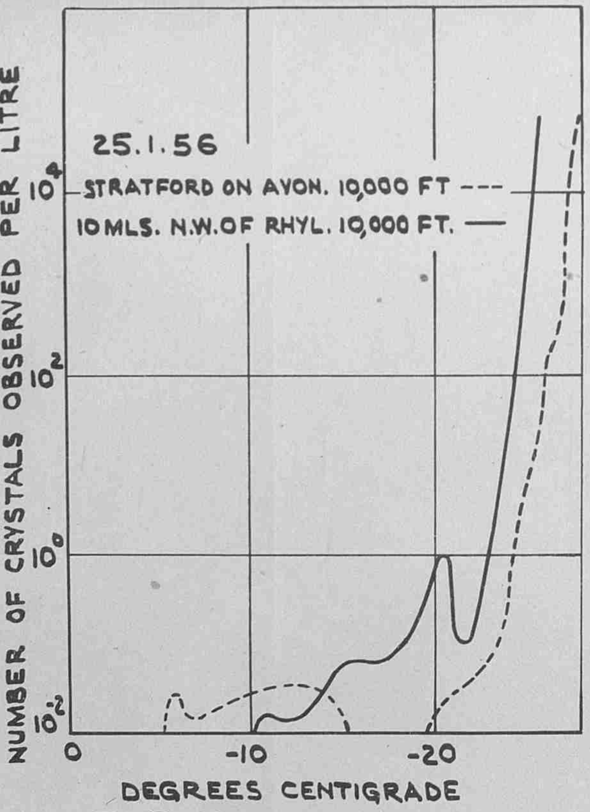

FIG. 11

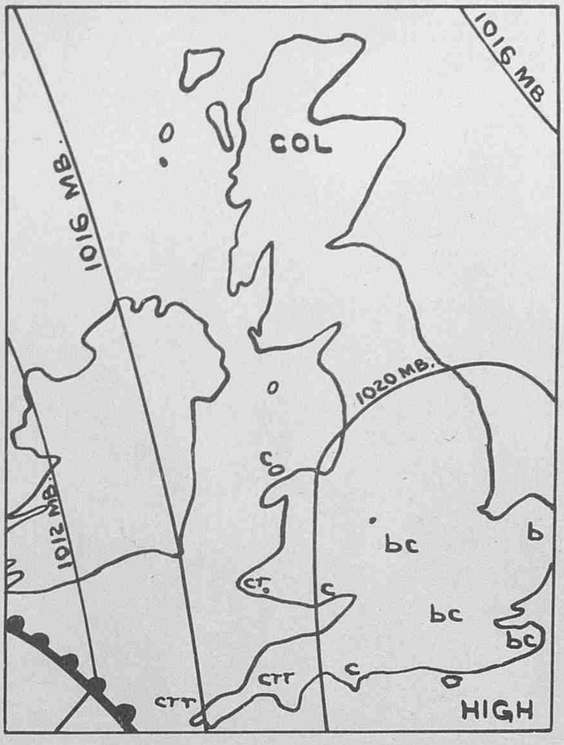
1016 MB
1016 MB.
COL
1020 MB.
1012 MB.
c
bc
b
CT
CTT
HIGH

SYNOPTIC CHART, 1200 G.M.T. 25.1.56.

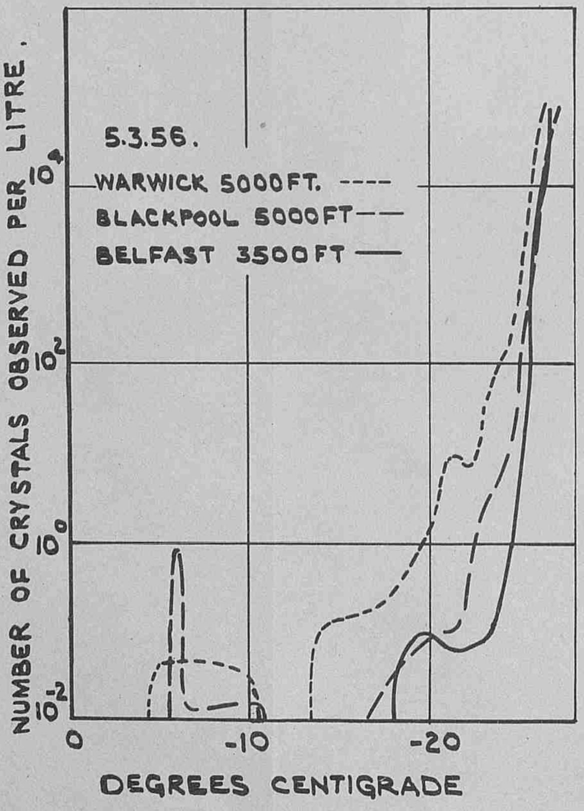

FIG. 12

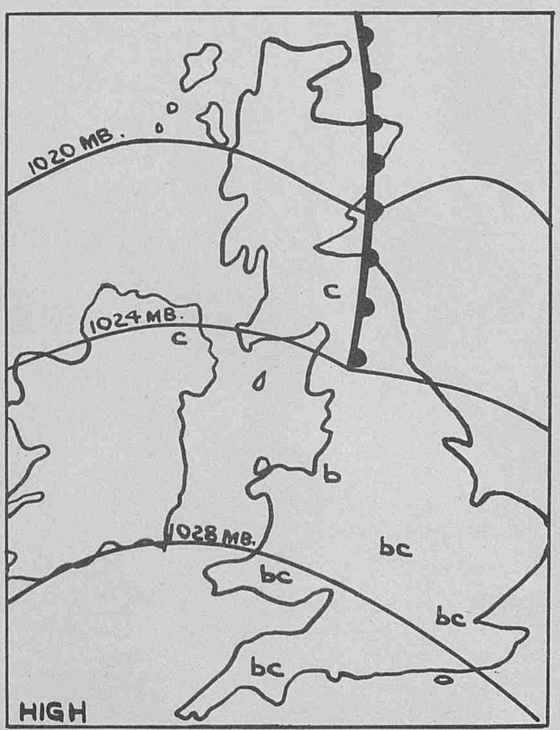
1020 MB.
1024 MB.
1028 MB.
c
b
bc
HIGH

SYNOPTIC CHART. 1200 G.M.T. 5.3.56.

VARIATION OF FREEZING NUCLEI IN THE HORIZONTAL.

13547

M.R.P. 1001

18th January, 1957

AD 223118

Index of M.R.Ps. Approved for General Distribution

Appendix 16 of M.R.P. 200

(Meteorological Office)

AIR MINISTRY

METEOROLOGICAL RESEARCH COMMITTEE

Addendum to M.R.P. 1001

M.R.P.	Title	Author
989	The measurement of surface wind	R. Frith

57

G.24265/PO/9/57/340

951	Index of M.R.Ps. approved for general distribution. (Appendix 15 of M.R.P. 200)	-
952	Convection from a small, continuous source of heat in a calm, neutral atmosphere (with an appendix on the bent-over plume)	P.J. Meade
953	The success achieved in forecasting upper winds by orthodox and statistical techniques	D.H. Johnson
955	Comments on statistical and orthodox forecasting	C.S. Durst
956	The use of a stream function in the Sawyer-Bushby two parameter model of the atmosphere	F.H. Bushby Vera M. Huckle
960	Development of thermometers for high-speed aircraft	D.D. Clark
961	A technique for studying the local atmospheric diffusion of airborne material (Porton Technical Paper No.527)	J.S. Hay F. Pasquill
965	Objective Analysis	D.H. Johnson
970	The harmonic representation of the annual temperature variation in different parts of the British Isles	J.M. Craddock
971	Variation of visibility in fog at Exeter Airport, and the time of fog dispersal	W.E. Saunders
972	Water loss from various cropped surfaces	N.E. Rider
973	Evaporation from a saturated rough surface into a turbulent air stream (Porton Technical Paper No. 533)	J.S. Hay
974	A vertical gustiness recorder for use with a captive balloon (Porton Technical Paper No. 536)	J.I.P. Jones
976	Further observations of humidity up to 50,000 feet made from aircraft of the Meteorological Research Flight in 1955	N.C. Helliwell J.K. Mackenzie M.J. Kerley
977	An electrical dewpoint hygrometer suitable for routine meteorological use	J. MacDowall
978	Long-period averages for the upper air	J.K. Bannon

/979

G.5233/JEK/1/57/340

At the time of issue this report has not been published. Any author desiring to quote this paper should refer to it as "A paper of the Meteorological Research Committee (London),
M.R.P. No. 1001
A copy is available in the Library of the Meteorological Office."

M.R.P. 1001
18th January, 1957

AIR MINISTRY
METEOROLOGICAL RESEARCH COMMITTEE

Index of M.R.Ps. Approved for General Distribution
Appendix 16 of M.R.P. 200

M.R.P.	TITLE	AUTHOR
951	Index of M.R.Ps. approved for general distribution. (Appendix 15 of M.R.P. 200)	-
952	Convection from a small, continuous source of heat in a calm, neutral atmosphere (with an appendix on the bent-over plume)	P.J. Meade
953	The success achieved in forecasting upper winds by orthodox and statistical techniques	D.H. Johnson
955	Comments on statistical and orthodox forecasting	C.S. Durst
956	The use of a stream function in the Sawyer-Bushby two parameter model of the atmosphere	F.H. Bushby Vera M. Huckle
960	Development of thermometers for high-speed aircraft	D.D. Clark
961	A technique for studying the local atmospheric diffusion of airborne material (Porton Technical Paper No.527)	J.S. Hay F. Pasquill
965	Objective Analysis	D.H. Johnson
970	The harmonic representation of the annual temperature variation in different parts of the British Isles	J.M. Craddock
971	Variation of visibility in fog at Exeter Airport, and the time of fog dispersal	W.E. Saunders
972	Water loss from various cropped surfaces	N.E. Rider
973	Evaporation from a saturated rough surface into a turbulent air stream (Porton Technical Paper No. 533)	J.S. Hay
974	A vertical gustiness recorder for use with a captive balloon (Porton Technical Paper No. 536)	J.I.P. Jones
976	Further observations of humidity up to 50,000 feet made from aircraft of the Meteorological Research Flight in 1955	N.C. Helliwell J.K. Mackenzie M.J. Kerley
977	An electrical dewpoint hygrometer suitable for routine meteorological use	J. MacDowall
978	Long-period averages for the upper air	J.K. Bannon

/979

G.5233/JEK/1/57/340

M.R.P.	TITLE	AUTHOR
979	Further observation of condensation trails	N.C. Helliwell J.K. Mackenzie
980	Further observations of large cumuliform clouds by the Meteorological Research Flight	G.J. Day
981	Average height of the standard isobaric surfaces over the area from the North Pole to 55°N in July	H. Heastie
983	The measurement of humidity at Britannia SØ 1952-53	R.A. Hamilton
984	Variation with height of rainfall below the melting level	W.G. Harper
985	A preliminary study of atmospheric waves using radiosonde data	G.A. Corby
986	The objective analysis of some 500 mb. charts	F.H. Bushby
987	Equivalent head-wind statistics for variable tracks	P. Graystone
988	On the development of an improved daylight illumination recorder	M.J. Blackwell D.B.B. Powell
989	The measurement of Surface Wind	R. Frith
990	The exhaust trail from jet engines	R.F. Jones
991	Droplet sampling in cumulus clouds A note on M.R.P. 991	W.G. Durbin B.C.V. Oddie
994	A synoptic study of anomalies of surface air temperature over the Atlantic half of the Northern Hemisphere	J.M. Craddock C.A.S. Lowndes
995	Meteorological research in aircraft	R.J. Murgatroyd
996	Condensation trails formed by jet aircraft	J. Briggs
997	A simple method for measuring atmospheric attenuation of light ("meteorological optical range" or visibility) at night	K.H. Stewart
998	The measurements of natural freezing nuclei made by the Meteorological Research Flight during January, 1956	R.J. Murgatroyd M.P. Garrod